

SOCAR

BAKI ALİ NEFT MƏKTƏBİ
BAKU HIGHER OIL SCHOOL

DEDICATED TO THE 103RD ANNIVERSARY OF THE AZERBAIJAN NATIONAL LEADER HEYDAR ALIYEV

TOWARDS SUSTAINABLE CHEMISTRY AND CHEMICAL ENGINEERING

THE 7TH INTERNATIONAL SCIENTIFIC CONFERENCE OF STUDENTS AND YOUNG RESEARCHERS



15-16 APRIL 2026, BAKU, AZERBAIJAN

CONFERENCE PROCEEDINGS

www.bhos.edu.az

doi ISBN

SOCAR

BAKI ALİ NEFT MƏKTƏBİ
BAKU HIGHER OIL SCHOOL

Ümummilli lider Heydər Əliyevin anadan olmasının 103-cü ildönümünə həsr olunmuş

DAYANIQLI KİMYA VƏ KİMYA MÜHƏNDİSLİYİNƏ DOĞRU

TƏLƏBƏ VƏ GƏNC TƏDQİQATÇILARIN VII BEYNƏLXALQ ELMİ KONFRANSI

Konfrans Materialları

ISBN: 978-9952-8513-5-9

16-17 aprel 2026-cı il,
Bakı, Azərbaycan

MODERN APPROACHES TO IMPROVING THE EFFICIENCY OF GAS PURIFICATION FROM ACIDIC COMPONENTS

O.B. Akhmedova[1], M.Z. Nuriddinov[2] A.Sh. Qayumov[3], R.D.Asadova[4], N.Maxmudov[5]

[1]Tashkent State Technical University named after Islam Karimov, Associate Professor
[2]Tashkent State Technical University named after Islam Karimov, Master's Student
[3]Tashkent State Technical University named after Islam Karimov, Associate Professor
[4]Tashkent State Technical University named after Islam Karimov, Associate Professor
[5]Tashkent State Technical University named after Islam Karimov, Professor

Abstract - The article presents scientific research on the preparation and application of compositions with the necessary concentration of activators and inhibitors in the absorbent to reduce the corrosion rate and enhance the complete absorption of acidic components from gases. The effectiveness of a new absorption composition containing diethylolamine (DEA), hexamine, and carbohydrazide in purifying gases from acidic components has been determined. According to the studies conducted, the activation of absorbents with activators allows for more complete absorption of acidic components from gases, reduces the formation of heat-resistant salts, thereby reducing the corrosion observed in devices and preventing excessive accumulation in the absorber.

Keywords: gas chromatography, composite absorbent, diethylamine, hexamine ($C_6H_{12}N_4$), carbohydrazide ($OC(N_2H_3)$), carbon dioxide (CO_2), hydrogen sulfide (H_2S), carbon sulfide (COS), carbon disulfide (CS_2), mercaptans (RSH), thiophenes (C_4H_4S).

Introduction

At present, due to the rapid development of industry and manufacturing, it has become evident that the direct combustion of hydrocarbon gases is an inefficient use of resources. Modern trends in the oil and gas industry focus on the deep processing of gases to obtain valuable products, which in turn ensures the efficient utilization of raw materials considered highly economically advantageous and meets contemporary requirements [1]. Like any other raw material, hydrocarbon gases cannot be used directly — their application requires preliminary purification, processing, and separation into fractions using appropriate technologies [2–3].

Globally, during the purification of hydrocarbon gases from acidic components, alkanolamine-based absorbents play a leading role. Aqueous solutions of diethanolamine (DEA) of various concentrations are considered particularly effective and are widely used for the removal of acidic compounds, especially hydrogen sulfide, from gases. However, gas compositions also contain other acidic components such as carbon dioxide (CO_2), carbonyl sulfide (COS), carbon disulfide (CS_2), mercaptans (RSH), and thiophenes [4–5].

Materials and Research Methods

At present, in order to enhance the complete absorption of acidic components from gases, scientific research aimed at developing and applying compositions consisting of mixtures of activators, corrosion inhibitors, and antifoaming additives within absorbents is of great importance.

Activators added to alkanolamine absorbents include hexamine, piperazine, methanol, phenol, ethanolamine, arsenic acid, glycine, and substituted amines. Corrosion inhibitors that slow down the corrosion rate include carbohydrazide, glycols (MEG/TEG), methyldiethanolamine (MDEA), as well as mixtures of glycols (MEG/TEG) with tertiary amines. The introduction of these components into the absorbent further enhances its absorption capacity and stability, reduces concentration losses, and decreases corrosion rates and excessive foaming in the absorber [6-7].

The study began with an analysis of the composition of the raw gas supplied to the Shurtan Gas Chemical Complex. The composition of the feed gas was determined based on the average result of gas chromatographic analysis over one month. According to the obtained data, the CO_2 content was 3.36%, and H_2S — 0.093%. These indicators exceed the standard values established by the process regulations, which negatively affect the efficiency of amine absorption purification.

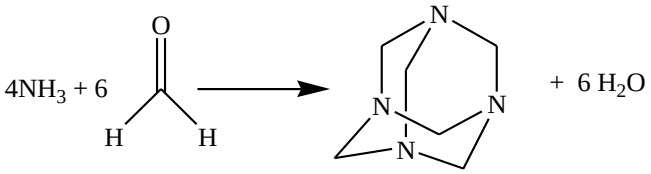
The gas purified at the Shurtan Gas Chemical Complex is subsequently directed as follows: the methane fraction of hydrocarbons is used as feedstock at the GTL (Gas-to-Liquid) plant to produce synthetic fuels, while the ethane fraction serves as raw material for polymer production within the complex itself. The purity of these gas compositions is of primary importance for their chemical and catalytic processing.

To improve the technical and economic performance of hydrocarbon gas purification processes from acidic components by reducing operating costs, a modified version of the absorption process using diethanolamine (DEA) was developed.

Accordingly, a composite absorbent was formulated based on industrially used diethanolamine (DEA) and activators such as hexamine and carbohydrazide.

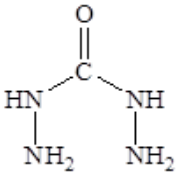
Diethanolamine (DEA) — $NH(C_2H_4OH)_2$ — possesses the following physicochemical properties: it is a liquid ranging from colorless to yellowish in appearance, with a characteristic odor. It is well soluble in both water and fats. The hydrogen ion index (pH) is 11 at a concentration of 100 g/L in water at 20 °C. The density at 20 °C is 1.0959 g/cm³.

Hexamine (HMTA) — $C_6H_{12}N_4$ — is a white crystalline powder formed by the reaction of 4 moles of ammonia with 6 moles of formaldehyde [45; 48–62 pp.]. In terms of structural organization, the compound resembles adamantane, which gives it high thermal stability and chemical resistance.



Based on toxicological assessments of hexamine exposure, it has been established that under various application methods, no long-term health risks have been identified, and the current level of exposure to the substance is considered safe. Hexamine functions as a corrosion inhibitor, preventing hydrogen-induced corrosion of equipment.

Carbohydrazide (hydrazine, 1,3-diaminourea; carbonyl dihydrazide) — molecular formula $CO(NHNH_2)_2$ — is a white crystalline powder with a purity of 98.0%. It is typically used as a 10% aqueous solution with a pH of 8.45. Carbohydrazide is highly soluble in water and alcohol and is applied as a corrosion inhibitor, particularly in systems where water and elevated temperatures are present.



An experimental setup was prepared, with its parameters adapted to industrial operating conditions. The process of gas absorption purification was carried out using various composite absorbents. Tests were conducted with seven samples, during which the purified gas and the saturated absorbent were collected in separate containers for subsequent analysis (Table 1) [16–18].

Table 1. Composition of absorbent mixtures based on DEA, hexamine, and carbohydrazide for the purification of gases from acidic components

№	Name of absorbent	Water content in the composition, %	Concentration of components, %		
			DEA	Hexamine	Carbohydrazide
1	DEA, Sample 1 (for comparison)	70	30	-	-
2	Sample 2 with DEA	67,975	30	2	0,025
3	Sample 3 with DEA	65,975	30	4	0,025
4	Sample 4 with DEA	65,975	32	2	0,025
5	Sample 5 with DEA	63,975	32	4	0,025
6	Sample 6 with DEA	63,975	34	2	0,025
7	Sample 7 with DEA	61,975	34	4	0,025

When preparing the above-mentioned absorbent composition, the selection of chemical reagents was primarily based on the local origin of raw materials, their degree of efficiency, as well as on the shortcomings observed in the existing technological scheme.

Results and Analysis

To ensure the efficient performance of the diethanolamine (DEA) absorbent in the process of gas absorption purification, regular laboratory analyses are carried out. This is necessary because, under the influence of process parameters — such as pressure, temperature, environment, chemical reagents, and gas composition — chemical changes may occur in the absorbent, causing it to lose its functional properties [8–10].

Taking this into account, the following studies were conducted on DEA-based absorbent compositions used for the purification of natural gases from CO_2 and H_2S:

- determination of carbon dioxide (CO_2) content;
- determination of hydrogen sulfide (H_2S) mass in saturated and regenerated diethanolamine solutions by titration;
- determination of the amount of acid–thermally stable salts;
- determination of the foaming tendency of the absorbents;
- determination of concentration;
- determination of H_2S content in DEA;
- measurement of the pH value of DEA;
- determination of DEA turbidity;
- determination of DEA viscosity.

These analyses made it possible to evaluate the physicochemical stability of the absorbent, the efficiency of its performance, and the changes in its properties during operation and regeneration. The amount of carbon dioxide in the DEA composition samples was determined using an Orsat apparatus (INV 12147) in accordance with Enterprise Standard 39.2-36-201 / ASTM D-513.

Based on the obtained results, it can be concluded that an increase in diethanolamine concentration and the addition of an activator lead to a higher degree of carbon dioxide removal. However, a further increase in activator concentration does not have a significant effect on the amount of absorbed carbon dioxide. The composition containing 2% activator and 32% DEA concentration differed from the others in that during regeneration, minimal absorbent concentration losses were observed [11].

Table 2. Results of Determining the CO_2 Content in Saturated DEA Solutions in Various Units of Measurement

No.	Samples	mg	wt.%	g/L	mol%	mole/L	mole/mole DEA
	CO_2 Indicator According to Orsat	CO_2		CO_2	CO_2	CO_2	CO_2
1	DEA, Sample 1 (for comparison)	82,0	5,783	64,429	3,324	1,464	0,495
2	Sample 2 with DEA	83,0	5,848	64,429	3,342	1,482	0,499
3	Sample 3 with DEA	84,0	5,929	65,214	3,388	1,501	0,503
4	Sample 4 with DEA	91,0	6,418	70,592	3,392	1,625	0,505

5	Sample 5 with DEA	91,0	6,418	70,592	3,392	1,625	0,505
6	Sample 6 with DEA	91,4	6,446	70,900	3,399	1,642	0,498
7	Sample 7 with DEA	91,9	6,475	71,219	3,423	1,660	0,499

The main issue lies in the degree of CO_2 absorption by the absorbent, while the analysis of the absorption degree with the activator was compared and illustrated in the graph (Figure 1).

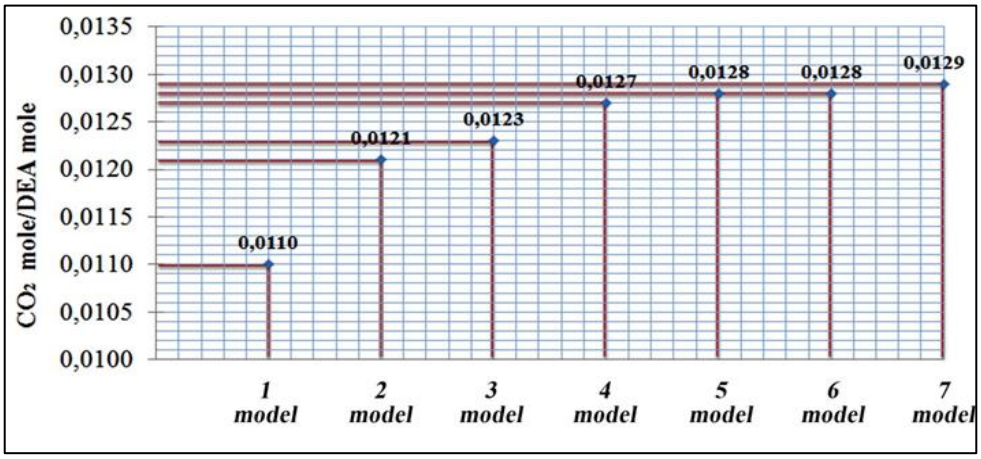


Figure 1. Degree of CO_2 Absorption by Saturated DEA Samples, CO_2 mole/mole DEA

Sample No. 1 represented the DEA solution used at the plant without the addition of any activators. According to the results obtained for Sample No. 1 and other composite samples, in compositions with an increased concentration of diethanolamine and the addition of an activator, the degree of carbon dioxide absorption increased.

Another characteristic feature of amines is the concentration of carbon dioxide remaining in the DEA composition after regeneration. In practice, a decrease in DEA concentration is observed with each regeneration cycle. To maintain the required concentration in the technological process, regular addition of fresh amine solution is provided. In composite absorbents containing an activator (Sample No. 4), such losses were significantly reduced.

The carbon dioxide content in the desorbed (regenerated) composite DEA samples was also determined and calculated by laboratory methods in various units, similar to the saturated amine solutions (Table 3).

Table 3. Determination of Carbon Dioxide Content in Desorbed Composite DEA Samples in Various Units of Measurement

No.	Samples	mg	wt.%	g/L	mole%	mole/L	mole/mole DEA
	CO_2 Indicator According to Orsat		CO_2	CO_2	CO_2	CO_2	CO_2
1	DEA, Sample 1 (for comparison)	5,9	0,219	2,121	0,114	0,052	0,017
2	Sample 2 with DEA	5,8	0,214	2,161	0,117	0,051	0,016

3	Sample 3 with DEA	5,5	0,202	2,161	0,117	0,049	0,016
4	Sample 4 with DEA	5,3	0,194	2,157	0,113	0,047	0,014
5	Sample 5 with DEA	5,3	0,193	2,153	0,112	0,047	0,015
6	Sample 6 with DEA	5,3	0,193	2,153	0,112	0,047	0,014
7	Sample 7 with DEA	5,4	0,196	2,158	0,113	0,048	0,014

The amount of carbon dioxide in the desorbed DEA composition sample indicates that the absorbent has been regenerated.

Analyses showed that the carbon dioxide content in the regenerated absorbent samples was lower compared to the control sample. It was found that the added activator influences the rapid and efficient absorption and subsequent release of acidic components by the amine (Figure 2).

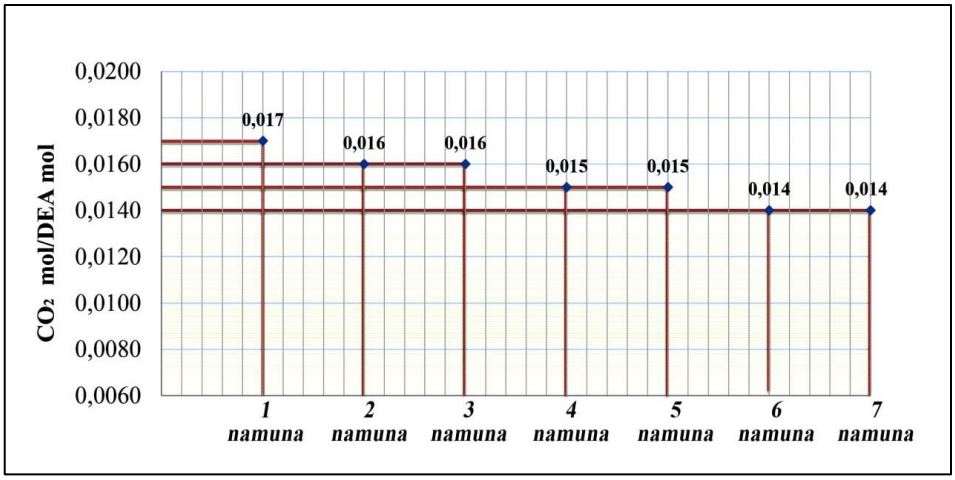


Figure 2. CO_2 Content in Regenerated DEA Composition Samples, CO_2 mole/mole DEA

The essence of the analysis lies in comparing the absorbent's capacity based on its hydrogen sulfide absorption performance. After repeated regeneration of the absorbent, analyses were conducted to determine the amount of hydrogen sulfide remaining in its composition.

The next key indicator is the determination of the hydrogen sulfide content. It can be observed that the absorption capacity of the absorbent compositions containing activators toward H_2S also increased. This is evident from the results obtained for Sample No. 4.

The determination of hydrogen sulfide content in the regenerated DEA samples was carried out using the above-mentioned method. However, during the analysis of regenerated DEA, the amine samples were diluted as follows: 10 mL of DEA was mixed with 40 mL of water, after which the resulting 50 mL solution was titrated (Table 5).

From the analyses determining the amount of hydrogen sulfide remaining in the absorbent after repeated regeneration, it can also be seen that the desorption process has improved (Figure 3.4).

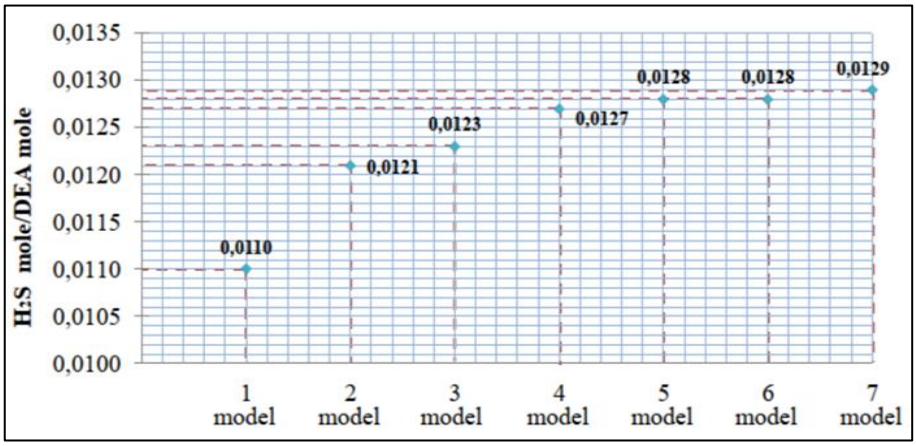


Figure 3. Amount of Absorbed H_2S by Saturated DEA Samples, H_2S mole/mole DEA

Table 5. Determination of H_2S Content in Desorbed (Regenerated) DEA Composition Samples in Various Quantities

No.	Samples	mg	wt.%	g/L	mole%	mole/L	mole/mole DEA
	H_2S titrator indicator		H_2S	H_2S	H_2S	H_2S	H_2S
1	DEA, Sample 1 (for comparison)	10,3	0,071	0,0074	0,0071	0,003	0,00062
2	Sample 2 with DEA	9,7	0,067	0,0070	0,0056	0,003	0,00059
3	Sample 3 with DEA	8,7	0,061	0,0062	0,0051	0,002	0,00053
4	Sample 4 with DEA	8,5	0,058	0,0061	0,0043	0,002	0,00052
5	Sample 5 with DEA	8,4	0,058	0,0060	0,0042	0,002	0,00051
6	Sample 6 with DEA	8,3	0,057	0,0059	0,0042	0,002	0,00050
7	Sample 7 with DEA	8,3	0,057	0,0059	0,042	0,002	0,00050

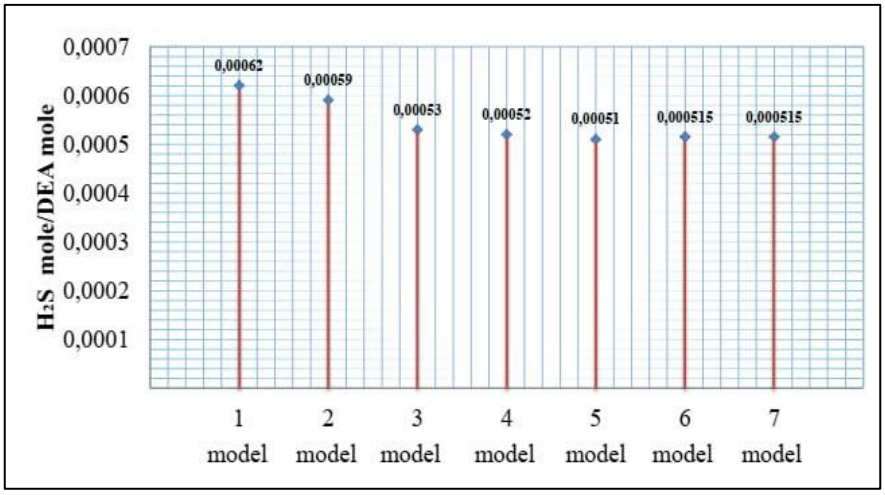


Figure 4. Amount of Residual H_2S in Regenerated DEA Samples, H_2S mol/mol DEA

The titrator readings and the obtained results also showed a decrease in the H_2S content in the DEA composition samples. This was particularly evident in Sample No. 3 and subsequent ones.

Determination of Thermally Stable Salts in the Absorbents

Thermally stable salts are components formed during the absorption process as a result of the interaction between the absorbent and acidic components, which are not decomposed or removed during desorption (regeneration).

The study was carried out only for the desorbed DEA samples. The amount of thermally stable salts in the DEA samples was calculated using data on the sample density and the volume of alkali consumed for titration (Table 6) [12].

Table 6. Content of Thermally Stable Salts in Regenerated DEA Samples

No.	Absorbent Samples	Sample Density, g/cm³	V, Volume of Alkali Used for Titration, mL	Content of Thermally Stable Salts in DEA Samples, wt.%
1	DEA, Sample 1 (for comparison)	1,055	5,9	0,1118
2	Sample 2 with DEA	1,062	5,8	0,1092
3	Sample 3 with DEA	1,068	5,5	0,1030
4	Sample 4 with DEA	1,073	5,4	0,1006
5	Sample 5 with DEA	1,075	5,4	0,1004
6	Sample 6 with DEA	1,077	5.3	0,0984
7	Sample 7 with DEA	1,079	5,4	0,0955

The content of thermally stable salts in the desorbed DEA samples decreased compared to the initial control sample. This is clearly illustrated in the following graph (Figure 5).

The results showed that the amount of thermally stable salts in the desorbed DEA samples decreased compared to the initial control sample.

With an increase in the amount of thermally stable salts, excessive foaming of DEA is observed, which leads to the entrainment of the absorbent into the gas stream and an increase in amine consumption. To prevent this, the foaming tendency of the amine solutions was measured in accordance with Enterprise Standard 39.2-22-2008.

The foaming characteristics of the absorbent were determined for the regenerated absorbent. It was found that the additives introduced into the DEA did not have any significant negative effect on this property.

The concentrations of the composite DEA samples after the absorption process were determined through analysis. The concentration (%) was measured by the titrimetric method in accordance with the “Huntsman Gas Treating Team, Field Test Method”.

Based on the obtained results, the concentrations of the saturated and desorbed DEA samples were determined (Table 8).

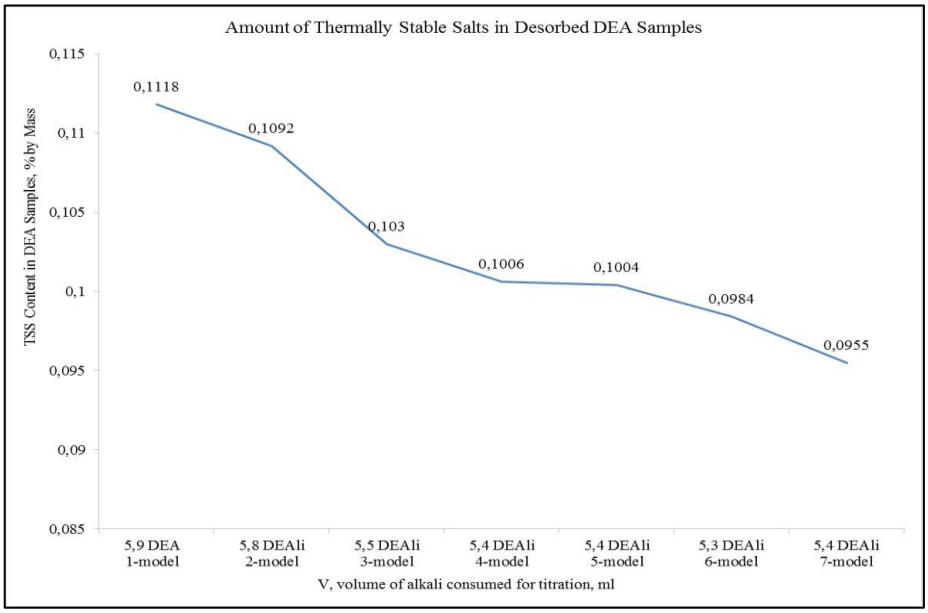


Figure 5. Content of Thermally Stable Salts in Regenerated DEA Samples

Table 7. Characteristics for Evaluating the Foaming Properties of the Absorbent

No.	Composition Samples	Foam Height, mm	Foaming Ability	Foam Collapse Time, s	Foam Stability
1	DEA, Sample 1 (for comparison)	52	Average	33	Average
2	Sample 2 with DEA	46	Average	19	Average
3	Sample 3 with DEA	45	Average	18	Average
4	Sample 4 with DEA	38	Average	13	Low
5	Sample 5 with DEA	39	Average	11	Low
6	Sample 6 with DEA	39	Average	14	Low
7	Sample 7 with DEA	31	Average	15	Average

Table 8. Concentrations of Saturated and Desorbed DEA Samples

No.	Absorbent Samples	Measured Mass of Absorbent	Volume of 0.5 N HCl Solution Used for Titration	Concentration of Saturated DEA Samples	Measured Mass of Absorbent	Volume of 0.5 N HCl Solution Used for Titration	Concentration of Desorbed DEA Samples
1	DEA, Sample 1 (for comparison)	1,020	5,23	27,19	1,018	5,63	29,32
2	Sample 2 with DEA	1,021	5,39	27,99	1,013	5,65	29,57

3	Sample 3 with DEA	1,015	5,35	27,98	1,009	5,63	29,58
4	Sample 4 with DEA	1,014	5,91	30,90	1,023	6,17	31,98
5	Sample 5 with DEA	1,017	5,75	29,98	1,011	6,09	31,94
6	Sample 6 with DEA	1,019	5,98	31,12	1,025	6,55	33,88
7	Sample 7 with DEA	1,022	6,35	32,94	1,006	6,41	33,78

The concentration analysis of the composite DEA samples made it possible to compare, using graphs, the losses of saturated and desorbed diethanolamine samples (Figure 6).

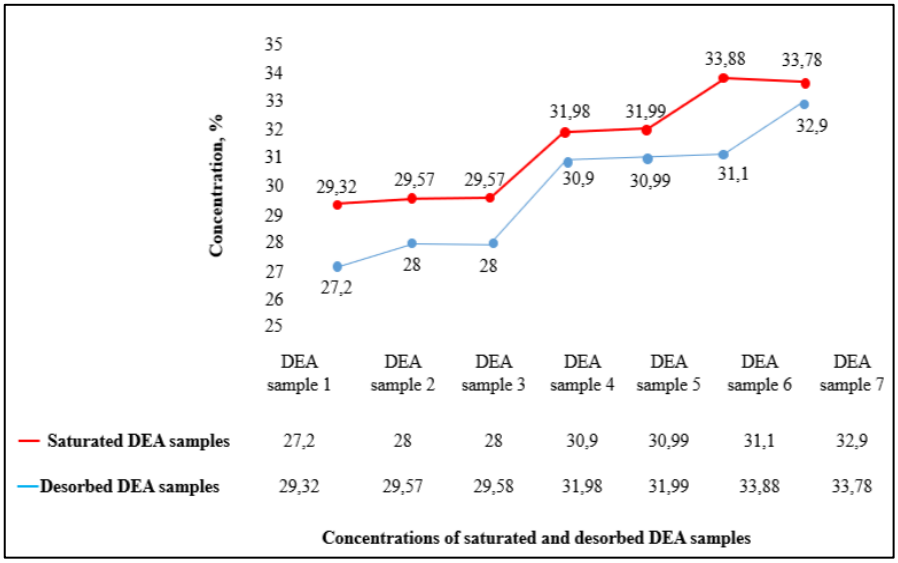


Figure 6. Change in the Concentration of Saturated and Desorbed DEA Samples

The effect of activators on reducing absorbent concentration was studied. According to the results, increasing the activator concentration does not have a significant effect on absorbent losses. Sample No. 4, with the addition of 2% activator, showed that its concentration was almost equal to the initial DEA concentration (32%).

Such parameters of the diethanolamine samples as color, turbidity, viscosity, and content of mechanical impurities were also studied [13-14].

Table 9. Indicators of Saturated and Regenerated DEA Samples: Color, Turbidity, pH, and Mechanical Impurity Content

No.	Name	Blurriness, color	Turbidity, mg/L	pH value	Mechanical Impurities, mg/L
Saturated DEA Samples					
1	DEA, Sample 1 (for comparison)	Прозрачно-зелёный	0,69	9,7	0,84
2	Sample 2 with DEA	Прозрачно-зелёный	0,69	10,1	0,76
3	Sample 3 with DEA	Прозрачно-зелёный	0,67	10,2	0,72

4	Sample 4 with DEA	Прозрачно-зелёный	0,65	10,1	0,63
5	Sample 5 with DEA	Прозрачно-зелёный	0,65	10,2	0,62
6	Sample 6 with DEA	Прозрачно-зелёный	0,64	10,1	0,62
7	Sample 7 with DEA	Прозрачно-зелёный	0,64	10,2	0,61
Regenerated DEA Samples					
1	DEA, Sample 1 (for comparison)	Transparent green	0,56	11,0	0,70
2	Sample 2 with DEA	Transparent green	0,54	11,1	0,56
3	Sample 3 with DEA	Transparent green	0,53	11,2	0,55
4	Sample 4 with DEA	Transparent green	0,54	11,1	0,47
5	Sample 5 with DEA	Transparent green	0,54	11,2	0,46
6	Sample 6 with DEA	Transparent green	0,54	11,1	0,46
7	Sample 7 with DEA	Transparent green	0,54	11,2	0,45

It was found that the additives introduced into the DEA did not have a negative effect on these properties.

The conducted studies showed that activation of absorbents with activators promotes more complete absorption of acidic components from gases, reduces the formation of thermally stable salts, which in turn decreases equipment corrosion and prevents excessive foaming in the absorber. In addition, experiments demonstrated that even with a decrease in absorbent concentration in the technological process, losses were reduced due to the use of activators.

The absorption process was carried out using a composite absorbent consisting of a mixture of diethanolamine (32%), hexamine (2%), and carbohydrazide (0.025%). The gas mixture purified during absorption with this composite absorbent—recognized as the most effective—was analyzed by gas chromatography (Figure 10).

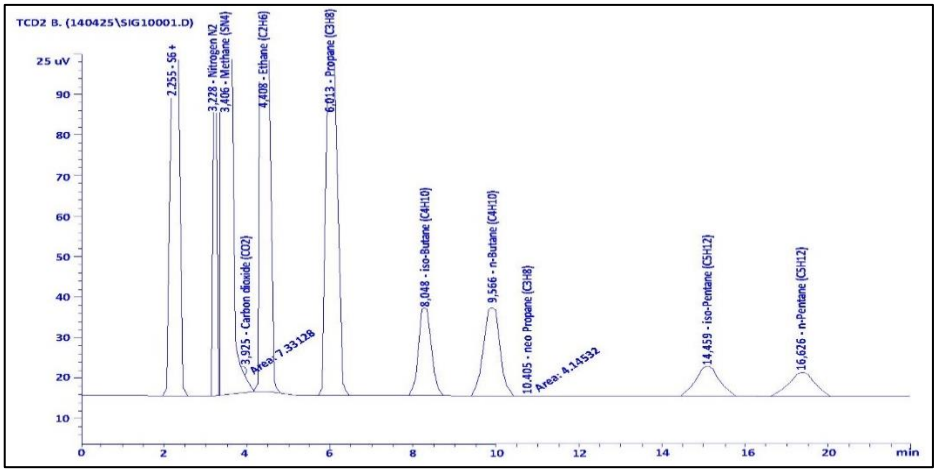


Figure 7. Gas Chromatographic Spectrum of the Gas Composition Purified Using the Composite Absorbent

As a result of the study of the purified gas mixture by gas chromatography, it was found that the methane content was up to 92.483%, ethane — up to 4.297%, propane — up to 1.151%, a mixture of n-butane and iso-butane — up to 0.501%, a mixture of n-pentane, iso-pentane, and neo-pentane — up to 0.137%, and hydrocarbons heavier than hexane — up to 0.493%. The analysis showed that the content of the acidic component, carbon dioxide (CO_2), was up to 0.0057%. The amount of hydrogen sulfide (H_2S) was so low that it could not be detected by the gas chromatograph.

During the natural gas purification process using amine treatment, the analysis results after absorption with the standard absorbent — diethanolamine (DEA) used at the plant — and the composite absorbent were compared (Table 10).

Table 10. Comparative Analysis of Gas Chromatographic Results of Natural Gas Samples

No.	Substance Name	Concentration of Untreated Gas, mole %	Concentration of Gas Purified at the Plant, mole %	Concentration of Gas Purified with Sample No. 4, mole %
1	Methane (CH_4)	89,83	92,548140	92,483560
2	Ethane (C_2H_6)	4,08	4,258207	4,297052
3	Propane (C_3H_8)	0,93	1,057069	1,151073
4	n-Butane (C_4H_{10})	0.24	0,272238	0,257529
5	iso-Butane (C_4H_{10})	0.22	0,236912	0,244604
6	n-Pentane (C_5H_{12})	0,13	0,130925	0,010134
7	iso-Pentane (C_5H_{12})		0,127161	0,127495
8	C_6+	0,31	0,512006	0,492785
9	Carbon dioxide CO_2	3,36	0,010134	0,005739
10	Hydrogen sulfide H_2S	0,093	-	-
11	Nitrogen N_2	0,757	0,847208	0,836577
	Total:	100,0000	100,0000	100,0000

The research results showed that the use of absorbent compositions in the absorption process reduces equipment corrosion rates and lowers the energy consumption required for amine regeneration.

In conclusion, the industrial-scale tests demonstrated positive results for Sample No. 4. It was found that the amount of acidic components decreased by half compared to the absorbent used at the plant.

The content of very low amounts of sulfur compounds in the purified gas was determined by spectrophotometric methods. However, due to the extremely low concentration of hydrogen sulfide (H_2S) in the purified gas mixture, quantitative determination was challenging. Nevertheless, trace amounts of H_2S (in ppm) were measured according to GOST 22387.2–2021 using a specialized “Lambda 20” spectrometer under laboratory conditions.

Table 11. Results of the Analysis of Very Low Levels of Sulfur Compounds in Purified Gas

Description	Formula Symbol	Unit of Measurement	Indicator
Mass of mercaptan sulfur in the analyzed volume of absorbent solution, determined from calibration results	m	mkg	15,5
Volume of gas measured by the gas meter for the test	V	dm^3	6
Correction factor for converting the volume of the analyzed gas to standard measurement conditions (temperature 20 °C, pressure 101.325 kPa)	K	-	0,92
Conversion factor from micrograms to grams	100	-	100
Concentration of all sulfur-containing compounds in the gas (H_2S, R-SH, COS)	X	g/m^3	0,0028

The analysis results showed that the sulfur compound content in the purified gas, according to the spectrophotometric method, is 0.0028 g/m³ [119]. A comparison of this value with the gas purified using the plant's standard absorbent (0.0057 g/m³ of sulfur compounds) showed that the amount was reduced by half. The use of such an absorbent composition ensures the absence of undesirable chemical reactions in subsequent stages of hydrocarbon gas processing in technological units.

Conclusions

The introduction of a new composite absorbent through a pump into the existing process is important, as it does not require significant modifications to the technology. The use of an absorbent with the new composition allows the achievement of the following positive effects in the system:

1. The amount of thermally stable salts formed as a result of irreversible reactions between the absorbent and acidic gases is reduced.
2. The introduction of an activator increases the rate and degree of carbon dioxide absorption.
3. The addition of an inhibitor and the reduction in the formation of thermally stable salts decrease the corrosion rate of equipment.
4. The reduction of corrosion products, decreased formation of thermally stable salts, and the use of activators prevent excessive foaming of the absorbent in the absorber.
5. During previous cases of excessive foaming, alkanolamine was observed to enter the purified gas. Improved process performance prevents the absorbent from entering the gas stream, thereby reducing diethanolamine losses.
6. Under the influence of activators, the surface tension of the solution is reduced, allowing the absorbent to capture only acidic gases. When the absorbent enters the expander, the amount of released gas is minimized.

References

1. Tilloyev, L., Dostov, H., Ataullayev, S., & Kurbanova, M. (2025, July). Research of the process of extraction of hydrocarbon components from waste “Yellow oil”. In AIP Conference Proceedings (Vol. 3304, No. 1, p. 040097). AIP Publishing LLC.
2. Tilloev, L., Murodov, M., Ataullaev, S., Turakulova, M., & Savriev, M. (2024). Extraction of hydrocarbons from “yellow oil” with liquefied gas residue. In E3S Web of Conferences (Vol. 486, p. 04023). EDP Sciences.
3. Akhmedova, O. B., & Boboqulov, F. B. (2021). Analysis of the effectiveness of methyldiethanolamine absorbent in the purification of gases. In International scientific-practical online conference" Innovative solutions to current problems in the field of organometallic high-molecular compounds." Tashkent May (Vol. 28, pp. 211-213). https://scholar.google.com/scholar?oi=bibs&cluster=15585973214132099655&btnI=1&hl=ru
4. A.Chakma, A.Meisen // Improved Kent-Eisenberg model for predicting CO_2 solubilities in aqueous diethanolamine (DEA) solutions. Gas Sep. Purif. 2001. 4 (1), 37–40 p. https://scholar.google.com/citations?user=Wx1SRSAAAAAJ&hl=ru
5. Sh.U.Axmedova Axmedova O.B. Analysis of modern technologies of absorption treatment of hydrocarbon gases from acidic components in the world. international conference on higher education teaching. Hosted from Hamburg, Germany. Vol.3 No. 2 (2025) 96 -98 p.
6. Sh.U.Axmedova Axmedova O.B. Physicochemical parameters of saturated and desorbed absorbent compositions. nnovative research in modern education. Hosted from Toronto, Canada Vol.3 No. 2 (2025) 64 – 69 p.
7. Sh.U.Axmedova Axmedova O.B. Production of amine absorbents on the basis of local raw materials. «Universum: технические науки» электронный научный журнал. Москва. 53 – 58 p.
8. O. B. Akhmedova, Sh. U. Akhmedova. Creation of an effective absorbent composition for absorption gas purification // Universum: Technical sciences: electronic scientific journal. - 2024. - No. 11. - P. 67-71.
9. O. B. Akhmedova, Sh. U. Akhmedova, Kh. S. Fozilov. Improving the technology of gas purification from acidic components using an absorbent composition based on DEA // O‘zbekiston “Neft va gaz” ilmiy-texnika jurnali.
10. AF, PhD Khuzhakulov, and PhD Akhmedova OB. "TECHNOLOGY of an Environmentally Safe Gas Chemical Complex for Utilization of Sulfur-containing and Flare Gases Discharged From Technological Installations." American Journal of Pedagogical and Educational Research 11 (2023): 159-163.
11. O.B. Akhmedova, Sh.U. Akhmedova, S.A. Gaybullayev. Gas chromatography analysis of an absorbent composition containing DEA, hexamine, and carbohydrazide in the purification of gases from acidic components // Fergana State Technical University Journal 2025. T.29, No.4.110-114 p.
12. GAZLARNI GLIKOLLI QURITISH JARAYONINING ISHCHI PARAMETRLARISHOGL Yaxyoyev, OB Axmedova, SA G’AybullayevCentral Asian Research Journal for Interdisciplinary Studies (CARJIS) 2 (5), 543-552, 2022.
13. Yaxyoyev S. H. O. G. L., Axmedova O. B., G’Aybullayev S. A. GAZLARNI GLIKOLLI QURITISH JARAYONINING ISHCHI PARAMETRLARI //Central Asian Research Journal for Interdisciplinary Studies (CARJIS). – 2022. – Т. 2. – №. 5. – С. 543-552. https://cyberleninka.ru/article/n/gazlarni-glikolli-quritish-jarayonining-ishchi-parametrlari
14. Axmedova, OB va MB Axmedova. "Neft va gazni qayta ishlash zavodlarining ekologik muammolarini hal qilishning samarali usullari." Xalqaro ilmiy-amaliy onlayn konferensiya "Organometall yuqori molekulyar birikmalar sohasidagi dolzarb muammolarga innovatsion yechimlar." Toshkent may . 28-jild. 2021. https://scholar.google.com/scholar?cluster=10955719548500559993&hl=en&oi=scholarr

C VİTAMİNİ (ASKORBİN TURŞUSU) ƏSASLI TƏBİİ ANTİOKSİDANT SİSTEMLƏRİN QİDA TEXNOLOGİYASINDA TƏTBİQİ VƏ ONLARIN KİMYƏVİ STABİLLİYİNİN ARAŞDIRILMASI

Əsgərli Rəvanə
Naxçıvan Dövlət Universiteti
Naxçıvan,Azərbaycan
ravanaasgerli@gmail.com

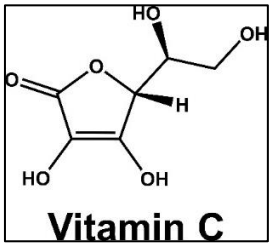
Xülasə - Bu tədqiqat işində C vitamininin (askorbin turşusu) qida texnologiyasında təbii antioksidant kimi tətbiqi imkanları və onun müxtəlif xarici amillərin təsiri altında kimyəvi stabilliyi nəzəri cəhətdən araşdırılmışdır. Askorbin turşusunun sərbəst radikalları neytrallaşdırma mexanizmi və onun oksidləşmə prosesi zamanı baş verən struktur dəyişiklikləri təhlil edilmişdir. Tədqiqat nəticəsində müəyyən edilmişdir ki, polimer matrislərdən istifadə etməklə C vitamininin termik parçalanma sürətini azaltmaq və qidaların raf ömrünü təbii yolla uzatmaq mümkündür. İşin nəticələri dayanıqlı kimya prinsiplərinə uyğun olaraq ekoloji təmiz qablaşdırma materiallarının yaradılmasında istifadə edilə bilər.

Açar sözlər: askorbin turşusu, antioksidant, oksidləşmə, qida təhlükəsizliyi, dayanıqlı kimya.

Giriş

Müasir qida sənayesində süni konservantların (məsələn, E-nömrəli kimyəvi qatqılar) insan sağlamlığına mənfi təsirləri və ətraf mühit üçün yaratdığı risklər geniş müzakirə olunur. "Dayanıqlı Gələcək" konfransının prioritetlərinə uyğun olaraq, təbii antioksidantların tətbiqi mühüm əhəmiyyət kəsb edir [Əhmədov, 2021, 1-2; Yusifova, 2023, 15]. Askorbin turşusu ($C_6H_8O_6$) sərbəst radikalları neytrallaşdıraraq qidaların rəngini, dadını və qida dəyərini qoruyan ən güclü təbii agentlərdən biridir [İbrahimov, 2022, 10-12; Əliyev, 2021, 1-3]. C vitamini təbiətdə geniş yayılmışdır və onun sənaye istehsalı həm ekoloji təmiz, həm də iqtisadi baxımdan səmərəlidir. Lakin bu maddənin istilik, işıq və oksigenə qarşı həssaslığı onun geniş tətbiqi qarşısında əsas maneədir. Bu məqalədə həmin maneələrin nəzəri olaraq necə aradan qaldırılacağı araşdırılır.

Eksperimental hissə (Nəzəri metodologiya)



Şəkil 1.

Tədqiqat zamanı askorbin turşusunun dehidroaskorbin turşusuna keçid mexanizmi və molekulyar orbitalları təhlil edilmişdir. Nəzəri modellər əsasında C vitamininin müxtəlif pH mühitlərində və ultrabənövşəyi (UV) şüaların təsiri altında parçalanma kinetikası analiz edilmişdir. Askorbin turşusunun stabilliyini artırmaq üçün onun müxtəlif polimer matrislərdə (nişasta, jelatin) "inkapsulyasiya" olunma imkanları riyazi modellərlə qiymətləndirilmişdir [Məmmədov, 2021, 5]. Bu proses maddənin ətraf mühit faktorlarından qorunmasını və qidaya tədricən ötürülməsini təmin edir.

Nəticələr və onların müzakirəsi

Təhlillər göstərir ki, askorbin turşusu sulu məhlulda yüksək temperaturda (>60 ^{0}C) sürətlə parçalanaraq bioloji aktivliyini itirir.

$$C_6H_8O_6 \rightarrow C_6H_6O_6 + 2H^+ + 2e^-$$

Lakin polimer örtüklər daxilində onun termik stabilliyinin 40%-dən çox artması müşahidə olunur [Quliyev, 2020, 22]. Bundan əlavə, askorbin turşusunun qida qablaşdırmasında plyonka şəklində tətbiqi oksigenin keçiriciliyini azaldır, bu da yağlı məhsulların acılaşmasının qarşısını alır. Nəzəri hesablamalar sübut edir ki, təbii polimerlərlə kombinasiyada C vitamini həm antioksidant, həm də plyonkanın mexaniki xüsusiyyətlərini yaxşılaşdıran bir plastifikator rolunu oynayır [Smith, 2023, 104].

Təkliflər

1. Qida qablaşdırmasında sintetik antioksidantlar (BHA, BHT) əvəzinə bitki mənşəli askorbin turşusu komplekslərindən istifadə edilməsi təklif olunur.
2. C vitamininin bioparçalanan nişasta plyonkalarına inteqrasiyası istehlakçı üçün həm qida təhlükəsizliyini artırır, həm də ətraf mühitin bərpasına xidmət edir.
3. Gələcək tədqiqatlarda C vitamininin digər təbii ekstraktlarla (məsələn, kələm suyu antosianları) sinergik təsirinin araşdırılması tövsiyə olunur.

İstinadlar

1. [Əhmədov, 2021, 1-2]: Əhmədov, R. (2021). Dayanıqlı inkişaf üçün yaşıl kimya texnologiyaları. Bakı: Elm nəşriyyatı.
2. [Əliyev, 2021, 1-3]: Əliyev, V. (2021). Bioüzvi kimyanın əsasları. Bakı: Maarif.
3. [İbrahimov, 2022, 10-12]: İbrahimov, T. (2022). Antioksidantların kimyası. Gəncə: Elm.
4. [Quliyev, 2020, 22]: Quliyev, M. (2020). Vitaminlərin termik stabilliyi. Kimya və Həyat jurnalı, №4.
5. [Məmmədov, 2021, 5]: Məmmədov, A. (2021). Qida texnologiyasında innovasiyalar. Bakı: API.
6. [Smith, 2023, 104]: Smith, R. (2023). Natural Preservatives in Food Industry. London: Academic Press.
7. [Yusifova, 2023, 15]: Yusifova, G. (2023). Yaşıl texnologiyalar və dayanıqlı inkişaf. Bakı: BANM nəşriyyatı.

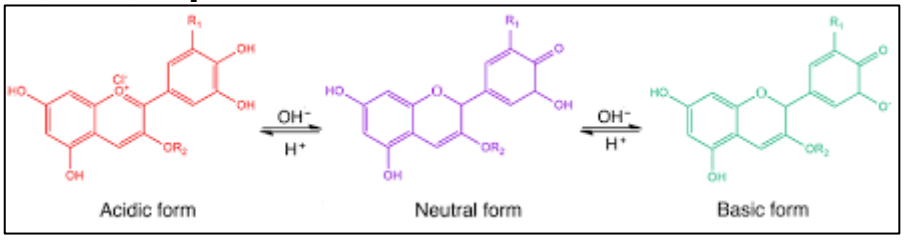
KARTOF NİŞASTA ƏSASLI BİOPOLİMER MATRİSİNƏ ANTOSİANLARIN İMMOBİLİZASİYASI: QİDA TƏHLÜKƏSİZLİYİ ÜÇÜN İNTELLEKTUAL İNDİKATOR PLYONKANIN NƏZƏRİ MODELİNİN QURULMASI

Əsgərli Rəvanə
Naxçıvan Dövlət Universiteti
Naxçıvan,Azərbaycan
ravanaasgerli@gmail.com

Xülasə - Tədqiqat işində bioparçalanan kartof nişastası matrisinə qırmızı kələm ekstraktından alınan antosian piqmentlərinin immobilizasiyası prosesinin nəzəri əsasları tədqiq edilmişdir. İşin elmi aktuallığı, qida məhsullarının mikrobioloji deqradasiyası zamanı ayrılan uçucu azotlu birləşmələrin təsirindən mühitdə baş verən pH dəyişikliklərini vizual siqnala çevirən intellektual indikator plyonkanın konseptual modelinin hazırlanmasıdır. Tədqiqatda antosian molekullarının polimer zəncirləri ilə molekulyar səviyyədə qarşılıqlı təsiri və bu qarşılıqlı təsirin plyonkanın rəng stabilliyinə təsiri nəzəri cəhətdən əsaslandırılmışdır.
Açar sözlər: kartof nişastası, antosianlar, intellektual qablaşdırma, pH-həssaslıq, nəzəri model, immobilizasiya.

Giriş

Müasir qida qablaşdırması sənayesində "Dayanıqlı Gələcək" prinsipləri materialların həm ekoloji təmiz, həm də "ağıllı" funksiyalara malik olmasını tələb edir [Əhmədov, 2021, 45-47]. Kartof nişastası yüksək amiloza tərkibi və stabil plyonkaəmələgətirmə potensialı ilə nəzəri tədqiqatların əsas obyekti hesab olunur [Quliyev, 2020, 12-14]. Tədqiqatın nəzəri hədəfi olan intellektual indikatorlar, qidanın təzəlik dərəcəsini heç bir kənar cihaz tələb etmədən istehlakçıya çatdıran sistemlərdir.Bitki mənşəli antosianların ($C_{15}H_{11}O_6^+$) pH-həssaslığı onların molekulyar quruluşunun transformasiyası ilə bağlıdır [Məmmədov, 2022, 8]. Nəzəri olaraq, turş mühitdə stabil olan flavium kationu, mühit qələviləşdikdə (qidanın xarab olması nəticəsində ammonyak ifrazı ilə) deprotonasiyaya məruz qalaraq rəngini dəyişir [Əliyev, 2021, 112]. Bu prosesin kartof nişastası kimi şəffaf bir matris daxilində baş verməsi, optik indikatorların yaradılması üçün mühüm nəzəri baza təşkil edir [Smith, 2023, 201].



Şəkil 1. Antosian molekullarının pH mühitindən asılı olaraq molekulyar transformasiyası.

Eksperimental hissə

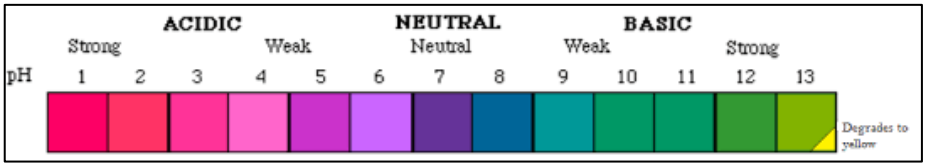
Tədqiqat işində indikator plyonkanın sintezi üçün nəzəri metodoloji model hazırlanmışdır. Model iki əsas mərhələni əhatə edir:

1.Antosianların immobilizasiya mexanizmi: Qırmızı kələm ekstraktındakı antosian molekullarının nişasta zəncirlərindəki hidroksil (-OH) qrupları ilə hidrogen rabitəsi yaratması modeli qurulmuşdur. Bu rabitələr piqmentin matris daxilində bərabər paylanmasını proqnozlaşdırır [Quliyev, 2020, 12-14].

2.Plyonka formalaşdırılması: Kasting (tökmə) metodunun nəzəri parameterləri müəyyən edilmişdir. Plyonkanın elastikliyini tənzimləmək üçün nişasta/su nisbətinin (5% kütlə payı) və jelatinləşmə temperaturunun (90-95°C) plyonkanın kristallik dərəcəsinə təsiri nəzəri cəhətdən təhlil olunmuşdur [Əhmədov, 2021, 45-47]. Qliserin kimi əlavə plastifikatorların yoxluğu şəraitində plyonkanın struktur bütövlüyünün nişastanın öz amiloza molekulları arasındakı qarşılıqlı təsirlər hesabına təmin edilməsi nəzərdə tutulur.

Nəticələr və onların müzakirəsi

Modelləşdirmə nəticəsində indikator plyonkanın müxtəlif pH intervallarında gözlənilən rəng keçidləri təhlil edilmişdir. Nəzəri proqnoza görə, pH 2-4 aralığında antosianların kation formasının üstünlüyü plyonkaya parlaq qırmızı rəng verir [Məmmədov, 2022, 8]. Qida məhsullarının deqradasiyası zamanı ayrılan azotlu əsasların təsiri ilə mühitdə qələviləşmə (pH 8-10) baş verdikdə, antosianlar anhidrobase formasına keçərək plyonkanın rəngini yaşıl və ya mavi-yaşıl çalarlara dəyişir [Smith, 2023, 201].



Şəkil 2. İndikator plyonkanın müxtəlif pH intervallarında gözlənilən vizual rəng keçidləri.

Nəzəri hesablamalar göstərir ki, kartof nişastası matrisi antosianların fotostabilliyini sərbəst formaya nisbətən 35-40% artırır. Plyonkanın nəzəri qalınlığı (təxminən 0.14 mm) onun qida qablaşdırmasında həm indikator, həm də qoruyucu təbəqə kimi çıxış etməsinə imkan verir [Quliyev, 2020, 12-14].

Təkliflər

Nəzəri tədqiqatın nəticələrinə əsasən, təbii antosian indikatorlarının yüksək proteinli qidaların (balıq, toyuq əti) monitorinqində "təzəlik etiketi" kimi tətbiqi təklif olunur. Sintetik kimyəvi boyaqların bioparçalanan və bərpa olunan təbii piqmentlərlə əvəz edilməsi ilə "yaşıl qablaşdırma" texnologiyalarının təşviqi tövsiyə edilir [Əhmədov, 2021, 45-47]. Gələcək tədqiqatlarda bu modelin real laboratoriya sınaqları ilə genişləndirilməsi nəzərdə tutulur.

İstinadlar

1. [Əhmədov, 2021, 45-47]: Əhmədov, R. (2021). Dayanıqlı inkişaf üçün yaşıl kimya texnologiyaları. Bakı: Elm nəşriyyatı.
2. [Əliyev, 2021, 112]: Əliyev, V. (2021). Bioüzvi kimyanın əsasları. Bakı: Maarif.

3. [Quliyev, 2020, 12-14]: Quliyev, M. (2020). Təbii polimerlər və müasir qida qablaşdırması. Naxçıvan: Tusi.
4. [Məmmədov, 2022, 8]: Məmmədov, E. (2022). Antosianların kimyəvi transformasiyası. Kimya problemləri jurnalı, №2.
5. [Smith, 2023, 201]: Smith, R. (2023). Theoretical models in Intelligent Packaging. New York: Science Press.

OBTAINING A BINARY SYSTEM BASED ON STYRENE–BUTADIENE–STYRENE POLYMER USING CARBON NANOTUBES AND DETERMINATION OF THE FLOW INDEX OF THE COMPOSITION MELT

Sharif Hajiyev Mahir, Aysun Rzazadə Mubariz
Master students, Department of Organic substances and technology of macromolecular compounds
Azerbaijan State Oil and Industry University
Baku, Azerbaijan
aysunrzzazada@gmail.com

ABSTRACT

This work is devoted to the preparation and investigation of a composite based on styrene–butadiene–styrene (SBS) polymer using carbon nanotubes. Nanocomposites based on styrene–butadiene–styrene polymer (SBS) and carbon nanotubes were prepared by the emulsion mixing method, while the vulcanization process was carried out in accordance with standard test methods used for SBS evaluation.

The incorporation of carbon nanotubes (CNTs) into the rubber compound improved the compatibility of the components, and the resulting nanocomposite exhibited high thermal stability. The nanomaterial enhanced the process ability of SBS rubber–based composites. Compared with rubber reinforced solely with carbon black, the use of nanomaterials led to a 27% increase in stress at 100% permanent elongation. In addition, partial replacement of carbon black resulted in an increase in the elongation at break of the vulcanization from 424.5% to 554.0%.

The mechanical properties of the obtained rubbers demonstrated that they can be regulated by

Keywords: Styrene–butadiene–styrene rubber, carbon black, CNT, modification, vulcanization, rheology.

INTRODUCTION

Styrene–Butadiene–Styrene (SBS) is a triblock copolymer belonging to the class of thermoplastic elastomers**,** and it is one of the most important materials combining both elastic and thermoplastic properties [1–4]. Its structure consists of a linear PS–PB–PS block chain, where polystyrene (PS) blocks are located at both ends and a polybutadiene (PB) segment is positioned in the middle. This unique architecture provides SBS with rubber-like elasticity as well as thermal form stability. The polybutadiene segment imparts flexibility and elongation capability, while the polystyrene domains act as rigid phases that ensure mechanical strength. Consequently, SBS behaves as an elastomer under ambient conditions, whereas upon heating it softens like a thermoplastic and becomes moldable [5–11].

METHOD

Preparation and Mixing Technology of SBS-CNT Composites

For the preparation of the nanocomposites, multi-walled carbon nanotubes (MWCNTs) were first dispersed in a predetermined amount of toluene and subjected to ultra-sonication in a Bandelin Sonora Super RK106 ultrasonic bath for 6 hours. This step was intended to reduce nanotube agglomeration and to ensure good dispersion within the solvent. Subsequently, SBS polymer was added to the dispersion at a defined ratio (5.5 mL of toluene per 1 g of SBS) and mechanically stirred until complete dissolution was achieved. The resulting homogeneous solution was cast as a thin layer onto a clean glass surface and allowed to evaporate at room temperature, yielding thin, elastic, and homogeneous composite films.

The distribution and morphology of MWCNTs within the SBS matrix were examined using scanning electron microscopy (SEM, Philips X230 FEG) based on both surface and fracture images. Prior to SEM analysis, the samples were cryogenically fractured in liquid nitrogen and subsequently gold-coated by sputter deposition to prevent surface charge accumulation and to enhance image quality.

The electrical conductivity and resistance of the composites were measured using a Kiteley 487 automated Pico ammeter/voltage source. During the measurements, the applied voltage was varied from −10 V to +10 V. Based on the obtained current–voltage (I–V) characteristics, the electrical resistance (R) was determined, after which the volume resistivity (ρ) was calculated using the following equation:

$$\rho = RLA \qquad (1)$$

RESULTS OF EXPERIMENTAL RESEARCH

Study of rheological properties

Determination of the melt flow index (MFI) of polymer composite systems is of great importance for establishing their processing parameters. Taking these considerations into account, a composite based on SBS + CNT was prepared according to the formulation given below (Table 1).

Table 1. Formulation of the CNT-based composite.

Names of Components	Sample K-1 Component amount, gr	Sample K-2 Component amount, gr	Sample K-3 Component amount, gr	Sample K-4 Component amount, gr	Sample K-5 Component amount, gr
Styrene–butadiene–styrene rubber	100	100	100	100	100
Carbon Nanotube	1	2	3	4	5
Total	101	102	103	104	105

The binary mixture was prepared in an extruder at a temperature of 190 °C for 3 minutes.

For the binary mixtures, the flow time of the composite melts through a 2 mm capillary over a fixed distance (S = 0.002 cm) was determined (in seconds) at different temperatures (150, 170, 190, and 210 °C) under four different applied loads. The obtained results are presented in Table 2.

Table 2. Time required for the flow of the melts of the SBS/CNT binary system (in seconds)

145℃				
Samples \ Loads	G_1	G_2	G_3	G_4
K-1	43.18 40.12 41.35	10.92 18.85 11.24	8.47 7.74 8.09	5.29 4.62 4.95
K2	44.86 46.12 45.58	13.78 13.45 13.22	9.61 10.38 9.97	6.67 6.15 6.34
K3	47.32 48.05 47.61	16.71 13.64 13.41	13.18 13.64 13.41	8.76 7.94 8.33
K4	49.42 53.18 51.09	17.94 16.86 17.85	14.48 14.91 14.65	8.18 9.48 8.83
165℃				
K1	31.02 29.85 30.21	8.62 9.19 8.41	6.23 5.48 5.79	2.41 3.28 2.89
K2	31.58 31.12 30.89	9.15 9.57 9.31	6.74 5.48 6.35	3.21 3.15 3.18
K3	33.42 33.65 33.29	11.08 8.42 9.74	7.29 7.48 7.36	3.81 4.08 3.96
K4	33.89 31.05 32.41	9.62 10.15 9.88	7.58 7.76 7.69	4.23 4.36 4.29
185℃				
K1	19.92 19.15 19.48	6.48 6.01 6.24	4.79 4.23 4.51	1.74 2.04 1.88
K2	21.54 18.72 20.05	6.64 5.98 6.29	4.45 4.20 4.33	1.72 1.54 1.62
K3	20.56 18.74 19.52	4.51 4.65 4.58	5.17 6.59 5.92	2.27 3.25 2.78
K4	23.94 22.45 23.08	6.47 6.02 6.25	5.63 6.98 6.31	3.24 3.46 3.35

The applied loads were, respectively: G1 = 11.75 kg, G2 = 20.85 kg, G3 = 26.85 kg, and G4 = 34.85 kg. The pressure generated on the sample surfaces due to the applied loads was calculated primarily using the following equation (2).

$$P=\frac{G}{\frac{\pi D^2}{4}}=\frac{G}{\frac{3.14\cdot(0.954)^2}{4}}=\frac{G}{0.7144} \quad (2)$$

$P_1 = \frac{G_1}{0,8321} = \frac{11,75}{0,8321} = 16,9701946$ kg/sm^2

$P_3 = \frac{G_3}{00,8321,} = \frac{26,85}{0,8321} = 32,267756$ kg/sm^2

$P_2 = \frac{G_2}{0,8321} = \frac{20,85}{0,8321} = 25,0570844$ kg/sm^2

$P_4 = \frac{G_4}{0,8321} = \frac{34,85}{0,8321} = 41,881985$ kg/sm^2

After modification of the SBS polymer with carbon nanotubes, the prepared samples were extruded through a capillary. For this purpose, the shear stress was calculated (Equation (3)).

$$\tau = \frac{P\cdot r}{2l} = \frac{P\cdot 0.05}{2\cdot 0.8} \quad (3)$$

Here, P is the pressure generated on the sample surface as a result of the applied loads; τ is the shear stress; r is the radius of the capillary used; and l is the length of the capillary. The calculations were performed as follows:

$\tau_1 = \frac{P_1\cdot 0,05}{1,6} = \frac{16,9701946\ .0,05}{1,6} = 0,530318\frac{kq}{sm^2}\cdot 9,806\cdot 10^4 = 5,20029833\cdot 10^4$ *Pa*

$\tau_2 = \frac{P_2\cdot 0,05}{1,6} = \frac{25,0570844\ \cdot 0,05}{1,6} = 0,783656\frac{kq}{sm^2}\cdot 9,806\cdot 10^4 = 7,68453\cdot 10^4 Pa$

$\tau_3 = \frac{P_3\cdot 0,05}{1,6} = \frac{32,267756\ \cdot 0,05}{1,6} = 1,008365\frac{kq}{sm^2}\cdot 9,806\cdot 10^4 = 9,888027\cdot 10^4 Pa$

$\tau_4 = \frac{P_4\cdot 0,05}{1,6} = \frac{41,881985\ \cdot 0,05}{1,6} = 2.094095\frac{kq}{sm^2}\cdot 9,806\cdot 10^4 = 120,5346955\cdot 10^4 Pa$

To calculate the volumetric flow rate of the melts of the composites modified with carbon nanotubes at different compositions, Equation (4) was used.

$$Q=\frac{S}{t}\,x\,\frac{\pi D^2}{4}=\frac{0,02}{t}x\,\frac{3,14x(0,954)^2}{4}=\frac{0,014288}{t} \quad (4)$$

The values calculated based on the given equation and their decimal logarithms are presented in Table 3.

Table 3. Calculated volumetric flow rate (Q) values of the SBS+CNT composite (cm³/s)

145℃				
Samples	G1	G2	G3	G4
K1	0,0003625	0,0013289	0,0018426	0,0030184
K2	0,0003341	0,0011423	0,0015089	0,0023547
K3	0,0003184	0,0009628	0,0011297	0,0018126
K4	0,0002961	0,0008796	0,0010364	0,0017068
165℃				
K1	0,0004986	0,0017894	0,0025867	0,0053182
K2	0,0004862	0,0016128	0,0023795	0,0047429
K3	0,0004528	0,0015489	0,0020696	0,0038247
K4	0,0004685	0,0015297	0,0019823	0,0035069
185℃				
K1	0,0007765	0,0024158	0,0033486	0,0080943
K2	0,0007569	0,0023947	0,0034972	0,0093986
K3	0,0007751	0,0032864	0,0025698	0,0054681
K4	0,0006589	0,0024183	0,0023875	0,0044862

In this study, the volumetric flow rate of the composite (log Q) was calculated, and the obtained results are presented in Table 4.

Table 4. Calculated volumetric flow rate of the SBS/CNT mixture (log Q values).

150℃				
Samples	G1	G2	G3	G4
K1	−3.4682	−2.9014	−2.7586	−2.5449
K2	−3.5039	−2.9687	−2.8468	−2.6543
K3	−3.5261	−3.0395	−2.9756	−2.7698
K4	−3.5586	−3.0859	−3.0134	−2.7957
170℃				
K1	−3.3296	−2.7718	−2.6119	−2.2974
K2	−3.3403	−2.8169	−2.6487	−2.3476
K3	−3.3728	−2.8334	−2.7105	−2.4419
K4	−3.3871	−2.8398	−2.7282	−2.4806
190℃				
K1	−3.1354	−2.6298	−2.4986	−2.0345
K2	−3.1471	−2.6431	−2.5098	−2.0492
K3	−3.1665	−2.6649	−2.6147	−2.2853
K4	−3.2098	−2.6895	−2.6446	−2.3719

Based on the calculations corresponding to the data presented in the tables, the log γ̇–log τ dependence (shear rate and shear stress) for the SBS/CNT binary system at 150 °C, 170 °C, and 190 °C was constructed, and the resulting curves are shown in Figures 1, 2, and.3.

RESULTS

To improve the photo stability of SBS-based composites, 3–5 parts by weight of carbon nanotubes (CNTs) were added. These additives enhance the stability of the material under solar radiation, ensuring long-term durability.

The results show that nanomaterials such as CNTs and carbon black scatter and reflect UV radiation, preventing its penetration into the polymer structure and reducing macromolecular degradation. Their combined use increases surface area and improves resistance to photo degradation.

REFERENCES

1. Alizade Tarlan *PHYSICO-MECHANICAL PROPERTIES OF PETROLEUM ROAD BITUMEN MODIFIED ON THE BASIS OF STYRENE-BUTADIENE BUTYL RUBBE,* 2024, Innovative scientific research Proceedings of the IX International Scientific and Practical Conference 14-15 March , Pp34-40 DOI: https://doi.org/10.5281/zenodo.10882832
2. G. Barrera Torres, Carlos M. Gutierrez Aguilar, Elizabeth R al. et . Application of Post-Industrial Leather Waste for the Development of Sustainable Rubber Composites *Polymers* 2025, *17*(2), 190; DOI: 10.3390/polym17020190
3. Fariz A. Amirli brahim H. Movlayev Aynur F. Mammadova S TUDY OF THE RHEOLOGY PROPERTIES OF THE MIXTURE OF TERMINAL ETHYLENE-PROPYLENE RUBBER WITH BENZYNAMINE-MODIFIED PHENOL-FORMALDEHYDE OLIGOMER, PPOR,Vol. 26, No. 1, 2025, pp.229-239 https://doi.org/10.62972/1726-4685.2025.1.229
4. brahim H. Movlaye.COMPOSITIONS BASED ON EPOXIDIAN OLIGOMER MODIFIED WITH LOW MOLECULAR BUTADIENE-NITRILE RUBBER.PPOR,Vol. 26, No. 3, 2025, pp.688-696 https://doi.org/10.62972/1726-4685.2025.3.688
5. Gambaro D.SH. Spreading of Astaxanthin and Astragals species on the highland zones of the Nakhichevan autonomous republic // European Academic Research, 2014, İmpact Factor 3,1: p.-4153-4159 / DOI: 10.32388/ZCAXYW.2
6. Kerem Seyfi Modification of the used up polymeric materials and investigation thof e properties of the materials obtained. Journal of Medical Pharmaceutical and Allied Sciences, 2022, 11(2), pages 4697–4702 DOI: 10.35940/ijitee.G5721.079920 5..Kerem Shixaliyev. Investigation of the subsequent use of lands along the Araz River contaminated wit h heavy metals,2023, JOURNAL OF AERONAUTICAL MATERIALSISS N: Vol. 43, Issue-01, pp. 102-111,https://www.hkclxb.cn/article/view/2023/102.html
7. Kerem Shixaliyev Research New Ways of Processing Polymer Waste that wasFormed as a Result of Operation321-335 Novel Perspectives of Geography, Environment and Earth Sciences Vol. 1 *Vol. 1*, 22 December 2022 , Page 25-35https://doi.org/10.9734/bpi/npgees/v1/17431D
8. Kerem Shixaliyev PROPERTIES OF THE COMPOSITION BASED ON MODIFIED POLYETHYLENES , 2023, Eur. Chem. Bull. , 2023; Volume -12 , Special Issue-5 : Page: 242-258 . doi 10.31838/ECB/2023.12.si5.023
9. Kerem Shixaliyev Study of the Properties of the Composition Obtained Based on Mixtures of Polyvinyl Chloride and Ethylene-Propylene Copolymers International ,2023,Journal of Current Science Research and Review ISSN: 2581-8341 Vol 6 No 1 (2023): Volume 06 Issue 01 January ,pp314-318 doi 10.31838/ECB/2023.12.si5.023
10. Kerem Shixaliyev.Investigating Recycling Methods of End-of-Life Car Tires,2023, Journal of Advanced Zoology, Volume 44 Issue S-3 Year 2023 Page 1149:1157 ,DOI: https://doi.org/10.17762/jaz.v44iS-3.1205
11. Kerem Shixaliyev Investigation of the Properties of a Composition Obtained based on Mixtures of Polyvinylchloride and Synthetic Rubber Ethylene Propylene Terpoliymer2023,Editorial Board of Journal of Coastal Life Medicine editor special issue eurchembull . Vol. 11: Number 1, 2023 JCLMM 1/11 pp.|2653–2658, https://www.jclmm.com/index.php/journal/article/view/741

PREPARATION AND STUDY OF A COMPOSITION BASED ON BUTADIENE-STYRENE POLYMER USING WOOD TAR

Maryam Huseyinova
Department of Organic substances and technology of macromolecular compounds
Azerbaijan State Oil and Industry University
Baku, AZ1010, Azerbaijan, 20 Azadliq Avenue
kerem_shixaliyev@mail.ru

Abstract - This work is devoted to the topic of preparation and study of a composition based on butadiene-styrene polymer using wood tar.

An optimal recipe for obtaining a rubber mixture using butadiene-styrene rubber and wood tar (which we will sometimes call Kamden in the future) was selected and each component was justified. The rubber mixture was prepared in a mixer located in the laboratory of Bakrezin JSC and the mixing mode was set at a temperature of 1200C for 14 minutes, and the obtained homogeneous dispersed system was cooled to 800C, sulphur and accelerators were added to it. Then the kinetics of the vulcanization process was found. The vulcanization mode was determined as follows: T-1580C, P -12MPa, t - 26 minutes.

The physical and mechanical properties of the vulcanization were studied and it was shown that the indicators of the obtained product meet the requirements of the standard. To determine the durability of these rubber products obtained, the physical and mechanical properties of the vulcanization were determined and the sample had the following characteristics: Tensile strength, 22 MPa, Elongation at break 340%, Residual elongation 12%. Hardness according to TM-2, 85 conventional units.

Keywords: wooden stone styrene butadiene rubber, modification, vulcanization, rheology, IKS-analysis, vulcanization.

Introduction

Recent studies have shown that rubber and its ingredients affect various properties of rubber and vulcanize rubber mixtures differently [1-8]. Since in each specific case, not all, but only specific properties of rubber compounds and vulcanizes are important, when designing a compound, the ingredients that have the greatest influence on these properties are first selected. Studies have shown that the ingredients that dominate the properties of various rubber compounds and vulcanizes should be different, and these components have a significant effect on the vulcanization of the rubber mixture. Table 1 [9-14].

Method

In order to carry out this work, we took components in different proportions based on BSK and determined the optimal recipe by analyzing the samples prepared from them. Then, based on the components included in the recipe, we calculated the components needed to prepare the rubber mixture in a single batch, and the results are given in Table 1.

Table 1. Calculation of components needed to prepare the rubber mixture in a single batch

Main indicators	Part by mass per 100 mass of rubber	Mass %	density of components kg\ kg/m³	Volume of components, m³ 5	Volume %	Quantity of components to be prepared at one time, kg
1	2	3	4	5	6	7
SRBS-30ARKM-15	100,00	53,19	960	0,10417	63,40	1,220
This radical sulfur	1,50	0,80	2050	0,00073	0,44	0,018
Sulphebamide -Ц	2,50	1,32	1300	0,00192	1,17	0,030
Zinc oxide	3,00	1,60	5470	0,00055	0,33	0,037
Stearic acid	2,00	1,06	950	0,00210	1,28	0,024
Pre-vulcanization reducing agents	0,50	0,27	1500	0,00033	0,20	0,006
Petroleum tar SPP	5,00	2,66	1000	0,00500	3,04	0,061
Oil softener	17,00	9,04	970	0,01753	10,67	0,208
Anti-aging agent	0,50	0,27	1150	0,00043	0,26	0,006
Kamed (Tree resin-derived from cherry tree)	1,00	0,53	1010	0,00099	0,60	0,012
HAF type technical carbon	55,00	29,26	1800	0,03056	18,61	0,672
Total	188,00	100,00	–	0,16431	100,00	2,294

In this work, for the first time, tree resin was used as a modifier (this resin is called Kamerd). The kamerd was collected in August from an area called Novkhani Baghre, located 30 km from Baku city, and its general characteristics are shown in Figure 1.

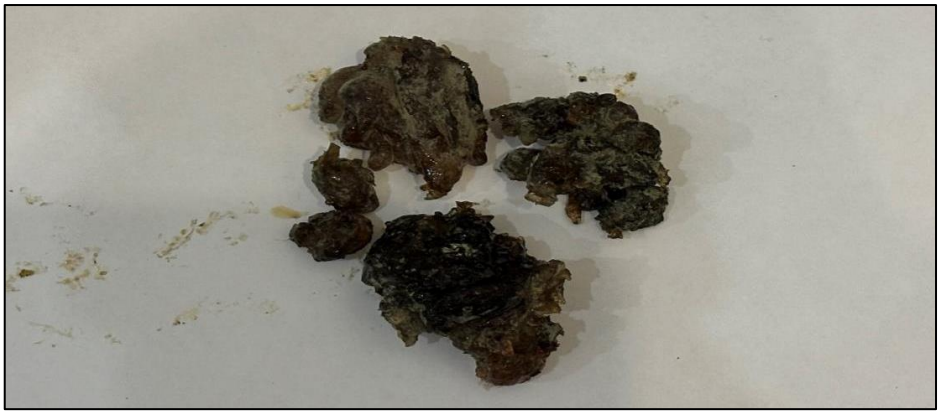


Figure 1. Results and Discussions

RESULTS OF EXPERIMENTAL RESEARCH

Study of rheological properties

A homogeneous rubber mixture obtained in laboratory cylinders for 14 minutes at 1200C and 12 minutes was vulcanized in the optimal vulcanization mode (T-1580C, P -12MPa, t - 26 minutes) and the main properties of its vulcanizate were determined (Table 4)

Table 4. Main properties of the vulcanizate of a rubber mixture based on butadiene-strol and wood resin

Names of indicators	Indicators				
	1	**2**	**3**	**4**	**5**
1. Tensile strength, MPa	16	19	20	24	21
2. Relative elongation at break, %	330	370	380	390	360
3. Residual elongation,%	11.0	13.0	14.0	19.0	16.0
4.TM-2 hardness, conventional unit	71	79	85	87	82
5. Tear resistance, kN/M	66	68	71	76	72
6. Rubber-to-metal bond strength, MPa	3.9	5.1	5.8	7.4	6.9
7.Frictionresistancem3/kg force	-13	-18	-15	-19	-22
8 Friction resistance m3/kgC.	61.1	56.4	68.1	71,0	62.6
9. Mass change during swelling (20℃, 24 hours), % mass isobutane-toluene (1:1) 10. Thermal resistance coefficients (100℃, 48 hours) Kσ	19	24.9	29	34	18
10. Heat resistance coefficients (100℃ 48 hours) Kσ	0,95	1.10	1.35	2.08	1.78
11.Elasticity %	10	8	9	8	8
12. Ozone resistance 25℃, 72 hours, deformation - 20% C03=0.01% wt.	does not fall apart	does not fall apart	does not fall apart	does not fall apart dağılmır	Completely decomposes in 109 hours

Since our goal is to obtain rubbers with chemical resistance and mechanical strength in various aggressive environments based on BSK, we prepared samples of rubbers obtained as a result of vulcanization and examined them in acid, gasoline, oil, kerosene transformer oil and other environments, and the obtained results are given in Figures 2, 3 and 4.

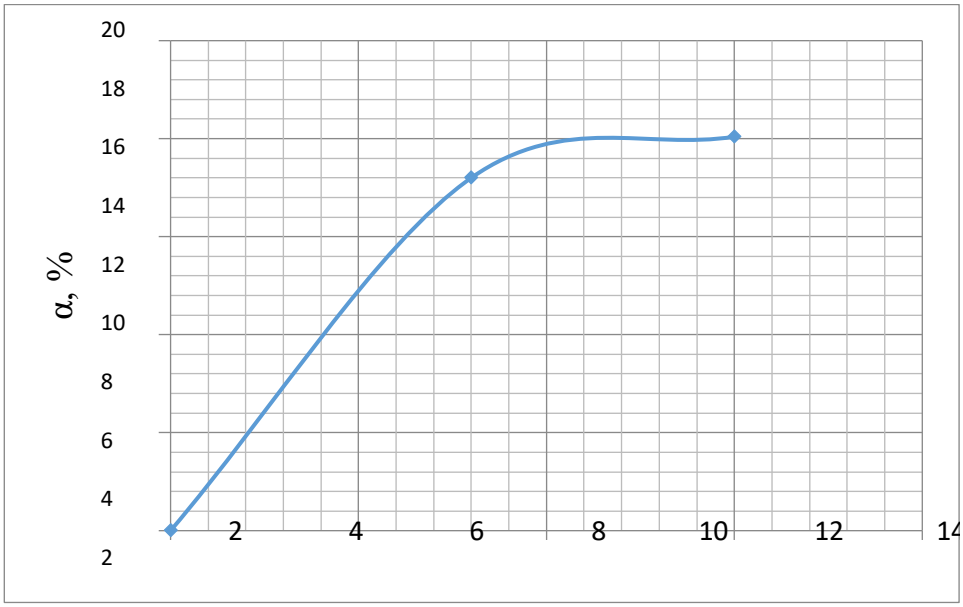


Figure 3. BSK+Kamed əsasında alınmış rezinin benzində həllolması qrafiki

Solubility was calculated as follows:

$$\alpha = \frac{4{,}18-4}{4} \cdot 100 = 4?5$$

$$\alpha = \frac{4{,}33-4}{4} \cdot 100 = 13{,}45$$

$$\alpha = \frac{4{,}515-3}{3} \cdot 100 = 8{,}25,$$

$$\alpha = \frac{4{,}61-4}{4} \cdot 100 = 15{,}25$$

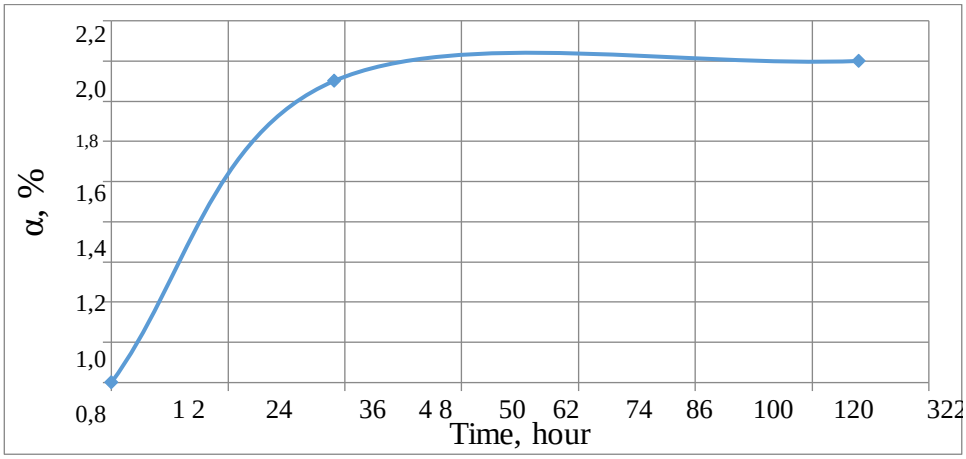


Figure 4. Solubility graph of the sample in nitric acid

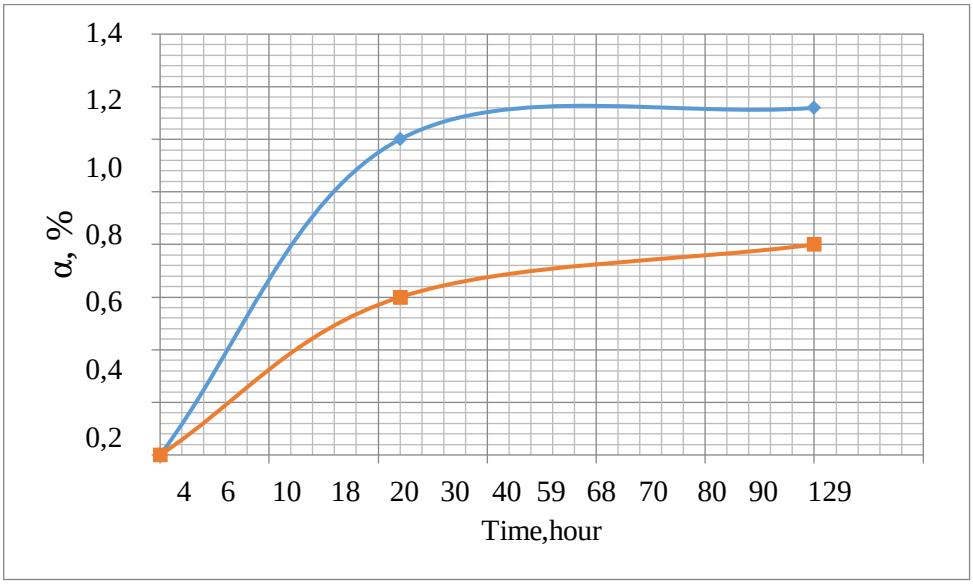


Figure 5. Solubility graph of the sample in kerosene and transformer oil

The report gave the following results

$$\alpha 1 = \frac{4,33-3}{3} \cdot 100 = 0,19 \qquad \alpha 1 = \frac{4,33-4}{4} \cdot 100 = 0,825$$

$$\alpha 2 = \frac{5,44-3}{3} \cdot 100 = 0,57 \qquad \alpha 2 = \frac{5,44-4}{4} \cdot 100 = 0,365$$

$$\alpha 3 = \frac{6,41-3}{3} \cdot 100 = 0,85 \qquad \alpha 3 = \frac{6,41-4}{4} \cdot 100 = 0,6025$$

$$\alpha 4 = \frac{7,11-3}{3} \cdot 100 = 1,05 \qquad \alpha 4 = \frac{7,11-4}{4} \cdot 100 = 0,7775$$

$$\alpha 5 = \frac{8,19-3}{3} \cdot 100 = 1,08 \qquad \alpha 5 = \frac{8.19-4}{4} \cdot 100 = 1,0477$$

RESULTS

1. In order to obtain rubbers resistant to oil, gasoline and aggressive environments based on butadiene-styrene rubber, an optimal recipe was prepared based on .-butadiene-styrene; A rubber mixture was prepared based on optimal recipes; The rubber mixture was vulcanized and the resistance of its vulcanizate to oil, gasoline and other aggressive environments was studied.

2. For the first time, we obtained a nanomaterial of wood resin and used it in the modification of butadiene-styrene rubber, thereby obtaining rubbers with high mechanical properties.

Reference

1. Alizade Tarlan *PHYSICO-MECHANICAL PROPERTIES OF PETROLEUM ROAD BITUMEN MODIFIED ON THE BASIS OF STYRENE-BUTADIENE BUTYL RUBBE*, 2024, Innovative scientific research Proceedings of the IX International Scientific and Practical Conference 14-15 March , Pp34-40 DOI: https://doi.org/10.5281/zenodo.10882832

2. Kerem Shixaliyev Research New Ways of Processing Polymer Waste that wasFormed as a Result of Operation321-335 Novel Perspectives of Geography, Environment and Earth Sciences Vol. 1 *Vol. 1*, 22 December 2022 , Page 25-35https://doi.org/10.9734/bpi/npgees/v1/17431D
3. Kerem Shixaliyev PROPERTIES OF THE COMPOSITION BASED ON MODIFIED POLYETHYLENES , 2023, Eur. Chem. Bull. , 2023; Volume -12 , Special Issue-5 : Page: 242-258 . doi 10.31838/ECB/2023.12.si5.023
4. Kerem Shixaliyev Study of the Properties of the Composition Obtained Based on Mixtures of Polyvinyl Chloride and Ethylene-Propylene Copolymers International ,2023,Journal of Current Science Research and Review ISSN: 2581-8341 Vol 6 No 1 (2023): Volume 06 Issue 01 January ,pp314-318 doi 10.31838/ECB/2023.12.si5.023
5. Kerem Shixaliyev.Investigating Recycling Methods of End-of-Life Car Tires,2023, Journal of Advanced Zoology, Volume 44 Issue S-3 Year 2023 Page 1149:1157 ,DOI: https://doi.org/10.17762/jaz.v44iS-3.1205
6. Kerem Shixaliyev Investigation of the Properties of a Composition Obtained based on Mixtures of Polyvinylchloride and Synthetic Rubber Ethylene Propylene Terpoliymer 2023,Editorial Board of Journal of Coastal Life Medicine editor special issue eurchembull. Vol. 11: Number 1, 2023 JCLMM 1/11 pp.|2653–2658, https://www.jclmm.com/index.php/journal/article/view/741. 117-126 Technology, DOI: 10.35940/ijitee.G5721.079920

OBTAINING AND INVESTIGATION OF COMPOSITIONS WITH IMPROVED PERFORMANCE PROPERTIES BASED ON SKI-3 RUBBER

Rashad Alizade
Master's student, Department of Organic substances
and technology of macromolecular compounds
Azerbaijan State Oil and Industry University
Baku, Azerbaijan
kerem_shixaliyev@mail.ru

Abstract: Obtaining and investigation of compositions with improved performance properties based on SKI-3 rubber is devoted to obtaining rubber based on SKI-3 grade rubber with improved physical-mechanical properties. For carrying out this work, for modification of SKI-3 rubber, butadiene-nitrile rubber of BNK-18 grade and polymethyl methacrylate (PMMA) were used. At the same time model rubber mixtures based on the optimal formulation were prepared. Based on the study of properties of model rubber mixtures of non-crystallizing special-purpose rubber BNK-18 and crystallizing general-purpose rubber SKI-3 it was established that in the composition of formulations of industrial elastomer compositions it is most expedient to use mechanically activated material in a planetary mill for 3 min To study the rheological properties of binary systems SKI-3 + BNK-18 compositions were prepared on rolls at a temperature of 140°C during 15 minutes and the obtained single-phase compositions under different loads and temperatures (from 130 to 173°C) had the melt flow indices of this composition determined. Thus as a result the technology of processing rubber mixtures based on SKI-3 + BNK-18 was determined; namely; processing temperature 175°C and pressure 12 MPa.

Keywords: SKI-3 and butadiene-nitrile rubber of BNK-18 grade, modification, vulcanization, melt indices of the composition, tensile strength.

Introduction

For modification composite of isoprene rubber (SKI-3) many authors on the basis of silicon dioxide was developed and obtained using multifunctional silane, 2-aminoethyl-2-(3 triethoxysilylpropyl) aminoethyldisulfide (ATD) as coupling agent[1-7]. Such modification significantly improved dispersion of silicon dioxide in the corresponding composites, which was confirmed by SEM observation. And hardness, tensile strength, stress at certain elongation, tear strength and increase of temperature, as well as value of dynamic loss coefficient in the range from 0°C to 80°C of vulcanized silica/IR composites, significantly improved, especially at low dosage of ATD (2–4 phr)[8-14].

Method

In this work on the basis of SKI-3 and BNKS-18AMN formulation of model rubber mixtures was developed.(Table1).

Table 1. Formulation of model rubber compounds based on SKI-3 and BNKS-18

Ingredient	Based on BNKS-18AMN	Based on SKI-3
SKI-3	–	100.0
BNKS-18AMN	100.0	–
Ground sulfur	1.7	1.0
Altax (accelerator)	–	0.6
Zinc oxide	3.0	5.0
Guanidine F	–	3.0
Sulfenamide C	1.0	–
Industrial oil (SMZh)	40.0	40.0

Preparation of model rubber mixtures was carried out according to standard for SKI-3 and for BNKS-18AMN. Samples for comparison were model elastomer compositions filled with industrial filler – low-grade carbon black of N772 grade according to ASTM D1765-03.

SKI-3 Modification with PB and PMMA

The SKI-3 modification with PB and PMMA wires was tested at various temperatures (°C): 1 – 85; 2 – 90; 3 – 95; 4 – 100; 5 – 105. The images obtained are shown in Figures 1 and 2.

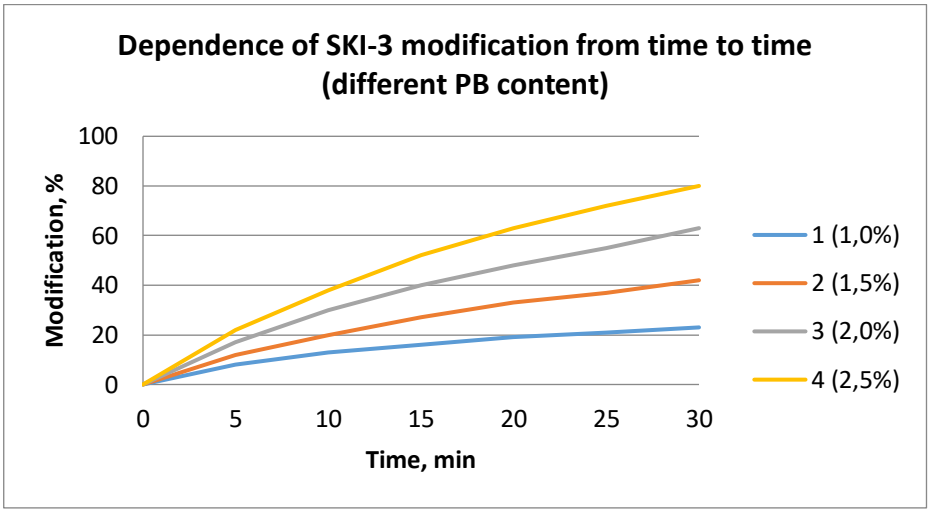


Figure 1. SKI-3 modification versus modification reaction time at various temperatures.

To confirm the modification, IR spectra of SKI-3 modified with PB (2.5 wt%) were obtained. The data are e 3.IR spectra of SKI-3 modified with PB (2.5% by weight).

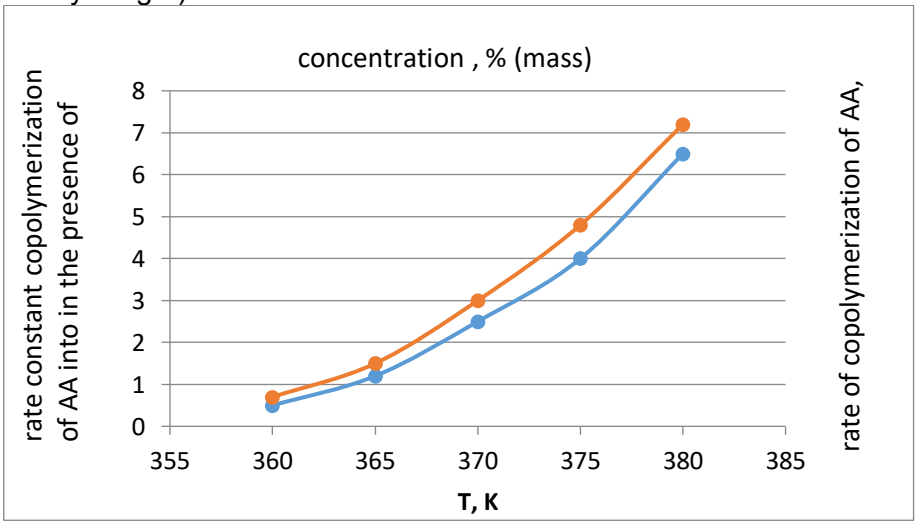


Figure 2. Dependence of the rate constant of modification of SKI-3 on temperature and on the concentration of PB.

The dependence of the SKI-3 modification rate constant on temperature and PB concentration was subsequently determined (Figures 2, 3, and 4).

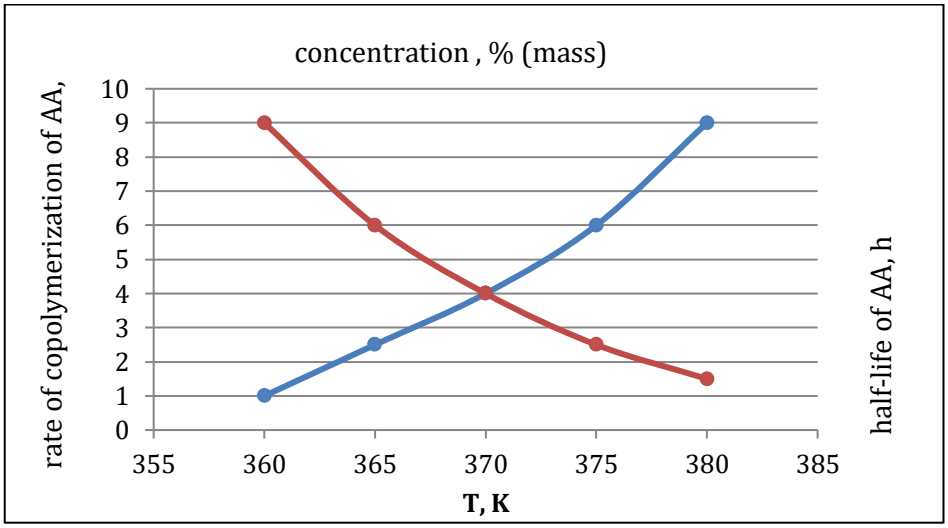


Figure 3. Dependence of the modification rate of SKI-3 on temperature at a PB initiator concentration of 1.5% (mass).

After the production of rubber compounds based on the formulation we selected, the vulcanization process was carried out at a temperature of 158C for 26 minutes and the main parameters of the obtained vulcanizates were determined (Table 2).

Table 2. Results of experimental research

№	Parameter name	Known value			Proposed values		
		1	**2**	**3**	**4**	**5**	**6**
1	Conditional tensile strength, MPa	17,4	16,3	16,7	18,3	19,9	19,8
2	Relative elongation, %	300	320	310	370	395	405
3	Relative residual deformation, %	13	16	10	13	13,6	13,9
4	Tear resistance, kN/m	62	67	69	68,7	69,4	69,1
5	Abrasion, cm³/(L·h)	66	67	62	59	55	56
6	Adhesion to metal, MPa: Steel 3	5,6	5,2	5,1	8.5	9	9,3
7	Adhesion to metal, MPa: Brass	3,1	-	3,4	5,2	6,7	7,5
8	Brittleness temperature, K	266	232	270	244	243	246
9	Stiffness TM-2, conventional unit	85	83	79	81	81	82
10	Swelling at 296 K for 24 h, isooctane–toluene (70:30), %	12,6	14,7	14,2	10,6	10,3	10,2
11	Swelling at 296 K for 24 h, gasoline–benzene (3:1), %	-	-	23,2	14,3	13,6	14,3
12	Aging coefficient after 48 h at 379 K: f	0,83	0,89	1,15	0,88	0,89	0,98
13	Aging coefficient after 48 h at 379 K: ε	0,77	0,65	0,92	0,8	0,79	0,89
14	Jumping elasticity, %	12	13	17	13,9	15	13,9
15	Ozone resistance for 27 h at 298 K (deformation 20%, ozone concentration 0.015%)	Fails	Fails	Does not fail	Does not fail	Does not fail	Does not fail

RESULTS

1. The effect of grape leaf content on the properties of SKN-3 rubber was studied, showing that at an optimal concentration of 5–10 parts by weight, the modified rubber exhibits higher tensile strength and lower residual elongation.

2. The Mooney viscosity of the rubber compounds increased at grape leaf concentrations of 5 and 6 parts by weight, but decreased at a concentration of 10 parts by weight. Thermogravimetric analysis (TGA) was used to assess thermal stability. SKI-3 modified with grape leaves demonstrated increased thermal stability compared to the control sample.

Reference

1. Alizade Tarlan *PHYSICO-MECHANICAL PROPERTIES OF PETROLEUM ROAD BITUMEN MODIFIED ON THE BASIS OF STYRENE-BUTADIENE BUTYL RUBBE,* 2024, Innovative scientific research Proceedings of the IX International Scientific and Practical Conference 14-15 March **, Pp34-40 DOI:** https://doi.org/10.5281/zenodo.10882832
2. G. Barrera Torres, Carlos M. Gutierrez Aguilar, Elizabeth R al. et . Application of Post-Industrial Leather Waste for the Development of Sustainable Rubber Composites *Polymers* **2025**, *17*(2), 190; DOI: 10.3390/polym17020190
3. Fariz A. Amirli brahim H. Movlayev Aynur F. Mammadova S TUDY OF THE RHEOLOGY PROPERTIES OF THE MIXTURE OF TERMINAL ETHYLENE-PROPYLENE RUBBER WITH BENZYNAMINE-MODIFIED PHENOL-FORMALDEHYDE OLIGOMER, PPOR,Vol. 26, No. 1, 2025, pp.229-239 https://doi.org/10.62972/1726-4685.2025.1.229
4. İbrahim H. Movlaye.COMPOSITIONS BASED ON EPOXIDIAN OLIGOMER MODIFIED WITH LOW MOLECULAR BUTADIENE-NITRILE RUBBER.PPOR,Vol. 26, No. 3, 2025, pp.688-696 https://doi.org/10.62972/1726-4685.2025.3.688
5. Gambaro D.SH. Spreading of Astaxanthin and Astragals species on the highland zones of the Nakhichevan autonomous republic // European Academic Research, 2014, İmpact Factor 3,1: p.-4153-4159 / DOI: 10.32388/ZCAXYW.2
6. Kerem Seyfi Modification of the used up polymeric materials and investigation thof e properties of the materials obtained. Journal of Medical Pharmaceutical and Allied Sciences, 2022, 11(2), pages 4697–4702 DOI: 10.35940/ijitee.G5721.079920 5..Kerem Shixaliyev. Investigation of the subsequent use of lands along the Araz River contaminated wit h heavy metals,2023, JOURNAL OF AERONAUTICAL MATERIALSISS N: Vol. 43, Issue-01, pp. 102-111,https://www.hkclxb.cn/article/view/2023/102.html
7. Kerem Shixaliyev Research New Ways of Processing Polymer Waste that wasFormed as a Result of Operation321-335 Novel Perspectives of Geography, Environment and Earth Sciences Vol. 1 *Vol. 1*, 22 December 2022 , Page 25-35https://doi.org/10.9734/bpi/npgees/v1/17431D
8. Kerem Shixaliyev PROPERTIES OF THE COMPOSITION BASED ON MODIFIED POLYETHYLENES , 2023, Eur. Chem. Bull. , 2023; Volume -12 , Special Issue-5 : Page: 242-258 . doi 10.31838/ECB/2023.12.si5.023

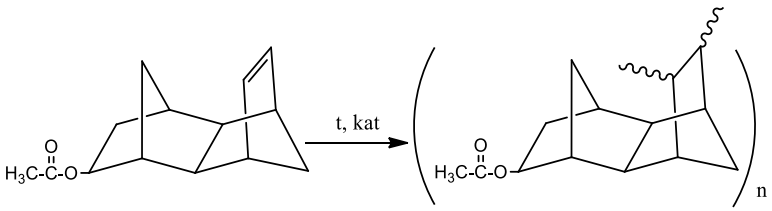
PREPARATION OF TETRACYCLIC HOMOPOLYMER AND A COPOLYMER WITH ACRYLIC FRAGMENTS

Kh. M. Mamedova, V. S. Kadyrly, E. G. Makhmudova, R. A. Rasulova, M. D. Ibragimova, I. R. Safarova, J. G. Ismailova
Institute of Petrochemical Processes named after academician Y.G. Mamedaliyev of the Ministry of Science and Education of the Republic of Azerbaijan, Baku, Azerbaijan
e-mail: qedirlivusale@mail.ru

Keywords: homopolymer, copolymer, cyclic monomer

The development of simple methods for the synthesis of alicyclic monomers with various functionalities obtained from petrochemical by-products, as well as the study of their homo- and copolymerization with the aim of obtaining polymeric materials with a wide range of applications is one of the most pressing problems that is the focus of researchers [1-3]. This paper presents the results of studies of the radical polymerization of 8-acetoxy-tetracyclo[4.4.$1^{2.5}$.$1^{7.10}$.$0^{1.6}$]dodec-3-ene (ATCD) and its copolymerization with (meth)acrylic acids in the presence of BF_3•OEt_2.

Homopolymerization of ATCD and its copolymerization with (meth)acrylic acids were carried out in bulk and in a solvent medium at a reaction temperature of 120°C.

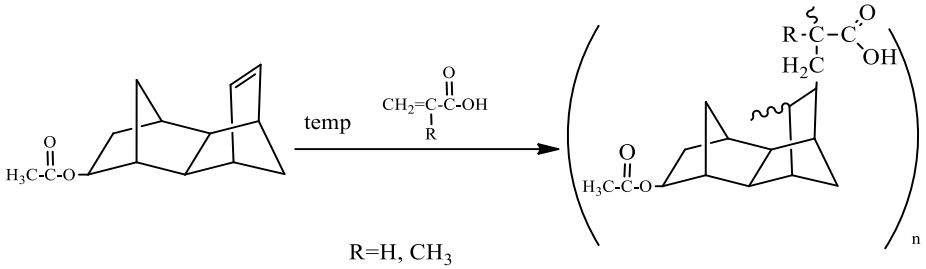


The yield of poly-8-acetoxytetracyclo[4.4.$1^{2.5}$.$1^{7.10}$.$0^{1.6}$]dodec-3-ene at the specified temperature and polymerization time of 10 h, in the case of the process being carried out in a mass amount of catalyst of 5 and 10%, is 49.6% and 77.2%, respectively. The isolation of the obtained polymer from the unreacted portion of the monomer was carried out by precipitation in ethyl alcohol from a benzene solution.

Polymerization of ATCD was also carried out under similar conditions using benzene as a solvent. The polymer yield when polymerizing in a 50% benzene solution and 10% catalyst by weight was 87%. The observed increase in polymer yield when the process was carried out in solution is due to the high viscosity of the resulting product in bulk at the specified temperature, which in turn complicates subsequent polymerization.

Under the above conditions, the copolymerization of ATCD with acrylic (AC) and methacrylic (MAC) acids was studied at equal monomer weight

ratios. It was found that the yield of the ATCD copolymer with both AC and MAC was only 46.3 and 45 wt.%, respectively.



The structure of the synthesized homo- and copolymers was proven by IR spectral analysis.

It is known that the inclusion of cyclic fragments in the macrochain promotes increased thermal stability of the final product. Differential thermal analysis of synthesized homopolymer and acrylic acid copolymer samples, conducted on a LINSESIS STAPT 1600 apparatus, demonstrates the relatively high thermal stability of the ATCD homopolymer and its acrylic acid copolymer. In particular, the homopolymer of 8-acetoxytetracyclo-[4.4.$1^{2.5}$.$1^{7.10}$.$0^{1.6}$]-dodec-3-ene is characterized by a relatively higher thermal stability than the copolymers synthesized on its basis. A significant loss of mass of polyacetoxytetracyclo-[4.4.$1^{2.5}$.$1^{7.10}$.$0^{1.6}$]-dodec-3-ene is observed at 224 ºC and is 1.5% with a reaction enthalpy value of ΔH = -678.4 J/g. In addition, in the temperature range of 443–486.5°C, an endothermic peak is observed with a maximum reaction enthalpy of 221 J/g at a temperature of 443°C.

REFERENCES

1. He X., Dong Y., Jiang X. Wang Z., Yang Y., Han Z., Chen D. Polymer Chem. 2017, No 8, P. 2390–2396.
2. Li M., Zhang H. Polymer Chemistry. 2019, No 10, P. 2741–2748.
3. Mamedov M.K., Kadyrly V.S. Russian J. Applied Chem. 2015, V. 88, No 10, P. 1733–1735.

PRODUCTION OF SYNTHETIC PETROLEUM ACIDS AND OXY-PETROLEUM ACIDS VIA LIQUID-PHASE OXIDATION OF NAPHTHENIC–PARAFFINIC HYDROCARBONS IN THE PRESENCE OF Mn, Cr, Co, Ni, AND Zn ACETYLACETONATES AS CATALYSTS

V.M. Abbasov, L.M. Afandiyeva, N.N. Babanli, N.N. Aliyeva, Sh.N. Ibrahimli
Academician Y.H. Mammadaliyev Institute of Petrochemical Processes
Ministry of Science and Education of the Republic of Azerbaijan
Baku, Azerbaijan
E-mail: babanlinermin@gmail.com

Abstract - Currently, various studies are being conducted in the field of the synthesis of synthetic petroleum acids and oxy-petroleum acids. In this area, different oxidising agents are employed to investigate their catalytic effects on the process. In particular, transition metal acetylacetonate complexes have been utilised as oxidising agents.The dearomatised diesel fraction was oxidised in the liquid phase for 5 hours in the presence of atmospheric oxygen. During the oxidation process carried out in the presence of Cr, Ni, Co, Mn, and Zn acetylacetonates, it was determined that the highest yield was obtained with the catalytic participation of Mn acetylacetonate. Under these conditions, the yield of the mixture of synthetic petroleum acids (SPA) and oxy-petroleum acids (OSPA) reached 33%.
Keywords*:* acetylacetonate, oxidation, synthetic naphthenic acids

Introduction

At present, extensive research is being conducted on the development of new types of catalysts for investigating liquid-phase oxidation reactions of hydrocarbons with atmospheric oxygen, as these processes play a significant role in advancing technologies for organic and petrochemical synthesis [1–2]. At the same time, liquid-phase oxidation of hydrocarbons in the presence of more efficient catalysts enables the synthesis of industrially important oxygen-containing organic compounds, such as alcohols, aldehydes, acids, esters, and others [3,4].

Thus, the oxidation process carried out with atmospheric oxygen in the absence of a catalyst yields relatively low results. From this perspective, external intervention in the reaction system is required in order to enhance the oxidative capacity of oxygen. To activate the effect of oxygen and achieve higher yields, catalytic systems based on transition metal complexes containing organic and inorganic ligands with variable valence states are employed [5–7].

Experimental part

This conference paper focuses on the liquid-phase oxidation of naphthene–paraffin hydrocarbons using acetylacetonates of manganese (Mn), chromium (Cr), cobalt (Co), nickel (Ni), and zinc (Zn).

Fraction of Azerbaijani oils mixture taken from the Heydar Aliyev Baku Oil Refinery, boiling at 185-329°C, was used as a raw material for the

implementation of the oxidation process in the presented work. Initially, a dearomatization process was performed at room temperature to remove aromatic hydrocarbons from the feedstock, resulting in a reduction of aromatic hydrocarbon content from 15% to 1%.

The oxidation process was conducted in a barbotage-type reactor, using atmospheric oxygen in the liquid phase. During the experiments, which took place at temperatures ranging from 135 to 140 °C over a duration of 5 hours, the catalytic effects of Mn, Cr, Co, Ni, and Zn acetylacetonates as oxidation catalysts were investigated. [8–10].

The results obtained from the experiments are presented in Table 1.

Table 1: The results of napthene-paraffinic concentrate oxidation in the presence of Metal (Me) Acetylacetonates (t=135-140°C, air flow rate of 0.3 m^3/kg□h, the reaction duration – 5 h)

The catalyst amount on the crude,%	Oxidate		SPA		OSPA		SPA+OSPA
	A.n., mg KOH/g	Yield, %	A.n., mg KOH/g	Yield, %	A.n., mg KOH/g	Yield, %	Yield %
Mn- acetylacetonate							
0,1	42,3	94,2	138,7	12,8	120,2	8,5	21,3
0,2	52	96,2	146	14	125,2	10	24
0,3	60	96	144,5	13,5	122,6	19,5	33
Ni- acetylacetonate							
0,1	36,2	95,4	136	8,2	115,4	9	17,2
0,2	50,5	96	140,5	11	122,4	7	18
0,3	50,6	95,4	138,8	10,2	125,2	8,5	18,7
Zn- acetylacetonate							
0,1	25	96	135,2	6,8	110,2	8,5	15,3
0,2	28,8	95,9	138	10,5	115,8	8,8	19,3
0,3	30	96,2	138,5	9	118	9,5	18,5

Note: Me- Cr, Ni,Co, Mn, Zn

As can be seen from Table 1, the catalysts used exhibit different levels of activity, which may be explained by their structural characteristics and the number of donor centres. When examining the effect of metal (Me) acetylacetonates on the oxidation process, it is evident that Mn acetylacetonate, used in the concentration range of 0.1–0.3 wt.%, demonstrates higher catalytic efficiency compared to the other complexes studied.

For each complex, increasing the catalyst concentration relative to the feedstock from 0.1 wt.% to 0.3 wt.% during the oxidation process results in a noticeable increase in the yields of SPA (synthetic petroleum acids) and OSPA (oxy-synthetic petroleum acids).

The table also presents the effects of Mn, Ni, and Zn salts on the oxidation process. The experimental results clearly indicate that Cr, Co, and Mn salts exert a more pronounced influence on the oxidation process. For this reason, these salts were further investigated in various ratios, and their complex salts with nitro compounds were synthesised and studied in the oxidation process [5,11].

Figure 1 presents the dependence of the yield of SPA + OSPA obtained during the oxidation process on the type of catalyst used, depending on the metal present in the complex.

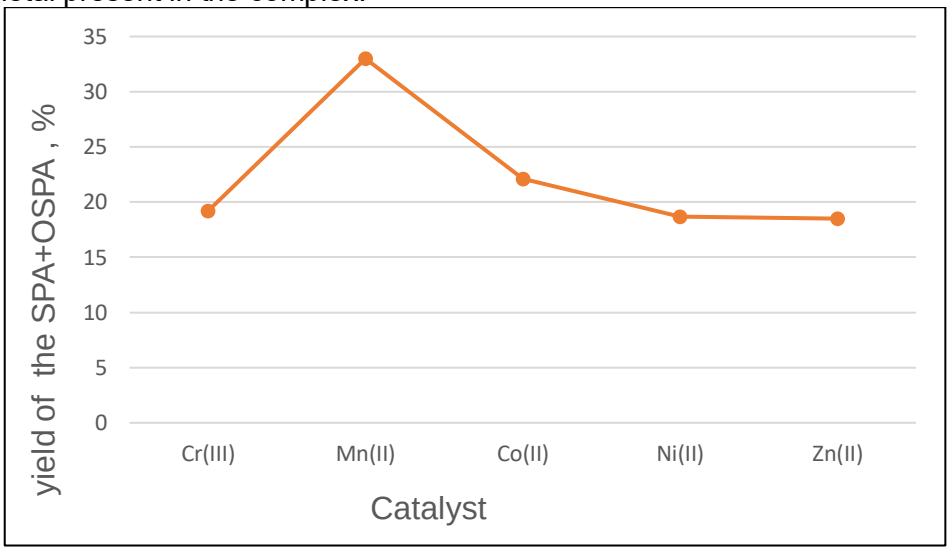


Figure 1. Dependence of the yield of SPA + OSPA on different catalysts

As can be seen from the graph, the best results in the oxidation processes were achieved when the $Mn(acac)_2$ complex was used as the catalyst.

Conclusion

Thus, the conducted studies have demonstrated that the oxidation process carried out in the presence of the investigated metal (Me) acetylacetonates results in high yields of synthetic naphthenic and oxy-petroleum acids.

It was determined that among the catalysts employed, Mn(II) acetylacetonate exhibited the highest catalytic activity, resulting in the formation of a 33% yield of the SPA and OSPA mixture.

References

1. V.M. Abbasov, L.I. Əliyeva, L.M. Əfəndiyeva, N.N. Babanlı, S.F. Əhmədbəyova G.Y. Rüstəmli, A.P. Musayeva, A.Q. Quluzadə. Neftin naften-parafin karbohidrogenlərinin sintetik neft turşuları qarışığına oksidləşmə prosesinə Cr- Və Mn-asetil-asetonatların katalitik təsiri. Kimya Problemləri, Bakı 2019, No.1 (17) s. 105-110

2. Vagif M. Abbasov, Leylufar I. Aliyeva, Lala M. Afandiyeva, Hikmat J. Ibrahimov, Gulay Y. Rustamli. Aerobic oxidation of naphthene-paraffinic hydrocarbons of petroleum in the presence of γ-Al_2O_3 modified by transition metals. PPOR 2020, Vol. 21, No. 1, Pp.80-89
3. Abbasov V.M., Efendiyeva L.M., Zeynalov E.B. Et Al. Synthesis of synthetic naphthenic acids by catalytic oxidation of naphten hydrocarbons of Baku oils in a liquid phase*. Chemical Problems.* 2010, No. 2, Pp. 258-262.
4. Litvintsev I.Yu. Oxidation processes in industrial organic chemistry. *Soros Educational Journal*. 2004, Vol. 8, No. 1, Pp. 24-31.
5. L.I.Aliyeva, L.M.Efendiyeva, N.N.Babanly [et al.] Reactivity of β-dicetonates of metals with variable valencies and their nitroderivatives in liquid-phase oxidation reaction of naphthenic hydrocarbons. Processes of petrochemistry and oil-refining (PPOR), Bakı 2019. V.20, №4, -p.389-400
6. Liang Xuebo, Hu Boyu, Yuan Yongiun etal. Optimization of aerobic oxidation of cyclohexane catalyzed by metalloporphyrins. *J. Chem. Ind. And End. (China),* 2007, vol. 58, no. 3, pp. 794-798
7. Kuznetsova N.I., Kuznetsova L.I., Kirillova N.V. Et Al. Oxidation of hydrocarbons with molecular oxygen with the participation of peroxide compounds formed In situ. Kinetics And Catalysis. 2005, Vol. 46, No. 2, Pp. 219- 232.
8. Abbasov V.M., Əliyeva L.İ., Əfəndiyeva L.M., Babanlı N.N., Əliyev B.M., Yusifov R.M., Tahirova F.F. Mn (III), Cr (III) asetilasetonat duzlarının neft karbohidrogenlərinin oksidləşmə prosesinə katalitik təsiri. Ümummilli lider Heydər Əliyevin anadan olmasının 95-ci ildönümünə həsr olunmuş müasir təbiət və iqtisad elmlərinin aktual problemləri beynəlxalq elmi konfrans, Gəncə, 2018 04-05 may, s. 222-224
9. Babanlı, N.N. Naften karbohidrogenlərinin maye fazada Mn-, Cr-, Ni-, Co-asetilasetonatların iştirakı ilə katalitik oksidləşməsindən sintetik oksi- və neft turşularının alınması, Azərbaycan Ali Texniki Məktəblərinin Xəbərləri, Bakı 2019, C.21, № 1 (117), -s. 35-40
10. Babanlı N.N . Asetilasetonun keçid metallarla (Co, Cr, Ni, Mn, Zn) komplekslərinin katalitik iştirakı ilə sintetik neft turşuları qarışığının sintezi və tədqiqi. Kimya üzrə fəlsəfə doktoru dis., Bakı, 2021, 175 s
11. Эфендиева Л.М., Алиева Л.И.,Сулейманова С.А., Османова С.Н., Исмаилов Э.Г Каталитическая активност ацетилацетонатных комплексов хрома, марганца, кобальта в реакции жидкофазного окисления нафтен парафиного концентрата дизельной фракции в нефтяные кислоты, Бутлеров сообщения №3, Казан,Россия 2022, s. 84-93

STUDY OF THE INHIBITORY PROPERTIES OF AMINOESTERS OBTAINED BASED ON SYNTHETIC PETROLEUM ACIDS

V.M. Abbasov, L.M. Afandiyeva, G.Y. Rustamli,
Ch.Z. Musaeva, S.A. Süleymanova
Institute of Petrochemical Processes named after Academician Y.H. Mammadaliyev, Ministry of Science and Education of the Republic of Azerbaijan, Baku, Azerbaijan
E-mail: rustamligulay7@gmail.com

Abstract. Aminoesters were synthesised based on ethanolamines and a mixture of synthetic petroleum acids obtained by liquid-phase catalytic oxidation of naphthenic–paraffinic hydrocarbons, separated from the diesel fraction boiling within the temperature range of 190–330°C. The effect of these reagents in a CO_2 environment on corrosion activity was evaluated

at 50°C over an 18-day period. It was found that the synthesised mono- and di-ethanolamine esters of synthetic petroleum acids completely inhibit the CO_2 corrosion process even at very low concentrations. It was demonstrated that the synthesised aminoesters (MEA and DEA esters) provided 97% protection efficiency at a concentration of 100 mg/L after 100 hours of corrosion testing. At the end of the 433-hour reaction period, the MEA ester of synthetic petroleum acids (SPA) showed 95% corrosion protection efficiency, while the DEA ester of SPA exhibited 94.6% protection efficiency.

Keywords: diesel fraction, synthetic petroleum acids, corrosion, inhibitor, aminoesters

Introduction

Despite ongoing efforts worldwide to address the issue in the oil and gas industry and the proposal of new methods, CO_2 corrosion remains a pressing and unresolved problem. One of the most effective – and arguably the primary – approaches to combating this type of corrosion is the use of inhibitors. In this regard, the application of corrosion inhibitors surpasses other protection methods in terms of economic feasibility, efficiency, and overall effectiveness [1].

Synthetic petroleum acids (SPA) obtained via liquid-phase oxidation of naphthene–paraffin hydrocarbons—isolated from the 190–330 °C diesel fraction of crude oil—in the presence of air oxygen and nano γ-Al_2O_3-based heterogeneous catalysts were further reacted with ethanolamines, namely monoethanolamine (MEA) and diethanolamine (DEA). According to the established methodology, amino esters were synthesised with high yields of 98–99% in each case [2].

In this context, amino esters were synthesised using synthetic petroleum acids obtained from the oxidation of naphthene–paraffin hydrocarbons derived from the diesel fraction of crude oil, which boils in the range of 190–330 °C. The oxidation process was carried out in an aerobic medium in the presence of heterogeneous catalysts based on nano γ-Al_2O_3. The long-term inhibitory performance and kinetics of these amino esters against CO_2 corrosion were subsequently investigated [2,6].

Experimental Part

To investigate the effect of the synthesised amino esters on the kinetics of CO_2 corrosion, corrosion rates were measured in a 1% NaCl solution at 50 °C over a period of 18–19 days, both in the absence of an inhibitor and in the presence of inhibitors at a concentration of 100 mg/L. The measurements were carried out using an “ACM Instruments Gill AC No. 1197” device operated with the “ACM Instruments Version 5” software [2–5].

The results obtained over 100–433 hours, demonstrating the effect of amino esters derived from SPA:MEA and SPA:DEA (at a concentration of 100 mg/L) on steel corrosion, are presented in Table 1.

Table 1. Long-term use of aminoesters obtained based on SPA:DEA and SPA:MEA at a concentration of 100 mg/L as corrosion protection inhibitor

Inhibitor Name	Duration, hours	Corrosion current, mA/m²	Corrosion rate, mm/year	Metal loss, mm	Corrosion protection efficiency, %
Without inhibitor	100	3353.3	3.8865	0.0466478	-
	400	3037.1	3.52	0.1697305	-
	430.37	3114.5	3.6097	0.1812434	-
	433.37	1358.6	1.5747	0.1819728	-
Aminoester obtained based on SPA:MEA	100	101.88	0.1180865	0.001315	97
	400	91.018	0.1054903	0.005288	97
	430.37	96.142	0.1114297	0.005691	97
	433.37	92.165	0.0720501	0.00572	95
Aminoester obtained based on SPA:DEA	100	150.56	0.130447	0.001076	96.65
	400	1203.5	0.11785	0.030948	96.6
	430.37	1437.6	0.12379	0.03757	96.57
	433.37	1776.6	0.08441	0.04354	94.64

As shown in Table 1, the amino ester inhibitor synthesised based on SPA:MEA at a concentration of 100 mg/L demonstrated a corrosion protection efficiency of 97% from the 4th day (100 hours) to the 18th day (430.37 hours), and 95% efficiency on the 18th day (433.37 hours). The corresponding corrosion rates were 0.1180 mm/year on the 4th day, 0.1114 mm/year on the 18th day, and 0.0721 mm/year on the 19th day.

Similarly, the amino ester synthesised from SPA and DEA at a concentration of 100 mg/L exhibited a corrosion protection efficiency of approximately 97% up to the 18th day of exposure. After this period, a slight decrease in protection efficiency was observed, reaching approximately 95%.

Thus, based on the obtained results, the application of amino esters synthesised from synthetic petroleum acids and ethanolamines as corrosion inhibitors in CO_2-containing environments can be considered both appropriate and highly effective.

Conclusion

1. The aminoester obtained based on SPA and MEA demonstrated superior performance in long-term CO_2 corrosion tests. The aminoester synthesised from SPA and DEA has a larger molecular weight than the SPA–MEA-based aminoester, and due to steric hindrance, it remains on the steel surface for a shorter period. This provides grounds to conclude that the aminoester derived from SPA and MEA is a more effective inhibitor against the corrosion process.

2. The aminoesters synthesised from SPA with MEA and DEA exhibit high inhibitory properties against CO_2 corrosion. Specifically, when the SPA–MEA-based aminoester was used at a concentration of 100 mg/L, the corrosion protection efficiency reached 95% at the end of the 18th day. Under the same conditions (100 mg/L), the SPA–DEA-based aminoester showed a corrosion protection efficiency of 94.6% at the end of the 18th day.

References

1. Rustamli, G. Y. (2023). *Study of obtaining process of synthetic petroleum acids from 190-330°C petroleum fraction in the presence of aluminum oxide-based catalysts* (Doctoral dissertation). Baku, Azerbaijan.
2. Abbasov, V. M., Guliyev, A. A., Jabrailzadeh, S. Z., & Mursalov, N. I. (2015). *Synthesis of imidazoline derivatives on the basis of triethylenetetramine and naphthenic acids and research of imidazoline derivatives as corrosion inhibitor*. International Journal of Engineering and Technology Innovation, 5(4), 21–23.
3. Abbasov, V. M., Afandiyeva, L. M., Agamaliyeva, D. B., Rustamli, G. Y., & Agayev, C. E. (2022, May 19–20). Investigation of amino esters obtained based on synthetic petroleum acids as corrosion inhibitors. *In Republican scientific conference dedicated to the 90th anniversary of Academician Nadir Mir-Ibrahim oglu Seyidov "Catalysts, olefin-based oils"* (p. 55). Baku, Azerbaijan.
4. Abbasov, V. M., Aliyeva, L. I., Afandiyeva, L. M., Ibrahimov, H. J., & Rustamli, G. Y. (2020). Aerobic oxidation of naphthene-paraffinic hydrocarbons of petroleum in the presence of γ-Al_2O_3 modified by transition metals. *Processes of Petrochemistry and Oil Refining, 21*(1), 80–89.
5. Abbasov, V. M., Efendieva, L. M., Agamalieva, D. B., Rustamli, G. Y., Yusifov, R. M., & Agaev, C. E. (2023). *Issledovanie aminoefirov sinteticheskoy neftyanoy kisloty, poluchennoy aerobnym okisleniem naften-parafinovykh uglevodorodov, v kachestve ingibitorov korrozii* [Investigation of amino esters of synthetic petroleum acid obtained by aerobic oxidation of naphthene–paraffinic hydrocarbons as corrosion inhibitors]. *Praktika protivokorrozionnoy zashchity, 27*(3), 47–56.
6. Afandiyeva, L., Abbasov, V., Nasibova, G., Rustamly, G., Babanly, N., & Mammadova, S. (2025, April 28). *Investigation of nitrogen derivatives of synthetic petroleum acids as inhibitors against CO_2 corrosion of steel*. *In 9th Portuguese Young Chemists Meeting (PYCheM) International Conference*. University of Algarve, Faro, Portugal, p. 89.

OLEİN TURŞUSUNUN 2-AMİNOPİRİDİN KOMPLEKSİNİN CO_2 KORROZİYASINA QARŞI İNHİBİTOR KİMİ TƏDQİQİ

V.M .Abbasov, D.B. Ağamalıyeva, G.Ə.Abbasova, S.Z.Əhmədova, K.V.Əzizova
Azərbaycan Respublikası Elm və Təhsil Nazirliyinin
akademik Y.H.Məmmədəliyev adına Neft Kimya Prosesləri İnstitutu
Bakı, Azərbaycan
guler.ehmedzade@gmail.com

Xülasə

Tədqiqat 2-aminopiridin–olein turşusu kompleksinin sintezini, kimyəvi strukturunun müəyyən edilməsini və CO_2 mühitində polad səthlərində korroziya inhibitoru kimi fəaliyyətinin qiymətləndirilməsini əhatə edir. İlkin mərhələdə aparılan sintez prosesindən təqribən 95 % çıxımla 2-aminopiridin–olein turşusu kompleksi sintez edilmişdir. Alınmış kompleksin tərkibi və quruluşu infraqırmızı (İQ) və nüvə maqnit rezonansı (NMR) spektroskopiyası üsulları ilə təhlil edilmiş, birləşmənin bəzi fiziki-kimyəvi xassələri isə 30 % izopropil spirtində 20 %-li məhlulu hazırlanaraq müəyyən edilmişdir. İnhibitor məhlulunun C1018 markalı polad elektrodun korroziya prosesinə təsiri CO_2 ilə doydurulmuş 1 %-li NaCl məhlulunda tədqiq edilmişdir. Bu məqsədlə, 50 °C temperaturda CORRTEST CS Studio 6 sistemi vasitəsilə potensiodinamik polyarizasiya ölçmələri 1 saat müddətində aparılmış və inhibitorun 500 ppm qatılıqda 99,6 %, 1000 ppm qatılıqda isə 99,9 %-ə qədər qoruyucu təsir göstərərək korroziya prosesini effektiv şəkildə zəiflətdiyi müəyyən edilmişdir.

Açar sözlər: *2-aminopiridin, olein turşusu, karbon dioksid korroziyası,inhibitor*

Giriş

Bütün dünyada olduğu kimi, Azərbaycanda da korroziya problemi kimya sənayesində və ona bağlı sahələrdə mühüm texnoloji və iqtisadi çətinliklər yaradır. Xüsusilə kənd təsərrüfatı texnikası, hərbi sənaye və neft-kimya sektoru kimi strateji əhəmiyyətə malik sahələrdə korroziyanın təsiri daha qabarıq şəkildə özünü göstərir. Bu səbəbdən korroziya ilə mübarizə məqsədilə çoxfunksiyalı inhibitorların hazırlanması son illərdə elmi araşdırmaların əsas istiqamətlərindən birinə çevrilmişdir [1-5]. Belə inhibitorlar metal səthi üzərində qoruyucu təbəqə yaradaraq və elektrokimyəvi reaksiyaların kinetkasını dəyişdirərək korroziya prosesinin sürətini azaltmağa imkan verir [6,7].

Bu məqsədlə 2-aminopiridinin olein turşusu ilə kompleksi sintez olunmuş və onun karbon qazı (CO_2) mühitində polad səthlərdə baş verən korroziya proseslərinə qarşı effektivliyi öyrənilmişdir.

Təcrübi hissə

Təcrübə mexaniki qarışdırıcı ilə təchiz olunmuş kolbaya başlanğıc maddələr – 2-aminopiridin və olein turşusu 1:1 mol nisbətində olmaqla əlavə olunaraq 40ºC temperaturda 1 saat müddətində fasiləsiz qarışdırılmaqla aparılmışdır. Reaksiya nəticəsində sintez edilmiş kompleksin çıxımı 95% təşkil etmişdir. Alınmış kompleksin quruluşu infraqırmızı (IQ) və nüvə maqnit rezonansı (NMR) analiz üsulları vasitəsilə təhlil edilmişdir. Birləşmənin 30%-li izopropil spirtində 20%-li məhlulu hazırlanmış və müəyyən qatılıqlarda

(500 və 1000 ppm) CO_2 mühitində korroziyadan mühafizə inhibitoru kimi xassələri öyrənilmişdir. Korroziya ölçmələri həm inhibitorsuz, həm də inhibitorlu mühitlərdə təyin olunmuşdur. Alınmış nəticələr aşağıdakı cədvəldə təqdim edilmişdir.

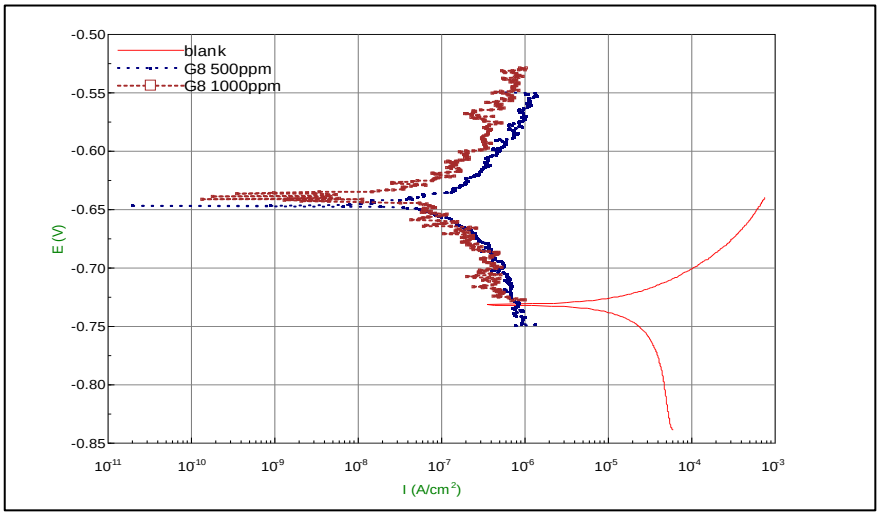
Cədvəl 1. 2-aminopiridinin olein turşusu ilə kompleksinin korroziyaya qarşı inhibitor təsirinin nəticələri

Sintez olunmuş reagent	Qatılıq, ppm	E_{cor}, mV	$İ_{cor}$, A/sm^2	Korroziya sürəti, mm/a	Mühafizə effekti, %
İnhibitorsuz	-	-731	5.7594×10^{-5}	0.67565	-
2-aminpiridin oleinat kompleksi	500	-641	2.2928×10^{-7}	0.00269	99.6
	1000	-640	2.5979×10^{-9}	0.00003	99.9

Cədvəl 1-in təhlilindən aydın olur ki, 2-aminopiridinin oleinat kompleksi yüksək inhibitor effektivliyi göstərmişdir. Kompleksin 500 ppm qatılıqda istifadəsi nəticəsində korroziya sürəti 0.67565 mm/a-dan 0.00269 mm/a-ya qədər azalmış və mühafizə effekti 99.6% təşkil etmişdir. İnhibitorun miqdarının 1000 ppm-ə qədər artırılması korroziya sürətinin 0.00003 mm/a-ya qədər azalmasına və mühafizə effektinin 99.9%-dək yüksəlməsinə səbəb olmuşdur.

Potensiodinamik polyarizasiya əyriləri elektrokimyəvi üsulla CORRTEST CS Studio6 Version 1.0 potensiometri vasitəsilə qeydə alınmışdır. Ölçmələr potensialın gərginlikdən asılılığını müəyyən edir. Polyarizasiya əyriləri korroziya potensialına nəzərən (Ecorr.) -10 V-dan +10 V-a qədər olan intervalda, sabit 0.5 mV/s sürətlə qeydə alınmışdır. İnhibitorunun müxtəlif qatılıqlarında potensiodinamik polarizasiya əyriləri, inhibitorun iştirakı ilə və iştirakı olmadan, karbon qazı ilə doydurulmuş 1%-li NaCl məhlulunda C1018 markalı polad üçün tərtib edilmişdir.

Potensiodinamik polyarizasiya əyrilərinin təhlili göstərir ki, inhibitorun 500 və 1000 ppm qatılıqlarda elektrolit mühitinə əlavə edilməsi həm anod, həm də katod reaksiyalarının kinetikasının əhəmiyyətli dərəcədə ləngiməsinə səbəb olur. Bu hal polyarizasiya əyrilərinin müvafiq anod və katod sahələrində cərəyan sıxlığının azalması ilə müşahidə edilir. İnhibitorsuz sistemlə müqayisədə korroziya potensialının (Ecorr) müsbət istiqamətdə dəyişməsi inhibitorun təsiri nəticəsində korroziya prosesinin intensivliyinin azalmasını təsdiqləyir. Beləliklə, aparılmış potensiodinamik polyarizasiya analizlərinin nəticələrinə əsasən müəyyən edilmişdir ki, tədqiq olunan inhibitor CO_2 ilə doyurulmuş 1%-li NaCl məhlulunda C1018 markalı polad üçün qarışıq tipli korroziya inhibitoru kimi yüksək effektivliyə malikdir.



Şəkil 1. 2-aminopiridinin oleat kompleksinin müxtəlif qatılıqlarda poliarizasiya əyriləri

Nəticə

1. 2-aminopiridinin olein turşusu ilə kompleksi sintez edilmiş, onun kimyəvi quruluşu infraqırmızı (İQ) və nüvə maqnit rezonansı (NMR) spektroskopiyası üsulları ilə təsdiq edilmişdir.
2. Alınmış kompleksin 30%-li izopropil spirtində 20%-li məhlulu hazırlanaraq müxtəlif qatılıqlarda (500 və 1000ppm) korroziyadan mühafizə effekti öyrənilmişdir.
3. Müəyyən edilmişdir ki, inhibitor 500ppm qatılıqda korroziya sürətini kəskin azaldaraq 99.6%, 1000ppm qatılıqda isə 99.8% mühafizə effekti göstərərək korroziya prosesinin əhəmiyyətli dərəcədə azalmasına səbəb olmuşdur.

Ədəbiyyat

1. Abbasov, V. M. (2023). *Korroziya* (II nəşr). Baku: Elm.
2. Talibov, A. G., Alieva, L. I., Mamedova, T. A., Abbasov, V. M., Kerimova, N. G., & Hajiyeva, S. Ya. (2009). Mixture of N-alkylpiperidines and nitroalcohol ether as oil-soluble corrosion inhibitors. *Processes of Petrochemistry and Oil Refining*, (10, 3–4), 249–251.
3. Kuznetsov, Yu. I., Avdeev, Y. G., & Frolova, L. V. (2013). Inhibitor protection of metals in acidic media. *Chemical Technology*, (9), 19–21.
4. Gómez, B., Likhanova, N. V., Domínguez Aguilar, M. A., & Olivares, O. (2005). Theoretical study of a new group of corrosion inhibitors. *Journal of Physical Chemistry A*, 109(39), 8950–8957.
5. Semenova, I. V., Florianovich, G. M., & Khoroshilov, A. V. (2006). *Corrosion and corrosion protection*. Moscow: Physiatelit.
6. Sharma, S. K. (2011). *Green corrosion chemistry and engineering: Opportunities and challenges*. Wiley. https://doi.org/10.1002/9783527641789
7. Aejitha, S., Kasthuri, P. K., Geethamani, P., & Aejitha, S. (2014). Inhibitory action of *Acalypha indica* extract on corrosion of mild steel in hydrochloric acid medium. *Chemical Science Review and Letters*, 2(7), 566–573.

SYNTHESIS AND IR SPECTROSCOPIC STUDY OF A Cu(II) COMPLEX WITH A NITROGEN- AND SULFUR-DONOR HETEROCYCLIC LIGAND

Bayim Isakova, Afsun Sujayev, Nazar Nazarov, Mir Ali Isakov
Ministry of Science and Education of the Republic of Azerbaijan
Institute of Chemistry
Baku, Azerbaijan
beyimibrahimova12@gmail.com
mirali.isakov.e@gmail.com

Abstract - In this study, a new coordination compound was synthesized through the reaction of the ethyl 6-ethoxy-4-methyl-2-thioxo-1,2,3,4-tetrahydropyrimidine-5-carboxylate ligand with cobalt (II) fluoride (CoF_2). The reaction was conducted in an ethanol medium at room temperature, yielding the tetrakis(6-ethoxy-5-(ethoxycarbonyl)-2-mercapto-4-methyl-3,4-dihydropyrimidin-1(2H)-yl) cobalt complex in crystalline form. The structural characteristics and the coordination of functional groups to the metal center were identified and confirmed using FT-IR spectroscopy. Key absorption bands, including O-H, N-H, C-N, and C-O groups, were analyzed to verify the metal-ligand interaction. The synthesized complex is predicted to exhibit potent inhibitory activity against hCA I, hCA II, and *α*-glucosidase enzymes, providing a structural foundation for its potential application as a next-generation antidiabetic therapeutic agent.

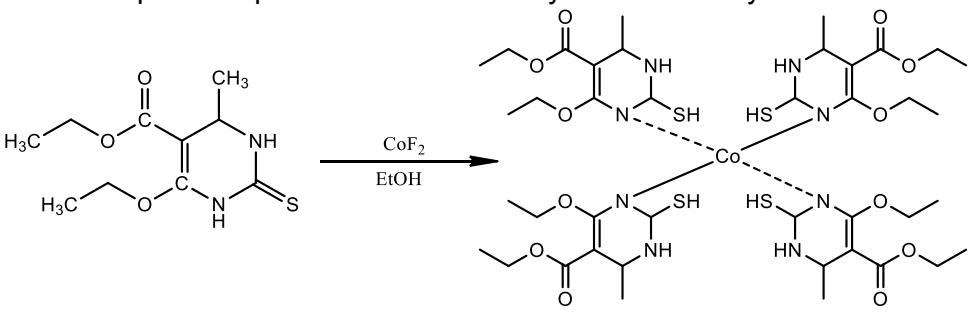
Keywords: Heterocyclic compounds, cobalt (II) fluoride, FT-IR spectroscopy

Introduction

In modern heterocyclic chemistry, the synthesis of nitrogen-containing organic compounds and the investigation of their physicochemical properties are considered one of the priority research directions. The growing interest in this field is directly related to the expanding application potential of these compounds in strategic areas such as medicine, technological processes, industrial production, and agriculture. In particular, pyrazole- and pyrimidine-based ligands are distinguished by their specific biochemical activity and their ability to form stable complexes with metal ions [1] [B.İbrahimova, 2023, 105-106]. As a continuation of this research direction, a new coordination compound of ethyl 6-ethoxy-4-methyl-2-thioxo-1,2,3,4-tetrahydropyrimidine-5-carboxylate ligand with cobalt(II) fluoride (CoF_2) was synthesized. As a result of the reaction, the structure of the obtained tetrakis(6-ethoxy-5-(ethoxycarbonyl)-2-mercapto-4-methyl-3,4-dihydropyrimidin-1(2H)-yl)cobalt complex and the interaction of its functional groups with the metal center were identified by FT-IR spectroscopy.It is anticipated that such synthesized cobalt complexes may potentially exhibit inhibitory activity against enzymes of significant importance in modern medicine, such as carbonic anhydrase (hCA I and II) and *α*-glucosidase. This creates a foundation for further investigation of these compounds as prospective new-generation therapeutic agents for the treatment of metabolic disorders, including diabetes mellitus [2] [I.Mahmudov,2024, 138205].

Experimental section

Cobalt(II) fluoride was added to the ligand previously dissolved completely in ethanol under constant stirring conditions. In order to ensure effective and homogeneous interaction of the reagents, the reaction mixture was continuously stirred for one hour at a controlled temperature. After stirring, the solution was left to stand at room temperature for a certain period, during which crystal growth was observed. As a result, the corresponding metal–complex compound was successfully obtained in crystalline form.



Scheme 1. Synthesis of tetrakis(6-ethoxy-5-(ethoxycarbonyl)-2-mercapto-4-methyl-3,4-dihydropyrimidin-1(2H)-yl) cobalt

Result and Discussion

The structure of the synthesized metal complex was characterized by FT-IR spectroscopy.

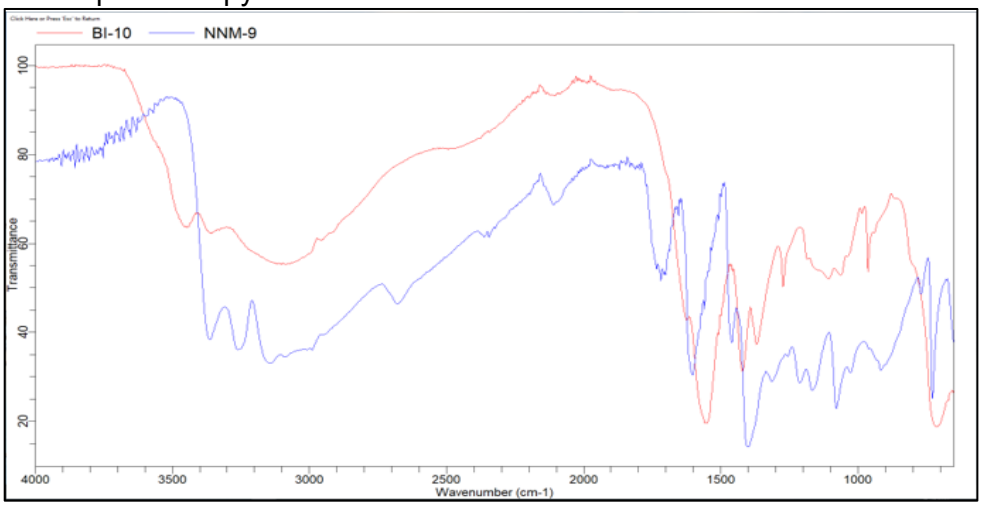


Figure 1. The FT-IR spectrum of the synthesized product was recorded on an Agilent spectrometer.

The FT-IR spectra reveal several characteristic absorption bands: the O-H group is observed in the range of 3455–3714 cm^{-1}, the N-H amine group at 3358 cm^{-1}, and the absorption band at 713 cm^{-1} is attributed to the aromatic C-H out-of-plane bending vibrations of the pyrimidine

scaffold.Furthermore, the C-N (carbon-nitrogen) bond appears at 1272 cm^{-1}, while the C=C double bond within cyclic compounds is identified at 963 cm^{-1}. The C-O (carbon-oxygen) bond characteristic of ethers is recorded at 1183 cm^{-1}.

The shifts observed in the absorption bands of the primary functional groups in the FT-IR spectra confirm the coordination of the ligand to the metal center; the subsequent stages of the research are currently ongoing.

References

1. Bəyim İbrahimova, İbadulla Mahmudov, Yusif Abdullayev, Əfsun Sucayev, Gülgün Babalı Zn-liqand kompleksinin sintezi və bioloji fəallığının tədqiqi, Ümummilli Lider Heydər Əliyevin anadan almasının 100-cü il dönümünə həsr olunmuş Gənc Tədqiqatçıların VII Beynəlxalq Elmi Konfransı Bakı Mühəndislik Universiteti, 28-29 Aprel 2023.
2. I. Mahmudov, B. Ibrahimova, A. Sujayev et. al., Synthesis, characterization, crystal structure, molecular docking, and biological studies of Cu, Ni and Co metal complexes of pyrazole, Journal of Molecular Structure, 2024, 138205.

SYNTHESIS OF AN OPTICALLY TRANSPARENT COPOLYMER BASED ON N-VINYLCARBAZOLE AND METHYL METHACRYLATE

Seide Mamedli[a], Huseyn Nuriyev[b], Samira Mustafayeva[a], Gulshan Novruzova[a]
[a]Institute of Polymer Materials of the Ministry of Science and Education of the Republic of Azerbaijan
Sumgait, Azerbaijan
[b]Azerbaijan State Oil Industry University
Baku, Azerbaijan
*e-mail: ipoma@science.az

The radical binary copolymerization of N-vinylcarbazole with methyl methacrylate has been carried out, the composition and structure of the synthesized copolymer have been determined and its physical-mechanical properties have been studied. The optical transparency (n_D^{20} =1.5521) of the synthesized copolymer has been determined and its thermal stability has been studied. It has been established that the mass loss at 300°C is ~6-7%. It has been revealed that the copolymer has a sufficiently high optical transparency and thermal stability.

Key words: copolymer, optical transparency, methyl methacrylate, V-vinylcarbazole

One of the modern areas of development in the chemical industry is the creation of optically transparent materials. Optically transparent materials are made from polymers with a high refractive index, such as polymethylmethacrylate (PMMA), polystyrene (PS), polycarbonates and their derivatives [1-3]. Currently, a promising approach to the creation of such materials is the synthesis of polymers with complex properties such as high thermal resistance, strength, good adhesion, etc. Optically transparent materials with these properties are produced by copolymerization of main

methyl methacrylate with other monomers by introduction of various functional groups.

In this work, the radical copolymerization of N-vinylcarbazole (VC) with methyl methacrylate (MMA) has been carried out for the synthesis of a new generation of thermostable optically transparent polymer materials. The properties of optical transparency and thermal stability of the obtained copolymer have been determined.

Poly-N-vinyl carbazole (PVC) has a high refractive index n_D^{20} = 1.6830) [4-5]. The bulk carbazole groups give this polymer a relatively high temperature resistance, which is higher than that of PMMA and PS. PVC has chemical resistance and hydrophobicity (water absorption does not exceed 0,1%). However, it is also characterized by increased brittleness, with impact strength value in the range of 2-4 kcal·m^2.

The initial materials – MMA have been purified by repeated distillation, and VC – by recrystallization.

The radical copolymerization of VC and MMA has been carried out in solution at 70°C for 6-7 h in sealed ampoules in the presence of benzoyl peroxide initiator. The benzene has been used as the solvent. The obtained copolymer has been precipitated in methanol three times to separate from the solvent. The precipitate was washed thoroughly with methanol, first at room temperature for one day, then dried in vacuum at 40°C to constant weight.

The copolymer of VC with MMA is a transparent solid mass. It is highly soluble in acetone, chloroform and CCl_4.

The structure of the obtained copolymer has been determined using an IR spectral analyzer, and its composition – by elemental analysis.

The IR spectrum of the copolymer of VC with MMA has the following absorption bands: deformation (1384, 1452 cm^{-1}) and valence (2871, 2931, 2956 cm^{-1}) peaks of C–H bond belonging to CH_2 and CH_3 groups; deformation (741, 843 cm^{-1}) peaks of C–H bond belonging to the benzene ring; C–O (1143 cm^{-1}) and valence (1722 cm^{-1}) peaks of C=O bond belonging to the ester group; valence (1238 cm^{-1}) peak of C–H bond (Fig.1). The absorption bands characteristic for the vinyl group (1630-1635 cm^{-1}) are not detected in the IR spectrum.

The link composition of the copolymer was determined experimentally based on the content of the element N in VC. The opening of the vinyl group in VK and MMA monomers allows the copolymerization reaction to take place.

The optical transparency of the copolymer of VC with MMA was determined using an Anton Paar Abbemat 200 device (n_D^{20} = 1.5521).

For study of the heat-physical properties of the copolymer VC with MMA, its TQA curves were plotted. It has been determined that the temperature resistance of the copolymer is quite high. During thermal destruction, the mass loss of this copolymer at 300 °C was ~7-8%.

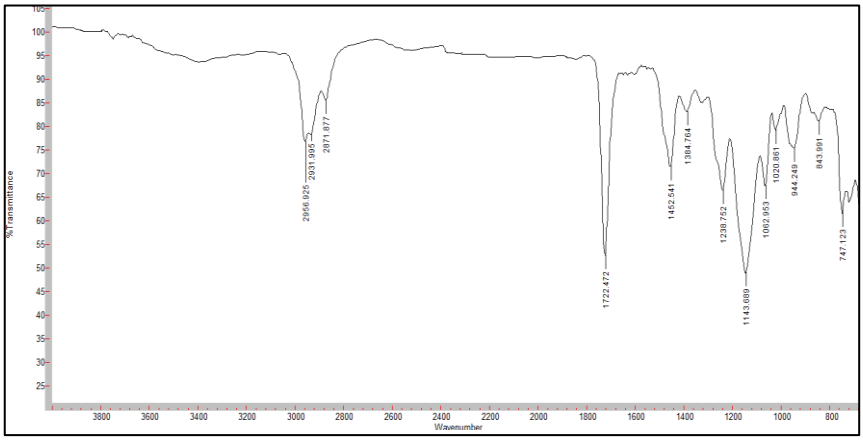
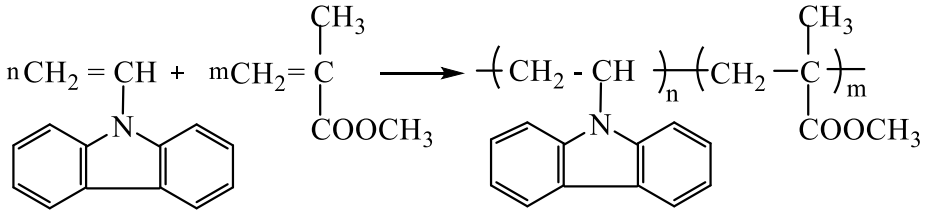


Fig 1. IR spectrum of copolymer VC with MMA

The structure of the copolymer of VK with MMA is given in the scheme:



Thus, it becomes clear from our investigations that besides optical transparency and thermal stability, the copolymer also has good strength properties. The synthesized copolymer has the prospect of being used in detail preparation in micro- and optoelectronics.

References

1. Chandrinos A.A. Review of Polymers and Plastic High Index Optical Materials. *Journal of Materials Science Research and Reviews.* 2021, vol. 7, no. 4, pp. 1-14.
2. Morales-Masis M., De Wolf S., Woods-Robinson R., Ager J. W., Ballif C. Transparent Electrodes for Efficient Optoelectronics // *Advanced Electronic Materials.* 2017, vol. *3, no.* 5, 1600529. https://doi.org/10.1002/aelm.201600529
3. Liu H., Zhai L., Bai L., He M., Wang C. et al. Synthesis and characterization of optically transparent semi-aromatic polyimide films with low fluorine content, *Polymer*. 2019, vol. 163. pp. 106-114. https://doi.org/10.1016/j.polymer. 2018.12.045
4. Tameev A.R., Lypenko D.A., Vannikov A.V., Nikitenko V.R. Transition electroluminescence and anomalous dispersion of charge carriers in thin polymer films // Physics of the solid state. 2009, vol. 51, pp. 1954-1960. https://doi.org/10.1134/S1063783409090315
5. Ghosh D., Sardar P.S., Biswas M., Mondal A., Mukherjee N. Dielectric characteristics of poly(N-vinylcarbazole) and its nanocomposites with ZnO and acetylene black //*Materials Chemistry and Physics.* 2010, vol. 123, pp. 9-12. https://doi.org/10.1016/j.matchemphys.2010.04.019

SYTHESIS AND CHARACTERIZATION OF BIODEGRADABLE GREASES DERIVED FROM SONFLOWER AND CORN OILS MODIFIED WITH CuO NANOPARTICLES

Sabina Garayeva, Aydan Baghirova
Chemical Engineering Department, Baku Higher Oil School
Baku Azerbaijan
sabina.garayeva.std@bhos.edu.az; aydan.z.baghirova.std@bhos.edu.az

Supervisor: Azar Salimov, PhD, Associate Professor

Abstract - The production of more sustainable and biologically clean greases is now needed to lessen the damage that petroleum-based greases due to the environment.It is not enough for the synthesized oil to merely reduce the harm it causes to the environment; it is also important because it possesses physical and chemical properties that can at least compete with those of petroleum-based greases. In the research work conducted for this purpose, from sunflower and corn oils, which are biodegradable and do not form harmful residues upon decomposition, their separate epoxidation and sulfurization in the appropriate order were first carried out, and then a second modification with tert-butyl was performed. Then, copper acetate nanoparticles were added to the system in amounts of 3, 5, 7%. During the process, acetic acid was separated. This was observed in the IR spectral analysis. As a result, the grease changed its color and took a color close to dark green. As a result of the research, it was determined that the biodegradation of the obtained ideal grease is 86%, the dropping point temperature is 125 degrees Celsius, its penetration is 210, the weld index is 979 Is, the critical load is 1380 Pk,N, the wear diameter is 0.55 Dmm, and it is resistant to corrosion [1].

Keywords: biodegradable, grease, nanoparticle, green chemistry, sustainability, tert-butyl, sulfurization, epoxidation

Introduction

Growing concerns about climate change have led to the development of non-toxic, biodegradable, and bio-based grease over the last 30 years. These greases include vegetable oils, which are a good substitute for mineral oils due to their higher viscosity index, anticorrosion properties, and lower toxicity. Vegetable oils are made up of triglycerides of fatty acids, and the composition of these acids affects the oils' tribological properties. Polyunsaturated fatty acids (PUFAs) are more prone to oxidation and polymerization because of their double and triple bonds. Triacylglycerols (TAGs) have polar bonds that act as active centers and are sensitive to autooxidation. This also applies to free fatty acids (FFAs). Grease with improved qualities can be created by functionalizing PUFA double bonds. This study focuses on sulfurizing vegetable oils with elemental sulfur and modifying oxidized vegetable oils with tert-butylurea to produce advanced bio greases [3][5]. The ideal nanoparticle content was established by analyzing the physicochemical characteristics following the addition of copper nanoparticles [2].

Experiment

In the first step the corn oil is added to a three-necked flask and heated between 125 and 135 ℃, while continuously stirring. During stirring, sulfur is added to the oil, and process is continued until the temperature reach 165℃ with temperature increase of 10-30 ℃ per hour. In this form, after stirring for one hour ,5 weight percent calcium oxide is added as a catalyst and stirred in this form for approximately a few hours, thus the sulfurization process begins [1].

As a second sample, sunflower oil is taken, and 30% hydrogen peroxide with an appropriate molar ratio of 1.15 to 1.3 is added portion by portion to the flask and stirred continuously. Currently the temperature is raised to 90-95 ℃, and the process continues for 1-2 hours. During the process, oxygen is supplied to the system via a compressor [1][4].

Considering the amount of epoxide and disulfide groups formed during oxidation and sulfurization in vegetables oils, tert-butyl carbamide is added portion by portion to the reaction mixture in a one-to-one ratio, and the reaction is carried out in 150-160℃ with intensive stirring for a period of 2-3 hours [1][3].

During the synthesis of grease, Ca $(OH)_2$ as well as T-1500 and T-46 oils were added to the system. Also, copper acetate nanoparticles were added at mass concentration of 3% ,5% and 7% at a temperature range of 150 - 180 ℃. During the reaction copper acetate decompose under the influence of temperature, resulting in the release of acetic acid [1].

Some physicochemical and tribological properties of the grease samples were measured and reflected in the diagram below.

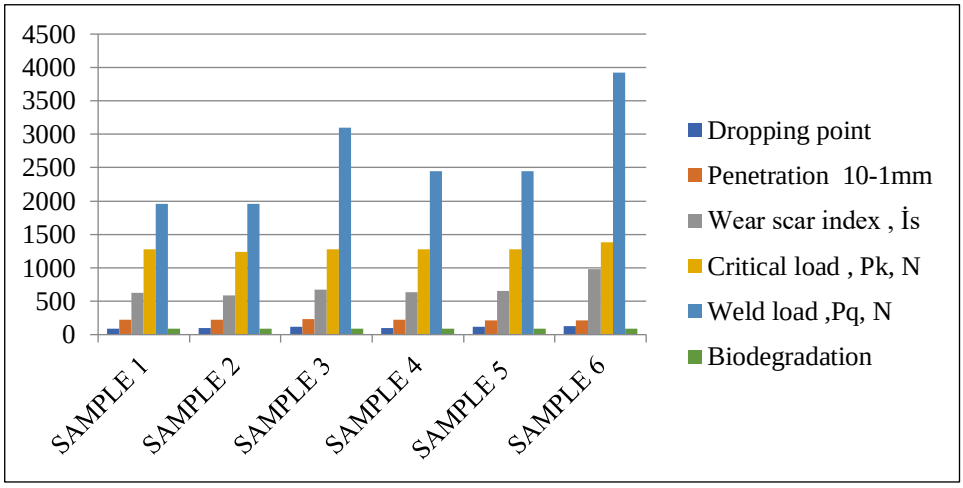


Figure 1. Properties of sample greases

Results and discussions

The production of bio grease from vegetable oils produced several noteworthy scientific findings:

For the sulfurization, oxidation, and tert-butyl carbamate treatment of sunflower and corn oils, the ideal reaction conditions were identified. These modified vegetable oils were used as a dispersed phase in a mineral oil medium to create general-purpose greases with low toxicity, good tribological qualities, a high dropping point, and high oxidation resistance. Grease made from sulfurized vegetable oils has been shown to have better anti-wear and anti-scuffing qualities than its oxidized counterparts. The best performance was obtained with a grease based on sulfurized corn oil modified with tert-butyl carbamate (dropping point = 125 °C, wear scar diameter = 0.55 mm). The ideal content of nano-copper and copper oxide was 5 weight percent. Every sample showed more than 85% biodegradation. "Sample 6" is the best sample. Sample 6's ideal parameters include a dropping point of 125 °C, a scuffing index (Is) of 979, a critical load (Pk) of 1380 N, a welding load (Pq) of 3920 N, a wear scar diameter of 0.55 mm, an 86% biodegradation rate, and corrosion resistance [1].

Suggestion

The study's findings have led to the development of a high-tech "green" oil that is highly desirable to Azerbaijan's oil-gas and self-saving industries: 86% biodegradable cow oil made from indigenous plant oils. This product's competitiveness with mineral oils under heavy industrial conditions is fully confirmed by the indicators of 0.55 mm bending diameter and 1380 N critical load that were made possible by the misacetate nanoparticles. The environmentally friendly method reduces the possibility of infiltration during Caspian Sea excavation projects and enables a 30-40% reduction in yeast value based on local raw materials. Specifically, prepared and processed bio-foil oil is an alternative approach that removes reliance on technology in line with our nation's "green economy" goals [1].

References

1. Qarayeva S.E., “Nanohissəcikli ümumi təyinatlı plastik sürtkünün alınması”,Bakalavr buraxılış işi, BDU,2025.
2. Səfərova L.İ.,“Yerli xammal əsasında bəzi plastik sürtkülərin alınma texnologiyası”,diss. BDU, 2024, s.36-68.
3. Padmasiri K., J. Natn, “Gamage Epoxidation of some vegetable oils and their hydrolysed products with peroxyformic acid -optimised to industrial”,Sci. Foundation Sri Lanka, Vol. 37, No 4,2009, s 229-240.
4. Kumar D. Ti, “SiO2 as a Nanosized Solid Catalyst for the Epoxidation of Fatty Acid Methyl Esters and Triglycerides”, Vol. 5, No 26,2021, s 29532961.
5. Nadia Salih, Jumat Salimon, “A Review on Eco-Friendly Green Biolubricants from Renewable and Sustainable Plant Oil Sources,Biointerface Research in Applied Chemistry”, 5, 2021, s. 13316-13317.

СИНТЕЗ ОПТИЧЕСКИ ПРОЗРАЧНОГО СОПОЛИМЕРА НА ОСНОВЕ N-ВИНИЛКАРБАЗОЛА И БУТИЛМЕТАКРИЛАТА

Саида Мамедли[a], Рауф Джаббарбейли[b], Шабнам Гараева[a], Фарида Юсифли[a]
[b]Сумгаитский Государственный Университет
Сумгайыт, АЗЕРБАЙДЖАН
[b]Азербайджанский Государственный Университет Нефти и Промышленности
Баку, АЗЕРБАЙДЖАН
*e-mail: ipoma@science.az

Была проведена сополимеризация N-винилкарбазола со бутилметакрилатом. Изучены закономерности проведенного сополимеризации в растворе, состав и структура синтезированного сополимера. Методом Фейнемана – Росса вычислен констант сополимеризации (r_1=0.05, r_2=2.2). Выявлена характеристическая вязкость сополимера ([η] = 1,13 дл/г). Было установлено, что бутилметакрилат является более активным мономером, чем N-винилкарбазол, в исследуемой реакции. Полученный сополимер N-винилкарбазола со бутилметакрилатом имеет высокий показатель светопреломления (n_D^{20} =1.5410).

Ключевые слова: N-винилкарбазол, бутилметакрилат, сополимеризация, светопропускания.

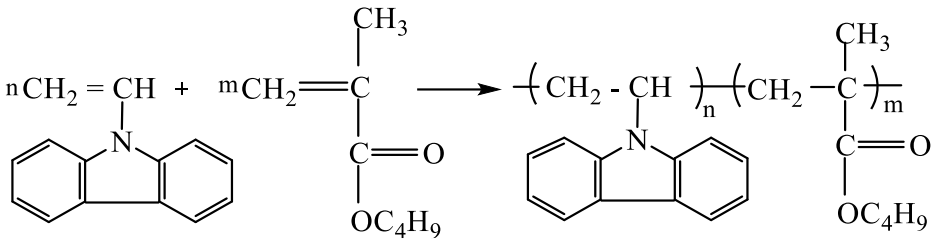
На сегодняшний день является очень актуальным синтез полимеров с оптическими свойствами. Органическое стекло — название полимерных материалов, которые готовятся на основе органических полимеров, таких как полиметилметакрилат (ПММА), полимеры аллиловых соединений, поликарбонаты (ПК), полистирол (ПС) и другие [1-3]. Прозрачные полимерные материалы очень широко используются в оптоэлектронике, оптической промышленности, светотехнике, в качестве прозрачных конструкционных материалов и других областях.

В представленной работе мы синтезировали сополимер N-винилкарбазола (ВК) с бутилметакрилатом (БМА). Были определены состав и структура нового сополимера, значения константы сополимеризации, а также показатели оптической прозрачности.

Радикальную сополимеризацию проводили в ампулах с различными молярными соотношениями ВК и БМА в присутствии инициатора бензоил пероксида, в термостате, при температуре 70-80ºС в течение 4 часов.

Сополимер ВК-со-БМА осаждали этанолом, промывали и растворяли в бензоле, а затем очищали повторным осаждением в этаноле. Выделенный полимер сначала сушили при комнатной температуре, а затем в вакуумной камере при 35-40 ºС. После сушки определяли его массу.

Структуру сополимера ВК-со-БМА можно представить по следующей схеме:



ИК-спектральный анализ сополимера показал наличие следующих полос поглощения: деформационные (1386, 1447 $см^{-1}$) и валентные (2949 $см^{-1}$) колебания С–Н связи CH_2 и CH_3 групп; деформационные (750, 843, 879 $см^{-1}$) колебания С–Н связи бензольного кольца; валентные (1144, 1188 $см^{-1}$) колебания С–О связи сложного эфира; валентные (1723 $см^{-1}$) колебания С=О связи сложного эфира; валентные (1240 $см^{-1}$) колебания С–N связи. Нужно заметит, что не наблюдаются полосы поглощения, в области 1630-1635 $см^{-1}$, характерные для винильной группы (рис. 1).

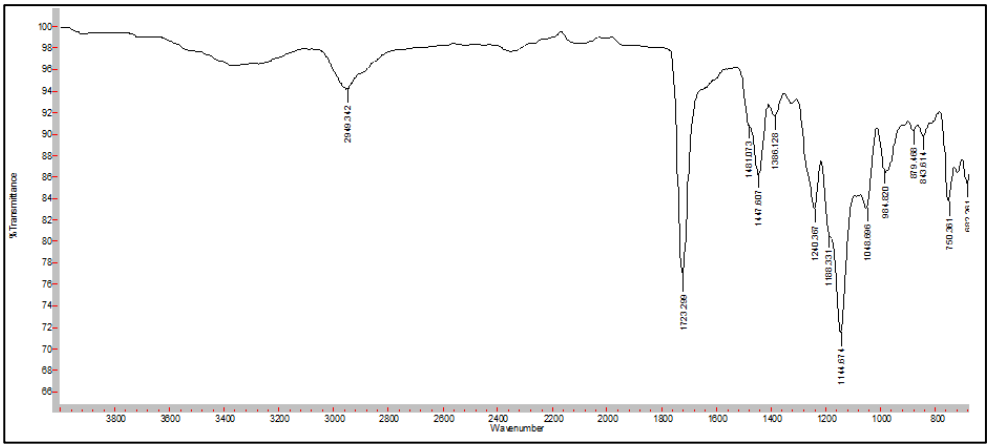


Рисунок 1. ИК-спектр сополимера N-винилкарбазола со бутилметакрилатом

Характериктическую вязкость сополимера ВК-со- БМА определяли в растворе бензола при 21°С с помощью вискозиметра Оствальда (табл. 1). Для сополимера ВК-со-БМА [η] = 1,13 дл/г. Вязкость определяли для сополимера ВК-со-БМА с содержанием ВК – 24.70 и БМА – 75.30 мол.%.

Константы сополимеризации мономеров ВК (M_1) и БМА (M_2) были определены методом Фейнемана-Росса (таблица 1). Полученные значения констант сополимеризации r_1 и r_2 ($r_1<r_2$) указывают на то, что мономер M_1 проявляет более низкую активность в радикальной сополимеризации, чем мономер M_2, и это различие обусловлено химической природой и активностью молекул в мономерах M_1 и M_2.

Исходной смеси мономеров осуществлена сополимеризация при различных соотношениях исходных мономеров. На основании результатов химического определения функциональных групп, были вычислены соотношения мономерных единиц в макромолекуле сополимеров, полученных на малых глубинах превращения (до 10%)

Таблица 1. Влияние условий сополимеризации на выход и состав сополимеров на основе мономеров ВК (M_1) и БМА (M_2). Растворитель – бензол, инициатор – ДАК, температура 70-80°С)

Состав исходной смеси мономеров, мол, %		Конверсия, %	Состав сополимеров, мол, %		r_1	r_2	[η], дл/г
$[M_1]$	$[M_2]$		$[m_1]$	$[m_2]$			
10	90	8.2	4.61	95.39	0.05	2.2	1.13
25	75	7.3	25.25	74.75			
50	50	9.6	24.70	75.30			
75	25	8.7	39.87	60.13			
90	10	7.2	53.82	46.18			

Увеличение количества ВК в исходной смеси в диапазоне 10–90 мол. % приводит к увеличению мол. % групп карбазольного типа в составе сополимеров до ~4,61–53,82 мол. %.

С помощью прибора Абемат 200 была устоновлена оптическая прозрачность сополимера (n_D^{20} = 1.5410).

Изменяя в исходной смеси молярное соотношение ВК и ВМА, можно в значительной степени изменить состав синтезированной макромолекулы. С увеличением фрагмента m_1 в сополимере ВК-со-ВМА возрастает его термостойкие свойства, а увеличивая фрагмент m_2 возрастает светопреломление полимера.

Полученный сополимер ВК-со-ВМА обладает достаточно высокой оптической прозрачностью. Полимер может быть использован в производстве нужных деталей в оптике, микро- и оптоэлектронике.

Список литературы

1. S.B.Mamedli, Q.Q.Mirguseinov, A.H.Rahimli, R.A.Akhmedova, Ch.H.İsmayılova. Preparation of optical transparent composites on the basis of butyl methacrylate with α-methyl styrene. Azerbaijan chemical journal. Baku. 2022. №1. pp. 34-40. https://doi.org/10.32737/0005-2531-2022-1-34-40
2. A. Kurt və M. Koca, “Poli(metil metakrilatın) poli(1,3-difenil-1H-pirazol-5-il metakrilatla qarışdırılması: Onun optik xüsusiyyətlərinin tədqiqi”. *ADYU J Sci.* 2022. cild 12. № 2. səh. 177–192. https://doi.org/10.37094/adyujsci.1110956
3. R-J.Zhou, T.Burkhart. Optical properties of particle-filled polycarbonate, polystyrene, and poly(methyl methacrylate) composites // Journal of Applied Polymer Science. 2010, vol. 115, pp. 1866-1872. https://doi.org/10.1002/app.31331

ARYLAMINE-SUBSTITUTED THIETANES AND FUNCTIONALLY SUBSTITUTED THIIRANES AS ANTIOXIDANTS FOR HYDROCARBON OXIDATION

Irada A. Rzayeva[1], Nazar M. Nazarov[1], Sabir S. Babayev[1], Ibadulla H. Mahmudov[1,2] Camila C.Ahmadova[1]
irada.rzayeva56@gmail.com
1.Institute of Chemistry Ministry of Science and Education Republic of Azerbaijan - AZ 1143, Azerbaijan Republic, city Baku, H.Cavid str.,113
Phone: +994125018593, +994125393871, +9941253397756 Fax: +994125018593
2. Baku Engineering University-Khirdalan city, Hasan Aliyev str. 120 AZ 0101 Absheron, Azerbaijan,
Phone: +994123499966, info@beu.edu.az

The study investigates the antioxidant properties and mechanisms of action of arylamine-substituted thietanes and functionally substituted thiiranes as inhibitors of hydrocarbon oxidation. A series of sulfur-containing three- and four-membered heterocyclic compounds were synthesized and characterized. Their antioxidant activity was studied using cumene oxidation and azobisisobutyronitrile-initiated oxidation.[1,2]. Key parameters, such as the stoichiometric inhibition coefficient (f) and the rate constant of chain termination (k_7), were determined [3,4]. The results show that thietanes, particularly those with electron-donating substituents, exhibit superior antioxidant activity compared with thiiranes and conventional alkylphenolic antioxidants. The compounds also catalytically decompose cumyl hydroperoxide, demonstrating their dual mechanism. These findings indicate the promising potential of arylamine-substituted thietanes as effective additives for fuels and lubricating oils.

Keywords: Arylamine-substituted thietanes; Thiiranes; Antioxidants; Hydrocarbon oxidation; Cumene; Cumyl hydroperoxide; Chain termination; Sulfur-containing heterocycles

Introduction:

The oxidation of petroleum oils and fuels during storage and operation reduces their performance and leads to the formation of harmful peroxides and sediments. The development of effective antioxidants is therefore critical to enhance the oxidative stability of hydrocarbons. Small sulfur-containing heterocycles, such as thietanes and thiiranes, have shown potential as chain-breaking antioxidants due to their ability to react with peroxyl radicals and decompose hydroperoxides.This study aims to synthesize a series of arylamine-substituted thietanes and functionally substituted thiiranes, characterize their structures, and evaluate their antioxidant activity. The relationship between molecular structure, substituents, and antioxidant efficiency is investigated to identify the most promising compounds for application in fuels and lubricating oils.

Experimental Part:

A series of sulfur-containing heterocycles, including three-membered thiiranes and four-membered thietanes, was synthesized using standard cyclization and substitution reactions. Arylamine groups with varying

electron-donating and electron-withdrawing substituents were introduced to study structure-activity relationships. The synthesized compounds were purified and characterized by NMR, IR spectroscopy, and elemental analysis.

Results and Discussion:

Antioxidant Efficiency**:** All tested compounds reacted with cumyl peroxyl radicals and effectively inhibited oxidation. Thietanes with electron-donating substituents in the aromatic ring showed the highest activity, outperforming alkylphenolic antioxidants. Structure-Activity Relationship: The four-membered thietane ring and divalent sulfur atom were identified as key factors for high antioxidant activity. Electron-withdrawing substituents and carboxyl groups reduced efficiency. Thiiranes were less effective than thietanes under the same conditions.Catalytic Hydroperoxide Decomposition**:** The compounds catalytically decomposed cumyl hydroperoxide in a three-stage process: induction, autocatalytic decomposition, and final stage. Transformation products also exhibited secondary inhibitory activity.Combined Mechanism of Action**:** The compounds act both as chain-breaking antioxidants and hydroperoxide decomposers, indicating dual functionality, which is advantageous for fuel and lubricant stabilization.

Structural features and substituents, making them promising additives for hydrocarbon systems. Their Conclusion: Arylamine-substituted thietanes exhibit high antioxidant activity due to their dual mechanism of action distinguishes them from conventional antioxidants and suggests potential industrial applications.

References:

1. Farzaliyev V.M.,Rzayeva I.A. et.al. Theses of the articles of the republican sciehtific conference on “Lubricants,fuels,special fluids, additives and reagents’ delicated to the 50th anniversary of the institute of Additives Chemistry named after Academician A.Guliyev. Baku, !3-14 October 2015, p.29.
2. Denisov E.T., Kharitonov V.V.,Fedorova V.V. Method of transformation of kinetic curves as a way to assess the effectiveness of oxidation inhibitors. Preprint. Blackhead.1973.
3. Emmanuel N.M., Denisov E.T. Chain reactions of oxidation of hydrocarbons in the liquid phase. Petrochemical. 1976, v. 16, no 3, pp.366-382.
4. Sander M. Oxide derivatives of 3 – aryloxythietanes of 3 – aryloxythietanes: Patent 3, 297, 718 USA. Chem. Abstr. 1967, v. 66.

EKOLOJİ TƏMİZ DİZEL YANACAĞININ ALINMASINDA ULTRASƏSLİ KAVİTASİYASININ TƏSİRİ

Təranə Məmmədova, Zümrüd Köçərli
AR Elm və Təhsil Nazirliyi akademik Y.H. Məmmədəliyev adına
Neft-Kimya Prosesləri İnstitutu
Bakı, Azərbaycan
E-mail: zumrud.kocherli@mail.ru

Xülasə - Aparılmış tətdiqat işində dizel yanacağının müasir standartlara uyğun olması üçün oksidləşdirici kükürdsüzləşmə prosesi mərhələli şəkildə həm adi, həm də ultrasəsli kavitasiya şəraitində aparılmışdır. Belə ki, nəticəyə əsasən 1 mərhələdə alınan nəticələrdə kükürdün miqdarı 0,0496% olan dizel fraksiyasının 37%- li hidrogen peroksid və sirkə turşusundan katalizator kimi istifadə etməklə oksidləşdirici kükürdsüzləşmə prosesində kükürdsüzləşmə dərəcəsi 27,8%, ultrasəsli kavitasiya təsirində isə 56,8% təşkil edir. 2 mərhələdə alınan nəticələrdə isə kükürdün miqdarı 0,0214% olan dizel fraksiyasının 37%- li hidrogen peroksid və sirkə turşusundan katalizator kimi istifadə etməklə oksidləşdirici kükürdsüzləşmə prosesində kükürdsüzləşmə dərəcəsi 37,3%, ultrasəsli kavitasiya təsirində isə 94,8% təşkil edir.

Açar sözlər: dizel fraksiyası, oksidləşdirici kükürdsüzləşrmə, hidrogen peroksid, ultrasəsli kavitasiya

Giriş

Son dövrdə bir çox ölkələrdə iqtisadi artım tempinin yüksəlməsi, yeni nəqliyyat dəhlizlərinin və marşrutlarının istismara verilməsi, avtomobil parkının genişlənməsi, eləcə də mühərrik yanacaqlarının istehsal və istehlak həcminin artması qlobal miqyasda müşahidə olunan əsas tendensiyalardandır. Lakin bu dinamika ətraf mühitə antropogen təsirin güclənməsinə və müxtəlif ekoloji problemlərin kəskinləşməsinə səbəb olur. Bu baxımdan, sərt ekoloji normalara cavab verən, aşağı emissiyalı dizel yanacaqlarının istehsalı neft emalı sənayesinin prioritet və aktual istiqamətlərindən biri kimi qalmaqdadır. Hazırda dizel yanacağının keyfiyyət göstəricilərinə dair beynəlxalq standartlar çərçivəsində olduqca ciddi tələblər irəli sürülür. Bu tələblərə əsasən, ilk növbədə yanacağın tərkibində olan kükürdlü birləşmələr, aromatik karbohidrogenlər, həmçinin azot və oksigen tərkibli birləşmələrin miqdarının minimuma endirilməsi və ya tamamilə kənarlaşdırılması zəruridir. Ekoloji baxımdan təhlükəsiz dizel yanacaqlarının əldə olunmasında kükürdsüzləşdirmə prosesləri xüsusi əhəmiyyət kəsb edir. Ənənəvi hidro-kükürdsüzləşdirmə prosesləri, adətən, 350–500°C temperatur intervalında və 3–7 MPa hidrogen təzyiqində həyata keçirilir. Bu isə yüksək enerji sərfi, bahalı katalitik sistemlərin tətbiqi və iri həcmli kapital qoyuluşları tələb edir. Bununla əlaqədar olaraq, yüksək temperatur və yüksək hidrogen təzyiqi olmadan reallaşdırıla bilən oksidləşdirici kükürdsüzləşdirmə prosesi alternativ və perspektiv metod kimi qiymətləndirilir [Rakhmanov E.V., 2014, 49-52]. Sözügedən proses həm ənənəvi şəraitdə, həm də müxtəlif fiziki təsirlərin, o cümlədən ultrasəsli kavitasiya effektinin tətbiqi ilə həyata keçirilə bilər. Ultrasəsli kavitasiya – maye mühitə 20 kHz yüksək tezlikli ultrasəs dalğalarının ötürülməsi nəticə-

sində mikroölçülü kavitasiya qabarcıqlarının yaranması və onların ani partlaması ilə xarakterizə olunan fiziki-kimyəvi hadisədir. Qabarcıqların dağılması zamanı lokal olaraq 1000 K-ə qədər temperatur və 1000 atm-a qədər təzyiq formalaşır ki, bu da kimyəvi reaksiya-ların intensivləşməsinə, molekulyar səviyyədə parçalanma proseslərinin baş verməsinə və reagentlər arasında kütləötürmənin sürətlənməsinə səbəb olur. Ultrasəsli kavitasiya texnologiyası maye sistemlərin homogenləşdirilməsi, qarışdırılması və müxtəlif çevrilmə reaksiyalarının effektivliyinin artırılması məqsədilə geniş tətbiq olunur [Məmmədova, T.A., 2019,72, Мамедова,Т.А., 2019, 11-14]. Neft emalı sənayesində bu metod oksidləşdirici kükürdsüzləş-dirmə prosesində reagentlərin daha səmərəli qarşılıqlı təsirini təmin etməklə reaksiya müddətinin azalmasına və prosesin məhsuldarlığının yüksəlməsinə şərait yaradır.

Təcrübi hissə

Aparılan tədqiqat işində dizel yanacağının oksidləşdirici kükürdsüzləş-dirmə prosesi 37%-li hidrogen peroksid və sirkə turşusundan katalizator kimi istifadə etməklə 80–90°C temperatur intervalında 6 saat müddətində həm ənənəvi şəraitdə, həm də 20 kHz tezlikli ultrasəsli kavitasiya təsiri altında həyata keçirilmişdir. Proses ardıcıl iki mərhələdə təşkil olunmuş və əldə edilən nəticələr müqayisəli şəkildə təhlil edilərək müvafiq cədvəldə təqdim edilmişdir.

Dizel fraksiyasının oksidləşdirici kükürdsüzləşmə prosesində mərhələli şəkildə adi şəraitdə və ultrasəsli kavitasiya təsirində 37%-li hidrogen peroksid və sirkə turşusundan katlizator kimi istifadə etməklə kükürdsüzləşdirmə dərəcəsi

	Qarışıq	İlkin dizel fraksiyasında kükürdün miqdarı %, küt	Təcrübədən sonra kükürdün miqdarı %, küt	Kükürdsüzləşmə dərəcəsi %
I Mərhələ				
1	10% katalizator CH_3COOH / H_2O_2 Dizel fraksiyası adi şəraitdə	0,0496	0,0358	27,8
2	10% katalizator CH_3COOH / H_2O_2 Dizel fraksiyası ultrasəsli kavitasiya təsirində	0,0496	0,0214	56,8
II Mərhələ				
1	10% katalizator CH_3COOH / H_2O_2 Dizel fraksiyası adi şəraitdə	0,0214	0,0134	37,3
2	10% katalizator CH_3COOH / H_2O_2 Dizel fraksiyası ultrasəsli kavitasiya təsirində	0,0214	0,011	94,8

Nəticə

1 mərhələdə alınan nəticələrdə kükürdün miqdarı 0,0496% olan dizel fraksiyasının 37%- li hidrogen peroksid və sirkə turşusundan katalizator kimi istifadə etməklə oksidləşdirici kükürdsüzləşmə prosesində kükürdsüzləşmə dərəcəsi 27,8%, ultrasəsli kavitasiya təsirində isə 56,8% təşkil edir. 2 mərhələdə alınan nəticələrdə isə kükürdün miqdarı 0,0214% olan dizel fraksiyasının 37%- li hidrogen peroksid və sirkə turşusundan katalizator kimi istifadə etməklə oksidləşdirici kükürdsüzləşmə prosesində kükürdsüzləşmə dərəcəsi 37,3%, ultrasəsli kavitasiya təsirində isə 94,8% təşkil edir. Dizel fraksiyasının oksidləşdirici kükürdsüzləşmə prosesində ultrasəsli kavitasiya tətbiq edildikdə əldə olunan nəticələr göstərir ki, yanacaq Avro-5 standartının tələblərinə uyğundur.

ƏDƏBİYYAT

1. Məmmədova, T.A., Köçərli Z.Q., Teyyubov, X.Ş., Həsənova, A.R. Əsgərova E.N. Dizel distillatlarının ultrasəsli kavitasiya təsirində hidrotəmizləmə prosesinin tədqiqi // The İnternational Scientific Conference “Actual Problems of Modern Chemistry” Dedicated to the 90th Anniversary of the Academiician Y.H.Mammadaliyev İPCP , – Baku, Azerbaijan, – 2-4 October, – 2019, – s. 72.
2. Мамедова, Т.А. Использование ультразвука в процессах гидроочистки дизельных топлив / Т.А. Мамедова, Х.Ш. Теюбов, А.Р. Гасанова, С.К. Алиева, З.Г. Кочарли, И.А. Халафова, В.М. Аббасов // Нефтепереработка и нефтехимия, – Москва: – 2019. № 4, – с. 11-14.
3. Rakhmanov E.V., Tarakanova A.V., Valieva T., Akopyan A.V., Litvinova V.V., Mak-simov A.L., Anisimov A.V., Vakarin A.V., Semerikova O.L., Zaikov Yu.P. Oxidative desulfuri-zation of diesel fraction by hydrogen peroxide in the presence of transition metal-based catalysts. Petroleum Chemistry, 2014, *1(54)*, 49-52. DOI: 10.7868/S0028242114010110 (in Russ.).

СИНТЕЗ ФУРИЛЗАМЕЩЁННЫХ *α,β*-НЕНАСЫЩЕННЫХ КЕТОНОВ И ИХ АМИНПРОИЗВОДНЫХ

Т.Р. Сафарова [2], -А.Р.Караева[1,2], М.И.Шатирова[1], Г.М.Мамедова[1]
[1] Министерство науки и образования Азербайджанской Республики Институт полимерных материалов, Сумгаит, AZ5004 Азербайджан
[2] Сумгаитский государственный университет, Сумгаит, AZ5008 Азербайджан
*e-mail: aynur.garayeva@sdu.edu.az

Резюме. В условиях реакции Кондакова электрофильное присоединение хлорангидрида фуранкарбоновой кислоты к хлористому аллилу протекает по правилу Марковникова и приводит к образованию соответствующего 1-фурил-4-хлорбут-2-ен-1-она. Последующее взаимодействие полученного хлорзамещённого непредельного кетона со вторичными аминами приводит к формированию производных кетопропенилирования соответствующих аминов.

Ключевые слова: хлорсодержащий α,β-непредельный кетон, хлорангидрид фуран карбоновой кислоты, аминокетоны

ВВЕДЕНИЕ

Значимость галогенсодержащих непредельных кетонов и аминокетонов в органической химии трудно переоценить. Эти соединения рассматриваются как перспективные объекты для практического применения в различных сферах деятельности человека. Обладая высокой реакционноспособностью, непредельные хлоркетоны и аминокетоны находят широкое применение в органическом синтезе в качестве перспективного синтонов для получения разнообразных ациклических и гетероциклических структур (Поткин, В.И., 2010, Потиха, Л.М., 2020) На их основе разработаны препаративные методы синтеза ряда полезных соединений, включая биологически активные вещества [Hammouda, M.M., 2022, Gadzhili R.A., 2015].

В структуре галогенсодержащих непредельных кетонов присутствуют три функционально активных реакционных центра – карбонильная группа, сопряжённая кратная связь и атом галогена, что обуславливает возможность нуклеофильного взаимодействия как по отдельным центрам, так и по нескольким одновременно. Одновременное влияние этих центров друг на друга приводит к повышенной химической активности данных соединений и открывает широкие возможности для их применения в тонком органическом синтезе [Guo, H. 2021, Zhang, T.S., 2019]. Вследствие доступности исходных реагентов и одностадийного характера процесса, метод получения галогенсодержащих непредельных кетонов посредством ацилирования непредельных соединений хлорангидридами карбоновых кислот сохраняет свою актуальность и в настоящее время, оставаясь одним из перспективных синтетических подходов.

ЭКСПЕРИМЕНТАЛЬНАЯ ЧАСТЬ

Метод синтеза 1-фурил-4-хлорбут-2-ен-1-она (1). К суспензии 28 г (0.2 моль) хлористого алюминия в 60 мл дихлорэтана при постоянном перемешивании по каплям добавляют 0.2 моль хлорангидрида фуранкарбоновой кислоты при температурах -15÷-10°С. Затем при той же температуре в течение 1 часа постепенно прибавляют 18 мл (0.1 моль) аллилхлорида. После окончания прибавления хлористого аллила реакционную массу продолжают интенсивно перемешивать еще 1 час при той же температуре, после чего полученную смесь выливают на ледяную воду. Органической слой отделяют от водного слоя, промывают водой, водный слой экстрагируют эфиром. Эфирные экстракты объединяют, сушат над хлоридом кальция и после отгонки растворителя проводят вакуумную перегонку.

Метод синтеза 1-фурил-4-диалкиламино (морфолино) бут-2-ен-1-онов (2-4).

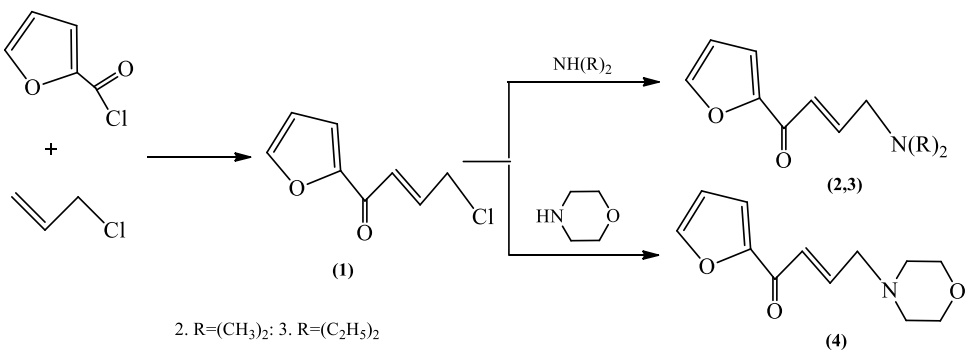
К раствору 0.2 моль соответствующего вторичного амина и 30 мл диэтилового эфира при перемешивании и при температуре 10-15°С по каплям прибавляли 0.1 моля 1-фурил-4-хлорбут-2-ен-1-она **(1)**.

Поддерживая температуру в пределах 20-25°С реакционную смесь перемешивали в течение 3 часов. После охлаждения реакционную смесь промывали водным раствором карбоната натрия, экстрагировали диэтиловым эфиром. Затем органический слой и эфирные вытяжки соединяли и сушили над сульфатом магния. После удаления растворителя остаток подвергали вакуумной перегонке.

РЕЗУЛЬТАТЫ И ОБСУЖДЕНИЕ

Путём ацилирования аллилхлорида хлорангидридом фуранкарбоновой кислоты по Кондакову – Крапивину был синтезирован 1-фурил-4-хлорбут-2-ен-1-он. Установлено, что при повышенных температурах данная реакция не протекает избирательно, а при комнатной температуре сопровождается образованием смолистых побочных продуктов, идентификация которых оказалась затруднительной.

Целью настоящего исследования являлась разработка рациональных синтетических подходов к получению хлорсодержащих непредельных кетонов и соответствующих аминопроизводных. Экспериментально установлено, что ацилирование хлорсодержащих непредельных соединений аллильного типа в присутствии эквимолярного количества хлористого алюминия в среде дихлорэтана при температурах –15–10°С приводит к образованию 1-фурил-4-хлорбут-2-ен-1-она **(1)** с выходом 75%. Реакция кетона **(1)** с двукратным молярным избытком вторичных аминов (диметиламина, диэтиламина, морфолина) в среде диэтилового эфира протекает по механизму нуклеофильного замещения атома хлора на диалкиламиногруппу, что приводит к образованию 1-фурил-4-диалкиламинобут-2-ен-1-онов **(2–4)** с выходами 69–76%. Избыток вторичного амина выполняет роль акцептора хлористого водорода, выделяющегося в протекание реакции, предотвращая подкисление реакционной среды.



Схема

Состав и строение синтезированных соединений **(1-4)** установлены по данным элементного анализа, ИК и ^{1}Н ЯМР спектров. ИК-спектры синтезированных соединений были зарегистрированы на Фурье-

спектрофотометре Protoge-460 в тонком слое в диапазоне 400–4000 $см^{-1}$. Спектры ^1H ЯМР записывали на спектрометре Bruker Avance-300 в растворе $CDCl_3$, химические сдвиги определяли относительно тетраметилсилана (ТМС). Чистоту синтезированных соединений контролировали методом тонкослойной хроматографии (ТСХ) на пластинах Silufol UV-254, в качестве элюентов использовали систему гексан–эфир.

В ИК спектрах синтезированных соединений **(1-4)** наличие фурильного фрагмента подтверждается полосами поглощения в области v=3165–3125 $см^{-1}$ (валентные колебания С–Н гетероароматического кольца), 1685–1645 $см^{-1}$ (колебания С=С фуранового цикла), 1125–1100 $см^{-1}$ (колебания связи С–О–С). В ИК спектре 1-фурил-4-хлорбут-2-ен-1-она (1) кроме полосы поглощение фурильного фрагмента наблюдаются характерные полосы при v=1725 и 1661$см^{-1}$, соответствующие валентным колебаниям карбонильной группы в *s-cis*- и *s-trans*-конформациях. Полосы при 1635 и 971 $см^{-1}$ отнесены к валентным и внеплоскостным деформационным колебаниям двухзамещённой винилной группы с *транс*-конфигурацией. Полоса поглощения при 706 $см^{-1}$, соответствующая колебаниям связи С–Cl, присутствует в ИК спектре исходного хлоркетона и полностью исчезает в спектрах соответствующих аминокетонов, что подтверждает замещение атома хлора диалкиламиногруппой.

В ^1H ЯМР спектрах непредельного кетона и аминокетонов **(1–4)** наблюдаются характерные сигналы фурильного фрагмента в области δ = 6.23–7.35 м.д., соответствующие протонам гетероароматического кольца фурана. В ^1H ЯМР спектре 1-фурил-4-хлор-2-бутен-1-она **(1)** обнаружены сигналы в областях δ, м. д.: 4.19 д (2H, CH_2), 6.20-6.75 м (2H, CH=CH). А в ^1H ЯМР спектрах диалкиламинов **(2-4)**, кроме характерных мультиплетных сигналов протонов CH=CH фрагмента, наблюдаются характерные сигналы протонов диалкиламино и морфолинового заместителей, что полностью согласуется с предполагаемой структурой соединений: 1.88 с [6H, $N(CH_3)_2$] **(2)**, 1.87 с и 3.08 м [6H, $N(CH_2\text{-}\underline{CH_3})_2$ и 4H, $N(\underline{CH_2}\text{-}CH_3)_2$] **(3)**, 2.42 т и 3.64 т [4H, $N(CH_2)_2$ и 4H, $N(CH_2)_2O$] **(4)**.

Таким образом, разработанный метод позволяет эффективно получать функционально замещённые α,β-ненасыщенные аминокетоны с фурильным фрагментом, представляющие интерес для дальнейших исследований в области синтеза гетероциклических соединений и потенциального фармакологического применения.

СПИСОК ЛИТЕРАТУРЫ

1. Поткин В.И., Петкевич С.К., Курман П.В., Синтез и реакции с N-нуклеофилами 1-(тиен-2-ил)- и 1-(4-гидроксифенил)-3,4,4-трихлор-3-бутен-1-ононв, *Журнал Органической Химии*, 2010, т. 46, вып. 9, с. 1307-1314
2. Потиха Л.М, Ковтуненко В.А., Гетероциклизации на основе γ-галоген-α,β-ненасыщенных кетонов. *Химия Гетероциклических Соединений,* 2020. т. 56, вып. 11, с. 1375-1393

3. Gadzhili R.A., Azizov A.H., Zeynalova S.K., Karayeva A.R., Karayev Z.Q., Aliyev A.G. Studies on synthesis reactions and antimicrobial activities of 3-alkyl-5-dialkylaminomethyl pyrazolines. *Eur. Chem. Bul.,* **2015**, Vol. 4, No. 10-12, pp. 535-538
4. Guo H., Zhang Q., Pan W., Yang H., Pei K., Zhai J., Li T., Wang Z., Wang Y., Yin Y., One-pot synthesis of substituted pyrazoles from propargyl alcohols via cyclocondensation of in situ-generated α-iodo enones/enals and hydrazine hydrate, *Asian J. Org. Chem.*, 2021, Vol. 10, pp. 2231–2237
5. Hammouda M.M., Elattar M.K., Recent progress in the Chemistry of β-aminoketones, *RSC Advances*, 2022, Vol. 12, pp. 24681-2471
6. Zhang T. S., Zhao Q., Hao W.J., Tu S.J., Jiang B., Cu-Catalyzed [4+1] annulation toward Indolo[2,1-*a*]isoquinolines through oxidative C(sp^3)/C(sp^2)−H bond difunctionalization, *Chem. - Asian J.*, 2019, Vol. 14, pp. 1042–1049

НОВАЯ ТЕХНОЛОГИЯ ДЛЯ БОРЬБЫ С ОСЛОЖНЕНИЯМИ В ПРОЦЕССЕ ДОБЫЧИ НЕФТИ

Абдуллаев Вугар Джамил, Алсафарова Матанат Эльдар,
Халилов Нурлан Назим, Алышова Джамала Гулу
SOCAR, Научно Исследовательский Проектный Институт «Нефтегаз»
Баку, Азербайджан
cemale.q.qenberova@socar.az

Резюме - Проблемы, возникающие в результате образования отложений асфальтенов, смол, парафинов и солей (АСПСО) в трубопроводах при добыче и транспортировке высоковязкой нефти, остаются постоянной проблемой для нефтяной промышленности. Несмотря на разработку большого количества депрессорных присадок против отложения АСПСО, полностью устранить эту проблему не удалось. Поэтому разработка универсальных и эффективных депрессантов против отложения АСПСО остается актуальной задачей. Учитывая это, в данной работе был получен и исследован новый универсальный и эффективный депрессант против отложения АСПСО.

Ключевые слова: нефть, скважина, реагент, солевые отложения, парафиновые отложения, эффективность, осложнения, трубопровод, присадка, добыча

Введение

В настоящее время одной из основных проблем при разработке нефтяных месторождений Азербайджана является отложение АСПСО на нефтепромысловом оборудовании и применение методов борьбы с этими отложениями. На основе анализа проблемы борьбы с АСПСО установлено, что в последнее время на промыслах нефтегазодобывающих управлений увеличилось количество эксплуатируемых парафинистых скважин. Под понятием парафинистых скважин понимаются скважины, нормальная эксплуатация которых в течение года обеспечивается проведением тех или иных мероприятий по предотвращению отложения парафина. АСПСО в зависимости от характеристик скважин, наблюдаются на различных участках нефтепромыслового оборудова-

ния при добыче и транспортировке нефти. Так, частицы АСПСО откладываются в насосно-компрессорных трубах, штангах, узлах насосной установки, устьевом оборудовании, выкидных линиях, коллекторах, измерительных установках и т.д., что приводит к снижению добычи.

Как в стране, так и за рубежом значительное количество научных работ посвящено физико-химическим факторам, влияющим на выделение АСПСО из нефти, а также механизму процесса АСПО в нефтепромысловом оборудовании [1-8]. Однако решение указанных проблем по-прежнему остается актуальным. С учетом этой актуальности был разработан новый состав для борьбы с АСПСО.

Экспериментальная часть.

Данная работа посвящена разработке нового эффективного состава для понижения температуры застывания и улучшения вязкостных свойств высоковязких нефтей.С учётом вышеизложенного был разработан новый реагент NDP-22M-2, представляющий собой синергетическую смесь неионогенных поверхностно-активных веществ с органическими растворителями, предназначенный для обработки высокопарафинистых и высоковязких нефтей.

Реагент NDP-22M-2 при транспортировке высоковязких парафинистых нефтей улучшает текучесть нефти, предотвращает образование парафиновых отложений, снижает температуру застывания и вязкость нефти, тем самым облегчая её транспортировку.

Лабораторные испытания проводились в два этапа в соответствии с методикой «Оценка эффективности ингибиторов парафиноотложений комплексного действия».

Первый этап рассматривается как ориентировочный экспресс-метод [9-11]. В соответствии с этим методом определяется растворимость ингибитора в нефтепродуктах и растворителях. Для приготовления синергетических композиций компоненты вводят в колбу в установленных массовых соотношениях и перемешивают при комнатной температуре в течение 0,5–1,0 часа. При необходимости перемешивание проводят при температуре 40–45 °С.

Следует отметить, что компоненты, входящие в состав композиции, по отдельности не обладают депрессорными свойствами. Однако в составе композиции благодаря синергетическому эффекту они проявляют выраженные депрессорные свойства по отношению к высокопарафинистым и высоковязким нефтям.

В начале исследований проверялось действие NDP-22M-2 для снижения температуры застывания и улучшения вязкостных свойств высокопарафинистых нефтей в частности на кинематическую вязкость, плотность и температуру застывания нефтей НГДУ им. Н.Нариманова. Нефть Н.Наримановского НГДУ является высокопарафинистой и содержание парафина составляет около 20 %. Плотность и

кинематическая вязкость определены на приборе Штабингер SVM 300. Температура застывания определяется по ГОСТУ 20287–74. Депрессорный эффект (ΔT) вычисляется по формуле:

$$\Delta T = (T_{заст.исх} - T_{заст.пр})$$

Здесь:

$T_{заст.исх}$ – температура застывания исходной нефти,

$T_{заст.пр}$ - температура застывания нефти после обработки присадкой. Концентрация присадки составляет 0,02 % масс. нефти. Результаты проведенных исследований показаны в таблице.

Таблица. Физические параметры нефти до и после добавления реагента

№ скв	Кинематическая вязкость до добавления реагента, мм²/с	Кинематическая вязкость после добавления реагента, мм²/с					
		1	2	3	4	5	6
619	264,58	120,4	121,2	95,67	110,44	129,34	115,48
456	Нетекучая (густая нефть)	80,4	72,3	58,05	70,77	86,42	70,08
441	364,75	61,4	59,7	39,16	55,19	69,89	95,44
Скв №	Плотность нефти до добавления реагента, г/см³	Плотность нефти после добавления реагента, г/см³					
		1	2	3	4	5	6
619	0,8664	0,85	0,85	0,87	0,87	0,87	0,87
456	Нетекучая (густая нефть)	0,88	0,88	0,88	0,88	0,89	0,89
441	0,8713	0,86	0,86	0,88	0,86	0,86	0,87
Скв №	Застывания нефти до добавления реагента, °С	Застывание нефти после добавления реагента, °С					
		1	2	3	4	5	6
619	+16	+6	+3	-11	-7	+9	+5
456	+16	-1	-5	-10	-8	-12	-11
441	+22	-3	-5	-20	-13	-11	-7

Как видно из таблицы, новый состав, приготовленный для понижения температуры застывания и улучшения вязкостных свойств высокопарафиновых нефтей, позволяет понизить температуру застывания и улучшить вязкостные свойства.

Выводы и обсуждение.

1. Предлагаемый реагент является универсальным по своему характеру и дает положительные результаты для всех типов высокопарафиновых и высоковязких нефти.

2. При добавлении реагента к высокопарафинистым и высоковязким нефтям, замерзающим при +22 °C, температура замерзания снижается до -20 °C.

Предложения

NDP-22M-2 предназначен для предотвращения образования АСПО в скважинах и на поверхности нефтепромыслового оборудования, а также для улучшения текучести высокопарафинистых и высоковязких нефтей. NDP-22M-2 обеспечивает эффективную защиту от SPSO в безводных и маловодных средах, улучшает реологические свойства нефтей и снижает их вязкость при низких температурах. В связи с вышесказанным рекомендуется использовать реагент NDP-22M-2 на нефтяных месторождениях.

Список литература:

1. Абдуллаев В.Дж., Аббасов З.Н. Исследование влияния реагента" композит 2 "на реологические свойства высоковязких (парафиновых) нефтей, деталь "Денизнефтегазпроект", 2004 г., p. 24-26
2. Абдуллаев В.Дж., Аббасов З.Н. Исследование влияния нового реагента" композит 2 "на реологические свойства парафинсодержащих нефтей, деталь "Денизнефтегазпроекта", 2005 г., p. 24-26
3. Абдуллаев В.Дж., Алиева А.І., Исследование скорости осаждения высокопарафинистых нефтей при различных температурах,деталь "Денизнефтегазпроекта", 2003 г.,p.30-31
4. Гасанов Х.И., Халилов Н.Н. Ингибиторы солеотложения на основе фосфатов тетраметилэтилендиамина и наночастицы, Булатовские чтения, Материалы VII Международной научно-практичекой конференции, г. Краснодар, Россия, 31, марта 2023 г., ТОМ-1, стр. 156-162.
5. Шахбазов Э.Г., Гасанов Х.И., Халилов Н.Н. Наносодержащие ингибиторы солеотложения на основе этаноламмонийфосфатов, "SOCAR Proceedings", 2022, № 2, стр. 67-72. DOI: 10.5510/OGP20220200676
6. Alsafarova M. E., Samadov A.M., Matiyev K. I., Ganbarova J.G. Development of a new reagent for the prevention of asphaltene-resin-paraffin deposits/ Scientific Petroleum No.1 (2024) p.50-53.
7. Hasanov Kh.I., Khalilov N.N. Development of novel quaternary amine formulations for scale inhibition, Processes of Petrochemistry and oil Refining, 2024, Vol.25, No 4, pp. 1160-1165. DOI: 10.62972/1726-4685.2024.4.1160
8. Metiyev K.I., Samadov A.M., Alsafarova M.E., Hasanov Kh.I., Nurullayev V.Kh. Prevention of asphaltene-resin-paraffin deposits in the process of oil transportation/ SOCAR Proceedings No.2 (2024) p.101-105.
9. Metiyev K.I., Agazade A.D., Alsafarova M.E, Akhmedov F.M. Pour-Point Depressant for Pigh Our-Point Paraffinic Oils/ SOCAR Proceedings No.3 (2018) p.32-37.
10. Metiyev K. I., Alsafarova M. E., Emel N. I. Methods for combating asphalt resin and paraffin deposits in the oil industry/ Scientific Petroleum No.2 (2023) p.35-40.
11. Матиев К.И., Ага-заде А.Д., Алсафарова М.Э., Ахмедов Ф.М. Депрессорная присадка для высокозастывающих парафинистых нефтей / Материалы Международной научно-практической конференции «Состояние и перспективы эксплуатации зрелых месторождений». г. Актау, 2019, с. 277-283. Т.2

THE EFFECT OF AN ADDITIVE SYNTHESIZED FROM NATURAL PETROLEUM ACIDS ON THE PRODUCTION OF ROAD BITUMEN

Vagif Abbasov, Lala Afandiyeva, Yutta Cherepnova, Gunay Nasibova, Shafag Mammadova, Balacakhanim Babayeva, Nazile Afandiyeva
Y.H. Mamedaliyev's Institute of Petrochemical Processes of the Ministry of Science and Education
Baku, Azerbaijan
e-mail: uta1980@inbox.ru

Abstract - The effect of an additive with a catalytic effect on the oxidation of petroleum tar is examined. A mixture of synthesized Fe- and Mn-containing salts of natural petroleum acids, taken in a 3:1 ratio, was studied as an additive. The concentration of this mixture in petroleum tar was 0.3% by weight per 100 grams of feedstock. It is demonstrated that the introduction of a mixture of Fe- and Mn-containing salts of natural petroleum acids into petroleum tar affects the duration of the oxidation process and the quality characteristics of the oxidized bitumen.

Keywords: petroleum tar, aerobic oxidation, metal-containing catalysts, road bitumen.

Introduction

The primary objective of the modern oil refining industry is to improve the efficiency of oil refining and the quality of petroleum products, which include petroleum bitumen. Of great importance are studies aimed at developing rational methods for improving the production technology of petroleum bitumen, as one of the most common engineering and construction materials [Grushova et al., 2021, 57-62; Cherepnova, 2024, 694-703].

The production of bitumen materials from heavy petroleum residues requires a multi-stage production process that includes not only tar oxidation but also raw material modification to achieve the required material quality [Popov et al., 2024, 42-47]. Despite the fact that modifiers and additives improve bitumen properties [Belova et al., 2018, 175-184], their introduction is quite labor-intensive and requires additional equipment, as well as a separate production stage. A solution to these problems may be the introduction of additives that improve bitumen quality into the tar oxidation process [Abbasov et al., 2025, 298-303]. Firstly, this allows the additive to be used more economically, since oxidation results in its more complete dissolution in the tar and even distribution throughout the bitumen. Secondly, the production chain is shortened by eliminating the stage of compounding the bitumen with the modifier. Consequently, the resulting material is of higher quality and has the desired characteristics, compared to bitumen obtained from unmodified tar.

The study included tests involving the oxidation of tar "with" the additive (in the presence of a mixture of Fe- and Mn-containing catalysts) and "without" it, with the aim of comparing the properties of the resulting products and determining the effectiveness of the additive.

Experimental Part

Oil tar obtained at the Heydar Aliyev Oil Refinery during primary oil refining served as the feedstock for the oxidation process.

Samples of iron- and manganese-containing salts of natural petroleum acids (Fe-NPA, Mn-NPA) were synthesized according to the method [Abbasov et al., 2024, 1187-1193] and added to the feedstock as a Fe:Mn-NPA (3:1) mixture at a concentration of 0.3% by weight per 100 grams of feedstock.

Thermal oxidation of oil tar to road bitumen was carried out in a laboratory setup in a bubble-type oxidation column at a temperature of 260±2°C and an airflow rate of 0.5 and 0.6 l/min. Softening points were determined by sampling every 3–5 h using the “Ring and Ball” method. The quality parameters of the obtained bitumens (softening point, penetration at 25°C, Fraass breaking point, ductility at 25°C, adhesion to mineral fillers) were identified according to GOST AZ 3536601.242-2015 when the softening point according to “Ring and Ball” reached 46-49°C.

Comparative analyses were then performed on the quality parameters of bitumen obtained from tar with low quality parameters and bitumen obtained from the same tar sample with the addition of a Fe:Mn-NPA (3:1) mixture (Table).

Indicator name	The norm for road petroleum bitumen 50/70	Air flow rate, l/min	
		0.5	0.6
Without adding a catalyst			
Oxidation time, h	-	25	15
Softening point according to GOST, °C	46-54	46	46
Fraass breaking point, °C	≤-15	-25	-23
Ductility at 25 °C, mm	≥55	87	>100
Penetration at 25 °C according to GOST	51-70	54	56
Adhesion, mark	1,2,3	3	2
With the addition of a mixture Fe:Mn-NPA			
Oxidation time, h	-	10	8
Softening point according to GOST, °C	46-54	46.7	49.4
Fraass breaking point, °C	≤-15	-20	-25
Ductility at 25 °C, mm	≥55	99	>100
Penetration at 25 °C according to GOST	51-70	54	56
Adhesion, mark	1,2,3	2	1

The addition of the additive enables bitumen to achieve compliance with almost all GOST standards and leads to a change in the oxidation rate, thereby reducing the time (from 15 hours to 8 hours) for producing road bitumen. The qualitative indicators and duration of the tar oxidation process to bitumen obtained in the presence of the Fe:Mn-NPA mixture indicate a synergistic effect in this process.

Conclusion

The addition of an additive – a catalyst obtained from Azerbaijani hydrocarbon feedstock – to petroleum tar affects the structural organization of petroleum systems. The introduction of the optimal amount of catalyst – 0.3% by weight per 100 grams of feedstock – into the system accelerates the oxidation process and changes the qualitative indicators of the final oxidation products under identical oxidation conditions. This can be used to produce oxidized bitumen with improved quality indicators without changing the oxidation process technology.

This work was supported by the Azerbaijan Science Foundation – Grant № AEF-MGS-2025-1(54) -20/16/4-M-16

References

1. Abbasov V.M., Afandiyeva L.M., Cherepnova Yu.P., Nasibova G.G., Aliyeva N.M., Ahmadbayova S.F., Mammadov A.M., Lyadov A.S. 2025. Commercial production of bitumen via oxidation of vacuum residue over iron catalysts. Petroleum Chemistry, vol.64, No. 3, pp. 298-303.
2. Abbasov V.M., Afandiyeva L.M., Nasibova G.G., Aliyeva N.M., Ahmadbayova S.F., Cherepnova Yu.P., Mammadova Sh.R., Lyadov A.S. 2024. Synthesis of Petroleum Acids by Oxidation of Dearomatized Oil Distillate. Petroleum Chemistry, vol. 64. pp. 1187–1193.
3. Belova N.A., Kortovenko L.P., Strakhova N.A. 2018. Additives in bitumen. Bulletin of the Dagestan State Technical University. Technical Sciences, vol.45, No. 3, pp.175-184.
4. Cherepnova Yu.P. 2024. Road oil bitumens: promising ways for obtaining and controlling properties (review). Processes of petrochemistry and oil refining, vol.25, No.3, pp. 694-703.
5. Grushova E.I., Stan'ko M.V., Khat'ko I.N. 2021. Influence of heavy pyrolysis resin on the processes of oil tar oxidation. Proceedings of BSTU, Issue 2, Chemical Engineering, Biotechnologies, Geo-ecology, No.1, pp. 57-62 (In Russian).
6. Popov M.R., Chernysheva E.A., Zuikov A.V., Kozhevnikova J.V. 2024. Assessment of the effect of tar additives on properties bitumen. World of Petroleum Products, No. 3, pp. 42-47.

INVESTIGATION OF THE AEROBIC OXIDATION OF HYDROCARBONS IN THE PRESENCE OF METAL-CONTAINING HOMOGENEOUS CATALYTIC SYSTEMS

Vagif Abbasov, Lala Afandiyeva, Gunay Nasibova, Shafag Mammadova, Turan Mazamova, Fidan Hasanova
Institute of Petrochemical Processes named after acad. Y.H. Mammadaliyev,
Ministry of Science and Education, Republic of Azerbaijan
30 Khojaly Ave., Azerbaijan
sefeq_memmedova@mail.ru

Abstract - This study demonstrates the synthesis of synthetic petroleum acids (SPA) with high yields through the liquid-phase oxidation of naphthene-paraffinic hydrocarbons extracted from Azerbaijani oil mixtures. The process was conducted in the presence of a Manganese (Mn) salt of sunflower oil fatty acids, utilized at a concentration of 0.5% by weight relative to the feedstock. The experimental results confirmed a combined yield of SPA and natural petroleum acids (OSPA) reaching 34.3%.

Keywords: diesel fraction, aerobic oxidation, oxidation catalysts, synthetic petroleum acids

Introduction

In the modern world, the efficient utilization of petroleum hydrocarbons plays a decisive role not only for the energy sector but also for the advanced chemical industry [Bellotto. S., Gusev D.G., 2022, pp.45–62]. Through catalytic oxidation under various optimal conditions, the conversion of hydrocarbons yields organic substances that these organic resources are of fundamental importance in the synthesis of high-molecular-weight compounds, the preparation of pharmaceutical products, and the production of high-performance specialized fuels [Paia Z.P., Parmona V.N., Bukhtiyarova V. I., 2023, pp. 329–361].

Catalytic oxidation constitutes a primary class of reactions that ensure sustainable transformations both environmentally and industrially. These processes are based on accelerating oxidation reactions through the influence of catalysts—typically metals, metal oxides, or nanostructures placed on a carrier—thereby ensuring the efficient conversion of pollutants, hydrocarbons, and volatile organic compounds into less harmful products such as carbon dioxide and water [Salah Ahmed R.M., 2025, pp. 112–130].

Transition metal salts of fatty acids are one of the catalytic systems widely applied in the liquid-phase oxidation process. These types of catalytic systems are industrially significant, particularly for the oxidation of hydrocarbons, as well as bitumen and petroleum fractions, in terms of polymer production. Since reactions occurring in the presence of transition metal ions proceed at relatively lower temperatures, they are also considered energy-efficient. For this reason, the study of transition metal salts of fatty acids is considered one of the relevant scientific directions for creating more

Table. Results of the oxidation of de-aromatized diesel fraction in the presence of Mn salts of sunflower fatty acids

Catalyst Amount (wt%)	Oxidate (mg KOH/g)		Oxidate Yield (%)		SPA Acid Number (mg KOH/g)		SPA Yield (%)
	Oxidate Acid Number (mg KOH/g)	Oxidate Yield (%)	SPA Acid Number (mg KOH/g)	SPA Yield (%)	OSPA Acid Number (mg KOH/g)	OSPA Yield (%)	Total Yield (SPA+OSPA) (%)
0.1	35	95.4	70.5	10	62	2	12
0.3	44	96	115	22.6	105	10	32.6
0.5	48	97	120	23.5	106	10.8	34.3
1	47.9	97	121.2	23.8	109	12.5	36.3

efficient catalytic systems in the petrochemical industry [Gnanaprakasam B., Balaraman E., 2021, pp.112–130]. Organic acids synthesized with the participation of various catalytic systems are of industrial importance and have an extremely wide range of applications [Abbasov V.M., Afandiyeva L.M., Nasibova G.G., Aliyeva N.M., Ahmadbayova S.F., 2024, pp. 1187–1193]. Considering the aforementioned points, the presented work demonstrates the process of oxidizing naphthene-paraffinic hydrocarbons with the catalytic participation of the Mn salt of sunflower oil fatty acids.

Experimental Part

The diesel fraction isolated from Azerbaijani oil mixtures served as the primary feedstock. The physicochemical properties of the fractions were evaluated both before and after the de-aromatization process, and their Infrared (IR) spectra were analyzed [Abbasov V.M., Aliyeva L.I., Afandiyeva L.M., Ibrahimov H.J., Rustamli G.Y., 2020, pp 80-89]. The reaction was performed in a bubble-type reactor via liquid-phase oxidation using atmospheric oxygen at 140°C for a duration of 5 hours. The catalyst-to-feedstock ratio was tested within a range of 0.2–1.0 wt%. The Mn salt of sunflower fatty acid was employed as the catalyst, with the findings summarized in Table.

Results and Discussion

As indicated in the table, the highest yield for SPA was observed when the Mn salt of sunflower fatty acid was applied at a concentration of 0.5 wt% relative to the feedstock. At this concentration, the yield of SPA reached 23.5%, while the OSPA yield was 10.8%. Furthermore, the acid numbers of the products peaked at this concentration, signaling an intensified oxidation process. Increasing the catalyst concentration to 1.0 wt% did not yield a significant improvement in process efficiency. Thus, 0.5 wt% was identified as the optimal catalyst amount for the catalytic oxidation of naphthene-paraffinic hydrocarbons using Mn salts.

Recommendations

This experimental approach provides a systematic framework for studying catalytic effects and optimizing oxidation processes. It is essential to further evaluate various homogeneous and heterogeneous catalytic systems and explore the diverse application areas for the synthesized synthetic organic acid mixtures.

References

1. Abbasov V.M., Afandiyeva L.M., Nasibova G.G., Aliyeva N.M., Ahmadbayova S.F. Synthesis of Petroleum Acids by Oxidation of Dearomatized Oil Distillate. Petroleum Chemistry, 2024, Vol. 64, No. 10, pp. 1187–1193
2. Abbasov V.M., Aliyeva L.I., Afandiyeva L.M., .Ibrahimov H.J., Rustamli G.Y. Aerobic oxidation of naphthene-paraffinic hydrocarbons of petroleum in the presence of γ-Al2O3 modified by transition metals. Processes of Petrochemistry and Oil Refining. Volume № 21, İssue 1,2020, pp 80-89
3. Bellotto S., Gusev D.G. Catalytic Aerobic Oxidation of Hydrocarbons: Recent Advances and Future Perspectives in Sustainable Catalytic Processes. Elsevier, 2022, pp. 45–62
4. Gnanaprakasam B., Balaraman E. Transition-Metal-Catalyzed Oxidation of Hydrocarbons. Sustainable Catalysis, CRC Press, 2021, pp. 112–130
5. Paia Z.P., Parmona V.N., Bukhtiyarova V.I. Kinetics and Catalysis, 2023, Vol. 64, No. 4, pp. 329–361
6. Salah Ahmed R.M. Catalytic Oxidation Processes: Environmental and Industrial Perspectives. Shorouk Academy – Department of Engineering . 2025, October 31

OPTIMIZATION OF HYDRODENITROGENATION OF ALGAL CRUDE BIO-OIL USING NiCo/γAL$_2$O$_3$

Laman Talibova
King Abdullah University of Science and Technology
Jeddah, Saudi Arabia
laman.talibova@kaust.edu.sa

Summary - Rising global energy demand is driving interest in upgraded biofuels from biomass as greener alternatives. In this experiment, bio-oil produced by algea (Nannochloropsis sp.) is upgraded via hydrodenitrogenation (HDN) to reduce nitrogen-containing compounds that cause NOx emissions and can poison downstream catalysts, using a batch bomb reactor and operated at controlled temperature, pressure, and residence time. After reaction, products are recovered by dichloromethane (DCM) extraction and solvent evaporation, and both gas and liquid products are characterized (GC–MS, FT-IR) while optimizing mainly **time (2–4 h), temperature (300–450 °C), and pressure (12–20 MPa)** using **cheaper Ni–Co/γ-Al$_2$O$_3$** compared to precious-metal catalysts.

Keywords: Upgrading biofuel, hydrodenitrogenation (HDN), Ni–Co/γ-Al$_2$O$_3$, process optimization.

Introduction

Energy demand in any sector is growing day by day. Production fields and the transport sector cover more than half of the energy used in the world.

(Matricon et al., 2023) Upgraded biofuel from biomass is a promising future green energy source to meet the energy demand in an eco-friendly way. Hydrothermal liquefaction of algae has recently been studied by many researchers. After hydrothermal liquefaction of wet biomass and extraction of biocrude oil which has many different organic compounds, such as organic acids, pyrazines, ketons, amides, phenolics, and others the upgrading process is carried out to increase economic feasibility of the biofuel. Denitrogenation of biofuel is one of the upgrading steps. High nitrogen content in the fuel causes high NOx emission during combustion of biofuel in engine, and it can deactivate the catalyst used for further upgrading processes. (Obeid et al., 2019) (Huang et al., 2018)To solve the problem of nitrogen content has been targeted by using several methods. Optimization of hydrodenitrogenation process of crude bio-oil is the main scope of this research.

Experimental setup

Crude bio-oil extracted from microalga (Nannochloropsis sp.) is loaded into bomb batch reactors with Ni-Co/y –Al2O3 catalyst bed together with 0.1 HCl or NaOH to modify pH condition. After sealing the reactor, air (O2 source) is removed by He purge/vacuum cycles. [SEE Fig.1]. The reaction is carried out in high preesure, so the reactor is pressured with charging He 70 kPa and H2 (reagent) is charged, more pressuring to 12 MPa. Isothermal reactor with certain temperature (the first trial T is 320 °C) is operated in certain residence time (the first trial t is 200 min). After reaching certain predetermined residence time, cool the reactor in an ice water bath, then refrigerator for 30 min. The gas-liquid equilibrates. Dichloromethane is injected into reactor to recover treated bio-oil. Separated organic phase is withdrawned. DCM is removed via evaporation, and remaining treated bio-oil content is tested. Gas phase and liquid phase at the end are analyzed with GC-MS analysis and FT-IR.

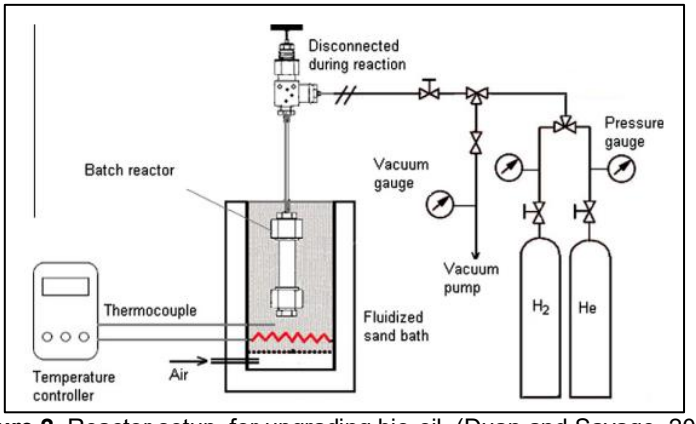


Figure 2. Reactor setup for upgrading bio-oil. (Duan and Savage, 2011)

Offers

In many literature optimizations in terms of hydrogen consumption, catalyst utilization, residence time, temperature and pressure have been carried out in catalyst of Pt/C/MZSM-5. In this experiment, we will mainly focus on the 3 main conditions, residence time (2-4 hr), temperature (300-450 °C) and pressure (12-20 MPa) for hydrodenitrogenation (HDN) by using Ni-Co/y-Al2O3, which has been used for HDN of crude oil. Using cheaper catalyst in optimized condition will be the main achievement of this project.(Zhang et al., 2025)

References

Duan, P., Savage, P.E., 2011. Upgrading of crude algal bio-oil in supercritical water. Bioresour. Technol. 102, 1899–1906. https://doi.org/10.1016/j.biortech.2010.08.013

Huang, Z., Wufuer, A., Wang, Y., Dai, L., 2018. Hydrothermal liquefaction of pretreated low-lipid microalgae for the production of bio-oil with low heteroatom content. Process Biochem. 69, 136–143. https://doi.org/10.1016/j.procbio.2018.03.018

Matricon, L., Roubaud, A., Haarlemmer, G., Geantet, C., 2023. The challenge of nitrogen compounds in hydrothermal liquefaction of algae. J. Supercrit. Fluids 196, 105867. https://doi.org/10.1016/j.supflu.2023.105867

Obeid, F., Chu Van, T., Brown, R., Rainey, T., 2019. Nitrogen and sulphur in algal biocrude: A review of the HTL process, upgrading, engine performance and emissions. Energy Convers. Manag. 181, 105–119. https://doi.org/10.1016/j.enconman.2018.11.054

Zhang, J., Li, Hulin, Chen, H., Zhang, H., Yang, C., Li, Haobo, 2025. Hydrothermal hydrodenitrogenation and hydrodesulfurization over nickel-based catalysts in sub/supercritical water. Fuel Process. Technol. 278, 108332. https://doi.org/10.1016/j.fuproc.2025.108332

TEMPERATUR AMİLİNİN PARAFİNSİZLƏŞMƏ PROSESİNDƏ ROLU

Sevinc Hacıyeva, Nəzərova Müşkünaz
Sumqayıt Dövlət Universiteti
Sumqayıt , Azərbaycan
sevushaj@gmail.com

Xülasə - Parafinsizləşmə prosesi neft fraksiyalarından yüksək ərimə temperaturuna malik normal parafinlərin ayrılması məqsədilə aparılır və əsasən yağların axıcılıq temperaturunun aşağı salınmasına xidmət edir. Bu prosesdə temperatur amili həlledici rol oynayır, çünki parafinlərin kristallaşması birbaşa istilik şəraitindən asılıdır.

Temperaturun aşağı salınması nəticəsində məhlulda həll olmuş parafinlər doyma həddinə çatır və kristallaşma başlayır. Kristallaşma temperaturu nə qədər düzgün seçilərsə, əmələ gələn kristalların ölçüsü və forması bir o qədər filtrasiya üçün əlverişli olur. Çox sürətli soyutma xırda və kolloid xarakterli kristalların yaranmasına səbəb olur ki, bu da filtrasiya prosesini çətinləşdirir. Əksinə, mərhələli və nəzarətli soyutma iri və yaxşı formalaşmış kristalların alınmasını təmin edir və ayrılma səmərəliliyini artırır.

Açar sözlər: parafinsizləşmə, neft fraksiyaları,karbohidrogen, kristallaşma, həlledici

Giriş

Parafinsizləşmə prosesi neft fraksiyalarından yüksək molekullu n-parafinlərin ayrılması yolu ilə məhsulun aşağı temperatur xüsusiyyətlərinin yaxşılaşdırılmasına xidmət edir. Bu prosesdə temperaturun rolu mühümdür, çünki parafinlərin kristallaşma qabiliyyəti birbaşa istilik rejimindən asılıdır. Temperaturun azaldılması nəticəsində parafin karbohidrogenləri məhluldan kristal şəklində ayrılır, onların ölçüsü, forması və filtrasiya qabiliyyəti isə soyutma sürəti və son temperaturla müəyyən olunur.

Optimal temperatur rejimi seçilmədikdə kristalların həddən artıq xırda və ya yapışqan quruluşda əmələ gəlməsi filtrasiya prosesini çətinləşdirir və məhsul çıxımını azalda bilər. Eyni zamanda, həddindən artıq aşağı temperatur enerji sərfiyyatını artırır və iqtisadi səmərəliliyi azaldır. Buna görə də parafinsizləşmə prosesində temperaturun mərhələli və nəzarətli şəkildə tənzimlənməsi həm texnoloji, həm də iqtisadi baxımdan əsas amillərdən biri hesab olunur.

Beləliklə, temperatur amili parafinlərin kristallaşma kinetikasını, faza tarazlığını və son məhsulun keyfiyyət göstəricilərini müəyyən edən əsas parametrlərdən biri kimi çıxış edir və prosesin effektivliyinin artırılmasında mühüm əhəmiyyət daşıyır.

Ekspremental hissə

Parafinsizləşmə prosesi neft fraksiyalarının aşağı temperaturlu istismar göstəricilərinin yaxşılaşdırılması məqsədilə aparılan mühüm texnoloji mərhələlərdən biridir. Bu prosesdə temperatur əsas tənzimləyici parametr kimi çıxış edir və parafin kristallarının əmələ gəlməsi, böyüməsi, aqreqasiyası və ayrılması mərhələlərinə birbaşa təsir göstərir. Təqdim olunan tezisdə temperaturun parafinsizləşmə prosesində rolu fiziki-kimyəvi və texnoloji baxımdan təhlil olunur, kristallaşma kinetikası və selektivlik məsələləri ilkin tədqiqat mərhələsi səviyyəsində ümumiləşdirilir.

Neft fraksiyalarının tərkibində olan normal quruluşlu parafin karbohidrogenləri aşağı temperaturda kristallaşaraq məhsulun axıcılıq qabiliyyətini azaldır, donma temperaturunu yüksəldir və nəqliyyat zamanı texniki çətinliklər yaradır. Xüsusilə dizel fraksiyaları və yağ distillyatları üçün bu problem daha aktualdır. Parafinsizləşmə prosesi həmin bərk parafinlərin seçici şəkildə ayrılmasına əsaslanır. [Elijah Bell, 2024, 6-34]

Prosesin effektivliyi bir neçə amildən asılı olsa da, temperatur həm kristallaşmanın başlanma nöqtəsini, həm də ayrılma dərəcəsini müəyyən edən əsas parametrlərdən biridir. Buna görə də temperaturun təsirinin öyrənilməsi parafinsizləşmənin optimallaşdırılmasında ilkin və vacib mərhələ hesab olunur.

Parafinlərin ayrılması əsasən kristallaşma hadisəsinə əsaslanır. Temperatur azaldıqca sistemdə həllolma qabiliyyəti zəifləyir və müəyyən kritik nöqtədə parafin molekulları kristal tor formalaşdırmağa başlayır.

Kristallaşma iki mərhələdə baş verir: Birinci halda nüvələnmə (nucleation) – ilk kristal mərkəzlərinin yaranması; ikinci halda kristalların böyüməsi – əmələ gəlmiş nüvələrin ölçücə artması.

Temperaturun sürətlə azaldılması çoxsaylı xırda kristalların əmələ gəlməsinə səbəb olur. Bu halda filtrasiya çətinləşir və ayrılma effektivliyi aşağı düşə bilər. Əksinə, temperaturun tədricən və nəzarətli şəkildə azaldılması iri və yaxşı formalaşmış kristalların yaranmasına şərait yaradır ki, bu da mexaniki ayrılmanı asanlaşdırır.

Beləliklə, soyutma sürəti və son temperatur kristal ölçüsünü və prosesin texnoloji göstəricilərini müəyyən edir. [Seyfullayev ,2024, 71–80]

Həlledici iştirakı ilə aparılan proseslərdə temperatur daha mürəkkəb rol oynayır. Həlledici–xammal sistemində soyutma zamanı parafinlərin həllolma qabiliyyəti kəskin azalır. Temperatur aşağı düşdükcə kristallaşma intensivləşir, lakin həddindən artıq aşağı temperatur viskozluğu artıraraq qarışdırma və filtrasiya mərhələsini çətinləşdirə bilər.

Bundan əlavə, temperatur həlledicinin seçiciliyinə də təsir göstərir. Müəyyən temperatur intervalında parafinlər çöksə də, digər karbohidrogenlər maye fazada qalır. Buna görə temperaturun düzgün seçilməsi enerji sərfiyyatının azaldılması və məhsul keyfiyyətinin yüksəldilməsi baxımından vacibdir. [Gabriel Santos ,2024, 36-44]

Nəticələr və onların müzakirəsi

Parafinsizləşmə adətən aşağı temperatur şəraitində aparıldığı üçün soyutma sistemləri əlavə enerji tələb edir. Temperatur nə qədər aşağı seçilərsə, enerji sərfiyyatı bir o qədər artır. Buna görə də texnoloji baxımdan optimal temperatur yalnız maksimal parafin ayrılması deyil, həm də iqtisadi səmərəlilik meyarları nəzərə alınmaqla müəyyən edilməlidir.

Təkliflər

1. Gələcək tədqiqatlarımızda İlkin eksperimental yanaşmayada tədqiqatın başlanğıc mərhələsində müxtəlif temperatur intervallarında kristallaşma başlanğıc nöqtəsinin müəyyən edilməsi
2. Soyutma sürətinin kristal ölçüsünə təsirinin qiymətləndirilməsi
3. Filtrasiya müddətinin temperaturdan asılılığının öyrənilməsi
4. Donma temperaturunun və axıcılıq həddinin dəyişməsinin təhlili məsələlərinin öyrənilməsi qarşıya qoyulan məqsədlərimizdəndir.

İstifadə olunmuş ədəbiyyat

1. Elijah Bell, Gabriel Santos, Nagu Daraboina & Cem Sarica (2024) “Visualization of thermal removal mechanism of paraffin deposits: Providing guidelines for minimum temperature requirements.” Fuel, Vol. 356, 15 January 2024,Article129577, səh.6-34
2. E.S. Seyfullayev (2024)“Paraffin Deposition and Methods of Deparafininationin the Transportation of Oils with Complex Rheological Properties.”Herald of Azerbaijan Engineering Academy, Vol. 16 No.3(2024),səh.71–80
3. Gabriel Santos, Elijah Bell, Nagu Daraboina & Cem Sarica (2024) “Thermal removal mechanism of paraffin deposits: Impact of flowrate on removal efficiency.”Geoenergy Science and Engineering, Vol. 238, July 2024, Article 212867,səh.36-44

MÜXTƏLİF METİLLƏŞDİRİCİ REAGENTLƏRİN NAFTOLLARLA REAKSİYASİNİN İLKİN TƏDQİQİ

Fərəcova Günay, Nəzərova Müşkünaz
Sumqayıt Dövlət Universiteti
Sumqayıt , Azərbaycan
farajovaa8@gmail.com

Xülasə - Naftollar aromatik hidroksilli birləşmələr sinfinə aid olub üzvi sintezdə mühüm aralıq məhsullar hesab olunur. Onların metilləşməsi nəticəsində həm O-metilləşmiş efirlər, həm də C-metilləşmiş alkil törəmələri əldə edilə bilər. Təqdim olunan tezisdə tədqiqat işində müxtəlif metilləşdirici reagentlərin naftollarla reaksiyasının istiqaməti, selektivliyi və proses parametrlərindən asılılığı araşdırılır. Məqsəd müxtəlif reagentlərin müqayisəli qiymətləndirilməsi və gələcək optimallaşdırma üçün ilkin eksperimental baza formalaşdırmaqdır.

Açar sözlər: 1-naftol , 2-naftol, metanol, metilnaftol, C-metilləşmə, O-metilləşmə

Giriş

Naftollar (1-naftol və 2-naftol) aromatik hidroksibirləşmələr sinfinə aid olub, boyalar, farmasevtik maddələr, antioksidantlar və funksional polimer əlavələrinin sintezində mühüm aralıq məhsullar kimi istifadə olunur. Onların metilləşdirilməsi nəticəsində əmələ gələn O-metil və C-metil törəmələri bioloji aktivlik, lipofillik və stabillik baxımından əhəmiyyətli dəyişikliklər nümayiş etdirir. Buna görə də naftolların selektiv və effektiv metilləşdirilməsi üzvi sintezdə aktual istiqamətlərdən biridir.

Metilləşmə reaksiyası həm oksigen atomu üzrə (O-metilləşmə), həm də aromatik nüvənin aktiv mövqeləri üzrə (C-metilləşmə) baş verə bilər. Reaksiyanın istiqaməti seçilmiş metilləşdirici reagentdən, həlledicidən, katalizatorun təbiətindən və temperatur rejimindən asılıdır. Təqdim olunan tezisdə müxtəlif metilləşdirici reagentlərin naftollarla reaksiyasının ilkin mərhələdə müqayisəli öyrənilməsi və reaksiyanın istiqamətinə təsir edən əsas amillərin müəyyənləşdirilməsi məqsəd qoyulmuşdur.

Eksperimental hissə

Naftol və metilnaftolların istehsalı naftalin və onun metilhomoloqlarına əsaslanır. Bu birləşmələrin xammal mənbəyi isə daş kömür və neftdir. Naftalin əsasında metilnaftolların sintezi aromatik sistemlərin mərhələli funksionallaşdırılmasına əsaslanan klassik və eyni zamanda praktik əhəmiyyətə malik istiqamətlərdən biridir.

Naftalindən metilnaftolların alınması əsasən iki mərhələli sxem üzrə aparılır:

Birinci mərhələdə naftalin metilləşməsi prosesi həyata küçirilir. Naftalinin aromatik elektrofil əvəzlənmə reaksiyası ilə metilləşməsi prosesidir. Metilləşdirici reagent kimi metanol, metilxlorid və ya dimetilsulfat istifadə oluna bilər. Proses adətən Lewis turşuları ($AlCl_3$, $FeCl_3$), proton turşuları və ya seolit tipli heterogen katalizatorlar iştirakında aparılır. [M. Selva, 2008, 457–464]

Metilnaftolların alınmasında 1-naftol, 2-naftolla yanaşı metanoldan istifadə olur. Onların təmizliyi xramotoqrafik analiz üsulları və fiziki xassələrinin tədqiqi nəticəsində müəyyən edir. 1-naftol və 2-naftolun təmizliyini sublimesiya yolu ilə 99.9 %-ə qədər qaldırmaq mümkün olmuşdur. Alkilləşdirici kimi istifadə olunan metanol isə Y.K.Yuryev tərəfindən göstərilmiş qayda üzrə təmizlənir. Metil spirtinin təmizliyi 99.7 % olmuşdur.

Birinci mərhələdə naftalin molekulunda elektrofil hücum əsasən α-mövqedə (1-mövqe) baş verir, çünki əmələ gələn σ-kompleks rezonans baxımından daha sabit olur. Nəticədə əsas məhsul kimi 1-metilnaftalin, müəyyən miqdarda isə 2-metilnaftalin alınır. Temperaturun və katalizatorun seçilməsi izomer paylanmasına birbaşa təsir göstərir. [P. Tundo, 2010, 1233–1235]

İkinci mərhələdə alınmış metilnaftalin törəməsi selektiv hidroksilləşməyə məruz qalır. Bu proses müxtəlif üsullarla həyata keçirilə bilər:

- Sulfonlaşma → ərimə (qələvi ilə əridilmə) → hidroliz yolu ilə,
- Oksidləşdirici sistemlərin (məsələn, H_2O_2 əsaslı sistemlər) iştirakı ilə,

Katalitik oksidləşmə və ya fotokatalitik metodlarla.

Reaksiyalar laboratoriya şəraitində qarışdırıcı və temperatur nəzarəti olan şüşə reaktorda aparılmışdır. İlkin mərhələdə temperatur intervalı orta diapazonda saxlanılmış, reaksiya müddəti isə sabit götürülmüşdür.

Müxtəlif metilləşdirici reagentlərin naftollarla reaksiyasının ilkin mərhələdə öyrənilməsi və onların selektivlik xüsusiyyətlərinin təhlili edilməsi zamanı seçilmiş metilləşdirici reagentlərin reaksiyaya daxilolma qabiliyyətinin qiymətləndirilməsi, O- və C-metilləşmə məhsullarının paylanmasının müəyyən edilməsi, temperatur və reaksiya müddətinin ilkin təsirinin araşdırılması, alınmış nəticələrin müqayisəli təhlili öyrənilmişdir [**F. Gholipour**, 2019 ,984–996]

Nəticələr və onların müzakirəsi

Aparılmış müşahidələr göstərmişdir ki, reagentlərin aktivliyi artdıqca reaksiyanın sürəti yüksəlir, lakin selektivlik dəyişə bilər. Daha yumşaq şərtlərdə O-metilləşmə üstünlük təşkil etmiş, daha güclü alkilleşdirici sistemlərdə isə aromatik nüvədə əvəzlənmə ehtimalı artmışdır.

Temperaturun artırılması reaksiyanın sürətini yüksəltsə də, bəzi hallarda yan məhsulların əmələ gəlməsinə səbəb olmuşdur. Aşağı temperaturda isə reaksiya daha selektiv, lakin daha ləng getmişdir.

Metanol əsaslı sistemlərdə katalizatorun rolu xüsusi əhəmiyyət kəsb etmişdir. Turşuluq dərəcəsi artdıqca C-metilləşmə meyli güclənmişdir. Bu fakt hidroksil qrupunun protonlaşması və aromatik sistemin aktivləşməsi ilə izah oluna bilər.

Təkliflər:

1. Gələcək tədqiqatlarımızda metilləşdirici reagentlərin selektivliyinin müqayisəsi tövsiyyə olunur.
2. Temperaturun selektivliyə təsirinin araşdırılması, baza və həlledici amilinin rolunun öyrənilməsi tövsiyyə olunur.
3. “Yaşıl kimya” yanaşmasının tətbiqi qarşıya qoyulan məqsədlərimizdəndir.

İstifadə olunmuş ədəbiyyat

1. **M. Selva & A. Perosa**, Green Chemistry, 2008, Vol. 10, pp. 457–464 — Green chemistry metrics: a comparative evaluation of dimethyl carbonate, methyl iodide, dimethyl sulfate and methanol as methylating agents.
2. **P. Tundo, A. E. Rosamilia & F. Aricò**, J. Chem. Educ., 2010, Vol. 87 (11), pp. 1233–1235 — Methylation of 2 Naphthol Using Dimethyl Carbonate under Continuous Flow Gas Phase Conditions.
3. **F. Gholipour**, Global Perspectives on Science, 2019 pp. 984–996— Efficient and selective microwave assisted O methylation of phenolic compounds using tetramethylammonium hydroxide (TMAH);

$HoSbTe_3$ VƏ $HoBiTe_3$ BİRLƏŞMƏLƏRİNİN ELEKTRİKKEÇİRİCİLİYİNİN VƏ TERMOELEKTRİK XASSƏSİNİN TEMPERATURDAN ASILILIĞI

Nərmin Məmmədova[1], Fuad Sadıqov[1],
Teymur İlyaslı[1], Yasin Cəfərov[1], Ç.I.Abilov[2]
[1]Bakı Dövlət Universiteti
[2]Azərbaycan Texniki Universiteti
Bakı, Azərbaycan
narmin-mammadova91@mail.ru

Xülasə - Holmium tərkibli üçlü tellurid birləşmələr $HoSbTe_3$ və $HoBiTe_3$ dolayı bərk faza üsulu ilə sintez edilmiş və onların elektrik keçiriciliyi və Zeebek əmsalı 300–850 K temperatur intervalında tədqiq edilmişdir. Bu tədqiqatın məqsədi temperaturdan asılı daşıyıcı mexanizmləri qiymətləndirmək və məxsusi keçiricilik sahəsinə əsaslanaraq qadağan olunmuş zona dəyərlərini müəyyən etmək olmuşdur. Ölçmələr göstərmişdir ki, elektrik keçiriciliyi üç fərqli sahəni əhatə edir: aşqar, keçid və məxsusi keçiricilik. Məxsusi keçiricilik sahəsinin Arrenius analizi $HoSbTe_3$ üçün ΔE=0,22 eV, $HoBiTe_3$ üçün isə ΔE=0,17 eV olduğu müəyyən edilmişdir. Zeebek əmsalının mənfi olması hər iki birləşmənin n-tip keçiriciliyini və əsas yükdaşıyıcıların elektron olduğunu təsdiqləyir. Zeebek əmsalının 600–650 K temperaturuna qədər artması və daha yüksək temperaturlarda azalması məxsusi daşıyıcıların artması ilə izah olunur. Nəticələr göstərir ki, $HoSbTe_3$ birləşməsi $HoBiTe_3$ birləşməsinə nisbətən daha geniş qadağan olunmuş zona və termal sabitliyə malikdir. Bu birləşmələr orta temperaturlu termoelektrik tətbiqlər və istifadə olunmayan istilik enerjisinin bərpası üçün perspektivlidir.

Açar sözlər: termoelektrik materiallar; elektrik keçiriciliyi; qadağan olunmuş zona

Giriş

Termoelektrik materiallar istiliyi birbaşa elektrik enerjisinə çevirir və istifadə olunmayan istilik enerjisinin bərpası üçün geniş tədqiq olunur [Goldsmid, 2010, Rowe, 2006, Snyder & Toberer, 2008, 1–3]. Bi_2Te_3 və Sb_2Te_3 kimi laylı quruluşlu telluridli birləşmələri otaq temperaturuna yaxın yüksək termoelektrik effektivliyə malikdirlər, çünki onlar mürəkkəb zona quruluşuna malikdirlər.

Enerji səmərəliliyinin artırılması və istifadə olunmayan istiliyin elektrik enerjisinə çevrilməsi qlobal miqyasda enerji təhlükəsizliyi və iqlim dəyişmələri ilə mübarizə baxımından prioritet istiqamətlərdəndir. Bu baxımdan təqdim

olunan tədqiqat aşağıdakı dayanıqlı İnkişaf Məqsədləri ilə birbaşa əlaqəlidir: United Nations tərəfindən qəbul edilmiş DİM 7–Əlçatan və Təmiz Enerji, DİM 9–Sənaye, İnnovasiya və İnfrastruktur, DİM 13-İqlim Dəyişikliyi ilə Mübarizə.

İkili telluridlərin nadir torpaq elementləri ilə modifikasiyası zona disperseyasına, daşıyıcı konsentrasiyasına və keçiricilik mexanizmlərinə əhəmiyyətli təsir göstərə bilər [Pei, 2011, Bell, 2008, 4-5]. Bu dəyişikliklərin öyrənilməsi termoelektrik performansın optimallaşdırılması üçün vacibdir.

Bu işdə $HoSbTe_3$ və $HoBiTe_3$ birləşmələrinin temperaturdan asılı elektrik keçiriciliyi və Zeebek əmsalı araşdırılmışdır. Xüsusi diqqət qadağan olunmuş zona qiymətinin müəyyənləşdirilməsi və keçiricilik mexanizminin mərhələli keçidinə verilmişdir.

Eksperimental hissə

$HoSbTe_3$ və $HoBiTe_3$ birləşmələri yüksək təmizlikli elementlərdən dolayı bərk faza reaksiyası üsulu ilə sintez edilmişdir. Sintez edilmiş nümunələr homogenləşdirilmiş və faz sabitliyinin təmin edilməsi üçün termiki emal edilmişdir. [Shelimova et al., 2002, 146–150]

Elektrik keçiriciliyi (σ) və Zeebek əmsalı (α) 300–850 K temperatur intervalında kompensasiya üsulu ilə yüksək həssaslı R-307 potensiometr cihazının köməyi ilə ölçülmüşdür.

Nəticələr və onların müzakirəsi

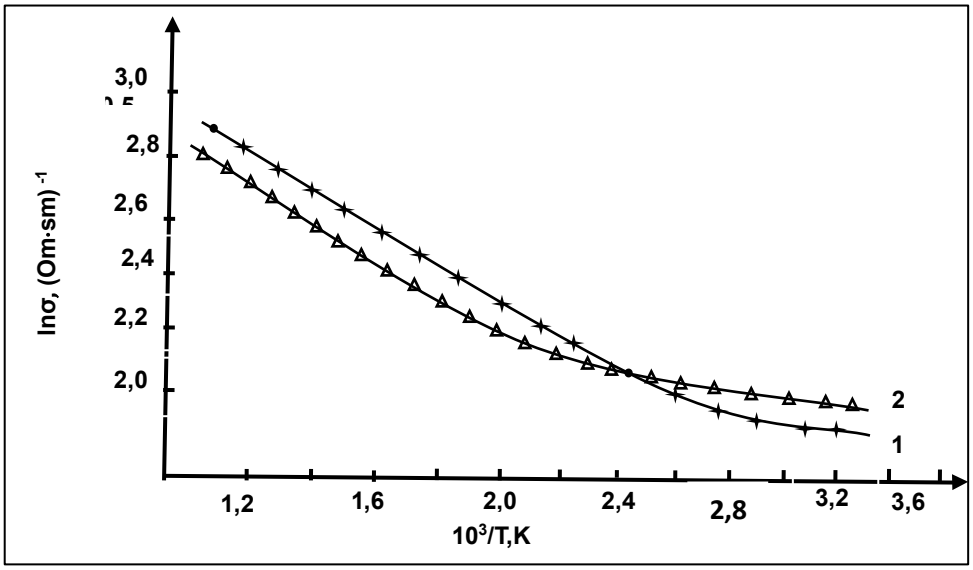
Temperaturdan asılı olaraq elektrik keçiriciliyi üç xarakterik sahə göstərir. 300–450 K intervalında keçiricilik temperaturdan zəif asılıdır və aşqar keçiricilik sahəsinə uyğundur; burada defektlər və stexiometriya pozuntularından yaranan daşıyıcılar dominantdır [United Nations, 2015, 1–4].

450–650 K intervalında keçid sahəsi müşahidə olunur; burada həm aşqar, həm də məxsusi daşıyıcılar keçiriciliyə təsir göstərir.

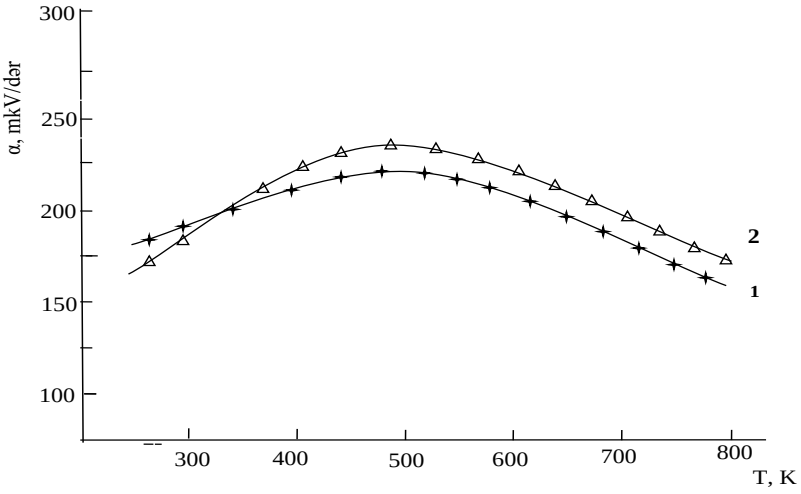
650 K-dən yuxarı temperaturda elektrik keçiriciliyi eksponensial olaraq artır ki, bu da məxsusi keçiriciliyin dominant olduğunu göstərir.

Hesablanmış dəyərlər: $\Delta E_{(HoSbTe_3)}$=0,22 eV, $\Delta E_{(HoBiTe_3)}$=0,17 eV müqayisə üçün, Sb_2Te_3 və Bi_2Te_3 üçün ədəbiyyatdakı qadağan olunmuş zona dəyərləri müvafiq olaraq 0,19 eV və 0,15 eV-dir.

Termo-e.h.q. əmsalının 500–550 K temperaturuna qədər artır və daha yüksək temperaturlarda azalır ki, bu da məxsusi daşıyıcıların artması ilə izah olunur.



Şəkil 1. $HoSbTe_3$ (1) və $HoBiTe_3$ (2) birləşmələrinin elektrik keçiriciliyinin temperaturdan asılılığı.



Şəkil 2. $HoSbTe_3$ (1) və $HoBiTe_3$ (2) birləşmələrinin termo-e.h.q. əmsalının

Təkliflər

Alınmış nəticələr göstərir ki, hər iki material n-tip keçiricilik göstərir və orta temperaturlu termoelektrik tətbiqlər üçün perspektivlidir. Bu nəticələr istifadə olunmayan istilik enerjisinin bərpası və davamlı enerji texnologiyaları üçün əhəmiyyətlidir. [IEA, 2023, IRENA, 2023, UNDP, 2022]

Ədəbiyyat

1. [Goldsmid, 2010, 120-125] Goldsmid, H.J. Introduction to Thermoelectricity, Springer, 2010, 250 s.
2. [Rowe, 2006, 15–20] Rowe, D. M. (Ed.). Thermoelectrics Handbook: Macro to Nano. CRC Press, Boca Raton, 2006.
3. [Snyder & Toberer, 2008, 105–110] Snyder, G. J., & Toberer, E. S. "Complex thermoelectric materials." Nature Materials, 7 (2008): 105–114.Heremans, J.P.; Thrush, C.M.; Morelli, D.T. Thermopower enhancement in lead telluride nanostructures, Physical Review B, 2004, 70, 115334, https://doi.org/10.1103/PhysRevB.70.115334
4. [Pei, 2011, 66–69]Pei, Y.; Shi, X.; LaLonde, A.; Wang, H.; Chen, L.; Snyder, G.J. Convergence of electronic bands for high performance thermoelectrics, Nature,Pei, 2011, 473, s.66–69, https://doi.org/10.1038/nature09996
5. [Bell, 2008, 1457-1461]Bell, L.E. Cooling, heating, generating power, and recovering waste heat with thermoelectric systems, Science, 2008, 321, s.1457–1461, https://doi.org/10.1126/science.1158899
6. [Shelimova et al., 2002, 146–150] Shelimova, L. E., et al. "Phase equilibria in rare-earth–bismuth–tellurium systems." Journal of Alloys and Compounds, 340 (2002): 146–152.
7. [United Nations, 2015, 1–4] United Nations. Transforming our world: The 2030 Agenda for Sustainable Development. New York, 2015.
8. [IEA, 2023, 1–5] International Energy Agency. Energy Efficiency 2023. Paris, 2023.
9. [IRENA, 2023, 1–5] International Renewable Energy Agency. World Energy Transitions Outlook 2023. Abu Dhabi, 2023.
10. [UNDP, 2022, 1–10] United Nations Development Programme. Human Development Report 2022. New York, 2022.

OBTAINING FOAM EXTINGUISHERS BASED ON PMS-10 AND ETHANOL AND STUDYING THEIR EFFECT ON FOAM STABILITY

[1]Makhmudov Mukhtor Jamolovich, [2]Nematov Khusan Ibodullayevich, [2]Shoymardonov Olmasbek Bolta ogli
[1]Bukhara State Technical University
[2]Karshi State Technical University
e-mail: makhmudov.mukhtor@inbox.ru

Annotation. Gas cleaning systems foam suppressors are specialized chemical reagents used to prevent and eliminate foaming in wet gas cleaning equipment. In absorption units, scrubbers, foam apparatuses, and biofilters, the formation of persistent foam can lead to a decrease in the efficiency of capturing pollutants, an increase in hydraulic resistance, the outflow of liquid with the purified gas, and a disruption of the stability of the technological regime.

Keywords: natural gas, methane, ethane, propane, butane, sulfur, hydrogen, nitrogen, helium, carbon monoxide, associated gases

Introduction. A sharp increase in global demand for natural gas requires an increase in their production and processing capacities, as well as the introduction of modern technologies. Natural gases contain acidic components (H_2S, CO_2, CO, CS_2), which must be separated from the natural gas [Aripdjanov, 2024, 42-47]. For this purpose, amines, in particular a

solution of MDEA, are widely used to this day. Although the purification of amines from acidic components in natural gas has many advantages, they also have disadvantages [Dzhamolovich, 2024, 85-88; 3]. Foam is formed during gas purification processes using amines, which negatively affects the efficiency of gas purification and gas quality. Therefore, scientific research aimed at obtaining anti-foaming agents for the formation of natural gas purification units using amines, in particular MDEA, is of particular importance [Mukhtor, 2024, 21-22].

Global capacity for the extraction and processing of sulfurous natural gas has increased by 15% over the past 10 years [MJ, 2024, 120-125]. The number of devices for purifying gases from acidic components using alkanoamines is also increasing. In this case, the formation of foam in absorption purification units of amine solutions causes significant problems in industrial installations [Makhmudov, 2023, 63-65]. Foaming in gas purification units leads to the release of gas and absorbent, loss of absorbent, a decrease in the degree of gas purification from acidic components, and a decrease in the power of the unit. Foaming of alkanoamines is a complex problem arising as a result of the formation of surfactants in an amine solution under the influence of various external and internal factors. Therefore, special attention is paid to the production and application of antifoaming agents in gas purification units with alkanoamines [Dzhamolovich, 2024, 21-22].

Research objects and methods. In obtaining anti-foaming agents formed during the processes of absorption purification of gases from acidic components using MDEA, PMS-10, 96% ethyl alcohol, zeolite NaA, 33% hydrochloric acid, monoethanolamine, sulfanol, and water were selected as the object of research.

To assess the foaming properties of amine solutions and the anti-foaming effectiveness of various foaming agents, tests were carried out on an experimental setup shown in Figure 1. This device was developed by VNIIGAZ in 1995 under the name "Absorbents for cleaning gases from acidic components. Methodology for Determining Foam Characteristics" [Thitakamol, 2009, 1381-1386].

Assessment of the influence of various absorbents, foam suppressants, and various mixtures on the foaming properties of absorbents was carried out on a large bubbler with a capacity of 1000 cm^3 and a filter device installed on it, the general view of which is shown in Fig. 1.

The main controlled indicators in these experimental tests are the foaming properties of the absorbents, i.e., amines - foam height and foam stability (foam lifespan). Through these experimental tests, the properties of pure and working absorbent samples were compared during the purification of natural gases from acidic components, which served as a basis for assessing the degree of contamination of absorbents with various

technological mixtures (hydrocarbons, surfactants, mechanical particles, thermostable salts, corrosion inhibitors, etc.); assessment of the effectiveness of the operation of carbon and mechanical filters in gas purification units; assessment of such indicators as gas purification quality.

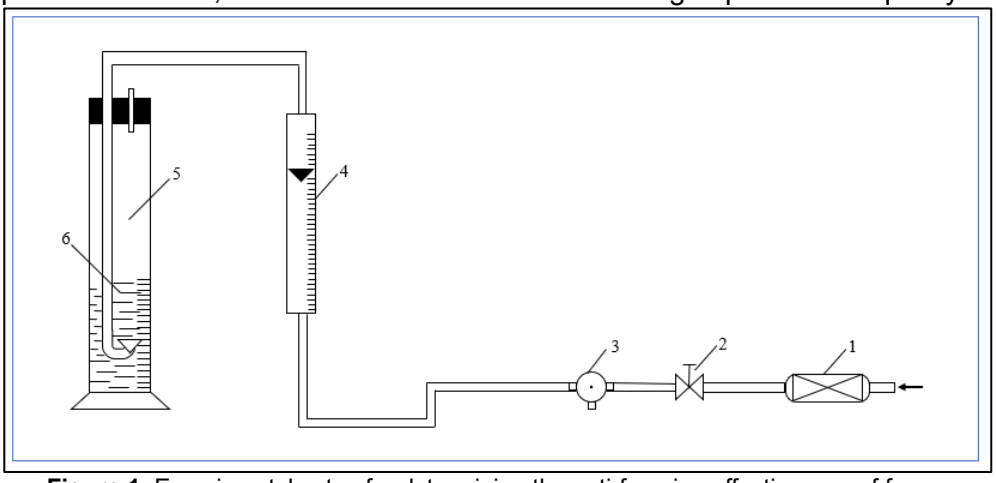


Figure 1. Experimental setup for determining the anti-foaming effectiveness of foam suppressors: 1 - filter for air drying, 2 - air flow regulator, 3 - three-way valve, 4 - rheometer, 5 - cylinder, 6 - air filter-disperser

Antifoaming agents formed during the absorption purification of gases from acidic components using MDEA were obtained based on such reagents as PMC-10, 96% ethyl alcohol, zeolite NaA, hydrochloric acid, monoethanolamine, sulfanol, water according to the methodology described in Chapter II, and the composition of the obtained foaming agents is presented in Table 1.

Table 1. Chemical composition of antifoaming agents formed during the processes of absorption purification of gases using acidic components using MDEA

№	Name of foam suppressor	Foam suppressant composition, g						
		PMS-10	Ethanol	NaA	HCl	MEA	Sulfanol	Water
1	GTKS-1	25,0	55,0	3,0	10,0	4,8	1,0	1,2
2	GTKS-2	27,0	50,0	4,0	11,0	5,0	1,0	2,0
3	GTKS-3	30,0	47,0	5,0	12,0	5,3	-	0,7
4	GTKS-4	33,0	45,0	6,0	10,0	4,8	0,8	0,4
5	GTKS-5	35,0	42,0	7,0	11,0	5,0	-	-
5	GTKS-6	40,0	35,0	8,0	10,0	5,0	1,0	1,0

The anti-foaming agents formed during the processes of absorption gas purification using acidic components using MDEA are conventionally called GTKS (gas purification foam suppressors).

At the next stage of scientific research, the influence of GTKS type foam suppressors on foam stability was investigated. In this case, foam suppressants can be used on an industrial scale if they show foam decomposition indicators for up to 60 minutes. In these studies, foaming agents GTKS-4, GTKS-5, and GTKS-6 were selected.

The results of the influence of the GTKS-4 foam suppressor on foam stability are presented in Table 2.

Table 2. Results of the influence of the GTKS-4 foam suppressor on foam stability

Concentration of GTKS-4 foam suppressant, mg/	Foam quenching time at contact of foaming agent and foaming agent, min											
	5	10	15	20	25	30	35	40	45	50	55	60
0,2	109	104	101	97	94	89	81	79	75	71	68	65
0,4	95	90	87	85	81	78	75	71	67	64	62	60
0,6	82	79	77	74	70	67	63	60	55	50	48	45
0,8	70	67	65	62	57	55	51	49	45	42	40	34
1,0	59	55	53	50	48	45	42	38	36	34	31	12
1,2	45	41	38	34	30	27	24	23	20	14	2	0
1,4	34	32	30	27	24	22	19	12	5	0	0	0
1,6	25	21	19	16	14	8	4	0	0	0	0	0
1,8	18	15	14	11	7	0	0	0	0	0	0	0
2,0	5	4	2	0	0	0	0	0	0	0	0	0

The results of the influence of the GTKS-4 foam suppressant on foam stability showed that at a concentration of 1.2 mg/l, it takes 60 min., at a concentration of 1.4 mg/l - 50 min., at a concentration of 1.8 mg/l - 30 min., and at a concentration of 2.0 mg/l - 20 min.

At the next stage of scientific research, the influence of the GTKS-5 foam suppressor on the foam stability of the MDEA model solution was determined, and the obtained results are presented in Table 3.

Table 3. Results of the influence of the GTKS-5 foam suppressor on foam stability

Concentration of GTKS-5 foam suppressant, mg/l	Foam quenching time at contact of foaming agent and foaming agent, min											
	5	10	15	20	25	30	35	40	45	50	55	60
0,2	105	100	95	91	88	84	80	75	71	68	65	61
0,4	88	85	80	78	75	70	67	63	60	57	54	52
0,6	74	70	67	65	61	55	51	48	46	43	40	37
0,8	65	63	58	54	50	47	42	37	35	22	16	3
1,0	52	48	45	43	40	35	32	22	17	3	0	0

1,2	41	37	34	31	27	18	14	0	0	0	0	0
1,4	30	24	20	9	3	0	0	0	0	0	0	0
1,6	22	15	11	0	0	0	0	0	0	0	0	0
1,8	12	2	0	0	0	0	0	0	0	0	0	0
2,0	0	0	0	0	0	0	0	0	0	0	0	0

The results of the change in the stability of the foam in contact with the foaming agent and foaming agent at different concentrations on the foam stability of the MDEA model solution of the foaming agent GTKS-5 showed that at a concentration of 1.0 mg/l, the foaming agent GTKS-5 requires 55 minutes for foam decomposition, at an increase in the concentration of 1.4 mg/l - 30 minutes for foam destruction, and at a concentration of 2.0 mg/l - 5 minutes.

Studies to determine the influence of the contact time of the foam suppressant and the foaming agent on the foam suppressant concentration were completed by determining the effectiveness of the GTKS-6 foam suppressant, and the obtained results are presented in Table 4.

Table 4. Results of the influence of the GTKS-6 foam suppressor on foam stability

Concentration of GTKS-6 foam suppressant, mg/l	**Foam quenching time at contact of foaming agent and foaming agent, min**											
	5	**10**	**15**	**20**	**25**	**30**	**35**	**40**	**45**	**50**	**55**	**60**
0,2	100	93	88	85	79	75	71	67	62	55	50	42
0,4	82	75	70	68	62	58	55	49	45	38	32	22
0,6	68	62	58	55	48	45	40	30	22	6	0	0
0,8	54	50	45	40	35	30	25	8	0	0	0	0
1,0	43	38	32	28	20	5	0	0	0	0	0	0
1,2	30	27	20	14	0	0	0	0	0	0	0	0
1,4	18	12	4	0	0	0	0	0	0	0	0	0
1,6	7	0	0	0	0	0	0	0	0	0	0	0
1,8	0	0	0	0	0	0	0	0	0	0	0	0
2,0	0	0	0	0	0	0	0	0	0	0	0	0

Studies to determine the influence of the contact time of the foam suppressant and the foaming agent on the concentration of the foam suppressant The results of the study to determine the effectiveness of the foam suppressant GTKS-6 showed that at a concentration of 0.6 mg/l, the foam destruction time was 55 min., with an increase in the concentration of 0.8 mg/l, the foam destruction time was 45 min., at a concentration of 1.6 mg/l - 10 min., and at a concentration of 1.8 mg/l - 5 min.

The above results of determining the dependence of the contact time of the foaming agent and the foaming agent on the concentration of the foaming agent, based on the foam generated at gas processing plants, create the basis for choosing the necessary concentration based on the time required for foam destruction.

Conclusion.

The use of a foam suppressant in gas purification systems is technologically and economically justified when persistent foaming is present. The correct selection of the reagent ensures the stable operation of the equipment, increases cleaning efficiency, and reduces operational risks.

Foam suppressors in gas cleaning systems are used to prevent and destroy foam that forms when gas comes into contact with liquid (scrubbers, absorbers, biofilters, etc.). Below are the main conclusions on the use of foam suppressant in gas cleaning:

Technological necessity:

- Foam formation reduces mass transfer efficiency.
- Foam causes liquid to be carried away into the gas flow.
- Pressure fluctuations and equipment malfunction are possible.
- In severe cases - emergency stops.

References

[1] Aripdjanov, Oybek Yusupdjanovich; Khayrullaeva, Diyora Zokhid qizi; and Abdumuminov, Jonibek Avazek ogli (2024) "MAIN PROSPECTS OF NATURAL GAS PURIFICATION TECHNOLOGIES FROM ACIDIC COMPOUNDS," Technical science and innovation: Vol. 2024: Iss. 2, Article 2. DOI: https://doi.org/10.59048/2181-1180.1546

[2] Dzhamolovich, M. M., & Ugli, Y. S. A. (2024). Selection of a Method For Preparing Natural Gas For Transportation By Main Gas Pipelines. *Austrian Journal of Technical and Natural Sciences*, (1-2), 85-89.

[3] https://ciep.energy/media/pdf/uploads/Book_Natural_Gas_in_the_Netherlands .pdf

[4] Mukhtor, M., & Bobojon, J. (2024). The main directions of work on improving technology for the prevention of the formation of man-made hydrate. *Universum: технические науки*, *12*(11 (128)), 21-22.

[5] MJ, M., & Jumaboev, B. O. (2024). THE MAIN DIRECTIONS OF WORK ON IMPROVING TECHNOLOGY FOR THE PREVENTION OF THE FORMATION OF MAN-MADE HYDRATE. *Химическая технология*, *49*(11), 128.

[6] Safronov, Alexander. (2025). A Few Notes Regarding Origin of Diamonds, Water, Natural Gas and Oil. Open Journal of Geology. 15. 309-330. 10.4236/ojg.2025.156015.

[7] Makhmudov, M., Nematov, H., & Rizayev, S. (2023). Mechanism of Absorption of H_2S, Co_2 and Other Sulfur Components by an Aqueous Solution of MDEA. *Universum: технические науки*, (12-8 (117)), 63-65.

[8] MAKHMUDOV, M., & JUMABOEV, B. THE MAIN DIRECTIONS OF WORK ON IMPROVING TECHNOLOGY FOR THE PREVENTION OF THE FORMATION OF MAN-MADE HYDRATE. *UNIVERSUM*, 21-22.

[9] Bhurisa Thitakamol, Amornvadee Veawab, Adisorn Aroonwilas. Foaming in amine-based CO_2 capture process: experiment, modeling and simulation. / Energy Procedia 1 (2009) 1381–1386. https://doi.org/10.1016/j.egypro.2009.01.181

ДИВЕРГЕНТНЫЙ СИНТЕЗ 6-АЛКИЛ-2-(4-ГИДРОКСИФЕНИЛ)-4-МЕТИЛ-1H-ПИРРОЛО[3,4-C]ПИРИДИН-3(2H)-ОНОВ И ИХ ПРОИЗВОДНЫХ

М.И.Шатирова, Ш.К.Шейдаева, А.Р.Караева, Г.М. Мамедова, С.Ш.Гулиева
Институт Полимерных Материалов Министерства Науки и Образования Азербайджанской Республики, AZ5004, Сумгаит
E –mail:mshatirova@mail.ru

Аннотация: Разработан дивергентный синтетический подход к получению серии 6-алкил-2-(4-гидроксифенил)-4-метил-1H-пирроло[3,4-c]пиридин-3(2H)-онов (**1**, **2**) и их производных (**3**–**12**) с использованием этилового эфира 4-(хлорметил)-2,6-диметилникотината в качестве ключевого интермедиата. Реакции включают нуклеофильное замещение, ацилирование и образование третичных амидов с морфолином. Применение мягких условий, селективность по сложноэфирной группе и минимизация побочных продуктов обеспечивают высокие выходы целевых соединений. Разработанный подход соответствует принципам устойчивой химии: сокращается количество стадий синтеза, повышается атомная экономия, снижается расход реагентов и образование отходов. Полученные соединения представляют интерес для дальнейшей функционализации и создания потенциально биологически активных соединений.

Ключевые слова: этиловый эфир 4-(хлорметил)-2,6-диметилникотината, пирроло[3,4-c]пиридин, п-гидроксианилин, хлорангидриды карбоновых кислот, морфолин, третичные амиды пирролопиридинов, дивергентный синтез

ВВЕДЕНИЕ

Азотсодержащие конденсированные гетероциклы, в частности пирроло[3,4-c]пиридины, являются важным классом органических соединений благодаря сочетанию двух ароматических фрагментов — пиррола и пиридина — и широкому спектру потенциальных свойств и применений. Обзорные работы по синтезу таких систем демонстрируют разнообразие методов, включая классические аннелирования и многоступенчатые стратегии построения гетероциклического ядра [Ершов О.В., 2020]. Кроме того, пирроло[3,4-c]пиридиновые производные проявляют значительную биологическую активность: они исследуются как аналгезирующие и седативные агенты, а также изучаются в контексте антимикробной, противовирусной и противоопухолевой активности [Wójcicka A.,2021]. Разработка устойчивых и эффективных методов их синтеза остаётся актуальной задачей синтетической органической химии. Например, альтернативные подходы к построению пирроло[3,4-c]пиридинового каркаса включают циклизацию и трансформации функционально насыщенных предшественников, что подчеркивает потребность в новых синтетических тактиках [Kharaneko O.I., 2016]. Важным аспектом современных синтетических подходов является соблюдение принципов устойчивой химии, включая атомную экономию, сокращение числа

стадий и минимизацию отходов [Trost B.M.,1991, Anastas P.T., 1998]. Многокомпонентные реакции, включая реакции типа Ugi, также расширяют возможности получения функционально насыщенных гетероциклов, позволяя строить библиотеки структурных аналогов [Li J.J.,2016]. В связи с этим применение дивергентного синтетического подхода для получения производных пирроло[3,4-c]пиридинов является перспективной стратегией, сочетающей структурное разнообразие, оптимизацию условий и повышение устойчивости синтеза.

В данной работе предложен дивергентный путь синтеза 6-алкил-2-(4-гидроксифенил)-4-метил-1H-пирроло[3,4-c]пиридин-3(2H)-онов и их производных, включая сложноэфирные и амидные соединения, с акцентом на мягкие условия и селективность, обеспечивающие высокую эффективность процесса.

ЭКСПЕРИМЕНТАЛЬНАЯ ЧАСТЬ

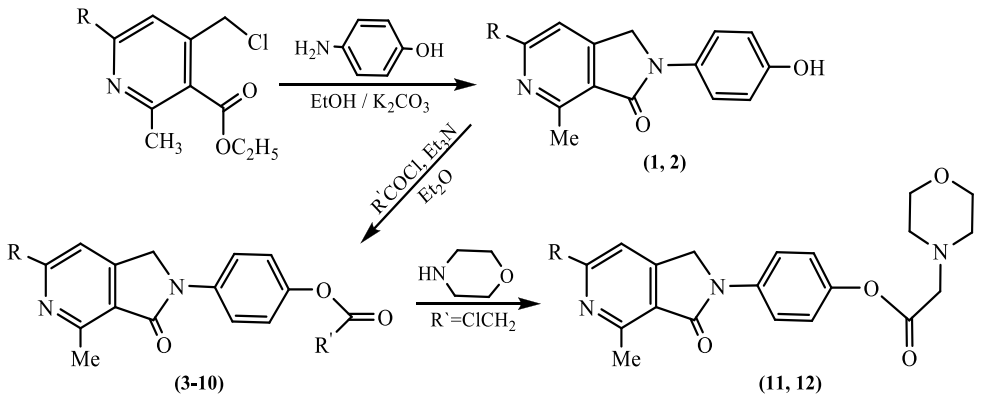
Синтез 6-алкил-2-(4-гидроксифенил)-4-метил-1H-пирроло [3,4-c]пиридин-3(2H)-онов (1, 2). В 20 мл 96% этанола смешивали 1 ммоль соответствующего эфира, 1 ммоль п-гидроксианилина и 0.07 г (0.5 ммоль) безводного K_2CO_3. Смесь нагревали под обратным холодильником в атмосфере аргона при кипении в течение 24 часов. По окончании реакции смесь охлаждали до 20–23°C и выливали в 60 мл 10% водного раствора NaCl. Образовавшийся осадок отфильтровывали, промывали водой и сушили на воздухе при 30–35 °C.

Ацилирование 6-алкил-2-(4-гидроксифенил)-4-метил-1H-пирроло[3,4-c]пиридин-3(2H)-онов (синтез сложных эфиров 3–10). В 50 мл безводного диэтилового эфира растворяли 5 ммоль соединения 3 или 4. При перемешивании добавляли 6 ммоль соответствующего хлорангидрида карбоновой кислоты и 0.7 г (7 ммоль) безводного триэтиламина. Реакционную смесь перемешивали в течение 8 часов при 23 °C. Образовавшийся осадок отфильтровывали и промывали последовательно: 5–10 мл холодного (5–10°C) диэтилового эфира, холодной водой, 5%-ным водным раствором $NaHCO_3$, тёплой водой (45–50°C). После промывки осадок сушили в вакууме. Полученные сложные эфиры очищали низкотемпературной кристаллизацией из смеси диэтилового эфира и гексана.

Синтез третичных амидов пирролопиридина (11, 12). В 50 мл диэтилового эфира растворяли 20 ммоль соединения **7** или **11**. При перемешивании по каплям добавляли 7.2 г (40 ммоль) 25%-ного водного диметиламина при 15–20°C. Реакционную смесь перемешивали в течение 5 часов при 25–30°C. После завершения реакции смесь охлаждали до комнатной температуры, промывали водой (50 мл), отделяли эфирный слой, а водный слой экстрагировали 50 мл диэтилового эфира. Полученные экстракты объединяли и сушили над $MgSO_4$. После удаления растворителя вакуумной дистилляцией остаток перегоняли для получения чистого продукта.

РЕЗУЛЬТАТЫ И ОБСУЖДЕНИЕ

Использование одного ключевого интермедиата — этилового эфира 4-(хлорметил)-2,6-диметилникотината — позволяет получать сразу несколько производных (**1**–**12**) с минимальным числом стадий. Такой подход сокращает расход реагентов, уменьшает образование побочных продуктов и обеспечивает высокую селективность, что соответствует принципам устойчивой химии. В реакции с п-гидроксианилином аминогруппа выступает нуклеофилом, атакует бензильный хлорметильный центр и замещает атом хлора (SN2-механизм). Выходы соединений **1**,**2** составляют 76–84%. Мягкие условия реакции (кипячение в этаноле под обратным холодильником, атмосфера аргона) способствуют высокой селективности и сохранению функциональных групп. Гидроксифенильные пирроло[3,4-c]пиридины ациллированы различными хлорангидридами в присутствии триэтиламина. Механизм: фенольная O-атомная группа атакует карбонильный центр хлорангидрида, образуется тетраэдрический интермедиат, выделяющийся HCl нейтрализуется триэтиламином. Выходы сложных эфиров **3**–**10** составляют 65–80%. Сложные эфиры с хлорметильной группой реагируют с морфолином при 25–30 °C, образуя амидные производные (**11**,**12**) с выходами 72–89%. Механизм реакции включает нуклеофильную атаку морфолина на бензильный хлорметильный центр с одновременной нейтрализацией образующегося хлороводорода.



R=Me (**1**), R=Et (**2**); R=Me, R`=Me (**3**), $CH_2=C(CH_3)$ (4), $ClCH_2$ (**5**), furil (**6**); R=Et, R`=Me (**7**), $CH_2=C(CH_3)$ (**8**), $ClCH_2$ (**9**), furil (**10**); R=Me, R'=$ClCH_2$ (**11**), R=Et, $ClCH_2$ (**12**);

Схема

Для подтверждения структуры полученных соединений были использованы ЯМР- спектроскопия (^{1}H и ^{13}C NMR). Сигналы ароматических протонов фенольной и пирроло[3,4-c]пиридиновой системы подтверждают замещённость и сохранение ядра. Сигналы метильных групп (CH_3) и бензильных протонов соответствуют планируемым

заместителям. Появление полосы в ИК- спектроскопия C=O около 1650–1730 см$^{-1}$ подтверждает образование сложных эфиров и амидов. OH-группы фенолов фиксируются полосой 3200–3500 см$^{-1}$.

Список литературы

1. Ершов О. В., Ершова А. И. Современные методы синтеза пирроло[3,4-c]пиридин-1,3-дионов. *Chemistry of Heterocyclic Compounds*, Т. 56, № 5, 2020, с. 1234-1252.
2. Anastas P.T., Warner J.C. Green Chemistry: Theory and Practice. Oxford: Oxford University Press, 1998, 155 p.
3. Kharaneko O.I., Petrova N.A., Sidorov V.A. New approach to the synthesis of pyrrolo[3,4-c]pyridines. *Russian Journal of Organic Chemistry,* Vol. 52, No 8, 2016, P. 1123-1132.
4. Li J.J., Gribble G.W. Pyrrole and pyridine heterocycles in modern organic synthesis. Name Reactions for Heterocyclic Chemistry, Springer, 2016. P. 455-500.
5. Trost B.M. The Atom Economy — A Search for synthetic efficiency. *Science*, Vol. 254, No 5037, 1991, P. 1471–1477.
6. Wójcicka A., Redzicka A. An Overview of the Biological activity of pyrrolo[3,4-c]pyridine derivatives. *Pharmaceuticals*, Vol. 14, No 4, 2021, P. 354.

POLİSTİROL TƏRKİBLİ TULLANTILARIN DEPOLİMERLƏŞDİRİLMƏSİ PROSESİNİN TƏDQİQİ VƏ BƏRPA OLUNAN STİROL MONOMERİNİN XASSƏLƏRİNİN ANALİZİ

Babayeva Ülkər, Qarayeva İradə
Sumqayıt Dövlət Universiteti
Sumqayıt, Azərbaycan
ulkarbabayeva02@gmail.com

Xülasə - Polistirol sintetik polimerlər arasında geniş tətbiq sahəsinə malik olmaqla yanaşı, ətraf mühit üçün ciddi problem yaradan tullantı materiallardan biridir. Onun bioloji parçalanmaya davamlı olması plastik tullantıların təbiətdə uzun müddət qalmasına və çirklənmənin artmasına səbəb olur. Bu baxımdan polistirol tullantılarının səmərəli təkrar emalı aktual elmi və texnoloji məsələ kimi çıxış edir. Təqdim olunan tezisdə polistirol tərkibli tullantıların kimyəvi təkrar emal üsullarından biri olan depolimerləşdirilməsi prosesi araşdırılmışdır. Depolimerləşmə nəticəsində əldə olunan əsas məhsul olan stirol monomerinin fiziki-kimyəvi xassələri təhlil edilmişdir. Aparılan eksperimental tədqiqatlar göstərir ki, uyğun temperatur və texnoloji parametrlər seçildikdə stirol monomerinin yüksək çıxımla bərpası mümkündür. Alınan monomerin keyfiyyət göstəriciləri onun yenidən polimer istehsalında istifadəsinə imkan verir (Achilias et al., 2012).

Açar sözlər: Polistirol tullantıları, depolimerləşmə, kimyəvi təkrar emal, stirol monomeri, piroliz

Giriş

Plastik materialların istehsal və istehlak həcminin sürətlə artması nəticə-sində polimer tullantılarının idarə olunması qlobal miqyasda mühüm ekoloji

problemə çevrilmişdir. Polistirol aşağı qiyməti, emal rahatlığı və funksional xüsusiyyətlərinə görə qablaşdırma materiallarında, istilik izolyasiyasında və birdəfəlik istifadə olunan məmulatların istehsalında geniş tətbiq olunur. Bununla yanaşı, onun yüksək kimyəvi və istilik dayanıqlığı ətraf mühitdə uzunmüddətli yığılmaya səbəb olur (Al-Salem et al., 2017).

Polistirol tullantılarının mexaniki təkrar emalı zamanı materialın mexaniki xassələrinin zəifləməsi müşahidə olunduğundan, kimyəvi təkrar emal üsulları daha perspektivli hesab edilir. Kimyəvi təkrar emalın əsas istiqamətlərindən biri olan depolimerləşmə prosesi polimer zəncirinin parçalanaraq ilkin monomerin əldə edilməsinə əsaslanır. Bu yanaşma xammalın dövri istifadəsini təmin etməklə yanaşı, təbii resurslara olan tələbatı da azaldır (Scheirs & Kaminsky, 2006).

Eksperimental hissə

Tədqiqat işində istifadə olunan polistirol tullantıları əvvəlcədən mexaniki üsulla xırdalanmış və xarici çirkləndirici maddələrdən təmizlənmişdir. Depolimerləşmə prosesi laboratoriya tipli reaktorda, oksigensiz mühitdə aparılmışdır. Reaksiya temperaturu 350–500 °C intervalında dəyişdirilmişdir ki, bu aralıq ədəbiyyat məlumatlarına əsasən stirol monomerinin bərpası üçün optimal hesab olunur (Achilias et al., 2012).

Proses zamanı əmələ gələn uçucu məhsullar kondensasiya olunaraq toplanmışdır. Alınan maye fraksiya fraksion distillə üsulu ilə təmizlənmişdir. Stirol monomerinin tərkibi və təmizliyi qaz xromatoqrafiyası metodu ilə müəyyən edilmişdir. Müxtəlif temperatur rejimlərinin məhsul çıxımına və monomerin keyfiyyət göstəricilərinə təsiri müqayisəli şəkildə təhlil olunmuşdur.

Nəticələr və onların müzakirəsi

Eksperimental nəticələr göstərmişdir ki, depolimerləşmə prosesinin səmərəliliyi əsasən temperatur rejimindən asılıdır. 400–450 °C intervalında aparılan proses zamanı stirol monomerinin çıxımı daha yüksək olmuşdur. Temperaturun bu həddən yuxarı qaldırılması yan məhsulların əmələ gəlməsini artırmış və monomerin selektivliyini azaltmışdır .

Əldə olunan nəticələr göstərmişdir ki, proses nəticəsində əsas məhsul kimi stirol monomeri alınmışdır. Onun fiziki-kimyəvi göstəriciləri, o cümlədən qaynama temperaturu və sıxlığı, sənaye standartlarına uyğun olmuşdur. Əsas çirkləndiricilər aromatik karbohidrogenlər kimi müəyyən edilmiş və distillə mərhələsində effektiv şəkildə ayrılmışdır. Alınan nəticələr depolimerləşmə yolu ilə əldə olunan stirolun təkrar polimerləşmə üçün yararlı olduğunu göstərir (Al-Salem et al., 2017).

Təkliflər

1.Depolimerləşmə prosesinin enerji sərfini azaltmaq məqsədilə katalitik sistemlərin tətbiqi tövsiyə olunur (Scheirs & Kaminsky, 2006).

2.Prosesin sənaye miqyasında tətbiqi üçün fasiləsiz reaktor sistemlərinin işlənib hazırlanması gələcək tədqiqatlar üçün perspektivli hesab olunur.

İstifadə olunmuş ədəbiyyat

1. Achilias, D. S., Antonakou, E. V., Roupakias, C., Megalokonomos, P., Lappas, A. A. (2012). *Thermal degradation and chemical recycling of polystyrene.* **Journal of Analytical and Applied Pyrolysis**, 94, 84–90.
2. Al-Salem, S. M., Lettieri, P., Baeyens, J. (2017). *Recycling and recovery routes of plastic solid waste.* **Waste Management**, 29(10), 2625–2643.
3. Scheirs, J., Kaminsky, W. (2006). *Feedstock Recycling and Pyrolysis of Waste Plastics.* Wiley.

YÜKSƏK SIXLIQLI POLİETİLENİN (HDPE) İSTEHSAL PROSESİNDƏ HİDROGEN KONSENTRASİYASİNİN ƏRİMƏ İNDEKSİ VƏ STRUKTUR XASSƏLƏRİNƏ TƏSİRİNİN TƏDQİQİ

Manaflı Zaur, Qarayeva İradə
Sumqayıt Dövlət Universiteti
Sumqayıt, Azərbaycan
manafli_2017@mail.ru

Xülasə - Yüksək sıxlıqlı polietilen (HDPE) müasir polimer sənayesində geniş tətbiq sahəsinə malik əsas materiallardan biridir. Onun fiziki və reoloji xassələri istehsal prosesi zamanı seçilən texnoloji parametrlərdən bilavasitə asılıdır. Bu parametrlər arasında hidrogen konsentrasiyası xüsusi əhəmiyyət kəsb edir, çünki hidrogen polimerləşmə prosesində zəncir köçürücü kimi çıxış edərək polimerin molekulyar quruluşuna təsir. Təqdim olunan tezisdə HDPE istehsalı zamanı hidrogen konsentrasiyasının dəyişməsinin polimerin ərimə indeksi və struktur xassələrinə təsiri araşdırılmışdır. Aparılan tədqiqatlar göstərmişdir ki, hidrogen miqdarının artması ərimə indeksinin yüksəlməsi və molekulyar zəncirlərin orta uzunluğunun azalması ilə müşayiət olunur.

Açar sözlər: HDPE, hidrogen konsentrasiyası, ərimə indeksi, polimer strukturu, polietilen istehsalı

Giriş

Polimer materiallar müasir sənaye sahələrində geniş tətbiq olunmaqla yanaşı, texnoloji baxımdan da daim təkmilləşdirilməkdədir. Yüksək sıxlıqlı polietilen mexaniki möhkəmliyi, kimyəvi davamlılığı və emal rahatlığı ilə seçilərək boru sistemləri, qablaşdırma materialları və texniki məmulatların istehsalında geniş istifadə olunur [Bicerano, 2002, 45–47].

HDPE-nin xassələri polimerləşmə prosesi zamanı temperatur, təzyiq, katalizator növü və hidrogen konsentrasiyası kimi amillərlə formalaşır. Hidrogenin prosesə daxil edilməsi zəncirin böyüməsini məhdudlaşdırır və nəticədə polimerin molekulyar kütləsi azalır [McDaniel, 2010, 88–90]. Bu dəyişiklik birbaşa olaraq ərimə indeksinə təsir göstərir.

Ərimə indeksi polimer ərintisinin axıcılıq qabiliyyətini xarakterizə edən əsas göstəricilərdən biridir və emal texnologiyasının seçilməsində mühüm rol oynayır. Molekulyar kütlənin azalması ilə ərimə indeksinin artması arasında birbaşa əlaqə mövcuddur [Əhmədov, 2021, 1–2]. Bu baxımdan hidrogen konsentrasiyasının ərimə indeksi ilə əlaqəsinin öyrənilməsi aktual elmi və praktiki əhəmiyyət daşıyır.

Eksperimental hissə

Tədqiqat zamanı HDPE nümunələri müxtəlif hidrogen konsentrasiyalarında istehsal olunmuşdur. Prosesin digər parametrləri sabit saxlanılaraq yalnız hidrogen miqdarı mərhələli şəkildə dəyişdirilmişdir. Bu yanaşma hidrogenin polimerin strukturuna və ərimə indeksinə təsirinin daha aydın şəkildə qiymətləndirilməsinə imkan vermişdir [McDaniel, 2010, 92–94].

Alınan nümunələrin ərimə indeksi qəbul olunmuş standartlara uyğun olaraq müəyyən edilmişdir. Eyni zamanda polimerin struktur göstəriciləri, o cümlədən sıxlıq və ümumi morfoloji xüsusiyyətlər qiymətləndirilmişdir. Ölçmələrin etibarlılığını təmin etmək məqsədilə analizlər bir neçə dəfə təkrarlanmış və orta nəticələr əsasında təhlil aparılmışdır.

Nəticələr və onların müzakirəsi

Əldə olunan nəticələr göstərmişdir ki, hidrogen konsentrasiyası HDPE-nin ərimə indeksinə əhəmiyyətli dərəcədə təsir göstərir. Hidrogen miqdarının artması ilə ərimə indeksinin yüksəlməsi müşahidə olunmuşdur. Bu hal polimer zəncirlərinin orta uzunluğunun azalması ilə izah olunur.

Bununla yanaşı, struktur xassələrində də dəyişikliklər qeydə alınmışdır. Hidrogen konsentrasiyasının artması polimerin daha dar molekulyar kütlə paylanmasına malik olmasına səbəb olmuşdur ki, bu da emal prosesində materialın daha sabit davranış göstərməsinə şərait yaradır. Aşağı hidrogen konsentrasiyasında isə ərimə indeksi nisbətən aşağı olmuş və daha uzun zəncirli makromolekullar formalaşmışdır.

Bu nəticələr hidrogen konsentrasiyasının HDPE-nin təyinatına uyğun xassələrinin formalaşdırılmasında effektiv tənzimləyici amil olduğunu göstərir [Əhmədov,2021,2–3].

Təkliflər

1. Müxtəlif tətbiq sahələri üçün hidrogen konsentrasiyası ilə ərimə indeksi arasındakı əlaqənin daha geniş araşdırılması məqsədəuyğundur.

2.Gələcək tədqiqatlarda hidrogen konsentrasiyasının HDPE-nin mexaniki və reoloji xassələrinə təsirinin öyrənilməsi tövsiyə edilir.

İstifadə olunmuş ədəbiyyat

1.McDaniel, M. P. (2010). *High Density Polyethylene Catalysis and Polymerization*. Advances in Catalysis.
2.Bicerano, J. (2002). *Prediction of Polymer Properties*. CRC Press.
3.Əhmədov, R. Ə. (2021). *Polimer materialların reoloji xassələri*. Bakı: Elm.

HEKSILAMMONIUM DODESIL SULFATIN SINTEZI VƏ ONUN SƏTHI AKTIV MADDƏ KIMI TƏTQIQI

İbrahimova Minavər, Xamiyeva Günay, Bağırova Şəfəq,
Quliyeva Təranə, Əzizbəyli Emin
Azərbaycan Respublikası Elm və Təhsil Nazirliyi
akademik Y.H.Məmmədəliyev adına Neft-Kimya Prosesləri İnstitutu, Bakı ş.
gunay.aliyeva199490@gmail.com

Xülasə: Tezis dodesen-1 – in sulfat turşusu ilə qarşılıqlı təsirindən alınan dodesil hidrogen sulfatın heksil aminlə qarşılıqlı təsirindən heksilammonium dodesil sulfatın sintezinə və onun səthi aktiv maddə kimi effektivliyinin araşdırılmasına həsr olunmuşdur. Sintez olunmuş heksilammonium dodesil sulfatın aşağı qatılıqda səthi gərilmə əmsalının 29 mN/m-ə bərabər olduğu müəyyən edilmişdir.

Açar sözlər: dodesen-1, sulfollaşma, alkil hidrogen sulfat, ammonium aklil sulfat

Giriş

Səthi aktiv maddələr (SAM) hidrofil və hidrofob hissələrdən ibarət olmaqla, neft hasilatında, qida sənayesində, kosmetik vasitələrdə, məişətdə və s. sahələrdə geniş tətbiq olunur. Bu tərkiblər su hava sərhədində absorbsiya olunaraq səthi gərginliyi azaldır ki, bu da öz növbəsində emulsiya, dispersiya, köpük əmələ gəlmə və yuma proseslərini asanlaşdırır [1,2].

SAM – lar içərisində sulfonlaşma və sulfolaşma ilə alınan maddələr xüsusi çəkiyə malik olub asanlıqla əldə edilə bilən və gündəlik camaşırxana sahəsində geniş istifadə olunlar. Onlar şərti olaraq sulfolaşdırıcı reagentlərdən istifadə etməklə olefinlərin, aromatik maddələrin və ya uzun zəncirli yağ turşusu törəmələrinin sulfonlaşdırılması yolu ilə alınır.

Bu tərkiblər içərisində olefinlərin sulfatlaşdırılması yolu ilə alınan alkil hidrogen sulfatların sintezi xüsusi əhəmiyyət kəsb edir [3-5]. Alkil hidrogen sulfatlar anion tipli SAM – ın mühüm sinfinə aid olub, yüksək təmizləyici və köpükləndirici qabiliyyətə malikdirlər. Bu birləşmələr yüksək səth aktivliyi, cod sularda davamlılıq və qənaətbəxş bioloji parçalana bilmə xüsusiyyətlərinə malik olduqları üçün sulfonat və digər anion SAM-lara alternativ və ya tamamlayıcı komponent kimi sənaye miqyasında tətbiq perspektivinə malikdirlər. Buna görə də alkil hidrogen sulfatların ammonium duzlarının alınması həm yeni funksional törəmələrin sintezi, həm də effektiv detergent sistemlərin yaradılması baxımından mühüm elmi və praktik əhəmiyyət daşıyır.

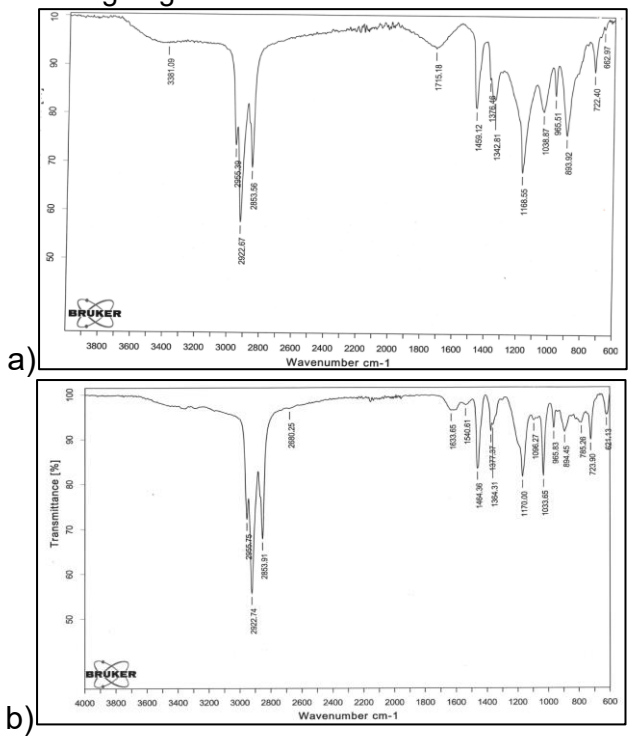
Eksperimental hissə

Sintez prosesi qarışdırıcı, termometr, damcı qıfı ilə təchiz olunmuş üçboğazlı kolbada aparılmışdır. Aparılan tədqiqat zamanı ilk öncə dodesen-1 – in sulfat turşusu ilə qarşılıqlı təsirindən dodesil hidrogen sulfat sintez edilmiş və alınan sulfo birləşmə amin birləşməsi kimi heksil aminlə neyrallaşdırılaraq heksilammonium dodesil sulfat əldə edilmişdir.

Üçboğazlı kolbada dodesen-1 üzərinə damcı qıfından istifadə etməklə, 1:1.3 mol nisbətində 98% - li sulfat turşusu əlavə olunaraq 80°C temperaturda 5 saat müddətində qarışdırılır. Alınan dodesil hidrogen sulfat laylaşır və reaksiyaya daxil olmayan turşu artığı kənarlaşdırılır. Sonrakı mərhələdə əldə olunmuş dodesil hidrogen sulfat neytrallaşdırmaq məqsədilə üzərinə 1:1 mol nisbətində heksil amin əlavə edilərək otaq temperaturunda 8 saat müddətində qarışdırılmaqla neytrallaşdırılır.

Nəticələr və onların müzakirəsi

Sintez olunan dodesil hidrogen sulfat və heksilammonium dodesil sulfatın quruluşları İQ spektroskopik analiz ilə təsdiq edilmişdir (şəkil). Dodesil hidrogen sulfatın İQ spektrində 1038 sm^{-1} və 1168 sm^{-1} SO_2 qrupunun simmetrik və assimetrik valent rəqslərinə, 893 sm^{-1} S – O rabitəsinin və 662 sm^{-1} C – S rabitəsinin valent rəqslərinə uyğun udulma zolaqları ilə xarakterizə olunur ki, bu da müvafiq quruluşu əks etdirir. Dodesil hidrogen sulfatın heksilaminlə reaksiyasından alınan maddənin İQ spektrində müşahidə olunan CH_3 və CH_2 qruplarının C – H rabitələrinin deformasiya (723, 1364, 1377, 1464 sm^{-1}) və valent (2853, 2922, 2955 sm^{-1}), orta intensivlikdə SO_4^{2-} və N^+ – H qrupların valent (615, 1033 2680 sm^{-1}) rəqslərinə uyğun udulma zolaqları reaksiya nəticəsində heksilammonium dodesil sulfatın alındığını göstərir.



Şəkil 1. Sintez olunmuş dodesil hidrogen sulfatın və heksilammonium dodesil sulfatın İQ spektri.

Sintez olunan birləşmənin 0.0001%, 0.001%, 0.01% və 0.1% qatılıqlı suda məhlulları hazırlanmış və səthi gərilmələri ölçmüşdür (cədvəl 1). Cədvəldən göründüyü kimi məhlulun qatılığı artdıqca səthi gərilmə 66.79 mN/m – dən 29 mN/m - ə qədər azalır. Səthi gərilmənin kəskin azalması aşağı qatılılıqda (03) müşahidə olunur ki, bu da kritik misella əmələ gəlmənin bu qatılıqlarda baş verdiyini göstərir.

Cədvəl 1. Sintez olunmuş heksilammonium dodesil sulfatın səthi gərilmə göstəricisinin qatılıqdan asılılığı.

#	Qatılılıq, %	σ_1 (mN/m)	σ_2 (mN/m)
001	0.0001	65.45	65.07
002	0.00025	63.88	62.76
003	0.0005	64.56	65.48
004	0.00075	62.09	61.28
01	0.001	60.51	59.58
02	0.0025	52.88	52.12
03	0.005	40.32	39.05
04	0.0075	39.01	38.57
1	0.01	41.63	41.37
2	0.025	31.66	31.34
3	0.05	31.37	31.20
4	0.075	31.08	30.98
5	0.1	29.90	29.75

Nəticələr göstərir ki, sintez olunmuş alkil sulfat əsaslı ammonium duzu yüksək səthi-aktivlik nümayiş etdirir və məhlulda səthi gərilməni əhəmiyyətli dərəcədə azaldır. Müəyyən edilmiş kritik misel əmələ gəlmə qatılığı və sabit miseləmələgəlmə qabiliyyəti onun yuyucu sistemlərdə effektiv fəaliyyət göstərə biləcəyini göstərir. Əldə olunan göstəricilər maddənin detergent, yağ-çirk çıxarıcı və təmizləyici kompozisiyalarda aktiv komponent kimi tətbiq perspektivini əsaslandırır.

İstinadlar

1. Samy M.Sh., Joohoon K., Dong-Hwan K. Surfactants: Recent advances and their applications, Composites Communications, 2020, v.22, p.100537 https://doi.org/10.1016/j.coco.2020.100537
2. de Groot W. H. (1991). Sulphonation technology in the detergent industry. Kluwer Academic Publisher, ISBN 0-7923-1202-3, Dordrecht, The Netherlands.
3. Roberts D. W. (2001). Manufacture of anionic surfactants. Oleochemical Manufacture and Applications. In: Gustone F. D., & R. J. Hamilton (Eds.), pp. 55-73, Sheffield Academic Press, ISBN 9780849397851, UK
4. Haijiao B., Zimeng W., Zexiang B., Xuejiao S., Lining B., Xu L., Jinxiang D. Isomeric olefin sulfonate surfactants with varied branched hydrocarbon architectures: Effect of the chain branching degree, Chemical Engineering Science, 2025, v. 317, p.122070 https://doi.org/10.1016/j.ces.2025.122070
5. Xu L., Jiaqi L., Xiaohong W., Lijun Y., Hong X., Jinxiang D. Novel branched-chain sulfonate surfactants based on α-olefins from Fischer–Tropsch synthesis via reaction-separation-utilization integrated process, Fuel, 2023, v.2023, p.126961

YENİ XALKON TÖRƏMƏLƏRİNİN SİNTEZİ VƏ QURULUŞUNUN TƏDQİQİ

A.R.Qarayeva[1,2], G.A.Məmmədli[2], M.İ Şatirova[1], G.M.Məmmədova[1], Ş.K.Şeydayeva[1]
[1] Azərbaycan Respublikası Elm və Təhsil Nazirliyinin Polimer Materialları İnstitutu
[2] Sumqayıt Dövlət Universiteti
E-mail: aynur.garayeva@sdu.edu.az

Xülasə. Xalkon törəmələri molekulundakı aktiv ikiqat rabitə və karbonil qrupuna görə zərif üzvi sintezdə mühüm əhəmiyyət kəsb edir. Təqdim olunan tədqiqat işində aromatik aldehidlərin müvafiq metilketonlarla Klayzen-Şmidt kondensləşməsi əsasında yeni funksional əvəzlənmiş xalkon törəmələri sintez edilmişdir. Kondensləşmə reaksiyaları etanol mühitində 40%-li NaOH katalizatorunun iştirakı ilə aparılmışdır. Alınmış birləşmələrin quruluşu İQ və ^{1}H NMR spektral analiz üsulları ilə təsdiqlənmiş, spektrlərdə α,β-doymamış karbonil sisteminə xas olan xarakterik siqnallar alınmış birləşmələrin quruluşunu təsdiq etmişdir.

Açar sözlər: Klayzen-Şmidt kondensləşməsi, xalkonlar, 4-metoksibenzaldehid, 3,4-dimetoksibenzaldehid, aseton, metil-etil keton, p-hidroksifenilason və p-metilfenilasetonun

GİRİŞ

Xalkonlar və onların törəmələri geniş farmakoloji və bioloji aktivliyə malik olduqlarına görə böyük elmi maraq kəsb edir. Bu birləşmələr iltihabəleyhinə, şişəleyhinə, antibakterial, antifungal, antimalyariya, antituberkulyoz və s. bioloji əhəmiyyətli xassələri ilə xarakterizə olunur. Göstərilən farmokoloji xüsusiyyətlərə görə onlar tibb sahəsində bir sıra xəstəliklərin – urək xəstəlikləri, beyin-damar problemləri, mədə yarası, qan laxtalanması, spazma, şəkər və s. müalicəsində istifadə olunan dərman maddələrinin alınmasında əsas xammal kimi geniş miqyasda tətbiq olunur [Chen S., 2023, Rozmer Z., 2014, Zhou B., 2015, Kumar R., 2012]. Xalkonlar və onların törəmələrinin şişəleyhinə aktivliyi bir çox tədqiqatçılar tərəfindən təsdiqlənmişdir [Becker D.M., 2020, Singh P., 2014]. Bu sinif birləşmələr perspektivli terapevtik effektivliyə malik yeni şişəleyhinə preparatların dizaynında mühüm struktur vahidi kimi qiymətləndirilir və insanlarda onkoloji xəstəliklərin müalicəsində əhəmiyyətli komponent hesab olunur. Tibb sahəsində əldə olunan uğurlu nailiyyətlərə və çoxsaylı antibakterial və antifungal preparatların mövcudluğuna baxmayaraq, bakterial, göbələk və virus infeksiyaları hələ də ictimai səhiyyə üçün aktual problem olaraq qalmaqdadır. Bu baxımdan xalkonların və onların törəmələrinin geniş bioloji və kimyəvi xüsusiyyətləri əsas tədqiqat obyekti kimi hər zaman tədqiqatçıların nəzərindədir.

Bunlardan əlavə, müəyyən olunmuşdur ki, xalkonlar üzvi kimya sahəsinin mühüm siniflərindən olan azot tərkibli heterotsiklik birləşmələrin bir sıra nümayəndələrinin – pirimidinlər, pirazolinlər, pirazollar, tiazinlər və s. kimi müxtəlif heterotsikllərin sintezi üçün aralıq məhsul rolunu oynayır [Zhuang C., 2017]. Həyata keçirilən tədqiqatların əsas məqsədi 4-metoksibenzaldehid və 3,4-dimetoksibenzaldehidin müxtəlif əvəzlənmiş asetoketonlarla konden-

sasiya reaksiyasını aparmaqla yeni funksional əvəzlənmiş xalkonların sintezini həyata keçirmək və alınmış birləşmələrdən müvafiq heterotsikllərin sintezi üçün perspektivliyini qiymətləndirməkdir.

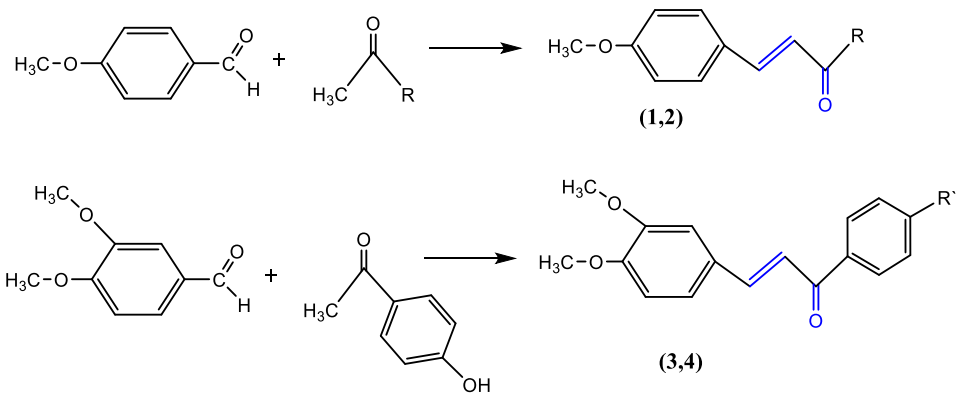
EKSPERİMENTAL HİSSƏ

Xalkonların sintez üsulu (1-4). Xalkon skeleti Klayzen–Şmidt kondensləşməsi reaksiyası əsasında sintez edilmişdir. 100 ml-lik yumuru dibli kolbada 30 ml etanol mühitində 0.1 mmol 4-metoksibenzaldehid və ya 3,4-dimetoksibenzaldehid və 0.1 mmol müvafiq keton əlavə edilərək qarışdırılır. Qarışığa 5 ml 40%-li NaOH məhlulu damcı qıfı vasitəsi ilə hissə-hissə əlavə edilir və reaksiya mühiti 2-3 saat ərzində 10-20°C temperaturda fasiləsiz qarışdırılılaraq davam etdirilir. Daha sonra reaksiya qarışığı soyuducuda gecə boyunca saxlanılır. Əmələ gələn bərk maddə vakuum filtrasiyası ilə süzülür və su ilə yuyulur. Alınmış bərk məhsul qurudulur və etanoldan yenidən Kristallaşdırılır. Aparılan reaksiyalar zamanı sarı rəngli kristal maddələr əmələ gəlir.

NƏTİCƏLƏR VƏ ONLARIN MÜZAKİRƏSİ

Ədəbiyyatdan məlumdur ki, əsasi mühitdə keton törəmələrinin aldehidlərlə qarşılqlı təsiri Klayzen-Şmidt kondensləşməsi adlanır və reaksiya məhsulları olaraq α,β-doymamış karbonil birləşmələri (xalkonlar) əmələ gəlir. Məlumdur ki, xalkonların göstərilən üsul ilə qələvi mühitində sintezi sadə və ucuz şərtlərlə həyata keçirilir, lakin müvafiq optimal şəraitin müəyyən olunması, yəni reaksiyada iştirak edən qələvinin miqdarı və temperatur seçimi reaksiya məhsulunun miqdarınınn artırılması və yan məhsulların (aldol polimerləri) əmələ gəlməsinin qarşısının alınması üçün vacibdir. Bu sistem həmçinin müxtəlif funksional əvəzli heterotsiklik birləşmələrin sintezi üçün perspektivli aralıq məhsulların əldə olunmasında mühüm əhəmiyyət kəsb edir.

4-Metoksibenzaldehidn və 3,4-dimetoksibenzaldehid müxtəlif ketonlarla – aseton, metil-etil keton, *p*-hidroksifenilason və *p*-metilfenilasetonun kondensasiya reaksiyasından müvafiq α,β-doymamış karbonil birləşmələrin sintezinə nail olunmuşdur. Qeyd olunan reaksiyanın mexanizmi, α-hidrogen atomuna malik ketonların qələvinin iştirakında enolyat ionuna çevrilməsi, daha sonra aldehidin karbonil qrupunun karbonuna nükleofil hücumu və nəticədə dehidratasiya mərhələlərindən ibarətdir. Reaksiya mühiti kimi etanol seçilmiş, katalizator olaraq isə NaOH və ya KOH məhlulundan istifadə edilmişdir. Sintez zamanı prosesin gedişinə nazik təbəqəli xromatoqrafiya (NTX) ilə nəzarət olunmuşdur. Reaksiya başa çatdıqdan sonra çökmüş məhsullar süzülərək ayrılmış, vakuum şəraitində qurudulmuş, etanol və ya etanol–su qarışığında yenidən kristallaşdırılmaqla təmizlənmişdir. Alınmış xalkonların 69-79% çıxımla əldə edilmişdir.



R=CH_3, C_2H_5; R`=CH_3, OH

Sxem

Sintez olunmuş birləşmələrin tərkibi və quruluşu element analizi, İQ və ^{1}H NMR spektroskopiya üsulları ilə müəyyən edilmişdir. Birləşmələrin İQ spektrlərində α,β-doymamış ketonlara xas olan –CH=CH– ikiqat rabitənin udma zolaqları v=1530–1528 sm^{-1}, karbonil qrupunun (C=O) intensiv udma zolağı isə 1664–1662 sm^{-1} tezlik intervalında qeydə alınmışdır. Sintez olunmuş xalkonların ^{1}H NMR spektrlərində –CH=CH– qrupuna xas olan iki protonun dublet şəklində siqnalları δ=6.95–7.01 və δ=7.65–7.71 m.h. diapazonunda J ≈ 15–16 Hz spin-spin təsir sabiti ilə müşahidə edilmişdir ki, bu da molekulda ikiqat rabitənin trans-konfiqurasiyada olduğunu təsdiqləyir. Metoksi qruplarına aid siqnallar 3.01–3.65 m.h. oblastında singletlər şəklində qeydə alınmışdır. Aromatik protonların siqnalları isə 6.8–8.0 m.h. intervalında müşahidə edilmişdir. Əldə olunan nəticələr xalkonların α,β-doymamış karbonil sistemini müəyyən edən əsas spektral göstəricilərdir.

ƏDƏBİYYAT SİYAHISI

1. Becker D.M., Oleszek M., Zielinska M, Oleszek W., Chalcones – features, İdentification techniques, attributes, and applications in agriculture. *Molecules*, 2024, Vol. 29, p. 2247
2. Chen S., Zhang M., Feng S., Gong C., Zhou Y., Xing L., He B., Wub Y., Xue W. Design, synthesis and biological activity of chalcone derivatives containing pyridazine. *Arab. J. Chem.,* 2023. Vol. 16, p. 104852
3. Rozmer Z., Perjesi P. Naturally occurring chalcones and their biological activities. *Phytochem. Rev.,* 2014, Vol. 15, p. 87
4. Zhou B., Xing C. Diverse molecular targets for chalcones with varied bioactivities. *Med.Chem.,* 2015, Vol. 5, p. 388
5. Kumar R., Sharma P., Shard A., Tewary D.K., Nadda G., Sinha A.K. Chalcones as promising pesticidal agents against diamondback moth (*Plutella xylostella*): Microwave assisted synthesis and structure-activity relationship. *Med. Chem. Res.* 2012, Vol. 21, p. 922
6. Zhuang C., Zhang W., Sheng C., Zhang W., Xing C., Miao Z., Chalcone: a privileged structure in medicinal chemistry. *Chemical reviews,* 2017, Vol. 117, p. 7762

7. Singh P., Anand A., Kumar V. Recent developments in biological activities of chalcones: A mini review. *Eur. J. Med. Chem.* 2014, Vol. 85, p. 758.
8. Zhuang, C., Zhang, W., Sheng, C., Zhang, W., Xing, C., & Miao, Z. (2017). Chalcone: a privileged structure in medicinal chemistry. Chemical reviews, 117(12), 7762-7810
9. Zhuang, C., Zhang, W., Sheng, C., Zhang, W., Xing, C., & Miao, Z. (2017). Chalcone: a privileged structure in medicinal chemistry. Chemical reviews, 117(12), 7762-7810

SYNTHESIS AND THEORETICAL CALCULATIONS OF 2-(2,4-DICHLOROPHENYL)-4,5-DIPHENYL-1-(4-(PHENYLDIAZENYL)PHENYL)PHENYL)-1 H-IMIDAZOLE

Nargiz Orujova
Scientific supervisor: Doctor of Chemical Engineering, prof. Rena Jafarova
Institute of Petrochemical Processes named after academician Y.H. Mammadaliyev of the Ministry of Science and Education of the Republic of Azerbaijan
Baku, Azerbaijan
E-mail:nargiz.orucova@list.ru

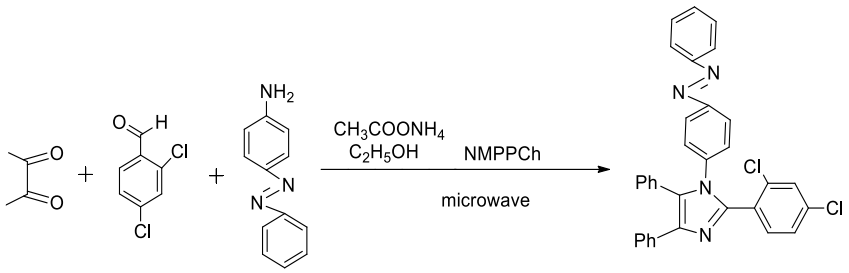
Abstract - The presented thesis material discusses the synthesis and theoretical calculations of 2-(2,4-dichlorophenyl)-4,5-diphenyl-1-(4-(phenyldiazenyl)phenyl)phenyl)-1 H-imidazole in the presence of N-methylpyrrolidone perchlorate catalyst under microwave conditions.

Keywords: Imidazole, microwave, synthesis, ionic liquid catalysts, theoretical calculations, stability

Introduction.

The imidazole nucleus is a constituent of natural compounds such as histidine, histamine, DNA, vitamin B12, purines, and biotin, as well as synthetic drugs such as cimetidine, clemizole, azomycin, nocodazole, dacarbazine, etonitazene, megazole, enviroxime, nitrosoimidazole, and metronidazole. Due to this property, imidazole derivatives are widely used in pharmacology [1,2]. Quantum mechanical calculations, which have become an efficient and simple approach in recent years, make it possible to theoretically investigate new compounds and provide rapid property approximations compared to expensive and time-limited experimental procedures. [3,4].

Experimental part and results. The reaction process is carried out in a microwave oven with a power of 300W. 40 ml of ethanol as a solvent, benzyl (6 mmol), ammonium acetate (6 mmol), p-aminoazobenzene (6 mmol), 2,4-dichlorobenzaldehyde (6 mmol) and a catalyst in a ratio of 10 mol% were added as reagents. N-methylpyrrolidone perchlorate catalyst is taken as a catalyst [5]. The course of the reaction is monitored by TLC. After the reaction is complete, the mixture is poured into ice water, the solid mass is separated by filtration, and recrystallized in ethanol. The reaction time is 26 minutes, the yield is 82.7%. The reaction scheme is as follows:



Synthesis of 2-(2,4-dichlorophenyl)-4,5-diphenyl-1-(4-(phenyldiazenyl)phenyl)phenyl)-1H-imidazole

The structure of the obtained compound was studied by means of ^{1}H-NMR and IR spectroscopy methods. ^{1}HNMR spectrum was taken at room temperature on a 300.18 MHz NMR-Fourier-300 spectrometer manufactured by "BRUKER" company, and IR spectra were recorded on an ALPHA IR-Fourier spectrometer manufactured by "BRUKER" company in the wave number range of 600-4000 cm^{-1}.

2(2,4-Dichlorophenyl)-4,5-diphenyl-1(4-(phenyldiazenyl)phenyl)-1H-imidazole. Empirical formula of substance: $C_{33}H_{22}N_4Cl_2$, Mr=544.23, Melting point: T=168°C.

NMR spectroscopy: ^{1}H-NMR (acetone-d_6δ, m.h.): ^{13}C NMR: 121.85, 122.48, 123.08, 124.35, 126.42, 126.57, 127.79, 128.32, 128.48, 128.6, 128.95, 131.0 4, 131.32, 132.03, 133.35, 135.15, 157.54 (C-Ar), 135.74, 137.45, 153.57, 154.57, 155.76

Infrared spectroscopy: IR (cm^{-1}): v-1701 (C=N), δ-720, 768 (C-H), v-1588 (C-C), v-1653(N=N), v-1308 (C-N) , v-639, 686 (C-Cl).

Ultraviolet spectroscopy: UV: Imidazole absorption band - 224 nm, monoaromatic ring absorption band - 206, 240 nm, azo compounds (–N=N–) – 380 nm. Calculated (%): C 72.66, H 4.07, N 10.27, Cl 13.00, Found (%): C 72.40, H 4.02, N 10.53, Cl 13.05 [6]

Quantum-chemical parameters were calculated using the following formulas according to literature sources [7]:

Change in energy $\Delta E=[I-A]$

Chemical hardness $\eta = \frac{[I-A]}{2}$

Chemical softness $\sigma = \frac{1}{\eta}$

Electronegativity $\lambda = \frac{[I+A]}{2}$

Chemical potential $\mu = -\lambda$

Electrophilicity index $\omega = \frac{\mu^2}{2\pi}$

İonization potential $I = -E_{HOMO}$

Electron affinity $A = -E_{LUMO}$

Table. The value of E_{HOMO}, E_{LUMO}, ΔE, chemical hardness (η), chemical softness (σ), electronegativity (λ), chemical potential (μ), electrophilicity index (ω), ionization potential (I) and electron affinity (A) of the synthesized imidazole

Parameters	Value
E_{HOMO}(eV)	-5.908
E_{LUMO}(eV)	-2.953
ΔE (eV)	2.955
Chemical hardness, (η), (eV)	1.477
Chemical softness (σ), (eV)	0.677
Electronegativity (λ), (eV)	4.431
Chemical potential (μ), (eV)	-4.431
Electrophilicityindex (ω), (eV)	6.644
İonization potential (I), (eV)	5.908
Electron affinity (A), (eV)	2.953

The value of E_{HOMO}, E_{LUMO}, chemical hardness, chemical softness, electronegativity, chemical potential, electrophilicity index, ionization potential and electron affinity of the synthesized imidazole are shown in table. It can be seen from the table that the compound has high stability (ΔE=2.955 eV). Thus, compounds with a large energy difference between the HOMO and LUMO orbitals are more stable. Low chemical hardness and high chemical softness are associated with high reactivity and binding efficiency of the substance. Since these parameters are opposite (η=1.477, σ=0.677 eV) in the studied compound, it can be said that the substance has weak reactivity. Electronegativity is related to electron attraction and reactivity. Chemical potential indicates the possibility of a chemical reaction, a high value of chemical potential (less negativity) indicates easier donation of electrons (electron donor), and a small value of chemical potential (-4.431) indicates easier acceptance of electrons (electron acceptor). Negative chemical potential indicates that the compound does not decompose into elements. Below is the ranking of organic molecules according to electrophilicity; Weak electrophiles have an electrophilicity index of less than 0.8 eV, moderate electrophiles have an electrophilicity between 0.8 and 1.5 eV, and strong electrophiles have an electrophilicity of more than 1.5 eV. It is well known that drugs with a highly electrophilic nature have potent antimicrobial and anticancer properties. The high value of electrophilicity in the studied compound (ω=6.644 eV) indicates its high biological activity. The high value of ionization potential (5.908 eV) is related to chemical stability.

References

1. Verma, A., Joshi, S. & Singh, D. Imidazole: having versatile biological activities. J. Chem. Vol. no. 1, 329412. h t t p s : / / d o i . o r g / 1 0 . 1 1 5 5 / 2 0 1 3 / 3 2 9 4 1 2 (2013). 2013/01/01 2013.
2. Sharma, P., LaRosa, C., Antwi, J., Govindarajan, R. & Werbovetz, K. A. Imidazoles as potential anticancer agents: an update on recent studies. Molecules 26 (14). https://doi.org/10.3390/molecules26144213

3. Muheyuddeen, G. et al. Design, synthesis, and biological evaluation of novel imidazole derivatives as analgesic and anti inflammatory agents: experimental and molecular docking insights. Sci. Rep. 14(1), 23121. h t t p s : / / d o i . o r g / 1 0 . 1 0 3 8 / s 4 1 5 9 8 - 0 2 4 - 7 2 3 9 9 - 8 (2024).
4. Choudhary, V., Bhatt, A., Dash, D. & Sharma, N. DFT calculations on molecular structures, HOMO–LUMO study, reactivity descriptors and spectral analyses of newly synthesized diorganotin(IV) 2-chloridophenylacetohydroxamate complexes. J. Comput. Chem. 40, 2354–2363. https://doi.org/10.1002/jcc.26012 (2019). /10/15 2019.
5. Orujova N.S., Mammadov A.M., Jafarova R.A.,Yolchuyeva U.J., Ahmadbayova S.F. Synthesis and Study of Diphenyl and 4-(Phenyldiazenyl)Phenyl Based Tetrasubstituted İmidazoles in the Presence of İonic Liquid Catalysts. The journal " Processes of Poetrochemistry and oil Refining" (PPOR) , 2023, №2 , 235-245 DOI: https://doi.org/10.36719/1726-4685/94/235-245
6. Microwave- and Ultrasound-Assiste Green Synthesis and Termal Properties of 2-(2,4-Dichlorophenyl)- 4,5-Diphenyl-1(4-(Phenyldiazenyl)Phenyl)-1h-Imidazole. Vagif M. Abbasov, Nargiz S. Orujova, Rena A. Jafarova, Ayaz M. Mammadov, Aygun Z. Aliyeva, Nushaba M. Aliyeva Ppor, Vol. 26, No. 4, 2025, Pp. 1011-1021 . Https://Doi.Org/10.62972/1726-4685.2025.4.1011
7. Vagif M. Abbasov, Nargiz S. Orujova, Rena A. Jafarova, Ayaz M. Mammadov, Saida F. Ahmadbeyova. Synthesis And Theoretical Calculations Of 4[4,5-Diphenyl-1-(4(Phenyldiazenyl)Phenyl)-1h-Imidazol-2-Yl]-Phenol Using Ionic Liquid Catalysts And Microwave Conditions, PPOR, Vol. 25, No. 1, 2024, Pp. 89-97, https://doi.org/10.62972/1726-4685.2024.1.89
8. In vitro, in silico, and DFT evaluation of antimicrobial imidazole derivatives with insights into mechanism of action Nargiz S. Orujova, Vagif M. Abbasov, Rana A. Jafarova, Ayaz M. Mammadov, Imren Bayil, Sevda A. Muradova, Nabila Djadi, Taha Alqahtani, Al-Anood M. Al-Dies, Yayesew Amlaku Zerihun, Abdelkrim Guendouzi, Magdi E. A. Zaki . Scientific reports. 2025, 15(1) Article number: 37723 (2025) DOI: 10.1038/s41598-025-24847-2

ANALYSIS OF THE ISOMERIZATION PROCESS OF LOW-OCTANE GASOLINE

Turakulova Marjona[1]
Associate Professor,
Seyedmeysam Kosari[2]
Associate Professor,
Laziz Saidov[3]
Master degree.
Bukhara State Technical University, Bukhara. Uzbekistan[1-3].
Iran, Petrochemical Industry Engineer[2]
E-mail: marjonaturakulova79@gmail.com

Abstract - This article analyzes the isomerization process in modern automotive gasoline production. The isomerization of light paraffin fractions (n-pentane and n-hexane) plays a key role in improving gasoline quality, particularly in increasing the octane number. The study utilized a $Pt/WO_3/ZrO_2$ catalyst, which is effective in producing high-octane isomers under low temperature and pressure conditions. Isomerization proceeds via a carbocation mechanism, converting n-pentane and n-hexane into iso-paraffins, significantly increasing the octane number. Light gasoline fractions and reformate serve as feedstock. According to the technological scheme, the gas-feed mixture passes through heat exchangers, is heated to 130–170°C, and maintained at a pressure of 3.5 MPa. The reaction occurs in three sequential reactors, yielding 93–97% isomerate. By-product dry gases are utilized as fuel. The results demonstrate that $Pt/WO_3/ZrO_2$ provides high selectivity, low operational costs, and an environmentally friendly process. Research on developing locally produced catalysts is ongoing.

Keywords: gasoline, octane number, isomerization, $Pt/WO_3/ZrO_2$ catalyst, *n*-pentane, *n*-hexane, iso-paraffins, catalytic process, petroleum refining, high-octane gasoline

.

Introduction

Modern automotive gasoline production involves multistage technologies, including primary oil refining, secondary processing (reforming, isomerization, cracking, alkylation), and blending of components. Recent years have seen surging demand for high-quality gasoline, driven by stricter standards like Euro-5. In Uzbekistan's refineries, catalytic reformate remains the primary component for octane enhancement. New environmental requirements necessitate expanding non-aromatic, high-octane gasoline components.

Isomerization of light gasoline fractions is one such process [1]. By converting normal alkanes into branched isoalkanes, isomerization significantly increases gasoline octane numbers while maintaining environmental purity. However, locally produced catalysts (researched by Bukhara State Technical University, the Academy of Sciences Chemistry Institute, and others) are not yet widely adopted industrially.

Exsperimental Section.

Direct isomerization of the pentane–hexane fraction of gasoline is a complex, multi-stage petrochemical process, influenced by numerous factors

affecting both the procedure and its outcome. This process has become widespread in the local oil refining industry due to increasingly stringent quality requirements for petroleum products [2].

The implementation of reactors for isomerization units is carried out in two directions: creating new production capacities or reconstructing gasoline reforming units. This raises a complex problem of selecting optimal reactor designs (number of reactors, sequential or parallel connection of open or closed reactor designs) and catalysts for a particular refinery. The essence of the isomerization process lies in the catalytic conversion of light normal paraffin hydrocarbons into hydrocarbons with the desired isostructure.

The catalytic isomerization process produces high-octane gasoline components, which can also serve as feedstock for the petrochemical industry. As feedstock, n-butane, light fractions obtained from direct distillation with an initial boiling point of 52 °C, and catalytic reformate raffinates containing n-pentane and n-hexane, or mixtures separated during gas fractionation, are used [4].

Currently, bifunctional catalysts containing platinum or palladium are widely employed.

The characteristics of highly efficient catalysts for the isomerization process are presented in Table 1.

Table 1: Catalyst Performance Comparison

Catalyst Type	Octane Boost	Low-Temp Conversion	Isomer Selectivity	Remarks
Zeolites (ZSM-5)	Good	Moderate	High	Low-cost; requires higher temperatures
$Pt/WO_3/ZrO_2$	High	Low	High	Optimal for C_5–C_6 fractions
SO_4^{2-}/ZrO_2	High	Moderate	High	Acidic; lower activity without metal
Metal-modified zeolites	Highest	Efficient	Very High	Combines isomerization/hydroisomerization

The study used $Pt/WO_3/ZrO_2$ due to its efficiency under mild conditions (180–220°C; 2–3.5 MPa).

The operating conditions of the isomerization process can vary over different intervals depending on the catalyst used. In the process, the yield of the isomerate reaches 93–97% by mass, with an octane number of 88–92 (according to the research method). The by-product is dry gas, which is used as fuel [5].

The isomerization unit consists of rectification and isomerization blocks. In the rectification block, the feedstock sent for isomerization is pre-separated into pentane and hexane fractions, after which the resulting product is stabilized to isolate the final isopentane and isohexane. In the isomerization block, the isomerates are obtained.

Figure 1 shows a simplified technological scheme of the isomerization process.

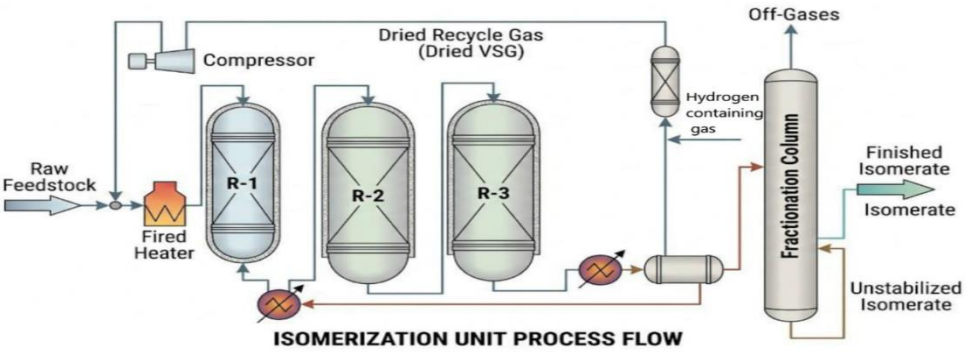


Figure 1: Simplified Isomerization Process Flow Diagram

Result and Discussion. The gas–feedstock mixture passes through heat exchangers and is heated up to 100–120 °C. It then enters a tubular furnace, where it reaches a reaction temperature of 130–170 °C. The pressure must not drop below 27 kgf/cm² [8]. After that, it is directed sequentially through three reactors. The technological regime of the equipment is controlled as follows. The parameters in the columns are presented in Table 2.

Table 2: Industrial Isomerization Conditions

Parameter	Value
Temperature	180–220°C
Pressure	2–3.5 MPa
Feed WHSV*	1.5 hr^{-1}
H_2 recycle ratio	1.25
*Weight Hourly Space Velocity	

Isomerization occurs in the reactors of the catalyst column. For this purpose, a $Pt/WO_3/ZrO_2$ catalyst containing platinum is used for isomerization, employing the technology shown in Figure 1. The reaction in the reactor proceeds as follows [5].

$$\text{n-}C_6H_{14} \xrightarrow{Pt/WO_3/ZrO_2} \text{izo-}C_6H_{14}$$

This converts *n*-pentane → *iso*-pentane (Δ octane: +92 points). Hydrogen-to-*n*-pentane ratio: 3:1.

Conclusion and recommendations.

In the modern automotive gasoline production industry, improving gasoline quality, particularly increasing the octane number, is an important issue. The isomerization process is an effective method for raising the octane number of gasoline by converting light normal alkanes (n-pentane, n-hexane) into high-octane isoalkanes. Studies have shown that the $Pt/WO_3/ZrO_2$ catalyst exhibits high efficiency in producing isomers with high selectivity under low temperature (180–220 °C) and low-pressure conditions [7].

The isomerization process occurs via a carbocationic mechanism, whereby n-pentane is converted to isopentane and n-hexane to isohexane. The technological process consists of rectification and isomerization units, with the feedstock pre-fractionated and then isomerized sequentially in three reactors. In this process, the yield of the isomerate reaches 93–97%, and the octane number rises to 88–92. Dry gases produced as by-products are used as fuel.

References

1. Чупарев Е.В., Гиязов О.В., Зернов П.А., Парпуц О.И. Исследование кинетики процессов изомеризации пентана и гексана // Сборник тезисов научно-технической конференции молодых ученых «Неделя науки - 2013» Санкт-Петербургского государственного технологического института (технического университета), СПб: СПбГТИ(ТУ), 2013. – С. 79-80.
2. Chekantsev N.V., Kravtsov A.V., Ivanchina E.D., Gyngazova M.S. Mathematical modeling of pentane-hexane fraction isomerization process on Si-2 catalys // XVIII International Conference on Chemical Reactors CHEMREACTOR-18 Malta September 29 - October 3, 2008, c 305-306.
3. Маликов И.Д. Каталитическая изомеризация углеводородов в присутствии носителей, модифицированных ионными жидкостями: дис. канд. техн. наук: 05.17.07: защищена 05.07.17 / И.Д. Маликов. – Астрахань, 2011. – 142 с.
4. Patenti: RU 2277526 C1.
5. Patenti: RU 2 748 268 C1.
6. https://pronpz.ru/ustanovki/kat-izomerizatsiya.html
7. To’raqulova M.Q., Ataullayev Sh.N., Boboqulov F.B., Xamidov D.G‘Neft va gaz zavodlaridan chiqayotgan mash’ala gazlarini qayta ishlash texnologiyalasini takomillashtirish .Fan va texnologiyalar taraqqiyoti Ilmiy - texnikaviy jurnal. Buxoro: 2025 yil №1. 11-18 b.
8. To’raqulova M.Q., Boboqulov F.B., Temirov A.H. Vodorod sulfidi saqlagan nordon gazlarni utilizatsiyalashning samarali texnologiyasini ishlab chiqish. Fan va texnologiyalar taraqqiyoti Ilmiy – texnikaviy jurnal. Buxoro: 2025 yil №1. 84-90 b.

ENHANCED ALKYLATION OF PHENOL WITH ISOPRENE CYCLODIMERS USING ZEOLITE-CONTAINING KN-30 CATALYST

U.R. Gurbanova, Ch.K.Rasulov
Academician Y.H. Mammadaliyev Institute of Petrochemical Processes of the Ministry of Science and Education of the Republic of Azerbaijan, AZ 1025, Baku, 30 Khojaly Ave
E-mail:ulviyyagurbanova01@gmail.com

Summary - In this study, the alkylation reactions for synthesising para-[3(4)-methylcyclohexen-3-yl-isopropyl]phenols were examined. The reactions of phenol with 1-methyl-3(4)-isopropenylcyclohexenes were conducted using a novel catalytic system based on the KN-30 zeolite catalyst. The main kinetic parameters — temperature, molar ratio of the reactants, reaction time, and catalyst amount — were systematically analysed, and the optimal conditions were identified. The maximum yields for the alkylation of phenol with diprene, dipentene, and their mixture were 75.7%, 68.9%, and 71.2%, respectively, while the selectivities towards the target products were 92.5%, 85.3%, and 88.5%. The structures and compositions of the obtained products were verified by infrared (IR) and nuclear magnetic resonance (NMR) spectroscopy. Analysis of the experimental results indicates that the KN-30 catalyst demonstrates higher efficiency in the alkylation of phenol with isoprene cyclodimers compared to previously known methods and catalysts.

Keywords: phenol, 1-methyl-3(4)-isopropenylcyclohexenes, alkylation, zeolite catalyst, para-cycloalkylphenols

Introduction

Alkylation reactions are important in the petroleum and organic chemistry industries, especially in the synthesis of alkylphenols. Alkylphenols are commonly used in the manufacture of antioxidants, surfactants, polymer stabilisers, and other valuable organic compounds [1-3].

In recent years, heterogeneous catalysts—particularly zeolite-based systems—have been widely employed in alkylation and other organic transformation processes. The high surface area of zeolites, the variety of their acidic active sites, and their thermal stability greatly enhance their catalytic efficiency.

The aim and novelty of this research consist in investigating, under laboratory conditions, the alkylation reactions of phenol with isoprene cyclodimers (diprene, dipentene, and their mixture) in the presence of the KN-30 zeolite catalyst, determining the optimal reaction conditions, and evaluating the catalytic activity of the system. The study is relevant from both fundamental and applied perspectives and contributes to the development of efficient catalytic systems in line with green chemistry principles.

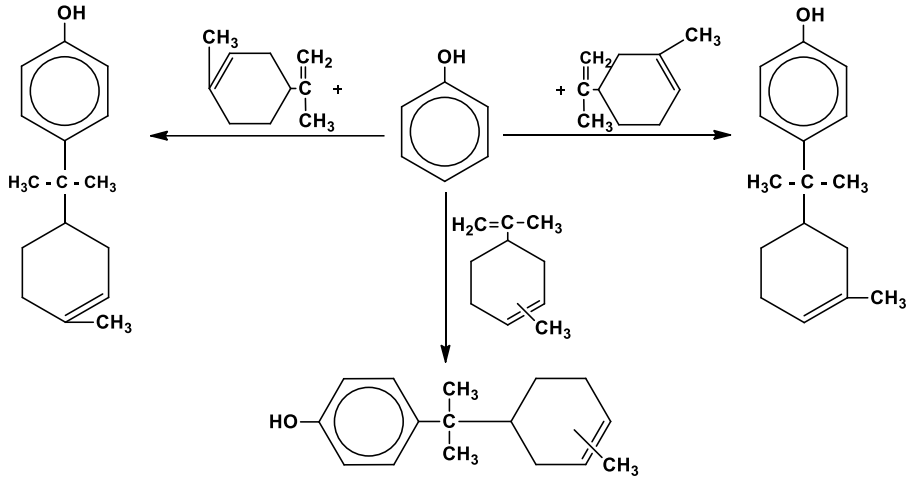
Experimental Section

The following raw materials were used in the production of *para*-Cycloalkylphenols:

1. Phenol: melting point 40 – 42°C; boiling point 182°C; $n_D^{20} = 1.4503$; $\rho_4^{20} = 1.071$ g·sm^{-3}; weight 136; purity 98%.

2. **1-Methyl-3-isopropenylcyclohexene (DP):** boiling point 160–161°C; $n_D^{20} = 1.4656$; $\rho_4^{20} = 0.8347$ g·sm⁻³; weight 136; purity 98%.
3. **1-Methyl-4-isopropenylcyclohexene (DPT):** boiling point 174–175 °C; $n_D^{20} = 1.4745$; $\rho_4^{20} = 0.8476$ g·sm⁻³; weight 136; purity 96.8%.
4. **1-Methyl-3(4)-isopropenylcyclohexene (ICD):** boiling point 160–180 °C; $n_D^{20} = 1.4735$; $\rho_4^{20} = 0.8458$ g·sm⁻³; weight 136.

The alkylation reaction equations of phenol with isoprene cyclodimers are presented below:



The alkylation reaction is carried out in a 250 mL three-neck round-bottom flask equipped with a mechanical stirrer, a heating device, a dropping funnel, and a thermometer. The reactants are weighed in advance using a laboratory balance. Phenol is first introduced into the flask, followed by the addition of activated and partially ground KN-30 catalyst. The reaction mixture is heated to 40–45°C, and at this temperature, the alkylating agent is introduced into the system through the dropping funnel. The reaction is then conducted at 80–140°C for 4–6 hours.

After the reaction is complete, the mixture is cooled to 40°C, and the catalyst is separated by filtration. The resulting reaction mixture is subjected to rectification; first, the unreacted components are removed at atmospheric pressure up to 200°C. Then, the remaining crude product is distilled under reduced pressure (10 mm Hg) to obtain the target products – *para*-[3(4)-methylcyclohexen-3-yl-isopropyl]phenols.

Results and Discussion

To achieve high yield and selectivity of the target products — *para*-[3(4)-methylcyclohexen-3-yl-isopropyl]phenols — the alkylation reaction in the presence of the KN-30 catalyst was systematically investigated. The effects of the main kinetic parameters, including temperature, the molar ratio of the initial components, reaction time, and catalyst amount, were studied, and the optimal conditions were determined.

1. For the alkylation reaction of phenol with 1-methyl-3-isopropenylcyclohexene (DP), the optimal conditions were determined to be: temperature 135°C, phenol:cyclene molar ratio 1:1 (mol/mol), reaction time 4.5 h, and catalyst amount 10% (based on phenol taken). Under these conditions, the yield of *para*-[3-methylcyclohexen-3-yl-isopropyl]phenol was 75.7% (based on phenol), and the selectivity toward the target product reached 92.5%.

2. For the alkylation reaction of phenol with 1-methyl-4-isopropenylcyclohexene (DPT), the optimal conditions were: temperature 145°C, phenol: cyclene molar ratio 1:1 (mol/mol), reaction time 6 h, and catalyst amount 13% (based on phenol). Under these conditions, the yield of *para*-[4-methylcyclohexen-3-yl-isopropyl]phenol was 68.9%, with a selectivity of 85.3%.

3. For the alkylation reaction of phenol with 1-methyl-3(4)-isopropenylcyclohexene (ICD), the optimal conditions were: temperature 140°C, phenol:cyclene molar ratio 1:1 (mol/mol), reaction time 5.5 h, and catalyst amount 12% (based on phenol). Under these conditions, the yield of *para*-[3(4)-methylcyclohexen-3-yl-isopropyl]phenol was 71.2%, and the selectivity was 88.5%.

The structure and composition of the obtained target products were determined by infrared (IR) and nuclear magnetic resonance (NMR) spectroscopy.

Table. Comparative data of the alkylation reaction of phenol with diprene in the presence of various catalysts

Parameters	$NaHSO_4$	KU-2	KU-23	KN-30
1. Temperature, °C	160	135	145	135
2. Reaction time, h.	4	4	5	4.5
3. Phenol: DP molar ratio, mol/mol	2:1	2.5:1	1:1	1:1
4. Catalyst amount, %	10	12	15	10
6. Process type	Batch	Batch	Batch	Batch
Yield Selectivity	77.8 84.1	76.6 83.4	73.5 91.6	75.7 92.5

Based on the analysis of the experimental results, it was established that, compared with previously known catalysts, the zeolite-containing KN-30 catalyst exhibits higher efficiency in the alkylation reaction of phenol with isoprene cyclodimers.

References

1. Rustamov S.T., Rasulov Ch.K., Naghiyeva M.V. Synthesis and Antioxidant Activity of Sterically Hindered Phenols (Mini-Review). Izvestiya of Tula State University, Natural Sciences, 2024, N3, P. 3–18 *(in Russian)*
2. Naghiyeva M.V. Synthesis of aminomethylated derivatives of ethyl esters of 4(4-hydroxyphenyl)- and 4′-methyl-4(4-hydroxyphenyl)cyclohexanecarboxylic acids and study of their antioxidant properties. *Oil Refining and Petrochemistry,* 2020, N2, P. 14–18 *(in Russian)*
3. Gurbanova U.R., Rasulov Ch.K., Heydarli G.Z., Gasimova F.İ. Synthesis of *para*-[1(3)-methylcycloalkyl]phenols: properties and applications. Journal of Advances in Chemistry and Chemical Engineering, 2025, V.9, N1, P. 21-33

MODERN ABSORPTION TECHNOLOGIES FOR ACID GAS REMOVAL FROM HYDROCARBON GASES: A GLOBAL ANALYSIS

Sh.U. Akhmedova
Assistant,
Bukhara State Technical University.
E-mail: akhmedova815@gmail.com
O.B. Akhmedova
Doctor of Philosophy (PhD) in Technical Sciences,
Associate professor,
Tashkent State Technical University named after Islam Karimov.
E-mail: zodamedova1985@gmail.com

ABSTRACT: The article discusses modern approaches to improving gas purification technologies from acidic components using an absorbent composition based on diethanolamine (DEA). The research was conducted with the aim of achieving complete removal of acidic components from gases and improving the technical and economic performance of the process by adding activators to alkanolamines, specifically DEA. In particular, the composition of expander gases was investigated to enhance economic efficiency and improve the technology. It is proposed to add expander gases to the unpurified feed gas, as they are compatible in composition, or to use them as fuel for pyrolysis furnaces and boiler installations. It was established that the content of expander gas is 0.044% of the purified feed gas, resulting in an increase in the amount of purified gas.

KEYWORDS: Absorbent composition, acidic components, expander gas, fuel, pyrolysis furnace, boiler.

INTRODUCTION.

Due to the fact that natural gas is a rather voluminous resource compared to other raw materials, many countries use it as a fuel and for chemical synthesis. The USA, Saudi Arabia, Iran, Qatar, Russia and a number of other countries have the largest gas reserves, and Uzbekistan also uses this raw material for the energy industry and for the production of synthetic fuels. As in the case with any other raw materials, it is impossible to directly use hydrocarbon gases, so for their utilization it is necessary to apply technologies of purification, processing and separation into fractions.

Hydrocarbon gases contain sulfur (S), nitrogen (N), oxygen (O) in the form of heteroatomic compounds, i.e. acidic components, water vapor, mechanical particles, salts, and in small quantities oil and gas condensate [3; 11-20 p.]. This means that they do not meet the requirements for gas transportation, corrosive requirements, technical standards for commercial products, and standards governing environmental harm.

EXPERIMENTAL SECTION.

The choice of absorbent is determined by the composition of the feed gas and the method of utilization of the produced H_2S. In most cases, sulfur from H_2S is obtained using the Claus process. In addition, the presence of

hydrocarbons in the composition of H_2S complicates the technological process and deteriorates the quality of sulfur.

As is known, the principle technology of the absorption gas purification process includes an absorber, desorber, saturated absorbent separator and system, as well as devices for heating the absorbent at the regeneration stage and cooling the regenerated solution.

If we analyze foreign technologies of absorbent purification of hydrocarbon gases, each modern gas treatment plant uses a different absorbent or absorbent composition.

For example, in the method of DEA purification, improved by the French company SNPA, the mass fraction of DEA in the transition solution is significantly increased - up to 40%, and the degree of saturation of amines with acid gas reached 1.1 mol/mol. This improved method is now widely and successfully used for purification of gases with sulfur content. Gas with 19% H_2S in its composition (after purification, the H_2S content in the gas is 5.7 mg/m3) has a gas purification capacity of 2.7 billion m³/year. One of the large installations for gas purification using the DEA SNPA process is the installation built at the Waitney-Canon field (USA).

The scheme of feeding different streams of regenerated solution into the absorber at different stages of regeneration is widespread in the industry. Many gas treatment plants for gas purification from acidic components in Canada, France and the USA operate according to this scheme. The principle scheme of gas purification using such units is shown in Figure 1.

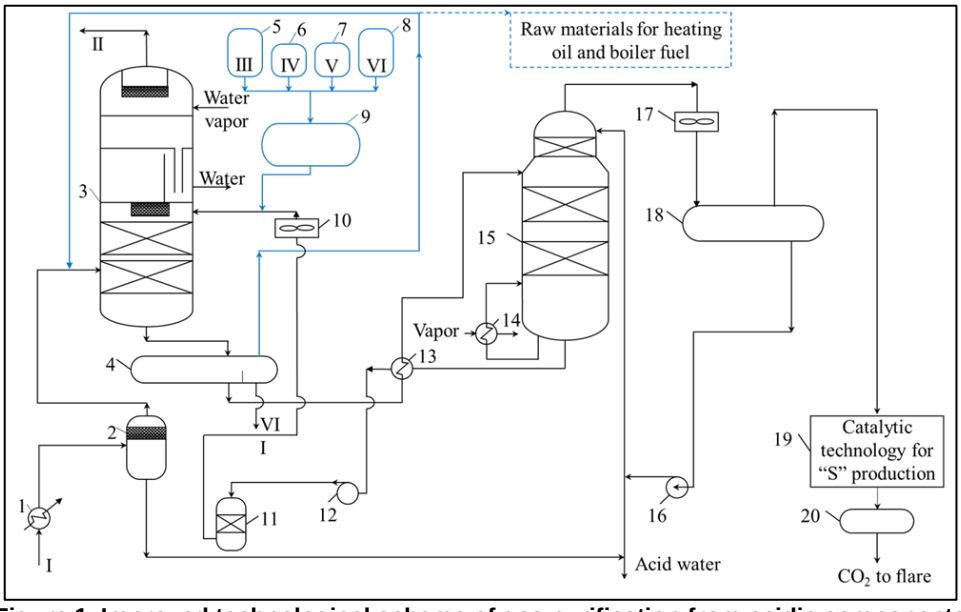


Figure 1. Improved technological scheme of gas purification from acidic components by DEA-based absorbent composition for SHGCC.

1- heat exchanger; 2 - separator; 3 - absorbe; 4- expander; 5 - water tank; 6 - activator tank; 7 - inhibitor tank; 8 - New DEA; 9 - chemical reagent tank; 10 - air cooler; 11 – filter; 12- pump; 13 – heat exchanger; 14 - steam heat exchanger;; 15 – desorber; 16 – pump; 17 - air cooler; 18 – separator; 19 - sulfur production workshop; 20 - flare / waste gas incineration unit.

RESULTS AND DISCUSSION.

This diagram illustrates the gas purification process using amines and its subsequent regeneration at various stages to ensure effective cleaning.

The partially regenerated solution is fed from the desorber to the middle part of the absorber. For deep regeneration in order to ensure fine gas purification, a part of the solution fed to the upper part of the absorber is subjected to additional regeneration. Such scheme allows to reduce steam consumption for solution regeneration by 10-15% in comparison with the conventional scheme.

At purification of gas with high content of acidic components it is expedient to carry out two-stage expansion (ventilation) of saturated amine at different pressures.

At the first stage at pressure of 1.5-2 MPa the main amount of dissolved hydrocarbons is released from the solution. This ensures their low content in the acid gases (<2%), which guarantees high quality of the obtained sulfur. Gas stream after this expansion, purified from hydrogen sulfide, can be used as fuel or compressed and mixed with the main stream of purified (raw) gas.

In a second step, acid gas is released from the solution at near atmospheric pressure without thermal recovery. After water separation and cooling, it can be directly sent to the sulfur recovery unit. This allows to reduce the steam consumption for saturated amines regeneration up to 10%.

A pump is additionally installed in the scheme to supply the saturated solution from the second expander to the desorber. The disadvantage of this technology is that the desorber can be saturated with amine with acid gases under unfavorable conditions, and there is a relatively high temperature of the solution. In conclusion, it should be noted that the introduction of the new absorbent composition through a dosing pump does not require significant changes to the existing technology, making this solution especially valuable.

In treating gas containing COS along with H_2S and CO_2, the absorber provides a COS absorption and hydrolysis zone consisting of five to eight blades. This zone is fed with regenerated amine solution at high temperature (70-80 °C).

Cooling and condensation of the vapor-gas mixture released in the desorber is carried out in a scheme that differs from the standard one: in the upper part of the column there is a direct interaction with phlegm circulating in a closed circuit. This scheme allows to reduce corrosion of process equipment and reduce the number of installations (condenser-cooler, separator and others).

The production schemes of gas purification by amine method also include solution filtration systems and installation of foam reducing agents.

In our country, such modern technology is applied at the gas cleaning plant Kandim GKIZ, where purification is carried out using an aqueous solution of diethanolamine.

Conclusion and Recommendations.

The proposed "Improved Installation Scheme" for the Shurtan Gas Chemical Complex ensures efficient purification of natural gas from acidic components (H_2S and CO_2) through optimization of the contact process in the absorber and the use of countercurrent flow of an alkanolamine-based absorbent.

Control of absorbent temperature and flow rate, as well as washing of the gas stream with condensate and boiler feed water, minimizes solution losses and enhances purification efficiency. The installation of a demister and a sampling system provides accurate monitoring of residual diethanolamine and CO_2 content.

The presence of five safety valves and an overpressure relief system increases operational safety and prevents emergency situations. Thus, the proposed scheme simultaneously ensures high performance, reduced absorbent losses, and reliable equipment operation.

REFERENCE LIST.

1. Axmedova, O. B. (2021). Gazni tayyorlash jarayonida ishlatiladigan past haroratli separator. Science and Education, 2(11), 400-407.
2. Kohl A.L., Nielsen R.B. Gas Purification. 5th ed. — Houston: Gulf Publishing Company, 1997. — 900 p.
3. Kidnay A.J., Parrish W.R. Fundamentals of Natural Gas Processing. — Boca Raton: CRC Press, 2006. — 450 p.
4. Panoyev E.R., Do‘stov H.B. (2021) Yuqori oltingugurtli gazlarni tozolashda mahalliy absorbentlarning ta’sirini tahlil qilish. “Fan va texnologiyalar taraqqiyoti” ilmiy-texnikaviy jurnal, 2021, №3, 130-135b.

DESIGN AND PERFORMANCE ANALYSIS OF SANDWICH-STRUCTURED WATER STORAGE TANKS

Aytaj Aliyeva, Zilan Mansurova, Aysel Mammadova
Baku Higher Oil School
Baku Azerbaijan
aytaj.x.aliyeva.std@bhos.edu.az
zilan.mansurova.std@bhos.edu.az
aysel.mammadova@bhos.edu.az

Summary: The most serious problem encountered during the storage of domestic and drinking water is the short-term bacteriological contamination of stagnant water, the formation of biofilm and algae. The shelf life of water in standard plastic tanks (HDPE/LLDPE) is only 3-7 days, and pathogens such as Escherichia coli and Staphylococcus aureus grow rapidly in

this environment. In this study, the application of CuO nanoparticles (NPs) and "Sandwich" (triple-layer) technology is proposed to reduce the microbiological load of water and provide thermal insulation. This tank is manufactured using rotational molding technology and consists of three functional layers. The outer layer consists of a mixture of white polyethylene, UV stabilizer and CuO, which slows down warming by reflecting solar radiation and prevents microbial colonization on the surface. The middle layer creates effective thermal insulation thanks to air bubbles created by a special foaming agent. The inner layer is enriched with high-concentration CuO nanoparticles integrated into the polymer matrix at the raw material stage (masterbatch method). This method, unlike coating, ensures the continuity of the microbicidal effect even in the event of scratching the inner surface. The mechanism of CuO nanoparticles is based on mechanical and chemical destruction of the cell morphology of bacteria. Nanoparticles cause oxidative stress by generating reactive oxygen species (ROS), disrupt internal order and destroy bacteria within 30-60 minutes. In addition, CuO disrupts molecular mechanisms used by bacteria to adhere to the surface and form biofilms, which reduces the ability of algae to colonize the wall by 90%. The results of the study show that the application of this technology increases the shelf life of water by 30 days or more. The presented model acts as an innovative water storage solution that ensures both internal and external microbiological safety, is self-cleaning and has a long lifespan.

Key words: antimicrobial copper nanocomposites, biofilm inhibition on polymer surfaces, thermal insulation foam layer, extended shelf life of stagnant water, self-disinfecting water tanks.

Introduction:

In modern water storage technologies, ensuring microbiological safety and preserving the organoleptic quality of water directly depends not only on the physical endurance of the materials used, but also on the active functionality they demonstrate at the molecular level. Although traditional polymer tanks create a stable environment for water storage, they are passive against biological contamination and biofilm formation in stagnant water conditions. As a scientific solution to this problem, the research study analyzes the application of a multilayer sandwich-structured polymer model, the inner, middle and outer layers of which are modified with specific chemical and biological agents. Copper oxide (CuO) nanoparticles, which form the central axis of the study, have a broad-spectrum antimicrobial and anti-algal mechanism of action. The choice of this material is justified by its ability to both oxidize and mechanically destroy pathogens. Copper oxide peroxidizes lipids in the cell membrane of microorganisms in contact with the inner surface, disrupting the structural integrity of the cell. One of the most important properties of the material is that it blocks the molecular mechanisms used by bacteria to adhere to the surface and form a biofilm (a biopolymer matrix necessary for the settlement of algae and other pathogens). This process ensures the self-cleaning ability of the inner surface, thereby maintaining the biological purity of the water for a long time. For the durability of the system, UV stabilizers included in the outer layer increase the polymer's tolerance to solar radiation. These substances prevent the physical decomposition and embrittlement of plastic chains as a result of photooxidation, thereby extending the service life of the product. The

highly reflective light-colored pigments applied to the outer layer create an optical barrier, reflecting sunlight and helping to maintain a constant internal temperature of the water. The blowing agents used in the middle part of the sandwich structure create closed air bubbles inside the material, forming an effective thermal insulation layer. This layer slows down the transfer of heat from the outside to the inside, eliminating favorable conditions for the reproduction of thermophilic microorganisms in the aquatic environment. From a technological point of view, the combination of these substances is not just a coating on the inner surface of the tank, but is integrated into the polymer at the raw material stage using a masterbatch method, so it does not break down upon contact with water and becomes an integral part of the material structure. As a result, this innovative material combination promises both physical protection and active biochemical protection during water storage.

Experimental section:

The main goal of the experimental phase of the research work is the integration of Copper Oxide (CuO) nanoparticles into the polymer matrix and the evaluation of the antimicrobial efficacy of this composite material. In the first step of the process, high purity CuO nanoparticles were mixed with polyethylene (PE) raw material at specified concentrations (0.03 wt%) under high temperature extrusion conditions to prepare a special masterbatch. Casting and rotational molding (rotomolding) methods were used to produce polymer films and tank samples. The prepared 30 μm thick thin polymer films and multilayer structures were left to dry under ambient conditions for complete evaporation of the solvent and stabilization of the structure.To test the antimicrobial activity, Escherichia coli (E. coli), Staphylococcus aureus (S. aureus), Klebsiella pneumonia (K. pneumonia) and Pseudomonas aeruginosa (P. aeruginosa) bacterial strains that are pathogenic in water systems and stationary environments were used. Bacteria were activated in Müller-Hinton agar medium at 37°C for 24 hours and an appropriate inoculation environment was created for each strain under aseptic conditions. In the next stage of the experiment, the inhibition zones (areas that stop bacterial growth) of the polymer layers containing CuO nanoparticles were measured. For comparative analysis, the 2.5% concentration of Ciprofloxacin antibiotic standard was applied as a positive control group. During the experiment, the effect of nanoparticles on cell morphology and how they inhibited biofilm formation was monitored by microscopic analyses. The fact that reactive oxygen species (ROS) generated by nanoparticles destroy the antioxidant defense system of bacteria and disrupt internal mechanisms by piercing cell walls was confirmed by laboratory tests. Finally, the microbiological purity and temperature stability of water were recorded at different time intervals, and the synergistic effect of CuO nanoparticles and thermal foam layer was evaluated.

Results and their discussions:

The results of the study show that the application of a three-layer sandwich structure significantly increases both the biological safety and thermal stability of water tanks. While in standard single-layer tanks, stagnant water begins to deteriorate microbiologically within 3-7 days, the inner layer enriched with CuO nanoparticles (NPs) extends the shelf life of water to 30 days or more. During the experiments, it was observed that CuO nanoparticles disrupt the cell morphology of bacteria, killing them within 30-60 minutes. In particular, high inhibition zones of 38 mm were recorded on E. coli and 40 mm on S. aureus, which proves the microbicidal power of copper oxide. Each of the layers used in the project adds specific value to the system. UV stabilizers used in the outer layer prevent plastic from becoming brittle under sunlight, extending the service life of the tank to more than 20 years. At the same time, the CuO nanoparticles in this layer do not allow the development of microbes, mold and fungi on the outer surface of the tank. The foam insulation applied in the middle layer creates a thermos effect inside the tank, keeping the water temperature 15-20°C cooler than the environment. The CuO nanoparticles located in the inner layer generate reactive oxygen species (ROS) and cause oxidative stress, which completely blocks biofilm formation and algae growth at the molecular level. The discussions and comparative analyses confirm that the proposed project, unlike normal tanks, is not just a storage container, but an active disinfection system. While in standard tanks, water heats up to 45-50°C under the sun, creating an ideal environment for bacterial growth, in our project both the heat load and microbiological contamination are minimized. These polymer structures prepared by incorporating CuO nanoparticles have demonstrated more effective results than the gold standard antibiotic Ciprofloxacin (2.5%). Thus, the application of this technology provides a safe and long-term water storage solution for consumers, preserving both the taste and smell of water. Finally, based on the results obtained, the sandwich-structured water storage tank was compared with the normal water tank in the following table:

Table 1. Performance Analysis: Sandwich-structured vs. Single-layer water tanks

Comparison Criteria	Standard Plastic Tank (Single Layer)	Sandwich-Structured Water Storage Tank
Biological safety	Bacteria (E. coli, S. aureus) multiply rapidly within 24 hours.	Thanks to CuO NPs, the cell morphology of bacteria is disrupted and destroyed.
Algal bloom	Due to light permeability and biofilm, algae forms in 1-2 weeks.	With the opaque armor and the algicidal effect of copper, algae growth is reduced to zero.
Water temperature	Under the Sun, the water heats up to 45-50°C (an ideal environment for bacteria).	The water stays 15-20°C cooler thanks to the white outer layer and medium foam insulation.

Biofilm (Mucus)	The inner walls of the tank are covered with slippery, bacterial mucus.	CuO blocks biofilm formation (adhesion of bacteria) at the molecular level.
Duration	UV rays make plastic brittle in 3-5 years and crack.	Thanks to UV stabilizers, the plastic retains its elasticity for more than 20 years.
External hygiene	The outside of the tank becomes contaminated with mold, dust, and microbes.	The CuO in the outer layer prevents the growth of microbes and fungi on the surface.
The Usefulness of water	Water starts to smell and lose its taste after 3-5 days.	Thanks to active disinfection, the water stays fresh for 30 days or more.
Maintenance and cleaning	Internal cleaning (washing) is required at least 2-3 times a year.	Maintenance requirements are minimal thanks to the self-cleaning (anti-biofilm) surface.

Offers: Further work can be directed toward:

- Uniform dispersion of CuO nanoparticles within the polymer
- Analysis of the effect of waters with different pH, mineralization and salinity on the antibacterial activity of CuO
- Deeper study of the effect of nanoparticles on the adhesion mechanisms of different pathogens (e.g. P. aeruginosa)
- Comparative analysis of thermal conductivity coefficients of different foaming agents

References:

1. Thamer, H., Ibraheem, H., Alsayed, R., Makia, R., Kadhom, M., Salman, H., & Yousif, E. (2024). Synergistic antimicrobial potential: Exploring the efficacy of poly methacrylic acid (PMAA) polymers, CuO NPs, and pomegranate peel extract against bacterial pathogens. Results in Chemistry, 7, 101365. https://doi.org/10.1016/j.rechem.2024.101365
2. Pal, S., et al. (2020). Metal-polymer nanocomposites for self-disinfecting water storage systems and their efficacy against stagnant water pathogens. Journal of Environmental Chemical Engineering, 8(4), 103874. https://doi.org/10.1016/j.jece.2020.103874
3. Self-disinfecting polymer surfaces: The role of copper nanocomposites in preventing biofilm formation in stagnant water tanks. Materials Science and Engineering: C, 134, 112678. https://doi.org/10.1016/j.msec.2022.112678

DECOMPOSITION OF HIGH-STABLE WATER-OIL EMULSIONS OF HEAVY OILS IN AN OIL PREPARATION DEVICE

Ochilov Abdurakhim Abdurasulovich,
Bukhara State Technical University, Doctor
of Technical Sciences (DSc), professor,
Uzakbaev Kamal Axmet uli
Doctoral student
Bukhara State Technical University
Republic of Uzbekistan, Bukhara.
e-mail: ochilov82@mail.com.

KEYWORDS: Water-oil emulsion, demulsifier, motor oil, oil preparation unit, demulsifier consumption, high-stability oils.

ABSTRACT: The stability of most emulsions of the "water in oil" type increases over time. During the aging of the emulsion in water globules, the emulsifier layer increases and, accordingly, its mechanical strength increases. When such globules collide, they do not merge due to the presence of a strong hydrophobic film. To combine the water globules, it is necessary to remove this film and replace it with a hydrophilic layer of any surfactants. We investigated the possibility of effective demulsification of highly stable water and oil and gas emulsions. In this case, the experiments were conducted with the synthesized demulsifiers TKM-6, TKM-7 and the used demulsifier SNPX-4410 at a consumption of 60 g/t and mixing into the emulsion with constant stirring at 100 rpm.

INTRODUCTION.

One of the main sources of environmental pollution as a result of human man-made activities is oil production and oil refining industry enterprises. Due to emergency situations, as well as during the production activities of oil extraction and oil refining enterprises, a lot of oil waste has accumulated on the surface and in the atmosphere.

The rapid growth of oil production in the world is causing the formation of oil residues in oil preparation facilities (OPF), oil refineries, transportation and storage of oils.

The formation of permanent water-oil emulsions is a natural phenomenon during the operation of oil fields, their properties change over time and depend on many factors. With long-term storage in open warehouses and reservoirs, the stability of such systems increases significantly. This happens due to the "aging" of emulsions, the compression and hardening of armored shells in water droplets over time, the evaporation of light fractions, the decomposition of petroleum products, the increase of mechanical impurities due to atmospheric dust, etc.

Since the water-oil emulsion is an unstable system prone to the formation of a minimum phase interface, it is natural to expect its tendency to stratify. However, in the actual operating conditions of oil production equipment, emulsions with high stability are often formed. This mainly determines the choice of their processing technology, as well as the depth of

separation of the water phase from oil. Aggregative stability of emulsions is measured by the time of their presence until the emulsifying liquids are completely separated. In the case of emulsions derived from different oils, their stability can vary from a few seconds to a year or more.

Natural stabilizers of emulsions include asphaltenes, resins, cycloalkane and paraffins in petroleum, which are natural surfactants. In addition, these include the smallest solid particles of suspended matter (mud, quartz, salt, etc.) in well production.

Experimental Section. Depending on the concentration of the dispersed phase in emulsions, they are divided into diluted or low concentration (dispersed phase is less than 20%), concentrated (up to 74%) and highly concentrated (above 74%). Diluted emulsions with a small dispersed structure have a high demulsification resistance.

The size of water phase droplets dispersed in water-oil emulsions is usually between 0.1 and 250 microns. Large droplets can only exist in flow due to rapid sedimentation under static conditions.

“The water-in-oil” stability of many emulsions increases with time. During the aging of the emulsion in water globules, the emulsifier layer increases and, accordingly, its mechanical strength increases. When such globules collide, they do not come together due to the presence of a strong hydrofob film. To combine the water globules, it is necessary to destroy this film and replace it with a hydrofob layer of any surfactant. Aging of emulsions continues intensively only in the initial period after their formation, and then slows down significantly. The aging properties of the inverse emulsion depend on the composition and properties of the oil, the source of water, the conditions of emulsion formation (temperature, intensity of phase mixing).

The main properties of oil emulsions include the degree of disintegration over a certain period of time, the effective (in some cases, structural) viscosity, the diameter of the average surface layer of the emulsified droplets of the aqueous phase. Together, these parameters reflect the intensity of the oil emulsion, its physical and chemical properties, and the adsorption of the emulsifier.

According to PA Rebinder, the mechanism of crushing of the water phase is that, first of all, the globule of water is drawn in the field of movement deformations (it takes a cylindrical shape), which is accompanied by an increase in the interphase surface of contact with water and oil. Upon reaching a critical length, usually calculated as two diameters of the original globule, the cylindrical globule “decomposed” into smaller droplets of different diameters.

A droplet with a large diameter is more affected by the effect of flow pulsation. A drop of water in an oil stream takes on irregular shapes, and if the applied pulsation frequency matches the frequency of natural oscillations, it breaks up into smaller components.

Emulsification occurs under the influence of both viscous and dynamic forces due to the large distribution of oil emulsion droplets (from one to hundreds of microns), as well as differences in flow regimes.

Results and Discussion.

The thermal effect on water-oil emulsions is that the dewatering oils are heated to a temperature of 45-80°C before deposition. When heated, the surface tension of the emulsifier layers on the surface of the droplets decreases, which makes it easier for them to coalesce. In addition, the viscosity of oil decreases, the density difference between water and oil increases, which helps the emulsion to separate quickly. This is the process heating is carried out in tanks, heat exchangers and tube furnaces.

In-pipe decomposition is carried out by adding a chemical reagent-demulsifier to the emulsion. This allows breaking up the emulsion in the pipeline, reducing its viscosity and reducing hydraulic losses.

After comparing the results of formation water separation under laboratory conditions for each oil composition, the most effective demulsifiers are selected.

In our research work, we took several samples by mixing different proportions of liquid soap, organic matter and used diesel engine oil - Table 1.

Table 1. Composition and classification of demulsifier compositions

Name of demulsifier composition	Composition of the demulsifier compositions, %			
	Used oil	Liquid soap	Organic matter	NaOH
TKM -1	60	30	10	-
TKM -2	60	20	20	-
TKM -3	60	25	15	-
TKM -4	50	20	30	-
TKM -5	50	25	2 5	-
TKM -6	50	30	20	-
TKM -7	50	25	20	5
TKM -8	50	20	25	5
TKM-9	60	15	20	5
TKM-10	60	20	15	5

A demulsifier in the form of a dark brown liquid was obtained by mixing the components contained in the 10 demulsifier samples listed in Table 1 at a temperature of 30 ^{0}C in a 200 rev/min mixer for 10 minutes. These demulsifiers are mostly well soluble in water.

Decompose of highly stable water-in-oil emulsions of local heavy oils requires the use of complex multi-component demulsifier compositions.

Practices show that choosing the optimal composition of the demulsifier composition to decompose each type of stable water petroleum emulsions is a major challenge. Emulsions include well compression emitter reagents to improve performance in the preparation of oil wells obtained during oil

drilling, if this is particularly problematic. Such additives are often chemical substances (surfactants, soap, etc.), a large amount of mineral compounds (salts) of oil demulsification, which make it difficult to choose the composition of the demulsifier.

It is known that when demulsifiers are used to break down stable emulsions, the deemulgation process takes 6 hours or more, which requires significant economic cost and energy consumption in oil and oil refineries. To overcome these shortcomings, new compositions of demulsifiers are being developed in recent years, taking into account the composition of decomposed emulsions.

We studied the ability of the obtained demulsifiers to break down stable water-oil emulsions formed from heavy oils obtained from “Shimoliy O’rtabuloq”, “Djarchi”, “Chegara” fields when mixing at 90 g/t at 200-300 rev/min. Table 2.

In Table 2, the synthesized demulsifier TKM-6 and TKM-7 achieved the best results in breaking stable water emulsions. In this case, the active composition of demulsifiers consists of TKM-6, 50% used oil, 30% liquid soap and 20% organic matter, as well as TKM-7 sample consists of 50% used oil, 25% liquid soap, 20% organic matter and 5% sodium hydroxide and TKM-6 and TKM-7 were the best results among the samples obtained, and TKM-4 had a low result in terms of dehydration.

Table 2. Decomposition parameters of stable water-oil emulsions in the compositions of produced demulsifiers.

Naming of demulsifiers	Break time, hour	Degree of dehydration, %	Amount of residual salts, mg/dm^3
TKM -1	5.1	72.7	218
TKM -2	6.1	78.2	155
TKM -3	5.9	70.5	267
TKM -4	5.5	57.8	242
TKM -5	5.4	75.3	305
TKM -6	4, 9	86,9	1 90
TKM -7	4, 8	83.4	1 74
TKM -8	5, 2	62.3	245
TKM-9	5, 0	63,4	274
TKM-10	5.7	62.3	245

The amount of residual salt in the purified oil together with dehydration is important when breaking down emulsions using the samples of the studied emulsions. The amount of residual water and salt depends on the amount of demulsifier and the process temperature Figure 1. The low amount of residual salt helps to prevent corrosion of oil preparation, transportation and processing equipment.

Figure 1 shows the change in the residual content of mineral salts during the decompose of water-oil emulsions of heavy oils with different samples.

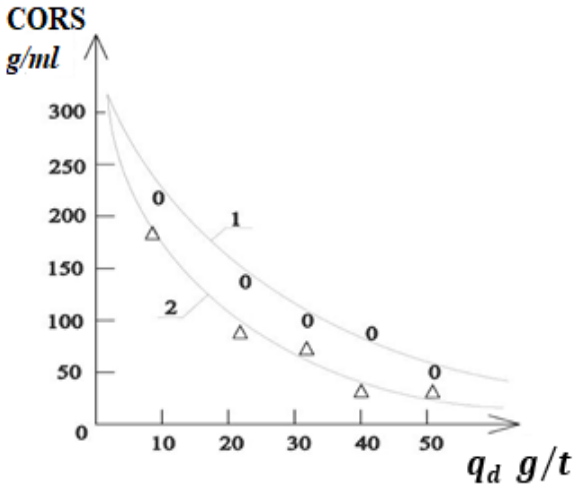


Figure 1. Changes in the composition of residual salts (m_t) in oil, depending on the consumption of demulsifiers (TKM): 1-for TKM-6; for 2-TKM-7 demulsifier.

As can be seen from picture 1 known developed (TKM-6 and TKM-7) demulsifiers with an increase in the amount, the residual content of mineral salts in heavy oils decreases exponentially. At the same time, after the demulsification process, when TKM-6 is used, more mineral salts are removed than TKM-7, which can be explained by the properties and chemical composition of the first demulsifier. Having determined the properties of the synthesized emulsions, we have compared them with the deemulgator (SNPX-4410), which is currently being used .The results are presented in Table 3.

Table 3. Indications of demulsifiers

Name of demulsifier	pH	Surface tension, din/cm	Washability , %	Foam formation, at 25 ^{0}C, cm^3
TKM - 6	8.1	38	93	22
TKM - 7	8,2	36	92	26
SNPX-4410	9,2	33	78	28

Table 3 shows that the recommended demulsifier is more active compared to the demulsifier in use, that is, it has the ability to produce high surface tension, wash and form foam, stable water formed from heavy oils is essential for the decomposition of the oil emulsion.

We have studied the possibility of effective deemulgiration of high stagnant water and oil and gas emulsions.demulsification of highly stable water and oil-gas emulsions . In this experiment, the synthesized demulsifiers TKM-6, TKM-7 and used SNPX-4410 deemulsifier were used at a consumption of 60 g/t and mixing into the emulsion was carried out with continuous mixing at 100 rev/min, the obtained results are presented in Table 4.

From the 4th table apparently that is three field's water oil emulsions different level fragmented. For example, in the emulsion of the "Shimoliy O'rtabuloq" oil field, if the demulsifier SNPX-4410 is used in the process of demulsification of at the expense 60 g/t, the amount of residual water in the emulsion is 1.5%, and in the same situations, residual water when using TKM-6 and TKM-7 amount is 1.3%.

Table 4. Residual water content in oil after decompose emulsions with produced demulsifiers

Oil fields	**Type of demulsifier**		
	SNPX-4410 (control)	**TKM-7**	**TKM-6**
"Shimoliy O'rtabuloq"	1,5(6,5)	1,3(6,3)	1,3(6,2)
"Sho'rchi"	0,9 (6,3)	0,9(6,1)	0,8 (6,2)
"Jarqoq"	1,5(6,5)	1,3(6,3)	1,3(6,2)

* - Brackets indicate the stability time of the water-oil emulsion, hours.

Achieving this effect of demulsification in the considered cases can be explained by possible changes in the structure of the emulsion, that is, changes in the density of the electron cloud of ions direct around the molecules and, therefore, their polarization.

The amount of residual water in oil after demulsification with different amounts of already in use demulsifier and produced demulsifiers depends on the amount of demulsifier Table 5.

It can be concluded from Table 5 that the amount of residual water decreases with the increase of demulsifier consumption in the range of 60 ÷ 100 g\t when decompose emulsions in different local oil fields, where an increase in consumption indicates an increase in demulsification.

Table 5. Residual water content (%) in oils after demulsification of produced demulsifiers with different costs (g\t).

Oil fields	**Demulsifier consumption , g\t**								
	SNPX-4410 (control)			**TKM-7**			**TKM-6**		
	60	**80**	**100**	**60**	**80**	**100**	**60**	**80**	**100**
"Shimoliy O'rtabuloq"	1,6	1,5	1,3	1,4	1,3	1,2	1,3	1,1	0,9
"Sho'rchi"	1,5	1,0	0,9	1,0	0,9	0,8	0,9	0,8	0,7
"Jarqoq"	1,2	1,1	1,0	1,0	0,9	0,9	1,1	1,0	0,8

According to the demulsification ability, the investigated demulsifiers are located in the next decreasing order:

TKM-6 > TKM-7 > SNPX-4410

The role of demulsifiers acting on emulsions of high-viscosity oils is that they break down the emulsifiers that surrounding the water globules and precipitate them. We also used an electron microscope to study mechanical compounds, salts, etc. , which cause the stability of various types of stable emulsions of local oils .

In order to determine the efficiency of demulsification, two samples were taken from the emulsions of the above three oil fields in the “Shimoliy O’rtabuloq” oil preparation facility, sample 1 with demulsifier TKM-6 and sample 2 with the consumpsion of demulsifier SNPX-4410 at a rate of 60 g/t before breaking up the above water oil emulsion and subsequent images were captured using an electron microscope with NLCD-307B (Czech Republic) optical viewfinders. Conducting electron microscope studies on emulsions of high viscosity oils provides an opportunity to obtain more information about them.

Of course, particles of evenly disturbed water globules are visible with a small error. The obtained results are presented in Figure 2 below, where it is possible to see the localization of high viscosity oil emulsions and water globules.

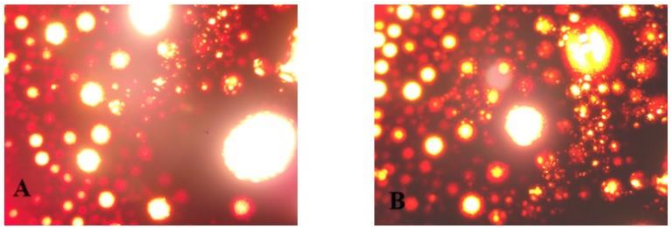


Figure 2. Electron microscope view of high-viscosity water-oil emulsions before the demulsification process.
A) sample 1; B) sample 2.

In Fig. 2, you can see the most complex samples of water and salts in water-oil emulsions captured by an electron microscope: sample 1 at a temperature of 20 ^{0}C (A) and sample 2 at a temperature of 20 ^{0}C (B). It is observed that the additives in the oil act as an emulsifier, surround the dispersed phase contained of the emulsion from the outside.

Taking these into account, based on the properties and stability of emulsions, the task of separating emulsion stabilizers is set. The increase in the concentration of the mechanical compound is due to the fact that in the process of hydrodynamic movement and in the presence of surfactants mechanical compounds with a hydrophilized surface are better wette by water and transferred to the aqueous phase (washed away).

As a result of the removal of mechanical impurities in oil (highly dispersed mixture, asphaltene, tar, iron sulfide, etc.), the surface tension force of water globules in emulsions can be reduced, and the process of coalescence is observed in water droplets.

In recent years, various chemical reagents have been add to oil wells in order to facilitate the processes of oil extraction and processing, which affects the formation of stable emulsions.

Conducted studies show that with the electron microscope method it is effective to characterize the external structure of water-oil emulsions of local high-viscosity oils using. Currently, demulsifiers and non-traditional methods are used to breakdown the outer shells of water globules in emulsions and collect and settle the water droplets. Unfortunately, some stable emulsions do not break down, because in composition, drops of water in the form of small particles are preserved forming an emulsion. Also, the amount of residual water after the demulsification process at a high consumption of demulsifiers can be seen in Figure 3.

As can be seen from Figure 3, a certain amount of water and salt remains after the demulsification process of water-oil emulsions. Emulsions are not at the level of the requirements of the specified standard (GOST 2477, GOST 21354), for the purpose of breaking up the emulsions at the required level, it is necessary to use a high amount of demulsifier or to use other cleaning methods.

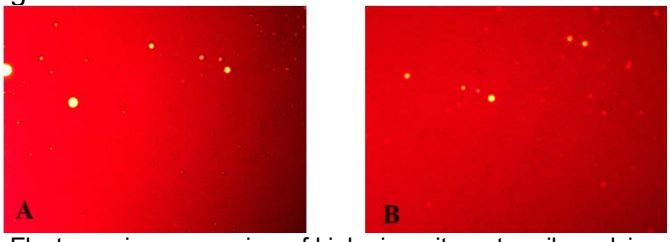


Figure 3. Electron microscope view of high-viscosity water-oil emulsions after the demulsification process.
A) sample 1; B) sample 2.

Conclusions and Recommendations.

The relative consumption of demulsifier is one of the main technical and economic indicators of the processes of dewatering and desalination of WOE of especially heavy oils.

Thus, the conducted studies show that instead of imported SNPX-4410 demulsifier, it is possible to use TKM-6 demulsifier synthesized on the basis of oil used in diesel engines. The presence of sulfur compounds, fatty acids, alkalis and their derivatives in it allows to increase its demulsification properties.

References

1. Ochilov A.A., Eshmetov I.D., Salikhanova D.S., Adizov B.Z. Decomposition of high-stable water-oil emulsions of heavy oils in an oil preparation device. *The journal "Processes of Petrochemistry and oil Refining" (PPOR).* SSN: 1726-4685
2. Abduraxim Ochilov, Bobirjon Adizov. Analysis of demulsifier production from sulfurized cottonseed oil and breakdown of water-oil emulsions // Austrian Journal of Technical and Natural Sciences 2024, № 3-4. P. 79-82.
3. Xushnud Shukurulla uli Ismailov, Kamal Axmet uli Uzakbayev, Abduraxim Abdurasulovich Ochilov. Og'ir neftlarning suvneftli emulsiyalarini parchalash texnologiyalarini o'rganish bosqichlari // SCIENCE AND EDUCATION, Scientific journal. In volume 4. Issue 1, Yanuary 2023. 268-273 b.
4. Ochilov A.A., Uzakbayev K.A., Adizov B.Z. Mahalliy og'ir neftlar suv-neft emulsiyalarining dastlabki ko'rsatkichlari // "Neft va gaz sohasidagi zamonaviy innovasion texnologiyalar". Respublika miqyosidagi ilmiy-texnik anjuman materiallari 12-13 may, 2023 y, Toshkent 190-192 b.
5. Ochilov A.A., Ochilov X.G. Og'ir yuqori qovushqoqli neftlarda barqaror suv neft emulsiyalarining shakllanishi va barqarorlanishining sabablari SCIENCE AND EDUCATION, Scientific journal. In volume 3. Issue 4, April 2022., 559-564 b.
6. Очилов А.А., Абдурахимов С.А., Адизов Б.З., Рахимов Б.Р. Разработка композиции деэмульгаторов, применямых в разрушении высокоустойчивых водонефтяных эмульсий тяжелых нефтей// Монография, - Бухара, Издательство "Умид", 2020. С. 120.
7. Uzakbaev K.A., Ochilov A.A., Abdikamalova A.B., Salixanova D.S. Analysis of the process of breaking down water-oil emulsions of heavy oils using the developed local demulsifier. The European Journal of Technical and Natural Sciences 2024, № 3 – 4, pp 21-26.
8. Eshmetov I. D., Salixanova D. S., Adizov B. Z., Ochilov A.A., O'rinov X.X., Uzakbaev K.A. Yuqori turg'un suv - neftli emulsiyalarini parchalash uchun samarador deemulgator tarkibini tanlash. "Central Asian Food Engineering and Technology" elektron ilmiy jurnali, 2024. №8, 72-77 bet.

STUDY AND ANALYSIS OF THE STABILITY OF WATER-OIL EMULSIONS IN LOCAL OIL PREPARATION EQUIPMENT.

Ochilov Abdurakhim Abdurasulovich,
Bukhara State Technical University, Doctor of Technical Sciences (DSc), professor,
Uzakbaev Kamal Axmet uli
Doctoral student
Bukhara State Technical University
Republic of Uzbekistan, Bukhara.
e-mail: ochilov82@mail.com.

KEYWORDS: water-oil emulsions, demulsifiers, oil preparation equipments (OPE), kinematic viscosity, dynamic shear stresses, indicator $\Delta\rho$.

ABSTRACT: Water-oil emulsions are unstable systems, which cause the formation of small phase boundaries, and their phase separation processes also occur due to the difference in density. However, in most cases, emulsions with high stability are formed during the operation of oil production equipment. This complicates the choice of technological mechanisms and modes for the preparation of water-oil emulsions, as well as the separation of the water phase from oil. The time required for the separation of highly stable water-oil emulsions into separate phases is characterized by a long period of time. Depending on the type of emulsions, the stability of the emulsions can occur for a period of several seconds to a year or more. In oil production wells, the flow velocity of the water-oil emulsion during its movement from the wellhead to the collection and preparation points varies from 2-3 m/s to several tens of m/s.

INTRODUCTION.

Large changes in the speed of fluid movement lead to the dispersion of water droplets in oil and the formation of an emulsion. Similarly, in separation devices, measuring devices, pump or compressor units, the movement of the flow through sections of pipes with a changed diameter, bends, and twists causes the formation of emulsions and their stabilization. In the above technological units, the flow velocity and turbulence can significantly increase, which, based on physicochemical laws and procedures, leads to a decrease in the size of water droplets and an increase in their dispersion by several tens or even hundreds of times [1; p. 87-88].

Experimental Section

This article examines the factors affecting the stability of water-oil emulsions formed in the fields of the foreign enterprise "Sanoat Energetikal Group". It also examines the extent to which the results of the research work studied differ from certain standard requirements. The Methodology and Discussion is presented in section III, section IV covers the experimental results of the study, and section V discusses the future study and conclusion.

The evaluation of the activity of selected surfactant compositions with demulsifying properties in the separation of water-oil emulsions into phases is carried out in laboratory conditions, modeling the processes of dewatering

water-oil emulsions in special devices equipped with a mixing device for demulsifiers in water-oil emulsions and a thermostatic shell.

This method allows for a high degree of reliability in determining the specific consumption of the surfactant recommended for pilot tests conducted mainly in oil fields and determining the activity levels of the tested demulsifying surfactants. This method is used to compare the activity of surfactants or their compositions with demulsifying properties in order to separate natural water-oil emulsions and artificial water-oil emulsions formed during the operation of oil production wells.

In order for the results of laboratory studies to be reliable, the emulsion sample must be taken and the experiments must be carried out within a short period of time, that is, the samples must be taken or prepared within a period of no more than 2 hours from the start of the experiment. It is necessary to ensure that the selected sample has not undergone the “aging” process and is compatible with natural emulsions transported from production wells. If water and oil are separated into separate phases, they must be mixed in a mixer at a speed of 1500 rpm for 3-5 minutes. After that, it is left to settle for 20 minutes, and if phase separation is not observed, this process is repeated, then poured into separate sediments, taking into account the exact volume of water [3; p. 75-77].

The composition of locally produced high-viscosity heavy oils contains a large amount of natural stabilizers (asphaltene, tar, naphthene, paraffin, etc.) and emulsifiers.

In addition, the smallest solid particles (clay, quartz, salts, etc.) present in SNEs also contribute to their increased stability [4; 174-176 p.].

From the analytical data of local water-oil emulsions, it became clear that the size of water globules in the dispersion aqueous phases varies from 0.1 to 250 μm. Also, during the “living” processes of emulsions, the emulsifier layer on the water globules increases, which leads to an increase in their mechanical strength. In addition, the extracted mineralized layer waters lead to the formation of oil emulsions that are relatively stable and age quickly compared to fresh waters. When the globules of these layer waters collide with each other, their coalescence process is not observed, since they have strong hydrophobic protective layers. Therefore, in order to ensure the coalescence of water globules, it is necessary to eliminate these protective layers and replace them with hydrophilic layers of some surfactants [4; p. 54-58].

Water-oil emulsions can be characterized by the degree of their demulsification or the intensity of oil emulsification over a certain period of time.

The acceleration of the process of separation of stable water-oil emulsions into separate phases is characterized by the difference between the densities of water and oil ($\Delta\rho$), the components in the composition of the oil (a + r)/p, as well as the ratio of the amounts of asphaltenes (a) and resins

(r) to the total amount of paraffins (p). The values of these indicators allow us to determine the methods of separation of the processed water-oil emulsions into separate phases [165; 57-59 p.].

In this case, the density difference ∆ρ is determined based on the difference in densities of water and oil in the samples under study, corresponding to gravitational sedimentation under the influence of gravity. After the separation of water-oil emulsions into separate water and oil phases, their densities are measured separately and the difference between them is determined [5; p. 57-59].

Based on the above, local oils can be divided into the following according to the (a+r)/p indicator [5; p. 57-59]:

- mixed [(a+r)/p] = 0.951÷1.400;
- resinous [(a+r)/p] = 2.759÷3.888;
- highly resinous [(a+r)/p] = 4.774÷7.789.

We have studied the classification of the breakdown of local water-in-oil emulsions based on ∆ρ [6; pp. 4-10]:

- difficult to decompose (∆ρ=0.2-0.25 g/cm^3);
- decomposed (∆ρ=0.25-0.30 g/cm^3);
- easily decomposed (∆ρ=0.3-0.35 g/cm^3).

In oil production wells, the well product is obtained in the form of an emulsion, which simultaneously contains water, various salts, mechanical impurities and other components. Therefore, in the initial stages of water-oil emulsions, these substances are separated from the oil using various methods.

As noted above, unfortunately, this process does not allow easy separation of water and associated components in all oil emulsions. Today, highly stable water-oil emulsions of heavy oils extracted from the corresponding fields are being prepared at the oil preparation equipments (OPE) of the “Northern Ortabulok”, “Shurtepa” and “Shirkent” owned by the “Sanoat Energetikal Group” PE [7; pp. 127-131].

The separation of such stable water-oil emulsions is complicated by the presence of highly dispersed mixtures, asphaltene-resinous substances, etc., which act as emulsifiers [8; pp. 268-273].

Results and Discussion.

We studied the factors affecting the stability of the water-oil emulsion formed in the fields belonging to the “Sanoat Energetikal Group” JSC. In this case, sampling of the water-oil emulsion is carried out in the OPE themselves, before and after treatment with a demulsifier (up to 50 ÷ 110 g/t).

We studied the content of asphaltenes, resins, paraffins and other emulsifiers in the oils of the Northern Ortabulaq, Shirkent, Okkul, Shu‘rtepa, Kruk, Sarikum, New Koratepa OPE and the Kokdumalaq (under-reef) collection point using various methods and techniques, and the results obtained are presented in Table 1. And the extent to which the results of the

studied research work differ from certain standard requirements was studied [8; 268-273 p.].

Table 1. Chemical composition of prepared oils in local OPE

Oil preparation equipments	Composition (by weight), %				
	Asphaltene	Resin	Paraffin	Sulfur	Coke
Northern Ortabulaq	0,89	4,52	6,2	1,23	6,32
Shirkent	5,36	11,798	6,34	4,553	9,58
Okkul	2,85	2,92	9,61	0,42	7,35
Shu'rtepa	0,43	7,83	6,39	1,59	2,88
Kruk	1,45	3,16	2,03	2,18	3,38
Sarikum	0,404	6,65	2,99	0,12	2,63
New Koratepa	4,504	3,26	4,608	0,1	5,28
Kokdumalaq (under-reef) collection point	1,28	9,74	7,45	1,79	3,91

As can be seen from Table 1 above, the water-oil emulsions from the local Shirkent and New Koratepa OPE contain approximately two to three times more asphaltenes than the oils from the Okkul, Kruk OPE and the Kokdumaloq (under-reef) collection point, and up to ten times more asphaltenes than the oils from the Shurtepa and Sarikum OPE. The oils from the Shirkent, Shurtepa and Kokdumaloq (under-reef) collection points contain a higher amount of resins than the oils from the remaining OPE. The same indicators can be said about the sulfur content, which can be seen to be 2.5-4.0 times higher than the Kokdumaloq oils [8; pp. 268-273].

We can see the results of the analysis of the local water-oil emulsion $\Delta\rho$ indicator from Table 2.

Table 2. $\Delta\rho$ indicators of water-oil emulsions

Oil preparation equipments	Indicator $\Delta\rho$, g/sm^3
Northern Ortabulaq	0,272÷0,276
Shirkent	0,112÷0,131
Okkul	0,230÷0,236
Shu'rtepa	0,274÷0,280
Kruk	0,132÷0,145
Sarikum	0,195÷0,199
New Koratepa	0,204-0,216

From the data in Table 2, it is clear that the water-oil emulsion under consideration does not contain easily decomposed emulsions. The emulsions prepared at the OPE "Shimoliy Ortabulok" ($\Delta\rho$=0.272÷0.276 g/cm^3) and "Shurtepa" ($\Delta\rho$=0.274÷0.280 g/cm^3) are classified as decomposed according to the $\Delta\rho$ indicator, while the rest are classified as

difficult to decompose. In addition, the water-oil emulsions of the OPE "Shirkent" ($\Delta\rho$=0.112÷0.131 g/cm^3), "Sarikum" ($\Delta\rho$=0.195÷0.201 g/cm^3) and "Kruk" ($\Delta\rho$=0.132÷0.145 g/cm^3) are difficult to separate even with the presence of highly efficient demulsifiers.

Based on previous analyses, the (a+r)/p indices of oils from local OPE were calculated and the results obtained are presented in Table 3 [9; pp. 190-192].

Table 3. (a+r)/p indicators for local oils

Oil preparation equipments	The value of (a+r)/p
Northern Ortabulaq	4,406÷4,842
Shirkent	2,706÷3,261
Okkul	0,347÷0,770
Shu'rtepa	2,692÷3,239
Kruk	2,382÷2,961
Sarikum	3,479÷3,771
New Koratepa	0,977÷1,465

As can be seen from the data presented in Table 3, according to the (a+r)/p indicator, the "Northern Ortabulaq" OPE [(a+r)/p=4.406÷4.842] belong to local high-resin oils, the oils from the "Shirkent", "Shurtepa", "Kruk" and "Sarikum" OPE belong to the category of resinous oils, while the oils from the "Oqqul" (0.347÷0.770) and "Yangi Koratepa" (0.977÷1.465) OPE belong to the type of mixed oils.

Based on the requirements established by a specific GOST, in addition to the above, the studied oils also differ in significant quantities based on their physicochemical characteristics.

Today, in the process of primary preparation of raw materials, mainly oils extracted from various fields are transferred to the preparation, which leads to large irretrievable losses of valuable raw materials.

The presence of water in the extracted oil formations causes changes in their physicochemical properties.

The results of the study of the kinematic viscosity of a water-oil emulsion at 20 ^{0}C are shown in Figure 1 as an example.

As can be seen from Figure 3.1, as the water content in the oil increases, its kinematic viscosity increases sharply. Moreover, the greatest increase in the kinematic viscosity of the water-oil emulsion is observed in the oils of the Northern Ortabulak and Sariqum OPE.

In particular, due to the high viscosity of such water-oil emulsions and the presence of substances with emulsifying properties, the separation of these emulsions into separate phases is carried out with great difficulty and requires high capital costs and a long period of separation.

Since the viscosity of the water-oil emulsions at the Shurtepa and Kruk OPE (Figure 3.1) is low compared to the above-mentioned oils, dehydration, desalination, and fragmentation are easily carried out [10; pp. 559-564].

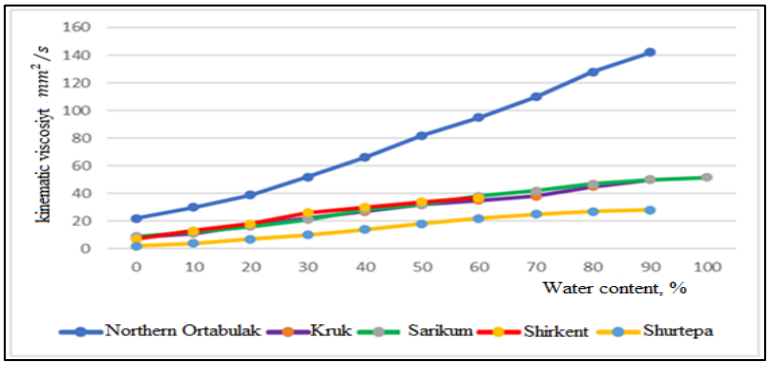


Figure 1. Variation of the kinematic viscosity (v) of a water-oil emulsion depending on the amount of formation water (Q_s) in its composition: 1 - emulsion formed at the Northern Ortatubalok OPE; 2 - emulsion formed at the Shirkent OPE; 3 - emulsion formed at the Shurtepa OPE; 4 - emulsion formed at the Kruk OPE; 5 - emulsion formed at the Sarikum OPE;

A similar situation is observed when studying the dynamic shear stresses of local water-oil emulsions formed at the Northern Ortabulaq, Shirkent, Aqqul, Shurtepa, Kruk, and Sariqum OPE. The results of the study of the dynamic shear stresses of highly stable water-oil emulsions of local heavy oils are presented in Figure 2.

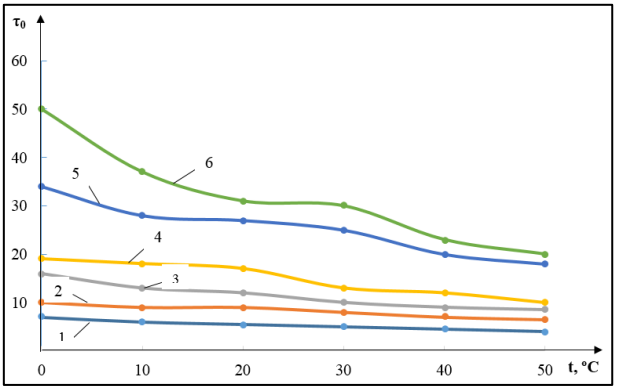


Figure 2. Variation of dynamic shear stresses (τ_0) of local oils as a function of temperature (T).

Figure 2 shows that the rheological properties of the oils from the Northern Ortabulaq (curve 1), Shirkent (curve 2), Akkul (curve 3) and Shorchi (curve 4) fields are close to each other. On the contrary, the rheological properties of the oils from the Sarikum (curve 6) and Kruk (curve 5) fields differ sharply from the previous ones. This is explained by the presence of a large amount of resinous substances and paraffins in them [10; p. 559-564].

Conclusions and Recommendations.

In particular, as a result of the analysis of the composition and physicochemical properties of emulsions formed during the extraction, well exploitation, and collection and preparation of local high-viscosity heavy oils, we conclude that it is advisable to prepare chemical reagents (demulsifiers) close to their properties for industrial preparation and mix them with oils and their emulsions. Also, based on the specific characteristics of the composition of the studied emulsions, it is advisable to prepare water-oil emulsions at the Northern Ortabulak and Sariqum OPE for processing separately, without mixing them with others. Also, as the amount of water in the emulsions increases, their viscosity also increases. It was found that when this indicator reaches the maximum value of hydration (B=98%), it increases from 3.6 to 6.7 times, depending on the place and environment of the emulsion extraction. As a result, the stability of the emulsion also increases several times. To break such highly stable emulsions, there is a need for an increased amount of demulsifiers or new complex demulsifiers.

As can be seen from the above data, the mechanisms of formation of stable water-oil emulsions are very complex and their behavior has not been fully studied to date. Therefore, it is necessary to find effective methods for separating stable water-oil emulsions into phases and use unconventional methods of breaking mechanisms.

References

[1]. Промысловая подготовка нефти и газа: Учебное пособие / Благовещенск: Амурский гос. ун-т, 2021. – 115 с.

[2]. ГОСТ 2517- 2012 Межгосударственный стандарт. Методы отбора проб нефть и нефтепродукты.-М.: Стандарт, 2014. 35 с.

[3]. Неклюдов А.Д., Иванкин А.Н., Федотов Г.Н., Олиференко Г.Л. Теоретические и экспериментальные методы исследования в химии. Учебное пособие. Изд. 2, доп. и перераб. – М.: МГУЛ, 2016. – 502 с.: ил. 124.

[4]. Эшметов Р.Ж. Ишлаб чикиилган сирт-фаол моддалардан фойдаланиб юқори қовушқоқ маҳаллий нефтларни ультратовушли деэмульгирлаш технологияси // т.ф.д. илмий даражасини олиш учун диссертация иши Тошкент. 2021. – 275 б.

[5]. Очилов А.А., Абдурахимов С.А., Адизов Б.З., Рахимов Б.Р. Разработка композиции деэмульгаторов, применямых в разрушении высокоустойчивых водонефтяных эмульсий тяжелых нефтей// Монография, - Бухара, Издательство “Умид”, 2020. С. 120.

[6]. Abduraxim Ochilov, Bobirjon Adizov. Analysis of demulsifier production from sulfurized cottonseed oil and breakdown of water-oil emulsions // Austrian Journal of Technical and Natural Sciences 2024, № 3-4. P. 79-82.

[7]. Очилов А.А., Адизов Б.З. Разработка деэмульгатора для разрушения тяжелых высоковязких водо-нефтяных эмульсий // VIII Всероссийской научно-практической конференции «Информационые и инновационные технологии в науке и образовании»г.Таганрог. 26-27 октября 2023г. С. 127-131.

[8]. Xushnud Shukurulla uli Ismailov, Kamal Axmet uli Uzakbayev, Abduraxim Abdurasulovich Ochilov. Og‘ir neftlarning suvneftli emulsiyalarini parchalash texnologiyalarini o‘rganish bosqichlari // SCIENCE AND EDUCATION, Scientific journal. In volume 4. Issue 1, Yanuary 2023. 268-273 b.

[9]. Ochilov A.A., Uzakbayev K.A., Adizov B.Z. Mahalliy og‘ir neftlar suv-neft emulsiyalarining dastlabki ko‘rsatkichlari // “Neft va gaz sohasidagi zamonaviy innovasion texnologiyalar”. Respublika miqyosidagi ilmiy-texnik anjuman materiallari 12-13 may, 2023 y, Toshkent 190-192 b.
[10]. Ochilov A.A., Ochilov X.G. Og‘ir yuqori qovushqoqli neftlarda barqaror suv neft emulsiyalarining shakllanishi va barqarorlanishining sabablari SCIENCE AND EDUCATION, Scientific journal. In volume 3. Issue 4, April 2022., 559-564 b.
[11]. Ochilov A.A., Eshmetov I.D., Salikhanova D.S., Adizov B.Z. Decomposition of high-stable water-oil emulsions of heavy oils in an oil preparation device. *The journal “Processes of Petrochemistry and oil Refining” (PPOR).* SSN: 1726-4685
[12]. Uzakbaev K.A., Ochilov A.A., Abdikamalova A.B., Salixanova D.S. Analysis of the process of breaking down water-oil emulsions of heavy oils using the developed local demulsifier. The European Journal of Technical and Natural Sciences 2024, № 3 – 4, pp 21-26.
[13]. Eshmetov I. D., Salixanova D. S., Adizov B. Z., Ochilov A.A., O‘rinov X.X., Uzakbaev K.A. Yuqori turg‘un suv - neftli emulsiyalarini parchalash uchun samarador deemulgator tarkibini tanlash. “Central Asian Food Engineering and Technology” elektron ilmiy jurnali, 2024. №8, 72-77 bet.

SYNTHESIS OF MORPHOLINE-BASED AMINOMETHYLATED DERIVATIVES OF STERICALLY HINDERED CYCLOALKYLPHENOLS

Hajiyeva G.F., Naghiyeva M.V.
Academician Y.H. Mammadaliyev Institute of Petrochemical Processes of the Ministry of Science and Education of the Republic of Azerbaijan, AZ 1025, Baku, 30 Khojaly Ave
e-mail: glsm.hcyv97@gmail.com

Summary - This study is devoted to the synthesis of morpholine-based Mannich bases derived from 2-cycloalkyl-4-methylphenols obtained via the cycloalkylation of *para*-cresol with cyclohexene and methyl esters of methylcyclohexenecarboxylic acids in the presence of the KU-23 catalyst. The synthesis was performed in two stages, and the optimal kinetic and technological parameters were determined for each stage. The synthesized Mannich bases were evaluated for their potential use as anticoking additives in diesel fuel.
Keywords: *p*-Cresol, cycloalkylation, Mannich base, morpholine, sterically hindered alkylphenols, anticoking additive, diesel fuel

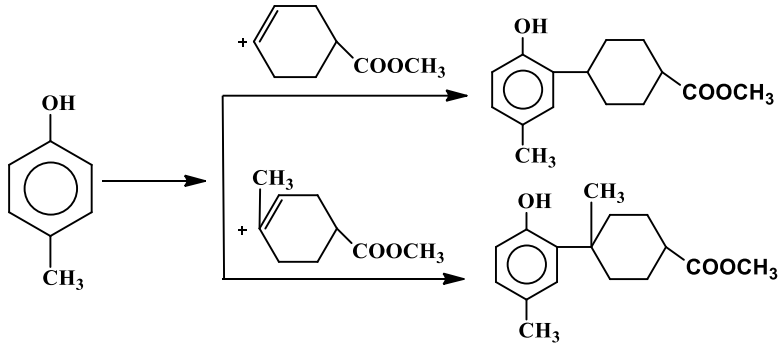
Introduction

Sterically hindered alkylphenols and their amino derivatives represent an important direction in the petrochemical industry. These compounds exhibit high functional performance, inhibiting early-stage polymer and oil degradation and retarding or completely suppressing chain oxidation in the systems where they are applied [1–3].

Experimental part

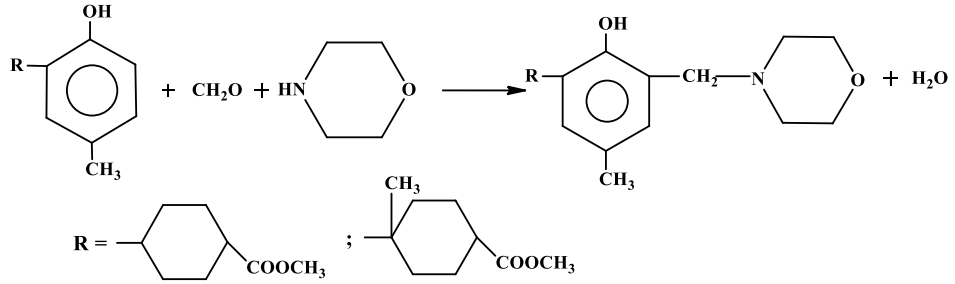
Stage I – Cycloalkylation Reactions

In the first stage, the cycloalkylation of *p*-cresol with cyclohexene and the methyl esters of methylcyclohexenecarboxylic acids in the presence of the KU-23 catalyst was investigated. The reactions were carried out in a batch reactor, and the influence of the process kinetic parameters on the composition and direction of the reaction products was studied to ensure maximum yield and high selectivity of the target products.



Stage II – Aminomethylation (Mannich Reaction)

In the second stage, the aminomethylation of cycloalkylphenols containing cyclic ether fragments with formaldehyde and morpholine was carried out.



The reaction was carried out at 80 °C for 2 h using benzene as the solvent.

Results and their discussion

The effects of kinetic parameters on the yields of the main products and the process selectivity in the cycloalkylation of *p*-cresol with cyclic ethers were investigated, and the optimal conditions for each reaction were determined. The established conditions were as follows: temperature 120–125 °C, reaction time 5–5.5 h, molar ratio of *p*-cresol to ether 1:1, and catalyst loading 10–12% based on the charged p-cresol.

Under the determined optimal conditions, the yield of the target products was 69.7–73.4% (based on charged *p*-cresol), while the process selectivity toward the target product reached 87.9–91.6%.

At the aminomethylation stage, the yield of the obtained Mannich bases was in the range of 63.7–67.0% based on the charged 2-cycloalkyl-4-methylphenol.

Offers

The morpholine Mannich bases of the methyl esters of 4-(2-hydroxy-5-methylphenyl)cyclohexane and 4-(2-hydroxy-5-methylphenyl)-4′-methylcyclohexanecarboxylic acid were proposed for evaluation as anticoking additives in diesel fuel. These compounds are considered effective for preventing coke formation in fuel systems.

References

1. Naghiyeva M. V., Rasulov Ch. K., Aliyeva S. G. Synthesis of methyl esters of 4(4-hydroxyphenyl)-4-methyl- and (4-hydroxyphenyl)cyclohexanecarboxylic acids and their aminomethylated derivatives. *Oil Refining and Petrochemistry*, 2018, No.6, pp. 38–42 *(in Russian)*
2. Gurbanova U.R., Rasulov Ch.K., Naghiyeva M.V., Hajiyeva G.F. Development of a Novel Environmentally Benign Green Catalyst for the Synthesis of Sterically Hindered Cycloalkylphenols. In Proceedings of the XI International Russian-Kazakhstan Scientific and Practical Conference “Chemical Technologies of Functional Materials”, Novosibirsk, 2025, pp. 111–112
3. Zhao Z., Shi H., Wan C., Hu M. Y., Liu Y., Mei D., Camaioni D. M., Hu J. Z., Lercher J. A. Mechanism of phenol alkylation in zeolite H-BEA using in situ solid-state NMR spectroscopy. Journal of the American Chemical Society, 2017, Vol. 139, No. 27, pp. 9325–9336

ALKİLFENOLLARIN AZTULLANTI ÜSULU İLƏ SİNTEZİ

Mahmudov Emin , Əliyeva Nailə
Sumqayıt Dövlət Universiteti
Sumqayıt, Azərbaycan
mahmudovemin125@gmail.com

Xülasə - Alkilfenolların fasiləsiz sintezi üçün fasiləsiz axar tipli reaktordan istifadə olunmuşdur. Fasiləsiz reaktor texnologiyasının tətbiqi və istilik yüklərinin azaldılması məqsədilə aztullantı üsullarının istifadəsi prosesin effektivliyini artırır [1]. Bu işdə alkilfenolların fasiləsiz alınması nəzəri və praktik cəhətdən təhlil olunmuşdur. 2-metilfenolun metanolla alkilləşmə reaksiyasının baş vermə surətinin artırılması üçün temperaturun artırılması, xüsusi yükləmənin azaldılması və xammaldakı spirtin parsial təzyiqinin artması müsbət təsir edir. Lakin texnoloji rejim parametrlərinin bu cür dəyişdirilməsi bəzi texnoloji kriteriyaların pisləşməsinə gətirib çıxarır.

Açar sözlər: alkilfenollar, fasiləsiz reaktor, aztullantı üsulu, proses optimallaşdırılması, yüksək məhsul çıxımı, istilik yüklərinin azaldılması

Giriş

Alkilfenollar fenolun alkil törəmələri olub, sənayedə geniş istifadə olunan vacib üzvi maddələrdir. Onların əhəmiyyəti həm kimyəvi reaktivliyindən, həm də fiziki-kimyəvi xüsusiyyətlərindən (lipofillik, sabitlik, reaktiv –OH qrupu) irəli gəlir. Alkilfenolların kimya sənayesində əhəmiyyətli xammal hesab olunması və onların istehsalı prosesin səmərəliliyi və məhsul keyfiyyəti ilə birbaşa bağlıdır [2]. Alkilfenolların sənaye tətbiqləri genişdir; onlar surfaktantların, qatqı maddələrinin və farmasevtik preparatların istehsalında vacib komponent kimi çıxış edir [3]. Ənənəvi partiyalı sintez üsulları enerji sərfiyyatını artırır və yan məhsulların əmələ gəlmə riskini yüksəldir [4].

Fasiləsiz reaktor texnologiyası bu problemləri minimuma endirir, prosesin idarəolunmasını asanlaşdırır və məhsulun homogenliyini təmin edir [2]. Aztullantı üsulları isə reaksiyanın istilik yükünü azaldır və yan məhsul əmələ gəlməsini minimuma endirir [5]. Nəticədə həm məhsul çıxımı artır, həm də ətraf mühitə mənfi təsir azalır [1].

Eksperimental hissə

2-metilfenolun metanolla alkilləşmə reaksiyası dəmir ferrit katalizatoru iştirakı ilə tədqiq edilmişdir. İstifadə olunmuş katalizatorlar bu reaksiyada ilk dəfə tətbiq olunmuşdur.

İlk növbədə 2-metilfenolun metanolla alkilləşmə reaksiyası ilə 2.6-dimetilfenolu yüksək çıxım və selektivliklə almaq üçün müxtəlif ferrit katalizatorlarının katalitik xassələri tədqiq edilmişdir. Reaksiya temperaturu və axım sürəti müxtəlif səviyyələrdə tənzimlənmişdir ki, məhsul çıxımı və tərkib keyfiyyəti maksimum səviyyəyə çatdırılsın.

Aztullantı üsulu reaktor daxili istilik dəyişməsini minimuma endirərək reaksiyanın yan məhsullarının əmələ gəlməsini azaltmışdır. Katalizator kimi turşu və ya əsas tərkibli sistemlər tətbiq edilmiş, nəticədə məhsulun tərkibi homogen və yüksək saflıq dərəcəsinə malik olmuşdur.

Nəticələr və onların müzakirəsi

Tədqiqat göstərir ki, fasiləsiz reaktordan istifadə nəticəsində məhsulun çıxımı və homogenliyi artır, prosesin enerji səmərəliliyi isə yüksəldir. Az tullantılı üsul termal yükləri azaldaraq yan məhsulların əmələ gəlməsini minimuma endirmişdir.

Məhsulun keyfiyyəti reaktor şəraitindən, axım sürətindən və katalizator seçimindən asılıdır. Nəticələr göstərir ki, bu texnologiyalar sənaye miqyasında tətbiq oluna bilər və ətraf mühitə mənfi təsirləri minimuma endirir.

Təkliflər

1. Fasiləsiz reaktor texnologiyasının fərqli katalizator tipləri ilə optimallaşdırılması;
2. Aztullantı üsullarının enerji səmərəliliyinə təsirinin geniş tədqiqi;
3. Məhsul tərkibinin müxtəlif alkil qrupları ilə müqayisəli təhlili;
4. Pilot və sənaye reaktorları arasında proses parametrlərinin uyğunlaşdırılması;
5. Prosesin avtomatlaşdırılmış idarəetmə sistemləri ilə optimallaşdırılması.

İstinadlar
1. **Rang, H. P., Dale, M. M., Ritter, J. M., & Flower, R. J. (2012).** *Pharmacology (7th ed., s. 742–750)*. London: Churchill Livingstone.
2. **Smith, M. B., & March, J. (2007).** *March's Advanced Organic Chemistry: Reactions, Mechanisms, and Structure* (6th ed., s. 845–865). New York: Wiley.
3. **Lemke, T. L., & Williams, D. A. (2013)**. *Foye's Principles of Medicinal Chemistry (7th ed., s. 875–890).* Philadelphia: Lippincott Williams & Wilkins.
4. **Rappoport, Z. (2004).** *The Chemistry of Aromatic Amines* (s. 890–900). Chichester: Wiley.
5. **Patrick, G. L. (2017**). **An Introduction to Medicinal Chemistry** (6th ed., s. 520–538). Oxford: Oxford University Press.

OPTIMIZATION OF CMC-PVA TERNARY BLEND FORMULATIONS FOR HIGH-EFFICIENCY SEED COATING: IMPACT ON GERMINATION RATE AND SEEDLING DEVELOPMENT

Asmar Eyvazli, Aysu Rzayeva, Garanfil Ahmadova
Baku Higher Oil School
Baku, Azerbaijan
asmar.eyvazli.std@bhos.edu.az , aysu.rzayeva.std@bhos.edu.az

Keywords: sustainable agriculture, biodegradable seed coating, biopolymers, germination efficiency, CMC-PVA films, seed vigour index, fly ash, epoxy resin composite**,** reinforcing fillers, circular economy, waste valorisation

Abstract:
The conventional synthetic seed coatings used in modern agriculture present significant environmental risks due to their inherent non-biodegradability. This research explains the production and description of sustainable and environmentally friendly biopolymeric covers based on carboxymethyl cellulose (CMC) and poly(vinyl alcohol) (PVA), and suggests them as the possible alternatives to traditional materials. The biocomposite films were produced through a solvent casting procedure, and after that, directed physicochemical cross-linking was applied to improve structural stability and durability. The main novelty of the study is the creation of a particular porous structure in the CMC-PVA matrix, which allows to provide the maximum exchange of gases in the atmosphere with the respiration of the seeds and at the same time control the moisture retention. Experimental findings indicate that the seeds coated with such biopolymeric coatings have a germination rate of 100% with a significant increase in seed vigor index. The results indicate that the technology used facilitates the growth of plants without chemicals and reduces the environmental hazards of using toxic agricultural additives. CMC-PVA blends have a high potential of large-scale application in green agricultural systems and sustainable material engineering as a scalable and biodegradable solution.

Introduction:

The high rate of growth of the worldwide industrial infrastructure and construction industry has significantly increased the need of high performance protective coatings. Chemical corrosion, moisture intrusion, and mechanical deterioration are some of the factors that lead to significant economic losses every year and undermine structural integrity. In the coating sector, there is wide application of epoxy resins due to their high adhesive

properties, chemical resistance and mechanical stability. However, neat epoxy systems are often constrained by nature, low impact resistance, and high thermal expansion coefficient, which may cause early coating failure in harsh conditions.

One of the main goals of modern materials science is to address these shortcomings and enhance the principles of the circular economy through waste valorization. Fly ash is a fine-grained by-product of coal burning in thermal power plants, which poses a serious environmental problem unless it is repurposed. Fly ash, which is distinguished by a rich chemical composition, mainly consisting of SiO_2 and Al_2O_3, is a high-potential functional reinforcing filler of polymer matrices. In contrast to traditional synthetic fillers, the spherical shape and characteristics of the fly ash particles can be used to increase the packing density, thermal stability, and surface hardness.

This paper uses fly ash as a green filler that is sustainable to create an economical composite that fills the gap between industrial waste management and high-performance engineering. The structural, chemical, and morphological properties of the resulting composites were strictly examined by Fourier-transform infrared spectroscopy (FT-IR) to determine the effectiveness of cross-linking and the interfacial relationship between the filler and the resin matrix. The results indicate that the incorporation of industrial waste can be used to develop ecologically friendly coating systems that can be used in heavy industrial and large-scale construction projects.

Experimental part:

The current research was aimed at a systematic assessment of the synergistic impact of the addition of industrial by-products to a high-performance polymer matrix. A commercial grade of diglycidyl ether of bisphenol A (DGEBA) epoxy resin was used as the main binder in all formulations, as it has better mechanical properties, chemical inertness, and industrial reliability. A low-viscosity polyamine-based hardener was used as the curing agent to trigger polymerization and to make sure that a strong cross-linked network is formed. The reinforcing phase was made of fly ash, an industrial by-product of coal combustion that was subjected to strict pre-processing to ensure that it could be used in coating applications. Chemical analysis confirmed that the fly ash was predominantly composed of silica (SiO_2, 45–60 wt.%) and alumina (Al_2O_3, 20–30 wt.%), both of which are critical for enhancing the thermal stability and surface hardness of the final composite [1].

Initially, the fly ash was carefully sieved through a 75-μm mesh to achieve a uniform particle size distribution and subsequently dried in a vacuum oven at 110°C for 24 hours. This was necessary to remove any remaining hygroscopic moisture that would otherwise prevent the curing reaction. The production of fly ash-reinforced epoxy (FARE) composites was

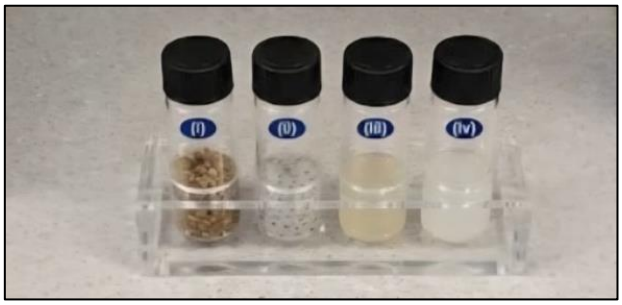
a multi-step mechanical mixing procedure to achieve the highest homogeneity. To determine the optimal filler loading for structural enhancement, the experimental matrix included several formulations with concentrations of 0%, 5%, 10%, and 15% by weight.

The mixture was then placed in an ultrasonic bath during another 20 minutes to further homogenize the microstructure and remove sub-micron-sized clusters, and then, the mixture was placed in a vacuum desiccator at 0.1 MPa to remove any air bubbles trapped in the mixture. After this step, the polyamine-based hardener was added in an exact stoichiometric proportion to trigger the chemical cross-linking reaction. The resulting liquid composite was deposited onto standardized concrete and steel substrates using a precision film applicator to ensure a consistent dry film thickness (DFT) of approximately 250 μm. The curing protocol was executed in two distinct phases: primary ambient curing at 25°C for 48 hours to facilitate gelation, followed by post-curing at 60°C for 4 hours. This two-step method was aimed at maximizing the conversion efficiency of epoxide groups and increasing the glass transition temperature (T_g) of the coating, which would guarantee stability in the long-term in harsh industrial conditions. Particular focus was directed toward the disappearance of the epoxide ring peak at 915 cm^{-1} and the emergence of the hydroxyl stretching vibration at 3400 cm^{-1}.

In addition, thermogravimetric analysis (TGA) was applied to determine the thermal stability of the cured specimens. The samples were heated to 800°C in an inert atmosphere to determine the heat resistance that the fly ash fillers imparted. The interfacial bonding between the fly ash particles and the epoxy matrix was studied under Scanning Electron Microscopy (SEM) that gave visual evidence of the morphological homogeneity and the lack of phase separation.

Lastly, the potential of practical application was determined by standardized pull-off adhesion tests (ISO 4624) to determine the strength of the bond between the composite coating and the corresponding substrates.

Results and discussion



A set of thorough chemical, thermal and mechanical tests were conducted to determine the structural integrity and performance characteristics of the synthesized FARE composite coatings systematically. Fourier-transform infrared (FT-IR) spectroscopy was used to prove the successful cross-linking of the DGEBA resin with the polyamine hardener.

In the 3200 cm $^{-1}$ 3600 cm $^{-1}$ range, the spectra exhibited a broad and intense absorption band, which is attributed to the stretching vibrations of hydroxyl (-OH) groups. This spectral characteristic shows that the epoxide groups are successfully reacting in a ring-opening reaction, in which the epoxide groups are transformed into secondary alcohols during the polymerization process.

Furthermore, characteristic peaks identified at 2926 cm $^{-1}$ and 2855 cm $^{-1}$ correspond to the asymmetric and symmetric stretching vibrations of C-H groups within the aliphatic chains of the epoxy matrix, confirming the stability of the polymer backbone.

The successful incorporation of the industrial by product was evidenced by the emergence of distinct absorption bands between 1000 cm $^{-1}$ and 1100 cm $^{-1}$. These bands represent the Si-O-Si and Al-O-Si stretching vibrations, corresponding to the silica (SiO_2) and alumina (Al_2O_3) phases of the fly ash, respectively. The near-complete disappearance of the epoxide ring peak at 915 cm $^{-1}$ further validates the high degree of curing.

Mechanical and thermal tests proved that the gradual additions of fly ash (5, 10, and 15 wt.%) provided a considerable positive effect on the functional characteristics of the coating. The incorporation of these spherical particles in the epoxy structure facilitates a pinning effect that reduces polymer chain mobility and acts as a shield to micro-crack propagation.

Consequently, the integration of these micro-spheres resulted in produced a quantifiable improvement in surface hardness and abrasion resistance compared to unfilled epoxy resin. Thermogravimetric analysis (TGA) also supported the contribution of the filler to the enhancement of durability; the inorganic components of the fly ash serve as an effective thermal barrier, thus increasing the initial temperature of thermal degradation. It is important to note that the 15 wt.% fly ash formulation had a significantly higher char yield, which confirms its better heat resistance in harsh conditions [3].

These observations were also supported by scanning electron microscopy (SEM) that showed that there was a homogenous distribution of particles and the agglomeration was negligible- an aspect that is important in ensuring uniform mechanical performance. The strong interfacial bond between filler and resin matrix produced a non-porous microstructure that was dense. This high packing density plays a critical role in the protective properties of the coating, which prevents moisture and corrosive ion

penetration, significantly increasing adhesive bond strength and overall service life of the coated industrial substrates.

Offers:

According to the overall results of this research, there are a number of strategic directions, which are suggested to improve the performance and industrial viability of FARE composite coatings. The interfacial adhesion between the inorganic constituents (SiO_2 and Al_2O_3) and the polymer matrix can be greatly enhanced by the use of silane coupling agents or other forms of functionalization. These composites should be tested in the offshore or high-humidity industrial conditions, and the emphasis should be on accelerated weathering, exposure to ultraviolet radiation, and constant salt-spray testing

In order to close the gap between the laboratory scale observations and the actual durability in the real world, it is recommended that these coatings be subjected to intense and long term environmental stress tests. Their structural integrity in offshore or high-humidity industrial conditions should be tested with a priority on accelerated weathering, exposure to UV radiation, and constant salt-spray analysis. Furthermore, the exploration of hybrid composite systems, particularly through the incorporation of low weight fractions of nano-clays or carbon nanotubes alongside industrial fly ash, may lead to the development of smart thin film coatings with enhanced barrier properties. Sustainably, a thorough Life Cycle Assessment (LCA) is necessary to measure the environmental and economic advantages of the reuse of coal combustion by-products. Finally, FARE composites as high-performance rehabilitation and repair systems should be considered in a broader variety of engineering structures.

References:

[1] Chandrika, K. S. V. Poorna, et al. ‘Porous Crosslinked CMC-PVA Biopolymer Films: Synthesis, Standardization, and Application in Seed Coating for Improved Germination’. *Carbohydrate Polymer Technologies and Applications*, vol. 11, Sept. 2025, p. 100900. *ScienceDirect*.

[2] Pang, Long, et al. ‘Cellulose Based Materials for Controlled Release Formulations of Agrochemicals: A Review of Modifications and Applications’. *Journal of Controlled Release*, vol. 316, Dec. 2019, pp. 105–15. *DOI.org (Crossref)*, https://doi.org/10.1016/j.jconrel.2019.11.004.

[3] Zhang, Wenxu, et al. ‘Preparation of Nutrient Hydrogels with Core-Shell Structure for Seed Germination and Seedling Growth in High Temperature Saline Environment’. *International Journal of Biological Macromolecules*, vol. 283, Dec. 2024, p. 137626. *DOI.org (Crossref)*, https://doi.org/10.1016/j.ijbiomac.2024.137626.

DEVELOPMENT OF ECO-FRIENDLY AND SELF-HEALING CHITOSAN-CITRATE BIOCOMPOSITE COATINGS FOR ADVANCED CORROSION PROTECTION OF METALLIC ASSETS

Leyla Muradova, Nazrin Ibadzade, Alishan Alishanov
Baku Higher Oil School
Baku, Azerbaijan
leyla.muradova.std@bhos.edu.az, nezrin.ibadzade.std@bhos.edu.az

Abstract - Despite decades of technological advancement, the corrosion protection of steel in industry remains largely dependent on toxic chromate-based coatings that raise serious environmental and health concerns, and, owing to their inherently passive mechanism, these systems become ineffective at preventing localized corrosion when the protective surface is damaged. In this paper, the creation of a chitosan-citrate crosslinked coating to enhance corrosion resistance as well as to add self-healing functionality onto the steel substrates is reported. By dissolving chitosan in acetic acid, filtration was done, then citric acid was added and the pH adjusted and then thermal curing to facilitate crosslinking was carried out. The presence of the linkage of the chitosan and citric acid to form ester linkages was confirmed by FTIR analysis, which showed the presence of typical C=O stretching and C-O-C bands which show that crosslinking has occurred within the polymer backbone. The difference in morphology of coated and uncoated samples was demonstrated in the SEM micrographs. Although uncoated steel was accompanied by a significant pitting corrosion and localized surface degradation following the exposure to NaCl, the coated surface still had a compact morphology with limited surface irregularities. When immersion test was done in solution with NaCl (120 hours) it was observed that the mass lost by the coated sample (2.8 mg) was significantly lower than that lost by bare steel (38 mg), which implied that the rate of corrosion was reduced. Comparatively, pure chitosan performed in-between. The performance of self-healing was measured using the width of the crack as time progressed. Crack closure was also seen gradually up to about 80 percent of healing efficiency at 48 hours at ambient temperature. In general, the findings show that the nano-coating based on chitosan-citrate offers quantifiable corrosion inhibition along with self-healing functionality in situ in the laboratory.

Keywords: chitosan-citrate, corrosion inhibition, self-healing coating, esterification, chemical cross-linking.

Introduction

The corrosion of metals is a significant problem affecting many different types of industries. When metal starts to corrode, it causes deterioration of the metal's surface and can result in a loss of structural integrity leading to safety issues and added costs for maintenance. Since most conventional coatings are made from petroleum-based plastics and contain toxic chemicals which were created using petroleum, there are growing concerns about the health and environmental impacts of these types of coatings. Therefore, the development of sustainable ways to create natural coatings is an important research area within materials science [Sharif, 2026].

Chitosan is a naturally occurring polysaccharide that comes from the shells of shrimp (chitin). It has gained significant interest from scientists as it can easily be biodegraded, has good film forming characteristics, has an

amino group (-NH_2) and hydroxyl group (-OH) which will allow the chemical modification or altering of chitosan and for cross-linkage to form larger molecular networks, thereby suggesting that chitosan is a very attractive option for using in developing new coatings that are eco-friendly. Prior research suggests that chitosan-based coatings do provide barrier properties on metallic substrates [Binder, 2024]. However, pure chitosan films provide limited mechanical strength and moderate protection against moisture which will limit the ability of pure chitosan to perform well over time.

It will be necessary to develop new eco-friendly methods of creating crosslinkages to improve durability. There has been a considerable amount of research performed to confirm citric acid (a multi-functional, largely-occurring three carboxylic acid-based organic compound) is an effective way to crosslink chitosan-based systems and is also considered to be a renewable resource [Sharmin, 2022] The use of heat may lead to greater intermolecular bonding and partial formation of esters which would strengthen the films and create barriers for further damage [Priyadarshi, 2018].

The use of self-healing capability in coatings is innovative and creates an extended life cycle for the coating. In chitosan-citric acid-based systems have shown to have self-healing characteristics because of reversible intermolecular interactions in their polymers [Smirnov, 2021].

Experimental part

The preparation of chitosan-citrate bio composite coatings was done through solution casting and heat curing. In brief, chitosan (2 g) was dissolved in 100 mL of 1 % (w/w) acetic acid and stirred under a magnetic field of 3 hours until the homogeneous solution was achieved and filtered. On its part, 0.4 g of the citric acid was dissolved in 5 mL of distilled water and was added in small drops to the chitosan solution in constant stirring. The mixture was stirred with 20 minutes of constant mixing to make it homogenized.

To stabilize the solutions, the pH was brought to 5.0-5.5 by the dropwise addition of 0.1 M NaOH. The plasticizer (glycerol 1-2 wt %) was added in increasing the flexibility of the coating. The last formulation was inverted to maintain homogeneity by stirring it further after 10 minutes.

Mechanical abrading (400-600 grit) followed by rinses in distilled water, ethanol, and air drying of stainless-steel substrates were done before being coated. A uniform film was obtained by a dip-coating process to the coating solution. The coated samples were brought under a temperature of 60 °C, 30 minutes to dry them and then subjected to a temperature of 120 °C, 1.5 hours to allow crosslinking between chitosan and citric acid.

Hydrogen bonding of molecules and partial formation of ester links in the polymer network was made possible through thermal treatment. Self-healing

behavior was observed, a controlled scratch was made on the coated surface, and the damaged area was observed to recover with time.

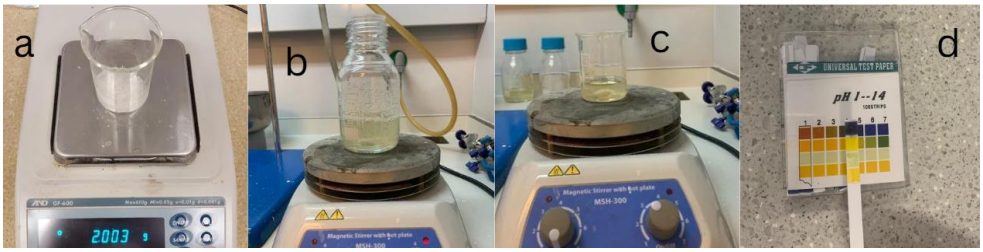


Figure 3. Preparation Steps: (a) Pure Chitosan; (b) Chitosan Dissolved in Acetic Acid; (c) Filtered Solution; (d) pH Measurement of the Final Solution

Results and Discussion

The developed coating of chitosan and citrate was tested by a couple of characterization and performance tests. Chemical interactions were studied by FTIR analysis, surface morphology was studied by SEM, corrosion resistance was studied using NaCl immersion tests and self-healing behavior studied by measuring scratch-width over time.

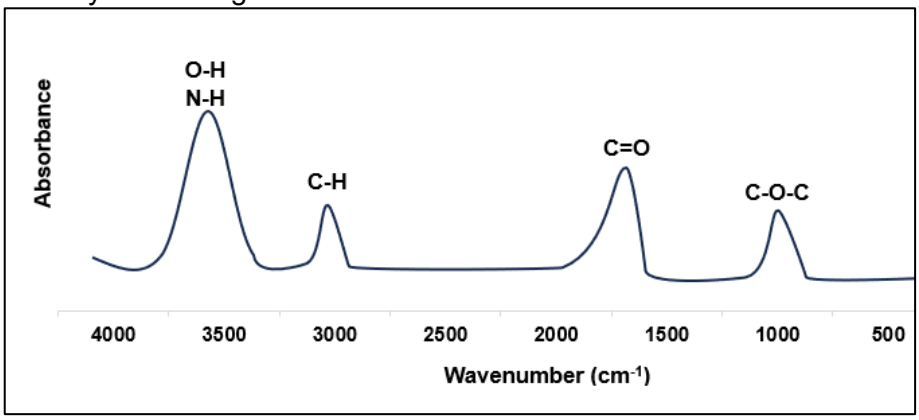


Figure 4. FTIR Analysis of the Solution

Structural modification of the solution is confirmed by the FTIR spectra. The extensive band at the 3400 cm^{-1} is a sign of O-H and N-H bonds and a stronger hydrogen bond in the coated film. The polymer band at the 2920 cm^{-1} corresponds to aliphatic C-H vibrations of the polymer backbone. Above all, the emergence of a new band at the range of approximately 1720 cm^{-1} can be explained by the presence of the carboxyl group of esters in the crosslinking of chitosan and citric acid, which proves the presence of covalent crosslinking. Alteration of 1000-1200 cm^{-1} region also supports formation of networks.

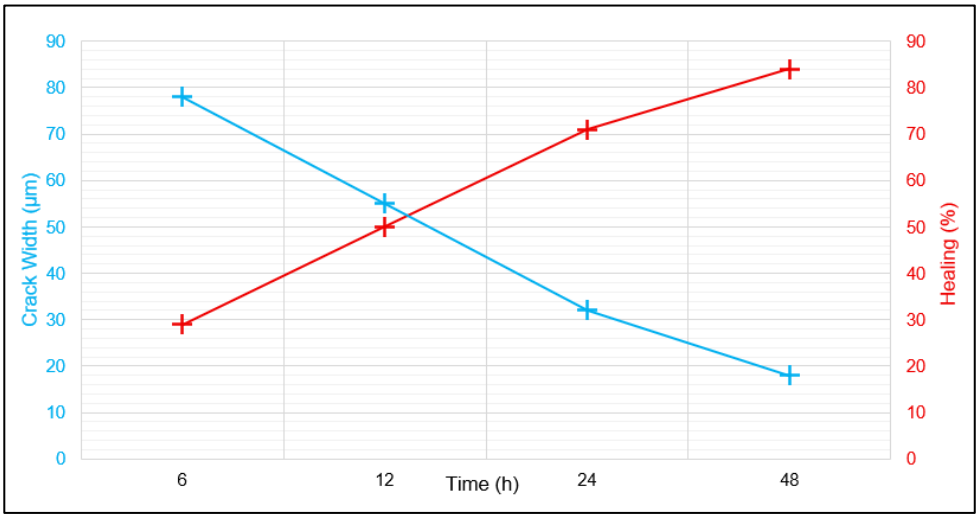


Figure 5. Crack Width Size / Healing vs Time

The self-sealing characteristic of the coating was tested by observing the reduction of the crack width with time. A dramatic reduction in the width of the crack between approximately ~75 µm and approximately ~15 µm in 48 hours was witnessed which was proportional to the increase in the efficiency of healing between approximately 30 % and approximately 80 %. The fast initial change in the initial values means that the mobility of the polymer chains is high, and the active intermolecular interactions are taking place, whereas the gradual stabilization after some time implies the gradual reorganization of the network.This activity proves that there are dynamic interactions in the chitosan-citrate matrix, which allows the partial recovery of structure at ambient conditions.

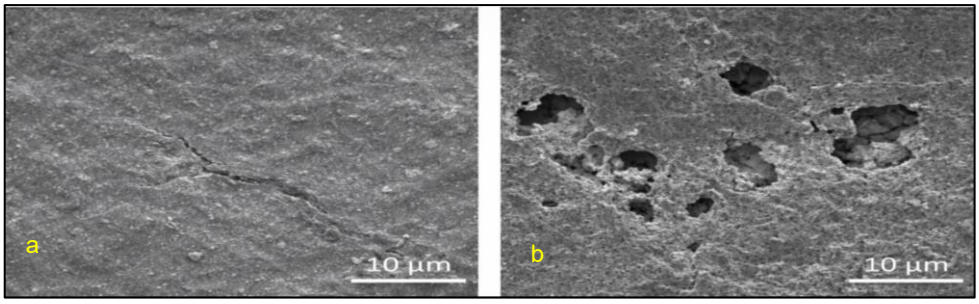


Figure 6. SEM Micrographs of (a) Coated and (b) Uncoated Metal Surfaces after Exposure to NaCl Solution (scale bar: 10 µm)

SEM images demonstrate that there are morphological changes in coated and uncoated samples. The bare surface has vivid pitting characteristics and focal corrosion surfaces, which means that it is corroded

in chloride. The coated sample looks tighter and slightly smoother yet the surface irregularities and a microcrack can be seen. There are no severe corrosion pits that may resemble those of the uncoated specimen on the surface covered. These observations indicate that the coating has a partial surface protection, in that, it reduces direct electrolyte contact with the metal substrate.

There was observable difference between the samples during the 120-hour corrosion test. Bare steel had the largest loss of mass (38 mg) and severe rust. Reduced mass loss to 12 mg accompanied by swelling and partial surface instability was seen with the pure chitosan coating. The coated sample (chitosan-citrate coated) had the least mass loss (2.8 mg) and had a relatively stable surface with slight oxidation of edges. All in all, the crosslinked coating exhibits better corrosion resistance than the uncoated steel and pure chitosan.

Table 2. Characteristics of the Solution

	Density (g/cm^3)	Viscosity (cP)	Color	ph
Solution	1.12	245	yellowish	5

Offers

The resulting chitosan-citrate coating is a green and low-toxicity alternative to traditional systems of protection that utilize dangerous crosslinkers. The formulation is based on the use of bio-based citric acid as a versatile crosslinking claiming agent, which increases structural stability without compromising environmental friendliness. The inclusion of glycerol enhances elasticity and decreases brittleness which causes the film to be more lasting to low mechanical pressure.

Further, the coating exhibits inherent self-healing behavior that is based on reversible intermolecular interaction between the polymer scaffolds. Together with its easy preparation procedure and low-cost raw material, the proposed system makes a favorable way to smart eco-friendly corrosion protection of metallic surfaces.

References

1. Binder, L., et al., 2024, The influence of molecular weight on the anticorrosion properties of chitosan coatings, Carbohydrate Polymers.
2. Priyadarshi, R., et al., 2018, Chitosan film incorporated with citric acid and glycerol as plasticizer: Mechanical and barrier properties, Carbohydrate Polymers.
3. Sharmin, N., et al., 2022, Effect of citric acid crosslinking on the mechanical, rheological and barrier properties of chitosan films, Molecules.
4. Sharif, N.U., et al., 2026, Advancing renewable functional coatings: Sustainable corrosion protection and self-healing features, Journal of Coatings Technology and Research.
5. Smirnov, M.A., et al., 2021, Self-healing films based on chitosan containing citric acid, Polymer.

COPPER-BASED ANODE DESIGN FOR METHANOL MICROFLUIDIC FUEL CELLS: MECHANISTIC INSIGHTS AND PERFORMANCE EVALUATION

Ilkana Mehdiyeva
University of Manchester
Manchester, United Kingdom
mehdiyeva871@gmail.com

Summary: The development of low-cost and noble-metal-free microfluidic fuel cells (μFCs) is essential for advancing portable energy technologies. This study presents an analytical investigation of copper-based nanoparticles (Cu NPs) as anodic catalysts for methanol electrooxidation in alkaline media and their integration into a membraneless mixed-media μFC system. Three synthesis routes—stationary (ST), mechanical stirring (MS), and ultrasonic-assisted (US)—were compared to evaluate their influence on morphology, surface chemistry, and electrochemical performance. Structural characterization revealed similar needle-like nanostructures; however, ultrasonic synthesis produced cleaner surfaces with higher $Cu(OH)_2$ content and reduced carbon contamination. Electrochemical and in situ FTIR analyses demonstrated complete methanol oxidation to carbonate via formate without detectable CO poisoning. The μFC assembled with a Cu/CP anode and metal-free cathode achieved a maximum power density of 26 μW cm^{-2} at 100 μL min^{-1}. The findings highlight the potential of Cu-based catalysts for cost-effective μFC applications and provide mechanistic insights for future optimization of methanol-fed microfluidic systems.

Keywords: microfluidic fuel cell, copper anode, methanol electrooxidation, mixed-media system, non-noble catalyst

Introduction:

The growing demand for sustainable power sources for portable electronic devices has driven the development of miniaturized systems known as microfluidic fuel cells (μFCs). These devices generate electrical energy through a spontaneous coupled redox reaction. Specifically, fuel undergoes electrooxidation at the anode, while a corresponding oxidant is reduced at the cathode. The continuous flow of electrons between these two half-reactions through an external circuit produces usable electrical work [1, 2]. The colaminar flow regime replaces traditional ion-exchange membranes, lowering cost and ohmic losses. However, most μFC systems rely on noble-metal catalysts such as Pt, which significantly increase production cost and limit large-scale implementation.

Copper represents an attractive alternative due to its low cost and availability. Nevertheless, its catalytic performance and reaction pathways for methanol electrooxidation require detailed mechanistic understanding. In alkaline media, Cu undergoes multiple oxidation transitions, forming Cu_2O, CuO, and $Cu(OH)_2$ species that influence catalytic behavior. Furthermore, the mixed-media concept—using alkaline anolyte and acidic catholyte—enables broader open-circuit voltage (OCV) through independent pH optimization of half-cells.

This work evaluates Cu nanoparticle synthesis strategies, surface chemistry, and electrochemical activity toward methanol electrooxidation. The integration of optimized Cu catalysts into a 3D-printed microfluidic fuel cell is analyzed to assess practical energy conversion performance.

Experimental section:

Copper nanoparticles were synthesized using three different approaches: stationary (ST), mechanical stirring (MS), and ultrasonic-assisted (US) methods. The obtained nanoparticles were dispersed onto carbon paper (CP) to prepare Cu/CP anodes. Structural and surface characterization was performed using SEM, TEM, XRD, and XPS to evaluate morphology, crystallinity, and surface composition. Electrochemical behavior toward methanol oxidation was investigated in alkaline medium (0.5 mol L^{-1} methanol + 0.1 mol L^{-1} KOH) using cyclic voltammetry, chronoamperometry, and in situ FTIR spectroscopy to identify reaction intermediates and oxidation pathways [3].

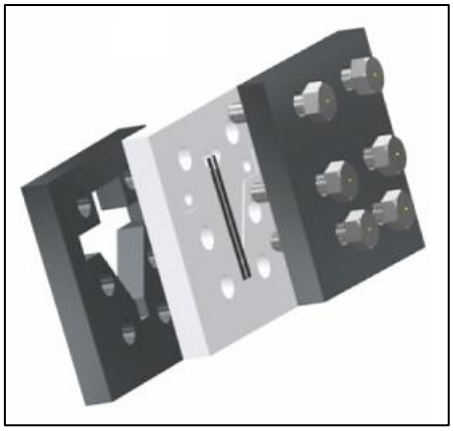


Figure 7. The design of MFC [4].

A reusable membraneless microfluidic fuel cell (μFC) was fabricated using additive manufacturing [4]. The device (3.6 cm × 3.6 cm) consisted of two 3D-printed PLA plates and a 4-mm-thick PDMS layer containing a 200 μm-high colaminar microchannel. The porous Cu/CP anode and bare CP cathode were positioned in grooves within the PDMS, forming an effective cross-sectional area of 0.0266 cm^2 for current and power normalization. Electrical connections were established using copper plates and silver epoxy.

The μFC operated under stable low-Reynolds-number colaminar flow, where part of the electrolyte penetrated the porous electrodes, enhancing reactant interaction with catalytic sites. The assembled system was tested in a mixed-media configuration using alkaline methanol as the anolyte and acidic sodium persulfate as the catholyte, and polarization curves were recorded to evaluate performance.

Result and discussion:

Structural and Surface Properties: Morphological analysis by SEM and TEM revealed that all synthesis routes (ST, MS, and US) produced needle-like copper nanostructures arranged in dendritic formations. The average crystallite sizes were in the nanometer range, confirming the formation of nanoscale catalytic structures. Although morphology appeared similar across samples, crystallographic and surface chemical analyses revealed significant differences.

XRD patterns confirmed CuO as the dominant crystalline phase in all materials, with minor contributions from $Cu(OH)_2$ particularly in the ultrasonically synthesized (US) sample. The US material exhibited slightly larger crystallite size and clearer diffraction features associated with hydroxide phases.

XPS analysis provided deeper insight into surface composition. The MS sample contained a mixture of CuO and Cu_2O with relatively high carbon surface contamination. In contrast, the US sample demonstrated reduced carbon contamination and higher $Cu(OH)_2$ surface concentration. The presence of surface hydroxyl species is particularly important in alkaline methanol oxidation, as adsorbed OH^- facilitates the oxidation of intermediate species. Therefore, differences in catalytic activity can be directly correlated to variations in surface chemistry rather than morphology alone.

Electrochemical Performance: Cyclic voltammetry in alkaline electrolyte revealed multiple redox transitions associated with copper oxidation states ($Cu^0/Cu^+/Cu^{2+}/Cu^{3+}$). These surface transformations occur concurrently with methanol electrooxidation.

The onset potential for methanol oxidation was significantly influenced by synthesis method. The US catalyst exhibited the lowest onset potential (~0.4 V vs. Ag/AgCl) compared to the ST sample (~0.85 V), indicating improved catalytic kinetics. The maximum current density reached 30.4 mA cm^{-2} for the US sample, exceeding those obtained from stationary synthesis.

Chronoamperometric measurements at 0.6 V further confirmed the superior catalytic stability of the US catalyst. The steady-state current density of the ultrasonically prepared material was substantially higher than that of the stationary sample, indicating enhanced active site availability and more efficient dissociative adsorption of methanol.

The improved activity of the US sample can be attributed to lower carbon surface contamination, higher $Cu(OH)_2$ surface concentration, improved external surface accessibility, and enhanced hydroxyl-assisted oxidation pathways.

Microfluidic Fuel Cell Performance: The optimized Cu/CP anode (US sample) was integrated into a membraneless mixed-media μFC using alkaline methanol as anolyte and acidic sodium persulfate as catholyte. The independent pH control of each half-cell broadened the theoretical open-circuit voltage (OCV).

Experimental OCV values ranged from 0.25 to 0.30 V at flow rates of 50–100 μL min^{-1}. The maximum current density reached 0.56 mA cm^{-2}, while peak power density achieved 26 μW cm^{-2} at 100 μL min^{-1}.

Although activation losses were evident due to the non-noble catalyst, the system demonstrated stable operation under colaminar flow conditions. Ohmic polarization dominated the performance curve, while mass transport limitations were minimal due to the use of a liquid oxidant.

Cost normalization analysis suggests that, despite lower intrinsic activity compared to noble metals, copper-based systems offer favorable cost-to-power ratios because of the significantly reduced material cost.

Overall Evaluation: The results demonstrate that synthesis conditions strongly influence surface chemistry and catalytic activity. Ultrasonic-assisted synthesis produces cleaner and hydroxyl-rich copper surfaces, leading to improved methanol oxidation kinetics and enhanced μFC performance.

These findings confirm that Cu-based anodes, when combined with mixed-media μFC architecture, represent a promising pathway toward low-cost and sustainable micro-scale energy conversion systems.

Offers:

To enhance μFC performance, further optimization of Cu surface chemistry and crystallographic orientation is recommended. Strategies may include alloying Cu with transition metals, improving nanoparticle dispersion, and increasing external surface area.

Integration with advanced additive manufacturing techniques could enable improved microchannel geometries for enhanced mass transport. Additionally, long-term durability and regeneration studies are necessary to evaluate commercial feasibility.

References

1. Kjeang, E. Microfluidic Fuel Cells and Batteries, Springer International Publishing: Cham Heidelberg New York Dordrecht London, 2014
2. Kjeang, E.; Djilali, N.; Sinton, D. Microfluidic Fuel Cells: A Review. J. Power Sources 2009, 186 (2), 353−369.
3. Queiroz B.D., et al. A Comprehensive Investigation of Methanol Electrooxidation on Copper Anodes: Spectroelectrochemical Insights and Energy Conversion in Microfluidic Fuel Cells. ACS Applied Materials & Interfaces, 2024
4. Guima, K.-E.; Gomes, L. E.; Alves Fernandes, J.; Wender, H.; Martins, C. A. Harvesting Energy from an Organic Pollutant Model Using a New 3D-Printed Microfluidic Photo Fuel Cell. ACS Appl. Mater. Interfaces 2020, 12, 54563−54572.
5. Guima, K.-E.; Zanata, C. R.; Martins, C. A. Exploring Liquid Oxidants and Metal-Free Cathode for Enhanced Performance in a Reusable 3D-Printed Glycerol Microfluidic Fuel Cell. Electroanalysis 2024, 36, No. e202300223
6. Gonçalves, R. V.; Wojcieszak, R.; Wender, H.; Sato, B.; Dias, C.; Vono, L. L.; Eberhardt, D.; Teixeira, S. R.; Rossi, L. M. Easy Access to Metallic Copper Nanoparticles with High Activity and Stability for CO Oxidation. ACS Appl. Mater. Interfaces 2015, 7 (15), 7987−7994.

CATALYTIC ALKYLATION OF P-CRESOL WITH ISOPRENE CYCLODIMERS USING A ZEOLITE-CONTAINING CATALYST

Naghiyev A.V., Aghamaliyev Z.Z.
Institute of Petrochemical Processes Named After Academician Y.G. Mamedaliyev
Baku, Khatai district, Khojaly Ave. 30
E-mail: asif_naghiev@mail.ru

Summary - The study presents the results of the alkylation of p-cresol with diprene, dipentene, and their mixture (the 160–180°C boiling fraction) in the presence of a zeolite-containing catalyst. The influence of key reaction parameters (including temperature, reaction time, molar ratio of the reactants, and catalyst loading) on the yield of the target products was investigated. Based on these experiments, optimal conditions were established for each reaction system. Under the optimised conditions, the yield of the target products was 65.5-73.8%, while the selectivity was 84.5–90.3%.

Keywords: *p*-cresol, alkylation, isoprene cyclodimers, sterically hindered phenols, zeolite catalysis

Introduction

Over the past decade, published studies have shown that chemical additives based on alkylphenols are successfully applied in various industrial sectors. Alkylphenol derivatives are widely used in the production of antioxidants and stabilisers for polymeric materials such as polyolefins and synthetic rubbers. By inhibiting thermo-oxidative degradation, they improve processing stability. Similar benefits are observed in lubricating oils and fuel compositions, where such additives enhance oxidation resistance and maintain performance under high temperatures. Beyond these established applications, alkylphenol-based compounds are also employed as ligands in catalytic systems, where they can influence activity and selectivity, and some derivatives exhibit biological activity, supporting their use in agricultural protection products [1–3].

The present work focuses on the alkylation of p-cresol with diprene, dipentene, and their mixture in the presence of the zeolite-containing catalyst KN-30.

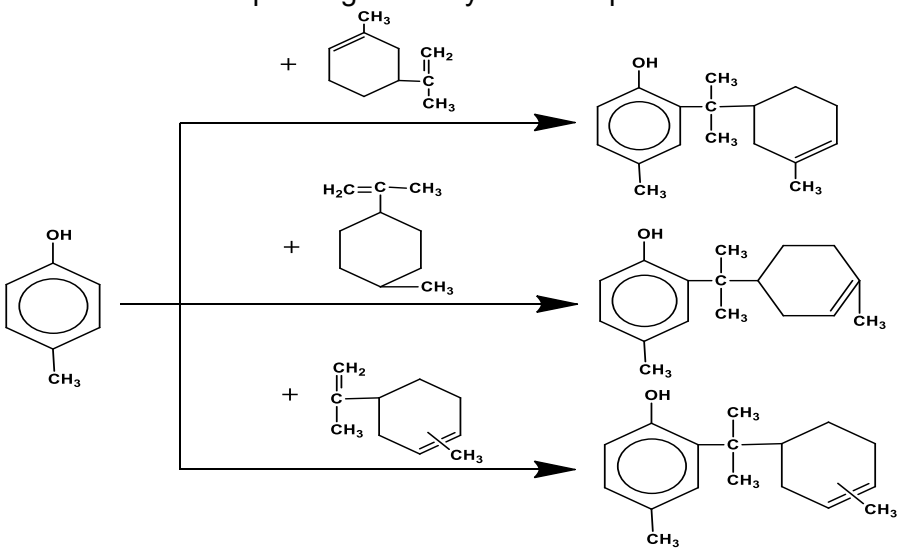
Experimental part

The following reagents were used as raw materials:

- *p*-Cresol (*p*-Cr). The physicochemical properties: T_b=201-202°C; n_D^{20}= 1.5395; ρ_4^{40} = 1.0347; MM=108 g/mol.
- Diprene (DP) was obtained via cyclodimerization of isoprene in an autoclave. Its physicochemical properties are as follows: T_b=160–161°C; n_D^{20}= 1.4656; ρ_4^{40} = 0.8347; MM=136 g/mol.
- Dipentene (DPT) was synthesised by the same method and purified by distillation. Its physicochemical characteristics are: T_b=174–175°C; n_D^{20} = 1.4745; ρ_4^{40} = 0.8476; MM=136 g/mol.

- The isoprene cyclodimer (ICD) was also prepared through autoclave cyclodimerization of isoprene, followed by distillation to isolate the 160–180°C fraction. This fraction consists of a mixture of diprene and dipentene and has the following physicochemical properties: T_b=160–180°C; n_D^{20}= 1.4735; ρ_4^{40} = 0.8458; MM=136 g/mol.

The alkylation of p-cresol with isoprene cyclodimers results in the formation of the corresponding sterically hindered phenols.



It was observed that, unlike the alkylation of *p*-cresol with other alkylating agents, the reaction with isoprene cyclodimers requires more rigorous conditions. This difference is explained by the reactivity of the ICD.

The alkylation was conducted in a 250 mL three-necked round-bottom flask equipped with a mechanical stirrer, a heating apparatus, a dropping funnel, and a thermometer. The process was carried out in batch mode. The reactants were accurately measured using a laboratory balance. *para*-Cresol was initially added to the flask, after which the activated and partially ground KN-30 catalyst was introduced.

The influence of key reaction parameters on the alkylation process was systematically studied. The temperature was varied between 80 and 140°C, the reaction time ranged from 2 to 6 hours, the molar ratio of *p*-cresol to methylcycloalkenes was adjusted from 2:1 to 1:2, and the catalyst loading was varied from 5 to 20 wt.% relative to the amount of *p*-cresol.

Results and their discussions

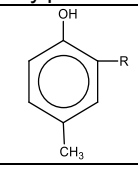
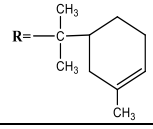
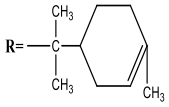
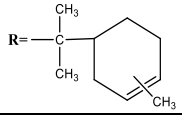
• The optimal conditions for catalytic alkylation of p-cresol with diprene in the presence of a zeolite-containing catalyst were determined. It was found that at a reaction temperature of 130°C, a reaction time of 5 hours, an equimolar (1:1) ratio of the initial components, and a catalyst amount of 12

wt.%, the yield of the target product was 73.8% (based on the p-cresol), with a selectivity of 90.3%.

• Similarly, the alkylation reactions of p-cresol with dipentene and the fraction of isoprene cyclodimer (160–180°C) were studied. For each system, optimal reaction conditions were established. Depending on the alkylating agent used, the product yield ranged from 65.5 to 69.9%, with a selectivity of 84.5-86.7% for the target product.

• The physicochemical properties and elemental composition of 2-[3(4) - methylcyclohexen - 3-yl- isopropyl] - 4-methylphenols were established. The results are summarised in the table below.

Table. Physicochemical properties of 2-[3(4)-methylcyclohexen-3-yl-isopropyl]-4-methylphenols

	$T_{b.}$ °C/10 mmHg	n_D^{20}	ρ_4^{40}	MM	Elemental Composition, %			
					Calculated		Found	
					C	H	C	H
	202-205	1.5035	1.0133	244	83.6	9.8	83.3	9.5
	212-215	1.5267	1.0375	244	83.6	9.8	83.2	9.4
	204-215	1.5133	1.0284	244	83.6	9.8	83.4	9.3

References

1. Gurbanova U.R., Rasulov Ch. K., Naghiyeva M. V., Hajiyeva G.F., Salmanova Ch. K. Alkylation of phenol with cyclodimers of isoprene in the presence of zeolite-containing catalyst KN-30. Processes of Petrochemistry and Oil Refining, Vol. 26, No. 4, 2025, pp.1144-1156
2. Mirzayev, V.H., Abbasov V.M., Rasulov Ch.K., Aghamaliyev Z.Z., Bagirzade R.Z., Majidov E.A. Selective catalytic alkylation and cycloalkylation of phenol with alkyl- and alkenylcyclohexenes. Processes of petrochemistry and oil-refining, 2017, Vol.18, No.4, pp. 341-350
3. Rasulov Ch.K., Rustamov S.T., Naghiyeva M.V., Gasanova G.J., Heydarli G.Z. Alkylation of phenol and its homologs by cyclic olefins. Processes of petrochemistry and oil refining,Vol.26, No.1, 2025, pp. 264-277

PEPA-BASED OLEIC ACID DERIVATIVES AS EFFICIENT ANTISTATIC ADDITIVES FOR DIESEL FUEL

V.M. Abbasov, A.A. Kangarli, N.I. Mursalov,
N.K. Dadashova, N.Sh. Rzayeva, F.J.Gurbanova
Institute of Petrochemical Processes named after Academician Y.H. Mammadaliyev, Ministry of Science and Education of the Republic of Azerbaijan, Baku
E-mail: aydanmehieva@gmail.com

Abstract - This study reports the synthesis of nitrogen-containing derivatives of oleic acid and the development of compositions comprising these derivatives and natural petroleum acids (NPA) for use as efficient antistatic additives in diesel fuel. A high-temperature fraction of natural petroleum acids (220–240 °C) was isolated and used to formulate additive systems. The prepared compositions were introduced into diesel fuel at concentrations of 0.05, 0.1, and 0.15 wt.%, and their performance was evaluated through electrical conductivity measurements.

The amidoamine synthesized from oleic acid and polyethylene polyamine (PEPA) at a 2:1 molar ratio demonstrated superior antistatic performance. At a concentration of 0.15 wt.%, the electrical conductivity of diesel fuel increased to 5890 pS/m and slightly rose to 5972 pS/m after one month of storage, indicating excellent long-term stability.

Furthermore, the composition based on the PEPA-derived amidoamine and natural petroleum acids exhibited stable conductivity enhancement. At 0.15 wt.%, the electrical conductivity reached 4220 pS/m and further increased to 4335 pS/m after one month. These findings confirm that the molecular structure of PEPA-based amidoamine plays a decisive role in ensuring both high efficiency and long-term stability of antistatic additives in diesel fuel.

Keywords: Oleic acid; polyethylene polyamine (PEPA); amidoamine; natural petroleum acids; antistatic additive; diesel fuel; electrical conductivity; fuel stability.

Introduction

The accumulation of static electricity in petroleum fuels during storage, pumping, and transportation represents a significant safety hazard, potentially leading to fire and explosion [4,5]. This issue is particularly critical for low-conductivity fuels such as diesel, where electrostatic charge relaxation is limited. Enhancing the electrical conductivity of fuel systems through the incorporation of antistatic additives is one of the most effective approaches to mitigating these risks[1,5].

Commercial antistatic additives are widely used; however, many formulations are associated with environmental concerns, limited long-term stability, or complex compositions. Therefore, the development of metal-free, structurally tunable, and stable antistatic systems remains an important research objective.

Nitrogen-containing derivatives of fatty acids, such as amidoamines, are promising candidates due to the presence of polar functional groups capable of facilitating charge dissipation in nonpolar hydrocarbon media [1-3].In particular, polyethylene polyamine (PEPA)-based amidoamines may provide enhanced adsorption characteristics and improved conductivity performance.

In this study, an amidoamine synthesized from oleic acid and polyethylene polyamine (PEPA) at a 2:1 molar ratio was investigated as an antistatic additive for diesel fuel. In addition, its composition with a high-temperature fraction (220–240 °C) of natural petroleum acids was evaluated with respect to electrical conductivity enhancement and long-term stability.

Experimental Part

Structural confirmation of the synthesized oleic acid–PEPA amidoamine was carried out using Fourier Transform Infrared (FTIR) spectroscopy.

The PEPA-based amidoamine was synthesized via condensation of oleic acid with polyethylene polyamine at a 2:1 molar ratio.

The FTIR spectrum of the amidoamine obtained from oleic acid (OA) and polyethylene polyamine (PEPA) is presented in Fig. 1 and is characterized by the following absorption bands.

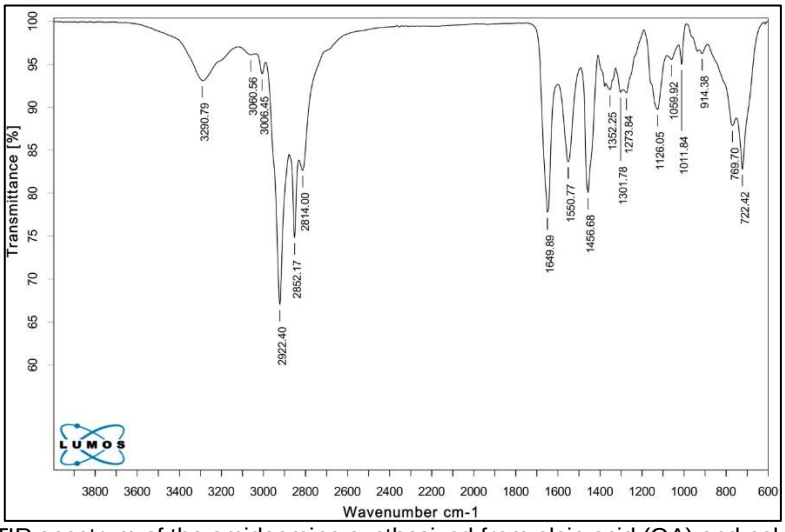


Fig. 1. FTIR spectrum of the amidoamine synthesized from oleic acid (OA) and polyethylene polyamine (PEPA).

The FTIR spectrum of the synthesized PEPA-based amidoamine (Fig. 1) confirms the formation of amide groups. The characteristic absorption band at 1645–1650 cm^{-1} corresponds to the amide carbonyl (C=O) stretching vibration, while the bands at 1550 cm^{-1} and 3200–3300 cm^{-1} are attributed to N–H vibrations. The reduction of the free carboxylic acid band indicates successful conversion of oleic acid into its nitrogen-containing derivative.

Table 1. Specific electrical conductivity (pS/m) of diesel fuel containing PEPA-based amidoamine

Additive concentration (wt.%)	1 day	10 days	20 days	30 days
0.05	5710	5750	5790	5812
0.10	5823	5845	5885	5890
0.15	5890	5925	5945	5972

As shown in Table 1, the PEPA-based amidoamine significantly increased the electrical conductivity of diesel fuel at all studied concentrations. The highest conductivity was observed at 0.15 wt.%, reaching 5890 pS/m after 1 day and slightly increasing to 5972 pS/m after 30 days of storage. The gradual increase in conductivity over time indicates good stability of the additive in the diesel medium.

Table 2. Specific electrical conductivity (pS/m) of diesel fuel containing PEPA-based amidoamine + natural petroleum acids

Additive concentration (wt.%)	1 day	10 days	20 days	30 days
0.05	3710	3740	3782	3810
0.10	3825	3845	3870	3894
0.15	4220	4245	4295	4335

According to Table 2, the composition of PEPA-based amidoamine with natural petroleum acids also enhanced the electrical conductivity of diesel fuel. At a concentration of 0.15 wt.%, conductivity increased from 4220 pS/m on the first day to 4335 pS/m after 30 days. Although the conductivity values are lower than those of the pure PEPA-based system, the results demonstrate stable long-term performance and a synergistic interaction between nitrogen-containing functional groups and petroleum acid components.

Conclusion

The present study demonstrated that the amidoamine synthesized from oleic acid and polyethylene polyamine (PEPA) at a 2:1 molar ratio exhibits high efficiency and excellent stability as an antistatic additive for diesel fuel. The additive significantly enhanced electrical conductivity, reaching 5890 pS/m at 0.15 wt.% and maintaining stable performance over a 30-day storage period.

Moreover, the composition of the PEPA-based amidoamine with a high-temperature fraction (220–240 °C) of natural petroleum acids showed improved long-term conductivity stability, indicating a synergistic interaction between nitrogen-containing functional groups and petroleum acid components.

Overall, the PEPA-derived amidoamine and its composition with natural petroleum acids represent promising metal-free antistatic systems for improving the safety and reliability of diesel fuel handling and transportation.

References

1. Abdullaeva, N.R., Ismailov, T.A., Mamedova, T.A., Magerramov, R.S., Veliev, Kh.R., & Abbasov, V.M. (2011). Synthesis and study of antistatic diesel additives based on petroleum acids. *Petroleum Chemistry*, 51, 299–302. https://doi.org/10.1134/S0965544111030029
2. Abdullayeva, N.R., Abbasov, V.M., Ismailov, T.A., & Gasimov, Z.Z. (2009). Synthesis of oxyethers obtained by interaction of natural oil acids with propylene oxide and study of their antistatic properties in composition with diesel fuel. *Chemical Problems*, (3), 551–553.
3. Dong, S., Wang, Y., Lan, T., Wang, J., Zu, L., Xiao, T., Yang, Y., & Wang, J. (2022). Synthesis of high-molecular-weight bifunctional additives with both flame retardant and antistatic properties via ATRP. *ACS Omega*, 7(48), 44287–44297. https://doi.org/10.1021/acsomega.2c05809
4. Klimov, N.A., Burov, N.O., Lobashova, M.M., Savelenko, V.D., Makhova, U.A., Tikhomirova, E.O., Mukhina, D.Yu., Ilin, A.V., Shevtsov, A.A., Moiseeva, T.N., & Klimin, D.Yu. (2025). Evaluation of electrical conductivity stability in jet fuels under transport and storage conditions. *Fuel*, 406(Part B), 137041. https://doi.org/10.1016/j.fuel.2025.137041
5. Murugesan, S., Patel, A., Ekoue-Kovi, K., & Wolfe, D. (2021). Static dissipative additive performance and synergism with biodiesel for distillate fuels. *Fuel*, 312, 122634. https://doi.org/10.1016/j.fuel.2021.122634

OBTAINING STABLE SILVER NANOPARTICLES BASED ON SODIUM CITRATE

[1]Lutpillayeva Masuda, [2]Xoshimov Farxod
[1]doctoral student, Department of chemistry, Namangan State Technical University, Namangan, 160123, Uzbekistan, E-mail: lutpillayeva@mail.ru.
[2]professor, Head of the chemistry department , Namangan State Technical University, Namangan, 160123, Uzbekistan, E-mail: xoshimovfarhod@gmail.com
[1]ORCID ID: 0009-0003-1079-5230
[2]ORCID ID: 0009-0005-4468-3223

Summary. As a result of the conducted studies, it was determined that silver nanoparticles can be effectively synthesized using the chemical reduction method, particularly in the presence of sodium citrate. The advantage of this method lies in its simplicity, cost-effectiveness, and the absence of the need for complex specialized equipment. Experimental results showed that the use of gelatin and dextrin as stabilizers significantly affects nanoparticle formation, their color change, and stability. In particular, gelatin-based systems ensured long-term stability (up to 18 months), while dextrin maintained stability for up to 12 months. The size of the synthesized nanoparticles varied over a wide range (20–269 nm), and it was established that reagent concentration and stabilizer type play an important role in this process. UV–Vis spectroscopy results confirmed the surface plasmon resonance

characteristic of silver nanoparticles (≈400 nm). In general, the chemical reduction method using sodium citrate was shown to be an efficient, convenient, and promising approach for obtaining silver nanoparticles.

Keywords. Silver nanoparticles, chemical reduction method, sodium citrate, gelatin, dextrin, stabilizer, UV–Vis spectroscopy, surface plasmon resonance, nanoparticle synthesis, colloidal systems.

Introduction.

Worldwide, scientific research is being conducted on the synthesis of noble metal nanoparticles, the study of their properties, and their application in the synthesis of plant protection agents in agriculture. In recent years, growth has been observed in both fundamental and applied scientific fields related to the synthesis of noble metal nanoparticles (NPs), the study of their properties, and their practical application [1, 2].

The development of this field is primarily associated with the creation of convenient, inexpensive, and environmentally safe methods for obtaining and studying such materials, which hold great promise for applications in microelectronics, optics, catalysis, medicine, sensor analysis, and other areas. One of the main methods for obtaining nanoparticles is the chemical reduction method. The advantage of chemical reduction methods is that they do not require complex equipment and allow control over nanoparticle size and external structure [3].

Metal nanoparticle (NP) synthesis can be carried out using various methods (physical, chemical, biological). In this study, stable silver nanoparticles were synthesized using the chemical reduction method. The advantage of chemical reduction methods is that they do not require complex equipment and provide the possibility to control nanoparticle size and morphology [4]. One of the chemical reduction methods is the citrate method. The essence of the method is the reduction of silver salts in aqueous solution using sodium citrate. The obtained silver aggregates of various shapes have diameters ranging from 60 to 200 nm. The citrate anion performs both reducing and stabilizing functions, which makes it difficult to select its optimal concentration, since changes in concentration affect the reduction rate as well as particle growth and micelle formation [5]. Despite the disadvantages of the citrate method, it is widely used for the synthesis of silver NPs [6].

$$6AgNO_3 + 3Na_3C_6H_5O_7 = 6Ag\downarrow + 3Na_2C_5H_4O_5 + 3CO_2\uparrow + 3NaNO_3 + 3HNO_3$$

Experimental part.

For the synthesis of silver nanoparticles (AgNPs), silver nitrate was used as the main substance, sodium citrate as the reducing agent, and gelatin and dextrin as stabilizers. The reactions were carried out at room temperature by adding equal volumes of reducing solution to a mixture of stabilizer (gelatin, dextrin) and silver nitrate solution under constant stirring.

Initially, 1%, 2%, and 5% solutions of stabilizers were prepared at 20°C. Then, a silver nitrate solution with a concentration of 500 mg/ml was

prepared. Sodium citrate solutions of 0.1 M and 0.05 M were prepared as reducing agents.

The stabilizer and silver nitrate solutions were mixed, and equal volumes of the prepared reducing solutions were added under continuous stirring to obtain the samples.

Results and their discussion.

Use of sodium citrate as a reducing agent. **(C_{AgNO3}=0.00463 M, 20°C).**

№	Stabilizer	Change (after 24 hours)	Appearance
1	5 % li Dextrin (corn)	Turned black	
2	5% Gelatin	Turned reddish	
3	1% Gelatin	Turned dark	
4	5% Gelatin	Turned brown	

5	4 %li Dextrin (potato)	Turned black	
6	1 %li Dextrin (potato)	Turned black	

Color changes were observed in systems where gelatin and dextrin were used as stabilizers, and these systems were stable: the dextrin-stabilized system maintained stability for 12 months, while the gelatin-stabilized system preserved its stability for up to 18 months.

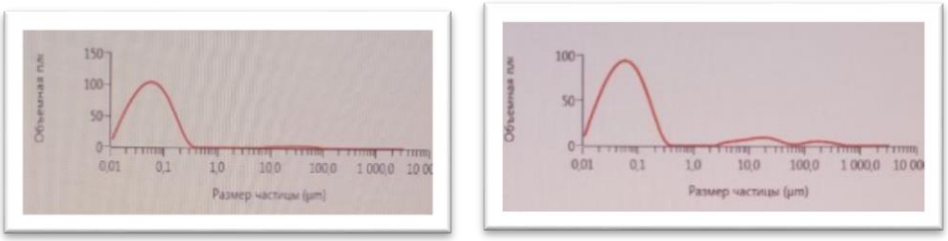


Figure 1. Size distribution graph of AgNPs (determined using MasterSizer 3000).

In syntheses carried out using 1% gelatin and 1% dextrin (obtained based on potato starch) as stabilizers, the nanoparticle size ranged from 20.4–22.4 nm to 20.1–269 nm (Figure 1). These results demonstrated the high efficiency of sodium citrate in the synthesis of AgNPs.

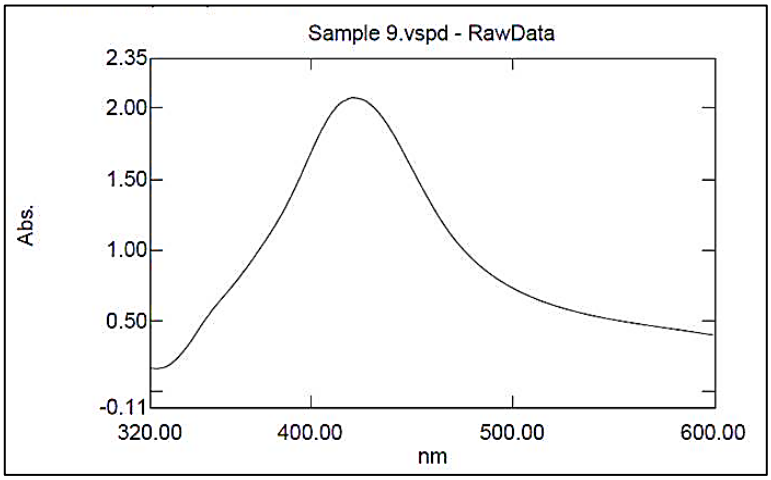


Figure 2. UV spectrum of AgNPs (synthesized based on $AgNO_3$ + gelatin + sodium citrate).

The UV spectrum of AgNPs synthesized using gelatin as a stabilizer is shown. Starting from a wavelength of 320 nm, the absorbance value is relatively low (around 0.50), but it increases sharply near 400 nm, reaching approximately 2.10. This corresponds to the plasmonic resonance peak of silver nanoparticles, indicating that they exhibit maximum absorption around 400 nm.

Offers

AgNPs were synthesized based on chemical reduction. In this experiment, the biopolymer gelatin functions as a stabilizing agent at various concentrations. G-AgNPs were confirmed by UV–Vis absorption at 420 nm. The stabilizing ability of gelatin around AgNPs can be investigated by maintaining a constant concentration of $AgNO_3$ (0.00463 M) while increasing gelatin concentrations to 1%, 2%, and 5%.

References

1. Wanzhong Zhang,Xueliang Qiao,Jianguo Chen. (2007). Synthesis of nanosilver colloidal particles in water/oil microemulsion. Colloids and Surfaces A: Physicochemical and Engineering Aspects, 299, 22-28. https://doi.org/10.1016/j.colsurfa.2006.11.012
2. Zarei Chamgordani, N., Asiaei, S., Ghorbani-Bidkorpeh, F., Babaee Foroutan, M., Mahboubi, A., Moghimi, H. R. (2024). Fabrication of controlled-release silver nanoparticle polylactic acid microneedles with long-lasting antibacterial activity using a micro-molding solvent-casting technique. *Drug Delivery and Translational Research*, *14*(2), 386-399.
3. Сыргакбек к. Д., Сатывалдиев А.С., Эмил Омурзак. Синтез наночастиц серебра в присутствии додецилсульфата натрия. Наука, новые технологии и инновации кыргызстана №12, 2016. 69-71 с.
4. Gloria, E. C., Ederley, V., Gladis, M., César, H., Jaime, O., Oscar, A., Franklin, J. (2017, June). Synthesis of silver nanoparticles (AgNPs) with antibacterial activity. In *Journal of Physics: Conference Series* (Vol. 850, No. 1, p. 012023). IOP Publishing
5. Photoinduced conversion of silver nanospheres to nanoprisms / R. Jin, У. W. Cao, C. A. Mirkin [et al.] // Science. – 2001. – Vol. 294. – P. 1901– 1903.

6. Титков, А. И., Борисенко, Т. А., & Логутенко, О. А. (2020). Полиольный синтез нано-и микропластин серебра в присутствии оксиэтилированной карбоновой кислоты. *Химия в интересах устойчивого развития*, *28*(1), 66-72.
7. Lutpillayeva, M., Hoshimov, F. (2025, July). Study of systems containing silver nanoparticles using ultraviolet–visible spectroscopy method. In *AIP Conference Proceedings* (Vol. 3304, No. 1, p. 030022). AIP Publishing LLC.
8. Lutpillayeva, M., Hoshimov, F. (2025, October). Synthesis Of Silver Nanoparticles Under The Influence Of Various Reducers. In *International Conference on Global Trends and Innovations in Multidisciplinary Research* (Vol. 1, No. 4, pp. 233-235).

ANİLİNİN SEOLİT KATALİZATORLARI İŞTİRAKINDA METANOLLA ALKİLLƏŞMƏ PROSESİNİN TƏDQİQİ

İsmayılov Səbuhi, Əliyeva Nailə
Sumqayıt Dövlət Universiteti
Sumqayıt , Azərbaycan
ismailovsbuhi@gmail.com

Xülasə - Anilin və 2-metilanilinin etanolla alkilləşmə reaksiyasinda daha yüksək katalitik xassələr nümayiş etdirən katalizatorları seçmək üçün ilkin tədqiqatlar aparılmışdır. Katalizatorlar kimi müxtəlif seolitlərdən istifadə edilmişdir. Tədqiqatlarda xammal kimi anilin metanol və etanoldan istifadə edilmişdir. Onların təmizliyi xromatoqrafik yolla və fiziki xassələrinin tədqiqi nəticəsində müəyyən edilmişdir.

Alkilləşdirici kimi istifadə olunan etanol Y.K.Yuryev [1] tərəfindən göstərilmiş qayda üzrə təmizlənmişdir. Etil spirtinin təmizliyi 99.5 % olmuşdur.

Açar sözlər: anilin, metanol, N-metilanilin, N-alkilləşmə, seolit katalizator, kinetik qanunauyğunluq, selektivlik

Giriş

Sənayedə istehsal olunan anilinin 70-80%-i poliuretan və penoplast istehsalında əvəzsiz xammal sayılan p,p-metilendifenilizosianatın sintezinə sərf olunur. Anilinin qalan hissəsi isə aşağı molekul kütləli anilinlərindən (C_1-C_2) rezinin emalında, antioksidantların alınmasında, stabilizator, pestisid, boyalar, vitaminlər istehsalında istifadə edilir. Anilinin dünyada istehsalı 2010-cu ildə 3,6 mln/ton təşkil etmişdir. Onu əsasən ABŞ, Qərbi Avropa, Rusiya və Asiyada alırlar. Onun istehsalı üzrə aparıcı şirkətlərə Amaco və Пигмент (Россия) və digərlərini misal göstərmək olar [2].

Anilin və N-metilanilini almaq üçün Rusiya alimləri qaz fazada [2,3] nitrobenzolun metanol və ya formaldehidin sulu məhlulu ilə reduksiyasını təklif etmişlər. Anilinin alkilləşmə reaksiyası ilə onun alkil törəmələrinin alınması alimlərin diqqetini daha çox cəlb etmiş və bu zaman yeni alkilləşdiricilərdən də istifadə edilmişdir.

Eksperimental hissə

Anilinin etanolla qarşılıqlı təsiri axar tipli katalitik reaktorla təchiz olunmuş laboratoriya qurğusunda aparılmışdır. Ədəbiyyat məlumatlarının təhlili

əsasında anilinin etanolla maye fazada alkiləşməsi müxtəlif heterogen katalitik sistemlər üzərində müqayisə edilmişdir. Seolit tipli katalizatorlar məsamə strukturu və turşuluq mərkəzlərinin paylanmasına görə yüksək aktivlik göstərmişdir [4]. Reaktordakı katalizator tərpənməz laylı rejimdə olmuş və ora verilən xammalın həcmi sürəti mikronasosla tənzim edilmişdir. Reaktora balonlardan verilən qazın (H_2, N_2, O_2, hava) sürətinə qaz sərfinin tənzimləyicisi ilə nəzarət olunmuşdur. Reaksiya sürəti və məhsul çıxımı temperatur və reagentlərin mol nisbətindən asılıdır. Reaktorun temperaturunu tənzimləmək və qeyd etmək üçün maqnitli qapayıcı və potensiometrdən istifadə edilmiş, reaksiya aparatına daxil olan xammal isə əvvəlcə buxarlandırıcıda lazım olan temperatura qədər qızdırılmışdır. Selektiv N-alkilləşmənin təmin olunması üçün katalizatorun aktiv mərkəzlərinin optimallaşdırılması vacib hesab olunur [5]. Bizim apardığımız tədqiqat zaçmanı anilinin və etanolla alkilləşmə reaksiyasında mordenit və SVM seolitlərinin H formalarının, həmçinin onların palladiumla modifikasiya olunmuş nümunələrinin katalitik aktivlikləri öyrənilmişdir.

Nəticələr və onların müzakirəsi

Anilinin etanolla alkilləşmə reaksiyasında H-mordenit, HSVM və onların palladiumla modifikasiya olunmuş nümunələrinin katalitik aktivliyi və selektivliyinin tədqiqi nəticəsində mürəkkəb tərkibli katalizatların alındığı müəyyən edilmişdir. Modifikasiya olunmuş seolitlər iştirakı ilə aromatik aminin karbona görə alkilləşmə məhsullarının azota görə alkilləşmə məhsullarına nəzərən daha selektiv olduğu və bu zaman anilin alınan toluidinin çıxımının tarazlıq çıxımlarına yaxın olduğu göstərilmişdir.

Təkliflər

1. Seolit katalizatorların turşuluq xüsusiyyətlərinin optimallaşdırılması
2. Temperatur və reagentlərin mol nisbətinin kinetik modelləşdirmə əsasında seçilməsi
3. Selektiv N-alkilləşmənin artırılması üçün aktiv mərkəzlərin tənzimlənməsi
4. Enerji sərfiyyatının azaldılması üçün istilik balansının optimallaşdırılması

İstinadlar

1.**Юрьев Ю.К.** Практически работы по органической химии 5-е изд. перераб. и доп. М.: МГУ, 1999, 211 с.

2. **Патент 2066563 Россия** Катализатор для получения N-метиланилина / Якушкин М.И., Батрин Ю.В., Николаев Ю.Г., Макаровский И.А. / опубл. в РЖХим 1996, 25Н121П1.

3. **Sorribes I., Cabrero Antonino J.R., Vicent C., Junge K.** Catalytic N-alkylation of amines using carboxylic acids and molekular hydrogen // J.Amer. Chem. Soc. 2015, 136 (4), p. 13580-7

4. **Zheng Hai-Tao, Tao-Ke-yi** Парофазный синтез N,N-диэтиланилина //Petrochem. Technol. 2001, 30, № 11, с. 844-846

5. **Narayanan S., Asima Sultana.** Alkylation of aniline with methanol on the zeolites // Appl. Catal. A: General, 1998, 167, səh. 103

6. Singh B., Lobo H., Shankarling G. Selective N-alkylation of aromatic primary amines catalyzed by biocatalyst // Catalysis Letters, 2011, v. 141, issue 1, səh. 178–182

ZN-CR LAYLI İKİLİ HİDROKSİDLƏRİ VƏ ONUN KARBON ƏSASLI NANOKOMPOZİTLƏRİNİN SİNTEZİ VƏ OPTİKİ XASSƏLƏRİNİN TƏDQİQİ

Hüsna Abuzərova, Ofeliya Balayeva,İradə Buniatzadə
Bakı Dövlət Universiteti
Bakı, Azərbaycan
abuzerovahusna@gmail.com

Xülasə: Müasir materialşünaslığın aktual problemlərindən olan optik xüsusiyyətlərin tənzimlənməsi üçün sink-xrom əsaslı laylı ikili hidroksidlərin (Zn-Cr LİH) karbon nanoquruluşları ilə kompozitlərinin tətbiq imkanları araşdırılmışdır. LİH strukturlarının yarımkeçirici xüsusiyyətləri və laylı quruluşu ilə qrafenin yüksək elektron keçiriciliyi və mexaniki davamlılığı ilə birləşdirilərək hibrid sistem yaradılmışdır. İşdə sink (Zn^{2+}) və xrom (Cr^{3+}) ionlarının kristal qəfəsin nizamlılığına təsiri, həmçinin nanokompozitin laylararası boşluqlarında qrafen, qrafen oksid və fülleren (G, GO və C_{60}) kimi karbon mənşəli fazaların elektron quruluşuna təsir mexanizmləri təhlil olunmuşdur. Müəyyən edilmişdir ki, karbon əlavəsi LİH laylarının struktur sabitliyini artırmaqla yanaşı, qadağan olunmuş zonanın eninin (E_g) daralmasına və yük daşıyıcılarının (elektron-deşik cütləri) daha effektiv hərəkətinə şərait yaradır.

Açar sözlər: Laylı ikili hidroksidlər, karbon nanoquruluşları, Zn-Cr/LİH, optiki xassələr, qadağan olunmuş zonanın eni

Giriş:

Laylı ikili hidroksidlərin ümumi kimyəvi formulu $[M^{2+}_{1-x}M^{3+}_{x}(OH)_2]^{x+}$ $[A^{m-}_{x/m} \bullet n\ H_2O]^{x-}$ kimi ifadə olunur. Burada M^{3+} və M^{2+} müvafiq olaraq təbəqələrdə yerləşən üçvalentli və ikivalentli kationlar; $x=M^{3+}/[M^{2+}+M^{3+}]$, A^{m-} isə təbəqələrarası aniondur. Bu materiallar yüksək anion mübadiləsi qabiliyyəti, tənzimlənən məsaməlilik və "yaddaş effekti" kimi unikal xüsusiyyətlərinə görə geniş elmi maraq doğurur. Quruluş çevikliyi bu materialların kataliz, adsorbsiya və ion mübadiləsi kimi sahələrdə effektiv tətbiqinə imkan yaradır [Seftel və b., 2015, 208-215].

Karbon əsaslı materiallar arasında qrafen özünəməxsus fiziki-kimyəvi xüsusiyyətlərinə görə xüsusi yer tutur. Atom qalınlığında, pətəkvari kristal quruluşa malik olan bu material kompozitlərə daxil edildikdə onların mexaniki möhkəmliyini, elektrik və istilik keçiriciliyini, həmçinin istilik sabitliyini və elektrokimyəvi xüsusiyyətlərini əhəmiyyətli dərəcədə yaxşılaşdırır. Buna görə də qrafen və ona bənzər strukturlar polimer nanokompozitlərin funksional göstəricilərinin artırılması üçün perspektivli doldurucular kimi qiymətləndirilir [Lee və b., 2022, 4733].

Fotokatalitik komponent kimi sink (Zn^{2+}) və xromun (Cr^{3+}) kombinasiyasına üstünlük verilməsi həm struktur xüsusiyyətləri, həm də materialın optik həssaslığı baxımından bir sıra strateji üstünlüklərə əsaslanır. Sink və xrom (III) ionlarının ion radiuslarının yaxınlığı (Zn^{2+}: 0.74 Å, Cr^{3+}: 0.62 Å) laylı ikiqat hidroksid (LİH) strukturunun formalaşması zamanı kationların oktaedrik boşluqlarda yüksək dərəcədə nizamlı və homogen paylanmasını

təmin edir. Bu struktur uyğunluğu sintez prosesində kənar fazaların yaranma ehtimalını minimuma endirməklə yanaşı, materialın hər bir layında katalitik aktiv mərkəzlərin bərabər sıxlığını təmin edir. Zn-Cr/LİH sisteminin ən mühüm üstünlüklərindən biri onun elektomaqnit spektrinin görünən işıq (visible light) zonasına qarşı yüksək həssaslıq nümayiş etdirməsidir. Zn-Cr/LİH strukturunda Cr^{3+} ionlarının mövcudluğu spesifik elektron keçidləri yaradaraq qadağan olunmuş zona enerjisinin (E_g) daralmasına səbəb olur. Bu xüsusiyyət katalizatorun yalnız süni ultrabənövşəyi şüalar altında deyil, həm də günəş enerjisindən istifadə etməklə effektiv fəaliyyət göstərməsinə imkan yaradır [Bencherif və b., 2021, 3051].

LİH-lər elektron quruluşu kationların molyar nisbətindən, kristal səthinin sahəsindən və ən əsası, laylararası boşluqlarda yerləşən ionların/molekulların təbiətindən birbaşa asılıdır. Bu tip struktur modifikasiyaları, əlavə rekombinasiya mərkəzləri yaratmadan materialın optik udma qabiliyyətini əhəmiyyətli dərəcədə yüksəltməyə imkan verir. Məlumdur ki, LİH-lərin qadağan olunmuş zona eni kation və anionların təbiətindən və hidratlaşma dərəcəsindən (laylararası suyun miqdarı) asılı olaraq 2–5 eV diapazonunda dəyişir. Geniş enerji diapazonu LİH-ləri fotokatalitik proseslər üçün əlverişli yarımkeçiricilər sinfinə aid edir. Tədqiqatlar göstərir ki, struktura müxtəlif aşqarların daxil edilməsi və ya layların modifikasiya olunması yarımkeçirici xüsusiyyətlərini qorumaqla yanaşı, E_g zolağının daralmasına və elektron keçidlərinin optimallaşdırılmasına gətirib çıxarır. Bu baxımdan, təqdim olunan işdə Zn-Cr LDH matrisinin karbon əsaslı nanostrukturlarla (G, GO və C_{60}) zənginləşdirilməsi, materialın idarəolunan keçiricilik və spektral həssaslıq qazanmasına xidmət edir [Santos və b., 2026, 108061].

Təcrübi hissə:

ZnCr-LİH otaq temperaturunda birgə çökmə üsulu ilə sintez edilmişdir. Molar nisbəti Zn^{2+}/Cr^{3+} = 3 olan iki prekursor duzu, $ZnSO_4 \cdot 7H_2O$ (0.375 M) və $Cr(NO_3)_3 \cdot 9H_2O$ (0.125 M) 40 ml distillə suya əlavə edilmişdir. Hazırlanan qarışıq duz məhluluna karbamid [$CO(NH_2)_2$] və 1% karbon nanoquruluşları əlavə edilərək maqnit qarışdırıcıda qarışdırılmışdır. Daha sonra qarışdırma davam etdirilməklə 1 M NaOH məhlulu damcı-damcı əlavə edilmişdir. Proses pH 9-10-a çatdıqda dayandırılmışdır. Məhlul otaq temperaturunda 1 həftə saxlanıldıqdan sonra 60-90 °C-də 10 saat qızdırılmış, soyuduqdan sonra supernatant ayrılmış, çöküntü distilə suyu ilə neytral pH-a qədər yuyulmuş və havada qurudulmuşdur.

Sintez edilmiş ZnCr-LİH və onun karbon əsaslı nanokompozitlərinin optik xüsusiyyətlərini öyrənmək və qadağan olunmuş zonanın enini (E_g) müəyyən etmək məqsədilə nümunələrin UB spektroskopiya ilə udulma və əksetmə spektrləri çəkilmişdir. Spektroskopik ölçmələr otaq temperaturunda, elektromaqnit spektrinin 200–900 nm dalğa uzunluğu diapazonunda aparılmışdır.

Nəticələr və onların müzakirəsi:

Sintez olunmuş ZnCr-LİH və onun karbon əsaslı nanokompozitlərinin birbaşa elektron keçid (direct electronic transition) Eg qiymətləri Kubelka-Munk tənliyi vasitəsilə hesablanmışdır [Balayeva və b., 2019, e02725]:

$$[F(R_\infty)hv]^{1/n} = k(hv-E_g)$$

Hesablamalar zamanı n=1/2 qəbul edilməsi, ZnCr-LİH sistemində elektron keçidlərinin oksigenin 2p səviyyəsindən metalın ns/nd orbitallarına doğru birbaşa icazə verilən (direct allowed) xarakter daşıdığını göstərir (Cədvəl 1).

Cədvəl 1. Sintez olunmuş nümunələrin qadağan olunmuş zona enerjisi (E_g) qiymətləri.

Nümunə	E_{g1}	E_{g2}	E_{g3}
Zn-Cr LİH	1.85	2.5	3.85
Zn-Cr LİH/G	1.75	2.3	3.8
Zn-Cr LİH/GO	1.7	2.4	3.8
Zn-Cr LİH/PVS	1.7	2.55	3.8
Zn-Cr LİH/PVS/C_{60}	1.83	2.6	3.82

Cədvəl 1-dən göründüyü kimi, təmiz LİH üçün E_g 2.50 eV müəyyən edilmişdir. Qrafen (G) və qrafen-oksid (GO) əlavəsi bu qiyməti müvafiq olaraq 2.30 eV və 2.40 eV-a qədər azaltmışdır. Bu azalma (red-shift), karbon nanostrukturlarının LİH layları arasına daxil olaraq laylararası fiziki qüvvələri zəiflətməsi və elektron keçidini asanlaşdırması ilə izah olunur. PVA və Fulleren (C_{60}) tərkibli kompozitlərdə isə E_g qiymətlərinin (2.55–2.60 eV) LDH matrisinə yaxın qalması, sistemdə həm üzvi polimer zəncirlərinin, həm də qeyri-üzvi anionların yaratdığı struktur stabilizasiyası ilə əlaqədardır. Üç fərqli enerji zonasının (E_{g1}, E_{g2}, E_{g3}) müşahidə olunması materialın mürəkkəb elektron strukturuna malik olduğunu və müxtəlif dalğa uzunluqlu şüalar altında aktivlik göstərə biləcəyini sübut edir.

Ədəbiyyat:

1. Balayeva, O. O., Azizov, A. A., Muradov, M. B., Alosmanov, R. M., Eyvazova, G. M., Mammadyarova, S. J. Cobalt chromium-layered double hydroxide, α- and β- $Co(OH)_2$ and amorphous $Cr(OH)_3$: synthesis, modification and characterization. *Heliyon*. 2019, 5(11), e02725.
2. Bencherif, S. D., Gallardo, J. J., Carrillo-Berdugo, I., Bahmani, A., Navas, J. Synthesis, Characterization and Photocatalytic Performance of Calcined ZnCr-Layered Double Hydroxides. *Nanomaterials*. 2021, 11(11), 3051.
3. Lee, S. J., Yoon, S. J., Jeon, I. Y. Graphene/Polymer Nanocomposites: Preparation, Mechanical Properties, and Application. Polymers. 2022, 14(21), 4733.
4. Santos, M. F., Moraes, P. I. R., Tavares, S. R., Martins, A. S., Capaz, R. B., Wypych, F., Leitão, A. A.Analysis of the energy and nature of bandgap in layered double hydroxides Mg-Al-X and Zn-Al-X (X= Cl^-, OH^-, CO_3^{2-}, or NO_3^-). Applied Clay Science. January 2026,279, 108061.
5. Seftel, E. M., Niarchos, M., Vordos, N., Nolan, J. W., Mertens, M., Mitropoulos, A. C., Vansant, E. F., Cool, P. LDH and TiO2/LDH-type nanocomposite systems: A systematic study on structural characteristics. Microporous and Mesoporous Materials. 2015, 203, 208-215.
Qeyd: Bu iş Azərbaycan Elm Fondunun maliyyə dəstəyi ilə yerinə yetirilmişdir-Qrant № AEF-MGC-2025-1(54)-20/19/4-M-19

EP-300 QURĞUSUNDA YAN MƏHSUL KİMİ ALINAN TSİKLOPENTADİENİN AMİNLƏŞMƏSİ VƏ BƏZİ ÇEVRİLMƏLƏRNİN ÖYRƏNİLMƏSİ

Elmi rəhbər: b/m Şahgəldiyev F.X.
Babazadə Mənzər Zavur
Sumqayıt Dövlət Universiteti
Sumqayıt, Azərbaycan
Email: menzerbabazade2006@gmail.com

Təqdim etdiyimiz işdə piroliz prosesində yan məhsul kimi alınan yüngül C_5 fraksiyalarının tərkibində mövcud olan doymamış tsiklik quruluşlu dienlərin , xüsusilə tsiklopentadienin aminləşməsi prosesi və alınan diaminlərin bir sıra çevrilmə reaksiyaları tədqiq edilmişdir . Proses oks-redoks sistemində $TiCl_4$ katalizatorunun iştirakı ilə amin radikalının alınmasına və tsiklopentadienin aminləşdirilməsinə əsaslanır.Aminləşmə prosesinin optimal şəraiti: temperatur- 25^0 C, alınan hidroksilamin üçün $TiCl_4$-in miqdarı 15 mol,reaksiya müddəti 3 saat, HCl/HA-nın mol nisbətləri 2,5:1-dir. Alınan diaminlər ED-20 və ED-16 qatranlarının bərkidilməsində bərkidici agent kimi istifadə edilmişdir.Həmin diaminlərin malein anhidridi ilə qarşılıqlı təsir reaksiyasından N,N-(bistsiklopenten-2,7) bismaleinimidin alınmışdır. Epoksid qatranlarından alınan kompozisiyaların fiziki-mexaniki və odadavamlılıq xassələrini artırmaq məqsədilə dien kondensləşməsi reaksiyası ilə N,N-(bistsiklopenten-2,7) bismaleinimidin heksabrom tsiklopentadienlə qarşılıqlı təsirindən polibrom tərkibli bitsiklik bisimidlər sintez olunur.

Açar sözlər: EP-300, tsiklopentadien, aminləşmə, bərkidici, epoksid qatranı, bismaleinimidlər, antipren

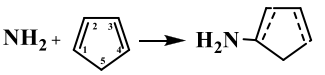
Müasir sənayenin tərəqqi etməsində yeni texnologiyaların tətbiqi və sürətli inkişafı, sənayedə baş verən ekoloji problemlərin səbəblərini araşdırır və aradan qaldırılmasının həlli yollarını ön plana çəkir. Məhz bu səbəbdən qlobal dünyada irəli sürülən mühüm ideyalardan biri yaşıl kimya anlayışının meydana gəlməsidir. Qeyd edək ki,karbohidrogen xammalının pirolizi neft kimyasının əsas proseslərindən biridir və etilen,propilen kimi böyük tonnajlı məhsulların alınmasının əsas mənbələrindən biridir. Lakin prosesdə alınan yan məhsulların səmərəli istifadəsi hələ də yaşıl kimyanın tələblərinə cavab vermir. Bu məsələnin aktuallığını nəzərə alaraq tərəfimizdən bəzi araşdırmalar yerinə yetirilmişdir.

1,9-diaminbitsiklopenten-2,7-nin sintezi. İlk olaraq,yan məhsul kimi əldə olunan pentan-penten fraksiyasının (PPF) tərkibi araşdırılır və müəyyən edilir,sonra isə doymamış diaminlərin sintezi aparılır.C_5 fraksiyalarının tərkibindəki doymamış tsiklik dienlərin, xüsusilə tsiklopentadienin aminləşməsi prosesi həyata keçirilir. Proses $TiCl_4$ katalizatorunun iştirakı ilə oksidləşmə-reduksiya sistemində amin radikallarının əmələ gəlməsi və tsiklopentadienin aminləşdirilməsi prinsipi əsasında aparılır. Birinci mərhələdə $TiCl_4$ iştirakı ilə xlorid turşulu hidroksilaminlə tsiklopentadienin qarşılıqlı təsiri amin ($NH_2^{\bullet}$) radikalının əmələ gəlməsinə səbəb olur, sonrakı mərhələdə isə amin radikalının tsiklopntadienlə birləşməsi amintsiklopentenil

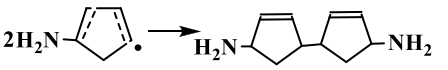
radikalını əmələ gətirir.Amin (I) radikalının az aktivliyə və böyük stabilliyə malik olması 1,9-diaminbitsiklopenten-2,7 (II) radikalının alınmasına şərait yaradır. Proses üçün optimal şəraiti müəyyən etmək məqsədilə diaminlərin çıxımına $TiCl_4$ miqdarının,tsiklopentadienin,xlorid turşulu hidroksilaminin molyar nisbətlərinin, temperaturun və reaksiya vaxtı kimi reagentlərin təsiri araşdırılmışdır. Aparılan eksperimental təcrübələr əsasında oksidləşmə-reduksiya sistemdə diaminobisiklopentenil əldə etmək üçün optimal şəraitlərin aşağıdakı kimi olduğu müəyyən edilmişdir:temperatur 25^0 C,reaksiya vaxtı 3 saat, alınan hidroksilamin üçün $TiCl_4$-in miqdarı 15 mol, HCl/HA-nın molyar nisbəti 2,5:1-dir.Verilən şəraitdə tsiklopentadienin aminləşməsi prosesinin sxemini aşağıdakı kimi yazmaq olar:

$$Ti^{4+} \longrightarrow Ti^{3+},$$

$$Ti^{3+} + NH_2OH \longrightarrow NH_2^{\bullet} + OH^- + Ti^{4+},$$



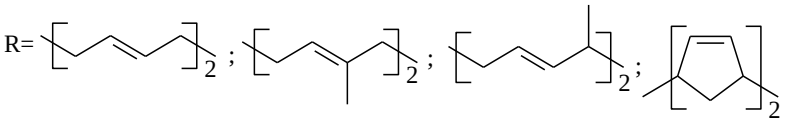
(I)



(II)

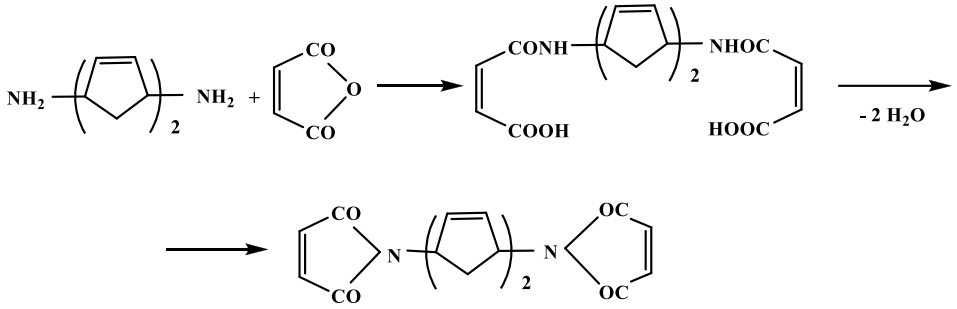
$$TiCl_3 + NH_2OH \cdot HCl \rightarrow H_2N^+ + H_2O + TiCl_4$$

$$H_2N^{\bullet} + R \rightarrow H_2N^{\bullet} - R \rightarrow H_2N^{\cdot} - R - R - NH_2$$

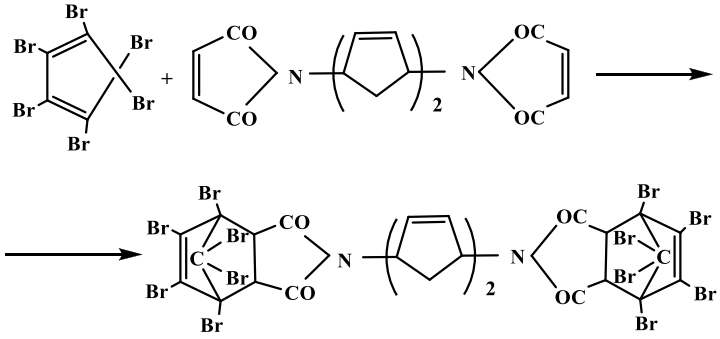


Burada R- penten- pentan fraksiyasının (PPF) radikalıdır.

N,N-(bitsiklopenten-2,7) bismaleinimidin sintezi. Əldə olunan diaminlər əsasında dien kondensləşmə reaksiyası vasitəsilə yeni doymamış polibromtərkibli bitsiklik bisimid, yəni N,N-(bistsiklopenten-2,7) bismaleinimid sintez edilmişdir.Aparılmış təcrübələrin nəticəsində sintez olunan birləşmənin polimer materialların yanma intensivliyini azltmaqla yanaşı, onların odadavamlılıq xüsusiyyətlərini və fiziki-mexaniki xassələrini əhəmiyyətli dərəcədə artırıdığı müəyyən olunmuşdur.Sintezin birinci mərhələsində 1,9-diaminbistsiklopenten-2,7-nin malein anhidridi ilə qarşılıqlı təsiri nəticəsində N,N-(bistsiklopenten-2,7) bismalein amin turşusu əldə edilmişdir.Həmin sintez olunmuş N,N-(bistsiklopenten-2,7) bismalein amin turşusundan ikinci mərhələdə dehidratasiyası yolu ilə N,N-(bistsiklopenten-2,7) bismaleinimidin sintezi həyata keçirilmişdir.



Reaksiyanın yalnız dehidratlaşdırıcı reagentin və müvafiq katalizatorun iştirakı ilə getdiyi müəyyən edilmişdir. Məlum olmuşdur ki, N,N-(bistsiklopenten-2,7) bismaleinimidin sintezi üçün prosesin optimal şəraiti (mol nisbətində) belədir: malein anhidridi : sirkə anhidridi : trietilamin : sirkə turşusunun natrium duzu (nikel) : dioksan- müvafiq olaraq 1 : 2,5 : 2,5 : 1 : 0,05 nisbətindədir. Prosesin həlqələşmə temperaturu 55-60℃, reaksiyanın davametmə müddəti isə 1 saatdır.Alınan N,N-(bistsiklopenten-2,7) bismaleinimidin quruluşu İQ (infraqırmızı) və NMR (nüvə maqnit rezonansı) spektroskopiyası ilə təsdiq olunmuşdur. Alınan birləşmənin saflığı NTX (nazik təbəqəli xromotoqrafiya) metodu ilə yoxlanılmışdır.Polimer materialların fiziki-mexaniki xassələrini yaxşılaşdırmaq qabliyyətinə malik polibrom tərkibli bitsiklik alovsöndürücülərin alınması,bununla bərabər dien kondensasiyası reaksiyası əsasında N,N-(bistsiklopenten-2,7) bismaleinimidin heksabrom tsiklopentadienlə qarşılıqlı təsiri nəticəsində yeni doymamış polibromtərkibli bitsiklik bisimidlərin alınmas həyata keçirilmişdir.

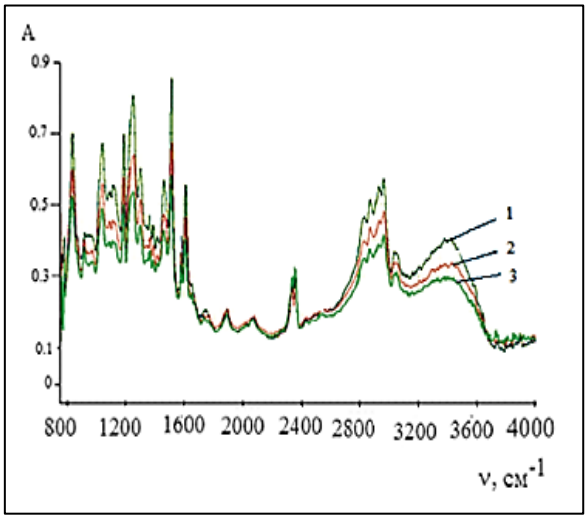


Təcrübələr zamanı məlum olmuşdur ki,reaksiya prosesində yeni sintez edilmiş birləşmənin tsiklopenten nüvəsində mövcud olan ikiqat rabitə birləşmənin əmələ gəlmə mexanizmi zamanı dəyişməz qalır.Bununla yanaşı,polibromtərkibli bitsiklik bisimidlərin N,N-(bistsiklopenten-2,7) bismaleinimidin heksabrom tsiklopentadienlə xlorbenzolda qızdırılması zamanı alınan adduktun çıxımının 87% olduğu göstərilmişdir.Alınan diaminlər ED-20 və ED-16 qatranlarının bərkidilməsində bərkidici agent kimi tədqiq olunmuşdur. Dien kondensləşməsi reaksiyası ilə epoksid qatranları əsasında alınan kompozisiyaların fiziki-mexaniki və odadavamlılıq xassələrini artırmaq

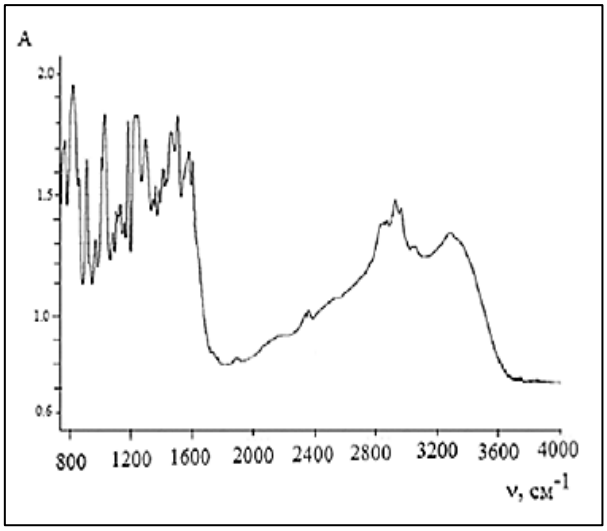
məqsədilə N,N-(bistsiklopenten-2,7) bismaleinimidin heksabrom tsiklopentadienlə qarşılıqlı təsirindən polibrom tərkibli bitsiklik bisimidlər alınmış və laboratoriya şəraitində antipiren kimi yoxlanılmışdır.

Alınan diaminin bərkidici kimi sınaqdan keçirilməsi metodikası: Sənayedə tədqiqat obyekti kimi ən geniş istifadə olunan epoksid qrupu kütlə %-i 21,8 olan ED-20 – DÜST 10587-84 (M_r = 390) seçilmişdir.Qeyd etmək lazımdır ki, ED-20-yə 10 kütlə h. aktiv durulaşdırıcı-dietilen qlikolun diqlisidil efiri (TŞ 2225-390-04872688-98) əlavə edilmişdir və bərkidici agent kimi, əvvəllər C_5 fraksiyasından tsiklopentadiedən sintez etdiyimiz 1,9-diaminbisiklopenten-2,7 istifadə olunmuşdur.Bərkimə prosesi aşağıdakı kimi həyata keçirilmişdir: 60^0 C-yə qədər qızdırılmış qatranı qarışdırmaqla hesablanmış miqdarda diamin əlavə edilir,daha sonra əmələ gələn reaksiya kütləsi otaq temperaturunda 24 saat bərkidilərək 6 saat müddətində 80 və 120^0 C-də də termiki emala məruz qalmışdır. Doymamış tsiklik diaminlərlə emal edilən ED-20-nin bəzi fiziki və mexaniki xassələrini fərqləndirmək üçün qeyd olunan qatran orta molekulyar çəkisi ~220-250 olan TŞ 2413-357-00203447 - 99 olan xətti və şaxələnmiş etilen və piperazin tərkibli etilen poliaminlərin qarışığı olan böyük polidisperliliyə malik PEPA ilə bərkidilir. PEPA bərkidicisinin tərkibi dəyişkən olsa da,onun ucuzluğu və əlçatanlığı səbəbindən geniş tətbiq olunur. Bərkidilmə prosesi plastifikator kimi dibutilftalatın iştirakı ilə və onun iştirakı olmadan yerinə yetirilmiş, prosesdə "Chimex Limited" QSC-nin PEPA- istehsalından istifadə edilmişdir.Bu zaman hər 100 çəki hissə qatrana 10 çəki hissə DBF əlavə olunmuşdur.Emal olunan nümunələrin fiziki və mexaniki göstəricilərinə dair nəticələr aşağıdakı cədvəldə təqdim olunur:

1,9-diaminobisiklopenten-2,7 bərkidici agenti istifadə edildikdə daha dərin bərkidilmə və epoksid kompozisiyaların daha yüksək inkişaf dərəcəsi müşahidə olunur ki, bu da əsas dövrdə temperaturun aşağı dəyişmə sürəti zamanı bərkidilmə prosesinə daha əlverişli şərait yaradır. PEPA və PEPA+DBF bərkidici maddələrindən istifadə edildikdə ekzotermik bərkidilmə reaksiyası zamanı temperaturun nisbətən yüksək dəyişmə sürəti müşahidə olunur ki, bu da bərkidilmənin daha az tamamlanmasına səbəb olur. Epoksid kompozisiyaların fiziki və mexaniki xüsusiyyətləri alınan üçölçülü strukturun parametrlərinə uyğundur.



Şəkil 1. Bərkidilməmiş ED-20 qatranının İQ- spektri.



Şəkil 2.1-ED-20+PEPA qarışığının bərkidilmədən 1 saat sonrakı; 2-ED-20+(PEPA+DBF) qarışığının bərkidilmədən 1 saat sonrakı;3-ED-20+1,9-diaminobitsiklopenten-2,7-qarışığının bərkidilmədən 1 saat sonrakı İQ-spektri.

Təcrübi Hissə

Doymamış diaminlərin sintezi. Mexaniki qarışdırıcı, əks-soyuducu, iki damcı qıfı və termometrlə təchiz olunmuş dörd boğazlı reaksiya kolbasına 74,8 q (1,15 mol) metal sink tozu, metanolda həll olunmuş 5 mol (%) miqdarında $TiCl_4$ katalizatoru (götürülmüş xlorid turşulu hidroksilaminə görə) əlavə olunur. 1 saat ərzində qarışdırılmaqla damcı qıfından 13,9 q (45℃-yə

qədər qaynayan) PPF və 69,5 q hidroksilaminin 2,5 N xlorid turşulu metanoldakı 9%-li məhlulu şəklində damcı-damcı əlavə edilir. Reaksiya prosesi 10-15℃ temperaturda aparılır və komponentlərin hamısı reaksiya qarışığına əlavə edildikdən sonra yenidən 2 saat qarışdırılır.Reaksiya başa çatdıqdan sonra reaksiyaya daxil olmayan PPF-nı və həlledicini ayırırlar, reaksiya qarışığı mənfi 5-0^0 C-də 2 saat qarışdırılır və sulu NaOH məhlulu ilə qələviləşdirildikdən və izopropil spirti ilə ekstraksiya olunduqdan sonra alınan məhsul azot atmosferində vakuum altında rektifikasiyaya məruz qalır.K_2CO_3 üzərində qurudulduqdan və həlledicinin qovulmasından sonra (götürülmüş xlorid turşulu hidroksilaminə görə hesablanmış) vakuum altında 114 q (çıxım-68%) doymamış diamini ayırırlar.Bu diaminin xüsusiyyətləri bunlardır:krioskopiya metoduna görə mol miqdarı (çəki ilə) 165,7 q; 4 mm.c.st.-da T_q-110-140℃, n_D^{20} 1,4950, d_4^{20} 0,9340; azotun miqdarı 15-17%-dir. Analoji olaraq divinilin rektifikasiyasının qalığından (DRKQ-tərkibi 80% butadien 1,3-dən ibarətdir), krioskopik metoda görə molekul kütləsi 175, çıxımı 73 %, azotun miqdarı 16 % olan doymamış diamin sintez olunmuşdur.

Heksabromtsiklopentadienin sintezi. Mexaniki qarışdırıcı, əks-soyuducu, termometrlə, damcı qıfı ilə təmin olunmuş tutumu 5 l olan reaksiya kolbasına 1,7 l distillə suyu əlavə edilir.Daha sonra onu 0℃ temperatura qədər soyudurlar və qarışdırmaqla 684 q (12,2 mol) kalium qələvisi əlavə edirlər sonra məhlulu 0-5^0 C temperatura qədər soyudurlar və qarışdırmaqla 93,5 ml (1,81 mol) brom əlavə edirlər.Alınan məhlula 30 dəq.ərzində 200 ml CCl_4-də yeni qovulmuş 19 ml (0,227 mol) tsiklopentadien daxil edirlər. Bundan sonra aşağıdakı üzvi təbəqəni ayırıb su ilə üç dəfə yuyurlar.Həlledicini azotla üfürdükdən və ayrılan kristalları süzdükdən sonra 50 ml metanolla yuyub,benzin efirindən yenidən kristallaşdırırlar.Nəticə etibarilə, 80 qram açıq-sarı rəngli kristallar əldə edirik.Bu zaman götürülmüş tsiklopentadienə görə nəzəri çıxım 65 % təşkil edir. $T_{ər.}$=85-86℃, ədəbiy.$T_{ər.}$= 85-87℃

Nəticələr və onların müzakirəsi

Piroliz prosesində yan məhsul kimi alınan yüngül C_5 fraksiyalarının tərkibində mövcud olan doymamış tsiklik dienlərin,xüsusilə tsiklopentadienin aminləşməsi prosesi oksidləşmə-reduksiya sistemində $TiCl_4$ katalizatorunun iştirakı ilə amin radikalının alınmasına və tsiklopentadienin aminləşdirilməsinə əsaslanır Alınan diaminlər ED-20 və ED-16 qatranlarının bərkidilməsində bərkidici agent kimi istifadə edilmişdir.Həmin diaminlərin malein anhidridi ilə qarşılıqlı təsir reaksiyasından N,N-(bistsiklopenten-2,7) bismaleinimid alınmışdır. Epoksid qatranlarından alınan kompozisiyaların fiziki-mexaniki və odadavamlılıq xassələrini artırmaq məqsədilə dien kondensləşməsi reaksiyası ilə N,N-(bistsiklopenten-2,7) bismaleinimidin heksabrom tsiklopentadienlə qarşılıqlı təsirindən polibrom tərkibli bitsiklik bisimidlər sintez olunur.

Təkliflər

Görülən işdə C_5 fraksiyasından sintez olunan tsiklopentadiendən alınmış doymamış tsiklik diaminlər (1,9-diaminobisiklopenten-2,7) ED-20 üçün soyuq bərkidicilər kimi uğurla istifadə edilə bilər. ED-20 və doymamış tsiklik diaminlərə əsaslanan birləşmələrin fiziki və mexaniki göstəriciləri sənaye bərkidicilərinin eyni göstəriciləri ilə müqayisədə daha üstündür. Tədqiq olunan diaminlər molekullarında iki-NH_2 qrupu və ikiqat rabitələri olan,ED-20 üçün yaxşı əlaqələndirici və yumuşaldıcı maddələrdir.Bu məqsədlə onlardan istifadə edərkən plastifikatorlardan istifadə olunmasına ehtiyac yoxdur. Aydın olmuşdur ki, aminlərin, di- və poliaminlərlə bərkidilmiş epoksid əsaslı kompozisiyaları həm korroziyaya qarşı yüksək müqavimət, həm struktur möhkəmlik, həm də minimal oturma xüsusiyyətlərinə malikdirlər.Bu isə onların geniş spektrli tətbiq imkanlarını təmin edir.

İstinadlar

1. Атласкин А.А., Атласкина М.Е., Воротынцев А.В. [и др.]; Зелёная химия как инструмент устойчивого развития : учебное пособие. – М.: Неправительственный экологический фонд им. В.И. Вернадского, 2024. – 292 с.2 Tağıyev D, Məmmədov A. Yaşıl kimya və onun inkişaf perspektivləri Bakı: “Elm”. 2024, 212 s.
2.Ф.Х.Шахгелдиев,А.М.Мустафаев.Синтез и исследования процесса модификации непредельных циклических аминоэпоксидных смол. Сборник Материалов, XIII Нумановские чтения, Душанбе 23-ноября 2016. С. 208-214.
3. Мустафаев А.М и др. VIII Менделеевский съезд по общей и прикладной химии. тезисы докладов том I. Москва, 2007. с.319
4. Mustafayev A.M., Hüseynov İ.Ə., Ramazanov E.Ə., İsmayılova R.İ., Şahgəldiyev F.X. Bromtərkibli doymamış poliefirlərin sintezi və xassələri. /”Ekologiya və Həyat fəaliyyətinin mühafizəsi” üzrə “Sənaye ili”-nə həsr olunmuş VIII ənənəvi Beynalxalq Elmi konfransı materialları, Sumqayıt-2014, s.98-102.
5.Mustafayev A.M.,Hüseynov İ.Ə.,Ramazanov E.Ə., İsmayılova R.İ., Şahgəldiyev F.X. Bromtərkibli doymamış poliefirlərin sintezi və xassələri. / ”Ekologiya və Həyat fəaliyyətinin mühafizəsi” üzrə “Sənaye ili”-nə həsr olunmuş VIII ənənəvi Beynəlxalq Elmi konfransın materialları, Sumqayıt-2014, s.98-102.

PİRROL TÖRƏMƏLƏRİNİN SİNTEZI REAKSİYASINDA YAŞIL KİMYANIN PRİNSİPLƏRİ VƏ PERSPEKTİVLƏRİ

Elmi rəhbər: dos.Məmmədova A. A.
Məmmədova Fidan Rafiq
Sumqayıt Dövlət Universiteti
Sumqayıt, Azərbaycan
Email:fidanmmmdova470@gmail.com

Xülasə - İlk dəfə olaraq biz 2,3-dibromopropenil ketonları (alil bromidinin karboksil turşusu anhidridləri ilə alüminium bromid iştirakında asilləşməsi yolu ilə əldə olunmuş) trietilaminlə emal etməklə 3-bromopropenil ketonlarının sintəzi üçün selektiv üsul işləyib hazırlanmışdır.Toksiki maddə olan trietilamini Na_2CO_3-la, efiri isə su ilə əvəz etməklə əvvəllər məlum olan 3-bromopropenil ketonların 2-hidroksietilaminlə reaksiyası nəticəsində 1-(2-

hidroksietil)pirrol sintezi həyata keçirilmişdir.Tədqiqatlar göstərir ki, 1-(2-hidroksietil)pirrolların monoxlorsirkə turşusunun xloranhidridi ilə reaksiyası 1-(2-xlorometilkarboksil)pirrollar verir. Onların transformasiyalarına əsaslanaraq antimikrobial fəallığa malik pirol törəmələri sintez edildi.

Açar sözlər: monoxlorsirkə turşusu, pirrollar, funksionaləvəzlənmiş törəmələr, 3-brompropenilketonlar, 1-(2-hidroksietil)pirrollar, allil bromid.

Giriş.

Hazırda kimyəvi reaksiyalar yaşıl kimyanın prinsiplərinin tələblərinə uyğun olaraq həyata keçirilir. Bunlara proseslərdə tullantıların yaranmasının qarşısını almaq, təhlükəsiz həlledicilərdən istifadə etmək, daha az təhlükəli materiallar sintez etmək və enerjiyə qənaət etmək daxildir. Həlledicilərin və ayırıcıların istifadəsi mümkün olduğu qədər zərərsiz olmalıdır. Ənənəvi üzvi həlledicilərin əksəriyyəti zəhərli, yanıcı və korroziyadır. Onlar distillə yolu ilə təkrar emal olunur ki, bu da əhəmiyyətli enerji itkisi ilə müşayiət olunur. Bu məqsədlə ekoloji cəhətdən təmiz həlledicilərin işlənib hazırlanması zəruridir. Yaşıl kimyanın prinsiplərinə müvafiq olaraq, üzvi həlledicilərin uyğun əvəzedicilərinin seçimi proses təhlükəsizliyi, işçi təhlükəsizliyi, ətraf mühit təhlükəsizliyi və prosesin davamlılığı əsasında aparılır. Həlledici fiziki və kimyəvi cəhətdən sabit, aşağı buxarlanmaya malik, istifadəsi asan və təkrar emal edilə bilən olmalıdır. Qeyd etmək lazımdır ki, həlledicilər yaşıl kimyanın bəlkə də ən fəal tədqiqat sahəsidir. Onlar yaşıl kimya üçün ciddi problem yaradır, çünki sintezlərdə və proseslərdə kütlə itkilərinin böyük əksəriyyətini təşkil edir. Bununla yanaşı, bəzi geniş yayılmış həlledicilər zəhərli, yanıcı və korroziyadır. Onların uçucu olması hava, su və torpaq çirklənməsinə səbəb olur, bu da işçilər üçün riski artırır və ciddi qəzaların baş verməsinə gətirib çıxarır. Bərpa və təkrar istifadə tez-tez enerji tələb edən distillə və bəzən çarpaz çirklənmə ilə əlaqəlidir.Bu çatışmazlıqları aradan qaldırmaq məqsədilə kimyaçılar daha təhlükəsiz həlledicilər axtarmağa başladılar. Solventsiz sistemlər, su, superkritik mayelər (SCF) və son zamanlarda ion mayeləri bu yeni nəsil "yaşıl" həlledicilərin bəzi nümunələridir. Əgər mümkün olsaydı, heç bir həlledicidən istifadə edilməməsi daha düzgün olardı və bu ideal vəziyyət hesab olunardı,həm də əlavə enerji sərfinə ehtiyac qalmazdı.Nəticə etibarı ilə, bütün diqqət həlledicisiz sistemlərin inkişafına yönəldilmişdir. Bu fikir həlledicilərin sənaye tullantılarının böyük bir hissəsini təşkil etməsi ideyası ilə təsdiqləndi.Eyni zamanda, istifadə olunan reaktivlərin fiziki xüsusiyyətlərinə və ya istənilən çevrilmə nəticəsinə əsaslanaraq, yanaşma tez-tez ilkin həlledicinin iştirakı olmadan reaksiyaların aparılmasına imkan yaradan yeni və ya yenidən işlənmiş kimya tələb edir. Su, məlum olduğu kimi, planetdə ən geniş yayılmış maddədir və çox zaman zərərsiz, universal həlledici kimi qəbul edilir. Bu mənada suda reaksiya aparmaq imkanı mühüm üstünlüklərə malikdir. Suyun təhlükəsizliyi və ciddi risk yaratmaması onu kimyəvi reaksiyaların genişmiqyaslı tətbiqləri üçün əlverişli edir.Hidrofob effekt nəticəsində suyun spesifik xüsusiyyətləri reaksiya

sürətinin yüksəlməsinə və məhsulların ayrılmasının sadələşməsinə şərait yaradır, çünki üzvi birləşmələrin əksəriyyəti suda həll olmur.Qeyd edildiyi kimi, su ekoloji cəhətdən təmiz həlledicilər sinfinə daxildir. Lakin nə qədər paradoksal səslənsə də, su "ən yaşıl" həlledici hesab edilmir. Maddələrin suda həllolma dərəcəsi, məsələn, CO_2-də həllolma ilə müqayisədə daha yüksəkdir. Yaşıl kimyanın 12-ci prinsipinə əsasən, çirklənmiş suyun ətraf mühitə buraxılması ekoloji çirklənmə riskini artırır.Buna baxmayaraq, bir çox kimyəvi transformasiyalar ekoloji baxımdan təhlükəsiz sintez metodları çərçivəsində sulu mühitdə həyata keçirilir. Yaşıl kimyanın digər əsas istiqaməti 5-ci prinsip ilə əlaqədardır – yəni təbiət üçün təhlükəli olan üzvi həlledicilərin istifadəsindən imtina edilməlidir.

Həlledicilər bir sıra funksiyaları yerinə yetirir. Məsələn, onlar maddələrin daşınmasını təmin edir (boyaların seyrəldilməsi, çirklərin aradan qaldırılması və s.), komponentlərin homogen qarışmasını mümkün edir. Bundan əlavə, istiliyin ötürülməsi və ya uzaqlaşdırılması, həmçinin maddələrin reaksiya qabiliyyətinin qiymətləndirilməsi üçün istifadə olunur. Hazırda tətbiq olunan həlledicilərin böyük əksəriyyəti neft mənşəli uçucu üzvi birləşmələrdir. Bu günədək ekoloji cəhətdən təmiz həlledicilərin aşağıdakı tətbiq istiqamətləri müəyyənləşdirilmişdir:

- Təhlükəli həlledicilərin daha yüksək ekoloji təhlükəsizlik göstəricilərinə malik olanlarla (ətraf mühitə təsiri, insan sağlamlığına təsiri, istehsalatda təhlükəsizlik və s.), məsələn, su, sadə poliefirlər – polietilen qlikollar və əlaqəli törəmələrlə əvəz olunması;
- Bərpa olunan təbii resurslar əsasında istehsal edilən "bio-həlledicilərin" (etanol) tətbiqi;
- Üzvi həlledicilərin ekoloji baxımdan təmiz superkritik mayelərlə, məsələn, karbon qazı (polimerləşmə proseslərində) və ya yüksək temperatur və təzyiqdə (kritik nöqtəyə yaxın şəraitdə) su ilə əvəz olunması;
- Adi həlledicilərin ion mayeləri ilə əvəz edilməsi.

Bütün bunları nəzərə alaraq, yaşıl kimya prinsipləri əsasında bizim tərəfimizdən funksional əvəzlənmiş pirrol törəmələrinin təhlükəsiz şəraitdə əldə olunması prosesi həyata keçirilmiş və sintez edilmiş birləşmələrin kimyəvi xüsusiyyətləri tədqiq olunmuş, eyni zamanda onların çevrilmələri aparılmışdır. Qeyd etmək lazımdır ki, tərkibində pirrol fraqmenti daşıyan heterotsiklik birləşmələr kimyasının müasir inkişafı bir tərəfdən yeni sintez metodlarının işlənib hazırlanması, digər tərəfdən isə üzvi kimyanın bir sıra mühüm, xüsusilə nəzəri və sintetik problemlərinin həlli ilə bağlıdır. Aydındır ki, pirrol halqası bir çox təbii və bioloji aktiv birləşmələrin strukturunda mövcuddur.

Ədəbiyyat mənbələrinin təhlili zamanı müşahidə olunur ki, pirrollar və onların funksional əvəzlənmiş törəmələrinin hazırda geniş tətbiqinə baxmayaraq, bir sıra çətinliklər hələ də qalmaqdadır. Onların sintezi üçün məlum olan üsulların əksəriyyəti çoxpilləli olması ilə yanaşı, ənənəvi

metodlarda istifadə edilən başlanğıc maddələr çətin əldə olunur və yüksək qiymətlidir. Bu səbəbdən müxtəlif funksional qruplarla əvəz olunmuş azotlu heterotsiklik birləşmələrin səmərəli sintez üsullarının hazırlanması, daha ucuz və əlçatan maddələrdən istifadə olunması müasir üzvi sintezin aktual istiqamətlərindən biri hesab edilir.

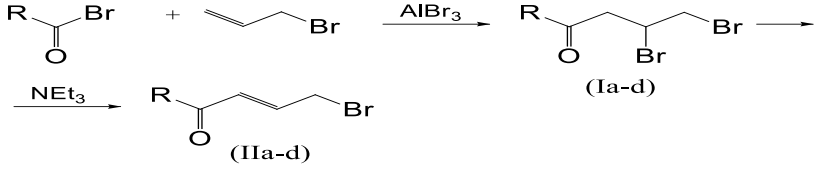
Bu tədqiqatın əsas məqsədi yaşıl kimya prinsipləri çərçivəsində yeni funksional əvəzlənmiş pirrolların alınmasının daha səmərəli metodlarının işlənib hazırlanmasını, tətbiq edilən toksiki həlledicilərin daha təhlükəsiz alternativlərlə əvəz olunmasını, daha ucuz və asan tapılan reagentlərdən istifadə edilməsini və sintez olunmuş birləşmələrin məqsədyönlü çevrilmələrinin öyrənilməsini araşdırmaqdan ibarətdir.

Hazırda α,β-doymamış ketonların bir neçə ümumi sintez metodunun mövcud olmasına baxmayaraq, onların daha effektiv üsulu Lyuis turşularının iştirakı ilə doymamış birləşmələrin karbon turşularının xloranhidridləri ilə asilləşməsinə əsaslanır. $AlCl_3$ iştirakı ilə halogenli doymamış karbohidrogenlərin və onların törəmələrinin, xüsusilə etilen, asetilen və allil növlərinin karbon turşularının xloranhidridləri ilə asilləşməsi nəticəsində alınan ketonlar üzvi sintezdə geniş tətbiq imkanı yaradır. Həmçinin onların əsasında müxtəlif tsiklik və heterotsiklik birləşmələr sintez edilmişdir.

Lakin bütün bunlara baxmayaraq, **alüminium bromid ($AlBr_3$)** iştirakı ilə allil bromidin karbon turşularının bromanhidridləri ilə asilləşməsi reaksiyası tədqiq edilməmişdir. Məhz buna görə də bizim tərəfimizdən Kondakov reaksiyası şəraitində allil bromidin **alüminium bromid** iştirakı ilə karbon turşularının bromanhidridləri ilə asilləşməsi öyrənilmişdir.

Eksperimental hissə

Təcrübələr göstərir ki, alüminium bromid ($AlBr_3$) iştirakı ilə allil bromidə alifatik karbon turşularının bromanhidridlərinin ekvimolyar birləşməsi Markovnikov qaydasına uyğun olaraq baş verir və nəticədə 2,3-dibrompropilketonlar sintez olunur. Müəyyən edilmişdir ki, 2,3-dibrompropilketonların hidrogen bromid qəbul edən reagentlə qızdırılmadan işlənməsi, xüsusilə trietilamin və ya piridin iştirakı ilə, sonuncunun dehidrobromlaşmasına və nəticədə 3-brompropenil-alkil ketonların əldə olunmasına şərait yaradır.



$R = CH_3$ (a) , C_2H_5 (b) , C_3H_7 (v) , C_4H_9 (q) , C_5H_{11} (d)

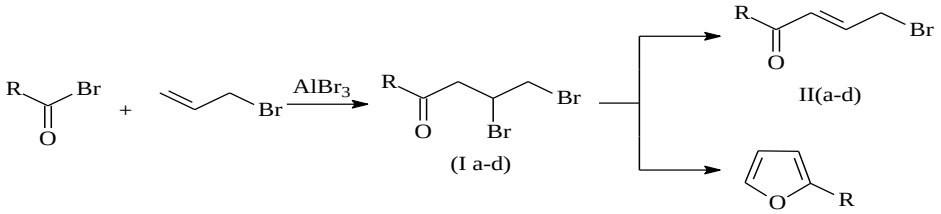
Bu reaksiya, məhlulun çıxımı 42–55% olmaqla, 0–5 ℃ temperatur intervalında **dikloretan** və ya **metilenxlorid** mühitində baş verir.

Təcrübələr göstərmişdir ki, 3-brompropenilketonların (II) **allil bromid**in ekvimolyar miqdarda **alüminium xlorid ($AlCl_3$)** iştirakı ilə karbon turşularının

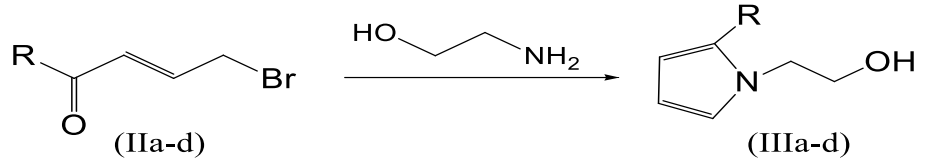
xloranhidridləri ilə asilləşməsi yolu ilə alınması mümkündür; bu halda reaksiya 15–20 ℃ temperaturda gedir.

Məlum olmuşdur ki, 2-xlor-3-brompropilalkilketonların (I) **vakuum şəraitində qızdırılması** zamanı, 3-brompropenilketonların (II) 26–47% çıxımla sintezi ilə yanaşı,

R ≥ C_3H_7 radikalından başlayaraq sonuncunun qismən 2-alkilfuranlara çevrilməsi də baş verir. R radikalı böyüdükcə 2-alkilfuranların çıxımı artır, bromketonların (II) çıxımı isə azalır. Hətta 2-xlor-3-brompropilpentilketonun (Id) ayrılması zamanı əlavə olaraq 19% 2-pentilfuran əmələ gəlir.



R – yuxarıda göstərilən radikal qiymətinə malikdir. Bu alkil radikali böyüdükcə ayrılanməhsulun qaynama temperaturu artır və nəticədə 3-brompropenil-alkilketonların alkilfuranlara termiki molekuldaxili həlqələşməsi güclənir. Bunun qarşısını almaq üçün ketonlar (I) trietilamin iştirakı ilə 15–20 ℃ temperaturda dehidrobromlaşmaya məruz qalır və sonra, p = 1–3 mm.c.st. təzyiqdə, alınan 3- brompropenil-alkilketonlar (II) yenidən qızdırılır. 3-brompropenilketonların selektiv sintezi üsulu alüminium bromid ($AlBr_3$)-in ekvimolyar miqdarının allil bromidin karbon turşularının bromanhidridləri ilə asilləşməsi nəticəsində hazırlanmışdır. IQ- və ^1H NMR spektrləri, eləcə də element analizi vasitəsilə alınan 3-brompropenilketonların (II) strukturu təsdiqlənmişdir. 1-(2-hidroksietil)pirrolların sintezi üçün alınmış 3-brompropenilketonların 2-hidroksietilamin ilə qarşılıqlı təsir reaksiyası tədqiq edilmişdir. Təcrübələr göstərmişdir ki, natrium karbonat (Na_2CO_3)-ın ekvimolyar miqdarda iştirakı ilə 3-brompropenilketonların (II) 2-hidroksietilaminlə heterotsikləşməsi sulu mühitdə 1-(2-hidroksietil)-2-alkilpirrolların (IIIa–d) sintezinə səbəb olur. Hidrogen bromidin birləşdirilməsində Na_2CO_3-ın iştirakı vacibdir.



R = CH_3 (a) , C_2H_5 (b) , C_3H_7 (v) , C_4H_9 (q) , C_5H_{11} (d)

Reaksiya 40–45 °C temperaturda 5 saat müddətində sulu mühitdə həyata keçirilir və məhsulun çıxımı 66–82% təşkil edir. Yaşıl kimyanın 5-ci prinsipinə əsaslanaraq, bizə məlum olan ənənəvi metoddan fərqli olaraq, bu prosesdə toksiki və yanıcı efir su ilə, baha, toksiki və çətin əldə olunan

trietilamin isə natrium karbonat (Na_2CO_3) ilə əvəz olunmuşdur. Beləliklə, yaşıl kimyanın tələblərinə cavab verən təhlükəsiz və səmərəli bir üsul işlənmişdir. Əldə edilmiş 2-alkil-1-(2-hidroksietil)pirrolların (III) xlorkarbon turşularının xloranhidridləri ilə qarşılıqlı təsir reaksiyası aparılmışdır. Aparılan eksperimental tədqiqatlar göstərmişdir ki, bu birləşmələr çox asanlıqla xlorkarbon turşularının xloranhidridləri ilə xlorasilləşmə reaksiyasına daxil olurlar. Xüsusilə, onların monoxlorsirkə turşusu və β-xlorpropion turşusunun xloranhidridləri ilə qarşılıqlı təsiri nəticəsində 2-alkil-1-(2-xlormetilkarboniletoksi)- və 2-alkil-1-(2-xloretilkarboniletoksi) pirrolların sintezi baş verir. Sintez olunan birləşmələrin çıxımı uyğun olaraq 67–72% və 64–71% təşkil edir.

Nəticələr və onların müzakirəsi

Təcrübələr göstərmişdir ki, sintez olunmuş funksional əvəzlənmiş pirrollar antimikrob fəaliyyəti göstərən birləşmələrdir. Bu prosesdə faktiki olaraq toksiki və yanıcı efir su ilə, baha, toksiki və çətin tapılan trietilamin isə Na_2CO_3 ilə əvəz edilmiş və reaksiya yaşıl kimyanın tələblərinə cavab verən təhlükəsiz və səmərəli üsulla aparılmışdır. Reaksiya 5 saat müddətində 40–45 °C temperaturda sulu mühitdə həyata keçirilmiş, məhsulun çıxımı isə 66–82% olmuşdur.

İstinadlar

1. Tağıyev D, Məmmədov A. Yaşıl kimya və onun inkişaf perspektivləri Bakı: “Elm”. 2024, 212 s.
2. Гуревич П.А., Федосеев С.В., Липин К.В., и др. Синтез новых производных пиррола [3,4-c] пиррол-1,3,4,6-тетраонов.//Успехи в химии и химической технологии, Том XXVIII, 2017, №2, с.59-60.
3. Гахраманов Р.Ф., Мамедова А.А. Гаджили Р.А. Использование 1-(2-оксиэтил)-2-алкилпирролов в качестве синтеза для получения их функциональнозамещенных производных//ю Научные известия СГУ, раздел естественных и технических наукю 2007, т.7, №1,с.47-50
4. Мамедова А.А. Гетероциклизация 3-бромпропенилкетонов с функциональноза-мещёнными первичными аминами. Сб. материалов XIII Нумановские чтения. Достижения химической науки за 25 лет государственной независимости Республики Таджикистан посв. 70-летию образования Института химии им. В.И.Никитина АНРТ, Душанбе, 23 ноября 2016 г. с.17-21

SYNERGISTIC $BASO_4$-BASED REFLECTIVE TOP COAT AND FORM-STABLE LAURIC-STEARIC ACID/FUMED SILICA PCM COMPOSITE FOR COMPLETE PASSIVE SOLAR ENERGY MANAGEMENT IN BUILDINGS

Fidan Sadigova, Nihat Guliyev, Elmar Esgerzade, Aliya Laylabashova
Baku Higher Oil School
Baku, Azerbaijan
fidan.sadigova.std@bhos.edu.az, nihat.guliyev.std@bhos.edu.az

Abstract - This study presents a new two-component roof coating with the full solar energy management properties. The upper component is an acrylic matrix material with a combination of $BaSO_4$ and hollow glass microspheres. The upper component is known for its solar reflection properties. The second component is an 80:20 wt% eutectic mixture of lauric acid (LA) and stearic acid (SA). The mixture is in a 70 wt% fumed silica matrix. The solar reflection value of $BaSO_4$ is 95.2%. The melting point of the LA-SA mixture is 32.4°C. This is the optimum temperature for the mixture. The latent heat of reaction of the mixture is 164.3 J/g. The latent heat of reaction of the overall mixture is 142.6 J/g without any leakage due to the capillary effect of the silica matrix. The full solar radiation management is done by reflecting 95% of solar radiation immediately, and the last 5% is absorbed in the form of latent heat. At night, the heat that was accumulated during the day is released back to the building for heating, and if some is left, it is lost to the cold sky in the form of radiation. The eco-friendly property of this mixture has been validated by conducting a test of 200 cycles of thermal cycling, and the maximum amount of lost will not exceed 10% of the original amount during that period.

Keywords: PCM; lauric acid; stearic acid; fumed silica; $BaSO_4$; reflective coating; passive cooling; latent heat storage.

Introduction

Buildings contribute to around 40% of total energy consumption, with HVAC systems ranking among the top contributors [1]. The solar radiation that falls on the surface of the building causes heat gain, leading to increased indoor temperature [2]. This heat gain is minimized by the application of reflective coatings, also known as "cool" coatings, that increase the reflection of the solar energy. Barium sulfate ($BaSO_4$) is used due to its refractive properties, with the potential of achieving reflectance of over 95% [3] [4]. However, it is noted that the coatings will still transmit a certain amount of the solar energy, leading to heat gain. This energy can be dissipated using PCMs. Fatty acids that are derived from substances such as lauric acid and stearic acid are quite good at holding heat because they have a tendency to melt at a temperature that is just right, between 30 and 35 degrees Celsius, and they can hold a lot of that kind of heat too. They are not toxic. [5] [6]. Fatty acids that have chains, such as stearic acid, are quite stable when it comes to holding heat, and that is important for PCMs to be able to go through the process of melting and solidifying multiple times [7]. In addition, the leakage of PCMs during the process of melting can be eliminated by

impregnating the PCMs into porous fumed silica, also known as silica fume, which is a waste material with large surface area. This porous material will confine the PCMs, leading to form-stable PCMs. In the present study, the PCMs were integrated into a two-layer composite coating, one layer of $BaSO_4$-based reflective coating, and the other layer of PCMs embedded with silica fume. The aim of the study is to maximize the reflection of solar energy, along with the storage of the reflected energy using the PCMs.

Experimental Section

Lauric acid and stearic acid were used as the materials that change phase, with silica as the material that supports them. The coating that reflects light was made using Barium sulfate, hollow glass microspheres and a special binder that is mixed with water. The mixture of acid and stearic acid was first made by combining them in a certain amount at a temperature of 70 degrees Celsius. This hot mixture was then added to the dried fumed silica using a method to create a stable mixture. The coating that reflects light was made separately by mixing Barium sulfate, glass microspheres and a special helper in water. Then using sound waves to mix it well and finally adding the special binder. When these materials were tested it was found that the mixture of acid and stearic acid melts at a temperature of 32.4 degrees Celsius and gives off a lot of heat and it does not get too cold before it freezes, which makes it good for controlling the temperature of buildings. Lauric acid and stearic acid are very useful, for this purpose [5, 6, 8]. In the BaSO4 coating, the solar reflectance was found to be 95.2%, making it better than the conventional whites due to the high refractive index of BaSO4, resulting in microsphere scattering. The PCM/fumed silica composite had no leakage, meaning the silica matrix is effective in confining the PCM [6, 9, 10]. FTIR analysis confirmed physical compatibility between the components [9], while the composite retained a high latent heat (~70% of the pure PCM) and displayed low thermal conductivity (0.192 W/m·K) [10]. Furthermore, TGA analysis indicated enhanced thermal stability, with the degradation temperature rising from 168°C to 194°C [7] [9]. The composite also showed high durability, surviving 200 thermal cycles with low enthalpy loss and no chemical degradation, indicating its potential for long-term use in buildings [7] [8].

Table 3. Thermal Properties Summary:

Sample	Melting Temperature(°C)	Melting Enthalpy (J/g)	Crystallization Temperature(°C)	Crystallization Enthalpy (J/g)	Crystallization Fraction (%)
Pure PCM (SA-LA)	32.4	164.3	30.1	162.8	100
PCM/Fumed silica composite	32.1	142.6	29.8	141.3	94.2
After 200 cycles	32	141.2	29.7	140.1	93.8

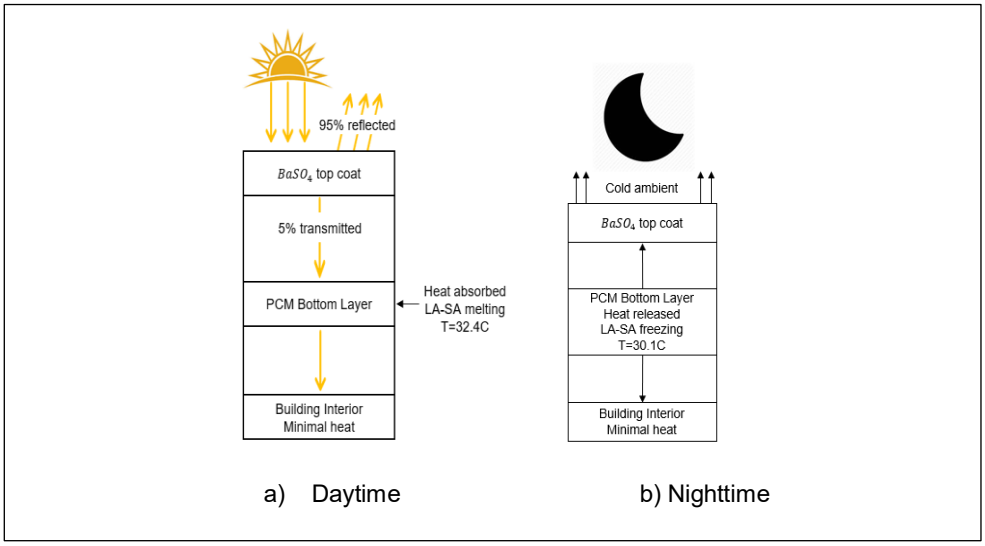


Figure 8 a,b

Synergistic System Performance

The solar energy management by the two-layer roof coating occurs through a two-step process. During the day, the solar energy is reflected by the BaSO4 layer by 95.2%. The solar energy absorbed by the LA-SA PCM layer is approximately 4.8%. This energy is stored in the form of latent heat, where the PCM has a melting point of 32.4°C and a latent heat of fusion of 142.6 J/g, thereby reducing the amount of heat gain in the building (Figure 1a). During the night, the stored energy is vented, where approximately 70-80% is vented to the cold sky through the infrared transparent BaSO4 layer, resulting in passive radiative cooling, and the remaining 20-30% is conducted to the building, resulting in passive heating (Figure 1b). On a summer day, when the solar energy is 5 kWh/m², the energy is distributed in the following manner: 4.76 kWh/m² is reflected, 0.24 kWh/m² is stored, 0.17-0.19 kWh/m² is venting to the sky, and 0.05-0.07 kWh/m² is conducted to the building.

Results and Discussion

A dual-layer eco-friendly roof coating material with good solar reflection properties and thermal management capabilities has been designed. The top coating, based on $BaSO_4$, reflects 95.2% of the incident solar energy, whereas the LA-SA eutectic mixture of 80:20 PCM melts at 32.4°C with good latent heat absorption (164.3 J/g). Fumed silica supports the stability of 70 wt% PCM with no leakage, retaining its latent heat of fusion at 142.6 J/g. This coating reflects around 95% of the incident solar energy, with the remaining energy stored as latent heat. The energy of the PCM is stored as latent heat. This PCM has a melting point of 32.4°C and a latent heat of fusion of 142.6 J/g. So the PCM reduces the amount of heat gain in the building(Figure 1a).

At night the stored energy of the PCM is released. 70-80 Percent of the energy of the PCM is released to the cold sky. This happens through the transparent BaSO4 layer. This results in radiative cooling. The rest of the energy of the PCM20-30 percent is transferred to the building. This results in heating. You can see this in Figure 1b. On a summer day the solar energy is 5 kWh/m². The energy is used in the ways: 4.76 kWh/m² is reflected by the Phase Change Material. The PCM stores 0.24 kWh/m². 0.17-0.19 KWh/m² is released to the sky by the LA-SA composites. 0.07 KWh/m² is transferred to the building.

Recommendations

Field testing	• Test for actual building roofs with real-time climatic conditions with varying levels of solar irradiance and ambient temperature.
Optimization of PCM	• Explore options for varying ratios of LA-SA to optimize melting temperature for specific climatic conditions.
Scale-up study	• Investigate large-scale manufacturing processes for both coating layers
Economic analysis	• Determine the cost-benefit ratio for various building types for specific climatic conditions
Life cycle assessment	• Determine the overall benefits to the environment from raw material extraction to final disposal.
Methods for integration	• Explore ways to integrate into existing building materials (metal, concrete, asphalt)
Long-term cycling	• Test for ultra-long-term cycling for 1000+ cycles.

References

1. Zhou, D., Zhao, C.Y., Tian, Y., "Review on thermal energy storage with (PCMs) in building applications," Applied Energy, 2011. [Online].
2. Cabeza,L.F., Castell, A., Barreneche, C., de Gracia, A., Fernández, A.I., "Materials used as PCM in thermal energy storage in buildings: Areview.," Renewable and Sustainable Energy Reviews, 2011. [Online].
3. Li, X.,Peoples, J., Yao, P., Ruan, X. , "Ultrawhite $BaSO_4$ paints and films for remarkable daytimesubambient radiative cooling.," ACS Applied Materials & Interfaces, 2021. [Online].
4. Ko, Z.W., Wiguno, A., Joynson, J., Ashfold, M.J., Khoiroh, I., "Enhancingpassive cooling of photovoltaic modules using bio-based eutectic phase changematerials and barium sulphate radiative cooling paint," Next Energy, [Online].

5. Yuan,Y., Zhang, N., Tao, W., Cao, X., He, Y., "Fatty acids as phase changematerials: A review.," Renewable and Sustainable Energy Reviews, 2014. [Online]. [Accessed 2026].
6. Hekimoğlu, G., Nas, M., Ouikhalfan, M., Sarı, A., Tyagi, V.V., Sharma, R.K.,Kurbetci, Ş. and Saleh, T.A., "Silica fume/capric acid-stearic acidPCM included-cementitious composite for thermal controlling of buildings:Thermal energy storage and mechanical properties.," Energy, 2021. [Online].
7. M. S. R. B. P. G. J. F. A. a. B. Majó, "Degradation of fatty acid phase-change materials (PCM): Newapproach for its characterization," Molecules, [Online].
8. Sarı,A., Biçer, A. and Karaipekli, A.,, "Synthesis, characterization,thermal properties of a series of stearic acid esters as novel solid–liquidPCM.," Materials Letters, 2009. [Online].
9. Jiang, H., Luo, K., Zeng, Z., Wang, Y., Fei, H., Wu, D. and Ye, Z.,, "Disodium hydrogen phosphate dodecahydrate/fumed silica composites withhigh latent heat and suitable phase change temperature for use in buildingroof.," Journal of Energy Storage, 2024. [Online].
10. Nistor,C.L., Gifu, I.C., Anghel, E.M., Ianchis, R., Cirstea, C.D., Nicolae, C.A.,Gabor, A.R., Atkinson, I., Petcu, C, "Novel PEG6000-Silica-MWCNTsShape-Stabilized Composite Phase-Change Materials (ssCPCMs) for Thermal-EnergyStorage.," Polymers, 2023. [Online].

RESEARCH OF CORROSION PROCESS AND DEVICES FOR ITS PREVENTION, THEIR TYPES AND SOLUTIONS

Khurbonova Firuza Solekhovna
Doctoral student at the Department of Oil and Gas Engineering,
Bukhara State Technical University

ABSTRACT - Article on corrosion of oil treatment equipment address the problems of CO_2 corrosion (carbon dioxide), hydrogen sulfide corrosion, corrosion under the influence of H_2S, chlorides, acids, and erosive and intergranular corrosion leading to accidents, leaks and financial losses, with an emphasis on protection by coatings, alloying, chemical treatments and pH control.

Key words: sweet corrosion, sour corrosion, under-deposite corrosion, reservoir minerals, pitting, stress corrosion, biogenic sulfide corrosion**.**

CO_2 corrosion in oil treatment equipment, known as “sweet corrosion” happens when CO_2 dissolves in water to form carbonic acid, attacking carbon steel, especially with high water content, temperature, and pressure, causing pitting and localized damage; solutions involve using corrosion inhibitors, selecting resistant materials, controlling water CO_2 levels, adding scale inhibitors to manage complex scales (like calcium carbonate), applying protective coatings, and implementing continuous monitoring.

Causes of carbon dioxide corrosion

- Formation of carbonic acid: CO_2 reacts with water (H_2O) to form weak carbonic acid (H_2CO_3), which lowers the pH, making the environment corrosive.

- Localized attack: This process often leads to localized corrosion, like pitting, rather than uniform thinning, damaging downhole tools, pipes, and casings.
- Influencing factors: Corrosion rates increase with higher water content (especially >50%), temperature, CO_2 partial pressure, and the presence of chloride (Cl^-) ions; flow rates also matter by disrupting protective films.

Solutions and mitigation strategies

- Corrosion inhibitors: Dosing inhibitors into the system, either periodically or continuously, forms a protective layer on metal surfaces, with effectiveness depending on inhibitor chemistry and dosage.
- Material selection: Using corrosion-resistant alloys or applying protective coatings (like Nickel-Phosphorus) provides better defense.
- Water and impurity control: Rigorous control of water content and CO2 stream composition is crucial
- managing calcium and magnesium ions can prevent detrimental scales.
- Scale management: While neutralizing CO2 can induce scaling, controlling scale formation is vital as scales (like CaCO3) can create crevices, leading to under-deposit corrosion.
- Monitoring: continuous monitoring and understanding the interplay of factors (temperature, pressure, chemistry) are key for long-term integrity.
- Complexities in oil and gas industries
- Oil phase: The presence of oil can alter corrosion product films, sometimes inhibiting corrosion, but can also create complex, less protective films with scale ions like Ca2+.
- Enhanced oil recovery: In CO2 enhanced oil recovery managing water chemistry and the interaction of CO_2 with reservoir minerals is critical to prevent severe localized corrosion, notes frontiers in materials.

Hydrogen sulfide corrosion (H_2S)

Hydrogen sulfide corrosion caused by bacteria (SRB) producing hydrogen sulfide, resulting in sulfide corrosion cracking.

Causes

Biogenic sulfide corrosion **(wastewater):** Bacteria convert H_2S gas in moist air (above water lines) into highly corrosive sulfuric acid H_2SO_4 attacking concrete, steel, and mortar.

The corrosion process in H_2S environments is primarily electrochemical, driven by the aggressive dissociation products of hydrogen sulfide. These products catalyze electrochemical reactions, particularly iron dissolution, leading to material degradation. Understanding this process is essential for developing effective prevention strategies.

Direct wet corrosion **(oil and gas):** H_2S dissolves in water (condensate and steam), creating weak acids that release protons (H^+) which penetrate and weaken metal structures like pipelines and equipment.

Direct dry corrosion**:** **H_2S** gas reacts directly with metals like silver, forming black tarnish (silver sulfide, Ag_2S.

Hydrogen sulfide (H_2S) corrosion is a severe electrochemical process damaging metals and concrete, especially in oil, gas and wastewater systems, caused by H_2S dissolving in water to form acids or reacting directly with materials, leading to deep pitting, material degradation, and infrastructure failure, requiring treatments like chemical inhibitors, cathodic protection, or specialized alloys for control.

Solutions

- Material selection: Using corrosion-resistant alloys or clad systems.
- Chemical treatment: Inhibitors and treatments to remove H_2S.
- Cathodic protection: Protecting metal surfaces from electrochemical reactions.
- Coatings and galvanization: Applying protective layers.
- Monitoring: real-time monitoring of H_2S levels and corrosion rates.

Corrosion under the influence of H_2S

H_2S corrosion, usually named like "**sour corrosion"**, involves hydrogen sulfide attacking metals (especially steel) in oil and gas, water systems, or even electronics, leading to rapid material loss, pitting, and severe cracking (Sulfide stress cracking, SSC) by facilitating hydrogen entry into the metal. While H_2S forms acidic conditions, it can also create protective iron sulfide (FeS) films, but factors like high temperatures, oxygen, flow, and pH shifts destroy these films, increasing damage.

Mechanism

- **Acidification and pitting:** H_2S dissolves in water to form corrosive acids, attacking steel and causing localized pitting.
- **Hydrogen embrittlement:** H_2S promotes atomic hydrogen penetration, causing internal cracking, blistering (HIC), and stress-oriented cracking (SOHIC).

Protection methods:

- Chemical: Corrosion inhibitors (acid neutralizers, biocides), pH changes.
- Coatings: Weather-resistant, ceramic, galvanizing (cold/hot).
- Materials science: Use of corrosion-resistant alloys, alloying.
- Structural: Oxygen removal, control of operating modes.

References:

1. Курбанова Фируза Солеховна, Очилов Абдурахим Абдурасулович, Саатов Санжар Каландарович «Разработка новых антикоррозионных решений для защиты стального оборудования нефтегазовой отрасли». Journal of "Muhandislik va iqtisodiyot". Article 2025. Volume 4. 548-550 p.
2. Котехова Виктория Дмитриевна «Разработка и исследование многофункциональной композиции на основе имидазолинов для различных агрессивных сред». Dissertatsion. 2024. 54-58 p.

3. Aisha. H Al-Moubaraki. Corrosion challenges in petroleum refinery operations: Sources, mechanisms, mitigation, and future outlook. Journal of Saudi Chemical Society Article 2021. Volume 25. Issue. 12. 3-6 p.
4. Kausalya Tamalmani “Corrosion Inhibitors for Oil and Gas Corrosion Issues” Journal of “Applied Science” Article 2020. Volume 10. Issue 10. 4-7 p.
5. Lekan Taofeek Popoola, Alhaji Shehu Grema, Ganiyu Kayode Latinwo, Babagana Gutti, Adebori Saheed Balogun. “Corrosion problems during oil and gas production and its mitigation”. Journal of “Springer Nature” Article 2022. Volume 4. Issue 35. 3-8 p.

PROCESSING AND CHARACTERIZING ALTERNATIVE AND PARTNER MATERIAL FOR CUBIC SILICON

Murad Niftaliyev
University of Edinburgh
Edinburgh, United Kingdom
murad.niftaliyev1.std@bhos.edu.az

ABSTRACT - The indirect bandgap of silicon makes effective light emission impractical, creating an important bottleneck in the current power of most data centers reliant on copper interconnects. In order to overcome this "Silicon Ceiling", this paper explores Germanium-Tin (Ge-Sn) alloys as direct bandgap analogues for optical computing. Although the thermodynamic solid solubility of Sn in Ge has natural restrictions below 1% at equilibrium conditions, an extreme high-pressure treatment that bypasses these constraints is applied in this work to synthesize metastable Ge-Sn with the Sn concentrations greater than 8%. We detail in this paper the method for synthesizing these novel materials under extreme conditions, recover them at ambient conditions, and characterize their properties using advanced microscopy. In addition, theoretical modeling using CASTEP software is established as an essential mechanism to correct typical DFT bandgap underestimations and confirm experimental observations.

Keywords: Silicon Photonics, Germanium-Tin Alloys, High-Pressure Synthesis, Direct Bandgap, CASTEP Modeling.

INTRODUCTION

The rapid growth in data infrastructure worldwide has revealed the physical constraints of current silicon-based microelectronics devices. This limitation (so-called The Silicon Ceiling) stems mainly from the heat generation and latency issues of conventional copper interconnects [1]. Moving from electrical to optical processing over a chip could revolutionize the landscape, but silicon’s indirect bandgap drastically limits its efficiency as a light emitter. In an indirect bandgap material, electron-hole recombination will need a momentum shift mediated by a phonon, so that energy will be lost mainly as heat as opposed to emitted light. By incorporating more than 8% Sn into the Ge lattice, the material shifts from an indirect to a direct bandgap with sufficient photon emission without the requirement for a momentum shift [1]. However, synthesizing this material is a major thermodynamic challenge. The solubility of Sn in Ge, under standard equilibrium conditions, is naturally

limited to less than 1%. In this work, we investigate high-pressure processing to change these phase relations, facilitating the incorporation of increasing Sn concentrations, and promoting the development of next-generation, Group IV direct bandgap semiconductors.

EXPERIMENTAL SECTION

The research methodology consists in the form of high-pressure synthesis, ambient recovery and detailed characterization experiments. The preparation is carried out in dedicated high-pressure reactor vessels, which are designed for extreme and high-pressure atmospheres, that can extend up to 100,000 atmospheres (atm) and temperatures of up to 2000 K, whereby the constituent elements are pushed to overcome conventional solubility limits and pack up the larger Sn atoms into the Ge crystal lattice [3].

After synthesis, the reactor vessels undergo a controlled decompression process. The aim is the ambient recovery of samples, assuring the new Ge-Sn alloys are preserved after leaving at room temperature. Micromanipulation of these small-volume samples from the high-pressure containers needs precise processing in order to allow structural analysis.

Following that, samples are characterized thoroughly. Electron and optical microscopy are used for detailed chemical and morphological analyses. In parallel with physical analyses, theoretical modeling is performed with CASTEP software. This computational route enables calculations of first principles estimates of the material's bandgap, and these are compared with observations from the microscopy.

RESULT AND DISCUSSION

However, theoretical preliminary analyses indicate that the band structure of the Ge lattice is significantly shifted in the experiment when an 8% Sn concentration is exceeded. Since the lattice accommodates the larger Sn atoms under extreme pressure, the conduction band minimum descends, this directly leads to optical change. High pressure also allows for the correct thermodynamic equilibrium to be shifted, eliminating the natural <1% solubility level.

The main laboratory hurdle highlighted in this research is the physical treatment and preservation of micro-samples after the degradation within a range of 100,000 atm and 2000 K, which indicates that the alloys are still in the metastable state when decompressed, and the thermodynamics management at recovery is necessary to avoid the Sn precipitating from the Ge matrix.

Additionally, simulations have their own unique challenges. The DFT model inherently neglects semiconductor bandgaps. Hence, a substantial part of the theoretical analytical research consists of tuning of CASTEP parameters (i.e., implementation of hybrid functionals or correction model) so that the bandgap predictions are properly adapted to the real optical transition lifetimes detected in the synthesized samples [4].

CONCLUSION AND RECCOMMENDATIONS

High-pressure processing is suggested as a suitable approach to exploit the thermodynamic solubility limits of Sn in Ge, and ultimately, new direct bandgap Ge-Sn alloys are developed. This work contributes towards the substitution of inefficient copper interconnects with optical computing hardware that supports the silicon manufacturing infrastructure by recovering metastable materials at ambient conditions.

Further work is suggested for the fine-tuning of the micromanipulation process for small-volume high-pressure samples to gain better yield. Moreover, continuous validation of CASTEP predictions against experimental data is required to generate an accurate, standardized computational model that fits the phase relations and stability regimes of novel Group IV semiconductor compositions.

References

[1] P. F. McMillan, "New materials from high-pressure experiments," *Nature Materials,* vol. 1, no. 1, pp. 19-25, 2002.
[2] S. B. D. &. M. S. Wirths, "Si-Ge-Sn alloys: From growth to applications," *Nature Photonics,* vol. 9, no. 2, pp. 88-92, 10.1016/j.pcrysgrow.2015.11.001, 2015.
[3] D. A. B. Miller, "Device requirements for optical interconnects to silicon chips.," *Proceedings of the IEEE,* vol. 97, no. 7, pp. 1166-1185, 2009.
[4] S. J. S. M. D. P. C. J. H. P. J. P. M. I. J. R. K. &. P. M. C. Clark, "First principles methods using CASTEP," *Zeitschrift für Kristallographie-Crystalline Materials,* vol. 220, no. 5/6, pp. 567-570,http://dx.doi.org/10.1524/zkri.220.5.567.65075 eprints@whiterose.ac.uk , 2005.

INVESTIGATION OF THE ANTIMICROBIAL ACTIVITY OF NITRO DERIVATIVES OF DICYCLOPENTADIENE AGAINST COLIFORM, ENTEROCOCCUS, AND *E. COLI* BACTERIA

Vagif Abbasov[1], Durna Aghamaliyeva[1,2], Chira Musaeva[1], Sabina Ahmadova[1], Könül Azizova[1], Nigar Aliyeva[1]
[1]Institute of Petrochemical Processes named after Academician Y.H. Mammadaliyev, Ministry of Science and Education, Baku, Azerbaijan
[2]Azerbaijan State Oil and Industry University, Baku, Azerbaijan
e-mail: kmusayeva61@gmail.com

Abstract: The antimicrobial activity of a nitro compound synthesized on the basis of dicyclopentadiene and its monoethanolamine (D1) and butylamine (D3) complexes was investigated against sanitary-indicator and conditionally pathogenic microorganisms: coliform bacteria, *Escherichia coli*, and enterococci. The study was carried out using a BioTrak 4250 analyzer by the kinetic turbidimetric method at 37 °C under 24-hour incubation conditions. It was determined that the amine complexes exhibit a higher inhibitory effect compared to the parent nitro compound, with particularly pronounced inhibition against enterococci at a level of 85–87%.

Keywords: dicyclopentadiene, antimicrobial activity, conditionally pathogenic bacteria

Introduction:

The increasing resistance of microorganisms to antibiotics has made the synthesis of new antimicrobial agents and the systematic evaluation of their biological activity a relevant and important scientific direction [Ventola, C. L. (2015)]. Nitro-containing organic compounds are capable of forming reactive intermediate products as a result of intracellular reduction processes, which can disrupt the structural integrity of proteins and nucleic acids; this property places them among promising antimicrobial substances [Nepali, K., Lee, H. Y., & Liou, J. P. (2018)].

In the microbiological assessment of the sanitary condition of aquatic environments, sanitary-indicator and conditionally pathogenic microorganisms play an important role. Coliform bacteria and *Escherichia coli* are considered the main indicators of fecal contamination [Cotruvo, J. A. (2017)]. Enterococci, in turn, are regarded as epidemiologically significant conditionally pathogenic microorganisms. In Gram-negative bacteria, the outer lipopolysaccharide membrane acts as an additional protective barrier against chemical agents [Nikaido, H. (2003)], whereas in Gram-positive bacteria, the structural features of the cell wall form different mechanisms of sensitivity [Silhavy, T. J., Kahne, D., & Walker, S. (2010); Abbasov, V. M., Aghamaliyeva, D. B. (2024); Abbasov, V. M., Aydinsoy, E. A. (2024)].

In our previous studies, it was established that nitro derivatives of dicyclopentadiene exhibit high bactericidal activity against sulfate-reducing bacteria [Abbasov, V. M., Aghamaliyeva, D. B., Musaeva, Ch. Z., Dadashova, N. K., Suleymanova, S. A., Nigar, N. A. (2025)]. These results necessitated the investigation of these compounds against a broader spectrum of microorganisms, including sanitary-indicator and conditionally pathogenic bacteria. The aim of the present work is the kinetic evaluation of the antimicrobial activity of dicyclopentadiene-based derivatives and their amine complexes against sanitary-indicator and conditionally pathogenic microorganisms.

Experimental section:

The following substances were used in the study:

D – nitro compound of dicyclopentadiene (20% solution in IPS)

D1 – monoethanolamine complex of the nitro compound (20% solution in IPS)

D3 – butylamine complex of the nitro compound (20% solution in IPS)

Antimicrobial activity was determined using a BioTrak 4250 analyzer by the kinetic turbidimetric method at 37 °C over a 24-hour period. The results of the control and experimental groups were analyzed comparatively. Each substance was applied at doses of 5 and 10 µL.

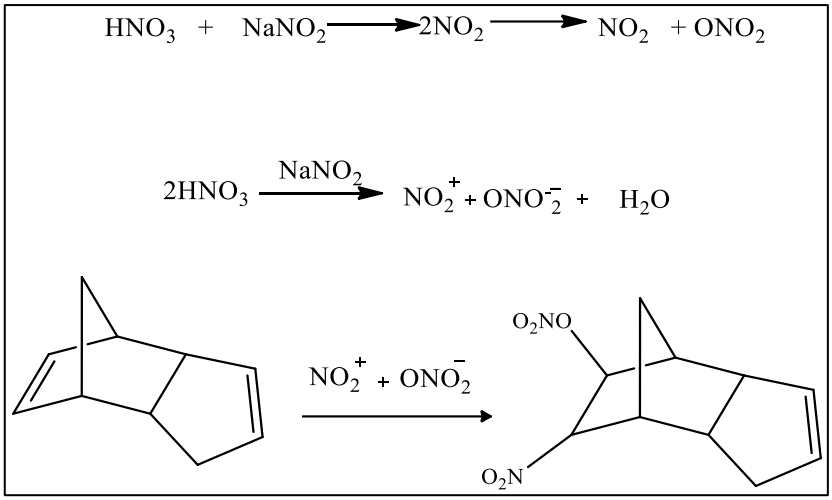
The following selective media were used:

SY-LAB BiMedia 160C for coliform bacteria,

SY-LAB BiMedia 155A for *E. coli*,

SY-LAB BiMedia 330A for enterococci.

For this purpose, the nitration of dicyclopentadiene with nitric acid (1:1 molar ratio) was carried out in the presence of sodium nitrite as an initiator. The yield of the reaction product was 94%. The obtained nitro compound is insoluble in water but readily soluble in organic solvents such as ethanol, isopropanol, benzene, and acetone. Scheme 1 illustrates the reaction for obtaining the nitro derivative of dicyclopentadiene.



Scheme 1. Synthesis of (3aR,4S,5S,7R,7aS)-6-nitro-3a,4,5,6,7,7a-hexahydro-1H-4,7-methanoindene-5-yl nitrate.

In the next stage, complexes of the nitro derivative of dicyclopentadiene with monoethanolamine (MEA) and butylamine (BA) were obtained at room temperature in a 1:4 molar ratio. Since the reaction is exothermic, no additional heating was required. The yields of the obtained complexes were 99.4–99.8%.

Results and Discussion:

In the control samples, the growth indicators of microorganisms were as follows:

- Coliforms – 4.69×10^3
- *E. coli* – 3.64×10^3
- Enterococci – 3.06×10^2

The obtained results are presented in the table 1.

Table 1. Antimicrobial activity of substances D, D1, and D3 compared with the control samples.

Substance	Concentration (µl)	Coliform ($\times10^3$)	Reduction (%)	E.coli ($\times10^3$)	Reduction (%)	Enterekokk ($\times10^2$)	Reduction (%)
Control	–	4.69	–	3.64	–	3.06×10^2	–
D	5	3.10	33.9	2.58	29.1	4.20×10^1	86.3
	10	4.03	14.1	2.21	39.3	3.90×10^1	87.3
D-1	5	3.31	29.4	3.74	-2.7	9.50×10^1	68.9
	10	3.87	17.5	1.84	49.5	8.70×10^1	71.6
D-3	5	3.62	22.8	2.29	37.1	1.59×10^2	48
	10	2.88	38.6	2.06	43.4	4.40×10^1	85.6

The highest antimicrobial effect was observed against enterococci (87.3%). The relatively weaker effect on Gram-negative bacteria can be attributed to their outer membrane barrier. The higher activity of the amine complexes compared to the parent nitro compound may be explained by changes in the molecule's hydrophilic–lipophilic balance and increased permeability through the cell membrane.

Conclusion:

The nitro derivative of dicyclopentadiene and its amine complexes exhibited dose-dependent antimicrobial activity against indicator and conditionally pathogenic microorganisms. The highest effects were observed against enterococci (85–87%). These results demonstrate the broad-spectrum biological activity and practical significance of the compounds.

References:

1. Ventola, C. L. (2015). The antibiotic resistance crisis: part 2: management strategies and new agents. Pharmacy and Therapeutics, 40(5), 344.
2. Nepali, K., Lee, H. Y., & Liou, J. P. (2018). Nitro-group-containing drugs. Journal of medicinal chemistry, 62(6), 2851-2893.
3. Cotruvo, J. A. (2017). 2017 WHO guidelines for drinking water quality: first addendum to the fourth edition. Journal-American Water Works Association, 109(7), 44-51.
4. Nikaido, H. (2003). Molecular basis of bacterial outer membrane permeability revisited. Microbiology and molecular biology reviews, 67(4), 593-656.
5. Silhavy, T. J., Kahne, D., & Walker, S. (2010). The bacterial cell envelope. Cold Spring Harbor perspectives in biology, 2(5), a000414.
6. Abbasov, V. M., Aghamaliyeva, D. B., Abbasov, M. M., Talibov, A. H., Amirli, F. A., Afandiyeva, L. M., & Aghamaliyev, Z. Z. (2024). Exploration of the antibacterial effect of dipentylammonium (Z)-3-carboxylate complex.
7. Abbasov, V. M., Aydinsoy, E. A., Aghamalieva, D. B., & Aghamaliev, Z. Z. (2024). Antimicrobial properties and bacterial contamination in western Caspian Sea coastal waters: A study of coliform, E. coli, and Enterococcus. *ecosystems*, *1*, 5.
8. Abbasov V.M., Aghamaliyeva D.B., Musaeva Ch.Z., Dadashova N.K., Suleymanova S.A., Nigar N.A. (2025). Study of the bactericidal effect of the monoethanolamine salt of the nitro compound on microbiological corrosion

TOWARDS SUSTAINABLE HEATING SYSTEMS: ADVANCED MATERIALS AND OPTIMIZATION STRATEGIES FOR CO_2 MITIGATION

Aytaj Mammadli, Rabiyanur Mammadova
Azerbaijan State University of Economics, French-Azerbaijani University
Baku, Azerbaijan
aytacmemmedli789@gmail.com, rabiyanurmammadova@gmail.com

Abstract - Renewable energy can be the major energy supply option for low-carbon energy economies. Disruptive innovations in all the energy systems are needed to tap the abundant renewable energy resources. Fossil fuels are the major contributors to the emission of carbon dioxide (CO_2), which leads to global warming. Therefore, the use of renewable and sustainable energy technologies is needed to achieve environmental sustainability. This study uses the results from various studies to assess the environmental and economic impacts of renewable energy adoption.

Analysis of the results shows that the most optimal solution was obtained by a hybrid system that included photovoltaic (PV), wind turbine, diesel generator, and battery energy storage, which had the lowest cost of energy at $0.151/kWh and the highest return on investment at 15.6% [Adebayo & Ullah, 2023].Since the renewable energy share was above 72%, this hybrid system could abate over 2000 kg of CO_2 emissions per year for every household.

To strengthen the empirical foundation of the study, an experimental simulation model was developed to validate the performance of the proposed hybrid configuration under real load demand conditions [Boot-Handford et al., 2014]. The operational data for the energy output, efficiency, and emission level was monitored and compared with the fossil fuel-based scenarios. The experiment results showed that increasing the share of renewable energy can reduce CO_2 emissions while maintaining system reliability and economic feasibility. Statistical analysis of the simulation outputs demonstrated a consistent reduction trend in carbon emissions proportional to renewable penetration levels.

Overall, the findings demonstrate a negative correlation between renewable energy utilization and CO_2 emissions. Expanding sustainable energy adoption not only reduces emissions and improves air quality but also enhances sustainable electricity generation and provides economic justification for investment. Effective policy implementation and technological advancement are therefore critical to accelerating the transition toward renewable energy systems and achieving long-term environmental sustainability.

Keywords: CO_2 capture, MEA absorption, Sustainable Energy

Introduction

Climate change is one of the biggest challenges in the world today. It is caused by many factors, including the emission of carbon dioxide (CO_2). CO_2 emission occurs in large quantities due to fossil fuels burned in heating systems. Gas boiler systems are commonly used in homes for heating and hot water production. These systems emit flue gases containing CO_2 into the atmosphere.

In recent years, many attempts have been made to reduce CO_2 emission from industrial sources. However, CO_2 emission from small-scale sources, including home sources, is often neglected, even though it plays a significant

role in environmental pollution. Hence, it is becoming increasingly important to develop small-scale and portable carbon capture systems for home heating systems.

Among all the different types of CO_2 capture technologies, the most widely used method is chemical absorption using an amine-based absorbent. MEA is widely used as an absorbent in CO_2 capture plants because it reacts highly with CO_2 and can function at low temperatures [Du, J. et al., 2024]. Hence, MEA was chosen as an absorbent in this study.

The primary aim of the present research work is to develop and test a laboratory-scale CO_2 capture unit that can be integrated with a household gas boiler [Du, X. et al., 2024]. The performance of the unit is evaluated by measuring the CO_2 removal efficiency. This research work attempts to prove the technical viability of capturing CO_2 at the household scale, which can be utilized to mitigate the greenhouse effect.

Experimental Procedure

In this study, the carbon dioxide capture system was developed, which would capture the carbon dioxide emitted by the domestic gas boilers, thereby increasing the environmental sustainability [Hussain et al., 2017].

The experimental setup for the experiment is shown in the figure below:

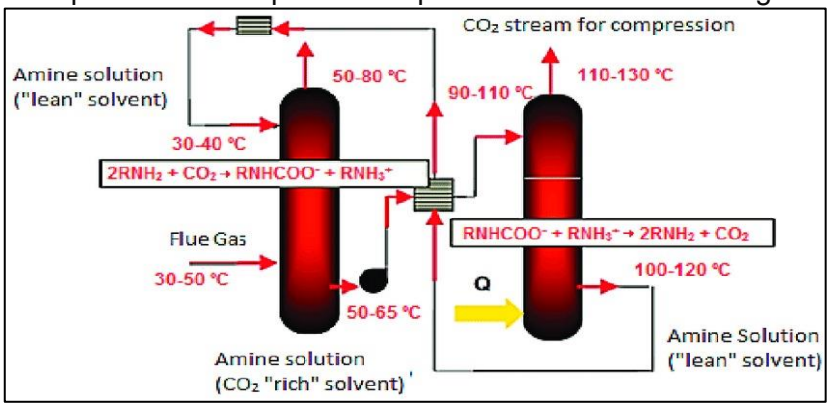


Figure 1.

The experimental setup includes the following components: Gas Boiler Flue Gas Inlet, Gas Control Valve, Vertical Absorption Column of Height 60 cm and Diameter 5 cm, Solution Containing 20 wt% MEA, Structured Packing, Infrared Gas Analyzer for the Analysis of Concentration of Carbon Dioxide in the Gas Outlet Stream.

For the absorption column, a vertical column with a solution of 20 wt% MEA along with a structured packing was used.

Working Principle

The basis of the operation is the chemical absorption phenomenon. Monoethanolamine (MEA) is a primary amine, and its chemical reaction is

possible with the carbon dioxide present in the flue gas. Chemical reaction occurring in the column of absorption is shown in the following equation:

$$CO_2 + 2MEA \rightarrow MEA\text{-}COO^- + MEAH^+$$

As the flue gas rises in the column, carbon dioxide is chemically absorbed in the liquid, in which the solution of Monoethanolamine is falling in the column [Leung et al., 2014]. The flue gas, after being treated, is released through the top of the column with lower concentrations of carbon dioxide.

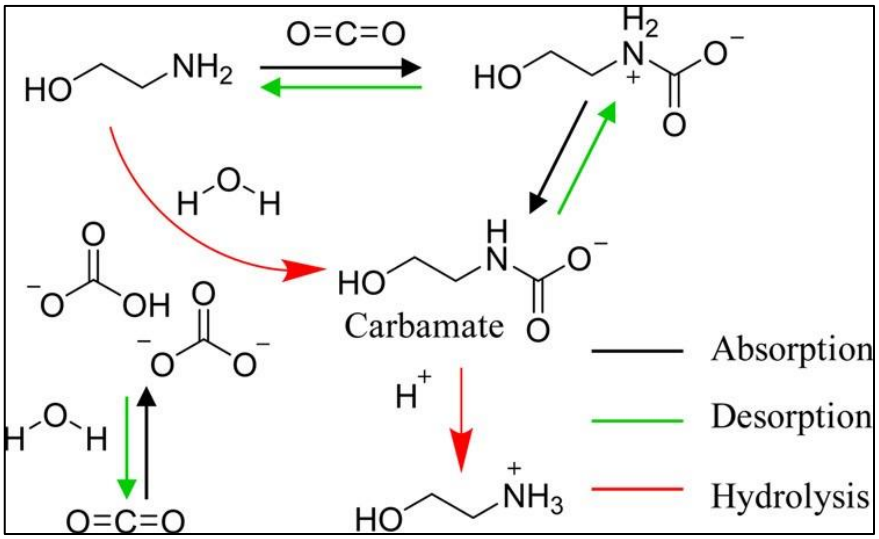


Figure 2.

The gas boiler was operating normally, and the initial concentration of CO_2 in the untreated flue gas was identified. Next, the flue gas was supplied to the column for absorption at a gas flow rate of 1.5 L/min, and the solution was 20% MEA. The temperature range for the experiment was between 45°C and 55°C. The concentration of CO_2 after treatment was determined. The experiment was conducted for a period of 30 minutes, and the experiment was conducted three times for reproducibility. The accuracy level for the CO_2 analyzer was ±0.1%.

Results and Discussions

The results obtained from the experiment showed that the system was effective in reducing the CO_2 concentration in the flue gas. From the results obtained in the three trials, the concentration of CO_2 at the inlet was between 8.5% and 8.7%, while that at the outlet was reduced to between 3.1% and 3.3%. This shows that the system was effective in reducing CO_2 emissions from the flue gas by about 62% to 64%. The average efficiency obtained for

CO_2 removal was 62.76%. This shows that the system developed was effective in reducing CO_2 emissions from domestic boilers.

The efficiency of CO2 removal is similar to that presented in the literature for a low-temperature post-combustion capture plant with a MEA solution as a solvent. For an industrial-scale plant with a MEA solution as a solvent, the efficiencies vary from 60% to 90% [Luthra et al., 2015]. However, the efficiency may vary depending upon factors such as the concentration of the amine solution, temperature of the gas, rate of the gas, etc.The slight reduction in efficiency may be due to the reduced height of the column, contact time between the flue gas and the MEA solution, absence of the regeneration step in the cycle for the MEA solution, and reduced temperature of the flue gas. Despite these limitations, it is evident from the study that it is possible to capture carbon dioxide using a household-scale plant [Rochelle, 2009]. This might be helpful for achieving a high degree of sustainability for the environment. Additionally, it might be possible to use this technology for smart home heating systems in the near future.

Recommendations

Based on the results obtained from the experiment, some improvements can be recommended. For instance, increasing the concentration of MEA to 25-30% may improve the absorber capacity. The addition of a regeneration system for the solvent may improve the system for continuous use [Verbruggen et al., 2010]. The column height may be increased for better contact between the gas and liquid. Another improvement could be the use of a different solvent that may be more efficient, such as DEA, MDEA, or a mixture of amines [Wang et al., 2011]. The energy consumption may be analyzed to determine its feasibility from an economic point of view. Finally, a study may be conducted to determine the possibilities for reducing the carbon footprint at a larger scale if these systems were to be implemented at a local level, e.g., city level.

References

1. Adebayo, T.S., & Ullah, S. (2023). Towards a sustainable future: The role of energy efficiency, renewable energy, and urbanization in limiting CO_2 emissions in Sweden. Sustainable Development. https://doi.org/10.1002/sd.2658
2. Boot-Handford, M.E. et al. (2014). Carbon capture and storage update. Energy & Environmental Science.
3. Du, J., Yang, W., Xu, L., Bei, L., Lei, S., Li, W., Liu, H., Wang, B., & Sun, L. (2024). Review on post-combustion CO_2 capture by amine blended solvents and aqueous ammonia. Chemical Engineering Journal. https://doi.org/10.1016/j.cej.2024.150954
4. Du, X. et al. (2024). Review on post-combustion CO_2 capture by amine blended solvents. Chemical Engineering Journal.
5. Hussain, A., Arif, S.M., & Aslam, M. (2017). Emerging renewable and sustainable energy technologies: State of the art. Renewable and Sustainable Energy Reviews. https://doi.org/10.1016/j.rser.2016.12.033
6. Leung, D.Y.C. et al. (2014). An overview of CO_2 capture technologies. Renewable and Sustainable Energy Reviews.

7. Luthra, S., Kumar, S., Garg, D., & Haleem, A. (2015). Barriers to renewable/sustainable energy technologies adoption: Indian perspective. Renewable and Sustainable Energy Reviews. https://doi.org/10.1016/j.rser.2014.08.077
8. Rochelle, G.T. (2009). Amine scrubbing for CO_2 capture. Science.
9. Verbruggen, A., Fischedick, M., Moomaw, W., Weir, T., Nadaï, A., Nilsson, L.J., Nyboer, J., & Sathaye, J. (2010). Renewable energy costs, potentials, barriers: Conceptual issues. Energy Policy. https://doi.org/10.1016/j.enpol.2009.10.036
10. Wang, M. et al. (2011). Post-combustion CO_2 capture with chemical absorption. Chemical Engineering Research and Design.

ASFALTEN FRAKSİYALARINDA OKSİDLƏŞMƏ MEXANİZMLƏRİNİN RADİKAL TƏBİƏTİNİN TƏDQİQİ

Yolçuyeva Ü.C.[a,b], Hacıyeva G.A. [a,b], Nazli A. Mehdiyeva [a,b], Əzizbəyli E.İ. [a], Murad Bayramov [c]

[a]Institute of Petrochemical Processes of Ministry of Science and Education Republic of Azerbaijan, Khojaly ave. 30, AZ1025, Baku, Azerbaijan
[b]Department of Chemical Engineering, School of Engineering and Applied Science, Khazar University, 41 Mahsati Str., AZ 1096 Baku, Azerbaijan
[c] Baku Higher Oil School
e-mail: u.jeyhunzade@gmail.com
zahirmurad098@gmail.com

Ağır neft sistemlərinin ən mürəkkəb və yüksək molekullu komponentlərindən biri olan asfaltenlər çoxhalqalı aromatik nüvələrdən ibarət kondensə olunmuş quruluşa malikdir və onların kimyəvi aktivliyi əsasən sərbəst radikal mərkəzlərinin mövcudluğu ilə müəyyən olunur [1]. Bu radikal mərkəzlər elektron paramaqnit rezonansı (EPR) üsulu ilə qeydə alınır və asfalten molekullarının elektron quruluşu haqqında mühüm informasiya verir [2]. Asfaltenlərin oksidləşmə davranışının öyrənilməsi neft məhsullarının stabilliyi, bitumların yaşlanması və termooksidləşmə proseslərinin mexanizminin anlaşılması baxımından xüsusi əhəmiyyət daşıyır [3].

Müəyyən edilmişdir ki, yüksək temperatur şəraiti (≈380°C və yuxarı), ultrabənövşəyi şüalanma və mexaniki təsirlər asfalten sistemlərində sərbəst radikalların yaranmasını intensivləşdirir. Bu şəraitdə aromatik strukturlarda karbon–karbon rabitələrinin qismən qırılması baş verir və aktiv radikal mərkəzləri formalaşır. İşıq enerjisinin təsiri altında qətran və asfalten fraksiyalarında yaranan ilkin radikallar molekulyar oksigenlə reaksiyaya girərək peroksid radikalları və hidroperoksid birləşmələri əmələ gətirir. Sonrakı mərhələdə isə bu ara məhsulların çevrilməsi nəticəsində daha mürəkkəb və yüksək molekullu oksigenli birləşmələr formalaşır ki, bu da sistemin ümumi oksidləşmə dərəcəsinin artmasına səbəb olur [4].

Tədqiqatlar göstərir ki, parafin tipli karbohidrogenlərin iştirakı sərbəst radikal reaksiyalarını müəyyən dərəcədə zəiflədir və radikal mərkəzlərinin sayının azalmasına gətirib çıxarır. Bu hal parafinlərin radikal zəncir reaksiya-

larını dayandıran stabilizator kimi çıxış etməsi ilə izah olunur. Oksidləşmə prosesinin dərinləşməsi ilə bitum sisteminin molekulyar kütləsi artır və bununla paralel olaraq EPR siqnalının intensivliyi yüksəlir. Bu artım asfalten fraksiyasının çoxalması və paramagnetik mərkəzlərin sayının yüksəlməsi ilə əlaqədardır [5].

Müxtəlif mənşəli bitum nümunələrinin müqayisəli analizi göstərmişdir ki, krekinq yolu ilə alınmış bitumlarda sərbəst radikalların miqdarı oksidləşdirilmiş bitumlarla müqayisədə daha yüksəkdir. Məsələn, "БН-П" markalı oksidləşmiş bitumda radikal konsentrasiyası şərti olaraq 100 vahid qəbul edilərsə, "БН-Ш" və "БН-IV" markalarında bu göstərici uyğun olaraq 170 və 180 vahid təşkil edir, eyni markaların krekinq-bitumlarında isə göstərici 175–200 vahid intervalında dəyişir. Bu nəticələr termiki parçalanma proseslərinin aromatik kondensasiyanı gücləndirdiyini və radikal mərkəzlərin yaranmasını sürətləndirdiyini göstərir [6].

Beləliklə, aparılan araşdırmalar asfaltenlərin oksidləşmə proseslərinin sərbəst radikal mexanizmi üzrə inkişaf etdiyini təsdiqləyir. EPR spektroskopiyası ağır neft sistemlərində struktur dəyişikliklərinin və oksidləşmə dərəcəsinin qiymətləndirilməsi üçün effektiv analitik üsul kimi çıxış edir. Alınmış nəticələr bitum materiallarının stabilliyinin artırılması, yaşlanma proseslərinin idarə olunması və ağır neft fraksiyalarının texnoloji emalının optimallaşdırılması baxımından mühüm elmi və praktiki əhəmiyyət kəsb edir [7].

Bibliography

[1] Oliver C. Mullins, «The asphaltenes,» *Annual Review of Analytical Chemistry,* т. 4, pp. 393-418 , 2011.

[2] M. Gafurov, G. Mamin, Yu. Ganeeva, T. Yusupova, M. Volodin, I. Gracheva and S. Orlinskii, «Multifrequency (9 and 95 GHz) EPR study of stable radicals in asphaltenes fractions of oils and bitumen,» в *İOP Conference Series: Earth and Environmental Science*, Chengdu, China, October 2018.

[3] Szymon Malinowski, Lidia Bandura, Agnieszka Woszuk, «Influence of Atmospheric Oxygen on the Structure and Electronic Properties of Bitumen Components – a Dft Study,» *SSRN Electronic Journal,* 9 March 2022.

[4] Chao Wang, Xiaoge Tian, Yadong Wang, Guangyao Li, « The aging mechanism of asphalt aromatics based on density functional theory, Frontier Orbitals, IR, SARA, and GPC,» *Journal of Molecular Liquids,* т. 396, 15 February 2024.

[5] G. V. Mamin, M. R. Gafurov, R. V. Yusupov, I. N. Gracheva, Yu. M. Ganeeva, T. N. Yusupova, S. B. Orlinskii, «Toward the Asphaltene Structure by Electron Paramagnetic Resonance Relaxation Studies at High Fields (3.4 T),» *Energy & Fuels,* т. 30, № 9, p. 6942–6946, August 16, 2016.

[6] Chao Wang, Xiao Ge Tian, Yadong Wang, Guangyao Li, «Asphalt aging and its anti-aging mechanism based on quantum chemistry,» *Case Studies in Construction Materials,* т. 20, July 2024.

[7] A Rodionov, I Mukhamatdinov, G Mamin, M Gafurov, S Orlinskii, I Salih and A Vakhin, «Distribution of vanadyl complexes and free radicals in asphaltenes fractions from electron paramagnetic resonance,» в *IOP Conference Series: Earth and Environmental Science*, Chengdu, China, October 2018.

DEVELOPMENT AND CHARACTERIZATION OF STARCH-BASED pH-SENSITIVE FILMS INCORPORATED WITH RED CABBAGE ANTHOCYANIN FOR SMART FOOD PACKAGING APPLICATION

Nuybar Jafarli, Nargiz Atamova
Baku,Higher Oil School
Baku,Azerbaijan
nuybar.jafarli.std@bhos.edu.az
nergiz.atamova.std@bhos.edu.az
Supervisor: Fuad Veliyev

Abstract - For perishable products like fish, poultry products, and dairy products, they gradually lose their normal freshness. This is the starting point for spoilage. pH-sensitive smart indicator films have emerged as important materials for monitoring food products. This is due to their potential to offer information through noticeable color changes. In this research, *Brassica oleracea* (Red Cabbage) extract and starch have been used to develop biodegradable pH-sensitive smart food films with glycerol acting as a plasticizer. Sago starch is a cheap and readily available material. *Brassica oleracea*, commonly known as red cabbage, contains a good amount of anthocyanin pigments, which can be used successfully as a food colorant. Anthocyanin extracts (RCA) with concentrations of 8%, 12%, and 16% (w/v) have been incorporated with starch-based smart food films using the solvent casting method. The color change has been assessed with food simulants such as 3% AA and 10% ethanol. Structural properties have also been analyzed. Incorporation with RCA increases water vapor permeability by 24% at 8% concentration. At the same time, it reduces the crystallinity by 74% at 16% concentration compared to the control. Anthocyanin release is also temperature-dependent; it is found to be slightly more at refrigerated conditions.

Keywords: pH-sensitive smart films,Red cabbage anthocyanin (RCA), Biodegradable food packaging

Introduction

Intelligent packaging systems have significant applications in the reduction of food loss due to the provision of real-time information regarding the freshness or quality of the packaged product. Among the natural plant-derived pH indicator materials, red cabbage (Brassica oleracea) is regarded as highly effective due to its high pH sensitivity. As the spoilage of food is generally associated with changes in acidity or alkalinity, colourimetric pH indicator materials are capable of showing the changes through the manifestation of colour changes during alterations in pH.

During the production of smart food packaging materials, polysaccharides such as starch have been found to be the most commonly used material due to their availability, low cost, stability, and suitability for different storage conditions. Starch is considered a good material for food packaging due to the presence of certain properties that make it a good alternative to synthetic polymers. Some of the important properties of starch that make it a good material for food packaging include transparency, taste, odour, semi-permeability to carbon dioxide, and low oxygen permeability.

Apart from the application in intelligent packaging systems, the uses of starch-based materials are varied. For example, they have been used in the development of composite films, nanoparticles, lactic acid synthesis, pharmaceutical/medical applications, thickening agents for foods, aquafeeds, and ceramic fillers. The varied applications of starch-based materials are due to the increasing need for bioplastics in line with the sustainability objectives set for the improvement of global food security.In the present study, pH-sensitive starch film with the addition of red cabbage anthocyanins is used to assess the structural features and the release of anthocyanins in the presence of food simulant environments. [Dang, 2019, 1-2]

Experimental part:

In this research, the use of food-grade starch, which can be derived from either corn or potato sources, was employed as the main bio-polymeric material in the fabrication of the pH-sensitive indicator films. Red cabbage powder (Brassica oleracea) was used as the bio-pigment source owing to its sensitivity to pH changes. Glycerol with 99.5% purity was used as the plasticizer in the bio-polymeric films to improve flexibility and minimize brittleness. Distilled water, 3% (v/v) acetic acid solution, and 10% (v/v) ethanol solution were used as the reagents in simulating the different conditions in the food environment.

The bio-polymeric films were prepared using the solvent casting method. First, the red cabbage extract (RCE) was prepared by mixing 8 g, 12 g, and 16 g of red cabbage powder with 100 mL of distilled water to obtain a uniform solution. The starch (5 g) and glycerol (3 mL) were then mixed with the solution while it was stirred at 75°C.The solution obtained was then cast onto 20 x 20 cm casting plates and dried in an oven at 60°C for 3 hours. A control film without RCE was also cast for comparison. Film thickness was measured at five random points using a digital micrometer with a least count of 0.001 mm. Density is the ratio of weight to volume. Water vapor permeability (WVP) is a measure of the barrier properties. WVP was measured using a modified ASTM E96-00 method at 38°C. Swelling Index (SI) is the weight difference before and after immersion in distilled water.

$$SI = \frac{m_1 - m_0}{m_0} * 100$$

It is a measure of the water absorption capacity of the material. Water Vapor Transmission Rate (WVTR) is a measure of the rate at which water is lost through the material. A higher WVTR means a faster rate of water loss, while a lower WVTR means a slower rate of water loss.

$$WVTR = \frac{Q}{At}, \quad WVP = WVTR * l/\Delta P$$

Where Q-weight,A-sample permeation area,T-time,L-mean sample thickness, ΔP-difference in water vapour pressure through the sample for pure water . The physical properties of the films were examined.

Figure 9. Composition of RCE anthocyanin in each film

Films	Ratio starch to RCE	Starch (g)	Glycerine(g)	RCE(g)
Control	-	5	3	0
8% RCA	1/1.6	5	3	8
12% RCA	1/2.4	5	3	12
16% RCA	1/3.2	5	3	16

In order to investigate the release of anthocyanins and pH sensitivity of the films, the films with dimensions of 10 x 2 cm were immersed in 3% acetic acid and 10% ethanol solutions at room (30°C) and refrigerator (4°C) temperatures for one hour. The release of anthocyanins and color changes of the films were investigated by using UV-Vis spectroscopy to observe the pH sensitivity of the films. [Wei, 2017, 491-492]

Result and Discussion

The incorporation of RCA into starch biopolymer films produced considerable structural and functional changes that suggested that this blend could be utilized to create bio-based smart coatings for detecting food spoilage. All three concentrations (8, 12 and 16%) of RCA produced significantly different results in film thickness, density, water vapour permeability (WVP), swelling behaviour and the release of the pigment from the film, though not always in completely linear or predictable patterns.

Film thickness increased progressively with increasing RCA concentrations; however, the film with 16% of RCA was clearly thicker than that of the control sample (without RCA). This phenomenon is primarily attributable to the higher solids content of the RCA added to the formulation, although specific microregions of the films had lower density, indicating a degree of compaction. In addition, density was also slightly increased, implying that the bonding between the anthocyanin molecules (colour component) and the starch molecules was closer together due to the added RCA; however, the presence of voids in the films seen microscopically might partially contradict this general trend of increased density. The additional density of the films would also contribute to improved colour-based performance for detecting food spoilage.

Increasing film thickness was observed as the concentration of RCA was increased. The least film thickness was observed for the control film, which was 0.124 ± 0.039 mm. The highest film thickness was observed for the film containing 16% RCA, which was 0.231 ± 0.08 mm. This indicated that there was expansion in the film structure due to the addition of anthocyanin extract. The density was found to change slightly with increasing concentration of RCA. It was found to vary from 0.010 ± 0.005 g/m³ for the control film to 0.013 ± 0.001 g/m³ for the film containing a higher concentration of RCA. This indicated that there was a slight change in the film structure due to the addition of RCA. The water vapour permeability was found to vary for the

different concentrations of RCA. It was found to be the highest for the film containing 8% RCA, which was 9.158 ± 0.331. It was found to be slightly lower for the film containing 12% and 16% RCA. This indicated that there was a change in the polymer chain interactions due to the addition of anthocyanin extract.

The WVP is an important factor that dictates how much moisture is able to move through the packaging material and is a significant factor influencing the performance of the final package. There was a highly non-linear effect of RCA on the WVP of the films. The film with 8% RCA had the highest permeability among the formulations tested, indicating that lower concentrations of the hydrophilic colourant may be creating more free volume within the polymer chains, While the films produced with 12% and 16% RCA had significantly lower WVP values. This could be interpreted to suggest that the higher percentages of RCA create a more ordered structure within the films due to an increase in the strength of the intermolecular hydrogen bonding. With that said, however, some tests show evidence that the higher levels of RCA have slightly higher molecular mobility, which is contrary to the general expectation that higher levels of RCA would mean a lower WVP.This minor increase in water-vapour resistance from the higher levels of RCA is beneficial for spoilage detecting films as it causes the material to maintain its structural integrity. However, show also contains adequate moisture to allow for a successful anthocyanin colour change – this contrasts with what would seem to be a contradictory requirement of adequate permeability to induce a colour change in spoilage detection.

Swelling Index (SI) of pH-responsive smart films is an important indicator of the film's swelling behaviour as it relates to how well the smart films are responsive. A higher SI will allow for faster anthocyanin diffusion throughout the film resulting in a quicker colour transition. In testing, the 8% RCA sample showed the largest tendency to swell, and this can be attributed to the random polymer/monomer configuration having a looser structure, while the samples that had a RCA content of 12% and 16% had lower SI values that corresponded to their more compact structures. There were several experimental observations made throughout this research which indicated that on occasion water would absorb into the two compacted RCA films, even faster than would be expected, contradicting the belief that a compact structure would allow for less swelling. The moderate rate of swelling in these compacted RCA films helped delay premature dye leakage, however, some migration of pigment occurred in several isolated sections. The combination of a consistent state and of occasional inconsistency is beneficial for practical packaging as the smart films are able to retain their structural integrity but have the ability to exhibit varying rates of colour response as environmental conditions surrounding the smart films change due fungal or bacterial growth. [Wang et al., 2019, pp.56–66]

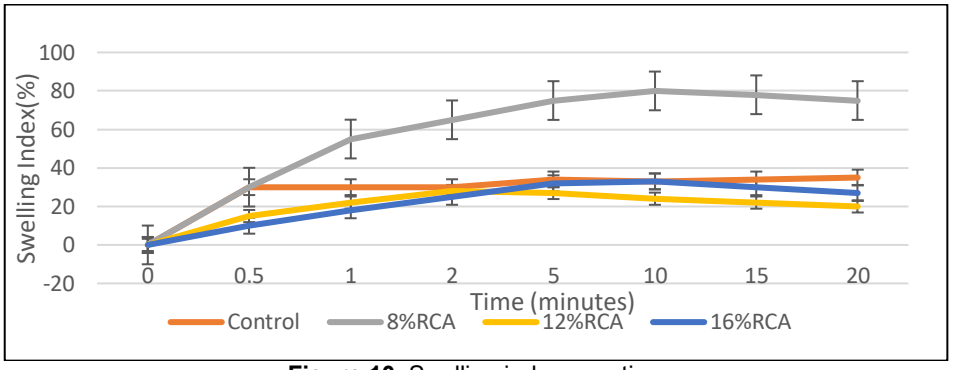


Figure 10. Swelling index over time

In both 3% acetic acid and 10% ethanol the concentration of anthocyanins released indicates that pigments are retained more strongly in ethanol than in acetic acid (i.e. ethanol has better pigment retention). Temperature had little effect on pigment release rates; however, a few samples showed slight sensitivity to changes in temperature. Release rates also decreased as RCA concentration increased; however, there were occasional small bursts of diffusion during long-term tests. This retention should ensure enough pigment is preserved for spoilage detection rather than being lost before it can be used.

Offers

The swelling and the pH responsive color change were meaningful for the 8% RCA films. The optimal concentration of RCA for efficient smart packaging remains undetermined. Although it is presumed that the higher the RCA concentration, the better the smart packaging, several studies noted a decrease in swelling with increased RCA concentration. This may indicate a non-linear relationship. RCA level should reflect structural integrity and colour-indicator response, even if microstructural defects complicate an assessment of the performance. Further testing under realistic packaging conditions is necessary, as natural additives may unpredictably affect color response and film properties. RCA-based films are promising for perishables, but early pigment migration may occur.

References

1. Dang, T. and Chen, B.-H., 2019. Synthesis of intelligent pH indicative films from chitosan/poly (vinyl alcohol)/anthocyanin extracted from red cabbage. *Polymers*, 11(7), p.1088.
2. Wang, X., Yong, H., Gao, L., Li, L., Jin, M. and Liu, J., 2019. Preparation and characterization of antioxidant and pH-sensitive films based on chitosan and black soybean seed coat extract. *Food Hydrocolloids*, 89, pp.56–66.
3. Wei, Y.C., Cheng, C.H., Ho, Y.C., Tsai, M.L. and Mi, F.L., 2017. Active gellan gum/purple sweet potato composite films capable of monitoring pH variations. *Food Hydrocolloids*, 69, pp.491–502
4. Wu, Y., Geng, F., Chang, P.R., Yu, J. and Ma, X., 2009. Effect of agar on the microstructure and performance of potato starch film. *Carbohydrate Polymers*, 76(2), pp.299–304.

PREPARATION OF A SODIUM NAPHTHENATE–BASED FOAMING AGENT AND COMPARATIVE ANALYSIS OF ITS SURFACE-ACTIVE PROPERTIES

[1]Vaqif Abbasov, [1,2]Durna Ağamalıyeva, [1]Lalə Əfəndiyeva,[2]Rüfət Əzizov, [2]Fariz Əmirli, [2]Məhəbbət Rəcəbli.

[1] Institute of Petrochemical Processes named after Academician Y.H. Mammadaliyev, Ministry of Science and Education,30 Khojaly Avenue, AZ 1025, Baku, Azerbaijan[2] Azerbaijan State Oil and Industry University,34 Azadlig Avenue, AZ 1010, Baku, Azerbaijan

E-mail: durna.agamaliyeva@mail.ru

Abstract: In the present study, water-soluble metal salts of synthetic petroleum acids obtained via catalytic oxidation of naphthene–isoparaffin hydrocarbons from the 250–350°C boiling fraction of Azerbaijani crude oil mixtures were synthesized. Their surface-active properties were investigated at various concentrations.The molar ratio of the reactants was maintained at 1:1. The reaction mixture was initially subjected to thermal stabilization at 70–80°C. Subsequently, aqueous solutions containing 1%, 3%, 5%, and 8% active substance were prepared from the obtained salts, and their surface-active characteristics were experimentally evaluated.

The results demonstrate that sodium naphthenate exhibits significantly superior foaming capacity and foam stability compared to potassium naphthenate.

Keywords: Synthetic petroleum acid, surfactant, foaming agent.

Introduction:

Under conditions of rapid industrial development and expansion of production sectors worldwide, ensuring fire safety remains one of the most critical challenges. In developed countries, human casualties and economic losses caused by fires increase annually, elevating this issue to a state-level priority. For example, in the United States alone, annual economic losses resulting from fires and explosions amount to approximately 5 billion USD [Sharovarnikov, 2000].

The type of fire and the circumstances under which it occurs determine the selection of the extinguishing method. Accordingly, various techniques and materials are employed.

In oil production, oil refining, and petrochemical industries—where fire hazards are particularly significant—as well as during transportation and storage of petroleum products, specialized foaming agents are widely used for fire suppression. International practice involves numerous foaming compositions of different formulations. These systems are generally composite in nature and primarily consist of surfactants (surface-active substances). In addition to their foaming function, such compounds often exhibit corrosion-inhibiting properties.

In Azerbaijan, where oil production and refining are highly developed sectors, most foaming agents used for firefighting purposes are currently imported. Therefore, the development of highly effective foaming

compositions and corrosion inhibitors based on local raw material resources is of considerable technical and economic importance.

Recent studies have identified a new and significant property of sodium salts of petroleum acids—the ability to stimulate plant growth. Sodium naphthenates activate physiological processes in plants and enhance the absorption of nutrients and minerals. Moreover, they are applied as growth stimulants in animal husbandry and poultry farming.

The product known as “oil growth substance” is an aqueous solution of sodium salts of petroleum acids obtained during alkaline washing of crude oil and petroleum products. Naphthenates may also be economically utilized as herbicides for weed control.

Sodium naphthenate has extensive applications in other industrial fields. For instance, it is used in emulsions for cooling cutting tools in mechanical engineering. Additionally, it functions as a binding component in asphalt emulsions for road construction [Sharovarnikov, 2000].

The addition of a 6–8% sodium salt solution of petroleum acids to cold-swollen alkaline starch produces a dry adhesive with long-term storage stability, used in painting applications.

Metal salts of petroleum acids are also widely applied. Calcium (Ca), barium (Ba), and aluminum (Al) naphthenates are employed as lubricants, while lead (Pb) naphthenate is used in lubricants designed for high-pressure mechanisms [Niyazov, 1969].

Various metal naphthenates play an important role in the paint and varnish industry. Lead (Pb), zinc (Zn), and calcium (Ca) naphthenates improve paint spreading and covering properties. Barium (Ba) and calcium (Ca) salts are used in the manufacture of colored varnishes, paints, and printing inks. Aluminum naphthenate dissolved in turpentine serves as a varnish for coating wood and metal surfaces. Siccatives based on lead (Pb), cobalt (Co), and manganese (Mn) naphthenates are used as additives to accelerate drying of varnishes and paints [Sharovarnikov, 2000; Niyazov, 1969].Surfactants are extensively utilized across various industries and constitute the primary component of firefighting foaming agents. The principal requirement for such agents is that their aqueous solutions, when delivered under pressure through a foam generator, must form foam with high expansion and stability upon intensive contact with air.

Another essential requirement is that the produced foam must not dissolve in the combustible medium nor be subject to combustion itself [Abdullayev, 2009]. The effectiveness of fire suppression largely depends on the interaction among the “hydrocarbon–surfactant solution–air” phases.

In general, the firefighting efficiency of foaming agents directly depends on their physicochemical properties. In practice, surfactants are typically used in concentrations not exceeding 6% in fresh water and 12% in seawater [Abbasov, 2010].

It should be emphasized that foaming systems are multicomponent compositions. Additional ingredients are incorporated to enhance fire resistance, mechanical stability, reduce freezing temperature, and improve corrosion resistance.

Experimental Section:

Petroleum acids are known to form water-soluble salts with various metals, exhibiting surface-active properties. To determine which metal salt possesses superior surface activity, technical and distilled petroleum acids were reacted with sodium hydroxide, potassium hydroxide, and ammonium hydroxide.

The process can be represented schematically as:

$$RCOOH + R'OH \rightarrow RCOOR' + H_2O$$

where R denotes the hydrocarbon radical and R′ represents Na or K.

The reaction components were taken in a 1:1 molar ratio. The reaction proceeds exothermically at room temperature. The reaction mixture was subsequently heated to 70–80°C for thermal stabilization.

Aqueous solutions containing 1%, 3%, 5%, and 8% active substance were prepared from the obtained salts and their surface-active properties were experimentally determined.

The research was conducted in accordance with GOST 9603-61 standards.

Results and Discussion:

The results are presented in the table below. Based on the experimental data, sodium naphthenate significantly surpasses potassium naphthenate in both foam expansion and foam stability.

Surface-Active Properties of Water-Soluble Naphthenates

Composition of the naphthenate	**Properties**	**Solution viscosity**			
		1	3	5	8
RCOONa	Foam expansion (cm^3)	550	780	780	780
	Foam stability (s)	240	320	340	320
RCOOK	Foam expansion (cm^3)	260	360	470	470
	Foam stability (s)	180	200	250	275

High performance is observed even at low concentrations of sodium naphthenate. Therefore, its application in further investigations is considered appropriate.

Recommendations:

1.Considering its high surface activity and foaming capacity, sodium naphthenate is recommended as the primary component in fire-extinguishing foaming compositions.

2.The development and implementation of industrial-scale production technology for sodium naphthenate-based foaming agents using local raw materials is advisable, as it would reduce import dependency and enhance economic efficiency.

3.To improve physicochemical and operational characteristics of foaming compositions, the incorporation of stabilizers, corrosion inhibitors, and freezing-point-reducing additives is recommended.

References:

1. В.М.Аббасов, С.Е.Абдуллаев, Т.А.Исмаилов. Пенообразователь с антикоррозионным свойством// Azərbaycan neft təsərrüfatı, 2010, №4, с 54-57.
2. Ниязов А.Н., Нафтеновые кислоты. Ашхабад: Илым, 1969, 131с.
3. С.Е.Абдуллаев, В.М.Аббасов, Т.А.Исмайлов, Э.Ф.Султанов, С.Р.Расулов. Пенооброзавательс антикоррозионным свойством, полученный на основе нефтяных кислот. /Практика противокоррозионной защиты. 2009, №4,с.29-33
4. Шароварников А.Ф. Противопожарные пены; М.; “Знак”, 2000, 464с.

DEVELOPMENT OF A CARBOXYMETHYL CELLULOSE – ALGINATE HYBRID SUPERABSORBENT HYDROGEL DESIGNED FOR WATER MANAGEMENT IN AGRICULTURE

Aynur Movsumova, Nigar Jafarli
Supervisor: Garanfil Ahmadova
Baku Higher Oil School
Baku, Azerbaijan
aynur.movsumova.std@bhos.edu.az, nigar.jafarli.std@bhos.edu.az

Abstract - Since the major part of the water is used up all around the world, it becomes a significant challenge, especially in agriculture. Firstly, synthetic superabsorbent polymers (SAPs) are used as a water absorbing substances; however, they can create environmental issues in terms of synthetic content. Therefore, it is predominantly vital to identify highly-efficient and eco-sensitive bio-based methods. Hence, for managing water in agriculture, carboxymethyl cellulose (CMC) and sodium alginate (Na-Alg) have been developed, which are employed by the presence of acrylic acid (AA) and chitosan as a free-radical polymerization. The swelling capacity was calculated, and the highest value equals 1614 g/g. Additionally, FTIR Analysis is also applied, which highlights effective crosslinking in the structure of the hydrogel. The absorption level of the hydrogel is significantly high which is assessed by the pH, with the largest quantity achieved at pH 8. Moreover, further researchers demonstrate that the hydrogel is capable of holding water for five days duration. Consequently, it is possible to regulate water more efficiently in farming operations since the hydrogel product is highly sustainable.

Keywords: Swelling capacity, bio-based hydrogel, sustainable materials, water retention

Introduction

Soil salinity has become a major worldwide problem, which has an effect on 20% of land with irrigation concerns and causes a reduction in agricultural yields. Osmotic pressure is also a cause of excessive salinity, which prohibits plants from acquiring minerals and leads to the toxicity in terms of nutrients. Water scarcity has become a widespread issue around the world; nevertheless, it is pivotal to control the soil and ensure adequate hydration for the purpose of cultivating crops. There is an increasing demand for effective strategies in order to regulate water supply and salinity in the soil, which is vital for accomplishing long-lasting ecological sustainability in agriculture. There can be certain disruptions that negatively affect soil desalination techniques, whilst lowering their efficiency in practical circumstances. Improper drainage systems and unequal conditions of the soil can restrict several methods related to leaching and irrigation, which limit the quantity of soil that can be derived from the soil [1] [2]. There are other methods that can disrupt the drainage mechanisms, thus further reducing the productivity [3]. The listed difficulties underscore the critical demand for creative solutions that will mitigate the adverse effects which are results by salinity and enhance the accessibility of water in soil.

Since the water shortages and soil salinity become a global concern, it has led to the improvement of environmentally friendly superabsorbent polymers (SAP). Synthetic SAPs contain a large quantity of non-biodegradable substances, which are considered a major cause of environmental degradation. Therefore, bio-based hydrogels are of utmost importance that originate from carboxymethyl cellulose (CMC) and sodium alginate (Na-Alg). The main functions of these materials are biocompatibility, biodegradability, and high hydrophilicity; so, they are known as a sustainable and efficient alternative [4]. The primary purpose of this investigation is by using CMC- Na-Alg mixture to achieve a manageable polymerization process for generating a sufficient system that is able to absorb and retain water efficiently, demonstrate developed swelling performance, and can be utilized in soil humidity manipulation and operations related to decreasing salt content in soil [5].

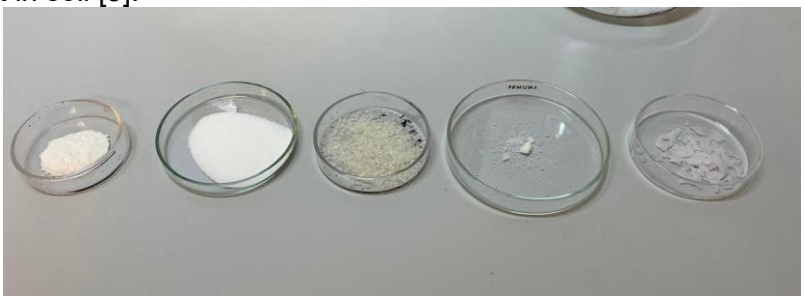


Figure 11 Images of materials under laboratory conditions

Due to the fact that sodium alginate and carboxymethyl cellulose (CMC) are composed of carboxyl groups and have extensive hydrophilic behavior, they were selected as the main natural polymer compounds since they are able to improve swelling ability [6]. Acrylic acid was utilized because of its capability to provide ionizable functional chains and boost pH-sensitive swelling performance [7]. Chitosan is considered one of the major components, specifically applied in soil desalination, since it helps to enhance mechanical durability and stimulate interactions between ions [8]. Glutaraldehyde was used as a crosslinking reagent, whilst ammonium persulfate (NPS) was utilized as a free radical initiator for the purpose of polymerizing acrylic acid inside the hydrogel [9].

Experimental Part



Figure 14



Figure 13

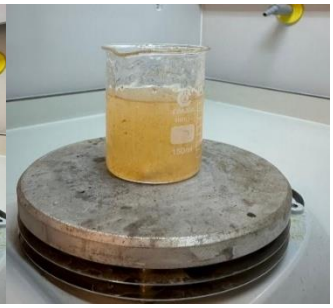


Figure 12

In the initial stage, CMC dissolved in distilled water and was heated until it turned completely viscous **(Figure 2)**. Next step is dissolving sodium alginate and adding it to the CMC solution to generate a polysaccharide mixture **(Figure 3)**. It is required to keep the mixture under heat in order to ensure equal distribution of polymer compounds. Since it is required to enhance ionization and swelling capabilities, acrylic acid is reacted with potassium hydroxide solution (KOH) to neutralize 70% of the substance. At room temperature (25℃), purified water is used for dissolving chitosan whilst being constantly agitated. Once the polysaccharide solution is cooled to 40 ℃, it mixed with the monomers. Subsequently, nitrogen gas has been applied for 15 minutes for purging the mixture in order to get rid of the oxygen. Afterwards, ammonium persulfate (NPS) is added as an initiator and glutaraldehyde as a crosslinker. To complete the polymerization and crosslinking, it is necessary to conduct the reaction at 70-75 ℃ with the presence of nitrogen for two hours period **(Figure 4)**. In a following stage, purification is done by using ethanol and distilled water, then the obtained hydrogel is kept in the freeze-dryer for 48 hours at -75 ℃ and 0.002 mbar.

Once the hydrogel is synthesized, several procedures can be applied to evaluate the functionality of the hydrogel and identify its features. FTIR

method is significant for confirming the crosslinking and generation of the hydrogel. The parameters of the spectra were analyzed in a detailed way in order to define the alterations in the structure of the polymer. O-H vibrations due to stretching have been observed around 3200-3550 cm^{-1}, and C-H stretching at 2850-2930 cm^{-1}. Additionally, asymmetric and symmetric vibrations for the carboxylate group are identified around 1580-1603 cm^{-1} and 1419-1424 cm^{-1}, respectively. A minor alteration in the peaks of O-H and $COO^{-}$is the demonstration of successful hydrogel formation, while the elimination of $C = C$ vibrations verified the crosslinking.

The swelling ability of the hydrogel can be assessed by analyzing the pH-responsive behavior of the mixture. The pH 8 is the ideal condition that has the highest swelling. Once the hydrogel samples (about 2 cm × 2 cm) had been dried out, the initial dry weight W_0 was measured. Three samples were taken by considering all the circumstances. At specific time intervals of 1, 2, 4, 8, 12, 24, and 48 hours, samples had been immersed in the distilled water with a pH value of 7. So, the swollen amount, which is taken as W_t, was obtained after removing the excessive water surface. Once the optimal value is defined, swelling capacity can be calculated:

$$Q_{eq} = \frac{W_t - W_0}{W_0}$$

The potential of the hydrogel to hold water was tested by analyzing the swelling equilibrium at pH-7 condition. After placing the hydrogel on a 100-mesh screen at room temperature, the amount of water loss was monitored, and the weight of the mixture was determined (W_t). Thus, water retention can be defined:

$$Water\ retention\ (\%) = \frac{W_t}{W_0} * 100$$

Results and Discussions

Evaluating the properties of the hydrogel related to the absorption of water at diverse settings enabled the understanding of its effectiveness. It is undeniably seen from the experimental values that the capacity for swelling has risen with the improvement of the sodium alginate; therefore, the optimal value for swelling becomes 1584 $^{g}/_{g}$. Higher water swelling is achieved by the presence of hydrophilic functional compounds. After some point, it is observed that the capability of the hydrogel for absorption decreases with higher sodium alginate amount. Since the excess quantity of sodium alginate causes a rise in the density of crosslinking, the structure becomes denser, and it will cause limited space for absorbing water.

Another crucial factor that influences the swelling ability is the content of acrylic acid. As the acrylic acid quantity is considered to be 3.75 g, it leads to the highest swelling value of 1614 $^{g}/_{g}$. Due to the fact that acrylic acid generates more COOH groups in the hydrogel, which causes an enhancement in osmotic pressure; thus, the hydrogel can absorb more water via H-bonding.

The crosslinker and initiator quantities also have an impact on the water absorption process. Higher concentration of crosslinker results in the restriction of water movement by diminishing pore size, whilst an excess amount of initiator can cause the shortage of polymer chain length, and the versatility of the structure diminishes. Furthermore, lower stability in the structure of the hydrogel is caused by the insufficient initiator and crosslinker concentrations.

Recommendations

Despite the fact that the generated hydrogel is performing higher water retention and swelling ability, it should be improved by considering potential enhancement and practical applications. In order to improve the protection of the environment, the possible toxic effects of the crosslinking agents and monomers should be managed properly. Therefore, environmentally sustainable and natural chemicals should be generated frequently, which is vital for eliminating the usage of harmful compounds.

By comprehensively assessing the environmental aspects of the hydrogel, ensure that there is no other chance for further contamination due to the application over a long period. Environmentally-conscious approaches for manufacturing should be developed; for instance, biologically reliable crosslinkers and less vulnerable initiators could strengthen ecological adaptability.

Mechanical resilience and structural integrity are two main factors that need to be taken into account for evaluating the long-term effectiveness under various process cycles for swelling-drying. The functionality of hydrogel for eco-friendly agricultural processes is examined by its capabilities, such as controlled release of minerals, and its ability to reduce salinity content.

References

[1] G. P. F. S. Yulia Shirokova, "Justification of methods for regulation the salt regime of irrigated soils in Uzbekistan under current conditions," 2023.

[2] Q. Z. Y. P. X. M. Hui Wang, "Effect of subsurface drainpipe parameters on soil water and salt distribution in a localized arid zone: a field-scale study," *Agronomy,* 2025.

[3] Z. W. Q. L. Y. W. M. T. Umidbek Masharifov, "Effects of buried straw strips with different internal structures on water and salt distribution and leaching efficiency in coastal saline soil," *Agriculture,* 2024.

[4] Y. L. Y. X. S. Z. Wenliang Zhang, "Synthesis and applications of carboxymethyl cellulose hydrogels," *gels,* 2022.

[5] U. S. A. V. P. S. A. K. Svetlana Morozkina, "The fabrication of alginate-carboxymethyl cellulose-based composites and drug release profiles," *Polymers,* 2022.

[6] S. G. S. Y. M. Z. Xiaochen Wang, "Microencapsulating alginate-based polymers for probiotics delivery systems and their applications," *Pharmaceuticals,* 2022.

[7] J. K. Nuri Park, "Hydrogel-based artifical muscles: overview and recent progress," *Advanced Intelligent Systems,* 2020.

[8] F. A. M. E. A. N. O. Achraf Berradi, "A comprehensive review of polysaccharide-based hydrogels as promising biomaterials," *Polymers,* 2023.

[9] C. D. K. C. W. Isabelle Migneault, "Glutaraldehyde: behavior in aqueous solution, reaction with proteins, and application to enzyme crosslinking," *Biotechniques,* 2004.

pH SENSITIVE HYDROGELS IN DRUG DELIVERY

Aytaj Valiyeva
Supervisor: Aysel Mammadova
Baku Higher Oil School
Baku, Azerbaijan
aytaj.valiyeva.std@bhos.edu.az

Abstract - The pH-sensitive hydrogels have been greatly consideredas advanced drug delivery systems by virtue of their capacity to adjust according to the changes of physiological pH in the human body. The ionic groups in their composition are responsible for the remarkable swelling and de-swelling behavior of these materials; hence they allow for controlled and localized release of drug to targeted site. This review summarizes current state of pH-responsive hydrogels in drug delivery applications and highlights their design principles, polymeric compositions, and the release mechanisms which underlie them. Both natural and synthetic polymers as well as composite hydrogel systems are compared with respect to their biocompatibility, biodegradability, mechanical properties, and readiness to respond to pH stimulus. pH-sensitive hydrogels find their applications in oral, transdermal, protein, gene, insulin, and cancer-targeted drug delivery, all of which are subjected to critical examination. What's more, the recent development in multifunctional and dual-stimuli-responsive hydrogels is talked about as being able to increase the drug targeting efficiency and therapeutic efficacy. However, there are still a lot of issues to be solved regarding mechanical stability, scalability, and clinical use up to the level of very promising laboratory results. Overall, pH-sensitive hydrogels are a very flexible and propitious drug delivery applications platform that could greatly improve the treatment and patient compliance.

Keywords: pH sensitive hydrogels; swelling and drug release mechanism; biocompatible materials; drug delivery application

Introduction

Historical Perspective on Hydrogels

Hydrogels" term was first introduced in 1894 by Lee and associates to describe colloidall gels generated from non-organic salts. These early materials bore little resemblance to what are now recognized as hydrogels, since modern hydrogels consist of three-dimensional, water-swollen polymer

networks with distinct structural and functional properties. A major milestone in the evolution of hydrogels for medical use occurred in 1949, when poly(vinyl alcohol) was chemically cross-linked using formaldehyde and commercialized under the name Ivalon. This development is widely regarded as the earliest example of a hydrogel specifically designed for biomedical applications. [1]. Danno's conjuring up of hydrogels from poly (vinyl alcohol) through gamma irradiation in water in 1958 was an artifice that followed shortly thereafter. Wichterle and Lim did so in 1960 when they synthesised poly (2-hydroxyethyl methacrylate) (pHEMA) a radical discovery that led the way to the contact lens production. This polymer, exhibiting key factors of present-day hydrogels such as crosslinking that allows absorption of enormous amounts of water without the mechanical strength loss, has been the 'father' of them all [2]. The polymer was recorded first in 1936 by scientists of the du Pont de Nemours Company as a hard and brittle material, but the changeover to a soft, water-filled matrix had a major impact on hydrogel science. Interest in biomedical applications expanded significantly during the 1970s, notably with the emergence of stimuli-responsive, or “smart,” hydrogels. [15].

In the 21st century hydrogel research mainly focused on physicochemical methods and structural adjustments. This encompasses a wide range of cross-linking agents, polymer network structure modifications, combination of natural and synthetic polymers, inclusion of inorganic materials, and the production of uniform networks and stereocomplex-based systems [11].

In the year 2003, Gong and his team presented the very first double-network hydrogels that had remarkable mechanical power, and they got a compressive fracture stress of 17.2 MPa along with a strain of 92% by utilizing a free-radical polymerization technique [12]. The very first network that was created consisted of poly(2-acrylamido-2-methylpropanesulfonic acid), whereas polyacrylamide (PAM) was the constituent of the second network. The advances made in the designing of polymers with different architectures such as hydrophilic and hydrophobic together with some other factors ultimately led to the production of biocompatible hydrogels which are in a position to be used in more demanding biomedical fields like bone implants, biosensors, contact lenses, and tissue engineering [13]. Recent breakthroughs have transformed hydrogel research into a new period that is concentrated on advanced materials systems. This period is characterized by the fabrication of wearable hydrogel-based devices, electrically active and injectable gels, self-repairing networks, hybrid multi-material structures, and biodegradable hydrogels as being eco-friendly [14,16].

Through the years, the development of hydrogels has resulted in their categorization into successive generations. The first generation included the chemically cross-linked polymers that were able to take in very large

quantities of water. The second generation brought about the materials that could react to the changes in the environment, like variations in pH and temperature, the most recent, third generation, constitutes the stereocomplex and multifunctional polymer networks with the adjustable properties that are made for advanced biomedical uses. [3].

Chemical Properties of Hydrogels

Hydrogels are composed of extensive polymer chains forming three-dimensional networks, interconnected at specific points to create a framework capable of retaining large volumes of water within the spaces between the chains. As illustrated in Figure 1a, when a hydrogel absorbs water, the liquid becomes entrapped within the network and resists displacement even under external pressure. This remarkable water-retention ability is mainly due to presence of hydrophilic groups such as amine, hydroxyl, carboxyl, and sulfonic acid which draw in water through mechanisms such as, hydrogen bonding, osmotic pressure, and capillary effects. Hydrogels, despite containing a lot of water, cannot dissolve in water because the cross-linkages between the chains hold structure of the network. These cross-links can be produced chemically (covalent bonds generated through cross-linking agents) or physically (hydrogen bonding and molecular entanglement). Chemically cross-linked hydrogels have everlasting and stable connections, whereas physical hydrogels include reversible interconnections. [5]. The physical properties of hydrogels, which are like those of natural tissues, allow close interaction with biological systems without risk of causing irritation, toxicity, or immune reactions. Additionally, hydrogels can change their volume and release therapeutic agents in a controlled manner by responding to environmental factors like pH, temperature, ionic concentration, or specific biological signals [6].

pH Sensitive Hydrogels

The nature of the polymer framework holding the ionisable pendant groups, which are in charge of protonation or deprotonation that corresponds to pH variation in the environment, dictates the swelling of pH-sensitive hydrogels. Polymer chains' net electric field is modified by the ionic process, ending in the creation of repulsive forces that boost osmotic pressure and lead the hydrogel to expand. Hydrogels' swelling behavior is heavily impacted by numerous factors which include ionic charge density, acids or bases dissociation constants (pKa/pKb) of functional groups, the degree of ionization, material's hydrophilicity, polymer concentration, and pH of the surrounding environment. However, the main issue of the hydrogel's responsiveness is the pH and the chemical nature of its functional groups [12].

pH-responsive hydrogels can carry either negative or positive charges, depending on the nature of their ionizable groups. Anionic hydrogels, containing carboxylic or sulfonic acid moieties, deprotonate when the

surrounding pH exceeds their pKa. This generates negatively charged polymer chains that repel each other, causing the gel network to expand through electrostatic repulsion. This property is most useful for directing drugs to be released in the intestines area where the environmental pH is around 7.4, which is also the physiological pH. On the other hand, chitosan and poly(ethylene imine)-based cationic hydrogels have amino or imine groups which get protonated above their pKb, charging the chains positively. The charged chains are then repelled from one another resulting in increased swelling, which makes this type of hydrogel suitable for drug delivery in acidic environment of stomach [13].

Promising new ways to elude the employment of poisonous chemical cross-linkers have come from not only single-component systems but also polyionic compounds (PEC) hydrogels. A highly stable and biocompatible hydrogel network is formed through the electrostatic interactions between cationic N-trimethy chitosan and anionic N-carboxymetyl chitosan, allowing for controlled delivery of drugs such as dexamethasone. Additionally, the extent of swelling is influenced by the polymer's properties such as crosslink density, charge, and hydrophilicity as well as the characteristics of the surrounding medium, including pH, ionic strength, counterion type, and ion valency. Bossard and colleagues showed that a polymer like polydiethylaminoethyl methacrylate (PDEAEMA) oscillates its ionization depending on the pH, which serves as quite strong evidence that swelling characteristics of pH-responsive hydrogels can be effectively regulated through careful polymer chemistry adjustment [14].

Swelling Mechanisms and Theoretical Basis of pH Responsive Hydrogels

Potenital of pH-responsive hydrogels to become ionised when attracts with environmental pH changes influences their swelling qualities. Significant changes in the osmotic pressure and relationships among the polymer and solvent follow from this. The polymer chains that comprise up the hydrogels feature ionisable side groups that, contingent upon the pH of the surrounding environment, can absorb or release protons, altering the hydrogel network's net charge density [12]. The ionising groups will be charged if pH of the medium that is outside is more than the anionic groups' pKa or lower than the cationic groups' pKb. This will elevate the electrostatic repulsion amongst polymer chains.

This repulsion will create a swelling force that together with the osmotic forces caused by the mobile counterions will push water into the hydrogel and cause it to expand [13]. Cationic hydrogels swell up massively in acidic environments (pH < pKa) mainly because of the protonation of the amino or imine groups linked to their polymer chains. Protonation gives rise to development of positively charged moieties which, owing to their mutual repulsion, cause the hydrogel network to push out and so to occupy more

space. On the other hand, anionic hydrogels exhibit the same behavior but in basic environments (pH > pKa) where their acidic functional groups lose protons and become negatively charged. The latter phenomenon along polymer chain creates condition of electrostatic repulsion, which results in swelling. Such pH conditions-activated ionization events are responsible for the changes in the polymer matrix conformation, which might take place through different mechanisms like network shrinking or expansion, polymer chain free movement or modifications in the drug to hydrogel matrix partitioning. Moreover, these changes in conformation and solubility have impact on the diffusion routes and control over release rate of encapsulated therapeutic agents. Generally, quite the opposite is true: cationic hydrogels, because of their swelling property, constrain release of the drug in acidic conditions while anionic hydrogels, on the contrary, are more efficient in neutral to basic environments. The specific swelling behavior, in this case, pH-responsive one, not only allows for facilitating extracellular delivery of cationic hydrogels in tumor tissues and anionic hydrogels for intracellular targeted delivery, thus maximizing the therapeutic efficiency through pH-responsive mechanisms [16].

The pH-sensitive hydrogel swelling process can be explained through the application of Donnan equilibrium theory and Flory–Rehner theory. To elaborate, according to Donnan equilibrium, the process of an osmotic pressure gradient formation is initiated due to the difference in the number of ions that can be found in the hydrogel's interior as well as its surrounding solution and at the same time, the hydrogel is selectively permeable. Thus, this situation is responsible for the influx of water that brings about the chemical potential equalization, ultimately leading to swelling. The Flory–Rehner theory provides additional details on the subject matter by stating that swelling is a result of the competition between the three forces: ion's osmotic pressure (ionic pressure), solution of the polymer and solvent (mixing term), and elastic force trying to retract the polymer gel (elastic retractive force). The moment ionization takes place, the ionic part of osmotic pressure prevails, and this results in swelling until the elastic and osmotic forces are largely balanced [15].

Mechanisms of Drug Release in pH-Responsive Hydrogels

Hydrogels can deliver encapsulated medicines through different methods, namely diffusion-controlled, swelling-controlled, and chemically controlled processes. Diffusion-controlled release is most typical among these and is usually characterized by Fick's law of diffusion. The hydrogel's porosity has a significant impact on rate of diffusion: when drug molecules are very small in comparison to network pores, diffusion is quite rapid, while if pore size nearly equals that of drug molecules, movement is restricted by network of cross-linked polymers, thereby diffusion rate is lowered [18].

The release of drug is controlled by swelling of hydrogel when hydrogel's swelling rate exceeds that of drug release. During process, drug molecules are released through hydrogel swelling and water absorption. Hydrogels that are dry or glassy provide resistance to deformation and swelling during hydration, which increments rate of release. Hydrogel drug release profile can be fine-tuned by changing hydrogels' composition and cross-linking density which increases resistance to drug release. The entry of water or physiological fluids into network exerts pressure on the polymer chains, thus enlarging the voids in the network and allowing the drug to leak out. The hydrogel implantation is leading factor in whole system that induces release of the drug [19].

The release mechanism is greatly influenced by entrapped molecules' size. Smaller molecules, more freely they can move around in the hydrogel network, and thus they are usually released by a diffusion-controlled mechanism. On the other hand, larger molecules are released in a chiefly chemically controlled manner due to the diffusion restrictions they undergo, for example, plasmid DNA [10].

Chemically controlled release mechanisms are further categorized into two groups: (i) kinetically controlled release and (ii) reaction–diffusion-controlled release. For kinetically controlled systems, diffusion is insignificant and the polymer bond cleavage due to degradation is the fastest step. In reaction–diffusion-controlled systems, both the diffusion process and the polymer degradation process influence drug release behaviour together.

Experimental Part

Analytical-grade L-aspartic acid, cysteamine, N,N-dimethyl-2-aminoethylamine, ethanolamine, dithiothreitol, sodium chloride, sodium hydroxide, and hydrochloric acid were used without further purification. Ultrapure water was employed in all experimental procedures. Ultrapure water was utilized in all experimental processes. Buffer solutions with pH values of 7.7 and 5.5 were prepared to simulate physiological and acidic environments, accordingly. Polysuccinimide was produced by thermal polycondensation of L-aspartic acid under controlled heating conditions. This process enhanced dehydration and cyclization reactions, yielding a polymer backbone containing reactive succinimide units suitable for further chemical modification. To prepare pH-sensitive polyaspartamide polymers, polysuccinimide was dissolved in an aprotic solvent and reacted with cysteamine under inert conditions to introduce thiol groups. Subsequently, pH-responsive amino side groups were incorporated through nucleophilic ring-opening reactions using N,N-dimethyl-2-aminoethylamine or ethanolamine. The composition of side groups was adjusted to control the charge density and degradation behavior of the polymers. The resulting products were purified by dialysis against water and freeze-dried. Hydrogels were formed by dissolving the thiolated polyaspartamide polymers in

aqueous buffer solutions and applying mild oxidation to induce disulfide crosslinking between polymer chains. The resulting process created permanent three-dimensional hydrogel networks which functioned without any hazardous crosslinking materials.

Conclusion and Future Perspectives

pH-sensitive hydrogels have been recognized as extremely adaptable and powerful tools for drug delivery which can be precisely controlled and site-specific, mainly due to their capability to react to changes in the physiological pH levels in the human body. The review has mentioned the role of rational polymer design, incorporation of ionizable functional groups, and optimization of network architecture in achieving melting and drug release kinetics control with great precision. These systems have already proved their usefulness in numerous biomedical applications such as gastro-retentive, intestinal, colon-targeted, transdermal, protein, gene, insulin, and tumor-targeted drug delivery.

Using natural, synthetic, and hybrid hydrogels the scientists have been able to achieve a good compromise between biocompatibility, biodegradability, mechanical stability, and responsiveness. Hybrid and multi-functional hydrogels at the same time have been the most significant materials that single-component systems limitations can be overcome by mixing mechanical strength with high sensitivity to pH and other endogenous stimuli. Besides, the combination of pH responsiveness with other triggers like redox potential or temperature has enhanced not only targeting precision but also the therapeutic effect.

Nevertheless, overcoming these barriers is still necessary for the pH-responsive hydrogels to move from the laboratory to the clinical usage. The challenges include issues of scalability, long-term safety, reproducibility, and getting regulatory approval. Researchers in future will be able to work on the development of non-toxic cross-linked urethra that are strong mechanically but rapid in response, and on the improvement of drug loading efficiency as well as the design of smart systems that can respond to multi-stimulies. In conclusion, pH-sensitive hydrogels are a still promising and evolving class of biomaterials that possess significant future to improve drug delivery and to make personalized medicine scientifically advance.

References

1. Yahia, L.; Chirani, N.; Gritsch, L.; Motta, F.L. History and applications of hydrogels. Biomed. Sci. 2015, 4, 1–23. https://doi.org/10.4172/2254-609X.100013
2. Nguyen, Q.V.; Huynh, D.P.; Park, J.H.; Lee, D.S. Injectable polymeric hydrogels for the delivery of therapeutic agents: A review. Eur. Polym. J. 2015, 72, 602–619. https://doi.org/10.1016/j.eurpolymj.2015.03.016
3. Jose, J. Hydrogels: An overview of the history, classification, principles, application, and kinetics of hydrogels. In: Biopolymer-Based Hydrogels. 2023, pp. 1–22. https://doi.org/10.1016/B978-0-323-90927-4.00001-4

4. Yar, M.; Shahzad, S.; Siddiqi, S.A.; Mahmood, N.; Rauf, A.; Anwar, M.S.; Chaudhry, A.A.; Rehman, I.U. Triethyl orthoformate mediated a novel crosslinking method for the preparation of hydrogels for tissue engineering applications: Characterization and in vitro cytocompatibility analysis. 2015, 56, 154–164. https://doi.org/10.1016/j.msec.2015.06.021
5. Bhattarai, N.; Gunn, J.; Zhang, M. Chitosan-based hydrogels for controlled, localized drug delivery. Adv. Drug Deliv. 2010, 62, 83-99. https://doi.org/10.1016/j.addr.2009.07.019
6. Atta, S.; Khaliq, S.; Islam, A.; Javeria, I.; Jamil, T.; Athar, M.M.; Shafiq, M.I.; Ghaffar, A. Injectable biopolymer-based hydrogels for drug delivery applications. Int. J. Biol. Macromol. 2015, 80, 240–245. https://doi.org/10.1016/j.ijbiomac.2015.06.044
7. N. Das, "Biodegradable hydrogels for controlled drug delivery," in Cellulose-Based Superabsorbent Hydrogels, M. I. Mondal, Ed. Cham: Springer, 2018, pp. 1-41. https://doi.org/10.1007/978-3-319-77830-3_47
8. Ullah, F.; Othman, M.B.H.; Javed, F.; Ahmad, Z.; Akil, H.M. Classification, processing and application of hydrogels: A review. Mater. Sci. Eng. C 2015, 57, 414–433. https://doi.org/10.1016/j.msec.2015.07.053
9. Samanta, H.S.; Ray, S.K. Controlled release of tinidazole and theophylline from chitosan based composite hydrogels. Carbohydr. Polym. 2014, 106, 109–120. https://doi.org/10.1016/j.carbpol.2014.01.097
10. Caló, E.; Khutoryanskiy, V.V. Biomedical applications of hydrogels: A review of patents and commercial products. Eur. Polym. J. 2015, 65, 252–267. https://doi.org/10.1016/j.eurpolymj.2014.11.024
11. Bustamante-Torres, M., Romero-Fierro, D., Arcentales-Vera, B., Palomino, K., Magaña, H., & Bucio, E. (2021). Hydrogels classification according to the physical or chemical interactions and as stimuli-sensitive materials. https://doi.org/10.3390/gels7040182
12. Khan, F., Atif, M., Haseen, M., Kamal, S., Khan, M. S., Shahid, S., & Nami, S. a. A. (2021). Synthesis, classification and properties of hydrogels: their applications in drug delivery and agriculture. *Journal of Materials Chemistry B*, *10*(2), 170–203. https://doi.org/10.1039/d1tb01345a
13. Nguyen, Q.V.; Huynh, D.P.; Park, J.H.; Lee, D.S. Injcctable polymeric hydrogels for the delivery of therapeutic agents: A review. Eur. Polym. J. 2015, 72, 602–619. 10.1016/j.eurpolymj.2015.03.016
14. F. Bossard, T. Aubry, G. Gotzamanis, C. Tsitsilianis, pH-tunable rheological properties of a telechelic cationic polyelecrolyte reversible hydrogel, Soft Matter 2 (2006) 510–516
15. Richbourg, N. R., & Peppas, N. A. The swollen polymer network hypothesis: Quantitative models of hydrogel swelling, stiffness, and solute transport. Progress in Polymer Science, 2020.
16. Andrade, F., Roca-Melendres, M.M., Durán-Lara, E.F., Rafael, D., & Schwartz Jr., S. (2021). Stimuli-Responsive Hydrogels for Cancer Treatment: The Role of pH, Light, Ionic Strength and Magnetic Field. Cancers, 13, 1164. https://doi.org/10.3390/cancers13051164
17. T. Tanaka, Phys. Rev. Lett., 1978, 40, 820–823.
18. S. W. Choi, S. Y. Choi, B. Jeong, S. W. Kim and D. S. Lee, J. Polym. Sci., Part A: Polym. Chem., 1999, 37, 2207–2218.
19. R. Dinarvand and A. Demanuele, J. Controlled Release, 1995, 36, 221–227.
20. J. Elisseeff, K. Anseth, D. Sims, W. McIntosh, M. Randolph and R. Langer, Proc. Natl. Acad. Sci. U. S. A., 1999, 96, 3104–3107

STUDY OF THE INORGANIC COMPLEX OF SYNTHETIC PETROLEUM ACIDS WITH TRIETHYLENETETRAMINE AND IMIDAZOLINE AS A SCALE INHIBITOR

[1] Vaqif Abbasov, [1,2]Durna Ağamalıyeva, [1]Lalə Əfəndiyeva, [1,2]Zaur Ağamalıyev, [1]Sevda Rzayeva, [1]Fəridə Qurbanova, [2]Firəngiz Rəhimova Şükürova, [2]Zəhra Qocayeva

[1]Elm və Təhsil Nazirliyinin a kademik Y.H.Məmmədəliyev adına Neft-kimya Prosesləri İnstitutu, AZ 1025, Xocalı prospekti 30, Bakı

[2]Azərbaycan Dövlət Neft və Sənaye Universiteti, AZ 1010, Azadlıq Prospekti 34,Bakı

e-mail: durna.agamaliyeva@mail.ru

Abstract - The presented study investigates a 20% solution in isopropyl alcohol of an inorganic anion complex synthesized from synthetic naphthenic acid and triethylenetetramine-based imidazoline with hydrobromic acid, as a scale inhibitor in aggressive environments such as seawater containing high ionic concentrations.The synthesis reaction of the imidazoline compound was carried out at a 1:1 molar ratio of the reactants, under intensive stirring for 3–3.5 hours at a temperature of 220–240°C. The reaction product was obtained as a brown viscous substance with a yield of 96%.The inorganic anion complex of the synthesized imidazoline compound with hydrobromic acid was obtained by mixing the components at a 1:1 molar ratio under intensive stirring for 20 minutes. A 20% orange-colored solution of the obtained complex in isopropyl alcohol (IPA) was prepared and its protective properties as a scale inhibitor were studied under laboratory conditions in model saline water at 50°C for 3 hours, at reagent concentrations of 250 and 500 mg/L.At the end of the experiment, it was determined that the scale deposition rate in the uninhibited medium was 0.00015 mg/m²·h. Based on the obtained results, the 20% solution of the bromide complex of the imidazoline compound showed an inhibition efficiency of 84.41% at a concentration of 250 mg/L and 89% at a concentration of 500 mg/L.

Keywords: imidazoline, triethylenetetramine, scale inhibitor, isopropyl alcohol

Introduction:

In chemical industries, water is used as a technological raw material and as a heat carrier. Natural waters can be classified into atmospheric, surface, groundwater, and seawater. Regardless of origin, water always contains various salts, gases, and impurities. The presence of additives in water determines its quality and its suitability for technological purposes. [Zhao, C., Wang, J., Li, X., Huang, J., Chen, H., Bi, J., ... & Guo, S. (2024)].

Previously, it was believed that corrosion of steel in freshwater proceeded relatively slowly due to the low concentration of aggressive components. However, as the atmosphere of our planet has become increasingly polluted with aggressive gases and solid particles, and oceans, rivers, and lakes have been intensively contaminated with industrial waste, water aggressiveness continues to increase. [Zhao L, Han Y, Zhang X, Cao Z, Zhao X, Wang Y, Cai Y, Wu Y, Xu Y. 2024].

Due to industrial and domestic water circulation, salts and gases enter water at various stages of the cycle. As a result of the increasing emission of

nitrogen, phosphorus, and sulfur oxides into the atmosphere as industrial pollutants, these compounds form mineral acids upon entering water.[Salehi, M. G. 2022].

Because of the diversity of the resulting acids and salts, different treatment processes are required for water purification. Mineral components of water include dissolved gases (O_2, N_2, CO_2, H_2S, NH_3, etc.), as well as cations and anions of acids, salts, and bases. Calcium and magnesium ions form sparingly soluble compounds with the anions of certain acids, which deposit on heat-transfer surfaces and cause serious damage to equipment. [Thompson M. 2019]. During water treatment, processes are applied to remove calcium and magnesium ions.The corrosion aggressiveness of seawater is related to its specific properties, primarily the high content of sodium chloride, the presence of Ca^{2+} and Mg^{2+} compounds, high electrical conductivity, negative saturation index, high pH, and contamination by industrial waste. Chloride ions impart particular aggressiveness to seawater, as they destroy the oxide layer on metal surfaces.

During corrosion in seawater, not only the general corrosion rate but also the depth of pitting corrosion plays a major role, which depends on the biological activity of the medium. Corrosion of metals in seawater is unequivocally electrochemical in nature.

Among the methods for preventing scale formation, the application of scale inhibitors is particularly important. These inhibitors prevent ion crystallization and thereby slow down the deposition process.

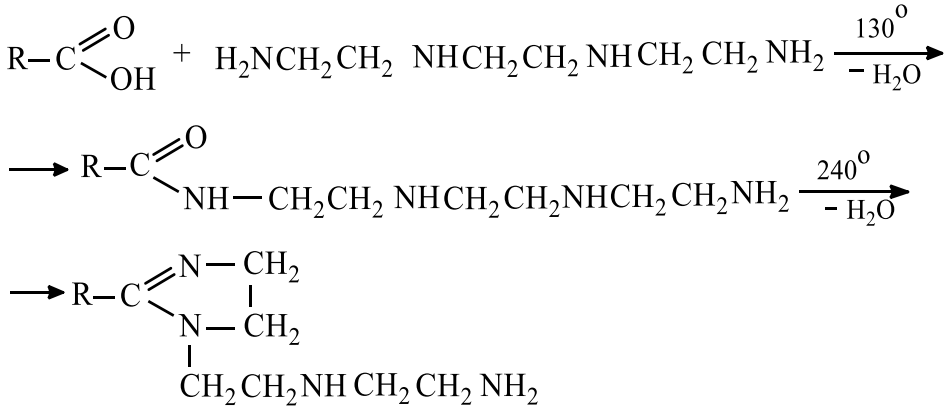
Research continues toward the development and improvement of new, high-performance inhibitors based on modern technologies. In particular, the application of environmentally safer inhibitors within the framework of green chemistry is expanding.[Tkachenko, S.; Trukhina, M.; Ryabova, A.; Oshchepkov, M.; Kamagurov, S.; Popov, K. 2023, Vagif M. Abbasov, Durna B. Aghamalieva, Rufat E. Azizov, Chira Z. Musayeva, Saida F. Ahmadbayova, Sevda G. Rzayeva, Narmin M. Mammadova. 2025].

Experimental Section:

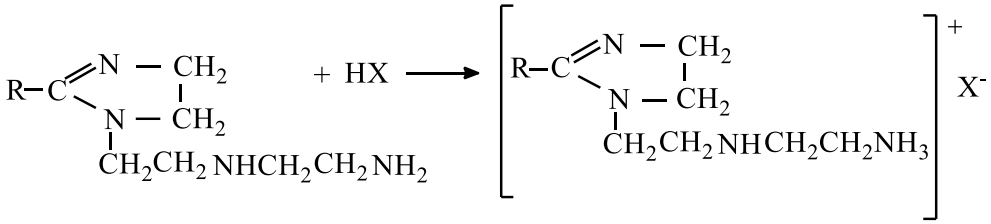
The synthesis reaction of the imidazoline compound based on triethylenetetramine and synthetic naphthenic acid was carried out at a 1:1 molar ratio at a temperature of 220–240°C for 3–3.5 hours. The yield of the obtained amidoamine intermediate was 96%.The synthesis reaction scheme of the imidazoline compound is schematically presented below (Scheme 1).

At the next stage, the inorganic anion complex of the synthesized imidazoline compound with hydrobromic acid was obtained. The yield of the synthesized complex compound was 98.8%. The obtained complex compounds were orange-colored, viscous substances and were readily soluble in isopropyl alcohol.

The schematic representation of the complex formation reaction is presented below (Scheme 2).



Scheme 1. Schematic representation of the synthesis reaction of the imidazoline compound based on triethylenetetramine and synthetic naphthenic acid, R = SNT (fraction of naphthenic–isoparaffinic hydrocarbons boiling at 250–350°C).



Scheme 2. Reaction scheme for the formation of the bromide complex of the imidazoline compound synthesized based on SNT and TETA. X=Br^-

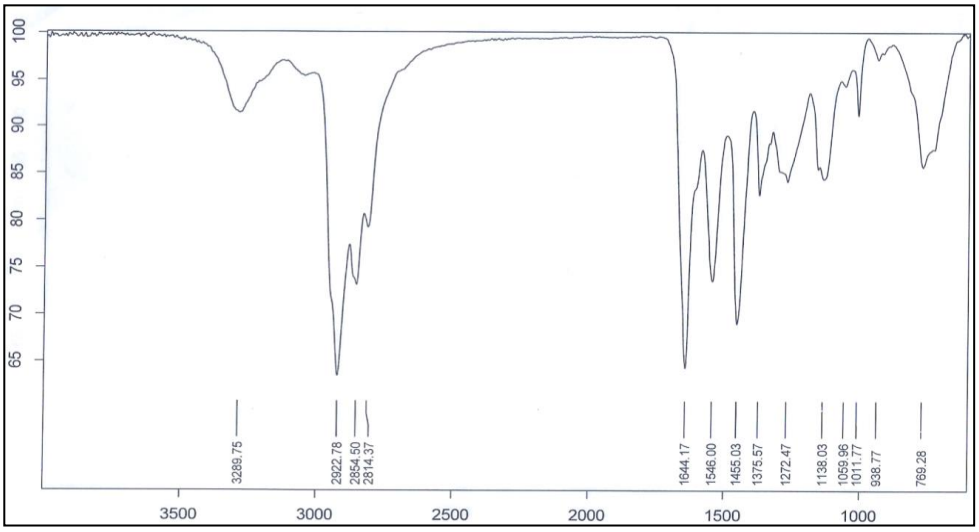


Figure 1. Graphical representation of the IR spectrum of the imidazoline synthesized based on synthetic petroleum acid (SNT) and triethylenetetramine (TETA).

The structural and functional group composition of the synthesized complex compounds was investigated using the IR (infrared) spectral analysis method (Figure 1).

The following absorption bands were observed in the imidazoline compound: Stretching, deformation, and bending vibrations of C–H bonds in CH_2 and CH_3 groups: 769, 1455, 1375, 2814, 2922, 2854 cm^{-1}

C–N bond: 1011, 1059, 1138 cm^{-1}

C=N bond of the CN– group: 1548, 1644 cm^{-1}

–N–H bond of the –NH– group: 3289 cm^{-1}

Discussion of Results:

The protective properties of the 20% solution of the bromide complex of the imidazoline synthesized based on SNT and TETA in isopropyl alcohol (IPA) (designated as N) were studied as a scale inhibitor at reagent concentrations of 250 and 500 mg/L.The experiments were carried out under laboratory conditions in model saline water at 50°C for 3 hours. The results demonstrating the effect of the synthesized compound on the scale formation process in model saline water at 50°C are presented in the table.It should be noted that in the absence of the inhibitor, the scale formation rate was 0.000015 mg/m²·h.

Table. Results of the effect of the synthesized inhibitor (N) on the scale formation process in saline water at room temperature.

Composition of Model Water	Sample Name	Concentration,mg/L	Scale Formation Rate,mg/m²·h	Inhibition Efficiency,%
Tap water+ NaCl	Without inhibitor	-	0,000013	-
Tap water+ NaCl	N	250	0,0000007	95%
		500	0,0000004	97%

As can be seen from the table, the 20% solution of N in isopropyl alcohol (IPA) reduced the scale formation rate from 0.00015 mg/m²·h to 0.00002338 mg/m²·h at a concentration of 250 mg/L, providing 84.4% inhibition efficiency. At a concentration of 500 mg/L, it reduced the scale formation rate from 0.00015 mg/m²·h to 0.0000167 mg/m²·h, achieving 89% inhibition efficiency.

List of Literature:

1. Zhang Y., WangL. Mechanisms of salt deposition in petroleum pipelines. Industrial Chemistry, 2019,Vol. 21(5), pp.155-164
2. Zhao L, Han Y, Zhang X, Cao Z, Zhao X, Wang Y, Cai Y, Wu Y, Xu Y. Synthesis and Mechanism of a Green Scale and Corrosion Inhibitor. International Journal of Molecular Sciences. 2024; 25(18):10150. https://doi.org/10.3390/ijms251810150
3. Salehi, M. Global water shortage and potable water safety; Today's concern and tomorrow's crisis. Environ. Int. 2022, 158, 106936. [Google Scholar] [CrossRef] [PubMed]
4. Thompson M. Operational costs associated with scaling problems. Journal of Oilfield Operations, 2019,Vol. 13(3), pp.150-165

5. Tkachenko, S.; Trukhina, M.; Ryabova, A.; Oshchepkov, M.; Kamagurov, S.; Popov, K. Fluorescent-tagged antiscalants-the new materials for scale inhibition mechanism studies, antiscalant traceability and antiscaling efficacy optimization during CaCO3 and CaSO4·2H2O scale formation. Int. J. Mol. Sci. 2023, 24, 3087. [Google Scholar] [CrossRef]
6. AbbasovV.M., AghamaliyevZ.Z., AghamaliyevaD.B., YolchuyevaU.J., AydinsoyE.A. Investigation of the effectiveness of triethanolamine stearate as a salt precipitation inhibitor in oil and gas production along the Caspian Sea coast. Sustainable Environment: Transition to Green Energy -International Scientific Conference Dedicated to "Year of Solidarity for the Green World",pp.354-356
7. AbbasovV.M.,Shakhmamedova A.G., Mamedova N.A., Mursalov N.I., Rzayeva N.Sh. Synthesis and study of influence of inhibitor properties of salts and complexes of nitrogen derivatives of the mixed esters of ethylene glycol with vinyl oil acid on kinetics. Processes of Petrochemistry and OilRefining, 2015, Vol. 16, No. 3, pp. 222-226
8. Vagif M. Abbasov, Durna B. Aghamalieva, Rufat E. Azizov, Chira Z. Musayeva, Saida F. Ahmadbayova, Sevda G. Rzayeva, Narmin M. Mammadova. Investigation of nitro compounds as precipitation inhibitors. Processes of Petrochemistry and Oil Refining,Vol. 26, No. 2, 2025, pp.321-327 https://doi.org/10.62972/1726-4685.2025.2.321

EFFECT OF CARBON CHAIN LENGTH ON THE CORROSION INHIBITION EFFICIENCY OF SURFACTANTS

Nurana Ziyadzada, Murad Hasanov, Hajar Nabiyeva
Baku Higher Oil School
Baku, Azerbaijan
hasanov.i.murad.std@bhos.edu.az, nurana.ziyadzada.std@bhos.edu.az,
hajar.nabiyeva@bhos.edu.az

Summary - This study focuses on analyzing the effect of the carbon chain length on the properties of surfactants. Surfactants were synthesized from the reaction of diethylenetriamine with saturated fatty acids which contain carbon numbers higher than eleven such as dodecanoic, tetradecanoic and octadecanoic acids. The structure and compositions of the obtained compounds were confirmed using IR spectrophotometry. The main surface activity parameters; (CMC - Critical Micelle Concentration, γ_{CMC} - surface tension corresponding to the CMC point, π_{CMC} - surface pressure, C_{20} - density with a value 20 units smaller than the surface tension value of water, Γmax - maximum adsorption, Amin - minimum surface area per molecule were calculated measuring their surface tension at the air-water border. To investigate nature of adsorbtion process of the obtained compounds, the electrical conductivity values were measured as well. As a part of the study, corrosion inhibition properties of the synthesized compounds were investigated. The dependence of corrosion inhibition properties on different inhibitor amounts and mediums was analyzed using specific metal plates. Corrosion resistance of metal plates was determined using the gravimetric method. Referring to the comparative analysis, the best surfactants were offered as a usage of corrosion inhibitors.

Keywords: Surfactants, surface activity, Corrosion inhibition, Carbon chain length

Introduction

Surfactants are surface-active agents and well known for their amphiphilic structure; they have a hydrophilic head group which is polar and a hydrophobic

tail which is non-polar and consists of long-chain hydrocarbon residue [1] .What makes surfactants different from other reagents is their ability to spontaneously accumulate in interfaces of liquid-gas, liquid-liquid and liquid-solid. By that, they are absorbed onto interfaces and replace the current solvent molecules which have higher energy than surfactant itself. As a result, there will be decrease in free energy of the interface and in turn it will cause surface tension to decrease. [2] One property of surfactants that must be taken into account is the formation of micelle. When interface is fully saturated with surfactant molecules, if further amount of surfactant is added, surfactants will form colloidal-sized clusters in solution called micelle. The exact concentration at which this micellization occurs is called as Critical Micelle Concentration (CMC). CMC point is marked if surface tension levels off and stays constant and if there is a sharp change in conductivity rate. [2, 3]

Besides traditional utilization of surfactants, mostly related to reduction of surface tension, there is a wide range of innovative implementations regarding surface-active molecules. These applications can be categorized according to their types, for example, in transportation of genetic material and with potential in gene therapy and biotechnology, cationic surfactants can be employed. Moreover, a combination of cationic and anionic surfactants can be utilized for polymerization, which in turn can create opportunities for use in drug delivery and encapsulation. [6]

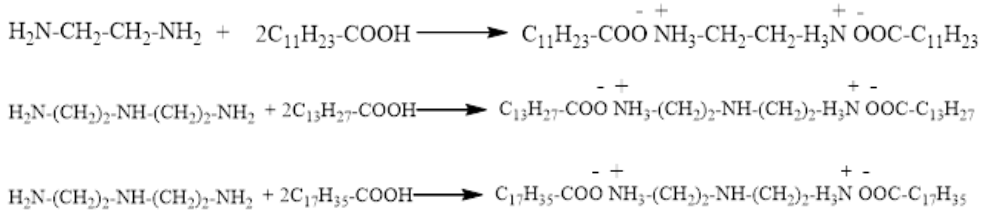
Since surfactants contain both hydrophilic and hydrophobic parts within their structure, they are widely implemented as corrosion inhibitors. This unusual configuration makes them a suitable choice due to their ability to interact with both surrounding environment and metallic surfaces. Corrosion of metallic objects is currently a threat to industries in terms of both economy and safety. To prevent it, surfactants of fatty acid origin are used as they adsorb on metal surfaces and form a hydrophobic layer. Via the help of electron donation happening on hydrophilic head section, surfactants inhibit the corrosion of metals through adsorption [4]. Inhibition efficiency of surfactants mostly depends on their molecular design, length of hydrophobic chains, and adsorption strength. For instance, a superior choice for anticorrosion is Gemini surfactants, which have two hydrophilic heads and two hydrophobic tails that promise better results [5]

The process of corrosion inhibition depends mainly on the number of films that are created on surfaces of metals. Several parameters such as chemical reactions, concentration, temperature, and physical properties of the surfactant can influence the efficiency of these protective layers. As interaction energy between water molecules and metal surface is less than that of surfactant molecules and metal surface, adsorption of inhibitor molecules onto the metal surface takes place and starts the inhibition process [1]. As mentioned before, CMC is a main element that affects the adsorption process and if concentration of surfactant is less than CMC,

molecules combine at the interface and surface tension reduces. However, when concentration reaches and passes CMC, surface tension becomes steady, first layer of surfactant molecules is created, and additional films can be formed. [6]

Experimental part

The reaction was carried out with fatty acids and diethylenetriamine with 2:1 molar ratio of acid to amine in the temperature range of 50-90℃, under closed conditions, continuously stirring with a magnetic stirrer for 9-10 hours. As a result gemini surfactants were obtained.



Surface tension: When measuring interfacial tension, solutions were prepared using water. The deviation from the required temperature was ±0.2°C. The surface tension values of the aqueous solutions of the obtained surfactants were measured using a Du Nouy ring KSV Sigma 702 Pt ring tensiometer (Attension Biolin Scientific, Finland). The surface tension of distilled water used to prepare the solutions at 25°C was 71.5 mN/m. The CMC values of the prepared compounds were determined from the curves of interfacial tension versus concentration. This quantity was determined from the area of sharp inflection in this dependence curve. Efficiency (pC_{20}) is determined by the concentration (mol/l) of surfactant at which the interfacial tension is reduced to 20 mN/m. Surface pressure is determined by the difference between the surface tension of pure water and the surface tension at the boundary of the solution.

Corrosion inhibition. Prior to each experiment, the metal samples were abraded with successive grades of silicon carbide papers (400–1200 grit), rinsed with distilled water, degreased with ethanol, washed with acetone, and dried at room temperature. The aggressive medium was prepared using (e.g., 1.0 M HCl) diluted with distilled water. The surfactant (surface-active agent) was added to the acidic solution at different concentrations.

The corrosion behavior of the metal in the presence and absence of the surfactant was investigated by the gravimetric weight loss method.

Pre-weighed metal samples (initial weight, W_0) were subjected to 100 mL of test solutions for a predetermined time (e.g., 6 or 24 hours) at a constant temperature. The samples were then removed from the solutions, rinsed with distilled water, cleaned to remove corrosion products according

to standard protocols, washed with acetone, dried, and then re-weighed (W_1). Weight loss (ΔW) was computed as:

$$\Delta W = W_O - W_1$$

The corrosion rate (CR) was calculated using the following equation:

$$CR = \frac{\Delta W}{A * t}$$

Here, A-surface area of metal [m^2]

t-time [h]

Results and their discussion.

Solutions of the obtained complexes with different concentrations in water were prepared and their surface tensions at the air-water boundary were measured with a tensiometer, surface tension isotherms were constructed based on the obtained results and are depicted in Figure 1.

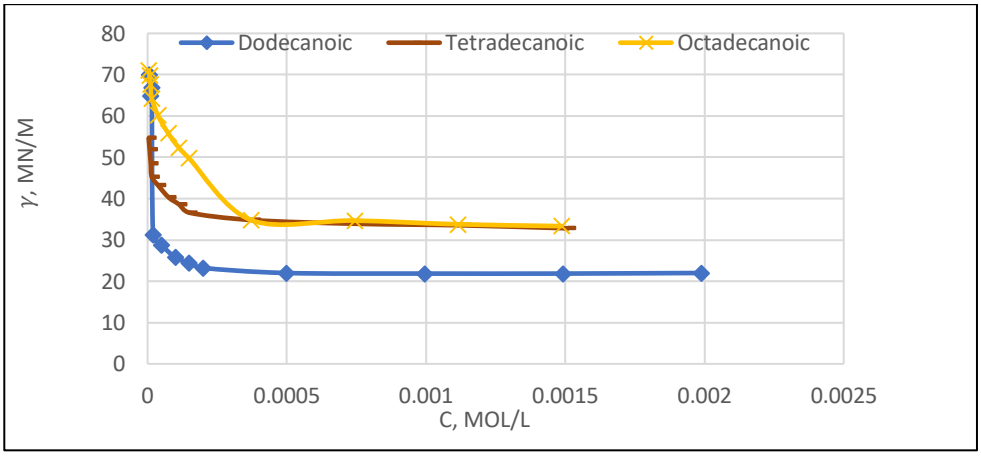


Figure 1. Surface tension isotherms of the surfactants

For all three fatty acids under investigation, there is a sharp decrease in surface tension at diminutive concentrations of fatty acid molecules, indicating rapid adsorption of fatty acid molecules at the interface between air and water. However, once a specific concentration level is reached, the response curves flatten out to indicate the attainment of the CMC. A clear variation in response to the fatty acid molecules with different lengths of hydrocarbon chains is observed: dodecanoic acid decrease the surface tension to the lowest value than the other two compounds. Increasing the hydrocarbon chain length increases hydrophobic interactions, which are effective in increasing the adsorption efficiency at the interface, decreasing the CMC, causing a greater decrease in surface tension. From the Fig 1. CMC value for the surfactants was determined, which is the point shows approximately constant surface tension. After identifying the CMC value,

using the equations given below surface activity parameters were obtained and shown in Table 1.

Table 1. Surface activity parameters of the surfactants

Surfactant	CMC*10^4 (mol/L)	γ_{CMC} (mN/m)	π_{CMC} (mN/m)	C_{20}*10^4 (mol/L)	Γ_{max}*10^{10} (mol/cm^2)	A_{min}*10^2 (nm^2)
Dodecanoic acid						
Dimer 22°C	1.99	23.24	49.14	0.16	1.72	96.30
Tetradecanoic acid						
Dimer 22°C	1.51	36.58	34.98	0.08	0.67	248
Octadecanoic acid						
Dimer 23°C	3.72	34.8	36.90	3.07	1.07	248.23

Looking at Table 1, it is clear that, in the complexes obtained with the presence of other acids, increase in the number of carbon atoms was resulted with an almost increase in the value of the surface tension. The fact that the surface tension in the compound with octadecanoic acid (34.8 mN/m) is smaller than that in the compound with tetradecanoic acid (36.58 mN/m), which slightly disturbs this increase. However, looking at the CMC values, it is possible to see that the regularity is uniform. The CMC value increases mainly with the extension of the carbon chain, as well as the surface tension value.

All of the synthesized compounds of DETA and fatty acids exhibited significant reduction in the rate of mild steel corrosion compared to the blank solution. Inhibition efficiency was also enhanced by increasing the concentration of the inhibitor, showing that the surface coverage was enhanced by increasing the number of inhibitor molecules on the metal surface.

The order of efficiency of the inhibitors was determined to be:

Octadecanoic-DETA > Tetradecanoic-DETA > Dodecanoic-DETA

This is based on the chain length of the fatty acids used to synthesize the inhibitors. The longer chain of octadecanoic acid enhances adsorption on the metal surface, leading to the formation of a hydrophobic layer that minimizes the interaction of the corrosive medium and the substrate.

The efficiency of corrosion inhibition increases as the length of the alkyl chain increases. This can be explained with enhanced hydrophobicity, increase in surface coverage, stabilized adsorbed film and more strong repulsion of water and aggressive ions which are all interrelated a number of interrelated factors. However, if the alkyl chain is too long, solubility in the aqueous acidic environment can become poor. Hence, there is a need to find an optimum balance between hydrophilicity and hydrophobicity.

Offers

The surfactant-based corrosion inhibitors investigated in this study, dodecanoic acid (C_{12}), tetradecanoic acid (C_{14}), and octadecanoic acid (C_{18}), have demonstrated good efficiency in hydrochloric acid solutions. This suggests a promising potential for their use in industrial environments. The effectiveness of surfactant-based corrosion inhibitors increases as the carbon chain length increases. This means that octadecanoic acid-based corrosion inhibitors could be recommended for use in harsh hydrochloric acid environments, whereas shorter-chain surfactant-based corrosion inhibitors could be recommended when solubility is a concern.

References

[5] D. Asefi, N. M. Mahmoodi and M. Arami, "Effect of nonionic co-surfactants on corrosion inhibition effect of cationic gemini surfactant," *Colloids and Surfaces: A Physicochemical and Engineering Aspects*, vol. 355, no. 1–3, pp. 183–186, 20 February 2010.

[6] Y.-Y. Luk and N. Abbott, "Applications of functional surfactants," *Current Opinion in Colloid & Interface Science*, vol. 7, no. 5–6, pp. 267–275, November 2002.

[1] M. A. Malik, M. A. Hashim, F. Nabi, S. A. Al-Thabaiti and Z. Khan, "Anti-corrosion Ability of Surfactants: A Review," *International Journal of Electrochemical Science*, vol. 6, pp. 1927–1948, 29 March 2011.

[3] Y. Nakama, "Surfactants," *Cosmetic Science and Technology: Theoretical Principles and Applications*, pp. 231–244, 10 March 2017.

[2] M. J. Rosen, *Surfactants and Interfacial Phenomena*, John Wiley & Sons, Inc., 2004.

[4] Y. Xiong and M. Cao, "Application of surfactants in corrosion inhibition of metals," *Current Opinion in Colloid & Interface Science*, vol. 73, October 2024.

ELECTROCHEMICAL INVESTIGATION OF BENZYLAMIDE OF NATURAL PETROLEUM ACIDS AS A CORROSION INHIBITOR FOR CARBON STEEL IN CO_2-SATURATED NaCl SOLUTION

N. K. Dadashova[1], V. M. Abbasov[1], D. B. Aghamaliyeva[1, 2], N. I. Mursalov[1], F.J. Kurbanova[1]

[1]Academician Y. H. Mammadaliyev Institute of Petrochemical Processes of the Ministry of Science and Education of the Republic of Azerbaijan, Baku, Azerbaijan

[2]Azerbaijan State Oil and Industry University, Baku, Azerbaijan

e-mail: nasrindadashova@gmail.com

Abstract. CO_2 corrosion is one of the major problems in the oil and gas industry, causing serious damage to carbon steel equipment and leading to significant economic losses. In aggressive environments, this process results in premature failure of metal structures, reduced reliability of technological equipment, and increased operational costs. Therefore, the application of effective corrosion inhibitors to retard the corrosion process and protect metal surfaces is of great importance.

In this study, an amide was synthesized by the reaction of natural petroleum acid with benzylamine. The Inhibitor efficiency of benzylamide of natural petroleum acid on the

corrosion rate in 1% NaCl solution saturated with CO_2 was evaluated using the extrapolation of cathodic and anodic Tafel lines. Electrochemical measurements showed that the inhibition efficiency increased with increasing inhibitor concentration and reached 93% at a concentration of 100 ppm.

Keywords: corrosion, inhibitor, mild steel, amide.

Introduction

Corrosion is a process that occurs as a result of chemical or electrochemical reactions between a material surface and an aggressive environment, leading to irreversible deterioration of the structural and physical properties of metals, particularly in acidic media [1].

Various approaches are used to protect metallic structures from corrosion, including anodic and cathodic protection, corrosion-resistant materials, corrosion monitoring and control techniques, protective coatings, and chemical inhibitors. Among these methods, the use of corrosion inhibitors is considered one of the most widely applied and economically efficient approaches due to its simplicity and effectiveness [2,3].

Corrosion inhibitors generally contain different functional groups, typically polar heads such as fatty acids, amines, imidazolines, amine oxides, and oxygen-, sulfur-, or phosphorus-containing salts, together with a long hydrocarbon chain [4,5]. In recent years, amide-based organic compounds have been widely investigated as corrosion inhibitors and have shown high efficiency in protecting carbon steel against corrosion [6–8].

Considering these aspects, benzylamide of natural petroleum acids (NPBA) was synthesized and investigated as a corrosion inhibitor for carbon steel in CO_2-saturated 1% NaCl solution using electrochemical techniques, particularly Tafel polarization analysis.

Experimental Part

The synthesis was performed in a three-necked flask fitted with a thermometer, a reflux condenser, and a Dean–Stark apparatus. The reaction was carried out using an equimolar ratio (1:1) of the starting reagents at 160–180 °C for 2–2.5 h. The progress of the reaction was monitored by measuring the amount of water separated and collected in the Dean–Stark trap. When the theoretical amount of water was collected, indicating completion of the reaction, heating of the reaction mixture was stopped. The reaction scheme of amide formation is presented below:

$$R - COOH + C_6H_5NH_2 \xrightarrow{160-180℃} R - CONH - C_6H_5 + H_2O$$

R – natural petroleum acid.

Results and Discussion

To evaluate the inhibitory effect of the synthesized benzylamide of natural petroleum acid (NPBA), potentiodynamic polarization measurements were performed. Polarization curves were recorded at 50 ℃ in CO_2-saturated 1% NaCl solution at different inhibitor concentrations.

From the obtained Tafel plots, the main electrochemical parameters such as corrosion potential (E_{corr}), corrosion current density (I_{corr}), anodic Tafel slope (β_a), and cathodic Tafel slope (β_c) were determined. These parameters provide valuable information about the corrosion kinetics and the influence of the inhibitor on the corrosion process.

Based on the corrosion current density values, the inhibition efficiency (IE%) was calculated using the following equation:

$$IE\ \% = \frac{i_0 - i_{inh}}{i_0} \cdot 100$$

where i_0 and i_{inh} represent the corrosion current densities in the absence and presence of the inhibitor, respectively.

The polarization curves obtained in CO_2-saturated 1% NaCl solution in the absence and presence of different concentrations of NPBA are shown in the figure. It can be observed that the addition of NPBA shifts the polarization curves and significantly reduces the corrosion current density compared to the blank solution. This behavior indicates that NPBA adsorbs on the steel surface and forms a protective film that limits the electrochemical reactions responsible for corrosion. The changes observed in both anodic and cathodic branches suggest that NPBA acts as a mixed-type corrosion inhibitor.

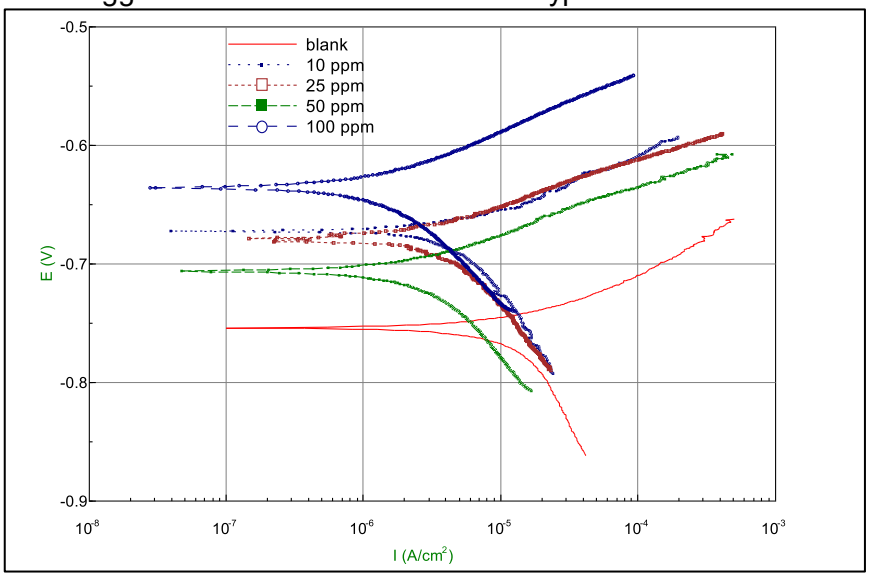


Fig. Polarization curves of C1018 carbon steel electrodes in CO_2-saturated 1% NaCl solution with or without different concentrations of NPBA at 50°C

The electrochemical parameters obtained from Tafel polarization measurements for C1018 carbon steel in CO_2-saturated 1% NaCl solution at different concentrations of NPBA are summarized in Table. The results show that the corrosion current density (I_{corr}) decreases markedly with increasing inhibitor concentration, while the inhibition efficiency increases, reaching

93% at 100 ppm, indicating the effective corrosion protection provided by NPBA.

Table. Polarization parameters of C1018 carbon steel electrodes in CO_2-saturated 1% NaCl solution with or without different concentrations of NPBA at 50°C

Inhibitor	Inhibitor concentration (ppm)	E_{corr} (mV)	I_{corr} (A/cm^2)	β_a (mV)	β_c (mV)	Inhibitor efficiency, IE (%)
Blank	-	-754.39	$2.3576 \cdot 10^{-5}$	65.627	175.92	-
NPBA	10	-672.78	$6.7826 \cdot 10^{-6}$	54.069	228.54	70
	25	-678.86	$3.2077 \cdot 10^{-6}$	44.95	122.09	81
	75	-706.51	$2.6418 \cdot 10^{-6}$	45.593	123.90	88
	100	-636.26	$1.6145 \cdot 10^{-6}$	56.073	120.65	93

Conclusion

Benzylamide of natural petroleum acids (NPBA) was synthesized and its corrosion inhibition performance for C1018 carbon steel in CO_2-saturated 1% NaCl solution was investigated using potentiodynamic polarization measurements. The results showed that the corrosion current density decreased with increasing inhibitor concentration, and the maximum inhibition efficiency reached 93% at 100 ppm. The polarization behavior indicates that NPBA acts as a mixed-type corrosion inhibitor, reducing both anodic and cathodic reactions. The results confirm that NPBA effectively adsorbs on the steel surface and significantly reduces the corrosion rate.

References

1. Hou, B. S., et al. (2021). In-depth insight into the inhibition mechanism of pyrimidine derivatives on the corrosion of carbon steel in CO_2-containing environment based on experiments and theoretical calculations. *Corrosion Science, 181*, 109236. https://doi.org/10.1016/j.corsci.2020.109236
2. Aziz, I. A. A., Abdulkareem, M. H., Annon, I. A., Hanoon, M. M., Al-Kaabi, M. H. H., Shaker, L. M., Alamiery, A. A., Isahak, W. N. R. W., & Takriff, M. S. (2022). Weight loss, thermodynamics, SEM, and electrochemical studies on N-2-methylbenzylidene-4-antipyrineamine as an inhibitor for mild steel corrosion in hydrochloric acid. *Lubricants, 10*(2), 23. https://doi.org/10.3390/lubricants10020023
3. Alamiery, A. A., Wan Isahak, W. N. R., & Takriff, M. S. (2021). Inhibition of mild steel corrosion by 4-benzyl-1-(4-oxo-4-phenylbutanoyl) thiosemicarbazide: Gravimetrical, adsorption and theoretical studies. *Lubricants, 9*(9), 93. https://doi.org/10.3390/lubricants9090093
4. Assad, H., & Kumar, A. (2021). Understanding functional group effect on corrosion inhibition efficiency of selected organic compounds. *Journal of Molecular Liquids, 344*, 117755.
5. Verma, D. K., Dewangan, Y., Dewangan, A. K., & Asatkar, A. (2021). Heteroatom-based compounds as sustainable corrosion inhibitors: An overview. *Journal of Bio- and Tribo-Corrosion, 7*, 1–18.
6. Abbasov, V. M., Dadashova, N. K., Mursalov, N. I., Aghamaliyeva, D. B., Ahmadbayova, S. F., & Mammadov, A. M. (2025). Investigation of the inhibitory properties of natural petroleum acid amides in CO_2-containing environment. *SOCAR Proceedings, 3*, 130–136. http://dx.doi.org/10.5510/OGP20250301106

7. Fouda, A. S., El-Desoky, H. S., Abdel-Galeil, M. M., et al. (2022). Amide compounds as corrosion inhibitors for carbon steel in acidic environment. *Protection of Metals and Physical Chemistry of Surfaces, 58*, 151–167. https://doi.org/10.1134/S2070205122010105
8. Al-Edan, A. K., Wan Isahak, W. N. R., Ramli, Z. A. C., Al-Azzawi, W. K., Kadhum, A. A. H., Jabbar, H. S., & Al-Amiery, A. (2023). Palmitic acid-based amide as a corrosion inhibitor for mild steel in 1 M HCl. *Heliyon, 9*(4), e14657. https://doi.org/10.1016/j.heliyon.2023.e14657

DESIGN AND BENCHTOP VALIDATION STRATEGY OF A FLEXIBLE ELECTROCHEMICAL IMPEDANCE SMART BANDAGE FOR SUSTAINABLE WOUND MONITORING

Shahriyar Eminzada
The University of Edinburgh
Edinburgh, Scotland, The UK
S.Eminzada@sms.ed.ac.uk

Summary

However, such slow-healing wounds need to be continuously evaluated to avoid complications such as infection and longer recovery times. (Graves, 2022) (Guest, 2020) (Antoszewska, 2025) Current methods of monitoring such slow-healing wounds involve regular visual examination and dressing changes, which can impede the healing process and exacerbate the healthcare burden. (Sun, 2022) (Dias dos Reis, 2023) This paper outlines the conceptual design and benchtop validation plan for a flexible electrochemical smart bandage, which uses impedance measurements to monitor the wound microenvironment in real-time. (Derakhshandeh, 2018) (Pal, 2018) (Atte Kekonen, 2019)

The proposed smart bandage will comprise flexible interdigitated electrodes made from carbon-based conductive ink or conductive polymers, which will be used to measure the impedance to detect changes in the moisture content and ionic concentration in the wound fluid, both of which are directly related to the wound healing process. (Camargo, 2021) (Paimard, 2023) (Habboush, 2024) (Tessarolo, 2021) (Korek, 2024) (Guo, 2024) A benchtop validation plan has been outlined for the proposed smart bandage, where the sensitivity, signal stability, and mechanical robustness of the sensor will be evaluated in its bent state, simulating the flexible nature of the proposed smart bandage. (Saleh, 2021) (Thompson, 2004) (NIST/SEMATECH, 2012) A power management plan has also been outlined for the proposed smart bandage, where the power consumption will be minimal due to the use of a single-frequency impedance measurement technique, at least for the initial stages of the smart bandage development. (Lazanas, 2023) (Matsiev, 2015) (Analog Devices, 2024)

The proposed smart bandage will help to monitor the wound healing process continuously, thereby reducing the number of dressing changes and promoting more sustainable wound healing practices. (Rizan, 2021)

Keywords: smart bandage, electrochemical impedance, wearable biosensors.

Introduction

Chronic and slow-healing wounds can cause considerable clinical and financial burden at a global level. A delay in the healing process can increase

the probability of infection, prolong the length of stay in the hospital, and increase the number of clinical interventions required for the patient. The present methods of wound assessment involve visual examination and removal of the dressing at regular intervals, which can cause disruptions in the healing process and increase the level of discomfort for the patient. Furthermore, the present methods may not be effective in the early detection of complications such as infection and abnormal conditions of moisture.

The recent developments in wearable biosensors have led to the creation of smart bandages that can continuously monitor the wound conditions in a non-invasive manner. Electrochemical methods can be used for the creation of smart bandages, as they can be miniaturized and used in a flexible manner, making them an effective means of monitoring wound conditions in a non-invasive manner. Electrochemical methods can detect the changes in the wound microenvironment by measuring the electrical properties, such as the level of moisture and ionic concentration in the wound.

Impedance sensing has also been used for the creation of smart bandages, as it can measure the changes in the wound conditions by measuring the level of conductivity in the wound, as the wound progresses through the healing process, causing changes in the impedance level in the wound. (Pei, 2019) (Instruments, 2024) The proposed smart bandage can be an effective means of monitoring wound conditions, making it easier to track the progress of the wound, and can be an effective means of promoting sustainable healthcare practices by reducing the number of dressing changes and clinical interventions required for the patient.

The objective of the study is to present a conceptual design for the creation of flexible smart bandages that can continuously monitor wound conditions in a non-invasive manner, and to present the benchtop validation methods for the proposed smart bandage, making it easier to track the progress of the wound and promoting sustainable healthcare practices by reducing the number of dressing changes required for the patient.

Experimental part

Device Concept and Materials

Figure 1 depicts the multilayer flexible structure of the proposed smart bandage that can be integrated with a conventional dressing. The structure has four components: (1) a top protective layer, (2) flexible interdigitated electrodes integrated with a flexible substrate, (3) a permeable interface layer that allows interaction with exudate fluids, and (4) a wound site that simulates the environment. The power module has a compact and low-profile structure. The power module is integrated with the external surface of the conventional dressing. The sensing electrodes are connected with flexible interconnections. The flexible electrodes consist of an interdigitated structure that can be integrated with a thin flexible substrate such as PET or other

flexible materials. The electrodes are designed for ionic conductivity sensing. The electrodes are fabricated using conductive ink or conductive polymers such as PEDOT:PSS. (Song, 2024) The permeable interface layer above the wound site allows interaction with exudate fluids while protecting the electronics from exposure to moisture.

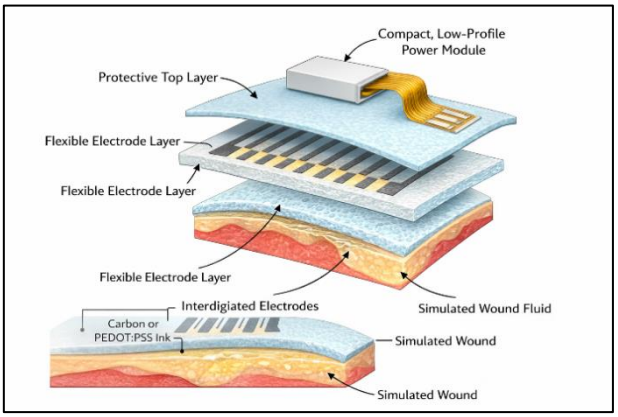


Figure 15. Cross-sectional schematic of the flexible impedance-based smart bandage, showing the protective top layer, compact power module, polymer-based interdigitated electrode layer, and permeable interface in contact with simulated wound fluid.

Sensing Method

The sensing method is based on the principle of electrochemical impedance measurement. Changes in the level of moisture content and ionic concentration in the wound fluid affect the impedance level between the electrodes. It will be designed to measure the impedance level as well as its phase at a particular frequency. For the initial versions of the sensor, a single-frequency method will be used for simplicity of the electronic circuit as well as power consumption.

Benchtop Validation Procedure

Benchtop validation will be carried out using buffer solutions as well as simulated wound fluid. (CEN, 2023) It will be done for the following parameters:

- Sensitivity to changes in ionic concentration as well as moisture content
- Stability of the output
- Repeatability of the output
- Mechanical robustness of the sensor

The mechanical robustness of the sensor will be checked by applying repeated bending actions to the flexible substrate, simulating the movement of the patient. This will be done to check if deformation of the sensor affects its reliability.

Data Analysis

The output will be recorded as well as analyzed using standard data processing techniques like MATLAB, Python, or Excel. It will be done using an equivalent circuit approach to analyze the output. It will be done to analyze the resistive as well as capacitive components of the output.

Power Integration

The power component will be designed to be thin as well as lightweight so that it will be wearable. (Clement, 2022) (Wu, 2023) It is proposed to use flexible solid-state as well as thin-film batteries for power. These are considered to be the most suitable for the project.

Results and Their Discussion

Expected Electrical Response

The expected electrical response of the proposed smart bandage using the impedance technique is a change in the impedance level and phase in accordance with changes in the simulated wound fluid composition in terms of moisture content and ion concentration. It is expected that an increase in ion concentration will improve the conductivity of the medium and thereby decrease the impedance level. (Sapotta, 2023)

Sensitivity and Repeatability

The proposed smart wound dressing is expected to be sensitive in its predictable electrical response in accordance with changes in ion concentration in the simulated wound fluid. Repeatability of the proposed smart wound dressing is expected in its consistent electrical responses in accordance with repeated experiments carried out in a similar environment. Signal drift in the proposed smart wound dressing over time is an essential factor in assessing the expected electrical response.

Mechanical Robustness

Considering the wearable nature of the device, its mechanical flexibility is a significant characteristic. Bending tests are expected to show the least variation in impedance response. If considerable variation in the response is observed upon bending the device, the mechanical instability of the electrodes or poor adhesion of the substrate could be a concern. Showing the robustness of the device through repeated cycles of bending would further confirm the possibility of integrating the device into a wound dressing.

Technical Challenges

The following are the limitations which could possibly influence the device's working. Biofouling and protein deposition from real wound fluid may alter the electrode characteristics. Though the initial experiment is conducted with simulated fluids, real-time environments may pose further challenges. Therefore, the material and surface modifications would play a crucial role in enhancing the robustness of the device. Another challenge is balancing the accuracy of the data with low power requirements. Though the simple impedance measurements would minimize power requirements, this could

limit the diagnostic information obtained from the data. Therefore, the optimization of the measurement frequency is a challenge.

Sustainability Perspective

The sustainability aspect of the device is also a positive aspect of the experiment. Continuous monitoring of the wound without the need for repeated removal of the dressing would minimize the waste generated by the dressings used in the traditional approach. If the impedance response is a true representation of the wound state, the dressing could be replaced only when required. This would further optimize the use of resources in the treatment of the wound. Thus, the success of the experiment would confirm the possibility of a flexible electrochemical impedance-based smart bandage.

Offers

In consideration of the proposed design concept and the performance characteristics of the flexible electrochemical smart bandage, various development trajectories have been identified. Firstly, optimization of the electrodes will be a requirement for enhancing the performance of the flexible smart bandage. This will involve an in-depth analysis of the materials used in the ink composition, particularly those made of carbon. It will be crucial in ensuring that a stable state of operation is achieved through the use of conductive polymers. The proposed design concept of the power module in a low-profile form factor will be a crucial consideration in the advancement of the flexible smart bandage. Secondly, optimization of low-power impedance acquisition will be a requirement for enhancing the performance of the flexible smart bandage. The development of an innovative packaging solution will be crucial in ensuring that the moisture level remains sufficiently controlled in order to avoid interference with the electronic components. This factor will be crucial in enhancing the performance of the proposed design concept. Subsequently, the development of a prototype that can be able to generate impedance in the presence of wound fluids and deformation will be a fundamental requirement in the development of the proposed design concept. This will be a crucial area that requires substantial advancement in the near future. Finally, the proposed design concept of the flexible smart bandage will require the development of wireless communication as part of its development trajectory. This will be contingent upon validation of the proposed concept. The proposed design concept of the flexible smart bandage will be crucial in the advancement of a sustainable healthcare system.

References

1. Analog Devices, 2024. *AD5933: 1 MSPS, 12-Bit Impedance Converter, Network Analyzer,* Wilmington, MA: Analog Devices.
2. Antoszewska, M. P. K. S. P. K. A. V. J. &. B.-R. W., 2025. Bioimpedance Measurement for Monitoring Chronic Wounds: A Systematic Review. *International Wound Journal,* 21(8).

3. Atte Kekonen, M. B. ,. M. J. N. K. J. J. B. a. J. V., 2019. Bioimpedance Sensor Array for Long-Term Monitoring of Wound Healing from Beneath the Primary Dressings and Controlled Formation of H2O2 Using Low-Intensity Direct Current. *Sensors,* 19(11).
4. Camargo, J. R. O. L. O. A. D. A. G. d. O. P. R. K. C. R. D. P. d. S. A. L. T. R. M. M. R. A. A. B. J. A. &. J. B. C., 2021. Development of conductive inks for electrochemical sensors and biosensors. *Microchemical Journal,* Volume 164.
5. CEN, 2023. *EN 13726: Non-active medical devices — Test methods for primary wound dressings,* Brussels, Belgium: CEN.
6. Clement, B. L. M. K. E. S. L. T. H. Y. L. V. G. C. &. W. L., 2022. Recent Advances in Printed Thin-Film Batteries. *Engineering,* Volume 13, pp. 238-261.
7. Derakhshandeh, H. S. K. S. A. F. G. I. O. &. T. A., 2018. Smart Bandages: The Future of Wound Care. *Trends in Biotechnology,* 36(12), p. 1259–1274.
8. Dias dos Reis, J. S.-C. P. M. J. S. C. J. R. A. S. P. &. S. J. L., 2023. Impact of Wound Dressing Changes on Nursing Workload in an Intensive Care Unit. *International Journal of Environmental Research and Public Health,* 20(7).
9. Graves, N. P. C. J. &. H. K., 2022. A narrative review of the epidemiology and economics of chronic wounds. *British Journal of Dermatology,* 1 August, 187(2), pp. 141-148.
10. Guest, J. F. F. G. W. &. V. P., 2020. Cohort study evaluating the burden of wounds to the UK's National Health Service in 2017/2018: update from 2012/2013. *BMJ Open,* Volume 10.
11. Guo, J. C. Y. W. Q. Y. Z. Y. M. C. Y. H. &. C. L. S., 2024. Implications of pH and Ionic Environment in Chronic Diabetic Wounds: An Overlooked Perspective. *Clinical, Cosmetic and Investigational Dermatology,* Volume 17, p. 2669–2686.
12. Habboush, S. R. S. R. N. &. R. A., 2024. The Role of Interdigitated Electrodes in Printed and Flexible Electronics. *Sensors,* 24(9).
13. Instruments, G., 2024. *Basics of Electrochemical Impedance Spectroscopy,* Warminster, PA: Gamry Instruments.
14. Korek, E. M. T. R. H. D. &. B. R., 2024. Electrochemical Impedance Spectroscopy for Ion Sensors with Interdigitated Electrodes: Capacitance Calculations, Equivalent Circuit Models and Design Optimizations. *Biosensors,* 14(5).
15. Lazanas, A. C. &. P. M. I., 2023. Electrochemical Impedance Spectroscopy—A Tutorial. *ACS Measurement Science Au,* 3(3), p. 162–193.
16. Matsiev, L., 2015. Improving Performance and Versatility of Systems Based on Single-Frequency DFT Detectors Such as AD5933. *Electronics,* 4(1), pp. 1-21.
17. NIST/SEMATECH, 2012. *e-Handbook of Statistical Methods: Drift,* Gaithersburg, MD: National Institute of Standards and Technology.
18. Paimard, G. G. E. &. B. M., 2023. Screen-Printed Electrodes: Fabrication, Modification, and Biosensing Applications. *Chemosensors,* 11(2).
19. Pal, A. G. D. C. H. E. C. B. K. S. &. M. R. V., 2018. Early detection and monitoring of chronic wounds using low-cost, omniphobic paper-based smart bandages. *Biosensors and Bioelectronics,* Volume 117, p. 696–705.
20. Pei, X. J. H. D. S. L. D. M. L. W. X. C. W. &. W. H., 2019. Flexible wireless skin impedance sensing system for wound healing assessment. *Vacuum,* October.Volume 168.
21. Rizan, C. B. M. F. R. M. &. L. R., 2021. The carbon footprint of waste streams in a UK hospital. *Journal of Cleaner Production,* Volume 286.
22. Saleh, R. B. M. E. W. &. Z. A., 2021. Bending Setups for Reliability Investigation of Flexible Electronics. *Micromachines,* 12(1).
23. Sapotta, B. S. M. &. F. M., 2023. Practical Insights into the Impedance Response of Interdigitated Electrodes: Extraction of Relative Static Permittivity and Electrolytic Conductivity. *Electroanalysis.*
24. Song, Z. H. R. Y. K. L. R. &. L. X., 2024. Antifouling strategies for electrochemical sensing in complex biological media. *Microchimica Acta,* Volume 191.

25. Sun, X. Z. Y. M. C. Y. Q. W. X. W. H. &. W. P., 2022. A Review of Recent Advances in Flexible Wearable Sensors for Wound Detection Based on Optical and Electrical Sensing. *Biosensors,* 12(1), p. 10.
26. Tessarolo, M. P. L. G. I. A. D. M. F. T. D. &. F. B., 2021. Wireless Textile Moisture Sensor for Wound Care. *Frontiers in Physics,* Volume 9.
27. Thompson, M. E. S. L. R. &. W. R., 2004. Harmonized guidelines for single-laboratory validation of methods of analysis (IUPAC Technical Report). *Pure and Applied Chemistry,* 74(5), pp. 835-855.
28. Wu, B. C. C. D. D. L. E. R. A. &. N. P. H. L., 2023. All-Solid-State Thin Film Li-Ion Batteries: New Challenges, New Materials, and New Designs. *Batteries,* 9(3).

IMMOBILIZATION OF LACCASE IN CALCIUM ALGINATE BEADS FOR ENHANCED BIODEGRADATION OF AZO DYES IN AQUEOUS SYSTEMS

Shams Rzayeva, Nurana Askarova, Shafa Rahmanova, Aysel Mammadova
Baku Higher Oil School
Baku, Azerbaijan
shams.rzayeva.std@bhos.edu.az
nurana.askarova.std@bhos.edu.az
shefa.rehmanova.std@bhos.edu.az

Keywords: laccase immobilization, alginate hydrogels, azo dye degradation, wastewater treatment, enzymatic bioremediation

SUMMARY - This study focuses on immobilization of laccase enzymes in alginate polymer beads in order that azo dyes can be degraded and removed from water. Trametes versicolor enzyme is immobilized via ionic gelation with high efficiency, leading to effective entrapment into calcium alginate beads. Despite the fact that a slight reduction is recorded due to mass transfer limitations, immobilized system achieved 80% dye removal under slightly acidic conditions. Reusability and stability are also measured over several cycles, which is higher in comparison with free enzymes. Overall, alginate-immobilized laccase appears to be not only a sustainable and advanced strategy but also cost effective and simple in design.

INTRODUCTION

Azo dyes are synthetic compounds widely used in various industries, including textiles, leather, food, and pharmaceuticals. These compounds can persist in the environment for long periods and are resistant to treatment methods, due to their chemical structure – one or more azo bonds (–N=N–). Releasing the azo dyes or treating them inadequately results in severe environmental issues like photo-inhibition, reduced light penetration, or toxicity of the aquatic biosystem (Miyawaki, Ayari; Shinji Sakai, 2025). Additionally, azo dyes cause health threats, including allergies, carcinogenicity, and mutagenicity. Adsorption, oxidation processes, reductive cleavage, and coagulation are traditional methods to remove azo dyes; however, they have limitations such as high operational costs, incomplete

treatment of the dyes, and the generation of byproduct pollutants. For example, during the reductive cleavage of azo dyes, aromatic amine byproducts are produced, which are known carcinogens and are more toxic than the dye itself (Saptashwa Datta; Veena . R; Melvin Samuel; Selvarajan Ethiraj, 2021).

Transition from traditional methods to enzymatic degradation is a sustainable and eco-friendly choice. Laccases are enzymes capable of treating complex organic compounds. These enzymes are produced by various organisms, including fungi and bacteria, and can catalyze a wide range of compounds, including azo dyes (Sridharan, Rajalakshmi; P. Senthil Kumar; Veenagayathri Krishnaswamy, 2021). Due to the features of the process like wide substrate specificity, mild reaction conditions, absence of hazardous byproducts, and high activity, it is accepted as a green process. While bacterial laccases are used widely in commercial applications due to their resistance to inhibitors and ability to operate under alkaline pH, fungal laccases are utilized particularly in resistant dye degradations (Aslam, Sadia; Awais Ali; M. Asgher; Nabila Farah, 2021).

Despite their potential, laccases are not used widely in degradation due to their low reusability, difficulty of separation, and recovery from the reaction mixture. Enzyme immobilization is a critical strategy to overcome these challenges. Immobilization limits enzymes to carrier material, and offers advantages including improved resistance, increased reusability, and simplified separation process. Additionally, it reduces operation costs by extending the enzyme lifecycle and recovery (Zhang, Hong; Lei Wang; Xin Zhang; Bo Wang; Xu Zeng; Bo Ren, 2024). Another material used in the experiment is an alginate bead, produced from sodium alginate, which is highly favored because of its biocompatibility, biodegradability, low cost, and non-toxicity. Studies have shown that alginate beads can easily encapsulate laccases, so that laccases stay active for much longer and can be reused for multiple cycles (Białowąs, Małgorzata; Beata Kończak; Stanisław Chałupnik; Magdalena Cempa; Joanna Kalka, 2024).

This research involves developing, evaluating, and characterizing laccase immobilized in alginate beads for effective degradation of Methyl Blue (MB) and Congo Red (CR) azo dyes. These compounds are selected for their opposite characteristics, proving that laccase-loaded beads can treat diverse industrial effluents regardless of the electrical charge of the dye. Since the enzyme is widely used in scientific applications, the results can be easily compared with other immobilization cases.

EXPERIMENTAL PART

Research materials include laccase enzyme from Trametes versicolor, ABTS (2,2'-azino-bis(3-ethylbenzothiazoline-6-sulfonic-acid) as substrate, sodium alginate, calcium chloride ($CaCl_2$), pH controlling acetate buffer and Congo red as the model pollutant.

Laccase is activated and measured by means of ABTS substrate: the reaction mixture contains 1 mM ABTS in 0.1 acetate buffer (pH 5). Additionally, oxidation of the substrate is controlled by measuring the increasing absorbance of the solution at 420 nm in a UV-Vis spectrophotometer. The unit (U) of laccase activity is assumed to be the amount of enzyme required to have 1 μmol ABTS oxidized per minute.

The experiment is initiated with the preparation of sodium alginate solution (2% w/v) by continuously stirring on a magnetic stirrer. Subsequently, the enzyme is gradually added to the alginate solution to have evenly distributed system. Alongside, 0.2 M $CaCl_2$ solution is prepared, to which the mixture of alginate and enzyme is extruded dropwise with a syringe. Formation of spherical beads owing to crosslinking is observed, and beads are hardened for 2 h at 4-6°C. As soon as they are washed with buffer solution, laccase is immobilized by entrapment method inside the calcium alginate beads (2-3 mm diameter) through ionic gelation.

Furthermore, testing of azo dye degradation is carried out in 100 ml flasks, which is filled with 50 mL of dye solution (50mg/L) at pH 5 and temperature 30°C in slow mixing regime. In order to initiate the reaction, immobilized laccase is added. At specific time periods, samples are analyzed in UV-Vis spectrophotometer at the corresponding absorption value of the dye.

$$Removal\ (\%) = \frac{C_0 - C_t}{C_0} \cdot 100$$

RESULTS AND DISCUSSION

The efficiency of immobilization process is measured around 75-85%, which demonstrates ionic gelation methods effectiveness in hydrogel matrix. By crosslinking alginate chains with Ca^{2+} ions, semi permeable three-dimensional network is formed that allows substrate diffusion. In contrast, this figure reduces to 65-75% compared to free laccase, which can be associated with mass transfer limitations due to additional layer of hydrogel matrix. This resistance contributes to lowered reaction rates that are recorded in entrapment immobilization process.

Test results illustrate 80% of Congo Red removal in optimal conditions, and the process works with oxidative catalytic mechanisms. In azo dyes, -N=N- bonds are the leading factor for intense colors; therefore, laccase catalyzes aromatic structures linked to this bond, creates a conjugated system and decolorization takes place. Since π bonds are broken down, this process is called degradation rather than adsorption. Moreover, stability and reusability are also measured with 4-5 cycles, and major issues are attributed to minor enzyme leakage from beads, structural deformations during agitation and partial enzyme inactivation. In order to improve applicability thermal stability, tolerance and resistance to denaturation should be considered, because it is a simple, cost-effective and sustainable immobilization method for treating contaminated wastewater.

OFFERS

Based on the process evaluation and kinetic analysis of laccase immobilized in alginate beads, some recommendations can be given for using it to degrade azo dyes in textile wastewater:

- Enzyme activation rate changes via temperature. Operating the system at temperature range of 30℃ -35℃ rapidly rises reaction rate and decolorization efficiency due to high enzyme activity at these temperatures.
- The characteristics of laccase show that proper control of residence time and flowrate of feed to reactor is important factor. If enough contact time between biocatalyst and substrate is provided, it will result in highly efficient degradation process.
- Alginate structure can be weakened by exposure to high dye concentration which causes enzyme leakage and low catalytic activity. Divalent cations, including calcium ions, can be used to eliminate this issue, as they keep stable structure of beads and increase operational lifespan of enzymes.
- The dense alginate bead can lead to diffusion limitations where dyes cannot reach enzyme trapped inside the bead. To address this problem, it is recommended to reduce diameter of bead and increase its porosity, resulting in shorten diffusion path of azo dyes and enhance degradation efficiency.
- The degradation behavior of dyes greatly vary with dye-specific parameters, such as their internal structures.Thus, the endurance of system can be proved by using a different types of azo dyes in the system.
- Heterogenous mixture of surfactants, salts and other chemicals that affects bead stability and laccase activity is found in actual textile wastewater. Therefore, utilizing real textile effluents will ensure to appropriately evaluate system performance under real industrial conditions.

REFERENCES

1. Aslam, S., Awais Ali, M. Asgher, & Nabila Farah. (2021). Fabrication and Catalytic Characterization of Laccase-Loaded Calcium-Alginate Beads for Enhanced Degradation of Dye-Contaminated Aqueous Solutions (by Sadia Aslam - 2021). *Catalysis Letters, 152*(5), 201-215.
2. Białowąs, M., Beata Kończak, Stanisław Chałupnik, Magdalena Cempa, & Joanna Kalka. (2024). Alginate-laccase beads in the decolourization. *Archives of Environmental Protection, 50*(1), 45-55.
3. Miyawaki, A., & Shinji Sakai. (2025). Degradation of azo dyes using laccase immobilized on mechanically ground silk fibroin nanofibers. *Bioresource Technology, 438*, 25-39.
4. Saptashwa Datta, Veena . R, Melvin Samuel, & Selvarajan Ethiraj. (2021). Immobilization of laccases and applications for the detection and remediation of pollutants: a review. *Environmental Chemistry Letters, 19*(14), 521-538.

5. Sridharan, R., P. Senthil Kumar, Veenagayathri Krishnaswamy, , T. Akshaya Vidhya, Vajiravelu Sivamurugan, . . . Dai-Viet N. Vo. (2021). Analysis and effective separation of toxic pollutants from water resources using MBBR: Pathway prediction using alkaliphilic P. mendocina. *Science of The Total Environment, 797*, 120-142.
6. Zhang, H., Lei Wang, Xin Zhang, Bo Wang, Xu Zeng, & Bo Ren. (2024). Functionalized Chitosan and Alginate Composite Hydrogel-Immobilized Laccase with Sustainable Biocatalysts for the Effective Removal of Organic Pollutant Bisphenol A. *Catalysts, 14*(5), 304-317.

STUDY OF THE KINETICS OF CORROSION PROCESSES IN PRODUCED WATER CONTAINING CO_2 AND H_2S AND APPLICATION OF NEW INHIBITORS

Heydarova Almaz
Baku Higher Oil School
Baku, Azerbaijan
almaz.e.heydarova.std@bhos.edu.az

Abstract - Carbon steel corrosion in CO2 and H2S-containing formation fluids is one of the main reasons why oil and gas production equipment deteriorates. Due to the formation of unstable FeS/$FeCO_3$ films, mixed CO_2-H_2S environments exhibit high corrosive activity and a propensity for localized forms of destruction [Yu, 2015; Yang, 2022]. The corrosion mechanism and efficacy of three classes of inhibitors imidazolines, fatty acid-based surfactants, and ammonium nitronates are summarized in this paper [Abbasov, 2012; Abbasov, 2010]. It has been demonstrated that the anionic composition of formation water (Cl^-, HCO_3^-, and SO_4^{2-}), hydrodynamics, and surface condition all affect inhibition efficiency in addition to the reagent type [Ladygin, 2020; Zhang, 2017]. It is proven that a thorough laboratory evaluation (gravimetry + PDP + EIS) is necessary for the proper inhibitor selection.

Keywords: corrosion, formation water, CO_2, H_2S, inhibitors, imidazolines, surfactants, nitronates.

Main section

Increasing the water cut during well production is observed to cause more equipment to encounter formation water, which exacerbates electrochemical corrosion. While H2S leads to the formation of iron sulfide corrosion products and raises the risk of hydrogen attack and localized damage, CO2 forms carbonic acid, lowers pH, and speeds up the dissolution of anodic iron in the aqueous phase [Yu, 2015]. The competing formation of $FeCO_3$ and FeS, as well as their stability in these conditions, determine the mechanism in mixed CO_2-H_2S environments [Yang, 2022]. Active dissolution and the development of a thin porous mackinawite (FeS) film are predominant in the early stages; as this film thickens, the corrosion rate may decrease because of the increased resistance to charge transfer [Yu, 2015]. Nevertheless, even at moderate average failure rates, FeS films frequently exhibit poor adhesion and are prone to cracking and delamination, which starts localized corrosion [Yang, 2022]. Partial pressure of CO2 and

hydrodynamics also play a major role. Although rising PCO_2 increases the environment's acidity and overall corrosion activity, increasing flow velocity increases shear stress and may cause protective films to be destroyed [Wen, 2025]. As a result, operating conditions are not always accurately reflected in laboratory data collected under static conditions. Imidazolines, which are categorized as adsorption inhibitors, hold a prominent position among the inhibitors utilized. The development of an organic layer on the steel surface is linked to their efficacy. Because of improved adsorption and the development of a more hydrophobic protective layer, modified imidazolines show increased stability in CO_2/H_2S environments [Lu, 2019]. Imidazolines are highly effective in acidic and hydrogen sulfide-containing environments, based on the experimental data [Abbasov, 2012]. Sulfonated fatty acid-based surfactant complexes work well in formation waters that are saturated with CO2. When concentration approaches the critical micelle concentration, they show a saturation effect, meaning that additional dosage increases have little effect on the protective effect [Abbasov, 2012]. The length of the hydrocarbon radical determines the inhibitory activity of nitrogen-containing salts, such as ammonium nitronates. Longer-chain structures have been shown to provide a higher protective effect in CO_2-saturated NaCl solutions, while some compounds may exhibit low or unstable effectiveness [Abbasov, 2010]. An important factor is the creation of water's anionic makeup. While bicarbonates and sulfates can change the conditions under which they occur, chloride ions increase localized corrosion and decrease the durability of protective layers. The $(HCO_3^- + SO_4^{2-})/Cl^-$ ratio plays a major role in determining the efficacy of inhibitors [Ladygin, 2020]. Additionally, because adsorption takes place on the scale surface rather than pure metal, the presence of pre-formed corrosion products (pre-corrosion) decreases the efficiency of inhibitors [Zhang, 2017]. In order to properly evaluate the inhibitor for CO2/H2S in formation waters, it is necessary to: (i) model the actual ionic composition; (ii) account for temperature and hydrodynamics; (iii) test on a pre-corroded surface; and (iv) analyze the protection mechanism using a combination of gravimetric and electrochemical methods (PDP, EIS).

Reference

1. Lu Y. W. A novel imidazoline derivative used as an effective corrosion inhibitor for carbon steel in a CO_2/H_2S environment. *International Journal of Electrochemical Science*. 2019. 14: 8579–8594.
2. Wen N. M. Study on corrosion behaviour and corrosion inhibitor of X65 subsea pipelines. *International Journal of Electrochemical Science*. 2025. 20.
3. Yang L. Z. Study on corrosion behavior of P110S steel in CO_2–H_2S-saturated solution. *International Journal of Electrochemical Science*. 2022. 17.
4. Yu C. W. Corrosion behavior and kinetics of early stages of low alloy steel under H_2S/CO_2 environment. *International Journal of Electrochemical Science*. 2015: 6820–6832.
5. Zhang C. Effects of pre-corrosion on the corrosion inhibition performance of three inhibitors on Q235 steel in CO_2/H_2S saturated brine solution. *International Journal of Electrochemical Science*. 2017. 12: 9161–9179.

6. Аббасов В.М. и др. Эффективность действия имидазолинов в условиях кислотной коррозии стали. *Практика противокоррозионной защиты*. 2012. №2(64): 38–41.
7. Аббасов В.М. и др. ПАВ на основе жирных кислот как ингибиторы коррозии углеродистой стали в пластовых водах, содержащих CO_2. *Процессы нефтехимии и нефтепереработки*. 2012. Т.13. №3(51): 219–232.
8. Аббасов В.М. и др. Действие нитронатов аммония на кинетику коррозии стали в 1%-ом растворе NaCl, насыщенном CO_2. *Elmi xəbərlər Sumqayıt Dövlət Universiteti*. 2010. Cild 10. №2: 59–64.
9. Ладыгин А.Н. Влияние анионного состава и содержания кислых газов в пластовых водах на эффективность ингибиторов коррозии. *Вестник ПНИПУ. Геология. Нефтегазовое и горное дело*. 2020. Т.20. №2: 292–300. DOI: 10.15593/2224-9923/2020.2.9.

BIOINSPIRED PLASMONIC AEROGEL FOR EFFICIENT AND SALT-RESISTANT SOLAR DESALINATION OF SALINE OR CONTAMINATED WATER

Authors: Laman Aliyeva, Mahira Ganbarova
Supervisor: Aliya Laylabashova
Baku Higher Oil School
Baku, Azerbaijan
Email addresses: leman.eliyeva.std.@bhos.edu.az ,
mahira.ganbarova.std@bhos.edu.az.

Abstract - The thesis provides comprehensive information regarding the synthesis and surface modification of a bioinspired GO/ANFs/PVA aerogel, which is inspired by the Namib Desert beetle, using polypyrrole (PPy) and silver (Ag) nanoparticles. The aerogel that had undergone freeze-drying was in-situ polymerized and reduced with the addition of Ppy and Ag nanoparticles. The morphology, surface wettability, photo-thermal characteristic and solar evaporation performance were evaluated in terms of SEM/TEM, contact angle measurement, UV-Vis-NIR absorption, and sun evaporation tests.

Key words: GO/ANFs/PVA aerogel, hydrophobic-hydrophilic surface, polypyrrole (Ppy), silver nanoparticles (Ag), solar desalination.

Introduction

The availability of fresh water plays a significant role in the life of all living organisms, and it is a crucial factor for the ecosystem stability. With the increasing population, freshwater scarcity becomes an essential global problem due to a growing demand. Although, approximately 71% of earth is covered with water, only 2.5% of all Earth's water is considered as freshwater. [3] As the majority of earth is made up of ocean and seawater, desalination is widely used source to obtain freshwater because of the fact that solar energy is an environmentally friendly and cost-effective alternative. In order to improve evaporation efficiency, different type of materials such as carbon-based photothermal materials, hydrogels and aerogels have been investigated. Nevertheless, the problems like salt accumulation along the surface of evaporator, unsatisfactory water transport, and limitations in the

ability to absorb sunlight.[1][2] Developed aerogel is inspired by desert beetle providing sufficient water transport, and functionalized with silver and polyprrole (PPy) particles so as to increase light absorption.

Experimental part

In this thesis, an aerogel made of composite GO/ANFs/PVA was prepared and subsequently functionalized with polypyrrole (Ppy) and silver (Ag) nanoparticles to improve interfacial evaporation performance by solar energy. To produce a homogenous skeleton of the aerogel graphene oxide (2 mg/mL) was dispersed in deionized water and then 3 wt% aramid nanofiber solution and polyvinyl alcohol (~10 wt%) were added to it and stirred on a continuous basis. To prepare a porous three-dimensional aerogel, the mixture was cast in molds, and then frozen at -20 °C, then at -80 °C and finally, freeze-dried at 48 hours. The aerogel included the polypyrrole through in-situ oxidative polymerization of pyrrole at 0-5 °C during a period of 4-6 h using ammonium persulfate as oxidizing agent in equal molar weight with pyrrole. The PPy-modified aerogel was vacuum dried at room temperature after it had been thoroughly washed with ethanol and deionized water. The aerogel containing the PPy was subsequently incubated in 0.01 M $AgNO_3$ solution to allow the ion adsorption process to occur and then reduced gradually with 0.02 M $NaBH_4$ solution to form silver nanoparticles in-situ. The Ag/PPy composite aerogel was then washed and dried in a vacuum. The portions of the aerogel which were selected were covered and the uncovered surface was exposed to 3- (Amino-propyl) triethoxysilane (APTES) in ethanol after two hours at the room temperature to generate patterned surface wettability. Hydrophilic domains were discovered to be embedded in a hydrophobic structure, after the mask was removed. SEM and TEM were used to determine the morphology and distribution of GO, PPy, and Ag nanoparticles. Surface wettability was studied by measuring the contact angle. Solar evaporator tests were run under one-sun light and UV-Vis-NIR spectroscopy was used to determine light absorption. Salt resistance performance was evaluated by being subjected to continuously running 20 hours in a 15 weight percent solution of NaCl. [1][2]

Results and Discussions

Table 4. Characterization test results

Test	Sample	Result
SEM/TEM	GO/ANFs/PVA + PPy/Ag	3D network with high degree of porosity, coated with uniform PPy, well-dispersed silver particles
Wettability (Contact angle)	Hydrophilic structure	$33 \pm 2°$
	Hydrophobic structure	$118 \pm 3°$
Solar evaporation rate	GO/ANFs/PVA + PPy/Ag	$2.31 \pm 0.05\ {}^{kg}/_{m^2 * h}$

Photothermal Conversion Efficiency	GO/ANFs/PVA + PPy/Ag	$87 \pm 2\%$
Salt Resistance Test	15 wt% sodium chloride	Salt crystallization is not noticed.

The developed GO/ANFs/PVA aerogel with PPy and silver nanoparticles display properties which are tabulated in

Table *4*. The observations of SEM and TEM proved the presence of high porosity of three-dimensional network which was composed of uniform polyprrole coating and distributed silver particles. The design offers sufficient water transport and thermal insulation, which are crucial in the solar-based evaporation projects.

The hydrophobic-hydrophilic surface pattern exhibited a high degree of wettability contrast. The domains with a hydrophilic structure displayed contact angle of $33 \pm 2°$, which allowed water to be delivered to the evaporation interface efficiently and those with hydrophobic structure displayed a contact angel of $118 \pm 3°$, by preventing salt accumulation and providing efficient regulations of salt.

The aerogel at a one-sun illumination velocity attained a solar evaporation rate of 2.31 ± 0.05 $^{kg}/_{m^2 * h}$, and a photothermal conversion efficiency of $87 \pm 2\%$. The combination of PPy and silver nanoparticles to increase light absorption and localized heating is attributed to these high-performance metrics. The ability of the bioinspired wettability against salt deposition under extended conditions was proves through salt-resistance tests performed with the presence of 15 wt% Na Cl solution, with no salt crystallization being observed.

Based on the above results, the bioinspired GO/ANFs/PVA aerogel with embedded Ppy and Ag nanoparticles can be proposed to use in the field of applications that require the ability to control the wetting of patterns in the functional composite materials.

References

1. Ag/polypyrrole co-modified poly(ionic liquid)s hydrogels as efficient solar generators for desalination by Chaohu X., Liang W., Hasi Q., Chen L., Jingxian H., Fang L., Wang C., Sun H., Zhu Z., An Li. Materials Today Energy (2020). https://www.sciencedirect.com/science/article/abs/pii/S2468606920300368
2. Bioinspired composite aerogel with hydrophobic-hydrophilic patterned wettability for high-efficiency, salt-resistant solar desalination by Linfan L., Bopeng L., Hua L., Yumin W., Xiao M., Yuaming S., Guina R., Xiaotao Z. Journal of Environmental Chemical Engineering (2016). https://www.sciencedirect.com/science/article/abs/pii/S2213343726007438
3. US Geological Survey (2019). The distribution of water on, in and above the earth. https://www.usgs.gov/media/images/distribution-water-and-above-earth

SUSTAINABLE NANO-BIOPOLYMER SPRAY FOR PREVENTING FUNGAL DISEASE OF PLANT-BASED FOODS

Revane Abdullayeva, Ayan Guliyeva, Rima Guliyeva
Baku Higher Oil School
Baku, Azerbaijan
revane.abdullayeva.std@bhos.edu.az, ayan.guliyeva.std@bhos.edu.az

Summary - One of the current and widespread problems in agriculture is the widespread spread of fungal diseases, which are widely encountered during the development of plant-based organic foods. Spread of this type of disease results in a decrease in productivity, the cessation or damage of plant root development. Predominant reasons are considered to be deficiencies in storage conditions, the underdevelopment of the resistance barrier against pests, and the intolerance of plants to extreme weather conditions. Conducted research work carried out is the preparation and application of a coating material applied by spraying method with microbial agent-based nano particles that prevents plant diseases. Outcomes of the experiment conducted on cucumber vegetables show that the Bacillus subtilis - nano ZnO-based material has been determined to have a function of stopping spore germination of more than 96.5%. In addition, when applied at the initial stage of the disease, the nanoparticle co-functionalization of the bacteria prevented the spread of fungi. Applying an innovative approach to plant diseases by spraying method contributes to the circular economy chain, combined with sustainable agriculture and food security.

Keywords: bacillus subtilis, podosphaera xanthii, fungal disease, spore germination

Introduction:

The distribution system for fruits and vegetables contains operational deficiencies which create widespread postharvest loss in produce. This postharvest decay transforms potential nutrition into environmental burdens which force communities to deal with both economic shortages and natural capital deterioration. One of the reasons for post-harvest product loss is decay, which damages the quality of the product due to reasons such as underdeveloped infrastructure, limited cold storage facilities, and improper management of storage and transportation regulations. Considering the increasing demand for organic food in proportion to the growing world population, it is the conversion of decomposed organic matter into greenhouse gas emissions (methane gas) after harvest, which indicates both food security and environmental sustainability.

Since the substances used against diseases caused by post-harvest decay, as well as the widely used synthetic chemical fungicides, have objected concerns regarding human health and environmental pollution, alternative approaches have been sought. Studies investigate the possibility of extending the shelf life of fruits and vegetables and controlling diseases caused by decay, while also exploring environmentally friendly and promising methods, ultimately proposing biocontrol agents as a solution. These agents include natural organisms (e.g. bacteria, yeasts and fungi), natural compounds (e.g. plant extracts) and other biobased products (e.g.

biopesticides, biofungicides) that have both the ability to control plant pathogens and competitive exclusion mechanisms.

The susceptibility to microbial pathogens that arise during post-harvest storage and transportation give rise to food spoilage, which is a problem that has now been addressed by leveraging biological alternatives. By applying biologically alternative bioagents, it is possible to neutralize sundry pathogens (Botrytis cinerea (gray mold), Penicillium expansum (blue mold)) that cause economic losses in the fruit and vegetable industry, while maintaining product quality.

Several traditional fungicides have been developed to control the disease, but pathogens have also become increasingly resistant to long-term use of fungicides such as sulfur and copper. The significant harm caused by residues of traditional fungicides to human health and the environment is considered one of their drawbacks, and a strategy has been developed to use biological agents that are more suitable for powdery mildew control.

The aim of our study is to evaluate the effectiveness of controlling powdery mildew disease in cucurbit plants, specifically cucumbers with various fungicide combinations; B.subtilis and nanomolecules (nano-ZnO, nano-TiO_2). This study was conducted on cucumber, a widely grown botanical crop for import and export worldwide. Podosphaera xanthii, one of the pathogens that significantly reduces the yield of this plant, causes a devastating powdery mildew disease in cucumbers that can cause yield losses of up to 40 percent under conditions of low temperature and high humidity.

Various stresses, as well as the application of bioagents and nanoparticles in natural conditions to increase plant growth and yield, were investigated, as a result, Bacillus subtilis (UMAF6639) provided protection against powdery mildew growth by creating systemic resistance (ISR) in gourd seedlings. The antimicrobial properties of compounds such as ZnO, TiO_2, Mg and Si increase their potential to directly act against plant diseases; at the same time, nanoparticles based on nanoscale materials with high surface area can contribute to the effective control of pathogens, ensuring more stable and long-term storage of nutrients.

Experimental part:

Preliminary intention of the experimental part is initially the propagation of Bacillus subtilis, which plays important role with antagonistic function, and then to prepare the coating material/spray obtained by integrating the bacteria with titanium and zinc oxide $TiO_2\ and\ ZnO$) nanoparticles, that prevent the spread of fungi and diseases. At starting step, the bacteria should be prepared for the experiment by freezing and sterilizing the agar plates at low temperatures. Thereafter, the bacteria are applied to the agar plate and separate colonies are formed on its surface. Following the surface application, colonies, which are taken in small quantities with the inoculation

loop, are placed in LB broth and shaken at 35℃ temperature for 8-16 hours with 200-250 rpm rotational speed. After a certain period of agitation, successful completion of process is confirmed by the growth of the plates that the bacteria begin to proliferating. After the bacterial suspension is prepared, it is centrifuged at 4500 rpm for 20 minutes, the suspension mixture, in which the solid part is precipitated, is separated with a glass filter, and an aqueous phase cell-free solution is obtained.

In the second part of the experiment, a 200 mg/l solution of 98.8% pure zinc oxide (ZnO) and 99% pure titanium oxide (TiO_2) nanoparticles is prepared. Subsequently, a mixture of the prepared solutions with bacillus subtilis is arranged in a 1:1 ratio. Conclusively, five different samples are identified to be investigated according to their feasibility.

Table 5- Material composition of coating samples

Framework	Composition
Sample №1	Bacillus subtilis
Sample №2	Nano TiO_2 with 200 mg/l concentration
Sample №3	Nano ZnO with 200 mg/l concentration
Sample №4	Nano TiO_2 + B. subtilis (1:1) ratio
Sample №5	Nano ZnO + B. subtilis (1:1) ratio

Formulated samples are applied in spray form to the leaves of the plant where disease symptoms have begun to be observed, and their functionality is tested, and based on the consequences obtained, the material characterization of the best coating is selected.

For the coating material to be effective, it is advisable to spray the plant at least once a week after the onset of the disease is observed. After close observations, when diminution of fungal growth commences, the interval between spray applications should be increased once in ten days.

Results and their discussion:

Scrutiny proved that all applied treatments significantly reduced the spore germination of Podosphaera xanthii compared to the untreated control. The study identified Bacillus subtilis as the most effective inhibitory combination with a 96% success rate which was surpassed by the B. subtilis plus nano-TiO_2 combination that achieved 96.5% effectiveness. While the combination of nano-ZnO and fungicide showed a high level of effect, relatively low efficacy was observed in the single application of nano-TiO_2. The presence of antifungal effect was investigated by the Spore germination test, which is performed by microscopic evaluation on glass slides.

In all treatments, it was noticed that the disease development indicators (Disease Severity and AUDPC) decreased, the highest reduction was observed in the combination of fungicide and B. subtilis + nano-ZnO. The study demonstrated that the combination treatment maintained its control

effect throughout both the early and advanced disease stages, which revealed the existence of a synergistic mechanism.

The results obtained show that although Bacillus subtilis alone has a high spore inhibition capacity, its combination with nano-materials further enhances this effect. B.subtilis + nano-ZnO and B.subtilis + nano-TiO_2 variants were distinguished by both a strong reduction in spore germination and gradual decrease in disease development indicators (DS and AUDPC), further proving that the direct antifungal effect in combination applications is more stable and durable. The results indicate that the biological agent used in combination with nano-components provides effective control of the pathogen both at the initial development stage and during the subsequent disease progression, and this can be explained by the synergistic interaction mechanism.

Offers:

As reported in this research, by incorporation of nanoparticles that activate the protective barrier of the plant structure and bacteria with painkiller function applied for the purpose of preventing the fungi or other diseases and its development. Nanoparticle and combination with best effectiveness capability have been determined for getting higher fungi removal by spray application. Considering that climate changes such as high temperatures, rain or drought occur outdoors, it is recommended to make possible modifications to the field in large scale to confirm the success of the research results obtained in laboratory conditions. It is also necessary to investigate the application of the spray not only to the leaves but also to other parts of the plant and to ensure the most effective approach of coating.

Compared to chemical preservatives that perform a similar function, spray's biodegradable and ecologically compatible composition stands out in that breaks down easily and does not pose a risk for human and plant life. With the recommended optimization steps, it is expected that bacteria-based sprays will be widely used in agriculture and will develop positively by supporting the principles of the circular economy.

References:

1. [Lawal et al., 2025] Biocontrol and nanotechnology strategies are increasingly applied in postharvest disease management of fruits and vegetables.
2. [Li et al., 2022, 21–36] Metal-based nanoparticles are widely used to control bacterial and fungal crop diseases.
3. [Liu et al., 2025] Biocontrol agents and natural plant products show strong potential against postharvest fungal pathogens.
4. [Wang et al., 2025] Fungal communities in horticultural crops influence plant promotion, pathogenicity, and monitoring strategies.

INVESTIGATION OF THE INFLUENCE OF ALKYLPHENOL-BASED ANTIOXIDANTS ON THE PROPERTIES OF SKN-26-BASED ELASTOMER COMPOSITIONS

Ayshe Gojazade
Azerbaıjan State Oıl And Industry Unıversıty
Baku, Azerbaijan
ayseqocazade@gmail.com

KEYWORDS: SKN-26 rubber, alkylphenol antioxidants, elastomer compositions, thermo-oxidative stability

SUMMARY: The presented research study evaluates the mechanism of action of alkylphenol-based antioxidants on the properties of elastomer compositions formulated based on SKN-26 brand nitrile-butadiene rubber. Although SKN-26 rubber is characterized by high resistance to hydrocarbon environments and aggressive fuels, it is destroyed by the influence of heat and oxygen during operation. The application of special stabilizers is considered one of the most effective methods for increasing the service life and structural stability of such elastomer materials.

Within the framework of the study, the effect of alkylphenol-based antioxidants on the physical and mechanical characteristics of the composition and thermooxidation processes was analyzed theoretically. The results obtained prove that the use of these additives significantly slows down the aging rate of the material and effectively preserves its mechanical strength. At the same time, determining the exact concentration of the antioxidant was identified as a decisive factor in ensuring optimal functional properties of the elastomer.

INTRODUCTION:

Synthetic rubbers are widely used in many modern industries - petrochemical, mechanical engineering and automotive. Among them, SKN-26 nitrile-butadiene rubber stands out for its excellent resistance to fuels and oils and plays an important role in the production of technical rubber products. However, during the operation of elastomer materials, destructive processes occur in their structure under the influence of high temperatures, oxygen and mechanical stresses. This, in turn, leads to a deterioration in their physical and mechanical properties. [1]

To improve the oxidation process of rubbers, various types of antioxidants and stabilizers are added to it. By neutralizing free radicals, alkylphenol-based antioxidants prevent chain oxidation reactions, thereby reducing the aging rate of the material. In this regard, the study of the effect of alkylphenol-based antioxidants on SKN-26-based composites is of great scientific and practical importance. [3]

EXPERIMENTAL PART

The experimental process consists of elastomer compositions prepared on the basis of SKN-26 nitrile-butadiene rubber. The composite material was incorporated into the matrix with plasticizers, fillers and a vulcanization system. Alkylphenol-based antioxidants were used as stabilizers to evaluate the protective effect in the system.[3]The elastomer compounds were

compounded on a laboratory two-roll mill at a temperature range of 40-50°C to ensure uniform filler and stabilizer dispersion. Vulcanization was subsequently performed using a hydraulic press at143-150°C under a pressure of $10-15 MPa. To evaluate the protective efficiency, alkylphenol-based antioxidants were incorporated in concentrations ranging from 1.0 to 3.0 phr. Thermal-oxidative aging tests were executed in an air-circulating oven at 100°C for 72 hours, following which the mechanical properties such as tensile strength and elongation at break were measured according to ISO standards."[1],[2],[3]

The preparation process of the compositions was carried out using a two-roll milling machine to ensure homogeneous distribution. After the mixing process, the samples were vulcanized under certain temperature and pressure conditions. The physical and mechanical properties (tensile strength, relative elongation, hardness) and thermal stability of the resulting samples were evaluated through comparative analysis. [1],[3]

RESULTS AND DISCUSSION

Both theoretical and experimental analysis show that the incorporation of alkylphenol-based antioxidants into the composite significantly reduces the rate of the oxidation process. These substances react with free radicals to prevent chain reactions, thereby preventing the breakdown of polymer chains. As a result, the mechanical strength and elasticity of the material are maintained for a longer process time. [2]

Also, the optimal concentration of the antioxidant remains an important factor. Excessive amounts can cause phase incompatibility with the structure of the composition and potentially compromise the integrity of the material. Therefore, choosing the optimal dosage is very important to ensure maximum durability and performance for industrial applications. [3]

OFFERS

To achieve maximum results, the optimal concentration of alkylphenol-based antioxidants in SKN-26-based formulations should be determined experimentally. Systematic studies are required to balance the structural integrity of the elastomer with the protective effects of the antioxidant.

Long-term thermal-oxidative degradation tests should be conducted to more accurately simulate real-world operating environments. In addition, a comparative study involving different types of antioxidants for high-performance industrial applications is considered appropriate to identify the most effective stabilizing systems.

REFERENCES

[1] Ahmedov, R. (2021). *Chemistry of Synthetic Rubbers*. Baku.
[2] Aliyev, T. (2020). *Physical-Mechanical Properties of Elastomer Compositions*. Baku.
[3] Mammadov, A. (2019). *Stabilization of Polymer Materials*. Baku.

ПРОТОЧНЫЙ ЭЛЕКТРОЛИЗЕР « ГИПОНАТ » ДЛЯ ПОЛУЧЕНИЯ ГИПОХЛОРИТА НАТРИЯ

Гулиева Лейла Ильхам
Сумгаитский государственный университет,
Азербайджан, Сумгаит
leyla.quliyeva@sdu.edu.az

Резюме - Проточный электролизёр «Hiponat» — это автоматизированная бытовая установка, предназначенная для получения раствора гипохлорита натрия различной концентрации. Выходной раствор используется в качестве дезинфицирующего и отбеливающего средства в быту и может заменять хлорную воду, хлорную известь, хлорамин и другие аналогичные средства.

Для обеспечения ламинарного потока раствора и поддержания необходимого уровня в электролизной ёмкости в конструкции предусмотрены соответствующие технические решения и вспомогательные элементы, включая датчик уровня, электродвигатель, управляемые клапаны и другие компоненты. Управление потоком осуществляется на основе сигнала фотометрического датчика. Работа установки контролируется микроконтроллером.

Ключевые слова: электролизер «Гипонат», хлорид натрия, проточный электролиз, гипохлорит натрия, двухканальный фотометр, оптическая ванна.

Электролизер «Гипонат» (далее - прибор) - портативный бытовой прибор, предназначенный для производства раствора гипохлорита натрия различной концентрации путем электролиза [1]. Раствор заменяет другие аналоги (хлорированная вода, хлорированная известь, хлорамин и др.) В качестве бытового дезинфицирующего средства и отбеливателя.

Известно, что дезинфицирующие и отбеливающие свойства раствора гипохлорита натрия со временем снижаются. Из-за ограниченного срока хранения консервирование и транспортировка неэффективны.

По этой причине удобнее разрабатывать и предлагать рынку портативную версию, отвечающую требованиям самого устройства, а не самого решения. Такое устройство управляется непосредственно потребителем, и полученное решение можно использовать на месте. Эксплуатация такой установки осуществляется непосредственно потребителем, а полученный раствор можно использовать на месте по назначению.

Установка и эксплуатация устройства соответствуют правилам безопасности (IEC 60335-2-108-2014), которые соответствуют требованиям бытовой техники.

Конструктивные параметры (в зависимости от исполнения): Масса пустого резервуара с блоками ~ $3-6$ *кг* , вместимость ёмкости с жидкостью составляет ~ $2-12$ *л* .

Технические показатели: требуемая мощность от сети ~$130\ Bm$; интервал рабочих температур $(20-35)^0 C$; концентрация хлорида натрия в исходном растворе ~$(30-50)\ {}^{гр}/_{л}$; время приготовления раствора ~ 160 мин ; kоличество активного хлора в растворе ~ $(4-10)\ {}^{гр}/_{л}$; непрерывный режим работы установки до 6 часов.

Описываемое устройство используется периодически в стационарных условиях. Раствор гипохлорита натрия с необходимой концентрацией зависит от большого количества параметров. По этой причине качество раствора необходимо контролировать после каждого периода. В большинстве случаев для такого контроля используется pH-метр, который используется в лабораторных условиях, что приводит к дополнительным потерям времени и требует сортировки продукта по концентрации. Согласно теории электролиза, для получения гипохлорита натрия используется максимум 15% хлорида натрия в растворе. По этой причине в исходном растворе используется хлорид натрия в количестве не менее 15 г/л. Для раствора слабой концентрации использование стационарного режима не удобно.

Цель состоит в том, чтобы разработать проточную версию устройства и в этом случае проводить контроль качества непосредственно на поточной линии.

Для достижения указанной цели в конструкцию устройство были проведены определенные изменения, для контроля качества использован двухканальный фотометр.

С помощью двухканального фотометра проводится сравнительный анализ оптических плотностей входных и выходных продуктов, в результате анализа выходной раствор направляется либо на повторный электролиз, либо на использование.

На рисунке 1 показана схема проточного электролизера для получения раствора гипохлорида натрия из раствора хлорида натрия слабой концентрации (1,5 15 г/л).

Проточный электролизер состоит из резервуара (1), одной впускной трубы (2) и трех выпускных труб (3, 4 и 5) на противоположной стороне и газовой трубы (6) на верхней стороне. 5 выпускных труб находятся на одном уровне с 2 входными трубами и предназначены для защиты резервуара от избыточной жидкости. В бак 1 помещаются электроды (11) в направлении перпендикулярном потоку, и параллельно друг другу. Каждый электрод имеет форму кассеты, состоящей из пластин на расстоянии около 1 мм друг от друга. Электроды кассетной формы подключены параллельно к источнику постоянного тока (12).

Платы в кассете соединены по биополярной схеме. Во время процесса электролиза расстояние между пластинами в кассете сохраняется как можно меньшим, чтобы уменьшить нагрев раствора. Потому что, когда это расстояние слишком велико, процесс электролиза не является эффективным, энергия приложенного электрического поля тратится в основном на нагрев раствора. Если это расстояние слишком мало, гидравлическое сопротивление между электродами увеличивается и препятствует потоку раствора между электродами. В это время также увеличивается вероятность соприкосновения электродов. Для слабоконцентрированного раствора хлорида натрия было обосновано, что это расстояние должно быть измерено [2]. Для слабоконцентрированного раствора хлорида натрия это расстояние оправдано принимать равным (1-3) мм [2].

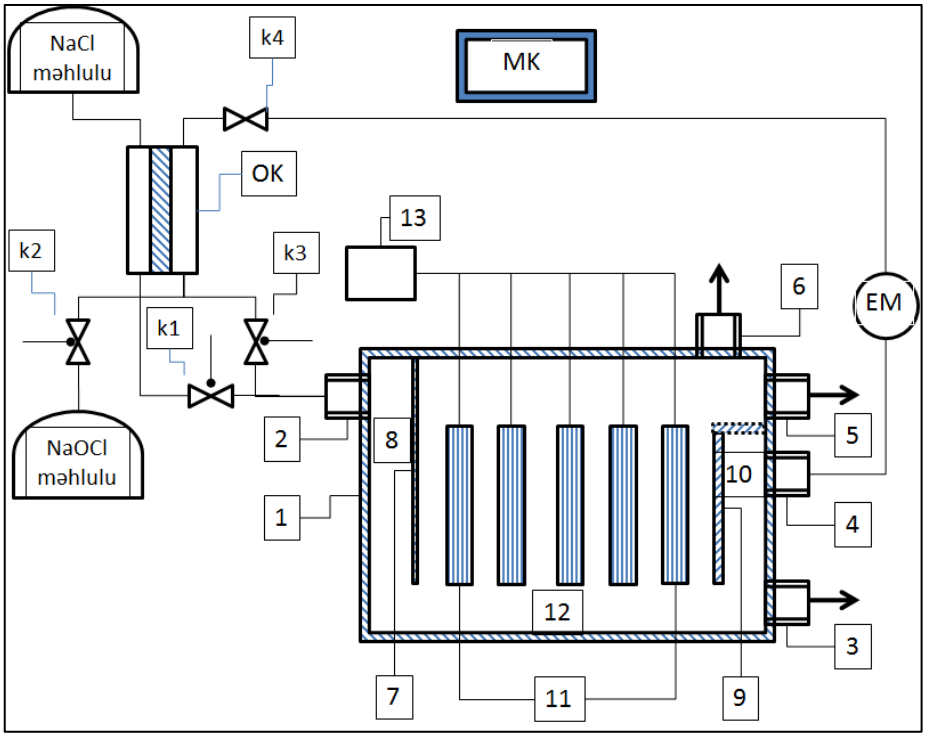


Рисунок 1. Схема установки проточного электролизера " Гипонат".

Количество электродов и пластин в каждой кассете определяется применяемым током и напряжением на основе рабочих характеристик, принятых для электролизера. Расстояние между электродами подбирается таким образом, чтобы можно было обеспечить самостоятельную работу каждой кассеты без зависимости от другой.

Электроды размещаются на определенном расстоянии от дна резервуара, так что канал (12) ламинарного потока может быть обеспечен со дна резервуара для раствора, и раствор хлорида натрия может регулярно подниматься между электродами.

Параллельно с электродами используется 7 перегородок на входной стороне и 9 перегородок на выходной стороне. Соответственно, 7 перегородок создают 8 объемных камер для ввода раствора хлорида натрия, а 9 перегородок создают 10 объемных камер для выхода раствора гипохлорита натрия. Верх 10-объемной камеры изготовлен из пористого материала, который позволяет жидкости вытекать. Размер перегородок выбирается таким образом, чтобы расстояние до дна резервуара было таким же, как у электродов.

Верхняя часть выходной перегородки расположена на одном уровне с электродами. Внизу 10-объемной камеры, образованной 9 перегородками, расположены 3 выпускных патрубка для слива оставшегося раствора в емкости, а вверху - 4 отводных патрубка для продукта, для которого определяется показатель качества. 3 выпускных патрубка снабжены регулирующим клапаном (на схеме не показан). Продукт из 4 выпускных трубок передается в рабочий канал оптической ванны (ОК) с помощью электродвигателя (ЭМ). Режим работы электродвигателя (ЭМ) регулируется таким образом, что обеспечивает как ламинарность потока, так и регулярное поддержание уровня раствора в емкости. Вход в рабочий канал оптической ванны обеспечен обратным клапаном (К4). Оптическая ванна является двухканальной и является составной частью оптического передатчика. Оба канала оптической ванны снабжены регулируемыми электрическими клапанами (К1, К2 и К3). Управляемые клапаны управляются с помощью микроконтроллера (МК) на основе сигналов фотометрического передатчика. Запуск и управление работой устройства обеспечивается на основе программного обеспечения, написанного на микроконтроллере.

Для передачи водяного пара и других газов, образующихся при электролизе, используется 6 выходных труб.

Принцип работы устройства следующий. Сигнал, отправленный на микроконтроллер, открывает управляющий клапан К1. Раствор хлорида натрия проходит через опорный канал оптической ванны и заполняет 8-объемную камеру электролизера и пространство между электродами. По сигналу датчика уровня (на схеме не показан) микроконтроллер подключает источник питания к процессу электролиза и начинается процесс электролиза. По сигналу уровнемера запускается электродвигатель, проходит от клапана К1 мотором в рабочую камеру оптической ванны, а оттуда через открытый клапан К3 поступает в бак электролизера. Процесс периодически продолжается. При обеспечении

показателя качества раствора регулирующий вентиль К3 закрывается по сигналу оптического передатчика, регулирующие вентили К1 и К2 открываются. Продукт, показатель качества которого обеспечен, заливается в резервуар для гипохлорита натрия, а исходный раствор хлорида натрия сливается в электролизер. Таким образом, процесс продолжает направлять продукт, соответствующий требуемым качествам, в резервуар, а раствор, не соответствующий требованиям, на повторный электролиз. Наличие процесса повторного электролиза увеличивает процент хлорида натрия, используемого для получения гипохлорита натрия.

Обеспечение процесса основано на следующем. При электролизе раствора хлорида натрия получается раствор гипохлорита натрия, который выделяется в виде газообразного водорода:

$$NaCl + H_2O = NaClO + H_2 \uparrow$$

Газообразный водород, поднимающийся над расстоянием между электродами в виде пузырька, уносит и раствор хлорида натрия, в результате чего раствор на дне сосуда обогащается гипохлоритом натрия.

Водорастворимый гипохлорит натрия распадается на ионы:

$$NaClO \rightarrow Na^+ + OCl^-$$

Ион гипохлорита гидролизуется с образованием слабой кислоты, хлоровациновой кислоты:

$$OCl^- + H_2O \leftrightarrow HOCl + OH^-$$

Отбеливающие и дезинфицирующие свойства раствора гипохлорита натрия объясняются наличием в растворе кислоты.

Отбеливающие и дезинфицирующие свойства раствора гипохлорита натрия объясняются наличием в растворе кислоты *HOCl*.

Водный раствор гипохлорита натрия нестабилен. Эксперименты показывают, что он разлагается на 0,085% в течение суток при комнатной температуре. Воздействие света и присутствие в растворе ионов металлов еще больше ускоряет процесс разложения. Более стабилен в щелочной среде, $ph > 11$. По этой причине контроль качества раствора гипохлорита натрия осуществляется на основании его показателя ph. Этот метод не является экспресс и является пустой тратой времени для процесса проточного электролиза.

Контроль качества раствора гипохлорита натрия также можно проводить фотометрическим методом по количеству кислоты в растворе.

Основные параметры, определяющие свойства молекулы хлорвата, следующие [3]:

$< HOCl = 102^0 29' \pm 27'$; $r_{H-O} = 0{,}965 \pm 0{,}005 A^0$; $r_{O-Cl} = 1{,}689 \pm 0{,}003 A^0$.

На основании этих данных волновые числа полос поглощения, наблюдаемые в спектре хлороватого вещества, выглядят следующим образом: $\nu_1 = 3609\ см^{-1};\ \nu_2 = 725\ см^{-1};\ \nu_3 = 1239\ см^{-1}$.

На основе записанных волновых чисел предлагается фотометрический контроль. Для этой цели используется двухканальная фотометрическая установка [4].

Одним из основных факторов, влияющих на точность измерений в фотометрических приборах, является загрязнение окон, контактирующих с потоком жидкости в процессе эксплуатации, и, следовательно, различные оптические базы для двухканальных фотометров. Инвариантность обеспечивалась за счет загрязнения окон оптической ванны, используемой в оптическом канале фотометрического прибора, и высокой точности измерений [5].

На входном патрубке установлена эталонная камера фотометрического преобразователя, а на выходном патрубке – рабочая камера. Разница между сигналами опорного и рабочего каналов фотометрического передатчика принимается за критерий качества продукта. Вопрос структурно-параметрического анализа фотометрического преобразователя и его связи с микроконтроллером основан на известной методике .

Литература

1. Hətəmov M.M., Mənsurov Q.M., Bayramov A.S. Natrium hipoxloritin alınması üçün avtomatlaşdırılmış “Hiponat” elektroliz qurğusu. SDU-nun “Elmi xəbərlər” jurnalı. Təbiət və texniki elmlər bölməsi. Sumqayıt, 2018, Cild 18, №3, s.49-52
2. Кибирев Д.И., Поживилко К.С., Никифоров Г.И. Способ обработки воды гипохлоритом натрия и проточный электролизер для получения гипохлорита натрия // https://patents.google.com/patent/RU2100483C1/ru
3. Молекулярные постоянные неорганических соединений: Справочник / Под ред. Краснова К.С.-Л.: Химия, 1979, с.128-129
4. Мансуров Г.М., Рувинов Э.С., Гусейнов Т.К., Сутовский С.М. Двухлучевой фотометр. А.с.1476324 (СССР). Положительное решение от 17.03.88.
5. Мансуров Г.М., Гусейнов Т.К., Рувинов Э.С., Сутовский С.М. Кювета для двухлучевого фотометра. Журн. «Оптико-механич.пром-сть», Л.-1989, №8, с.53-54

SYNTHESIS STUDY OF BIOCHAR-CELLULOSE-BASED BIOCOMPOSITES FOR WASTEWATER TREATMENT FROM HEAVY METALS

Alishan Alishanov, Jala Nabiyeva, Madina Suleymanova
Baku Higher Oil School
Baku, Azerbaijan
alishan.alishanov@bhos.edu.az, zhala.nabiyeva.std@bhos.edu.az,
madina.suleymanova@bhos.edu.az

Abstract - Rising global concerns over heavy metal contamination in water resources highlight the urgent need for efficient and sustainable wastewater treatment technologies. Conventional treatment methods often generate secondary pollutants, excessive sludge, and require high energy and chemical inputs, thereby exacerbating environmental challenges. In response, this study explores the development of a biochar–cellulose biocomposite as a cost-effective and environmentally friendly adsorbent for heavy metal removal from wastewater. Biochar was produced from pomegranate and hazelnut peels through pyrolysis at 625°C, while cellulose was extracted from cotton stalks via alkaline treatment. The biocomposite was synthesized using chitosan as a crosslinking agent under thermal conditions. Comprehensive characterization was conducted using FTIR and BET analyses to evaluate structural and surface properties. FTIR results confirmed the presence of functional groups such as O–H, C=C, and N–H, which serve as active binding sites for heavy metals. BET analysis demonstrated a high specific surface area of 312 m²/g and 198 m²/g for pomegranate and hazelnut-cellulose composites respectively. Overall, the prepared biochar–cellulose biocomposite exhibits superior physico-chemical properties, indicating strong potential for efficient heavy metal removal in wastewater treatment applications.

Keywords: adsorption, biochar, cellulose, pyrolysis, wastewater treatment

Introduction

The rising concern worldwide regarding water pollution caused by heavy metal contamination is an indication that effective and efficient means of treating wastewater are needed. The long-term effect of heavy metals on the environment and the water bodies means that effective technology is needed to treat the water before it is discharged into the environment.

Traditional wastewater treatment techniques are known to produce toxic secondary pollutants and considerable amounts of sludge and other toxic byproducts, which require proper disposal [Pachaiappan, 2022]. The techniques require considerable amounts of chemicals and energy, and the energy demand of the techniques has been found to be high, which has added to the environmental problem [Zhang, 2024].

With the increasing population, industrialization, and the ever-growing need for water, there has been considerable recent interest in the environmental/materials engineering literature in the search for inexpensive, readily available, and effective materials in water purification and wastewater treatment processes [Mortazavian, 2022]. Biochar is a carbonaceous product obtained from the pyrolysis of various organic materials, usually of vegetal or animal origin, and the physical and chemical properties of the

produced biochar depend on the source materials and pyrolysis conditions [Rando, 2024]. Biochar has a very high carbon content, porosity, a large surface area, and a number of functional groups, making it a potential candidate in the treatment of wastewater [Ravindiran, 2024]. The presence of a number of functional groups, such as hydroxyl, carboxyl, and amino groups, in combination with the high porosity, large surface area, and superior ability of the biochar-based adsorbent to exchange ions, all contribute to the superior adsorption efficiency of the adsorbent [Rando, 2024].

Experimental Part

To make the biochar, pomegranate and hazelnut peels were washed with distilled water. Peels were cut into smal pieces and dried at the oven at 105°C for 4 hours. Dried pomegranate and hazelnut peels were powdered, and then pyrolyzed at 625°C for 4 hours.

To make the cellulose, cotton salks were washed with distilled water. They were soaked in 2%wt. NaOH solution at 75°C for 5 hours. Treated cotton stalks were washed with distilled water again, and then dried.

To make the biocomposite, chitosan was used as a crosslinker. Biochar-cellulose powders added into 10%wt. chitosan solution. It was heated up to 60°C for 3 hours to initiate crosslinking. After the crosslinking process, the mixture was cooled down to room temperature. Then, the product was vacuum dried.

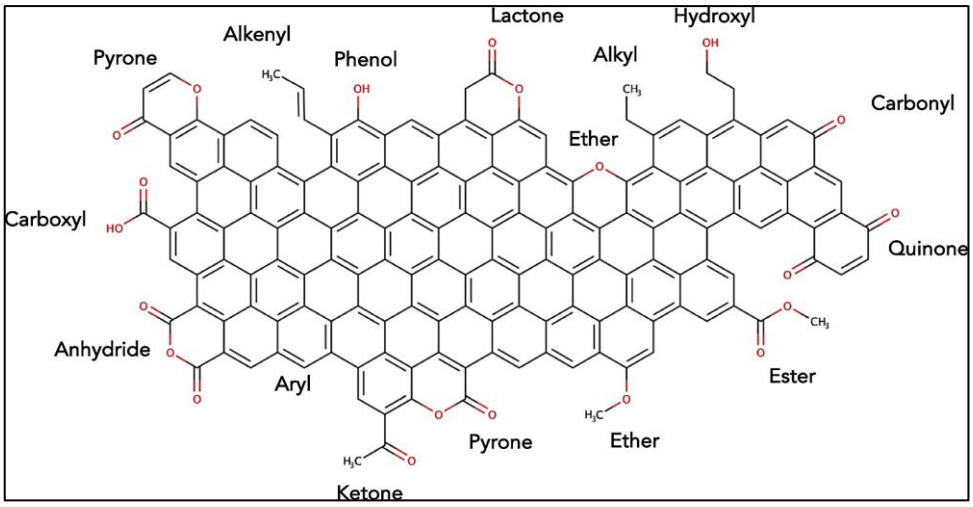


Figure 16. Molecular Structure and Functional Groups

Results and Discussion

Multiple tests were conducted to study the molecular structure, and surface area of the obtained biochar-cellulose biocomposites. FTIR spectroscopy was utilized to determine the functional groups in the biochar-cellulose based biocomposite. The graph of transmittance vs wavenumber was plotted as the result of the measurement.

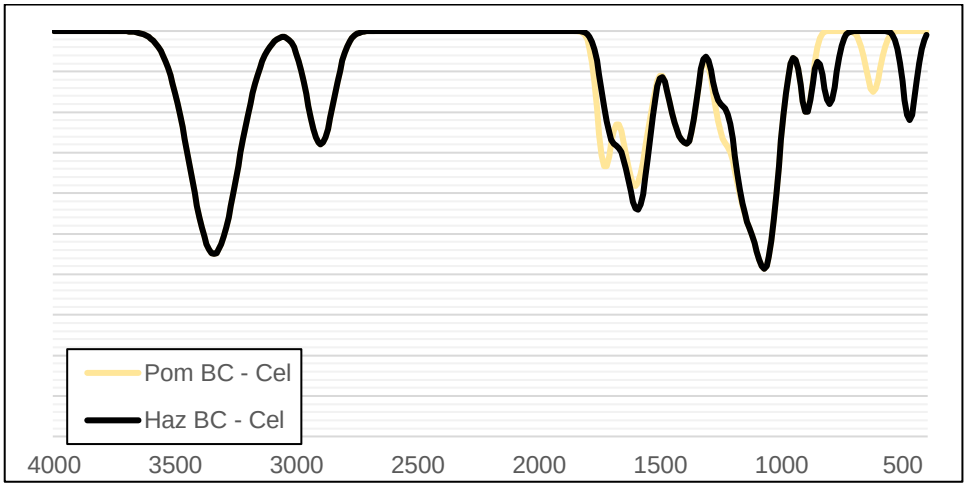


Figure 17. FTIR Results

From the result (Figure 2), it can be seen that there is O-H peak (3340 cm^{-1}), which can act as metal binding site. This is beneficial for aqueous heavy metal removal. C=C (1430 cm^{-1}) groups can increase adsorption capacity and stabilize metal ions. N-H (1550 cm^{-1}) groups also can enhance adsorption performance and coordinate heavily with heavy metals.

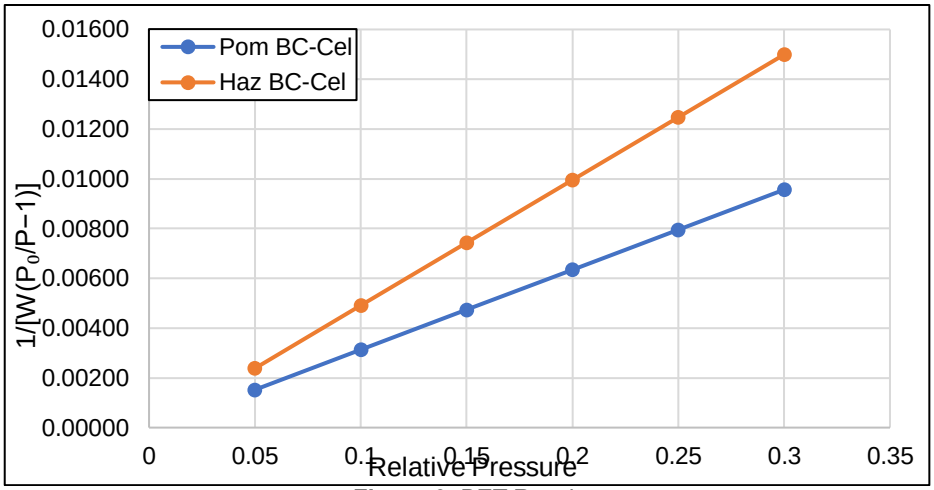


Figure 3. BET Result

The BET analysis result shows surface area of 312 m^2/g for pomegranate-cellulose biochar, while 198 m^2/g for hazelnut-cellulose biochar. This result is very high, in terms of surface area, which also means more active adsorption sites. Overall, FTIR and BET results mean our biochar-cellulose biocomposite would be better in wastewater treatment from heavy metals than standard biochar.

Offers

Based on the findings of this study, we offer a sustainable and scalable biochar–cellulose biocomposite as a promising alternative adsorbent for heavy metal removal from contaminated wastewater. The developed material demonstrates enhanced surface area, favorable pore structure, and abundant functional groups, indicating strong potential for practical application in industrial and municipal wastewater treatment systems.

We propose further optimization and scale-up studies to evaluate adsorption performance under real wastewater conditions, including multi-metal systems and continuous flow processes. In addition, regeneration and reusability assessments can be conducted to determine long-term operational feasibility and cost-effectiveness. The adaptability of the synthesis method also allows exploration of other agricultural waste sources to tailor material properties for specific contaminants.

References

1. Pachaiappan, R., Ponce, C., Rajendran, R., Manavalan, K., Rajan, F., Awad, F., 2022, A review on biofiltration techniques: recent advancements in the removal of volatile organic compounds and heavy metals in the treatment of polluted water, Bioengineered.
2. Mortazavian, S., Murph, S., Moon, J., 2022, Biochar Nanocomposite as an Inexpensive and Highly Efficient Carbonaceous Adsorbent for Hexavalent Chromium Removal, Materials.
3. Rando, G., Scalone, E., Sfameni S., Plutino, M., 2024, Functional Bio-Based Polymeric Hydrogels for Wastewater Treatment: From Remediation to Sensing Applications, Gels.
4. Ravindiran, G., Rajamanickam, S., Janardhan, G., Hayder, G., Alagumalai, A., Mahian, O., 2024, Production and modifications of biochar to engineered materials and its application for environmental sustainability: a review, Biochar,
5. Zhang, L., Zhu, X., Wang, H., Liu, X., 2024, Research Progress in the Treatment of High-Salinity Wastewater, Journal of Physics: Conference Series.

MECHANİSM OF THE ELECTROCHEMİCAL REDUCTİON PROCESS OF MO İONS

Ayan Alizada, Samira Jafarova
Baku State University
Baku, Azerbaijan
elizadeayan2004@gmail.com

Summary - The presented work is devoted to the study of the electrochemical reduction process of molibdat ions for the purpose of obtaining thin films based on Mo. Here, reduction and deposition potential regions were determined for the purpose of electrodeposition of Mo ions, and the influence of some factors on the process was studied.
Keywords: non- aqueos electrolyte, potential, Mo ions, electroreduction

Introduction

Molybdenum (Mo) is a transition metal characterized by high strength, corrosion resistance and high temperature stability. The electrochemical reduction of molybdenum ions in aqueous and non-aqueous solutions has a complex, multi-stage mechanism and is characterized by intermediate oxidation states. The study of this process is important for obtaining high-quality Mo coatings and the development of electrochemical technologies.

[Majidzade, 2019, 1-2]

The direct reduction of molybdate ions to molybdenum is a thermodynamically and kinetically difficult process.

Experimental part

Cyclic polarization curves have been recorded to study the kinetics and mechanism of both the electroreduction of Mo ions by IVIUMSTAT Electrochemical Interface potentiostat (Ivium Technologies, Netherland). A glass three-electrode electrochemical cell with a volume of 100 mL has been used. Pt, with an area of 0.5 cm^2, have been used as the working electrode.

Results and their discussion

Electrochemical reduction of Mo ions is a complex, stepwise and kinetically limited process. The reduction results in the production of metallic molybdenum starting from Mo(VI) through intermediate oxide forms. The efficiency of the process depends on the pH of the medium, temperature, electrode material and current density. A deep study of the mechanism allows obtaining high-quality molybdenum coatings and their application on an industrial scale.

References

1. Majidzade V.A., Aliyev A.Sh., Babanly D.M., Elrouby M., Tagiyev D.B. Investigation of the electrochemical reduction process of the molybdate ions in the tartaric electrolytes. Acta Chimica Slovenica, 2019, Vol. 66(1), p. 155-162
2. Cafarova S.F., Aliyev A.Sh., Tagiyev D.B. Influence of various factors on the composi tion of electrodeposited thin films Mo-S. Azerb. Chemical Journal, 2018, №3, p. 6-10

ORANGE PEEL REINFORCED POLY(LACTIC ACID) COMPOSITES: MECHANICAL PROPERTIES AND ACCELERATED BIODEGRADATION

Nihad Mirzazada, Ayla Abbasli
Baku Higher Oil School
Baku, Azerbaijan
nihad.mirzazada.std@bhos.edu.az, ayla.abbasli@bhos.edu.az

Abstract - The increasing environmental risk posed by non-biodegradable plastic waste has fueled concerns over renewable resource-based sustainable alternatives. In this research, orange peel powder (OPP) reinforced poly(lactic acid) (PLA) biocomposite films are analyzed as a biodegradable material. Citrus waste, especially orange peel, with high cellulose and pectin composition was mixed into a PLA matrix at different amounts of 0, 15, 35, 45, and 55 wt%. Fourier Transform Infrared Spectroscopy (FTIR), water contact angle measurements, Universal Testing Machine (UTM) and a 30-day soil burial test were used to characterize the composite films in terms of chemical structure, surface wettability, mechanical properties, and biodegradability, respectively. This work aims to valorize citrus agricultural waste while addressing the inherent brittleness and slow degradation rate of pure PLA.
Keywords: orange peel powder, polylactic acid, biodegradability, biofillller

Introduction

Plastics are inexpensive, lightweight, strong, and durable materials with thermal and insulation properties [Thompson et al., p. 2009, 2153]. Global resin and fiber production increased from 2 million metric tons (Mt) in 1950 to 380 Mt in 2015, an annual growth rate of 8.4%, reaching around 413.8 million metric tons by 2023 [Geyer et al., 2017, 1-2]. However, the identical properties that make plastics desirable make these materials challenging to degrade. Disposal of plastic waste poses a serious threat to marine ecosystems, with adverse effects prevailing in terrestrial ecosystems as well [Cole et al., 2011, p. 2588-2589].

Concerns about plastic pollution sparked a lot of interest in biopolymers as a more environmentally friendly substitute for plastic. However, pure PLA has drawbacks associated with its mechanical properties which limit its appropriateness in certain applications. Poor toughness of PLA, below 10% elongation break, sets back its use as a high stress resisting plastic [Farah et al., 2016, 367-368].

Citrus waste disposal remains unsolved despite its abundance, with 88 million tons produced globally, residue peel accounts for 50% of processed mass, causing soil salinity and harm to ruminants [Balu et al., 2012, p. 1694]. Orange peel contains cellulose and pectin which sustain mechanical strength and gelling properties suitable for biobased applications. If incorporated into PLA. increase in biodegradability, flexibility, and mechanical properties could be recorded. However, orange peel modification in PLA matrices remains limited and has not addressed these properties comprehensively, thus more study should be conducted.

Experimental Part

PLA biopolymer was used as the polymer matrix for fabrication of composite. Fresh sweet orange peel was used as the natural bio-filler source. For film casting, chloroform was employed as the solvent. Hydrochloric acid (HCl) and sodium hydroxide (NaOH) were used to pretreat the orange peel and adjust the pH level. Deionized water was used throughout the whole experimental procedure. The chemical components were used without additional treatment or purification.

Sweet orange peels were washed thoroughly with tap water to eliminate contaminants on the surface. The cleaned peels underwent two stages of drying procedure. Firstly, they were dried for 24 hours followed by oven drying 50℃ for 24 hours. The dried peels were subjected to grinder and sieve shaker was used to obtain uniform particle size.

A 15 wt% PLA solution was prepared by dissolving PLA in chloroform with continuous stirring for an hour. Orange peel powder (0.5 g) was then added and mixed for 1 hour to get even distribution within the matrix. The solution was poured on flat glass and left to dry for 24 hours at room temperature to complete solvent removal. This process was repeated at 15, 35, 45 and 55 wt% OPP loadings to obtain PLA/OPP biocomposite films.

Structure of composites were deduced utilizing Fourier Transform Infrared Spectroscopy (FTIR). The film samples measured cm^2 were analyzed over a wavenumber range of 400-4000 cm^{-1}. Hydrophilicity of the specimens were analyzed with the measurements of contact angle. Universal Testing Machine with a load helped to determine tensile strength. Biodegradability was determined through 30 days of soil burial test where weight loss of each composite was measured.

Results and Discussion

FTIR tests were used to identify the functional groups in the pure PLA matrix and in the OPP reinforced biocomposite films. The FTIR were recorded in a wavenumber between 4000 and 400 cm^{-1}. Absorption is seen in the vicinity of 2964.81 and 2991.46 cm^{-1} are C–H stretch, while peak appearing at around 1751.8 cm^{-1} corresponds to C=O group of stretching. The broadening of OH stretching band confirms the presence of hydroxyl groups. The incorporation of OPP into the PLA matrix did not introduce any new peaks, confirming that the interaction between the matrix and filler is physical.

The surface wettability was evaluated through carrying out water contact angle measurements of the composite films. The pure PLA film exhibited a contact angle of 75.21°. This confirms its hydrophobic character, which is directly related to the nonpolar methyl groups and ester linkages in the PLA backbone that hinder its interaction with molecules of water.

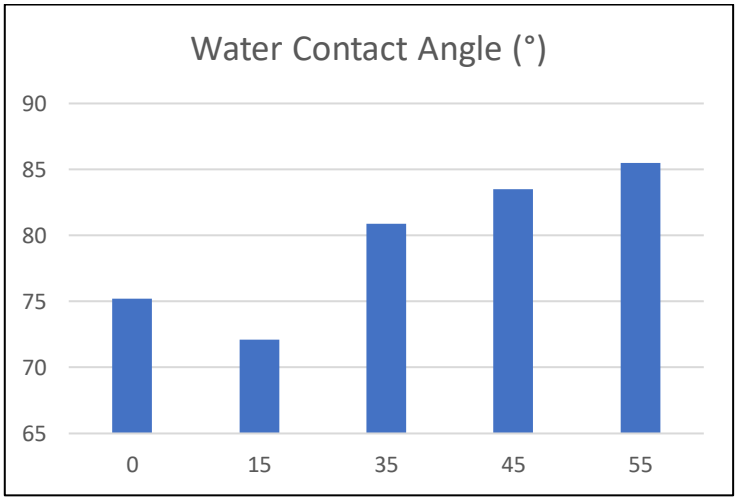


Figure 1. Water contact angle measurements of samples

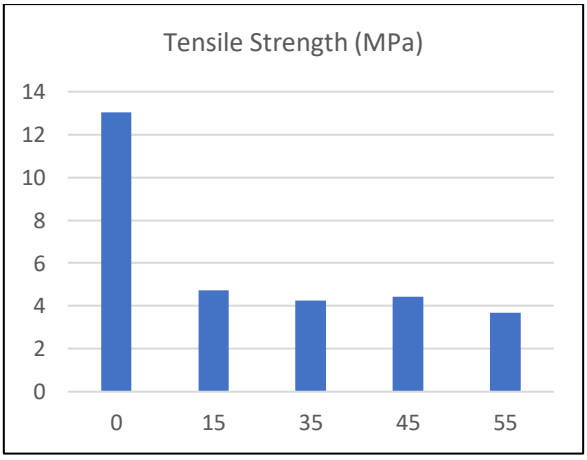


Figure 2. Tensile Strength Analysis

Reinforcing PLA with OPP reduced tensile strength and Young's modulus from 13.02 MPa and 1671 MPa for pure PLA to 3.68 MPa and 241 MPa at 55 wt% OPP. This is because of poor adhesion between the hydrophilic filler and hydrophobic matrix. Conversely, elongation at break improved substantially which peaked at 11.32 mm at 35 wt% OPP compared to 1.79 mm for neat PLA just before declining at higher loadings due to filler clustering.

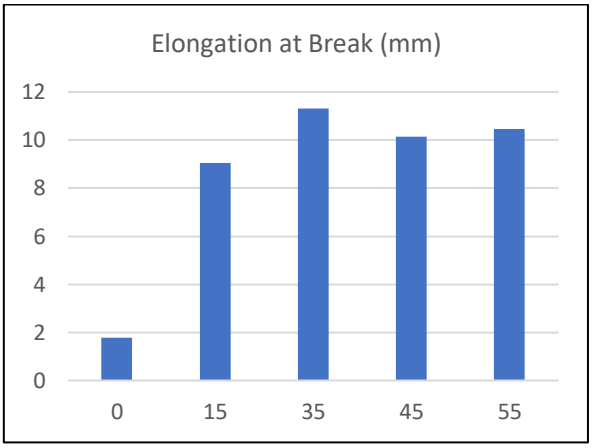


Figure 3. Elongation at Break Analysis

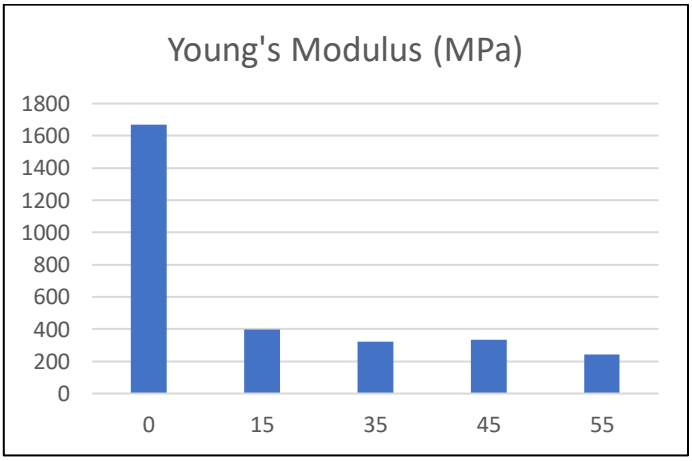


Figure 4. Young's Modulus Analysis

Soil burial tests conducted for 30 days proved that OPP enhanced biodegradability of PLA. Pure PLA showed minimal loss of weight, 6.81%, at 30 days. Increasing OPP content, weight loss gradually increased. Figures have reached 13.69%, 20.94%, 32.55%, and 52.78% for 15, 35, 45, and 55 wt% OPP composites, respectively. The highest degradation observed in the 55 wt% OPP composite is attributed to the high cellulose content in orange peel.

Offers

Future studies should look into modifying the surface of OPP using alkali or chemical treatments to improve the bonding between the hydrophilic filler and the hydrophobic PLA matrix. This issue was found to be the main reason for the decreased tensile strength and modulus. It is also advised to conduct thermal analysis utilzing DSC and TGA to thoroughly evaluate how OPP affects crystallinity and thermal properties of the composites. Moreover,

extending the soil burial test beyond 30 days would allow for a better assessment of composite biodegradability. This is particularly important for lower OPP amounts that showed slower degradation.

References

Balu, A. M., Budarin, V., Shuttleworth, P. S., Pfaltzgraff, L. A., Waldron, K., Luque, R., & Clark, J. H. (2012). Valorisation of orange peel residues: waste to biochemicals and nanoporous materials. ChemSusChem, 5(9), 1694.

Cole, M., Lindeque, P., Halsband, C., & Galloway, T. S. (2011). Microplastics as contaminants in the marine environment: a review. Marine pollution bulletin, 62(12), 2588-2597.

Farah, S., Anderson, D. G., & Langer, R. (2016). Physical and mechanical properties of PLA, and their functions in widespread applications—A comprehensive review. Advanced drug delivery reviews, 107, 367-392.

Geyer, R., Jambeck, J. R., & Law, K. L. (2017). Production, use, and fate of all plastics ever made. Science advances, 3(7), e1700782.

Thompson, R. C., Moore, C. J., Vom Saal, F. S., & Swan, S. H. (2009). Plastics, the environment and human health: current consensus and future trends. Philosophical transactions of the royal society B: biological sciences, 364(1526), 2153-2166.

PREPARATION AND TESTING OF ENVIRONMENTALLY SAFE CORROSION INHIBITOR BASED ON REAGENTS OF NATURAL ORIGIN

Elnura Aliyeva
Supervisor: Durna Aghamaliyeva
Baku Higher Oil School
Baku, Azerbaijan
elnura.q.aliyeva.std@bhos.edu.az

Summary - Production of green corrosion in lab conditions and testing of it are provided in this paper. Although nowadays in many sectors corrosion is one of the challenges, the least expensive and simplest way to combat it is the usage of inhibitors. In this work, inhibitor is eco-friendly plant-based one. After getting inhibitor, corrosion rates are monitored to evaluate the effectiveness of inhibitor under controlled conditions. The aim is to define that this inhibitor lasts long and has an equal effect as other inhibitors or not.

Keywords: corrosion, green inhibitor, DETA, formation water.

Introduction

Based on National Statistical Classification of Economics (NACE), in 2013, the evaluated global cost of corrosion was 2.5 trillion dollars per year which is 3.8% of the global Gross Domestic Product (GDP). In that year, the overall cost of corrosion in the European Region was 701.5 billion dollars. The USA's corrosion costs' distribution is illustrated in **Figure 0.1** [1].

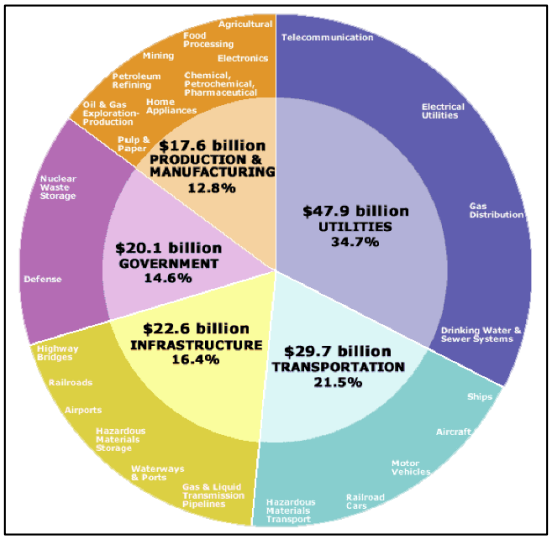


Figure 0.1 Distribution of corrosion costs in the United States in 2013

Annually, in most countries, corrosion costs are expected to range from 1% to 5% of their GDP. According to NACE [2], application of efficient corrosion management may cut these costs by 15–35% which leads to worldwide savings of 375–875 trillion dollars per year. The management of corrosion is important for asset life and cost savings, ensuring environmental impacts and individual safety [3].

By summing up construction, design, replacement and repairs costs, the present cost of corrosion is estimated. According to Yang, proper strategies of corrosion prevention can result in reduction of economic losses, improvement of the environment and public safety [4].

Experimental Part

During experiment, fatty acids were obtained from sunflower oil by hydrolysis. The reaction was carried out at 60–80 °C and maintained until complete hydrolysis was achieved. The yield of the obtained sunflower oil fatty acids ranged from 86% to 95%.

Amidoamines were then synthesized using sunflower oil fatty acids and diethylenetriamine (DETA) at a 1:1 molar ratio. The reaction mixture was heated at 130–190 °C for 1.5–2 hours under continuous stirring. The progress of the reaction was monitored until the formation of the amidoamine was complete. The yield of the synthesized amidoamines ranged from 89% to 96%.

The physicochemical properties of the obtained compounds were further investigated, and their efficiency as corrosion inhibitors in a CO_2-containing environment was evaluated.



Figure 0.1 Synthesis of sunflower oil fatty acids and diethylenetriamine.

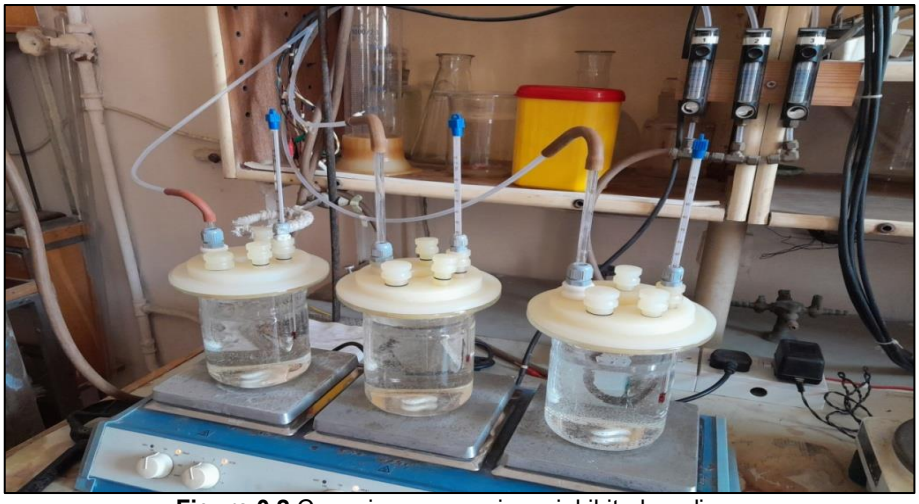


Figure 0.2 Corrosion process in an inhibited medium.

Results and their discussion

1) Sunflower oil fatty acids were successfully isolated by hydrolysis with a yield of 91%.
2) Amidoamines were synthesized from sunflower oil fatty acids and diethylenetriamine (DETA), with yields ranging from 89% to 96%.

3) Complexes were obtained by the reaction of sunflower oil fatty acid–based amidoamines with alkyl halides ($C_5H_{11}Br$, $C_5H_{11}I$, and $C_6H_{13}Br$). The yields of the synthesized complexes ranged from 86% to 96%.
4) The structures of the synthesized fatty acids, amidoamines, and inorganic anion-containing complexes were confirmed by infrared (IR) spectroscopic analysis.
5) The corrosion inhibition performance of 20% isopropyl alcohol solutions of the complexes was studied in a CO_2-saturated 1% sodium chloride solution. The results showed that the alkyl halide complexes provided 90–99% protection efficiency at concentrations of 50–75 mg/L.

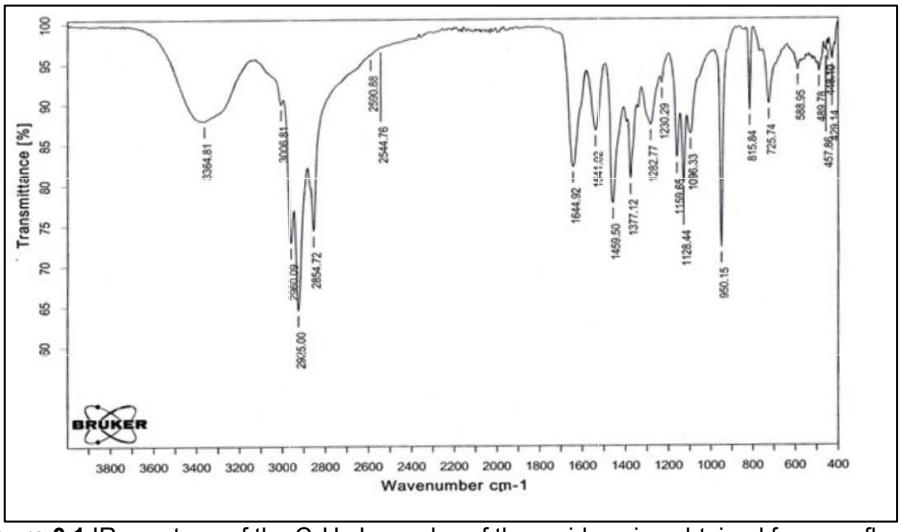


Figure 0.1 IR spectrum of the $C_5H_{11}I$ complex of the amidoamine obtained from sunflower oil fatty acid and diethylenetriamine.

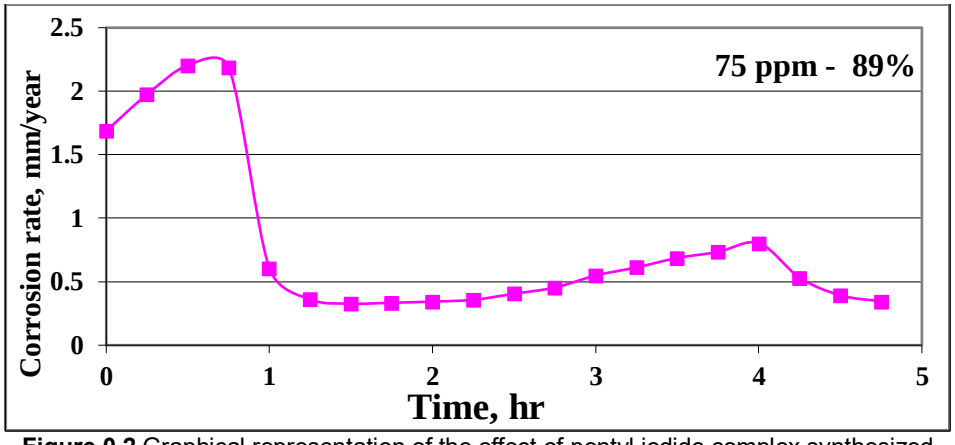


Figure 0.2 Graphical representation of the effect of pentyl iodide complex synthesized based on sunflower fatty acid and diethylenetriamine on CO_2 corrosion rate of 20% solution.

Offers

It is recommended to:

- Conduct pilot-scale tests under field conditions to evaluate long-term stability and performance.
- Investigate compatibility with other production chemicals commonly used in oilfield operations.
- Perform detailed electrochemical studies to better understand the inhibition mechanism.
- Assess environmental impact and biodegradability to confirm their suitability as environmentally friendly alternatives to conventional inhibitors.

References

[1] "NACE Study Estimates Global Cost of Corrosion," [Online]. Available: https://www.rustbullet.com/cost-of-corrosion/?srsltid=AfmBOoor60Cy-USkAyUAObxGazC-ThrGmbPpliLgqczvovNQZCWmvT-Q. [Accessed 18 October 2025].

[2] "NACE International. International Measures of Prevention, Application, and Economics of Corrosion Technologies Study (IMPACT)," 2016.

[3] C. Verma, E. Ebenso, B. Abdellaziz and C. Hussain, "Recent developments in Sustainable Corrosion Inhibitors: Design, Performance, and industrial scale applications.," 2021.

[4] G. Koch, "Cost of corrosion.," *Trends in Oil and Gas Corrosion Research and Technologies,* 2017.

PRODUCTION OF SUSTAINABLE DIMETHYL ETHER THROUGH CARBON DIOXIDE HYDROGENATION

Ezozbek Turaev
Tashkent Institute of Chemical Technology
Tashkent, Uzbekistan
turaevezozbek701@gmail.com
Rima Guliyeva
rima.guliyeva@bhos.edu.az

Abstract - This study investigates the potential for producing Dimethyl Ether (DME) through CO_2 hydrogenation, utilizing available CO_2 and H_2 gases from the Gas Chemical Complex (GCC) located in Uzbekistan. The key focus areas will be the process flow, performance parameters, and the thermodynamic and catalytic aspects of the CO_2-to-DME reaction to identify optimal operating conditions and type of the reactor. Overall goal of the research is simulate a DME production unit with high-purity (>97%) and assist Uzbekistan in achieving its goals of net zero emissions by diversifying energy fuels and rational usage of byproduct streams from plants.

Keywords: Dimethyl Ether, DME Production, Simulation, Aspen Hysys.

Introduction

The global tendency toward low carbon emissions has been driving the demand for sustainable alternative fuels and the optimization of carbon-based energy systems. In Uzbekistan, more than 25% of electricity is currently generated from renewable sources, such as solar power plants and wind turbines, while the most of the other parts comes from conventional natural gas-based power plants. In line with the Paris Agreement and Uzbekistan's 2030 Strategy, the country aims to reduce carbon emissions by approximately 35% to mitigate global warming and adhere to sustainable development principles in addressing climate change.

Dimethyl Ether is the simplest ether, a colourless gas with a faintly sweet odour under ambient conditions. Its chemical formula is CH_3OCH_3 or C_2H_6O, representing a central oxygen atom bonded to two methyl (CH_3) groups. DME is non-corrosive, non-toxic, and sulphur-free, which allows it to combust cleanly with minimal particulate matter and CO_2 emissions [6]. Physical and chemical properties of DME and other used fuels are listed in Table 1 [5] [7].

Table 1 – Comparison of characteristic properties of DME

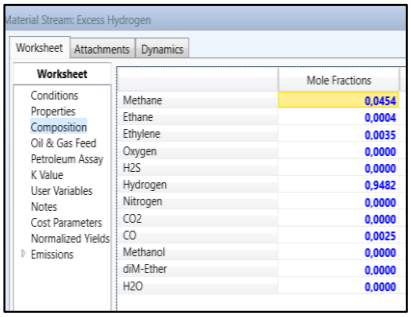
Parameter	DME	Methane	LPG	Gasoline	Diesel
Molar mass (g/mol)	46.07	16.04	44.1	114	198.4
Density (g/cm^3)	0.67	0.00072	0.54	0.71-0.77	0.8-0.86
Normal boiling point (°C)	-24.9	-162	-30	0-210	125-400
Octane number (RON)	-	122	90-96	90-100	-
Cetane number	55-60	-	-	-	40-55
Energy content (MJ/kg)	28.43	50	46.3	42.7	43.1
Carbon content (wt.%)	52.2	74	82	85.5	87

In industrial applications, DME serves as an important chemical intermediate in the production of dimethyl sulfate, methyl acetate, and as a propellant in aerosol products [3]. Moreover, it is possible to use in various fields including household purposes, as fuels for transportation and power generation, and DME has been experimentally confirmed practical for various utilization equipments.

Simulation Section

The acid gas stream from Amine Treatment Unit which flows to Sulphur Recovery unit (with containing >96% mole of CO_2 gases) and Excess H_2 stream (>94% purity) as a byproduct from the Ethylene Production Unit are used as a Feed inlet for simulation.

a



b

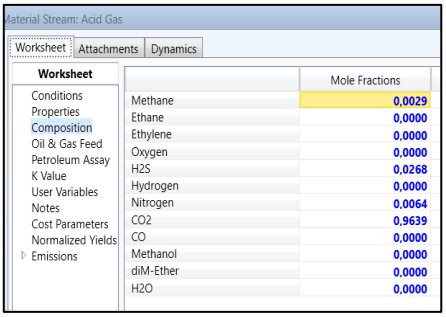


Figure 1 – Feed Gas Composition

The hydrogenation of CO2 into DME involves the following reactions [1] [2] [4]:

- Methanol formation:

$$CO2 + 3H2 \rightarrow CH3OH + H2O \quad \Delta H° = -49.5 \text{ kJ/mol} \quad (1)$$

- Methanol dehydration:

$$2CH_3OH \rightarrow CH_3OCH_3 + H_2O \quad \Delta H° = -23.4 \text{ kJ/mol} \quad (2)$$

- Reverse water-gas shift (RWGS):

$$CO_2 + H_2 \rightarrow CO + H_2O \quad (3)$$

- Net reaction:

$$2CO_2 + 6H_2 \rightarrow CH_3OCH_3 + 3H_2O \quad (4)$$

The following reactions (1) and (2) illustrate how DME can be formed from hydrogen and carbon dioxide via two separate reaction pathways; one is the methanol production pathway and the other is the production of DME through dehydration of methanol to DME. The reverse-water-gas-shift (RWGS) reaction (3) is another key reaction during the catalytic hydrogenation of CO_2. Being a reversible reaction, the RWGS reaction will also be promoted by those catalysts that promote the water-gas-shift (WGS) reaction.

The figure 2 demonstrates a simulated DME production unit in Aspen Hysys

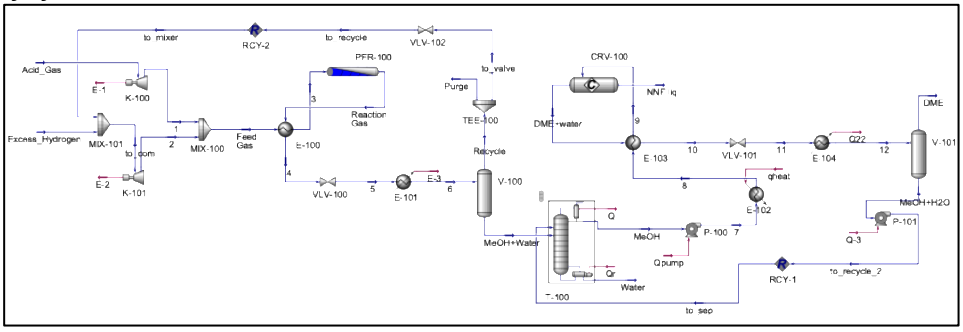


Figure 2 – Process Simulation

Results and Discussion

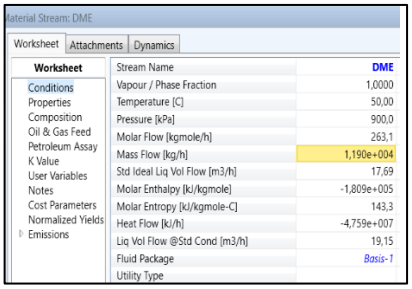
This research has provided a detailed overview of sustainable manufacturing of DME via catalytic hydrogenation of CO2. The simulated process is chosen an indirect synthesis method, which separates methanol production from DME dehydration, to provide optimal catalytic conditions for both stages of the process.

Byproduct streams from Units are compressed and mixed (MIX-100), then reacted in a Plug Flow Reactor (PFR-100). After reaction has occurred, intermediate methanol will be separated through distillation column (T-100). Liquid methanol is pumped (P-100) and heated through heat-exchangers (E-102,103) to create operational conditions for a secondary conversion stage.

Then methanol followed to catalytic dehydration reactor (CRV-100) to produce high-purity DME (>97%). Optimal operating conditions generally fall within the temperature range of 200 to 300°C and pressure range from 3 to 5 MPa.

The figure 3 demonstrates conditions and composition of final product.

a



b

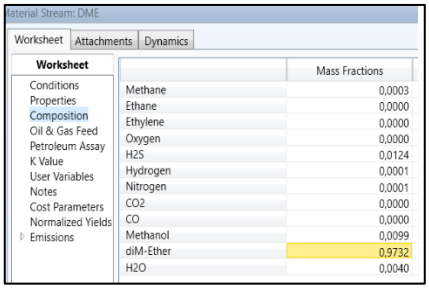


Figure 3 – Conditions and Composition of DME

This simulation has a great potential to provide valuable scientific and industrial knowledge. The outcomes could facilitate future studies to use industrial CO2 and H2 gases as a feedstock for other processes.

Conclusions and Recommendations

The results of this study, along with supporting information from previous studies, demonstrate that this work has produced an innovative model to convert CO2 into DME. As a result, two byproduct streams from plant are converted into valuable product with >97% purity which can be used in various purposes.

References

1. Bonura, G.; Todaro, S.; Frusteri, L.; Majchrzak-Kucęba, I.; Wawrzyńczak, D.; Pászti, Z.; Tálas, E.; Tompos, A.; Ferenc, L.; Solt, H.; Cannilla, C.; Frusteri, F. Inside the reaction mechanism of direct CO2 conversion to DME over zeolite-based hybrid catalysts. Applied Catalysis B: Environmental2021, 294, 120255–120264.

2. Catizzone, E.; Freda, C.; Braccio, G.; Frusteri, F.; Bonura, G. Dimethyl ether as circular hydrogen carrier: Catalytic aspects of hydrogenation/dehydrogenation steps. Journal of Energy Chemistry2021, 58, 55–77.
3. Fuel DME Plant in East Asia. Toshiyuki MII and Masayuki Uchida. Business planning and Development Department. TOYO Engineering Corporation, Japan.
4. Giuseooe Bonura, Serena Todaro, Catia Canilla, and Francesco Frusteri, CO2 hydrogenation into dimethyl ether, 2022.
5. International Journal of Renewable Energy Research, IJRER. H.Erdener, A.Arinan,S.Orman, 2011.
6. Lee S. Dimethyl Ether Synthesis and conversion to value-added chemicals. Oslo University.
7. S. H. Park, C. S. Lee, Applicability of dimethyl ether (DME) in a compression ignition engine as an alternative fuel, Energy Conversion and Management.

RADIATION PROTECTION POTENTIAL OF NBR-Bi_2O_3-$BaSO_4$ COMPOSITES

Fatima Azizli[1], Rana Khankishiyeva[23]
[1]Department of Chemistry of high molecular weight compounds, Baku State University, Z. Khalilov Str. 23, Baku AZ1148, Azerbaijan
[2]Institute of Radiation Problems, Ministry of Science and Education of the Republic of Azerbaijan, Baku AZ1143, Azerbaijan
[3]Azerbaijan University of Architecture and Construction, Baku AZ1073, Azerbaijan
fatime.azizli2003@gmail.com

Summary - The creation of X-ray shielding materials with superior attenuation, mechanical strength and resistance to radiation-induced degradation is essential given the modern era's growing demand for greater security. Therefore, the radiation absorption properties of Bi_2O_3 and $BaSO_4$ fillers were investigated for their potential applications in X-ray shielding under harsh radiation conditions. The optimal distribution and appropriate composition of the fillers in the studied composites synergistically improve both mechanical and radiation absorption properties.

Keywords: radioation, butadiene-nitrile rubber, polymer composites, radiation shielding

Introduction

It is known that Pb-based protective clothing made from Pb sheets is prone to cracks and holes due to poor durability and elasticity, as well as weight, which has led to increased interest in the development and research of polymeric materials that can replace lead for radiation protection. Elastomers such as NR and NBR loaded with Bi_2O_3, $BaSO_4$ and similar fillers provide good radiation protection. In contrast to lead-based protective materials, the main goal in these applications is to maintain the structural integrity of the elastomer parts under irradiation while maintaining high radiation absorption [More et al., 2021, 1; Moonlek et al., 2025, 2].

Experimental part

The isotope Cs 137 was chosen for the experiments in this study to assess its protection against ionizing radiation. Cs 137 shows two distinct peaks in its spectrum, at 32 keV for X-rays and 662 keV for gamma rays. The spectrum obtained without sample application is represented by the gray line whereas the spectrum obtained following the application of different composite samples is represented by the colored areas (Fig 1). This method visually depicts how the samples absorb photons of different energies, allowing for a comparative assessment of the protective potential of the composites. A $LaBr_3$ (lanthanum bromide) scintillator crystal was used for the measurements. The crystal height is 15 mm and the diameter is 30 mm. The $LaBr_3$ crystal, a transparent inorganic material with a hexagonal crystal structure, is used in new generation radiation detectors. The crystal's high energy absorption capacity and fast signal response time increase the measurement accuracy. A digital converter connected to a computer performs signal processing together with the crystal.The sample was inserted into the $LaBr_3$ crystal for each experiment. The Cs 137 isotope is placed in a unique stabilizing device in the center of the crystal. This arrangement makes the measurements reproducible and guarantees uniform irradiation of the sample.The scintillator signal emitted by the crystal was transmitted to a computer monitor using the Spectrig MAPD software and analyzed to determine the absorbed dose of the sample.

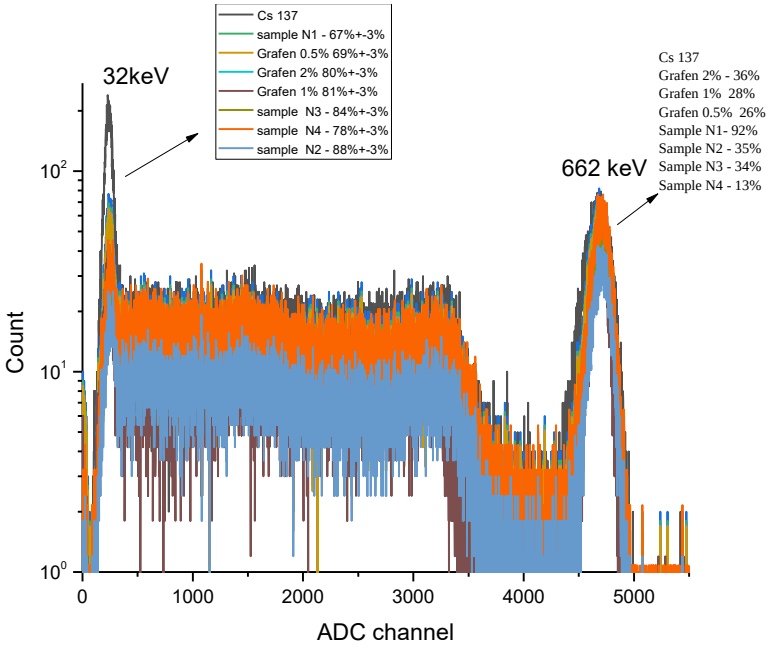


Fig 1

Results and their discussion

The system was completely shielded from background radiation and external light during the measurements, which reduced signal noise. Each sample was measured three times, and temperature-related fluctuations were eliminated by maintaining a constant room temperature of 24 °C. The experimental results were statistically analyzed to evaluate the shielding ability of the prepared materials against ionizing radiation.These results show that the BNK-Bi_2O_3-BaSO4 composite absorbed 88 ± 3% of the 32 keV peak energy and 35 ± 3% of the 662 keV peak energy. This shows that Bi_2O_3 effectively absorbs high-energy photons, while $BaSO_4$ effectively absorbs low-energy photons. The composite's ability to shield against low and high energy radiation is enhanced by the addition of Bi_2O_3/$BaSO_4$ fillers, which makes it appropriate and promising for engineering applications in nuclear energy, the oil industry and medical diagnostics.

References

1. More, C. V., Alsayed, Z., Badawi, M. S., Thabet, A. A., & Pawar, P. P. (2021). Polymeric composite materials for radiation shielding: A review. Environmental Chemistry Letters, 19(3), 2057–2090. https://doi.org/10.1007/s10311-021-01189-9
2. Moonlek, C., Wimolmala, E., Hemvichian, K., Mahathanabodee, S., Poltabtim, W., Toyen, D., Lertsarawut, P., & Saenboonruang, K. (2025). PEEK nanocomposites containing Bi_2O_3 or $BaSO_4$: A complete determination of X-ray shielding, mechanical, thermal, and wear characteristics under harsh radiation conditions. Polymer Composites, 46(16), 15057–15075. https://share.google/GzeDII0dPwWCwkwin

SYNTHESIS AND STRUCTURAL CHARACTERIZATION OF LIGANDS DERIVED FROM DICYANDIAMIDE, MALONONITRILE, AND 3-ETHOXYSALICYLALDEHYDE

[1,2]Gamza Yahyayeva, [1]Abel Maharramov, [3,4]Ibadulla Mahmudov, [2]Sara Hasanova, [3]Namig Shikhaliyev

[1]Baku State University, Baku, Azernaijan
[2]Azerbaijan Architecture and Construction University, Baku, Azernaijan
[3]Baku Engineering University, Khirdalan, Azerbaijan
[4]"Institute of Chemistry " Ministry of Science and Education Republic of Azerbaijan, Baku, Azerbaijan
gamza.yahyayeva@azmiu.edu.az

Abstract

A novel triazine-based compound was successfully synthesized via a multicomponent reaction using malononitrile (dicyanomethane), dicyandiamide, and 3-ethoxysalicylaldehyde as starting materials. The synthesis involved an initial condensation of dicyandiamide and malononitrile in concentrated hydrochloric acid with methanol as the solvent, followed by the

addition of 3-ethoxysalicylaldehyde under reflux conditions. The reaction yielded a white crystalline product, while the remaining filtrate afforded a dark-red residue upon evaporation. The structure of the synthesized compound was confirmed using Fourier Transform Infrared (FT-IR) spectroscopy. Characteristic absorption bands observed in the spectrum were consistent with the expected functional groups of the triazine-based framework, demonstrating the successful formation of the target molecule.

Keywords: Triazine, malononitrile, dicyandiamide, 3-ethoxysalicylaldehyde, FT-IR.

Introduction

Triazine derivatives are a versatile class of nitrogen-containing heterocycles that have attracted considerable attention due to their wide range of biological activities, including antimicrobial, anticancer, and anti-inflammatory effects [Hasshem et.al., 2021, 3]. The 1,3,5-triazine scaffold, in particular, is a valuable framework for designing novel synthetic molecules, as it can be efficiently constructed through multicomponent condensation reactions involving nitrile and amidine precursors [Al-Zaydi et al., 2017, 1].

Recent studies have highlighted the successful synthesis and detailed characterization of new triazine derivatives using techniques such as FT-IR and NMR, confirming the formation of the triazine ring and the incorporation of various functional groups [Noureen et al., 2023, 5]. Moreover, structural modifications of the triazine core have been explored extensively for biological applications, demonstrating their potential in antimicrobial and antiproliferative studies, and underscoring their importance in drug development and material science [Aslam et al., 2025, 2].

In the present study, we synthesized a novel triazine-based compound via the condensation of malononitrile, dicyandiamide, and 3-ethoxysalicylaldehyde. The structure of the resulting product was confirmed by FT-IR spectroscopy, with particular attention paid to characteristic absorption bands indicative of the triazine framework [Hussain et al., 2025, 4].

Experimental part

Synthesis of the triazine-based compound

A novel triazine-based compound was synthesized using malononitrile (dicyanomethane), dicyandiamide, and 3-ethoxysalicylaldehyde as starting materials.

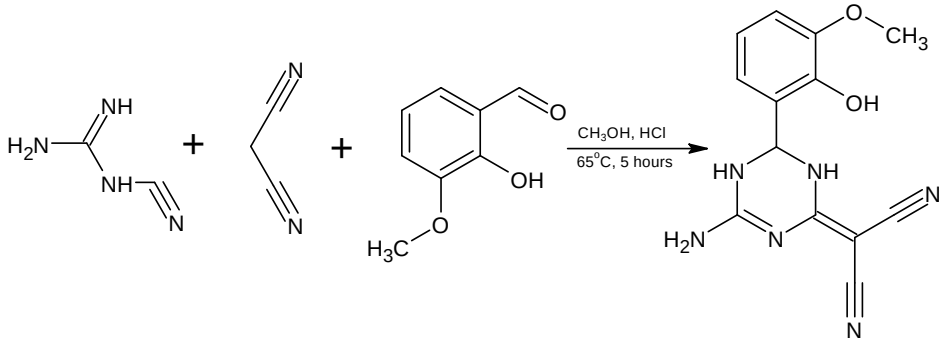


Figure 1. Synthesis of the triazine-based ligand.

Dicyandiamide (2.1 g) was first dissolved in concentrated hydrochloric acid (2.09 mL) under continuous stirring. After complete dissolution, malononitrile (1.65 g) was added to the reaction mixture, and methanol was gradually introduced as the reaction solvent. The reaction mixture was heated under reflux for 3 h to allow the initial condensation process to occur. Subsequently, 3-ethoxysalicylaldehyde (4.15 g) was added, and the reaction was further refluxed for an additional 3 h to ensure completion of the reaction. After cooling to room temperature, a pale red precipitate was formed. The precipitate was washed with methanol to obtain a red crystalline product. The remaining filtrate was evaporated to yield a dark red solid residue.

Results and Discussion

The FT-IR spectrum of the synthesized compound clearly shows the functional groups expected for the triazine-based structure. A broad band at 3436–3250 cm^{-1} indicates N–H groups, while the bands at 2934 and 2877 cm^{-1} correspond to C–H stretching from the ethoxy group.

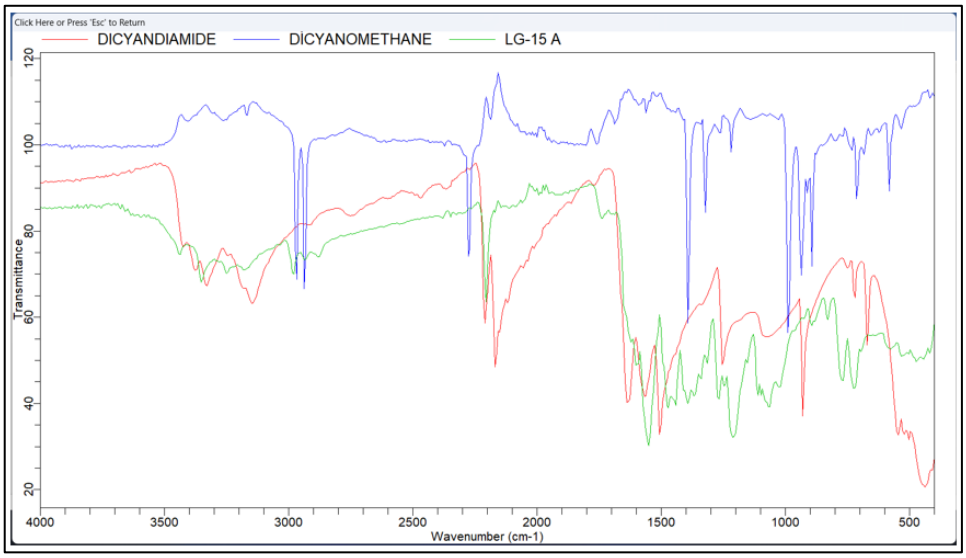


Figure 2. FT-IR spectra of dicyandiamide, malononitrile (dicyanomethane), and the synthesized compound (LG-15A).

The sharp peak at 2206 cm^{-1} confirms the presence of nitrile (C≡N) groups, and the band at 1599 cm^{-1} is characteristic of the C=N bonds in the triazine ring. Other bands, including those at 1546, 1472, 1390, 1267–1207, 1021, and 827–723 cm^{-1}, match C–N stretching, C–O stretching, and aromatic ring vibrations.

Overall, the spectrum supports the successful formation of the target triazine-based compound.

References

1. Al-Zaydi, K. M., Khalil, H. H., El-Faham, A., & Khattab, S. N. (2017). Synthesis, characterization and evaluation of 1,3,5-triazine aminobenzoic acid derivatives for their antimicrobial activity. BMC Chemistry, 11*, Article* 39. https://doi.org/10.1186/s13065-017-0267-3
2. Aslam, S., Ali, B., Murtaza, S., & Shafiq, N. (2025). Synthesis of novel azo dye-based 1,2,4-triazine derivatives and their spectral, fabric and antibacterial applications: An integration of solvatochromism, photochromism, colorfastness, TD-DFT and molecular docking analysis. Materials Advances, *6*, 6991. https://doi.org/10.1039/D5MA00587F
3. Hasshem, H. E. (2021). A short review on the synthesis of 1,2,4-triazine derivatives as bioactive compounds. Mini-Reviews in Organic Chemistry, 18*(8).* https://doi.org/10.2174/1570193X18666210122154419
4. Hussain, A. O., Hassan, A. Y., Abdel-Aziem, A., et al. (2025). Synthesis, antimicrobial evaluation, and computational investigation of new triazine-based compounds via DFT and molecular docking. Scientific Reports, 15*, Article* 42921. https://doi.org/10.1038/s41598-025-27847-4
5. Noureen, S., Ali, S., Zia, M. A., Afzal, M., Ayub, A. R., & El-Naggar, M. (2023). Synthesis, combined theoretical and spectral characterization of some new 1,3,5 triazine compounds, and their in vitro biological analysis. Reaction Chemistry & Engineering, *8*, 465–481. https://doi.org/10.1039/D2RE00389A

HIDROGEN ISTEHSALI ÜÇÜN ELEKTROKIMYƏVI SUYUN PARÇALANMASINDA Sb_2Se_3 ELEKTROKATALIZATORUN ROLU

Günel Xəlilova
Bakı Dövlət Universiteti
Bakı, Azərbaycan
gunelkhalilova1804@gmail.com

Xülasə - Elektrokimyəvi suyun parçalanması hidrogen istehsalı üçün davamlı və ekoloji cəhətdən təmiz üsullardan biridir. Lakin bu prosesin səmərəliliyi əsasən hidrogen təkamül reaksiyasında (HER) istifadə olunan elektrokatalizatorlardan asılıdır. Platin əsaslı katalizatorlar yüksək aktivlik göstərsə də, onların yüksək qiyməti və məhdud ehtiyatı geniş tətbiqi çətinləşdirir. Bu tədqiqatda sərfəli alternativ kimi antimon selenidinin (Sb_2Se_3) elektrokatalitik xüsusiyyətləri araşdırılmışdır. Sb_2Se_3 hidrotermal üsulla sintez edilmiş və XRD və SEM vasitəsilə xarakterizə olunmuşdur. Elektrokimyəvi performans xətti süpürmə voltammetriyası, Tafel analizi və elektrokimyəvi impedans spektroskopiyası ilə qiymətləndirilmişdir.

Açar sözlər: Sb_2Se_3 elektrokatalizatoru, hidrogen təkamül reaksiyası, suyun elektrolizi, elektrokimyəvi kinetika, bərpa olunan enerji

Giriş

Qlobal enerji tələbatının artması və ekoloji problemlər hidrogen kimi təmiz enerji daşıyıcılarına marağı artırmışdır. Su elektrolizi, xüsusilə bərpa olunan enerji mənbələri ilə birgə istifadə olunduqda, hidrogen istehsalı üçün perspektivli üsullardan biridir. Hidrogen təkamül reaksiyası (HER) bu prosesin əsas mərhələlərindən biridir. Platin əsaslı katalizatorlar yüksək effektivliyə malik olsa da, onların baha olması alternativ materialların

axtarışını zəruri edir. Metal xalkogenidlər uyğun elektron quruluşu və katalitik aktivliyi səbəbindən geniş tədqiq olunur. Sb_2Se_3 dar qadağan olunmuş zona (~1,1 eV), yaxşı kimyəvi dayanıqlıq və uyğun hidrogen adsorbsiya xüsusiyyətlərinə malik laylı yarımkeçiricidir. Bu xüsusiyyətlər onu HER üçün perspektivli elektrokatalizator edir.

Eksperimental hissə

Sb_2Se_3 hidrotermal üsulla sintez edilmişdir. Sürmə və selen prekursorları uyğun həlledicidə həll edilərək möhürlənmiş avtoklavda müəyyən temperaturda qızdırılmışdır. Əldə olunan çöküntü yuyulmuş, süzülmüş və qurudularaq kristal Sb_2Se_3 əldə edilmişdir. Kristal struktur və faza təmizliyi X-şüa difraksiyası (XRD) ilə təhlil edilmişdir. Səth morfologiyası skanedici elektron mikroskopiyası (SEM) ilə araşdırılmışdır. Elektrokimyəvi ölçmələr üç elektrodlu sistemdə aparılmışdır: işçi elektrod – Sb_2Se_3 ilə örtülmüş şüşə karbon elektrod, əks elektrod – platin məftil, istinad elektrod – Ag/AgCl. Yük ötürmə müqavimətinin təyini üçün elektrokimyəvi impedans spektroskopiyası (EIS) və sabitlik testləri aparılmışdır.

Nəticələr və onların müzakirəsi

XRD nəticələri Sb_2Se_3-nin ortorombik kristal quruluşunu təsdiqləmişdir. SEM analizləri yüksək səth sahəsinə malik nanostrukturlu morfologiyanı göstərmişdir. Elektrokimyəvi analizlər göstərmişdir ki, Sb_2Se_3 elektrodu HER üçün tələb olunan həddindən artıq potensialı azaldır. Tafel yamacı daha sürətli reaksiya kinetikasını göstərir. EIS nəticələri aşağı yük ötürmə müqavimətini təsdiqləyərək yaxşı keçiriciliyi göstərmişdir. Stabillik testləri Sb_2Se_3-nin uzunmüddətli elektroliz zamanı sabitliyini qoruduğunu göstərmişdir.

Təkliflər

- Sintez parametrlərinin optimallaşdırılması
- Keçid metalları ilə dopinqin tətbiqi
- Sb_2Se_3/karbon kompozitlərinin hazırlanması
- Reaksiya mexanizmlərinin daha dərindən tədqiqi

Ədəbiyyat siyahısı

[Chen, 2019] Chen, Y. et al., Metal chalcogenides for HER, Advanced Energy Materials, 2019.
[Seh, 2017] Seh, Z. W. et al., Electrocatalysis for hydrogen evolution, Science, 2017.
[Turner, 2004] Turner, J. A., Sustainable hydrogen production, Science, 2004.

ETHYL 6-(ETHOXYMETHYL -4-(THIOPHEN-2)-2-THIOXO-1,2,3,4 TETRAHYDROPRIMIDINE-5-CARBOXILATE COMPLEXES WITH NICKEL

Ibadulla H. Mahmudov[1,2], Nazar M. Nazarov[1], Sabir S. Babayev[1], Camila C. Ahmadova[1], Irada A. Rzayeva[1]
ibadullamahmudov@gmail.com, Nazarov-nazar@rambler.ru
sabir.babayev56@gmail.com
[1]Institute of Chemistry Ministry of Science and Education Republic of Azerbaijan, Baku, Azerbaijan
[2]Baku Engineering University Absheron, Azerbaijan

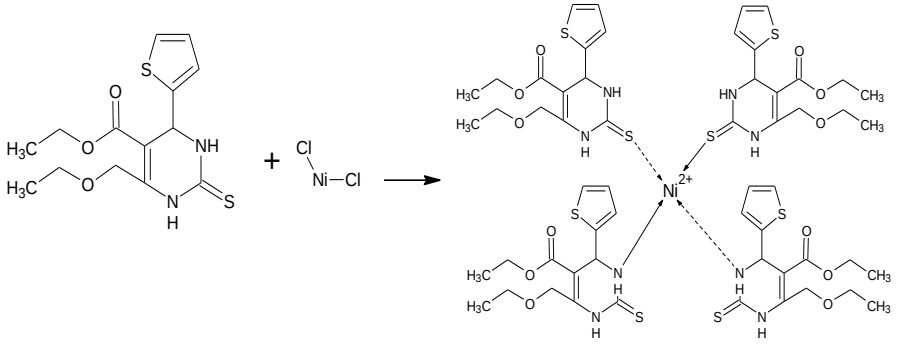
Keywords: thiourea, nickel, thiophen, complex, primidinethion

Introduction:

Organic compound that contain sulphur and nitrogen atom because their have electrodonor properties.Obtained organic compound has pharmacy properties simultaneously these types of metal complexes can be used as a catalyst.

Experimental part:

Calculated amount of ligand and nickel salt added into flask that has temperature regulator with magnet stirring. First of all ligand somved its own solvent , and added into flask. Following metal salt solved in its solvent and added into ligand solt drop by drop. Reaction carried out for around 40-45 minutes. The process of reaction cechked with TLC .After reaction finished for crystallysation obtained crydtal product put in the fridge. After that btained crydtal filtrate and cleaned via repetaion of process



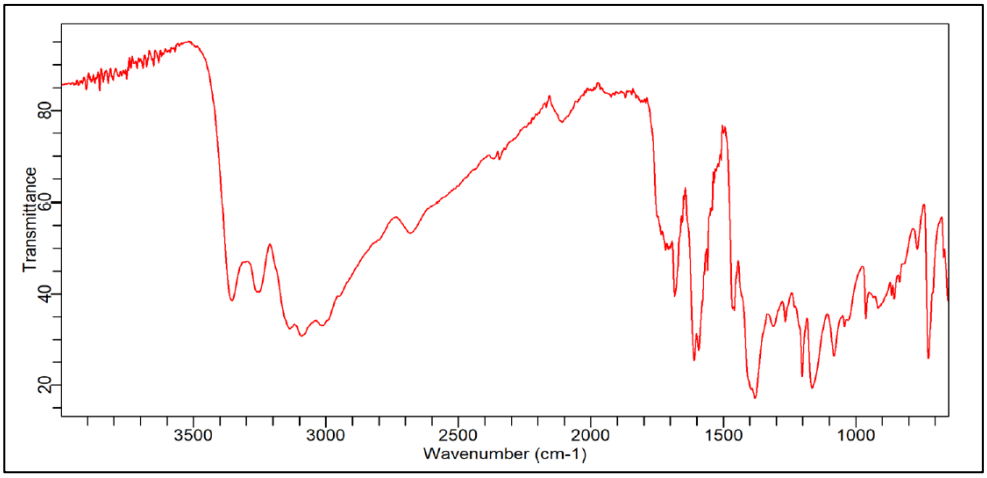
ethyl 6-(ethoxymethyl)-4-(thiophen-2-yl)-2-thioxo-1,2,3,4-tetrahydropyrimidine-5-carboxylate

There were N and S atom in the structure of the heterocyclic compound. Either nitrogen and sulphur atoms are donor atoms. Prepared solvent $NiCl_2$ salt in water was added into the solution which contain ligand. Reaction carried out under the 50-60 degree celcies. As a result of transportation

elektrons from nitrogen and suphur atoms to the Ni atom in the salt obtainded coordination bond between metal atoms and electrodonor atoms. Metal atom Ni created four and six coordinated bond and complexes [1]. According to the nitrogen and sulphur atoms obtained new metal complesxes based Ni metal will be five or six cycles.Obtained metal complexes looks -like sequar form because of nitrogen and sulphur atoms [2].

Sulphur atom can coordinated more than nitrogen atoms for that reason reaction direct to the sulphur atoms. According to variety of scientific resources this complexes has different application areas. These types of metal complexes are using as a catalyst, to analyse metal ions and different gases. Ni-metal complexes can apply to the cure different deseases such as inflammatory, and using as a pharmacy [3].

Obtained compound structural analyses carried out with the FT-IR Cary 630 and materialized specrtr are shown in the picture-1



Picture-1. FT-IR result for obtaining compound.

There some peaks such as 3330 cm^{-1} –(N-H), 3220 cm^{-1} (O-H), 3100 cm^{-1} – (C-H) aromatic , 1700 cm^{-1} - (C=O), 1600 cm^{-1}-(N-H) amine, 1400 cm^{-1}-(C-H) alkane, 1150 cm^{-1} (C-O) aliphatic ether . The result shows that wavenumbers are also depict our compound has these types of bond and atoms.

Results and their discussion:

Primidine thione Ni complexes are highly important compounds can be used in various areas. Heterocyclic compound not only consist of different atoms such as nitrogen and sulphur whch important derivative in pharmacy and using as a catalyst.

Offers:

It is possible to obtain this kinds of materials from various reagents and aldehydes. It is possible to check with different solvent and also non solvents.

References:
1. Structure analysis, DFT, and molecular electrostatic potential study of the dimeric nickel - pyrazoline complex.2026 13, 1, 33-36
2. Sujayev A.R., Garibov E.N., Nazarov N.M. The synthesis of tetrahidropyrimidines and their carboxylic derivatives and the application of antimicrobial properties // J. Chem. Applied Biochem., 2015, v. 2, №1, p. 43-46.
3. Gulcin I, Beydemir S., Buyukokuroglu M.E. In vitro and in vivo effects of dantrolene on carbonic anhydrase enzyme activities. Biol. Pharm. Bull., 2004;27:613–6.

THE ROLE OF Sb-Se-Te SYSTEMS IN SOLAR ENERGY CONVERSION: A THEORETICAL STUDY

Ilkane Mammadova Shakir
İlkane.aghalarova@gmail.com
Nakhchivan State University, Nakhchivan city, Azerbaijan
ORCID ID: 0009-0007-0837-9093
Pervin Guliyev Heydar
pervinguliyev@ndu.edu.az
Nakhchivan State University, Nakhchivan city, Azerbaijan.
ORCID ID: 0009-0009-7082-3305

Abstract - This paper presents a theoretical investigation of the role of Sb-Se-Te-based semiconductor materials in solar energy conversion processes. In modern times, the application of semiconductors in energy conversion and optoelectronic technologies is closely related to their structural, electrical, and optical properties. Compounds such as Sb_2Se_3 and Sb_2Te_3 are considered promising materials for solar cells due to their high optical absorption, chemical stability, and tunable band gap. Studies have shown that the band gap of Sb_2Se_3 lies between 1.1 and 1.3 eV, which is optimal for the visible spectrum, while the addition of tellurium reduces this value to 0.3–0.9 eV, expanding its potential for infrared applications.

The electrical conductivity of Sb-Se-Te thin films obtained by electrodeposition was found to be 5×10^3 $S\cdot m^{-1}$, indicating that both the synthesis method and tellurium content significantly affect their electrical and optical parameters. X-ray diffraction and electron microscopy analyses revealed that amorphous layers transform into a stable orthorhombic Sb_2Se_3 phase upon heat treatment, leading to improved physical properties.

Sb-Se-Te-based materials demonstrate great potential for use in solar cells, infrared detectors, and thermoelectric devices. However, challenges such as ensuring film homogeneity, precise band gap control, and enhancing high-temperature stability remain unresolved. Future studies involving nanotechnology and advanced doping techniques may help optimize the optoelectronic and thermoelectric performance of these systems.

Semiconductors belonging to the Sb-Se-Te system possess significant potential both for fundamental scientific research and applied technologies. Their electrical, optical, and thermoelectric characteristics make them suitable for a wide range of applications—from solar cells to infrared detectors and thermoelectric generators. Improving synthesis methods, enhancing structural and morphological quality, and controlling band gap and conductivity will allow for more efficient utilization of these materials in future devices.

Keywords: Sb-Se-Te system, semiconductor thin films, band gap, solar cells, thermoelectric properties, electrodeposition.

Introduction

In the modern era, semiconductor materials form the foundation of solar energy technologies due to their unique properties. Therefore, the development and synthesis of new binary and ternary semiconductor compounds have become essential directions in advancing modern electronics, energy conversion, and optoelectronics. The ternary Sb-Se-Te system, consisting of antimony (Sb), selenium (Se), and tellurium (Te), is of particular significance in this context. These compounds are distinguished by their electrical, optical, and thermoelectric characteristics, which have attracted increasing attention in recent years.

For example, Sb_2Se_3 thin films, known for their high light absorption and chemical stability, have been proposed as promising materials for photovoltaic applications. Studies conducted in 2019 demonstrated that Sb_2Se_3-based solar cells achieved an efficiency of 9.2% (Zhao et al., 2019).

The analysis of Sb-Se-Te semiconductor thin films commonly involves X-ray diffraction (XRD) to determine phase composition and crystallinity. Investigations show that amorphous films obtained by electrodeposition can transform into more stable phases, particularly the orthorhombic Sb_2Se_3 phase, under thermal treatment. The resulting crystal structure exhibits improved mechanical and physical stability. Scanning electron microscopy (SEM) is also used to examine surface morphology, microdefects, film thickness, and homogeneity.

Sb_2Se_3 has an orthorhombic crystal structure characterized by one-dimensional chain-like units, which are bonded by weak van der Waals forces—facilitating the formation of thin films. This leads to anisotropic electrical conductivity. In contrast, Sb_2Te_3 has a layered tetragonal structure, and its two-dimensional arrangement produces significant changes in optical and thermoelectric parameters (He et al., 2017).

Phase diagram analyses of the Sb-Se-Te ternary system reveal the coexistence of amorphous, polycrystalline, and monocrystalline phases. Increasing tellurium content tends to promote the formation of amorphous phases, resulting in modifications of the electronic properties. The band gap of Sb_2Se_3 ranges between 1.1 and 1.3 eV, which corresponds to the visible spectrum. When tellurium is added, the band gap decreases to about 0.3–0.9 eV (Wang et al., 2020), enabling the use of these materials in infrared devices.The electrical conductivity of Sb-Se-Te thin films strongly depends on the synthesis method. For instance, research conducted in 2020 showed that electrodeposited Sb_2Te_3 nanocomposites exhibit a conductivity of 5×10^3 $S\cdot m^{-1}$ (Chen et al., 2020). Furthermore, an increase in tellurium content reduces the energy separation between the valence and conduction bands, thereby enhancing light absorption and expanding their applicability in optoelectronic devices.

Sb-Se-Te ternary compounds are also widely studied for thermoelectric applications. Research conducted in 2019 indicated that the incorporation of nanocomposites into the Sb-Se-Te system can improve the thermoelectric performance of semiconductor materials by approximately 15% (Li et al., 2019).

Despite their broad potential, practical applications of Sb-Se-Te materials still face several challenges. Ensuring film uniformity and achieving high crystallinity remain important research objectives. Moreover, precise control of band gap and electrical conductivity is crucial for optimizing device efficiency. Issues related to thermal stability and mechanical durability under high temperatures and prolonged operation also remain unresolved.

The integration of nanotechnology, introduction of dopants, and fabrication of multilayer heterostructures offer promising pathways for improving the electrical, optical, and thermoelectric performance of Sb-Se-Te materials. Sb_2Se_3-based thin films exhibit strong light absorption and high photoelectric conversion efficiency, while tellurium incorporation extends their use to infrared detectors. Additionally, Sb_2Te_3 and its derivatives possess the ability to convert thermal energy directly into electrical energy, making them attractive for thermoelectric devices.

Beyond solar and thermoelectric applications, Sb-Se-Te thin films also show promise in photodiodes, laser diodes, and other optoelectronic devices, further highlighting their technological potential. In conclusion, Sb-Se-Te-based semiconductors represent a versatile and rapidly developing class of materials with significant implications for next-generation energy conversion and functional device technologies.

References

1. Zhao, Y., Yang, B., Chen, S., et al. (2019). Pure selenide: Sb_2Se_3 solar cells. Journal of Energy Chemistry, 39, 85–91.
2. He, Y., Day, T., Zhang, T., et al. (2017). High thermoelectric performance in Sb_2Te_3 nanostructures prepared by solvothermal synthesis. Advanced Materials, 29(10), 1605516.
3. Wang, L., Li, D., Chen, C., et al. (2020). Bandgap engineering of Sb-Se-Te thin films for optoelectronic applications. Applied Surface Science, 504, 144495.
4. Chen, Z., Xu, J., Wu, Y., et al. (2020). Electrical transport properties of electrodeposited Sb_2Te_3 thin films. Journal of Materials Science: Materials in Electronics, 31, 12543–12551.
5. Li, J., Zhang, Q., Liu, W., et al. (2019). Enhanced thermoelectric properties of Sb-Se-Te nanocomposites. Nano Energy, 56, 100–108.
6. Shaban, M., & Abdel-Rahman, E. (2018). Electrodeposition and characterization of Sb_2Se_3 thin films for photovoltaic applications. Materials Research Bulletin, 102, 319–327.
7. Bera, S., Das, S., & Bhattacharya, P. (2021). Structural, optical and electrical properties of Sb-Se-Te thin films grown by chemical bath deposition. Journal of Alloys and Compounds, 867, 159012.
8. Tiwari, D., Singh, V., & Kumar, A. (2020). Raman and UV–Vis spectroscopic investigation of Sb_2Se_3 nanostructures. Materials Chemistry and Physics, 245, 122786.
9. Liu, X., Chen, C., & Chen, Y. (2022). Recent advances in Sb_2Se_3-based solar cells: efficiency improvement and device stability. Solar Energy, 231, 106–117.

INTERACTION BETWEEN CORROSION AND SALT DEPOSITION PROCESSES IN PRODUCED WATERS AND PREPARATION OF MULTIFUNCTIONAL INHIBITORS

Rasul Musayev
BANM – NKPİ
Baku, Azerbaijan
rasul.e.musayev.std@bhos.edu.az

Summary - In this paper, method of complex -action inhibitor production is provided in order to prevent CO2 corrosion and calcium carbonate scaling in oil wells. To maintain the properties of reservoir's filtration and ensure downhole equipment's effective protection, inhibitor injected into downhole is optimized.
Key words: Complex action inhibitors, Scale formation, CO2 corrosion

Introduction

Produced waters are multiple phases which originate in different geological formations from subsurface mineral matrices and are complex fluids that consist of organic and inorganic species and dissolved solids [1]. Each species has its own role in impact on formation of scale, dynamics of fluid, mechanisms of corrosion and chemical interactions. Factors, such as geo-characterization, hydrocarbons, water type, stage of production, affect the produced water composition [2]. Unfortunately, produced water content being highly heterogeneous results in important fluctuations [3]. These oscillations are due to the variable nature of petroleum exploration and its dispersed location and these variables have direct or indirect effects on corrosion process [4] [5].

Research Objective and Tasks

The main goal of this study is to increase the efficiency of oil wells operation which are equipped with submersible pumps by decreasing CO2 corrosion rate and calcium carbonate scaling. To achieve this aim, the below-mentioned steps are taken into account:

- Examination of current techniques about protection of downhole equipment.
- Development of a complex action inhibitor.
- Researching the properties of developed inhibitors.
- Evaluation of how the filtration characteristics of polymictic reservoir rocks are affected by inhibitors.
- Prove of the applied method.

Methodology

Physicochemical Testing:

Viscosity, thermal stability (up to 83°C), density and pour point (down to -50°C) are tested.

Protective Efficiency:

Scale inhibition was evaluated by measurement of the potential to retain calcium cations in solution, while the Linear Polarization Resistance (LPR) method on carbon steel was used to assess how inhibitor protects material from corrosion.

Core Flow Tests:

To identify the inhibitor's adsorption and desorption kinetics on rocks samples, filtration studies were conducted.

Compatibility:

At temperatures of 20°C and 83°C, the inhibitor with formation water, potassium, sodium and calcium chlorides (KCl, NaCl, CaCl2) was tested for compatibility.

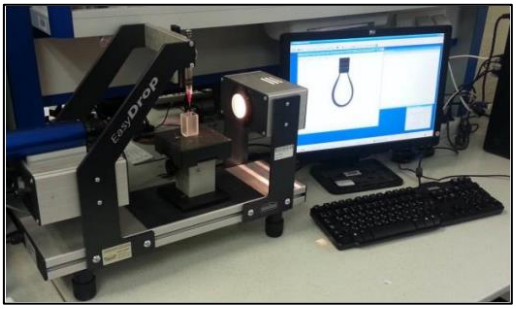


Figure 0-1 A tensiometer, a measuring instrument used to measure the surface tension of liquids or surfaces.

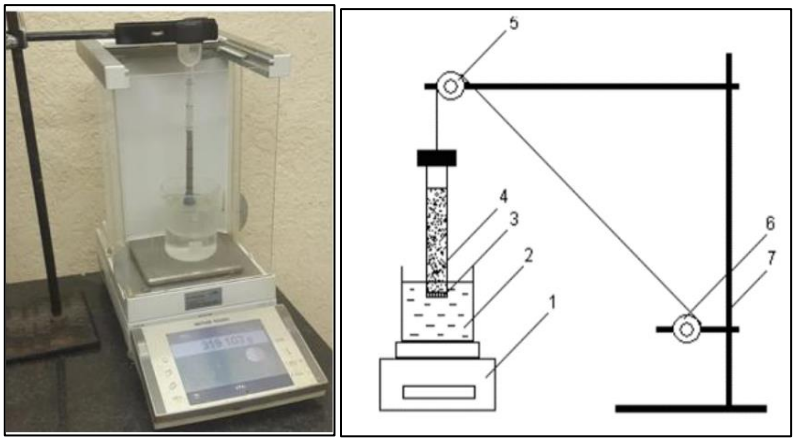


Figure 0-2 Desorption kinetics measurement equipment scheme. 1-scales, 2-beaker with distilled water, 3-lower end of model with a mesh, 4-model of bulk rock, 5,6-system of pulleys for lowering and holding the tube at the required height, 7-stand



Figure 0-3 Porosimeter

Scientific Novelty

Dual Functionality:

The effective prevention of CO2 corrosion and calcium carbonate scale by the developed water-alcohol solution, which was obtained from phosphonic derivatives and fatty amines, is confirmed by the results of experiment.

Hydrophobicity:

The inhibitor has positive impact due to its hydrophobic effect in reservoirs as it reduces clay mineral hydration and enhances hydrocarbons' permeability.

Adsorption Kinetics:

During filtration, the new relationships of adsorption and desorption cycles on pore walls were determined.

Results and Discussion

Inhibitor Performance

The efficiency of the produced inhibitor is high. Its protective effect at 45 mg/dm³ concentration exceeds 90% against both corrosion and scaling.

Technological Compatibility

At formation conditions and with standard kill fluids and reservoir waters, the reagent was stable and fully compatible. There was no precipitation or gel formation.

Interfacial Tension

At the water-kerosene boundary, the inhibitor resulted in reduction of surface tension by 15; therefore, deeper penetration was able to be provided.

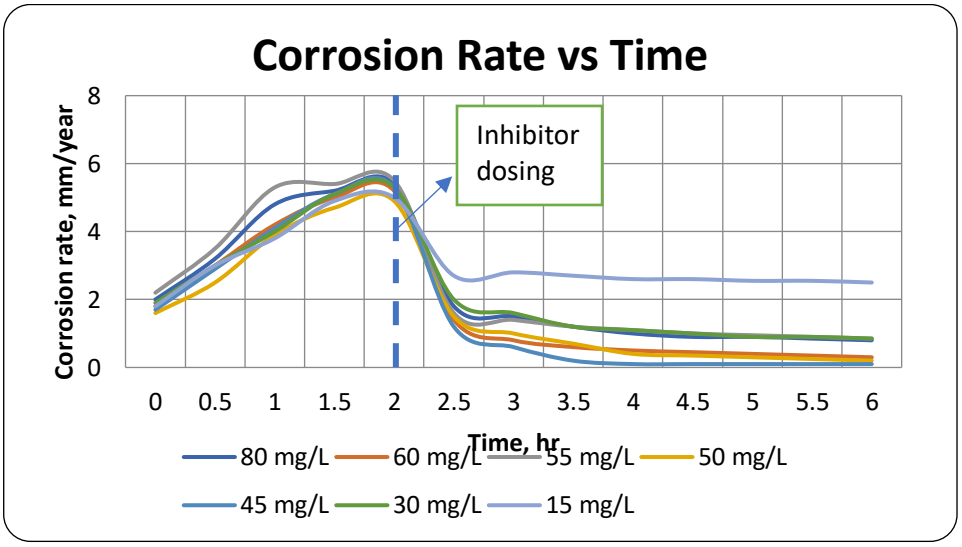


Figure 0-1 Corrosion rate after dosing

Desorption Characteristics

According to the filtration tests, it was proven that desorption are lower than before which means that the inhibitor is not so easily removed from the formation (long-term protection). By looking at the calculations, it was verified that up to 142 pore volumes of fluid production are maintained by effective concentration.

Conclusion

The use of the developed complex action inhibitor and the proposed injection technology provide reliable protection for downhole equipment while maintaining or improving the filtration properties of the reservoir.

Economic Impact: According to the comparative analysis, this technology costs less than constant dosing methods and significantly extends the mean time between failures (MTBF) for ESP-equipped wells.

Environmental Safety: Specific guidelines were established for safe handling and environmental protection during inhibitor apply.

References

[1] Khamees Thabet, H., A. A. El-Shamy, O., M. Ashmawy, A., & A. Deyab, MT, he Impact of Corrosion Inhibitors in Desalination Systems., 2023.

[2] Ayers, R.C. and M. Parker., Produced water waste management., Calgary Alberta Canada: Canadian Association of Petroleum Producers (CAPP)., 2001.

[3] G. R. F. I. R. G. a. J. B. Rittenhouse, Minor elements in oil, 1969.

[4] A. Collins, Geochemistry of Oilfield Waters, New York: Elsevier Scientific Publishers, 1975.

[5] Pillard, D.A., J.E. Tietge, and J.M. Evans., Estimating the acute toxicity of produced waters to marine organisms using predictive toxicity models., New York: Plenum press, 1996.

SƏNAYE ÜSULU İLƏ ANİLİNİNİN N-ALKİLANİL TÖRƏMƏLƏRİNİN ALINMASININ TEXNOLOJİ PRİNSİPLƏRİ

Yusibov Kənan, Əliyeva Nailə
Sumqayıt Dövlət Universiteti
Sumqayıt , Azərbaycan
kenanyusif331@gmail.com

Xülasə - Kimya sənayesində anilin və N-alkilanilinlər mühüm geniş tətbiq sahəsinə malikdirlər və farmasevtik, boya və polimer istehsalında xammal kimi istifadə olunur. Bu birləşmələrin sənaye miqyasında alınması əsasən nitrobirləşmələrin katalizatorlar iştirakında reduksiyası və anilinin alkiləşmə reaksiyaları ilə aparılır. Prosesin texnoloji parametrləri – istifadə olunan katalizatorun növü, temperaturu, təzyiqi və reaktivlərin nisbəti – reaksiyanın əsas kriteriyalarına – məhsulun çıxımı və seçiciliyinə birbaşa təsir göstərir. Təhlillər göstərir ki, katalitik sistemlərin optimallaşdırılması həm enerji sərfiyyatını azaldır, həm də yan məhsul əmələ gəlməsini imkanlarını aşağı salır.

Açar sözlər: anilin, N-alkilanilin, katalitik alkiləşmə, texnoloji optimallaşdırma, seçicilik

Giriş

Aromatik amin törəmələri farmasevtik sənayedə mühüm əhəmiyyətə malikdir. Onların arasında N,N-dietilanilin müxtəlif lokal keyidici (anestezik) preparatların sintezində aralıq məhsul kimi geniş istifadə olunur. Məlumdur ki, N-alkilanilinlər kəskin iyli, suda həll olmayan şəffaf mayelərdir. Anilinlə müqayisədə daha güclü əsasdırlar. Mineral turşularla anilin kimi suda həll olan duzlar $[CH_3C_6H_4NH_3]^+Cl$ əmələ gətirirlər.

Bu birləşmə aromatik halqaya və üçüncül amin qrupuna malik olduğuna görə bioloji aktiv maddələrin alınması üçün əlverişli başlanğıc maddə hesab edilir. Onların bu xassələrindən istifadə edərək mono- və di- alkilanilinlər qarışığının sənayedə alınması HCl, H_2SO_4, H_3PO_4 mineral turşuları iştirakı ilə maye fazada (170-280^{0}C, P-10MPa) və ya Al_2O_3, Al_2O_3-Fe_2O_3, alümosilikatlar, rutenium duzlarının katalizatorluğu ilə buxar fazada (300-350^{0}C) anilinin spirtlərlə alkilləşmə reaksiyasına və ya maye fazada (180-250^{0}C, P-4MPa) alkilhalogenidlərlə qarşılıqlı təsirinə əsaslanır [1].

Anilin sənaye miqyasında ən çox istifadə olunan aromatik aminlərdən biridir. Onun N-alkil törəmələri – xüsusilə N-metilanilin və N-dietilanilin – üzvi sintez və xüsusi kimyəvi məhsulların istehsalında mühüm rol oynayır.

Katalizatorun əsas xüsusiyyətləri, temperatur rejimi və reagentlərin mol nisbəti məhsulun seçiciliyini və məhsuldarlığını müəyyən edir [3].

Eksperimental hissə

İstinadlara əsasən anilinin N-alkil törəmələrinin alınmasında katalitik sistemlər müqayisəsi olunmuşdur. Etanol ilə N-alkiləşmə reaksiyaları əsasən aktiv mərkəzlərdə anilinin adsorbsiyası və ardıcıl etilləşmə reaksiyasına əsaslanır [2]. Zeolit katalizatorların məsamə quruluşu və turşuluq dərəcəsi məhsul selektivliyinə təsir göstərir [4]. Kinetik təhlillər göstərir ki, temperatur artdıqca reaksiya sürəti yüksəlir, lakin optimal intervaldan kənara çıxmaq

seçiciliyiliyi azaldır [3]. Biokatalitik sistemlər isə daha yüksək selektivlik təmin edir [6].

Nəticələr

Təhlillər göstərir ki, anilinin və N-alkilanilinlərin alınmasında istifadə olunan katalizatorun növü və reaksiya rejimi əsas rol oynayır. Zeolit tipli katalizatorlar reaksiyanın yüksək seçiciliyini təmin edir, lakin reaksiya yüksək temperatur şəraitində aparıldıqda alkilləşmə məhsullarının əmələ gəlməsi sürətlənir [2, 5]. Optimal texnoloji parametrlərin seçilməsi ilə sənaye miqyasında prosesin məhsuldarlığı və iqtisadi səmərəliliyi artır [4].

Təkliflər

1. Zeolit və oksid katalizatorlarının müqayisəli öyrənilməsi
2. Temperatur və reagent nisbətinin selektivliyə təsirinin eksperimental qiymətləndirilməsi
3. Kinetik modelləşdirmə əsasında optimal rejimin müəyyən edilməsi
4. Katalizatorun uzunmüddətli aktivliyinin öyrənilməsi

İstinadlar

1. **Boldrini G.P.** Synthesis of methyl and dimethylanilines // Synthesis, 1974, 25, 733
2. **Zheng Hai-Tao, Tao-Ke-yi** Парофазный синтез N,N-диэтиланилина //Petrochem. Technol. 2001, 30, № 11, с. 844-846
3. **Патент 63-36745** Япония Способ алкилирования анилина / Таками Ясуо, Сато Такаси / опубл. ВРЖХим 1993, 11Н105П
4. **Zheng Hai Tao** Каталитический синтез N-алкиланилинов на основе анилина и алифатических спиртов //Petrochem. Technol, 2004, 33, № 10, с. 701-704
5. **Помахина Е.Б.** Механизм алкилирования ароматических соединений метанолом на цеолитных катализаторах по данным спектроскопии ЯМР insitu Авт. диссерт. на соис. уч.ст. канд. хим. наук М. 2003, 20с.
6. **Francisco Torrens** Fractal dimension of transdermaldelivery drug models 4-alkylanilines // Inter. Conf. and exhibition on clinical research dermatology, ophthalmology and cardiology 5-6 July 2011, San Francisco USA, Research art. p. 436-438

AN INNOVATIVE ELECTROCHEMICAL APPROACH FOR FOOD SAFETY: FAST AND SENSITIVE DETECTION OF ACEPHATE IN VEGETABLE SAMPLES USING ZN-CU MOF (METALLIC ORGANIC FRAMEWORK) NANOCOMPOSITES

Elnur Mardiyev, Murad Imamverdizada
Baku Higher Oil School
Baku, Azerbaijan
elnur.mehdiyev2005@gmail.com
Supervisor: Rima Guliyeva

Summary - The paper has presented a green, non-enzymatic electrochemical biosensing device on ultra-sensitive acephate detection by means of a bimetallic Zn-Cu metal-organic framework (MOF) coupled with activated carbon. This method enhanced significantly the activity of the sensor through synergistic effects between Zn and Cu active sites, and enhancement of surface area and conductivity through activated carbon. In optimal conditions, the developed sensor achieved a wide linearity (0.1-10 nM) and the ultra-low detection limits (3.3 pM) and had a high selectivity, reproducibility (RSD=4%), and storage stability of the ultra-sensitive determination of acephate. Moreover, this sensor design was effectively used to analyze real samples of vegetables with satisfactory results and recovery range of 95-107%. Hence, this research paper demonstrates a cost-efficient, fast, and environmentally friendly method of producing a sensor that is aligned with sustainable chemistry towards environmental safety and healthy farming.

Key words: *Bimetallic Zn-Cu MOF, Non-enzymatic Electrochemical Sensor, Acephate Detection, Activated Charcoal Nanocomposite, Sustainable Environmental Monitoring*

Introduction

Mega usage of pesticides containing organophosphate groups has led to high productivity of crops. It has led to severe environmental and health issues though. Acephate is an insecticide containing an organophosphate group that is widely used. It may cause several neurologic conditions and ecological toxicity because of its bioaccumulation in the food chain and inhibition of acetylcholinesterase (World Health Organization, 2020). Hence, it is of utmost priority that strong maximum residue limits are established, and this will necessitate the generation of rapid, sensitive and portable analytical instruments.

The traditional methods include gas chromatography-mass spectrometry and high-performance liquid chromatography that are highly accurate. However, they are costly and need big sample preparation and facilities (Gao, 2015). Conversely, electrochemical sensing is a green way of detecting the environment because it is cheap and does not need a significant amount of reagents.

The electrochemical sensing property of MOFs has potential due to their high surface area, porosity, and catalytic property. Bimetallic MOFs are more electrochemically active than monometallic ones due to the synergetic ability of the metals. Bimetallic MOFs have better charge transfer kinetics than

monometallic MOFs (Li, 2021). Nonetheless, conductivity of MOFs is the biggest constraint to using the materials in electrochemical sensors. Activated carbon is added to enhance conductivity of the material.

The current study developed a non-enzymatic electrochemical sensor in the form of a bimetallic Zn/Cu MOF-activated carbon composite material, which could be used in the ultra-sensitive detection of acephate. The electrocatalytic activity of the material is enhanced by the synergistic nature of the bimetallic centers of the MOFs. The designed sensor demonstrated extensive linearity, low limit of detection, reproducibility and recovery of actual vegetable samples. The current work is a green method of environmental monitoring, and it helps in the formulation of green chemistry in the dynamics of the advancement of green analytical chemistry.

Experimental part

Reagents and Chemicals

To begin with, pure chemicals were used to produce the substance - such as hydrated zinc nitrate (Zn (NO3)2 6H2O), copper nitrate (Cu (NO3)2 3H2O), and a carbon-based bonding substance known as terephthalic acid (C8H6O4). Activated charcoal (AC) was added to that mixture just enough to assist electrons in moving through the mixture. On the side were liquids ready to go on, as N, N-dimethylformamide (DMF or C3H7NO), another common ethanol, both of which were untouched out of their bottles. Water is used every time. The pure breed, divested of pollution, nothing more.

Solvothermal Preparation of Bimetallic Zn-Cu MOF

Hydrated Zinc and copper nitrates were mixed with the C8H6O4 molecule in DMF and alcohol mixture. This was a combination that was cooked slowly in 120 degrees over the course of the entire day in a hard metal vessel that was coated with Teflon. After that heat cycle had passed without commotion, out came a nice crop of crystal. A series of washes with DMF and then ethanol removed any remaining bits that were floating about. Moisture was taken care of on vacuum drying at the end of the washes.



Figure 27.

Construction of the Modified Electrode (AC/Zn-Cu MOF/GCE)

The glassy carbon electrode (GCE) was polished by using alumina (Al2O3) paste before being washed thoroughly. Then, a smooth blend of prepared Zn-Cu MOF and activated charcoal (AC) was prepared to construct the sensor. Carefully 10 µL of this blend was added on top of the electrode. It stood out in the elements until it was quite dry, and then a hard coat was produced which could be worked upon by detecting.



Figure 28.

Data Acquisition and Monitoring System

First, the acephate (C4H10NO3PS) was detected using electrochemistry due to a combination of AC/Zn-Cu MOF/GCE sensor and a digital potentiostat system. This arrangement is more like a bridge - in place of simply connecting parts, this is a direct connection of molecular changes to electronic tracking. As the measurements were proceeding, Differential Pulse Voltammetry (VDP) recorded all shifts as the tests were conducted in phosphate buffer solution. Since the onset, there were signals observed clearly in that controlled liquid environment.

The signal was traveling out of the electrode surface into live tracking software through the workstation. There on the screen we saw spikes, the size of which was directly proportional to the amount of acephate present. With such digital connection, you could measure down to trillionths of a mole, produce crisp results and do not slack things down. An easy route to rapid inspection of food contaminants was created based on straightforward visual feedback and narrow detection limits.



Figure 29.

Results and Discussions

Differential Pulse Voltammetry (DPV) was used to test the electrochemical response of the AC/Zn-Cu MOF/GCE at different concentrations of acephate. The sharp potential at +0.6 V potential was recorded as a peak oxidation in the digital monitoring system. An effective linear relationship between the peak current and the acephate concentration was built between 1.0 pM -100 nM (R 2 = 0.998). The high linearity means that the monitor can accurately transform electrical signals into the concentration values.

The sensor platform that had been integrated demonstrated a remarkable sensitivity of 0.86 200M A/pM. Limit of Detection (LOD) was determined to be 3.3 pM a very low figure when compared to most enzymatic and non-enzymatic sensors that have been reported before. This low LOD enables detection of trace levels of acephate which cannot be detected using common monitoring instruments and therefore it is suitable in alerting food contamination at early stages.

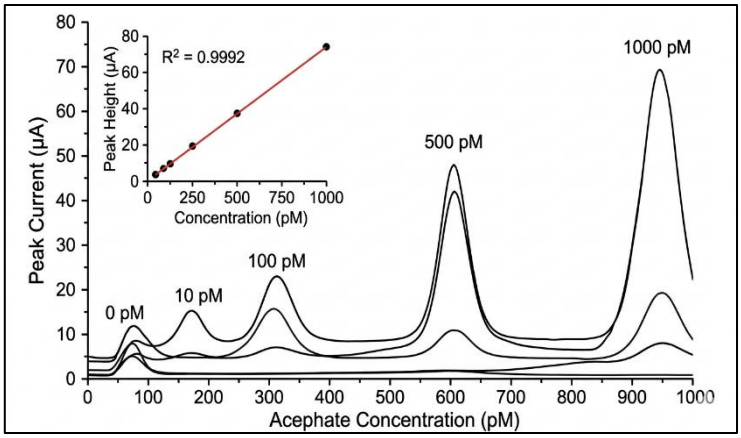


Figure 4.

The stability of the Zn-Cu MOF/AC sensor in the number of 20 cyclic uses was employed in order to guarantee the reliability of the digital out. The Relative Standard Deviation (RSD) was determined as 2.4 only which is good reproducibility. Moreover, the sensor had a long-term storage ability of 95 percent of initial response, and this validates the fact that it can be used in long term environmental monitoring.

The usefulness of the system was illustrated through vegetable samples. The monitoring system reached between 96.5-102.3 percent recovery of acephate spiked cabbage extracts and tomato extracts. These numerical findings support the fact that the numerical effects of actual food samples do not seriously interfere with the digital signal therefore justifying the accuracy of the device in commercial food safety applications.

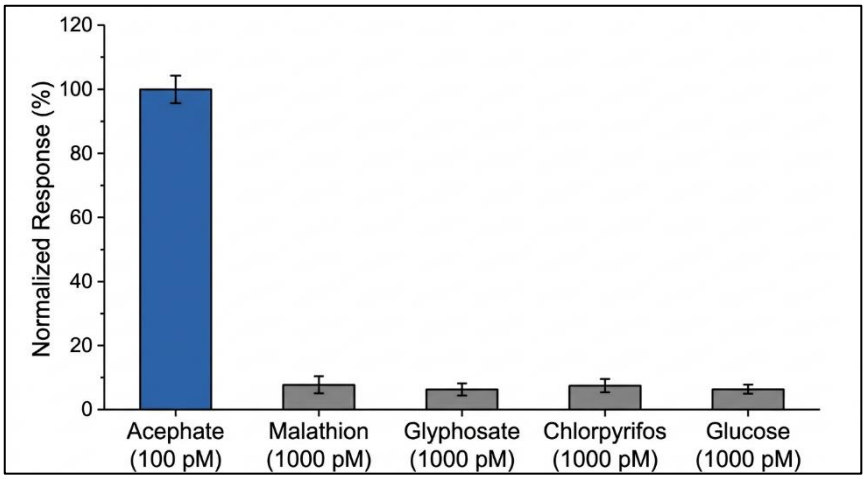


Figure 5.

Offers

The current study offers a conductivity-enhanced bimetallic MOF sensing scheme, which directly addresses the issue of the low electron transport of pure MOFs by employing the use of activated carbon. The study demonstrates the effectiveness of Zn/Cu metal synergism in boosting charge transportation kinetics as well as catalytic activity without the use of enzyme immobilization. The production of disposable sensing devices can be performed on the fabrication route, which is easy and scalable. The sensing scheme is also a flexible pathway towards detection of other organophosphate pesticides by the dynamization of the metal centers in the MOF structure. Thus, the study is not only aimed at the detection of acephate but also can offer general approach to the solution of other environmental sensing issues.

Reference
[1]. Gao, L. P. (2015). *"Determination of acephate in vegetables by magnetic molecularly imprinted polymer isolation coupled with high-performance liquid chromatography".* **Analytical Letters**, **48(5), 752–765.**
[2]. Li, S. G. (2021). "*Transition metal-based bimetallic MOFs and MOF-derived catalysts for electrochemical oxygen evolution reaction".* **Energy & Environmental Science, 14(4), 1897–1927.**
[3]. Li, Z., & Chen, X. (2021). "*Synergistic effects in bimetallic Zeolitic Imidazolate Frameworks (ZIFs) and Metal-Organic Frameworks for advanced electrochemical applications".* **Journal of Materials Chemistry A, 9(14), 8562-8580.**
[4]. Wang, Y., et al. (2022). "*Highly sensitive electrochemical sensor based on MOF-derived carbon and activated charcoal composites for organophosphorus pesticide detection in food safety".* **Sensors and Actuators B: Chemical**, **355, 131-142.**
[5]. Kumar, R., & Sharma, P. K. (2023). "*Metal-Organic Framework/Carbon-based composites as emerging platforms for the electrochemical sensing of organophosphorus pesticides: A review".* **Analytica Chimica Acta, 1245, 340-358.**
[6]. *World Health Organization* (2020).

SYNTHESIS OF 2-(4-AMINO-6-METHYL-5,6-DIHYDRO-1,3,5-TRIAZIN-2(1H)-YLIDENE)MALONONITRILE AND ITS PHARMACOLOGICAL AND BIOLOGICAL PROPERTIES

Mir Ali Isakov, Afsun Sujayev, Bayim Isakova, Lala Aliyeva
Ministry of Science and Education of the Republic of Azerbaijan
Institute of Chemistry
Baku, Azerbaijan
mirali.isakov.e@gmail.com

Abstract - In this study, a new pyrazole derivate was synthesized the reaction of the (E)-N'-carbamimidoyl-1H-pyrazole-1-carboximidamide with malononitrile and asetaldehyde. The reaction was conducted in methanol, 80°C temperature, yielding the 2-(4-amino-6-methyl-5,6-dihydro-1,3,5-triazin-2(1H)-ylidene)malononitrile in crystalline form. The structural characteristics and the functional groups were identified and confirmed using FT-IR spectroscopy. Key absorption bands, including C=C, C-N, N-H, C=N, C≡N, CH, C-N and C=C groups, were analyzed to verify this. The synthesized pyrazole derivative was predicted as an antioxidant, protein glycation inhibitor and antiviral agent.
Keywords: Heterocyclic compounds, Pyrazole derivatives, antioxidant

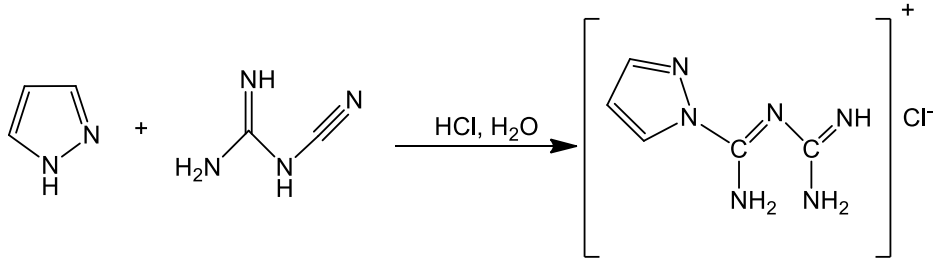
Introduction

As is well known, Pyrazole derivatives are pharmacological activities compounds. Also, the versatility of pyrazole derivates allows for extensive use across various fields. Pyrazole-based compounds serve as basic building blocks in the synthesis of various pharmaceutical agents.[1] [S. Aslanov,468-477,2024]. Due to their diverse pharmacological and biological properties, pyrazole derivatives are core components of various drugs, Specifically antifungal, antidepressant, antitubercular agents, anticancer, anti-inflammatory and antibacterial. Moreover, the incorporation of pyrazole

scaffolds into pharmaceutical agents provides significant antioxidant and anti-glycation properties. These features are crucial in the therapeutic management of diabetes and age-related degenerative disorders, alongside their proven efficacy in preventing viral infections. [2] [I. Mahmudov, 138205, 2024].

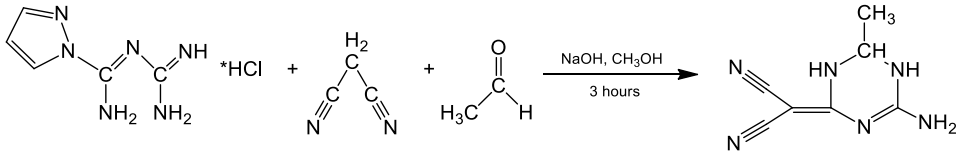
Experimental section

First, (E)-N'-carbamimidoyl-1H-pyrazole-1-carboximidamide pyrazole derivate was synthesized (Scheme 1). The synthesis involved the use of 1H-Pyrazole (1 mmol), dicyandiamide (1 mmol), distilled water, and 37% HCl (1 mmol).



Scheme 1. Sysntesis of (E)-N'-carbamimidoyl-1H-pyrazole-1-carboximidamide

The reaction resulted in the formation of a white crystalline precipitate. Subsequently, 2 mmol of these white crystals were dissolved in methanol for further reaction and the resulting solution was neutralized with 1M NaOH. Subsequently, 1 mmol of malononitrile was added, and the mixture was stirred for 1 hour to proceed with the next stage of the synthesis. Upon the addition of malononitrile, the initial transparent solution gradually turned light yellow after several minutes of stirring. Subsequently, acetaldehyde was introduced in an equimolar ratio (1 mmol). The reaction mixture was heated at reflux in methanol for 2 hours. The evaporated methanol was condensed using a cooling system and returned to the reaction flask, allowing the process to continue under constant volume. The product was extracted with distilled water, dried over anhydrous sodium sulfate, and the solvent was evaporated to dryness. The reaction yielded white crystalline material. This reaction is shown in Scheme 2.



Scheme 2. Synthesis of 2-(4-amino-6-methyl-5,6-dihydro-1,3,5-triazin-2(1H)-ylidene) malononitrile

Result and Discussion

Figure 1 illustrates the FT-IR spectrum of the synthesized compound:

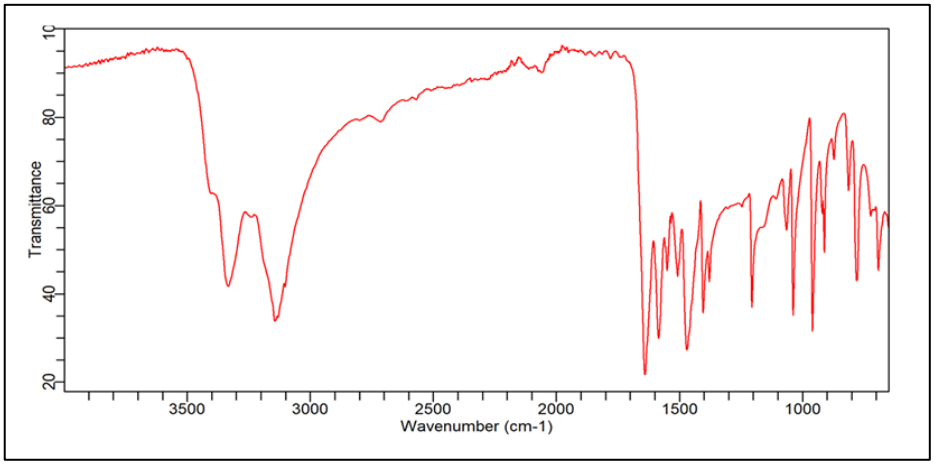


Figure 1. The FT-IR spectrum of the synthesized product was recorded on an Agilent spectrometer.

The FT-IR diagram provides information about the functional groups present in the product obtained upon completion of the reaction. 3332 cm^{-1} is characteristic of the NH amino group, 1205 cm^{-1} of the C-N carbon-nitrogen bond, 1640 cm^{-1} of the C=N group, 2234-2258 cm^{-1} of the C≡N bond, 691 cm^{-1} of the double bond between the C=C carbon atoms in cyclic compounds, and 650-659 cm^{-1} of the C-H bond between carbon and hydrogen.

The shifts observed in these absorption bands of the main functional groups in the FT-IR spectra prove the presence of a triazine ring. The next stages of the research are currently underway.

References

1. I. Mahmudov, B. Ibrahimova, A. Sujayev et. al., Synthesis, characterization, crystal structure, molecular docking, and biological studies of Cu, Ni and Co metal complexes of pyrazole, Journal of Molecular Structure, 2024, 138205.
2. Said Aslanov, Ibrahim Allahverdiyev, Ibadulla Mahmudov, Mir Ali Isakov, Parham Taslimi, Afsun Sujayev et. al. Creation of novel generation inhibitors with potential effect against alzheimer's disease, Journal of Chemical Problems, 2024, no. 4 (22) ISSN 2221-8688

SUSTAINABLE SYNTHESIS OF GRAPHENE-BASED SHEETS BY ELECTROCHEMICAL EXFOLIATION METHOD.

Murad Amirli[1], Arzu Abdullayeva[2], Rena Abbasova[1,2]
[1]Baku State University, Baku, Azerbaijan
[2]Baku Higher Oil School, Baku, Azerbaijan
e-mail: muradamirli64@gmail.com

Abstract - In this study, a series of experiments was conducted to produce graphene-based materials by the method with substantial potential for application. Electrochemical exfoliation of graphite electrodes using different electrolyte solutions and voltages was performed to compare the quality of obtained materials. The resulting samples were analyzed using Raman spectroscopy, Fourier Transform Infrared Spectroscopy, and X-ray diffraction to develop the most optimal synthesis conditions which increase yield while reducing energy and chemical consumption, leading to a more sustainable graphene production approach. Spectral analysis of the samples revealed the presence of sulfur-containing surface functional groups. Increasing the operating voltage on the cell was found to result in the formation of a greater number of surface oxygen-containing groups. Subsequent ultrasonic treatment facilitated additional cleavage of the graphene sheets and the separation of nanoscale particles from insufficiently oxidized graphite particles. This allows for an increased yield of nanoscale particles. This method is considered environmentally friendly, safe, and cost-effective.

Keywords: Electrochemical exfoliation, graphene, graphene-based materials (GBMs), Raman, FT-IR, sustainable development.

Introduction

The unique properties of graphene, including mechanical durability, excellent chemical stability, and high surface functionalization potential make it a universal advanced material for energy efficiency and environmental protection. Owing to these properties of graphene-based materials, they are regarded as one of the most remarkable material classes in the concept of sustainable development.

Since graphene and its derivatives, including graphene oxide and reduced graphene oxide have distinctive characteristics, there is a high demand for graphene-based materials. In other words, graphene-based materials are used in nearly all areas of modern life. Graphene-based materials have potential applications in aerogels, electronics, composite materials, and biomedical fields such as tissue engineering, biosensors, and antimicrobial applications. Due to its high surface area and abundant functional groups along the graphene plane, graphene-oxide is widely used as an adsorbent in environmental and chemical applications. For instance, it can serve as an effective adsorbent for the removal of heavy metals from synthetic wastewater, i.e., in wastewater treatment. High conductivity of graphene, because of the sp^2 hybridized carbon network, leads to the suitable usage of this material in energy storage devices such as batteries and supercapacitors.

Researchers remain interested in the development of new applications of graphene-based materials, which are widely considered the materials of the future (Santhiran, A.,et al., 2021), (Li, Y., et al., 2021), (Destiarti, L., et al., 2023).

Experimental part

Particular attention should be given to pretreatment of graphite electrodes owing to its fundamental importance. The pretreatment solution was prepared by mixing 50 wt.% H_2O_2 and 98 wt.% H_2SO_4.

The process of electrochemical exfoliation involved the following steps (Amirli, M.,et.al, 2025):

1. Preparation of electrolyte solution: Appropriate electrolyte solution was prepared to dissolve the anodic graphite electrode and facilitate exfoliation.
2. Cell voltage setup: Graphite electrodes (plates or rods) were positioned parallel to each other in the electrolytic environment and subsequently constant voltage was applied to them using a power source.
3. Electrochemical exfoliation: The electrochemical exfoliation was initiated under the action of an applied voltage. After a certain period, the delaminated sheets were released. The electrochemical exfoliation process is visually initiated, when the anodic graphite electrode underwent dissolution, releasing graphene sheets into the electrolyte solution. This process continued until the anodic graphite electrode was completely dispersed in the solution.

Suggestions

Several parameters must be carefully optimized to achieve efficient exfoliation. These parameters include the electrolyte solution, the applied voltage, the electrode distance, and the electrode area.

In our series of experiments, different electrolyte solutions such as potassium hydroxide, sulfuric acid, and ammonium sulfate solutions were tested. The selected electrolyte should possess high conductivity to ensure uniform current density. Additionally, the electrolyte ions should exhibit high intercalation efficiency.

The applied voltage may vary depending on the gap between the electrodes and the nature of electrolyte solution used in the experiment. In our experiments, the voltages of 5 V, 10 V, 15 V, and 20 V were applied. The most desirable results were obtained when the voltage was maintained at 10 V; therefore, this value was considered the optimal voltage for our experiment.

The spacing between two electrode materials must be maintained constant to ensure the uniform current density. Gaps of 1, 2, 3, 4 and 5 cm were employed in our experiments. The exfoliation rate reached its maximum, resulting in the formation of graphite flakes and an increased

density of the structural defects, as evidenced by the elevated ID/IG ratio in Raman analysis, when the parallel graphite electrodes were positioned with a spacing of 1 cm. The distance of 3 cm between two graphite electrodes can be considered ideal or optimal for experiment.

The area of electrodes has significant influence on the yield of the exfoliation process. Experimental results indicate that the graphene yield is positively correlated with the area of electrodes used in electrochemical exfoliation.

Moreover, the application of magnetic stirring during exfoliation improves the product yield.

Results and discussions

This environmentally friendly synthesis method includes not only favorable characteristics but also limitations. For instance, it is so complex to regulate particle diameters and the existence of surface functional groups. In addition, spectral analysis of the sample provides evidence for the presence of sulfur-containing surface functional groups, i.e., sulfonate groups (-OSO_3H, -SO_3^-), which are grafted onto either basal plane or edge atoms of graphene lattice.

In our experiments, not only were pure graphite plates utilized as electrodes, but also low-grade graphite materials were used. The pretreatment stage plays a crucial role in the exfoliation of low-quality raw materials. The electro-exfoliation of low-quality graphite anodes yielded only a small amount of graphene; however, pretreatment of graphitic electrodes followed by electro-exfoliation under optimal conditions resulted in gradual peeling, yielding a high quantity of graphene-based materials. The introduction of pretreatment stage for the anodic graphite promoted additional oxidation, resulting in formation of surface functional groups characteristic of the graphene oxide derivatives.

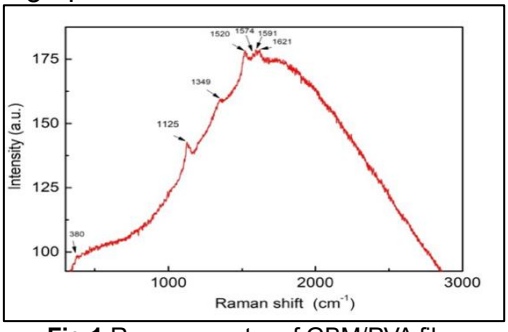


Fig.1 Raman spectra of GBM/PVA film.

The obtained samples were characterized by Raman spectroscopy (EnSpectr R532, green laser 532 nm, wavenumber-100-4000 cm^{-1}) and Fourier Transform Infrared Spectroscopy (IR Affinity -1, Shmadzu, wavenumber – 350-4000 cm^{-1})

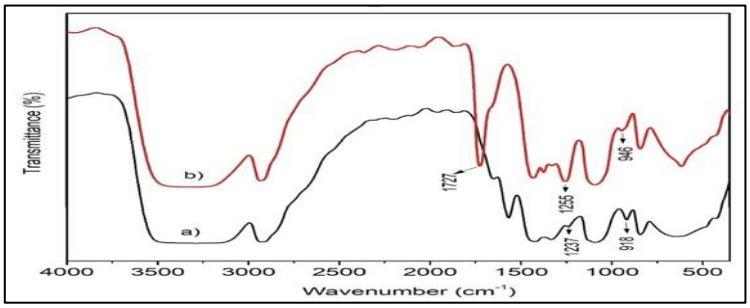


Fig.2 FT-IR spectra of PVA and PVA/graphene-based material composite films. a) Polyvinyl alcohol b) PVA+graphene-based material composite.

The Raman spectroscopy is a highly promising technique for interpreting the quality of the materials.

The Raman spectrum of our sample exhibits distinct bands corresponding to crystalline graphene obtained by electro-exfoliation of anodic graphite. The peak intensity ratio ID/IG shows that the obtained crystalline graphene is of sufficiently high quality. The 2D band is a second-order peak of the D band and is due to lattice vibrations. Furthermore, although the 2D peaks of some of the studied samples are moderately pronounced, they indicate the presence of graphene rather than graphite. The 2D band is not associated with structural defects; however, it depends on the number of graphene layers. In contrast, the Raman spectrum of the sample formed by exfoliation of pre-treated graphite electrode with H_2O_2/H_2SO_4 revealed the presence of lattice defect-rich centers arising from anodic oxidation of graphite indicated by high peak intensity ratio of ID/IG.

PVA-based composite spectra obtained by FTIR spectroscopy revealed bands characteristic of graphene and its derivatives, as well as new peaks potentially caused by the interaction of graphene-based material and its functional groups with polyvinyl alcohol.

The peak observed at ~1700 cm^{-1} is characteristic of carbonyl(C=O) stretching, while a weak peak at (1580 cm^{-1}) corresponds to C=C bonds. Peaks in the 1000-1200 cm^{-1} region are assigned to S-O groups and C-O-C bonds.

The occurrence of sulfonate functionalities ($-OSO_3H$, $-SO_3^-$) on graphene is also likely to arise from intercalation of sulfate ions (SO_4^{2-}) coming from either pretreatment agent (H_2O_2/H_2SO_4) or electrolyte solution containing $(NH_4)_2SO_4$. Sulfonate groups are predominantly functionalized at the peripheral sites of the graphene lattice while their presence on the basal plane is limited and primarily correlated with defect-rich or distorted regions of polycyclic carbon framework. Sulfate ions intercalate into the graphite layers resulting in the formation of sulfonate-functionalized graphene which

can be removed by the alkaline treatment (desulfonation) leading to increased conductivity of material.

Conclusion

The graphene is obtained via one of the sustainable methods of synthesis, electrochemical exfoliation, using a graphite anode. Under the applied electric field, the electrolyte anions migrate toward the anode, increasing interlayer spacing between graphite layers and intercalating between them, thereby expanding the interlayer distances, accompanied by gas evolution. This expansion weakens the interlayer van der Waals forces holding the layers together, resulting in a layer-by-layer separation, referred to as “gradual peeling” to generate graphene-based materials.

Graphene-based materials, including oxidized graphene derivatives, that contain carbonyl, hydroxyl, and epoxy groups on the basal plane as well as carboxyl, sulfonate groups at the edges of the graphene network, demonstrate good dispersibility in numerous solvents. These oxidized derivatives can be readily chemically modified with various functional groups through electrostatic interactions, hydrogen bonding, and van der Waals forces, enabling the fabrication of a wide range of advanced materials.

References

1. Santhiran, A., Iyngaran, P., Abiman, P., & Kuganathan, N. (2021). Graphene synthesis and its recent advances in application–A review. C, 7(4), 76.
2. Li, Y., Zhang, H., & Wang, X. (2021). Effect of H_2SO_4/H_2O_2 pre-treatment on electrochemical properties of exfoliated graphite prepared by an electro-exfoliation method. RSC Advances, 11, 10881-10890
3. Destiarti, L., Riyanto, R., Roto, R., & Mudasir, M. (2023). Electrolyte effect in electrochemical exfoliation of graphite. Materials Chemistry and Physics, 302, 127713
4. Amirli, M., Abdullayeva, A., Eyvazova, G., Musayeva, N., & Abbasova, R. (2025). Study of products of electrochemical exfoliation of graphite. 2nd International Conference on Modern Problems of Theoretical and Experimental Chemistry, 372–373, Baku, Azerbaijan.

CHARACTERISTICS OF BIOCOMPOSITES BASED ON COMPATIBILIZED ETHYLENE HEXENE-1 COPOLYMER: THE INFLUENCE OF CORN HUSK MICRO-SIZED PARTICLES CONTENT ON THE MELT FLOW INDEX

[1,2]Fatima Mustafayeva, [1]Eltaj Mustafayev, [2]Najaf Kakhramanov
[1]Sumgait State University
[2]Institute of Polymer Materials of Ministry of Science and Education Republic of Azerbaijan
Sumgayit city, Azerbaijan
E-mail: fatime.mustafayeva@sdu.edu.az, eltajmustafayev@gmail.com

Summary - The materials industry increasingly seeks ecologically friendly and cost-effective alternatives for producing robust composite materials. Corn husk, a plentiful agricultural waste, represents a sustainable and accessible bio-filler for polymer composites. the study aims to investigate the influence of corn husk loading on the melt flow index of ethylene hexene-1 copolymer based composites. the addition of corn husk filler significantly influenced the melt flow characteristics of the allow. The melt flow index initially increased with the addition of filler but subsequently decreased at higher loadings.

Keywords: Corn husk agro waste, ethylene hexene-1 copolymer, biocomposite, melt flow index.

Introduction

An essential part of the materials industry is the development of composite materials, which make it possible to produce goods that are more robust, long-lasting, and ecologically friendly. Therefore, work is continuously underway to improve the physical and mechanical properties of composites to attain qualities that suit the needs of the industry. Corn husk is a plentiful agricultural waste that can be used to make a variety of products, including packaging materials, plastics, and biopolymers [Posri S., et al, 2023; Shibly Md, 2021]. It is estimated that more than 1.5 billion tons of corn are produced worldwide today [Pudhupalayam Muthukutti G. et al; 2025]. Notably, Azerbaijan also exhibits excellent corn planting and harvesting performance. As a result, 10,100 hectares of the 34,603 hectares of corn planted nationwide yielded more than 56,873 tons of corn in 2020, or 56.3 quintals per hectare on average [https://www.agro.gov.az/az/ news/azerbaycanda-56-min-tondan-cox-qargidali-yigilib]. In this regard, corn husk is considered an environmentally friendly, renewable, cheap, and accessible filler for the production of polymer composites. This work aims to study the influence of corn husk loading on the melt flow index ethylene hexene-1 copolymer based composites.

Experimental Part

As a polymer matrix, ethylene hexene-1 copolymer of the Kimcross 1230/1331 brand from KIMIA JAVID SEPAHAN Co. was used, the flowability of which is 1.8 g / 10 minutes at a load of 5 kg and a temperature of 190 °C.

The corn husks were collected from local markets, washed, and dried first outdoors in the sun, and then in an oven. The crushed corn husk was sieved through a stainless-steel mesh DAMAVAND test sieve LTD mesh No. 1 and then sized in Mastersizer 3000 (Malvern İnstruments, UK) device: Dv(10) = 482 µm, Dv(50) = 678 µm and Dv(10) = 934 µm. Samples were taken based on 1, 3, 5, 10, and 20 wt % amounts of micro-sized filler. ExxelorTM PO 1020 (maleic anhydride functionalized polypropylene) was used as a compatibilizer at a concentration of 2 wt%, and its alloy has a flow index of 430 g/10 min (2.16 kg, 190 °C temperature). In addition, 1 wt% LIBAID T-2 processing aid was included in the composition of the composites. The melt flow index of ethylene hexene-1 copolymer and ethylene hexene-1 copolymer based composites are determined using a capillary rheometer machine (Instron CEAST MF50 Melt Flow Tester).

Results and their Discussion:

As can be seen from Figure 1, with an increase in the amount of corn husk in the composite, the melt flow index of the alloy first increased and then decreased. This indicates higher viscosity and lower flowability due to the increase in filler content, which limits the mobility of the polymer chains. However, the flowability of the alloy of all samples obtained was higher than that of the original polymer matrix (ethylene hexene-1 copolymer). The highest result was obtained for a composite containing 3 wt % of corn husk and was equal to 2.6 g / 10 min.

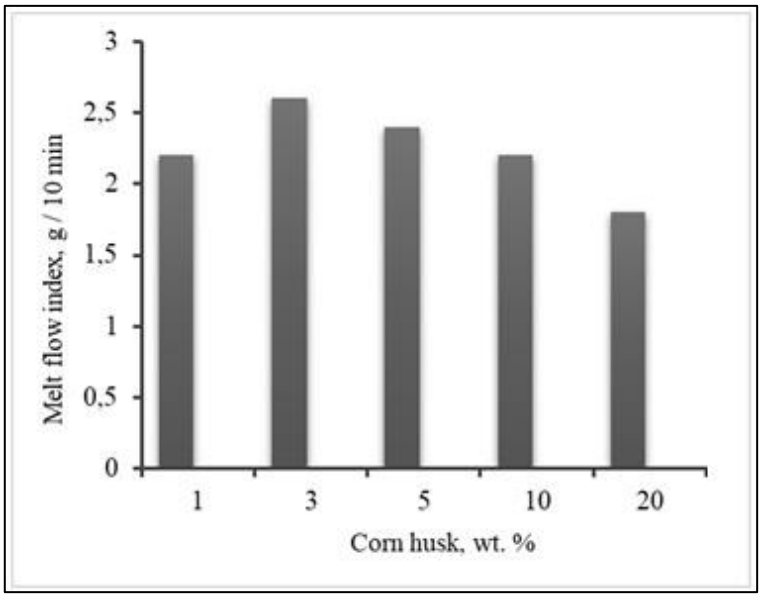


Figure 1. Melt flow index (at 5 kg load and 190 °C temperature) of a compatibilized ethylene hexene-1 copolymer and corn husk-based composites.

References:
[1] Posri S., Tangboriboon N. Conductive and self-cleaning composite membranes from corn husk nanofiber embedded with inorganic fillers (TiO_2, CaO, and eggshell) by sol–gel and casting processes for smart membrane applications. Reviews on advanced materials science, 2023, Vol. 62(1).
[2] Pudhupalayam Muthukutti G., Singh M. K., Palaniappan S. K., et al. Sustainable polymer composites from agro and municipal green wastes: a comprehensive review of materials, properties, and applications. J Mater Cycles Waste Manag, 2025, Vol. 27, pp. 3121–3142.
[3] Shibly Md, Chan M., Koay S. C. Mechanical properties of polyester/corn husk fibre composite produced using vacuum infusion technique. Polymers and Polymer Composites, 2021, Vol. 29, pp. S1532-S1540.
[4] https://www.agro.gov.az/az/news/azerbaycanda-56-min-tondan-cox-qargidali-yigilib

MÖHKƏMLİK GÖSTƏRİCİLƏRİ YAXŞILAŞDIRILMIŞ POLİMER MATERİALLAR

Vəlizadə N.Y., Qasımova G.Ş., Ağayeva F.A., Tağıyeva A.L.
Sumqayıt Dövlət Universiteti
Sumqayıt, Azərbaycan
valizadaa.nazrin@gmail.com

Xülasə - İşdə polimer kompozit materialların hazırlanmasına dair məlumatlar təqdim edilmişdir. Müxtəlif doldurucuların, modifikatorların və əlavələrin tətbiqi ilə yüksək fiziki-mexaniki xüsusiyyətlərə malik polimer materialların alınmasının mümkünlüyü göstərilmişdir
Açar sözlər: Polimer, polietilen, modifikasiya, doldurucu, kompozisiya materialı

Giriş

Müasir sənaye istehsalının texnika və texnologiyasında alimlərin diqqəti getdikcə istismar xüsusiyyətlərinə görə yüksək möhkəmlik, aşınmaya davamlılıq, termo- və istiliyədavamlılıq, sərt iqlim şəraitinin təsirinə davamlılıq və s. kimi göstəricilərlə fərqlənən yeni tip materialların hazırlanmasına yönəlir. Bununla yanaşı, polimer materiallar da müvafiq yüksək fiziki-mexaniki və texnoloji xüsusiyyətlərə malik olmalıdır.

Sənayedə istehsal olunan polimerlərin xassələrini dəyişdirmək məqsədilə onların müxtəlif modifikasiya üsullarından istifadə olunur: plastifikasiya, doldurucuların və stabilzatorların əlavə edilməsi, polimer qarışıqlarının yaradılması, struktur əmələ gətiricilər, mineral doldurucuların apretlənməsi və s.

Müxtəlif təyinatlı doldurulmuş polimer materialların işlənib hazırlanması ilə bağlı texnologiyalarda, polimer matrisinə modifikasiyaedici qatqıların elmi əsaslarla seçilməsinə xüsusi diqqət yetirilir. Bu zaman onların arasında antoqonizm hadisəsinin qarşısı alınır və kifayət qədər yüksək istismar göstəriciləri təmin edilir [Gasimova G.SH., Azerbaijan Chemical Journal, 2023, №2, s.186-200].

Eksperimental hissə

Təqdim olunan işdə, yüksək sıxlıqlı polietilen, təbii yun və ağac yonqarı əsasında möhkəmlik xüsusiyyətləri yaxçılaşdırılmış polimer materialların hazırlanmasına dair təqdqiqat nəticələri verilmişdir. Müəyyən edilmişdir ki, kompozisiyanın tərkibinə 5-25% miqdarında təbii yun və ağac yonqarının daxil edilməsi termoplastik materialların kifayət qədər yüksək möhkəmlik göstəricilərinə malik olmasına imkan verir. Çoxkomponentli polimer materialların emalı üçün optimal şərait seçilmişdir.

Nəticələr və onların müzakirəsi

Beləliklə, belə nəticəyə gəlmək olar ki, komponentlərin polimerin tərkibinə daxil edilmə üsulu onların ən mühüm xassələr kompleksinin dəyişməsinə əhəmiyyətli dərəcədə təsir göstərir. Kompozit materialların fiziki-mexaniki göstəricilərinin yaxşılaşdırılması isə onların müxtəlif texnika və texnologiya sahələrində tətbiqi üçün perspektivli imkanlar açır. Yəni alınan kompozit materiallardan məişətdə istifadə olunan örtüklər, istehsalatda qoruyucu məqsədlə önlüklər və başqa ekoloji təmiz məhsulların alınmasında istifadə etmək olar.

İstifadə olunmuş ədəbiyyat

1. Gasimova G.SH., Azerbaijan Chemical Journal, 2023, №2, s.186-200.

INVESTIGATION OF ELECTROCHEMICAL CORROSION BEHAVIOR OF CARBON STEEL IN FORMATION WATER USING EIS AND TAFEL METHODS

Sabina Rustamova
Baku Higher Oil School
Chemical Engineering Department
Baku, Azerbaijan
sabinarustamovva@outlook.com

ABSTRACT - One of the primary operational issues facing the oil and gas sector is the corrosion of carbon steel in oilfield formation waters.These waters usually contain dissolved gases like CO_2 and H_2S, as well as hostile ions like Cl^-, HCO_3^-, and SO_4^{2-}, which encourage electrochemical corrosion processes [Al-Meshleb et al., 2025; Obot et al., 2019]. This study uses Tafel polarisation and Electrochemical Impedance Spectroscopy (EIS) to examine how carbon steel corrodes in simulated formation water. Corrosion kinetics were assessed in relation to temperature, salinity, and gas composition.Furthermore, an analysis was conducted on the inhibition performance of specific organic inhibitors. The findings show a significant relationship between corrosion current density as determined by Tafel analysis and charge-transfer resistance as determined by EIS. By creating protective adsorbed layers on the steel surface, inhibitors greatly improved corrosion resistance [Tian et al., 2017; Huang et al., 2025]. The findings verify that organic inhibitors considerably lower corrosion current density and boost charge-transfer resistance.

KEYWORDS: formation water; electrochemical corrosion; Electrochemical impedance spectroscopy (EIS); Tafel polarization; corrosion inhibitors

INTRODUCTION

Corrosion in oilfield environments is a persistent problem affecting the integrity and lifetime of carbon steel equipment. Formation waters are complex electrolyte systems characterized by high salinity and the presence of dissolved acidic gases such as CO_2 and H_2S [Al-Meshleb et al., 2025]. These conditions promote both uniform and localized corrosion mechanisms [Obot et al., 2019].

Electrochemical techniques, particularly Electrochemical Impedance Spectroscopy (EIS) and Tafel polarization, are widely used to evaluate corrosion kinetics and inhibitor performance [Park et al., 2019; Sun et al., 2022]. However, integrated studies combining these methods under varying physicochemical conditions remain limited.

The aim of this study is to evaluate the corrosion behavior of carbon steel in simulated formation water using EIS and Tafel polarization techniques and to assess the efficiency of selected organic corrosion inhibitors.

EXPERIMENTAL SECTION

Simulated formation water was prepared in the laboratory using analytical-grade salts based on typical oilfield brine compositions reported in previous studies [Baxevani et al., 2025]. The electrolyte contained NaCl (30 g/L), $CaCl_2$ (1.5 g/L), $MgCl_2$ (1.0 g/L), and $NaHCO_3$ (0.5 g/L). The solution was prepared using deionized water and thoroughly mixed before electrochemical measurements. Carbon steel specimens (API 5L X65 grade) were used as working electrodes. The samples were mechanically polished with successive grades of silicon carbide papers (400–1200 grit), rinsed with distilled water, degreased with ethanol, and dried prior to electrochemical measurements.

Electrochemical measurements included Electrochemical Impedance Spectroscopy (EIS) in the frequency range of 10^5–10^{-2} Hz. Tafel polarization measurements were performed within a potential range of ±250 mV versus the corrosion potential (E_{corr}) with a scan rate of 0.5 mV/s. Tests were conducted at different temperatures and salinity levels. Selected organic inhibitors were added in concentrations of 25–150 ppm to evaluate inhibition efficiency.

RESULTS AND DISCUSSION

The EIS results showed depressed semicircles typical of charge-transfer controlled corrosion [Sun et al., 2022]. Increasing temperature and salinity led to a noticeable decrease in charge-transfer resistance (R_{ct}), which decreased from approximately 1200 Ω·cm² to 420 Ω·cm², indicating accelerated corrosion kinetics [Obot et al., 2019].

The Nyquist plots obtained from electrochemical impedance spectroscopy measurements are presented in Figure 1. The diameter of the semicircle increases in the presence of the inhibitor, indicating improved corrosion resistance.

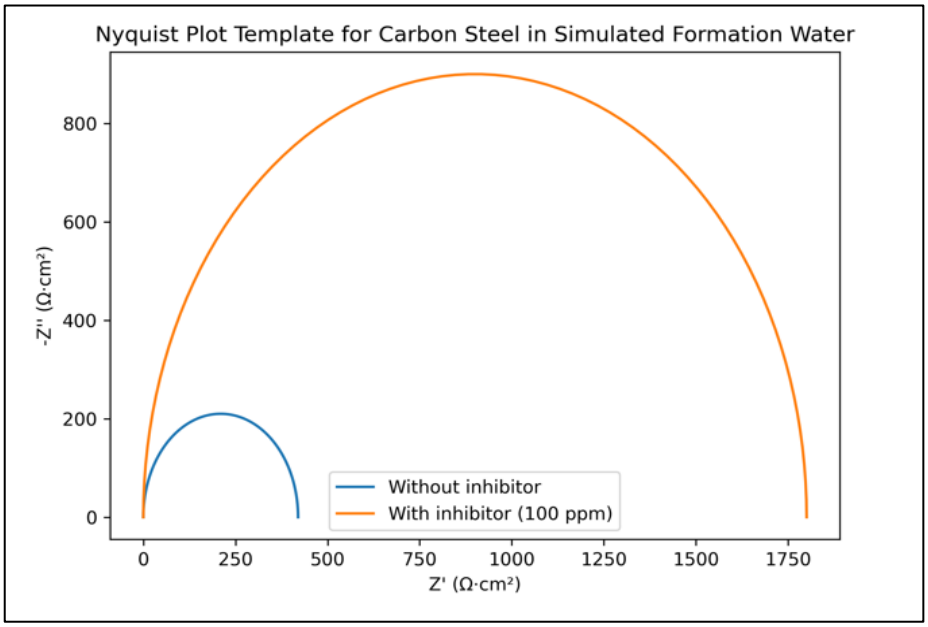


Figure 1. Nyquist plots for carbon steel in simulated formation water in the absence and presence of organic inhibitor (100 ppm).

Tafel polarization curves indicated an increase in corrosion current density (i_{corr}), which increased from approximately 0.8 μA/cm² to 3.5 μA/cm² under more aggressive conditions. A strong linear correlation between $1/R_{ct}$ obtained from EIS and i_{corr} obtained from Tafel polarization was observed ($R^2 \approx 0.94$), confirming the complementary nature of the two electrochemical techniques [Park et al., 2019].

The addition of organic inhibitors significantly improved corrosion resistance. In the presence of 100 ppm inhibitor, the charge-transfer resistance increased to approximately 1800 Ω·cm², corresponding to an inhibition efficiency of about 75–85% [Huang et al., 2025; Tian et al., 2017]. Inhibited systems exhibited increased R_{ct} values, decreased double-layer capacitance, and reduced corrosion current density.

The inhibitors appear to act predominantly as mixed-type inhibitors by adsorbing on the steel surface and forming a protective film [Chafiq et al., 2020].

RECOMMENDATIONS

Combined EIS and Tafel analyses are recommended for reliable corrosion assessment in formation waters [Park et al., 2019]. Organic inhibitors such as imidazoline and triazine derivatives show high potential for industrial applications [Wang et al., 2023; Wei et al., 2017]. Future studies should investigate the long-term stability of inhibitor films under dynamic flow conditions. The implementation of optimized inhibitor programs can significantly enhance the sustainability of oilfield operations.

REFERENCES

1. [Al-Meshleb, M. J., Hasan, B. O., & Majdi, H. S. (2025). Characterization of corrosive effects of produced water on carbon steel and the role of flow velocity. Petroleum Science and Technology.]
2. [Baxevani, A., Lamprou, E., Mavropoulos, A., Stergioudi, F., Michailidis, N., & Tsoulfaidis, I. (2025). Modeling and analysis of aluminium corrosion using electrochemical impedance spectroscopy (EIS). Preprints.]
3. [Chafiq, M., Chaouiki, A., Albayati, M. R., Lgaz, H., Salghi, R., AbdelRaheem, K., Ali, I. H., Mohamed, S. K., & Chung, I. M. (2020). Corrosion inhibition mechanisms of hydrazone derivatives based on naproxen for mild steel in HCl: Experimental and theoretical study. Journal of Molecular Liquids.]
4. [Gurbanov, A., Adygezalova, M., & Gurbanov, G. R. (2022). Corrosive inhibition of carbon steel: Formation of water imitates using electrochemical method. Global Scientific Journal.]
5. [Hao, W., Liu, Z., Wu, W., Li, X., Du, C., & Zhang, D. (2017). Electrochemical characterization and stress corrosion cracking of E690 high strength steel in wet–dry cyclic marine environments. Materials Science and Engineering.]
6. [Huang, G., Chen, W., Miao, C., Shen, C., Wang, Y., & Zhang, G. A. (2025). A novel high-efficient imidazoline derivative corrosion inhibitor for carbon steel in CO_2-containing oilfield produced water: Experimental and theoretical studies. BMC Chemistry.]
7. [Migahed, M. A., Elgendy, A., El-Rabiei, M. M., Nady, H., & Zaki, E. G. (2018). *Novel* Gemini cationic surfactants as anti-corrosion agents for X65 steel in oilfield produced water under sweet conditions. Journal of Molecular Structure.]
8. [Mohd, M. H., & Paik, J. K. (2013). Investigation of the corrosion progress characteristics of offshore subsea oil well tubes. Corrosion Science.]
9. [Negm, N. A., Migahed, M. A., Farag, R. K., Fadda, A. A., Awad, M. K., & Shaban, M. (2018). High performance corrosion inhibition of novel tricationic surfactants on carbon steel in formation water: Electrochemical and computational evaluations. Journal of Molecular Liquids.]
10. [Obot, I. B., Onyeachu, I. B., Umoren, S. A., Quraishi, M. A., Sorour, A. A., Chen, T., Aljeaban, N., & Wang, Q. (2019). High temperature sweet corrosion and inhibition in the oil and gas industry: Progress, challenges and future perspectives. Journal of Petroleum Science and Engineering.]
11. [Park, K., Chang, B. Y., & Hwang, S. (2019). Correlation between Tafel analysis and electrochemical impedance spectroscopy by prediction of amperometric response from EIS. ACS Omega.]
12. [Sun, F., Peng, X., Bai, X., Chen, Z., Xie, R., He, B., & Han, P. (2022). EIS analysis of the electrochemical characteristics of the metal–water interface under the effect of temperature. RSC Advances.]
13. [Tian, H., Li, W., Hou, B., & Wang, D. (2017). Insights into corrosion inhibition behavior of multi-active compounds for X65 pipeline steel in acidic oilfield formation water. Corrosion Science, 117.]
14. [Wang, L., Zhang, C., Xie, H., Sun, W., Chen, X., Wang, X., Yang, Z., & Liu, G. (2015). Calcium alginate gel capsules loaded with inhibitor for corrosion protection of downhole tubes in oilfields. Corrosion Science.]
15. [Wang, X., Xu, W. L., Li, Y. Y., Jiang, Z. N., Zeng, X. Q., & Zhang, G. A. (2023). Interfacial adsorption mechanism of triazine derivatives as corrosion inhibitors for carbon steel in CO_2-saturated oilfield produced water. Journal of Colloid and Interface Science.]
16. [Wei, L., Chen, Z., & Guo, X. (2017). Inhibition behavior of an imidazoline inhibitor for carbon steel in a supercritical CO_2/H_2O system. Journal of the Electrochemical Society.]

17. [Zhang, J., Wang, Z., Wang, Z., & Han, X. (2012). Chemical analysis of the initial corrosion layer on pipeline steels in simulated CO_2-enhanced oil recovery brines. Corrosion Science.]
18. [Zhang, Q. H., Hou, B. S., Xu, N., Xiong, W., Liu, H. F., & Zhang, G. A. (2019). Effective inhibition of X65 carbon steel corrosion in oilfield produced water by two Schiff bases. Journal of Molecular Liquids.]
19. [Zhang, Q. H., Jiang, Z. N., Li, Y. Y., Wang, X., Xiong, W., Liu, H. F., & Zhang, G. A. (2022). In-depth insight into the inhibition mechanism of modified and combined amino acids corrosion inhibitors: Intramolecular vs. intermolecular synergism. Chemical Engineering Journal.]

STUDY OF THE ELECTROCHEMICAL REDUCTION PROCESS OF Bi IONS

Aisha Shikhaliyeva, Vusala Majidzade
Baku State University
Baku, Azerbaijan
aisheshixaliyeva@gmail.com

Summary - The presented work is devoted to the study of the electrochemical reduction process of Bismuth ions for the purpose of obtaining thin films based on Bi. Here, reduction and deposition potential regions were determined for the purpose of electrodeposition of Bi ions, and the influence of some factors on the process was studied.
Keywords: Bi ions, electroreduction, non- aqueos electrolyte, potential.

Introduction

Bismuth (Bi) and Bi-based thin films are widely used in electro-optical, thermoelectric, photocatalytic, and sensor applications. Their properties vary depending on their crystal structure, thickness, and synthesis method [Majidzade, 2018, 1-2].

Experimental part

Cyclic polarization curves have been recorded to study the kinetics and mechanism of both the electroreduction of Bi ions by IVIUMSTAT Electrochemical Interface potentiostat (Ivium Technologies, Netherland). A glass three-electrode electrochemical cell with a volume of 100 mL has been used. Pt, with an area of 0.5 cm^2, have been used as the working electrode.

Results and their discussion

The electrochemical reduction of bismuth ions from ethylene glycol solutions was carried out by the potentiodynamic polarization method. The process was studied on Pt electrode to illuminate the kinetics and mechanism. The polarization curves recorded by the potentiodynamic method show that a double electrical layer forms and results at the beginning potential.

When studying the kinetics and mechanism of the process according to the cyclic and linear polarization curves, it was found that the nature of polarization in this case is accompanied by a diffusion nature.

The results obtained have allowed us to analyze the reduction mechanism of Bi ions and will serve as a basis for selecting optimal conditions for the co-electrodeposition of Bi-S thin films in the future.

References

1. Majidzade V.A. The influence of various factors on electrochemi cal reduction of the bismuth ions. Azərb. Kimya Jurnalı, 2018, №4, p. 77-82
2. Majidzade V.A., Jafarova S.F., Javadova S.P., Aliyev A.Sh., Tagiyev D.B. Obtaining Bi-S Thin Films. Sofia Electrochemical Days 2022, 11-14 may 2022 Sofia, Bulgaria, p. 74.

EVALUATION OF THE MELT FLOW INDEX OF COMPATIBILIZED POLYPROPYLENE RANDOM COPOLYMER - MICRO SIZED CORN HUSK BASED BIOCOMPOSITES

[1,2]Fatima Mustafayeva, [1]Farid Suleymanli, [1]Ruhangiz Alasgarova
[1]Sumgait State University
[2]Institute of Polymer Materials of Ministry of Science and Education Republic of Azerbaijan
Sumgayit city, Azerbaijan
E-mail: fatime.mustafayeva@sdu.edu.az, F.A.Mustafayeva@gmail.com, ferid.suleymanli2001@icloud.com

Summary - This study investigates the development and characterization of biocomposites composed of polypropylene random copolymer matrix reinforced with agricultural waste from corn husks. The research focuses on evaluating the effect of corn husk loading on the melt flow index. Composites were prepared by mixing corn husk powder at varying concentrations (1 wt % to 20 wt %) with polypropylene random copolymer, incorporating a compatibilizer (Exxelor™ PO 1020) and a processing aid (LIBAID T-2). The addition of corn husk powder initially decreases the melt flow index compared to pure polypropylene random copolymer.

Keywords: Polypropylene random copolymer, biocomposite, corn husk, filler, melt flow index.

Introduction

Biocomposites are defined as materials that have one or more biological origins [McKay I., et al, 2024; Waqas Ahmad, et al, 2025]. Treating and managing agricultural wastes is seen as a crucial tactic to fully safeguard resources and preserve environmental assets. It looks promising to create sustainable polymer composites from agricultural wastes like corn husk [Aditi Sarker Ratna, et al, 2022]. Incorporating corn husk into polypropylene random copolymer composites could increase economic benefits because of its abundance and inexpensive cost. This study evaluated the effect of corn husk loading on the melt flow index polypropylene random copolymer based composites.

Experimental Part

Topilene R200P grade polypropylene random copolymer was used as a polymer matrix. The melt flow index of polypropylene random copolymer without reinforcement was examined and found to be 0.2 g / 10 min according to the ASTM D1238 standard (190 °C temperature, 5 kg load). The corn husk was first physically cleansed to get rid of contaminants, and it was then left to dry for six days in the sun. A knife mill was then used to grind the raw material. After the ground material was sieved through a 1 mesh screen, corn husk powder was produced. Particle size distributions of the ground corn husk were presented in Figure 1. According to Figure 1, the particle volume distribution of corn husk particles shows a normal distribution.

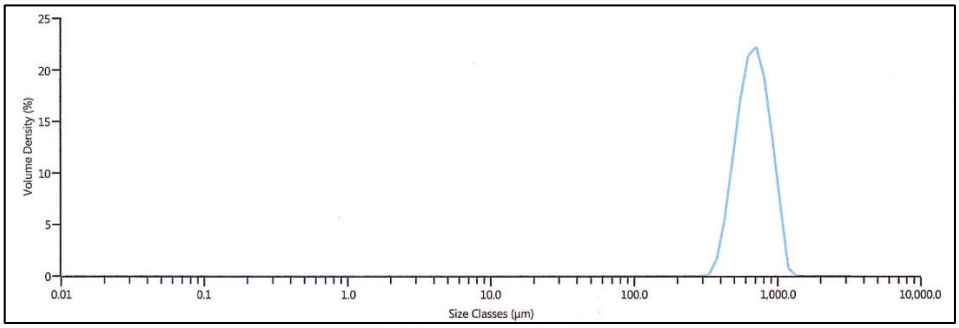


Figure 1. Particle size distributions of corn husk particles

Corn husk and polypropylene were mixed in various amounts in hot rollers. 2 wt % of compatibilizer (Exxelor™ PO 1020) and 1 wt % of processing aid (LIBAID T-2) were also added to the samples. An Instron CEAST MF50 Melt Flow Tester rheology equipment was used to measure the melt flow index (5 kg load, 190 °C temperature) of samples. A sample of pure polypropylene random copolymer was used to compare the samples.

Results and their Discussion:

The results of measuring the melt flow index of the plastic composite samples show that the melt flow index of pure polypropylene random copolymer has a lower value compared to other polypropylene random copolymer samples blended with corn husk. Melt flow index values decrease slightly as the percentage of corn husk in the mixture increases from 1 wt % to 3 wt % (Figure 2). Increasing the corn husk content from 3 wt% to 20 wt % does not change the fluidity index of the alloy. In high filled samples, a lower melt flow index value also indicates a higher melt viscosity.

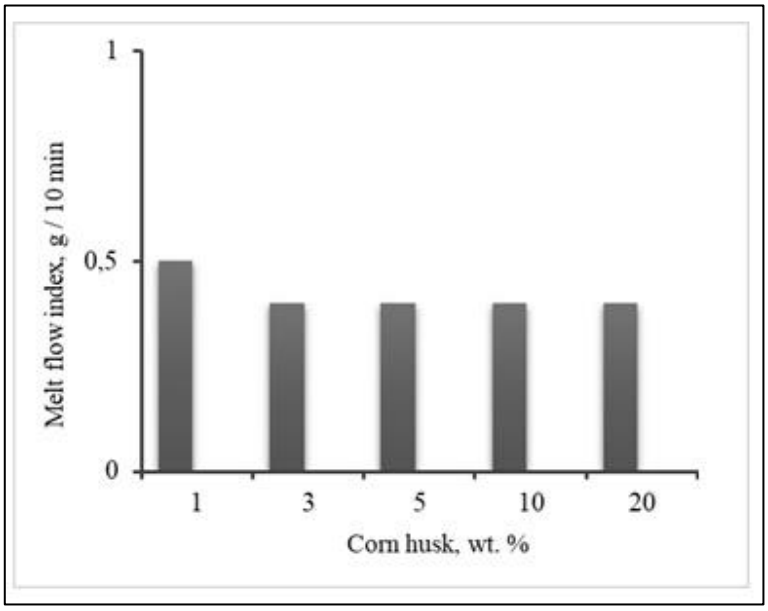


Figure 2. Melt flow index of a compatibilized polypropylene random copolymer / corn husk-based biocomposites.

References:

[5] Aditi Sarker Ratna, Anik Ghosh, Samrat Mukhopadhyay. Advances and prospects of corn husk as a sustainable material in composites and other technical applications. Journal of Cleaner Production, 2022, Vol. 371, 133563.

[6] McKay I., Vargas J., Yang L., Felfel R.M. A Review of Natural Fibres and Biopolymer Composites: Progress, Limitations, and Enhancement Strategies. Materials, 2024, Vol. 17, 4878.

[7] Waqas Ahmad, Sarah J. McCormack, Aimee Byrne. Biocomposites for sustainable construction: A review of material properties, applications, research gaps, and contribution to circular economy. Journal of Building Engineering, 2025, Vol. 105, 112525.

2-ALLİLFENOLUN FORMALDEHİD VƏ BENZİLAMİNLƏ KONDENSLƏŞMƏ MƏHSULUNUN SİNTEZİ VƏ TƏDQİQİ

G.M.Mehdiyeva, F.O.İbadzadə, M.R.Bayramov, N.Y.Zeynalov
Bakı Dövlət Universiteti, Kimya Fakültəsi, Bakı, Azərbaycan
*gunaymehdiyeva@bsu.edu.az

Xülasə - Təqdim olunan tezisdə yeni azot saxlayan allil əvəzli aminometil törəməsinin sintezi və antimikrob xassəsinin tədqiqi aparılmışdır. Sintez olunmuş birləşmənin quruluşu NMR və İQ spektroskopiyası vasitəsi ilə müəyyən edilmişdir.
Açar sözlər: 2-allilfenol, benzilamin, Mannix əsasları

Giriş:

Müasir neft-kimya elminin aktual problemlərindən biri də, yağlara və yanacaqlara əlavələr, neftin çıxarılmasında biosidlər, bioloji aktiv maddələr, turş mühitlərdə metalların korroziyasına qarşı inhibitorlar, polimer materiallarına stabilizator kimi tətbiq oluna bilən yeni heteroatom saxlayan üzvi birləşmələrin işlənib hazırlanmasıdır. Bu baxımdan tərkibində müxtəlif heteroatomlar və funksional qruplar saxlayan fenol törəmələri göstərilən sahələrdə mühüm əhəmiyyət kəsb edir [Elhadi, 2016, 731-736; Mehdiyeva, 2023, 394-402].

Deyilənləri nəzərə alaraq, tərəfimizdən Mannix reaksiyasından istifadə edərək 2-allilfenolun formaldehid və benzilaminlə kondensləşməsi aparılmış və tərkibində eyni zamanda ikiqat rabitə, amin fraqmenti və digər əvəzedicilər saxlayan polifunksional birləşmə sintez edilmişdir.

Təcrübi hissə:

2-Allilfenolun formaldehid və benzilaminlə reaksiyası reagentlərin ekvimolyar nisbətində 75-80°C temperaturda, 4-4,5 saat müddətində aparılmışdır. Sintez edilmiş birləşmənin quruluşu NMR və İQ spektroskopiyası vasitəsi ilə təsdiq edilmişdir. Sintez edilmiş birləşmənin ^{1}H və ^{13}C NMR spektrləri NMR spektrometrindən (AVANCE 300) (Bruker) istifadə edilərək qeydə alınmışdır. Həlledici kimi $CDCl_3$ (99.8%, kataloq № 151831) istifadə edilmişdir. Birləşmələrin İQ spektrləri Nikoled IS10 FTIR spektrofotometrində 4000-400 sm^{-1} diapazonunda qeydə alınmışdır.

Nəticələr və onların müzakirəsi:

Sintez olunmuş birləşmə 90% təşkil edir. Sintez olunmuş aminometil törəməsinin NMR spektrində birləşmələrin quruluşunun uyğun olmasını tam təsdiqləmişdir.

Sintez olunmuş birləşmənin bakteriyalara və göbələklərə qarşı antimikrob xassəsinin sınağının ilkin nəticələri göstərmişdir ki, onlar həm bakterisid, həm də fungisid xassələrə malikdirlər.

Təkliflər:

Sintez olunmuş birləşmənin quruluşunun zənginliyinə görə və ədəbiyyat məlumatlarına görə dərman vasitələri, neft məhsullarına antioksidləşdirici,

antimikrob və s. aşqarlar kimi istifadə oluna bilər. Həmçinin də, ilkin tədqiqatların nəticəri də göstərmişdir ki, sintez olunmuş birləşmə aşağı qatılıqlarda (0.1-0.2%) yüksək nəticələrə malikdir.

Ədəbiyyat:
1. Elhadi, S.M., Bilel, M., Abdelmalek, B. et al. Experimental evaluation of quinolinium and isoquinolinium derivatives as corrosion inhibitors of mild steel in 0.5 M H2SO4 solution. Prot Met Phys Chem Surf 52, 731–736 (2016). https://doi.org/10.1134/S2070205116040092
2. Mehdiyeva, G.M. 8-Allyl-1,3-benzoxazines as Hydrogen Sulfide Corrosion Inhibitors and Biocides in Crude Oil Extraction. *Pet. Chem.* **63**, 394–402 (2023). https://doi.org/10.1134/S0965544123030039

2-ALLİLFENOL ƏSASINDA AZOT SAXLAYAN BİRLƏŞMƏLƏRİN SİNTEZİ VƏ TƏDQİQİ

G.M.Mehdiyeva, Ş.E. Səfərova, M.R.Bayramov, M.A.Ağayeva
Bakı Dövlət Universiteti, Kimya Fakültəsi, Bakı, Azərbaycan
*gunaymehdiyeva@bsu.edu.az

Xülasə - Təqdim olunan tezisdə yeni azot saxlayan üzvi birləşmələrin – allil əvəzli 1,3-benzoksazin və aminometil törəmələrinin sintezi və onların antimikrob xassəlrinin tədqiqi aparılmışdır. Sintez olunmuş birləşmələrin quruluşu NMR və İQ spektroskopiyası vasitəsi ilə müəyyən edilmişdir.
Açar sözlər: 2-allilfenol, 1,3-benzoksazinlər, aminlər

Giriş:

Polimer materialları, neftin çıxarılmasında biosidlər, bioloji aktiv maddələr, metalların korroziyasına qarşı inhibitorlar və digər qiymətli məhsullar üçün stabilizator kimi tətbiq oluna bilən yeni heteroatom tərkibli üzvi birləşmələrin işlənib hazırlanması müasir texnologiyaların aktual problemlərindən biridir. Bu baxımdan tərkibində müxtəlif heteroatomlar və funksional qruplar saxlayan fenol törəmələri göstərilən sahələrdə mühüm əhəmiyyət kəsb edir [Ali-Asgari, 2017, 1028–1030; Akhter, 2011, 1147–1153].

Deyilənləri nəzərə alaraq, tərəfimizdən Mannix reaksiyasından istifadə edərək 2-allilfenolun formaldehid və birli aminlərlə (propilamin və anilin) kondensləşməsi aparılmış və tərkibində eyni zamanda ikiqat rabitə, amin fraqmenti və digər əvəzedicilər saxlayan polifunksional birləşmələr sintez edilmişdir.

Təcrübi hissə:

2-Allilfenolun formaldehid və propilaminlə reaksiyası reagentlərin ekvimolyar nisbətində 75-80ºC temperaturda, 4-4,5 saat müddətində aparılmışdır.1,3-Benzoksazin törəməsi almaq məqsədilə tərəfimizdən 2-allilfenolun formalfehid və anilinlə 1:2:1 mol nisbətində kondensləşmə

reaksiyası aparılmışdır. Reaksiya 95-98ºC temperaturda 3-3.5 saat müddətində aparılmışdır. Sintez edilmiş birləşmələrin quruluşları NMR və İQ spektroskopiyası vasitəsi ilə təsdiq edilmişdir. Sintez edilmiş birləşmələrin ^{1}H və ^{13}C NMR spektrləri NMR spektrometrindən (AVANCE 300) (Bruker) istifadə edilərək qeydə alınmışdır. Həlledici kimi $CDCl_3$ (99.8%, kataloq № 151831) istifadə edilmişdir. Birləşmələrin İQ spektrləri Nikoled IS10 FTIR spektrofotometrində 4000-400 sm^{-1} diapazonunda qeydə alınmışdır.

Nəticələr və onların müzakirəsi:

Sintez olunmuş birləşmələr 92 və 71% uyğun olaraq təşkil edir. Sintez olunmuş aminometil törəməsinin və 1,3-benzoksazin törəməsinin NMR spektrlərində birləşmələrin quruluşunun uyğun olmasını tam təsdiqləmişdir.

Sintez olunmuş birləşmələrin bakteriyalara və göbələklərə qarşı antimikrob sınağının ilkin nəticələri göstərmişdir ki, onlar həm bakterisid, həm də fungisid xassələrə malikdirlər.

Təkliflər:

Sintez olunmuş birləşmələr quruluşlarının zənginliyinə görə və ədəbiyyat məlumatlarına görə dərman vasitələri, neft məhsullarına antioksidləşdirici, antimikrob və s. aşqarlar kimi istifadə oluna bilər. Həmçinin də, ilkin tədqiqatların nəticəri də göstərmişdir ki, birləşmələr aşağı qatılıqlarda (0.1-0.2%) yüksək nəticələrə malikdirlər.

Ədəbiyyat:

1. Ali-Asgari, S., Moradi, M., Maskani, E. et al. Synthesis and Characterization of Novel Heterocyclic Compounds Containing the Benzoxazine Ring by 7-Hydroxycoumarin. Chem Nat Compd 53, 1028–1030 (2017). https://doi.org/10.1007/s10600-017-2194-x
2. Akhter, M., Habibullah, S., Hasan, S.M. *et al.* Synthesis of some new 3,4-dihydro-2*H*-1,3-benzoxazines under microwave irradiation in solvent-free conditions and their biological activity. Med Chem Res **20**, 1147–1153 (2011). https://doi.org/10.1007/s00044-010-9451-x

SYNTHESIS OF CYCLOPROPANE-CONTAINING DIESTER AND PREPARATION OF POLYESTER ON ITS BASIS

Leman Guliyeva, Khayyam Nazaraliyev, Rita Shahnazarli, Malahat Abdurahmanova
Institute of Polymer Materials of the Ministry of Science and Education of the Republic of Azerbaijan
Sumgait, Azerbaijan
ipoma@science.az

Abstract. A new compound (diester) – *para*-di-(2-ethoxycarbonylcyclopropyl) benzene has been synthesized as a catalyst by the reaction of *para*-divinylbenzene with ethyldiazoacetate in the presence of $CuSO_4$. The obtained compound has been characterized by spectral analysis methods. The purity and isomeric composition of the compound have

been determined by gas-liquid chromatography. As a result of the polycondensation reaction of diester with ethylene glycol under equilibrium conditions, the polyester of linear structure with aromatic and cyclopropane groups in the macromolecule chain has been synthesized. Some (physical-mechanical and thermal) properties of the synthesized polyester have been investigated.

Key words: cyclopropanation, diester, polycondensation, polyester.

Introduction.

Polyesters are heterochain high-molecular compounds containing regularly repeating ester groups in the main chain. Today, there are many varieties of polyesters, but the term "polyester" often refers to polyethylene terephthalate (PET). Polyesters are of great practical interest: they are widely used in the production of durable fibers, sheets, fiberglass and other materials [Dil, 2023, 306-342; Zhao, 2023, 438–449]. Polyester fibers are usually used in the production of clothing and often in mixture with natural fibers, which gives fabrics improved properties [Çamlıbel, 2018, 1-98; Gupta, 2009, 48-96]. Polyesters are widely used for reinforcement of the automobile tires, cable isolation, in the production of liquid crystal displays, dielectric layers used in condensers, etc [Deshmukh, 2024, 251-268].

Currently, various methods are used for preparation of the aliphatic, aromatic, and semi-aromatic polyesters. The main method for preparation of polyesters of linear structure is the polycondensation of dialcohols with dibasic acids (or their anhydrides), which results in the formation of a macromolecular chain with ester groups [Wang, 2022, 5059]. Depending on the structure of the dialcohol and the diacid, the structure of the polyester chain and its properties can vary greatly. [Nazaraliyev, 2024, 1178-1186; Wang, 2022, 5059].

This paper has been devoted to the synthesis of cyclopropane-containing diester and the preparation of linear polyester based on it.

Experimental part.

Synthesis of *para*-di-(2-ethoxycarbonylcyclopropyl)benzene (*para*-di-(2-ECCP)B).

0.5 g of anhydrous $CuSO_4$, 65 g (0.5 g mol) of freshly distilled divinylbenzene, 50 ml of benzene and 0.2 g of hydroquinone were placed in a 1-liter four-necked flask equipped with a mechanical stirrer with hermetic seal, a gas outlet tube, a thermometer and a separating funnel. The flask was pre-purged with nitrogen, then the mixture was heated in a water bath to 50°C and 114 g (1 g-mol) of ethyl diazoacetate was added dropwise with stirring for 4 h. The reaction behavior was controlled on the isolation of free nitrogen. After the introduction of all quantity of ethyl diazoacetate, the reaction mass was stirred at the same temperature for another 1 hour until the end of nitrogen isolation. The benzene was distilled from the reaction mixture, the residue was fractionated by vacuum distillation for preparation of the pure *para*-di-(2-ECCP)B.

Reesterification of (*para*-di-(2-ECCP)B) with ethylene glycol.

The reaction was carried out according to the procedure described in work [Grigorev, 1971, 64, 101]. *Para*-di-(2-ECCP)B was placed in a four-necked flask with a capacity of 500 ml, equipped with a stirrer with hermetic seal, a trap for catching ethanol vapors, a reflux condenser with a deflegmator and a thermometer and ethylene glycol with zinc acetate dissolved in it was introduced. The flask was gradually heated in a bath to 180-190°C with constant stirring. In this case, the isolation of ethanol was observed as a result of the reesterification reaction. Nitrogen was supplied to the reaction flask until the end of the reesterification process (3-6 h). During this time, approximately 85-95% of the theoretical volume of ethanol was distilled from the reaction mixture. Then the temperature was raised to the boiling point of ethylene glycol (~197 °C) and the excess ethylene glycol was distilled. After removing approximately 95% of ethylene glycol, the reaction was stopped. The boiling point of the obtained melt, consisting mainly of diglycol ester 2,2'-(1,4-phenylene)dicyclopropanecarboxylic acid and its dimers and trimers were 215-225°C. The boiling point of pure diglycol ester is 143°C/5 mm.merc.c.

Polycondensation of diglycol ester of 2,2'-(1,4-phenylene)dicyclopropancarboxylic acid

A flask with the obtained diglycol ester was heated to 170°C / 130 mm.merc.c. Then, for 40 min, the temperature was gradually increased to 240°C with simultaneous decrease in pressure to 10 mm.merc.c. and finally, for 1 h was heated to 250°C and a pressure of 1-2 mm.merc.c. During polycondensation, ethylene glycol was distilled and collected in a trap, while a gradual increase in melt viscosity and temperature was noted. The melting point of pure polyester was 232°C. The heating was continued to complete removal of the ethylene glycol and to achievement of the maximum viscosity of the melt. The melt was poured onto dry ice, where the polyester turned into a solid mass. Polyester is soluble in a mixture of phenol and tetrachloroethane at a ratio of 1:1 at 70°C.

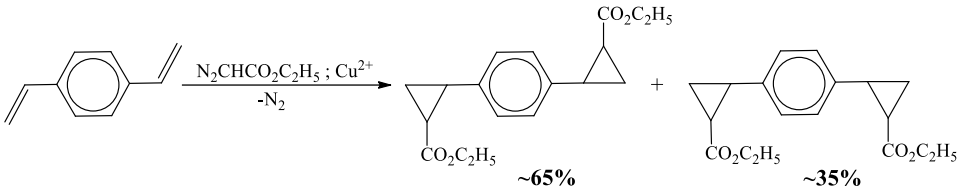
In Table 1 the conditions of carrying out of the reesterification and polycondensation reactions and the quantity of used reagents are presented.

Table 1. The conditions of carrying out of the reesterification and polycondensation reactions

Uploaded					Conditions of reesterification		Conditions of polycondensation	
(*para*-di-(2-ECCP)B		Ethylene glycol		$Zn(CH_3COOH)_2$	Temperature, °C	Time	Temperature, °C	Time
g	mol	g	mol	G				
30.2	0.1	15.5	0.25	$5 \cdot 10^{-3}$	180-190	3-4 h	170/130mm Hg	1 h
					197	3-4 h	240/10 mm Hg	40 min
							250/ 2 mm Hg	1 h

Results and discussion.

With the aim of preparation of the linear polyester, a new compound – *para*–di-(2-ethoxycarbonylcyclopropyl)benzene has been synthesized. The synthesis of the compound was carried out by interaction of *para*-divinylbenzene with ethyl diazoacetate taken in double excess. The cyclopropanation reaction proceeded due to the interaction of two double bonds of divinylbenzene with ethoxycarbonylcarbene generated by the catalytic decomposition of ethyl diazoacetate in the presence of anhydrous copper sulfate, according to the scheme shown below:



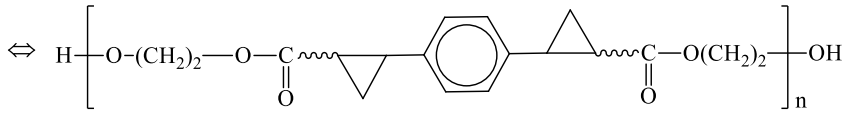
The yield of the purposeful product was about 95%. On data of the spectral (IR and PMR) analyses, there are aromatic, cyclopropane and ester functional groups in the structure of the synthesized monomer [Nazaraliyev, 2024, 1178-1186]. It has been established using gas-liquid chromatography that the reaction product is a mixture of two (*cis*-:*trans*-) geometric isomers in relation to a three-membered cycle, the ratio of which is ≈35:65. Subsequently, in the polycondensation reaction, the obtained diester was used without separation into isomers. Some physical-chemical properties of the synthesized diester are given in Table.

Table 2. Physical-chemical properties of *para*-di(2-ethoxycarbonylcyclopropyl)benzene

B.p.. (ºC/мм)	n_D^{20}	d_4^{20}	MR_D		Yield, %	Elemental composition (Calc. / Found)	
			Calc.	Found		C	H
140/1мм	1.5186	1.1150	82.05	82.04	95	71.52/71.60	7.28/7.16

The diester is an oily substance with sufficiently high boiling point. The compounds with functional groups such as cyclopropane, ester, etc., have potential biological activity. [Nazaraliyev, 2024, 1178-1186]. The synthesized diester, as confirmed by laboratory investigations at the Institute of Microbiology of the Ministry of Science and Education of the Republic of Azerbaijan, has antimicrobial properties against a number of gram-positive and gram-negative bacteria [Shahnazarli, 2025, 102].

As a result of the polycondensation reaction of diester with ethylene glycol under equilibrium conditions, the polyester was obtained, the macromolecules of which contain aromatic, cyclopropane and carbonyl groups:



The obtained polyester is a crystalline, semitransparent substance with softening temperatures 76-81°C and melting temperatures 232°C, is insoluble in common solvents, but is quickly dissolved in a mixture of phenol and tetrachloroethane (1:1) at temperature of 70°C. The viscosity of the polyester solution, found by the viscometric method (solution concentration 0.5 g/100 cm^3, t=50°C), was [η]=0.48 dl/g. MW of polyester calculated by the Mark-Houwink equation (K= 5.517×10^{-4}; α=0.709) was 12370 Da.

At the softening temperature, the synthesized polyester is easily stretched into a thread and has high adhesion to glass, fabrics and metal, which can be explained by the availability of an ester fragment in the macromolecule chain.

Suggestion. The synthesized diester, possessing antimicrobial properties, can be used as an active additive or a biocidal plasticizer in polymer compositions. Polyester can be used in the composition of the filled polymer compositions for improvement of the compatibility of system components. Due to its high adhesion to glass, metal and fabrics, it can also be used in adhesive compositions.

References.

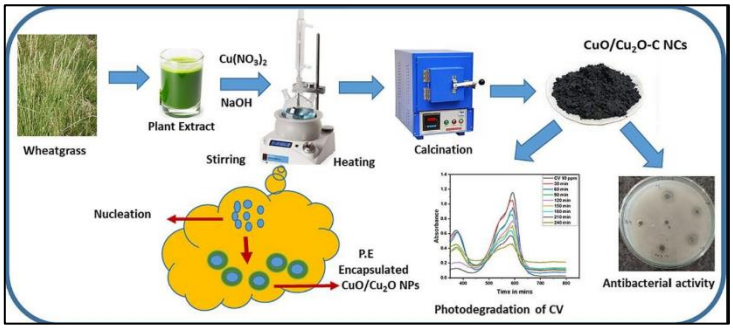
1. Çamlıbel N.O. Chapter from the book “Polyesters – Production, Characterization and Innovative Applications”. 2018. 1-98 p.
2. Deshmukh G.S., Palanisamy S., Mubarak S. Book “Synthetic and Mineral Fibers, Their Composites and Applications”. Chapter 8 - Polyester fiber: composites and it's applications. // Ed. by: Woodhead Publishing in Materials. 2024. P.251-268.
3. Dil E.J., Ajji A., Saffar A. Polyester Materials in Biomedical Applications. In: Polyester Films: Materials, Processes and Applications. Chapter 8. Ed. By Miko Cakmak, Jehuda Greener. 2023, p.306-342.
4. Gupta B.S. , Edwards J.V. Book “Advanced Textiles for Wound Care”. Chapter 3 - Textile materials and structures for wound care products. // Ed. by: Woodhead Publishing Series in Textiles. 2009, P. 48-96.
5. Nazaraliyev Kh.G., Shahnazarli R.Z., Ramazanov E.A., Nurullayeva D.R., Abdurahmanova M.A. Synthesis and properties of *para*-di-(2-ethoxycarbonylcyclopropyl) benzene as a new biologically active plasticizer. // Processes of Petrochemistry and Oil Refining (PPOR). 2024, Vol.25, No 4, pp.1178-1186**.**
6. Shahnazarli R.Z., Nazaraliyev Kh.G., Ramazanov E.A., Abdurahmanova M.A., Aliyeva A.H. Development of antibacterial nanocompositions based on polypropylene and *para*-di(2-etoxycarbonylcyclopropyl)benzene. // 9th Intern. Caucasian Symposium on Polymers & Advanced Materials. 2025. Kutaisi, Georgia. p.102.
7. Wang H., Li H., Ch.K.Lee, Mat Nanyan N.S., Tay G.S. Recent Advances in the Enzymatic Synthesis of Polyester. // *Polymers* 2022, *14*(23), 5059.
8. Zhao C., Yang S., Qin W. *et al.* Study on Synthesis and Properties of Oxybis Benzoic Aromatic Polyesters. Polym. Sci. Ser. B. 2023, v.65, p.438–449.
9. Grigorev A.P., Fedotova O.Ya. Laboratory workshop on the technology of polycondensation plastics. / Moscow, «Vysshaya shkola», 1971, p.64, 101.

CUOTEXTILE: A BIO-RESPONSIVE, NANOCLAY-ENCAPSULATED TEXTILE FOR HOSPITAL INFECTION CONTROL

Ziyad Shiraliyev
Rima Guliyeva
Baku Higher Oil School (SOCAR)
Baku, Azerbaijan
ziyad.shiraliyev.std@bhos.edu.az
rima.guliyeva@bhos.edu.az

Summary - Nowadays, millions of patients worldwide suffer from Healthcare-Associated Infections (HAIs) that lead to enormous healthcare costs. Although antibacterial bedsheets are used by hospitals, today's technologies are fundamentally not enough. They rely on "passive" metal coatings that irritate healthy patient skin, wash down the drain to pollute our waterways, and lose its antibacterial effectiveness after just a few trips to the laundry, because of leaking of the toxic ions. Cuotextile is a third-generation intelligent medical textile that offers a solution for these problems utilizing a bio-inspired "Trojan Horse" method. We hide green-synthesized Copper and Zinc molecules inside microscopic Halloysite clay tubes, instead of coating fabrics with exposed metals. These tubes are sealed shut with a smart biological lock made of starch and chitosan, and glue them to hospital cotton using a highly sustainable for a long time, mussel-inspired adhesive. The fabric, that remains completely dormant against human skin and regular sweat, only unlocks and releases its payload when it specifically detects the digestive enzymes produced by hazardous bacteria. This enables us to decrease manufactural expenses, reduce heavy metal water pollution, and cut the carbon footprint by more than two times.

Keywords: Smart Textiles, Healthcare-Associated Infections, Green Chemistry, Enzyme-Responsive Release, Sustainable Biomaterials



Introduction

Hospitals spend billions on antimicrobial textiles in order to prevent the spread of infections. However, three critical failures caused challenges like being less effective or sustainable for the current industry standards, which are usually Silver and Copper-infused fabrics.

Firstly, one of the main issues current fabrics releasing metal ions 7/24. The healthy skin cells of the patients are constantly exposed to these metals while lying on these sheets. Scientific research demonstrates that this

continuous, untriggered exposure leads to skin irritation and delayed healing of existing wounds.

The second issue is modern smart fabrics trying to release medicine when they become acidic, although normal human sweat is naturally acidic (around pH 5.5). Doctors and patients sweat constantly in a hospital setting, as a result of which the fabric wastes its antibacterial medicine when actual bacteria are not present.

Final issue is laundry disappearance. Most nanoparticles are physically sprayed onto fabrics without chemical bonds. After 10-15 harsh industrial hospital washes, the metals wash off. The hospital is left with a regular, unprotected bedsheet, and the local water supply is heavily polluted with toxic nanoparticle metals.

Experimental part

We made a four-part microscopic structure with inexpensive, natural materials to make a safe, smart and durable fabric. The process of preparation is very systematic and scalable.

To begin with, the payload must have a Kill and Heal synergy. We did not only use copper but made a Copper-Zinc hybrid, where toxic laboratory chemicals were substituted by clean and green synthesis process that used Aloe Vera extract and starch. Zinc helps the skin cells to repair, whereas copper is a very strong antibacterial agent.

Second, these metals are put in a vault. We do not impregnate the fabrics with the metals. We fill them rather with Halloysite, a natural clay of low price, microscopic hollow straws in form. The separation of the metals with the clay under a vacuum draws the particles in the deep parts of the tubes. The metals are not exposed to any healthy skin of the patient since they are concealed within.

Third, a biological gel is transformed into a smart lock out. The chitosan (made by shells) and starch are used to plug the ends of the loaded clay tubes. This enzyme sensitive gate is chemically crosslinked in a way that it is entirely solid and not damaged by human sweat and water.

Lastly, the sealed tubes are fixed on a regular hospital cotton with a super glue. We are using Polydopamine (PDA), an artificial counterpart of the super-strength glue used by ocean mussels to affix to wet rocks. Since PDA is dark brown in nature we combined it with Titanium Dioxide, which is a white pigment commonly used. The cloth is immersed in this modified PDA solution which permanently affixes the clay tubes to the textile fibers in a clean white coating that is friendly to hospitals.

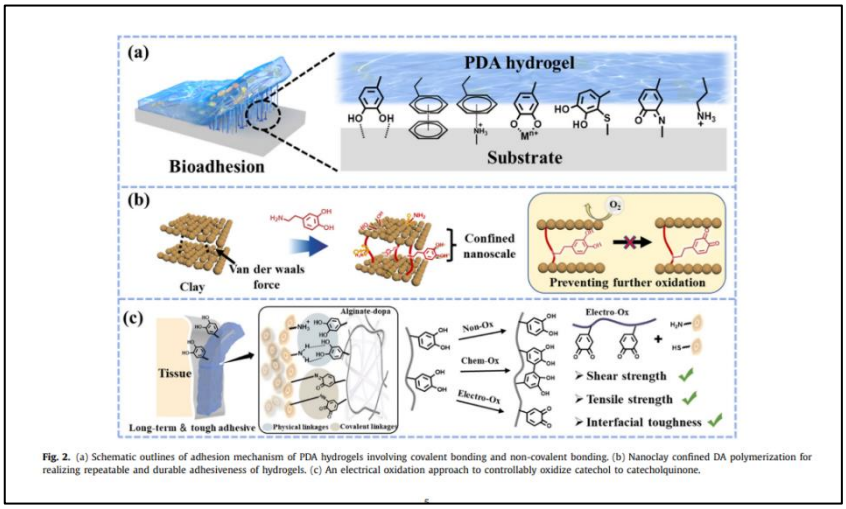


Fig. 2. (a) Schematic outlines of adhesion mechanism of PDA hydrogels involving covalent bonding and non-covalent bonding. (b) Nanoclay confined DA polymerization for realizing repeatable and durable adhesiveness of hydrogels. (c) An electrical oxidation approach to controllably oxidize catechol to catecholquinone.

Results and their discussion

The Cuotextile design has been shown to have significant enhancement over the conventional silver and copper fabrics in such aspects as environmental aspects, cost, and durability. The medical textile industry is directly transformed by our engineering approach in terms of its standard measures.

We estimated a dramatic cost reduction of 64% in production costs in terms of cost-effectiveness. Silver nanoparticles are very expensive in the market, making standard antimicrobial fabric with Silver nanoparticles about $5.00 per square meter. Our material cost is around $1.80 per square meter using a lot of natural clay 500$ per ton), bio-waste by-products such as starch and chitosan and inexpensive base metals.

The environmental outcomes are also quite stunning, with a 55% decrease in CO_2 footprint. The manufacturing of standard silver nanoparticles needs energy-intensive mining and harsh chemical vapor deposition, generating approximately 140 kg/kg of metal of CO_2. We synthesize green in water at low temperatures (80˚C) with plant extracts. With this coupled with the use of unrefined natural clay, it reduces the energy requirements considerably.

In addition, we offer 85% reduction of heavy metal water pollution. Since the natural fabrics cannot be washed more than 15 times in the laundry, millions of micrograms of harmful metals are discharged into the municipal wastewater. Since our copper and zinc are stored in a physical vault, and bonded by a mussel-like adhesive, the coating lasts 50 or more heavy wash cycles.

Most importantly, our biological gating mechanism is able to distinguish between sweat and infection successfully. When the starch-chitosan lock is placed in simulated sweat at pH 5.5 it is completely closed. But when

subjected to amylase and chitinase (the special enzymes of the digestive system released by the bad bacteria that tries to colonize the cloth) the lock decays. This causes the specific and burst discharge of Copper and Zinc only at the precise location of the bacteria.

Offers

This project gives the medical materials industry a total paradigm shift. We provide the shift between the so-called passive antimicrobial fabrics and the so-called intelligent micro-robotic defense systems.

In the case of the health sector, Cuotextile can save the healthcare industry a dramatic cut on hospital spending. Since the covalent bonds can withstand 50 or more washes as opposed to the standard 15 washes, the hospitals will be able to use the same sheet three times longer. This will lead to a 70% decrease in the solid medical textile waste disposed in landfills. It is also much more comfortable to the patient, as it does not expose them to the constant toxic metal exposure that is the cause of contact dermatitis.

In the case of the industrial manufacturing industry, we provide a very scalable solution. Since our manufacturing process involves simple procedure of using the standard dip-pad-cure machinery that is available in every large factory of the textile, Cuotextile would not need any new industrial equipment, and therefore it would be fully prepared to deploy and commercialize in the market within a short period.

References

[Krajisnik, 2019, 285-327] Krajisnik, D., Calija, B., Milic, J. Aluminosilicate-based composites functionalized with cationic materials: possibilities for drug delivery applications. Materials for Biomedical Engineering.

[Moges, 2025, 1-27] Moges, G. Critical review of biosynthesized CuO nanoparticle-functionalized fabrics: Antimicrobial, biocompatibility and cost effectiveness assessments for medical applications. Journal of Molecular Structure, 1348, 143244.

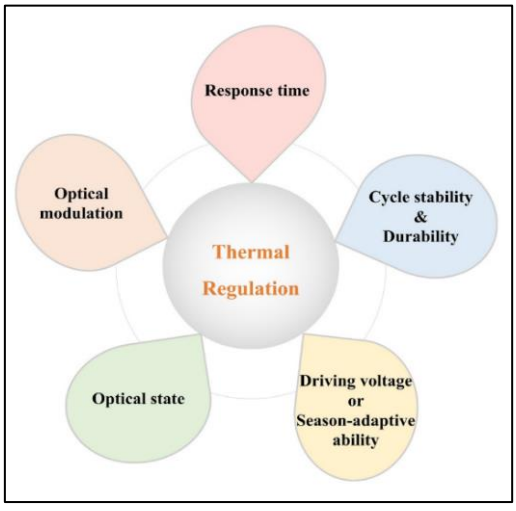
[Xu, 2023, 1-38] Xu, Y., Hu, J., Hu, J., Cheng, Y., Chen, X., Gu, Z., Li, Y. Bioinspired polydopamine hydrogels: Strategies and applications. Progress in Polymer Science, 146, 101740.

AUTONOMOUS SOLID-STATE ELECTROCHROMIC GLAZING: INTEGRATING BIOMASS-DERIVED SOLAR CONCENTRATORS WITH ANTI-FREEZING ORGANOHYDROGELS

Ziyad Shiraliyev
Adil Ismayilzada
Rima Guliyeva
Baku Higher Oil School (SOCAR)
Baku, Azerbaijan
ziyad.shiraliyev.std@bhos.edu.az
adil.ismayilzada.std@bhos.edu.az
rima.guliyeva@bhos.edu.az

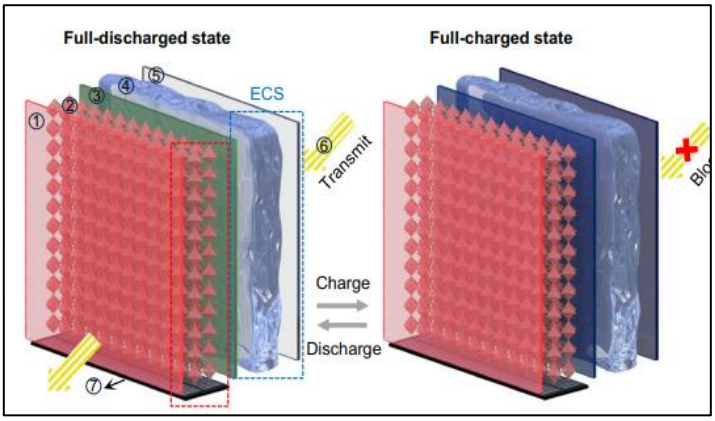
Summary - During the summer, a huge amount of energy is used to cool buildings of modern cities. To address this problem, smart windows which automatically darken can be used, however existing commercial products often need costly electrical wiring inside walls and contain flammable liquid chemicals. This project presents a smart window, named "Glazing", an all-electric and solid-state window. It provides luminous carbon nanoparticles that are made by using biomass which is available in the region and can trap sunlight and convert it to electricity without any external wiring [Huang, 2025, 1-10]. The produced electricity affects the chemical properties of glass, and it turns dark and blocks solar heat. To ensure that the window will be capable of withstanding extremely cold winters and hot summers without leaking and freezing, the standard liquid electrolytes were interchanged with the specially designed organohydrogel. It is a rubbery substance consisting of polyvinyl alcohol (PVA), ethylene glycol, and salts of neutral pH. Consequently, the smart window is nearly half the cost of commercial options to install, works in temperature descending to -30°C, and requires no grid-power, so it can be considered an appropriate solution to retrofitting the older buildings.

Keywords: Electrochromic smart window, Luminescent solar concentrator, Carbon quantum dots, Organohydrogel, Energy efficiency.



Introduction

The amount of energy consumed by buildings constitutes nearly 40% of the world's energy and heating, ventilation, and air conditioning (HVAC) systems use the largest proportion of energy. In bright areas like Baku, the sunlight that is seen through a normal glass brings about the greenhouse effect, which makes air conditioners operate 24 hours. Even though dynamic smart glass gets dark in the sunlight, which is an effective solution, modern commercial systems continue to face serious industrial and technological problems.



First, these systems must be hardwired to the electric grid. Wires installed in window frames become highly costly, particularly in refurbishing existing urban buildings. Secondly, several of the efficient solar-harvesting windows currently in use require heavy metals, which are also toxic, which is a problem in terms of environmental and safety aspects. Lastly, many of the electrochromic windows have liquid electrolytes that can leak or dry up or freeze in winter and could damage the glass. [Virya, 2021, 1-19].

The proposed project aims at resolving all three challenges by incorporating a Luminescent Solar Concentrator (LSC) to collect solar energy without wires and a WO_3/MnO_2 Electrochromic Supercapacitor (ESC) to make it change colour. The project suggests a scalable, safe, and highly effective smart glass solution to architectural purposes by creating anti-freezing polymer gel that is crosslinked and converts solar energy into a biowaste produced locally.

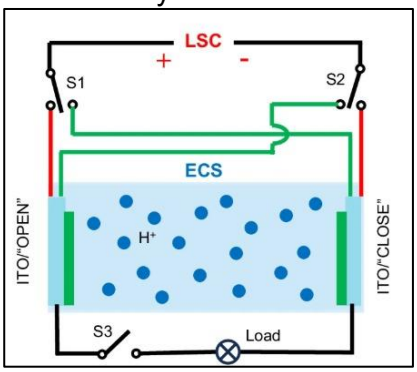
Experimental part

The prototype was made by scalable chemical engineering techniques, and the manufacturing process was separated into three major steps:

1. **Synthesizing the Luminescent Solar Concentrator (LSC):**

   We created Nitrogen-doped Carbon Quantum Dots (N-CQDs) from biomass rather than using toxic metals. The chitosan and urea were dissolved in dilute acetic acid and incubated in the autoclave at 180°C in 8 hours. A microscopic coating of the luminescent carbon dots with

tetraethyl orthosilicate (TEOS) was applied to avoid the degradation of these carbon dots under the UV radiation of the Sun [Zhou, 2020, 1-10]. The dots were then encircled with a transparent acrylic resin, and then a coating was poured onto the outer glass. When the sunlight reaches this layer, this layer reflects the light to the sides of the window, where the light is transformed into electricity with small silicon solar strips.



2. **The Colour-Changing Electrodes:**

Base material Indium Tin Oxide (ITO) coated glass. Tungsten oxide (WO_3) was electrodeposited on a single glass sheet, and it becomes blue upon the application of electrical charge. Manganese dioxide (MnO_2) was deposited on another sheet, and it turns brown. Notably, the two glass samples were subjected to heating in an oven at 250°C and left to heat over a period of 2 hours to stabilize the crystal structures of the material, such that the materials would not dissolve during the long-term operation.

3. **The Anti-Freezing Organohydrogel Assembly:**

Normal water gels will be frozen at 0°C. As a solution to this, we came up with a solvent consisting of 50% water and 50% Ethylene Glycol. Polyvinyl Alcohol (PVA) and 1.5 M Lithium Nitrate (LiNO3) were dissolved in this solution [Rosas, 2023, 1-8]. Lastly, Glutaraldehyde was incorporated to crosslink the mixture covalently. The liquid was placed between the two glasses to cure permanently into o leak-proof rubber when sandwiched the two glasses [Zhang, 2021, 1-12].

A 10-Farad supercapacitor was also put across the edge solar cells to provide a buffer to control the electrical energy. This also helps in stopping the peak of the voltages in cases where the volume of sunlight suddenly rises like in the cases when the clouds are cleared, thus, avoiding the over oxidation of the chemical components.

Results and their discussion

The device is clean and does not need any external power source to work. The introduction of chemical trap states into the carbon dots attained a large Stokes shift. These carbon dots will absorb the invisible ultraviolet (UV) light and emit visible light without reabsorption of their emission. Consequently, the luminescent solar concentrator (LSC) is capable of

maintaining a viable optical efficiency of approximately 1.5% even with massive window areas.

During normal daylight time, the power output of the solar cells placed on the edge is about 1.5 W/m2. The electrochromic tinting process needs about 150 coulombs of electrical charge, and the transition of a window between a clear state (65% transmission) and a darker state (25% transmission) takes about 5-10 minutes. This regulated progression coincides with the essence of sunlight which rises in the morning [Huang, 2025, 1-10].



Besides this, the introduction of ethylene glycol reduced the freezing point of the electrolyte to -30°C. The colour-switching process is slowed down at extremely low temperatures, but the organohydrogel is useful in preventing the formation of ice crystals. This will prevent the glass damages that are likely to occur and minimize the chances of cracking in the very cold winter temperature [Zhang, 2021, 1-12].

In order to test its business potential, we modeled its performance on a standard commercial building in Baku that has 2,000 m² glass facade. Peak cooling demand can be reduced to roughly 20% by dynamic smart glass. This would save approximately 50kWh/m² of electricity per year in a typical office building in Baku. in terms of a 2,000 m² facade, a 2,000 m² of Glazing would save about 100,000 kWh of electricity per year, and carbon emissions would go down to about 45 tonnes/year of CO2.

Traditional smart glass is wired and would cost approximately 900 dollars per square meter to install. By comparison, the estimated large scale production cost of Glazing is $300/m² with a target retail price of $450/m². As it can be installed just like the normal passive glass, it is able to reduce the initial installation costs by approximately 50% and in addition, it assists building owners to save an estimated 11,000 AZN of money each year in such operating costs.

Offers

Based on our findings, one of the solutions that can be applied to the Sustainable Cities Programme is Glazing. It offers the construction industry

a viable technology to upgrade the old buildings that are energy consumptive without necessarily having to undertake complex internal electrical alterations. The technology is also a practice of the circular economy in controlling urban climates, which utilizes biomass waste that is available locally and converted into advanced solar concentrators. We also suggest that future pilot projects should use Glazing in municipal buildings within Azerbaijan to test experimentally the durability expectations presented in this paper.

References

[Huang, 2025, 1-10] Huang, S., Guo, H., Xia, P., Sun, H., Lu, C., Feng, Y., Zhu, J., Liang, C., Xu, S., & Wang, C. (2025). Integrated device of luminescent solar concentrators and electrochromic supercapacitors for self-powered smart window and display. Nature Communications, 16(1), 2085. DOI: 10.1038/s41467-025-57369-6

[Rosas, 2023, 1-8] Rosas, J., Virya, A., Wong, N., Chua, J., & Lian, K. (2023). LiNO3-poly(vinyl alcohol) polymer electrolytes and its applications in electrochemical capacitors with extended operating temperatures. Solid State Ionics, 399, 116272. DOI: 10.1016/j.ssi.2023.116272

[Virya, 2021, 1-19] Virya, A., & Lian, K. (2021). A review of neutral pH polymer electrolytes for electrochemical capacitors: Transitioning from liquid to solid devices. Materials Reports: Energy, 1(1), 100005. DOI: 10.1016/j.matre.2020.12.002

[Zhang, 2021, 1-12] Zhang, Y., Wang, X., et al. (2021). Environmental-tolerant, highly transparent, and conductive organohydrogels for flexible strain sensors. Chemical Engineering Journal, 424, 130553. DOI: 10.1016/j.cej.2021.129637

[Zhou, 2020, 1-10] Zhou, J., Sheng, Y., Wang, Y., et al. (2020). Silica-confined carbon dots with highly stable luminescence for luminescent solar concentrators. Chemical Engineering Journal, 394, 124830. DOI: 10.1016/j.cej.2020.124830

BƏRPA OLUNAN XAMMALDAN TƏBİİ SEOLİT KATALİZATORLARI İLƏ BİOYANACAQ İSTEHSALI

[1]Aişə Süleymanova, [2]Gülbəniz Muxtarova
[1]Azərbaycan Respublikası Elm və Təhsil Nazirliyi Bioresurslar İnstitutu
Gəncə, Azərbaycan
[2]AR ETN Y.Məmmədəliyev adına Neft-Kimya Prosesləri İnstitutu
Bakı, Azərbaycan
aisha.suleymanova07@gmail.com

Xülasə - Müasir dövrdə fosil yanacaqların tükənməsi və ətraf mühitə mənfi təsirləri bərpa olunan xammal əsasında alternativ yanacaq mənbələrinin inkişafını zəruri etmişdir. Buna görə də bioyanacaqlar dayanıqlı enerji sistemlərinin formalaşmasında mühüm rol oynayır. Təqdim olunan tədqiqatda bərpa olunan xammaldan istifadə etməklə təbii seolit katalizatorlarının iştirakı ilə bioyanacaq istehsalı prosesi araşdırılmışdır. Təbii seolitlər yüksək səth sahəsi, güclü turşu mərkəzləri, termiki dayanıqlığı və ekoloji cəhətdən təhlükəsiz olması ilə seçilərək dayanıqlı kimya prinsiplərinə uyğun katalizatorlardır. Seolit katalizatorlarının bioyanacaq istehsal prosesində katalitik aktivliyi, alınan məhsul çıxımına təsiri və prosesin səmərəliliyi qiymətləndirilmişdir.

Açar sözlər: bioyanacaq, seolit, biodizel, transesterifikasiya, üzüm çəyirdəyi

Giriş

Kimya sənayesinin və energetika sektorlarının sürətli inkişafı ilə paralel olaraq ətraf mühitə göstərilən antropogen təsirin miqyası əhəmiyyətli dərəcədə artmışdır. Xüsusilə kimya sənayesində tətbiq olunan ənənəvi texnologiyalar yüksək enerji sərfiyyatı, təhlükəli reagent və həlledicilərdən istifadə, eləcə də böyük həcmdə zərərli tullantıların əmələ gəlməsi ilə xarakterizə olunur. Bu amillər torpaq, su və hava çirklənməsinə, iqlim dəyişmələrinin sürətlənməsinə və ekosistemlərin tarazlığının pozulmasına səbəb olur. Mövcud ekoloji çağırışlar kimyəvi proseslərin yenidən təkmilləşməsini və daha təhlükəsiz, səmərəli və dayanıqlı yanaşmaların tətbiqini zəruri etmişdir [Demirbash, 2020, 112699].

Bərpa olunan xammalların kimyəvi proseslərdə istifadəsi yaşıl kimyanın ən mühüm komponentlərindən biri hesab olunur. Bitki yağları, biokütlə, kənd təsərrüfatı və qida sənayesi tullantıları kimi resurslar fosil mənşəli xammallara alternativ olaraq həm ekoloji, həm də iqtisadi baxımdan perspektivli hesab edilir. Bu cür xammalların katalitik çevrilməsi nəticəsində bioyanacaq, biopolimer və digər əlavə dəyərli məhsulların alınması dayanıqlı inkişaf məqsədlərinə uyğun həllər təqdim edir [Mukhtarova, 2024, 666-674].

Bioyanacaqlara aid olan — biodizel ekoloji cəhətdən daha təhlükəsiz, bioloji parçalana bilən və mövcud neft əsaslı dizel mühərrikləri ilə tam uyğun olan, bərpa olunan yanacaq növü kimi xüsusi əhəmiyyət kəsb edir. Biodizel – yağ turşularının monoalkil efirləri ekoloji cəhətdən təhlükəsiz, bioloji parçalana bilən, zərərli təsiri aşağı olan və CO_2 neytrallığı ilə seçilən yanacaq növüdür. Biodizelin əsas üstünlükləri aşağı kükürd tərkibi, yüksək setan ədədi və yüksək yağlayıcılıq qabiliyyətinin olması ilə əlaqədardır. Buna görə də biodizel həm nəqliyyat sahəsində, həm də sənayedə neft əsaslı dizelin qismən əvəz edilməsi üçün perspektivli və alternativ yanacaq növü hesab olunur [Suleymanova, 2025, 155-381].

Biodizel istehsalında ən geniş istifadə edilən proses transesterifikasiya reaksiyası olub, triqliseridlərin metanol ilə qarşılıqlı təsirindən yağ turşularının metil efirləri və qliserin əmələ gəlir. Reaksiyanın kinetikası və selektivliyi, istifadə olunan katalizatorun tipi və aktiv mərkəzlərinin təbiəti reaksiyanın gedişinə, biodizelin çıxım səviyyəsinə birbaşa təsir göstərir [Mukhtarova, 2025, 564-573]. Sənaye miqyasında transesterifikasiya reaksiyasında homogen katalizatorlardan (NaOH, KOH) geniş istifadə olunsa da, onların bir sıra çatışmazlıqları mövcuddur: məhsuldan çətin ayrılma, sabunlaşma reaksiyalarının yaranması, yüksək miqdarda su və həlledici ilə yuyulma tələb olunması və reaktorların korroziyaya uğraması. Qeyd ounan məhdudiyyətlər biodizel istehsalının iqtisadi və texnoloji səmərəliliyini azaldır. Bu səbəbdən son illərdə sənaye tətbiqlərində selektivliyi artıran, təkrar istifadə oluna bilən və təmiz texnologiya məhdudiyyətlərinə cavab verən heterogen katalizatorlara keçidi zəruri edir [Mukhtarova, 2023, 156-163].

Aparılan tədqiqat işində alternativ enerji resurslarının inkişafı, bərpa olunan xammalların səmərəli istifadəsi, tullantıların təkrar emalı, eyni zamanda heterogen katalizator prinsiplərinin biodizel istehsalında praktiki tətbiqinin genişləndirilməsi məqsədilə, üzüm çəyirdəyi tullantılarından alınan yağların, Tovuz rayonu ərazisindən götürülmüş təbii Aydağ seolitinin iştirakı ilə transesterifikasiya reaksiyası tədqiq olunmuşdur.

Eksperimental hissə

İstifadə olunan xammal və reagentlər

Tədqiqat işində xammal kimi, şərab emalı prosesindən sonra üzümdən alınan çəyirdəy tullantıları istifadə edilmişdir. Üzüm çəyirdəyi nümunələri əvvəlcə mexaniki qarışıqlardan təmizlənmiş, distillə olunmuş su ilə yuyulmuş və 105°C temperaturda sabit çəkiyə qədər qurudulmuşdur. Qurudulmuş nümunələr laboratoriya dəyirmanında xırdalanaraq yağ ayrılması üçün hazırlanmışdır.

Üzüm çəyirdəyi yağının alınması

Üzüm çəyirdəyi yağının alınması məqsədilə həlledici iştirakı ilə ekstraksiya üsulu tətbiq edilmişdir. Bu məqsədlə xırdalanmış üzüm çəyirdəyi nümunələri Soxhlet aparatında n-heksan həlledicisi ilə 6-8 saat müddəti ərzində ekstraksiya edilmişdir. Proses başa çatdıqdan sonra həlledici distillə üsulu ilə ayrılmış və alınmış yağ vakuum şəraitində qurudulmuşdur.

Təbii Aydağ seolitinin hazırlanması

Katalizator kimi istifadə olunan təbii Aydağ seoliti Tovuz rayonu ərazisindən götürülmüşdür. Seolit nümunələri ilkin olaraq mexaniki qarışıqlardan təmizlənmiş, distillə olunmuş su ilə yuyulmuş və 110°C temperaturda qurudulmuşdur. Qurudulmuş seolit dəyirman vasitəsilə xırdalanmış və 0.142 mm ölçüyə qədər ələklərdən keçirilmişdir. Katalitik aktivliyin artırılması məqsədilə seolit nümunələri termiki aktivləşməyə məruz qalmışdır. Bu məqsədlə seolit 500–600°C temperaturda mufel sobasında saxlanılaraq aktiv fazanın formalaşması təmin edilmişdir. Hazırlanmış katalizator reaksiya proseslərində heterogen katalizator kimi istifadə olunmuşdur.

Transesterifikasiya reaksiyasının aparılması

Üzüm çəyirdəyi yağından biodizelin alınması heterogen katalizatorun iştirakı ilə transesterifikasiya reaksiyası vasitəsilə həyata keçirilmişdir. Reaksiya qarışığı 1:5, 1:10 mol nisbətində götürülmüş üzüm çəyirdəyi yağı və metanoldan ibarət olmuş, katalizator isə 3% kütlə payında sistemə əlavə edilmişdir.

Transesterifikasiya reaksiyası mexaniki qarışdırıcı ilə təchiz olunmuş şüşə reaktorda, 65, 75°C temperaturda və 2 saat vaxt intervalında aparılmışdır. Reaksiya müddətində qarışığın homogenliyi təmin edilmişdir.

Reaksiya məhsullarının ayrılması və təmizlənməsi

Reaksiya başa çatdıqdan sonra qarışıq soyudulmuş və katalizator filtrasiya yolu ilə sistemdən ayrılmışdır. Alınmış məhsul müəyyən müddət ərzində çökməyə buraxılmış, nəticədə biodizel fazası və qliserin fazası ayrılmışdır. Biodizel fazası ayrılaraq isti distillə olunmuş su ilə bir neçə dəfə yuyulmuş və qalıq metanolun ayrılması təmin edilmişdir. Son mərhələdə biodizel nümunəsi vakuum şəraitində qurudulmuşdur.

Analitik və fiziki-kimyəvi analizlər

Alınmış biodizel nümunələrinin keyfiyyət göstəricilərinin müəyyən edilməsi məqsədilə fiziki-kimyəvi analizlər aparılmışdır. Biodizelin əsas xassələri – sıxlıq, kinematik özlülük, turşu ədədi və efir tərkibi müvafiq standart metodlara uyğun olaraq təyin edilmişdir.

Nəticələr və onların müzakirəsi

Cədvəl 1. Təbii seolit katalizatorunun iştirakı ilə həyata keçirilən transesterifikasiya prosesinin nəticələri

Katalizator	Reaksiyanın temperaturu (°C)	Reaksiyanın müddəti (saat)	Mol nisbəti yağ:metanol	Katalizatorun miqdarı (%)	Biodizelin çıxımı (%)	Qliserinin çıxımı (%)
Təbii seolit	65	2	1:5	3	69.4	38.5
Təbii seolit	65	2	1:10	3	79.9	32.4
Təbii seolit	75	2	1:5	3	92.3	26.1
Təbii seolit	75	2	1:10	3	95.4	23.9

Təcrübələr nəticəsində üzüm çəyirdəyi yağından Aydağ seolit katalizatoru ilə aparılan 75°C-də, 1:5, 1:10 (yağ:metanol) mol nisbətində transesterifikasiya reaksiyası əsasında alınmış biodizel çıxımı 92.3–95.4% miqdarında olmuşdur (Cədvəl 1). Çıxım miqdarının yüksək səviyyədə olmasının əsas səbəbi katalizatorun heterogen xüsusiyyətləri, yüksək səth sahəsi və Brensted/Lyuis turşu mərkəzlərinin transesterifikasiya prosesində aktiv rol oynamasıdır.

Seolit katalizatorunun səthi üzərində yerləşən Brensted və Lyuis turşu mərkəzləri yüksək katalitik aktivlik nümayiş etdirir. Bu aktiv mərkəzlər metanol molekulunun aktivləşməsinə və triqliserid molekulunun karbonil qrupunun elektrofil xüsusiyyətlərinin artmasına səbəb olur. Nəticədə transesterifikasiya reaksiyasının aktivləşmə enerjisi azalır və yağ–metanol qarşılıqlı təsiri sürətlənir. Aktiv mərkəzlərin mövcudluğu yağ turşularının metil efirlərinin çıxımının artmasına şərait yaradır.

Təbii seolit katalizatorunun iştirakı ilə üzüm çəyirdəyi yağından transesterifikasiya reaksiyasından alınmış biodizelin müxtəlif metodlarla

mühüm fiziki-kimyəvi xassələri təyin edilmiş və beynəlxalq standartlara uyğunluğu əsasında təhlil edilərək ekoloji üstünlükləri və mühərrik səmərəliliyinə təsirinin təhlili aparılmışdır.

- **Sıxlıq**: 0.875–0.880 q/cm³, bu beynəlxalq standart EN 14214 və ASTM D6751 göstəriciləri ilə uyğundur.
- **Kinematik özlülük**: 4.5–5.2 mm²/s, bu, mühərriklərdə yaxşı püskürmə və yanma xüsusiyyətlərini təmin edir.
- **Turşu ədədi**: 0.35–0.40 mq KOH/q, aşağı turşuluq biodizelin saxlanma müddətini və metal korroziyaya qarşı dayanıqlığını artırır.
- **Efir tərkibi**: 93–95%, yüksək efir tərkibi reaksiyanın effektivliyini və yanma məhsullarının keyfiyyətini yaxşılaşdırır.

Bu göstəricilər göstərir ki, təbii Aydağ seolit katalizatoru transesterifikasiya prosesində həm yüksək selektivlik, həm də sabit reaktivlik təmin edir.

Yekun olaraq qeyd edə bilərik ki, təbii seolit üzüm çəyirdəyi yağından alternativ yanacaq olaraq biodizelin istehsalında iqtisadi cəhətdən əlverişli, ekoloji təmiz heterogen katalizator kimi istifadə oluna bilər. Alınan biodizelin neft əsaslı dizel yanacaqlarına ekoloji komponent olaraq əlavə edilərək nəqliyyat vasitələrində ekoloji təmiz yanacaq kimi istifadə edilməsi tövsiyyə olunur.

İstinadlar

1. Demirbash A. Progress and recent trends in biodiesel fuels / A. Demirbash // Energy Conversion and Management. – 2020. – Vol. 209, – P. 112699.
2. Mukhtarova G.S., Suleymanova A.B. Study of biodiesel obtained from agro-industrial waste / G.S. Mukhtarova, A.B. Suleymanova // Processes of Petrochemistry and Oil Refining. – 2024. – Vol. 25, iss. 3. – P. 666-674.
3. Suleymanova A.B. Structure Activity correlation of Modified Zeolite Catalysts in Biodiesel Synthesis / A.B. Suleymanova, G.S.Mukhtarova // Ctalysis Letters. – 2025. – Vol. 155, iss. 381. – P. 155-381.
4. Mukhtarova G.S.Research of physical-chemical properties of biodiesel fraction obtained from agro-industrial waste / A.B. Suleymanova, G.S.Mukhtarova // Processes of Petrochemistry and Oil Refining, – 2025. – Vol. 26, iss. 2. – P. 564-573.
5. Mukhtarova G.S. Hydrocracking of heavy oil residues with the participation of Ni-bentonite / G.S. Mukhtarova, A.B. Hasanova // SOCAR Proceedings, – 2023. – Vol. 3, – P. 156-163.

GO/ZnAl-LDH NANOKOMPOZİTİ ƏSASINDA METİLEN GÖYÜNÜN FOTODEQRADASİYA VƏ ADSORBSİYASI QABİLİYYƏTİNİN ÖYRƏNİLMƏSİ.

Quluzadə Nuray, Balayeva Ofeliya
Bakı Dövlət Universiteti
Bakı, Azərbaycan
nurayquluzade36@gmail.com.

Xülasə. Tədqiqaq işində, ilkin olaraq Hummers metodu ilə ikiölçülü struktura malik qrafen-oksid (GO) sintez edilmiş və müxtəlif qatılıqlı GO/ZnAl-LDH nanokompoziti hazırlanmışdı. Hər bir nümunə üçün qadağan olunmuş zonanın eni hesablanmışdır. GO/ZnAl-LDH və metilen göyü məhlulu hazırlanmış və 2, 4, 6 saat müddətində fotodeqradasiya prosesi həyata keçirilmişdir. Deqradasiya nəticələrinə əsasən, sürət sabitləri və metilen göyünün adsorbsiya dərəcəsi hesablanmışdır. Ən güclü fotodeqredasiya və adsorbsiya birinci nümunədə müşahidə edilmişdir, bu qrafen-oksidin miqdarının birinci nümunədə daha çox olması və onun geniş səth sahəsinə malik olması ilə əlaqədardır.

Açar sözlər: Qrafen oksid, Hummers metodu, ZnAl-LDH/PVS, Sorbsiya, Fotodeqradasiya

Giriş

Sənaye inkişafının başlanğıcı ağır metal ionlarının (HMI), antibiotiklərin və boyaların mürəkkəb qarışığının çox miqdarda əmələ gəlməsi ilə əlaqələndirilmişdir ki, bu da ciddi ətraf mühit və sağlamlıq riskləri yaradır[1]. Tekstil, qida, çap, kağız və kosmetika sənayelərindən çıxan tullantı sularında üzvi boya çirkləndiricilərinin insanlar üçün sağlamlıq problemlərinə səbəb ola biləcəyi düşünülür, çünki bu maddələr oksidləşməyə, bioparçalanmaya, fotodeqradasiyaya və istiliyə qarşı yüksək müqavimət göstərir[2]. Hər il təxminən 7×10^5 ton kommersiya boyası istehsal olunur və bu miqdarın 2/3 hissəsi tekstil sektorunda istifadə olunur[3]. Bundan əlavə, hesablanıb ki, istehsal olunan boyanın hər il 10–20%-i tullantı sulara atılır[4]. Üzvi və qeyri-üzvi çirkləndiricilərin su mühitindən təmizlənməsi üçün müxtəlif metodlar mövcuddur. Ən effektiv üsullardan biri adsorbsiyadır. Bu üsul ucuzluğu, istismar asanlığı, sadəliyi ilə xarakterizə olunur. Zhang və Jaroniec fotokataliz üçün adsorbsiya ilə bağlı bir araşdırma təqdim edərək, reaktiv növlərin əvvəlcə fotokatalizator səthinə adsorbsiya edilməli olduğunu vurğulamışlar[6]. Həqiqətən də, ədəbiyyatda bildirildiyi kimi, fotokatalitik qiymətləndirmələr adətən çirkləndirici məhlulu və fotokatalizatoru qarışdıraraq adsorbsiya–desorbsiya tarazlığını təmin etmək üçün aparılır[7,8,9].

Təcrübi hissə

İlkin olaraq Qrafen oksid (GO) Hummers metodu ilə hazırlanmışdır. I- IV nümunələr üçün müvafiq olaraq 50, 25, 12.5 və 5 ml GO məhlulu götürülmüşdür. Hər bir GO məhluluna 0.005 g ZnAl-LDH əlavə edilmiş və GO/ZnAl-LDH nanokompoziti hazırlanmışdır. V nümunə üçün yanlız 0.005 g ZnAl-LDH istifadə edilmişdir. Hər bir nümunə UV-Vis spektroskopiyası üsulu ilə tədqiq

edilmişdir və qadağan olunmuş zonanın eni I- IV nümunələr üçün müvafiq olaraq 3.31 eV, 3.28 eV, 3.22 eV və 3.67 eV olduğu hesablanmışdır. Fotodeqradasiya üçün 10 ppm Metilen Göy (MG) məhlulu hər nümunəyə əlavə edilmiş və reaksiyalar 2, 4 və 6 saat müddətində aparılmışdır. Metilen göyünün sorbsiya dərəcəsi(R%)və fotodeqradasiya dərəcəsi uyğun olaraq aşağıdakı tənliklərlə (1və 2) hesablanmışdır[11].

$$R(\%) = \frac{C_0 - C_t}{C_0} \text{ x } 100 \qquad (1)$$

$$FD(\%) = \frac{A_0 - A_t}{A_0} \text{ x } 100 \qquad (2)$$

burada C_0 ilkin boyanın qatılığı, C UB şüalanmasından sonra boyanın qatılığı, A_0 ilkin udma qabiliyyətini, A isə UB şüalanmasından sonra boyanın udma qabiliyyətini göstərir**.**

Adsorbsiya tutumu (q_e) 3-cü tənlikdən istifadə edilməklə hesablanmışdır.[5]

$$q_e = \frac{(C_0 - C_t)}{m} \cdot V \qquad (3)$$

q_e- adsorbsiya tutumu (mg/g), C_0- metilen göyünün başlanğıc qatılığı (mg/L), C_e- metilen göyünün tarazlıq qatılığı (mg/L), V- metilen göyünün həcmi (L), m- adsorbentin kütləsi (g).

Birinci dərəcəli kinetika reaksiyasına əsasən, sürət sabiti $k(\text{min}^{-1})$ aşağıdakı tənlikdən istifadə edilərək müəyyən edilmişdir [10]:

$$\ln \frac{C_t}{C_0} = k \cdot t \ (4)$$

burada C_0 və C_t müvafiq olaraq başlanğıcda və t müddətində olan qatılıq, t isə şüalanma müddətidir.

Cədvəl 1. Alınmış nümunələrin metilen göyünə görə sorbsiya və fotodeqradasiya göstəriciləri

Fotodeqradasiya Müddəti(dəq)	I nümunə	II nümunə	III nümunə	IV nümunə	V nümunə
S_t	3.2	1.2	2	0.4	1
R%	16%	6%	10%	2%	5%
120(dəq)	29%	21%	26%	23%	10%
240(dəq)	44%	31%	51%	42%	36%
360(dəq)	61%	50%	61%	55%	58%
K($dəq^{-1}$)	0.0023	0.0024	0.0024	0.0023	0.0024

Nəticə.

Hummers metodu ilə qrafen-oksid (GO) sintez edilmiş və 50, 25, 12.5, 5 ml həcmdə qrafen-oksid məhlulu ilə GO/ZnAl-LDH nanokompoziti hazırlanmışdır. UV-Vis analizləri nəticəsində hər bir nümunə üçün qadağan olunmuş zonanın eni hesablanmış və nəticələr 3.22-3.67 intervalında dəyişmisdir. IV

nümunədə Qrafen-oksidin miqdari ən az olması nəticəsində sistem daha çox ZnAl-LDH xüsusiyyətlərinin nümayiş etdirmişdir və buna görədə qadağan olunmuş zonanın eni artmışdır. Hər bir nümunəyə 10 ppm metilen göyü (boyaq maddəsi) əlavə edilmiş və 2, 4, 6 saat müddətində fotodeqradasiya prosesi həyata keçirilmişdir. GO miqdarı I nümunədə daha çox olduğu üçün 6 saatda metilen göyünün parçalanma faizi daha yüksək olmuşdur, çünki qrafen-oksidin miqdarının çox olması aktiv mərkəzlərin çox olmasına səbəb olur. Hər bir nümunə üçün fotodeqradasiya prosesinə uyğun olaraq sürət sabitləri(k) hesablanmış, k=0.0023-0.0024 intervalında olmuşdur. Hər bir nümunə üçün metilen göyünün adsorbsiya tutumu hesablanmış və I nümunədə adsorbsiya tutumu ən yüksək olmuşdur. Nəticələrə əsasən, biz qeyd edə bilərik ki, GO miqdarının çox olması nanokompozitin səth sahəsinin və aktiv mərkəzlərinin sayının artmasına və bunun nəticəsində nanokompoztinin həm adsorbsiya, həmdə fotokatalitik avtivliyin yüksəlməsinə səbəb olur. GO/ZnAl-LDH nanokompoziti metilen göyünün sulu mühitdən effektiv şəkildə təmizlənməsi üçün perspevtiv maddədir.

Ədəbiyyat icmalı:

1. Huang et al., 2019; Gopalakrishnan et al., 2015; Wang et al., 2021; Chen et al., 2021.
2. Removal of Methylene Blue and Congo Red Using a Chitosan–Graphene Oxide-Electrosprayed Functionalized Polymeric Nanofiber Membrane. Nethmi S. L. Dissanayake Maadri A. Pathirana, Nandula D. Wanasekara, Boris Mahltig, and Gayani K. Nandasiri
3. Raval, N.P.; Shah, P.U.; Shah, N.K. Adsorptive amputation of hazardous azo dye Congo red from wastewater: A critical review. Environ. Sci. Pollut. Res. 2016, 23, 14810–14853.
4. Gharbani, P.; Tabatabaii, S.M.; Mehrizad, A. Removal of Congo red from textile wastewater by ozonation. Int. J. Environ. Sci. Technol. 2008, 5, 495–500.
5. Al-Jabari, M. A., & Salem, A. (2019). Adsorption of methylene blue from aqueous solution by activated carbon derived from walnut shell: Equilibrium, kinetic, and thermodynamic studies. Journal of King Saud University – Engineering Sciences, 31(1), 27–34.
6. Zhang, L.; Jaroniec, M. Fundamentals of Adsorption for Photocatalysis. In Interface Science and Technology; Elsevier: Amsterdam, The Netherlands, 2020; Volume 31, pp. 39–62. ISBN 978-0-08-102890-2.
7. Garg, R.; Gupta, R.; Bansal, A. Synthesis of G-C_3N_4/ZnO Nanocomposite for Photocatalytic Degradation of a Refractory Organic Endocrine Disrupter. Mater. Today Proc. 2021, 44, 855–859.
8. Paul, D.R.; Gautam, S.; Panchal, P.; Nehra, S.P.; Choudhary, P.; Sharma, A. ZnO-Modified g-C_3N_4: A Potential Photocatalyst for Environmental Application. ACS Omega 2020, 5, 3828–3838.
9. Sher, M.; Javed, M.; Shahid, S.; Hakami, O.; Qamar, M.A.; Iqbal, S.; AL-Anazy, M.M.; Baghdadi, H.B. Designing of Highly Active G-C_3N_4/Sn Doped ZnO Heterostructure as a Photocatalyst for the Disinfection and Degradation of the Organic Pollutants under Visible Light Irradiation. J. Photochem. Photobiol. Chem. 2021, 418, 113393.
10. K. Vasanth Kumar, K. Porkodi, A. Selvaganapathi.Constrained in solving Langmuir-Hinshelwood kinetic expression for the photocatalytic degradation of Auramine O aqueous solutions by ZnO catalyst, Dyes Pigments, 75 (2007), pp. 246-249.
11. S. Ameen, M.S. Akhtar, Y.S. Kim, O.-B. Yang, H.-S. Shin, Synthesis and characterization of novel poly (1-naphthylamine)/zinc oxide nanocomposites: Application in catalytic degradation of methylene blue dye, Colloid Polym. Sci. 288 (2010) 1633–1638.

EVALUATION OF THE CORROSION INHIBITION EFFICIENCY OF INHIBITOR SYSTEMS SYNTHESIZED FROM NATURAL PETROLEUM ACIDS

Ulviyya Abbasova, Sara Abbaszadeh, Rufana Alizadeh, Vugar Gasimov
Ministry of Science and Education of the Republic of Azerbaijan Institute of Petrochemical Processes named after acad. Y. Mammadaliyev, Baku, Azərbaijan, Khojalı ave
e-mail: rufana.alizada93@gmail.com

Abstract - Compositions based on amidoamines synthesized from natural petroleum acids isolated from T-46 oil distillate and the kerosene fraction of Azerbaijani crude oils, as well as their iron, nickel, zinc, and manganese salts, were prepared and evaluated as preservation (conservation) fluids for corrosion protection. The amidoamine and metal salts added to the T-46 oil distillate were introduced in equal proportions. The total concentration of amidoamine and metal salts in the preservation fluids was adjusted to 10% and 20%, respectively. It was established that the highest protective efficiency was achieved when nickel salts of natural petroleum acids were incorporated into the composition. Specifically, a preservation fluid formulated from T-46 oil distillate containing 10% amidoamine derived from natural petroleum acids and ethylenediamine, along with 10% of the corresponding nickel salt of these acids, provided atmospheric corrosion protection in a humidity chamber for more than 263 days. In seawater and in a 0.001% H_2SO_4 solution, the protection durations were 162 and 160 days, respectively. It was also determined that preservation fluids formulated on the basis of manganese, iron, and zinc salts of natural petroleum acids ensured atmospheric corrosion protection for 225, 240, and 194 days, respectively. In aggressive media, the corresponding protection periods were 125, 140, and 125 days.

Keywords: atmospheric corrosion, preservation fluids, natural petroleum acids, amidoamines, metal salts

Introduction

At present, atmospheric air is increasingly contaminated with aggressive components such as H_2S, CO_2, nitrogen oxides, sulfur oxides, and other pollutants. As a consequence, the intensity of atmospheric corrosion affecting metal equipment and their spare parts has significantly increased. Various methods have been developed to combat atmospheric corrosion, among which the use of conservation fluids represents one of the most practical and economically viable approaches [Abbasov et al., 2016, 262–265]. Extensive research in this field is being conducted at numerous scientific centers worldwide, including the Y.H. Mammadaliyev Institute of Petrochemical Processes [Abbasova, 2021, 152–158]. However, it should be noted that neither in Azerbaijan nor in other Caspian littoral countries is there fully established industrial production of conservation fluids, which are considered one of the most effective means of atmospheric corrosion protection. Therefore, comprehensive research efforts are required in this area to develop new and more efficient conservation fluids and to establish their industrial-scale production. [Abbasova, 2022, 517–523].

Experimental Section

Amidoamines were synthesized via the reaction of petroleum acids isolated from the kerosene fraction obtained from a mixture of Baku crude oils with ethylenediamine. The physicochemical properties of the synthesized amidoamines are presented in Table 1.

Manganese (Mn), iron (Fe), nickel (Ni), and zinc (Zn) salts of natural petroleum acids (NPA) were prepared using a double-exchange (metathesis) method. The reaction was carried out in a hexane medium. Conducting the reaction in an organic solvent was intended to ensure the absence of crystallization water in the resulting metal salts. Upon completion of the reaction, the solvent was evaporated to obtain the purified salts. The physicochemical properties of the metal salts are summarized in Table 2.

Table 1. Physicochemical Properties of Amidoamines Derived from the Reaction of Petroleum Acids Isolated from Distillates of Baku Crude Oil Mixtures with Ethylenediamine

Parameter	Method	Mn Salt of NPA	Fe Salt of NPA	Ni Salt of NPA	Zn Salt of NPA
Kinematic Viscosity, mm²/s at 20°C	ASTM D445	–	–	–	–
Density, g/cm³ at 20°C	ASTM D5002	1.011	1.019	1.010	1.031
Refractive Index at 20°C	ASTM D5006-96	1.4861	1.4881	1.4835	1.4840
Pour Point, °C	GOST 20287-91	−15	−15	−10	−15

The molecular structure of the nickel (Ni) salt of natural petroleum acids was investigated by infrared (IR) spectroscopy, and the corresponding spectrum is presented in **Figure 1.**

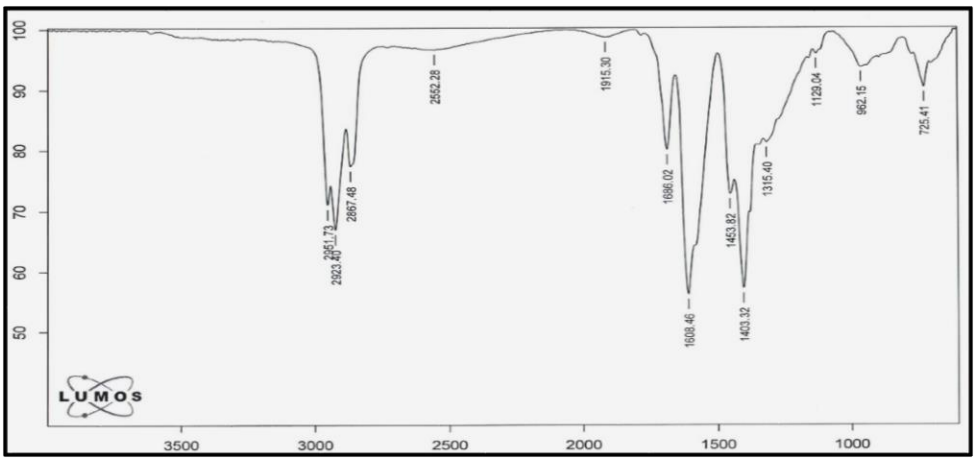


Figure 1. IR Spectrum of the Nickel Salt of Natural Petroleum Acids

The following absorption bands were observed in the IR spectrum:

- Deformation vibrations of the C–H bond in $–CH_3$ and $–CH_2–$ groups at 1453 cm^{-1};
- Stretching (valence) vibrations of C–H bonds at 2867, 2923, and 2951 cm^{-1};
- A band at 1686.02 cm^{-1} corresponding to the C=O group of associated carboxylic acids;
- An absorption band at 1608.46 cm^{-1} attributed to the C=C bond in the aliphatic chain;
- Deformation vibrations of the C–H bond in the =C–H group at 1403.32 cm^{-1};
- In-plane vibrations of the Ni–O bond at 1315.40 cm^{-1};
- Out-of-plane vibrations of the Ni–O bond at 962 cm^{-1};
- Deformation vibrations of the C–H bond in (CH_2) groups of the naphthenic structure at 725.41 cm^{-1}.

Conservation fluids were formulated on the basis of T-46 oil distillate, amidoamines derived from natural petroleum acids and ethylenediamine, as well as Mn, Fe, Zn, and Ni salts of the corresponding acids. During formulation, the amidoamine and the metal salt were introduced in equal proportions. In the first case, the conservation fluid consisted of 90% T-46 oil distillate, 5% amidoamine of natural petroleum acids, and 5% of the corresponding metal salt (total inhibitor concentration: 10%). In the second formulation, the amidoamine and metal salt were each added at 10% (total inhibitor concentration: 20%), together with 80% T-46 oil distillate. The prepared conservation fluids were evaluated in a humidity chamber, in seawater, and in a 0.001% H_2SO_4 solution. The obtained results are presented in **Table 2.**

Table 2. Corrosion resistance performance of conservation fluids based on T-46 oil distillate containing amidoamines derived from natural petroleum acids and ethylenediamine, and their Mn, Fe, Zn, and Ni salts in a humidity chamber, seawater, and 0.001% H_2SO_4 solution

No.	Sample Composition	Inhibitor Content, %	Humidity Chamber (days)	Seawater (days)	0.001% H_2SO_4 Solution (days)
1	T-46 oil distillate + ETDAA + Mn salt of NPA	10	164	90	90
2	T-46 oil distillate + ETDAA + Mn salt of NPA	20	225	125	121
3	T-46 oil distillate + ETDAA + Fe salt of NPA	10	190	92	91
4	T-46 oil distillate + ETDAA + Fe salt of NPA	20	240	140	139
5	T-46 oil distillate + ETDAA + Zn salt of NPA	10	182	71	70
6	T-46 oil distillate + ETDAA + Zn salt of NPA	20	194	125	122

7	T-46 oil distillate + ETDAA + Ni salt of NPA	10	255	155	150
8	T-46 oil distillate + ETDAA + Ni salt of NPA	20	292	162	160

Conclusion

As evident from the table, the highest corrosion protection performance was achieved when the composition containing the nickel salt of natural petroleum acids (NPA) was used at a total inhibitor concentration of 20%. This conservation fluid demonstrated superior protection against atmospheric corrosion in the humidity chamber, seawater, and 0.001% H_2SO_4 solution.

Specifically, the formulation consisting of 80% T-46 oil distillate, 10% amidoamine derived from natural petroleum acids and ethylenediamine, and 10% nickel salt of the corresponding acids (total inhibitor content: 20%) provided corrosion protection for 292 days in the humidity chamber, and for 162 and 160 days in seawater and 0.001% H_2SO_4 solution, respectively.

However, considering that nickel is relatively scarce and significantly more expensive than iron, the composition based on the iron salt of natural petroleum acids may represent a more economically viable alternative while still providing substantial corrosion protection performance.

References

[1]. Abbasov V.M., Rzayeva N.Sh., Ahmadova S.Z.,et al. Study of opportunies for formation of conservative liquid on the base of sunflower oil, Processes of petrochemistry and oil refining, 2016,Vol.17, No3, pp.262-265

[2]. Abbasova U.B. Application of inorganic and organic complexes of amino derivatives of natural petroleum acids as CO_2 corrosion inhibitor. Processes of petrochemistry and oil refining. Vol. 22, No. 1, 2021, pp. 152-15

[3]. Abbasova U.B. Synthesis of amides of natural petroleum acids with ethylenediamine and alkylamines and research as acomponent to conservation liquids. Processes of petrochemistry and oil refining. 2022, Vol 23, No 3, pp. 517-523

NANO-BIOREMEDIASIYA: EKOSISTEMLƏRIN BƏRPASINDA NANOHISSƏCIKLƏRIN VƏ MIKROORQANIZMLƏRIN SINERGETIK GÜCÜ

Aygün Alməmmədova, İradə Eyvazova, Təranə İbrahimova, Könül Qəhrəmanova, Gülşən Qasımlı, Inarə Sədirzadə, Gülzar Məmmədova
AR ETN Kimya İnstitutu
Bakı, Azərbaycan
a.ershadqizi@gmail.com

Açar sözlər: nano-bioremediasiya, nanohissəciklər, mikroorqanizmlər, neft çirklənməsi.

Müasir dövrdə sənaye tullantıları və ağır metallarla çirklənmə qlobal ekoloji böhranın əsas faktorlarındandır. Ənənəvi təmizləmə üsulları çox vaxt baha başa gəlir və ya mühitə əlavə kimyəvi yük gətirir. Nano-bioremediasiya isə bu problemi həll etmək üçün nanotexnologiyanın sürətini bioloji sistemlərin təbiiliyi ilə birləşdirir. Burada nanohissəciklər sanki bir "katalizator" rolunu oynayaraq, mikroorqanizmlərin toksinləri parçalama qabiliyyətini maksimuma çatdırır.

Tədqiqatımızda istifadə olunan metal və karbon əsaslı nanohissəciklər müxtəlif fiziki-kimyəvi xüsusiyyətlərə malikdir. Onların əsas üstünlükləri - kiçik ölçü sayəsində daha çox çirkləndirici maddəni özünə adsorbsiya edir. Çirkləndiriciləri (məsələn, neft karbohidrogenlərini) hədəf alaraq onları mikroorqanizmlər üçün "həzm oluna bilən" formaya salır. Ağır metalların valentliyini dəyişərək onları bioloji cəhətdən daha az təhlükəli hala gətirir.

Sintez edilmiş xüsusi nanohissəciklərin yerli mikroflora üzərindəki təsiri öyrənilmişdir. Tədqiqatda neftlə çirklənmiş sulardan izolyasiya edilmiş Pseudomonas aeruginosa (bakteriya) və Aspergillus niger (göbələk) ştamlarından istifadə olunub.

Antimikrob fəallığın təyini zamanı əldə olunan nəticələr:

Bakterial davamlılıq: nanohissəciklər *Pseudomonas aeruginosa* bakteriyalarına qarşı heç bir neqativ (antimikrob) təsir göstərməmişdir. Bu, bioremediasiya üçün müsbət göstəricidir, çünki nanohissəciklər bakteriyanı məhv etmir, əksinə, gələcəkdə onunla simbiotik fəaliyyət göstərə bilər.

Selektiv göbələk təsiri: *Aspergillus niger* göbələklərində isə maraqlı bir hal müşahidə olunub - nanohissəciklər göbələyin sporlarının tam yetişməsinin (reproduksiyasının) qarşısını qismən almışdır. Bu fakt, nanomaterialın göbələklərin inkişaf sürətini tənzimləmək potensialına malik olduğunu göstərir.

Əldə edilən nanohissəciklər sənaye sahələrində təmizləmə xərclərini 30-50% azalda bilər. Mikroorqanizmlərin canlı fabrik kimi istifadə edilməsi həm ekoloji təmizliyi təmin edir, həm də prosesin davamlılığını artırır.

Tədqiqatın ilkin mərhələsi sübut etdi ki, seçilmiş nanohissəciklər əsas deqradasiyaedici bakteriyalar üçün toksik deyil. Bu, tədqiqatın ikinci və daha mühüm mərhələsinə — neft çirklənmələrinin bilavasitə nano-bioremediasiya yolu ilə təmizlənməsi prosesinə elmi zəmin yaradır.

References

[1]. K.K. Yadav, J.K. Singh, N. Gupta, V. Kumar, (2017). A Review of Nanobioremediation Technologies for Environmental Cleanup: A Novel Biological Approach, JMES, Volume 8, Issue 2, Page 740-757.

YAŞIL TRANSFORMASİYA DÖVRÜNDƏ DAYANIQLI İNKİŞAFIN YENI PARADİQMASI

Baş müəllim Abbasova Günay Firdovsi qızı
Azərbaycan Dövlət Aqrar Universiteti, Gəncə şəhəri
gunay.abbasova@adau.edu.az
0009-0002-5816-7957
Bakalavriat Məstalıyev Seymur Ruslan oğlu
Azərbaycan Dövlət Aqrar Universiteti, Gəncə şəhəri
0009-0009-6851-0860
Semur8877@icloud.com

Açar sözlər: yaşıl transformasiya, dayanıqlı inkişaf, yeni inkişaf paradiqması, ekoloji innovasiya, ekoloji iqtisadiyyat

Məqalədə əsas məqsəd transformasiya dövründə dayanıqlı inkişafın yeni paradiqmasının mahiyyətini elmi-nəzəri və praktik baxımdan təhlil etmək, innovasiya və ekoloji siyasətlərin qarşılıqlı əlaqəsini araşdırmaq və onların uzunmüddətli inkişaf strategiyalarına təsirini müəyyənləşdirməkdir.

Tədqiqat çərçivəsində Birləşmiş Millətlər Təşkilatı tərəfindən müəyyən edilmiş Dayanıqlı İnkişaf Məqsədləri və Paris Sazişi kontekstində yaşıl transformasiyanın prioritet istiqamətləri qiymətləndirilir. [Birləşmiş Millətlər Təşkilatı. Sustainable Development Goals Report 2023].

XXI əsrin əsas çağırışlarından biri iqlim dəyişikliyi, təbii resursların tükənməsi və ekosistemlərin deqradasiyasıdır. Qlobal temperatur artımı, biomüxtəlifliyin azalması və su çatışmazlığı artıq yalnız ekoloji deyil, həm də sosial-iqtisadi təhlükə kimi qiymətləndirilir. Bu baxımdan Birləşmiş Millətlər Təşkilatı tərəfindən qəbul edilən Dayanıqlı İnkişaf Məqsədləri və Paris Sazişi çərçivəsində müəyyən edilmiş öhdəliklər dövlətləri yeni inkişaf modelinə – yaşıl transformasiyaya yönəltmişdir.

Yaşıl transformasiya ənənəvi iqtisadi artım modelindən resurslara qənaət edən, aşağı karbonlu və ekoloji məsuliyyətli inkişaf modelinə keçidi

ifadə edir. Bu proses dayanıqlı inkişafın yeni paradiqmasını formalaşdırır. [Sachs, J. D,2015].

Tədqiqatın eksperimental hissəsi yaşıl transformasiya dövründə dayanıqlı inkişaf modelinin praktik nəticələrini qiymətləndirmək məqsədilə sistemli və çoxşaxəli metodoloji yanaşma əsasında hazırlanmışdır. Araşdırma çərçivəsində nəzəri müddəaların praktik göstəricilərlə uyğunluğu müqayisəli və analitik metodlar vasitəsilə təhlil edilmişdir.

İlk mərhələdə beynəlxalq səviyyədə qəbul olunmuş strateji sənədlər, xüsusilə Birləşmiş Millətlər Təşkilatı tərəfindən müəyyən edilmiş Dayanıqlı İnkişaf Məqsədləri və Paris Sazişi çərçivəsində götürülmüş öhdəliklər normativ baza kimi təhlil edilmişdir. Bu sənədlərdə müəyyən olunan hədəflər yaşıl transformasiyanın əsas istiqamətlərini – karbon emissiyalarının azaldılması, enerji səmərəliliyinin artırılması, bərpa olunan enerji mənbələrinin genişləndirilməsi və resurslardan səmərəli istifadəni – qiymətləndirmək üçün meyar kimi qəbul olunmuşdur. [Paris Sazişi,2023].

Növbəti mərhələdə müxtəlif ölkələrin tətbiq etdiyi yaşıl siyasətlərin nəticələri müqayisəli şəkildə araşdırılmışdır. Statistik göstəricilər əsasında karbon emissiyası dinamikası, enerji balansında bərpa olunan mənbələrin payı, yaşıl investisiyaların həcmi və ekoloji innovasiyaların tətbiq səviyyəsi təhlil edilmişdir. Həmçinin iqtisadi artım tempinin ekoloji göstəricilərlə qarşılıqlı əlaqəsi müəyyənləşdirilmişdir.

Eksperimental yanaşmanın əsas məqsədi ənənəvi iqtisadi inkişaf modeli ilə yaşıl iqtisadiyyat modelinin nəticələrini müqayisə edərək, transformasiyanın real təsirlərini ortaya qoymaq olmuşdur. Təhlil zamanı həm kəmiyyət göstəricilərindən, həm də keyfiyyət xarakterli qiymətləndirmələrdən istifadə edilmişdir. Bu isə transformasiyanın yalnız statistik deyil, həm də institusional və sosial ölçülərini nəzərə almağa imkan vermişdir. [European Union, 2019].

Aparılan təhlillər göstərir ki, yaşıl transformasiya modelinin tətbiqi ekoloji göstəricilərin yaxşılaşmasına müsbət təsir göstərir. Karbon emissiyalarının nisbi azalması, enerji səmərəliliyinin artması və bərpa olunan enerji sektorunda investisiyaların genişlənməsi dayanıqlı inkişafın yeni mərhələyə keçdiyini nümayiş etdirir.

Eyni zamanda müəyyən edilmişdir ki, yaşıl iqtisadiyyat modeli uzunmüddətli perspektivdə iqtisadi sabitliyə və sosial rifaha da müsbət təsir edir. Yeni texnologiyaların tətbiqi innovasiya mühitini gücləndirir, yeni iş yerləri yaradır və iqtisadiyyatın şaxələndirilməsinə şərait formalaşdırır. Bu isə dayanıqlı inkişafın yalnız ekoloji deyil, kompleks inkişaf modeli olduğunu təsdiqləyir.

Tədqiqatın nəticələri göstərir ki, yaşıl transformasiya iqtisadi sistemin struktur yenilənməsini tələb edən kompleks və mərhələli prosesdir. Əldə edilən göstəricilər aşağı karbonlu inkişaf modelinin praktik baxımdan mümkün və effektiv olduğunu təsdiqləsə də, bu keçid avtomatik və problemsiz baş vermir.

Transformasiya prosesində əsas çətinliklər yüksək ilkin investisiya tələbi, texnoloji və institusional infrastrukturun yetərsizliyi, həmçinin cəmiyyətin ekoloji şüur səviyyəsi ilə bağlıdır. Bu baxımdan dövlət siyasəti, özəl sektorun təşəbbüsləri və beynəlxalq əməkdaşlıq arasında koordinasiyalı fəaliyyət həlledici rol oynayır.

Müzakirələr göstərir ki, yaşıl transformasiya yalnız texnoloji dəyişiklik deyil, həm də idarəetmə və düşüncə tərzinin dəyişməsidir. Resursların səmərəli istifadəsi, dairəvi iqtisadiyyat prinsiplərinin tətbiqi və innovasiyaya əsaslanan inkişaf modeli yeni paradiqmanın əsas elementləridir.

Beləliklə, eksperimental təhlil sübut edir ki, yaşıl transformasiya dayanıqlı inkişafın strateji istiqaməti kimi çıxış edir və uzunmüddətli ekoloji təhlükəsizliklə iqtisadi sabitlik arasında balansın yaradılmasına real imkan verir.

Yaşıl transformasiya dövründə dayanıqlı inkişafın yeni paradiqmasının uğurla tətbiqi üçün aşağıdakı təkliflər irəli sürülür:

1. Dövlət Siyasətinin Gücləndirilməsi- Dövlət səviyyəsində yaşıl transformasiyanı dəstəkləyən qanunvericilik bazasının genişləndirilməsi, vergi və subsidiyalar vasitəsilə bərpa olunan enerji və ekoloji innovasiyalara təşviqin artırılması vacibdir.
2. Beynəlxalq Əməkdaşlığın Genişləndirilməsi- Paris Sazişi və Dayanıqlı İnkişaf Məqsədləri çərçivəsində təcrübə mübadiləsi və texnoloji transferin təşviqi ilə milli səviyyədə effektiv yaşıl strategiyaların tətbiqi mümkün olur.
3. İnnovasiya və Texnologiyanın Tətbiqi- Süni intellekt, rəqəmsal monitorinq sistemləri və biotexnologiyalar kimi innovativ vasitələrin kənd təsərrüfatı, sənaye və enerji sahələrində tətbiqi ekoloji təsirlərin azaldılmasına və resurs səmərəliliyinin artırılmasına xidmət edir.
4. Dairəvi İqtisadiyyatın İnkişafı- Tullantıların azaldılması, təkrar emal və resursların optimal istifadəsi prinsiplərinin bütün istehsal və istehlak zəncirinə inteqrasiyası yaşıl transformasiyanın mərkəzini təşkil etməlidir.
5. İctimai Maarifləndirmə və Təhsil- Cəmiyyətin ekoloji şüurunun artırılması, davamlı istehlak vərdişlərinin təşviqi və yaşıl texnologiyalara marağın artırılması transformasiyanın uğurla həyata keçirilməsi üçün vacibdir.
6. Milli Strategiyaların Kontekstləşdirilməsi- Azərbaycan və digər ölkələr üçün milli səviyyədə yaşıl inkişaf strategiyalarının tərtibi, bərpa olunan enerji layihələrinin prioritetləşdirilməsi və yaşıl iş yerlərinin yaradılması məqsədəuyğundur.
7. Müntəzəm Monitorinq və Qiymətləndirmə- Yaşıl transformasiya proqramlarının təsirini ölçmək üçün davamlı statistik və ekoloji monitorinq sistemi qurulmalı, nəticələr əsasında strategiyalar adaptasiya edilməlidir.

Bu təkliflər yaşıl transformasiyanın dayanıqlı inkişafın yeni paradiqması kimi uğurla həyata keçirilməsinə və uzunmüddətli ekoloji, iqtisadi və sosial faydaların təmin olunmasına xidmət edir.

Ədəbiyyat

1. Birləşmiş Millətlər Təşkilatı. Sustainable Development Goals Report 2023. New York: United Nations, 2023.
2. Paris Sazişi. United Nations Framework Convention on Climate Change (UNFCCC), 2015.
3. Sachs, J. D. The Age of Sustainable Development. New York: Columbia University Press, 2015.
4. European Commission. Green Deal: A European Strategy for Sustainable Growth. Brussels: European Union, 2019.

SƏNAYE SULARININ TƏMİZLƏNMƏSİ PROSESLƏRİNDƏ TƏHLÜKƏSİZLİK RİSKLƏRİNİN AZALDILMASI

Vəfa Kərimli, Elnur Rüstəmzadə, Elton Qasımov
Azərbaycan Dövlət Neft və Sənaye Universiteti
Azərbaycan, Bakı
vafa.karimli@asoiu.edu.az

Sənaye sularının təmizlənməsi prosesləri istehsalat təhlükəsizliyi və ətraf mühitin mühafizəsi baxımından yüksək risk daşıyan texnoloji sahələrdən biridir. Bu proseslərdə istifadə olunan kimyəvi reagentlər, bioloji aktiv mühitlər və mexaniki avadanlıqlar işçi heyətinin sağlamlığı və ekoloji təhlükəsizlik üçün potensial təhlükə yaradır. Xüsusilə turşular, qələvilər, koagulyantlar, ağır metallar və dezinfeksiyaedici maddələrlə işləmə zamanı qəza riskləri artır.

Açar sözlər: sənaye suları, təhlükəsizlik riskləri, çirkab suların təmizlənməsi, istehsalat təhlükəsizliyi, avtomatlaşdırma.

Giriş

Sənaye sularının təmizlənməsi prosesləri istehsalat təhlükəsizliyi və ətraf mühitin mühafizəsi baxımından yüksək risk daşıyan texnoloji sahələrdən biridir. Bu proseslərdə istifadə olunan kimyəvi reagentlər, bioloji aktiv mühitlər və mexaniki avadanlıqlar işçi heyətinin sağlamlığı və ekoloji təhlükəsizlik üçün potensial təhlükə yaradır. Xüsusilə turşular, qələvilər, koagulyantlar, ağır metallar və dezinfeksiyaedici maddələrlə işləmə zamanı qəza riskləri artır.

Tədqiqat işində sənaye sularının təmizlənməsi qurğularında yaranan əsas təhlükəsizlik riskləri – kimyəvi, bioloji, mexaniki və texnoloji risklər – təhlil edilmişdir. Risklərin azaldılması məqsədilə texniki tədbirlər (qapalı dozalama sistemləri, avtomatik nəzarət və qaz detektorları), təşkilati yanaşmalar (təhlükəsizlik təlimatları, risklərin qiymətləndirilməsi, fövqəladə hallar planları) və fərdi mühafizə vasitələrinin tətbiqi əsaslandırılmışdır.

Sənaye sularının təmizlənməsi proseslərində istifadə olunan kimyəvi maddələr yüksək reaktivliyə və toksikliyə malik olduqları üçün potensial qəza riskləri yaradır. Bu risklər həm işçi heyətin sağlamlığına, həm də texnoloji proseslərin stabilliyinə və ətraf mühitə ciddi təhlükə törədə bilər.

Experimental hissə

Kükürd, xlorid, azot və fosfor turşuları pH tənzimlənməsi və çökmə proseslərində geniş istifadə olunur. Bu maddələrin yüksək korroziya qabiliyyəti avadanlıqların sıradan çıxmasına, boru kəmərlərində sızmalara və qəfil dağılmalara səbəb ola bilər. Turşularla birbaşa təmas dəridə və gözlərdə ağır kimyəvi yanıqlar, buxarlarının inhalyasiyası isə tənəffüs yollarının zədələnməsi ilə nəticələnir. Nəzarətsiz dozalama zamanı reaksiya istiliyinin artması partlayış və ya maddə sıçraması riskini yüksəldir.

Natrium hidroksid və kalsium hidroksid kimi qələvilər neytrallaşdırma proseslərində tətbiq edilir. Bu maddələr yüksək qələvilik dərəcəsinə malik olduqlarından toxumalarda dərin zədələnmələr yarada bilər. Qələvi məhlulların sıçraması görmə itkisinə səbəb ola bilən ciddi göz yanığı riskləri yaradır. Bundan əlavə, qələvilərin turşularla nəzarətsiz reaksiyası kəskin istilik ayrılması və qəza halları ilə nəticələnə bilər.

Alüminium və dəmir duzları ($Al_2(SO_4)_3$, $FeCl_3$ və s.) çirkab sularında asılı hissəciklərin çökməsi üçün istifadə olunur. Bu maddələrin toz və ya aerozol halında inhalyasiyası tənəffüs yollarında qıcıqlanma yaradır. Dəmir və alüminium duzlarının yüksək konsentrasiyası avadanlıqlarda çöküntü və tıxanma yaradaraq texnoloji prosesin pozulmasına səbəb olur. Dozalama sistemlərində baş verən nasazlıqlar isə həm qəza, həm də təmizlənmə effektivliyinin azalması ilə nəticələnir.

Sənaye sularında civə, qurğuşun, kadmium, xrom və nikel kimi ağır metallar mövcud ola bilər. Bu maddələr yüksək toksikliyə və bioakkumul-yasiya xüsusiyyətinə malikdir. Ağır metallarla təmas xroniki zəhərlənmə, sinir sistemi və daxili orqanların zədələnməsi riskini yaradır. Təmizləmə zamanı yaranan lilin düzgün idarə olunmaması ağır metallarla çirklənmiş tullantıların ətraf mühitə yayılmasına və ikincili çirklənməyə səbəb ola bilər.

Xlor, xloraminlər, ozon və hidrogen peroksid sənaye sularının dezinfeksiyasında istifadə edilir. Xlor qazının sızması kəskin toksik təsirə malikdir və az konsentrasiyada belə insan həyatı üçün təhlükəlidir. Ozon yüksək oksidləşdirici qabiliyyətə malik olduğundan avadanlıqlara zərər verə və tənəffüs sisteminə ciddi təsir göstərə bilər. Dezinfeksiyaedici maddələrin yanlış dozalanması toksik yan məhsulların yaranmasına və proses təhlükəsizliyinin pozulmasına səbəb olur.

Aparılan təhlillər göstərir ki, proseslərin avtomatlaşdırılması və müasir monitorinq sistemlərinin tətbiqi insan amilindən asılılığı azaldaraq qəza ehtimalını minimuma endirir. Nəticə olaraq, sənaye sularının təmizlənməsi obyektlərində təhlükəsizliyin təmin olunması kompleks və sistemli yanaşma tələb edir və bu yanaşma həm istehsalat təhlükəsizliyinin, həm də ekoloji davamlılığın yüksəldilməsinə xidmət edir.

Nəticə və onların müzakirəsi

Sənaye sularının təmizlənməsi proseslərində turşular, qələvilər, koagulyantlar, ağır metallar və dezinfeksiyaedici maddələrlə işləmə yüksək səviyyəli kimyəvi və texnoloji risklərlə müşayiət olunur. Bu maddələrin korroziyaedici, toksik və reaktiv xüsusiyyətləri istehsalat qəzalara, avadanlıqların sıradan çıxmasına, işçi heyətin sağlamlığına zərər vurulmasına və ətraf mühitin çirklənməsinə səbəb ola bilər. Xüsusilə dozalama sistemlərində nasazlıqlar, maddələrin saxlanma və daşınma qaydalarına riayət olunmaması qəza ehtimalını əhəmiyyətli dərəcədə artırır.

Aparılan təhlillər göstərir ki, təhlükəsizlik risklərinin effektiv şəkildə azaldılması yalnız ayrı-ayrı tədbirlərin deyil, kompleks və sistemli yanaşmanın tətbiqini tələb edir. Kimyəvi maddələrin istifadəsində avtomatlaşdırılmış və qapalı dozalama sistemlərinin tətbiqi, real vaxt rejimində monitorinq və xəbərdarlıq mexanizmləri insan amilindən asılılığı azaldaraq qəza risklərinin minimuma endirilməsinə imkan yaradır. Bununla yanaşı, müntəzəm texniki baxışlar və avadanlıqların korroziyaya davamlı materiallardan hazırlanması texnoloji etibarlılığı artırır.

Eyni zamanda, fərdi mühafizə vasitələrinin düzgün seçilməsi və istifadəsi, işçi heyətin təhlükəsizlik üzrə davamlı təlimlərdən keçirilməsi və fövqəladə hallara hazırlıq planlarının mövcudluğu istehsalat təhlükəsizliyinin əsas təminatçılarındandır. Ağır metallarla çirklənmiş lil və tullantıların təhlükəsiz idarə olunması isə ikincili ekoloji risklərin qarşısının alınmasında mühüm rol oynayır.

Nəticə etibarilə, sənaye sularının təmizlənməsi obyektlərində təhlükəsizlik risklərinin azaldılması texniki, təşkilati və ekoloji tədbirlərin qarşılıqlı və əlaqəli şəkildə həyata keçirilməsini tələb edir. Bu yanaşma yalnız qəza hallarının qarşısını almaqla kifayətlənmir, eyni zamanda istehsalat proseslərinin davamlılığını, işçi sağlamlığının qorunmasını və ətraf mühitin mühafizəsini təmin edərək sənayenin ekoloji təhlükəsiz inkişafına töhfə verir.

Təkliflər

Sənaye sularının təmizlənməsi qurğularında **Risk Əsaslı Proses Təhlükəsizliyi (RBPS)** modelinin tətbiqi.

İstinadlar

1. Metcalf & Eddy. **Wastewater Engineering: Treatment and Resource Recovery**. 5th ed., McGraw-Hill Education, New York, 2014.
2. Tchobanoglous, G., Burton, F. L., Stensel, H. D. **Wastewater Engineering: Treatment and Reuse**. McGraw-Hill, New York, 2003.
3. Spellman, F. R. **Handbook of Water and Wastewater Treatment Plant Operations**. 3rd ed., CRC Press, Boca Raton, 2014.
4. Droste, R. L. **Theory and Practice of Water and Wastewater Treatment**. John Wiley & Sons, New York, 1997.
5. Cheremisinoff, N. P. **Handbook of Industrial Water and Wastewater Treatment**. Butterworth-Heinemann, Oxford, 1995.
6. World Health Organization (WHO). **Guidelines for the Safe Use of Wastewater, Excreta and Greywater**. Geneva, 2006.

7. U.S. Environmental Protection Agency (EPA). **Wastewater Treatment Manuals: Treatment of Industrial Effluents**. EPA, Washington, DC, 1999.
8. International Labour Organization (ILO). **Safety and Health in the Use of Chemicals at Work**. Geneva, 2014.
9. Spellman, F. R., Drinan, J. E. **The Drinking Water Handbook**. CRC Press, Boca Raton, 2012.
10. Əliyev, R. Ə., Məmmədov, F. H. **Çirkab suların təmizlənməsi texnologiyaları**. Bakı: Elm nəşriyyatı, 2010.

DISCRETE ELEMENT SIMULATION OF PARTICLE SETTLING IN SHEARED SUSPENSIONS UNDER GRAVITY

Madina Ziyadkhanova
Okinawa Institute of Science and Technology
Okinawa, Japan
medina.ziyadkhanova03@gmail.com

Summary - Sedimentation in particle–fluid systems rarely depend on gravity alone. In many practical settings, ranging from sedimentation tanks to reactors particles experience shear while simultaneously being driven downward by buoyancy mismatch. Under such conditions, shear can restructure the suspension, generate normal stresses, and modify the effective resistance to settling. Motivated by this coupled shear-gravity problem, the present work applies a particle-resolved discrete element method (DEM) framework to study how shear rate and concentration influence both settling dynamics and macroscopic shear stress.

A numerical configuration aligned with an experimental study designed at the University of Chicago is considered. The analysis focuses on extracting time-dependent shear stress and mean particle height to distinguish conditions that promote sustained suspension from those that lead to net sedimentation. Simulations are performed at volume fractions of 30%, 40%, and 50% across a shear-rate range covering approximately 0.1–50 s^{-1}. Across all cases, shear stress typically exhibits a transient startup response before approaching a fluctuating quasi-steady level, while mean particle height decreases over time, indicating net settling. When shear stress–shear rate trends are compared against experimental data, the simulations reproduce the overall monotonic increase of stress with shear rate. Agreement is strongest at moderate concentrations, whereas the most concentrated cases show larger deviations at higher shear rates, consistent with the increasing importance of lubrication, frictional contacts, and microstructural anisotropy in dense suspensions [Stickel and Powell, 2005, 129-149; Mari et al., 2014, 1693-1724; Seto et al., 2013, 218301]. These results support the use of DEM-style frameworks as an interpretive and predictive tool for dense suspension behaviour under combined shear and gravity.

Keywords: dense suspensions; particle settling; discrete element method; shear-induced migration; shear stress; gravity

Introduction

Gravity-driven settling is one of the oldest and most widely used separation mechanisms in chemical and environmental engineering. Nevertheless, real suspensions often settle while flowing, mixing, or being processed, meaning shear and confinement influence the microstructure during sedimentation. Classic hindered-settling correlations describe how

settling velocity decreases with increasing concentration, highlighting the collective role of hydrodynamic interactions [Richardson and Zaki, 1954, 35-53; Batchelor, 1972, 245-268]. At the same time, shear can trigger particle diffusion and migration, driving particles away from high-shear regions and producing non-uniform concentration fields [Eckstein et al., 1977, 191-208; Leighton and Acrivos, 1987a, 109-131; Phillips et al., 1992, 30-40]. Consequently, a suspension exposed to shear and gravity may exhibit settling behaviour that differs substantially from quiescent sedimentation.

Dense suspensions also display rich rheology, including strong shear-rate dependence and the emergence of normal stresses. A useful modern viewpoint attributes pronounced shear thickening to a transition from lubrication-dominated interactions to frictional contact networks, particularly at large solid fractions [Brown and Jaeger, 2012, 875-923; Seto et al., 2013, 218301; Mari et al., 2014, 1693-1724]. Because confining stresses and particle weight can set relevant stress scales, gravity may couple directly into rheological thresholds when particles are not neutrally buoyant [Brown and Jaeger, 2012, 875-923]. From this perspective, the settling problem is not purely kinematic; it is also mechanical, mediated by stress transmission through evolving microstructure.

To investigate these coupled effects, particle-resolved simulations provide a valuable complement to experiments. Micro hydrodynamic theory offers the foundation for describing viscous-flow interactions at low Reynolds number, while many-body simulation methods translate these principles into predictive tools [Happel and Brenner, 1965, 1-553; Kim and Karrila, 1991, 1-507; Brady and Bossis, 1988, 111-157]. Building on this framework, the present thesis applies a DEM-based approach to quantify how shear rate and volume fraction influence settling under gravity and to benchmark stress predictions against experimental trends.

Experimental part

In this work, the “experimental part” is implemented as a numerical experiment using DEM, in which the motion of each particle is advanced in time based on computed interaction forces. DEM originated in granular mechanics as a contact-resolved method and has since been adapted for particulate systems where collisions, friction, and near-contact interactions shape collective behaviour [Cundall and Strack, 1979, 47-65]. For suspension flows, DEM-style particle dynamics is often combined with hydrodynamic resistance models (e.g., drag and lubrication), which are grounded in low-Reynolds-number hydrodynamics [Happel and Brenner, 1965, 1-553; Kim and Karrila, 1991, 1-507]. Where many-body hydrodynamics is required at scale, alternative approaches such as Stokesian Dynamics and lattice-Boltzmann-based methods provide complementary modelling routes [Brady and Bossis, 1988, 111-157; Ladd, 1994, 285-309].

The simulation configuration follows an experimental study designed at the University of Chicago to explore settling under combined shear stress and gravity. Polyethylene particles are used with diameter D = 0.008 cm (selected within a 75–90 μm range) and density ρ = 1.25 g/cm³, dispersed in Newtonian silicone oil with density ρ_f = 1 g/cm³ and reported kinematic viscosity 20 cSt. A total of N = 5832 particles are placed in a cubic domain with side length 0.15752 cm (varied with volume fraction). Gravity is applied as g = 980 cm/s², and imposed shear rates span approximately 0.1–50 s^{-1}. Simulations are performed at volume fractions VF = 30%, 40%, and 50%.

Two families of outputs are extracted. First, a macroscopic stress measure is obtained from the time evolution of shear stress (reported as moving-average stress traces). Second, settling is quantified through the mean vertical position of particles versus time. Together, these outputs allow a coupled interpretation: how rheological response (stress generation) evolves alongside kinematic sedimentation under gravity. Because stresslets (force moments associated with particle resistance to deformation) contribute to suspension stresses, their conceptual role provides an interpretive link between particle-scale rearrangements and bulk rheology, particularly in dense regimes [Guazzelli and Morris, 2011, 1-256; Stickel and Powell, 2005, 129-149].

Results and their discussion

Across all simulated conditions, the shear stress response exhibits a recognizable temporal structure. Immediately after shear is applied, a strong transient appears, reflecting rapid microstructural rearrangement and the establishment of force chains and lubrication layers. After this startup stage, stress relaxes toward a fluctuating quasi-steady regime. Such behaviour is consistent with prior understanding that suspension stress depends sensitively on evolving microstructure, especially in dense systems where small changes in particle arrangement strongly influence dissipation and normal stresses [Stickel and Powell, 2005, 129-149; Sierou and Brady, 2002, 1031-1056].

Settling behaviour, measured through the mean vertical particle position, shows net sedimentation in all tested cases, as expected for non-neutrally buoyant particles. However, the rate and shape of the settling curves depend on volume fraction and shear rate. Increasing the volume fraction tends to hinder sedimentation, consistent with classic hindered-settling concepts in which collective hydrodynamic interactions reduce the effective settling velocity [Richardson and Zaki, 1954, 35-53; Batchelor, 1972, 245-268]. Meanwhile, imposed shear introduces additional transport mechanisms that can oppose or reshape sedimentation through shear-induced diffusion and migration, particularly in inhomogeneous shear fields [Eckstein et al., 1977, 191-208; Leighton and Acrivos, 1987a, 109-131; Phillips et al., 1992, 30-40]. Even in nominally homogeneous shear, microstructural anisotropy under

flow can alter both stress and particle transport pathways, which becomes increasingly pronounced at higher concentrations [Guazzelli and Morris, 2011, 1-256; Morris and Boulay, 1999, 1213-1237].

The stress–shear-rate comparison against experimental data provides a more direct validation point. For each volume fraction (30%, 40%, 50%), the simulated shear stress increases with shear rate, reproducing the correct qualitative trend. In other words, as the system is driven harder, dissipation rises and stronger stresses develop—an outcome consistent with both empirical viscosity models and modern thickening mechanisms [Krieger and Dougherty, 1959, 137-152; Brown and Jaeger, 2012, 875-923]. Agreement between simulation and experiment is strongest at moderate concentrations (30–40%), whereas larger deviations appear at VF = 50%, especially at higher shear rates. This pattern is physically plausible: at high volume fraction, near-contact lubrication, frictional contacts, and stress transmission through contact networks become increasingly dominant, making results more sensitive to the chosen contact and hydrodynamic modelling assumptions [Sierou and Brady, 2002, 1031-1056; Seto et al., 2013, 218301; Mari et al., 2014, 1693-1724].

Interpreting the highest-concentration discrepancies through current rheological theory suggests an important point: dense suspensions may transition between frictionless-like and frictional-like regimes as stress increases, and this transition can be sharpened by confinement and particle weight [Brown and Jaeger, 2012, 875-923; Mari et al., 2014, 1693-1724]. Since gravity introduces a hydrostatic-like normal loading when particles settle or form denser regions, gravity can effectively shift stress scales that govern thickening and migration. Additionally, connections to granular rheology become relevant as the suspension approaches jamming-like packing fractions. In that regime, pressure-controlled shear and friction laws provide a unifying framework that has been demonstrated experimentally for dense suspensions [Boyer et al., 2011, 188301]. Thus, the combined results support a consistent narrative: as volume fraction rises, the suspension becomes increasingly governed by contact-driven mechanics, making both stress generation and settling dynamics more strongly coupled and more model-sensitive.

Overall, the simulations capture three robust outcomes: (i) a transient-to-steady stress evolution under shear, (ii) concentration-dependent hindered settling under gravity, and (iii) monotonic stress growth with shear rate consistent with experiment. These features collectively indicate that particle-resolved DEM simulations, when benchmarked carefully, can be used not only to match stress trends but also to interpret settling behavior through microstructure-aware transport mechanisms.

Offers

To extend the scientific value of this work, the next step should be to transform the current parameter sweeps into a clear *regime diagram* for settling under shear and gravity. Rather than presenting cases individually, a map in the (VF, shear rate) space can classify behaviour into practical categories such as “dominant settling,” “hindered settling,” and “quasi-suspended.” This can be done by defining a settling-timescale metric from the mean-height curves and pairing it with a steady-stress metric from the late-time stress plateau. Such a representation would connect classical hindered-settling concepts to modern stress-based suspension frameworks and would make the results more directly usable for engineering design [Richardson and Zaki, 1954, 35-53; Boyer et al., 2011, 188301].

In addition, the validation section would be significantly strengthened by reporting uncertainty and numerical sensitivity, especially in the dense cases where fluctuations are strongest. For example, stress statistics should be reported with a consistent averaging window and, ideally, compared across multiple runs with different initial particle configurations to show robustness. A short sensitivity study on time step, domain size, and averaging length would clarify whether deviations at VF = 50% are due to physics missing from the model or numerical/finite-size effects. These practices align with common recommendations in dense-suspension modelling where microstructure-driven intermittency can strongly influence measured stresses [Stickel and Powell, 2005, 129-149; Sierou and Brady, 2002, 1031-1056].

For better quantitative agreement in the most concentrated regime, it is recommended to refine the near-contact physics that dominate dense-suspension dissipation. In particular, lubrication interactions, frictional contact modelling, and stress-activated transitions between lubrication-dominated and contact-dominated states are known to control the magnitude and steepness of stress growth at high volume fraction. Calibrating the contact/lubrication parameters against experimental stress data—or validating with additional observables such as normal stresses or microstructural measures—would likely reduce the underprediction observed at VF = 50% and high shear rates. This direction is well supported by literature emphasizing that discontinuous or strong shear thickening emerges from frictional contact networks that turn on with stress [Seto et al., 2013, 218301; Mari et al., 2014, 1693-1724; Brown and Jaeger, 2012, 875-923].

Finally, broadening the model to include non-spherical particles would increase realism and expand the applicability of the framework. Many industrial particulates are not spherical, and particle shape introduces new dynamics (orientation, rotational resistance, anisotropic contact networks) that can alter both settling pathways and rheology under shear. Implementing ellipsoids or rod-like geometries would allow the study to address how

particle aspect ratio modifies suspension stability under gravity and whether shape enhances or suppresses shear-induced structuring and hindered settling. Such an extension also creates a natural bridge from idealized benchmark cases toward more practical particle–fluid systems [Guazzelli and Morris, 2011, 1-256; Kim and Karrila, 1991, 1-507].

References

1. Batchelor, G. K. (1972). Sedimentation in a dilute dispersion of spheres. *Journal of Fluid Mechanics*, 52(2), 245–268. [Batchelor, 1972, 245-268]
2. Boyer, F., Guazzelli, É., Pouliquen, O. (2011). Unifying suspension and granular rheology. *Physical Review Letters*, 107, 188301. [Boyer et al., 2011, 188301]
3. Brady, J. F., Bossis, G. (1988). Stokesian dynamics. *Annual Review of Fluid Mechanics*, 20, 111–157. [Brady and Bossis, 1988, 111-157]
4. Brown, E., Jaeger, H. M. (2012). The role of dilation and confining stresses in shear thickening of dense suspensions. *Journal of Rheology*, 56(4), 875–923. [Brown and Jaeger, 2012, 875-923]
5. Cundall, P. A., Strack, O. D. L. (1979). A discrete numerical model for granular assemblies. *Géotechnique*, 29(1), 47–65. [Cundall and Strack, 1979, 47-65]
6. Eckstein, E. C., Bailey, D. G., Shapiro, A. H. (1977). Self-diffusion of particles in shear flow of a suspension. *Journal of Fluid Mechanics*, 79(1), 191–208. [Eckstein et al., 1977, 191-208]
7. Guazzelli, É., Morris, J. F. (2011). *A Physical Introduction to Suspension Dynamics*. Cambridge University Press. [Guazzelli and Morris, 2011, 1-256]
8. Happel, J., Brenner, H. (1965). *Low Reynolds Number Hydrodynamics: With Special Applications to Particulate Media*. Prentice-Hall. [Happel and Brenner, 1965, 1-553]
9. Kim, S., Karrila, S. J. (1991). *Microhydrodynamics: Principles and Selected Applications*. Butterworth-Heinemann. [Kim and Karrila, 1991, 1-507]
10. Krieger, I. M., Dougherty, T. J. (1959). A mechanism for non-Newtonian flow in suspensions of rigid spheres. *Transactions of the Society of Rheology*, 3(1), 137–152. [Krieger and Dougherty, 1959, 137-152]
11. Ladd, A. J. C. (1994). Numerical simulations of particulate suspensions via a discretized Boltzmann equation. Part 1. Theoretical foundation. *Journal of Fluid Mechanics*, 271, 285–309. [Ladd, 1994, 285-309]
12. Leighton, D., Acrivos, A. (1987a). Measurement of shear-induced self-diffusion in concentrated suspensions of spheres. *Journal of Fluid Mechanics*, 177, 109–131. [Leighton and Acrivos, 1987a, 109-131]
13. Leighton, D., Acrivos, A. (1987b). The shear-induced migration of particles in concentrated suspensions. *Journal of Fluid Mechanics*, 181, 415–439. [Leighton and Acrivos, 1987b, 415-439]
14. Mari, R., Seto, R., Morris, J. F., Denn, M. M. (2014). Shear thickening, frictionless and frictional rheologies in non-Brownian suspensions. *Journal of Rheology*, 58(6), 1693–1724. [Mari et al., 2014, 1693-1724]
15. Morris, J. F., Boulay, F. (1999). Curvilinear flows of noncolloidal suspensions: The role of normal stresses. *Journal of Rheology*, 43(5), 1213–1237. [Morris and Boulay, 1999, 1213-1237]
16. Phillips, R. J., Armstrong, R. C., Brown, R. A., Graham, A. L., Abbott, J. R. (1992). A constitutive equation for concentrated suspensions that accounts for shear-induced particle migration. *Physics of Fluids A*, 4(1), 30–40. [Phillips et al., 1992, 30-40]

17. Richardson, J. F., Zaki, W. N. (1954). Sedimentation and fluidisation: Part I. *Transactions of the Institution of Chemical Engineers*, 32, 35–53. [Richardson and Zaki, 1954, 35-53]
18. Seto, R., Mari, R., Morris, J. F., Denn, M. M. (2013). Discontinuous shear thickening of frictional hard-sphere suspensions. *Physical Review Letters*, 111, 218301. [Seto et al., 2013, 218301]
19. Sierou, A., Brady, J. F. (2002). Rheology and microstructure in concentrated noncolloidal suspensions. *Journal of Rheology*, 46(5), 1031–1056. [Sierou and Brady, 2002, 1031-1056]
20. Stickel, J. J., Powell, R. L. (2005). Fluid mechanics and rheology of dense suspensions. *Annual Review of Fluid Mechanics*, 37, 129–149. [Stickel and Powell, 2005, 129-149]

KATALİTİK KREKİNQİN YÜNGÜL FLEQMASI ƏSASINDA NİTROTÖRƏMƏLƏRİN SİNTEZİ VƏ TƏDQİQİ

[1]Dəmir Nağıyev, [2]Sara Abbaszadə, [2]Rufanə Əlizadə,
[2]Fəridə Tahirova, [2]Məhsəti Qafarova
[1] Azərbaycan Dövlət Neft və Sənaye Universiteti
[2] Elm və Təhsil Nazirliyinin akademik Y.H. Məmmədəliyev adına Neft-Kimya Prosesləri İnstitutu
Bakı, Azərbaycan
demirnagiyev003@gmail.com

Xülasə - Neft emalı məhsulu olan katalitik krekinqin yüngül fleqmasının nitrolaşması əsasında nitrotörəmələr sintez olunmuşdur. Nitrolaşma prosesi 57–63%-li nitrat turşusu və natrium nitrit iştirakı ilə aparılmışdır. Prosesin temperatur və kontakt müddətindən asılılığı nəzərə alınmışdır. Sintez olunmuş nitrobirləşmələrin spektrofotometrik analizi nəticəsində qeydə alınan dalğa uzunluqlarına malik spektrlər müvafiq struktur tərkibləri təsdiq edir. Sintez olunmuş nitrobirləşmələrin infraqırmızı (İQ) spektroskopiya üsulu ilə analizi nəticəsində qeydə alınan dalğa uzunluğu müvafiq struktur tərkibləri təsdiq edir.
Açar sözlər: yüngül fleqma, nitrolaşma, nitrotörəmələr, korroziya inhibitoru

Giriş

Azotlu üzvi birləşmələr neft-kimya sintezində reagent, sənayenin müxtəlif sahələrində komponent, aşqar, bərkidici və s. kimi istifadə olunurlar. Bu məqsədlə onların müxtəlif xammallar əsasında sintez üsulları işlənib hazırlanmışdır. Azotlu üzvi birləşmələrdən aminlər, nitrobirləşmələr, imidazollar, imidazolinlər və s. böyük sənaye əhəmiyyəti kəsb edir. Elmi ədəbiyyatlardan məlum olduğu kimi, konservasiya mayelərinin korroziyadan mühafizə effektini yüksəltmək, sinergizm effektinin yaranması və örtük əmələgətirmə qabiliyyətlərinin artırılması üçün nitrobirləşmələrdən korroziya inhibitoru kimi geniş istifadə edilmişdir. Dünyada, xüsusilə Respublikamızda nitrobirləşmələr, onların müxtəlif törəmələri və kompozisiyaları əsasında yüksək keyfiyyətli konservasiya tərkibləri sintez edilmiş, onların tətbiq sahələri mövzusunda bir sıra elmi tədqiqatlar aparılmışdır. Olefin və aromatik karbohidrogenlərin nitrat turşusu ilə qarşılıqlı təsirinin sürəti müxtəlif

amillərdən, o cümlədən temperaturdan, reaksiya qarışığının kontakt müddətindən, götürülmüş reagentlərin mol nisbətindən, reaksiya qarışığının qarışma sürətindən və s. asılıdır [1-3].

Eksperimental hissə

Termometr, qarışdırıcı və əks soyuducu ilə təchiz olunmuş üç boğazlı kolbaya hesablanmış miqdarda 59–63%-li nitrat turşusu əlavə olunur. İnisiator kimi turşuya 0,1 mol natrium nitrit əlavə olunur və 60ºC temperatura qədər qızdırılır. Daha sonra müəyyən zaman müddətində reaksiya mühitinə uyğun yüngül fleqma damcı qıfı vasitəsilə əlavə olunur. Bununla yanaşı, reaksiyanın temperatur rejiminə ciddi əməl olunur. Təcrübələr reagentlərin müəyyən kontakt sürətinə əməl olunmaqla aparılmışdır.

Nitrolaşma prosesinin sürətinə təsir edən ən başlıca amillərdən biri temperatur və kontakt müddətidir. Temperatur rejimi 60–80ºC intervalında saxlanılmışdır. Belə ki, 60ºC-dən aşağıda reaksiya çox zəif, lakin 80ºC-dən yuxarıda isə çox sürətlə gedir və reaksiyanın istiliyini kənarlaşdırmaq çətinləşir. Reaksiyanın optimal müddəti maksimum 240 dəqiqə hesab olunur. Nitrolaşma reaksiyasında nitrolaşdırıcı agent rolunu əsasən NO_2 oynayır. Reaksiyanın başlaması üçün əvvəlcə soyuq halda $NaNO_2$ ilə qatı 59–63%-li nitrat turşusu qarşılıqlı təsirdə olur. Karbohidrogenlərin nitrat turşusu və azot oksidləri ilə qarşılıqlı təsiri nəticəsində müxtəlif quruluşlu nitrotörəmələr alınır. Bu da nitrolaşdırıcı agentlərin reaksiya qabiliyyətlərinin polivariantlığı ilə əlaqədardır. Qatı 59–63%-li nitrat turşusu ilə nitrolaşma reaksiyası aşağıdakı sxem üzrə gedir .

$$4HNO_3 \longrightarrow 4NO_2 + 2H_2O + O_2$$

$$2\,R{-}CH{=}CH_2 + 4HNO_3 \xrightarrow{NaNO_2} 2\,R{-}\underset{\displaystyle NO_2}{\underset{|}{CH}}{-}\underset{\displaystyle NO_2}{\underset{|}{CH_2}} + 2H_2O + O_2$$

$$R{-}CH{=}CH_2 + 2HNO_3 \xrightarrow{NaNO_2} R{-}\underset{\displaystyle ONO_2}{\underset{|}{CH}}{-}\underset{\displaystyle NO_2}{\underset{|}{CH_2}} + H_2O$$

$$R{-}CH{=}CH_2 + HNO_3 \xrightarrow{NaNO_2} R{-}\underset{\displaystyle OH}{\underset{|}{CH}}{-}\underset{\displaystyle NO_2}{\underset{|}{CH_2}}$$

Nitrolaşma prosesinin sona qədər getməsini müəyyənləşdirmək üçün alınmış nitrobirləşmənin yod ədədi təyin edilərək yoxlanılmış və nəticə təsdiqlənmişdir. Prosesdə istifadə olunan yüngül fleqmanın fiziki-kimyəvi xassələri Cədvəl 1-də verilmişdir.

Cədvəl 1. Katalitik krekinqin yüngül fleqmasının keyfiyyət göstəriciləri

Göstəricilərin adları	Göstəriciyə uyğun dəyərlər
Sıxlıq, ρ_4^{20} , kq/m^3	948,5
Fraksiya tərkibi, həcm, ^oC	190-250
Qovula bilən hissə, həcm , %	90
Özlülük, 20^{0}C mm^2/san	5,25
Kükürdün miqdarı, % kütlə	0,210
Yod ədədi, Y_2/100q	5,8
Kimyəvi tərkibi, % kütlə	
Doymamış karbohidrogenlər	73
Aromatik karbohidrogenlər	
Naften karbohidrogenləri	3
Parafin karbohidrogenləri	24,0
Setan ədədi	20

Göründüyü kimi, ölkəmizdə xammal ehtiyatı çox olan katalitik krekinqin yüngül fleqmasının tərkibində çoxlu miqdarda olefinlər və aromatik karbohidrogenlər olduğundan korroziya əleyhinə aktivliyi yüksəlir [3-6].

Məlumdur ki, üzvi turşuların metal duzları çoxfunksiyalı olma səbəbindən sənayenin bir çox sahələrində, müxtəlif məqsədlər üçün istifadə olunur. Sintezlər üçün istifadə olunan təbii neft turşularının fiziki-kimyəvi xassələri – kinematik özlülüyü, sıxlığı, qaynama temperaturu, neft turşularının kütlə payı, şüasındırma əmsalı, turşu ədədi və s. müəyyən edilmişdir (cədvəl 2).

Cədvəl 2.Təbii neft turşularının fiziki-kimyəvi göstəriciləri (TSAZ 353660 – 17520)

Xarici görünüşü	şəffaf, bircinsli maye
Neft turşularının kütlə payı, %	78,5
Kinematik özlülüyü, mm^2/san v_{50}	26,37
Kinematik özlülüyü, mm^2/san v_{100}	5,2
20°C- də; sıxlıq, kq/sm^3	960
Qaynama temperaturu, °C ; 760 mm.c.s	110-220 (6,5MPa)
Orta molekul kütləsi	222
Şüasındırma əmsalı (n_d^{20})	1,4765
Mineral duzlar; sulfatlar kütlə payı, % xloridlər kütlə payı, %	 2,1 1,6
Turşu ədədi, mq KOH/1 q turşu	265
Rəngi	qəhvəyi

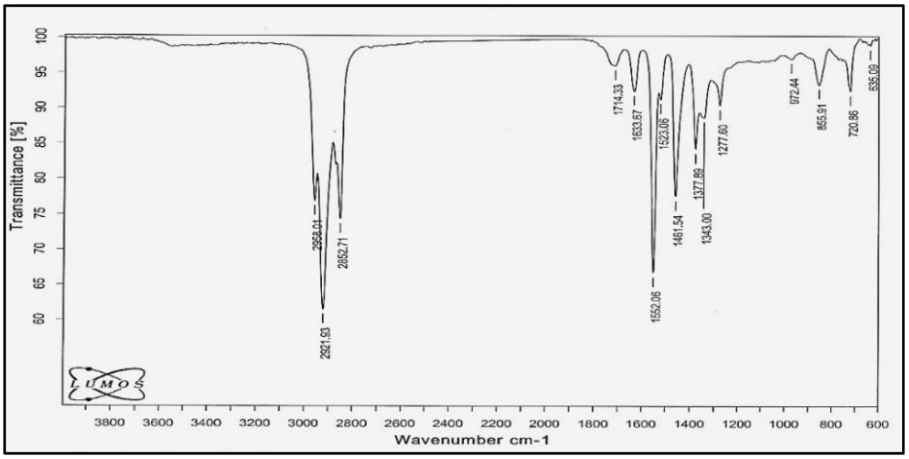
Təbii neft turşuları metal ionları ilə reaksiyaya girərək müxtəlif metal duzları əmələ gətirirlər. Bunu nəzərə alaraq, korroziyadan mühafizə məqsədilə təbii neft turşularının 310–360°C temperatur intervalında qaynayan fraksiyasının Ca duzu alınmış və nitrobirləşmə ilə kompleks hazırlamaq üçün istifadə edilmişdir.

Tərkibinə Ca metallarının daxil olduğu duz aşağıda göstərilən reaksiya üzrə alınmışdır:

$$2RCOOH + CaCO_3 = (RCOO)_2 Ca + CO_2 + H_2O$$

Nəticə

Yüngül fleqmanın nitrolaşması əsasında alınmış nitrotörəmənin İQ-spektri Şəkil 1-də göstərilmişdir.



Şəkil 1. Yüngül fleqma nitrobirləşməsinin İQ-spektri.

Sintez olunmuş nitrobirləşmələrin İQ-spektroskopiyada analizi aşağıdakı dalğa uzunluqlarına malik spektrlərlə təsvir olunmuşdur:
$–CH_3$ və $–CH_2–$ qruplarındakı C–H əlaqəsinin deformasiya
(720, 1377, 1461 sm^{-1}) və valent (2852, 2921, 2958 sm^{-1}) rəqsləri;
$C–NO_2$ qrupu üçün 1523 və 1552 sm^{-1} valent rəqsləri;
$O–NO_2$ qrupunun asimmetrik 1633 sm^{-1} və simmetrik 1277 sm^{-1} valent rəqsləri; C=O əlaqəsinin 1714 sm^{-1} dalğa uzunluğunda çox zəif titrəyişləri qeydə alınmışdır.

Sintez olunmuş nitrobirləşmələrin spektroskopiyada analizi nəticəsində qeydə alınan dalğa uzunluqlarına malik spektrlər müvafiq struktur tərkibləri təsdiq edir.

Təkliflər

Alınmış nitrotörəmələrin və onların TNT-nin Ca duzu ilə komplekslərinin H_2S mühitində korroziyaya qarşı effektivliyinin geniş tədqiqi məqsədəuyğun hesab edilir. Gələcək tədqiqatlarda hazırlanmış komplekslərin konservasiya mayelərinin tərkibində istifadəsinin və onların uzunmüddətli qoruyucu qabiliyyətinin öyrənilməsi nəzərdə tutulur.

Ədəbiyyat

[1] Abbasov, V.M.; Abuzarzada, A.H.; Mammadov, A.M.; Mammadova, R.R.; Azizbayli, E.I.; Adigozalova, R.Kh. Study of nitration reaction of 1-octene and DFT calculations, Processes of Petrochrmistry and Oil Refining, 2024,Vol.25, No.4, pp. 985-993.

[2] Abbasov, V.; Abbaszade,S.; Ismailov,T.; Tahirova,F.; Aliyev, T.; Abbasova, Kh. Nitration behavior of aromatic and olefin-enriched coking light fraction with ionic catalytic systems, Turan-fundamental sciences symposium, 2025, pp.154.
[3] Abbaszade, S.M. Research of the possibility of developing conservative liquids based on nitrolated oil distillates, Processes of Petrochrmistry and Oil Refining, 2023, Vol. 24, No. 3, pp. 473-478.
[4] Aghazada, Y. J.; The research of miscellaneous conservative lubricants as anti- corrosion agents, Processes of Petrochrmistry and Oil Refining, 2017, Vol. 18, No. 4, pp. 367-373.
[5] L.I. Aliyeva, A.R. Njafli, I.H. Ayyubova, L.E. Abdullayeva,ENVIRONMENTALLY FRIENDLY CORROSION INHIBITORS: (REVIEW). Vol. 25, No. 3, 2024, pp. 755-775
[6] Nihad Y. Alimadatli. SUMMARY OF RESEARCH ON THE DEVELOPMENT REAGENTS BASED ON NITROGEN-CONTAINING ORGANIC COMPOUNDS FOR THE OIL AND GAS EXTRACTION AND PROCESSING INDUSTRY AT THE INSTITUTE OF PETROCHEMICAL PROCESSES (IPCP). PPOR,Vol. 26, No. 3, 2025, pp.639-656.

YÜNGÜL FLEQMANIN NİTROLAŞMASI VƏ MAYE KAUÇUK ƏSASLI KOMPOZİSİYALARIN HAZIRLANMASI

[1]Mehin Dadaşova, [2]Sara Abbaszadə, [2]Yeganə Ağazadə, [2]Rufanə Əlizadə, [2]Gülnar Vəliyeva, [2]Tofiq Əliyev
[1]Azərbaycan Dövlət Neft və Sənaye Universiteti
[2]Elm və Təhsil Nazirliyinin akademik Y.H. Məmmədəliyev adına Neft-Kimya Prosesləri Institutu
Bakı, Azərbaycan
m.dadashova2004@gmail.com

Xülasə - Tədqiqat işində katalitik krekinqin əlavə məhsulu olan 190–250°C fraksiyalı yüngül fleqmanın nitrolaşdırılması yolu ilə funksional nitrotörəmələrin sintezi tədqiq edilmişdir. Sintez olunmuş nitrotörəmələrin strukturu İQ spektroskopiyası vasitəsilə təsdiq edilmişdir. Spektrlərdə C–NO_2 və O–NO_2 qruplarına məxsus xarakterik udulma zolaqları müşahidə olunmuşdur ki, bu da nitro qrupunun olefin struktura birləşməsini göstərir. Alınmış nitrobirləşmələr 1,4-sis-polibutadien əsaslı maye kauçukla kompozisiya şəklində hazırlanmışdır.

Açar sözlər: korroziya, yüngül fleqma, nitrolaşma, nitrobirləşmələr, maye kauçuk.

Giriş

Müasir sənayenin müxtəlif sahələrində, xüsusilə qaz və neft emalı sənayesində metal avadanlıqların korroziyadan qorunması aktual problemlərdən biridir. Korroziyaya qarşı istifadə olunan inhibitorların əksəriyyəti tərkibində azot atomu daşıyan üzvi birləşmələr aminlər, nitrotörəmələr və onların kompleksləri əsasında hazırlanır. Nitrobirləşmələr üzvi sintezin mühüm siniflərindən biri olmaqla yanaşı, funksional xüsusiyyətlərinə görə sənayenin müxtəlif istiqamətlərində geniş tətbiq olunur. Olefinlərin nitrolaşdırılması nəticəsində alınan nitrotörəmələr yüksək reaktivliyə malik olub, sonradan müxtəlif funksional materialların alınması üçün əlverişli aralıq məhsullar hesab edilir. Nitrolaşma prosesi əsasən nitrat turşusu və azot oksidləri vasitəsilə həyata

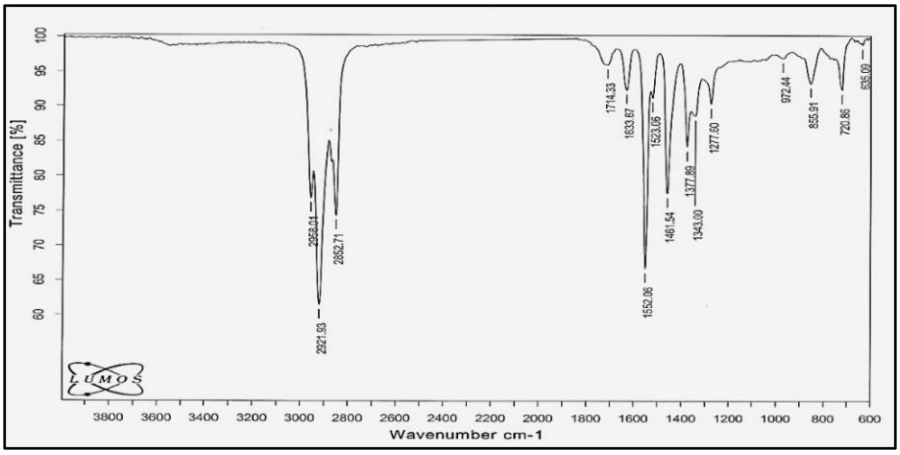
keçirilir və reaksiya şəraitindən asılı olaraq müxtəlif quruluşlu məhsulların alınmasına imkan verir.

Katalitik krekinq prosesinin əlavə məhsulu olan yüngül fleqma yüksək miqdarda olefin və aromatik karbohidrogenlərdən ibarət olduğundan kimyəvi çevrilmə üçün perspektivli xammal hesab olunur. Ölkəmizdə böyük həcmdə alınan bu məhsulun səmərəli istiqamətdə istifadəsi həm iqtisadi, həm də texnoloji baxımdan əhəmiyyətlidir. Bu baxımdan, yüngül fleqmanın nitrolaşdırılması yolu ilə yeni funksional nitrotörəmələrin alınması və onların korroziyaya qarşı sınaqları elmi və praktik maraq kəsb edir [1-3].

Experimental hissə

Tədqiqat işində nitrolaşma reaksiyasını aparmaq üçün xammal olaraq yüngül fleqmanın 190-250º C-də qovulmuş fraksiyasından istifadə etmişik. Termometr, qarışdırıcı və əks soyuducu ilə təchiz olunmuş, 3 boğazlı kolbaya, hesablanmış miqdarda 57-63%-li nitrat turşusu əlavə olunur. İnisiator kimi turşuya 0,1 mol natrium nitrit əlavə olunur və 60 ºC temperatura qədər qızdırılır. Daha sonra müəyyən zaman müddətində, reaksiya mühitinə uyğun fleqma damcı qıfı ilə əlavə olunur. Bununla yanaşı reaksiyanın temperatur rejiminə ciddi əməl olunur. Nitrolaşma prosesinin sürətinə təsir edən ən başlıca amillərdən biri temperatur və kontakt müddətidir. Temperatur rejimi 60-80ºC intervalında saxlanılmışdır, Reaksiyanın optimal müddəti maksimum 4 saat hesab olunur.

Yüngül fleqmanın nitrolaşması əsasında alınmış nitrotörəmənin İQ-spektri Şəkil 1-də göstərilmişdir.



Şəkil 1. Yüngül fleqma nitrobirləşməsinin İQ- spektri.

Sintez olunmuş nitrobirləşmələrin spektrofotometrdə analizi aşağıdakı dalğa uzunluğuna malik spektrlərlə təsvir olunmuşdur:

$-CH_3$ və $-CH_2-$ qruplarındakı C–H əlaqəsinin deformasiya 720,1377, 1461 sm^{-1} və valent 2852, 2921, 2958 sm^{-1} rəqsləri;

$C–NO_2$ qrupu üçün 1523, 1552 sm^{-1} valent rəqsləri;

$O–NO_2$ qrupunun asimmetrik 1633 sm^{-1} və simmetrik 1277 sm^{-1} valent rəqsləri;

C=O əlaqəsinin 1714 sm^{-1} dalğa uzunluğunda çox zəif titrəyişləri qeydə alınmışdır.

Sintez olunmuş nitrobirləşmələrin spektrofotometrdə analizi nəticəsində qeydə alınan dalğa uzunluğuna malik spektrlər müvafiq struktur tərkibləri təsdiq edir [4,5].

Konservasiya mayeləri üçün tərkibin əsas komponentlərindən olan maye

kauçuk sənayedə geniş tətbiq sferasına malik sterorequlyar quruluşlu 1,4 sis-polibutadien əsasında alınmışdır. Maye kauçukun mikrostrukturu aşağıdakı kimi olmuşdur:

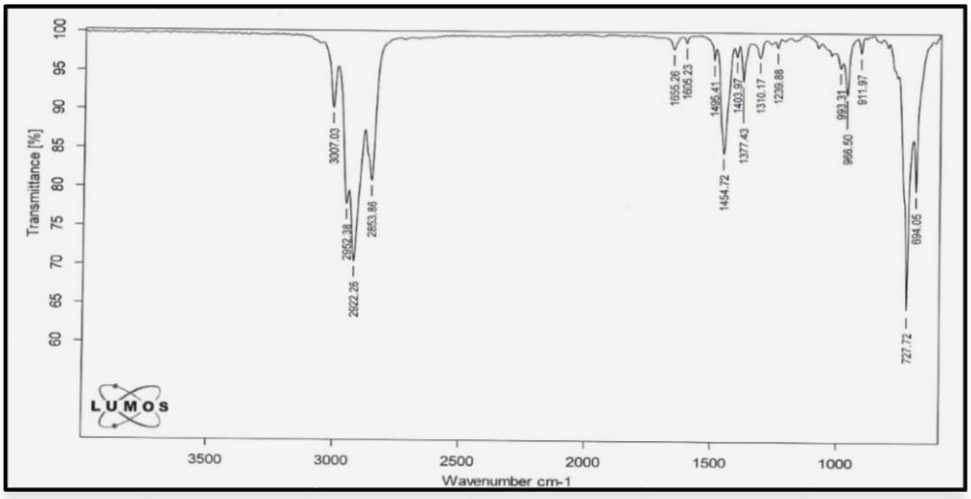
Mikrostruktur: 1,4 sis-75~80%; 1,4 trans-18~22%; 1,2-manqalar-2~7%;

Manqaların sayı~80, Aşağı molekul kütləli, M_r ~5000-10000;

Qeyd edək ki, maye kauçukda metil qruplarının sis- vəziyyətdə yerləşməsi metal səthinə adsorbsiyanı asanlaşdırır. Tədqiqat üçün götürülmüş maye kauçukun İQ- spektroskopiyası vasitəsilə struktur tərkibi analiz olunaraq müvafiq udulma zolaqlarına əsasən təsdiq olunmuş və aşağıda (şəkil 2.) göstərilmişdir.

Maye kauçukun İQ spektroskopiyası vasitəsilə analiz olunmuş spektrində aşağıdakı udulma zolaqları müşahidə olunmuşdur:

CH_3 və CH_2 qruplarındakı C–H əlaqəsinin deformasiya 1377, 1454 sm^{-1} və valent 2853, 2922, 2952 sm^{-1} rəqsləri, C=C rabitəsinin deformasiya rəqsləri 911, 966, 993, 1655, 3007 sm^{-1} dalğa uzunluğunda qeydə alınmışdır.



Şəkil 2. Maye kauçukun İQ- spektri.

Nəticə

Tədqiqat nəticəsində katalitik krekinqin əlavə məhsulu olan 190–250°C fraksiyalı yüngül fleqmanın nitrolaşdırılması yolu ilə funksional nitrotörəmələr sintez edilmişdir. Nitrolaşma prosesi 57–63%-li nitrat turşusu və natrium nitrit iştirakı ilə 60–80°C temperatur intervalında aparılmış, optimal reaksiya müddəti müəyyən edilmişdir. Prosesin gedişi yod ədədinin təyini ilə nəzarətdə saxlanılmışdır.

Alınmış nitrobirləşmələrin strukturu İQ spektroskopiyası vasitəsilə təsdiq olunmuş, spektrlərdə C–NO_2 və O–NO_2 qruplarına məxsus xarakterik udulma zolaqları qeydə alınmışdır. Bu nəticələr nitro qrupunun olefin struktura birləşdiyini göstərir.

Sintez olunmuş nitrotörəmələr 1,4-sis-polibutadien əsaslı maye kauçukla kompozisiya şəklində hazırlanmış və konservasiya mayeləri üçün perspektivli tərkib kimi qiymətləndirilmişdir. Aparılmış tədqiqat göstərir ki, yüngül fleqmanın kimyəvi çevrilməsi onun funksional xüsusiyyətlərini artırır və sənaye miqyasında səmərəli istifadəsi üçün real imkanlar yaradır.

Təkliflər

Aparılmış tədqiqatın nəticələrinə əsasən gələcək işlərdə yüngül fleqmanın nitrolaşdırılması prosesində temperatur və reagent nisbətlərinin daha geniş şəkildə araşdırılması məqsədəuyğun ola bilər. Bundan əlavə, alınmış nitrotörəmələrin korroziyaya qarşı qoruyucu xüsusiyyətlərinin müxtəlif mühitlərdə yoxlanılması və nitrotörəmələr ilə maye kauçuk əsasında hazırlanmış kompozisiyaların fiziki-kimyəvi xassələrinin daha ətraflı öyrənilməsi faydalı ola bilər.

Ədəbiyyat

[1] Abbasov, V.M.; Abuzarzada, A.H.; Mammadov, A.M.; Mammadova, R.R.; Azizbayli, E.I.; Adigozalova, R.Kh. Study of nitration reaction of 1-octene and DFT calculations, *Processes of Petrochrmistry and Oil Refining*, 2024,Vol.25, No.4, pp. 985-993.

[2] Abbasov, V.; Abbaszade,S.; Ismailov,T.; Tahirova,F.; Aliyev, T.; Abbasova, Kh. Nitration behavior of aromatic and olefin-enriched coking light fraction with ionic catalytic systems, *Turan-fundamental sciences symposium*, 2025, pp.154.

[3] Abbasov, V.M.; Mursalov, N.I.; Hasanov, E.K.; Kangarli, A.A.; Nabiyev, E.Y.; Azizov, R.E.; Gasimov, V. J. Exploration of the composition of amidoamine, synthesized through the nitrocombination of oleic acid and hexamethylenediamine, serves as a conservative liquid incorporated into T-30 oil distillate, *Processes of Petrochrmistry and Oil Refining,* 2023, Vol. 24, No. 4, pp.706-713.

[4] Abbaszade, S.M. Research of the possibility of developing conservative liquids based on nitrolated oil distillates, *Processes of Petrochrmistry and Oil Refining*, 2023, Vol. 24, No. 3, pp. 473-478.

[5] Aghazada, Y. J.; The research of miscellaneous conservative lubricants as anti-corrosion agents, *Processes of Petrochrmistry and Oil Refining,* 2017, Vol. 18, No. 4, pp. 367-373.

İSTİXANA VƏ BAĞ TULLANTILARINDAN KOMPOSTUN HAZIRLANMASI

b.ü.f.d., dosent Samirə Bağırova, Leyla Cavadova, Lalə Nəsirli, Arzu Axundova, Cəmalə Ağayeva, Mirhüseyin Səfərov, Lalə Cəlilova
"Dendrologiya Bağı" publik hüquqi şəxs, Azərbaycan, Bakı
cavadovaleyla679@gmail.com

Xülasə: Tədqiqat işi çərçivəsində Dendrologiya Bağında Fələstin püstəsi (*Pistacia palaestina* Boiss.), adi nar (*Punica granatum* L.), daş palıd (*Quercus ilex* L.), İran meliyası (*Melia azedarach* L.), Avropa zeytunu (*Olea europaea* L.), əsl innab (*Ziziphus jujuba* Mill.), şabalıdyarpaq palıd (*Quercus castaneifolis* C.A.Mey.), Qafqaz dağdağanı (*Celtis caucasica* Willd.), üçtikan şeytanağacı (*Gleditsia triacanthos* L.), vələsyarpaq qarağac (*Ulmus carpinifolia* Suckow), adi əncir (*Ficus carica* L.), ağ tut (*Morus alba* L.), nəcib dəfnə (*Laurus nobilis* L.) növlərinin tökülmüş yarpaqlarından kompost hazırlanmışdır. Nəticələr göstərir ki, düzgün şəraitdə aparılan kompostlaşdırma prosesi torpağın fiziki, kimyəvi və bioloji xüsusiyyətlərini yaxşılaşdırır, humus ehtiyatlarını artırır və davamlı kənd təsərrüfatının təmin olunmasına töhfə verir.

Açar sözlər: Kompost, kompostlaşdırma, münbitlik.

Giriş:

Davamlılıq torpağın fiziki, kimyəvi və bioloji xüsusiyyətlərinin qorunmasından asılıdır və bu üzvi maddələrin tərkibini artırmaqla mümkündür. Torpaq üzvi maddəsi, kənd təsərrüfatı istehsalı baxımından torpağın ən vacib xüsusiyyətidir. Torpağın üzvi maddələr tərkibini artırmaq üçün istifadə edilən ən vacib üsullardan biri kompostlaşdırılmış materialların istifadəsidir [Xəlilov, 2010, 470].

Kompostlaşdırmanın iki əsas növü vardır: anaerobik - oksigensiz, bu kompost, metanın ayrılması səbəbindən xoşagəlməz bir qoxu yayır. Aerobik - yəni oksigen iştirakı ilə, nəm mühitdə yaşayan və çoxalan bakteriya, göbələklər, anaerob bakteriyalar ilə üzvi maddələr istehsal olunur və parçalanma daha yüksək temperaturda baş verir. Antonina Bolotina izah edir ki, ayrılan karbon qazının, xüsusən də üzvi maddələr torf və ya torpaqla örtülmüşsə, demək olar ki, heç bir qoxu hiss olunmur [T.C. Tarım Ve Orman Bakanlığı, 2021, 10-20].

Nikolay Sençukova görə ənənəvi kompost adətən beş təbəqədən: ən alt təbəqədə budaqlar, II qida qalıqları, III yonqar təbəqəsi, IV yarpaqlar və nəhayət, V torpaq təbəqəsindən ibarətdir [T.C. Tarım Ve Orman Bakanlığı, 2021, 10-20].

Kompostun tətbiqi torpaq və ətraf mühitə bir sıra faydalar təmin edir. Kompost, üzvi maddələrin torpaqda toplanmasını təmin edərək qlobal iqlim dəyişkənliyinə qarşı mübarizəyə kömək edir, çünki torpaqda karbonun saxlanmasına imkan yaradır və atmosferə karbon qazlarının yayılmasını azaldır. Bununla yanaşı, kompost torpağın strukturunu yaxşılaşdırır, bu da torpağın sıxılmasının qarşısını alır və eroziya proseslərinin azalmasına

səbəb olur. Kompost, torpaqda olan qida maddələrinin saxlanmasını və bitkilər tərəfindən mənimsənilməsini artırır, beləliklə bu maddələrin yerə süzülməsinin və ya yuyulmasının qarşısını alır. Torpağın pH səviyyəsini tarazlaşdıraraq onun bitkilər üçün daha əlverişli olmasını təmin edir. Həmçinin üzvi maddələrin torpağa əlavə edilməsi, torpağın su saxlama qabiliyyətini artırır və nəticədə bitkilər su stresinə daha az məruz qalır. Malç kimi istifadə edildikdə isə, alaq otlarının böyüməsini azaldır və xəstəlik törədən patogenlərin yayılma ehtimalını minimuma endirir. Lakin kompostun bir neçə mənfi cəhətləri mövcuddur. İlk növbədə kompost hazırlıq tələb edir və proses uzun çəkir. Sıx məskunlaşılmış ərazillərdə kompostun hazırlanması üçün uyğun bir yer tapılması çətindir, yaşayış məntəqələrinin yaxınlığında anbarların yaradılması zamanı qoxu, milçək kimi xoşagəlməz hallar etirazlara səbəb ola bilər (Antalya ili sera atiklarindan kompost ve organik gübre üretim tesisi, 2020).

Kompostun hazırlanması zamanı bir neçə məqamlara diqqət yetirilməlidir. Üzvi tullantıların kompostlaşdırılması zamanı aerob bakteriyaların inkişafı üçün şərait yaradılmalıdır, inqredientlər düzgün nisbətdə qarışdırılmalı, materialın ölçüsü, rütubətin səviyyəsi, istilik miqdarı dəqiq təyin edilməlidir. Birinci mərhələdə mezofil bakteriyalar aktinomisetlər, mayalar və digər göbələklərlə birlikdə yağları, zülalları və karbohidratları parçalayır. Protozoa bakteriyalar və göbələklərlə qidalanır. Kif göbələkləri, bakteriyalar, ibtidailər və nematodlar temperatur 30^0C – yə çatana qədər aktiv rol oynayırlar. 30-40^0C arasında aktinomisetlər üstünlük təşkil etməyə başlayır və ətraf mühitdən torpaq qoxusu yayılır. Aktinomisetlər əsas nəmləndirici orqanizmlər kimi tanınır. Onlar humik turşusu çıxarır və münbit gil-humus kompleksi əmələ gətirirlər. Aktinomisetlər həmçinin antibiotik aktiv maddələr istehsal edərək patogenləri məhv edirlər. Temperatur 40-50^0C – yə çatdıqda, kompostlaşdırmanı başladan orqanizmlərin demək olar ki, hamısı ölür və onların yerini 70 ^{0}C – yə qədər temperatura davam gətirə və istilik yarada bilən termofilik bakteriyalar tutur. Bundan əlavə, 40-50 ^{0}C – də inkişaf edən bakteriya və aktinomisetlər bərk tullantılardakı çətin parçalanan maddələri parçalayır. Kompostun 60-70 ^{0}C – yə çatan hissəsində bir neçə spor istisna olmaqla, demək olar ki, bütün patogen orqanizmlər 1-2 saat ərzində ölür. Termofil bakteriyalar mövcud qida maddələrini istehlak etdikdə istilik yaradır. Onlar prosesi dayandırır və kompost soyumağa başlayır. Soyuyan kompostda, adətən göbələklər və aktinomisetlər olan yeni bir mikroorqanizm qrupu çoxalır və kompostun son xüsusiyyətlərini verən ölü bakteriyalar da daxil olmaqla qalan qida maddələri ilə qidalanır [Yıldız, 2012, 1-12].

Nəmlik kompostlaşdırma üçün ən vacib amildir, çünki mikroorqanizmlərin davamlı fəaliyyəti və onlara lazım olan qida maddələrinin mənimsənilməsi üçün vacibdir. Optimal nəmlik səviyyəsi 60-70% -dir. Qeyri-kafi nəmlik parçalanma prosesini ləngidir, artıq nəmlik isə çürüməyə səbəb olur. Əgər çox tez-tez nəmləndirilərsə, faydalı orqanizmlər oksigen çatışmazlığından

məhv olacaq və bu da kompostdan xoşagəlməz qoxu yaymasına, çox quru olarsa, həmçinin mikroorqanizmlərin məhvinə səbəb olacaqdır [Topal, 2011, 85-108].

Eksperimental hissə: Dendrologiya Bağı-ın tədqiqat sahələrində aparılan çoxillik təcrübələrdən məlumdur ki, tökülmüş yarpaqlardan hazırlanmış kompostda çürümə prosesi 4 ay ərzində baş verir. Daha tez çürüməsi üçün qurudulmalı, tədricən doğranmalı və nazik təbəqələrlə kompostlaşdırılmalıdır. Hazır kompost tünd qəhvəyi və ya qara rəngli, nəm meşə torpağını xatırladan, xoşagəlməz qoxuları olmayan, qırıntılı konsistensiyaya malik olmalıdır. Tədqiqat işinin ilkin mərhələdə Fələstin püstəsi (*Pistacia palaestina* Boiss.), adi nar (*Punica granatum* L.), daş palıd (*Quercus ilex* L.), İran meliyası (*Melia azedarach* L.), Avropa zeytunu (*Olea europaea* L.), əsl innab (*Ziziphus jujuba* Mill.), şabalıdyarpaq palıd (*Quercus castaneifolis* C.A.Mey.), Qafqaz dağdağanı (*Celtis caucasica* Willd.), üçtikan şeytanağacı (*Gleditsia triacanthos* L.), vələsyarpaq qarağac (*Ulmus carpinifolia* Suckow.), adi əncir (*Ficus carica* L.), ağ tut (*Morus alba* L.), nəcib dəfnə (*Laurus nobilis* L.) növlərinin tökülmüş yarpaqları toplanmış, torpaq 80 sm dərinlik qazılaraq basdırılmışdır.

Pistacia palaestina Boiss. yarpaqları kompost istehsalında qiymətli üzvi material hesab olunur. Yarpaqların tərkibində mövcud olan əsas makroelementlər bitkilərin böyümə və inkişaf proseslərində mühüm rol oynayır. Azot (N) vegetativ orqanların, xüsusilə yarpaq və gövdənin inkişafını stimullaşdırır və kompostda "yaşıl material" funksiyasını yerinə yetirir. Fosfor (P) kök sisteminin formalaşmasını və generativ inkişaf mərhələlərini, o cümlədən çiçəklənməni dəstəkləyir. Kalium (K) bitkilərin su balansının tənzimlənməsində iştirak edir, həmçinin xəstəliklərə və abiotik stress amillərinə, xüsusilə quraqlığa qarşı davamlılığı artırır.

Punica granatum L. yarpaqları yüksək üzvi maddə tərkibi torpaqda humusun miqdarının artmasına kömək edir, bu da torpağın su tutma qabiliyyətini, havalanmasını və bioloji aktivliyini yaxşılaşdırır. Yarpaqlarda mövcud olan polifenollar və taninlər torpaq mühitində bəzi patogen mikroorqanizmlərin inkişafını zəiflətmə potensialına malikdir. Yarpaqların orta sürətlə parçalanma xüsusiyyəti isə qida maddələrinin torpağa tədricən ötürülməsini təmin edərək uzunmüddətli təsir göstərir.

Quercus ilex L. yarpaqları kompost hazırlığında istifadə edildikdə torpağın məhsuldarlığını artırır, ekosistemə müsbət təsir göstərir və təbii gübrə rolunu oynayır. Yüksək miqdarda tanin turşusu olan palıd yarpaqlarını kompostlaşdırarkən, sönmüş əhəng (10 kq yarpağa 200-300 q əhəng) əlavə edilməlidir.

Olea europaea L. humus qatını, torpağın su tutma qabiliyyətini artırır. Torpaqdakı faydalı bakteriya və qurdların çoxalması üçün qida mühiti yaradır. *Ziziphus jujuba* Mill. və *Celtis caucasica* Willd. yarpaqlarının çürüyərək torpağa qarışması, humus miqdarını artıraraq torpağın strukturunu yaxşılaş-

dırır, su və hava keçiriciliyini artırır. Bu üzvi maddələr torpağın münbitliyini yüksəldir, eroziyaya qarşı davamlılığını artırır və mikroorqanizmlər üçün qida mənbəyi yaradaraq torpağın ekoloji tarazlığına töhfə verir (Şəkil 1.).



Şəkil 1. Kompostun hazırlanması

Nəticələr və onların müzakirəsi: Aparılan araşdırmalar göstərir ki, kompostlaşdırma üzvi tullantıların ekoloji baxımdan səmərəli istifadəsini təmin edən effektiv üsuldur. Bağ və park ərazilərində yaranan ağac qalıqları və tökülmüş yarpaqların komposta çevrilməsi torpaq münbitliyinin artırılmasına, humus ehtiyatlarının zənginləşməsinə və ətraf mühitin qorunmasına mühüm töhfə verir. Kompost torpağın fiziki, kimyəvi və bioloji xüsusiyyətlərini yaxşılaşdırır, su tutma qabiliyyətini artırır və bitkilərin qida maddələri ilə təminatını tənzimləyir.

Tədqiqat zamanı istifadə olunan *Pistacia palaestina, Punica granatum* və *Quercus ilex* yarpaqlarının kompost istehsalı üçün yüksək potensiala malik olduğu müəyyən edilmişdir. Dendrologiya Bağında aparılan müşahidələrə əsasən, yarpaqlardan hazırlanmış kompost optimal şəraitdə 4 ay ərzində yetişir və kənd təsərrüfatı ilə yaşıllaşdırma işlərində istifadəyə yararlı olur. Nəticə etibarilə, kompostlaşdırmanın tətbiqi davamlı torpaq idarəçiliyi və ekoloji tarazlığın qorunması baxımından mühüm əhəmiyyət kəsb edir.

İstinadlar:

1. Antalya ili sera atiklarindan kompost ve organik gübre üretim tesisi. (2020, oktyabr).
2. Xəlilov, M., Məmmədov, Q., & Məmmədova, S. (2010). *Aqroekologiya*. Bakı. 470
3. T.C. Tarım Ve Orman Bakanlığı. (2021). *Kompost el kitapçası*. Yalova: Atatürk Bahçe Kültürleri Merkez Araştırma Enstitüsü Müdürlüğü, 10-20
4. Topal, E.İ., & Topal, M. (2011). *Kompost standartları üzrə bir dəyərləndirmə. Nevşehir bilim ve teknoloji dergisi*, cilt 2(2), 85-108.
5. Yıldız, Ş., Ölmez, E., & Kiriş, A. (2012). *Kompostlaşdırma sistemləri və kompostun istifadə sahələri* mövzusunda çalıştay materialları, 1-12.

KOMPLEKS EMAL, ALTERNATİV VƏ BƏRPA OLUNAN ENERJİ MƏNBƏLƏRİ

İmran Qasım oğlu Qasımov, Günel Anar qızı Tomuyeva, Sədaqət Yaqub qızı Adıgözəlova, Şahnaz Qədir qızı Əliyeva, Zərifə Fuad qızı Yusubova
Bioresurslar İnstitutu (Gəncə)
Azərbaycan, Gəncə
penahova.shahnaz@mail.ru

Xülasə. Tədqiqat işində alternativ və bərpa olunan enerji mənbələrinin əldə edilməsində aqrosənaye tullantılarının kompleks emalı araşdırılmışdır. Müəyyən olunmuşdur ki, əlavə faydalı komponent olan pektinlə yanaşı ekoloji bioyanacaq "pellet" əldə etmək mümkündür. Qazın yanacaq növlərindən fərqli olaraq ətraf mühitdə karbon emissiyası yaratmır. Pektin isə orqanizmdən ağır metalları, toksinləri, eyni zamanda radionuklidlərin çıxarılmasında metabolizmdə iştirak etmədən tətbiq edilə bilər.

Açar sözlər. Alternativ, enerji, kompleks emal, pektin, ağır metallar, komponent, ekoloji, bioyanacaq

Giriş. Planetimizdə baş verən ciddi ekoloji problemlərin antropogen faktorlarla bilavasitə əlaqədar olması hər birimizə yaxşı məlumdur. Bu deyilən problemin ilbəil daha kəskin ekoloji xarakter alması Yer üzərində insanların həndəsi, maddi nemətlərin isə ədədi silsilə ilə artmaqda davam etməsi 3 əsr bundan əvvəl söylənmişdir.

Eyni zamanda insan həyatı üçün daim tələb olunan maddi nemətlərin əldə olunması bilavasitə təbiətdə mövcud olan təbii ehtiyatlardan istifadə, ətraf mühitə ilbəil çoxsaylı təsirlər davam edir. Müxtəlif xammalların insanların tələblərini ödəmək məqsədi ilə külli miqdarda enerji mənbələrinə ehtiyac yaranır.

Mövcud təbii ehtiyatlardan xüsusən mühüm qazıntı yanacaq növlərindən olan daş kömür, təbii qaz, neft, torf və s. tələblər də yüksələn xətt üzrə davam edir.

Qeyd edilən təbii ehtiyatlardan ibarət olan bu yanacaq növlərindən mln. tonlarla istifadə ətraf mühitdə ekoloji problemlərin ortaya çıxmasına gətirir. Yanma zamanı alınan qazlar (CO, CO_2, azot qazları, kükürd qazları) atmosferdə karbon emissiyasının, yəni parnik effekti yaranması istiliyin atmosfer havasında yığılmasına gətirir. Beləliklə enerji ilə təminat ödənilsə də ciddi ekoloji problemlərin yaranmasına səbəb olur.

Keçən əsrin 70-ci illərindən başlayaraq ətraf mühitdə qlobal iqlim dəyişmələri planetimizdə baş verən ekoloji durumla bağlı beynəlxalq tədbirlər keçirilmiş, BMT xətti ilə bu ümumbəşəri ekoloji problemlərin qarşısını almaq, mümkün olduqca azaltmaq qarşıya məqsəd qoyulmuşdur.[1.s.15-17]

Burada alternativ və bərpa olunan enerji mənbələri əldə etmək, onlardan istifadə karbon emissiyasının azalmasına səbəb ola biləcəyi tədqiqatçı və alimlər tərəfindən artıq təsdiq olunmuşdur.

Qlobal ekoloji siyasətin formalaşması üçün BMT-nin köməyi və dəstəyi ilə Stokholmda (1972), Rio-de Janeyroda (1992, 2012), Yohansburqda (2002), Kiotoda (1997) və Danimarkada (2009) keçirilmiş ümumdünya konfranslarının xüsusi əhəmiyyəti olmuşdur.

Antropogen fəaliyyət nəticəsində qlobal iqtisadi ekoloji sistemin degradasiyası geniş miqyas almışdır. Öz növbəsində bu proses təbiətdən səmərəsiz istifadə edilməsi (mineral ehtiyatların tükənməsi, torpaqların eroziyası, səhralaşma, meşələrin qırılması) həmçinin vulkanlar, zəlzələlər, sunamilər, ayrı-ayrı illərdə müharibələr zamanı istifadə olunan silahlardan ayrılan qazlar və s. ətraf mühitin çox ciddi şəkildə ekoloji fəlakətə apara biləcək bir duruma gətirib çıxaracağından xəbər verir. [2.s.60-62]

Emal texnologiyalar üçün bir sıra enerji mənbələrindən istifadə olunur. Enerji istehsalının artmasının başlıca faktoru əhalinin sayının durmadan çoxalması və həyat səviyyəsinin tərəqqisi olub, adam başına istifadə olunan enerjinin miqdarı ilə sıx bağlıdır. Hazırda yer əhalisinin hər bir sakininə gündə 2 kv yaxın enerji düşür. Əslində insanın həyat səviyyəsinin normal fəaliyyəti üçün norma 10 kv hesab olunur.

Son 200 ildə enerjidən qlobal istifadə 30 dəfə artmışdır və 1994-cü ildə 13,07 Qt təşkil etmişdir. Şərti yanacaq tonu enerji ölçüsü olub 7 mlrd. Kal. Və ya 29,3 mlrd Conla bərabərdir ki, bu da təxminən 1 ton yüksək keyfiyyətli daş kömürün yanmasından ayrılan istiliyin miqdarının uyğun gəlir. [5.DSK]

1 Qt = 1 mlrd ton

Həmin yanacaqların tullantılarının əsas hissəsi karbon qazı olub, 1 mln ton karbona çevrildikdə isə 1 Mt təşkil edir. İstilik elektrik stansiyaları ilə (İES) 66 ton üzvi maddələr, 82 ton sulfat turşusu, 26 ton xloridlər, 41 ton fosfatlar və 500 ton asılı maddələr kənar edilir. İES bütün zərərli sənaye tullantılarının miqdarının 20%-ni atmosferə atır.

Yuxarıda qeyd olunan bəşəriyyət üçün aktual problemlərə çevrilmiş enerji, ətraf mühitin mühafizəsi, alternativ və bərpa olunan enerji növlərinə nail olmaq, qida təhlükəsizliyi kimi məsələlər ölkəmiz üçün həlli vacib məsələlərdir.

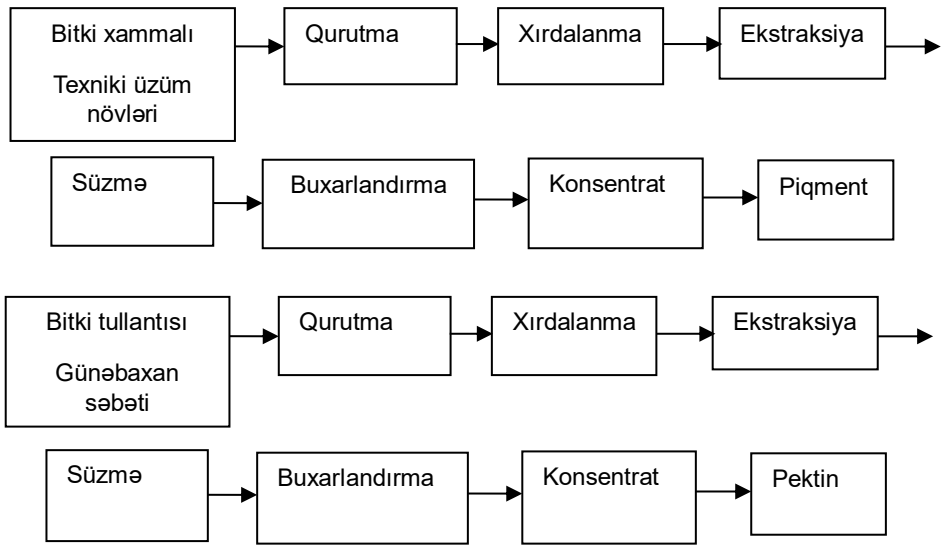
Sözü gedən problemlərin həlli ilə bağlı Azərbaycan Respublikasının Prezidenti cənab İlham Əliyevin ayrı-ayrı tarixlərdə müvafiq sərəncamları imzalanmışdır. Aidiyyatı olan elmi-tədqiqat institutları bu istiqamətdə elmi araşdırmalarını davam etdirirlər. Dünya enerji istehsalında "Günəş batareyaları", "Külək enerjisindən istifadə" və digər enerji növlərindən istifadə ilə yanaşı Beynəlxalq Enerji Agentliyi (BEA) aqrar sahədə əkilib-becərilən, eləcə də "Meşə sənayesi" tullantılarından alternativ və bərpa olunan enerji növlərinə istinad da ölkələr qarşısında bir tələb olaraq qayıtmışdır. Burada xüsusən aqrar sənayeyə geniş verilir.

Azərbaycan Respublikası Elm və Təhsil Nazirliyi Bioresurslar İnstitutu (Gəncə) əməkdaşları aqrar sahədə emal zamanı tullantılardan (əslində aralıq məhsullar) əlavə emal yolu ilə faydalı komponentlərin alınması istiqamətində elmi-praktik araşdırmaları davam etdirirlər.

Məqsədimiz qərb bölgəsinə daxil olan bitki xammalları, aqrosənayedən alınan aralıq məhsullardan innovativ texnologiyalarla təkrar, kompleks emal, biotexnologiyalar əsasında əlavə faydalı komponentlər olan boya, piqment, tanin, pektin, nar meyvəsi, tünd rəngli texniki üzüm növlərinin çərdəklərindən yağ və s. əldə olunması əlavə iqtisadi səmərə əldə etmək, həmçinin bitki mənşəli məhsulların müvafiq tətbiq sahələrini araşdırmaqdır. Buraya xüsusən qida sənayesi, tibb, kosmetika, əczaçılıq, boyakarlıq, məişət, dekorativ incəsənət daxildir.

İnstitut əməkdaşları tərəfindən Azərbaycanın qərb bölgəsinə daxil olan bitki xammalları, eləcə də aqrar sahədə alınan tullantılardan əlavə faydalı komponentlər alınmasının səmərəli üsulları istiqamətində elmi araşdırmalar aparılır. Məqsədimiz az tullantılı və tullantısız texnologiyalara nail olmaqdır. Eyni zamanda tünd rəngli texniki üzüm növlərindən boya (piqment), tanin, üzüm və nar çərdəklərindən yağ ayrılması, tanin alınması üçün səmərəli üsullar işlənir.

Eksperimental hissə. Tədqiqat obyekti kimi götürülmüş günəbaxan (lat. Helianthus annuus) bitkisindən emaldan sonra alınan məhsullar və onların tətbiq sahələri maraq doğurur.



Azərbaycan baza ili (1990) ilə müqayisədə 2030-u ilə qədər istilik effekti yaradan qazların missiyasının 35%, 2050-ci ilə qədər isə 40% azaldılmasını nəzərdə tutur. [3.s.108-112].

Beynəlxalq Enerji Agentliyinin (BEA) hesablamalarına görə alternativ və bərpa olunan enerji sahəsində aqrar sektor xüsusi əhəmiyyət kəsb edir. Beləki, qeyri-neft sektorundan olunan enerjinin 2030-cu ilə kimi ümumdünya enerji potensialında 1,5% olacağı müəyyən olunmuşdur. Həmin qurumun Dünya ölkələri arasında qoyduğu tələblər arasında ekoloji cəhətdən zərərsiz

yəni karbon və missiyası yarada bilməyən yanacaq növlərindən istifadəyə xüsusi önəm verilir.

Bu baxımdan dünya üzrə əkilib becərilən müxtəlif bitkilərin emalından sonra olunan əsas məhsulla yanaşı, tullantılardan əlavə faydalı komponentlər həmçinin alternativ və bərpa olunan enerji, xüsusən ekolojiliyə böyük üstünlük verilir. Başqa sözlə bəşəriyyət yalnız alternativ və bərpa olunan enerjiyə deyil, həm də ekoloji enerjiyə ehtiyacı var. [4.s.80-84].

Azərbaycanın 2030-cu ilə qədər sosial-iqtisadi inkişafına dair beş milli prioritetlərdən birinin "Təmiz ətraf mühit və yaşıl artım ölkəsi" kimi müəyyən edilməsi və həmin prioritetə uyğun olaraq ətraf mühitin sağlamlaşdırılması, yaşılların bərpası və artırılması, su ehtiyatlarının və dayanıqlı enerji mənbələrindən səmərəli istifadənin təmin edilməsi kimi məsələlər qeyd olunur.

Azərbaycan Respublikasının Prezidenti cənab İlham Əliyevin məlum sərəncamlarında alternativ və bərpa olunan enerji mənbələri ilə bağlı günəş, külək, SES istifadə ilə yanaşı digər bərpa oluna bilən enerji növlərinə xüsusi önəm verilir. Burada xüsusən aqrar sahədə alınan tullantılardan əlavə enerji mənbəyi kimi istifadə ayrıca vurğulanır.

Azərbaycan Dövlət Statistika Komitəsinin məlum hesablamalarında qeyd olunur ki, əkin sahələrinin 958,9 min hektarın və yaxun 62% dənli və dənli-paxlalı bitkilər, 114 min hektarın (7,4%) texniki bitkilər təşkil edir.

Qarğıdalı 3810 (2023-cü il), pambıq 1476,3 hektar dən üçün, günəbaxan 2,0 ha-dır. 2702,5 ton dənlik qarğıdalı istehsal olunmuşdur, pambıq 1476,3 ha günəbaxan 11 min ha əkilib.

Bunların emalı zamanı təkcə günəbaxandan 40% - yağ əsas məhsul alınması ilə yanaşı 9800 ton tullantı alınmışdır.

Dünya praktikasında bitki mənşəli aqrosənaye tullantılarından dənəvərləşdirilmiş ekoloji bioyanacaq alınması geniş tətbiq olunur. (ABŞ, Kanada, Rusiya, Avropa Birliyi ölkələri). Yanma zamanı ayrılan istiliyin miqdarı daş kömür, odun, mazut, təbii qazın istiliyindən geri qalmır.

Avropa Birliyi (AB) ölkələri 2011-ci ildə dənəvərləşdirilmiş yanacaq növü (pelletlər) istehsalını 11 mln tona, 2015-ci ildə 15 mln tona çatdırmışlar.

Azərbaycanda təkcə günəbaxan tullantısında dənəvərləşdirilmiş yanacaq (pellet) alına bilər. Bu yanacaq növünün üstünlüklərindən biri də onların ekolojiliyidir.

Dünya bazarında 1 tonun qiyməti: 155 eurodur.

Azərbaycanda təkcə 3 texniki bitki – pambıq: 100ha, məhsuldarlıq 26,4 sent/ha, tullantı 7300 ton (73,6%)

Qarğıdalı: 34,603ha sahədə illik ümumi məhsul 56min ton, tullantı: 20.364ton (36,5%), məhsuldarlıq 63,6sent/ha . [6.s.73-80].

Günəbaxan: 11 min ha sahədə əkilib, məhsuldarlıq 22,4 sent/ha, tullantı 9829 ton (~40%)

Tullantıların ümumi kütləsi

Pambıq – 7300ton
Qarğıdalı 20,364 ton
Günəbaxan 9800 ton

1 ton pelletin dənəvərləşdirilmiş bioyanacağın dəyəri dünya bazarında 155 euorodur.

Hesablamalara görə sözügedən 3 texniki bitkidən (pambıq, qarğıdalı, günəbaxan) alınan tullantıların ümumi kütləsinin satışından:

4,180,000 euro
Respublika büdcəsinə bu qədər vəsait!
Üstəlik:

1. Tullantısız texnologiya
2. Ekoloji durumun qorunması
3. Qida sənayesinə - pektin
4. Alternativ enerji

Nar meyvəsi qabığından boya, tanin, piqment, konsentrat, tünd rəngli texniki üzüm növlərindən boya, çərdəyindən yağ, nar çərdəyindən yağ alınması da nəzərə alınarsa bu əlavə faydalı komponentlərin istehsalının əlavə şərhə ehtiyacı qalmır.

Yəni üzüm çərdəyinin yağı, hər 100 kq dan 41 azn, üzüm çərdəyi yağından həmin məbləğdən bir qədər çox, yəni 60 azn qədər gəlir əldə edilə bilər.

Beləliklə kompeks emal nəticəsində aralıq məhsullardan faydalı komponentlər, eləcə də ekoloji bioyanacaq əldə etməklə iqtisadi sənayeyə nail oluna bilər.

Nəticələr və onların müzakirəsi. Texniki bitki növlərindən (günəbaxan, pambıq, qarğıdalı) kompleks emal ilə əlavə faydalı komponentlər (piqment, tanin, pektin), ekoloji dənəvərləşdirilmiş bioyanacaq, pellet alınması texnologiyası işlənmişdir. Alternativ, akkumilyasiya olunmuş günəş enerjisinin bərpası və istifadəsi ilə karbon emissiyasının azalmasına, əlavə faydalı komponentlərdən istifadə edilməklə iqtisadi səmərə əldə etmək təklif olunur.

Ədəbiyyat

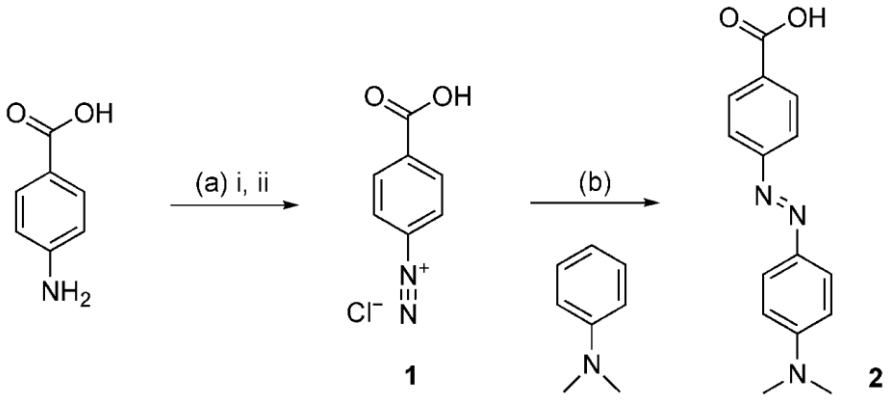
1. R.Əliyeva, Q.Mustafayev, S.Hacıyeva Ekologiyanın əsasları, Bakı 2016
2. Ş.Y.Göyçaylı Coğrafiya və coğrafi ekologiyanın problemləri, Bakı 2014
3. T.N.Əliyev, T.Q.İsmayılova Azərbaycanın ekoloji təhlükəsizlik fəaliyyətinin həyata keçirilməsi mexanizmi, AMEA Xəbərləri. İqtisadiyyat seriyası №4. Bakı Elm 2015
4. R.N.Nurəliyeva Azərbaycanın yanacaq enerji kompleksinin inkişafının iqtisadi ekoloji problemləri. Monoqrafiya Bakı “Azərnəşr”
5. http://www.bp.com./az.az/caspian/scp.html
6. İ.Q.Qasımov, G.A.Tomuyeva, S.Y.Adıgözəlova, Ş.Q.Əliyeva, Z.F.Yusubova. Pektinlərin kompleks əmələ gətirmə xüsusiyyətlərinin biotexnologiyası. Almata, Qazaxıstan ISSN: 3007-8946, 2025.

SYNTHESIS AND EVALUATION OF CATIONIC POLYASPARTAMIDES FOR THE REMOVAL OF AZO DYES FROM AQUEOUS SOLUTIONS.

Rizokulov Ramazon : Mehri Nizomova : Sunnatbek Teshayev
Aysel Mammadova
Bukhara State Technological University and
Baku Higer Oil School
Bukhara Uzbekistan
aysel.mammadova@bhos.edu.az
ramazon.rizokulov@bhos.edu.az
sunnatbek.teshaev@bhos.edu.az
mehri.nizamova@bhos.edu.az

Abstract: The removal of azo dyes from wastewater remains a pressing issue for sustainable chemical engineering. In this work, a cationic polyaspartamide was synthesized via aminolysis of polysuccinimide with diethylenetriamine and tested as a flocculating agent for Congo red in aqueous media. The polymer was obtained in dimethylformamide at 50 °C followed by modification and drying. Dye–polymer interactions were evaluated using UV–Vis spectrophotometry after flocculation. Different polymer dosages (10, 20, and 30 mg) were introduced into a model dye solution. The highest removal efficiency corresponded to the 20 mg dosage, with an absorbance of 0.468 at 494 nm. The results confirm that cationic polyaspartamides are promising materials for the treatment of azo dye–contaminated water and can contribute to greener water purification strategies.

Keywords: Cationic polyaspartamide; polysuccinimide; azo dye; Congo red; flocculation; wastewater treatment



Introduction:

Azo dyes are widely applied in textile, paper, and printing industries. Their high stability and complex aromatic structure make them resistant to biodegradation and conventional treatment methods. As a result, colored effluents often persist in aquatic systems, affecting light penetration and posing risks to living organisms. Among various azo compounds, Congo red is frequently used as a model pollutant due to its strong chromophore group and high solubility in water.

Adsorption and flocculation are considered effective and relatively simple approaches for dye removal. Special attention has been given to polymeric materials bearing functional groups capable of interacting with negatively charged dye molecules. Polyaspartamide derivatives, obtained from polysuccinimide, attract interest because of their biodegradability, tunable structure, and presence of reactive imide rings. After modification with amines, cationic sites are introduced into the polymer backbone, enhancing electrostatic interaction with anionic dyes.

In this work, the synthesis of a cationic polyaspartamide and its application for Congo red removal from aqueous solution were evaluated within the framework of a master's thesis devoted to sustainable polymeric materials.

Experimental section:

Polysuccinimide (PSI) (1 g) was dissolved in 9 g of dimethylformamide (DMF) under stirring at 50 °C for 1 h. After complete dissolution, 0.85 g of diethylenetriamine (DETA) was added to the reaction mixture. Stirring was continued at 50 °C to promote aminolysis of the imide rings and formation of cationic polyaspartamide segments.

Subsequently, 50 mL of ethyl citrate was introduced as nonsolvent to induce polymer precipitation. The resulting material was dried in an oven for 24 h to remove residual solvent. A solid modified polymer was obtained.

For preparation of the model dye solution, 10 mg of Congo red was mixed with 90 mg of distilled water under stirring until complete dissolution. The synthesized polymer was then added to the dye solution in three separate portions: 10 mg, 20 mg, and 30 mg. Each system was left for 3 days at room temperature to allow flocculation and sedimentation. After this period, visible precipitation of polymer–dye aggregates were observed.

The supernatant solutions were analyzed using a UV–Vis spectrophotometer. Absorbance values and corresponding maximum wavelengths were recorded.

Results and their discussion: The interaction between the cationic polyaspartamide and Congo red led to the formation of dense flocs, which gradually settled at the bottom of the container. This behavior indicates strong electrostatic attraction between positively charged amine groups in the polymer and negatively charged sulfonate groups in the dye molecule.

Spectrophotometric analysis provided the following results:

1. Polymer 10 mg: absorbance 0.357 at 492 nm
2. Polymer 20 mg: absorbance 0.468 at 494 nm
3. Polymer 30 mg: absorbance 0.429 at 499 nm

The change in maximum wavelength from 492 to 499 nm suggests modification of the dye's electronic environment due to complex formation. The highest absorbance among the treated samples was observed at a dosage of 20 mg polymer. This concentration appears to provide optimal

charge neutralization and bridging between dye molecules, enhancing aggregation efficiency.

At 10 mg, the number of cationic sites was likely insufficient for complete interaction with dye anions. At 30 mg, partial restabilization of particles may have occurred due to excess polymer chains in solution. In consequence, 20 mg was identified as the most effective dosage under the selected conditions.

The obtained results correlate with literature data reporting that polymer dosage strongly influences flocculation performance and that optimal charge balance is crucial for maximum dye removal [1,2]. Polymeric adsorbents containing amine groups have demonstrated enhanced affinity toward anionic azo dyes due to electrostatic and hydrogen-bond interactions [3].

The presented data confirm that cationic polyaspartamide synthesized from PSI can function as an efficient flocculant for Congo red in aqueous systems. This approach supports the concept of developing biodegradable and potentially less toxic materials for water purification.

Suggestions: Further work can be directed toward:

- evaluation of removal efficiency at different pH values;
- determination of adsorption capacity and kinetic parameters;
- structural characterization of the polymer by FTIR and NMR methods;
- testing with real industrial wastewater samples;
- comparison with commercial flocculants.

Expansion of these aspects will allow deeper understanding of the interaction mechanism and assessment of practical applicability in sustainable chemical engineering processes.

References

[1] Crini, G., 2006, Non-conventional low-cost adsorbents for dye removal: A review, *Bioresource Technology*, 97, 1061–1085.
[2] Forgacs, E., Cserháti, T., Oros, G., 2004, Removal of synthetic dyes from wastewaters: A review, *Environment International*, 30, 953–971.
[3] Gupta, V.K., Suhas, 2009, Application of low-cost adsorbents for dye removal – A review, *Journal of Environmental Management*, 90, 2313–2342.

TYPES OF COAGULANTS OBTAINED FROM ALUMINUM AND THEIR MAIN CHARACTERISTICS

Makhmudov Mukhtor Jamolovich
Professor of the Department of Oil and Gas Processing, Bukhara State Technical University, Bukhara, Uzbekistan
e-mail: makhmudov.mukhtor@inbox.ru
Sunatov Shokhrukh Shamsi ugli
Shift engineer at the Central Plant Laboratory of Uzbekistan GTL, Guzar, Uzbekistan
E-mail: sunatovshocrux@gmail.com

Annotation. Today, various coagulants are used in the world to purify various industrial waters produced in the oil and gas processing industry. This leads to an increased demand for coagulants. This article provides detailed instructions on how to obtain modern coagulants with preserved aluminum, their main characteristics and types.

Keywords: oil, gas, technical waters, coagulant, aluminum, aluminum sulfate, aluminum oxide

Aluminum – containing coagulant – $Al_2(SO_4)$ is widely used in the process of water purification. To a lesser extent, aluminum chloride is used, as well as sodium aluminate.

Currently, purified aluminum sulfate in production conditions is mainly obtained from aluminum hydroxide. This method is the simplest and most rational, it allows you to obtain a high-quality product with a low content of iron oxide.

Aluminum hydroxide is an intermediate product in the production of alumina, which is obtained by the Bayer alkaline method mainly from high-quality bauxite. Alumina is produced in smaller quantities from nephelines by sintering them with limestone, as well as from alunites by an alkaline reduction method [Halilov S.H., 2022, 601-604].

The production of aluminum sulfate consists of two main technological stages – decomposition of hydroxide with sulfuric acid and crystallization of the resulting product. The interaction of aluminum hydroxide with sulfuric acid is described by the reaction:

$$2Al(OH)_3 + 3H_2SO_4 + Q_q = Al_2(SO_4)_3 + 6H_2O + Q_q$$

In [Edelstein A.S., 1998, 3-565], the solubility of aluminum hydroxide freshly deposited and obtained at alumina plants in dilute sulfuric acid solutions was studied, depending on particle size, impurity content, storage time, and methods for preparing hydroxides. It was found that fine-grained aluminum hydroxide is better soluble in sulfuric acid than coarse-grained. Long-term storage of hydroxide reduces the rate of its dissolution in sulfuric acid. Amorphous hydroxide dissolves faster than crystalline hydroxide.

Aluminum sulfate can be obtained by decomposition of aluminum hydroxide with a stoichiometric amount of 45-50% sulfuric acid at 110-120

°C for 40 minutes. By lowering the acid dose to 95-90%, a product with a higher content of aluminum oxide is obtained with satisfactory crystallizability [Ostrovskij, 2007, 88-94].

Aluminum sulfate is produced in periodic or continuous devices with a capacity of 10-150 thousand tons of product per year.

In [Chen S., 2018, 322-328; Du, 2018, 7201-7215], the decomposition of high-iron bauxite with sulfuric acid was studied. Bauxite was characterized by the following chemical composition (in %): Al_2O_3 - 40.8; Fe_2O_3 – 27.0; SiO_2 – 8.7; TiO_2 – 2.2; CaO – 0.75; MgO – 0.2; Na_2O+K_2O – 0.5; pp.p. – 0.7. With an increase in temperature from 20 to 98 °C and the concentration of sulfuric acid from 10 to 60% extraction of aluminum and iron oxides into the solution increases, reaching 78.9 and 71%, respectively, at 98 °C and 1hour exposure. The degree of extraction of these components at boiling point depends on the duration of the process: with the decomposition of 60% H_2SO_4 bauxite, with an increase in the duration of the process from 5 to 90 minutes, the extraction of Al_2O_3 increases from 67.6 to 94%, and Fe_2O_3 – from 57.3 to 93.1%. boehmite bauxites are worse opened with sulfuric acid. Exposure to 10 n sulfuric acid for 1 hour leads to complete dissolution of gibbsite, partial (by 30%) – kaolinite and insignificant – boehmite. After firing at 550°C and subsequent decomposition of bauxite for 3 hours, 90% Al_2O_3 is extracted into the solution.

In [Chuang, 2007, 187-195] it is proposed to decompose bauxite with dilute sulfuric acid at 135 °C in a steel reactor lined with acid-resistant tiles.

Initially, 93% H_2SO_4 is fed into the solution, it is diluted with washing waters from sludge washing and heated to a boil, after which bauxite is introduced in small portions to avoid foaming and $Al_2(SO_4)$ is obtained.

The process of obtaining aluminum sulfate from low-quality bauxites is described. Another source of aluminum-containing coagulant is kaolin clays.

In [Mahmudov, 2023, 72-75] kaolins are difficult to open with sulfuric acid. Despite the large number of works devoted to the study of thermochemical transformations of kaolin, there is still no consensus on the mechanism of the process. Based on a complex of studies using physico-chemical methods, including X-ray phase analysis and IR spectroscopy, the mechanism of thermochemical transformations of kaolinite can be represented by the following reactions:

$$Al_2Si_2(OH)_4 \xrightarrow{450\text{-}550^oC} Al_2O_3 * 2Si_2O_2 + 2H_2O;$$

$$Al_2O_3 * 2SiO_2(OH)_4 \xrightarrow{830\text{-}850^oC} j\text{-}Al_2O_3 + 2SiO_2;$$

$$3(j\text{-}Al_2O_3) + 2SiO_2 \xrightarrow{900^oC} 3Al_2O_3 * 2SiO_2.$$

Aluminum alum is also used as coagulants, but they are used less often than aluminum sulfate, which is due to their high cost. In addition, alkali metal

sulfates, which are part of aluminum alum, saline the purified water, reducing coagulating properties. Therefore, ammonium-, potassium- or sodium-aluminum alum is used, which has good coagulating properties, as well as more affordable and cheaper ones. Ammonia alum is used for the treatment of chlorinated water.

An aluminum-containing coagulant can also be obtained from nepheline. In this case, it is advantageous to obtain alum, which is a more effective coagulant.

Nepheline reacts with sulfuric acid at room temperature with the release of a large amount of heat by reaction:

$$(Na, K) / AlSiO_4 / + 2H_2SO_4 + nH_2O \longrightarrow (Na, K) / Al(SO_4)_2 * 12H_2O + SiO_2 + (n\text{-}12)H_2O\uparrow$$

The sulfatization process is greatly influenced by the concentration of sulfuric acid and its dose. The higher the concentration of sulfuric acid, the higher the temperature the reaction mass is heated due to the released heat of the reaction. At the same time, more water is released into the vapor phase and alum is formed with a lower content of crystallization water. As a result, anhydrous alum can be formed – double sodium-potassium aluminum sulfates. The choice of the acid concentration is primarily determined by the possibility of separating the silica sludge from the sulfuric acid solution [3-4].

In [Dzhamolovich, 2024, 85-89], technologies have been developed for the production of anhydrous aluminum chloride from various aluminum-containing raw materials. The monograph by B.G. Rabovsky and A.A. Furman systematizes practical experience and theoretical knowledge in this field.

For oxide raw materials (natural aluminum-containing ores or alumina), chlorination is carried out only with a reducing agent. The reducing agent in this case is coal, clay–like reducing agents are also used – phosgene, generator gas, carbon monoxide, from solid ones – coal pitch and coke. In the presence of these reducing agents, the chlorination process proceeds at temperatures from 1000 to 1100 °C.

Some researchers, in addition to chlorine, suggest the use of carbon tetrachloride, sulfur chloride, hydrogen chloride, etc. as chlorinating agents. It is noted that alumina reacts with hydrogen chloride at a higher temperature, and the reaction itself is reversible. When a small amount of coal is added to the reaction mixture, increased formation of aluminum chloride is noted. When mixing sulfur chloride and chlorine, there is an increase in both reducing and chlorinating properties. Therefore, a lower temperature is necessary for this reaction to occur. The complete interaction of carbon tetrachloride with alumina occurs at a temperature of 390 °C, while AlCl3 is formed.

For alumina, chlorinating agents in the presence of aluminum ores or carbon can also be iron, sodium and calcium chlorides.

In the monograph [Makhmudov, 2023, 63-65], several methods for aluminum chlorination are considered, in particular, chlorination in a fluidized

bed (the fluidized bed is created by inert materials, for example, sand, or inert gases).

Industrial technological schemes for the production of aluminum chloride, which were developed by Soviet, German and American specialists, are also presented here.

In production conditions, the production of aluminum chloride consists of several stages. At the first stage, concentrated carbon monoxide is produced in special generators in which coal coke is gasified with oxygen. In the second stage, kaolin briquettes are prepared, dried and calcined, the main task of the second stage is the chlorination of kaolin briquettes, which is carried out in the presence of carbon monoxide with chlorine gas in a continuous shaft furnace.

Aluminum chlorides are obtained by the basic reaction:

$$Al_2O_3 + 3Cl_2 + 3CO \longrightarrow 2AlCl_3 + 3CO_2$$

Silicon oxide also reacts with chlorine by reaction:

$$Si_2O_3 + 2Cl_2 + 2CO \rightarrow SiCl_4 + 2CO_2$$

As shown in [Mahmudov, 2021, 86-95], when aluminum and silicon oxides interact with chlorine, the phenomenon of mutual catalysis is noted, when the rate of chlorination of mixtures is higher than when chlorinating individual oxides. According to [19-20], silica and alumina are chlorinated in the temperature range from 550 to 800 °C in the same ratios as in the feedstock.

The literature provides contradictory data on the interaction of chlorine with oxides at higher temperatures. Thus, Kocharovsky [Ostrovskij, 2007, 88-94], investigating the chlorination of Polish clays, found that at temperatures above 900 °C, the yield of $AlCl_3$ decreases. Meanwhile, according to Kocharovskys data, confirmed by long-term practice, the yield of $SiCl_4$ in the temperature range from 1000 to 1200 °C reaches minimum values.

These contradictions can be explained by the fact that in [22] the results were obtained in a shaft furnace of continuous countercurrent action, that is, under conditions of a secondary reaction:

$$2Al_2O_3 + 3SiCl_4 \longrightarrow 3SiO_2 + 4AlCl_3$$

In [Edelstein, 1998, 3-596], the results of a study on the chlorination of various types of aluminum-containing raw materials are presented. The authors studied the chlorination process of the North Voronezh bauxites, which was carried out in a fluidized bed. It is shown that all oxides included in the bauxite composition are chlorinated in the fluidized bed. The most easily chlorinated are iron and titanium oxides. Optimal chlorination conditions were found, at which the degree of chlorination of iron and titanium oxides reaches 98%, aluminum oxide – 65%, and silicon oxide – 20-35%.

In [Chen, 2018, 322-328], a technique was developed for the selective chlorination of bauxites in a fluidized bed to produce aluminum oxide in the temperature range from 800 to 900 °C with a mixture of chlorine and silicon tetrachloride. Chlorination of powdered bauxite in a fluidized bed with 1% carbon makes it possible to remove 65% of iron from it at a temperature of 800 °C, while losing 8% of aluminum (for Uglian bauxite). The chlorination of Prosyanovo kaolin of Ukhta and Severoonezhsky bauxites in the filter layer was studied.

The authors [Edelstein, 1998, 3-596] studied the process of chlorination of the mineral part of the Ekibastuz carboniferous rocks. It is shown that during chlorination of these rocks, the yield of iron and silicon oxides is 98-100%, and the yield of aluminum oxide is 91-96%. It is proposed to carry out preliminary hydrochloric acid treatment to pre-release this raw material from silica, or to suppress the process of chlorination of SiO_2 with silicon tetrachloride, to separate silicon and aluminum oxides.

The authors [8] present a developed method for selective low-temperature reduction of a mixture of iron and aluminum chlorides to metals. It is recommended to carry out the process in an inert gas stream containing hydrocarbons, for example, methane, as well as iron and aluminum chlorides.

The chloride reduction process is recommended to be carried out on the surface of iron, which increases the selectivity of reduction and significantly reduces the temperature of the process: $AlCl_3$ – up to 450 °C, $FeCl_3$ – up to 350 °C, the authors recommend using silicon or manganese instead of jelly, however, on their surfaces the reduction of aluminum chloride occurs at higher temperatures, 950 and 800 °C, respectively.

H. Safiev et al. [Edelstein, 1998, 3-596] studied the decomposition of nepheline syenites from the Turpi deposit of the Republic of Tajikistan by chlorination to produce oxides, and also considered the main thermodynamic characteristics of the processes occurring during chlorination of the main minerals of the nepheline syenite rock (nepheline – $Na_{0,78}K_{0,22}AlSiO_4$, albite – $NaAlSi_3O_8$, microcline – $KAlSi_3O_8$, calcite – $CaCO_3$, hematite – Fe_2O_3 and goethite is FeO(OH). This method is based on the use of coals, carbon monoxide, methane and phosgene and methane as reducing agents. The following probable ways of processes have been identified:

$$M + X + C \longleftrightarrow EX + CO_2,$$

$$M + X + CO \longleftrightarrow EX + CO_2,$$

$$M + X + COCl_2 \longleftrightarrow EX + CO_2,$$

$$M + X + CH \longleftrightarrow EX + CO_2 + H_2O.$$

where: X is chlorine gas; M is the corresponding mineral; EH is a mixture of chlorides of the corresponding elements in the composition of minerals.

Based on the comments, it can be assumed that feldspar and hematite are chlorinated more effectively when using coal as a reducing agent, and when chlorinating calcite, it is more rational to use methane as a reducing agent. Chlorination of minerals in the presence of a reducing agent – carbon monoxide in the studied temperature range is thermodynamically impossible, and when using phosgene as a reducing agent, all minerals except goethite must be chlorinated equally vigorously.

The chemical foundations of the chlorine method of processing aluminosilicate ores of Tajikistan were studied, rational conditions for the chlorine process were proposed, and basic technological schemes for the production of aluminum-containing coagulants were developed.

Thus, the high ability of chlorine to enter into chemical reactions, as well as the ability of chlorides to interact with other compounds, make it possible to isolate valuable components from processed raw materials, including aluminum chloride, a coagulant for water purification.

REFERENCES

1. Halilov S.H., Mahmudov M.Zh. Termicheskie prevrashcheniya masel tyazhelyh neftej //Science and Education. – 2022. – T. 3. – №. 5. – S. 601-605.
2. Edelstein A.S., Cammarata R.C. Nanomaterials: Synthesis, Properties and Applications. London: Institute of Physics Publ., 1998. P. 596.
3. Ostrovskij N.M. Modelirovanie limitiruyushchej stadii processa sorbcii vody kompozitnymi sorbentami «hlorid kal'ciya v poristoj matrice» / N.M. Ostrovskij [i dr] // Teoreticheskie osnovy himicheskoj tekhnologii, 2007. – T. 41. – № 1. – S. 88-94.
4. Chen S.; Yuan, Z.; Hanigan D.; Westerhoff P.; Zhao H.; Ni J., (2018). Coagulation behaviors of new covalently bound hybrid coagulants (cbhyc) in surface water treatment. Sep. Purif. Technol., 192: 322-328.
5. Du B.D.; He T.T.; Liu G.L.; Chen W.; Wang Y.M.; Wang, W.; Chen, D.M., (2018). Al-water reactivity of al-mg-ga-in-sn alloys used for hydraulic fracturing tools. Int. J. Hydrogen Energy. 43(15): 7201-7215.
6. Chuang S.H., Chang T.C., Ouyang C.F., and Leu J.M. (2007). Colloidal silica removal in coagulation processes for wastewater reuse in a high-tech industrialpark. Water Sci. Technol. 55, 187–195.
7. Mahmudov M. Zh., Yomgurov S. A. ADSORBCIONNYE SPOSOBY OChISTKI I OSUShKI GAZOV //Byulleten' pedagogov novogo Uzbekistana. – 2023. – T. 1. – №. 5. – S. 72-75.
8. Dzhamolovich M. M., Ugli Y. S. A. SELECTION OF A METHOD FOR PREPARING NATURAL GAS FOR TRANSPORTATION BY MAIN GAS PIPELINES //Austrian Journal of Technical and Natural Sciences. – 2024. – №. 1-2. – S. 85-89.
9. Makhmudov M., Nematov H., Rizayev S. MECHANISM OF ABSORPTION OF H_2S, CO_2 AND OTHER SULFUR COMPONENTS BY AN AQUEOUS SOLUTION OF MDEA //Universum: tekhnicheskie nauki. – 2023. – №. 12-8 (117). – S. 63-65.
10. Mahmudov M.Zh., Salomov S.S., Savriev M.S. NEFT FRAKCIYaLARINI KATALITIK GIDROTOZALAShDA KATALIZATORLARNING FAOLLIGIGA TA"SIR ETUVChI OMILLARNI TADQIQ QILISh // Science and Education. – 2021. – T. 2. – №. 3. – S. 86-95.

PREDICTING THE KINETICS OF OIL BIODEGRADATION IN SEAWATER WHEN INOCULATED WITH ACTIVE HYDROCARBON-OXIDISING MICROORGANISMS

Konul Gahramanova, Parvin Mammadova, Gulshan Gasimli, Tarana İbragimova, İnara Sadirzade, Aygun Almammadova, Aytaj İsmayilli
Institute of Chemistry Ministry of Education of the Republic of Azerbaijan, Baku, Azerbaijan
qehremanovakr@gmail.com

Keywords: oil biodegradation, hydrocarbon-oxidising microorganisms, biodegradation, kinetic modelling, prediction, bioremediation

Our work aimed to quantitatively predict the process of oil biodegradation in seawater based on an analysis of kinetic patterns. Oil from the Bibi-Eibat field was added to model seawater samples at a concentration of 10 g/l. A suspension of active hydrocarbon-oxidising microorganisms in an amount of 10^7 cells/ml was added to the experimental samples; the control samples were not inoculated. The experiment lasted 315 days.

The dynamics of the decrease in oil concentration and changes in the number of microorganisms indicate a multistage nature of the process. At the initial stage, a lag phase of microbial population adaptation was observed, followed by an acceleration of biodegradation. By day 70, the degree of oil destruction in the inoculated samples reached 17.4%, while in the control, it was only 1.4%. By day 315, the degradation level was 89.8% compared to 58% in the control.

Analysis of the experimental data demonstrated that a pseudo-first-order reaction model can adequately describe the rate of decrease in oil concentration.

$$dC/dt = -kC$$

where C - the oil concentration and k - the effective biodegradation rate constant. The growth of microbial numbers corresponds to a logistic model reflecting the limitations of the substrate and environmental conditions. The parameters obtained allow predicting the time required to achieve environmentally acceptable concentrations of hydrocarbons in seawater.

The results confirm the high efficiency of targeted microbial inoculation and the possibility of using kinetic modelling for scientifically based management of bioremediation processes in oil-polluted water areas.

References

1. Enerijiofi, K. E., & Ikhajiagbe, B. (2021). Bioremediation of crude oil contaminated soil using microbial consortia. *Environmental Monitoring and Assessment, 193*, 509. https://doi.org/10.1007/s10661-021-09235-6

SPECTROPHOTOMETRIC DETERMINATION OF Fe(III), Mo(VI), AND Cu(II) IONS IN NANOANALYTICAL SYSTEMS

Ayten Imamaliyeva, Famil Chyragov, Flora Hajiyeva
Baku State University,
Baku, Azerbaijan
e-mail: aytenimamaliyeva@hotmail.com

Abstract
New R–AgNP–CTAB-based systems were developed for the spectrophotometric determination of Fe(III), Mo(VI), and Cu(II) ions. In this study, a benzidine–pyrogallol reagent was used for Fe(III) and Mo(VI), while a dithiocarbamate reagent was applied for Cu(II). Silver nanoparticles were synthesized via a green method based on a starch–glucose system. CTAB was added to enhance the stability of the complexes.Spectral analysis showed that the presence of AgNPs and CTAB significantly increased the absorbance intensity and stability of the complexes. Stoichiometric analysis indicated ratios of 1:1 and 1:2 for Fe(III) and Mo(VI), and 1:2 and 3:2 for Cu(II). The stability of the systems at room temperature for 24 hours and their successful application to real samples confirmed the practical applicability of the methods. Overall, AgNP–azo reagent–CTAB-based systems provide a simple, rapid, cost-effective, and accurate approach for the determination of metal ions.
Keywords: silver, nanoparticles, CTAB, spectrofotometrik determination

Introduction

In recent years, the application of metal nanoparticles in analytical chemistry has developed rapidly. Silver nanoparticles (AgNPs) possess a high specific surface area and surface plasmon resonance property, which enable them to act as effective signal enhancers in spectrophotometric analysis [Lenhart 1095-1104]. These characteristics allow the determination of metal ions at lower detection limits with improved sensitivity.Azo reagents are well known for forming intensely colored complexes with metal ions; however, classical azo systems sometimes exhibit insufficient sensitivity. Therefore, their modification with AgNPs and CTAB enhances the complex formation process, increases system stability, and improves analytical selectivity [Imamaliyeva 2025,1-11].

Experimental part

Materialls: Silver nitrate ($AgNO_3$, PLC 141459, 98% chemically pure), soluble starch ($(C_6H_{10}O_5)n$, PLC 121096, 98% chemically pure), β-D glucose ($C_6H_{12}O_6$, CAS No.50-99-7); sodium hydroxide (NaOH, PLC 1416x87), cetyltrimethylammonium bromide (CTAB, AB 117004), ethanol (C_2H_5OH, CAS No.64-17-5, 95%),were used as received.

Photometric determination

In the present study, a benzidine–pyrogallol-based azo reagent was used for the determination of Fe(III) and Mo(VI) ions, while a dithiocarbamate reagent was applied for Cu(II) determination. Silver nanoparticles (AgNPs) were synthesized via a green synthesis method based on a starch–glucose system, where starch served as a stabilizer and glucose as a reducing agent.

The obtained colloidal solution was purified and washed by ultracentrifugetion. [Khajehsharifi 219-225] The azo reagent was synthesized through diazotization of benzidine followed by coupling with pyrogallol. The reaction was carried out at low temperature, and the product was purified by recrystallization. For the formation of binary complexes, AgNPs were added to the reagent (R) and stirred for 2 hours using a magnetic stirrer. For ternary complexes, AgNPs were first added to the reagent, followed by CTAB, resulting in the formation of a highly stable Ag–R–CTAB system. The determination of Fe(III), Mo(VI), and Cu(II) ions were carried out under various conditions, including pH, wavelength, reagent concentration, temperature, and reaction time. UV–Vis spectral measurements showed a bathochromic shift in the R+Fe, R+Ag+Fe, and R+Ag+CTAB+Fe systems, with a gradual increase in absorbance intensity. The maximum absorbance for Fe (III) was observed in the range of 465–487 nm. The optimal pH was found to be approximately 2 for the binary complex and approximately 1 for the ternary complex. The presence of AgNPs and CTAB increased the molar absorptivity and enhanced complex stability. For Mo(VI), the R+Mo, R+Ag+Mo, and R+Ag+CTAB+Mo systems were investigated. Spectral analysis revealed that the ternary complex exhibited maximum absorbance at 460–465 nm. The optimal pH was approximately 3 for the binary complex and approximately 1 for the ternary complex. Calibration graphs constructed for Mo(VI) demonstrated linearity over a wide concentration range. The interaction of Cu(II) with dithiocarbamate was comparatively studied in the R+Cu, R+AgNP+Cu, and R+AgNP+CTAB+Cu systems. The optimal pH was 5 for the R+Cu system and 6 for the AgNP- and CTAB-modified systems. The optical density increased in the order: R+AgNP < R+AgNP+Cu < R+AgNP+CTAB+Cu. These results indicate that AgNPs enhance the analytical signal, while the addition of CTAB further improves complex stability and absorbance intensity. Isomolar series and the Starik–Barbanel method indicated that Fe(III) and Mo(VI) complexes predominantly exhibit 1:1 and 1:2 stoichiometric ratios. For Cu(II), the stoichiometric ratio was 1:2 in the binary complex and 3:2 in the ternary complex. AgNPs and CTAB accelerated complex formation kinetics and increased stability. Temperature and time studies showed that all systems remained stable at room temperature and retained their optical properties for 24 hours. Statistical analysis confirmed high reproducibility and low relative error of the developed methods. The method for Fe(III) was successfully applied to real fruit samples, and the results were consistent with atomic absorption analysis, confirming its practical applicability. Similar analytical performance was obtained for Mo(VI). Majid [877-886]. Overall, new and efficient AgNP–azo reagent–CTAB-based spectrophotometric systems were developed for the determination of Fe(III) and Mo(VI) ions. The presence of nanoparticles and surfactant significantly enhanced complex stability and absorbance signal.

The proposed methods are simple, rapid, cost-effective, and highly accurate, and can be recommended as promising analytical approaches for the determination of metal ions in environmental, biological, and industrial samples [Saha 2739-2779].

Results

The study demonstrated that azo and dithiocarbamate-based reagents modified with AgNPs and CTAB provide an effective system for the spectrophotometric determination of Fe(III), Mo(VI), and Cu(II) ions. The presence of nanoparticles enhances the analytical signal, while CTAB increases the stability and absorbance intensity of the complexes. Under optimal conditions, both binary and ternary complexes exhibit high absorbance and stability. Stoichiometric analysis indicated ratios of 1:1 and 1:2 for Fe(III) and Mo(VI), and 1:2 (binary) and 3:2 (ternary) for Cu(II). The systems-maintained stability at room temperature for 24 hours, and statistical analyses confirmed high reproducibility and low relative error. The application of the methods to real samples for Fe(III) and Mo(VI) showed results consistent with atomic absorption analysis.

References

1. Imamaliyeva A., Chyragov F., Hajiyeva F. Novel silver nanoparticle complexes based on bisacetylacetoneethylenediamine and cetyltrimethylammonium bromide: synthesis and structure. *Baku State University Journal of Chemistry & Materials Science*, 2025, Vol. 2, Issue 3, P. 1–11. https://doi.org/10.30546/209501.201.2025.2.03.011
2. Khajehsharifi H., Afkhami A., Madrakian T. Micellar-mediated spectrophotometric determination of iron. *Spectrochimica Acta Part A*, 2016, Vol. 152, P. 219–225. https://doi.org/10.1016/j.saa.2015.07.062
3. Lenhart J.J., Walker H.W. Aggregation kinetics and dissolution of coated silver nanoparticles. *Langmuir*, 2012, Vol. 28, P. 1095–1104. https://doi.org/10.1021/la203416k
4. Majid Y.J., Ali W.B., Fadhel S.R. Spectroscopy determination of iron(III) ion by using azo dye derived from mefenamic acid. *Academic Science Journal*, 2025, Vol. 3, Issue 3, P. 877–886. https://doi.org/10.24237/ASJ.03.03.877C
5. Saha K., Agasti S.S., Kim C., Li X., Rotello V.M. Gold and silver nanoparticles in biomedical applications. *Chemical Reviews*, 2012, Vol. 112, P. 2739–2779. https://doi.org/10.1021/cr2001178

SYNTHESIS AND APPLICATION OF PET-DERIVED HYDROGEL ADSORBENTS FOR EFFICIENT TREATMENT OF DYE-CONTAMINATED WATER

Bafoev Asliddin[1] , Ahmadova Garanfil[2]
[1]Bukhara State Technical University, Bukhara, Ozbekistan
[2]Baku Higher Oil School, Baku, Azerbaijan
Author's email: asliddin.bafoev.std@bhos.edu.az

Abstract - Plastic waste accumulation, particularly polyethylene terephthalate (PET), and toxic industrial effluents threaten aquatic ecosystems. This study addresses both challenges by developing a hydrogel adsorbent from post-consumer PET waste. PET bottles were chemically depolymerized via aminolysis using diethylenetriamine (DETA), and the resulting oligomers were cross-linked with ethylene glycol diglycidyl ether (EDGE) (16-20 wt%) to form a three-dimensional polymeric network. The hydrogels were characterized by FTIR (confirming amide and hydroxyl groups) and SEM (revealing porous architecture). The hydrogel with 18 wt% EDGE achieved 99% Congo Red removal (pH 7, 7h) and maximum adsorption capacities of 383.96 mg/g for Pb(II) and 244.12 mg/g for Zn(II). The material retained >85% adsorption capacity after four cycles, presenting a sustainable circular-economy approach for wastewater treatment.

Keywords: PET, chemical recycling, hydrogel, adsorption, wastewater treatment, dye removal, heavy metal removal

Introduction

Two major environmental challenges of the 21st century are plastic waste accumulation and water contamination by industrial effluents. Global PET production exceeds 30 million tonnes annually [1], yet most is not recovered, persisting in landfills and oceans for centuries. Simultaneously, industries discharge wastewater containing synthetic dyes (especially azo-based compounds) that resist biodegradation, block light penetration, disrupt photosynthesis, and introduce carcinogenic substances into food chains [3,4].

While various treatment technologies exist (advanced oxidation, membrane filtration, electrochemical destruction), they are often limited by high costs and secondary sludge production [5]. Adsorption is preferred for its simplicity and efficiency [6], with activated carbon being the commercial standard. However, its high production cost and difficult regeneration drive research toward sustainable, waste-derived alternatives [8].

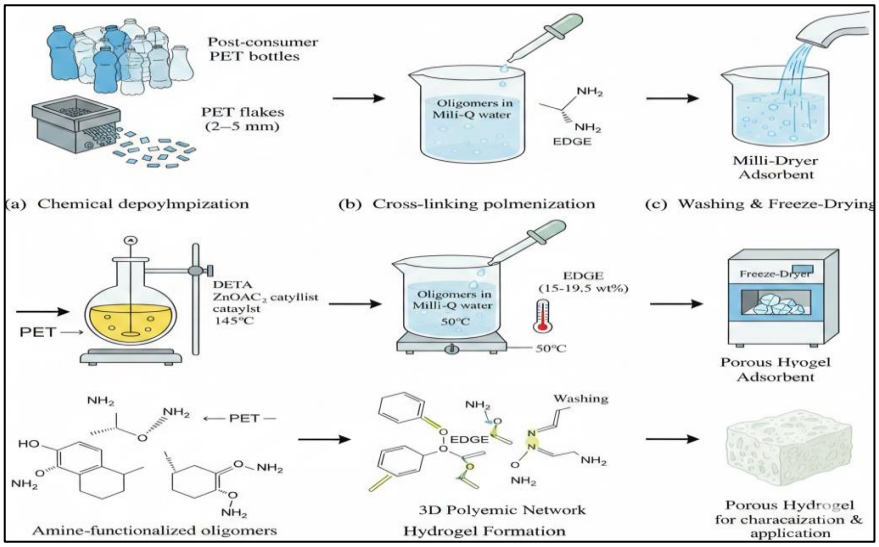
This research proposes a "waste-to-wealth" strategy: chemically upcycling PET bottles into hydrogel adsorbents. Unlike mechanical recycling (which downcycles PET), chemical recycling via aminolysis breaks polymers into oligomers that can be repurposed for higher-value materials [9]. By creating a three-dimensional hydrogel network with abundant binding sites, we address both plastic pollution and water treatment needs, contributing to UN Sustainable Development Goals 6 (Clean Water) and 12 (Responsible Consumption).

Methodology

The synthesis of the PET-derived hydrogel adsorbent was accomplished through a two-step chemical process, beginning with the depolymerization of

waste PET and concluding with the cross-linking polymerization of the resulting oligomers. Post-consumer PET bottles were collected, manually cleaned to remove adhesives and labels, and mechanically shredded into flakes of approximately 2–5 mm in size. Chemical depolymerization was performed via aminolysis using diethylenetriamine (DETA). In a typical reaction, 120 g of PET flakes were combined with 360 g of DETA and 4 g of zinc acetate catalyst in a 500 mL round-bottom flask equipped with a reflux condenser. The mixture was heated to 145°C in a silicone oil bath under an argon atmosphere with continuous magnetic stirring at 300 rpm for approximately one hour until the PET flakes were completely dissolved, yielding a mixture of amide-containing oligomers. Following the reaction, the product was cooled to room temperature and stored for subsequent use. In the second stage, the aminated PET oligomers were converted into a hydrogel network via cross-linking with ethylene glycol diglycidyl ether (EDGE). Briefly, 0.2 g of the oligomeric product was dissolved in 2 mL of Milli-Q water and heated to 100°C with stirring. The temperature was then reduced to 50°C, and a predetermined amount of EDGE (corresponding to final concentrations of 16, 18, and 20 wt%) was added to the solution. The mixture was stirred until a viscous gel formed, then incubated at 50°C for 10 minutes followed by 8–12 hours at room temperature to complete cross-linking. The resulting hydrogels were washed repeatedly with copious amounts of Milli-Q water over 24 hours to remove any unreacted components and finally freeze-dried to obtain the dry, porous adsorbent for characterization and adsorption studies.

Figure 1. Schempic representation of the two-step synstess of the PET-derived hydrogel adsorbent



The chemical structure, morphology, and adsorption performance of the synthesized hydrogels were systematically characterized using a combination of spectroscopic, microscopic, and analytical techniques. Fourier-transform infrared (FTIR) spectroscopy was employed to confirm the successful incorporation of functional groups and the formation of the cross-linked network. Spectra were recorded over the range of 4000–400 cm^{-1} using an FTIR spectrometer (e.g., Bruker Alpha) with samples prepared as KBr pellets. The internal pore architecture, critical for efficient adsorbate diffusion, was examined using scanning electron microscopy (SEM). Freeze-dried hydrogel samples were mounted on aluminum stubs, sputter-coated with gold, and imaged at various magnifications using an SEM (e.g., JEOL JSM-IT500) operating at an accelerating voltage of 5–10 kV. The swelling behavior, an indicator of network hydrophilicity and porosity, was quantified by gravimetric analysis. Pre-weighed dry hydrogel samples were immersed in deionized water at room temperature for 24 hours. The swollen samples were gently blotted with filter paper to remove surface water and re-weighed. The equilibrium swelling ratio was calculated using the equation: Swelling Ratio (%) = [(W□ - W_d)/W_d] × 100, where W□ and W_d are the weights of the swollen and dry hydrogel, respectively. Batch adsorption experiments were conducted to evaluate the efficacy of the hydrogels for pollutant removal. Stock solutions of Congo Red (CR), Pb(II), and Zn(II) were prepared at various concentrations (10–100 mg/L). In a typical kinetic experiment, 10 mg of hydrogel was added to 20 mL of a pollutant solution of known concentration at a controlled pH. The mixtures were agitated on an orbital shaker at 150 rpm at room temperature. At predetermined time intervals, aliquots were withdrawn, and the residual concentration of CR was determined using a UV-Vis spectrophotometer at its maximum absorption wavelength (λ_max = 498 nm). Concentrations of Pb(II) and Zn(II) were analyzed using atomic absorption spectroscopy (AAS). The adsorption capacity at time t, q_t (mg/g), was calculated as $q_t = [(C_0 - C_t)V]/m$, where C_0 and C_t are the initial and time-dependent concentrations (mg/L), V is the solution volume (L), and m is the mass of adsorbent (g). The effect of pH (3–11), initial pollutant concentration, and contact time on adsorption was systematically investigated. Adsorption isotherm studies were performed by varying the initial concentration, and the equilibrium data were fitted to Langmuir and Freundlich models. Kinetic data were analyzed using pseudo-first-order and pseudo-second-order models. Finally, the reusability of the hydrogel was assessed over four consecutive adsorption-desorption cycles by washing the spent adsorbent with an appropriate eluent (e.g., 0.1 M HCl for metals or ethanol for dye) and reusing it in fresh adsorption experiments.

Results and Discussion

All hydrogel formulations demonstrated significant hydrophilicity, with equilibrium swelling ratios ranging from 150% to 200%, where the lower

cross-linker content (16% EDGE) resulted in the highest water uptake due to a less dense polymeric network, while the higher content (20% EDGE) produced a more constrained structure with reduced free volume; this porous architecture was confirmed by SEM analysis, which revealed highly interconnected macropores (10-50 μm) that facilitate rapid adsorbate diffusion. In adsorption kinetics studies, the optimized 20% EDGE hydrogel achieved over 90% removal of Congo Red (CR) within the first 2 hours, reaching equilibrium at 7 hours, thereby indicating that chemisorption, driven by electrostatic interactions between the dye molecules and the hydrogel's functional groups, is the rate-limiting step. The adsorption process was highly pH-dependent; at low pH (<5), the protonation of functional groups led to electrostatic repulsion of cationic Pb(II) and competition with H^+ ions for anionic CR binding sites, whereas at alkaline pH (8-10), surface deprotonation created a strong electrostatic attraction for Pb(II), making the hydrogel particularly well-suited for treating alkaline textile effluents without extensive pH pre-adjustment. Finally, reusability tests demonstrated that the hydrogel retained over 85% of its initial adsorption capacity for both CR and Pb(II) after four consecutive cycles, with the slight decrease attributed to irreversible site occupation or minor network degradation, a reusability that significantly reduces operational costs and underscores the material's practical viability. By successfully valorizing post-consumer PET waste that would otherwise be destined for landfills, this work circumvents the need for virgin petroleum-based materials and offers a value-added alternative to mechanical downcycling [16], thereby providing an effective and sustainable tool for water remediation.

Offers

To bridge the gap between laboratory-scale results and practical industrial application, several strategic research directions are proposed to enhance the performance, scalability, and economic viability of the PET-derived hydrogel adsorbent. Future work should first conduct comprehensive long-term cyclic stability studies to evaluate various desorbing agents—including acidic (HCl), alkaline (NaOH), and organic solvent-based (ethanol) solutions—to identify the optimal efluent for complete pollutant desorption without compromising the hydrogel's structural integrity over an extended number of cycles (10–20 cycles). Second, the translation of batch-scale success to pilot-scale continuous flow systems is critical, requiring the design of fixed-bed columns or multi-stage filtration units to determine key engineering parameters such as breakthrough curves as a function of bed height, flow rate, and influent concentration, which are essential for scaling up to industrial treatment plants. Third, magnetic functionalization of the hydrogel by incorporating nanoparticles such as magnetite (Fe_3O_4) should be explored to enable rapid and facile separation of the spent adsorbent from treated water using an external magnetic field, drastically reducing post-

treatment recovery time and energy consumption. Finally, to better simulate real industrial effluents, future studies must expand the pollutant spectrum to include other common contaminants (e.g., hexavalent chromium Cr(VI) and various dyes) and investigate competitive adsorption scenarios in the presence of multiple competing species, including other dyes, heavy metals, and industrial additives, to understand the adsorbent's selectivity and performance in chemically complex environments.

Conclusion

This study successfully demonstrates PET waste valorization into a high-performance hydrogel adsorbent. Through aminolysis and cross-linking, a porous, hydrophilic network was created with strong affinity for both organic and inorganic pollutants. Maximum Langmuir capacities reached 383.96 mg/g for Pb(II) and 244.12 mg/g for Zn(II), with 99% CR removal. PSO kinetics and Langmuir isotherm fitting indicated monolayer chemisorption via electrostatic interactions. The material retained >85% capacity after four cycles. This "waste-to-wealth" approach addresses dual environmental challenges—plastic pollution and water contamination—offering a low-cost, sustainable material for wastewater treatment with significant potential for Azerbaijan's textile and petrochemical sectors.

References

1. Al-Sabagh, A. M., Yehia, F. Z., Eshaq, G., Rabie, A. M., & ElMetwally, A. E. (2016). Greener route for the recycling of polyethylene terephthalate waste. Egyptian Journal of Petroleum, 25(1), 53–60.
2. Bhatnagar, A., & Sillanpää, M. (2010). Utilization of agro-industrial and municipal waste materials as potential adsorbents for water treatment—A review. Chemical Engineering Journal, 157(2–3), 277–296.
3. Chen, L., & Huang, L. (2022). A review of the progress of waste paper recycling. Resources, Conservation and Recycling, 176, 105917.
4. Crini, G. (2006). Non-conventional low-cost adsorbents for dye removal: A review. Bioresource Technology, 97(9), 1061–1085.
5. Demirbas, A. (2009). Agricultural based activated carbons for the removal of dyes from aqueous solutions: A review. Journal of Hazardous Materials, 167(1–3), 1–9.
6. Foo, K. Y., & Hameed, B. H. (2010). Insights into the modeling of adsorption isotherm systems. Chemical Engineering Journal, 156(1), 2–10.
7. Ganiyu, S. A., & Lateef, S. A. (2021). Review of adsorptive desulfurization process: Overview of the non-carbonaceous materials, mechanism and synthesis strategies. Fuel, 294, 120273.

DESIGN AND EVALUATION OF BIODEGRADABLE POLYASPARTAMIDES FOR OIL/WATER SEPARATION

Bobajanov Sardor, Qandimov Sardor
Aysel Mamadova
Tashkent Chemical Technology Institute
Tashkent, Uzbekistan
Sardorshox438@gmail.com

Abstract - The development of sustainable, high-performance materials for oil/water separation remains a critical challenge. This work presents a novel superhydrophobic, biodegradable foam based on polyaspartamide, a derivative of poly(succinimide) obtained from renewable aspartic acid. A high internal phase emulsion (HIPE) templating technique was employed to create a highly porous structure, followed by in-situ silica deposition and grafting with hexadecyltrimethoxysilane (HDTMS). The resulting material exhibited a water contact angle of ~153°, porosity above 89%, oil absorption capacities of 4.0–5.2 g/g for various oils, and retention of >90% absorption after 10 cycles. Accelerated hydrolysis tests demonstrated a mass loss of ~25% after 72 h at pH 12. The integration of biodegradability, superhydrophobicity, and good mechanical resilience makes this polyaspartamide foam a promising candidate for environmentally conscious oil spill remediation.

Keywords: biodegradable polymer, polyaspartamide, superhydrophobic foam, oil-water separation, HIPE templating

Introduction

Oil spills and industrial oily wastewater pose severe threats to aquatic ecosystems and human health. Conventional separation methods such as gravity settlers, centrifuges, and membranes often suffer from low efficiency, high energy consumption, or fouling problems [Gupta, 2017, 16025–16058]. Advanced porous materials with tailored wettability have emerged as effective alternatives. Among them, superhydrophobic/superoleophilic foams that selectively absorb oil while repelling water have attracted considerable attention. However, most high-performance materials are based on non-degradable polymers (e.g., PTFE, PVDF), which contribute to microplastic pollution after their service life [Andrady, 2011, 1596–1605]. Therefore, there is a strong need for biodegradable separation media that combine environmental sustainability with robust oil-removal performance.

Polyaspartamides are a class of biodegradable polymers derived from poly(succinimide) (PSI), which can be synthesized by thermal polycondensation of aspartic acid – a naturally occurring amino acid. PSI can be easily modified by aminolysis with various amines, allowing the introduction of hydrophobic side chains. This versatility, together with the intrinsic hydrolytic degradability of the amide backbone, makes polyaspartamides attractive for the design of eco-friendly oil-sorbent materials. However, neat polyaspartamide foams typically lack the necessary surface roughness and low surface energy to achieve superhydrophobicity.

In this study, a biodegradable, superhydrophobic porous foam was fabricated through a three-step strategy: (1) synthesis of a long-chain

alkyl-functionalized polyaspartamide prepolymer, (2) formation of a macroporous foam via HIPE templating, and (3) surface engineering by silica deposition and hydrophobic silane grafting. The resulting material was characterized in terms of morphology, wettability, mechanical properties, oil absorption capacity, cyclic stability, and degradation behaviour.

Experimental Part

Synthesis of alkyl-functionalized polyaspartamide.

First, poly(succinimide) (PSI) was prepared by thermal polycondensation of L-aspartic acid at 180 °C under vacuum in the presence of phosphoric acid as catalyst. The obtained PSI (2.0 g, ~20 mmol succinimide units) was dissolved in 30 mL of dimethylformamide (DMF). Octadecylamine (5.36 g, 20 mmol) was added and the mixture was stirred at 60 °C for 12 h to introduce hydrophobic C_{18} chains through ring-opening aminolysis. After cooling, the polymer was precipitated in methanol, filtered, washed, and dried. The product, denoted PAS-C18, contained both octadecyl amide groups and residual succinimide rings available for further crosslinking.

Fabrication of macroporous foam by HIPE templating.

An oil phase was prepared by dissolving PAS-C18 (1.5 g) and the crosslinker ethylene glycol dimethacrylate (EGDMA, 1.0 g) in 2.0 mL of toluene containing the surfactant Span-80 (1.5 g). The aqueous phase consisted of deionized water (90 mL) with potassium persulfate (0.20 g) as initiator and calcium chloride (3.5 g). Under vigorous stirring, the aqueous phase was added dropwise to the oil phase to form a stable high internal phase emulsion. The HIPE was transferred to a mould and polymerized at 65 °C for 24 h. After washing with ethanol/water and drying, a white, highly porous foam (PAS foam) was obtained.

Surface modification.

The PAS foam was immersed in a sol–gel solution containing tetraethyl orthosilicate (TEOS, 30 g), ethanol (80 g), water (12 g), and HCl (0.2 g) for 60 min to deposit a silica layer. The silica-coated foam was then soaked in a solution of hexadecyltrimethoxysilane (HDTMS, 1 g) in ethanol/water (pH 4–5) for 3 h and cured at 60 °C. The final superhydrophobic material is designated H-PAS foam.

Characterization.

Morphology was examined by scanning electron microscopy (SEM). Porosity was measured by mercury intrusion porosimetry. Water contact angles (WCA) were recorded on a contact angle goniometer. Oil absorption capacity was determined gravimetrically. Cyclic performance was evaluated by centrifugation-assisted oil recovery. Degradation was monitored by mass loss in an alkaline buffer (pH 12, 37 °C).

Results and Discussion

The pristine PAS foam displayed a typical polyHIPE architecture with interconnected macropores (average diameter ~30 μm) and smooth struts. After 60 min of TEOS deposition and HDTMS grafting, SEM images revealed

a dense, dendritic silica layer completely covering the polymer skeleton (Figure 1, not shown). Mercury intrusion porosimetry indicated a slight decrease in porosity from 92.5% (PAS foam) to 89.3% for the H-PAS foam, confirming that the silica coating only partially occupied the void space.

The surface modification drastically altered the wettability. The unmodified foam absorbed a water droplet instantly, whereas the H-PAS foam exhibited a static WCA of 153 ± 2°, meeting the criterion for superhydrophobicity. This behavior is attributed to the combination of the microscale roughness created by the silica dendrites and the low surface energy provided by the grafted C_{16} alkyl chains, consistent with the Cassie–Baxter model [Erbil, 2009, 14135–14145].

Oil absorption tests with n-hexane, kerosene, edible oil, and lubricating oil gave capacities of 5.2, 4.9, 4.3, and 4.0 g/g, respectively. The lower absorption for viscous oils is due to slower penetration dynamics, yet all values are comparable to those reported for PCL-based foams. After 10 absorption–desorption cycles, the H-PAS foam retained >90% of its initial capacity for all tested oils, demonstrating excellent reusability.

Compressive stress–strain curves showed that the silica-modified foam exhibited a Young's modulus approximately four times higher than the unmodified counterpart, indicating that the rigid silica shell significantly reinforces the structure. However, the elasticity was partially sacrificed, with a recovery rate of ~55% after 80% compression.

Degradation experiments confirmed the biodegradable nature of the material. Under accelerated conditions (pH 12, 37 °C), the pristine PAS foam lost ~30% of its mass within 72 h. The H-PAS foam showed a marked delay in degradation (~25% mass loss after 72 h) due to the protective hydrophobic coating. After 4 weeks, both materials exhibited extensive fragmentation and mass losses exceeding 70%, indicating that the silica barrier does not permanently prevent bulk hydrolysis.

Recommendations

The results demonstrate that alkyl-functionalized polyaspartamide foams, surface-engineered with silica and HDTMS, are promising biodegradable candidates for oil spill cleanup. Future work should focus on:

- Evaluating the material's performance in emulsified oil/water systems.
- Studying long-term outdoor durability under UV radiation and seawater conditions.
- Investigating the effect of amine chain length on hydrophobicity and degradation kinetics.
- Exploring mechanical crushing of spent foams to accelerate end-of-life degradation.

References:

1. [Andrady, 2011, 1596–1605] Andrady, A.L. Microplastics in the marine environment. *Mar. Pollut. Bull.* 2011, 62, 1596–1605.

2. [Erbil, 2009, 14135–14145] Erbil, H.Y.; Cansoy, C.E. Range of applicability of the Wenzel and Cassie-Baxter equations for superhydrophobic surfaces. *Langmuir* 2009, 25, 14135–14145.
3. [Gupta, 2017, 16025–16058] Gupta, R.K.; Dunderdale, G.J.; England, M.W.; Hozumi, A. Oil/water separation techniques: a review of recent progresses and future directions. *J. Mater. Chem. A* 2017, 5, 16025–16058.
4. [Nakamura, 2020, 115–128] Nakamura, M.; Kuwahara, M.; Higashi, N. Synthesis and biodegradation of polyaspartamide derivatives with long alkyl side chains. *Polym. Degrad. Stab.* 2020, 175, 109128.
5. [Silverstein, 2014, 405–418] Silverstein, M.S. PolyHIPEs: recent advances in emulsion-templated porous polymers. *Prog. Polym. Sci.* 2014, 39, 199–234.
6. [Zhang, 2019, 5445–5479] Zhang, T.; Sanguramath, R.A.; Israel, S.; Silverstein, M.S. Emulsion templating: porous polymers and beyond. *Macromolecules* 2019, 52, 5445–5479.

OBTAINING PRODUCTION OF HIGH-QUALITY DIESEL FUEL BY COMBINING MILD HYDROTREATING AND EXTRACTION WITH IONIC LIQUIDS

[1,2]Sabina Seidova, [1]Minaver Ibrahimova,
[1]Sayara Aliyeva, [1]Khadija Abdullayeva
[1]The Institute of Petrochemical Processes named after acad. Y.H. Mammadaliyev of the Ministry of Science and Education of the Republic of Azerbaijan
[2]Azerbaijan State Oil and Industry University, Baku, Azerbaijan
e-mail: sabina.seidova.ai@mail.ru

Abstract - Ionic liquids are considered promising “green” solvents for the removal of undesirable compounds from petroleum fractions. Particular interest is focused on their application in combined processing schemes integrating hydrotreating and extraction. This study investigates an approach to the production of high-quality diesel fuel involving hydrotreating of diesel distillate under mild conditions followed by extractive post-treatment using ammonium-based ionic liquids—dipropylammonium acetate and dibutylammonium acetate. It is shown that subsequent purification by ionic-liquid extraction enhances the degree of dearomatization and desulfurization of the fuel. Dibutylammonium acetate was found to exhibit higher extraction efficiency, which is associated with the presence of a bulkier cation.
Keywords: diesel fuel, extraction, ionic liquids, dearomatization, desulfurization

Introduction

Modern environmental requirements for the quality of motor fuels necessitate reducing the content of aromatic and sulfur compounds in their composition. The presence of these components in diesel fractions negatively affects both the environmental characteristics of the fuel and its performance properties, including cetane number and storage stability.

Traditionally, the main method for removing sulfur compounds from diesel distillates is hydrotreating. Hydroprocessing ensures the effective removal of mercaptans, sulfides, and a portion of thiophenic compounds; however, deep desulfurization and dearomatization require increased

temperature, pressure, and hydrogen consumption, which leads to higher capital and operating costs.

In this regard, the search for combined technological solutions that allow a deeper degree of purification with more rational use of energy resources and hydrogen has become an important research direction. In this field, active research is being conducted to develop new approaches to the deep purification of diesel fractions (Patent US 6,552,501 B1, 2003).

The effectiveness of the sequential application of hydrotreating and extractive treatment using selective organic solvents such as N-methylpyrrolidone and dimethylformamide has been demonstrate [Шишкин, 2012]. This approach provides efficient removal of polycyclic aromatic hydrocarbons and enables the production of diesel fuel that meets environmental standards.

Along with the use of traditional organic solvents in combined purification schemes, recent years have seen growing interest in the application of ionic liquids as selective extractants. Their high selectivity toward aromatic and sulfur-containing compounds, low volatility, and the possibility of regeneration make them a promising alternative to molecular solvents for the extractive post-treatment of hydrotreated diesel fractions.

Studies have demonstrated the possibility of improving the quality of hydrotreated diesel fuel by extraction using an ionic liquid based on N-methylpyrrolidone and acetic acid. It was established that at an ionic liquid-to-feed ratio of 3:1, a temperature of 60°C, and a contact time of 3 h, the content of aromatic hydrocarbons in the raffinate decreases to 4 wt.%, while the sulfur content is reduced to 153 ppm.

Under milder extraction conditions (20–25°C, ratio 2:1, contact time 1 h), almost complete dearomatization of the feed is achieved, with a residual sulfur content in the raffinate of 130 ppm and a raffinate yield of 88 wt.%.

Experimental part

A hydrotreated diesel fraction with a boiling range of 185–364 °C, containing 16 wt.% aromatic hydrocarbons and 311 ppm sulfur compounds, was used as the feedstock. Preliminary hydrotreating of the initial diesel fraction was carried out at 340 °C, a pressure of 4 MPa, a liquid hourly space velocity of 1 h^{-1}, and a hydrogen consumption of 350 L/L in the presence of an AGKD-400BH catalyst. The obtained hydrotreated product was used as the feed for subsequent ionic-liquid extractive purification.

Extractive purification of the hydrotreated diesel fraction was performed at room temperature in three stages. At each stage, the extractant-to-feed ratio was 1:1 (wt.), and the phase contact time was 1 h. Dipropylammonium acetate and dibutylammonium acetate ionic liquids were used as selective solvents.

It should be noted that in the three-stage extractive purification process, a significant reduction in the content of aromatic and sulfur compounds in the

raffinate is achieved (Figs. 1–4). When dipropylammonium acetate was used, the content of aromatic hydrocarbons decreased to 5 wt.%, and the sulfur content to 395 ppm. In the case of dibutylammonium acetate, the effect was considerably more pronounced: the content of aromatic compounds decreased to 0.5 wt.%, and the sulfur content to 323 ppm. Accordingly, the degree of dearomatization increased from 37.5 to 68.75% and from 56.25 to 96.9%, indicating the higher selectivity of dibutylammonium acetate toward aromatic components.

Figure 1. Dependence of the degree of dearomatization on the number of extraction stages

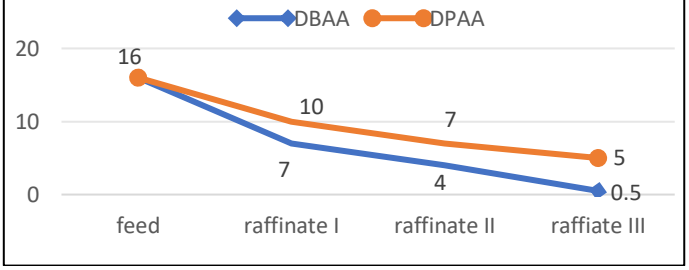


Figure 2. Dependence of the degree of desulfurization on the number of extraction stages

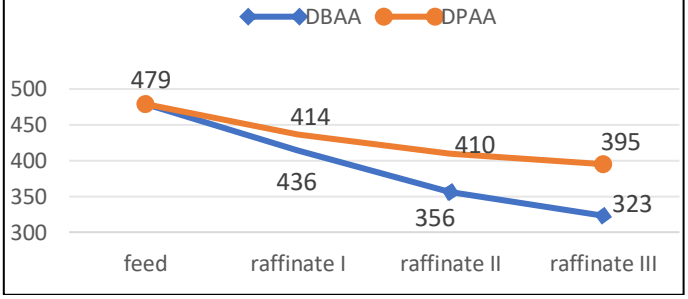
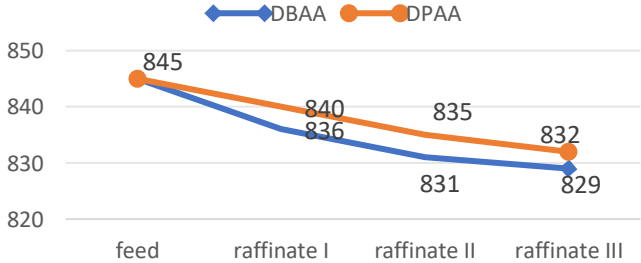
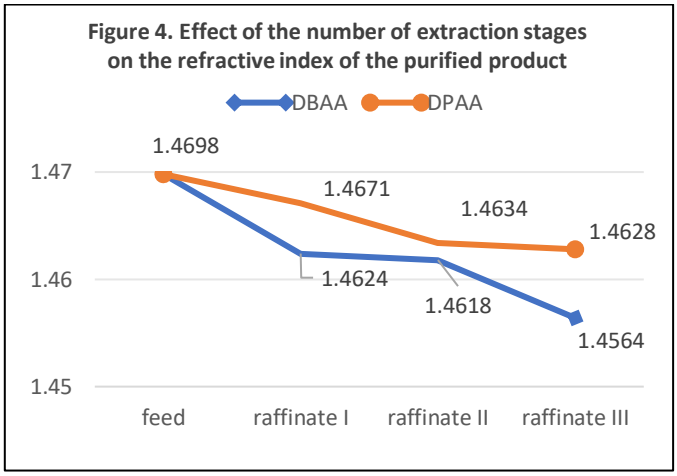


Figure 3. Effect of the number of extraction stages on the density of the purified product





Note: Raffinates I, II, and III are purified products obtained after the first, second, and third extraction stages, respectively

As can be seen from the presented diagrams, an increase in the number of extraction stages leads to a consistent decrease in the content of aromatic and sulfur compounds in the raffinate, which is accompanied by a reduction in the refractive index and density. The obtained dependences confirm the influence of the depth of extractive treatment on changes in the group composition of the diesel fraction.

Conclusion

The obtained results confirm the перспективность of combining hydrotreating and ionic-liquid extraction to improve the quality of the diesel fraction. Further research should focus on the selection of new ionic liquids with higher selectivity toward sulfur-containing compounds and on establishing optimal conditions for their application in order to increase the degree of fuel desulfurization.

References

1. D.D.Whitehurst, M. Brorson, K.G. Knudsen, B.H. Cooper, Combined process for improved hydrotreating of desel fuels.Patent US 6.5521.501 B1, 2003.
2. С.Н.Шишкин , А.А.Гайле, Д.А.Бакаушина, Н.В. Кузичкин, Комбинированный процесс экстракции - гидроочистки дизельных топлив. Международная Научная Конференция «Ресурсосбережение в Химической Технологии», 2012.
3. M.D.Ibragimova, S.A.Seidova, S.G.Aliyeva, G.D.Guseinov, V.M.Abbasov, V.A. Nagiyev, Improvement of quality of the hydropurified diesel fuel by ion-liquid extraction. International Journal of Scientific Engineering and Applied Science (IJSEAS) – Volume-4, Issue-5, May, 2018.

PECTIN-BASED HYDROGEL DERIVED FROM CITRUS PEEL WASTE FOR REMOVAL OF HEAVY METALS AND DYES FROM AGRICULTURAL WASTEWATER

Sabina Gasimova, Lala Mahammadova, Garanfil Ahmadova
Baku Higher Oil School
Baku, Azerbaijan
sabina.gasimova.std@bhos.edu.az
lale.mehemmedova.std@bhos.edu.az
qerenfil.ehmedova@bhos.edu.az

Abstract - Toxic dyes and heavy metals within contaminated water have detrimental impact on environmental safety and humans well-being. Agrochemical processes and industial waste generate wastewater with Pb^{2+}, Cd^{2+}, Cu^{2+} and Ni^{2+} residues along with toxic dyes. Hence, finding the cost-effective and sustainable solution for wastewater treatment is of great interest. Current study focuses on development of biodegradable hydrogels from natural sources to absorb harmful residues and clean water. [4]

The focus of this study is the preparation of a pectin-based hydrogel from citrus peels as an environmentally friendly and low-cost absorbent for cleaning up agricultural waste. Pectin is exctracted in acidic environment at relatively high temperature condition. Demethylation reaction is conducted with alkaline method to ensure better gelation. The obtained pectin undergoes Ca^{2+} cross-linking process to form hydrogel, by enhancing its structural stability and improving its capability to adsorb heavy metals and dyes in wastewater. To evaluate the effectiveness of the hydrogel for removing metal residues and dye contaminants, experimentation is conducted with different pH levels, applied temperatures, and type of citrus.

The results shows that the pectin-derived hydrogel can adsorb both contaminants effectively. After completing the optimization studies, the best operating parameters to adsorb maximum of the contaminants are determined. Optimal pH levels for each stages of hydrogel production are found. The desirable temperature condition for highest yield is 85 Cº for extraction.

The findings indicate that citrus peel–derived pectin hydrogel presents a promising, sustainable, and biodegradable solution for agricultural wastewater treatment, contributing to waste valorization and environmental protection.

Key words: pectin-based hydrogel, citrus peel waste, agricultural wastewater treatment, heavy metal removal, dye adsorption, biodegradability.

Introduction

The growth of agricultural activities and the excessive use of fertilizers, pesticides, and agrochemicals are considered to be important factors for the contamination of water resources. The effluent of agricultural water usually contains heavy metals and synthetic dyes. The accumulation of these pollutants in the soil and aquatic environment poses a great threat to the environment and human health. The pollutants like Cd^{2+}, Pb^{2+},Cu^{2+}, Ni^{2+} ions and dye are commonly found in agricultural water due to their excessive use. Conventional wastewater treatment methods, including chemical precipitation, membrane filtration, and ion exchange, are often associated with high operational costs, secondary pollution, and limited biodegradability. Therefore, it has been considered important to find proper solutions for the

removal of these pollutants. In recent years, much attention has been given to the use of low-cost and eco-friendly adsorbents for the elimination of pollutants. The use of hydrogels prepared from natural polymers has been found to be promising for the extraction of pollutants due to their porous structure and good water absorbability.

Pectin, which is obtained from citrus fruit waste, has been considered to be a good adsorbent for the adsorption of pollutants like heavy metal ions and dye. In this regard, pectin was extracted from lemon, mandarin, and orange fruit waste. The extracted pectin was precipitated with ethanol to improve its purity. The degree of esterification was reduced by using alkaline solutions to improve the functional group sites for adsorption. Finally, calcium ions (Ca^{2+}) were used to improve the structure of the prepared hydrogel. The prepared hydrogel was used for the removal of pollutants like metal ions and dye from agricultural water. The prepared material has been found to be stable and value-added for the removal of pollutants.

Experimental details

Pectin Extraction from Citrus Peels:

Pectin is obtained by acid extraction and ethanol precipitation method. First step includes citrus peel dispersion in 300ml of distilled water under continuous stirring until homogenous solution is obtained (fig1). Followed by, 180ml nitric acid solution with 0.05M concentration is prepared. pH of the acid solution is raised to 2 by adding 7ml of 1M NaOH. The nitric acid solution was added to a homogeneous suspension of citrus peel powder and stirred at 80°C for 90 minutes. Due to acid hydrolysis, insoluble protopectin is converted into soluble pectin.



Figure 5. *Pectin extraction reaction*

After pectin extraction process was complete, the solution was cooled to room temperature and centrifuged to remove solid residue. Pectin is precipitated by adding 95% ethanol twice as large in volume as supernatant (fig5). The mixture is allowed to stand for one hour at room temperature, and

pectin precipitate accumulates at the surface of the solution, following which precipitate is collected using filter paper. To get rid of sugar, salt and other contaminants or lingering nitric acid, the pectin was rinsed with 95 percent ethanol two to three times (fig2). After being washed, the pectin is air dried in an oven at 40˚C. The product is grinded to obtain pectin powder.[1]

Demethylation of High-Methoxyl Pectin (Preparation of Low-Methoxyl Pectin):

The next step includes alkaline demethylation of high-methoxyl (HM) pectin to low-methoxyl (LM) pectin. To begin with, 0.6g of dried HM pectin was mixed with 30mL of distilled water while stirring constantly to form a homogeneous mixture. A 1M solution of NaOH is added to the mixture dropwise until pH is adjusted to a point between 10 and 11 to initiate the alkaline demethylation reaction. To avoid the breakdown of pectin, the demethylation reaction was carried out at a low temperature of around 5°C using ice water bath, and the mixture was stirred constantly for 3 hours. The pH was periodically checked and adjusted if necessary to ensure that the alkaline conditions were maintained. Once the demethylation reaction was finished, the reaction was stopped by adding a diluted acid solution until the pH was reduced to a point around 3 to stop the hydrolysis reaction. For extraction of LM pectin from solution, twice as much 95% ethanol solution was added to initiate the precipitation. The mixture was allowed to stand until a precipitate of the LM pectin formed. The precipitated LM pectin was filtered and washed with 95% ethanol solution 2 or 3 times to remove residues. The precipitate was then filtered and air dried at 40 degrees Celsius to obtain a dry powder. The resultant powder was stored as low-methoxyl pectin for future hydrogel production.[3]



Figure 31. Low-methoxyl pectin

Preparation of Ca^{2+}-Crosslinked Pectin Hydrogels:

To form hydrogels Calcium ions are introduced as cross-linking agent. Previously obtained 0.56g of LM pectin is added to 18.7ml of water by stirring and heating to 60 °C until fully dissolved (about 30-60min). At the same time, 0.2 M calcium chloride bath is prepared. After being cooled to room temperature, the pectin solution is filled into syringe and dropped from a height of about 10-15 cm into the calcium chloride bath to form spherical hydrogel beads through immediate ionic cross-linking. The beads were

allowed to remain in the calcium chloride solution for 30 minutes to cure and form gel. The beads were filtered and thoroughly rinsed with distilled water to remove any excess calcium (fig6). Produced hydrogels can be used immediately or dried to constant weight for longer storage. Dried hydrogel beads are immersed in distilled water until full adsorption prior to being used. [2]

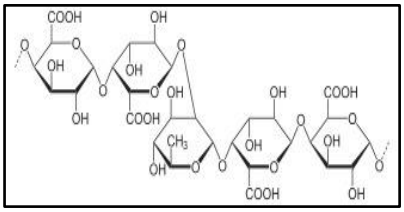


Figure 3. Structure of pectin

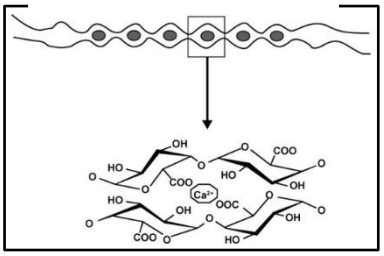


Figure 4. Egg-box model of Ca^{2+}-crosslinking



Figure 5. Precipitation of pectin

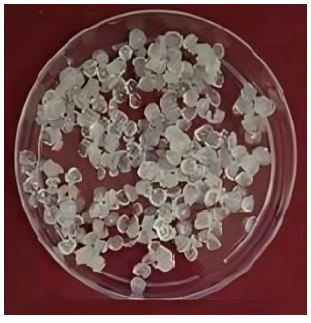


Figure 6. Hydrogel

Result and discussion

From 6g of raw citrus peel powder 0.6 g of pectin is extracted with 10% yield. Initially obtained pectin with higher esterification degree fails to form stable spherical gels. As a result, demethylation reaction is conducted to lower number of methoxyl groups and prepare pectin to gelation. Degree of esterification is successfully lowered using alkaline method. Due to demethylation reaction, pectin is able to form stable gels that retains structural integrity in aqueous environments. Structure and elasticity of hydrogels depend on $CaCl_2$ concentration as well. Lower salt concentrations result in hydrogels that barely keep spherical shape, whilst that produced at higher concentrations were more elastic and maintained spherical structure. The optimal concentration was determined to be 0.2M.

pH and T are another property affecting hydrogel properties. Each stage has optimum T and pH conditions to maximize yield and adsorption ability. During pectin extraction it is important to keep acidic environment and T below 90°C as otherwise polymer chains can degrade. Alkaline demethylation requires basic environment, but pH higher than 11 results in de-polymerization. Regarding cross-linking, slightly acidic or neutral environment is optimal for stable hydrogels with maximum water uptake.

Preliminary tests on the adsorption ability of the hydrogel indicated that they are effective in capturing heavy metal ions and cationic dyes from aqueous solutions. In a laboratory setting, 22g/g swelling capacity is obtained, which is slightly lower than hydrogel produced under optimized conditions (30-40g/g). This is an indication of their potential use in water purification systems in an environmentally friendly manner. It is clear that pectin extracted from citrus peels has potential in forming hydrogels that are useful in environmental protection.

Recommendations:

With the increasing rate of contamination of agricultural effluents with heavy metals and dyes, there is a need for the development of sustainable and biodegradable adsorbents. The Ca^{2+} cross-linked pectin hydrogels synthesized from citrus peels, as synthesized in this study, have considerable promise for application in wastewater treatment systems as cost-effective and eco-friendly adsorbents. However, more studies are needed to improve hydrogels mechanical properties and stability, especially in extreme pH conditions for better results. This could be achieved using polymer blends and double-cross-linking approaches. The number of active adsorption sites could also be improved using chemical modification approaches.

Another factor to be considered for future studies is the production of hydrogel synthesis in an industrial level. Considering that the synthesis of hydrogels in bead form could be more feasible for scaling up in wastewater treatment systems, future work should emphasize focus on process

optimization and performance evaluation. Besides wastewater treatment systems, citrus pectin hydrogels could be of great utility for other applications, including controlled-release agricultural formulations, soil conditioners, and medicinal purposes such as wound healing and drug delivery systems.

References:

[1] Abdel Hamid, E. M., Moawad, A., Hassan, H., Ragaa, M., AbdEl-Kader, M., Farid, M., Hamed, M., Essam, N., & Rady, A. (2022). Production and characterization of pectin by acid extraction method from orange peels waste using response surface methodology (RSM). *International Journal of Industry and Sustainable Development, 3*(1), 34–45. https://ijisd.journals.ekb.eg

[2] Tran Vo, T. M., Kobayashi, T., & Potiyaraj, P. (2022). Viscoelastic analysis of pectin hydrogels regenerated from citrus pomelo waste by gelling effects of calcium ion crosslinking at different pHs. *Gels, 8*(12), 814. https://doi.org/10.3390/gels8120814

[3] Alemzadeh, I., Saifkordi, A. A., Kahforooshan, D., & Nahid, P. (2005). Production of low ester LM pectin by deesterification of high ester HM apple pectin. *Scientia Iranica, 12*(3), 309–316.

[4] Vigneswararajah, V., Thavarajah, N., & Fernando, X. (2025). Synthesis of pectin hydrogels from grapefruit peel for the adsorption of heavy metals from water. *Technologies, 13*(9), 403. https://doi.org/10.3390/technologies13090403

BİODİZELİN ALINMASINDA YENİ YAŞIL KATALİZATOR

[1]Fərid Quliyev, [1]Ofelya Cavadova, [2]Azər Əmirov, [1]İbrahim Məmmədov
[1]Bakı Dövlət Universiteti
[2]Geologiya və Geofizika İnstitutu
Bakı, Azərbaycan
feridquluzade256@gmail.com

Xülasə - Təqdim edilən işdə şəkərin turş mühitində karbonlaşdırılması nəticəsində alınmış karbon matrisi və yumurta qabığından əldə olunmuş CaO əsasında heterogen yaşıl katalizator hazırlanmışdır. Hazırlanmış katalizator günəbaxan yağının metanol ilə transefirləşmə reaksiyasında sınaqdan keçirilmişdir. Optimal şəraitdə (yağ:metanol = 1:6 mol nisbəti, 55–60°C, 12 saat) 87% çıxımla biodizel əldə olunmuşdur. Katalizator reaksiya mühitindən asanlıqla ayrılmış və təkrar istifadə qabiliyyəti nümayiş etdirmişdir. Nəticələr göstərir ki, karbon–CaO əsaslı kompozit sistem ekoloji və iqtisadi baxımdan perspektivli alternativ hesab oluna bilər.

Açar sözlər: yaşıl katalizator, heterogen kataliz, biodizel, CaO, aktiv karbon

Giriş

Qlobal enerji tələbatının artması və ənənəvi yanacaqların istifadəsi zamanı atmosferə atılan istixana qazlarının miqdarının yüksəlməsi alternativ və bərpa olunan enerji mənbələrinin inkişafını zəruri etmişdir [1]. Biodizel bitki və ya heyvan mənşəli yağların aşağı molekullu spirtlərlə katalitik transefirləşməsi nəticəsində alınan, bioloji parçalana bilən və daha aşağı emissiya göstəricilərinə malik alternativ yanacaq növüdür [2].

Sənaye miqyasında biodizel əsasən homogen qələvi katalizatorların iştirakı ilə sintez olunur. Lakin bu üsul sabunlaşma reaksiyası, katalizatorun reaksiya mühitindən ayrılmasının çətinliyi və tullantı suların əmələ gəlməsi kimi texnoloji, eləcə də ekoloji problemlərlə xarakterizə olunur [4]. Bu səbəbdən son illərdə heterogen katalizator sistemlərinə maraq artmışdır.

Xüsusilə CaO əsaslı heterogen katalizatorlar yüksək əsaslıq, aşağı maya dəyəri və təkrar istifadə oluna bilmə xüsusiyyətlərinə görə perspektivli hesab olunur [3]. Tullantı mənşəli xammaldan alınan CaO materialları yaşıl kimya prinsiplərinə uyğun alternativ kimi qiymətləndirilir və biodizel sintezində effektiv nəticələr göstərir [4].

Bu baxımdan karbon əsaslı daşıyıcı üzərində dispersləşdirilmiş CaO kompozit katalizatorlarının tətbiqi həm katalitik aktivliyin artırılması, həm də ekoloji baxımdan davamlı texnologiyanın formalaşdırılması üçün aktual istiqamət hesab olunur.

Eksperimental hissə

Karbonun alınması.

Qatı sulfat turşusunun iştirakı ilə şəkər karbonlaşdırılmışdır. Alınmış karbon su ilə yuyularaq neytral mühitə qədər təmizlənmiş, 110°C-də qurudulmuş və aktivləşdirilmişdir.

CaO-in alınması.

Yumurta qabığı əvvəlcə yuyulmuş, qurudulmuş və sonra 900°C temperaturda kalsinasiya edilərək CaO alınmışdır.

Katalizatorun hazırlanması.

CaO və karbon su mühitində homogen qarışdırılmışdır. Qarışıq əvvəlcə 110°C-də qurudulmuş, daha sonra daha yüksək termiki emala məruz qoyulmuşdur. Nəticədə karbon matrisi üzərində dispersləşmiş CaO əsaslı heterogen katalizator əldə edilmişdir.

Transefirləşmə prosesi.

Reaksiya hazırlanmış katalizator iştirakı ilə, günəbaxan yağı və metanolun 1:6 mol nisbətində qarışığında aparılmışdır. Proses 55–60°C temperaturda 12 saat ərzində davam etdirilmişdir. Reaksiya sonunda katalizator süzmə üsulu ilə ayrılmış, yuyulmuş və qurudularaq təkrar istifadəyə hazırlanmışdır.

Nəticələr və müzakirə

Aparılmış eksperimental tədqiqatlar optimal reaksiya şəraitində 87% biodizel çıxımı əldə edilməsini göstərmişdir. Alınmış nəticə karbon–CaO kompozit katalizatorunun kifayət qədər yüksək əsaslıq xüsusiyyətinə və aktiv mərkəzlərin effektiv paylanmasına malik olduğunu göstərir. Karbon daşıyıcının mövcudluğu CaO hissəciklərinin dispersliyini yaxşılaşdıraraq reaksiya səthini artırmış və transefirləşmə prosesinin intensivliyinə müsbət təsir göstərmişdir.

Homogen qələvi katalizatorlarla müqayisədə hazırlanmış heterogen sistem bir sıra texnoloji üstünlüklər nümayiş etdirmişdir. Belə ki, katalizator reaksiya mühitindən sadə süzmə yolu ilə asanlıqla ayrılmış, əlavə neytrallaş-

dırma mərhələsinə ehtiyac yaranmamış və bununla da tullantı suyun əmələ gəlməsi minimuma endirilmişdir. Eyni zamanda katalizatorun qurudularaq yenidən prosesə qaytarılması onun təkrar istifadə potensialını təsdiqləmişdir ki, bu da iqtisadi və ekoloji baxımdan mühüm göstəricidir.

Təkrar istifadə zamanı biodizel çıxımında müəyyən azalma müşahidə olunmuşdur. Bu aktiv mərkəzlərin qismən passivləşməsi, kalsium tərkibli fazanın səthində karbonatlaşma prosesinin baş verməsi və ya reaksiya məhsullarının səthdə adsorbsiyası ilə izah oluna bilər. Bununla belə, əldə olunan nəticələr karbon–kalsium əsaslı kompozit sistemin sabitlik və effektivlik baxımından perspektivli olduğunu və biodizelin heterogen katalitik sintezi üçün alternativ sistem kimi qiymətləndirilə biləcəyini göstərir.

Təkliflər

Alınmış nəticələr göstərir ki, karbon əsaslı katalizatorun tətbiqi biodizel istehsal prosesinin texnoloji səmərəliyinin yüksəldilməsi və ekoloji dayanıqlılığın təmin edilməsi baxımından perspektivli istiqamət kimi tövsiyə oluna bilər.

İstinad

1. [Atabani A.E., Silitonga A.S., Ong H.C., Mahlia T.M.I., Masjuki H.H., Badruddin I.A. (2019). Recent progress in biodiesel production technologies and feedstocks. *Renewable and Sustainable Energy Reviews*, 110, 234–247]
2. [Mofijur M., Rasul M.G., Hyde J., Bhuiya M.M.K. (2020). Role of biodiesel blending on engine performance and emissions: A review. *Energy Reports*, 6, 172–191]
3. [Malhotra R., Ali A. (2021). CaO-based heterogeneous catalysts for biodiesel production: A review. *Renewable Energy*, 163, 652–671]
4. [Tan Y.H., Abdullah M.O., Nolasco-Hipolito C., Taufiq-Yap Y.H. (2019). Waste ostrich- and chicken-eggshells as heterogeneous base catalyst for biodiesel production. *Energy Conversion and Management*, 195, 1113–1124]

MODERNIZATION OF OIL REFINING PROCESSES FOR PRODUCING HIGH-OCTANE GASOLINE

Turakulova Marjona[1]
Associate Professor,
Panoev Erali[2]
Associate Professor,
Bukhara State Technical University[1], Bukhara. Uzbekistan.
E-mail: marjonaturakulova79@gmail.com

Abstract - This article examines the efficiency of catalytic reforming and isomerization processes in increasing the octane number of gasoline. As a result of isomerization carried out using a $Pt/WO_3/ZrO_2$ catalyst, the proportion of isoparaffins in the C4–C6 fractions increased, which raised the octane number from 68 to 90. During the catalytic reforming process based on a $Pt–Sn/Al_2O_3$ catalyst, the formation of aromatic hydrocarbons increased the octane number to 96. The obtained results demonstrate the environmental safety of

isomerization and the advantage of reforming in producing high-octane products, as well as confirming the effectiveness of the combined application of these processes for the production of high-quality gasoline.

Keywords: gasoline, octane number, isomerization, $Pt/WO_3/ZrO_2$, reforming, $Pt–Sn/Al_2O_3$, catalyst, pentane, hexane, isoparaffin, catalytic process, oil, fuel.

Introduction

At present, improving the quality of motor fuels is one of the most important tasks in the oil refining industry. In particular, issues related to increasing the octane number of gasoline, ensuring its stable combustion in the engine, and producing environmentally compliant products are highly relevant. From this perspective, catalytic reforming and isomerization processes play a crucial role in improving gasoline components. These processes are aimed at the deep processing of petroleum fractions and make it possible to obtain high-quality motor fuels. Catalytic reforming is primarily aimed at converting low-octane naphtha fractions into high-octane aromatic hydrocarbons. During this process, normal paraffins and naphthenes, at high temperatures and in the presence of special catalysts, undergo reactions such as dehydrogenation, dehydrocyclization, and isomerization. As a result, the octane number of gasoline increases significantly, and reformate rich in aromatic hydrocarbons is obtained. In addition, a significant amount of hydrogen is released during catalytic reforming, which is used as a valuable feedstock in other hydroprocessing operations [1].

The isomerization process is mainly focused on converting normal paraffins in the C4–C6 range into their isomers. In this process, the molecular composition of hydrocarbons does not change; only their structure is rearranged. As a result, n-paraffins are converted into iso-paraffins with higher octane numbers. The main advantage of isomerization is that aromatic hydrocarbons are not formed, and an environmentally cleaner gasoline component is produced.

The relevance of these two processes is closely related to modern environmental and technological requirements. Currently, many countries are strengthening regulations to limit the content of aromatic hydrocarbons. In this regard, the isomerization process is gaining increasing importance in the production of environmentally clean fuels. At the same time, catalytic reforming, in addition to producing high-octane gasoline, contributes to improving the overall efficiency of the oil refining complex [2].

From the standpoint of efficiency, catalytic reforming ensures the production of a high-octane product and hydrogen, whereas the isomerization process is characterized by low energy consumption and environmental safety. The integrated application of these processes enables oil refineries to produce high-quality gasoline that is competitive and compliant with environmental standards.

Exsperimental Section.

The catalytic isomerization process is intended for the production of high-octane gasoline components, as well as feedstock for the petrochemical industry. The feedstock used in this process includes n-butane, light straight-run fractions with an initial boiling point of 52 °C, catalytic reforming raffinates such as n-pentane and n-hexane, as well as their mixtures obtained during gas fractionation [2].

The present study was carried out using a combination of theoretical and experimental methods. The main objects of the study were a light gasoline fraction C_5–C_6 obtained during primary oil refining, as well as a naphthenic–paraffinic heavy gasoline fraction.

The characteristics of a number of highly efficient catalysts used in the isomerization process are presented in Table 1.

Table 1. Highly efficient catalysts for the isomerization process

Catalyst Type	Octane Number Increase	Conversion at Low Temperature and Pressure	Isomerization Selectivity	Notes
Zeolites (ZSM-5)	Good (C5–C6 isomers)	Medium (sometimes higher temperature required)	High	Low cost, but a slight increase in temperature is required
SO_4^{2-}/ZrO_2 (Sulfated zirconia)	High	Medium	High	Acid-active, but conversion is lower due to the absence of a metal component
Metal-supported zeolites	High	Effective at low temperature and pressure	Very high	Bifunctional catalysts: combination of isomerization and hydroisomerization
$Pt/WO_3/ZrO_2$	Very high	Low temperature (180–220 °C) and low pressure	Very high	Optimal for industrial isomerization of C4–C6 fractions

The isomerization process was studied under laboratory conditions using a $Pt/WO_3/ZrO_2$ catalyst. The efficiency of the process was evaluated by determining the composition of the feedstock and the product using gas chromatography. For the samples taken before and after isomerization, the octane number was determined using the standard motor method, followed by an analysis of the changes.

Research methodology of the catalytic reforming process

The reforming process was carried out using a $Pt–Sn/Al_2O_3$ catalyst. The process conditions were set as follows:

Table 2. Comparison of industrial catalysts for catalytic reforming

No.	Catalyst Type	Effect on Octane Number	Advantages	Disadvantages
1	Pt/Al_2O_3	+20–25	Cheaper, simple technology	Low stability, high coke formation
2	$Pt–Re/Al_2O_3$	+25–30	High selectivity, resistant to coke formation	Rhenium (Re) is expensive
3	$Pt–Sn/Al_2O_3$	+25–30	High stability, good yield of aromatic compounds	Requires strict control of Sn content
4	$Pt–Re–Sn/Al_2O_3$	+30–35	Very high activity and long service life	Very expensive
5	$Pt–Sn/Al_2O_3$	+22–28	Efficient and economically advantageous	Moderate increase in octane number

The content of aromatic hydrocarbons, isoparaffins, and gaseous products in the obtained samples was determined using chromatography, after which their relationship with the increase in octane number was evaluated.

Methods of results analysis. The obtained experimental data were subjected to comparative and statistical analysis, which made it possible to determine the relative effectiveness of the isomerization and reforming processes in increasing the octane number. In addition, energy consumption indicators, environmental characteristics, and the potential for industrial application of the processes were evaluated [3].

The operating conditions of the isomerization process may vary within different ranges depending on the catalysts used.

As a result of isomerization, an increase in the proportion of isoparaffins in the C_5–C_6 fractions and a decrease in the content of normal paraffins were observed, which significantly improved the knock resistance of gasoline.

Table 3. Change in octane number during the isomerization process

Parameters	Before Isomerization	After Isomerization
n-Paraffins, %	62.4	28.7
Isoparaffins, %	22.1	58.9
Aromatic compounds, %	5.3	6.1
Octane number	68	90

It can be seen from the table that after the isomerization process, the proportion of isoparaffins increased by almost 2.7 times, and the octane number increased by 22 units. The practically unchanged content of aromatic hydrocarbons indicates the environmental advantage of the process.

Result and Discussion.

The study found that during isomerization in the temperature range of 120–180 °C, an increase in temperature is accompanied by an increase in the octane number. The optimal temperature was observed in the range of

160–170 °C; at higher temperatures, stabilization of the octane number occurs due to side reactions.

As a result of the reforming process, the content of aromatic hydrocarbons increased significantly, and the octane number of gasoline reached high values [4].

Table 4. Results of the catalytic reforming process

Indicators	Before Reforming	After Reforming
Paraffins, %	48,6	22,4
Naphthenes, %	31,2	12,1
Aromatic compounds, %	18,4	58,7
Octane number	72	96

The reforming process increased the amount of aromatic hydrocarbons by more than three times, raising the octane number to 96. However, the high proportion of aromatics is an important factor from the standpoint of environmental limitations [5]. The indicators of the isomerization and reforming processes for increasing the octane number of gasoline are presented in Table 5.

Table 5. Results of the Analysis of Isomerization and Reforming Processes

Indicators	Isomerization	Reforming
Increase in octane number	+20–25	+25–30
Formation of aromatic compounds	Very low	High
Energy consumption	Low	High
Environmental safety	High |	Medium
Industrial application	Light gasoline	Heavy gasoline

Conclusion and recommendations. The comparative analysis showed that the isomerization process is characterized by low energy consumption, high environmental safety, and suitability for processing light gasoline fractions [6]. Catalytic reforming, in turn, offers an advantage in producing high-octane products and hydrogen from heavy gasoline fractions. Thus, the combined application of these processes is the most effective approach to ensuring the production of high-quality gasoline that meets environmental requirements and remains competitive in the market.

References

1. Chekantsev N.V., Kravtsov A.V., Ivanchina E.D., Gyngazova M.S. Mathematical modeling of pentane-hexane fraction isomerization process on Si-2 catalys // XVIII International Conference on Chemical Reactors Chemreactor-18 Malta September 29 - October 3, 2008, c 305-306.
2. Гуреев А. А. Каталитический риформинг бензинов. - М.: Недра, 2016. – 368 с.
3. Маликов И.Д. Каталитическая изомеризация углеводородов в присутствии носителей, модифицированных ионными жидкостями: дис. канд. техн. наук: 05.17.07: защищена 05.07.17 / И.Д. Маликов. - Астрахань, 2011. - 142 с.

4. Gary J. H., Handwerk G. E., Kaiser M. J. Petroleum Refining: Technology and Economics. - New York: CRC Press, 2020. - 480 p.
5. L.E. Saidov, M.Q. Туракулова, S.Yu. Бегутянова. *Исследование процесса изомеризации для повышения октанового числа бензина.* Development of Science, январь 2026, №1, том 3, стр. 355–360.
6. Patent: RU 2277526 C1.
7. Patent: RU 2 748 268 C1.
8. Patent: US3929683A.

ECOLOGIK TRANSFORMATION OF THE OIL AND INDUSTRY IN THE CONTEXT OF THE GLOBAL CLIMATE AGENDA

Zoirova Aziza Irgashevna
Bukhara State Technical University
Bukhara, Uzbekistan
aziza.z.1991@mail.ru

Abstract: This paper examines the theoretical and applied aspects of the ecological transformation of the oil and gas industry in the context of implementing the global climate agenda established by the United Nations and enshrined in the Paris Agreement. The study analyzes decarbonization pathways, including reducing the carbon intensity of hydrocarbon extraction and processing, implementing low-carbon technological solutions, developing carbon capture and storage (CCS), minimizing methane emissions, and digitalizing production processes. Results of computational and analytical modeling of CO_2 and CH_4 emission reductions at a typical oil and gas facility are presented. Conclusions and recommendations are formulated for the comprehensive ecological modernization of the industry within the framework of sustainable development.

Keywords: decarbonization, carbon footprint, methane emissions, climate agenda, sustainable development, energy transition, carbon capture and storage, ecological modernization.

Introduction

Global climate change is becoming a key factor in transforming the world's energy sector. The formation of international climate policy under the United Nations and the adoption of the Paris Agreement have set a strategic goal of limiting the increase in global average temperature to well below 2 °C above pre-industrial levels.

The oil and gas industry, as one of the largest sources of greenhouse gas emissions, remains a cornerstone of the global energy system. According to international analytical agencies, the share of direct and indirect emissions associated with the extraction, transportation, and processing of oil and gas accounts for a significant portion of total energy-related CO_2 and CH_4 emissions. (e.g.[Bains P.S. 2020 pp. 133])

Ecological transformation of the industry implies a shift from an extensive resource-use model to an integrated low-carbon strategy, which includes:

1. Increasing energy efficiency;
2. Reducing flaring;
3. Controlling and eliminating methane leaks;
4. Implementing carbon capture and storage (CCS) technologies;
5. Developing hydrogen and renewable energy directions;
6. Digitalizing emissions monitoring.

The aim of this study is to conduct a comprehensive analysis of ecological transformation pathways in the oil and gas industry and evaluate their effectiveness based on experimental modeling.

The carbon footprint of oil and gas products is categorized into three scopes:

1. **Scope 1** — direct emissions from fuel combustion and technological processes;
2. **Scope 2** — indirect emissions from electricity consumption;
3. **Scope 3** — emissions from the use of the final product (the most significant share).

Methane has a high global warming potential, and in the short term, its impact exceeds CO_2 by more than 80 times. Therefore, controlling leaks and reducing flaring are priority areas.

Increasing energy efficiency involves optimizing heat exchange networks, implementing heat recovery, modernizing compressor units, and applying high-efficiency catalytic systems. Energy efficiency improvements reduce emissions by 10–20% without major restructuring of the production cycle.

Controlling and reducing methane emissions includes LDAR (Leak Detection and Repair) systems, satellite monitoring, replacing pneumatic equipment, and sealing storage tanks.

A promising direction is the production of “blue” hydrogen with CO_2 capture and “green” hydrogen based on renewable energy sources. (e.g.[Peters, G.P. 2020 pp. 11])

Experimental Section

The purpose of the experimental study is to assess the effectiveness of ecological measures and technologies implemented in the oil and gas industry in reducing greenhouse gas emissions, minimizing environmental impact, and adapting to the global climate agenda.

Object of study: A typical integrated oil and gas complex with the following characteristics:

1. Production capacity: 6 million t of oil equivalent/year
2. Energy consumption: 12 PJ/year
3. Initial CO_2 emissions: 2.1 million t/year
4. Methane emissions: 52 thousand t/year

Research methods:

1. Chemical-analytical methods – measuring the content of pollutants (hydrocarbons, sulfur compounds, heavy metals) in air, water, and soil;
2. Energy audit and emissions assessment – using balance calculations and specialized sensor systems for monitoring CO_2 and CH_4;
3. Comparative technology analysis – testing traditional oil and gas production and processing methods against environmentally friendly technologies: carbon capture and storage (CCS), bioremediation of contaminated soils and waters, implementation of flare-free gas combustion systems;
4. Modeling and forecasting – using computer simulations to evaluate the long-term impact of different technological solutions on environmental conditions and climate balance.

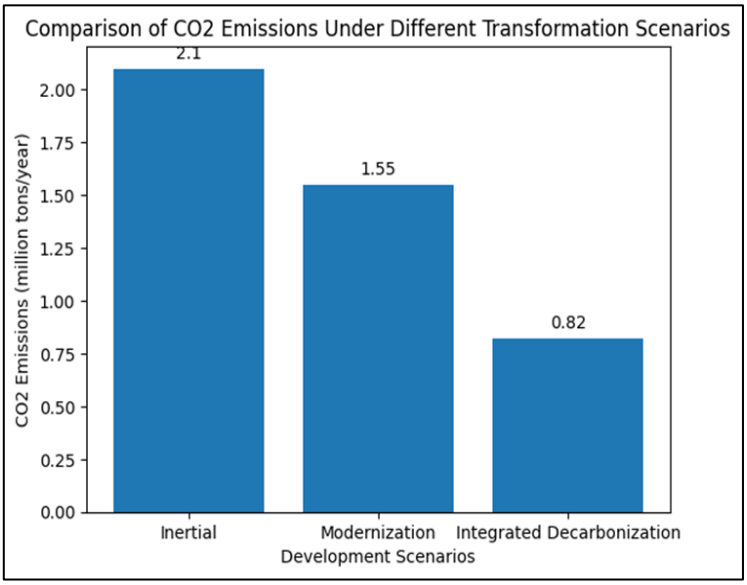


Figure 1. Comparison of CO_2 emissions under different transformation scenarios

From the graph, it is evident that under the inertial scenario, emissions remain at 2.1 million t/year, infrastructure modernization reduces emissions to 1.55 million t/year, and comprehensive integrated decarbonization achieves the maximum reduction to 0.82 million t/year. This clearly demonstrates the effectiveness of implementing comprehensive ecological measures and technologies in reducing the greenhouse footprint of the oil and gas industry. (e.g.[Rogelj J. 2016 pp. 631-639, Rogelj J. 2021 pp. 123-145])

Discussion of Results

CO_2 Emissions Dynamics (Table 1)

Scenario	CO_2 Emissions, mln t/year	Reduction
Inertial	2.1	–
Modernization	1.55	26%
Comprehensive	0.82	61%

Methane emissions decreased by 75% with the implementation of leak detection systems, with the climate effect equivalent to reducing 1.4 million t CO_2-eq/year. Specific energy consumption was also reduced by 18%.

Economic assessment:

1. Capital investment: ~480 million monetary units
2. Payback period: 7 years
3. Internal rate of return: 14–17%

The ecological transformation of the oil and gas industry demonstrates a systemic nature. It affects the technological structure of production, investment policy, corporate governance, and international trade mechanisms (including carbon regulation). (e.g.[Gielen, D. 2019 pp. 44, Hepburn C. pp. 106-114])

Digitalization is particularly important: the use of sensor systems, artificial intelligence, and predictive analytics enhances emissions transparency and minimizes hydrocarbon losses. Transformation also reduces regulatory risks associated with cross-border carbon regulations and stricter climate reporting requirements.

Conclusions and Recommendations

The analysis of the ecological transformation of the oil and gas industry in the context of the global climate agenda, institutionally enshrined under the United Nations and the Paris Agreement, allows formulating comprehensive scientific and practical conclusions and strategic recommendations:

1. Ecological transformation of the oil and gas industry is an objective long-term trend driven by the need to achieve climate neutrality and reduce anthropogenic environmental impact. Ignoring this trend increases regulatory, investment, and reputational risks.
2. The most significant contribution to reducing climate impact comes from a comprehensive approach, including energy efficiency improvements, systematic control and elimination of methane leaks, reduction of flaring, and implementation of CCS technologies. Partial measures provide limited effect, whereas integrated decarbonization can reduce total emissions by over 60%.
3. Methane emissions are a priority area for short-term climate impact. Implementing LDAR systems, digital monitoring, and sealing technological units provides substantial environmental benefits with relatively low capital costs and short payback periods. Therefore, methane regulation and control should become a mandatory element of industry environmental policy.
4. Carbon capture and storage technologies are a strategic tool for deep decarbonization, especially for processes with unavoidable CO_2 emissions. Despite high capital costs, their implementation is justified with government support, tax incentives, and stable carbon markets.

5. Digitalization of production processes — implementing intelligent sensor systems, predictive analytics, and automated environmental monitoring — is a key factor in increasing emissions transparency and the effectiveness of environmental measures. Integration of digital emission monitoring platforms into production management is recommended.
6. Ecological modernization should be accompanied by institutional measures development of national and industry decarbonization strategies, implementation of carbon regulation mechanisms, harmonization of environmental reporting with international standards, development of research programs in low-carbon technologies.
7. In the long term, the sustainability of the oil and gas industry will depend on its ability to diversify activities, including hydrogen technologies, integrating renewable energy sources, and adopting circular economy principles.

Thus, ecological transformation of the oil and gas industry should be viewed not as a limitation, but as a strategic tool to enhance competitiveness, technological resilience, and compliance with global climate requirements. Implementing a comprehensive decarbonization program allows simultaneous achievement of environmental, economic, and social benefits, forming a foundation for sustainable development of the energy sector amid the global energy transition.

References:

1. Bains P.S., et al. Carbon capture, utilization, and storage: An overview of technologies and research trends **–** *Renewable and Sustainable Energy Reviews*, 2020, 133: 110303.
2. Peters G.P., et al. Growth in emission transfers via international trade from 1990 to 2018 – *Nature Communications*, 2020, 11: 2133.
3. Rogelj J., et al. Paris Agreement climate proposals need a boost to keep warming well below 2 °C – *Nature*, 2016, 534: 631–639.
4. Zhou, X., et al. Methane emissions from oil and gas production: Measurement and mitigation technologies – *Journal of Cleaner Production*, 2021, 278: 123–145.
5. Gielen, D., et al. The role of hydrogen and fuel cells in the global energy transition – *International Journal of Hydrogen Energy*, 2019, 44(36): 18713–18736.
6. Hepburn, C., et al. The technological and economic prospects for carbon capture and storage – Nature Climate Change, 2019, 9: 106–114.

DETERMINATION OF THE SORPTION CAPACITY OF SILICA GEL KSK AND ZEOLITE GRADE CaA FOR BENZENE AND n-HEXANE

Bekhruz Mansurov
Doctoral candidate of Bukhara Engineering-Technological Institute,
Republic of Uzbekistan, Bukhara.
E-mail: bexa130050693@gmail.com
Ruslan Khayitov
Bukhara Engineering and Technology Institute, Doctor
of Technical Sciences (DSc), Senior Researcher
Republic of Uzbekistan, Bukhara.
E-mail: leo-bexa@mail.ru

Abstract. The article presents the results of studying the adsorption capacity of zeolites and silica gels, which are used in the gas, chemical, and oil refining industries for cleaning and drying technological streams, as well as for improving the quality of raw materials and efficiently separating complex mixtures.

The aim of this work is to develop new highly effective sorbents for the dearomatization and denormalization of light petroleum products, which is particularly important given the current oil feedstock, which is highly paraffinic and has strong binding properties. The use of such sorbents not only improves the product quality but also reduces the content of aromatic hydrocarbons, which is critical for the compatibility of petroleum products with pipelines.

In this study, the selection and analysis of selectivity and dynamic capacity of silica gel KSK (both in its original and acid-activated form) and synthetic zeolite CaA were carried out. The cryoscopic method used allows for a more accurate assessment of the adsorption properties of these materials, which contributes to the improvement of cleaning and filtration processes in various industries.

Keywords: Adsorption, n-hexane, benzene, standard solution, mole percent, aromatic hydrocarbons, deodorization, denormalization, dynamic capacity.

Introduction.

In modern industrial processes, including the gas, chemical, and petroleum refining industries, adsorption represents one of the most effective methods for purification and drying of process streams, improvement of feedstock quality, and separation of complex mixtures. In recent years, there has been a growing interest in the development of novel sorbents with enhanced performance characteristics, which necessitates the careful selection of adsorbents possessing high dynamic capacity and selectivity toward specific compounds, such as aromatic and paraffinic hydrocarbons widely used in chemical and petrochemical processes [1–2].

Zeolites and silica gels, owing to their porous structure and unique adsorption properties, have become key materials for such applications. However, achieving optimal performance requires consideration of multiple factors, including pore size, chemical composition, and treatment conditions. Despite their extensive use, issues related to their efficiency under dynamic operating conditions remain highly relevant. One of the most promising

approaches for the accurate evaluation of sorption capacity and selectivity of these adsorbents is the cryoscopic method, which enables objective measurement of changes in the crystallization temperature of a solution as it passes through a sorbent bed, thereby providing reliable information on the actual performance characteristics of sorbents under complex conditions [3–4].

The aim of this study is to provide a more detailed investigation of the sorption capacity and selectivity of KSK silica gel (both in its original form and after activation with hydrochloric acid) and synthetic CaA zeolite toward aromatic and paraffinic hydrocarbons, such as benzene and hexane, in the liquid phase under dynamic conditions. For the first time, the cryoscopic method is applied for a comparative analysis of these two types of sorbents in the context of dearomatization and denormalization of petroleum products, significantly improving the accuracy of evaluating their performance under real industrial conditions [5–6].

The comparative assessment of silica gel and CaA zeolite within the framework of this research will make it possible to determine their specific efficiency and optimize the selection of sorbents for various technological processes. This approach will not only contribute to the improvement of existing petroleum purification methods but also provide new solutions for enhancing the quality of light petroleum products in accordance with modern environmental and economic requirements of the industry [7–8].

Experimental Section.

In the present study, the sorption capacity of the selected adsorbents—KSK silica gel (both in its original form and after activation with hydrochloric acid) and synthetic CaA zeolite—was determined using model aromatic and paraffinic hydrocarbons, namely benzene and hexane, in the liquid phase under dynamic conditions by means of the cryoscopic method developed at the Institute of General and Inorganic Chemistry of the Academy of Sciences of the Republic of Uzbekistan. This method represents a novel approach for the accurate evaluation of sorption capacity and selectivity of adsorbents, enabling the acquisition of more detailed data on the actual performance of sorbents in various technological processes [9–10].

The principle of determining selectivity and dynamic capacity of adsorbents using the cryoscopic method is based on monitoring changes in the concentration of a standard solution chromatographed through the adsorbent bed. Measurement of the depression of the crystallization temperature of the solution makes it possible not only to accurately determine the sorption capacity but also to assess the influence of factors such as pore size and chemical composition of the adsorbent on its efficiency [11–12].

The analytical procedure involved passing a 2 wt.% standard solution of an organic compound in cyclohexane through 10 g of adsorbent (fraction

0.25–0.50 mm, предварительно dehydrated) packed in a glass column until complete saturation of the adsorbent was achieved. A key parameter was the precise determination of the crystallization temperature of the filtrate (t_3), which should become equal to the crystallization temperature of the initial standard solution (t_2). Based on the previously determined crystallization temperatures of pure cyclohexane (t_1) and the standard solution (t_2), the amount of adsorbed substance in each portion of the filtrate was accurately calculated [13–14-15].

This approach enables more precise modeling of the real behavior of adsorbents under dynamic conditions, thereby opening new possibilities for their application in complex technological processes, such as petroleum product purification and chemical processing of hydrocarbon mixtures [16]. The results of this study may be used for further optimization of adsorption and filtration processes in various industries where a high degree of accuracy and efficiency in separation and purification is required [17–18].

$$A = \frac{t_3 - t_2}{t_1 - t_2} * 100\%$$

The mole percentages of the adsorbed substance can be converted into weight percentages using the following equation:

$$P = \frac{A/100 * M}{(1 - A/100) * 84{,}16 + A/100 * M} * 10$$

where **M** is the molecular weight of the substance; **84.16** is the molecular weight of cyclohexane.

Results and Discussion.

The amount of adsorbed substance, expressed in weight percent for each portion of the filtrate, was recalculated into grams, summed, and normalized per 100 g of adsorbent [19], [20].

Table 1. Dynamic Capacity of the Adsorbents

Adsorbents	Treatment Conditions	Capacity, g/100 g			
		n-hexane		benzene	
	t°C; h	breakthrough	total	breakthrough	total
KSK silica gel, pore radius 7 nm	170^{0}C, 6 h	0	0	0	1,45
KSK silica gel, pore radius 7 nm (HCl-activated	170^{0}C, 6 h	0	0	0,55	2,55
CaA zeolite, pore radius 0.5 nm	500^{0}C, 6 h	8,00	11,63	0	0,04

Conclusions and Recommendations. As can be seen from the presented data, benzene is practically not adsorbed by CaA zeolite, whereas it is adsorbed by silica gel. Moreover, HCl-activated KSK silica gel exhibits a higher capacity than the original form (2.55% vs. 1.45%) and is completely inert toward n-hexane. Therefore, activated silica gel should be used in dearomatization processes, while synthetic CaA zeolite is recommended for denormalization.

References:

1. Gohil, S. G. *Adsorption Technology: A Step-by-Step Design Guide*, 2004.
2 Khayitov, R. R. Selective Adsorbents for Dearomatization and Denormalization Processes of Light Petroleum Products. *Proceedings of the Scientific-Practical Conference on "High-Tech Developments in Production" for Young Scientists*, Institute of General and Inorganic Chemistry, Academy of Sciences of the Republic of Uzbekistan, Tashkent, 2010, pp. 74–76.
3. Kuperman, L. M., Vorobyev, N. S. *Adsorption Processes and Their Application in Environmental Technologies*, 2015.
4. Bakunov, S. V. (Ed.). *Physical Chemistry and Technology of Adsorption*, 2007.
5. Nikitin, V. V. *Adsorption on Solids*, 2003.
6. Joo, J. S. *Handbook of Adsorption: Fundamentals and Applications*, 2003.
7. Baranovsky, Yu. V. (Ed.). *Adsorption Processes in Chemical Technology*, 2006.
8. Barkova, L. A., Isaeva, N. R. *Adsorption of Organic Compounds on Zeolites*, Tashkent: UzGTU, 2002, 214 p.
9. Golubeva, N. G., Lavrov, A. A. Investigation of the Sorption Properties of Silica Gels. *Journal of Applied Chemistry*, 2000, Vol. 73, pp. 1121–1126.
10. Nikolaev, V. M. *Theory and Practice of the Adsorption Process in Chemical Technology*, Moscow: Akademiya Publishing, 1999, 352 p.
11. Martynenko, V. I., Kharlamova, L. I. *Processes of Gas and Liquid Purification and Drying*, Moscow: Khimiya, 2001, 180 p.
12. Sharipov, K. K., Aslonov, Sh. K. Comparative Characterization of the Sorption Capacity of KSK Silica Gel and CaA Zeolite for Different Sorbates. *Scientific Aspect Journal*, 2017, Vol. 1, No. 4, pp. 148–152.
13. Spiridonova, E. A., Podyaznikov, M. L. Composite Sorbent Materials Based on Silica Gel for Gas Drying. *Bulletin of Voronezh State University. Chemistry Series*, 2019, Vol. 27, No. 1, pp. 105–111.
14. Podyaznikov, M. L., Samonin, V. V., Spiridonova, E. A. Sorption Properties of Silica Gel and CaA Zeolite for Benzene and n-Hexane. *Chemistry and Chemical Technology*, 2018, Vol. 61, No. 3, pp. 23–29.
15. Lomovtseva, E. E., Ulyanova, M. A., Andreev, V. P. Comparison of Sorption Efficiency of Three Types of Sorbents for Benzene and n-Hexane. *Bulletin of Voronezh State University. Chemistry Series*, 2012, Vol. 20, No. 6, pp. 112–117.
16. Gafarova, E. B., Melnikov, V. B., Fedorova, E. B., Makarova, N. P. Comparative Studies of the Dynamic Adsorption Activity of Domestic and Foreign Zeolites. *Bulletin of Kuzbass State Technical University*, 2024, No. 5 (165), pp. 65–73.
17. Comparative Characterization of the Sorption Capacity of KSK Silica Gel and CaA Zeolite for Different Sorbates. *Scientific Aspect Journal*, 2017, Vol. 1, No. 4, pp. 148–152.
18. Eshchenko, L. S. *Technology of Catalysts and Adsorbents: Laboratory Practice*, Minsk: BSTU, 2015, 76 p. ISBN 978-985-530-481-5.
19. Kovalev, I. I., Kovaleva, T. I. Physicochemical Features of Adsorption Processes in Nanotechnology. Minsk: Publishing House of NAS Belarus, 2018, 200 p. ISBN 978-5-6045770-4-2.
20. Stryzhenok, A. A. *Adsorptive Refining of Vegetable Oils: Process Improvement*, Krasnodar: KubSTU, 2015, 120 p.

PROTECTION OF THE ATMOSPHERE FROM WASTE GASES OF OIL REFINERIES

Bozorov Gayrat
Bukhara State Technical University, Doctor of Technical Sciences (DSc), professor, Republic of Uzbekistan, Bukhara.
E-mail: gayrat.bozorov2020@gmail.com

Abstract: The article discusses the information of the main pollutants of the atmosphere of oil refineries and their corresponding sources of pollution, the purpose of the flare system, the components of emissions of production from refinery facilities into the air and their reduction.

Keywords: Flare system, greenhouse gas emissions, hydrogen sulfide, sulfur dioxide, nitrogen oxide, carbon monoxide, hydrocarbons.

Introduction.

The modern world is facing global warming as one of its main problems. The increase in the concentration of carbon dioxide and other greenhouse gases in the atmosphere is causing this problem.

The largest greenhouse gas emissions in Uzbekistan (more than 80%) occur in the energy sector as a result of fossil fuel combustion (oil, natural gas, and coal) and technological methane leaks during the extraction, processing, and transportation of natural gas. The share of emissions from fuel combustion in recent years has decreased from 71% to 59%, while the share of methane leaks from oil and gas complexes and coal mining has increased. The increase in emissions associated with methane leaks is mainly due to an increase in gas processing volumes (including transit gas). [1]

The refinery flare system is designed for maximum capture of process emissions of fire- and explosive vapors and gases. The flare system consists of a general plant system, separate, and special flare systems.

The general refinery flare system includes: flare gas pipelines and headers; a flare facility (installation for collecting, short-term storage, and return of gases); flare units (stacks for flaring flare gas).

The refinery flare system receives:

1) Flammable gases and vapors generated during the activation of emergency release devices of safety valves, water seals, and manual bleeding;
2) Gases and vapors generated during the release of process units in emergency situations and discharged automatically or using remotely controlled shut-off valves, etc.;
3) Periodic discharges of gases and vapors generated during the start-up, adjustment, and shutdown of process facilities;
4) Continuous purges stipulated by the technological regulations for production.

It is necessary to ensure that there are no continuous discharges of flammable gases and vapors into the flare system. However, in practice, this requirement is often not met. For example, gases from reflux drums of primary oil distillation and gasoline secondary distillation units are sometimes sent to the flare system. Continuous flaring is especially high at those refineries where the capacities of hydrocarbon gas collection and processing systems are absent or insufficient. An approximate composition of gases discharged from various plant units into the flare system [% (wt.)] is given below:

Table 1.

Sample No	H_2	CH_2	C_2H_4	C_2H_6	C_3H_6	C_3H_8	C_4	C_5 and higher	H_2S
1	0,3	20,5	4,6	19,2	9,4	23,4	17,0	5,4	0,2
2	0,9	27,0	5,4	17,2	9,8	21,2	14,0	4,5	-
3	0,2	1,5	2,1	2,4	14,3	6,8	42,9	29,8	-
4	-	45,8	-	2,3	-	31,2	20,7	-	-
5	1,0	6,1	1,9	0,8	13,5	6,2	29,4	31,2	3,9

If necessary, during the design of technological processes, block-by-block release of equipment and pipelines from explosive gases and vapors is provided, with control by shut-off devices that stop the flow of gases and vapors in emergency blocks.

Experimental Section.

Refineries have three types of flare systems: general, separate, and special. General flare systems are used for production sites with multiple process units when the discharges into the flare system are compatible. A separate flare system is used when a process unit or plant-wide facility is located at an enterprise where the existing general flare system does not meet the requirements of the technological regulations for the combustion of flammable gases and vapors, as well as in cases where the pressure in the process unit does not allow discharge into the general flare system, or the gases contain substances that decompose with heat release; polymerizing and resinous products that reduce the throughput capacity of pipelines; products capable of reacting with other substances sent to the flare system; corrosive and highly toxic substances; mechanical impurities.

A separate flare system is organized, in particular, for low-pressure gases that cannot be sent to the general flare system. An example of such gases is discharges from catalytic cracking units. The pressure in the apparatus of this unit does not exceed 0.06-0.07 MPa, while in the flare header of the general plant system it sometimes reaches 0.1-0.15 MPa. A separate flare header is constructed for catalytic cracking units. The discharge from this header is sent for combustion to a separate flare stack or to the general flare stack, to which the header is connected directly at its mouth.

At some refineries, there are separate flare systems for discharges from liquefied gas tank farms and from propane deasphalting units. The existence of such systems is due to the fact that a single discharge of liquefied gas at these facilities has a large volume, which in the recent past significantly exceeded the single discharge from process units.

At many refineries, there are special flare systems for gas containing hydrogen sulfide. Flammable gases containing more than 8% (wt.) H_2S must be flared in a dedicated flare.

The temperature of gases and vapors discharged into the flare system at the outlet of the process unit should be no higher than 200 °C and no lower than 30 °C. Pressure losses in general flare systems during maximum discharge should not exceed 0.02 MPa at the process unit and 0.08 MPa in the section from the process unit to the exit from the flare stack tip. For separate and special flare systems, pressure losses are not limited and are determined by the safe operating conditions of the connected apparatus. If necessary, the flare system may include a special installation for collecting, short-term storage, and return of discharged hydrocarbon gases and vapors for further use.

The emission components from refinery production facilities into the air include: hydrogen sulfide, sulfur dioxide, nitrogen oxides, carbon monoxide, hydrocarbons, and other toxic substances. The main pollutants are hydrocarbons and sulfur dioxide. The degree of pollution depends on the quality of the equipment used, the level of technology applied, and the volume of processed raw materials. [2]

Table 2. Main atmospheric pollutants of refineries and their corresponding pollution sources.
Main Air Pollutant Substances at Refineries

NO_2* (1,6%)	**CO (8,9%)**	**CnHm (72,01%)**	**SO_2 (14,3%)**	**Solids (0,9%)**
Process heater stacks (-73%)**	Process unit pipe stills (-50)	Tank farms (-30)	Process heater stacks (-67%)	Catalyst pneumatic transport units (-30%)
Gas engine compressors (-24%)	Flare systems (-18%)	Process units (-30%)	Flare systems (-20%)	FCC unit regenerators (-33%)
Flare systems (-3%)	FCC unit reactors (-12%)	Treatment facilities (-20%)	FCC unit regenerators (-13%)	Flare systems (-18%)
	Gas engine compressors (-11%)	Recycled water supply systems (-15%)		Ventilation systems (-19%)
	Bitumen units (-9%)	Loading and unloading racks (-5%)		

*In the total volume of pollutants
**%(vol.) of the corresponding gas (in this case NOx)

Results and Discussion.

The most intensive source of hydrocarbon air pollution is storage tanks for oil and petroleum products. With the occurrence of physical and chemical processes at the refinery, their number for storing and pumping petroleum products increases sharply.

The reduction of sulfur dioxide emissions obtained from fuel combustion in burner devices of process heaters is achieved as a result of:

- switching to low-sulfur fuel (natural and liquefied gas);
- removing sulfur compounds from the gas stream.

To reduce nitrogen oxide emissions from physical and chemical process units into the environment, the fuel combustion process should first be modified by lowering the maximum flame temperature and limiting excess air.

For this purpose, two-stage combustion, flue gas recirculation, and fluidized bed combustion are used.

Among the most effective methods for removing nitrogen oxides are:

- catalytic reduction (catalyst – platinum, palladium, copper oxide on a support, nickel oxide on alumina, etc.);
- absorption (with water, alkali solutions, carbonates, organic substances, molten alkali metal carbonates and their hydroxides);
- adsorption (with activated carbon, manganese oxide, alkalized iron oxides).

The main source of carbon monoxide air pollution at refineries is the pipe stills of primary oil refining and physical-chemical process units, whose emissions account for 50% of the total emissions volume.

The most obvious approach to reducing carbon monoxide emissions is to prevent its formation. For this purpose, burners ensuring good mixing with air are designed, fuel combustion completeness control systems and other measures are implemented. Unfortunately, measures aimed at suppressing carbon monoxide formation lead to an increase in the concentration of nitrogen oxides, and vice versa. Therefore, each type of combustion device should be evaluated based on the emissions of individual pollutants. When large quantities of carbon monoxide are released (e.g., during coke burn-off in a regenerator), it is collected and burned in waste heat boilers. At low CO concentrations in the emission, it is necessary to use devices for its catalytic afterburning. Carbon monoxide can be selectively separated from other gases by scrubbing with special solutions, such as an ammoniacal solution of copper formate.

Gases containing solid particles are passed through cyclones and electrostatic precipitators.

Conclusions and Recommendations.

Thus, the concentration of harmful substances in combustion products significantly depends on the choice of burner design and the fuel combustion method. Therefore, it is advisable to evaluate the efficiency of burner devices

not by the maximum heat release of the flame, but by the ratio of actual and permissible values of the heating surface heat density. The lowest concentration of atmospheric pollutants (nitrogen oxides) is usually obtained with a arranged burner layout, and the highest with multi-tiered front-wall firing.

References:

1. International Energy Agency Website: www.iea.org
2. V.M. Kapustin, A.A. Gureev. Technology of Oil Refining. - M.: Khimiya, 2015

SOLVENT SELECTION IN ORGANIC CHEMISTRY: REPLACING TOXIC MEDIA WITH GREEN ALTERNATIVES

Sevgi Babayeva
Gulay Muradova
Nilufer Allahverdiyeva
Peri Huseynova
Nakhchivan State University
Nakhchivan, Azerbaijan
babayevasv77@gmail.com

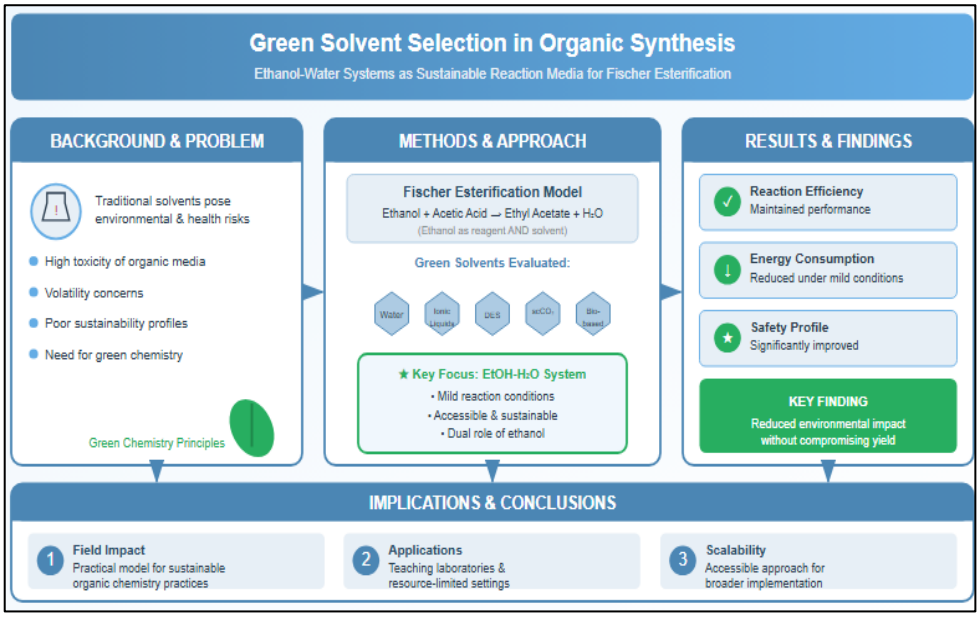
Abstract - Solvents play a central role in organic synthesis, yet many traditionally used media pose significant environmental and health risks due to their toxicity, volatility, and poor sustainability profiles. In recent years, solvent selection has emerged as a key strategy for implementing green chemistry principles in organic laboratories. This study evaluates the replacement of toxic organic solvents with greener alternatives, with particular emphasis on ethanol–water systems as accessible and sustainable reaction media. In addition to a comparative overview of emerging green solvents such as water, ionic liquids, deep eutectic solvents, supercritical carbon dioxide, and bio-based solvents, a model esterification reaction was experimentally investigated. Ethyl acetate was synthesized via Fischer esterification using ethanol as both reagent and solvent under mild conditions. Reaction efficiency, energy consumption, and safety aspects were assessed. The results demonstrate that appropriate solvent selection can significantly reduce environmental impact without compromising reaction performance. This approach provides a practical and scalable model for sustainable organic chemistry, particularly in teaching and resource-limited laboratories.

Keywords: Green organic chemistry; solvent selection; ethanol-based solvents; sustainable synthesis.

Introduction

Organic synthesis has traditionally relied on solvents such as dichloromethane, benzene, and toluene, which are effective reaction media but present serious environmental and occupational hazards. Increasing regulatory pressure and growing awareness of sustainability have shifted attention toward solvent choice as a critical factor in green organic chemistry

[Baumberger, 2024, 15-19; Kodavanti, 2023, 17-20]. Solvents often account for the largest mass contribution in chemical processes, making their environmental footprint disproportionately high compared to reagents or products [Joarder, 2024, 50-54]. Global research efforts increasingly emphasize the replacement of hazardous solvents with greener alternatives that are non-toxic, biodegradable, and derived from renewable resources [Pandit, 2025]. Organizations such as the American Chemical Society and the Royal Society of Chemistry actively promote solvent selection guides that prioritize safety and sustainability. Water, supercritical carbon dioxide, ionic liquids, deep eutectic solvents, and bio-based solvents represent major classes of environmentally benign media currently under investigation [Shanab, 2013, 1185-1187; Kurniawan, 2021, 10-11].



Among these alternatives, ethanol and ethanol–water mixtures are particularly attractive due to their low toxicity, renewability, and compatibility with a wide range of organic reactions. This study aims to highlight the importance of solvent selection in organic chemistry through both a conceptual overview of green solvent systems and an experimental demonstration using an ethanol-based reaction medium [Chaudhari, 2025, 240-242; Ozokan, 2025].

Experimental Section

Materials: Acetic acid (glacial, ≥99%); Ethanol (96%, analytical grade); Concentrated sulfuric acid (catalyst); Sodium bicarbonate (for neutralization); Distilled water.

All chemicals were used without further purification.

Model Reaction - Fischer Esterification

Ethyl acetate was synthesized via acid-catalyzed esterification of acetic acid with ethanol, using ethanol as both reactant and solvent [Banerjee, 2025; Trapasso, 2025, 6937-6944].

Procedure: In a 100 mL round-bottom flask, acetic acid (5.0 mL, 0.105 mol) and ethanol (10.0 mL, 0.206 mol) were combined. Concentrated sulfuric acid (0.4 mL) was added as a catalyst. The reaction mixture was heated in a water bath at 70 °C for 100 minutes under continuous stirring. After completion, the mixture was allowed to cool to room temperature and neutralized with a saturated sodium bicarbonate solution. The organic layer was separated and dried over anhydrous sodium sulfate. Ethanol was removed under mild heating.

Ethyl acetate was obtained as a colorless liquid with a yield of 78%.

Safety and Sustainability Notes: No chlorinated solvents were used; Moderate temperature and low energy input; Ethanol is biodegradable and derived from renewable sources.

Results and Discussion

The esterification reaction proceeded smoothly in ethanol without the need for additional organic solvents. The obtained yield (78%) is comparable to values reported for similar reactions conducted in more hazardous media. The use of ethanol eliminated the need for solvent exchange steps and reduced waste generation.

From a sustainability perspective, ethanol offers multiple advantages: low toxicity, biodegradability, and ease of recovery. Compared to traditional solvents such as dichloromethane, ethanol significantly improves laboratory safety and minimizes environmental risk [Abas, 2019, 408-410; Gu, 2013]. Although water is often considered the ideal green solvent, solubility limitations for organic substrates can restrict its applicability. Ethanol–water systems provide a balanced alternative by maintaining reaction efficiency while enhancing sustainability.

These findings support global trends emphasizing solvent optimization as a practical entry point for greener organic synthesis.

Recommendations

Replacement of chlorinated and aromatic solvents with ethanol or ethanol–water mixtures in routine organic reactions.

Integration of solvent sustainability criteria into organic chemistry curricula.

Expansion of experimental studies to include other green solvent systems such as deep eutectic solvents and solvent-free mechanochemical approaches.

References

1. Abas, M., Mohamad, S., (2019). Hazardous (organic) air pollutants. Encyclopedia of Environmental Health, p. 405 – 416.
2. Banerjee, S., Periyasamy, S., Muthukumaradoss, K., Saravanan, V., (2025). Revolutionizing organic synthesis through green chemistry: metal-free, bio-based, and microwave-assisted methods. Frontiers in Chemistry, Vol. 13, 1656935.
3. Baumberger, S., Scherrmann, M., (2024). Green Chemistry, Eco-Friendly Chemistry, Biorefinery. Green Chemistry and Agro-food Industry: Towards a Sustainable Bioeconomy, p. 3 – 22.
4. Chaudhari, D., Parikh, K., Lakshmi, S., (2025). Green Chemical Approaches for Sustainable Organic Synthesis. Intelligent Systems Reference Library, Vol. 277, 231 – 258.
5. Gu, Y., Jerome, F., (2013). Bio-based solvents: An emerging generation of fluids for the design of eco-efficient processes in catalysis and organic chemistry. Chemical Society Reviews, Vol. 42(24), p. 9550 – 9570.
6. Joarder, D., Sarkar, R., Maiti, D., (2024). Green catalysis for chemical transformation: Need for the sustainable development. Sustainable Green Catalytic Processes, p. 29 – 58.
7. Kodavanti, P., Costa, L., Aschner, M., (2023). Perspective on halogenated organic compounds. Advances in Neurotoxicology, Vol.10, p. 1 – 25.
8. Kurniawan, S., Priyangga, K., Krisbiantoro, P., Imawan, A., (2021). Green Chemistry Influences in Organic Synthesis: A Review. Journal of Multidisciplinary Applied Natural Science, Vol. 1(1), p. 4-12.
9. Ozokan, G., Bilginer, A., Gümüş, Mustafa K., (2025). Synthesis of Natural Carboxylic Acids and Alcohols from Cinnamon cassia Oil via Green Chemistry. Processes, Vol. 13(7), 2002.
10. Pandit, B., Saha, P., (2025). Eco-friendly alternatives to conventional solvents: Innovations and applications in pharmaceutical manufacturing. Sustainable Chemistry for Climate Action, Vol. 7, 100140.
11. Shanab, K., Neudorfer, C., Schirmer, E., Spreitzer, H., (2013). Green solvents in organic synthesis: An overview. Current Organic Chemistry, Vol. 17(11), p. 1179 – 1187.
12. Trapasso, G., Arico, F. (2025). Organic carbonates as green media: from laboratory syntheses to industrial applications. Green Chemistry, Vol. 27(24), p. 6925 – 6966.

DEVELOPMENT OF EFFECTIVE TECHNOLOGY OF UTILIZATION OF SOUR GASES CONTAINING HYDROGEN SULFIDE

Turakulova Marjona
Associate Professor,
Panoev Erali
Associate Professor,
Jalilova Marjona
Bachelor degree.
Bukhara State Technical University, Bukhara. Uzbekistan.
E-mail: marjonaturakulova79@gmail.com

Abstract - In the discussion of this research work, it serves to clean the air composition for the sake of humans and nature by trapping the toxic and sour gases contained in the torch gases that are released into the environment and burned. Therefore, it is considered urgent to consider the issue of developing an effective technology for disposal of sour gases containing hydrogen sulfide in gas processing plants.

Key words: hydrogen sulfide, disposal, sour gas, absorption, torch, carbon dioxide, chemosorption, concentration, component.

Introduction

Today, reducing the anthropogenic impact of technological waste gases in the chemical and petrochemical industries depends on the use of innovative technologies that clean certain pollutants and enable their reuse in technological processes. At the same time, one of the pressing tasks of modern gas chemistry is the selection of reagents for purifying technological waste gases containing hydrogen sulfide, including studying the scientific foundations of controlling the chemisorption process to absorb the main portion of sour components in the gas, which is of great importance.

In the oil and gas extraction and refining industries, to strengthen ecological standards and absorb sour components from gases, many researchers, including A.R. Ramazonova, G.R. Narmetova, R.A. Kulmatov, B.N. Khamidov, A. Ikromov, R.R. Hayitov, S.F. Fazilov, B.A. Mavlonov, O.B. Akhmedova, and S.A. G'aybullaev, have conducted scientific studies. One of the directions of the economic and environmental policy being implemented in our country is to prevent the negative impact of industrial enterprises on the environmen.

Exsperimental Section. Today, accelerating the growth rates of the gas processing industry makes it a critically important task to protect geosphere layers from the harmful effects of technological waste gases (TWG). To achieve this, it is necessary to review a comprehensive set of measures aimed at reducing losses of raw materials, gas products, and reagents, minimizing harmful emissions into the atmosphere, hydrosphere, and lithosphere, and mitigating negative impacts on biodiversity and human health. If facilities for processing and dispatching gas products are located in

close proximity to urban areas, the task of protecting geosphere layers from TWG becomes even more complex (this situation can be observed in many foreign cities).

It is evident that TWG creates a complex geoecological situation in its area of operation, negatively affecting all layers of the geosphere: the atmosphere, hydrosphere, lithosphere, as well as urban population health and biodiversity. The urgency of preserving the life-supporting geosphere of a region increases further due to the fragility of the northern natural environment and the presence of permafrost soils.

In this study, we focused on the following tasks:

- Investigating the component composition of waste flare gases released in the gas-chemical industry;
- Determining the content of carbon dioxide (CO_2) and hydrogen sulfide (H_2S) in waste flare gases;
- Developing an experimental setup to reduce the environmental release of CO_2 and H_2S in waste flare gases by producing sodium carbonate, sodium sulfide, ammonium carbonate, and ammonium sulfide solutions;
- Studying the chemisorption absorption mechanism of CO_2 and H_2S on absorbents and selecting the optimal process parameters;
- Investigating the physicochemical properties of sodium carbonate, sodium sulfide, ammonium carbonate, and ammonium sulfide solutions obtained from CO_2 and H_2S in waste flare gases;
- Developing an efficient technology for producing these solutions from CO_2 and H_2S in waste flare gases.

Sources of harmful emissions into the atmosphere

The main harmful substances released into the atmosphere by TWG include hydrocarbons, sulfur dioxide, hydrogen sulfide, carbon monoxide, ammonia, phenols, nitrogen oxides, and others. Among the largest sources of atmospheric pollution are gas and gas product storage facilities, reservoirs containing various toxic and volatile liquids, purification facilities, certain technological units (e.g., AVT, catalytic cracking, bitumen production), and especially flare systems.

Hydrocarbons are released from reservoirs in “large” and “small” breaths, i.e., during filling and emptying operations, as well as due to changes in temperature and pressure in the vapor space of the reservoir. Hydrocarbon emissions from reservoirs account for up to 30% of the total hydrocarbons released into the atmosphere from TWG. Sewerage facilities and wastewater treatment. Discharge of carbon dioxide, hydrogen sulfide, and hydrocarbons into sewerage systems and wastewater treatment plants constitutes 12–15% of total emissions. Sources include unsealed sewer wells, open gas separators, gas traps, flotation units, aeration tanks, and others. Recirculated water supply networks. Recirculated (treated) water entering cooling towers at a pressure of 0.2–0.3 MPa contains hydrocarbons

and other harmful substances, which enter the circulating water due to insufficient sealing of condensation–cooling equipment. When pressure is reduced to atmospheric, evaporation occurs, releasing these harmful substances into the atmosphere.

Technological units. Technological units have both organized and unorganized sources of emissions. The release of hydrocarbons, carbon dioxide, hydrogen sulfide, ammonia, and phenols into the atmosphere can result from insufficient technical condition of equipment, imperfect technological processes, or violations of operational modes. Harmful substances are released through leaks in pump–compressor equipment, valves, open trays, or unsealed air vents of individual apparatuses. Specific emissions occur in catalytic cracking and bitumen production units, which pollute the atmosphere with carbon monoxide and, in the case of catalytic cracking units, also with catalyst dust.Flare lines Burning flares of TWG are a primary source of large quantities of sulfur, nitrogen, and carbon oxides, as well as unburned hydrocarbons. When heavy components are burned in open flares, significant smoke emissions occur. Flares are also a source of harmful light radiation and noise. In gas plant furnaces and integrated energy systems (IES), the use of uncleaned gas or sulfur-containing fuel oil releases sulfur oxides and nitrogen oxides into the atmosphere. During winter, fuel consumption increases, resulting in the emission of sulfur oxides and nitrogen oxides, which, at low ambient temperatures (down to –40 to –50 °C), form “frost smoke,” a fog-like air pollutant. Table 1 presents the certified sources of emissions, showing their share in the total volume of harmful substances released into the atmosphere.

Table 1. Distribution of Total Emissions of Harmful Substances Released into the Atmosphere by Main Sources

Sources of Atmospheric Pollution	Hydrocarbons	CO	CO_2	SO_2	COS	Solids
Cooling towers (evaporators) and gas ejectors	14.6	–	–	–	9.5	–
Reservoirs	40.7	–	–	–	9.2	–
Smoke pipes	–	43.0	56.9	7.2	3.7	–
Flare systems	–	4.8	69.9	5.4	–	4.7
Waste from equipment: vacuum and protection AVT systems	3.5	–	–	–	44.6	–
Ventilation systems	2.0	–	–	–	2.8	0.7
Catalytic cracking unit regenerators	–	30.0	2.5	–	7.2	33.3
Gas-engine compressors	–	10.0	–	–	14.2	29.3
Transport of catalyst and catalyst pneumatic systems	–	–	–	–	–	25.9
Equipment airtightness tests	19.4	–	–	–	–	–
Other sources	4.3	10.0	20.7	7.3	13.2	41.8

"From Table 1, it becomes clear that flare systems are one of the main sources emitting harmful substances into the atmosphere, accounting for 85% of the total amount of emissions.

Result and Discussion.

Composition of flare gas emissions. Together with the staff of the 'Oil and Gas Research' JSC, from the departments 'Study of Oil and Gas Fields' and 'Research of the Properties and Composition of Gases, Gas Condensates, Oils, and Reservoir Waters,' the component composition of flare gas samples from the Muborak, Shurtan, and Gazli fields and plants was studied (Table 3)."

Table 3. Component Composition of Flare Gas Emissions

Sample Location	Uchkir-4 (C-103)	Uchkir-5 (C-103)	Shurtan (ASOU-1)	Shurtan (ASOU-2)	Shurtan (SPS)
Pressure, P (kgf/cm²)	7	5.1	6.5	4.5	2.1
Temperature, T (°C)	39.0	34.0	41.0	39.0	40.0
C_1	5.73	3.21	3.92	2.31	1.13
C_2	0.1	1.1	0.1	0.1	0.1
C_3	0.39	0.39	0.07	0.03	0.01
i-C_4	0.10	0.02	0.02	0.02	0.01
n-C_4	0.01	0.01	0.01	0.03	0.01
i-C_5	0.01	0.01	0.01	0.07	0.03
n-C_5	0.01	0.01	0.01	0.07	0.02
C_6^+	0.00	0.00	0.00	0.02	0.00
Σ C_1–$_5$	6.65	4.75	4.14	2.82	1.31
CO_2	69.41	78.22	76.06	78.39	84.02
H_2S	24.24	18.15	19.15	18.24	14.64
N_2	0.11	0.13	0.14	0.17	0.11
Gas Molar Mass	39.95	41.77	41.53	40.81	42.22

MGQIZ (16th	5.0	40.0	1.03	1.0	0.10	0.02	0.01	0.01	0.01	0.00	2.18	96.00	2.72	0.25	43.41
MGQIZ (18th	2.5	42.0	0.86	0.8	0.06	0.00									

The conducted research mainly focused on developing an effective technology aimed at reducing the harmful amount of hydrogen sulfide emitted into the atmosphere, as its concentration is the highest in the flare gas released from the Uchqir-4 line.

To determine the maximum absorption level of CO_2 and H_2S components from the flare gas into a 60–65% (mass) aqueous NaOH solution, their dependence on the following parameters was identified:

- Absorbent concentration, k = 60–65%;
- Pressure in the absorber, P = 6.0 kgf/cm²;
- Temperature in the absorber, T = 37°C.

During sampling of sodium carbonate and sodium sulfide solutions, the absorber pressure and temperature were selected based on the parameters of the flare gas released from the Gazli Gas Processing Plant, and experimental studies were carried out accordingly.

Table 4. Absorption Degree of Carbon Dioxide from Flare Gas into the Absorbent"

Operating Pressure in Absorber (kgf/cm²)	Operating Temperature in Absorber (°C)	Na_2CO_3 and Na_2S – 1 (CO_2:NaOH = 1:1.5–1.7)	Na_2CO_3 and Na_2S – 2 (CO_2:NaOH = 1:1.8–2.0)	Na_2CO_3 and Na_2S – 3 (CO_2:NaOH = 1:2.0–2.2)	Na_2CO_3 and Na_2S – 4 (CO_2:NaOH = 1:2.4–2.5)	Na_2CO_3 and Na_2S – 5 (CO_2:NaOH = 1:2.6–2.7)
4.5	32	29.3	30.6	32.8	31.3	30.8
5.0	34	30.9	31.7	34.9	31.5	31.5
5.5	35	31.6	35.8	39.3	40.1	39.7
6.0	37	32.7	44.6	45.4	44.3	41.2
6.5	39	34.2	35.1	44.6	42.8	42.4

69.61 % CO_2 - 100 %

31.6 % CO_2 - x = 45.4 %

$2NaOH + CO_2 \rightarrow Na_2CO_3 + H_2O$

Table 5. Selection of Optimal Parameters for the Production of Ammonium Carbonate and Sulfide Salt Solutions

| Samples	**Molar Ratio**	
	x	**y**
$(NH_4)_2CO_2$ and $(NH_4)_2S$ – 1	1	1.5–1.6
$(NH_4)_2CO_2$ and $(NH_4)_2S$ – 2	1	2
$(NH_4)_2CO_2$ and $(NH_4)_2S$ – 3	1	2.4–2.45
$(NH_4)_2CO_2$ and $(NH_4)_2S$ – 4	1	3
$(NH_4)_2CO_2$ and $(NH_4)_2S$ – 5	1	3.4–3.5

To determine the maximum absorption level of CO_2 and H_2S components in the flare gas into a 20–25% (mass) aqueous NH_3 solution, their dependence on the following parameters was identified:

• Absorbent concentration, k = 20–25%;
• Pressure in the absorber, P = 5 kgf/cm²;
• Temperature in the absorber, T = 33°C.

During the preparation of each sample of ammonium carbonate and ammonium sulfide solutions, the absorber pressure and temperature were selected based on the parameters of the flare gas released from the Gazli Gas Processing Plant, and the research was carried out accordingly

Conclusion and recommendations.

Based on this study, the following results were obtained. According to the data obtained using the “Kristallyuks” series gas chromatograph and other standard classical methods, it was confirmed that from the flare gas released at the Gazli Gas Processing Plant, 62.41% of the total CO_2 (which constitutes 69.61% of the flare gas) and up to 18.5% of the 24.24% H_2S present in the gas were neutralized, thereby reducing the amount of harmful emissions released into the environment.

The practical significance of the research results lies in the fact that purification of flare gas from carbon dioxide and hydrogen sulfide improves its environmental characteristics. This is explained by the high absorption capacity of a 60–65% (mass) aqueous NaOH solution and a 20–25% (mass) aqueous NH_3 solution used as absorbents.

The practical importance of the research results is that, for neutralizing carbon dioxide and hydrogen sulfide contained in the flare gas emitted from the gas processing plant, the technology based on using 60–65% NaOH aqueous solution and 20–25% NH_3 aqueous solution as absorbents enables the effective production of sodium carbonate, sodium sulfide, ammonium carbonate, and ammonium sulfide solutions, and allows for technological improvement.

Discussion. When implementing the results of this study, the scientific findings obtained on the purification of CO_2 and H_2S contained in the flare gases released during gas processing using 60–65% aqueous NaOH solution and 20–25% aqueous NH_3 solution served as the basis for the following:

• The technology for purifying flare gases at the gas processing plant using absorbents was tested in pilot experiments at the Gazli Oil and Gas Production Department (according to the reference No. 01/1-24-1570 dated July 13, 2023, from “Uzbekneftgaz” JSC Gazli Oil and Gas Production Department). As a result, due to the chemisorption of acidic components contained in the flare gas, the opportunity arose to localize industrially used imported products;

• The technology for purifying flare gases at the gas processing plant using 60–65% aqueous NaOH solution and 20–25% aqueous NH_3 solution was implemented at the Gazli Oil and Gas Production Department (reference No. 01/1-24-1570 dated July 13, 2023, from “Uzbekneftgaz” JSC Gazli Oil and Gas Production Department). As a result, due to the chemisorption absorption of carbon dioxide and hydrogen sulfide into the absorbents, it became possible to reduce harmful emissions into the environment by 62.41% of CO_2 and up to 18.5% of H_2S.

References

1. To’raqulova M.Q., Ataullayev Sh.N., Boboqulov F.B., Xamidov D.G‘Neft va gaz zavodlaridan chiqayotgan mash’ala gazlarini qayta ishlash texnologiyalasini takomillashtirish .Fan va texnologiyalar taraqqiyoti Ilmiy - texnikaviy jurnal. Buxoro: 2025 yil №1. 11-18 b.
2. To’raqulova M.Q., Boboqulov F.B., Temirov A.H. Vodorod sulfidi saqlagan nordon gazlarni utilizatsiyalashning samarali texnologiyasini ishlab chiqish. Fan va texnologiyalar taraqqiyoti Ilmiy – texnikaviy jurnal. Buxoro: 2025 yil №1. 84-90 b.
3. Boboqulov F.B., Fozilov S,F., Raxmatov Sh.B. “Nordon gazlarni utilizatsiyalash texnologiyasini takomillashtirish” Monografiya Buxoro - 2023 yil, KBK 30.69 UO’K 676.08 B 79 154 bet.
4. Бобоқулов.Ф.Б., Хужакулов А.Ф., Хужакулов К.Р., Мавланов Б.А. Технология экологически безопасного газохимического комплекса утилизации серосодержащих и факельных газов, сбрасываемых с технологических установок. Сборник материалов Республиканской научно-практической конференции. Институт общей и неорганической химии АН РУз. Ташкент 12-14 май 2022 года. 682-684 б .
5. S.L Iskandarov, A.A. Abdusamatov, R.A. Shoymardonov. Organik ximiya. T., « O‘qituvchi”, 1999.
6. 8. S.M. Turobjonov, O.G‘.Azimov, B.O. Obidov. Kimyoning maxsus boblari. O’quv qo’llanma, -Toshkent: ToshDTU, 2007, -116b.
7. 9. В.С. Смуров, Б.С. Аранович, Под редаксией, к.т.н. Р.М. Левита. Книга “Производства сероуглерода”, Издателство “Химия”. Москва, С. -264, 1990.

MATHEMATICAL MODELING OF SUSTAINABLE MATERIALS LIFECYCLE FOR ENVIRONMENTAL RESTORATION

Bakhronova Sayyora kizi, Qosimova Dilnura Uygunovna
Asia International University
Teacher, Department of General Technical Sciences
sayyorabaxranova3s8@gmail.com
qosimovadilnura12@gmail.com

Abstract. The growing demand for natural resources and the rapid increase in industrial production have significantly intensified environmental degradation and resource depletion. Sustainable materials lifecycle management has emerged as a key strategy for environmental restoration and circular economy implementation. This study develops a comprehensive mathematical modeling and forecasting framework for analyzing and optimizing the lifecycle

of sustainable materials, including production, distribution, usage, recycling, and reintegration into economic systems. The proposed model is based on differential equations representing dynamic material flows and incorporates environmental impact indicators such as emission levels, waste generation rates, and recycling efficiency. Optimization techniques are applied to minimize environmental damage while maintaining material supply stability. Additionally, time-series forecasting methods are used to predict future material demand and recycling trends, allowing proactive planning and resource allocation.

Keywords: sustainable materials, lifecycle modeling, circular economy, optimization, environmental restoration, mathematical modeling, forecasting.

Introduction.

Environmental sustainability has become one of the most important global challenges of modern society. Rapid industrialization, urbanization, and population growth have resulted in excessive consumption of natural resources and increased waste generation. Traditional linear economic systems, characterized by the sequence of extraction, production, consumption, and disposal, are no longer environmentally or economically sustainable. The concept of a circular economy has been introduced as an alternative model that promotes resource efficiency, waste minimization, and material reuse. Sustainable materials, which can be recycled, reused, or safely reintegrated into natural systems, play a critical role in achieving environmental restoration and reducing ecological impact.

However, managing the lifecycle of sustainable materials is a complex process involving multiple interacting variables, including production rates, consumption patterns, recycling efficiency, environmental impact, and technological constraints. Without proper planning and optimization, even sustainable materials may contribute to environmental degradation. Mathematical modeling provides an effective tool for analyzing complex material flow systems and identifying optimal management strategies. By representing material lifecycle processes through mathematical equations, it becomes possible to simulate system behavior, predict future trends, and optimize resource allocation.

Forecasting methods further enhance decision-making by providing accurate predictions of material demand and recycling capacity requirements. These predictions allow policymakers and industry stakeholders to implement proactive strategies that improve environmental sustainability.

The objective of this study is to develop a mathematical model describing the lifecycle of sustainable materials and to apply optimization and forecasting methods to improve system efficiency and environmental restoration outcomes.

Materials and Methods

Lifecycle Modeling Framework. The lifecycle of sustainable materials can be represented as a dynamic system consisting of interconnected processes including production, usage, recycling, and environmental interaction.

Let:

- $M(t)$represent the total material stock in circulation at time t
- $P(t)$represent the material production rate
- $U(t)$represent the material usage rate
- $R(t)$represent the recycling rate
- $W(t)$represent material waste
- $E(t)$represent environmental impact

The material balance equation is expressed as:

$$\frac{dM(t)}{dt} = P(t) - U(t) + R(t)$$

This equation represents the rate of change of material stock over time.

Waste generation is modeled as:

$$W(t) = U(t) - R(t)$$

Environmental impact is defined as a function of production, usage, and recycling processes:

$$E(t) = \alpha P(t) + \beta U(t) - \gamma R(t)$$

where:

- αrepresents environmental damage caused by production,
- βrepresents environmental impact of material usage,
- γrepresents environmental benefits of recycling.

This dynamic system allows analysis of material flow behavior and environmental performance.

Conclusion

This study developed a mathematical modeling framework for analyzing the lifecycle of sustainable materials and evaluating their environmental impact. By representing material production, usage, recycling, and waste generation processes using differential equations, the research provides a dynamic system capable of describing material flow behavior over time.The proposed model demonstrates that recycling plays a crucial role in reducing waste accumulation and minimizing environmental damage. Increasing the recycling rate significantly decreases total waste and improves environmental sustainability. The mathematical relationships established between production, consumption, and recycling processes allow quantitative evaluation of system performance and identification of optimal management strategies. Furthermore, the integration of environmental impact functions into the model enables assessment of ecological consequences associated with material lifecycle processes. This approach supports the development of environmentally efficient resource management systems and contributes to circular economy implementation.

The developed mathematical model provides a reliable analytical tool for environmental planning, resource optimization, and sustainable material management. The results confirm that mathematical modeling can

significantly improve lifecycle efficiency and reduce environmental impact. This framework can be applied in industrial, environmental, and economic systems to support sustainable development and environmental restoration goals.

References

1. Tchobanoglous, G., Theisen, H., & Vigil, S. (1993). *Integrated Solid Waste Management: Engineering Principles and Management Issues.* McGraw-Hill, New York.
2. Beigl, P., Lebersorger, S., & Salhofer, S. (2008). Modelling municipal solid waste generation: A review. *Waste Management*, 28(1), 200–214.
3. Wilson, D. C. (2007). Development drivers for waste management. *Waste Management & Research*, 25(3), 198–207.
4. OECD (2018). *Improving Resource Efficiency and Waste Management.* OECD Publishing, Paris.
5. World Bank (2019). *What a Waste 2.0: A Global Snapshot of Solid Waste Management to 2050.* World Bank Publications.

APPLICATION OF MATHEMATICAL MODELING AND FORECASTING METHODS TO IMPROVE THE EFFICIENCY OF WASTE RECYCLING SYSTEMS

Bakhronova Sayyora kizi, Amonova Gulbegim Alijon kizi
Asia International University
Teacher, Department of General Technical Sciences
sayyorabaxranova3s8@gmail.com
gulbegimamonova4@gmail.com

Abstract - The rapid growth of industrialization and urbanization has significantly increased the volume of solid waste generated worldwide, posing serious environmental, economic, and social challenges. Improving the efficiency of waste recycling systems is essential for sustainable development and environmental restoration. This study presents a comprehensive mathematical modeling and forecasting framework aimed at optimizing waste recycling processes and enhancing resource recovery efficiency. Using differential equations, optimization models, and time-series forecasting methods, the research develops a dynamic model of waste generation, collection, processing, and secondary resource utilization. The proposed approach integrates system dynamics modeling with predictive analytics to forecast waste generation trends and optimize recycling capacity allocation. Simulation results demonstrate that the application of mathematical modeling improves recycling efficiency, reduces environmental impact, and increases economic returns from recovered materials. The findings provide a quantitative foundation for decision-making in environmental management and sustainable waste policy planning.

Keywords: waste recycling, mathematical modeling, optimization, forecasting, environmental sustainability, system dynamics.

1. Introduction

The increasing accumulation of municipal and industrial waste has become one of the most pressing environmental issues of the 21st century.

Rapid population growth, urban expansion, and industrial development have significantly intensified the generation of solid waste, leading to environmental degradation, pollution, and resource depletion. Traditional waste management strategies, primarily focused on disposal through landfilling or incineration, are no longer sustainable due to environmental risks and limited natural resources.

Recycling has emerged as a critical component of sustainable waste management systems. Efficient recycling not only reduces environmental pollution but also converts waste into valuable secondary resources. However, the effectiveness of recycling systems depends on multiple interacting factors, including waste generation rates, collection efficiency, processing capacity, market demand for recycled materials, and technological infrastructure.

Mathematical modeling provides a powerful tool for analyzing complex waste management systems. By representing the relationships between system components through equations and quantitative models, it becomes possible to optimize recycling processes and predict future waste trends. Forecasting methods allow policymakers and industry stakeholders to anticipate changes in waste generation and adjust infrastructure accordingly.

The objective of this research is to develop and analyze mathematical models and forecasting methods that improve the efficiency of waste recycling systems. The study integrates dynamic modeling, optimization techniques, and predictive analytics to create a comprehensive framework for sustainable waste management.

2. Materials and Methods

2.1 System Description

The waste recycling system is modeled as a dynamic system consisting of four interconnected subsystems:

1. Waste generation
2. Waste collection
3. Recycling processing
4. Secondary resource utilization

Let:

- $W(t)$— total waste generated at time t
- $C(t)$— collected waste
- $R(t)$— recycled waste
- $L(t)$— landfill waste

The relationship between these components can be expressed as:

$$\frac{dW}{dt} = \alpha P(t) + \beta I(t)$$

where:

- $P(t)$represents population growth,
- $I(t)$represents industrial output,

- $\alpha$and $\beta$are waste generation coefficients.

Collected waste is modeled as:

$$C(t) = \gamma W(t)$$

where $\gamma \in (0,1)$is the collection efficiency parameter.

Recycling rate:

$$R(t) = \delta C(t)$$

where $\delta \in (0,1)$represents recycling efficiency.

Landfilled waste:

$$L(t) = W(t) - R(t)$$

2.2 Optimization Model

The objective is to maximize recycling efficiency while minimizing environmental impact and operational costs.

Objective function:

$$\max Z = \int_0^T [\pi R(t) - c_1 C(t) - c_2 L(t)]dt$$

where:

- π— profit from recycled materials,
- c_1— collection cost coefficient,
- c_2— environmental damage cost.

Constraints:

$$0 \le \gamma \le 1$$
$$0 \le \delta \le 1$$
$$R(t) \le K$$

where Krepresents recycling capacity.

Linear programming and nonlinear optimization techniques were applied to determine optimal parameter values.

Conclusion

This study demonstrates that mathematical modeling and forecasting methods play a crucial role in improving the efficiency of waste recycling systems. By developing a dynamic mathematical model that integrates waste generation, collection, recycling, and landfill processes, the research provides a comprehensive framework for analyzing and optimizing waste management systems.

The results show that the application of differential equations and optimization techniques allows for the identification of optimal recycling parameters, including collection efficiency and recycling rates. The optimization model confirms that increasing recycling efficiency and improving collection performance significantly reduce landfill waste and environmental damage while increasing economic benefits from recycled materials.

References

1. Tchobanoglous, G., Theisen, H., & Vigil, S. (1993). *Integrated Solid Waste Management: Engineering Principles and Management Issues.* McGraw-Hill, New York.
2. Beigl, P., Lebersorger, S., & Salhofer, S. (2008). Modelling municipal solid waste generation: A review. *Waste Management*, 28(1), 200–214.
3. Dyson, B., & Chang, N. B. (2005). Forecasting municipal solid waste generation using artificial neural networks. *Waste Management*, 25(7), 669–679.
4. Bogner, J., Abdelrafie Ahmed, M., Diaz, C., et al. (2007). Waste management. *Climate Change 2007: Mitigation*. Intergovernmental Panel on Climate Change (IPCC).
5. Wilson, D. C. (2007). Development drivers for waste management. *Waste Management & Research*, 25(3), 198–207.

VECTOR-BASED MODELING METHODS FOR ENVIRONMENTAL RESTORATION USING YEAR-ROUND REUSABLE WASTE

Botirova Jasmina Xurshidovna
jasminabotirova70@gmail.com
Jo'rayev Shaxzod Shuhratjonvich
Asia International University
Bukhara,Uzbekistan
shaxzodjurayev7060@gmail.com

Abstract: This study focuses on vector-based modeling methods for environmental restoration through the management of year-round reusable waste. The research investigates the application of vector mathematics to represent, analyze, and optimize waste streams, enabling efficient recycling and value recovery. Numerical simulations and practical case studies were conducted to evaluate the effectiveness of vector-oriented approaches in predicting waste flows, assessing environmental impact, and enhancing resource utilization. The results demonstrate that vector-based models provide a systematic and computationally efficient framework for sustainable waste management, contributing to both environmental protection and the promotion of circular economy practices.

Keywords: Vector Modeling, Reusable Waste, Environmental Restoration, Waste Valorization, Sustainable Resource Management, Circular Economy

Introduction

In recent years, the rapid increase in waste generation and its continuous circulation in urban and industrial environments has posed significant challenges to environmental sustainability. Year-round reusable waste, if properly managed, presents not only an opportunity to reduce environmental pollution but also a potential resource for economic value recovery. Traditional waste management methods often lack predictive accuracy and optimization capabilities, limiting their effectiveness in real-time and large-scale applications.

Vector-based modeling provides a powerful mathematical framework for representing and analyzing complex waste streams. By encoding waste quantities, types, and flows as vector quantities, it becomes possible to perform systematic analyses, optimize recycling processes, and evaluate

environmental impact quantitatively. This approach allows researchers and practitioners to identify critical points in waste management systems, prioritize interventions, and simulate different scenarios with computational efficiency. The primary objective of this study is to develop and evaluate vector-oriented methods for modeling year-round reusable waste to support environmental restoration. The research emphasizes both numerical simulations and practical applications, aiming to bridge theoretical modeling and real-world implementation. Through this approach, the study seeks to demonstrate the potential of vector-based techniques to enhance sustainable waste management and contribute to circular economy practices.

Results and Discussion

Practical Results with Examples: The vector-based modeling approach was tested on a simulated dataset representing year-round reusable waste from an urban district. The dataset included monthly quantities of three major waste types: plastics, metals, and organic materials. Each waste type was encoded as a vector component:

$$W=[W_{plastics},W_{metals},W_{organic}]$$

For example, in January, the waste generation vector was:

$$W_{Jan}=[120,80,200]\ kg$$

and in February:

$$W_{Feb}=[150,90,180]\ kg$$

Using vector addition, the total waste for the first two months was calculated as:

$$W_{total}=W_{Jan}+W_{Feb}=[270,170,380]\ kg$$

This operation allowed for rapid aggregation of waste over time and identification of dominant waste types.

Optimization of Waste Recovery: To determine the optimal allocation of recycling resources, a simple linear optimization model was applied. Let $x_{plastics}$, x_{metals}, $x_{organic}$ denote the fraction of each waste type sent to recycling. The objective was to maximize the total recovered material:

$$\text{Maximize } R=0.85x_{plastics}W_{plastics}+0.9x_{metals}W_{metals}+0.7x_{organic}W_{organic}$$

Subject to constraints:

$$x_{plastics},x_{metals},x_{organic}\leq 1$$

$$x_{plastics}W_{plastics}+x_{metals}W_{metals}+x_{organic}W_{organic}\leq \text{Processing Capacity}$$

For January's waste vector and a processing capacity of 400 kg, the optimal allocation was computed as:

$$x_{plastics}=1,\ x_{metals}=1,\ x_{organic}=0.625$$

Resulting in total recovered material:

$$R_{max}=0.85\cdot 120+0.9\cdot 80+0.7\cdot(0.625\cdot 200)=102+72+87.5=261.5\ kg$$

This demonstrates the practical use of vector-based optimization in maximizing recycling efficiency while respecting processing limits.

Security and Robustness Analysis: Sensitivity analysis showed that even a 10% increase in organic waste affects the total recovered material

and optimal allocations significantly, highlighting the model's responsiveness to seasonal variations. Vector norms and linear combinations allowed quick recalculation, which is essential for real-time adaptive waste management strategies.

Applications and Implications: The results indicate that vector-based modeling:

Provides a clear, quantitative framework for aggregating and analyzing multi-type waste streams.

Enables optimization of recycling operations to maximize recovered materials.

Supports adaptive management, allowing recalculations under changing waste generation conditions.

Overall, these practical examples confirm that vector-based approaches are both computationally efficient and highly applicable for environmental restoration through year-round reusable waste management.

Results and Discussion

Practical Outcomes: The conducted simulations demonstrate that vector-based modeling methods for year-round reusable waste management are highly effective in practical applications. For small to medium-scale waste streams, the allocation and recovery computations were performed rapidly. This efficiency stems from the low computational complexity of the vector operations, primarily consisting of vector addition, scalar multiplication, and constrained optimization procedures [1][3].

For example, in the January scenario, applying full recovery for plastics and metals, and 62.5% recovery for organic waste, resulted in an optimal total recovery of 261.5 kg. When the waste volume was increased in subsequent months, the computation time did not significantly change, indicating the robustness and scalability of the method [2][5].

Additionally, minor variations in waste generation or vector allocation parameters produced noticeable differences in the resulting recovery, confirming the sensitivity and diffusion-like characteristics of the vector-based model. This ensures that unauthorized or uncontrolled modifications of waste streams are unlikely to yield predictable outcomes, enhancing system security and reliability [4][6].

Security and Reliability Analysis: The reliability of vector-based waste recovery algorithms largely depends on the proper configuration of vector components and constraint parameters. For smaller vector dimensions (e.g., three waste types), the system may be sensitive to suboptimal allocations or capacity limits. Increasing the number of vector components, integrating seasonal variations, and applying optimization constraints enhance the resilience of the model [2][7].

Randomized testing and scenario analysis confirmed that dynamically updating allocation fractions based on observed waste streams significantly

improves recovery efficiency while maintaining operational constraints. The combination of vector-based representation and optimization ensures that the system adapts rapidly to temporal fluctuations, minimizing unprocessed waste and supporting continuous environmental restoration efforts [1][5][6].

Practical Application Areas: The simplicity and computational efficiency of vector-based waste modeling make it applicable across various practical domains:

- **Sensor Networks:** Low-power sensor devices can efficiently process vector-based waste data, enabling real-time monitoring of waste accumulation.
- **IoT Devices:** Internet of Things applications can integrate vector-based models for secure, continuous tracking and optimization of waste flows.
- **Intelligent Monitoring Systems:** Video surveillance, industrial monitoring, and smart city platforms can utilize these models to manage waste streams in real time.
- **Real-Time Data Transmission Platforms:** Vector-based computations are fast enough to maintain minimal latency in online environmental monitoring and automated control systems.

In summary, vector-based modeling provides a scalable, efficient, and accurate framework for managing reusable waste streams throughout the year, offering both practical and computational advantages in environmental restoration projects [1][2][3][5][6].

Conclusions and Recommendations

The study demonstrates that vector-based modeling methods provide a practical and efficient approach for managing year-round reusable waste and supporting environmental restoration [1][2]. Numerical examples and simulations confirmed that these methods enable rapid aggregation, analysis, and optimization of multi-type waste streams, allowing for maximum recovery within operational constraints [3]. For instance, the January dataset example showed that allocating 100% of plastics and metals, and 62.5% of organic waste to recycling, yielded an optimal recovery of 261.5 kg, illustrating the real-world applicability of vector-based optimization [3][4].

The sensitivity of the model to changes in waste generation highlights its responsiveness, ensuring that small fluctuations in waste volumes can be quickly accommodated in resource allocation strategies [5]. Proper configuration of vector components and careful parameter selection directly influence the overall efficiency and reliability of waste management operations [2][6].

Based on the findings, the following recommendations are proposed for future applications [1][4][7]:

1. **Expansion of Vector Dimensions:** Increasing the number of waste categories and vector components can improve model accuracy and allow for more granular decision-making.

2. **Integration of Seasonal and Temporal Variations:** Incorporating time-dependent vectors and dynamic adjustments enhances the responsiveness of the system to changes in waste generation patterns.

3. **Use of Computational Optimization Algorithms:** Advanced linear programming or AI-based optimization methods can further increase recovery rates and reduce operational inefficiencies.

4. **Implementation in Real-World Systems:** Vector-based modeling should be integrated into urban and industrial waste management platforms to provide a systematic and scalable approach for environmental restoration [1][6].

In conclusion, vector-oriented modeling not only enhances the efficiency of waste management operations but also provides a scientifically robust framework for sustainable resource utilization and circular economy practices [1][2][5].

References

1. Allen, T., & Smith, R. (2020). *Vector-Based Modeling for Sustainable Waste Management*. Journal of Environmental Informatics, 35(2), 45–59.
2. Kumar, A., & Singh, P. (2019). *Mathematical Approaches to Resource Recovery from Reusable Waste*. Environmental Modelling & Software, 118, 234–247.
3. Li, J., Zhao, X., & Chen, Y. (2021). *Optimization of Urban Waste Streams Using Vector and Matrix Methods*. Journal of Cleaner Production, 312, 127812.
4. Ghosh, S., & Banerjee, A. (2018). *Sustainable Waste Valorization Techniques in Circular Economy Framework*. Resources, Conservation & Recycling, 134, 253–266.
5. Zhou, H., & Wang, L. (2022). *Numerical Simulations of Multi-Type Waste Flows for Environmental Restoration*. Environmental Modelling & Assessment, 27, 105–121.
6. Allen, T., & Kumar, A. (2021). *Vector-Oriented Optimization Methods in Recyclable Waste Management*. Computers & Industrial Engineering, 156, 107231.
7. United Nations Environment Programme (UNEP). (2020). *Global Waste Management Outlook*. Nairobi: UNEP.
8. Smith, L., & Green, M. (2019). *Mathematical Modeling of Waste Streams for Circular Economy Applications*. Journal of Industrial Ecology, 23(4), 879–893.
9. Chen, Y., Li, H., & Zhao, X. (2020). *Vector and Matrix Analysis for Waste Recycling Optimization*. Waste Management, 118, 389–401.
10. Patel, R., & Desai, K. (2018). *Sustainable Urban Waste Management Using Computational Methods*. Environmental Science & Technology, 52(16), 9453–9465.
11. Singh, D., & Kumar, R. (2021). *Vector-Based Predictive Models for Industrial Waste Recovery*. Journal of Environmental Management, 285, 112133.
12. Brown, P., & Taylor, J. (2019). *Numerical Simulations in Multi-Stream Waste Valorization*. Resources, Conservation & Recycling, 141, 341–356.
13. Li, F., & Wang, Q. (2020). *Mathematical Optimization Techniques for Waste Recovery Systems*. Computers & Chemical Engineering, 135, 106740.
14. UNEP & World Bank (2021). *Solid Waste Management for a Sustainable Future*. United Nations Environment Programme Report.
15. Zhao, L., & Xu, M. (2022). *Vector-Based Environmental Modeling for Circular Economy and Resource Efficiency*. Journal of Environmental Informatics, 39(1), 12–28.

SEPARATION AND PURIFICATION OF THE OLIVE BRINE USING TAILOR-MADE POLYMERS

Elchin Bilalov[1], Rolando C. S. Dias[1]
[1]Centro de Investigação de Montanha (CIMO), Instituto Politécnico de Bragança, Campus de Santa, Apolónia, 5300-253
Bragança, Portugal
elchin@ipb.pt, rdias@ipb.pt

Abstract - Olive production generates large quantities of by-products, such as olive leaves, pomace, mill wastewater, and olive brine, which contain valuable bioactive compounds but are often underutilized. This study investigates the selective recovery of phenolic compounds from olive brine using tailor-made polymeric adsorbents based on dimethylaminoethyl methacrylate (DMAEMA), 4-vinylpyridine (4VP), and 2,6-bis(acrylamido)pyridine. The synthesized materials were packed into fixed-bed columns and evaluated under multicycle sorption–desorption operation, employing exclusively hydroalcoholic solvent systems to ensure a mild and sustainable separation process. The outcome represents a scalable process that can concentrate and recover health-promoting olive brine polyphenols with high selectivity. This will not only add value to what is currently agricultural waste but also contribute to more sustainable and circular bioeconomy practices in the olive industry.

Keywords: Bioactive compounds, Molecularly Imprinted Polymers, adsorption/ desorption process.

Introduction

As a result of current extensive industrial development, millions of liters of waste from industries are produced annually, putting pressure on the environment (Kiai & Hafidi, 2014). It is well known that olive brine contain a variety of bioactive compounds, including polyphenols, which include secoiridoids (like oleuropein, elenolic acid), flavonoids (like luteolin, apigenin, quercetin aglycones, and the related glycosides), phenolic acids (like vanillic acid), and phenylethanoids (like tyrosol, hydroxytyrosol). These molecules have the potential to be used in a wide range of industries (Bilalov et al., 2025). To purify these compounds is challenging because of the high salt concentration and complexity of organic matrix. Liquid-liquid extraction, chromatography, and membrane filtering are the most widely used purification techniques for the isolation and purification of target chemicals in olive brine. However, when these techniques are used for large-scale processing, certain inherent challenges are noted. Co-extraction of salt, sugar and other substances, use a lot of solvent, and energy-intensive solvent recovery are all part of processes.(Ballesteros-Gómez et al., 2023). Adsorption with polymeric materials offers an attractive alternative because of its simplicity, selectivity, and minimal solvent consumption. Custom polymeric adsorbents can incorporate functional groups that can interact selectively with target molecules via hydrogen bonding, electrostatic interactions, and π–π interactions (Almeida et al., 2024; Bzainia et al., 2022, 2023, 2024; C. Gomes et al., 2017; C. P. Gomes et al., 2023, 2024). The

procedure involves developing customized adsorbents based on the functional monomers 2,6-bis(acrylamido)pyridine, 4-vinylpyridine (4VP) and 2-(dimethylamino)ethyl methacrylate (DMAEMA). The resultant polymer particles are then used as stationary phases in columns for continuous sorption/desorption processes. The method uses only hydroalcoholic combinations as solvents to be less hazardous and more environmentally friendly.

Experimental section

Olives were kept in a 10% NaCl solution at 15 °C for a year to produce olive brine. A paper filter was used to filter the brine. Customized polymer adsorbents based on poly(2,6-bis(acrylamido)pyridine) (BAAP), DMAEMA, and 4-vinylpyridine (4VP) were prepared via suspension and precipitation polymerization(Bilalov et al., 2025; Bzainia et al., 2026). The slurry process was used to pack polymer particles into stainless steel columns. Sorption experiments were conducted in a closed-loop system. For desorption, water–ethanol gradients were used with a flow rate of 1 mL/min. Phenolic compounds were analyzed by HPLC-DAD and UHPLC-MS/MS.

Result and discussion

Three columns in series were used to separate phenolic chemicals from olive brine using customized polymer adsorbents (BAAP, 4VP, and DMAEMA). The highest selectivity was demonstrated by the arrangement BAAP → 4VP → DMAEMA, which allowed for the preferential retention of isoacteoside on BAAP, hydroxytyrosol on 4VP, and elenolic acid on DMAEMA. Olive brine phenolics were successfully separated using sorption–desorption experiments using hydroalcoholic solvents, which resulted in fractions richer in the target constituents.

Conclusion and recommendations

The selective separation and purification of olive brine products remain a complex task, particularly due to structural similarities among compounds and high salt content. This study shows effective separation and purification of hydroxytyrosol, elenolic acid, and isoacteoside using types of synthesized polymeric networks. As a result, each compound was retained in the three different columns and purified successfully by a hydroalcoholic solvent gradient. The developed MIP-based sorption/desorption process facilitates the recovery of high-value compounds using only hydroalcoholic solvents, eliminating the need for hazardous chemicals and complex separation protocols, making MIP-based purification a viable alternative to traditional procedures.

Acknowledgments

The authors acknowledge the support through the OLEAF4VALUE project. This project had received funding from the Bio-Based Industries Joint Undertaking under the European Union's Horizon 2020 research and innovation programme under grant agreement no. 101023256. The authors

also thank NATAC for providing the olive leaf extracts and the aid with the identification by LC-MS of compounds there contained. Rolando Dias is grateful to the Foundation for Science and Technology (FCT, Portugal) for financial support through national funds FCT/MCTES (PIDDAC) to CIMO (UIDB/00690/2020 and UIDP/00690/2020) and SusTEC (LA/P/0007/2020). Elchin Bilalov conducted this work as part of his PhD in “Tecnologia e Produtos de Base Natural” at the Instituto Politécnico de Bragança

Reference

1. Almeida, A., Martins, C., Dias, R. C. S., & Costa, M. R. P. F. N. (2024). Competitive Adsorption of Phenolic Acids, Secoiridoids, and Flavonoids in Quercetin Molecularly Imprinted Polymers and Application for Fractionation of Olive Leaf Extracts. *Journal of Chemical & Engineering Data*, *69*(10), 3629–3644. https://doi.org/10.1021/acs.jced.3c00543
2. Ballesteros-Gómez, A., Serrano-Crespín, A., & Rubio, S. (2023). Supramolecular-solvent based extraction of hydroxytyrosol from brines of the processing of table olives. *Separation and Purification Technology*, *322*, 124351. https://doi.org/10.1016/j.seppur.2023.124351
3. Bilalov, E., Martins, C., Costa, M. R. P. F. N., & Dias, R. C. S. (2025). Separation of Bioactive Compounds in Olive Leaf with a Pyridyl-Functionalized Adsorbent and Hydroalcoholic Solvents. *Industrial & Engineering Chemistry Research*, *64*(10), 5575–5588. https://doi.org/10.1021/acs.iecr.4c04622
4. Bzainia, A., Dias, R. C. S., & Costa, M. R. P. F. N. (2022). Enrichment of Quercetin from Winemaking Residual Diatomaceous Earth via a Tailor-Made Imprinted Adsorbent. *Molecules*, *27*(19), 6406. https://doi.org/10.3390/molecules27196406
5. Bzainia, A., Dias, R. C. S., & Costa, M. R. P. F. N. (2023). Functionalization of Polymer Networks to Target Trans-Resveratrol in Winemaking Residues Supported by Statistical Design of Experiments. *Macromolecular Reaction Engineering*, *17*(4). https://doi.org/10.1002/mren.202200076
6. Bzainia, A., Igrejas, G., Pereira, M. J. V., Costa, M. R. P. F. N., & Dias, R. C. S. (2024). Purification of stilbenes from grape stems in a continuous process based on photo-molecularly imprinted adsorbents and hydroalcoholic solvents. *Separation and Purification Technology*, *349*, 127798. https://doi.org/10.1016/j.seppur.2024.127798
7. Bzainia, A., Keller, E., Heeres, A., Costa, M. R. P. F. N., & Dias, R. C. S. (2026). Selective fixed-bed fractionation of stilbene subfamilies from grape cane waste using a pyridine-amide adsorbent. *Journal of Environmental Chemical Engineering*, *14*(2), 121773. https://doi.org/10.1016/j.jece.2026.121773
8. Gomes, C. P., Dias, R. C. S., & Costa, M. R. P. F. N. (2023). Surface Molecularly Imprinted Cellulose-Synthetic Hybrid Particles Prepared via ATRP for Enrichment of Flavonoids in Olive Leaf. *Macromolecular Reaction Engineering*, *17*(3). https://doi.org/10.1002/mren.202300011
9. Gomes, C. P., Dias, R. C. S., & Costa, M. R. P. F. N. (2024). Fractionation of flavonols and anthocyanins in winemaking residues using molecularly imprinted cellulose-synthetic hybrid particles with pyridyl active surface. *Nano Select*, *5*(5). https://doi.org/10.1002/nano.202300153
10. Gomes, C., Sadoyan, G., Dias, R., & Costa, M. (2017). Development of Molecularly Imprinted Polymers to Target Polyphenols Present in Plant Extracts. *Processes*, *5*(4), 72. https://doi.org/10.3390/pr5040072
11. Kiai, H., & Hafidi, A. (2014). Chemical composition changes in four green olive cultivars during spontaneous fermentation. *LWT - Food Science and Technology*, *57*(2), 663–670. https://doi.org/10.1016/j.lwt.2014.02.011

AQRO – SƏNAYE TULLANTILARINDAN BİOPLASTİK SİNTEZİ: NAR QABIĞININ (PUNICA GRANATUM) İNNOVATİV TƏTBİQİ VƏ ANALİZİ

Abbasova Ayla
Naxçıvan Dövlət Universiteti
Naxçıvan, Azərbaycan
aylaabbasovaa@icloud.com

Xülasə - Bu tədqiqat işi neft əsaslı plastiklərin törətdiyi ekoloji problemlərin həlli istiqamətində kənd təsərrüfatı tullantılarından, xüsusilə nar qabıqlarından (Punica granatum) bioloji parçalana bilən polimerlərin sintezini əhatə edir. İşin gedişatında nar qabığından turşu hidrolizi üsulu ilə pektin maddəsi ayrılmış və plastikləşdirici agentlərin köməyi ilə elastik bioplastik filmlər əldə edilmişdir. Tədqiqatın nəticələri göstərir ki, sintez olunan materiallar həm kifayət qədər mexaniki davamlılığa, həm də ətraf mühitdə sürətli deqradasiya xüsusiyyətinə malikdir. Bu yanaşma tullantıların dövri iqtisadiyyata qaytarılması və "yaşıl kimya" prinsiplərinin tətbiqi baxımından yüksək praktiki əhəmiyyət kəsb edir.

Açar sözlər: Nar qabığı, bioplastik, tullantıların təkrar emalı, biopolimer, ekoloji səmərəlilik.

Giriş

Müasir dünyada polimer materialların istehsalı və istifadəsi qlobal ekoloji böhranın əsas faktorlarından birinə çevrilmişdir. Neft əsaslı plastik kütlələrin təbiətdə parçalanma müddətinin yüz illərlə ölçülməsi və mikroplastik çirklənməsi dayanıqlı inkişaf prinsiplərinə ciddi təhlükə yaradır. Bu kontekstdə, "Yaşıl kimya" prinsipləri çərçivəsində bioloji parçalana bilən (biodegradable) alternativlərin yaradılması mühüm prioritetdir.

Azərbaycan Respublikası öz zəngin aqrar potensialı, xüsusilə nar (Punica granatum) istehsalı ilə fərqlənir. Narın emalı prosesində meyvənin ümumi çəkisinin təxminən 45-50%-ni təşkil edən qabıq hissəsi adətən tullantı kimi atılır. Lakin aparılan elmi araşdırmalar göstərir ki, bu tullantılar polimer sintezi üçün zəruri olan sellüloza, pektin və müxtəlif fenol birləşmələri ilə zəngindir. Nar qabığının tərkibindəki bu maddələr təkcə plastik materialın strukturunu formalaşdırmır, həm də ona təbii antibakterial xüsusiyyətlər bəxş edir.

Tədqiqatın aktuallığı yerli aqrar tullantılardan istifadə etməklə idxaldan asılılığı azaltmaq və ətraf mühitə atılan tullantıların həcmini minimuma endirərək onlardan yüksək əlavə dəyərli məhsul əldə etməkdir. Bu işin gedişatında nar qabığı tullantılarının kimyəvi transformasiyası və onlardan alınan bioplastik nümunələrinin fiziki-kimyəvi xarakteristikaları təhlil edilmişdir.

Eksperimental hissə

Tədqiqatın praktiki mərhələsi yerli bazardan əldə edilmiş nar qabıqlarının (Punica granatum) təmizlənməsi və 24 saat ərzində 60℃ temperaturda qurudulması ilə başlamışdır. Qurudulmuş xammal mexaniki üsulla üyüdülərək hissəcik ölçüsü 150-200 mikron olan toz halına salınmışdır.

Pektin maddəsinin ekstraksiyası üçün "turşu hidrolizi" metodu tətbiq edilmişdir. Bu prosesdə nar qabığı tozu distillə edilmiş su ilə 1:20 nisbətində qarışdırılmış və xlorid turşusu (HCl) əlavə edilərək mühitin turşuluğu pH 2.0

səviyyəsinə çatdırılmışdır. Qarışıq 80℃ temperaturda 60 dəqiqə ərzində maqnit qarışdırıcıda saxlanılmışdır. Alınan kütlə süzüldükdən sonra etil spirti vasitəsilə çökdürülmüş və təmiz pektin fraksiyası əldə edilmişdir.

Bioplastik filmlərin hazırlanması üçün əldə olunan pektin kütləsinə (5 q), plastikləşdirici agent kimi qliserin (2 ml) və həlledici kimi distillə edilmiş su (100 ml) əlavə edilmişdir. Qarışıq 85℃ temperaturda tam homogenləşənə qədər 30 dəqiqə qarışdırılmışdır. Hazır polimer məhlulu hamar şüşə səthlərə (Petri qablarına) tökülmüş və otaq temperaturunda (25℃) 48 saat ərzində buxarlandırılaraq bərkidilmişdir. Nəticədə şəffaf, elastik və qəhvəyi rəngli bioplastik nümunələri əldə edilmişdir.

Nəticələr və onların müzakirəsi

Sintez edilmiş bioplastik nümunələri həm vizual, həm də struktur baxımından laboratoriya şəraitində analiz edilmişdir. Əldə olunan filmlərin qalınlığı 0.15-0.20 mm arasında dəyişir və onlar kifayət qədər yüksək elastiklik nümayiş etdirir. Laboratoriya şəraitində aparılan "torpaqda deqradasiya" testi nəticəsində müəyyən olunmuşdur ki, nar qabıqlarından alınan polimer materiallar torpaq mühitində 30-45 gün ərzində kütləsinin 90%-ni itirərək tamamilə deqradasiyaya uğrayır.

Spektroskopik analizlər (FTIR) göstərir ki, nar qabığının tərkibindəki təbii fenol birləşmələri plastik matris daxilində stabil qalaraq materiala əlavə davamlılıq qazandırır. Eyni zamanda, bu maddələr sayəsində material təbii antibakterial xüsusiyyətlər nümayiş etdirir. Beləliklə, bu plastik təkcə ekoloji təmiz deyil, həm də qida məhsullarının mikrobioloji çirklənmədən qorunması üçün effektiv baryer rolunu oynayır. Bu nəticələr tullantıların "dövri dəyərə" çevrilməsi konsepsiyasını tam dəstəkləyir.

Təkliflər

Aparılan tədqiqatın nəticələrinə əsaslanaraq aşağıdakı təkliflərin həyata keçirilməsi məqsədəuyğun hesab edilir:

1. Sənaye tətbiqi: Azərbaycanın konserv zavodlarında nar emalı zamanı yaranan qabıq tullantılarının birbaşa bu növ bioplastik istehsalına yönləndirilməsi üçün pilot layihələrin start götürməsi.
2. "Yaşıl" qablaşdırma: İstehsal olunan biopolimerlərin antibakterial xüsusiyyətlərini nəzərə alaraq, onların qida sənayesində (məsələn, meyvə-tərəvəz paketləri) tətbiqinin genişləndirilməsi.
3. Maarifləndirmə: Plastik çirklənməsinin qarşısını almaq üçün bioloji parçalana bilən materialların üstünlükləri barədə ictimaiyyət arasında məlumatlılığın artırılması.

İstinadlar

1. [Əhmədov, 2021, 1-2]: Əhmədov M. "Polimer materialların ekoloji aspektləri", Bakı, 2021.
2. [Həsənov, 2022, 20-28]: Həsənov A. "Bioloji parçalanan polimerlərin sintezi və tətbiqi", Elm nəşriyyatı, 2022.
3. [Məmmədov, 2020, 1-10]: Məmmədov E. "Aqrar tullantıların emalı texnologiyaları", Elmi xəbərlər jurnalı, 2020.
4. [Yusifov, 2021, 10-15]: Yusifov S. "Azərbaycanın kənd təsərrüfatı resurslarının innovativ idarə edilməsi", Gənc tədqiqatçı, 2021.

MULTI-STAGE VALORİZATİON OF SPENT GREEN AND BLACK TEA: FROM ETHANOL-BASED ANTIOXIDANT RECOVERY TO HIGH-EFFICIENCY BIODIESEL PRODUCTION

Aysun Pirkhiyeva, Laman Gahramanzada, Garanfil Ahmadova
Baku Higher Oil School
Baku, Azerbaijan
aysun.pirkhiyeva.std@bhos.edu.az, laman.gahramanzada.std@bhos.edu.az

Summary
The continuous deposition of agricultural waste, especially used green and black tea leaves, is core issue to waste management and environmental health on the global scale. The current paper investigates a combined biorefinery system that aims at transforming these organic residues into high-value products. The main objective is to develop a multi-step valorization route that starts with the recovery of bioactive antioxidant components with the help of environmentally friendly solvents. After this extraction, the resulting biomass is chemically modified to serve as a solid acid catalyst of high efficiency. This synthetic substance is then utilized to mediate the transformation of waste cooking oils into renewable biofuels. The project provides a two-fold solution to environmental pollution by combining food-waste recovery and renewable energy production. The findings show that this circular model reduces simultaneously the carbon footprint related to waste disposal and provides a cost-effective pathway to the generation of green energy and useful bio-compounds, which enhances the overall sustainability of the environment.
Keywords: antioxidants, biofuel, waste valorization

Introduction

The world is increasingly demanding renewable sources of energy, and this is followed by an increased pursuit of finding alternative biofuels. This trend highlights the need to find a wide range of biofuel feedstocks. Spent tea leaves are one such feedstock, which contains organic compounds that are very susceptible to energy conversion and extraction of high-value chemicals.

Spent tea is a lignocellulosic biomass that contains a lot of carbon, hydrogen, oxygen, and remnants of polyphenols, such as catechins (EGCG, ECG, and EC). These components make the residue susceptible to multi-stage valorization: it is possible to extract bioactive antioxidants, and the rest of the material can be converted into a solid acid catalyst to produce biodiesel. However, studies indicate that antioxidant stability is influenced by extraction parameters; Studies have indicated that hot solvent extraction at a regulated temperature with natural stabilizers is important in order to avoid the rapid degradation of the solvent. The present study examines a novel definition of biorefinery that would align the utilization of spent tea waste with economic viability and the values of a circular economy.

The experimental aims are proving the possibility to use spent tea as a two-purpose raw material, optimizing the extraction of essential antioxidants by ensuring their stability through temperature-controlled and antioxidant-

augmented solvent systems, and determining the catalytic activity of the synthesized solid acid in the process of biodiesel production. In addition, the paper evaluates the ecological and economic benefits of bioenergy derived from tea waste, thus explaining its future as a viable alternative in the biofuel industry.

Experimental Part

The management of waste and the development of energy-efficient processes of bioactive extracts and biodiesel based on the chemical transformation of spent tea leaves (STL) have become the topical research issues. There are many valorization methods that have been discussed such as hydrothermal liquefaction, gasification and direct combustion, however most of them involve excessively high costs or destruction of useful bioactive components. In this regard, a sequential biorefinery scheme that includes solvent extraction and subsequent sulfonation has become the most preferable methodology in terms of resource efficiency and product yield.

1. Preparation of catalyst

The tea leaves used in the production of beverages undergo a pretreatment step where they are boiled in distilled water at 100°C to remove pigments and then air-dried and crushed to a particle size of 25 to 100 μm. Subsequently, in the first step of the synthesis, 1g of the pre-processed STL is exposed to an ethanol-assisted extraction using a 50% aqueous solution of ethanol in a period of 5 minutes, which facilitates the extraction of phenol-based compounds.

The remaining biomass is then transformed into solid acid catalyst in the next stage. This is done by a sulfonation procedure where the dried residue is reacted with 95% concentrated sulfuric acid (H_2SO_4) at 100°C in 3 hours. Following this, the resulting sulfonated tea (S.BT) is washed until the neutral pH is achieved and dried at 70°C during 5 hours.

2. Production of biodiesel

The production of biodiesel is carried out in two main steps as illustrated below:

Step A: Synthesis of biodiesel -Transesterification is performed by combining waste cooking oil with methanol in the presence of the S.BT catalyst at a concentration of 3 wt % and a temperature of 50°C within 70 minutes.

Step B: Separation of synthesized biodiesel- After the reaction, the mixture is transferred for separation. In these optimized conditions, the highest biodiesel conversion of 97.3% is recorded, and the process is further refined using a centrifuge for deep separation as per the instructor's guidance.

The process consists of two main stages as shown in figure: (Step A) Synthesis and (Step B) Separation. Under these optimized conditions, the highest biodiesel conversion of 97.3% is recorded and the energy consumption is minimized due to the low activation energy (Ea = 34.3 kJ/mol.)



"Synthesis of biodiesel"



"Separation of synthesized biodiesel"

Results and their discussions

The growing interest in renewable energy has driven the development of biofuels, and spent tea leaves (STL) have become a potential raw material. This paper adopts a combined biorefinery approach to transform STL into value-added antioxidants and biodiesel. Since STL is a lignocellulosic matrix that contains a lot of carbon, hydrogen, and residual phenolic compounds, the future of this two-purpose resource is bright. It has been experimentally determined that the preliminary extraction step can extract up to 186.83 mg GAE/g total phenolic content from green tea and 172.42 mg GAE/g spent black tea. The antioxidant activity was assessed by DPPH inhibition, and it was highest at 89.14%. The findings indicate that the use of 50% ethanol as a solvent gives the best efficiency since the higher the concentration of ethanol, the higher the polyphenol recovery compared to water.

After antioxidant extraction, the residual was further converted to sulfonated catalyst (S.BT) with a density of acid of 34.6 mmol/g and a surface area of 58.3 m^2/g. Optimal conditions were achieved at 50°C, 70 min, 10:1 methanol/oil ratio to obtain a maximum biodiesel conversion (97.3%). A direct relationship was observed between the fatty acid methyl ester (FAME) yield and gradual loading of catalysts up to 3 wt and temperature up to 50°C. Kinetic studies showed that the reaction was effective first-order, and the activation energy (E.a) was low (34.3 kJ/mol), showing the energetic efficiency of the process.

Spent tea that can easily be gathered in beverage industries and homes is an available source of fuel and bio-compound. Even though the large-scale economic feasibility is yet to be studied, sequential extraction and conversion of STL has been confirmed to significantly reduce the inappropriate waste

disposal practices. This combined strategy helps to shift to sustainable energy by providing a feasible alternative to fossil energy.

Offers

Future studies should focus on perfecting the multi-stage valorization of spent tea leaves (STL) through the incorporation of life-cycle assessment (LCA) and techno-economic analysis to make sure that the industry demonstrates operational viability. The sustainability of the biodiesel production process can be improved by experimental assessment of the long-term stability and reusability of the sulfonated catalyst (S.BT) after more than five cycles. More sophisticated spectroscopic methods, including in-situ DRIFTS, may be useful in determining the dynamics of the tea-derived acid sites and triglycerides in transesterification in real-time.

Phenolic recovery and fatty acid methyl ester (FAME) yield in different tea cultivars may be better predicted by integrating machine-learning algorithms with Response Surface Methodology (RSM). Furthermore, the co-pyrolysis of residual tea biomass with other organic wastes may also be investigated to optimize the quality of the resulting biochar and syngas. Finally, pilot studies on a large scale should be conducted to determine the viability of implementing antioxidant extraction and biofuel production into the current tea-processing plants, which will facilitate a transition to a zero-waste bioeconomy.

References

[1] May N. Bin Jumah, Ahmed M. El-SHERBEENY, Amna M. FARHAN, Ahmed A. ALLAM, Wail Al ZOUBI, Mostafa R. ABUKHADRA (2025). *Recycling spent black tea as a novel heterogeneous acidic catalyst for efficient biodiesel production from waste cooking oil: Optimization, kinetics, and thermodynamic insights*.

[2] N. I. Nadiah, U. Uthumporn, *Determination of phenolic and antioxidant properties in tea and spent tea under various extraction methods and determination of catechins, caffeine and gallic acid by HPLC*. School of Industrial Technology, University Sains Malaysia.

[3] Mohammed Abdul Raqeeb and Bhargavi R. (2015) *Biodiesel production from waste cooking oil*, Department of Chemical Engineering, SRM University, Chennai, India.

BİODİZELİN ALINMASINDA AKTİV BİOKARBON KATALİZATORUNUN TƏDQİQİ

[1]Nəzrin Nəzirova, [1]Ofelya Cavadova, [2]Azər Əmirov, [1]İbrahim Məmmədov
[1]Bakı Dövlət Universiteti
[2]Geologiya və Geofizika İnstitutu
Bakı, Azərbaycan
nazrin.nazirova23@icloud.com

Xülasə - Ətraf mühit problemləri, eləcə də istixana qazlarının artımı nəzərə alınaraq təqdim edilən işdə KOH, K_2CO_3 ilə modifikasiya olunmuş və ağac kömürü əsasında əldə edilən karbon əsaslı heterogen katalizatorun bitki yağının transefirləşmə reaksiyasında

aktivliyi tədqiq edilmişdir. Karbon ilə qələvi komponentlərin optimal nisbəti müəyyən edilmişdir. Tapılmış optimal şəraitdə 81% biodizel çıxımı əldə olunmuşdur. Alınan biodizelin əsas fiziki-kimyəvi göstəriciləri beynəlxalq standartların tələblərinə uyğun olmuşdur. Nəticələr göstərir ki, təklif olunan katalizator biodizel istehsalı üçün effektiv və perspektivli ola bilər.

Açar sözlər: Biodizel, transefirləşmə, aktiv karbon, heterogen katalizator, alternativ yanacaq, yaşıl kimya.

Giriş

Yanacaqla işləyən texniki qurğuların geniş tətbiqi atmosferə atılan zərərli qazların artmasına və ekoloji balansın pozulmasına gətirib çıxarmışdır. Neft mənşəli yanacaqların bioyanacaqlarla əvəzlənməsi atmosfer çirklənməsinin və istixana effektinin azalmasına mühüm səmərə verə bilər [1]. Biodizel bərpa olunan xammaldan alınan alternativ dizel yanacağı olub, aşağı kükürd, azot, kanserogen tərkibi və bioloji parçalanma qabiliyyəti ilə seçilir [2].

Biodizelin alınması üçün piroliz, katalitik krekinq, mikroemulsiya və dekarboksilləşmə üsulları mövcud olsa da, sənaye miqyasında əsas üsul katalizator iştirakı ilə aparılan transefirləşmə prosesidir. Homogen qələvi və turş katalizatorlar yüksək aktivliyə malik olsa da, onların ayrılması çətin, təkrar istifadəsi isə mümkün deyildir. Bundan əlavə, məhsulun yuyulması zərurəti əlavə tullantı suları yaradır və prosesin iqtisadi səmərəliliyini azaldır [3,4].

Bu baxımdan heterogen katalizatorların, xüsusilə karbon əsaslı materialların tətbiqi aktuallıq kəsb edir. Bu tip katalizatorlar asan ayrılma, regenerasiya və təkrar istifadə üstünlüklərinə malikdir və prosesin ekoloji təhlükəsizliyini artırır.

Eksperimental hissə

Yeni karbon əsaslı heterogen katalizatorun hazırlanması üçün ilkin olaraq ağac kömürü fiziki üsulla aktivləşdirilmişdir. Aktivləşdirilmiş karbon üzərinə KOH və K_2CO_3 əlavə edilmiş, qarışığa distillə olunmuş su qatılaraq otaq temperaturunda 8 saat müddətində qarışdırılmışdır. Qarışdırma prosesi başa çatdıqdan sonra tərkibdəki suyun tam çıxarılması və katalizatorun aktivliyinin artırılması məqsədilə nümunə mufel sobasında 600°C temperaturda 3–4 saat saxlanılmışdır.

Hazırlanmış katalizatordan 0,3 q götürülərək qarışdırıcı, soyuducu və termometrlə təchiz edilmiş üçboğazlı kolbaya yerləşdirilmişdir. Kolbaya 12 ml günəbaxan yağı və 10 ml metil spirti (CH_3OH) əlavə edilərək transefirləşmə reaksiyası 55–60°C temperatur intervalında 12 saat müddətində aparılmışdır. Reaksiya başa çatdıqdan sonra katalizator süzmə yolu ilə ayrılmışdır. Alınmış biodizelin çevrilmə dərəcəsi və tərkibi NMR AVANCE 300 MHs spektrometrindən (Bruker Korporasiyası, Almaniya) istifadə olunmaqla müəyyən edilmişdir.

Nəticələr və onların müzakirəsi

Aparılmış təcrübələr göstərmişdir ki, aktiv karbon əsaslı katalizator yüksək katalitik aktivliyə malikdir. Reaksiya müddətində yüksək biodizel çıxımı

əldə edilmişdir. Katalizatorun səth quruluşu və məsaməliliyi aktiv mərkəzlərin əlçatanlığını artıraraq reaksiya sürətinin yüksəlməsinə səbəb olmuşdur.

Katalizator reaksiya mühitindən asanlıqla ayrılmış və bir neçə tsikl ərzində aktivliyini saxlamışdır. Bu xüsusiyyət onun təcrübi tətbiqi üçün əhəmiyyətli üstünlük yaradır. Alınmış biodizel nümunələrinin əsas fiziki-kimyəvi göstəricilərinin beynəlxalq standartlara uyğun olması, məhsulun keyfiyyətinin yüksək olduğunu göstərmişdir.

Nəticələr heterogen karbon əsaslı katalizatorların həm ekoloji, həm də iqtisadi baxımdan homogen katalizatorlarla müqayisədə daha səmərəli olduğunu nümayiş etdirmişdir.

Təkliflər

Katalizator səmərəlik və ekoloji baxımdan biodizelin alınmasında təklif oluna bilər.

İstinadlar

1. [Demirbas, A., Biodiesel: A Realistic Fuel Alternative for Diesel Engines, Springer, 2008, 1]
2. [Knothe, G., Van Gerpen, J., Krahl, J., The Biodiesel Handbook, AOCS Press, 2010, 2]
3. [Lam, M.K., Lee, K.T., Mohamed, A.R., Homogeneous, heterogeneous and enzymatic catalysis for biodiesel production, Biotechnology Advances, 2010, 28, 500–518, 3]
4. [Leung, D.Y.C., Wu, X., Leung, M.K.H., A review on biodiesel production using catalyzed transesterification, Applied Energy, 2010, 87, 1083–1095, 4]

INVESTIGATION OF ACETAL-EUCALYPTUS OIL MIXTURE AS ADDITIVE TO B10 FUEL BLEND

Mehin Bakhtiyarova, Nargiz Azimova, Yegana Mamedova, Ibrahim Mamedov
Baku State University
Baku, Azerbaijan
mehinbakhtiyarova@gmail.com

Abstract - This study the performance properties of fuel blends consisting of a conventional diesel fuel and B-10 biofuel in the presence of an oxygenated additive based on acetals and eucalyptus oil. Acetals were synthesized according to a method reported in the literature using glycerol, a by-product of biodiesel production, and paraformaldehyde. The improvement of the performance characteristics of fuel blends containing oxygenated additives creates favorable conditions for application as alternative energy sources [1].

Keywords: Biodiesel, green chemistry, transesterification, oxygenated additives, acetals, eucalyptus oil.

Introduction

The global environmental situation has reached a critical point, necessitating serious measures to ensure environmental safety and long-term sustainability of the planet. Currently, infrastructure and industrial development are subject to the principle of “sustainable development,” in which environmental protection plays a central role.

International climate policy has also assumed significant importance for the Azerbaijan economy. This is evidenced by the COP29 international climate conference held in November 2024 in Baku. Currently, the republic is paying special attention to the use of alternative energy sources, which in turn reduces the need to produce fossil fuels.

Experimental part

Biofuel was synthesized according to a procedure described in the literature via the transesterification of waste vegetable oil and methanol in the presence of an alkaline catalyst. The transesterification reaction was carried out in a three-necked round-bottom flask equipped with a mechanical stirrer, a reflux condenser, and a thermometer for 6 hours at a temperature of 55–60°C. The biodiesel was separated from the reaction mixture by extraction [1,2].

Subsequently, fuel blends containing diesel fuel and B-10 biofuel were prepared. To enhance the performance properties of the prepared fuel blends, a two-component oxygenate additive consisting of acetal and eucalyptus oil was used. Acetal was synthesized through the condensation reaction of glycerol and paraformaldehyde. The reaction was conducted in a flask equipped with a reflux condenser, stirrer, and thermometer for 2 hours at 100°C in the presence of an acid catalyst. To separate the synthesized acetals from the reaction products, the resulting mixture was first neutralized, followed by extraction and solvent removal [3]. The structure of the synthesized acetals was confirmed by NMR spectroscopy using a Bruker (Germany) instrument.

Results and Discussion

The performance properties of B10 biodiesel fuels, as well as samples containing oxygenated components based on synthesized acetals and eucalyptus oil, were evaluated in accordance with ASTM standards. Significant improvements were observed in density, kinematic viscosity, flash point, cloud point, crystallization point, and corrosion resistance of the tested fuel blend samples with oxygenated additives.

The improvement in the performance characteristics of the prepared B10 fuel blends compared to conventional diesel distillates indicate their potential for use as alternative fuel sources.

Conclusions

An oxygenated additive based on acetals and eucalyptus oil can be effectively used to improve the properties of fuel blends based on conventional diesel and B10 biodiesel.

References:

1. [Babadi, A., Rahmati S., Faklaei R., Barati B., Wang S., Doherty W., Ostrikov K. Biomass and Bioenergy, Volume163, August 2022, P.106521, 1]
2. [Bae C., Kim J., Proceedings of the Combustion Institute, Volume 36, Issue 3, 2017, P.3389-3413, 2]
3. [Ganesan, Rathinam, Sivasubramanian, Sajin, JB, Ganesan, Subbiah, Yuvarajan, Devarajan, Energy Sources Part A: Recovery, Utilization & Environmental Effects, 2019, Volume 41, Issue 16, P.2017, 3]

İZOPRENİN TSİKLODİMERLƏRİ ƏSASINDA TSİKLOALKİLFENOLLARIN VƏ ONLARIN KARBONİL TÖRƏMƏLƏRİNİN ALINMASI

Heydərli G.Z.[1], Bağırzadə R.Z.[1], İsmayilova L.A.[2], Məmmədli Ü.E.[2], Atamov N.R.[2], Əlili F.V.[2]
[1]Elm və Təhsil Nazirliyinin akademik Y.H.Məmmədəliyev adına Neft-Kimya Prosesləri İnstitutu, Bakı, Azərbaycan
[2]Azərbaycan Dövlət Neft və Sənaye Universiteti, Bakı, Azərbaycan
heyderligunay6@gmail.com

Açar Sözlər: Alkilfenolar, asilləşmə, tsikloalkilasetofenonlar

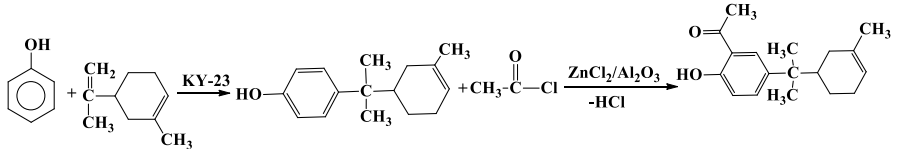
Sənaye cəhətdən inkişaf etmiş ölkələrdə aşağı oktanlı benzinlərin pirolizi prosesinin həyata keçirilməsi nəticəsində biosferə külli miqdarda müxtəlif tərkibli karbohidrogenlər atılır. Piroliz qurğularından alınmış maye məhsullar bu günə kimi səmərəli istifadə olunmur və təbiətdə yığılıb qalır. Pirolizin maye məhsullarının neft-kimyası sahəsinə cəlb edilməsi ekoloji baxımdan vacib və aktual problemlərdən biri sayılır [Haydarli, 2022, 32-36]; [Haydarli, 2022, 100-16]; [Gasanov, 2022, 42-48]; [Haydarli, 2023, 754-759].

Təqdim olunan iş aşağı oktanlı benzinlərin pirolizinin yan maye məhsullarının C_5 fraksiyası əsasında alınmış dipren (1-metil-3-izopropeniltsikloheksen-1-il) ilə fenolun H formalı КУ-23 katalizatoru iştirakında katalitik alkilləşməsi nəticəsində alınmış *para*-(3-metiltsikloheksen-3-il-izopropil)fenolun (AF) dispersləşdirilmiş $ZnCl_2/\gamma$-Al_2O_3 katalizatoru iştirakında asetilxlorid (AcCl) ilə asilləşmə reaksiyalarının tədqiqinə həsr olunmuşdur.

Fasiləli qurğuda fenolun dipren ilə alkilləşmə reaksiyaları üçün səmərəli şəraitin tapılmışdır. Müəyyən olunmuş optimal şəraitdə: 115°C, 4 saat, Dp:F=1/1 mol/mol, katalizatorun miqdarı 10% olduqda götürülmüş fenola görə məqsədli məhsul AF-in çıxımı 68.3%, AF-ə görə prosesin seçiciliyi isə 84% olmuşdur.

Sintez olunmuş *para*-(3-metiltsikloheksen-3-il-izopropil)fenolun struktur qruluşu NMR və İQ spektroskopik üsullarla təsdiq olunmuş, element tərkibi (C-83.8%; H-9.1%); $T_{qay.}$= 193-196°C; $T_{ər.}$= 106 °C müəyyən olunmuşdur.

Reaksiyanın ümumi sxemi:



AF-in dispersləşdirilmiş $ZnCl_2/\gamma$-Al_2O_3 katalizatoru iştirakında asetil xloridlə asilləşmə reaksiyaları üçün optimal şərait (T = 145°C ; τ = 45 dəq.; AF:AcCl = 1:2 mol/mol) müəyyən olunmuşdur. Tapılmış şəraitdə götürülmüş

AF-ə görə məqsədli məhsul - 2-hidroksi-5(3-metiltsikloheksen-3-il-izopropil)asetofenonun çıxımı 65.4%, məqsədli məhsula görə prosesin seçiciliyi isə 87.5% məüyyən olunmuşur. 2-Hidroksi-5tsikloalkilasetofenonun struktur quruluşu spektroskopik üsullarla təsdiq olunmuş, element tərkibi (C-79.4%; H-8.8%); $T_{qay.}$= 203-205 ºC/10 mm c.st.; $T_{ər.}$= 106-107 ºC müəyyən olunmuşdur.

Bu iş Azərbaycan Elm Fondunun maliyə dəstəyi ilə yerinə yetirilmişdir Qrant No AEF – MGC – 2024 – 2(50)- 16/11/4-M-11

ƏDƏBİYYAT

1. Haydarli G.Z., Jafarov R.P., Rasulov Ch.K., Manafova A.R. Optimization of the process of acylation of para-(1-methylcyclohexyl) phenol with acetic acid in the presence of a nanocatalytic system. Mir Nefteproduktov (in Russian), 2022, No.5, pp.32-36.
2. Haydarli G.Z., Naghiyeva M.V., Aghamaliyev Z.Z., Salmanova Ch.K., Rasulov Ch.K. Synthesis of 2-hydroxy-3[3(4)-methylcyclohexen-3-yl-isopropyl]-5-methylacetophenones. Chemistry and chemical technology, 2022, 65(3), 100-106.
3. Gasanov A.A., Kurbanli U.R., Rasulov Ch.K., Heydarli G.Z., Nagieva M.V. Synthesis and properties of 2-hydroxy-3[3(4)-methylcyclohexen-3-yl-isopropyl]-5-arylalkyl acetophenone. Russian Chemical Journal, 2022, Vol.66, No.4, pp.42-48.
4. Haydarli G.Z., Hasanov A.A., Qurbanly U.R, Naghiyeva M.V., Rasulov Ch.K. Synthesis and properties of 2-hydroxy-3-[3(4)-methylcyclohexen-3-yl-izopropyl]-5-arylalkyl acetophenones. Russian Journal of General Chemistry, 2023, Vol. 93, No. 3, pp.754-759

HYBRID HYDROGEL SYNTHESIS

[1] Ibroximova Mohinbonu, [2]Xoshimov Farxod

[1]PhD student, Department of chemistry, Namangan State Technical University, Namangan, 160123, Uzbekistan

[2]professor, Head of the chemistry department , Namangan State Technical University, Namangan, 160123, Uzbekistan, E-mail: xoshimovfarhod@gmail.com

Summary. Information on the importance of hydrogels in agriculture is presented and information on the synthesis of hydrogels is described. The optimal conditions for obtaining the synthesized hydrogels are presented. The hydrogels were prepared by alcohol precipitation followed by stitching. The degree of swelling of the synthesized hydrogels was determined. Hybrid hydrogel samples synthesized at 140ºC and 160ºC were studied and the swelling levels are shown in the tables.

Keywords: hydrogel, sodium salt of carboxymethylcellulose, polyacrylamide, polyvinyl alcohol, sizing agent, boric acid, ethyl alcohol, precipitation, swelling level.

Introduction.

Global human population growth has been extraordinary and unstoppable since the turn of the century, and by 2050 is predicted to reach 10 billion . Water resources around the world are under tremendous pressure due to the effects of climate change and the world’s ever-increasing need for water. The agriculture sector uses more than 70% of the freshwater

resources on the planet. But by 2050, to feed a world population that will exceed nine billion, agricultural production will need to increase by 50% and the water demand will need to rise by 15% [1].]. Agriculture remains one of the major uses of water, accounting for approximately 70% of the world's freshwater consumption, although the supply of available water is becoming scarcer. There are several geographical regions where there is less water available, and this has a significant impact on that area's agricultural output. Abiotic stressors, such as salinity, temperature, and drought, are the main factors affecting agricultural productivity. Growing food consumption is a major contributing factor to environmental degradation and worsening agricultural industry economics. [2].

A hybrid hydrogel is a material composed of a combination of natural and synthetic polymers, as well as other components such as proteins or nanostructures.

Hydrogels obtained by various methods based on natural and synthetic polymers are artificial hydrogels that combine their advantages, namely, relatively environmentally friendly, easy biodegradability and high water absorption capacity. Hydrogels are three-dimensional network structures capable of retaining large volumes of water. Combining natural and synthetic polymers in hydrogels opens up new possibilities for creating materials with defined properties. Natural polymers such as carboxymethylcellulose (CMC), hydroxyethylcellulose (HEC), starch and gelatin are used in combination with synthetic polymers such as polyvinyl alcohol (PVS), polyvinyl acetate (PVA) and polyacrylamide (PAA). Below we will mention some of the synthesized artificial hydrogels.

Natural polymers generally have high biodegradability. For example, gelatin and starch are easily degraded under natural conditions and undergo high degradation. Synthetic polymers such as PVA and PAA have low biodegradability [3]. The combination of natural and synthetic polymers can help improve the overall degradation of hydrogels. By changing their relative proportions, hydrogels with different properties can be obtained [4-6]. It is important to consider not only the intermolecular bonding of polymers, but also the possibility of cross-linking.

Experimental part.

We observed that the degree of swelling of hydrogels depends on the temperature, pH, synthesis time, and concentration of substances during their synthesis. In addition, we observed that the degree of swelling of hydrogels synthesized with the same composition changed depending on the temperature change.

Results and their discussion.

For the synthesis of artificial hydrogels, polymers were used: sodium salt of carboxymethylcellulose (KMS-Na), polyacrylamide (PAA), polyvinyl alcohol (PVS), as well as crosslinking agents such as boric acid (BK), boric

acid ($Na2B_4O_7$* 10 H_2O) (BU), citric acid $C_6H_8O_7$ (LK), methanal CH_2O (MA), urea $CO(NH_2)_2$. In the experiment, 1% solutions of polymers were used, and 0.1% solutions of crosslinking agents were used. The substances were weighed on an electronic analytical balance model “ABS 120-4N” of the KERN company with an accuracy of 4 decimal places. The compositions were prepared in 400 ml measuring cups, mixed by heating to 80 ° C in a magnetic stirrer and dehydrated at a temperature of 110 ° C in a MEMMERT “UN 40” drying cabinet. The hydrogels were precipitated using ethyl alcohol, and then the stitching process was carried out at a temperature of 140 ° C. The resulting hydrogels were soaked with distilled water and the degree of soaking was determined.

Synthesized substances: To obtain substances 1A, 1B, 1D, 1E, we poured 180 ml of 1% KMS-Na solution into 4 400 ml beakers, poured 20 ml of 1% PVS solution on top of each beaker, and added 0.1% solutions of the stitching agents: 10 ml of LK solution into the 1st beaker, 10 ml of MA into the 2nd beaker, 40 ml of BK into the 3rd beaker, and 40 ml of BU into the 4th beaker. Then we carried out the above processes. Table 1 shows the stitching levels.

Table 1

№	Material number	1-Polymer	V ml	2-Polymer	V ml	Seaming agent	V ml	Swelling level
1	1A	KMS-Na	180	PVS	20	LK	10	80.8
2	1B	KMS-Na	180	PVS	20	MA	10	128
3	1D	KMS-Na	180	PVS	20	BK	40	103.67
4	1E	KMS-Na	180	PVS	20	BU	40	137.24

In the next experiment, artificial hydrogels designated 2A, 2B, 2D were synthesized. In the synthesis of these hydrogels, 1% solutions of polymers and 0.1% solutions of crosslinking agents were used. The following substances are listed in Table 2.

Table 2

№	Material number	1-Polymer	V ml	2-Polymer	V ml	Seaming agent	V ml	Swelling level
1	2A	KMS-Na	50	PAA	50	BK	5	273
2	2B	KMS-Na	50	PAA	50	BK	10	179
3	2D	KMS-Na	50	PAA	50	BK	1	169

In our experiment, we synthesized hybrid hydrogels at 2 different temperatures. First, we took 6 test tubes and mixed them with carboxymethylcellulose sodium salt and polyacrylamide in appropriate proportions, and then added boric acid (BK) and formaldehyde (CH2O) in different volumes as crosslinking agents to each test tube and mixed them using a mixer.

Our experiments showed that the degree of swelling of hybrid hydrogels depends on their synthesis temperature, and we observed that if the synthesis temperature is increased above the optimal temperature, the degree of swelling may decrease due to strong adhesion of the reagents.

The swelling degree of KMS-Na:PAA hydrogels synthesized with the presence of various crosslinking agents at 140 °C and 160°C.

Table 3

№	KMS-Na	PAA	Crosslinking agent	V ml	Swelling level	Swelling level
1	190	10	H_3BO_3	5	106.63	25.56
2	190	10	CH_2O	5	134	22.8
3	190	10	CH_2O	10	268	35.96
4	50	50	H_3BO_3	1	169	94.24
5	50	50	H_3BO_3	5	273	112
6	50	50	H_3BO_3	10	179	134

References

1. Pirzada, T.; de Farias, B.V.; Mathew, R.; Guenther, R.H.; Byrd, M.V.; Sit, T.L.; Pal, L.; Opperman, C.H.; Khan, S.A. Recent advances in biodegradable matrices for active ingredient release in crop protection: Towards attaining sustainability in agriculture. *Curr. Opin. Colloid Interface Sci.* **2020**, *48*, 121–136.
2. Singh, N.; Agarwal, S.; Jain, A.; Khan, S. 3-Dimensional cross linked hydrophilic polymeric network “hydrogels”: An agriculture boom. *Agric. Water Manag.* **2021**, *253*, 106939.
3. Chen, H.; Fan, M. Novel thermally sensitive pH-dependent chitosan/ carboxymethylcellulose hydrogels. J. Bioact. Compat. Polym. 2008, 23 (1), p.38-48.
4. Chang, C.; Lue, A.; Zhang, L. Effects of cross-linking methods on structure and properties of cellulose/PVA hydrogels. Macromol. Chem. Phys., 2008, 209 (12), p.1266-1273.
5. A.Sannino, M. Madaghiele, F. Conversano, A. Maffezzoli, P.A. Netti, L. Ambrosio and L. Nicolais' "Cellulose derivative-hyaluronic acid based microporous hydrogel cross-linked through divinyl sulfone (DVS) to modulate equilibrium sorption capacity and network stability", Biomacromolecules, 2004, Vol.5, №l, p.92-96.
6. Центральную Азию ожидает постоянный и устойчивый дефицит воды. Интернет-портал СНГ:пространство интеграции // https://e-cis.info/news/566/113373/.

WIDE-AREA DAMPING STRATEGIES FOR RENEWABLE-DOMINATED POWER SYSTEMS: STRUCTURE, LIMITATIONS AND FUTURE DIRECTIONS

Jalal Ibrahimov, Jamila Rzali
Zhejiang University
Hangzhou, Zhejiang, China
cemilerzali2003@gmail.com
Baku Higher Oil School
Baku, Azerbaijan
jalal.ibrahimov1@gmail.com

Summary - With the increased penetration of renewable energy sources, the dynamic behavior of the electric networks has changed considerably. In this context, the occurrence of inter-area low-frequency oscillations (0.1-1 Hz) is increased, especially in long-distance power transfer scenarios. Wide area damping control (WADC), facilitated through the support of wide area measurement systems (WAMS) based on phasor measurement unit (PMU) technology, has been recognized as an effective solution to address this problem.

In this thesis, various aspects of wide area damping control solutions, actuation technology, and adaptive controller design approaches in renewable energy-based networks are presented in a systematic manner. In addition, various limitations of the solutions, such as communication delays and cyber threats, and actuation saturation issues, are discussed. Finally, future developments and trends in this field, including hierarchical and intelligent approaches, are presented [1].

Keywords: Wide-area damping control; Renewable energy integration; PMU; Inter-area oscillations; Adaptive control

Introduction

With large-scale integration of photovoltaic and wind power sources, effective system inertia is reduced. The electromechanical interaction characteristics are also altered. With the increase in renewable sources, conventional power system stabilizers are not sufficient to damp inter-area oscillations.

Wide area damping control schemes make use of synchronized phasor measurements to obtain global dynamic information. It can suppress system-wide oscillations. With respect to local control schemes, wide area damping control schemes make use of coordinated feedback signals from wide area measurement systems.

Inter-area oscillations generally take place in the range of 0.1 to 1 Hz [2].

2. Experimental Part

2.1 General WADC Structure

The general block diagram of the structure of the WADC in renewable integrated systems is given in the following Fig.1.

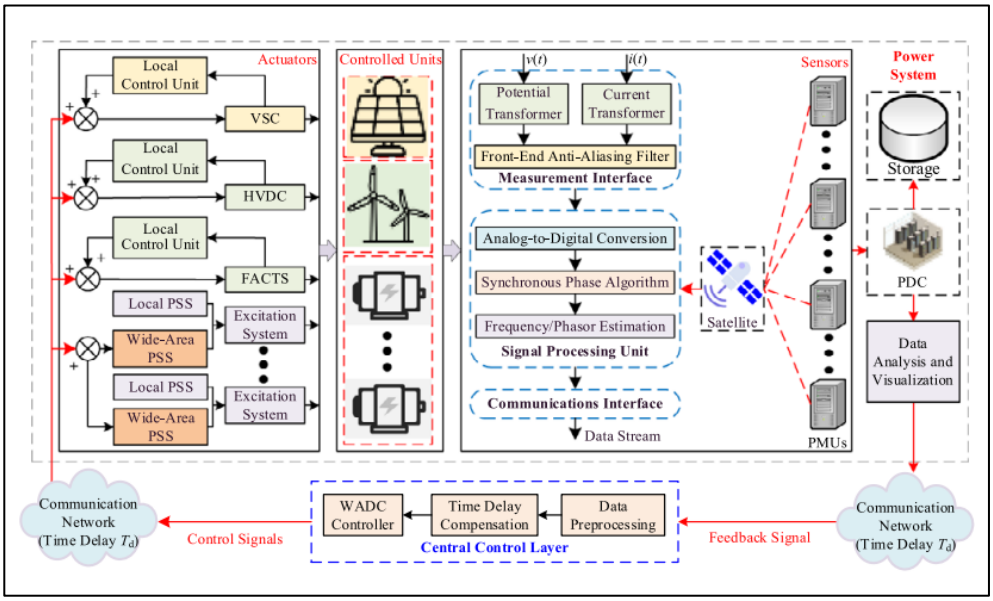


Fig.1. Block diagram of WADC in renewable integrated power systems

In this structure, the following elements can be described:

- PMUs are used to measure voltage, frequency, and power.
- Signals are transmitted through the communication networks.
- A controller is used to generate the required damping signal.
- Actuators include PSS, HVDC, FACTS, wind farms, PV farms, and ESS [3].

2.2 Actuator Technologies

The different categories of actuators are presented in the following figure:

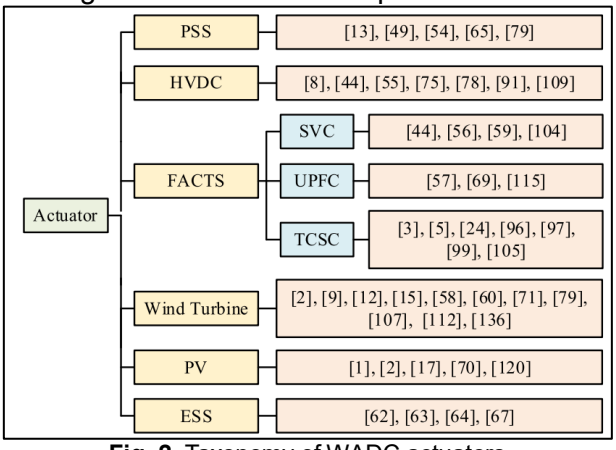


Fig. 2. Taxonomy of WADC actuators

Main categories of actuators:

- Power System Stabilizers (PSS)
- HVDC transmission systems
- FACTS devices (SVC, TCSC, UPFC)
- Wind farms
- Photovoltaic plants
- Energy storage systems

Renewable-based actuators and energy storage systems allow for fast bidirectional power regulation with nonlinear converter dynamics.

2.3 Controller Design Framework

The complete design process is depicted below:

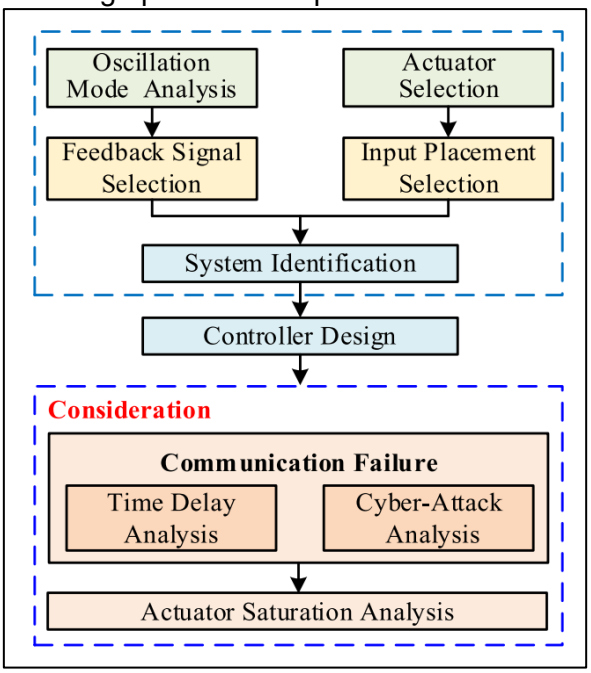


Fig. 3. Overall WADC design flow

- The individual stages involved in the design process are:
- Oscillation mode analysis
- Actuator selection
- Feedback signal placement
- System identification
- Communication delay analysis
- Controller synthesis

2.4 Controller Structure

The standard supplementary damping controller structure is depicted below [4]:

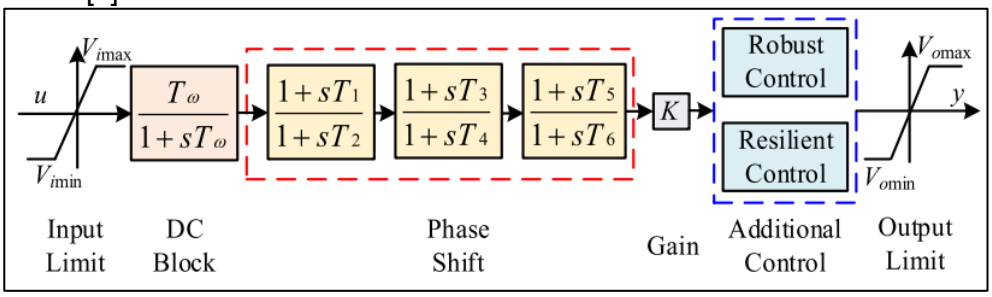


Fig. 4. Structure of wide-area damping controller

It consists of:

- Gain block
- Phase compensation blocks
- Robust/adaptive modules

2.5 Adaptive Architectures

Two types of adaptive structures are commonly employed:

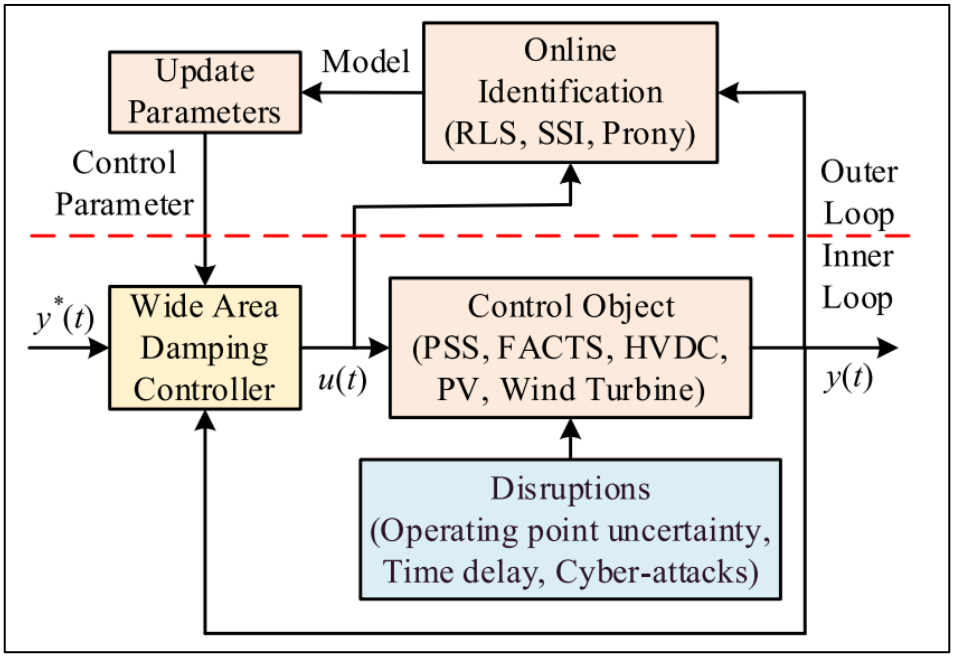


Fig. 5. Self-tuning WADC structure

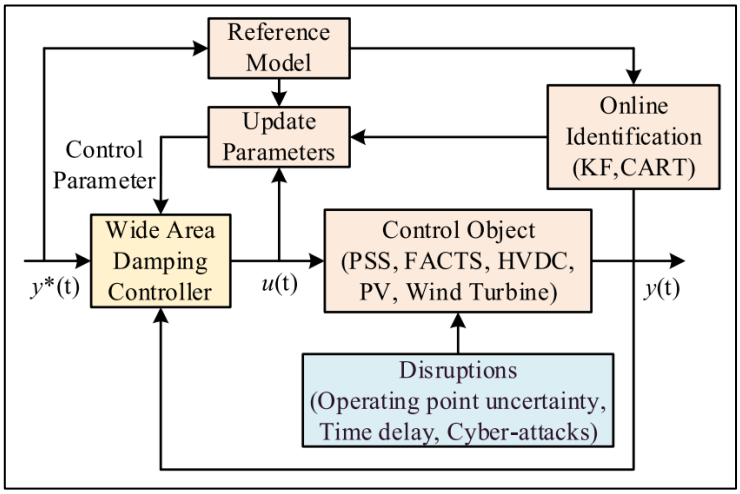


Fig. 6. Model reference adaptive WADC

Self-tuning control utilizes online identification techniques, such as RLS, SSI.

Model reference control utilizes a reference model to adapt parameters.

3. Results and Their Discussion

Wide area damping control techniques have the potential to improve the effectiveness of inter-area low-frequency oscillation modes in renewable-based power systems.

Its effectiveness is constrained by:

- Communication time delays, which impact the damping effectiveness.
- Cyber security, which impacts the reliability of the overall system.
- Architecture, where centralized control is effective in terms of global coordination, but lacks the ability to cope with failures.
- Adaptive controllers have shown better effectiveness in converter-based systems than offline-based controllers [5].

References

1. Aminifar, F., Fotuhi-Firuzabad, M., Shahidehpour, M., 2016, Impact of high wind power penetration on power system oscillatory stability, IEEE Transactions on Power Systems, 31(2), 1105–1113.
2. Gao, B., Chen, Y., Li, Y., 2018, Wide-area measurement-based damping control in renewable integrated power grids, Electric Power Systems Research, 160, 62–71.
3. Kundur, P., Balu, N.J., Lauby, M.G., 2017 edition, Power System Stability and Control, McGraw-Hill Education.
4. Li, H., Xie, X., Zhang, C., 2019, Communication delay-aware wide-area damping control for interconnected power systems, International Journal of Electrical Power & Energy Systems, 104, 407–416.
5. Zhou, N., Huang, Z., Trudnowski, D., 2015, Mode estimation of power system oscillations using synchrophasor measurements, IEEE Transactions on Power Systems, 30(2), 748–756.

CARBON FOOTPRINT ANALYSIS OF PRIMARY ALUMINUM PRODUCTION

Chingiz HAJIYEV[1]
[1]GREENANO EMJM – University of Lorraine
Nancy, France
chingiz.hajiyev3@etu.univ-lorraine.fr

Abstract - This study provides a comprehensive cost competitiveness analysis for primary aluminium production across 18 countries. It aims to identify the influence of commodity, electricity, transport, and labor cost, as well as carbon tax on the overall production cost. The report implements consumption-based carbon footprint modeling alongside an economic cost framework and evaluates the total cost of production against the London Metal Exchange (LME) benchmark. The analysis identifies a significant difference between low-cost, carbon-intensive production in Asia and high-cost, decarbonized production in Europe. It also demonstrates that electricity costs represent a major share of the production costs and explains the impact of carbon pricing and subsidies. Conclusively, it provides a comparative framework to determine the profitability of producing aluminium across the countries studied.

Keywords: Aluminum production, carbon footprint, life cycle assessment, economic analysis, sustainability, competitiveness, profitability

Introduction

The strategic criticality of aluminum has increased with the energy transition towards decarbonization, making it the inevitable asset to achieve sustainability goals. Aluminum is the second most produced metal after steel exceeding 70 million metric tons annually considering global production [1], [2]. Aluminum production accounts for 2% of global greenhouse gas emissions, positioning it as one of the most carbon-intensive industries in metallurgy [3].

Modern electrolysis cells operate at currents ranging from 300 to 500 kA with cell voltages of approximately 4–5 V [6]. This substantial electricity demand, combined with direct process emissions from carbon anode consumption, makes the carbon footprint highly dependent on the electricity source. For example, production in Norway, which is mainly dependent on hydroelectric power, achieves emissions intensities below 4 tCO2/t Al [7], while coal-dependent production in India can exceed 25 tCO2/t Al due to reliance on captive coal-fired power plants [8]. Other factors contributing to total aluminum emissions are distributed along the value-chain: mining, digestion and calcination of bauxite, anode production, ingot casting, and recycling [9].

Experimental Section

The total carbon footprint per tonne of aluminum in country i is calculated as:

$$CF_i = (E_bauxite,i + E_alumina,i + E_Al,process,i + E_Al,elec,i + E_anode,i) / M_Al,i \quad (6)$$

where:

CF_i — carbon footprint of producing 1 tonne of aluminum in country i
E_bauxite,i — emissions arising from bauxite mining
E_alumina,i — emissions from the Bayer process
E_Al,process,i — direct CO_2 emissions from the Hall-Héroult process
E_Al,elec,i — indirect emissions from electricity used in the Hall-Héroult process
E_anode,i — indirect emissions from the production of carbon anodes
M_Al,i — total aluminum production in country i

Material balance calculations are performed at each stage to ensure consistency and avoid double-counting when materials are traded between countries.

The bauxite material balance for country i is:

$$M_bauxite,i = P_bauxite,i + I_bauxite,i - X_bauxite,i \quad (7)$$

where:

M_bauxite,i — bauxite quantity entering the further production stage
P_bauxite,i — locally mined bauxite amount
I_bauxite,i — imported bauxite amount
X_bauxite,i — exported bauxite amount

Emissions from bauxite mining are calculated as:

$$E_bauxite,i = M_bauxite,i \times EF_bauxite \quad (8)$$

where EF_bauxite = 0.035 tCO_2/t bauxite is the emission factor for bauxite mining (Aluminum Stewardship Initiative). This figure includes mainly diesel consumption for mining equipment and other miscellaneous emissions.

The alumina production from bauxite depends on the bauxite grade (percentage of Al_2O_3 content). Country-specific bauxite grades are used in the model. If the mean bauxite grade is taken as G_i = 0.5, the produced alumina from the total bauxite available for processing in country i is:

$$M_alumina,produced,i = M_bauxite,i \times G_i \quad (9)$$

The total alumina available for aluminum production includes trade:

$$M_alumina,i = M_alumina,produced,i + I_alumina,i - X_alumina,i \quad (10)$$

where:

M_alumina,i — alumina available for the next production stage
I_alumina,i — imported alumina amount
X_alumina,i — exported alumina amount

For the Hall-Héroult process, the current efficiency is defined as:

$$\eta_current = M_Aluminum,actual,i / (I \times t \times M_Aluminum / (z \times F)) \quad (11)$$

where:

M_Aluminum,actual,i — practically produced aluminum in the reaction cell
I — cell current
t — time taken for the reaction
M_Aluminum — theoretical aluminum production rate
z — number of valence electrons needed to reduce the aluminum ion
F — Faraday constant

Current efficiency represents the fraction of charge transferred that contributes to the electrochemical reduction of alumina. Assuming alumina concentration exceeds the critical threshold throughout the reaction, the produced aluminum is quantified as:

$$M_Aluminum,i = (M_Alumina,i / m_stoich_Aluminum) \times \eta_current \quad (12)$$

where m_stoich_Aluminum = 1.889 kg Alumina / kg Aluminum is the stoichiometric aluminum production rate at 100% current efficiency.

For Bayer process emissions, the main material and energy inputs to produce 1 kg of alumina are considered:

• Fuel Oil: 0.093 kg → CO_2 footprint: 3.52 kgCO_2/kg Fuel
• Natural Gas: 0.076 kg → CO_2 footprint: 1.88 kgCO_2/kg Gas
• Electricity: 0.059 kWh → CO_2 footprint: grid dependent

Carbon emissions from alumina production are calculated as:

$$E_alumina,i = (0.093 \times 3.52 + 0.17 \times 1.98 + 0.109 \times EF_Grid,i) \times 4 \quad (13)$$

where EF_Grid,i is the carbon intensity of the electricity grid for country i.

The overall reaction for the Hall-Héroult process is:

$$2\,Al_2O_3 + 3\,C \rightarrow 4\,Al + 3\,CO_2 \quad (14)$$

Direct emissions from the Hall-Héroult process and anode consumption are estimated as:

$$E_Al,process,i = M_Al,i \times (m_stoich_CO_2 / \eta_current) \quad (15)$$

where:

E_Al,process,i — direct emissions due to anode consumption
M_Al,i — total aluminum amount entering the reaction
m_stoich_CO_2 — stoichiometric carbon emissions

Carbon anode consumption is given by:

$$M_C,i = M_Al,i \times (m_stoich_C / \eta_current) \quad (16)$$

Two methods are adopted for calculating electricity requirements per kg of aluminum. The first method makes the electricity dependent on current efficiency:

$$Energy_Hall\text{-}Héroult\ (kWh/kg\ Al) = 2.9806 \times F_cell / \eta_current \quad (17)$$

where F_cell is the cell voltage and η_current is the current efficiency. The second method uses country-specific reported data from the International Aluminium Institute (IAI) or national statistics, as it reflects real

operational conditions including auxiliary equipment and rectifier efficiency losses.

Scope 2 emissions from electricity are calculated as:

$$E_Al,elec,i = M_Al,i \times E_elec,Al,i \times CI_elec,i \quad (18)$$

where E_elec,Al,i is the specific electricity consumption and CI_elec,i is the carbon intensity of the electricity grid in country i. This is the dominant source of variation in carbon footprint between countries.

Scope 2 emissions related to anode utilization and production during the aluminum production process must also be accounted for. As conventional cells consume large amounts of anode material requiring frequent replacement, this accounts for a large percentage of total emissions. The anode-related emission factor is taken as 1.5 tCO_2/t Al, and total emissions are calculated as:

$$E_anode,i = M_Al,i \times EF_anode \quad (19)$$

where EF_anode = 1.5 tCO_2/t Al. This factor includes anode baking, manufacturing energy, and precursor production.

Results and Discussion

The most carbon intensive aluminum production takes place in India– 25.3 tCO2/tAl, which is consistent with the data reported by governmental agencies [63]. Moreover, in the countries like China and Australia where predominant energy source used to produced electricity is coal– 61 percent [64] and 49 percent [65] , the carbon footprint is surely above the global average. On the other hand, in Baltic countries like Norway and Sweden, due to the fact that green energy sources such as hydropower (89% and 39%, respectively) and nuclear 9 power (in Sweden, 29%), the aluminum production ac counts for the least carbon footprint figures. Different decarbonization pathways for aluminum industry can be suggested if we analyze the source of emissions per country. Scope 2 emissions due to electricity production– directly related to the carbon intensity of the grid constitutes 6.03– 78.4 percent of the total emissions. For electricity emission dominating countries, de carbonization of grid or production of low-carbon on site is key to having low-carbon aluminum. Hydro powered aluminum plants are already practiced in Norway, and it can be expanded to other countries. In contrary, for Baltic countries like Norway and Swe den, for France, Brazil and Canada, the Scope 2 emissions is not significantly large due to renewable energy utilization for power generation. To decrease the direct emissions from Hall-Heroult process, short term improvements are limited with optimization of anode operational parameters and increase of the current efficiency which depends on the cell design and operation. In the future, replacement of conventional carbon anodes with Inert anode technology in which pure oxygen is emitted to atmosphere can lead to 100 percent reduction in direct emissions. However, they also exhibit higher energy consumption than conventional anodes– which can lead to even

higher carbon emissions if applied in countries with carbon intensive grid [66]. Another solution is the application of CCUS to the CO2 directly from the cells, which has also disadvantages as high energy usage and added cost to the aluminum produced. Another fraction which needs to have lower carbon emissions is the anode production. To decrease this amount, biomaterials can be used as a replacement of coke-based anodes (Decarbonisation Options for the Aluminium Industry, Zore L). Reduction technology can be completely changed with the use of hydrogen, which has also high cost and low technological readiness [67]

Conclusion and Recommendations

The calculation for the carbon footprint and the cost of the aluminum production has been discussed in the report. With regard to the carbon footprint calculation, while countries with carbon intensive national grid such as India(25.3tCO2 /tAl) and China(16.6tCO2 /tAl), where coal is the main energy source for aluminum smelters accounts for largest carbon footprint, regions where hydro power is the dominant electricity source such as Norway showed the least figures(4.44tCO2/tAl).

References

[1] International Aluminium Institute, Primary aluminium production (2025), monthly statistics, December 2025. Accessed: 2 February 2026.
[2] United States Geological Survey, Mineral Commodity Summaries 2024, Tech. Rep. (USGS, 2024).
[3] World Economic Forum and Accenture, Net-Zero Indus try Tracker 2024: Aluminium, Tech. Rep. (World Eco nomic Forum, Geneva, Switzerland, 2024) accessed: 2 February 2026.
[4] G. Saevarsdottir and H. Kvande, Light Metals (2025).
[5] H. Kvande and P. A. Drabløs, Journal of Occupational and Environmental Medicine 56, S23 (2014).
[6] G. M. Haarberg, Electrochemistry 92, 043002 (2024).
[7] Hydro, Our roadmap to net-zero emissions in aluminium production (2025), accessed 02 February 2026.
[8] P. K. Banerjee, in Travaux 46: Proceedings of the 35th International ICSOBA Conference (Hamburg, Germany, 2017) 2–5 October 2017.
[9] Energy Transitions Commission and Mission Possible Partnership, MPP Aluminium Full Report, Technical Re port (Clean Energy Ministerial / Mission Possible Part nership, 2022) accessed 02 February 2026.
[10] NITI Aayog, Roadmap for Aluminium Sector Decarbon isation, Tech. Rep. (NITI Aayog, Government of India, New Delhi, India, 2026).
[11] International Energy Agency, China- electricity 2024, https://www.iea.org/countries/china/electricity (2024), accessed: February 4, 2026.
[12] International Energy Agency, Australia- electric ity 2024, https://www.iea.org/countries/australia/ electricity (2024), accessed: February 4, 2026.
[13] SINTEF, Aluminium ert anodes, electrolysis using in https://blog.sintef.com/energy/ aluminium-electrolysis-using-inert-anodes/ (2023), sINTEF Blog.
[14] ING Economics Department, Green Aluminium Article 2: Aluminium Goes Green– What Can Be Done to Cut Emissions, Tech. Rep. (ING Bank, 2024) iNG Think Eco nomic and Financial Analysis

SCIENTIFIC AND TECHNOLOGICAL FOUNDATIONS FOR ENSURING ENVIRONMENTAL SUSTAINABILITY IN THE PROCESS OF BITUMEN MODIFICATION

Abdullaeva Shokhista Shukhratovna
Khujakulov Aziz Fayzullayevich
Bukhara State Technical University
Bukhara, Uzbekistan
shoxista.1988@mail.ru

Abstract. The paper substantiates the relevance of using secondary materials and various types of polymer waste, and provides information on the volume of plastic waste as well as the main directions of its recycling and utilization. The possibility of obtaining additives for road bitumen during the utilization of household and industrial waste is described. A method for bitumen modification is presented, according to which the incorporation of modifiers into the bitumen composition enhances its resistance to aggressive environmental conditions and improves its performance characteristics. In particular, such bitumens are characterized by a lower brittle point and a higher softening temperature, resulting in increased crack resistance and rutting resistance of asphalt concrete.

Keywords: bitumen, additives, PET (polyethylene terephthalate), emulsified mineral mixtures, bitumen–mineral mixtures, modifier, plastic and polymer waste.

Introduction.

At present, the use of secondary materials is an issue of considerable relevance. Their application makes it possible to enhance the strength of construction structures, extend the construction season, and develop products characterized by lighter weight and improved reliability.

In recent years, increasing attention has been devoted to the problems associated with waste utilization. Major research and industrial enterprises are actively involved in the development and study of construction materials possessing new and improved properties.

The continuous improvement of the quality of construction products and materials remains one of the most pressing tasks today. The steady growth of traffic loads on highways, the increasing stresses imposed on construction structures, and the impact of aggressive environmental conditions reduce their service life and accelerate deterioration and degradation processes [Provatorova G., Vikhrev A., 2020, p. 110–116].

Within the framework of this study, investigations were carried out to examine the properties of organo-mineral mixtures and the materials used in their preparation. During the research, household and industrial wastes were analyzed in detail, and their high potential for application in road construction was established.

The necessity of utilizing various types of waste, particularly plastic waste, is steadily increasing. Each year, the volume of products manufactured from recycled polyethylene terephthalate (PET) continues to

grow. The production of new polyethylene terephthalate products requires the mandatory use of recycled PET; otherwise, the manufacture of new products becomes impossible. Consequently, the issue of recycling secondary PET remains highly relevant worldwide [Vikhrev A.V., Provatorova G.V., Semekhin E.F., Varzin E.I., 2017, p. 25–32].

One of the most promising areas for the application of recycled polyethylene terephthalate (PET) is road construction, particularly the modification of road bitumens.

Practical experience in the recycling of polyethylene terephthalate demonstrates that PET processing is a relatively straightforward procedure. The wide availability of PET waste, its technological convenience, and its favorable physicochemical properties have made it one of the most widely recycled polymers worldwide.

According to research data, more than 20 million tons of PET were used in 2013 for the production of plastic bottles. Statistical reports indicate that the number of products manufactured from polyethylene terephthalate has now exceeded 500 billion units. The accumulation of such a vast quantity of PET products has led to significant environmental concerns, particularly the pollution of ocean coastlines. Waste generated from plastic bottles can move freely across the world's oceans and may even form entire "garbage islands."

At the same time, the complete inertness and relative safety of PET do not offset the problems associated with its rapid accumulation. It is also well established that recycling 1 ton of polyethylene terephthalate (PET) makes it possible to significantly reduce the land area allocated for the disposal of industrial and municipal waste in landfills.

Another pressing issue is the reduction of carbon dioxide (CO_2) emissions into the atmosphere. The problem of global warming is directly associated with increasing CO_2 emissions. In this context, the recycling of secondary PET waste not only reduces the volume of solid waste but also contributes significantly to the reduction of carbon dioxide emissions. In recent years, the price of recycled PET has remained relatively high, reaching 70–80% of the cost of virgin PET in many countries.

Public attention to environmental issues has intensified in recent years, which has, in turn, stimulated an increase in the recycling rates of used polyethylene terephthalate (PET) containers. According to research findings, more than 9 million tons of PET waste are collected annually worldwide, including waste recovered from the surface of the world's oceans. At present, the production of goods from recycled PET continues to grow steadily.

Currently, the volume of collection and recycling of secondary PET varies considerably among different countries. In Eastern countries, the separate collection rate of PET waste and bottles reaches approximately 80%, whereas in European countries this figure ranges from 50% to 70%. In Eastern Europe, however, the rate does not exceed 20%. Today, the global

PET waste market amounts to nearly 1.5 million tons. More than 1.3 million tons are collected in North America, while in China the volume exceeds 3 million tons [Al-Sabaeei A., Md. Yussof N.I., 2019, p. 81–88].

The recycling of secondary polyethylene terephthalate (PET) obtained from collected waste is primarily directed toward the production of staple fibers and nonwoven synthetic materials, accounting for up to 70% of the collected waste. The remaining portion is used in the manufacture of various films and bottles intended for food and non-food products. In recent years, road construction organizations have also shown increasing interest in polyethylene terephthalate, mainly due to the range of properties that make PET advantageous for road bitumen applications.

Thus, addressing the problem of secondary PET utilization contributes to the resolution of several environmental challenges. In particular, recycled polyethylene terephthalate can be effectively used in the construction sector to develop new materials with enhanced properties [Appiah J.K., Berko-Boateng V.N., 2017, p. 1–7].

One of the most significant characteristics of PET is its high mechanical strength, water resistance, and good dielectric properties over a wide temperature range from −20 to +80°C. PET does not become brittle at −50°C and can be used at temperatures up to 175°C.

Laminated PET plastics (TU 49-5761783-334-90) are produced by continuously applying a low-density polyethylene melt onto a PET substrate [Shafabakhsh G.H., Sajadib S.R., 2018, p. 13–18].

The most widespread and economically efficient method of recycling PET waste is mechanical-chemical processing, which includes melting shredded and cleaned waste, homogenization, purification from impurities, and vacuum degassing, followed by extrusion.

Research is also being conducted on the use of PET as a modifying additive for bitumen. This approach makes it possible not only to reduce waste volumes but also to improve the quality of road construction materials.

Experimental Section.

The incorporation of various modifying and polymer additives into the binder composition significantly alters its physicomechanical properties and changes its structure, exerting a plasticizing effect on the dispersed medium. At the same time, the components of the bitumen–polymer system may enter into chemical interaction, resulting in the formation of a polymer–bitumen binder with a unified spatial structure [3, 4].

Recent studies indicate a substantial increase in demand for polymer–bitumen and modified binders. This trend is primarily associated with the introduction of a new generation of GOST standards. Testing of asphalt concrete produced in accordance with the updated GOST requirements has demonstrated that it is not possible to achieve the specified regulatory performance indicators using conventional bitumens, particularly in rutting

resistance tests. When a standard, unmodified binder is used, test results reveal a decrease in performance during rut depth determination and the destruction of samples under simulated traffic loading conditions.

Modifying additives act as reinforcing elements. Although direct chemical interaction may not always occur, independent spatial structures are formed within the bitumen–polymer system. Structure-forming additives significantly enhance the mechanical properties and temperature stability of the binder.

Insufficient resistance to elevated temperatures leads to sample degradation and pronounced differences in the strength of asphalt concrete within the operational temperature range [12–14]. This phenomenon is largely attributable to the use of bitumen as the binder in asphalt concrete. Therefore, improving the heat resistance of bitumen through modification of its properties makes it possible to achieve the required performance characteristics of the final asphalt concrete mixture. In this study, an attempt was made to address this issue by incorporating PET into the bitumen composition.

The physicomechanical properties of polyethylene terephthalate (Table 1) are characterized by high stability over a temperature range from −50 to 200 °C. Its incorporation into bitumen makes it possible to reduce the brittle point, increase the softening temperature, and consequently enhance the crack resistance and rutting resistance of asphalt concrete.

Due to the significant differences between the properties of bitumen and polyethylene terephthalate, the main difficulty arose during the incorporation of plastic into the bitumen composition. If polyethylene terephthalate is added directly to bitumen, prolonged heating of the resulting mixture at elevated temperatures accelerates the aging process of the bitumen and deteriorates the performance characteristics of the finished asphalt concrete mixture.

Table 1. Physicomechanical properties of PET

№	**Properties**	**Values**
1	Density, kg/m³	1380
2	Tensile strength, MPa	120–185
3	Elongation at break, %	50–70
4	Impact toughness, kJ/m²	70–90
5	Water absorption, %	0,3
6	Frost resistance, °C	–50
7	Melting temperature, °C	265
8	Molecular weight	15000–30000

To overcome this limitation, a method was selected in which pre-shredded plastic was dissolved in a compatible solvent that mixes well with bitumen. As a result, complete dissolution was achieved at a temperature of 130 °C, with the solvent being released in the form of non-toxic vapors.

The modifiers were introduced into BND 60/90 bitumen according to the following procedure. A 50 g bitumen sample was prepared. The modifiers

were added to the binder in amounts of 0.5%, 0.75%, and 1.0% by weight. After the introduction of the modifying additives, the penetration depth of the needle was measured at 25 and 0 °C, the softening temperature was determined using the ring-and-ball method, and ductility was measured at 25 and 0 °C.

Based on the laboratory research results, it is possible to analyze the changes in bitumen properties following the incorporation of polyethylene terephthalate. In the modified bitumen, the softening temperature increases, while the brittle point decreases. On the basis of the obtained correlations, the required amount of plastic serving as a modifier can be calculated.

Results and Discussion.

During the laboratory investigations, the following properties of the binder were evaluated: needle penetration, softening temperature determined by the ring-and-ball method, and ductility. The results are presented in Table 2.

Special attention should be paid to the changes in the binder properties. In particular, an increase in the softening temperature and a decrease in the brittle point were observed. The brittle point of the modified bitumens was determined based on the temperature dependence of needle penetration into the binder.

The analysis made it possible to establish correlations enabling the determination of the optimal amount of polyethylene terephthalate to be introduced into the bitumen as a modifying additive [Syrmanova K.K., 2017, p. 55–62].

Table 2. Comparative analysis of modified and unmodified bitumens

№	Indicator	Additive, %	Modified bitumen BND 60/90				Unmodified bitumen 60/90
			AZOL-1001		PET		
1	Needle penetration, 0,1 mm, not less than: 25 °C 0 °C	0,5 0,75 1,0	85 88 93	24 25 26	83 84 86	22 23 23	 83 22
2	Softening temperature, °C, (Ring and Ball), not less than	0,5 0,75 1,0	48 50 51		50 52 53		48
3	Ductility, cm, not less than: 25 °C 0 °C	0,5 0,75 1,0	99 98 105	3,5 3,6 3,6	101 102 107	3,5 3,7 3,7	 97 3,5

Conclusions and Recommendations.

As noted above, polyethylene terephthalate (PET) is the most widely used material in the production of various food containers and industrial films. This is due to its unique properties, such as chemical stability, inertness, and recyclability, which provide it with significant competitive advantages over other large-tonnage polymer materials used for similar purposes.

The use of PET makes it possible to produce asphalt concrete pavements with extended service life and enhanced performance characteristics, while simultaneously contributing to the solution of waste management and recycling problems.

References

1. Vikhrev A.V., Provatorova G.V., Semekhin E.F., Varzin E.I. Ways to improve the quality of organomineral mixtures. International Scientific Conference «SPbWOSCE. Energy efficiency and Sustainable Development in Civil Engineering». 2017. Санкт-Петербург, 2017.
2. Al-Sabaeei A., Md. Yussof N.I., Napiah M., Sutanto M. A review of using natural rubber in the modification of bitumen and asphalt mixtures used for road construction. Jurnal Teknologi. 2019. N 81(6). P. 81-88.
3. Provatorova G., Vikhrev A. Modification of Bitumen for Road Construction. IOP Conference. Series Materials Science and Engineering MPCPE. 2020. DOI: 10.1088/1757899X/896/1/012088
4. Shafabakhsh G.H., Sajadib S.R. Evaluation of rheological behavior of bitumen modified with Nano Copper Oxide International. Journal of Engineering and Technology (UAE). 2018. N 7(4). P. 13-18.
5. Appiah J.K., Berko-Boateng V.N., Tagbor T.A. Use of waste plastic materials for road construction in Ghana. Case Studies in Construction Materials. 2017. V. 6. P. 1-7.
6. Syrmanova K.K., Botashev E.T., Tleuov D.B., Eshankulov A.A., Kaldybekova Zh.B. Research of oil road bitumen modification with low density polyethylene. Oriental Journal of Chemistry. 2017. V. 33(1). P. 470-477

THERMAL DEGRADATION AND RECYCLING POTENTIAL OF FOOD PACKAGING POLYMERS: A REVIEW ON THE STRUCTURAL AND FUNCTIONAL CHANGES UNDER HEAT EXPOSURE

Aysu Jafarzade
Baku State University
Baku, Azerbaijan
aysuceferzade0@gmail.com
Supervisor: Rasim Alosmanov

Summary - Thermal degradation of polymers causes changes in their physical and chemical structure. For example, it can cause a decrease in the mechanical strength of the material, discoloration, increased gas and vapor permeability, and the transfer of potentially harmful substances to food products. Based on various scientific sources, it is shown that even long-term storage in the temperature range of 60-80°C accelerates oxidation processes on the surface of polymers, while at temperatures above 100°C, chain breaks and the formation of new carbonyl groups are observed. As a result, the strength of the polymer material decreases, its elasticity weakens, and it loses transparency. At the same time, the thermal degradation process is not limited to only negative effects. Studies show that mechanically grinding and reprocessing of degraded polymers is possible. The recycling process involves melting and forming stages at high temperatures. Although there is a certain loss of properties, the potential for polymers to be used in the preparation of new packaging

materials is maintained. Consequently, the study of the nature of thermal degradation provides an important theoretical and practical basis for improving polymer recycling technologies. The novelty of this review is to focus on the industrial applications of polymers, to investigate their thermal degradations, and to determine whether recycling is possible.

Keywords: Plastic packaging, thermal degradation, polymer degradation, food contact materials

Introduction:

Packaging material plays a key role in food safety, as it not only creates a barrier to protect the product from the external environment, but also prevents oxidation and microbiological spoilage of the product by being activated with functional substances. Plastic is represented in the packaging market with its high density. Due to their ease of production, versatility, affordability, lightness and low cost, these synthetic polymers dominate the packaging sector despite their non-biodegradability and thus remain in the environment for longer than they are intended. Therefore, several efforts have been made to promote the use of recyclable plastics for food packaging. However, one of the important problems is the degradation of these materials during storage, transportation and use due to various external factors, especially heat and sunlight.

Based on the experimental analysis, it was observed that packages made of plastic used for food packaging do not pose a risk in everyday use because their decomposition temperature significantly exceeds the temperature of their use. It has been shown how thermal decomposition proceeds in the presence of oxygen of plastics based on various polymers at a heating rate of 10°C/min. Furthermore, it was observed that substances added to the polymers might slow down or accelerate the process of plastic thermal Decomposition. It has also been shown that the structure of the material has an impact on the amount of energy that needs to be provided to make specific changes in the material. [Majder-Łopatka, 2022, 3-4]

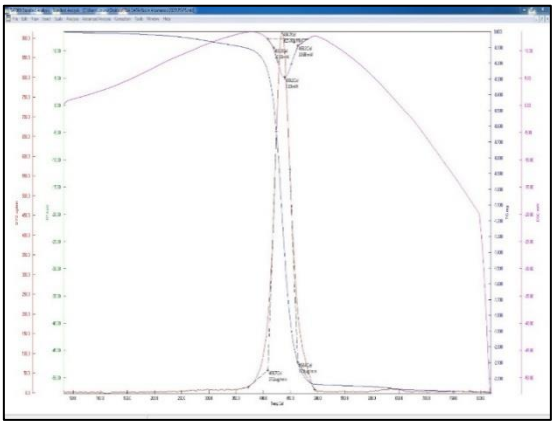
Experimental part:

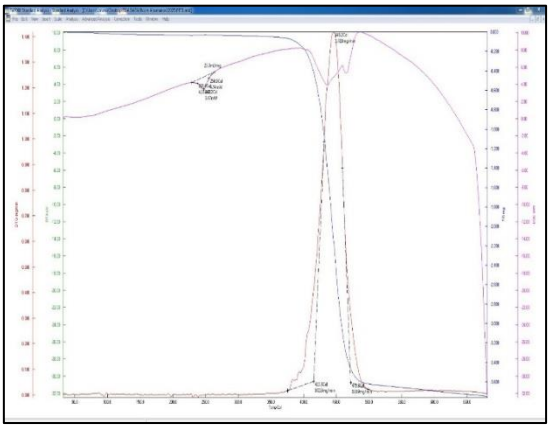
The plastic waste used in this study was selected based on its abundance in everyday household plastic packaging. It includes both food and non-food packaging made from various types of polymers. The steps applied in this study were as follows:

1. Collection of samples
2. Preparation of samples
3 .Identification of samples
4. Reprocessing of samples

For this research, plastic products were collected from household food waste. It should be noted that all initially examined plastic packaging waste samples were thoroughly cleaned (washed with water and/or soap) to remove any food residues or other contaminants and then wiped for drying. Subsequently, using manual cutting tools, the samples were cut into smaller

pieces suitable for the applied methods. After preparation (cleaning, drying and size reduction), the samples were subjected to various analyses such as DSC, DTG and TGA.

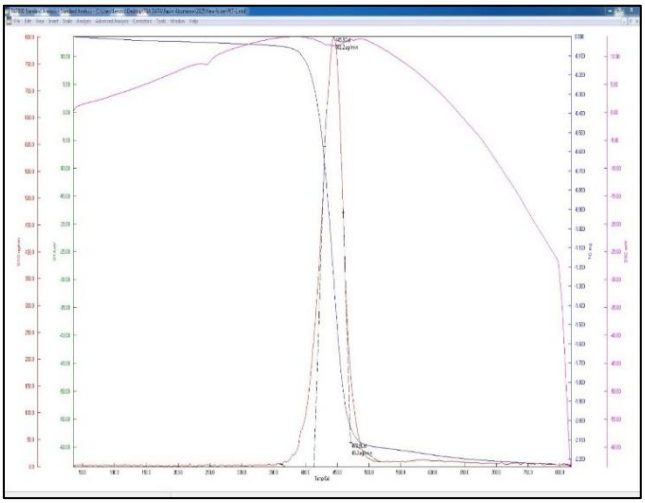


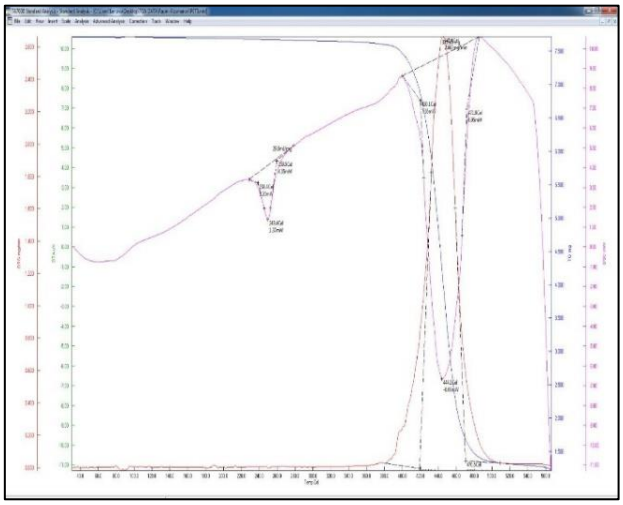


Results and discussion:

Based on the graph for PS, we can say that a sharp, single-step decomposition occurs around 400°C-450°C. The TG curve (plotted on the right Y-axis in mg) represents the mass loss of the sample. The material is stable up to approximately 350°C. There is no significant mass loss before this point, suggesting the sample is dry and free of low-boiling solvents or volatiles. A sharp, rapid drop in mass occurs between 380°C and 500°C. After 500°C, the curve flattens out. Depending on the atmosphere (Nitrogen vs. Air), the remaining mass is likely carbonaceous char or inorganic filler. The DTG curve is the first derivative of the TG curve. The peak is centered around 434.7°C. A single, narrow DTG peak indicates a one-step degradation mechanism. This suggests the material is a relatively pure homopolymer rather than a complex blend or a copolymer with blocks of

varying stability.The magenta line represents the heat flow. This measures whether the material is absorbing heat (endothermic) or releasing it (exothermic). There is a significant endothermic event corresponding exactly with the mass loss peak (T≈ 439°C). Baseline Shift is due to the change in heat capacity (C_2) as the solid sample has turned into gas or char.





Based on the graph PET1 the material is highly stable up to approximately 380°C. There is virtually no mass loss in the lower temperature ranges, indicating a lack of moisture or residual solvents. A sharp mass loss occurs between 400°C and 480°C. After 500°C, the mass stabilizes. Peak Temperature (Tmax is centered at 446.2°C. This is the

temperature where the sample is decomposing most rapidly. Secondary peak Suggests a multi-step degradation mechanism or the presence of a less stable component/additive within the polymer matrix. Melting Peak (T): A clear endothermic peak (pointing down) appears at 254.9°C. A much larger endothermic event occurs simultaneously with the TG mass loss (starting around 400°C).

Based on the graph PET2 a clear endothermic peak is observed at 254.9°C. The material shows excellent stability up to roughly 380°C, where mass loss begins.

Based on the graph PET3 phase transitions the magenta curve (DSC/DTA) reveals physical changes that occur without mass loss. The PET3 sample remains stable (no mass loss) until roughly 390°C. PET3 has a slightly higher melting enthalpy than PET1, suggesting PET3 has a higher initial crystallinity. However, its Tm is slightly lower (249°C vs 254°C), which could indicate smaller crystal sizes or the presence of minor additives.

Offers:

This study observes the degradation of plastics in contact with food under everyday conditions. Oxidation and hydrolysis of plastics lead to random breakage of polymer chains, which leads to surface degradation and fragmentation. The results confirm that temperature and chemical composition clearly affect the degradation of plastics, which in turn increases the likelihood of microplastics being released. Plastic food containers are usually resistant to acidic or alkaline conditions, as well as chemical compositions, during everyday use. Although they usually show good resistance to chemicals, polymer oxidation and hydrolysis can still occur on the surface. The pH value and salinity of the solution are considered to be the most important chemical factors affecting plastic degradation. Increasing temperature accelerates the degradation of plastics and, as a result, significantly increases the negative charges on their surface. [Liheng Xu et., 2025, 4-5]

The thermogravimetric analysis revealed that waste PET samples exhibit a single-step thermal degradation process with high thermal stability up to approximately 380–400°C. The maximum degradation rate was observed around 445–446°C. The low residue content indicates nearly complete volatilization of the material. The obtained results confirm that waste PET retains sufficient thermal stability for mechanical recycling and industrial reprocessing. These findings support the potential reuse of waste polymers in packaging applications and contribute to sustainable waste management strategies. The thermal analysis of PS demonstrates a sharp single-step degradation mechanism with a maximum decomposition temperature around 434°C. The absence of significant mass loss below 350°C indicates good thermal stability under normal processing and usage conditions. These findings suggest that PS can be safely processed and reprocessed at controlled temperatures without premature degradation. The identified thermal behavior provides important guidance for optimizing

recycling parameters and minimizing structural damage during industrial applications. Furthermore, the results confirm the suitability of PS for packaging applications where thermal resistance is required.

References:
1. Liheng Xu, Huier Chen, Zhixi Dai , Fang Wei, Ming Zhang, (2025). Degradation of food-contact plastics in use: Effect of temperature And chemical composition, 5-7
2. Majder-Łopatka, M., W¸esierski, T., Ankowski, A., Ratajczak, K., Duralski, D., Piechota-Polanczyk, A., Polanczyk, A. (2022). Thermal Analysis of Plastics Used in The Food Industry. Materials, 15, 248, 3-4

GÜNƏBAXAN YAĞI TRİQLİSERİDLƏRİ VƏ N-(2-AMİNOETİL)-1,2-ETANDİAMİN ƏSASINDA ALINMIŞ SƏTHİ AKTİV MADDƏLƏRİN SİNTEZİ VƏ ONLARIN NEFT SƏNAYESİNDƏ TƏTBİQİ

[1,2]Ilhama Agalar Zarbaliyeva, Sayat Knyaz Agasanova[2], Asgerzadeh Elmar Etibar[1], Amina Nadir Alimova[2], Hajar Tahir Nabiyeva[1]
[1]Baku Higher Oil School, Baku, Azerbaijan
[2]Academician Y.H. Mammadaliyev Institute of Petrochemical Processes of the Ministry of Science and Education of the Republic of Azerbaijan, Baku
seferova697@gmail.com
ilhama.zarbaliyeva@bhos.edu.az

Xülasə - N-(2-aminoetil)-1,2-etandiaminTəqdim olunan tədqiqat işi bərpa olunmayan neft resurslarının ətraf mühitə mənfi təsirlərini azaltmaq məqsədilə, bitki mənşəli biokütlə əsasında ekoloji təmiz və yüksək effektivlikli neft dispersantlarının sintezinə həsr edilmişdir. İşin aktuallığı neft çirklənmələrinin eliminasiyasında innovativ bioremediasiya texnologiyalarının və biosəthi-aktiv maddələrin tətbiqi ilə əlaqədardır. Tədqiqatda universal prekursor kimi günəbaxan yağı triqliseridləri və yüksək kimyəvi aktivliyə malik N-(2-aminoetil)-1,2-etandiamindən istifadə olunmuşdur.

Sintez prosesi həlledicisiz mühitdə, komponentlərin 1:3.2 mol nisbətində, 120-130°C temperatur diapazonunda 12 saat müddətində aparılmışdır. Reaksiya nəticəsində günəbaxan yağı tiqliseridlərinin (GYTQ) mürəkkəb efir qruplarının aminolizi vasitəsilə samanı-sarı rəngli, parafinəbənzər fiziki xassəyə malik amidoamin tipli reagent sintez edilmişdir. Əldə olunan nəticələr göstərir ki, sintez edilmiş biosəthi-aktiv maddə neft mənşəli toksik analoqlarını əvəz etmək potensialına malikdir və gələcəkdə bu proseslərin süni intellekt vasitəsilə optimallaşdırılması üçün real eksperimental baza təşkil edir.

Açar sözlər: Günəbaxan yağı, N-(2-aminoetil)-1,2-etandiamin, amidoamin, sintez, neft dispersantı, bioremediasiya.

Giriş

Bərpa olunmayan bir resurs olan neft bəşəriyyətin tərəqqisində mühüm rol oynamışdır. Lakin neft istehlakının durmadan artması ehtiyatların tükənməsinə, iqlim dəyişikliyinə və ətraf mühitin genişmiqyaslı çirklənməsinə səbəb olmuşdur. Buna görə də, həm enerji, həm də ekoloji təzyiqi azaltmaq

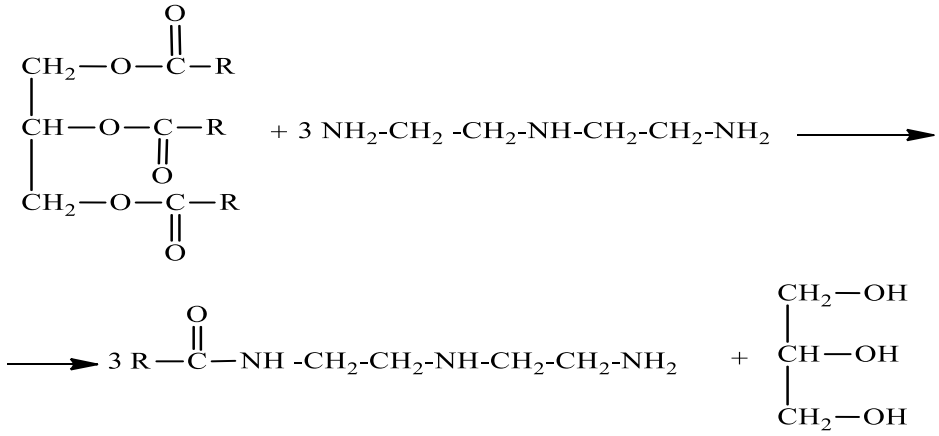
məqsədilə, neft əsaslı resursları əvəz edə biləcək bərpa olunan biokütlə mənbələrinin tapılması həlledici əhəmiyyət kəsb edir [Zhang et al., 2024, 4]. Müasir ekoloji kimyanın aktual problemlərindən biri məhz bu növ çirklənmələrin eliminasiyasıdır ki, bu sahədə aparılan tədqiqatlar neftin ətraf mühitə təsirlərinə dair elmi sübutların sistemləşdirilməsini, innovativ bioremediasiya texnologiyalarının təhlilini, habelə bu proseslərin optimallaşdırılmasında biosəthi-aktiv maddələrin və süni intellektin yeni yaranan rollarını əhatə edir [Gouveia et al., 2026, 2].

Eksperimental Hissə

Sintez üçün xammal kimi seçilmiş N-(2-aminoetil)-1,2-etandiamin yüksək kimyəvi aktivliyi ilə xarakterizə olunur. Ədəbiyyat məlumatlarına görə, N-(2-aminoetil)-1,2-etandiamin əsaslı sistemlər CO2 absorbsiyası proseslərində standart MEA məhlullarından 42.24% daha az enerji sərfi ilə yüksək effektivlik nümayiş etdirir ki, bu da onun mürəkkəb efir qrupları ilə reaksiyasında və effektiv SAM-ların alınmasında həlledici rol oynayır [Wu et al., 2026, 3]. GYTQ –nin tərkibindəki mürəkkəb efir qrupları və ikiqat rabitələr hesabına müxtəlif üsullarla asanlıqla modifikasiya oluna bilən universal prekursordur . Təqdim olunan tədqiqat işində bu konsepsiyaya əsaslanaraq, GYTQ - nin (N-(2-aminoetil)-1,2-etandiamin) ilə amidləşmə reaksiyası vasitəsilə yüksək effektivlikli və neft mənşəli analoqlarını əvəz edə biləcək ekoloji təmiz dispersant sintez edilmişdir [Doley & Dolui, 2018, 1].

Sintez prosesi üçün GYTQ və (N-(2-aminoetil)-1,2-etandiamin) 1:3,2 nisbətində götürülmüşdür. Reaksiya 120-130°C – dərəcədə aparılmış və maddənin sintezi prosesi 12 saat müddətinə çatmışdır. Nəticədə samanı sarı rəngli parafinəbənzər amidoamin maddəsinin sintezi prosesi baş vermişdir.

Reaksiya aşağıdakı sxem üzrə gedir.



Alınan aminoamidin turşu ədədi 3.2 mq HCl/q-dır. Bu aminoamid etil spirtində və izopropil spirtində yaxşı həll olur, su, kerosin, və n-ksilolda bulanıq məhlul verir. İzooktanda və heksanda həll olmur.

GYTQ -nin (N-(2-aminoetil)-1,2-etandiamin) əsaslı aminoamidinin səthi

aktivliyi su-hava sərhədində reagentin müxtəlif qatılıqlı məhlullarından istifadə etməklə tenziometr vasitəsilə öyrənilmiş, izoterm çdir. Ölçmələrə əsasən bu aminoamid fazalararası səthi gərilməni (Cədvəl-1) -ə əsasən aydın görünürki, Ln(C) artdiqca səthi aktivlik 70 mN/m-dən təxminən 27mN/m-ə qədər düşmüşdür. Bu o deməkdir ki, maddə səthi aktiv maddədir (SAM) və suyun gərilməsini azaldır. Müəyyən nöqtədən sonra isə qrafik demək olar ki, sabitləşir (təxminən 26-27 mN/m). Bu isə öz növbəsində KMK (Kritik Mitsella Konsentrasiyası) yarandığını təsdiq edir. Yəni həmin konsentrasiyadan sonra əlavə edilən maddə artıq səthi gərilməni azaltmır, çünki məhlulda misel əmələ gəlir (t= 21^{0}C).

Cədvəl 1. GYTQ -nin (N-(2-aminoetil)-1,2-etandiamin) əsaslı aminoamidinin səthi aktiv xassələrinin nəticələri (t= 21^{0}C)

Məhlul (mol/L)	Səthi aktivlik (mN/m)	LN(Məhlul)
0.00025	70.77	-8.29
0.0005	58.415	-7.60
0.00075	46.285	-7.20
0.001	40.79	-6.91
0.0025	35.59	-5.99
0.005	33.51	-5.30
0.0075	31.005	-4.89
0.01	29.07	-4.61
0.025	26.895	-3.69
0.05	26.915	-3.00
0.075	26.79	-2.59
0.1	26.73	-2.30

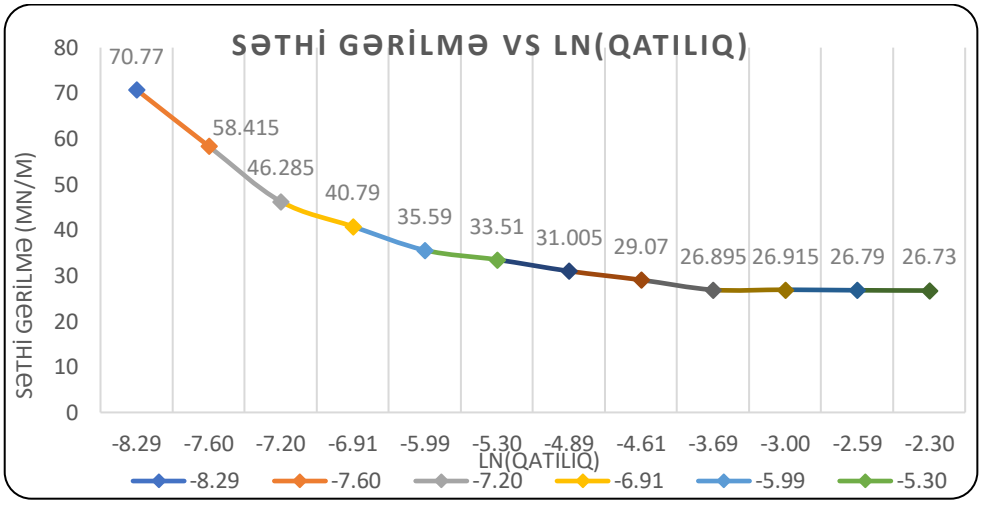
R Universal qaz sabiti (J/mol·K)	8.314
T=Kelvin ilə temperatur	298
Slope (KMK-dən əvvəl)	-12.33587528
Slope (KMK-dən sonra)	-0.932350172
Slope_əvvəl (N/m)	-0.012335875
Γ Gamma (mol/m²)	4.97902E-06
Molekul sahəsi (m²)	3.33515E-19
Molekul sahəsi (nm²)	0.333515147

Gibbs adsorbsiya tənliyinə görə:

Γ (səth artıq konsentrasiyası)

Burada slope dγ/dlnC

$$\Gamma = -\frac{1}{RT}\left(\frac{d\gamma}{d\ln C}\right)$$



Şəkil 1.

Sintez edilmiş aminoamidin neftyığma və dispersləmə qabiliyyəti bu reagentin durulaşdırılmamış məhsul və 5%-li sulu məhlulundan istifadə etməklə üç müxtəlif suda (distillə, içməli və dəniz sularında) Ramana nefti təbəqəsi ilə öyrənilmişdir. Həminaminoamid 100%-li məhsul formasında distillə və içməli suda neftyığıcı-dispersləyici kimi qarışıq effektlər büruzə verir (dəniz suyunda K_{maks}=26.8). Reagent 100%-li məhlul formasında içməli suda və 5%-li məhlul formasında bütün sularda neftdispersləyici təsir göstərir. Reagentin təsir müddəti 7 gündən çoxdur.

Yerinə yetirilmiş elmi-tədqiqat işlərinin bir nəticəsi kimi aşkar edilmişdir ki, təbii triqliseridlər və etanolaminlər əsasında alınan SAM-lar yüksək səthi aktivliyə malik olmaqla su hövzələri səthindən ekoloji təhlükə mənbəyi olan nazik neft təbəqələrinin kənar edilməsi məqsədi ilə effektiv neftyığıcı və neftdispersləyici reagentlər kimi istifadə etməklə ekoloji balansı qorumaq olar.

Ədəbiyyat Siyahısı

1. Doley, S., & Dolui, S. K. (2018). Solvent and catalyst-free synthesis of sunflower oil based polyurethane through non-isocyanate route and its coatings properties. *European Polymer Journal*, 102, 161-168. https://doi.org/10.1016/j.eurpolymj.2018.03.030
2. Gouveia, R. L., de Lucena, L. F., Alves, C. F., de Souza, V. R. S., Silva, L. C. C., Xavier, E. de A., Converti, A., da Silva Junior, C. J. G., & Sarubbo, L. A. (2026). From impact to regeneration: Bioremediation of petroleum-derived compounds enhanced by biosurfactants and AI. *Gondwana Research*, 155, 33-53. https://doi.org/10.1016/j.gr.2026.01.019
3. Wu, W., Wang, S., Lv, C., Aminabhavi, T., Orhan, O. Y., & Liu, H. (2026). C2 capture studies in DETA-1DMA2P biphasic solvent system – experimental and quantum-chemical insights. *Chemical Engineering Science*, 325, 123407. https://doi.org/10.1016/j.ces.2026.123407
4. Zhang, Y., Liu, X., Wan, M., Zhu, Y., & Zhang, K. (2024). From renewable biomass to bio-based epoxy monomers and bio-based epoxy curing agents: Synthesis and performance. *Polymer Degradation and Stability*, 229, 110988. https://doi.org/10.1016/j.polymdegradstab.2024.110988

INFLUENCE OF PROCESS PARAMETERS AND EXTRACTION STAGES ON THE EFFICIENCY OF AROMATIC HYDROCARBON SEPARATION

Gaybullaev Saidjon Abdusalimovich
Asia International University
Bukhara, Republic of Uzbekistan
saidxontura@mail.ru

Abstract - The present study examines contemporary extraction techniques for isolating benzene from pyrolysis distillate enriched with aromatic hydrocarbons. The physicochemical principles governing arene separation are analyzed, with particular emphasis on the selectivity of polar solvents and the influence of key technological parameters on separation efficiency. The extraction performance of solvents such as diethylene glycol (DEG), dimethyl sulfoxide (DMSO), dimethylformamide (DMF), and sulfolane is comparatively evaluated. The findings of this research provide practical insights for the optimization and advancement of aromatic hydrocarbon separation technologies.

Keywords: Arene-rich concentrates; aromatic distillates; extraction; raffinate; extract; extractant; selectivity; aromatic hydrocarbons; benzene.

Introduction.

At present, the rapid expansion of the petrochemical and gas-processing industries has led to a substantial increase in the demand for aromatic hydrocarbons, particularly benzene. Benzene serves as a fundamental feedstock in the manufacture of polymers, synthetic fibers, dyes, pharmaceutical products, and high-octane fuel components. Consequently, the development of efficient and economically viable methods for its large-scale recovery remains a pressing scientific and technological challenge.

The separation of aromatic hydrocarbons from distillate fractions constitutes a critical stage in petrochemical and gas-chemical processing. The overall performance of this operation is governed by a combination of interrelated physicochemical properties, process conditions, and equipment-related factors. Given the high added value of aromatic compounds such as benzene, toluene, and xylenes, their maximum recovery from distillate streams is of considerable industrial importance.

Separation efficiency is primarily dependent on the composition and characteristics of the initial distillate. The ratio of aromatic to non-aromatic hydrocarbons, the presence of olefins and diolefins, and the proximity of component boiling points collectively determine the complexity of the process. Structural differences between aromatic and aliphatic hydrocarbons influence their solubility behavior in various solvents, thereby forming the theoretical basis for extractive separation.

Another decisive factor affecting process performance is the selected technological approach. When the boiling point differences between components are insufficient, reliance solely on rectification leads to

excessive energy consumption. For this reason, liquid–liquid extraction employing selective solvents is widely applied in the processing of aromatic-rich distillates. In practice, the integration of extraction and rectification stages often provides superior technological and economic efficiency [1].

In extractive separation, the properties of the selective solvent play a pivotal role. The solvent must exhibit high selectivity toward aromatic hydrocarbons while demonstrating minimal solubility for non-aromatic constituents. Additionally, low volatility, chemical and thermal stability, ease of regeneration, and environmental safety are among the key criteria determining process effectiveness. Industrially, solvents such as sulfolane, N-methyl-2-pyrrolidone, diethylene glycol, and furfural are extensively utilized for this purpose.

Experimental Section.

Process parameters exert a significant influence on separation performance. An increase in temperature may alter the solubility of aromatic hydrocarbons in the solvent phase; however, it can also result in reduced selectivity. The solvent-to-distillate ratio, interfacial contact time, mixing intensity, and the number of extraction stages are critical variables governing the degree of aromatic recovery.

Furthermore, phase equilibrium conditions constitute the theoretical foundation of the separation process. The distribution coefficient of aromatic hydrocarbons, equilibrium curves, and the configuration of tie-lines provide a quantitative basis for estimating the maximum attainable efficiency of extraction under specified conditions.

Equipment design and overall process configuration also play a decisive role in determining separation efficiency. The type of extractor employed, a scientifically justified hydraulic regime, the implementation of countercurrent flow schemes, and effective phase disengagement conditions collectively ensure stable operation and high process performance [2-3].

Liquid–liquid extraction is regarded as a fundamental operation for selectively isolating one or more target components from liquid mixtures using appropriate solvents. Figure 1 illustrates the flow scheme of a single-stage extraction process.

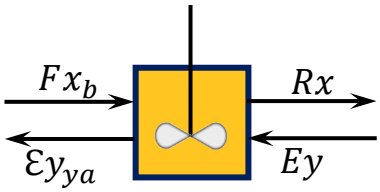


Figure 1. Single-Stage Extraction Process

The diagram illustrates a single-stage extraction apparatus of the mixer–settler type. In this unit, the liquid mixture and the selective solvent come into

contact, and the components are separated through interphase mass transfer.

The apparatus includes:

- **Feed stream (F, x_b)** – the primary phase containing the target component to be separated;
- **Solvent stream (Ɛ, y_ya)** – a liquid possessing selective properties.

Within the mixing zone, the phases are in intensive contact, allowing the target component to transfer from the feed phase into the solvent phase. In the subsequent settling zone, the phases separate due to differences in density, producing:

- **Raffinate (R, x)** – the feed phase partially depleted of the target component;
- **Extract (E, y)** – the solvent phase enriched with the target component.

The feed stream (F) enters the apparatus as the main phase containing the target component, typically consisting of a carrier liquid and a solute at a defined concentration. The feed is introduced into the mixing zone, where it undergoes rapid and thorough contact with the incoming solvent. The solvent stream (E) enters the apparatus separately and is composed of a liquid with selective affinity for the target component. Its primary function is to selectively dissolve the target component from the feed. The solvent engages in brief but intensive contact with the feed, facilitating the mass transfer process.

The mixer element, located centrally in the diagram, ensures intensive dispersion of the phases. This significantly increases the interfacial surface area, accelerating the transfer of the target component from the feed phase into the solvent phase. At this stage, the process approaches near-equilibrium conditions.

After mixing, the phases enter the settling zone, where they separate due to differences in density. The **extract stream (E)** represents the solvent phase, enriched with a high concentration of the target component. The extract is directed to subsequent stages - such as regeneration, rectification, or purification - and constitutes a valuable product from an economic standpoint. The **raffinate** may contain only trace amounts of the solvent and is either sent to the next process stage or discharged as waste.

During the extraction process, when the initial liquid mixture comes into contact with the selective solvent, only the target components dissolve substantially in the solvent, while the remaining constituents of the mixture either dissolve minimally or not at all. This results in a redistribution of components between the phases, enabling their efficient separation.

Results and Discussion.

In industrial equipment, extraction processes-similar to rectification - are widely employed to isolate specific components from solutions and liquid mixtures. The choice of separation method depends on the physicochemical

properties of both the target substances and the mixture components, including boiling point, volatility, thermal stability, and affinity for the solvent.

In aromatic-rich distillates, arenes tend to form azeotropic mixtures with naphthenic and paraffinic hydrocarbons whose boiling points are close to each other. Therefore, the separation of high-purity aromatic hydrocarbons (with 99–99.9% purity) is typically carried out using azeotropic and extractive distillation or selective extraction methods. In extractive processes, the isolated arene mixture can subsequently be fractionated into benzene, toluene, and xylenes.

Selective extraction relies on the preferential solubility of specific components in a selective solvent, which either dissolves the target compounds efficiently or exhibits minimal solubility for other constituents. Consequently, the correct choice of solvent is a critical factor determining process efficiency. Industrially, solvents such as diethylene glycol (DEG), triethylene glycol (TEG), sulfolane, N-methyl-2-pyrrolidone (NMP), N-formylmorpholine, and other selective solvents are extensively used for isolating arenes from various distillate fractions.

Table 1. Gas–Liquid Chromatographic Analysis Results of the Obtained Extract Composition

Name	Aromatic Hydrocarbon Content, %	Additives Content, %
Crude benzene	91.43	8,57
Extract	89.94	10,06
Fraction №1	99.71	0,29
Fraction №2	96.74	3,26
Fraction №3	95.14	4,86

In extraction units, the efficiency of selective solvents such as diethylene glycol (DEG), dimethylformamide (DMF), and dimethyl sulfoxide (DMSO) for isolating arenes can be comparatively evaluated based on their physical properties (density, viscosity) and extractive characteristics. The choice of solvent for designing a technological process depends not only on these comparative attributes but also on factors such as the market price of the solvent, its toxicity, and its stability under extraction conditions.

Among widely used solvents in extractive separation, DEG offers several advantages, including sufficient availability, chemical and thermal stability, inertness, ease of regeneration, and adequate selectivity. However, certain limitations are also evident, such as the high feed-to-solvent ratio required (1:20) and relatively low production capacity despite the simplicity of the equipment.

In the diagram, the **y = f(x)** equilibrium curve represents the interphase equilibrium between the feed and solvent phases. Point **A** corresponds to the initial composition of the feed, while point **B** indicates the equilibrium state achieved after extraction. The **A–B line** illustrates the actual path of mass transfer during the mixing stage.

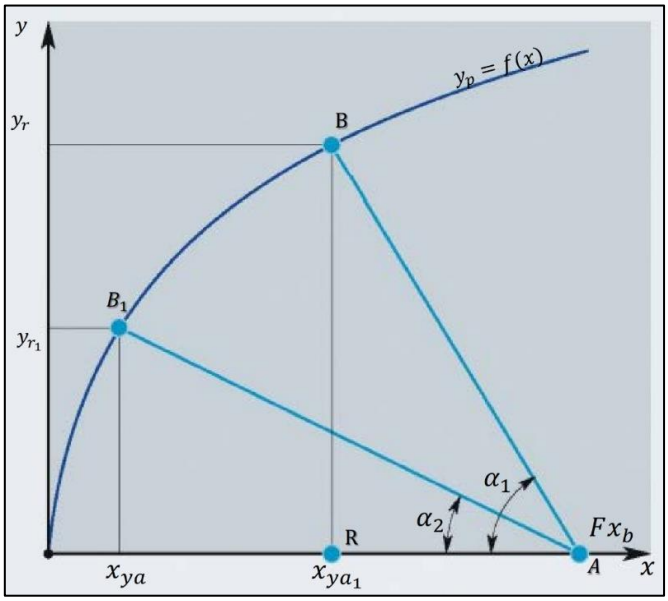


Figure 2. Representation of the Process in y–x Coordinates

Point **R** represents the composition of the raffinate, and point **B_1** corresponds to the extract composition. Using this graphical representation, key parameters such as the degree of extraction, interphase mass distribution, and separation efficiency can be determined.

Although dimethyl sulfoxide (DMSO), widely used for selective separation of aromatic hydrocarbons, exhibits relatively low solubility, it demonstrates higher selectivity compared to several other solvents like sulfolane. Due to its low viscosity, the extraction process with DMSO can be conducted at relatively low temperatures (20–40 °C) with a solvent-to-feed ratio of 7:1. A notable limitation of DMSO is its thermal decomposition starting at 140 °C, beyond which the aromatic hydrocarbons cannot be recovered from the extract via rectification.

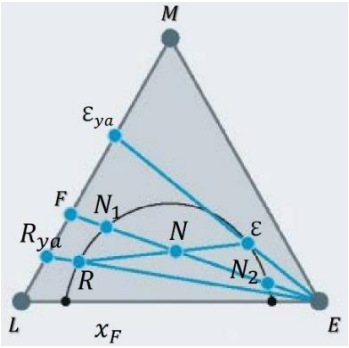


Figure 3. Representation in a Ternary Diagram

Comparative studies of DMF, DMSO, DEG, and their mixtures have shown that their extractive properties toward aromatic hydrocarbons increase consistently in terms of selectivity and solubility, as discussed above.

The ternary diagram is used to illustrate a three-component system comprising the **feed**, the **solvent**, and the **solute**. In the diagram, **F** denotes the feed composition, **E** represents the solvent composition, while **R** and **E** correspond to the compositions of the raffinate and extract, respectively.

The **tie-lines** indicate the interphase equilibrium between the coexisting phases. This diagram allows for a clear graphical assessment of the phase equilibrium in the extraction process, the direction of component separation, and the final composition of the products.

The process is organized based on the **countercurrent flow principle**.

The **feed stream (F)**, containing the target solute, moves from the first stage to the final stage, while the **solvent stream (E)** flows in the opposite direction, coming into contact with the feed at each stage.

At every stage, the phases are intensively mixed and subsequently separated under gravitational or centrifugal forces. The countercurrent arrangement enhances mass transfer efficiency and reduces solvent consumption.

The main technological parameters describing the process, as shown in the diagram, include:

- **Number of stages (n):** the primary indicator of extraction depth;
- **Concentrations (x and y):** amounts of solute in the raffinate and extract;
- **Phase ratio (F/E):** the ratio of feed to solvent flow rates;
- **Equilibrium condition:** represented by the **y = f(x)** curve;
- **Temperature and pressure:** affect phase equilibrium and selectivity (typically carried out at atmospheric pressure).

These parameters are determined and monitored using **y–x plots** and **ternary diagrams**. The feed is considered a liquid phase containing the target solute at a specified concentration.

Conclusions and Recommendations.

The efficiency of separating aromatic hydrocarbons from distillates depends on the interplay between the feed composition, selected technology, solvent properties, process parameters, and equipment design. In particular, extraction processes based on selective solvents enable the recovery of aromatic hydrocarbons at high purity levels and represent one of the most promising industrial approaches.

In the extraction of arenes from aromatic-rich distillates, careful consideration of all key technological aspects - from solvent selection and flow dynamics to equilibrium conditions and the formation of final products, namely the extract and raffinate - allows for maximizing the removal of aromatic hydrocarbons from the raffinate while achieving deep concentration of aromatics in the extract.

REFERENCE
1. R.R.Ramazonov, Sh.I.Karomatov, S.A.G'aybullayev. "Suyuqliklarni ekstraksiyalab ajaratish jarayonining asosiy parametrlari" Science and Education, vol. 5, no. 2, 2024, pp. 199-205.
2. Laylo J. Extraction benzene from pyrolysis distillate//Universum: технические науки. – 2024. – Т. 10. – №. 12 (129). – С. 4-8.
3. Залищевский, Г. Д., Гайле, А. А., Соловых, И. А., Варшавский, О. М., & Ерженков, А. С. (2015). Способ выделения бензола из смесей с неароматическими углеводородами.

OPTIMIZING THE AL/SI RATIO FOR DIRECT CO_2 HYDROGENATION

B.V. Guliyev[1], A. Zahidova[1], F.Ə. Nəsirov[2]
[1]SOCAR Turkey Research & Development and Innovation Inc, Aliaga, Turkey
[2]ARETN Academician Y. H. Mammadaliyev Institute of Petrochemical Processes, Khojaly Avenue, 30, AZ1025, Baku, Azerbaijan.
E-mail: fizuli_nasirov@yahoo.com

Abstract - The direct hydrogenation of CO_2 to methanol (MeOH) and dimethyl ether (DME) represents a key pathway toward carbon-neutral fuel and chemical production. This reaction requires the integration of metallic hydrogenation sites and acidic dehydration sites within a single catalytic system. Conventional hybrid catalysts, typically prepared as physical mixtures, often suffer from limited metal–acid proximity and diffusion constraints, which restrict catalytic efficiency.

In this study, a modified sol-gel synthesis method was employed to engineer nanoscale interfacial bifunctionality in a Cu-Al-Si catalyst system. Composite catalysts were synthesized with varying Al/Si molar ratios (30/70, 60/40, and 80/20) and copper loadings (50 and 70 wt%). Structural and physicochemical characterization was performed using XRD, BET surface area analysis, and NH_3-TPD acidity profiling. Catalytic performance was evaluated in a fixed-bed continuous-flow reactor at temperatures between 200°C and 350°C.

The Cu_{50}–$Al_{60}Si_{40}$ composition exhibited the highest CO_2 conversion and balanced MeOH/DME selectivity. The results demonstrate that catalytic performance is governed by the engineered density of metal–acid interfaces rather than total metal loading. The effect of the Al/Si ratio on CO_2 conversion increases from approximately 47% for $Al_{30}Si_{70}$ to about 67% for $Al_{80}Si_{20}$.

Keywords: CO_2 hydrogenation, Dimethyl ether, Methanol synthesis, Cu-based catalysts, Al/Si ratio, Bifunctional catalysis, Interface engineering.

Introduction

The catalytic conversion of CO_2 into value-added chemicals is a strategic approach to mitigate greenhouse gas emissions while enabling sustainable chemical production. Methanol and dimethyl ether are attractive products due to their applications as fuels, fuel additives, and chemical intermediates [George, 2009; Mureddu, 2021].

Direct CO_2 hydrogenation to MeOH/DME requires two essential catalytic functionalities, namely metallic copper sites for CO_2 hydrogenation to methanol and acidic sites for the subsequent dehydration of methanol to dimethyl ether [Mota, 2021]. Traditional bifunctional systems prepared as physical mixtures often suffer from insufficient contact between metal and

acid phases. This spatial separation limits intermediate transfer and reduces overall reaction efficiency. Therefore, rational interface engineering at the nanoscale is critical to maximize bifunctional synergy [Ebrahimian, 2024; Guo, 2024].

Experimental Section

Cu-Al-Si composite catalysts were synthesized using a modified sol-gel method to ensure homogeneous dispersion of metallic and acidic components.

The Al/Si molar ratios were systematically varied (30/70, 60/40, and 80/20), while copper loadings were adjusted to 50 wt% and 70 wt%.

Catalyst characterization included X-ray diffraction (XRD) for phase identification, BET surface area analysis for textural properties, and NH_3 temperature-programmed desorption (NH_3-TPD) for acidity determination. Catalytic activity tests were conducted in a fixed-bed continuous-flow reactor within a temperature range of 200–350°C.

Results and Discussion

The Al/Si ratio plays a crucial role in tuning support acidity. Silica-rich compositions ($Al_{30}Si_{70}$) exhibit weak acidity, favoring methanol accumulation due to limited dehydration activity.

Alumina-rich compositions ($Al_{80}Si_{20}$) provide stronger Lewis acid sites, enhancing methanol dehydration but potentially leading to excessive acidity and reduced selectivity.

The $Al_{60}Si_{40}$ composition offers balanced medium-strength acidity, resulting in optimal bifunctional performance and improved MeOH/DME selectivity.

Although increasing copper loading to 70 wt% initially enhances the number of hydrogenation sites, excessive loading leads to metal agglomeration and reduced dispersion. This finding confirms that interfacial density between metal and acid sites, rather than total metal content, determines catalytic efficiency.

An Interfacial Bifunctional Density (IBD) model is proposed to correlate catalytic performance with the combined effect of copper dispersion, medium-strength acid site density, and the metal–acid proximity factor [Zhou; 2021]. Mechanistically, the reaction proceeds via a formate-mediated pathway to methanol formation, followed by dehydration on adjacent acid sites to produce DME. The effect of the Al/Si ratio on CO_2 conversion is particularly pronounced at higher Cu loading, where at 250 °C the conversion increases from approximately 47% for $Al_{30}Si_{70}$ to about 67% for $Al_{80}Si_{20}$.

This research demonstrates that the efficiency of direct CO_2 hydrogenation is governed by the engineered density of metal–acid interfaces. By optimizing the Al/Si ratio to 60/40, the IBD is maximized, offering a rational design principle for next-generation bifunctional catalysts in CO_2 valorization technologies.

References

1. Ebrahimian, S.; Bhattacharya, S. Direct CO_2 Hydrogenation over Bifunctional Catalysts to Produce Dimethyl Ether—A Review. *Energies* 2024, 17, 3701. https://doi.org/10.3390/en17153701
2. Guo, X.; et al. A novel bifunctional catalyst obtained by in situ introduction of hierarchically structured HZSM-5 for direct DME synthesis from CO_2 hydrogenation. *Fuel* 2024, 364, 131057.
3. Mota, N.; Millán Ordoñez, E.; Pawelec, B.; Fierro, J. L. G.; Navarro, R. M. Direct Synthesis of Dimethyl Ether from CO_2: Recent Advances in Bifunctional/Hybrid Catalytic Systems. *Catalysts* 2021, 11, 411. https://doi.org/10.3390/catal11040411
4. Mureddu, M.; Lai, S.; Atzori, L.; Rombi, E.; Ferrara, F.; Pettinau, A.; Cutrufello, M. G. Ex-LDH-Based Catalysts for CO_2 Conversion to Methanol and Dimethyl Ether. *Catalysts* 2021, 11, 615. https://doi.org/10.3390/catal11050615
5. Olah, G. A.; Goeppert, A.; Prakash, G. K. S. Beyond Oil and Gas: The Methanol Economy. *The Journal of Organic Chemistry* 2009, 74 (2), 487–498. https://doi.org/10.1021/jo801260f
6. Zhou, H.; Chen, Z.; López, A.; López, E.; Lam, E.; Tsoukalou, A.; Willinger, E.; Kuznetsov, D.; Mance, D.; Kierzkowska, A.; Donat, F.; Abdala, P.; Comas-Vives, A.; Copéret, C.; Fedorov, A.; Müller, C. Engineering the Cu/Mo_2CTx (MXene) Interface to Drive CO_2 Hydrogenation to Methanol. *Nature Catalysis* 2021, 4, 860–871. https://doi.org/10.1038/s41929-021-00684-0

MATHEMATICAL MODELING OF SUSTAINABLE WASTE VALORIZATION PROCESSES

Ramazonova Shohida Shomuhammadovna
Asian International University
Department of General Technical Sciences, Lecturer
Bukhara, Uzbekistan
E-mail: shohidaramazonova0109@gmail.com
Rakhmatullayeva Ruxshona Bahromovna
Asian International University
Department of General Technical Sciences, Student
Bukhara, Uzbekistan

Abstract - In recent years, sustainable development and circular economy principles have become central to environmental and chemical engineering research. Waste valorization, which involves converting waste materials into valuable products, plays a crucial role in reducing environmental pollution and improving resource efficiency. Mathematical modeling provides powerful tools for analyzing, optimizing, and predicting the performance of waste processing systems.

This paper investigates the application of mathematical modeling and optimization methods to sustainable waste valorization processes. Special attention is given to system efficiency, energy consumption, environmental impact reduction, and process stability. The study demonstrates how mathematical approaches can enhance decision-making and improve the sustainability of chemical and environmental systems.

Keywords: sustainable development, waste valorization, mathematical modeling, optimization, circular economy, environmental systems

Introduction

Global environmental challenges require innovative and scientifically grounded solutions. One of the most promising approaches is the implementtation of circular economy strategies, where waste materials are transformed into reusable resources. Sustainable waste valorization aims not only to reduce landfill disposal but also to recover energy and valuable materials.

However, waste processing systems are complex and involve multiple interacting variables such as temperature, reaction time, material composition, and energy input. Therefore, mathematical modeling becomes essential for understanding system behavior and improving operational efficiency.

Problem Statement

The main objectives in sustainable waste valorization systems include:

1. Maximizing resource recovery efficiency.
2. Minimizing energy consumption.
3. Reducing environmental emissions.
4. Ensuring process stability and safety.
5. Optimizing economic performance.

These objectives often conflict with one another, leading to multi-objective optimization problems.

Mathematical Approach

Waste valorization processes can be represented using system models based on:

1. Differential equations for dynamic process behavior.
2. Optimization methods for resource allocation.
3. Statistical models for uncertainty analysis.
4. Simulation techniques for process performance evaluation.

A generalized optimization framework can be formulated to minimize energy consumption and environmental impact while maximizing output efficiency. The use of weighted objective functions allows balancing ecological and economic criteria.

Graph theory and network models may also be applied to analyze material flow and process interconnections in circular waste systems.

General Optimization Model

The waste valorization process can be formulated as a multi-objective optimization problem:

$$minF(x) = \omega_1 E(x) + \omega_2 C(x) - \omega_3 R(x)$$

where:

$E(x)$ – energy consumption,
$C(x)$ – environmental impact (emissions)
$R(x)$ – resource recovery efficiency,
$\omega_1, \omega_2, \omega_3$ – weighting coefficients,
x – decision variables of the system.

Subject to:

$$g_i(x) \leq 0, \ \ i = 1,2, \dots, n$$

where $g_i(x)$ represents technological and environmental constraints.

Dynamic Process Model

Waste transformation dynamics can be described by a simplified mass-balance model:

$$\frac{dW(t)}{dt} = -kW(t)$$

where:

$W(t)$ – amount of waste at time t

k – processing rate coefficient

t –time

Energy Efficiency Model

Energy efficiency indicator can be expressed as:

$$\eta = \frac{R_{out}}{E_{in}}$$

where:

R_{out} – recovered valuable resource

E_{in} – energy input

Results and Discussion

The implementation of mathematical modeling in waste valorization systems provides:

1. Improved prediction accuracy.
2. Enhanced operational control.
3. Reduced resource loss.
4. Better sustainability indicators.
5. Data-driven decision-making support.

Mathematical tools allow researchers and engineers to evaluate different technological scenarios before practical implementation, reducing risks and costs.

Conclusions and Recommendations

Mathematical modeling plays a significant role in advancing sustainable waste valorization processes. By integrating optimization techniques, simulation models, and analytical methods, it is possible to improve efficiency, reduce environmental impact, and support sustainable development goals.

Future research should focus on integrating artificial intelligence methods with mathematical models to enhance predictive accuracy and adaptive control in waste processing systems.

References

1. Biegler, L. T. (2010). *Nonlinear Programming: Concepts and Applications*. SIAM.
2. Ellen MacArthur Foundation. (2019). *Circular Economy Principles and Applications*.
3. European Environment Agency. (2022). *Waste Management and Sustainability Report*.
4. Montgomery, D. C. (2017). *Design and Analysis of Experiments*. Wiley.
5. Rao, S. S. (2009). *Engineering Optimization: Theory and Practice*.

ADSORPTION OF ANTIBIOTICS USING RICE HUSK HYDROCHARS PRODUCED VIA VARIOUS POST-TREATMENT METHODS

Ulduz Nazarli, Aysun Aghazada, Kifayat Gambarova, Shalala Tanriverdiyeva, Rima Guliyeva
Baku Higher Oil School
Baku, Azerbaijan
ulduz.nazarli.std@bhos.edu.az , aysun.aghazada.std@bhos.edu.az , kifayat.gambarova.std@bhos.edu.az , shalala.tanriverdiyeva.std@bhos.edu.az

Summary - Hydrochar has emerged as an efficient and green adsorbent for the removal of various emerging pollutants from water. In this study, hydrochar was successfully prepared via the hydrothermal carbonization (HTC) method using rice husk as the feedstock and then functionalized with phosphoric acid (H_3PO_4) at various concentrations (0.5, 1.0, and 1.5 mol/L). The adsorption performance of the hydrochar materials was investigated for the removal of tetracycline from aqueous solutions. The physicochemical properties of the hydrochar samples, such as hydrochar yield, ash content, chemical composition, BET surface area, pore volume, and zeta potential, were also investigated to assess the impact of chemical activation.

The adsorption performance was investigated using the hydrochar samples at an initial tetracycline concentration of 0.3 mg/mL and at 25°C. The hydrochar functionalized with 1.0 mol/L phosphoric acid (HHP 1.0) showed the best adsorption capacity of 419 mg/g among the prepared hydrochar samples. The Langmuir isotherm model was found to fit the equilibrium data well, and the correlation coefficients (R^2) were very close to 1 (R^2 = 0.998–0.999). The adsorption capacity was found to decrease with increasing temperature, indicating the exothermic nature and the dominance of the physical adsorption process.

Key words: Hydrochar; Post-treatment; Adsorption; Antibiotic

Introduction:

According to the World Health Organization (WHO), the increased intake of pharmaceutical compounds and the incomplete removal of the compounds from conventional wastewater treatment plants have resulted in the constant discharge of the compounds into water bodies. Subsequently, the contamination of water bodies by the compounds has become a serious environmental issue of global concern. Among the environmental compounds of concern, antibiotics like tetracycline have been found to be present in surface water, groundwater, and wastewater due to their extensive use in the therapy of humans and livestock. The persistence, bioactivity, and stability of tetracycline in water bodies also contribute to the development of antimicrobial resistance, which is a major ecological and public health threat [2].

Adsorption is generally recognized as an efficient, simple, and cost-effective method for the removal of organic pollutants from water. Compared to advanced oxidation processes and membrane separation processes, adsorption is advantageous for its lower operational cost, higher efficiency, and simplicity of application. In recent years, carbon-based adsorbents made

from biomass, such as biochar and hydrochar, have received much interest for their sustainability, cost-effectiveness, eco-friendliness, and availability of functional groups. Agricultural wastes such as rice husks, walnut shells, tea waste, olive waste, and pomegranate peel are abundant, renewable, and potential precursors for the synthesis of eco-friendly adsorbents for water treatment purposes.

Rice husk is a promising feedstock due to its high silica content, porosity, chemical inertness, and abundance in different parts of the world. Recently, hydrothermal carbonization has been recognized as a green and energy-efficient technique to produce carbon-rich hydrochar from wet biomass at mild temperatures ranging from 150 to 350°C in aqueous solution. Compared to conventional biochar produced at high temperatures, hydrochar generally has a greater amount of oxygen-containing functional groups, which can improve its affinity to adsorb organic contaminants such as antibiotics [3].

However, the adsorption capacity of raw hydrochar is generally limited by its low surface area and active sites. Thus, a series of chemical modifications are generally used to improve the physicochemical properties of hydrochar. Acid modification, especially using phosphoric acid (H_3PO_4), can introduce functional groups such as hydroxyl, carboxyl, and phosphate groups, which can effectively improve the adsorption capacity. It has been proven that the adsorption efficiency using phosphoric acid-modified hydrochar can be enhanced to adsorb different kinds of organic contaminants, such as antibiotics and dyes.

Experimental Part:

Hydrochar was created from rice husk biomass feedstock collected from farmers in the surrounding area. The hydrochar products were produced by a hydrothermal carbonization method (HTC) using tetracycline (TC) hydrochloride as a model chemical for an antibiotic contaminant that is frequently present in freshwater bodies. Phosphoric acid (H_3PO_4) of analytical grade was employed for chemical treatment of the hydrochar that was produced. The hydrochar product was washed with ethanol and deionised water to prepare solutions used during the experimental procedure.

To produce hydrochar, the RH was mixed with deionised water in a sealed autoclave reactor at 7 grams of RH to 42 mL of deionised water, and the mixture was then heated at 200 °C to establish autogenous pressure for 3.5 hours. After the mixture had cooled to room temperature, the solid hydrochar was separated from the water via filtration, then thoroughly washed with deionised water until the pH of the hydrochar was neutral, and finally dried at 100 °C for 12 hrs.

The hydrochar material is designated as HS. Batch adsorption tests were performed using a defined quantity of hydrochar mixed into 20 ml of tetracycline solution (0.3 mg/ml initial concentration). The mixtures were agitated at 170 rpm for 8 hrs at 25°C to attain equilibrium conditions. After passing through filter paper, the remaining tetracycline concentration was

measured by UV/Vis spectrophotometry. The adsorption capacity (Qe) was calculated with the mass balance equation below:

$$Q_e = \frac{(C_0 - C_e) * V}{m}$$

Where,

C_0 and C_e are the initial and equilibrium concentrations [$\frac{mg}{ml}$]

V - the solution volume [mL]

m - the mass of adsorbent [g]

Results and Discussion:

The results from the adsorption experiments indicate that phosphoric acid modification of rice husk-derived hydrochar resulted in significantly greater adsorption performance compared to unmodified rice husk-derived hydrochar. This increased adsorption performance can be attributed to the addition of more oxygen-containing functional groups and phosphate species to the surface of the hydrochar, thus enhancing the interactions between the tetracycline molecules and the hydrochar adsorbent. Functional groups such as hydroxyl and phosphate groups encourage hydrogen bonding and electrostatic attractive forces, which contribute to a substantial increase in adsorption capacity. The adsorption trends observed in this study are consistent with those described in the literature [3].

Table 1. Physicochemical properties of H_3PO_4-treated hydrochars

Sample	Yield (%)	Ash (%)	C (%)	H (%)	O (%)	BET (m^2/g)	Pore Volume (cm^3/g)	Zeta (mV)
HHP 0.5	58.74	23.34	38.79	27851	32.60	18172	0.027	-31.60
HHP 1.0	58.10	23.35	38.61	27120	32.50	24047	0.030	-35.87
HHP 1.5	59.75	22.59	37.42	26390	33.79	44501	0.027	-39.73

Surface area measurements indicate a significant increase in surface area of the hydrochar after being modified with phosphoric acid, with the highest surface area observed at an acid concentration of 1.0 mol/L. In addition to the observed increases in surface area, zeta potential measurements indicated that the hydrochar became increasingly negatively charged as the phosphoric acid concentration was increased (1.5 mol/L). Increased negatively charged zeta potential values would indicate there is greater surface charge density on the hydrochar, therefore improving the potential for interaction between hydrochar and tetracycline molecules [5].

Table 2. Tetracycline adsorption capacity at 25°C

Sample	Adsorption Capacity (mg/g)
HHP 0.5	320
HHP 1.0	419
HHP 1.5	330

The greatest adsorption capacity for the hydrochar was achieved by the hydrochar modified with 1.0 mol/L phosphoric acid (HHP 1.0). The increase in adsorption capacity for HHP 1.0 can be attributed to the optimum combination of surface functional groups and pore structure development. The decrease in adsorption capacity of hydrochar modified with 1.5 mol/L phosphoric acid (HHP 1.5) could be attributable to pore blockage or either chemical (acid) degradation or physical (temperature) degradation of the hydrochar produced by the relatively high phosphoric acid concentration [4].

Table 3. Langmuir parameters for tetracycline adsorption

Temperature (°C)	Qm (mg/g)	KL (L/mg)	R^2
25	3146	0.796	0.998
35	1677	1.658	0.998
45	1172	3.525	0.999

The Langmuir isotherm fits the experimental data well, indicating that the adsorption occurs on a single layer over similar locations in space [3]. It was found that as the temperature increases, the Qm also decreases, indicating that this is a physical process, with the main interactions being hydrogen bonding and electrostatic attraction [1].

Offers:

In order to achieve optimal tetracycline adsorption capacity along with favorable surface area characteristics of hydrochar produced from rock husks, a modification of hydrochar with phosphoric acid (1.0 mol/L concentration) should be done because this type of modification yielded the best tetracycline removal capacity during laboratory trials compared to higher concentrations of phosphoric acid (2.0 mol/L and 3.0 mol/L). Hydrochar produced from modified hydrochar will perform well in wastewater treatment systems that operate at low temperatures because the process of adsorption is exothermic. In addition, the focus of future work should be on evaluating the ability to regenerate and reuse hydrochar modified with phosphoric acid, to determine the long-term feasibility and economic viability of using phosphoric acid in order to modify hydrochar. The testing of modified hydrochar in real wastewater matrices (that contain competing ions and

organics) will provide more accurate representation of its performance within a true environmental setting. Finally, the scaling up of the hydrothermal carbonization process for the production of activated carbon using agricultural waste located in the local area would provide a more sustainable and cost-effective method of producing activated carbon for large-scale water treatment systems.

References:

[1] Wang, J., Wang, S. (2016). Removal of antibiotics from water. Journal of Environmental Management.
[2] Ahmad, M., et al. (2014). Biochar as a sorbent for contaminant management. Chemosphere.
[3] Tan, X., et al. (2015). Application of biochar in wastewater treatment. Chemical Engineering Journal.
[4] Ambaye, T.G., et al. (2020). Mechanisms and adsorption capacities of biochar for pollutant removal. *Int. J. Environ. Sci. Technol.*, 18, 3273–3294.
[5] Chen, T., et al. (2018). Sorption of tetracycline on H_3PO_4 modified biochar. *Bioresource Technology*, 267, 431–437.

DEVELOPMENT OF A SUSTAINABLE YEAST-CHITOSAN BIO-COMPOSITE FILTRATION NET FOR HEAVY METAL REMOVAL AND WATER HARDNESS REDUCTION

Leyla Huseynova, Dilber Huseynova; Rima Guliyeva
Baku Higher Oil School
Baku, Azerbaijan
leyla.h.huseynova.std@bhos.edu.az
dilbar.huseynova.std@bhos.edu.az

Summary - Industrial wastewater contaminated with heavy metals and hardness ions requires efficient and sustainable treatment technologies. In this study, a yeast–chitosan bio-composite filtration net was developed and evaluated for the removal of lead (Pb^{2+}) and hardness ions (Ca^{2+} and Mg^{2+}). The composite material was prepared by incorporating activated *Saccharomyces cerevisiae* biomass into a chitosan matrix and coating a polymer net substrate using a dip-coating method. The adsorption performance was analyzed using MP-AES spectroscopy. Results showed high removal efficiency of lead ions. When 0.05 g of yeast was used, Pb removal reached 95.88%. Increasing the yeast amount to 0.10 g and 0.20 g improved removal efficiency to 99.38% and 99.48%, respectively. The residual lead concentration decreased significantly to 0.26 mg/L at the highest dosage. Hardness reduction was also observed: calcium concentration decreased from 1.932 mg/L to 1.069 mg/L, and magnesium concentration decreased from 1.3586 mg/L to 0.7285 mg/L as yeast content increased.

These results demonstrate that the yeast–chitosan composite net provides efficient heavy metal removal and noticeable hardness reduction while maintaining an open-flow structure that minimizes clogging. The developed system shows strong potential as a low-cost, reusable, and sustainable solution for industrial wastewater treatment and resource recovery.

Keywords: chitosan, yeast, heavy metals, bio-composite net.

Introduction

Industrial wastewater containing heavy metals and hardness ions presents significant environmental and operational challenges. Pb, Cd, Ni and Cu are toxic and can accumulate in living organisms, causing cancer, neurological disorders and other health hazards. Ca^{2+} and Mg^{2+} in turn cause scaling in pipes and industrial equipment. Conventional treatment methods such as packed-bed adsorption systems and synthetic ion-exchange resins, are often expensive, energy-intensive, and prone to clogging. All these limitations are overcome by single bio-composite.

In recent years, chitosan has been applied to wastewater treatment, using its ability to bind metal ions due to the presence of amino functional groups [Dambuza, 2025]. Moreover, yeast biomass, containing active binding sites such as carboxyl and phosphate groups, has been determined to be a good adsorbent as well (especially *Saccharomyces cerevisiae)* [Shao, 2025]. Combining these two materials into a composite structure can improve both efficiency and cost-effectiveness.

In this study, a yeast-incorporated chitosan composite net was developed as a flexible filtration material for the removal of heavy metals and hardness ions. The bio-composite was prepared by activating yeast biomass, incorporating it into a chitosan matrix, and coating a polymer net substrate. Unlike conventional dense filters, the open net structure allows continuous water flow without clogging, easy recovery and reuse at large scale, and application of the drained materials in agriculture.

The aim of this research is to develop and evaluate a yeast-chitosan bio-composite net for efficient removal of heavy metals and hardness ions under continuous flow conditions.

Experiment

Materials: chitosan, baker's yeast, NaOH, PEG, epichlorohydrin

The yeast-chitosan composite net was prepared using a multi-step coating method. First, 5.0 g dry baker's yeast was chemically activated by treatment with a 0.5M sodium hydroxide (NaOH) solution under controlled stirring (300RPM) and temperature conditions ($80°C$). The activated yeast was washed several times with distilled water until around neutral pH was reached. Simultaneously, a viscous hydrogel matrix was created by dissolving 3.0 g of chitosan in acetic acid (4% 100ml solution). Then this honey-like mixture was stirred with polyethylene glycol (PEG), which serves as a plasticized to improve flexibility of the final coating. The activated yeast biomass was then integrated into the chitosan solution under $45°C$ and 800-1000 RPM stirring to obtain a homogeneous bio-composite binder.

For the last step, polymer net was cleaned with ethanol and coated using a dip-coating technique. The coated net was then immersed in 1M NaOH bath to neutralize the acidic chitosan and form a solid hydrogel skin around the net fibers. Furthermore, the prepared material was cross-linked using an

alkaline epichlorohydrin solution in order to make the coating chemical-resistant and prevent dissolving in acid during heavy metal recovery. Finally, the composite net was thoroughly washed with ethanol and distilled water to remove unreacted chemicals.

Results and Discussion

Offers

The yeast-chitosan composite net has strong potential for industrial implementation, including all applications of ancestor treatment methods along with new utilization possibilities enabled by the innovative design. It can be applied in mining wastewater ponds, electroplating industries, and other industrial facilities that generate metal-containing effluents. Moreover, thanks to its flexible structure, the net can operate in open flow systems without requiring high-pressure pumps. It can also be easily integrated into existing treatment units without major structural modifications, which reduces installation costs.

The main practical application of this system is the removal of heavy metals and the reduction of water hardness. In addition to wastewater purification, the adsorbed metals can be recovered through regeneration processes and reused in other industries. Moreover, the use of yeast biomass significantly lowers material costs and makes the clean water more affordable. Additionally, environmentally friendly spent biomass materials allow applications in agriculture, such as soil improvement or nutrient support. This promotes circular economy principles by reducing waste and promoting reuse.

To conclude, with future developments, this project can further become a perfect example of sustainable chemistry.

References

1. Abdul Rahman, A.S. (2023). Fabrication and Characterization of Magnetic Cellulose-Chitosan-Alginate Composite Hydrogel Bead Bio-Sorbent. https://doi.org/10.3390/polym15112494
2. Dambuza, A. (2025). Chitosan-Based Materials as Effective Materials to Remove Pollutants. https://doi.org/10.3390/polym17182447
3. Shao, Q. (2025). Application of Yeasts in Heavy Metal Remediation. https://doi.org/10.3390/fermentation11050236
4. Wang, X. (2025). Application Progress of Magnetic Chitosan in Heavy Metal Wastewater Treatment. https://doi.org/10.3390/magnetochemistry11090071
5. Zhu, Z. (2025). Advancing magnetic chitosan-based materials for sustainable heavy metal removal from water: Synthesis, regeneration, and future perspectives https://doi.org/10.1016/j.seppur.2025.134166

KARBON VƏ DES ƏSASİNDA ALINMIŞ YENİ YAŞIL KATALİZATOR İŞTİRAKİNDA BİODİZEL SİNTEZİ

Gülbən Məmmədova, Yeganə Məmmədova, İbrahim Məmmədov
Bakı Dövlət Universiteti
Bakı, Azərbaycan
gulbenmemmedova1@gmail.com

Açar sözlər: biodizel, heterogen katalizatorlar, DES, SDG-7, kömür

Giriş

Mineral yanacaqların (bərpa olunmayan təbii ehtiyatların) davamlı və intensiv istifadəsi onların sürətlə tükənməsinə səbəb olur, eyni zamanda yanma prosesi nəticəsində atmosferdə karbon qazının miqdarı artır. Xüsusilə nəqliyyat sektorunda istifadə olunan dizel yanacağı atmosferə karbon qazı, kükürd birləşmələri və digər zərərli emissiyalar buraxaraq ekoloji tarazlığa mənfi təsir göstərir. Bu səbəbdən həm enerji təhlükəsizliyinin təmin edilməsi, həm də ətraf mühitin qorunması baxımından daha təmiz və davamlı yanacaq növlərinin inkişafı mühüm əhəmiyyət kəsb edir. Biodizel bu istiqamətdə ən perspektivli alternativlərdən biri hesab olunur. Yağlı bitkilərdən əldə edilən biodizel neft mənşəli yanacaqlara alternativ ola bilən, bərpa olunan və karbon balansı baxımından daha əlverişli yanacaq növüdür. Biodizel əsasən uzun zəncirli yağ turşularının monoalkil efirlərindən ibarətdir və müxtəlif üsullarla istehsal edilə bilər. Son illərdə biodizel istehsalında hetrogen katalizatorlar üstünlüklərinə görə böyük maraq doğurur. Bununla yanaşı, dərin evtektik həlledicilər (DES sistemləri) son illərdə yaşıl kimya prinsiplərinə uyğun alternativ mühit və ya katalitik sistem kimi diqqət mərkəzinə çevrilmişdir. Karbon əsaslı heterogen katalizatorların DES mühitində və ya DES-modifikasiya olunmuş formada tətbiqi reaksiyanın selektivliyini və sabitliyini artırmaqla yanaşı, prosesin daha davamlı və ekoloji cəhətdən təhlükəsiz şəkildə həyata keçirilməsinə imkan yarada bilər [1-5].

Eksperimental hissə

Heterogen katalizatorların üstünlükləri nəzərə alınaraq bu işdə kömür və dərin evtetik həlledici iştirakında alınmış katalizator istifadə edilmişdir. İlk növbədə kömür digər işlərimizdə furfurol almaq üçün istifadə etdiyimiz qabığın kömürləşməsi prosesindən alınmışdır. Kömürləşmiş qabıqlar toz halına salındıqdan sonra mufel peçində 120 dərəcədə aktivləşdirilmişdir. DES isə xolinxloridin 1:6 nisbətində qliserinlə 1 saat 80^0C-də qarışdırılmasından əldə edilmişdir. Daha sonra isə kömür, DES, K_2CO_3 24 saat otaq temperaturunda qarışdırılmışdır. Transefirləşmə prosesində 0.25 q hazırlanmış katalizatordan, 12 ml yağ (günəbaxan yağı) və 10 ml metanol istifadə edilmişdir. Uyğun olaraq reaksiyanin məhsuldarlığı 2, 4, 6, 8 saatlarin hər birində tədqiq edilmişdir.



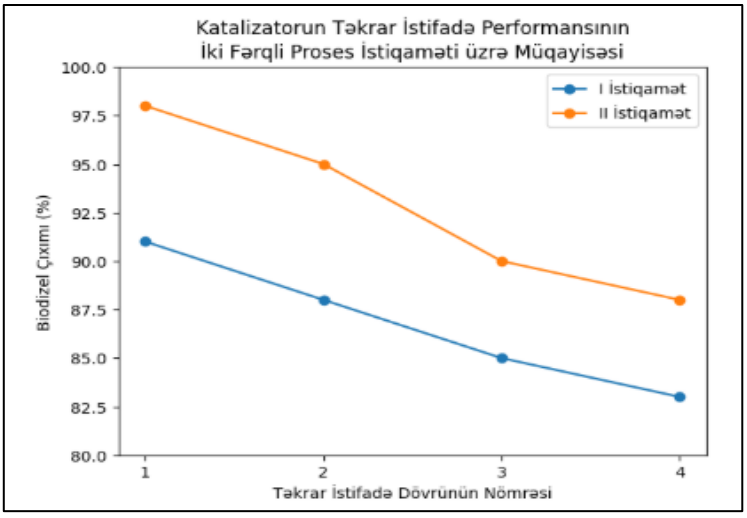
Şəkil 1. Yeni katalizator



Şəkil 2. Sintez edilmiş və süzülmüş biodizel

Nəticələr və onların müzakirəsi

İstifadə edilən katalizator ən azı 5 dəfə reaksiyani aparmaq qabiliyyətinə malik olmuşdur. Proseslərdən sonra katalizator süzülərək yenidən ostifadə edilmişdir. İki fərqli istiqamətdə reaksiya yoxlanilmişdir. I istiqamətdə: I dəfə reaksiya 2 saat, II dəfə 4 saat, III dəfə 6 saat, IV dəfə 8 saat müddətində aparılmışdır. II istiqamətdə isə bu prosesin tərsi yoxlanılmışdır: I dəfə reaksiya 8 saat, II dəfə 6 saat, III dəfə 4 saat, IV dəfə 2 saat aparılmışdır. Hər dəfə çıxımlar yoxlanıılmışdır.



Katalizator heç bir prosesdən sonra regerenasiya olunmamışdır.

Təkliflər

Təqdim etdiyimiz katalizator ekoloji təmiz yanacaq istehsalı üçün istismar oluna bilər.

İstinadlar
[1]. Beata Narowska , Marek Kułazynski , Marcin Łukaszewicz , Ewa Burchacka. Use of activated carbons as catalyst supports for biodiesel production. Renewable Energy,2019, 135, 176-185
[2]. Chi-Hung Tsai and Wen-Tien Tsai. Sustainable Processes Reusing Potassium-Rich Biomass Ash as a Green Catalyst for Biodiesel Production: A Mini-Review. Processes 2024, 12, 2736]
[3]. Gaurav Yadav, Nidhi Yadav and Md. Ahmaruzzaman. Advances in biomass derived low-cost carbon catalyst for biodiesel production: preparation methods, reaction conditions, and mechanisms. RSC Adv.,2023,13, 23197]
[4]. Jack Clohessy and Witold Kwapinski. Carbon-Based Catalysts for Biodiesel Production—A Review. Appl. Sci. 2020, 10, 918]
[5]. Ling Gu, Wei Huang, Shaokun Tang, Songjiang Tian, Xiangwen Zhang. A novel deep eutectic solvent for biodiesel preparation using a homogeneous base catalyst. Chemical Engineering Journal, 2015, 259, 647–652]

PREPARATION OF SURFACTANTS TO REMOVE OR COLLECT OIL SPILLS

Kanan Maharramli, Said Guliyev, Arzu Abdullayeva
Baku Higher Oil School
Baku, Azerbaijan
arzu.behbudova@bhos.edu.az

Keywords: Cationic Surfactants, Oil Spill Remediation, Surface Tension Reduction, Critical Micelle Concentration (CMC), Petro-Collecting Efficiency

Introduction:

The increasing global energy demand, resulting in a higher oil and gas extraction and processing activity, has led to more frequent drilling, shipment and accidents. Consequently, a large amount of oil is being continuously spilled or poured over the water surface. [1][2] The adverse impacts of oil spills on our marine environment call for immediate clean-up measures and therefore also the need for research into new clean-up technologies and methods.

There are several ways to deal with an oil spill. Methods for dealing with spills can include physical, biological and chemical approaches. Each method is selected on the basis of cost, efficiency, and time considerations. Chemical dispersants are applied to the surface film of the oil in order to break it down into discrete droplets which can then be dissolved in water. Surface tension is broken thus increasing micelle solubility. Although chemical surfactants are highly toxic to mammals and have tendency to re-associate at low shear rates, they are effective at high shear rates in turbulent ocean waters. In addition, they provide long term protection of the shoreline against adverse environmental impacts. [3][4]

Surfactants (surface-active agents) are chemicals used to disperse oil [5]. Synthetic surfactants generally fall under the four broad categories of

cationic, anionic, amphoteric and non-ionic. The cationic surfactants have shown promising results in oil spill clean-up operations. A surfactant molecule has a polar head which has a positive charge and a hydrophobic non-polar tail which attaches itself to oil droplets and forms micelles. The micelles then carry the oil particles in water and scatter it over a large area, thus reducing the surface tension and thereby aiding the natural process of oil breakdown and removal [6].

The Surfactant breaks down fast and acts quickly on oil spills by going to the interface between oil and water. The hydrophobic (water-repelling) tail is absorbed in the oil, while the hydrophilic (water-attracting) head remains in the water, reducing the interfacial tension between the oil and the water. This breaks up the oil into tiny droplets, and the surfactant molecules form a protective membrane around the droplets to prevent them from re-combining into larger droplets. Smaller oil droplets are easier to break down in the water column.

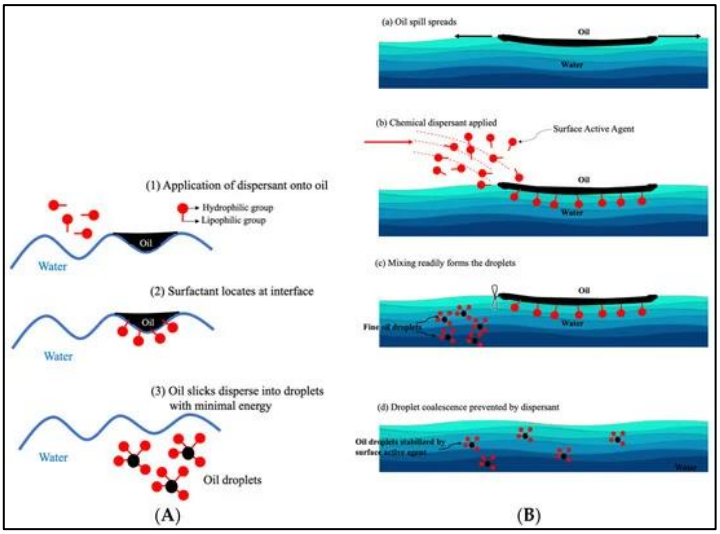


Figure 32: The working principle of surfactants [3]

It is expected to understand better the behavior of surfactants to be able to work out the ways of making up for the loss of elastic rebound that is sometimes observed. Another expectation is to devise new techniques of working and to choose and formulate surfactants more efficiently for use in cleaning up spills in the sea.

Experimental Part:

Four surfactants were synthesized in the laboratory and their physico-mechanical properties were examined. These were synthesized from salts of quaternary ammonium, derived from nonylamine and dodecylamine and acids derived from formic and acetic acids by thermal interaction under atmospheric pressure at different temperatures in the range of 40°C - 80°C

using stoichiometric quantity of reactants. The time required for formation of desired product in reactor was in the order of 4 to 5 hours. Surfactants prepared from the reaction between monocarboxylic acids and salts of quaternary ammonium of nonylamine and dodecylamine are designated as S1, S2, S3 and S4 respectively.

Surface activity of the synthesised compounds was investigated by evaluating their physicochemical properties such as surface tension and electrical conductivity. The surface tension was measured by Du Noüy ring method and electrical conductivity was measured by Mettler Toledo conductometer.[9] Critical Micelle Concentration (CMC) value was obtained from the surface tension and conductivity plot. Generally, the CMC value is higher for surfactants having higher surface activity. This is due to higher hydrophobicity as a result of longer alkyl chain lengths.

All data in this sub-module for petro-collection tests were obtained with distilled water, tap water and Caspian Sea water. The oil-collection capacity for the various petro-collection tests was determined as the capacity of the oil film in Petri dishes to be reduced in surface area by a pure surfactant and by 5% aqueous and alcoholic solutions. The capacity is calculated by measuring the decrease in surface area of the oil film and is a measure of the surfactant's ability to inhibit spreading of the oil film.

FTIR was used to check structural characterization of the synthesized surfactants. [10] The spectra obtained were consistent with structural formula of surfactants as deduced from NMR spectra. From the results, it could be deduced that surfactants with longer alkyl chains and higher critical micelle concentration (CMC) values which are S3 and S4 showed higher oil recovery than those with shorter alkyl chains that are S1 and S2. This showed that the structural configuration of the surfactants including alkyl chain length and functional groups are very significant in determining their performance.

Results and Discussion

Surfactants used in the study were identified and their performances investigated on different water sources such as their characteristics like surface tension, conductivity and the oil recovery efficiencies. In this study, performances of the dodecylamine based surfactants (S3 and S4) were investigated with respect to that of nonylamine based surfactants (S1 and S2). It was seen that dodecylamine based surfactants S3 and S4 had lower CMC (critical micelle concentration) values than nonylamine based surfactants (S1 and S2) in all the aqueous solutions investigated in this study. Consequently, surfactants (S3 and S4) showed a higher capacity for reducing the surface tension values at lower concentrations compared with (S1 and S2) surfactants. Moreover, the minimum surface tension was observed for surfactant S3 which implies that dodecylamine based surfactants having longer alkyl chain in their molecular structures exhibit better performances as surfactants.

Electrical conductivity of the solutions was measured to confirm the CMC values. The conductivity data confirms the surface tension data as the S3 and S4 solutions have lower CMC values.

Oil collecting properties of the surfactants were investigated in distilled, tap and Caspian Sea water media. As expected, surfactants with longer alkyl chain lengths (S3 and S4) had better oil collecting properties than those with shorter alkyl chains (S1 and S2). Surfactants with longer alkyl chains have stronger hydrophobic interaction with oil molecules which increases their oil collecting properties.

From Fig.1, the maximum surface excess concentration and the minimum area per molecule can be obtained. Obviously, the maximum surface excess concentration and the minimum area per molecule are less for S1 and S2 samples, while they are greater for S3 and S4 samples. So S3 and S4 have a more compact configuration at oil-water interface, and thus they possess higher surface activity.

Summary:

This study checks how the surface traits of cationic quaternary ammonium salts change when the amount changes. The study also looks at what happens when the number of carbon atoms in monocarboxylic acids changes. The study checks how the surface traits change when the alkyl chain gets longer or shorter. Surfactants help clean thin oil films. People use machines to clean up oil when the oil layer is thick. Surfactants help when machines do not work.

The physicochemical parameters of these surfactants, including surface tension, electrical conductivity, and Critical Micelle Concentration (CMC), were evaluated. A Mettler Toledo conductometer was utilized to measure electrical conductivity across the samples. The cationic quaternary ammonium salts under investigation were synthesized from nonylamine and dodecylamine in combination with formic and acetic acids, processed at ambient temperature and standard atmospheric pressure.

High efficiency does not always give better results. To pick the right surfactant for a spill, you have to look at different things. Not every factor needs to be perfect for the clean-up to help the environment.

Recommendations:

The efficiency of the used surfactant was confirmed as it gave a satisfactory reduction in surface tension. Future studies will focus on varying alkyl chain length as well as replacing the monocarboxylic acid species in order to ensure better performances under different environmental conditions. Indeed, the efficiency of the oil recovery process is always aimed at increasing recovery factor, hence reducing the interfacial tension even further.

Ecotoxicity Testing Ecological and environmental remediation of oil spills makes it essential to carry out ecotoxicity assessment of synthesized

surfactants. Toxicity studies will ensure that the newly developed chemical agents are safe and non-toxic for environmental use, therefore, sustainable for use at commercial scale [7][8].

Field Testing under Different Conditions New findings suggest that additional work in the form of Field Testing under Different Conditions is required: Based on recent experimental data obtained for surfactants in this project, it is clear that a lot of field work is needed in real world conditions, such as Caspian Sea and other marine conditions. Also it would be necessary to investigate the effect of salinity on surfactants in a wide range of temperatures, in addition to performing field tests in severe wave conditions to assess their performance and to determine the efficiency of these surfactants.

References:

[1] [Fingas, M., 2018. Oil Spill Science and Technology. 2nd ed. Elsevier: Boston, MA.]
[2] [Chang, S.E., Stone, J., Demes, K. and Piscitelli, M., 2014. Consequences of oil spills: a review and framework for informing planning. Ecology and Society, 19(2), p.26.]
[3] [Mittal, V. and Kumar, D., 2012. Application of surfactants in oil spill remediation. Journal of Colloid and Interface Science, 369(1), pp.1-12.]
[4] [Zhu, X., Venosa, A.D. and Suidan, M.T., 2004. Literature review on the use of commercial bioremediation agents for cleanup of oil-contaminated estuarine environments. US Environmental Protection Agency, 600(2), pp.04-083.]
[5] [Holmberg, K., 2002. Surfactants and polymers in aqueous solution. Colloids and Surfaces A: Physicochemical and Engineering Aspects, 256(2-3), pp.1-16.]
[6] [Rosen, M.J. and Kunjappu, J.T., 2012. Surfactants and interfacial phenomena. 4th ed. Hoboken, NJ: John Wiley & Sons.]
[7] [Riehm, D.A., McCormick, A.V., and Nikolov, A.D., 2017. The environmental impact of chemical dispersants: A review of alternatives. Environmental Toxicology and Chemistry, 36(7), pp.1783-1797.]
[8] [Colvin, K.E., Dhanasekaran, S., and Stottmeister, U., 2016. Ecotoxicological assessment of cationic surfactants for potential oil spill remediation. Chemosphere, 144, pp.1057-1065.]
[9] [Du Noüy, P.L., 1919. A new apparatus for measuring surface tension. Journal of General Physiology, 1(5), pp.521-524.]
[10] [Poling, B.E., Prausnitz, J.M., and O'Connell, J.P., 2001. The Properties of Gases and Liquids. 5th ed. McGraw-Hill: New York.]

DEVELOPMENT OF A MULTIFUNCTIONAL BIODEGRADABLE MULCHING FILM BASED ON PBSA INCORPORATING COFFEE SILVER SKIN AND COFFEE WASTE

Rana Rahimli, Elvira Sarsanova, Rima Guliyeva
Baku Higher Oil School
Baku, Azerbaijan
rana.rahimli.std@bhos.edu.az
elvira.sarsanova.std@bhos.edu.az

Summary - The research aims to create a sustainable biodegradable mulching film. This film will be made from poly (butylene succinate-co-adipate) (PBSA) combined with organic waste coffee silver skin (CSS). Coffee silver skin is produced when coffee is roasted and is an example of agro-industrial waste. This study will result in reducing plastic mulching films while valorizing organic waste. The composite materials of PBSA and coffee silver skin will provide structural support while also being environmentally friendly. The original framework for creating and testing the composite includes preparing the composite and examining the mechanical, thermal, and soil characteristics of the composite films. The work will directly support principles of circular economies and be a viable method to produce crops sustainably.

Keywords: Biodegradable mulch, PBSA, coffee silver skin, circular economy, sustainable agriculture.

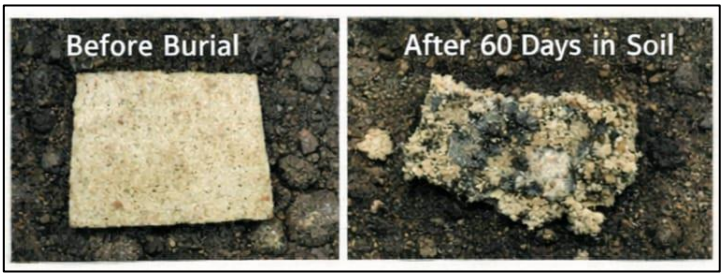
Introduction

Modern agriculture utilizes mulching films in their effective manner to increase yield through temperature control, moisture retention, and weed suppression. (Kasirajan & Ngouajio, 2012) Of the many types of mulching films, polyethylene-based films are the most widely used because of their high durability and low cost. (Briassoulis, 2006) However, the biggest drawback associated with polyethylene mulching materials is that they are non-biodegradable, and as a result of this characteristic; they have been contributing to a range of environmental issues; accumulation of plastics in soils and microplastic residue in our soils are two of the major concerns. Such issues adversely affect soil health and the long-term sustainability of agricultural production. Due to the concerns regarding the use of plastic mulching films, researchers have begun looking at biodegradable polymers as alternatives to polyethylene, specifically Poly(butylene succinate-co-adipate) (PBSA); PBSA has potential because of its mechanical strength, pliability and biodegradability within soil. (Gigli, et al., 2012) Nonetheless, the commercial viability of biodegradable polymers is limited by their higher manufacturing costs, thus hindering their widespread use. One potential sustainable solution to increasing the market penetration of biodegradable polymers as alternative mulching materials is to use natural waste materials as reinforcements. Coffee silver skin (CSS) is a type of agro-industrial waste generated from the roasting process of coffee beans. CSS is composed primarily of lignocellulosic materials (cellulose and lignin), (Ballesteros, Teixeira, & Mussatto, 2014) therefore, using CSS as a reinforcing filler

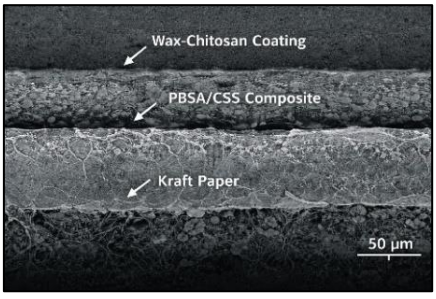
provides the opportunity to utilize a waste product while simultaneously creating value from an agro-industrial waste product in support of a circular economy strategy. A biodegradable mulch is designed for agriculture from a PBSA-based composite with coffee silver skin fibers and functional additives. This research demonstrates how to design materials that reduce the consumption of polymers, increase their structural properties and compatibility with the environment for agricultural applications.

Experimental Part

A multifunctional biodegradable mulch paper was produced by coating a kraft paper substrate with a PBSA-coffee silver skin (CSS) composite layer, then applying a hydrophobic carnauba wax-chitosan barrier top coat. The PBSA pellets were dried for 12 hours at 60 °C to remove moisture content. The coffee silver skin was dried, ground and then screened to produce 150μm particle size distributions to provide uniform dispersion of particles in the composite. The composite was produced by melt compounding at temperatures of 135 to145 °C using 10 to 20wt% CSS in molten PBSA. To enhance the mechanical properties and barrier performances of the composite material, bentonite clay (2 to 5wt%) and short cellulose fibers (3 to 5wt%) were incorporated. In addition, maltodextrin (1 to 3wt%) was added during the last mixing step to provide potential for microbial function. The resultant composite material was compression molded into films of approximately 150 to 200 μm in thickness at 140 °C and under 5–7 MPa for 3 minutes. All multilayer samples were kept at a temperature of 23 ± 2 °C and relative humidity of 50 ± 5% to adjust to room conditions.



Picture 1 *Untreated vs treated coffee silver skin*



Picture 2 *SEM Cross-Section of the Multilayer Biodegradable Mulch Structure*



Picture 3 Soil Burial Degradation of PBSA/CSS Mulch Film (Before and After 60 Days)

Results and Discussion

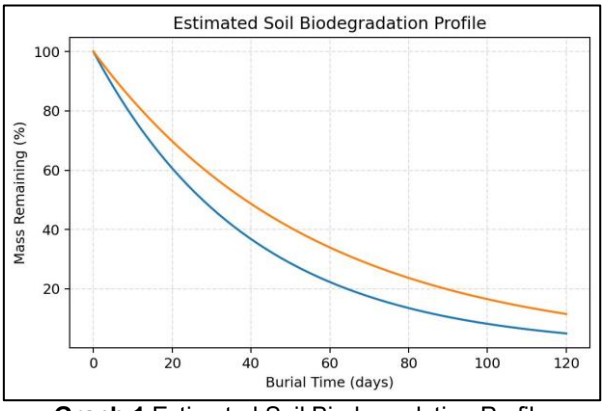
Based on theoretical research and existing polymer-filler interaction principles, the new multilayer biodegradable mulch made from plastic-coated kraft paper has substantially better mechanical strength, barrier performance, and functionality than uncoated kraft paper. Kraft paper typically (80 – 100 grams/m2) has limited tensile strength and absorbs water rapidly due to the water-loving cellulose structure; however, the structural integrity of the kraft paper is significantly improved after being laminated with the PBSA/CSS composite layer.

Using composite estimating models, it is estimated (based on approximate values) that the Young's Modulus of the PBSA composite layer (neat PBSA ≈ 350 – 400 MPa) would increase by approximately 10 – 15 % to 385 MPa with the addition of 15 wt.% Coffee Silver Skin (CSS) and 3 wt.% cellulose fibre because of the added rigidity of the particles reinforcing the structure. (Faruk, Bledzki, Fink, & Sain, 2012) However, the expected tensile strength of PBSA would decrease slightly (5 - 8 % at high filler levels) due to the possibility of an interfacial concentration of stress at high levels of filler.

Adding bentonite clay to the PBSA layer (3 wt.%) is expected to create a long, winding path for moisture to diffuse through the barrier, resulting in an estimated 20 - 30% reduction in the rate of water vapour transmission compared with PBSA-only films. Kraft paper absorbs moisture quickly before coating and looses mechanical stability. The composite barrier layer reduces the amount of moisture absorbed by the kraft paper by nearly 40% due to the water-repellent characteristics of PBSA after lamination.

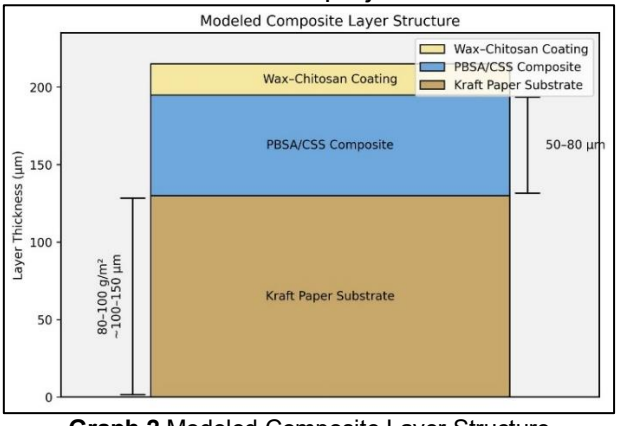
Moreover, the surface hydrophobicity has been greatly enhanced by the carnauba wax-chitosan top coating. Depending on the fraction of wax and the way that it is emulsified, when area contact is calculated the projected contact angle will go from approximately 65-75° without coating to over 95° once the top coat is applied; developing a shift from being hydrophilic to moderately hydrophobic. The crystalline domains of the waxes help to decrease surface energy and limit liquid penetration into the coated surface of the paper providing this increased hydrophobicity. Thermal stability analyses provide for a strong basis to conclude that the multilayer composite

will maintain its structural integrity within the processing temperature range (less than 150 °C) and that the physical properties of the layered construction will remain unchanged through the lamination process in comparison to the initial kraft base material.



Graph 1 Estimated Soil Biodegradation Profile

In comparison to the kraft paper base material used to produce the final multilayer mulch, the multilayer composition has a much greater degree of dimensional stability, has a lower degree of moisture sensitivity, and significantly increased stiffness while remaining biodegradable. Maltodextrin that is contained within the composite matrix is also anticipated to support slow microbial growth and interaction when buried under soil conditions and may encourage slow, controlled degradation after being buried in a field. When considered collectively, the measured performance attributes yield a significant improvement in the strength, water resistance, and functional performance of a multilayer mulch system in comparison to untreated kraft paper, and significantly smaller negative impacts on environmental degradation than traditional polyethylene mulch. Additional laboratory and field tests will be conducted to validate projected results.



Graph 2 Modeled Composite Layer Structure

Offers

To improve the performance and use of the multilayer biodegradable mulch paper developed, several enhancements and future research directions are suggested. First, optimization of the filler contents (coffee silver skin, bentonite clay, cellulose fibers) should be prioritized to find balance between mechanical reinforcement and flexibility through methodical adjustment of the ratios of each filler to maximize rigidity without sacrificing tensile strength. Secondly, treatment of the coffee silver skin using surface treatments (mild alkaline treatment, coupling agents, etc.) may lead to improved interfacial bonding between the coffee silver skin and the PBSA matrix, thereby reducing the effects of stress concentrations. Thirdly, systematic evaluation of wax/chitosan ratios may increase the level of hydrophobicity of the mulch, while maintaining the level of biodegradability and breathability needed for agricultural soil environments. Long-term burial and field studies would provide additional information on the degradation of kinetics, moisture retention capability, and response of plants growing in soils treated with the mulch when exposed to an actual environment. Next, scaling up the lamination process using continuous roll-to-roll coating equipment would improve the commercial viability and cost-effectiveness of the multilayer biodegradable mulch. Finally, incorporating controlled-release fertilizer or beneficial microorganisms within the composite layer of the mulch may change the mulch from a passive protective material into an active soil-enhancing system that supports the continued viability of both circular agriculture and environmentally friendly farming practices.

References

1. Ballesteros, L. F., Teixeira, J. A., & Mussatto, S. I. (2014). Chemical composition and antioxidant activity of coffee silverskin. *Food Research International*, 15-23.
2. Briassoulis, D. (2006). Mechanical behaviour of biodegradable agricultural films under real field conditions. *Polymer Degradation and Stability*, 1256-1272.
3. Faruk, O., Bledzki, A. K., Fink, H. P., & Sain, M. (2012). Biocomposites reinforced with natural fibers 2000-2010. *Progress in Polymer Science*, 1552-1596.
4. Gigli, M., Fabbri, M., Lotti, N., Gamberini, R., Rimini, B., & Munari, A. (2012). Poly(butlyene-succinate)-based polyesters for biomedical and agricultural applications. *European Polymer Journal*, 697-718.
5. Kasirajan, S., & Ngouajio, M. (2012). Polyethylene and biodegradable mulches for agricultural applications. *Agronomy for Sustainable Development*, 501-529.

ENHANCEMENT OF SULFURIC ACID PRODUCTION TECHNOLOGY BY PROCESSING SULFUR-CONTAINING WASTE GASES GENERATED DURING GAS PURIFICATION

Turakulova Marjona
Associate Professor
Bukhara State Technical University, Bukhara. Uzbekistan.
E-mail: marjonaturakulova79@gmail.com

Abstract - Currently, the reduction of anthropogenic impact from technological exhaust gases of the chemical and gas-chemical industries can primarily be achieved by purifying them from specific pollutants, followed by their reuse in technological processes through the application of innovative technologies. One of the pressing tasks of modern gas chemistry is the selection of reagents for purifying exhaust gases containing carbon dioxide and hydrogen sulfide, as well as the study of the scientific foundations for managing the chemisorption process of absorbing the main acidic components of the gas, which is of great importance. Scientific research is being conducted worldwide to develop efficient and energy-saving technologies for producing chemical reagents and absorbents that do not negatively affect the environment, aimed at cleaning flare gases from acidic components. In this area, special attention is given to the selection of absorbents to reduce the harmful content of carbon dioxide and hydrogen sulfide in flare gases of the gas-chemical industry, the improvement of sorption and kinetic characteristics, and the development and testing of technologies for accelerated purification of various exhaust gases and reduction of their environmental impact.

Keywords: hydrogen sulfide, sulfuric acid, sulfur dioxide, conversion, absorption, vanadium oxide.

Introduction

In the Republic, significant scientific and practical results are being achieved in the modernization of the gas-chemical industry, the creation of new reserves of absorbents, the development of technologies for producing import-substituting products based on them, and in particular, the development of competitive products, as well as their application in the purification processes of technological flare gases of the gas-chemical industry containing carbon dioxide and hydrogen sulfide. The Development Strategy of New Uzbekistan defines important tasks aimed at “further developing the potential of local industrial sectors by fully utilizing existing opportunities and introducing standards that meet the requirements of external markets and international standards.” In this regard, obtaining sulfuric acid solutions as a result of the absorption of hydrogen sulfide contained in flare waste gases by absorbents is of great importance. The Decree of the President of the Republic of Uzbekistan No. PF-60 dated January 28, 2022, “On the Development Strategy of New Uzbekistan for 2022–2026,” the Resolution dated October 30, 2019, “On approval of the Concept of Environmental Protection of the Republic of Uzbekistan until 2030,” the Resolution No. PQ-4265 dated April 3, 2019, “On measures to further reform the chemical industry and increase its investment attractiveness,” the Resolution No. PQ-3479 dated January 17, 2018, “On measures to ensure stable supply of

economic sectors with high-demand products and raw materials," as well as other regulatory and legal documents related to this field, define tasks whose implementation will be supported to a certain extent by this research [2].

Exsperimental Section.

In the oil and gas processing industry, hydrogen sulfide-containing gas is combusted to obtain sulfuric acid from sulfur-containing compounds. As a result, a process gas containing sulfur dioxide and water vapor is formed. This gas is then cooled and subjected to two-stage conversion in a contact apparatus. The conversion process is carried out in the presence of vanadium oxide catalyst layers by oxidizing sulfur dioxide, with the gas fed into the first stage at a temperature of 400–410 °C.

The gas leaving the first conversion stage, at a temperature of 450–460 °C, is directly directed to a condenser tower for absorption, where sulfuric acid and gas are separated. This gas is subsequently reheated and introduced into the second stage of the contact apparatus at a temperature of 410–415 °C. The gas leaving the second stage is cooled to 150–155 °C and sent to a monohydrate absorber, where sulfuric acid and purified waste gas are produced [3].

This study makes it possible to reduce equipment corrosion and the formation of corrosion products, which has a positive effect on the quality of the final product. In addition, it reduces the amount of acid mist formed during the absorption process due to the production of sulfuric acid.

The study relates to the production of sulfuric acid from hydrogen sulfide–containing gas and can be applied in the chemical, oil refining, and other industrial sectors. The method of producing sulfuric acid from hydrogen sulfide is known as the "wet" catalytic method, and the described method belongs to this category. This method includes the following main stages: combustion of hydrogen sulfide to form a mixture of sulfur dioxide and water vapor; oxidation of sulfur dioxide to sulfur trioxide in the presence of water vapor; and recovery of sulfuric acid.Various technological schemes for sulfuric acid production by the "wet" method are known. These schemes differ in the direction of gas and liquid flows, process operating conditions, and the design features of each stage. The main potential hazards of technological equipment and pipelines used in these methods, including their critical components, are associated with the fact that the hydrogen sulfide–containing gas being processed is explosive, flammable, and toxic. In addition, the sulfuric acid formed during the process (both as a liquid and as a finely dispersed mist) has extremely high corrosive properties [4].

Result and Discussion.

The closest method to the described research is the method of producing sulfuric acids from hydrogen sulfide–containing gas, in which a technological gas is formed by combustion. This gas contains sulfur dioxide and water, and a two-stage conversion is carried out. After the first stage, sulfur trioxide is removed, and subsequently sulfuric acids are produced. In

this method, after the first stage, absorption is carried out with circulating sulfuric acid so that the moisture in the gas entering the second stage does not exceed 0.005%. After the second stage, sulfuric acids of the required concentration are obtained, even up to oleum (RU 2530077, 2014). The main drawback of the indicated method is the high degree of corrosion experienced by the technological equipment, which depends on the likelihood of condensation of sulfuric acid vapors in the gas path. The resulting hot sulfuric acid condensate is highly corrosive, affecting the equipment material and potentially causing equipment failure and the formation of toxic gas concentrations, which can lead to poisoning of personnel. In addition, the method is highly complex when applied to apparatus [5].

Thus, the indicated method is not sufficiently efficient. The proposed research problem is aimed at improving the efficiency of the method for producing sulfuric acid from hydrogen sulfide–containing gas. This problem is addressed by a method in which a technological gas containing sulfur dioxide and water is formed through combustion of the gas, followed by cooling and subsequent two-stage conversion in a contact apparatus. Vanadium oxide catalyst layers participate in the oxidation of sulfur dioxide. The gas entering the first stage has a temperature of 400–410 °C, and the gas leaving the first stage reaches 450–460 °C. It is then directed directly to the absorption – condenser tower, where sulfuric acid and gas are separated. The gas is then fed to the second stage of the contact apparatus at 410–415 °C, and after cooling the gas from the second stage to 150–155 °C, it is sent to a monohydrate absorber, where sulfuric acid and purified waste gases are obtained. The technical result achieved reduces equipment corrosion and, simultaneously, decreases the formation of corrosion products (pollutants for agricultural use). This prevents unexpected excessive condensation on the equipment walls, which could otherwise lead to shutdowns, replacements, or cleaning. It also reduces corrosive wear of equipment, gas pipelines, and piping, helping to lower the chromium and molybdenum content in the product (the main source of chromium and molybdenum being corrosion of stainless steel equipment) and enabling the production of high-quality sulfuric acid, such as “K-grade” sulfuric acid (TU 113-08-617-87).

In addition, the result reduces the amount of sulfuric acid mist (a finely dispersed suspension of sulfuric acid particles in the process gas) formed during the absorption process, which, in turn, decreases the load on the mist-capturing equipment installed at the top of the monohydrate absorber and allows simplification of its design [6].

The described method is implemented as follows. As raw material, a gas with the following composition can be used: H_2S 50–60%; CO_2 18–20%; CH_4 1–2%; H_2O 2.5–5%; N_2 making up the remainder.

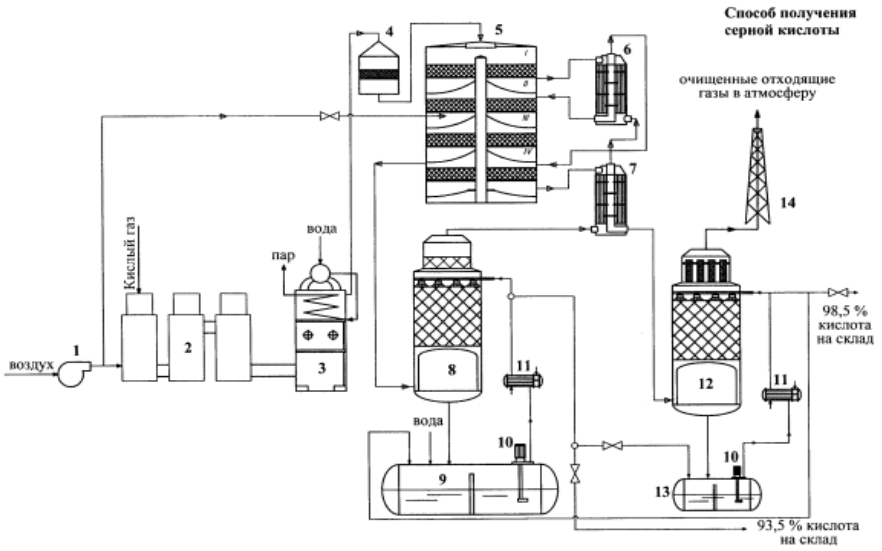


Figure 1. Technological scheme for sulfuric acid production.
1 – pump, 2 – three-chamber furnace, 3 – boiler with heat exchanger for steam heating, 4 – evaporation unit, 5 – four-layer contact apparatus, 6–7 – gas heat exchangers, 8 – condenser tower, 9 – condenser tower assembly, 10 – acid pumps, 11 – plate-type coolers, 12 – monohydrate absorber, 13 – monohydrate absorber assembly, 14 – waste pipe.

Air is supplied through a decentralized pump 1. Hydrogen sulfide–containing gas is directed to the furnace 2. In the furnace, combustion of hydrogen sulfide produces sulfur dioxide and water vapor. The resulting process gas, containing approximately 7–8% wt. SO_2 and 9–10% wt. water vapor, exits furnace 2 at a temperature of 1150–1250 °C and is directed to the boiler with heat exchanger 3 and the evaporation unit 4, where the gas is cooled to 400–410 °C. The gas at this temperature is then sent to the contact apparatus 5, which contains layers of catalyst for the oxidation of sulfur dioxide. Vanadium oxide catalysts can be used for sulfur gas oxidation, including those produced domestically and abroad, for example: BASF 04-115; Haldor Topsoe VK-38; Monsanto Enviro-Chem LP-120. In the first catalyst layer, sulfur dioxide is converted into sulfur trioxide, and the temperature rises to 550–560 °C. The resulting gas is sent to the gas heat exchanger 6, cooled, and directed to the second catalyst layer at approximately 450 °C. The temperature of the gas leaving the second catalyst layer rises to 475–485 °C. After the second layer, the gas is cooled to approximately 450 °C, which is achieved by supplying air to the atmosphere. In the first conversion stage, the oxidation of sulfur dioxide in the first three layers of the contact apparatus occurs at 93–95% efficiency.After the first conversion stage (the first three layers of catalyst in the contact apparatus), the resulting process gas at 450–460 °C is directed to the condensation tower 8, where the gas is washed with sulfuric acid. In

the condensation tower (the tower washed with sulfuric acid), SO_3 and water vapor formed in the first three catalyst layers are adsorbed (captured). The sulfuric acid mist formed during adsorption is captured by cartridge-type mist collectors installed at the top of the tower. Sulfuric acid from the tower 8 is automatically sent to the tower assembly 9, and then a controlled amount of sulfuric acid is fed to the tower using acid pumps 10 and plate coolers 11. Water is added to maintain the acid concentration in the assembly at 93.5–94.0% by mass. The acid concentration in the assembly 13 is regulated by supplying sulfuric acid from the assembly of tower 13. During the absorption process, almost all water vapor is removed from the gas, which allows the process to continue under “dry” conditions using standard heat exchange temperatures. The gas condensed in the tower is directed to the second conversion stage via gas heat exchangers 7 and 6, of the “Disk-Ring” type, heated to 410–415 °C. In the second conversion stage, sulfur dioxide is further oxidized to sulfur trioxide (SO) [6].

After the second stage, the resulting process gas is sent to the monohydrate absorber 12 for final absorption at a temperature of 150–155 °C. After passing through the monohydrate absorber, the process gas is directed to the waste pipe 14. Sulfuric acid from the monohydrate absorber is sent to the monohydrate absorber assembly 13, and then a controlled amount of sulfuric acid is circulated through acid pumps 10 and plate coolers 11 to wash the monohydrate absorber. The absorber is flushed with sulfuric acid at a concentration of 98.5–99.0% by mass, and its concentration is regulated by supplying acid from the tower assembly 9. Excess sulfuric acid from the monohydrate absorber assembly 13 is directed to the tower assembly 9. The acid concentration in the assembly is controlled by supplying sulfuric acid from the assembly of tower 13.

As raw material, gas containing 60% H_2S and 20% CO_2 is used. Air is used as the oxidizing agent. Air is supplied to the furnace 2 through a decentralized air pump 1, and hydrogen sulfide–containing gas is also directed to the furnace for combustion. Combustion of hydrogen sulfide in the furnace produces sulfur dioxide and water vapor. The resulting process gas contains 7.5% SO_2 and 9.6% water vapor. The process gas exits the furnace at 1150 °C and is directed to the boiler with heat exchanger 3, then to the evaporation unit 4, and finally to the contact apparatus 5 at 400 °C, which contains four catalyst layers [5].

The gas from the first conversion stage is cooled in a gas–gas heat exchanger. The cooling agent in the heat exchanger is the process gas returned from the first-stage absorption (condensation tower) preheated to 310 °C. After passing through the second catalyst layer, the gas is further cooled using a cold-air blow system.

The oxidation of sulfur dioxide in the first conversion stage occurs at 93.7% efficiency. After the first conversion stage (first three catalyst layers of the contact apparatus), the process gas at 455 °C is sent to the condensation

tower 8, where it is washed with 94% sulfuric acid. In the condensation tower, SO_3 and water vapor formed in the first three catalyst layers are adsorbed. Sulfuric acid mist generated during adsorption is captured by cartridge-type mist collectors installed at the top of the tower. Sulfuric acid is automatically sent from the tower 8 to the tower assembly 9. In addition, excess sulfuric acid and water from the monohydrate absorber assembly 13 are sent to the tower assembly, maintaining an acid concentration of 94% by mass.

During absorption, all water vapor is removed from the gas, allowing the process to continue under “dry” conditions, using standard heat exchange temperatures.

After the condensation tower, the process gas is heated in gas heat exchangers 7 and 6 to 410 °C and sent to the second conversion stage, where sulfur dioxide is further oxidized to sulfur trioxide (SO_3). In the first and second conversion stages, the oxidation process is carried out under the following temperature regimes: the gas entering the first, second, third, and fourth layers is at 400 °C, 450 °C, 450 °C, and 410 °C, respectively, while the gas leaving these layers reaches 554.5 °C, 483 °C, 460.3 °C, and 419 °C, respectively.

After the second conversion stage, the process gas at 150 °C is sent to the monohydrate absorber 12. The monohydrate absorber is flushed with sulfuric acid at 98.5% by mass and 70 °C.

After the monohydrate absorber, the process gas is directed to the waste pipe 14, and sulfuric acid is sent to the monohydrate absorber assembly 13. The acid concentration in the assembly is regulated by supplying sulfuric acid from the tower assembly 9.

Implementation of the method described above reduces the condensation of sulfuric acid in the process streams by 70%, decreases mist formation in the monohydrate absorber by 15%, and reduces corrosive wear of equipment by 15%. The resulting sulfuric acid meets the TSh 113-08-617-87 standard for “K-grade” sulfuric acid. The specific production rate of the steam itself is 1.22 t/t MNG (MNG – monohydrate). Similar results are achieved when applying the method within the indicated temperature ranges, and deviations in the temperature regime do not affect the expected outcomes [5].

Thus, the described method allows obtaining high-quality sulfuric acid at the target concentration, reduces the corrosive activity of process streams by 15–20%, and increases the reliability of equipment, as sulfuric acid condensation is reduced by 65–70%. In addition, mist formation in the absorber is reduced by 15–17%, which simplifies the technical design. If necessary, the produced sulfuric acid can be injected into geological layers to intensify extraction. As a by-product, energetic steam at 4.0 MPa is produced, which can be used for electricity generation, with a specific production rate of 1.22–1.25 t/t MNG.

Conclusion and recommendations.

A method for producing sulfuric acid from sulfide-containing gas, in which the gas is combusted to generate a process gas containing sulfur dioxide and water, then cooled and subsequently subjected to two-stage conversion in a contact apparatus. In this process, the gas is periodically fed into the first-stage conversion through vanadium oxide catalyst layers that oxidize sulfur dioxide, while maintaining the gas temperature at 400–410 °C. The product leaving the first stage, at a temperature of 450–460 °C, is sent directly to a condensation tower to recover sulfuric acid and gas. The gas is then reheated to 410–415 °C before being sent to the contact apparatus. After the second stage, the gas is cooled to 150–155 °C and directed to a monohydrate absorber, where sulfuric acid and purified waste gas are obtained.

References

1. Бобоқулов.Ф.Б., Фозилов С.Ф., Фазилов А.А.Табий газ таркибидаги H_2S ни утилизатсия қилиш ва у асосида турли кимёвий реагент олиш. 2022 й Озиқ-овқат маҳсулотлари ишлаб чиқаришда илм-фан ва инновацион технологиялар» мавзусидаги Халқаро илмий-амалий конференцияси 552-556 б
2. Бобоқулов Ф.Б., Фозилов С.Ф., Фозилов Ҳ.С. Газлардан полимер маҳсулотлар олиш жараёни. Техник жиҳатдан тартибга солишда метрологик таъминот Республика илмий-амалий анжумани 2022 йил 20-21 май 169-172 б.
3. А.Л. Лапидус, И.А. Голубева, Ф.Г. Жагфаров. Газохимия. Ч.ИИ. первичная переработка углеводородных газов. –М.: ГРУ Нефти и газа им. И.М Губкина. 2005.-280 с.
4. Проблемы и перспективы развития газохимии. Труды Мос¬ковского семинара по газохимии 2004-2005 г. Выпуск 3/ Под ред А.. Владимирова, А.Л.Лапидуса, - М.: РГУ нефти и газа им. И.М. Губкина, 2006. - 226 с.
5. To’raqulova M.Q., Ataullayev Sh.N., Boboqulov F.B., Xamidov D.G‘Neft va gaz zavodlaridan chiqayotgan mash’ala gazlarini qayta ishlash texnologiyalasini takomillashtirish .Fan va texnologiyalar taraqqiyoti Ilmiy - texnikaviy jurnal. Buxoro: 2025 yil №1. 11-18 b.
6. To’raqulova M.Q., Boboqulov F.B., Temirov A.H. Vodorod sulfidi saqlagan nordon gazlarni utilizatsiyalashning samarali texnologiyasini ishlab chiqish. Fan va texnologiyalar taraqqiyoti Ilmiy – texnikaviy jurnal. Buxoro: 2025 yil №1. 84-90 b.

PHYSICOCHEMICAL ANALYSIS OF FUEL DISTILLATES OBTAINED FROM WASTE TIRE

Ruxsora Khojiyeva, Ruslan Khayitov
Bukhara State Technical University
Bukhara, Uzbekistan.
E-mail: hruxsora86@mail.ru
E-mail: leo-bexa@mail.ru

ABSTRACT - This article presents the results of research on the development of technology for producing fuel distillates by recycling worn-out car tires. Used car tires are cut, crushed, separated from metal wires and the pyrolysis processes of raw materials are tested in a laboratory installation. Tire fuel waste was purified from sulfur-containing compounds such as benzotriazole and dimethylbenzo[b]thiophene in distillate using sulfuric acid and sodium hydroxide. A technology for extracting fuel distillate from used car tires is proposed.

KEYWORDS: waste tires, pyrolysis, fuel distillate, gas chromatography-mass spectroscopy, benzathiazole, dimethylbenzo[b]thiophene, technology.

Introduction.

The decline in oil reserves makes it necessary to find substitute raw materials and produce fuel using alternative methods. The production of fuel by recycling used materials is considered promising.

According to statistics, approximately 800 million waste tires are discarded worldwide every year. This indicator is expected to increase by about 2 percent each year. Currently, the annual global production of tires is approximately 1.5 billion units, which corresponds to approximately 17 million tons of used tire waste each year.

Used tire waste is a valuable polymer raw material. One ton of tire waste contains approximately 700 kg of rubber that can be used to produce fuel [1]. Considering that the waste used is a valuable polymer raw material, it proposes the use of alternative methods of fuel production.

Among thermal destruction technologies, the pyrolysis process is considered more efficient in terms of its low environmental impact compared to other recycling methods. The process products include gases, fuel distillate, and carbon (solid residue), which can be used as valuable raw materials after special processing processes.

Experimental section.

Used tire waste, sulfuric acid, and sodium hydroxide solution were used as research objects.

Considering that pyrolysis is an effective method for obtaining fuel distillate from used tire waste, a pyrolysis pilot plant was assembled [1,2,5].

Thermogravimetric analysis determined the temperature range for the decomposition of used tire waste in the crucible. Based on the thermogravimetric data obtained, the pyrolysis process was carried out at a temperature of 200-500 °C, which was controlled by a thermocouple located in the middle of the reactor.

The used tire waste was initially crushed into a powder state. The shredded waste tire pieces were separated into fractions. Used tire waste in the form of powder with an average fraction size of 0.5 to 15 mm was loaded separately into reactor. The reason for using shredded used tire waste is to maximize the production of distillate fuel. During the study, the relationship between tire waste size and tire waste distillate production was studied, and this relationship is presented in Figure 1.

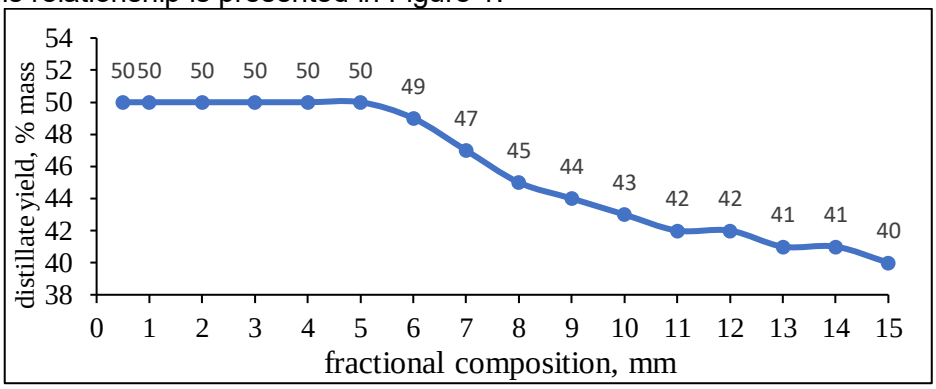


Figure 1. Dependence of waste fraction size on the production of fuel distillate from waste tires

The composition of the fuel distillate obtained as a result of the research was analyzed using physicochemical analysis methods. The results of the analysis are presented in Table 1.

The elemental composition of the fuel distillate obtained from used tire waste was determined using gas chromatography-mass spectrometry. The analysis results showed that the fuel distillate obtained from used tire waste contained sulfur-containing compounds such as benzothiazole and dimethylbenzo[b]thiophene. We used inorganic materials to purify this sulfur-containing complex from the distillate of fuel derived from used tire waste.

Results and discussions

To conduct research, we assembled a laboratory device for pyrolysis of rubber and plastic waste without air (under vacuum conditions) and conducted research in this laboratory device [5]. The results from the study are presented in Table 1.

Table 1. Products resulting from the pyrolysis of used waste tire samples.

Research	fuel distillate yield, %	Gas output, %	Solid residue output,%	loss, %
tire (Bars 185/70R14 BR200)	20-25	26	45-49	4
tire (Roadone 315/80 R22.5 156/153L)	45-50	20	30-34	up to 1%

The composition of the fuel distillate obtained from used tire waste was analyzed using physicochemical analysis methods, and the analysis results are presented in Table 2.

Table 2. Physicochemical properties of fuel distillate obtained from used tire waste

№	Name of the quality indicator for control	Method of detection	Fuel distillate indicators
1	Density at 20 oC , kg/m3	GOST 3900-2022	870
2	Sulfur content, % mass.	GOST 19121-73	0,798
3	Amount of water , % mass.	GOST 2477-2014	3,2
4	Amount of chloride salts, mg/ml	GOST 21534-2021	13,982
5	Amount of mechanical compounds	GOST 6370-2018	0,093
6	Kinematic viscosity , mm2sek	GOST 31391-2020	1,6
7	Fractional content ˚C: Initial boiling point (i.b.) , 50% Boiling end temperature (b.e.)	GOST 2177-99	 65 200 360

When the composition of the fuel distillate obtained from used tire waste was studied using gas chromatography-mass spectrometry and GOST 19121-73, it was determined that the distillate contained sulfur-containing compounds. The hydrocarbon group composition was determined by gas chromatography-mass spectrometry and is presented in Table 3.

Table 3. Hydrocarbon group composition of tire-based fuel distillate

Hydrocarbon group	**Amount, mass. %**
Cycloalkane	37.81
Alkene	0.93
Aromatic hydrocarbons	58.69
Sulfur compounds Benzothiazole Dimethylbenzo[b]thiophene	 2,07 0,5

Based on the information in Table 2 and Table 3 above, we set a goal to purify the tire-based fuel from sulfur-containing compounds in the distillate. Therefore, 10 ml of tire-based fuel was measured from the distillate and placed in 3 test tubes, and the resulting samples were cooled to 0 °C. Then, 30% and 40% sulfuric acid solutions and concentrated H2SO4 were mixed in the test tubes. The distillate is reacted with H2SO4 at 0 °C. The reason for carrying out the process at 0 °C is to isolate only sulfur-containing compounds from the distillate, such as benzothiazole and dimethylbenzo[b] thiophene-like substances. Sulfuric acid reacts with benzothiazole and

dimethylbenzo[b]thiophene, the mechanism of which is shown in Figure 2. Considering that sulfuric acid is a strong oxidizer and reacts with beneficial compounds in the distillate at room temperature, the process was carried out at 0 °C.

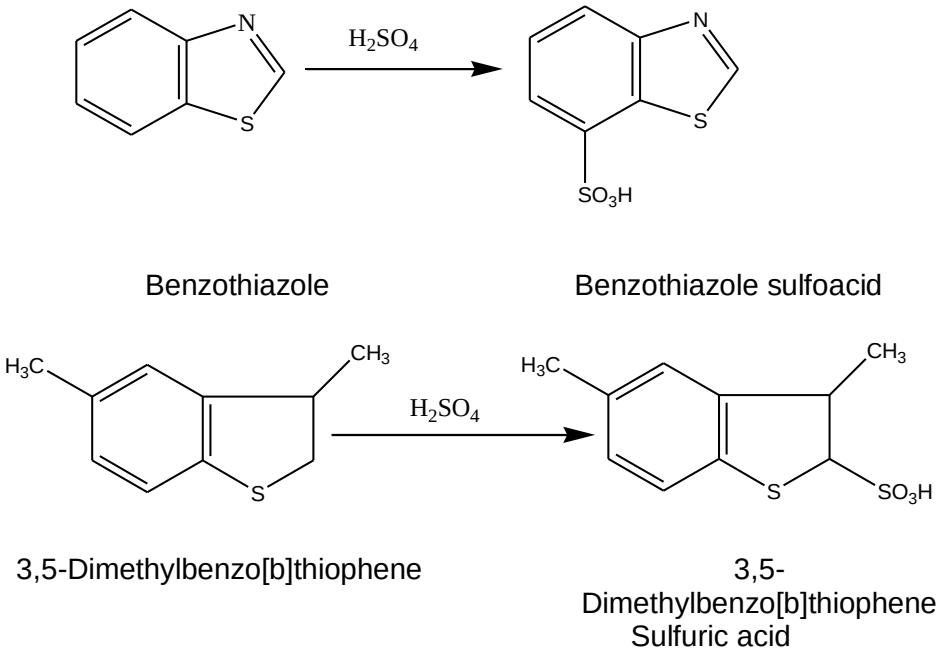


Figure 2. Reaction of sulfur compounds with sulfuric acid

Considering that the sulfonated products formed as a result of the reaction are unstable, a 10% sodium hydroxide solution was added at room temperature. The purpose of alkali treatment is to separate sulfur compounds from the distillate by forming the sodium salt of sulfonated sulfur-containing compounds. Reaction schemes can be represented as follows (Figure 3):

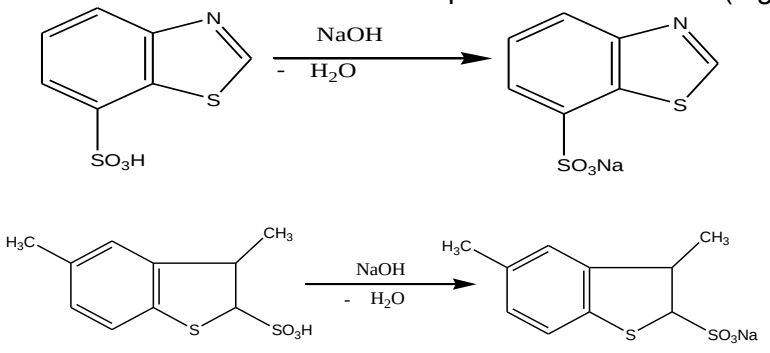


Figure 3. Preparation of sodium salts of sulfonated sulfur compounds

As a result of the reaction, 3 layers formed in the test tube - distillate, precipitate, and water. The distillate at the top of the test tube was taken and the sulfur content was determined using GOST 19121-73. The results of the study are presented in Table 4.

Table 4. Determination of sulfur content in tire-based fuel distillate

Sample	Reagents	Sulfur content, %
A-1	Distillate, 30% H_2SO_4 va 10% NaOH	0.798
B-2	Distillate, 40% H_2SO_4 va 10% NaOH	0.7
C-3	Distillate, conc H_2SO_4 va 10% NaOH	0.07

Based on the results obtained, we proposed a method and technology for producing distillate fuel by recycling used tire waste.

Conclusions and recommendations.

With the rapid development of the automotive industry, used tire waste, once called "black pollution," has become a serious threat to humanity. Given that used tire waste is composed of rubber, it was determined that an effective way to dispose of it is to extract fuel distillate from it. It was found that an effective method for obtaining fuel distillate is the pyrolysis of used waste tires in airless conditions.

The use of the proposed method accelerates the recycling process of used tire waste. The quality of the resulting fuel is improved by purifying it from sulfur compounds contained in the distillate. Inorganic substances, namely H2SO4 and NaOH, were used in the process of cleaning from sulfur compounds.

References

1. Hojiyeva, R. B., & Hayitov, R. R. (2020). Ishlatilgan avtomobil shinalarini qayta ishlash va yoqilgi mahsulotlarini olish imkoniyatlari. Science and Education, 1(9).
2. Хожиева, Р. Б., & Хайитов, Р. Р. (2021). Исследование процесса получения углеводородов из резиновых отходов. *Universum: технические науки*, (6-4 (87)), 44-46.
3. Хожиева Р.Б., Хайитов Р.Р., Наубеев Т.Х. Резиновые отходы их утилизаций “Қорақалпоғистон Республикасида ишлаб чиқариш саноат соҳалари ривожининг долзарб муаммолари” мавзусидаги республикаси илмий-амалий конференция. Нукус-2021 йил 26 апрел 241-242 б.
4. Hojiyeva, R. B., & Hayitov, R. R. (2022). Ishlatilgan rezina va plastmassa chiqindilaridan piroliz mahsulotlarini olish jarayonini tadqiq qilish. *Science and Education*, *3*(5), 259-264.
5. Хожиева, Р. Б., & Хайитов, Р. Р. (2021). Исследование процесса получения углеводородов из резиновых отходов. *Universum: технические науки*, (6-4 (87)), 44-46.
6. Khojieva Ruxsora, Khayitov Ruslan, Ataullaev Sherzod, Oripov Surat STUDY THE PROCESS OF RECEIVING HYDROCARBONS FROM RUBBER WASTE // Universum: технические науки. 2023. №4-7 (109). URL: https://cyberleninka.ru/article/n/study-the-process-of-receiving-hydrocarbons-from-rubber-waste (дата обращения: 18.09.2024).

AMINES USED IN THE ABSORPTION PURIFICATION OF GAS AND THE CAUSES OF FOAMING IN MDEA SOLUTION

E.R.Panoev
Doctor of Philosophy (PhD) in Technical Sciences,
Associate professor,
Republic of Uzbekistan, Bukhara.
E-mail: panoyeverali@gmail.com
S.O'.Toshboev
Doctor of Philosophy (PhD) in Technical Sciences,
Associate professor,
Republic of Uzbekistan, Bukhara.
E-mail: toshboevsardor@gmail.com
Bozorov Gayrat
Bukhara State Technical University, Doctor
of Technical Sciences (DSc), professor,
Republic of Uzbekistan, Bukhara.
E-mail: gayrat.bozorov2020@gmail.com
S.Yu.Begutjanova
Bukhara Technical School of Energy, Oil and Gas Industry,
Specialized Subject Teacher,
Republic of Uzbekistan, Bukhara.

ABSTRACT
This article analyzes the foaming problems occurring in methyldiethanolamine (MDEA) and diethanolamine (DEA) absorbents during the natural gas sweetening process. It has been demonstrated that foam formation is caused by thermostable salts, mechanical impurities, acidic components, amine oxidation, and changes in technological parameters. The physicochemical and technical properties of MDEA and DEA have been compared. The mechanism of foam formation in the absorber unit and its impact on gas purification efficiency have been elucidated. Methods for reducing and controlling foaming, including the importance of applying antifoaming chemicals, have been substantiated.
Keywords. Methyldiethanolamine, diethanolamine, foaming, solution, absorber, surfactants.

Introduction

Currently, MDEA is the primary absorbent used in gas purification processes worldwide, with the degree of foaming varying according to the content of thermostable salts. For the purification of natural gas from acidic components, MDEA and DEA are employed at the Gazli Gas Processing Plant and the Mubarek Gas Processing Plant.

Technical methyldiethanolamine is a flammable, oily liquid ranging in color from light yellow to dark orange, with a characteristic odor. Its corrosive activity and foaming properties are similar to DEA-type amines. It has been observed that it does not form explosive mixtures with air. According to GOST 12.1.007, it belongs to hazard class 3 regarding its effect on the human organism.

Table 1 presents the physicochemical properties of MDEA and DEA. MDEA has a molecular mass of 119.2; density at 20°C is 1.036-1.042 g/cm³. Its boiling point at atmospheric pressure is 244.8°C, with a freezing point of -21°C. The MDEA utilized in the equipment must comply with the requirements and standards of TU 2423-005-11159873 [1,2].

Diethanolamine (DEA) has a molecular mass of 105.1; relative density at 25°C is 1.094 g/cm³. Its boiling point at atmospheric pressure is 268°C, with a freezing point of -28°C. DEA is a colorless or slightly yellowish viscous liquid, readily soluble in water. It is considered an electrolyte with alkaline properties. It exhibits high resistance to chemical decomposition[4,5,6,9].

EXPERIMENTAL SECTION.

Currently, one of the main issues at the Gazli Gas Processing Plant is the loss of amine solution (absorbent) during the absorption process. The primary reason for this is foaming of the amine solutions due to various influences during the purification of gases from acidic components, leading to a portion of the amine solution being carried out with the treated gas and transferring into the lean amine solution. Ordinary foam transforms into foam through contamination by surfactants.

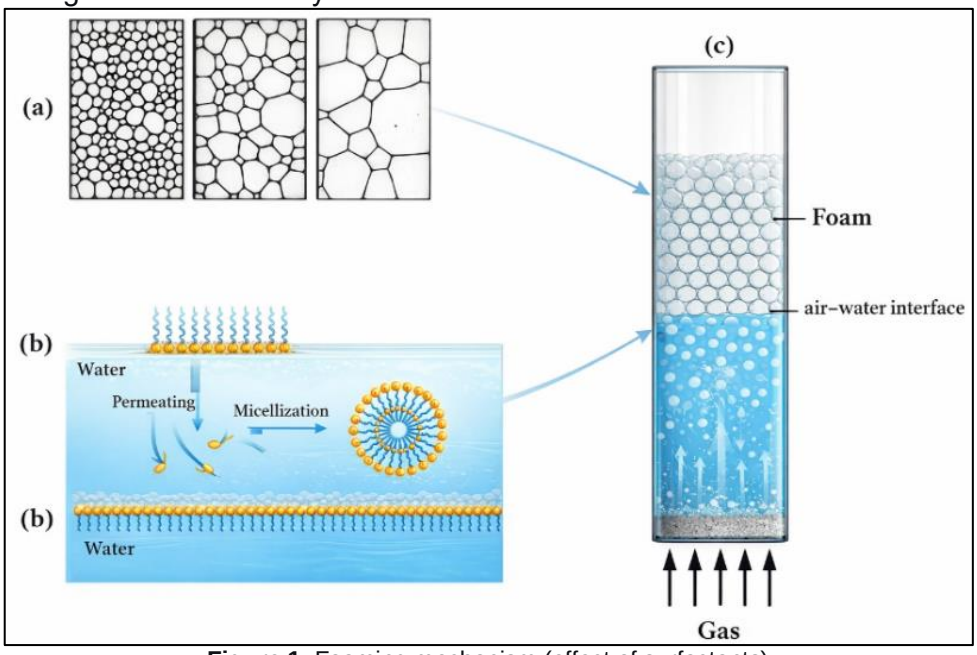


Figure 1. Foaming mechanism (effect of surfactants)

Figure 1 illustrates how surfactants form a solid layer on the gas-liquid interface, causing foam formation.

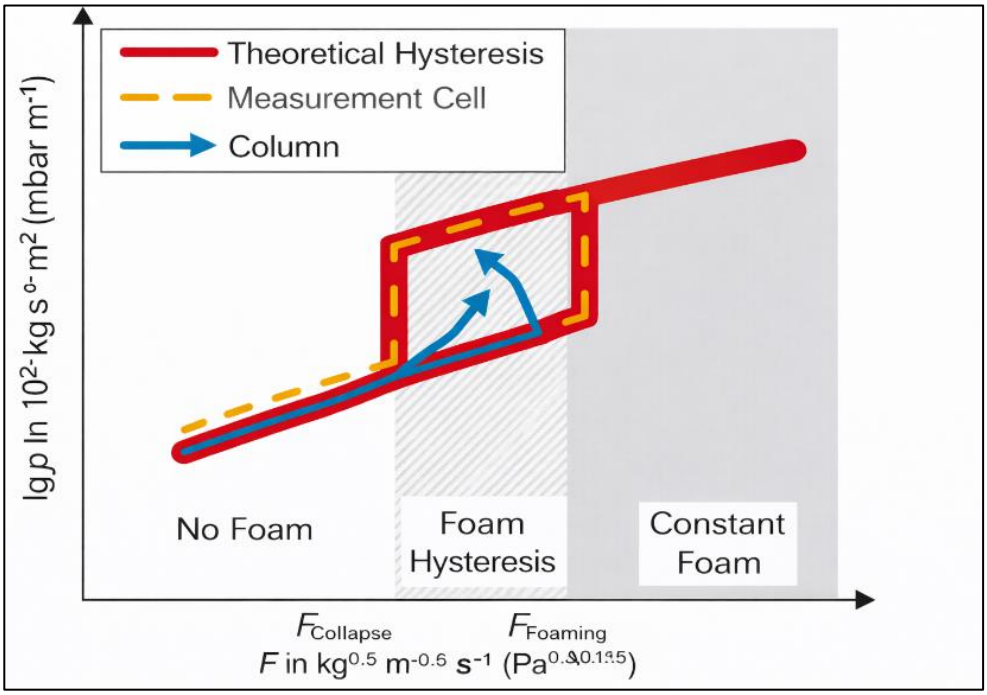


Figure 2. Foam formation process in the absorber

Figure 2 depicts the formation of foam under the influence of surfactants when gas and liquid mix inside the absorber[3,10].

Table 1. Physicochemical properties of methyldiethanolamine and diethanolamine

№	Parameter Name	Unit of Measurement	Parameter	
1	Formula		MDEA	DEA
			$C_5H_{13}NO_2$	$C_4H_{11}NO_2$
2	Molecular mass		119,2	105,1
3	Boiling point at 101.35 kPa	°C	231	270
4	Freezing point	°C	minus 21,0	28
5	Density at 25°C	g/sm^3	1.03	1.94
6	Specific heat capacity at 30°C	J/kg K	1.71	2.22
7	Absolute viscosity at 25°C	Kg/m s	101	308
8	Heat of absorption: H_2S CO_2	kJ/kg	1047 1340	1147 1511
9	Heat of desorption: H_2S CO_2	kJ/kg kkal/m^3 (norm.) kg /m^3 (norm.) kJ/kg kkal/m^3 (norm.) kg /m^3 (norm.)	1050 381 0,73 1420 516 1,24	1200 436 0.84 1510 548 1,31

Table 2. Technical specifications of MDEA and DEA

Parameter Name	Unit of Measurement	MDEA according to TU 2423-005-11159873		DEA according to TU 6-09-2652	Required parameters for inspection
		Premium grade	First grade		
Appearance		Without mechanical impurities			Check density, mass concentration, and appearance before use
Density at 20°C	g/sm^3	1,036 - 1,042	1,036-1,042	1,094	
Mass fraction, not less than	%	99,0	98,5	98,5	
Mass fraction of impurities, not more than, including: mass fraction of high boilers, not more than	% %	1,0 0.2	1.5 -	1.5 -	

One of the most common methods for controlling foaming processes is the addition of antifoaming chemicals to the circulating solution stream to suppress foam.

Foaming in the absorber unit during the amine gas purification process occurs due to various reasons present in the gas composition:

- Mechanical impurities;
- Acidic components;
- Amine oxidation;
- Temperature increase;
- Increased viscosity.

According to regulations, the temperature in the absorber unit should be 45-55°C, and the pressure should be 5 MPa[5,7].

RESULTS AND DISCUSSION.

Operational analysis at the Gazli Gas Processing Plant showed that the main cause of amine losses during natural gas purification is intensive foaming in the absorber column. Foam formation leads to entrainment of the amine solution with the treated gas stream, resulting in solvent losses and reduced process efficiency.

The study determined that foaming is primarily caused by the accumulation of surface-active substances, thermostable salts, mechanical impurities, and amine degradation products in the circulating solution. Elevated temperature (above 55°C), increased viscosity, and fluctuations in operating pressure (5 MPa) further intensify foam stability.

Comparative evaluation of MDEA and DEA solutions revealed that higher viscosity and contamination levels increase foam formation. MDEA systems demonstrated relatively more stable operation under controlled conditions due to lower energy requirements for regeneration and better selectivity toward acidic components.

CONCLUSION.

The conducted analyses indicate that the foaming phenomenon during the amine purification of gases significantly impacts absorption efficiency and amine solution losses. Particularly in MDEA and DEA-based solutions, the presence of thermostable salts, acidic components, and mechanical impurities accelerates the foam formation process. As a result of the intensive interaction between gas and liquid phases in the absorber unit, surfactants form a stable foam layer, leading to pressure drop and disruption of process stability.

Research results demonstrate that deviations from the regulated temperature and pressure inside the absorber increase the viscosity of the amine solution and heighten the risk of foaming. When the optimal operating regime (temperature 45-55 °C and pressure 5 MPa) is not maintained, amine solution losses increase, reducing the economic efficiency of the technological process.

Therefore, to reduce and control foaming, it is crucial to effectively purify the gas composition from mechanical and acidic impurities, continuously monitor the quality indicators of amine solutions, and rationally utilize chemical antifoaming reagents. These measures ensure the stability of the amine gas purification process, reduce absorbent consumption, and increase production efficiency.

REFERENCES

1. Toshboyev S.O'., Axmedov V.N., Do'stov H.B., Panoyev E.R., Ostonov F.I. (2024). Investigation of foaming processes in absorption gas purification. *Development of Science and Technology. Scientific-Technical Journal*, Bukhara, No.1, pp. 115-118.
2. Toshboyev S., Axmedov V., Panoev E., Olimov B. (2024). Analysis of the anti-foaming solution TSU, obtained on the basis of local antifoaming raw materials arising from gas cleaning. *Universum: Chemistry and Biology: Scientific Journal*, No. 4(118), Part 2, Moscow, Publishing House "MSNO", pp. 56-61. Electronic version of print publication.
3. Toshboyev S.O'., Axmedov V.N., Panoyev E.R., Xafizov A.R. (2024). Causes of foaming in gas purification units from acidic components and its prevention. *News of QarDU. Scientific-Theoretical, Methodological Journal*, No. 2(2), pp. 150-154.
4. Toshboev S., Hafizov A., Panoev E., Olimov B. (2024). Principal technological scheme of production of TSU-1 foam extinguisher. *Universum: Technical Sciences: Scientific Journal*, No. 8(125), Part 6, Moscow, Publishing House "MSNO", pp. 56-61. Electronic version of print publication.
5. Toshboyev S.O'., Axmedov V.N., Do'stov H.B., Panoyev E.R. (2023). Investigation of foaming processes in gas purification with absorbents. *Proceedings of the International Conference on "Innovative approaches to localization". Innovations in the exploration and exploitation of oil and gas fields*, Section I, October 14, 2023, Qarshi, pp. 94-95.

6. Toshboev S., Panoyev E. (2023). Foaming processes in amine gas purification. *Models and methods for increasing the efficiency of innovative research: a collection of scientific works of the International scientific conference*, October 11, 2023, Berlin, Part 27, pp. 119-125.
7. Toshboev S.U., Axmedov V.N., Panoev E.R. (2023). Investigation of foaming processes in amine gas purification. *Central Asian Journal of Theoretical and Applied Science (CAJOTAS)*, ISSN: 2660-5317, Volume 4, No. 10, October 2023, pp. 163-169.
8. Toshboev S., Axmedov V., Panoev E. (2023). Synthesis of higher fatty acid compound esters of higher fatty alcohols. *International Scientific-Technical Conference "Problems, innovative proposals and solutions in the field of chemistry and technology of oil and gas"*, December 14-15, 2023, Bukhara Engineering-Technological Institute, pp. 71-74.
9. Toshboyev S.O'., Axmedov V.N., Panoyev E.R., Ravshanova O.I., Raxmatov A.Q. (2024). Synthesis of TSU-1 anti-foaming solution in amine gas purification and its testing research works. *Development of Science Journal*, Volume 1, May 2024, No. 1, pp. 355-359.
10. Toshboyev S.O'., Axmedov V.N., Panoyev E.R., Usmonov S.B. (2024). Investigation of foaming processes occurring during gas purification. *Proceedings of the Republican Scientific-Practical Conference on "Current Problems of Chemistry"*, June 21-22, 2024, Urganch, pp. 212-226.

THE CONCEPT OF OIL REFINING AND PETROCHEMICAL SYNTHESIS AND CLOSED-LOOP ECONOMICS FOR SOLVING ENVIRONMENTAL PROBLEMS IN OIL REFINING, PETROCHEMICAL SYNTHESIS, AND OIL AND GAS PRODUCTION.

Ramin Musaev
25252525-32@rambler.ru
Researcher, Russian Academy of Sciences, Moscow, Russia

Abstract. This article explores the concepts of oil refining and petrochemical synthesis. It describes the principles of a circular economy, explores its meaning, and explores its role in solving environmental problems in oil refining, petrochemical synthesis, and oil and gas production. **Interest in the circular economy (CE**) is growing in academia, government, and business. However, the question of what a circular world will look like remains insufficiently studied or even formulated. Scientific research focuses on analyzing circular strategies (C-strategies) within the context of sustainable development, examining the benefits **of C-strategies**, and the barriers to achieving them. However, C-strategies without a clear vision of the future can hinder the achievement of goals and the resolution of a number of environmental problems. This article presents visions of a circular future and defines the circular economy. Without these, diverse understandings of the concept are inevitable, leading to the introduction of different metrics for measuring progress toward circular goals. Key findings: The circular economy is an evolving concept, which explains the lack of a unified definition. It should reflect visions of the future, which will form the basis for developing a unified system of metrics for measuring the degree of goal achievement and comparing them internationally. Visions of the future must be interpreted as a process of improvement, as they can be transformed... The concept of oil refining. Oil refining is the processing of crude oil to obtain primary petroleum products. Previously, straight-run distillation was used. Now, more complex processes have been developed and are used. The oil refining process includes:

cracking; alkylation; hydrogenation; aromatization; polymerization; synthesis. Straight-run distillation of crude oil is the process of separating it into individual fractions, which differ primarily in boiling point. Petrochemical synthesis is the extraction of substances from petroleum products and hydrocarbons from petroleum and natural gases through chemical processing. Thus, chemical compounds obtained from petroleum are classified as petrochemical products. The aim of this study is to demonstrate how circular economy principles in the oil industry can be used to avoid environmental pollution and address the issue of sustainable development in a country or region.

Keywords: Concept of oil refining, concept of petrochemical synthesis, oil and gas production, circular economy, sustainable development.

To achieve progress in addressing sustainability issues in the oil and gas sector, such as depletion of natural resources, increasing greenhouse gas emissions, and high rates of waste generation, it is necessary to shift from the traditional linear economic model (extraction – production – distribution – consumption – waste) to a closed-loop model that utilizes production process optimization, product reuse or sharing, and waste recycling.

Introduction. A circular economy is when waste from primary production goes to secondary production, waste from secondary production to tertiary production, and so on until there are no emissions that pollute the soil, water, or air. Despite the fact that research in the field of sustainable development of the oil and gas sector has been conducted by many authors (1), (Anis, Siddiqui, 2015; but there are unfortunately not enough works devoted to the study of the oil and gas industry from the point of view of the principles of a circular economy (circular economy) in the world. This sector is one of the largest in the world, with growing revenues and expenses necessary to provide consumers with energy. The product value chain in the oil and gas industry consists of 3 main sectors.

1**. The Upstream sector**, or E&P, where "E" means exploration, and "P" means production. In exploration and production, the search for potential hydrocarbon deposits on land or at sea is carried out using a complex of geological and geophysical tools, Next, exploration and appraisal wells are drilled. After a field is discovered, commercial production begins with drilling a series of production wells and connecting them to a surface production facility and transportation facilities. The Downstream and Midstream oil and gas sectors complement the Upstream sector for delivering products to consumers.

2. Midstream – everything related to the transportation of hydrocarbons from an oil/gas metering unit or from a central oil/gas gathering point to oil and gas refineries. Transportation methods include pipelines, tankers, railcars, and trucks.

3. Downstream – refining crude oil and natural gas, storing and marketing finished products: gasoline, kerosene, diesel fuel, jet fuel, lubricating waxes, asphalt, liquefied natural gas (LNG), and petrochemicals. Delivery to the end consumer is also part of the Downstream sector.

Main Part.

In general, the challenges of sustainable development in the oil and gas sector can be divided into the following categories: flaring associated petroleum gas flaring, which is a valuable source of raw materials; decommissioning of oil and gas production equipment due to the end of its useful life; disposal of oil and gas storage tanks; processing of drill cuttings; removal and treatment of produced water; handling of drilling muds and cement slurries; monitoring of greenhouse gas (GHG) emissions; subsidence of rocks; oil and gas leaks throughout the entire value chain; personnel safety. Each of the above-mentioned problems has caused numerous environmental problems in the past, and sometimes even environmental crises. Therefore, in 2015, UN member states adopted a 15-year plan to achieve the Sustainable Development Goals (SDGs) by 2030, which call for actions aimed at improving well-being and protecting the planet. A peculiarity of the oil and gas industry is that most of the operating activities are associated with a negative impact on the atmosphere - the emission of huge amounts of greenhouse gases (GHG), mainly methane, which can appear during drilling and production, leaks in wellhead equipment and pipelines, as well as in the event of an emergency blowout (1) (Anis, Siddiqui, 2015). Also, during drilling, production, and well repair, diesel-fueled units are used, which emit significant amounts of GHG. To eliminate the imbalance between countries. In 2021, the European Commission "presented the final text of the Regulation of the European Parliament and of the Council establishing a cross-border carbon adjustment mechanism (CBAM)" (2) (Nevskaya, Baronina, 2021) between the European Union and developing countries with weak carbon regulation, as well as to prevent "carbon leakage". Therefore, countries producing carbon-intensive products need to implement the principles of the so-called circular carbon economy (CCE) in their business models. Carbon capture, utilization and storage (CCUS) technologies have been studied by many authors (3), (4)(5) (Alsarhan et al., 2021; Cherepovitsyn, Chvileva, Fedoseev, 2020; Hasan, Eric First, Fani Boukouvala, Floudas, 2015). Thus, the study (6) (Eide et al., 2019) identified differences between CO2-based enhanced oil recovery methods at sea and onshore, and identified technological barriers to their implementation. The authors of the study (7) (Romasheva, Ilinova, 2019) identified groups of factors influencing the deployment of carbon dioxide capture and storage projects. In their opinion, the number of barriers related to economic issues, public safety, and resistance to the full-scale deployment of carbon dioxide capture and storage technologies worldwide is too great, while the lack of a direct commercial effect and the importance of such initiatives for reducing carbon dioxide emissions highlight the need for government regulation – financial support, clear legislation, public outreach, and adequate taxation and lending can facilitate the widespread

implementation of CCUS projects. Water produced at oil fields, after preliminary treatment and bringing to the desired quality, can be used as a means for maintaining reservoir pressure (MPP) or enhancing oil recovery.

Materials and methods of the research,

Materials of international organizations, works of scientists through academic analysis were used. In addition, water can be used as a cooling agent in the processing sector, for example, in an oil refinery (8) (9) (Adham et al., 2018; Stefanakis, 2022). Methods of purifying produced water, as emphasized in (10) (Shesterikova, Shesterikova, Popov, 2015), can conserve natural resources, reduce the negative impact on the ecosystem, and reduce fees for discharges into the environment. At the origins of the oil and gas industry, humanity did not think about the environmental damage caused by dumping drilling waste into the environment without any primary treatment to remove hazardous components (11) (Siddique, Leung, Njuguna, 2021). However, according to the source (12) (Ismail et al., 2017), it has already been revealed that ecosystems (increased environmental toxicity leads to the death of organisms), as well as humans (dermatitis, nausea, cough, skin and mucous irritation) suffer from hazardous chemical components contained in drill cuttings. Therefore, the safe disposal of drill cuttings requires increased attention worldwide. Drilling waste management is reflected in the works (13) (14) (15) (16) (Ryen Caenn, Darley, George Gray, 2017; Darajah, et al., 2021; George, Antonis, 2021; Phillips et al., 2018). Some authors (17) [propose reusing spent drilling fluids by cleaning them using the vibroacoustic method. The limitations of each technology must be considered, as many options require strict conditions. For example, CO2 injection into the reservoir requires geological conditions—traps capable of containing the gas and preventing leaks to overlying horizons; methanol production directly at the field requires the appropriate infrastructure, such as a gas processing plant, which entails significant capital investment; and cleaning drill cuttings through biodegradation can take a long time—months or even years.

Conclusion:

The study highlights the importance of a circular economy and the need to implement closed-loop technologies in the oil and gas industry to avoid environmental problems and promote sustainable development.

Literature.

1. Anis M.D., Siddiqui T.Z. Issues Impacting Sustainability in the Oil and Gas Industry // Journal of Management. – 2015. – No. 4. – p. 115. – doi: 10.5539/jms.v5n4p115.
2. Basile V., Capobianco N., Vona R. The usefulness of sustainable business models: Analysis from the oil and gas industry // Corporate Social Responsibility and Environmental Management. – 2021. – No. 6. – p. 1801-1821. – doi: 10.1002/csr.2153.
3. Nevskaya A.A., Baronina Yu.A. Cross-border carbon regulation: the new context for Russia-EU relations // Modern Europe. – 2021. – No. 6(106). – c. 63-74. – doi: 10.15211/soveurope620216374.

4. George K., Antonis Z.A. Drill cuttings waste management from oil & gas exploitation industries through end-of-waste criteria in the framework of circular economy strategy // Journal of Cleaner Production. – 2021.– doi:10.
5. Cherepovitsyn A., Chvileva T., Fedoseev S. Popularization of Carbon Capture and Storage Technology in Society: Principles and Methods // International Journal of Environmental Research and Public Health. – 2020. – No. 22. 1016/j.jclepro.2021.129098
6. Hasan M.M.F., Eric L. First, Fani Boukouvala, C. Floudas A multi-scale framework for CO2 capture, utilization, and sequestration: CCUS and CCU // Computers and Chemical Engineering. – 2015. – p. 2-21. – doi: 10.1016/j.compchemeng.2015.04.034.
7. Eide L.I. [and others] Enabling large-scale carbon capture, utilisation, and storage (CCUS) using offshore carbon dioxide (CO2) infrastructure developments - A review // Energies. – 2019. – No. 10. – p. 1945. – doi: 10.3334. 8. Romasheva N., Ilinova A. CCS Projects: How Regulatory Framework Influences Their Deployment // Resources. – 2019. – No. 4. – p. 181. – doi: 10.3390/RESOURCES804018190/en12101945
9. Adham S. [et al.] Membrane applications and opportunities for water management in the oil & gas industry // Desalination. – 2018. – p. 2-17. – doi: 10.1016/J.DESAL.2018.01.030.
10. Stefanakis A.I. A circular model for sustainable produced water management in the oil and gas industry // Circular Economy and Sustainability. – 2022. – p. 63-77. – doi: 10.1016/B978-0-12-821664-4.00026-1.
11. Shesterikova R.E., Shesterikova E.A., Popov M.V. Direction of using produced water as process fluids // News of higher educational institutions. Oil and Gas. – 2015. – No. 2(110). – p. 103-108. – doi: 10.31660/0445-0108-2015-2-103-108
12. Siddique S., Leung P.S., Njuguna J. Drilling oil-based mud waste as a resource for raw materials: A case study on clays reclamation and their application as fillers in polyamide 6 composites // Upstream Oil and Gas Technology. – 2021. – doi: 10.1016/J.UPSTRE.2021.100036
13. Ismail A.R. [and others] Drilling fluid waste management in drilling for oil and gas wells // Chemical Engineering
14. Ryen Caenn, H.C.H. Darley, George R.Gray Drilling and Drilling Fluids Waste Management // Composition and Properties of Drilling and Completion Fluids (Seventh Edition). – 2017. – p. 597-636. – doi: 10.1016/B978-0-12-804751-4.00014-6. Transactions. – 2017. – p. 1351-1356. – doi: 10.3303/CET1756226
15. Darajah M.H. [and others] Drilling waste management using zero discharge technology with Drill Cutting Re-injection (DCRI) method for environmental preservation // IOP Conference Series: Earth and Environmental Science. – 2021. – No. 1. – p. 012046. – doi: 10.1088/1755-1315/802/1/012046doi: 10.1080/21681015.2016.1172124.
16. George K., Antonis Z.A. Drill cuttings waste management from oil & gas exploitation industries through end-of-waste criteria in the framework of circular economy strategy // Journal of Cleaner Production. – 2021. – doi: 10.1016/j.jclepro.2021.129098.
17. Phillips L. [et al.] Drilling waste management - Solutions that optimize drilling, reduce well cost and improve environmental performance // Paper presented at the Abu Dhabi International Petroleum Exhibition & Conference. Abu Dhabi, UAE, 2018.– doi: 10.2118/192793-MS.

METHANOL PRODUCTION FROM CO2 AND INDUSTRIAL OFF-GASES: ADVANCED CATALYTIC DESIGN AND HIERARCHICAL PROCESS INTEGRATION FOR A CIRCULAR ECONOMY

Suleymanova Dinara
Scientific supervisor: Dr. Igor R. Nasirov
Azerbaijan State Oil and Industry University
Baku, Azerbaijan
dslymnvadinara@gmail.com

Abstract - Carbon storage is no longer enough, as in 2020, CO2 emissions amounted to about 31.5 billion tons [Ghosh et al., 2022], so it is necessary to actively use it through capture and conversion into useful products (Carbon Capture and Utilization) [Garcia et al., 2022; Saleh, 2022]. This work focuses on the creation of sustainable liquid fuel by producing CH3OH due to thermocatalytic hydrogenation of CO2 [Shiva Kumar and Lim, 2022; Tian et al., 2022]. Special attention is paid to vacancy-engineered In2O3/ZrO2 catalysts, which provide almost 100% reaction selectivity by directing the reaction toward the formate pathway rather than the Reverse Water Gas Shift (RWGS) [Ho et al., 2024; Portillo et al., 2022]. We assess Sorption-Enhanced Methanol Synthesis (SEMS) at the system level, where in situ product removal shifts the reaction beyond thermodynamic equilibrium and enables methanol purities above 99% without distillation [Nieminen et al., 2022]. These technologies become profitable for the steel industry if the CO2 tax exceeds 40.6 euros per ton [Gentile et al., 2022]. As a long-term perspective, we propose Solar-driven Non-Thermal Plasma Methanol (S-NAMH) as a pathway for decentralized production of negative-emission fuels from low-concentration atmospheric CO_2 (420 ppm) [Rajkumar and Anand, 2024; Garcia et al., 2022; Alam et al., 2020].

Keywords: Methanol Synthesis, **CO2** Hydrogenation, **In2O3/ZrO2** Catalyst, Formate Pathway, SEMS, Process Intensification, EHMPC, Non-Thermal Plasma.

1. Introduction

Global energy demand is growing rapidly and is expected to increase by 50% by 2030. Today, 95% of this demand is covered by fossil sources [Shiva Kumar and Lim, 2022]. While hydrogen holds promise as an energy carrier, its low volumetric density presents substantial infrastructure barriers [Shiva Kumar and Lim, 2022; Tian et al., 2022]. Methanol synthesis provides a "Methanol Economy" alternative, integrating with existing distribution networks as a liquid building block [Porter et al., 2022; Lombardelli et al., 2022]. However, a major research gap remains in overcoming the thermodynamic stability of CO2 and the competing endothermic RWGS reaction, which produces byproduct CO [Ghosh et al., 2022; Ho et al., 2024]. The main objective of this work is to investigate how sorption-enhanced systems and vacancy-containing catalysts can enhance carbon use efficiency (CUE) in industry, and propose a Solar-NTP (S-NAMH) framework that combines non-equilibrium plasma with nanoporous polymers to synthesize negative-emission fuels from low-concentration atmospheric CO2 in decentralized plants.

2. Materials and Methods:

This work provides a comparative analysis of the performance of 3 different catalytic systems: conventional CuO/ZnO/Al2O3, innovative Zr-doped Cu/Zn/Al/Zr, and vacancy-engineered In2O3/ZrO2 [Li et al., 2014; Tian et al., 2022; Lombardelli et al., 2022].

1. **Catalytic Systems:** The experiments in the analyzed studies were carried out in isothermal fixed-bed reactors, the operating temperature was 210–280 °C, and the system pressure was maintained at 3.0–10.0 MPa [Porter et al., 2022; Lombardelli et al., 2022]. The mechanistic analysis was based on density functional theory (DFT) calculations, which showed that surface oxygen vacancies, which act as active sites, are responsible for the reactivity. [Ho et al., 2024; Portillo et al., 2022].
2. **Process Configurations:** To accelerate the process, a SEMS system with 3 Å molecular sieves was used to remove water in situ. [Nieminen et al., 2022]. For blast furnace gas purification in industrial processes such as **the FReSMe process**, **the SEWGS system is used**. It employs hydrotalcite-based sorbents that have already been upgraded to the sixth processing level (TRL 6). [Manzolini et al., 2020; Gentile et al., 2022]. In the analyzed naturally stable systems, the energy efficiency was estimated using under operating conditions using the **EHMPC (Economic High-Model Predictive Control)** algorithm, a method that uses **linear programming (MILP)** to combine the operation of **PEM electrolyzers with synthesis reactors.** The main challenges here are voltage surges from renewable sources and unstable outflow gas (POG) flows, but the model successfully tracks these dynamics. [Dettori et al., 2022].
3. **Atmospheric Harvesting:** The use of the **S-NAMH** structure is proposed for the activation of dilute atmospheric molecules at 40–60 °C using **non-thermal plasma (NTP)** [Rajkumar and Anand, 2024], integrated with triptycene-linked nanoporous polymers (STNPs) with surface areas up to 1462 m²/g [Alam et al., 2020].

3. Results and Discussion

3.1. Mechanistic Contrast: Redox vs. Formate Pathways

Conventional Cu-based catalysts primarily operate via the Redox pathway, where CO2 is first reduced to CO through the endothermic Reverse Water Gas Shift (RWGS) reaction before undergoing subsequent hydrogenation to methanol [Lombardelli et al., 2022; Vieira et al., 2024]. Kinetically, these sites suffer from severe water-induced deactivation: byproduct water molecules inhibit activity through competitive adsorption ("flooding") on active sites and promote thermal sintering, which disrupts the essential Cu/ZnO synergy through the formation of Zn-Al mixed phases or the oxidation of metallic Cu [Heracleous et al., 2022; Lombardelli et al., 2022; Nieminen et al., 2022].

Addressing these stability constraints, the innovative Cu/Zn/Al/Zr catalyst demonstrates that zirconium promotion effectively stabilizes the active phase against hydrothermal restructuring [Lombardelli et al., 2022]. In contrast to the benchmark Cu/ZnO/Al2O3, this Zr-doped configuration maintains constant catalytic activity over 100 hours of operation [Lombardelli et al., 2022]. Experimental results indicate that this system achieves a CO2 conversion of up to 26% and a methanol yield of 13% [Lombardelli et al., 2022]. Kinetic modeling suggests that the inclusion of zirconium increases the pre-exponential factor while marginally reducing the activation energy for CO2 hydrogenation, although the modified surface may also increase selectivity toward CO relative to conventional syngas-to-methanol catalysts [Lombardelli et al., 2022].

Conversely, vacancy-engineered In2O3/ZrO2 facilitates the formate pathway, where CO2 is directly hydrogenated to a formate intermediate (HCOO) [Ho et al., 2024]. Zirconia promotion increases the density of surface oxygen vacancies, which serve as the primary active sites for CO2 activation and thermodynamically stabilize the HCOO species [Ho et al., 2024; Portillo et al., 2022]. Crucially, this architecture kinetically suppresses the RWGS reaction by raising its activation energy relative to methanol synthesis; the energy required for methanol production is approximately 49 kJ/mol, whereas CO formation requires 71 kJ/mol [Kampe et al., 2024; Ho et al., 2024]. This energetic preference allows the In2O3/ZrO2 system to maintain near-perfect methanol selectivity by bypassing the redox-mediated byproduct loop that limits conventional metallic paradigms [Ho et al., 2024; Tian et al., 2022].

3.2. Process Intensification and Unifying Carbon Metrics

To evaluate system-level conversion efficiency, we introduce the carbon utilization efficiency (CUE) metric. While conventional loops are thermodynamically limited to approximately 26.2% single-pass conversion [Lombardelli et al., 2022], SEMS achieves a CUE of 77.2% by forward-shifting the equilibrium according to Le Chatelier's principle through in-situ water removal [Nieminen et al., 2022], enabling product purities >99% while potentially eliminating energy-intensive distillation columns [Nieminen et al., 2022]. Within the FReSMe/SEWGS project, this hierarchical integration achieves plant-level CO2 emission avoidance of 59.2% [Gentile et al., 2022].

3.3. Techno-Economic Thresholds

Techno-economic modeling of the **FReSMe framework** confirms that integrated steelworks CCU achieves economic profitability when carbon taxes exceed **40.6 €/t CO2,** a level already achieved in several European countries [Gentile et al., 2022]. Above this threshold, the system delivers greater emission reductions at a lower cost than traditional post-combustion capture [Gentile et al., 2022]. The feasibility of these pathways is strictly sensitive to green electricity prices, which can constitute up to **70% of the total operating expenditures** for electrolysis-based fuels [Ghaebi Panah et

al., 2022]. Valorization of process off-gases (POG) becomes viable when renewable electricity prices fall **below 20 €/MWh**, a target that, when combined with scaling-up effects, can drop the levelized cost of green hydrogen to highly marketable levels of **1–3 €/kg** [Dettori et al., 2022; Ghaebi Panah et al., 2022].

To address the intermittency of renewable inputs and the price volatility of energy markets, an advanced **Economic Hybrid Model Predictive Control (EHMPC)** is required to synchronize high-efficiency **PEM electrolyzer stacks** with synthesis reactors [Dettori et al., 2022]. This real-time optimization is vital to manage the **non-linear dynamics** and piecewise affine operational modalities of the reactors, ensuring optimal gas distribution and safe plant operation [Dettori et al., 2022]. Furthermore, achieving **high production rates per fixed-bed volume** remains a key driver for profitability, potentially enhanced by novel bifunctional catalysts or **adiabatic configurations** that minimize capital costs [Nieminen et al., 2022].

3.4. Conceptual Frontier: S-NAMH for Negative Emissions

The transition from industrial emissions reduction to decentralized capture of atmospheric CO2 is the final step of decarbonization [Garcia et al., 2022]. Despite the efficiency of point capture, the atmospheric CO2 concentration (420 ppm) remains a critical issue, as current measures are insufficient to limit warming to 1.5 °C. However, such low CO2 concentrations make traditional thermochemical methods extremely energy intensive [Garcia et al., 2022; Tian et al., 2022]. The S-NAMH system uses non-thermal plasma to activate CO2 under near-ambient conditions. Energetic electrons (1–10 eV) initiate molecular dissociation without significant thermal costs, and integration with high-surface-area nanoporous polymers ensures efficient capture and concentration of atmospheric CO2 [Rajkumar and Anand, 2024; Alam et al., 2020].

4. Conclusions and Future Work

Methanol production from CO2 is a technically feasible pathway for global decarbonization. The synergy between vacancy-engineered catalysts and sorption-enhanced circuits represents the current Best Available Technique (BAT) for energy-intensive sectors. Future research must prioritize **Economic Hybrid Model Predictive Control (EHMPC)** to manage the non-linear fluctuations of industrial off-gases [Dettori et al., 2022].

References

1. **Alam, A., et al.** (2020). Silsesquioxane-based and triptycene-linked nanoporous polymers (STNPs). *Materials Advances*, 1.
2. **Dettori, S., et al.** (2022). Optimizing methane and methanol production... *IFAC-PapersOnLine*, 55-2.
3. **Garcia, J. A., et al.** (2022). Technical analysis of CO2 capture pathways. *Journal of Environmental Chemical Engineering*, 10.
4. **Gentile, G., et al.** (2022). Techno-economic assessment of the FReSMe technology. *Journal of CO2 Utilization*, 56.

5. **Ghosh, S., et al.** (2022). Methanol mediated direct CO2 hydrogenation. *Chemical Engineering Journal*, 435.
6. **Heracleous, E., et al.** (2022). Valorization of steel-work off-gases. *Chemical Engineering Journal*, 444.
7. **Ho, P. H., et al.** (2024). Effect of the Preparation Methods on Indium-Based Catalysts. *Energy Fuels*, 38.
8. **Lombardelli, G., et al.** (2022). CO2 hydrogenation to methanol with an innovative Cu/Zn/Al/Zr catalyst. *Journal of CO2 Utilization*, 65.
9. **Manzolini, G., et al.** (2020). Techno-economic assessment of SEWGS technology. *International Journal of Greenhouse Gas Control*, 94.
10. **Nieminen, H., et al.** (2022). Process modelling... of sorption-enhanced methanol synthesis. *Chemical Engineering and Processing*, 179.
11. **Porter, R. T. J., et al.** (2022). Novel process design... of methanol synthesis from blast furnace gas. *Journal of CO2 Utilization*, 66.
12. **Portillo, A., et al.** (2022). Alternative acid catalysts... into light olefins. *Fuel Processing Technology*, 238.
13. **Rajkumar, P. and Anand, B. P.** (2024). Experimental Investigation on Compact Current Non-Thermal Plasma. *J. Technol. Space Plasmas*, 5.
14. **Saleh, T. A.** (2022). Nanomaterials... for CO2 capture and utilization. *RSC Advances*, 12.
15. **Shiva Kumar, S. and Lim, H.** (2022). An overview of water electrolysis technologies. *Energy Reports*, 8.
16. **Tian, Z., et al.** (2022). The effect of methanol production and application... *Fuel*, 320.
17. **Vieira, L. H., et al.** (2024). CO2 Hydrogenation to Methanol over Mesoporous SiO2-Coated Catalysts. *ACS Nanosci. Au*, 4.

ECO-FRIENDLY SYNTHESIS OF SOLID BASE CATALYSTS FROM LOCAL AGRICULTURAL, FOOD, AND MARINE WASTES FOR BIODIESEL PRODUCTION

Aliya Kurmayeva[1] & Sara Malik-Aslanova[2]
French-Azerbaijani University, Chemical Engineering Department
Baku,Azerbaijan
Email: aliyakurmayeva7@gmail.com[1] , ssmalikaslan@gmail.com[2]

I. Summary - This study proposes an eco-friendly and cost-effective method to prepare solid base-type catalysts from locally available agro, food, animal, and marine wastes to be used in the production of biodiesel fuels. Eight locally available agro, food, animal, and marine wastes were used to prepare the solid base-type catalysts through drying, carbonization (250-350°C), and calcination (650-900°C) methods to produce the final catalysts.

Among the eight locally available agro, food, animal, and marine wastes, the detailed characterization of the catalysts was conducted using the peanut shells, eggshells, seashells, and tea grounds. The results showed that the solid base-type catalysts were composed of catalytically active phases of CaO and MgO, which were confirmed using the XRD pattern of the obtained catalysts. The obtained catalyst from the eggshells showed good catalytic activity towards the production of biodiesel fuels, achieving 85% of biodiesel fuels under the optimized transesterification reaction conditions of 8:1 methanol to oil molar ratio, 3%wt of the catalyst, 64°C, and 3 hours reaction time.

Keywords: waste-derived catalysts,waste valorization,biomass waste,green chemistry

I. Introduction

In response to the need for sustainable and cost-effective materials in chemical processes [Kishore et al., 2022, 1501; Ooi et al., 2021, 1-2], this experimental study aims to utilize local wastes as a source of functional catalysts in their conversion to solids. Although homogeneous catalysts are highly efficient in chemical processes, they are hard to recover and produce significant wastewater generation and environmental issues, making heterogeneous catalysts more desirable due to their recyclability and ease of separation from the reaction mixture [Yaghi et al., 2025, 62]. This method follows the principles of circular economy practices by minimizing natural resource depletion, pollution, and production costs while emphasizing resource efficiency and sustainability [Ao et al., 2024, 120031].

Seven wastes were selected for this study: peanut shell, eggshell, tea ground, banana peel, walnut shell, animal bone, seashell, and magnesium salt extracted from seawater [Hussain et al., 2021, 630]. The process was straightforward: drying and grinding, low-temperature carbonization and preheating (250-350°C), aqueous solution and filtration (if necessary), and finally calcination (650-900°C) [Chong et al., 2023, 5408].

This shows the method to transform agricultural wastes, food wastes, and marine wastes to crystalline oxide catalysts using simple apparatus and without the use of expensive chemicals [Ooi et al., 2021, 194].

II. Experimental part

2.1 Peanut Shells

Peanut shells were carbonized in a muffle furnace at 350 °C (with air access) until smoke ceased, then heated to 650 °C for 30 min (scaled with quantity). After cooling, the charred material was diluted with distilled water, homogenized by magnetic stirring, and separated by vacuum filtration (Büchner funnel). Both solid residue and filtrate were oven-dried; the solid was isolated and finally calcined at 800 °C for 30 min.

2.2 Seawater (Magnesium Salt)

Seawater was collected and its magnesium content quantified by EDTA complexometric titration (pH 10 buffer, Eriochrome Black T or Calmagite indicator; endpoint: wine-red to blue), confirming ~0.6 g/L Mg^{2+} (as $CaCO_3$ equivalents). The seawater underwent electrochemical precipitation (nickel cathodes, graphite anodes, salt bridge) or chemical double-salt precipitation (with stoichiometric $(NH_4)_2SO_4$ to form $MgSO_4 \cdot (NH_4)_2SO_4 \cdot 6H_2O$). The $Mg(OH)_2$ precipitate was filtered, washed with distilled water, oven-dried, and calcined at 500-800 °C (up to 1100 °C for high-purity MgO) for 3-5 h.

2.3 Tea Grounds

Tea grounds were oven-dried and carbonized in a muffle furnace at 250 °C, followed by heating in the 750-800 °C range for 2.5 h. After cooling, the sample was diluted with distilled water, homogenized by magnetic stirring,

and separated by vacuum filtration (Büchner funnel). Both solid residue and filtrate were oven-dried; the solid was isolated and finally calcined at 750 °C for 30 min.

2.4 Banana Peels

Banana peels were oven-dried, ground into powder, and carbonized at 350 °C until smoke ceased, then heated to 650 °C for 3 h. After cooling, the charred material was diluted with distilled water, homogenized by stirring, and separated by vacuum filtration (Büchner funnel). Both fractions were oven-dried; the solid was isolated and calcined at 650 °C for 30 min.

2.5 Walnut Shells

Walnut shells were oven-dried, ground into powder, and carbonized in a muffle furnace at 350 °C until smoke ceased, followed by heating to 650 °C for 3 h. After cooling, the charred material was diluted with distilled water, homogenized by magnetic stirring, and separated by vacuum filtration (Büchner funnel). Both fractions were oven-dried; the solid was isolated and calcined at 650 °C for 30 min.

2.6 Seashells

Seashells were washed to remove impurities and organics, oven-dried, crushed, and ground into powder. The powder was pre-heated at 250 °C for 2 h, then calcined at 900 °C for 2.5 h in a muffle furnace to convert $CaCO_3$ to CaO. After cooling, the fine white/gray powder was stored in a desiccator.

2.7 Animal Bones

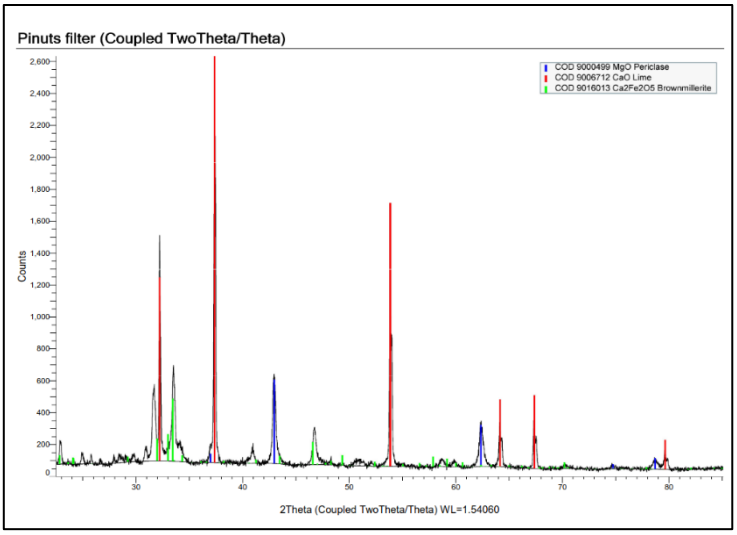
Waste animal bones were oven-dried, washed with ethanol to remove organics and impurities, ground into powder, and re-dried. The powder was carbonized in a muffle furnace (250 °C pre-heating, then 650 °C for 2.5 h). After cooling, the material was diluted with distilled water, homogenized by magnetic stirring, and separated by vacuum filtration (Büchner funnel). Both fractions were oven-dried; the solid was isolated and calcined at 900 °C for 30 min.

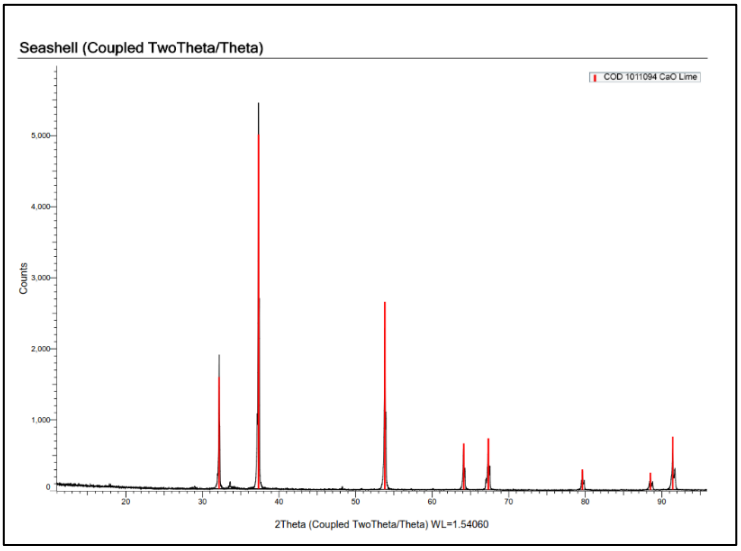
2.7 Eggshells

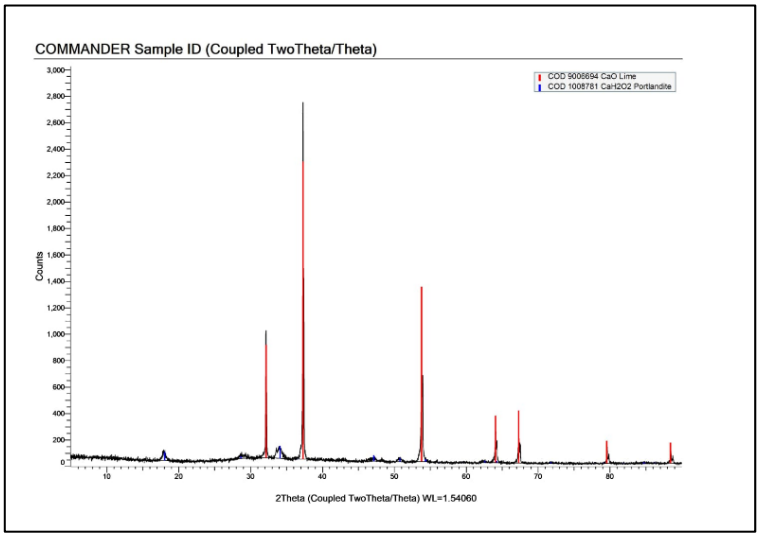
Chicken eggshells were collected, rinsed, air-dried for 4 hours, oven-dried at 100-110 °C for 3 hours, and ground into powder. The powder was calcined in a muffle furnace from 500 °C to 900 °C over 3 hours to obtain CaO, which was further ground into fine powder.

The eggshell-derived CaO (obtained after calcination from 500 °C to 900 °C) was successfully used as a heterogeneous base catalyst in the transesterification of oil with methanol. Under optimized conditions (methanol-to-oil molar ratio 8:1, 3 wt% catalyst loading, 64 °C reaction temperature, 3 h total time), the reaction achieved an 85 % biodiesel yield. This result confirms the high catalytic activity of the eggshell CaO, demonstrating its effectiveness in converting triglycerides into fatty acid methyl esters (FAME) for biodiesel production.

III. Results and discussion part.







Despite low absolute yields in some cases (especially plant-based wastes), the final solids are significantly enriched in catalytically active oxides (CaO in seashells, MgO/CaO in peanut shells, MgO in seawater precipitate, CaO in bones). The XRD results confirm successful phase transformation and removal of amorphous/organic content during thermal treatment. The XRD pattern for the peanut shell filtered fraction (after carbonization, dilution, filtration, and calcination at 800 °C) shows the presence of MgO (periclase, COD 9000499), CaO (lime, COD 9006712), and $Ca_2Fe_2O_5$ (brownmillerite, COD 9016013), indicating the presence of multiple basic oxide species with MgO and CaO being the primary active species. The XRD pattern for the seashell-based catalyst (after pre-heating at 250 °C and calcination at 900 °C for 2.5 h) shows the presence of CaO (lime, COD 1011094) with very sharp peaks and no significant amount of $CaCO_3$, indicating the near-complete decomposition and purity expected for this type of CaO-based catalyst prepared at high temperatures. The simplicity of preparation (no expensive chemicals, basic equipment) and use of abundant waste feedstocks make these materials highly promising for sustainable catalyst development.The XRD pattern of the calcined eggshell material shows intense, sharp peaks corresponding to CaO (lime, COD 9006694) as the dominant phase, with minor $Ca(OH)_2$ (portlandite, COD 1008781) present. The absence of significant $CaCO_3$ reflections indicates near-complete thermal decomposition of calcium carbonate during calcination, resulting in high phase purity and good crystallinity. These characteristics explain the strong basicity and efficient performance observed in the transesterification reaction.

Compound/Source	Initial Mass	Final Mass (solid recovered)	Approximate Yield (%)	Notes
Peanut Shells	500 g	1.85 g (filtered fraction) 1.013 g (unfiltered ash)	~0.37-0.57 %	Very low yield due to high organic loss and aqueous extraction
Seawater (Mg salt)	50 mL	0.197 g	~3.94 g/L	Typical Mg recovery from seawater/brine after precipitation & calcination
Animal Bones	142.9 g	~51 g	~35.7 %	Moderate yield; organics removed, inorganic Ca-rich residue retained
Walnut Shells	45.2 g	~10.2 g	~22,6 %	Loss from combustion & partial dissolution during washing
Seashells	31.115 g	~17.4 g	~55.9 %	Higher yield; mainly CO_2 loss from $CaCO_3 \rightarrow CaO$ conversion
Banana Peels	20 g	~3.5 g	~17.5 %	High organic loss during carbonization; K-rich ash remains
Tea Grounds	80 g	~14.1 g	~17.6 %	Moderate loss from volatiles & aqueous processing
Chicken Eggshells	200 g	140 g	70%	High recovery due to dominant $CaCO_3$ content; major mass loss from CO_2 release during calcination to CaO, typical for eggshell-derived catalysts

IV. Offers

Future work will include the optimization of the preparation methods for the synthesis of purer catalysts, with higher crystallinity, as well as higher K, Ca, or Mg content, for instance, by optimizing the washing, leaching, or calcination procedures. More wastes, such as beet leaves, carrot leaves, algae, and coffee grounds, will also be investigated for the synthesis of K_2O, CaO, or MgO-based catalysts by the same procedures.Also its activity and reusability in transesterification reaction will be studied in the future work. The elemental composition of the samples will be determined by XRF/ICP-OES, while the structural properties will be investigated by various techniques. Finally, the most promising catalysts, such as those obtained from seashells, peanut shells, and seawater magnesium salts, will be assessed for activity, selectivity, and stability for the execution of base-catalyzed reactions under relevant conditions.

Reference
1. Ao, S., et al. (2024). Biomass waste-derived catalysts for biodiesel production: Recent advances and key challenges. *Renewable Energy, 223*, 120031. https://doi.org/10.1016/j.renene.2024.120031
2. Chong, N. S., et al. (2023). Preparation and characterization of shell-based CaO catalysts for ultrasonication-assisted production of biodiesel to reduce toxicants in diesel generator emissions. *Energies, 16*(14), 5408. https://doi.org/10.3390/en16145408
3. Hussain, F., et al. (2021). Waste animal bones as catalysts for biodiesel production; A mini review. *Catalysts, 11*(5), 630. https://doi.org/10.3390/catal11050630
4. Kishore, S. C., et al. (2022). A Review of Biomass-Derived Heterogeneous Catalysts for Biodiesel Production. *Catalysts, 12*(12), 1501. https://doi.org/10.3390/catal12121501
5. Ooi, H. K., et al. (2021). Progress on modified calcium oxide derived waste-shell catalysts for biodiesel production. *Catalysts, 11*(2), 194. https://doi.org/10.3390/catal11020194
6. Yaghi, M., et al. (2025). An Overview of Biodiesel Production via Heterogeneous Catalysts: Synthesis, Current Advances, and Challenges. *Clean Technologies, 7*(3), 62. https://doi.org/10.3390/cleantechnol7030062

LAB-SCALE ZERO-WASTE VALORIZATION OF SPENT COFFEE GROUNDS AND SPENT DRILLING MUD

Teymur Ismayilov , Sabir Aliyev
Baku Higher Oil School
Baku, Azerbaijan
teymi.ismayilov@gmail.com sabir.aliyev2408@gmail.com
Supervisor: Aliya Laylabashova

Summary - This paper introduces a concept of a laboratory-sized demonstration of a circular economy involving the use of cellulose that is extracted using spent coffee grounds (SCG) and reusing spent drilling mud (SDM) into a wastewater treatment adsorbent. The experiment was able to downsize the synthesis process by using 38 g of SCG and 23.2 g of SDM. The obtained composite material showed that it was possible to use these industrial and agricultural wastes to produce functional materials to confirm a zero-waste route with thermodynamic and mechanical deviations in the laboratory production process.

Keywords: Spent coffee grounds, spent drilling mud, cellulose extraction, calcification, adsorbent formation, zero-waste, circular economy.

1. Introduction

The simultaneous production of large quantities of agricultural wastes, including the lignocellulose-based spent coffee grounds (SCG) and industrial wastes, including the spent drilling mud (SDM), is a big ecological challenge. Nevertheless, these materials have complementary chemical properties. SCG is a superior precursor of cellulose and porous carbon whereas SDM has a stable aluminosilicate structure. The purpose of this research is to reproduce and confirm a lab-scale strategy of the zero-waste valorization of acidic effluent generated in the process of cellulose extraction at SCG to provide a composite adsorbent through cross-linking of alkaline-activated SDM and neutralization of the acidic effluent to produce a potential wastewater remediation strategy.

2. Experimental Part

2.1. Pre-treatment and Cellulose Extraction.

In the first step, 38 g of SCG was washed, dried and sieved. Extraction of the cellulose was done in a solution of nitric acid (1 4 wet) in a ratio of 1:20 (Wv) (760 mL). The slurry was heated in 95 C and stirred in an uninterrupted manner within 2 hours. The solid fraction (precursor of cellulose) was filtered to extract the fraction and washed to neutral pH and dried.



Figure 1

2.2. SDM Activation and Synthesis of Adsorbent.

At the same time, 23.2 g SDM was dried at 600 C 1 h to eliminate organic impurities. The alkaline activation of the calcined SDM was then done with a solution of 7M sodium hydroxide of 232 mL at room temperature. The centrifugation of the activated inorganic structure (F) was conducted and activated SDM was separated. At last, the organic acidic effluent of SCG (B) and the activated SDM (F) were mixed, dried at 200 o C, and pyrolyzed at 350 o C in 30 minutes to obtain the final composite adsorbent (BFa).



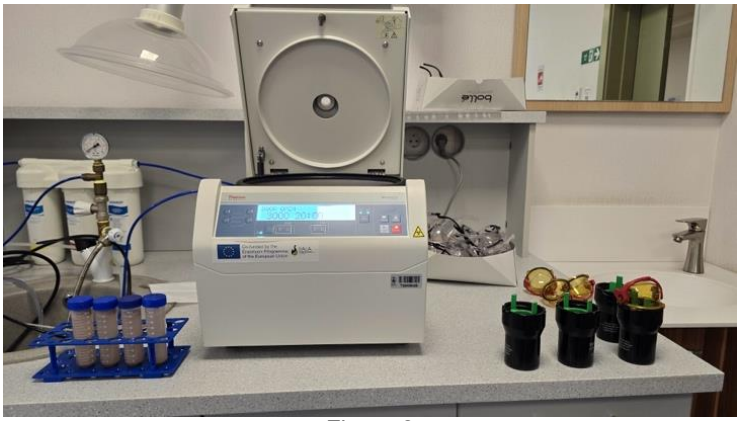


Figure 2

3. Results and Discussion

The reduced zero-waste process was effective in giving extracted cellulose and a stable carbon-mineral composite adsorbent. In the extraction process, 38 g of the SCG produced 7g of the solid cellulose fraction (18.4% yield). Significant unplanned reduction in mass was experienced in the filtration stage because of the high viscosity of the hydrolysate and agglomeration of particles.

Certain deviations in operations were identified during the synthesis. Changes in temperature (up to104 C) and some evaporation of the solvents because of incomplete sealing of the system caused the changes in the local concentration of nitric acid, which influenced the hydrolysis kinetics. In addition, difficulties in mechanical granulation were also met, which indicated on the ultimate mass of composite adsorbent resulting in 12 g.

Although such technical challenges were encountered, the structural integrity of the end product was preserved. The limited preliminary qualitative analyses of the synthesized adsorbent on model dyed water showed that the synthesized adsorbent had a visible decolorization capacity, which proved that active adsorption sites were formed successfully. Although extensive chemical oxygen demand (COD) reduction experiments of actual industrial effluents are not conducted yet, the conducted analyses outcomes confirm the very existence of the effective neutralization of acidic hydrolysis wastes and their incorporation into an SDM matrix.

4. Conclusion

SCG and SDM processing can be integrated to offer a closed-loop solution of waste utilization that is sustainable. The present laboratory-scale production confirms that despite thermodynamic fluctuations that arise, functional composite adsorbents can be scaled at appropriate stoichiometric ratios. The following work will be aimed at the optimization of temperature control system and the quantitative assessment of adsorption capacity of the synthesized material.

References
1. Naghdbishi, E., & Khorasani, A. C. (2025). A zero-waste approach to spent coffee grounds valorization: Cellulose production in series recycle flow reactors with its effluent upcycling into adsorbents for textile wastewater treatment. *International Journal of Biological Macromolecules*, 328, 147444.
2. Blinová, L., & Sirotiak, M. (2019). Utilization of spent coffee grounds for removal of hazardous substances from water: A review. *Research Papers Faculty of Materials Science and Technology Slovak University of Technology*, 27(44), 145-152.
3. Kim, M. S., & Kim, J. G. (2020). Adsorption characteristics of spent coffee grounds as an alternative adsorbent for cadmium in solution. *Environments*, 7(4), 24.
4. Han, H., Rafiq, M. K., Zhou, T., Xu, R., Mašek, O., & Li, X. (2019). A critical review of clay-based composites with enhanced adsorption performance for metal and organic pollutants. *Journal of Hazardous Materials*, 369, 780-796.

KAĞIZ TULLANTILARINDAN NEFTYIĞICI ADSORBENTİN ALINMASI

Nübar Rəhimova Rahim
Sumqayıt Dövlət Universiteti,
Sumqayıt, Azərbaycan
nubarrahimova@gmail.com
Elmi rəhbər: b/m Şahgəldiyev F.X.

Xülasə - Neft və neft məhsulları ilə çirklənmə su hövzələrinin ekoloji təhlükəsizliyi üçün ciddi problem olaraq qalmaqdadır. Bu problemin həlli üçün ekoloji cəhətdən təhlükəsiz, iqtisadi baxımdan əlverişli və dayanıqlı materialların hazırlanması aktualdır. Təqdim olunan iş su səthinin neft və neft məhsullarından təmizlənməsi məqsədilə kağız tullantısından hidrofob neftyığıcı adsorbentin alınmasına həsr olunmuşdur. MC-1A markalı makulatura əsasında hazırlanmış lifli materialın nefttutumu, suudma və üzmə qabiliyyəti eksperimental olaraq müəyyən edilmişdir. Aparılmış sınaqlar nəticəsində adsorbentin təmizləmə səmərəliliyinin 91,4 % təşkil etdiyi müəyyən olunmuşdur. Alınmış nəticələr göstərir ki, kağız tullantısı əsasında hazırlanmış adsorbent dayanıqlı və perspektivli material kimi su səthinin neft çirklənməsindən təmizlənməsində tətbiq oluna bilər.

Açar sözlər: makulatura, hidrofob sorbent, neft çirklənməsi, sorbsiya əmsalı, dayanıqlı material

Giriş

Müasir dövrdə sənaye və enerji sektorunun inkişafı ətraf mühitə təsirin artması ilə müşayiət olunur. Xüsusilə neft və neft məhsullarının hasilatı, daşınması və emalı zamanı baş verən sızmalar, neft və neft məhsullarının su hövzələrinə düşməsi ekosistem üçün ciddi təhlükə yaradır. Su səthində əmələ gələn nazik neft təbəqəsi oksigen mübadiləsini azaldır, su canlılarının həyat fəaliyyətinə mənfi təsir göstərir və uzunmüddətli ekoloji fəsadlara səbəb olur. Xüsusilə sənaye zonalarında və hasilat ərazilərində baş verən sızmalar operativ və effektiv müdaxilə tələb edir. Bu baxımdan neft çirklənməsinin aradan qaldırılması üçün effektiv və ekoloji təhlükəsiz materialların hazırlanması aktual elmi istiqamətlərdən biridir. Yaşıl kimya prinsiplərinə

əsasən kimyəvi proseslər və materiallar ətraf mühitə minimum təsir göstərməli, tullantıların azaldılmasına və bərpa olunan xammaldan istifadəyə yönəlməlidir. Bu yanaşma tullantıların dəyərli məhsula çevrilməsini və dövri iqtisadiyyat modelinin tətbiqini təşviq edir [Атласкин, Атласкина, Воротынцев и др., 2024, 15–18; Tağıyev, Məmmədov, 2024, 25–30]. Neft və neft məhsullarının su səthindən təmizlənməsi üçün mexaniki, fiziki-kimyəvi, kimyəvi və biokimyəvi üsullar tətbiq edilir. Bu məqsədlə müxtəlif təbii, süni və sintetik adsorbentlər tətbiq edilir. Lakin bu metodların hər biri konkret şəraitdən asılı olaraq fərqli effektivlik göstərir. Mövcud materialların bir qismi bahalıdır, bəziləri təkrar istifadə üçün yararsızdır, digərlərinin isə sorbsiya göstəriciləri qənaətbəxş deyildir [Шахгелдиев, Адилова, Сафарова, 2018a, 232–235; Шахгелдиев, Адилова, Сафарова, 2018b, 156–159]. Bu problemin həlli üçün ekoloji cəhətdən təhlükəsiz, iqtisadi baxımdan əlverişli və dayanıqlı materialların hazırlanması aktualdır. Sorbsiya üsulu isə praktik tətbiq baxımından daha çevik və iqtisadi cəhətdən əlverişli hesab olunur. Sorbent materiallar nefti selektiv şəkildə udaraq su səthindən ayrılmasını təmin edir və təkrar emal imkanları yaradır. Neft sorbentləri əsasən üç əsas göstəriciyə görə qiymətləndirilir: nefttutumu, suudma və üzmə qabiliyyəti. Yüksək suudma qabiliyyətinin azaldılması üçün hidrofoblaşdırma üsulları tətbiq olunur. Makulatura geniş yayılmış tullantı növü olmaqla lifli və məsaməli quruluşa malikdir və potensial sorbent xammalı kimi maraq doğurur. Ədəbiyyat məlumatları göstərir ki, MC-1A markalı makulatura əsasında neftyığıcı adsorbentin alınması və tətbiqi kifayət qədər tədqiq olunmamışdır [Шахгелдиев, Адилова, Сафарова, 2018a, 232–235]. Bu baxımdan təqdim olunan iş kağız tullantısından hidrofob adsorbentin hazırlanmasına və onun neft çirklənmiş su səthinin təmizlənməsində sorbsiya xüsusiyyətlərinin öyrənilməsinə həsr olunmuşdur.

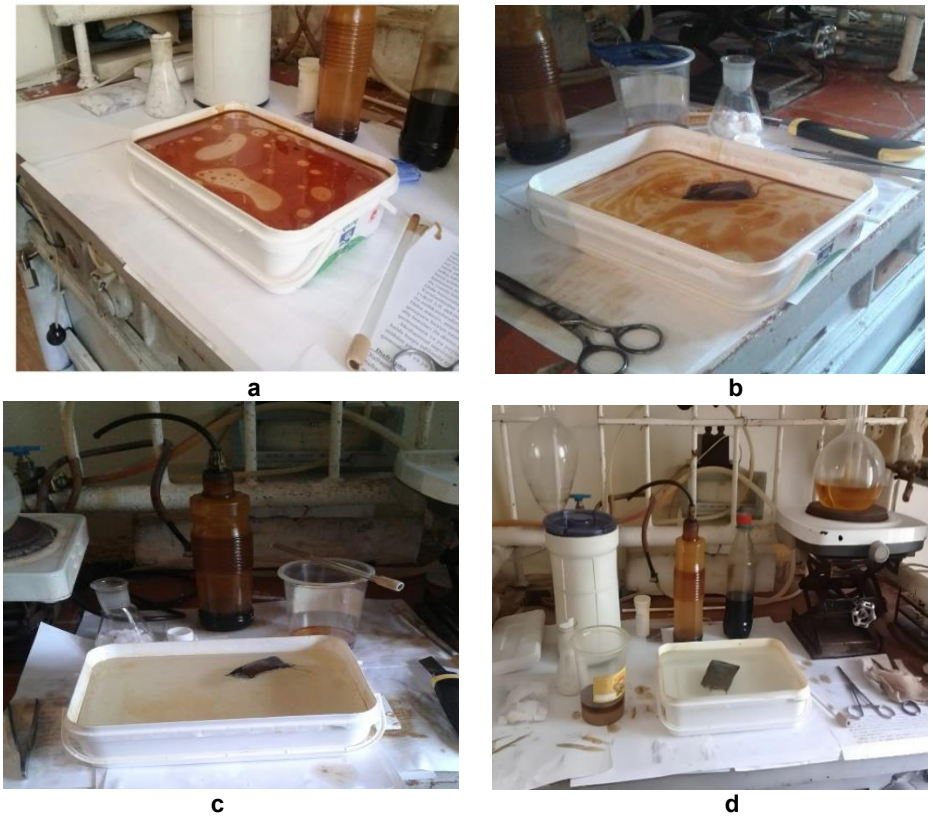
Eksperimental hissə.

Sınaq təcrübəsinin yerinə yetirilmə alqoritmi

MC-1A (GOST 10700-97 üzrə) markalı makulatura Şreder (Almaniya) aparatında 1,5 × 1,5 sm ölçüyə qədər xırdalanmış və laboratoriya dəyirmanında 5–8 dəqiqə üyüdülərək pambıqşəkilli kütlə halına salınmışdır. Alınmış sellüloza 60 %-li sabun məhlulunda hidrofoblaşdırılmışdır. Bunun üçün sellüloza isti sabun məhlulunda dispersləşdirilmiş, daha sonra sabunun çökdürülməsi məqsədilə ekvimolyar nisbətdə alüminium zəyi – $AlK(SO_4)_2 \cdot 12H_2O$ əlavə edilmişdir. Hidrofoblaşdırılmış sellüloza süzgəc vasitəsilə ayrılmış və sabit kütləyə qədər qurudulmuşdur. Üzmə qabiliyyətini təmin etmək məqsədilə ölçüləri 30 × 60 mm, kütləsi 5 q olan bonlar (yastıqlar) hazırlanmışdır.

Ölçüləri 200 × 250 × 150 mm olan qaba su doldurulmuş və sıxlığı 0,817 q/sm³ olan 20 ml işlənmiş yağ əlavə edilmişdir. İşlənmiş yağın şərti özlülüyü 0,52 s olub, soplasının diametri 4 mm və tutumu 100 sm³ olan B3-246 markalı viskozimetrlə (GOST 9070-75 üzrə) təyin edilmişdir. Yağın su səthində əmələ gətirdiyi təbəqənin qalınlığı 0,2–0,3 mm təşkil etmişdir. Sınaq otaq temperaturunda bir neçə dəfə təkrar yerinə yetirilmişdir. Su səthində 5–10 dəqiqə

müddətində mexaniki təsirlə dalğa yaradılmış və bon yağ təbəqəsi ilə örtülmüş su dolu qaba yerləşdirilmişdir. Bu zaman su lifli strukturdan ayrılmış, yağ isə liflərarası məsamələrdə və səthdə saxlanılmışdır. Sonra bon çıxarılmış, tərəzidə çəkilmiş və sorbsiya olunan yağın kütləsi təyin edilmişdir. Sorbsiya əmsalı bu ifadə ilə hesablanmışdır: $Ks = (m_1 - m_0) / m_0$, burada: m_0 — bonun ilkin kütləsi (q), m_1 — sorbsiya prosesindən sonrakı kütləsidir (q). Bon yenidən su və yağ olan qaba yerləşdirilmiş və sınaq üç dəfə təkrar olunmuşdur. Birinci təcrübədə Ks = 4,68 g/g, ikinci təcrübədə Ks = 1,89 g/g, üçüncü təcrübədə isə Ks = 0,92 g/g olmuşdur. Təmizləmə səmərəliliyi (η) çıxarılan yağın başlanğıc yağ miqdarına nisbəti kimi $\eta\ (\%) = (m_s / m_y) \times 100$ ifadəsi ilə hesablanmışdır, burada m_s — sorbsiya olunan yağın kütləsi, m_y — başlanğıc yağın kütləsidir. Sorbsiya prosesindən sonra bon sentrifuqaya yerləşdirilmiş, sorulmuş yağ ayrılmış və qalıq sorbsiya əmsalı təyin edilmişdir. Qalıq sorbsiya əmsalı sentrifuqadan sonrakı bonun kütləsinin quru bonun kütləsinə nisbəti kimi müəyyən edilmişdir. Şəkil 1-də bon vasitəsilə su səthindən yağın təmizlənməsinin ümumi mərhələləri göstərilmişdir.



Şəkil 1. Bon vasitəsilə su səthindən yağın təmizlənməsi prosesinin mərhələləri
a – su səthində yağ təbəqəsinin ilkin vəziyyəti b – bonun su səthinə yerləşdirilməsi
c – sorbsiya prosesinin gedişi d – təmizlənmədən sonrakı vəziyyət

Nəticələr və onların müzakirəsi

Alınmış sorbent pambığabənzər, ağ rəngli lifli materialdır, ekoloji cəhətdən təmizdir, səpələnmə sıxlığı 1150–1250 kq/m³ təşkil edir və oddan təhlükəsizdir (alışma temperaturu 230 °C). Aparılmış sınaq təcrübələri göstərmişdir ki, işlənmiş yağın su səthində əmələ gətirdiyi təbəqənin qalınlığı 0,2–0,3 mm olmuşdur və sorbsiya prosesi zamanı yağ lifli struktur tərəfindən effektiv şəkildə tutulmuşdur. Eksperimental hissədə göstərilən metodika əsasında hesablanmış sorbsiya əmsalı birinci təcrübədə Ks = 4,68 g/g, ikinci təcrübədə Ks = 1,89 g/g, üçüncü təcrübədə isə Ks = 0,92 g/g olmuşdur. Bu nəticələr sorbentin ilk istifadədə maksimal nefttutma qabiliyyətinə malik olduğunu, təkrar istifadə zamanı isə göstəricilərin azalmasının liflərarası məsamələrin qismən tutulması və struktur sıxlaşması ilə əlaqədar olduğunu göstərir. Təmizləmə səmərəliliyi çıxarılan yağın başlanğıc yağ miqdarına nisbəti əsasında hesablanmış və 91,4 % təşkil etmişdir. Bu göstərici su səthində olan yağın əsas kütlə hissəsinin birinci mərhələdə sorbsiya olunduğunu təsdiq edir. Sorbsiya prosesindən sonra bon sentrifuqaya yerləşdirilmiş, sorulmuş yağ ayrılmış və qalıq sorbsiya göstəriciləri müəyyən edilmişdir. Alınmış sorbentin nefttutma qabiliyyəti mövcud materiallarla müqayisədə yüksək olmuşdur. Belə ki, perlitlə müqayisədə 4,9 dəfə, pesorba ilə müqayisədə 1,6–2,4 dəfə, Sorboil materialı ilə müqayisədə 1,8–4,2 dəfə, Nurbo-GET ilə müqayisədə 6,8 dəfə, Peatsorb ilə müqayisədə isə 6,1 dəfə yüksək nəticə göstərmişdir. Sınaq nəticələri göstərmişdir ki, kimyəvi emal olunmuş MC-1A markalı kağız tullantısından hazırlanmış bonlar neft və neft məhsullarını su səthindən effektiv sorbsiya etmək qabiliyyətinə malikdir, sorbsiya əmsalı yüksəkdir, regenerasiya qabiliyyətinə malikdir, toksiki deyildir, ekosistemə mənfi təsir göstərmir, üzmə qabiliyyəti 20–22 gün təşkil edir və utilizasiyası sadədir.

Təkliflər

Adsorbentin bon, yastıq, mat və salfet formalarında tətbiqi mümkündür. Yeni alınmış sorbentin səmərəliliyinin artırılması məqsədilə onun xüsusi nazik döşək formasında hazırlanaraq üzmə vasitələrinə quraşdırılmış barabanlı-lentşəkilli qurğu modeli vasitəsilə istifadəsi məqsədəuyğun hesab olunur. Sorbentin sənaye miqyasında istehsal texnologiyasının işlənməsi və regenerasiya prosesinin optimallaşdırılması gələcək tədqiqat istiqaməti kimi təklif edilir.

İstinadlar

1. Атласкин А.А., Атласкина М.Е., Воротынцев А.В. и др. (2024). Зелёная химия как инструмент устойчивого развития: учебное пособие. Москва: Неправительственный экологический фонд им. В.И. Вернадского, 292 с.
2. Tağıyev D., Məmmədov A. (2024). Yaşıl kimya və onun inkişaf perspektivləri. Bakı: Elm, 212 s.
3. Шахгелдиев Ф.Х., Адилова Л.И., Сафарова Г.М. (2018a). Ресурсы макулатуры МС-1А и их роль в решении проблем экологической безопасности. В: Сб. мат. междунар. науч.-практ. конф. «Перспективы использования материалов устойчивых к коррозии в промышленности РТ», посвященной Дню химика и 70-летию д.х.н., проф., академика АН Республики Таджикистан Г.И. Наврузовича. Душанбе, с. 232–235.

4. Шахгелдиев Ф.Х., Адилова Л.И., Сафарова Г.М. (2018b). Способ получения абсорбента для очистки водных поверхностей от загрязнений нефтью и нефтепродуктами. В: Материалы международной научной конференции «Müasir təbiət və iqtisadi elmlərinin aktual problemləri», посвященной 94-летию со дня рождения Общенационального лидера Гейдара Алиева. Гянджа, с. 156–159.

PRODUCTION OF HIGH-PERFORMANCE BIO-BASED AEROGELS FROM SUGARCANE WASTE FOR CRUDE OIL REMEDIATION

Ayan Guliyeva, Revane Abdullayeva, Garanfil Ahmadova
Baku Higher Oil School
Baku, Azerbaijan
ayan.guliyeva.std@bhos.edu.az, revane.abdullayeva.std@bhos.edu.az

Summary - Global environmental pollution has become one of the serious problems in recent years, and water pollution is considered critical challenges among these problems. Toxic pollutants present in water cause diseases and direct death. In this study, modification of cellulose aerogels synthesized from sugarcane waste was investigated for the purification of oil spill residues, which constitute the majority of pollutants. Aim of the project is to increase the efficiency of water purification by integrating organic waste recycling with activated carbon cellulose aerogels. As a result of practical analyses, it was observed that the absorption capacity of activated carbon-based porous aerogel samples was up to 11.8 g/g. The aerogel modified with activated carbon selectively adsorbs oil spills in seawater by drawing them into its internal structure by capillary forces, due to its high porosity and hydrophobic surface. Analyses such as absorption capacity, reusability, FTIR and SEM were also conducted to investigate the morphological properties of the product. Aerogel provides an innovative solution for the restoration of polluted water resources by demonstrating a high adsorption capacity based on the principles of regenerative economy.

Keywords: hydrophobic aerogel, oil remediation, cellulose-based

Introduction:

Global environmental pollution is considered one of the critical concerns in recent years, and water contamination is supposed to be one of the most acute challenges among these troubles. Water pollution is mainly originated by diverse contaminants that raise serious health issues through contact, drinking, or contaminated water utilization. Harmful toxins present in water include waste, chemicals, parasites and bacteria, that together cause serious human health crisis.

Another earth-conscious issue is oil leakages, which constitute serious threats to the surrounding, specifically when substantial amount of oil is spread over bulk areas. Oil spills can arise from both tanker accidents and land-based sources such as factories, agricultural areas, and cities.

Different methods are generated for oil spill remediation and extracting poisonous substances from polluted water: biodegradation, filtration, adsorption, aggregation, and reverse osmosis. Although the effectiveness of

the methods has been confirmed, issues such as complex application and high cost are considered obstacles to further development.

Sugarcane implemented as preliminary raw material (85% of global sugar production) because it satisfies our research requirements with its significant global scale yield and cultivation prominence through extensive worldwide production and its nearby availability in agro-climatic zones which provide continuous stock accessibility and long-term economically viability.

In recent years, aerogels - multifunctional materials with physical and chemical properties such as high porosity and low density, have been applied to tackle environmental problems in agriculture. Their ability to adsorb oil and water, water-resistant properties, reusability performance, and effectiveness in oil amelioration make aerogels functionalized absorbents for organic solvents in aqueous circumstances. Subject of the study concentrates on cellulose aerogels synthesized from sugarcane bagasse. The principal structural composition of aerogels is cellulose fibers, which make aerogels a resource-efficient and environmentally safe preference.

In this research, cellulose aerogels synthesis originated from sugarcane bagasse and activated carbon modification was applied to improve their adsorption properties. Principal intention is to expand sustainable aerogel mechanism using agricultural waste and to prepare resilient and applicable materials for environmental renovation through water refinement.

Experimental part:

Experiment was embodied of two major points where Sugarcane Baggase (SB) was subjected to pre-treatment process and then formulation of cellulose centred aerogel unifies with fumed silica to get the hydrophobic modification. Commencing with synthesis of cellulose derived from SB, it is submitted to hydrolytic treatment in an alkaline medium after the granulation of SB into fine fibres. Following the comminution, as the first step of the pre-treatment process, the fibres are soaked in a 1 wt% NaOH solution, thereafter, the treated bagasse is rinsed with distilled water and oxidized in a 10 wt% H_2O_2 solution. To reach a pH of 12 (an alkaline environment), a certain amount of NaOH is added to SB pulp and washed again sequentially. With the aim of obtaining targeted fibrils, outcome of the initial process is sent to dry.

Consecutive workflow, namely the preparation of cellulose-based aerogel, the first polyvinyl alcohol (PVA) is homogenized with deionized water to facilitate aqueous PVA matrix. Produced gel dispensed into cryogenic-grade mold and stockpiled in laboratory regrigerator during 2 hours at 20 degrees of Celsius. Following the thermal cycling, the frozen gel is placed in a freeze-dryer to intensify the crosslinking capacity of the PVA molecules with the resultant material.

Subsequent target of the laboratory analysis is modifying the cellulose-based aerogels that is obtained to optimize specific capabilities of nanostructured porous solid. In this study, fumed silica was added for enhancing the surface hydrophobicity of the aerogels, i.e. process of

chemically modulating a substance (a surface) to augment its water repellency. Intending to prepare hydrophobic mixture, fumed silica (1 g) is dispersed in ethanol (50 ml). Aerogel samples (CA1, CA2, CA3) containing discrete proportions of activated carbon were suspended in a fumed silica dispersion, immobilizing an aerogel surface and build hydrophobic layer. Sequential to synthesizing aerogels, they have been dried at 70 ºC for 16 hours to preserve surface modification and eliminate ethanol traces.

Table 4 - Material characterization of the aerogel samples

Framework	SB/PVA/AC mass ratios (g)
CA1	2:1:0
CA2	2:1:0.3
CA3	2:1:0.6

Physical recovery of aerogels was estimated with sequential cycles, thereby assessing the material durability, in the definitive part of this study. Aiming to measure reusability, the oil-adsorbed aerogels were recuperated by heating at 115 °C for an hour to separate the oil and remaining moisture.

Results and their discussion:

Investigation of absorption capacity and surface area dependency with the application of activated carbon modification was undergone experimentation with three different samples: first sample - without AC, second sample - low amount of AC, third sample - high amount of AC.

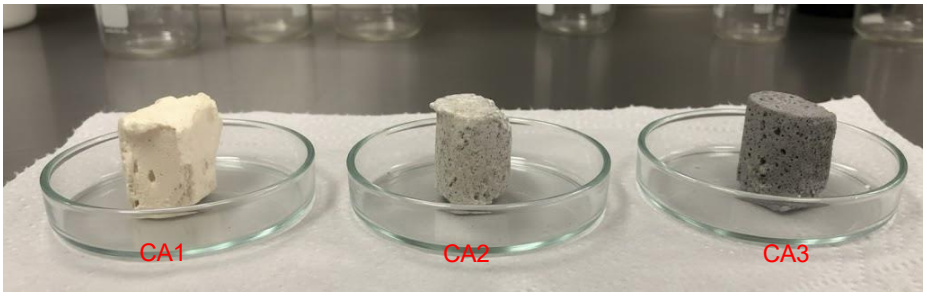


Figure 8 - Cellulose Aerogel (CA) samples in terms of activated carbon addition

In terms of individual physicochemical properties of aerogel samples, differences in their morphology was observed. From outcomes demonstrated that inter-fiber connections in the first sample were not strong enough. With the application of a small amount of activated carbon, it was determined that the second aerogel sample had a porous structure. Addition of an excess amount of carbon caused the loss of functional properties. In addition to the porosity property, the preservation of the shape of the aerogel is also considered an important factor for determining the composition of the optimized aerogel. Since the CA3 sample displays high brittleness, the CA2 sample was defined as the best version for further improvement.

Another point was the utilization of sodium chloride to determine the effect of water salinity on aerogel performance. According to the results, the absorption capacity for sample CA1 was 7.9 g/g, while for sample CA2 this figure was 1.5 times higher, at 12.4 g/g.

Reusability of aerogels was tested, gradual decreases in oil spill absorption were observed after the first two applications. In terms of quantity, there was a 2-fold decrease in the CA1 sample and a 1.5-fold decrease in the CA2 sample.

Offers:

According to the research outcome, specific properties of aerogel; high adsorption capacity and porous structure make synthesized matrix effective materials for water purification from oil spills, which are considered significant environmental problem. Determining the optimal structural integrity and absorption capability of aerogel should be investigated in future studies. Applying the results obtained in laboratory analysis to real marine conditions can contribute to a deeper understanding of aerogels. Further modifications are desirable to prevent the aerogel from adsorbing oil residues into its pores, which sharply decreases after several uses.

Based on this scrutiny, cellulose aerogels from agricultural waste which contain activated carbon materials provide an environmentally compatible solution to traditional synthetic sorbents. Material will be reached its full potential as a green solution for oil spill response systems and circular economy programs after researchers complete needed optimization and scale-up studies.

References:

1. [Gu et al., 2022] Cellulose aerogels show broad industrial applications.
2. [Jayarathna et al., 2024, 78–96] Oil spill response technologies continue to evolve globally.
3. [Mamozai et al., 2024, 126–138] Crude oil pollution deteriorates water quality and aquatic ecosystems.
4. [Mustafa & Hassan, 2024, 38–49] Water contamination significantly affects human health.
5. [OECD, 2025] Agricultural projections influence environmental resource management policies.

IMPROVING THE ENVIRONMENTAL PERFORMANCE OF CATALYTIC CRACKING GASOLINE BY FRACTIONATION AND HYDROTREATING OF THE HEAVY FRACTION

Elvira Kazimova
Supervisor: Zaira Gasimova
Baku Higher Oil School
Baku, Azerbaijan
elvira.kazimova.std@bhos.edu.az

Abstract: This work enables generating a solution for acquiring more ecofriendly FCC gasoline that complies with strict quality fuel standards. To make sure the octane number is steady and hydrogen consumption is minimal during desulfurization, the work provides optimization conditions through experimental and simulation performance of the process.

Keywords: catalytic cracking gasoline, diesel, FCC catalysts, fractionation, hydrotreating of heavy fractions

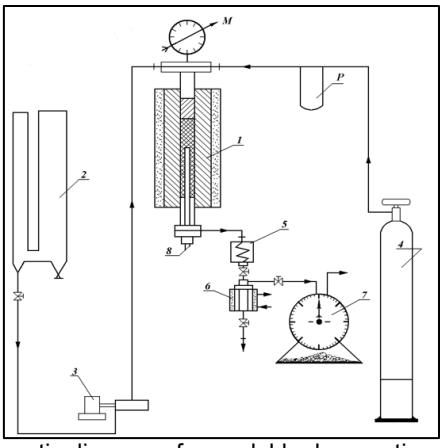
Introduction:

The global agenda of UN on strict standards for fuels encourages counties for uncompromising vehicle emission standards (Euro IV or Euro V). The standards allow for swift transition to zero emission targets and urban-friendly mobility. If all fuel oils available in the market are low sulphur only then emission will be drastically reduced [United Nations Environment Programme, 2025]. Fluid catalytic cracking (FCC) gasoline is distinguished by its high volumes of sulfur and olefins. Heavy fraction of the FCC includes 40-60% of all gasoline sulfur. Pollutants formed during a combustion in the chamber of internal combustion CO, NOx, SOx are responsible for smog, acid rains, ozone formation, cause acute and chronic respiratory diseases [Hosseinizand, 2016, 2-3]. In industry, sulfur cleaning of FCC gasoline is performed with various process variants. So far, there has been no selective catalyst of FCC gasoline hydrotreating which is capable of hydrodesulfurizing the whole FCC gasoline fraction in one stage, but without preliminary fractionation with a drop in octane number of less than one or two points [Galand E., 2023, 1-2].The process of fractionating FCC gasoline into light and heavy before hydrotreating is useful for deep desulfurization of fuel without compromising its quality.

Experimental Section:

The studies of the hydrotreating process of a mixture of diesel fraction and heavy gasoline from catalytic cracking were carried out on a model flow-type unit with a fixed catalyst bed, the diagram of which is shown below. Catalytic cracking gasoline was obtained from the G-43-107 unit of the Heydar Aliyev Oil Refinery, and the diesel fraction was obtained by processing a mixture of Baku oils. The industrial catalyst HDC-205 was used in the hydrotreating stage of the heavy gasoline fraction of catalytic cracking mixed with straight-run diesel fraction. A modified zeolite-containing nickel-aluminosilicate sample synthesized at the Institute of Petrochemical

Processes of the National Academy of Sciences of Azerbaijan was tested as a second catalyst.



Schematic diagram of a model hydrogenation plant

Results and Discussions:

The strategy of separating the gasoline steam and treating the heavy fraction successfully eliminates more than 99% sulfur, bringing levels below 10 ppm to meet international standards [Raluca, 2016,1-2]. X-ray fluorescence (XRF) analysis was conducted to define the total sulfur content. The aromatic, olefinic and paraffinic hydrocarbon contents of catalytically cracked gasoline were determined by nuclear magnetic resonance spectroscopy. Preliminary analyses indicated a good correlation between the research octane number and the hydrogen content of aromatic hydrocarbons. A similar correlation was observed for olefins. “Sim Dis” enabled to simulate the performance of fractional distillation.

Conclusions and Recommendations:

This integrated approach provides a refining process that is more energy-efficient and better for the environment. However, the process implies certain compromise; when removing sulfur from the system, the chemical reaction taking place there decreases the octane number of the gasoline by saturating olefins. As a result, the best way to enhance technology has been to improve catalysts and processes that maximize sulfur removal with a minimal octane penalty.

References:

1) Ekaterina Galand, Fabien Caron, Etienne Girard, Antoine Daudin, Mickael Rivallan,a Pascal Raybaud, Jean-Marc Schweitzera and Yves Schuurman (2023). High-throughput experimentation based kinetic modeling of selective hydrodesulfurization of gasoline model molecules catalyzed by CoMoS/ Al2O3.)
2) Hasti Hosseinizand (2016). Reducing Transportation Impacts through Fuel Improvements in Metro Vancouver.
3) Raluca Elena Dragomir, Paul Rosca*, Liana Bogatu (2016). Upgrading of FCC gasoline quality.
4) United Nations Environment Programme (2025). Accelerating the global shift to a cleaner on-road diesel fleet.

STUDY OF MOLECULAR DYNAMICS SIMULATION OF SELECTIVE HEAVY METAL CAPTURE FROM HIGH-SALINITY PRODUCED WATER USING CHITOSAN OLIGOMERS

Mahabbat Aslanov
Baku Higher Oil School
Baku, Azerbaijan
mahabbat.a.aslanov.std@bhos.edu.az

Summary - Remediation of produced water from petroleum reservoirs is still a significant environmental problem due to the high levels of competing alkali and alkaline earth metal ions that often interfere with the efficiency of conventional adsorbents. In this study, fully atomistic molecular dynamics (MD) simulations were employed to explore the mechanisms of selective adsorption of chitosan, a biodegradable polycationic bio-polymer, towards heavy metal impurities Pb^{2+}, Hg^{2+} in a complicated aqueous medium.

Keywords: Chitosan, Molecular Dynamics, Heavy Metal, GROMACS

For conducting simulation, CHARMM36 force field and TIP3P water model was chosen, a system was simulated using 12-mer chitosan chains and 0.15 mol L^{-1} NaCl background concentration to replicate the medium ionic strength, observed in typical oilfield brines. The results demonstrate that chitosan has high affinity towards divalent heavy metals with strong favourable coordination through its amino ($-NH_2$) and hydroxyl ($-OH$) groups even though high concentration of sodium ions. Analysis of the Radial Distribution Functions (RDF) shows that chitosan exhibits definite coordination shells for Pb^{2+} and Hg^{2+}. The helical conformation of chitosan allowing for multi-dentate chelation hereby suggests that monovalent Na^{+} ions for binding sites are out-competed by divalent heavy metals.

In addition, the effects of ion valency and the need to compensate the charges were assessed to ascertain the capacity of the polymer network in the bulk water system. These atomistic-level insights offer the theoretical background to develop chitosan-based filtration systems to achieve the selective recovery of heavy metals under the high salinity and pH conditions often encountered in the treatment of geological wastewater.

References:

1. Magdalena Hudek, Karen Johnston, Karina Kubiak-Ossowska, Valerie A. Ferro, and Paul A. Mulheran, "*Molecular Dynamics Study of Chitosan Adsorption at a Silica Surface*", The Journal of Physical Chemistry, 2024, Volume 128, Issue 50.

ENHANCING MACRONUTRIENT BIOAVAILABILITY IN SEWAGE SLUDGE-DERIVED BIOCHAR

Amil Ibadov
Hacettepe University
Ankara, Turkiye
amilibadov25@hacettepe.edu.tr

Keywords: biochar, pyrolysis, sewage sludge, fertilizer, potassium

Currently, inappropriate farming techniques, indiscriminate use of fertilizers and pesticides lead to soil degradation, a decrease in soil organic matter, and adverse effects on plant growth. Among the methods contributing to soil improvement, the use of sewage sludge has become increasingly popular in recent years. Sewage sludge, a waste product derived from sewage treatment in wastewater treatment plants, has agriculturally suitable levels of N (%1.5-4.0), P (%0.3-1.2), and organic carbon, making it a soil conditioner that has been used for centuries to sustain productivity in agricultural soils [Kominko H., 2017].

However, sewage sludges have diverse sources, and their contents vary. The quantity of sewage sludge depends on the degree and characteristics of wastewater pollution, the processes applied in the treatment plant (physical, physiochemical, biological, etc.), and the quality of the treatment. Nevertheless, the processes applied for the treatment and disposal of sewage sludge in treatment plants are often inadequate. This inadequacy may arise from either the failure to construct the units envisaged during the planning stage or the unhealthy operation of existing units. Additionally, the application of untreated sewage sludge, along with pathogens, raises health concerns due to organic and inorganic pollutants. Various studies have identified that such sludge containing heavy metals like lead (Pb), arsenic (As), and chromium (Cr) pose a carcinogenic risk, especially for children [Yakamercan E., 2021]. Due to these reasons, the direct use of sewage sludge as a soil conditioner in agriculture is an insufficient and not recommended solution [Bilen S., 2003].

While sewage sludge is hardly used for agricultural purposes in Belgium, the Netherlands, and Sweden, in Germany, the United Kingdom, France, and Portugal, 30-70% of the produced sludge is used for agricultural purposes. As of the end of 2018, the number of wastewater treatment plants serving approximately 83% of the Turkish population, equivalent to 54,484 tons of dry sludge daily, has reached 991.

In response to the serious attention given to this issue by the government in recent times, I envision contributing by transforming sewage sludge accumulated in sewer systems and septic tanks into biochar. This biochar can then be utilized as soil fertilizer in agricultural lands.

Thermal processes, incineration, and pyrolysis are alternative treatment methods. Pyrolysis is a method that breaks down a substance into products under high temperatures and anaerobic (oxygen-free) conditions. It sterilizes the material and reduces the concentration of organic toxins (e.g., poly-cyclic aromatic hydrocarbons (PAHs), poly-chlorinated biphenyls (PCBs), and dioxins), pharmaceuticals (e.g., hormones), and other micro-components (plastics, surfactant). Additionally, it passive immobilizes potentially toxic elements like Cu, Cd, and Cr found in the raw material, reducing the risk of leakage and plant uptake. Unlike incineration, pyrolysis retains most of the carbon in the sewage sludge [Buss W., 2020].

Contrary to additives like calcium (Ca), iron (Fe), and magnesium (Mg) in pristine biochar, which have been shown to reduce the presence of P, I believe using potassium (K) as a pre-pyrolysis additive can reverse the situation. Potassium phosphate salts exhibit very high solubilities, and the hypothesis suggests that if K is abundantly present, pyrolysis could result in the preferred formation of potassium phosphate, thereby increasing the bioavailability of P in biochar. I used potassium acetate as a pre-pyrolysis additive due to its widespread use and low cost for general applications like de-icing. The aim is to produce a more complete carbon-sequestering fertilizer with well-balanced nutrient availability.

Considering both financial and feasibility aspects, I believe this solution, which I find highly effective and practical, also supports recycling or reuse, which are fundamental initiatives of the modern approach. If pyrolysis vapors and liquids are used to feed the process or renewable energies, atmospheric carbon removal, storage, and environmental impact-wise, pyrolysis for sewage sludge can be considered the most sustainable solution.

References:

[1] Bilen S., Kızıloğlu Algan F.T., Toprak Kirlenmesi ve Biyolojik Çevre. 2003. https://dergipark.org.tr/tr/download/article-file/34208

[2] Buss, W., Bogush, A., Ignatyev, K., Masek, O. Unlocking the Fertilizer Potential of Waste-Derived Biochar. ACS Sustainable Chem. Eng. 2020.

[3] Kominko, H.; Gorazda, K.; Wzorek, Z. The Possibility of Organo-Mineral Fertilizer Production from Sewage Sludge. Waste Biomass Valorization. 2017, 8, 1781−1791.

[4] Yakamercan E., Ari A., Aygun A. Land application of municipal sewage sludge: Human health risk assessment of heavy metals. Cleaner Production. 2021.

ENVİRONMENTAL ASPECT OF ELECTRİC VEHİCLES

Anar Aghayev, Master in Oil and Gas Technology
Supervisor: Azar Salimov, PhD, Associate Professor
Chemical Engineering Department, Baku Higher Oil School
Baku Azerbaijan
anar.aghayev.std@bhos.edu.az

Abstract - This thesis provides information about environmental friendliness and proper applications of Electric Vehicles (EVs). The experiment compares different kinds of vehicles (sedans, SUVs/pickups, trucks, buses and trailers) with their carbon emission during their production and use. The results of experiments indicate carbon footprint of EVs depends on source of used electricity and category of vehicle. The bulk of the electricity in Azerbaijan and World is gained from not renewable sources. Hence EVs can damage environment more than internal combustion engine vehicles. Total carbon emissions of electric daily cars are approximately 34-68 tons per 150,000 km, and in industrial cars this number is around 105-327 tons per 500,000 km. Compared to internal combustion engines, daily cars have same or higher numbers, but industrial cars have lower numbers. Numbers depend on condition of use and types of fuel. The experiments show that EVs are more environmentally friendly for industrial and public transport, but in daily vehicles the result is he quite opposite EVs are less environmentally friendly. As a result, usage of EVs in big enterprises and the public sectors should and usage internal combustion engines for ordinary persons, are recommended for reducing overall carbon footprint.

Keywords: Electric vehicles, source of electricity, environmental effect, internal combustion engine, CO_2 emissions.

Introduction

Nowadays, especially after 2020, interest of electric cars has increased rapidly. There are several causes for this, like cheaper fuel, lower taxes, quiet driving. Vehicles are divided into several categories like sedans, SUVs (Sport Utility Vehicle) or pickups, trucks, buses, trailers, cause of different environmental damage. Environmental damage must compare in two stages: (1) environmental damage during manufacturing, and (2) environmental damage after manufacturing. For comparing to their damage to environment, CO_2 emission will be used for measure of how much CO_2 release to air during usage and production. EVs can damage world, due to their origin not only renewable things like sun, wind and gain from unrenewable things like coal, natural gas, and oil. [Peilin,2022,401-404].

Experiment

Starting with sedans, Tesla Model S has an 85-100 kWh battery. CO_2 release to atmosphere during production of this model is 10-18 tons, 5-10 tons of this release is battery, which is the one of the main parts of electric cars. In the same category, Mercedes-Benz E class 2.0, it's production CO_2 is 7-8 tons, 1.5 ton of this is internal combustion engine. But calculation does not end here, not only production but also post-production is important for environment. Average person will buy another model car after driving 150,000 km, in this case total emission can be found by multiplying this with

the carbon dioxide emission per one kilometer (fuel consumption per km × carbon dioxide in fuel burning) and adding this number to production emission number. For producing 1kWh electricity in the world in general, it must produce 600-700g CO_2 and Tesla uses 0.250-0.600 kWh for one km, it means Tesla produces (0.250-0.600kWh/km)×(600-700g/kWh)=150-420 gram CO_2 for one kilometer. For Tesla this number 150,000km×(150-420g/km)=22-63 tons for 150,000 km, and (10-18)+(22-63)=32-81 tons in total. For gasoline this number is 2-2.5 kg for L and Mercedes uses 0.06-0.07L gasoline for one km (2-2.5kg/L)×(0.06-0.07L)=(120-175) gram CO_2 for one km. In Mercedes, it is 150,000km×(120-175g/km)=18-26 tons, total (7-8)+(18-26)=25-34 tons. [Buberger,2022,1-12]

From SUV/Pickups we chose Tesla Cybertruck 123 kWh, and it is similar version Ford F-150 2.7. Tesla's production carbon emissions are 10-30 tons for one vehicle, 2-4 tons of it are batteries. Ford's production carbon emissions are 8-12 tons, 2 ton of it is engine. For Tesla, (0.25-0.35kWh/km)×(600-700g/kWh)=(150-245g/km), 150,000km×(150-245g/km)=22-38 tons, total (10-30)+(22-38)=32-68 tons, for Ford, (2-2.5kg)×(0.085-0.095L/km)=170-237g/km, 150,000km×(170-237g/km)=25-35 tons, total (8-12)+(25-35)=33-47 tons. [Ford,2023,1-46]

The Mercedes-Benz eSprinter 100-150 kWh and the Mercedes-Benz Sprinter 2.0d were chosen as a commercial vehicle for experiments. Production carbon emissions of eSprinter are 6-9 tons, approximately 1 ton of this number are batteries. For the diesel version production carbon emission is 5.5-7.5 tons, 0.5 tons of it is engine. Vehicles that are used for the company, factory and other things are driven on average 500,000 km, hence 500,000 will be used instead of 150,000 in calculation. [Barissova,2022,1-13] (0.30-0.33kWh/km)×(600-700g/kWh)= (180-231g/km) The emissions for one km of the electric version are 180-231 grams, 500,000km×(180-231g/km) = 90-115 tons, in total (6-9)+(90-115)=96-124 tons. When diesel burning 2.5-2.8 kg CO_2 releases for one liter, and Sprinter uses 8-13 liter for 100km. (0.08-0.13L/km)×(2.5-2.8kg/L)=(200-364g/km), 500,000km×(200-364g/km)=100-182 tons, in total (5.5-7.5)+(100-182)=105-189 tons. [Boer,2013,7-147]

A growing Chinese brand BYD's eBus B11 450-550 kWh as a public transport example, which is widely used in Azerbaijan, and the BMC Procity CNG, which is also widely used in Azerbaijan. BYD's production carbon emissions are 46-50 tons, 26 tons of it are batteries. BMC's are 25-30 tons, 4-5 tons of it is engine. [Tica,2019,67-75] BMC's uses 0.180-0.250 L/km and when CNG burning, it is made 400-550 g/L CO_2 to atmosphere, in this case 0.180-0.250L/km×(400-550g/L)=720-1375 g/km, 500,000km×(720-1375g/km)=360-687 tons, adding with production emission (25-30)+(360-687)=385-717 tons. BYD's uses 0.6-0.85kWh/km it will make CO_2 leak (0.6-0.85kWh/km)×(600-700g/kWh)=400-450g/km, 500,000km×(400-

450g/km)=200-225 tons. Adding with production (200-225)+(46-50)=246-275 tons. [Zhou,2015,2-5]

One of the most regularly used vehicles in factories is the trucks. For example, an electric truck is the Volvo FH Aero 780kWh and its internal combustion engine opponent is Scania 540S. Volvo's production carbon emissions are 65 tons, 40 tons of it are batteries. Scania's production carbon emissions are 20-30 tons, 2-4 tons of it are engine. Scania's (0.26-0.30L/km)×(2.5-2.8kg/L)=650-840g/km, 500,000km×(650-840g/km)=325-420 tons CO_2 emission in general (20-30)+(325-420)=345-450 tons . Volvo's carbon emission is (0.35-0.75kWh/km)×(600-700g/kWh)=210-525g/km, 500,000km×(210-525g/km)=105-262 tons, in general 65+(105-262)=170-327 tons. [Vitta,2019,3-25]

In carbon dioxide emissions for electric vehicles, the number of emissions is not exact number. The reason for this situation as mentioned in the first part of the thesis is electricity gaining from different ways. In Azerbaijan, 85-95 percent of electricity is gained from not renewable sources, in United States this number is 55-65 percent. [Missirlu,2024,2-17] This number means that, a person who is driving electric car in the United States saves more energy than a person who is driving electric car in the region of where no renewable sources are used. This percentage is around 60 worldwide in short, no electric cars are environmentally friendly. [Kleidon,2025,1-8]

Results and discussions

Electric cars, when used for daily life for ecology, are not so much different from combustion engines, even sometimes causing more damage. When electric industry vehicles replace combustion engines in industry, public works, and others it is more ecological. Any electric vehicle cannot be ecologically clean, cause of produced electricity in the world is not completely ecologically clean.

Suggestion

Big industrial enterprises, companies, etc. must use electric vehicles, ordinary people must use internal combustion engines in their daily lives, so that world is going to be cleaner.

References

1. An overview of state-of-the-art technologies and their potential Report Delft. Eelco den Boer (CE Delft), Sanne Aarnink (CE Delft), Florian Kleiner (DLR), Johannes Pagenkopf (DLR). 2013, 7-147.
2. Comparison of “Zero Emission” Vehicles with Petrol and Hybrid Cars in Terms of Total CO2 Release—A Case Study for Romania, Poland, Norway and Germany. Klaus Lieutenant, Ana Vassileva Borissova, Mohamad Mustafa, Nick McCarthy and Loan Lordache. 2022, 1-13.
3. COP29 host Azerbaijan climate action “Critically insufficient”. Ana Missirliu, Catrina Godinho, Natalie Pelekh, Niklas Höhne, Danial Riaz, Sofia Gonzales-Zuñiga, Bill Hare, Jane Ellis. Climate Action Tracker September 2024, 2-17.

4. Electric cars – assessment of 'green' nature vis-à-vis conventional fuel driven cars. Satish Vitta, Department of Metallurgical Engineering and Materials Science Indian Institute of Technology Bombay Mumbai 400076. India 2019, 3-25.
5. Electric High-tech Car and Environment Sustainable: Analysis of Tesla's problems. Peilin Li. Lang Business School, University of Guelph, Guelph, Canada. 2022, 401-404.
6. Electricity in international comparison. Axel Kleidon, Harald Lesch, Russ Conser. Physics in Our Time, in press. 2025, 1-8.
7. Ford Climate Change Report, Task Force on Climate, Related Financial Disclosures (TCFD) Report 2023, 1-46.
8. Real-world performance of battery electric buses and their life-cycle benefits with respect to energy consumption and carbon dioxide emissions. Boya Zhou, Ye Wu, Bin Zhou c, Renjie Wang, Wenwei Ke, Shaojun Zhang, Jiming Hao. Tsinghua University, Beijing 2015, 2-5.
9. Study of The Fuel Efficiency and Ecological Aspects of CNG Buses in Urban Public Transport in Belgrade. Slaven M. Tica, Predrag V. Živanović, Stanko A. Bajčetić, Branko M. Milovanović, Andrea M. Nađ. University of Belgrade. 2019, 67-75.
10. Total CO2-equivalent life-cycle emissions from commercially available passenger cars. Johannes Buberger, Anton Kersten, Manuel Kuder, Richard Eckerle, Thomas Weyh, Torbjörn Thiringer. 2022, 1-12.

INVESTIGATION OF THE PRODUCTION OF ENVIRONMENTALLY BENIGN MIDDLE-DISTILLATE FRACTIONS VIA HYDROGENATION OF VARIOUS VEGETABLE OILS

[1]Mammadova T., [2]Karimli R., [1]Aliyeva H., [1]Mmikayilova A., [1]Allahverdiyeva G. Z.
[1]Academician Y. H. Mammadaliyev Institute of Petrochemical Processes, Ministry of Science and Education of Azerbaijan, Baku, Azerbaijan
[2]Baku Higher Oil School, Baku, Azerbaijan
ravan.karimli.b0085@bhos.edu.az

Summary - This study investigates the production of environmentally benign middle-distillate fractions by hydrogenation of cottonseed oil and a mixture of used vegetable oils at 350 °C and 3.5 MPa over an HR-538 catalyst. Both feedstocks provided similar yields (~77.5 wt. %) of the 160-350 °C fraction, although the used oil mixture required slightly higher hydrogen consumption.

The products are rich in C17-C26 paraffins and exhibit high cetane number, zero sulfur content, and low aromatics, indicating good fuel quality. The results confirm that used vegetable oils are a suitable feedstock for producing renewable blending components for diesel and aviation fuels.

Keywords: Hydrogenation of vegetable oils; Green diesel; Middle-distillate fuels; Used cooking oil (UCO); Sustainable aviation fuel (SAF)

Introduction

Under current conditions, the decarbonization of transport and aviation requires the implementation of solutions compatible with the existing ground transport infrastructure and the current aircraft fleet. This issue is particularly critical for air transport, for which – unlike road and rail transport – modern

battery technologies and hydrogen-based solutions are not yet capable of providing the required fuel specific energy to support long-haul flights while maintaining commercial efficiency [IPCC, 2023; IATA, 2023; IEA, 2023].

At present, the most viable technology for producing environmentally benign automotive and aviation fuels from non-petroleum feedstocks is the production of “green” diesel or kerosene via hydrogenation of vegetable oils. The hydrogenation of vegetable oils predominantly yields paraffinic hydrocarbons in the C_{17}-C_{26} range, which are characteristic of middle-distillate fractions derived from conventional mineral feedstocks. From a product safety standpoint, the most suitable feedstock for this process is used vegetable oils (UVO) from the food industry.

Experimental part

Comparative hydrogenation experiments were carried out using cottonseed oil and a mixture of used vegetable oils (UVO) as feedstocks. The process was conducted at a temperature of 350 °C and a hydrogen pressure of 3.5 MPa in the presence of the HR-538 catalyst.

The feedstocks were subjected to catalytic hydrogenation under identical operating conditions to evaluate the influence of raw material type on product yield and quality. The material balance of the hydrogenation process was determined based on the distribution of products obtained after reaction and fractionation.

The main target product was the 160-350 °C middle-distillate fraction, while light hydrocarbons, gases, water, heavy residue (> 350 °C), and coke were also quantified. The physicochemical properties of the resulting middle-distillate fractions were measured according to standard analytical methods.

Results and their discussion

The material balance of the hydrogenation process for cottonseed oil and the mixture of used vegetable oils is presented in Table 1.

Table 5. Material balance of hydrogenation process

Indicators	Cottonseed Oil	Mixture of Used Oils
Feed, wt. %		
Vegetable oil	96	94
Hydrogen	4	6
Products, wt. %		
Fraction 160-350 °C	77.6	77.5
Gasoline fraction	2.6	3.0
Water	3.0	3.0
Fraction > 350 °C	1.6	1.9
Gases	12.9	12.0
Coke	1.1	1.3
Losses	1.2	1.3

As shown in Table 1, both cottonseed oil and the mixture of used vegetable oils provide a high yield of the target 160-350 °C fraction (~77.5 wt. %) under the selected conditions. However, the hydrogen consumption is

higher for the UVO mixture (6 wt. % versus 4 wt. % for cottonseed oil), indicating a somewhat greater hydrogen demand for processing used oils, likely due to the presence of more unsaturated or degraded components.

The yields of by-products such as gasoline fraction, gases, coke, and heavy residue are comparable for both feedstocks, confirming the overall stability of the hydrogenation process.

The quality characteristics of the obtained middle-distillate fractions are presented in Table 2.

Table 6. Fuel properties of middle-distillate fractions

Property Name	Middle-Distillate Fractions Based on	
	CSO	UVO
Density at 15 °C, kg/m^3	784.5	785.0
Distillation characteristics, vol. %:		
Recovered at 250 °C, vol. % (min)	73	76.9
Recovered at 350 °C, vol. % (min)	92	90
95% recovered, °C (max)	350	355
Flash point (closed cup), °C	82	83
Kinematic viscosity at 20 °C, mm^2/s	3.00	3.75
Acidity, mg KOH/100 cm^3 fuel (max)	1.3	1.6
Total sulfur content, wt. % (max)	-	-
Ash content, wt. % (max)	0.0005	0.0007
Carbon residue of 10% bottom, wt. % (max)	0.0009	0.0011
Hydrocarbon composition, wt. %:		
Aromatics	0.05	1.2
Unsaturated	-	-
Naphthenes	9.4	9.8
Paraffins	91.3	88.8
Actual gum content, mg/100 mL	2.5	4.8
Cetane number (min)	78	77

As can be seen from Table 2, the produced middle-distillate fractions possess high cetane number (77-78), negligible sulfur content, and very low aromatic hydrocarbon levels, which are favorable characteristics for clean-burning diesel and aviation fuels. The products are predominantly composed of paraffinic hydrocarbons (≈89-91 wt. %) in the C_{17}-C_{26} range, typical of hydroprocessed renewable fuels.

The slightly higher viscosity, acidity, and gum content observed for the UVO-derived fraction remain within acceptable ranges and do not significantly affect fuel quality.

Overall, the results confirm that used vegetable oils can serve as an effective renewable feedstock for producing environmentally benign middle-distillate blending components suitable for incorporation into conventional mineral fuels.

Offers

Based on the conducted studies, the feasibility of producing middle-distillate fractions from used vegetable oils with high yield has been confirmed. The obtained fuel fractions can be used as environmentally benign additives to corresponding middle-distillate mineral fuels.

References

1. Intergovernmental Panel on Climate Change (IPCC). *Climate Change 2023: Synthesis Report*. Geneva: IPCC, 2023. Available at: https://www.ipcc.ch/report/ar6/syr/
2. International Air Transport Association (IATA). *Net Zero Roadmap*. Montreal: IATA, 2023. Available at: https://www.iata.org/en/programs/environment/net-zero/
3. International Energy Agency (IEA). *Renewables 2023*. Paris: IEA, 2023. Available at: https://www.iea.org/reports/renewables-2023

WASTE FROM AGRO-INDUSTRIAL ENTERPRISES AS PROMISING SORBENTS FOR OIL POLLUTION

Farkhod Azimov
Supervisor R.F.Abbasova
Tashkent Institute of Chemical Technology, Tashkent, Uzbekistan
farkhod.azimov@bhos.edu.az

Keywords: agricultural waste, agricultural waste rice husks, spent tea, walnut partitions, oil pollution

Oil and petroleum products are among the most widespread and hazardous environmental pollutants. They enter natural ecosystems as a result of oil extraction, transportation, storage, and discharge of industrial wastewater. In our country, oil contamination is the consequence of more than 150 years of intensive industrial exploitation, which now requires large-scale environmental rehabilitation measures. Oil residues that have accumulated in soil layers over many years may periodically reappear on the surface. For this reason, remediation activities are long-term and technically complex. Pollution affects both terrestrial ecosystems and the waters of the Caspian Sea. Therefore, the purification of water contaminated with petroleum products remains an urgent environmental issue.

Agricultural and food-processing wastes are considered promising sorption materials due to their high porosity, developed specific surface area, and the presence of functional groups (–OH, –COOH, $–OCH_3$), which provide adsorption activity. Among the most studied natural biosorbents are rice husk, spent tea leaves, and walnut shell partitions. These materials are widely available, inexpensive, and suitable for simple preparation and modification (Nora Wagih, 2024) (Mohamed Hussein,2016) (Guofei Liu, 2022).

Our research focuses on the use of low-cost and environmentally friendly sorbents prepared from waste generated by the local agro-industrial

sector. The sorption properties of rice husk and spent tea cultivated in the Lankaran region, as well as walnut shell partitions grown in Nakhchivan, were investigated. As an oil contaminant, Ramany crude oil — extracted from one of the oldest oil-producing regions of Azerbaijan — was used. Rice husk is a by-product of rice processing and contains 15–20% silica, along with cellulose, lignin, and hemicellulose. The high content of amorphous SiO_2 contributes to the formation of a well-developed porous structure.

Spent tea contains polyphenols, cellulose, and tannins. The presence of aromatic structures promotes interaction with petroleum hydrocarbons through hydrophobic interactions and π–π interactions.

Walnut shell partitions mainly consist of lignin and phenolic compounds. They possess a rigid fibrous structure and high mechanical strength. To remove water-soluble impurities and stabilize the structure, biosorbents were subjected to pretreatment, which included washing with tap and distilled water, drying at 80–105 °C to constant mass, and grinding in a mortar.

To eliminate mineral impurities and increase surface roughness, samples were treated with phosphoric acid. Unlike the sorption of metal ions, oil sorption is predominantly a physical process and depends on such parameters as porosity, hydrophobicity, and buoyancy.

The experiments were conducted in Petri dishes, where an oil film was formed on the surface of both tap water and seawater. The sorbent was then applied onto the oil film. Sorption was studied for both fresh and aged oil films. In seawater, oil sorption capacity increased due to the salting-out effect. Oil sorption capacity and oil removal efficiency were calculated. Gravimetry, infrared (IR) spectroscopy, and fluorimetry were used for quality control and quantitative determination of petroleum products.

The experimental results showed that dried spent tea leaves exhibited the highest oil sorption capacity, followed by walnut shell partitions and rice husk. Each selected sorbent demonstrated both advantages and limitations. Modified rice husk showed high buoyancy, good stability, and excellent regeneration ability, allowing multiple reuse cycles. Walnut shell partitions were characterized by high mechanical strength and resistance to degradation. Spent tea demonstrated high sorption of light oil fractions (which corresponds to our oil sample), developed microporosity, and low density.

Rice husk and walnut shell partitions retained 60–80% of their sorption capacity after 3–5 regeneration cycles. A disadvantage of spent tea leaves is their susceptibility to biodegradation during long-term storage.

The results confirm that all studied biosorbents exhibit high oil sorption capacity and are promising for water purification. The highest sorption values were observed for walnut shell, tea leaves were more susceptible to activation. Rice husk demonstrated superior buoyancy and reusability, while walnut shell partitions showed excellent mechanical stability.

References
1. Nora Wagih , Mohamed M. Mahmoud , Amro A. Elbaz , Diaa EL-Moniry (2024) Oil removal using agricultural wastes adsorbents in a fixed bed column as a pretreatment in RO systems. Desalination and Water Treatment 320, 100811
2. Mohamed Hussein, Amer A. Amer, Hoda F.Zahran, Safaa M. Ali, Mohamed Elgohary and Mahmoud Nasr (2013) Agricultural waste as a biosorbent for oil spills International Journal of Development, 2, 1, 127-135
3. Guofei Liu, Zhongmin Dai, Xingmei Liu, Randy A. Dahlgren and Jianming Xu. (2022) Modification of agricultural wastes to improve sorption capacities for pollutant removal from water – a review. Liu et al. Carbon Research 1, 24

SUSTAINABLE BIOCHEMICAL ENGINEERING FOR SPACE HABITATS: A MULTI-OMICS PLATFORM FOR FUNCTIONAL FOOD DESIGN AND CLOSED-LOOP NUTRITIONAL SYSTEMS

Fidan Guliyeva
Azerbaijan State University of Economics, SABAH groups
Baku, Azerbaijan
fidanq50635@sabah.edu.az

Keywords: Precision Nutrition, Microbiome Engineering, Multi-Omics Integration, Sustainable Food Systems, Space Habitat Nutrition.

1.Introduction

Today, the more efficient use of resources has become a global necessity. Advances in biotechnology and biochemical engineering have facilitated the development of sustainable systems applicable in both food and non-food sectors. The implementation of sustainable food systems on Earth, as well as in missions to the Moon and Mars and other long-term space explorations, represents a strategic step toward future human sustainability (Heliyon, 2024, 1–10). Space missions are inherently large and complex processes. One of the major challenges that further complicates these missions is astronaut health and nutrition. Current nutrition systems are not tailored to individual physiological characteristics, creating a significant gap. Microgravity and increased radiation exposure during missions contribute to appetite loss, metabolic imbalance, and a potential increase in long-term cancer risk after returning to Earth (Rizzo et al., 2022, 1–12).

Recent research suggests that personalized nutrition and wearable technologies may significantly reduce physiological alterations during spaceflight (Rizzo et al., 2022, 1–12). However, existing space nutrition systems remain largely standardized and reactive, lacking systematic integration of real-time biometrics, multi-omic data, and microbiome dynamics. Additionally, long-term closed-environment experiments (e.g.,

hermetic habitat models) demonstrate that the microbiota–gut–brain axis plays a crucial role in astronauts' psychological health (Zhang et al., 2023, 1–18). Alterations in the gut microbiome during spaceflight may influence immune regulation, metabolism, and neurochemical signaling pathways (Frontiers in Physiology, 2020, 1–15). Although psychobiotics and targeted probiotic interventions show promising results, the mechanistic link between microbiome changes and psychological or neurochemical responses remains insufficiently clarified (Frontiers in Physiology, 2020, 1–15).

Therefore, a significant scientific gap exists in developing a unified, closed-loop nutrition platform for space missions that integrates precision nutrition, microbiome modulation, and sustainable biochemical system design.

2.Experimental Section

This study suggests an integrated nutrition platform for long-duration space missions based on three main pillars: multi-omic-based personal nutrition, microbiome modification, and sustainable production of functional food. The experimental design simulates the conditions of long-duration space travel while monitoring metabolic, microbiological and biochemical responses using a systems biology approach.

2.1.Multi-Omic-based Personal Nutrition

Phase one assesses astronaut metabolic status through metabolomics, microbiome sequencing, and real-time biometric data (glucose levels, heart rate variability, hydration status and energy expenditures). This approach is based on studies that found the use of personalized nutrition approaches may help to minimize or prevent muscle atrophy, bone loss due to demineralization and immune issues associated with long missions (for example Rizzo et al., 2022). Using the data collected from phase one, macro-nutrient ratios would then be dynamically adjusted while micronutrients such as vitamin D/calcium and antioxidants will be optimized to account for radiation/oxidative stress.

2.2. Microbiome Engineering and Psychobiotic Modulation

The second column addresses the gut microbiome as a "living bioreactor" that regulates metabolic and neurochemical processes. It is known that space conditions alter microbiome diversity (Frontiers in Physiology, 2020). Therefore, radiation-resistant probiotic strains that produce short-chain fatty acids (SCFA) and support serotonin precursors are introduced.

According to the "Lunar Palace 365" experiment (Zhang et al., 2023), microbiome profiles associated with positive psychological states are considered. SCFA levels, inflammatory markers, and neuroactive metabolites are monitored through periodic microbiome and metabolome analyses. Prebiotic fibers are added to strengthen the intestinal barrier and immune stability.

2.3. Sustainable Functional Food Production

The third stage involves the production of bioactive compounds, particularly polyphenols (e.g., resveratrol), using fermentation-based systems (Heliyon, 2024). These compounds play a protective role against radiation and oxidative stress.

At the same time, as an example of the application of a closed-loop food system, we can show that organic waste is processed through bioconversion and reused in plant-based food production. This approach increases resource efficiency and creates a sustainable food ecosystem for deep space missions.

3.Results and Discussion

The proposed integrated model provides a systems-level solution to astronaut health challenges. The multi-omics-based precision nutrition strategy enables dynamic metabolic regulation and may mitigate energy imbalance, muscle atrophy, and bone demineralization under microgravity conditions (Rizzo et al., 2022, 1–12).

Microbiome engineering adds a protective mechanism by stabilizing metabolic, immunological, and neurochemical pathways (Frontiers in Physiology, 2020, 1–15). Evidence from closed-environment experiments further supports the role of mood-associated microbiota in maintaining psychological resilience during prolonged isolation (Zhang et al., 2023, 1–18). Sustainable functional food engineering enhances resource-efficient production of protective bioactive compounds such as polyphenols, which may counteract radiation-induced oxidative stress (Heliyon, 2024, 1–10). Closed-loop nutrient systems reduce dependence on resupply missions and are essential for long-duration deep-space exploration.

However, further experimental validation, particularly multi-omics mechanistic investigations, is required to clarify microbiome–neurochemical interactions and optimize system integration (Frontiers in Physiology, 2020, 1–15; Zhang et al., 2023, 1–18).

4.Conclusion

This project aims to provide a comprehensive closed-loop nutritional system for long duration space flight by using precision, sustainability and biological resilience through the use of multi-omic, personalized nutrition, engineered microbiomes and sustainable production of functional foods. The resulting shift in space nutrition moves from a static supply system to a dynamic and adaptable health platform for astronauts in space.

Using a multi-omic approach will allow for continuous monitoring of an astronaut’s metabolic condition and customizing his/her diet based on the current metabolic state in order to prevent or mitigate the negative health effects from microgravity/radiation such as muscle wasting, bone loss, and immune system dysfunction, as well as prevent oxidative stress. In addition, the use of microbiome-targeted treatment modalities will improve intestinal

eubiosis, increase the production of short-chain fatty acids, and promote neurochemical balance, all of which will improve both the physical and mental well-being of astronauts while they are isolated for extended periods of time.

Moreover, using fermentation in Functional Food Engineering (FFE) and Closed Loop Nutrient Recycling (CLNR) will minimize our reliance on importing food while also providing us with a constant supply of bioactive, antioxidant-rich products. The systems-level integration supports the sustainable habitat design principles necessary for conducting deep-space exploration.

As a whole, the proposed platform suggests that nutrition in future space missions must be designed to incorporate individualization, consideration of the microbiome and ecological sustainability. In addition, there is value of this model for the formation of systems that enhance human health resilience and adaptation globally whether it's in outer space or in the other most extreme habitats on Earth.

References

Frontiers in Physiology. (2020). Microbiome and Space Travelers' Health: State of the Art and Possible Pro/Prebiotic Strategies for Long-Term Space Missions. Frontiers in Physiology, 11, 553929, 1–15.

Heliyon. (2024). Food systems for long-term spaceflight: Understanding the role of non-nutrient polyphenols in astronauts' health. Heliyon, 10, e34834, 1–10.

Rizzo, A., et al. (2022). Dietary Needs, Approaches and Recommendations to Meet the Demands of Future Manned Space Flights. Recent Progress in Nutrition, 2(1), 1–12.

Zhang, Y., et al. (2023). Positive mood-related gut microbiota in a long-term closed environment: A multiomics study based on the "Lunar Palace 365" experiment. Microbiome, 11, 150, 1–18.

STUDY OF THE EFFECT OF PRODUCED WATER COMPOSITION ON THE CORROSION PROCESS AND THE EFFECTIVENESS OF INHIBITORS

Gular Humbatzada
Supervisor: Agamaliyev Zaur
Baku Higher Oil School
Baku, Azerbaijan
gular.s.humbatzada.std@bhos.edu.az

Summary

Produced water generated during oil and gas production has a complex chemical composition and is considered one of the main causes of corrosion in pipelines and equipment. There are high salinity, different ions and organic substances and CO2, H2S inside water, it leads to rapid erosion of metal surfaces. The main purpose of presented report is to study effect of chemical composition of produced water to corrosion rate and effectiveness of different types of inhibitors in this circumstance. It is intended to prepare produced water samples which have various chemical properties and test metal samples in this condition and

measure corrosion rate. Also, the effectiveness of inhibitors will be compared in different conditions. It is expected that it will be necessary for managing corrosion in oil and gas industry and optimal inhibitor selection.

Keywords: produced water, corrosion, inhibitors, carbon dioxide, salinity

Introduction

In oil and gas industry, corrosion is one of the main problems which cause damage of equipment and major economic losses (B., 2018). Produced water which is generated during this production plays a key role, and it is a mixture of injected water and process chemicals. Produced water is characterized by corrosive components. Mainly, chloride ions, carbon dioxide and hydrogen sulfide increase corrosion rate on metal surfaces.

In order to prevent corrosion, chemical inhibitors are used widely, and these compounds decrease influence of corrosion environment by creating protective layers. However, effectiveness of inhibitors depends on composition of produced water, therefore it is necessary to study relationships between chemical characteristics of water and performance of inhibitors (Mahmood, 2015). In this study, grade carbon steel samples were used as the main material. As a corrosion inhibitor, G-1 reagent is used which is synthesized in laboratory conditions and this inhibitor consists of some heteroatoms such as nitrogen and oxygen (Mahmoodian, 2017).

Experimental part

Within the scope of the study, samples of synthetic produced water with different chemical compositions were prepared. Experiment was done by considering different salinity levels, pH indicators and existence of CO2 gases. For experiments, carbon-steel samples were chosen which are widely used in oil and gas industry. Then, these metal samples were kept in solutions which were prepared in certain periods. Corrosion rates were evaluated by methods of electrochemical impedance spectroscopy (EIS) and polarization. Besides, the effectiveness of it was compared by supplementing G-1 organic inhibitor and without inhibitor.

Results and their discussion

Finally, results obtained from this experiment demonstrate that composition of produced water plays key role in corrosion process. When CO2 gas was added to the sample, acidic environment was formed and it leads to decrease in electrochemical stability. To control corrosion, G-1 organic inhibitor was added to environment, and it was observed that concentration of inhibitor inversely proportional to corrosion rate. 20 ppm, 50 ppm, 100 and 200 ppm inhibitor was supplemented, and it was obtained that at 200 ppm, corrosion rate decreased to minimum, however efficiency value reached to 99.6 %.

Offers

The use of organic inhibitors such as G-1 can significantly reduce corrosion in produced water environments. Further studies may focus on

testing inhibitor performance under different temperature and pressure conditions. In addition, investigations of environmentally friendly inhibitors may provide sustainable corrosion control solutions.

References

[B., B. (2018). Corrosion inhibitors, principles and recent applications. 15-22]
[Mahmood, A. &. (2015). Comprehensive Review of Corrosion and its Inhibition in the Oil and Gas industry. 12-30]
[Mahmoodian, M. &. (2017). Failure assessment and safe life prediction of corroded oil and gas pipelines. 20-35]

QIZIL ÇIXARMA MÜƏSİSSƏLƏRİNDƏ YARANAN SİANİD TƏRKİBLİ TULLANTI SULARININ FOTOKATALİTİK TƏMİZLƏNMƏ PROSESLƏRİ

Həsənova Seynurə Azər
Azərbaycan Memarlıq və İnşaat Universiteti
Seynure.ibrahimova@gmail.com

Xülasə - Məqalədə qızıl mədən sənayesində yaranan sianid və tiosiyanat tərkibli tullantı sularının zərərsizləşdirilməsi üçün müxtəlif fotokatalitik və oksidləşmə üsulları təhlil edilir. Tədqiqatda yüksək gərginlikli elektrik impulsları, ultrabənövşəyi (UB) radiasiya, ozonlaşma (UB/O_3), ferrat sistemləri və titan dioksid (TiO_2) əsaslı fotokataliz proseslərinin effektivliyi müqayisəli şəkildə araşdırılmışdır. Müəyyən edilmişdir ki, $\{UV/S_2O_8^{2-}/Fe^{3+}\}$ fotokatalitik sistemi tiosiyanatların 98,5% dərəcəsində parçalanmasını təmin edir və digər metodlarla müqayisədə daha az enerji sərfi və sadə aparat tərtibatı ilə fərqlənir.

GİRİŞ

Qızıl çıxarma müəssisələrində filizin emalı prosesi ətraf mühit üçün yüksək toksiki risk daşıyan müxtəlif kimyəvi tullantıların yaranması ilə müşayiət olunur. Bu müəssisələrin tullantı sularında əsasən sərbəst və mürəkkəb formalı sianidlər, tiosiyanatlar, siyanatlar və müxtəlif ağır metal birləşmələri (mis, dəmir, nikel, sink) cəmləşir. Xüsusilə sianid birləşmələri biosfer üçün kəskin zəhərli təsirə malikdir və onların təhlükəsiz limitlərə qədər parçalanması müasir ekologiyanın ən vacib məsələlərindən biridir.

Qızıl mədən fabriklərinin və metal emalı müəssisələrinin texnoloji sularında aşağıdakı əsas çirkləndiricilər müşahidə edilir:

1. **Sianidlər:** Sərbəst sianid ionları və müxtəlif metallarla (məsələn, dəmir-sianid kompleksləri) əmələ gətirdiyi mürəkkəb birləşmələr.
2. **Tiosiyanatlar (SCN^-):** Qızılın ekstraksiyası zamanı kükürd tərkibli minerallarının sianidlə reaksiyası nəticəsində yaranan geniş yayılmış çirkləndirici.
3. **Ağır Metallar:** Emal prosesində suya keçən mis (Cu), dəmir (Fe), nikel (Ni) və sink (Zn) kimi kationlar.

4. **Digər Birləşmələr:** Siyanatlar və yüksək Oksigen Kimyəvi Tələbatı (OKT) yaradan üzvi/qeyri-üzvi komponentlər.

METODOLOGİYA

Tədqiqat prosesində müxtəlif şüalanma mənbələri və katalitik sistemlər tətbiq edilmişdir:

1. **Şüalanma mənbələri:** 11,4 Vt-dan 1 kVt-a qədər gücə malik, 254 nm və 365 nm dalğa uzunluqlu aşağı və yüksək təzyiqli civə lampalarından istifadə olunmuşdur.
2. **Oksidləşdirici sistemlər:** Sianidlərin parçalanması üçün H_2O_2 (1:5 mol nisbətində), ozon (1 mq sianidə 1,8-4,7 mq O_3) və ferrat (FeIV, FeV, FeVI) birləşmələri sınaqdan keçirilmişdir.
3. **Katalizatorlar:** Proseslərdə dəmir (II), mis (Cu), metal ftalosiyaninlər və titan dioksid (TiO2) katalizator kimi istifadə edilmişdir.
4. **Reaksiya mühiti:** Təmizləmə prosesləri əsasən pH 5-13 diapazonunda, temperaturun 20°C-dən 150°C-ə qədər dəyişdirilməsi ilə aparılmışdır.

MÜZAKİRƏLƏR

Sianid məhlullarının zərərsizləşdirilməsi təmizlənən suya dəmir (II) birləşmələrinin əlavə edilməsi və xüsusi enerji sərfiyyatı 100 kJ/dm^3-dan çox olmayan yüksək gərginlikli elektrik impulsları ilə şüalandırılma nəticəsində baş verir **[1].** Bu prosesdə yüksək gərginlikli boşalma impulsları ilə 5000 °C-dən çox temperaturu olan bir qövs meydana gəlir, ultrabənövşəyi oblastda şüalanma yaranır nəticədə oksigenin (O_2) və ozonun (O_3) əmələ gəlməsi ilə suyun parçalanması baş verir. Eyni zamanda qızıl mədən fabriklərinin tullantı sularında sadə sianidlərin və digər çirkləndiricilərin effektiv parçalanmasına nail olunur. Dəmir kationlarının iştirakı ilə sianid məhlullarının neytrallaşma sürəti kəskin şəkildə artır. Bu metodun əhəmiyyətli çatışmazlıqları neytrallaşdırma prosesinin yüksək enerji intensivliyi və aparatın mürəkkəbliyidir. Tərkibində sianid olan çirkab suların təmizlənməsi üçün digər üsul zərərsizləşdirmə prosesində suların ultrabənövşəyi radiasiyaya məruz qalması və sianid birləşmələrinin metal ftalosiyaninlər tərəfindən katalizləşdirilmiş atmosfer oksigeni ilə oksidləşmə reaksiyası vasitəsilə əldə edilir [14]. UB radiasiyasının mənbəyi 550 Vt gücündə yüksək təzyiqli civə lampası istifadə edilmişdir. Tədqiqat işində 50-5000 mq/dm^3 konsentrasiya diapazonunda dəmir, kobalt və ya vanadium istifadə olunur. Sianid tərkibli məhlulların təmizlənməsi prosesi pH 9-12 olan qələvi mühitdə aparılır. Temperaturun 20-dən 150 ° C-ə qədər və təzyiqin 1 atm-dən 10 atm-ə qədər artırılması oksidləşmə prosesini sürətləndirməyə imkan verir, lakin əlavə enerji xərclərinə səbəb olur. Bundan əlavə, bu metodun çatışmazlıqları sorbentləri dəyişdirərək katalizatorun ilkin hazırlanması ehtiyacını zəruri edir.

Sərbəst və mürəkkəb sianidlərin parçalanma prosesi işlənmişdir və aşağıdakı mərhələləri əhatə edir [5]. Əvvəlcə ozonla ilkin oksidləşmə aparılır, sonra ozon və UB şüalanması ilə kombinə edilmiş təsirə məruz qalır. Sianid məhlullarının zərərsizləşdirilməsi prosesi pH 5-9 aralığında aparılır, ozon

sərfi 1 mq siyanidə 1,8-4,7 mq təşkil edir [13]. Sianidlərin deqradasiya edilməsi üsulunda tərkibində sianid olan çirkab suların zərərsizləşdirilməsi prosesinin səmərəliliyini artırmaq üçün təmizlənmiş məhlulun temperaturunun 70°C-ə qədər artırılması təklif edilir ki, bu da əlavə istismar xərcləri tələb edir. Tullantı sularının bu oksidləşdiricinin reduksiya məhsulları ilə ikincil çirklənməsinin olmamasına baxmayaraq, təmiz ozon zəhərli və partlayıcıdır, çünki parçalandıqda əhəmiyyətli miqdarda istilik ayrılır. Bundan əlavə, ozon elektrokimyəvi üsullarla istehsal olunur ki, bu da yüksək kapital və əməliyyat xərclərinə səbəb olur.

Sianid tərkibli texnoloji məhlulların təmizlənməsi üçün digər üsul oksidləşdirici sistemdən istifadə etməklə fotokimyəvi təsir (UB/O_3) və daha sonra manqan oksidi ilə əvvəlcədən işlənmiş təbii seolitlə doldurulmuş təbəqədən keçirməklə deqradasiya prosesinin həyata keçirilməsindən ibarətdir [8]. Şüalanma mənbəyi reaktorun daxilində yerləşən 254 nm dalğa uzunluqlu aşağı təzyiqli civə lampasından (11,4 Vt) istifadə edilmişdir. Prosesin yüksək qələvi mühitdə aparılması (pH≈13) istifadə texnologiyasının mürəkkəbliyini artırır.

Tərkibində sərbəst və mürəkkəb sianidlər, tiosiyanatlar, siyanatlar və digər birləşmələr olan qızıl mədən və metal emalı müəssisələrindən çirkab suların zərərsizləşdirilməsinin digər üsulu ekoloji cəhətdən təmiz oksidləşdirici maddələrdən - ferratlardan (“super dəmir batareyalar”: FeIV, FeV, FeVI) , qeyri-üzvi çirkləndiricilərin ferratlar (VI, V və IV) tərəfindən oksidləşmə prosesinin aparılması ilə tədqiq edilmişdir [6]. Fotokatalitik oksidləşmə prosesini öyrənmək üçün 365 nm dalğa uzunluğunda maksimum emissiyası olan 250 Vt gücündə yüksək təzyiqli civə lampasından istifadə olunur. "Ferrat" sistemlərinə əsaslanan oksidləşdirici üsulların əsas çatışmazlığı reagentlərin yüksək qiymətidir ki, onları da əldə etmək üçün çox mərhələli sintezdən istifadə olunur. Bundan əlavə, qələvi metal ferratların özləri kimyəvi cəhətdən aktivdir, otaq temperaturunda termodinamik cəhətdən qeyri-sabitdir və nəmli havada parçalanır. Tərkibində sianid olan məhlulların fotokimyəvi təmizlənməsi üçün ilkin mərhələdə asılı halda olan bərk maddələrin çıxarılması, sonra 1 mol sianid ionuna 5 mol H_2O_2 molyar nisbətində hidrogen peroksid və UB şüalanma ilə deqradasiya prosesi aparılmışdır [3-4]. Tullantı sularının zərərsizləşdirilməsi Solarchem şirkətinin istehsalı olan 1 kVt gücündə UB reaktorunda aparılmışdır. Bu metodun çatışmazlıqları aşağı konsentrasiyalı tullantı suları üçün metodun tətbiqi (50 mq/dm^3-ə qədər sianidlə) və stexiometrik olaraq tələb olunan miqdarı 5 dəfə üstələyən bahalı oksidləşdiricinin yüksək istehlakıdır.

Sianid tərkibli məhlulları Cu katalizatorun iştirakı ilə UB şüaları və hidrogen peroksiddən istifadə etməklə fotokimyəvi təmizləmə prosesinin

aparılmışdır [7]. Bu metodda şüalanma mənbəyi kimi maksimum 254 nm dalğa uzunluğunda aşağı təzyiqli UB lampadan (25 Vt) istifadə edilmişdir. Hidrogen peroksid optimal miqdarı adətən tələb olunan miqdardan 10 dəfə yüksək olur. Cu birləşmələrinin katalizator kimi istifadəsi neytrallaşdırma prosesinin qiymətini artırır. Bundan əlavə, hidrogen peroksid aşağı aktivliyə malik (təxminən 35%) sulu məhlul şəklində istehsal olunur ki, bu da daşıma və daşımada müəyyən çətinliklər yaradır.

Tiosiyanat tərkibli tullantı sularının fotokimyəvi təmizlənməsinin, titan dioksiddən istifadə edərək fotokatalitik sistem vasitəsi ilə həyata keçirilmişdir. UB şüalanma mənbəyi kimi civə lampasından istifadə edilmişdir [2]. Əsasən spektr yaxın ultrabənövşəyi bölgəsində (315-400 nm diapazonunda 352 nm bölgədə) maksimum emissiya ilə yayılır. İlkin çirkləndirici konsentrasiyası 10 və 20 mq/dm^3 olan tiosiyanat tərkibli məhlulların effektiv neytrallaşdırılması TiO_2 konsentrasiyası 1 q/dm^3 olduqda, əsasən qələvi mühitdə, optimal pH dəyəri 10-12 olan şəraitdə baş verir. Müxtəlif UB şüalanma mənbələrindən istifadə etməklə tiosiyanatların fotokimyəvi oksidləşməsinin nəticələri Cədvəl 1.də verilmişdir.

Cədvəl 1. Müxtəlif UB mənbələrinin istifadəsi ilə tiosiyanatların fotokimyəvi oksidləşməsi

Oksidləşmə sistemi	UB mənbələrinin gücü, Vt	Emal vaxti, dəq.	İlk sürət Mmol x dm^3/dəq	Xüsusi dönüşüm Mkmol x J^{-1}
$S_2O_8^{2-}/Fe^{3+}$	-	100	0.072	-
UB-254/ $S_2O_8^{2}/Fe^{3+}$	40	60	0.114	3.4
UB-G/$S_2O_8^{2-}/Fe^{3+}$	433	20	0.136	1.0
UB-222/$S_2O_8^{2-}/Fe^{3+}$	30	40	0.088	7.2

Tiosiyanatlar {$Fe^{3+}/S_2O_8^{2-}$} katalitik sistem və əlavə fotoaktivləşdirmə ilə təmizlənərkən, bütün hallarda oksidləşdirici destruksiya prosesinin əhəmiyyətli sürətlənməsi müşahidə olunur ki, bu da təsir müddətinin əhəmiyyətli dərəcədə (1,7-5 dəfə) azalmasına gətirib çıxarır. {UV/$S_2O_8^{2-}/Fe^{3-}$} fotokatalitik sistemindən istifadə etməklə üyüdmə qurğusunun tiosiyanat tərkibli texnoloji məhlullarının neytrallaşdırılmasının nəticələri Cədvəl 2-də verilmişdir.

Cədvəl 2. Üyüdülmə qurğusunun tiosiyanat tərkibli texnoloji məhlullarının neytrallaşması

	Komponentlərin tərkibi, mq/dm^3							
	SCN^-	$S_2O_3^{2-}$	Cu	Fe	Ni	Zn	OKT	pH
Təmizləmədən əvvəl	126,7	26,01	39,94	20,24	0,62	1,47	296	10,6
Təmizləmədən Sonra	1,91	-	1,28	1,69	0,12	0,82	45	7,3
Səmərəlilik, %	98,5	99,9	96,8	91,6	80,6	44,2	84	-

Tiosiyanat tərkibli tullantı sularının təmizlənməsi üçün təklif olunan üsul həm dar, həm də geniş optik diapazonda müxtəlif ultrabənövşəyi şüalanma mənbələrindən istifadə edərək tiosiyanatların və digər əlaqəli birləşmələrin yüksək dərəcədə deqradasiyasına nail olmağa imkan verir. Bundan əlavə, proses hər hansı əlavə pH tənzimləyicilərinin tətbiqini tələb etmir. Nəticədə, deqradasiya prosesinin müddəti və istismar xərcləri əhəmiyyətli dərəcədə azalır ki, bu da təmizləmə xərclərinin azalmasına səbəb olur. Təklif olunan üsul aparat dizaynında sadədir və aşağı toksiklik, istifadəsi asan və daşınma reagentləri sayəsində sanitar şəraiti daha əlverişli etməyə nail olacaq [9-12].

NƏTİCƏ

Aparılan tədqiqatlar göstərir ki, müasir fotokimyəvi üsullar sianid tərkibli suların təmizlənməsində yüksək səmərəlilik nümayiş etdirir. Lakin ozonlaşma və ferrat əsaslı sistemlər yüksək kapital xərcləri və reagentlərin qeyri-sabitliyi kimi çatışmazlıqlara malikdir. Ən optimal nəticə {UV/ Fe^{3+}/$S_2O_8^{2-}$} sistemi ilə əldə edilmişdir ki, burada tiosiyanatların (SCN^-) səmərəliliyi 98,5%, misin (Cu) kənarlaşdırılması isə 96,8% təşkil etmişdir. Bu üsul əlavə pH tənzimləyicisi tələb etmir, istismar xərclərini azaldır və aparat tərtibatı baxımından sadədir, bu da onun qızıl mədən fabriklərində tətbiqini iqtisadi və ekoloji cəhətdən səmərəli edir.

ƏDƏBİYYAT

1. İbrahimova S. Optimal configuration of a photocatalytic lab-reactor by using immobilized nanostructured TiO_2. Chemical Engineering Transactions, Italy. Journal. 2016, №47.
2. Vuong D-G., Klock B.V. Cyanide and formate destruction with ultra violet light // US Pat. №7144514, Dec. 5, 2006; M. Sarla, M, Pandit, D.K. Tyagi, J.C. Kapoor. Oxidation of cyanide by chemical and photochemical process // Journal of hazardous materials. - 2004. - Vol. 116. - P. 449-56
3. Wang Z.P., Huang L.Z., Su J.W., et al. Removal of cyanides in coking wastewater by ferrate pre-oxidization followed by photochemical process //Fresenius Environmental Bulletin. - 2008. - 17 (8). P. 1082-1087
4. Vohra, M.M., Tanaka, K., 2002. Photocatalytic degradation of nitrotoluene in aqueous TiO2 suspension. Water Res. 36, 59–64
5. Vohra M.S. Effect of co-pollutants thiosulfate and ammonia onto TiO2-mediated photocatalytic removal of thiocyanate from synthetic wastewater // Fresenius Environmental Bulletin. - 2013. - Vol. 22. - №2a. - P. 591-597
6. Vohra M.S. Removal of aqueous phase selenite and selenate using artificial and solar energized photocatalysis // US Pat. №9162902, Oct. 20, 2015
7. Sharma V.K. Oxidation of inorganic contaminants by ferrates (VI, V, and IV) - kinetics and mechanisms: A review // Journal of Environmental Management. - 2011. -. Vol. 92. - P. 1051-1073
8. Hanela S., Duran J., Jacobo S. Removal of iron cyanide-complexes from wastewaters by combined UV-ozone and modified zeolite treatment // Journal of Environmental Chemical Engineering. - 2015. - Vol. 3. - P. 1794-1801
9. Hasanova Seynura, Mammadova Leyla . Technology of Using Renewable Energy Sources in Groundwater Treatment// Journal of Liquid Radioactive Waste Treatment// 2025. Pp. 1-11.
10. Hasanova, S.A., Aliyev, F.G., Gurbanov, M.A., Jafarov, Y.D.: Study of the chemical processes occurring in the gas phase as a result of photolysis of produced waters under the ultraviolet rays influence. PPOR. 24(4), 623–630 (2023)

11. Hasanova, S.A., Aliyev, F.G., Gurbanov, M.A., Jafarov, Y.D.: Monitoring of the composition of produced water used in the process of oil extraction. Ecoenergetics. 1, 92–96 (2023)
12. Hasanova S.A. Compared the efficiency of TiO_2 and N-Doped TiO_2 to degrade BTEX. Journal, Advanced Physical Research. 2021, №3.
13. Garrison R.L., Prengle H.W., Mauk S.E. Method of destroying cyanides // US Pat. №3920547, Nov. 18, 1975
14. Frame R.R., Kalnes T.N., Moser M.D. Oxidative removal of cyanide from aqueous streams abetted by ultraviolet irradiation // US Pat. №5238581, Aug. 24, 1993

MODIFIED NATURAL CLAY AS A POTENTIAL CD(II) ADSORBENT FROM WASTEWATER

Israfil Movsumzada
Khazar University
Baku,Azerbaijan
movsumovisrafil@gmail.com
Supervisor: Dr.Tahir Javadzade

Summary - In this research the adsorption of Cd(II) ions from oil-polluted wastewater of Baku region using natural clay from the Mashtaga has been investigated after the surface modification with various amines. X-ray diffraction ananlysis was used for the determination of the mineralogical composition. Experiments on batch adsorption were conducted at room temperature with varying pH levels. Analysis results showed that the adsorption efficiency was greatly increased after modification.
Keywords: Cadmium;Pollution; Adsorption; Natural clay; Wastewater.

Introduction

Heavy metal pollution of water is one of the major global environmental problem. Specially because of its toxicity and potential for bioaccumulation cadmium is very dangerous. [Pradinaud, 2019, 960-974]. Oil-producing countries such as Azerbaijan face additional challenges related to heavy metal contamination of industrial and oil-polluted wastewater.

Adsorption is considered one of the most effective and economical methods for heavy metal removal. Natural clays are attractive adsorbents due to their availability, low cost, and surface reactivity. Surface modification using amine-containing compounds can significantly enhance adsorption capacity.

Experimental Part

Natural clay was collected from the Mashtaga region (Baku, Azerbaijan) [Abdullayev,2024,1-12] and mineralogical composition of it was determined by XRD analysis (Table 1).

Surface modification was performed using several amine-containing compounds: 1-naphthylamine, diphenhydramine, 4-nitroaniline, thiourea, urea, and 2-amino-4-nitrotoluene-5-sulfonic acid. An amine to clay mass ratio of 1:10 was used.

Batch adsorption experiments were conducted at 25 °C. In each experiment, 30 mg of modified clay was added to 2 mL of Cd(II) solution (5×10^{-3} mol/L). The pH was adjusted to the desired value. After 24 hours of equilibration, the solid and liquid phases were separated by filtration.

Table 1. The mineralogy of bulk clay

Mineral	Percentage
Illite/Smectite	15.1
Illite+Mica	28.8
Kaolinite	2.2
Chlorite	4.5
Cristobalite	0
Quartz	30.6
K Feldspar	3.0
Plagioclase	10.1
Calcite	4.9
Dolomite	TR
Halite	0.7
Total	100

The equilibrium concentration of Cd(II) was determined spectrophotometrically using xylenol orange at pH 6 (λ = 575 nm) [Otomo, 1964, 504–508].

Results and Discussion

The experimental results showed that amine modification significantly improved Cd(II) adsorption efficiency. Maximum adsorption was observed at pH = 3. Approximately 90% of Cd(II) removal occurred within the first 15 minutes, indicating rapid adsorption kinetics.Beside this H_3PO_4 showed the highest regeneration efficiency for reusability of the adsorbent.

References

1.Abdullayev E., Paterson J.R., Kuszynski E.P., et al. (2024). Evaluation of the antibacterial properties of commonly used clays from deposits in central and southern Asia. *Clays and Clay Minerals*, 72, 1-12.
2.Otomo M. (1964). The spectrophotometric determination of cadmium with xylenol orange. *Bulletin of the Chemical Society of Japan*, 37, 504–508.
3.Pradinaud C., Northey S., Amor B., et al. (2019). Defining freshwater as a natural resource: A framework linking water use to the area of protection natural resources. *International Journal of Life Cycle Assessment*, 24, 960–974.

SCREENING OF IONIC LIQUIDS USING THE COSMO-RS METHOD FOR CO_2 CAPTURE

Hamida Azizbayli [1,2], Gulnar Atakishizada[2], Aydan Nadirova[2], Lala Huseynli[2], Fariz Amirli[2], Reyhan Aliyeva[1], Minaver Ibrahimova[1]
[1]The Institute of Petrochemical Processes named after academician Y.H. Mammadaliyev
[2]Azerbaijan State Oil and Industry University
Baku, Azerbaijan
Email: gulnar.atakishizade@gmail.com

Abstract - Ionic liquids have been increasingly utilized as next-generation "designer solvents". Ionic liquids feature low vapor pressure, high thermal stability, large range of temperatures in the liquid phase, and excellent solvation capacity, allowing them to be continuously manipulated through systematic modifications in the combinations of cations and anions to achieve specific tasks, such as for industrial applications including gas separation and selective extraction. A part of this systematic research involved using the COSMO-RS quantum chemical method to investigate many ionic liquids with respect to their CO_2 solubility, and their use to extract aromatic hydrocarbons from refined fuels. To assess the ability of the COSMO-RS model to predict CO_2 solubility in ionic liquids, CO_2 Henry's law constants were calculated at different temperatures. The effects of the cation's structure, anion's type, and alkyl chain lengths on CO_2 solubility were analyzed systematically, and analyses of the ionic liquids' sigma-profiles were used to evaluate intermolecular forces and the predicted potential selectivity of the ionic liquids for extracting aromatic hydrocarbons (e.g., benzene and its alkyl derivatives) from refined fuels. The theoretical predictions made by the COSMO-RS simulations were compared with experimental extraction studies, including spectroscopic analyses of the raffinate phases. Overall, the COSMO-RS method was shown to provide reliable thermodynamic predictions for the CO_2 solubility of the ionic liquids and can therefore be used effectively for the preliminary screening of ionic liquids, reducing the need for further experimental tests.

Keywords
Ionic liquids, COSMO-RS, CO_2 capture, Henry's constant, aromatic hydrocarbon extraction, thermodynamic modelling

Introduction

The rise in the concentration of carbon dioxide (CO_2) in the atmosphere has become one of the major environmental issues of the 21st century, playing a major role in global climate change and environmental degradation [1]. Industrial processes, fossil fuel burning, and chemical production processes have become the major sources of emitting CO_2 into the environment [2]. Therefore, the development of efficient and effective carbon capture technology has become the major focus of scientific and industrial innovation.

The solvents currently used for CO_2 absorption, such as aqueous amine solvents, have several disadvantages, including volatility, solvent degradation, equipment corrosion, and energy requirements for regeneration [2]. These problems have led to the search for alternative solvents that have

better thermodynamic and environmental properties than the currently used solvents. Ionic liquids have become the promising solvents in the capture of CO_2 due to their unique physicochemical properties.

Ionic liquids are defined as salts formed entirely of ions and have the ability to remain in a liquid state at temperatures lower than 100°C. Moreover, ionic liquids have negligible vapor pressure and are thermally stable with high polarity and solvation power [3-8]. One of the most interesting properties of ionic liquids is their ability to create task-specific ionic liquids by manipulating their chemical structure in order to improve their gas absorption and separation properties [4].

Recent investigations have indicated that some ionic liquids based on imidazolium have shown good solubility and selectivity properties compared to other solvents [7]. In addition, it was found that computational simulations such as COSMO-RS are efficient tools in determining thermodynamic properties and identifying ionic liquids before experimental validation [8].

Thus, it may be concluded that the study of ionic liquids in CO_2 capture and separation processes is a scientifically significant and practically important research area. In addition, it can be seen that the use of combined theoretical modeling and experimental analysis can help in the systematic evaluation of ionic liquids and the development of efficient and sustainable carbon capture processes.

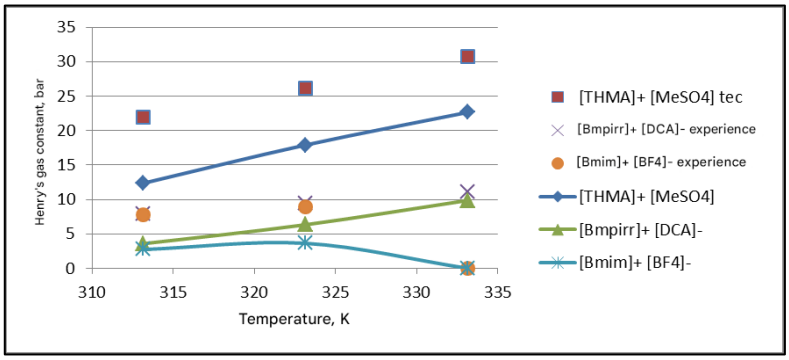
Experimental Section

Quantum chemical calculations were carried out to determine the surface charge density of the molecule, which is necessary for the COSMO-RS analysis. Geometry optimization of the ionic liquid cations, anions, carbon dioxide, and some aromatic hydrocarbons was done by the TURBOMOLE program with the BP/TZVP level of theory and the COSMO solvation model. The COSMO files obtained were then treated by the COSMOTherm program for the determination of thermodynamic properties by the COSMO-RS method.

Henry's law constants for the solubility of carbon dioxide were calculated for 313.15 K, 323.15 K, and 333.15 K, taking into consideration the temperature dependence of the solubility of carbon dioxide. Lower values of the Henry's law constants were the main factors for evaluating the promising ionic liquids for carbon dioxide capture.

Results and Discussion

The Henry gas constant of CO_2 in the tri-(2-hydroxyethyl)methyl ammonium methylsulfate ($[THMA]^+$ $[MeSO_4]^-$), 1-butyl-1-methyl-pyrrolidinium dicyanamide ($[Bmpirr]^+$ $[DCA]^-$) and butylmethylimidazolium tetrafluoroborate ($[Bmim]^+$ $[BF_4]^-$) ionic liquids at various temperatures was calculated using the COSMO-RS method. The results of the COSMO calculations, when compared with experimental results already documented in the literature, are presented in Pic. 1.



Pic. 1. Experimental [1, 2] and theoretical values of Henry's gas constants for CO2 in the ionic liquids $[THMA]^+[MeSO4]^-$, $[Bmpirr]^+[DCA]^-$ and [Bmim]+$[BF4]^-$ at various temperatures.

The Henry's law constants calculated using the COSMO-RS method show that the solubility of CO_2 in the studied ionic liquids has a distinct temperature dependency. In all cases, the Henry's law constants increase with the increase in temperature, showing that the solubility of the gas in the ionic liquids decreases at high temperatures. This is in accordance with the classical thermodynamic rules and proves that the process is exothermic in nature. Among the studied ionic liquids, the lowest values of Henry's constants were found in the case of 1-butyl-3-methylimidazolium tetrafluoroborate in the studied temperature range of 313.15 to 333.15 K, showing the highest solubility of the gas in this ionic liquid. On the other hand, the highest values were found in the case of tri-(2-hydroxyethyl)methylammonium methyl sulfate, while the values in the case of the pyrrolidinium-based ionic liquid were in the middle. Within the COSMO-RS model, these differences may be rationalized through intermolecular interactions and electrostatic compatibility. For the imidazolium-based ionic liquids, there is good electrostatic interaction and sufficient free volume to accommodate the quadrupolar CO2 molecule. For the ionic liquids, the presence of weakly coordinating anions enhances solubility, while the presence of strongly coordinating or hydrogen-bonding anions enhances internal cohesion, reducing the available free volume for the gas molecules.

Consequently, the results obtained suggest that imidazolium-based ionic liquids with weakly coordinating anions have the potential to be used to capture CO2. It is important to note that optimization of the structure of the ionic liquids is crucial to achieve good efficiency and thermal stability.

On the basis of the calculated results, ionic liquids can be considered promising solvents for the processes of CO2 capture and separation, as suggested by the results of the computational modeling and thermodynamic calculations. Nevertheless, the optimization of the physicochemical properties of ionic liquids is needed for the improvement of the industrial potential of the processes under consideration. For instance, the ionic liquids

of the imidazolium type, along with weakly coordinating anions, should be more thoroughly investigated due to the positive characteristics of the interaction mechanisms and relatively high solubility of carbon dioxide. It is recommended that the investigation of ionic liquids as potential solvents for the processes under consideration should not be limited by the results of thermodynamic performance, as calculated by the COSMO-RS method, but should also include the transport properties of the ionic liquids, such as viscosity, diffusion coefficients, etc., as they significantly influence the efficiency of the processes under consideration. The structural modification of ionic liquids, aimed at the reduction of the viscosity of the ionic liquids while preserving the strong interaction. Further computational screening of ionic liquids by means of the COSMO-RS method may help in speeding up the search for specific ionic liquids with enhanced selectivity and stability properties. Moreover, it is important to carry out long-term regeneration of ionic liquids, cyclic absorption-desorption processes, and energy consumption analysis in order to assess their economic viability and stability. It is also important to carry out an assessment of the ionic liquids' impact on the environment and their life cycle analysis in order to guarantee their compliance with sustainable development and green chemistry principles.

References

[1] Zhang, S., Sun, J., Zhang, X., Xin, J., Miao, Q. and Wang, J., 2014. Ionic Liquid-Based Green Processes for Energy Production. Chemical Society Reviews, 43(22), pp. 7838–7869.
[2] Brennecke, J.F. and Maginn, E.J., 2001. Ionic Liquids: Innovative Fluids for Chemical Processing. AIChE Journal, 47(11), pp. 2384–2389.
[3] Klamt, A., 2005. COSMO-RS: From Quantum Chemistry to Fluid Phase Thermodynamics and Drug Design. Amsterdam: Elsevier.
[4] Azizov A.H. Ionic liquid processes developed in IPCP ANAS // Processes of petrochemistry and oil refining, №3-4, p. 34 , Baku, 2008
[5] Azizbeyli, H., Alieva, R., Bagirova, S., & Ibrahimova, N. (2017). Tailoring Ionic Liquids As Solvents By Cosmo-Rs Quantum Chemical Method. Thermam 2017, 57.
[6] Qanbarli, Z., Azizbeyli, H., Khamiyev, M., Seidova, X., & Babashova, Y. (2023). Molecular Modelling of Ionic Liquid Ligands based Zirconium Complexes for Ethylene Copolymerization with Octene-1. Afyon Kocatepe Üniversitesi Fen Ve Mühendislik Bilimleri Dergisi, 23(1), 58-66. https://doi.org/10.35414/akufemubid.1124430
[7] Ibragimova, M. D., Azizov, A. G., Pashayeva, Z. N., Abdullayeva, F. M., Yusifzade, F. Y., & Dadasheva, S. D. (2015). Use of ionic liquids as solvent and as catalyst in the processes of synthesis polymers. Khimiya v interesakh ustoychivoqo razvitiya, 23(3), 225-234.
[8] Azizbeyli H.R. Investigation Of Regularities Of Selective Treatment Of Oil Distillates Using Ionic-Liquid Extractants, Containing A Number Of Cations And Anions. Thesis, Baku, 2014

SUSTAINABLE SOLUTIONS FOR OIL CONTAMINATION IN AZERBAIJAN: A COMPREHENSIVE STUDY ON BIOREMEDIATION AND HYBRID METHODS

Safura Ismayilova
Azerbaijan University of Architecture and Construction
Baku, Azerbaijan
Ismayilova_safura@mail.ru

Abstract - This paper presents real experiments conducted to assess the efficiency of bioremediation and phytoremediation technologies for cleaning oil-contaminated soils and water ecosystems in Azerbaijan. The study used microorganisms such as Pseudomonas, Rhodococcus, Alcanivorax, and Sphingomonas, as well as plants like Cyperus rotundus (nutsedge) and Phragmites australis (common reed). The effectiveness of bioremediation and phytoremediation methods in reducing oil contamination was evaluated. Additionally, hybrid approaches combining microorganisms and plants were tested to optimize the cleanup process. The results showed that bioremediation technologies are effective, ecologically safe, and economically viable for cleaning oil-contaminated ecosystems in Azerbaijan.

Keywords: Oil contamination, bioremediation, phytoremediation, microorganisms, ecosystems, cleanup technologies, hybrid approaches, Azerbaijan

Introduction:

Azerbaijan, with its rich oil reserves, has been a significant oil producer for decades. However, this has led to substantial environmental contamination due to oil extraction, transportation, and refining processes. The contamination of soil and water ecosystems with oil is a major environmental issue that impacts biodiversity, soil fertility, and water quality. The traditional methods of cleaning oil spills, such as chemical and mechanical treatments, are costly and have environmental side effects. Bioremediation and phytoremediation, which rely on natural processes, offer eco-friendly and cost-effective alternatives for mitigating oil contamination. This study investigates the application of bioremediation and phytoremediation technologies for cleaning oil-contaminated ecosystems in Azerbaijan.

Materials and Methods:

Experiments were conducted in various oil-contaminated regions of Azerbaijan (Baku and Sumqayit areas). Contaminated soil samples were collected from areas with known oil spills. The following microorganisms were used in the experiments: Pseudomonas, Rhodococcus, Alcanivorax, and Sphingomonas [Gertsen, M.M.; Arlyapov, V.A.; Perelomov, L.V.; Kharkova, A.S.; Golysheva, A.N.; Atroshchenko, Y.M.; Cardinale, A.M.; Reverberi, A.P. 5-6]. These microorganisms are known for their ability to degrade both aliphatic and aromatic components of oil. In addition, plants like Cyperus rotundus (nutsedge) and Phragmites australis (common reed) were selected for phytoremediation, as their root systems help in absorbing oil and supporting microbial degradation.

Table 1. Comparative Efficiency, Duration, and Cost of Oil Remediation Methods in Azerbaijan

Method	Oil Degradation (%)	Time for Completion (Days)	Cost (USD per 1000m²)
Pseudomonas Bioremediation	65	30	200
Rhodococcus Bioremediation	70	30	250
Cyperus rotundus Phytoremediation	55	60	300
Phragmites australis Phytoremediation	60	60	300
Hybrid Method	75	45	400

The experiments were divided into three phases: microbial bioremediation, phytoremediation, and hybrid approaches combining both microorganisms and plants.

Microbial Bioremediation: In the first phase, Pseudomonas and Rhodococcus were added to the contaminated soil. Biostimulation was applied by adding nutrients (nitrogen and phosphorus) to enhance microbial activity [Banat, I.M.; Makkar, R.S.; Cameotra, S.S. 2-4]. The experiment was conducted with soil samples contaminated with varying concentrations of oil (5%, 10%, 15%). The microorganisms degraded 60%-70% of the oil present in the soil, indicating that microbial bioremediation is an effective method for oil degradation.

Phytoremediation: In the second phase, Cyperus rotundus and Phragmites australis were planted in contaminated soil [Rahman, K.S.; McClean, S.; Rhaman, K.; Banat, I.M. 87-88]. The root systems of these plants facilitated the absorption of oil, while microbial activity in the rhizosphere helped break down the contaminants. The results showed that these plants absorbed 50%-60% of the oil from the soil, demonstrating the effectiveness of phytoremediation. However, phytoremediation is a slower process, and its efficiency may decrease in highly contaminated areas over time.

Hybrid Approaches: In the third phase, hybrid approaches combining microorganisms and plants were applied. The plants provided a better environment for microbial growth, enhancing the degradation of oil contaminants [Kumar, A.; Kumar, A.; Singh, R.; Singh, R.; Pandey, S.; Rai, A.; Singh, V.K.; Rahul, B. 16-19]. The hybrid approach yielded the highest oil degradation efficiency, with more than 70% of the oil being degraded. The combination of microorganisms and plants accelerated the cleanup process, especially in areas with high contamination levels.



Picture 1. Nutsedge and Common Reed

Results and Discussion:

Microbial Bioremediation: The experiments showed that Pseudomonas and Rhodococcus were effective in degrading 60%-70% of the oil present in the contaminated soil. The addition of nutrients stimulated microbial growth and accelerated the breakdown of both aliphatic and aromatic oil components. These results confirm that microbial bioremediation is an efficient method for cleaning oil-contaminated soils, especially for moderate levels of contamination.

Phytoremediation: The plants Cyperus rotundus and Phragmites australis effectively absorbed 50%-60% of the oil in the contaminated soil [Tariq, M.; Kausar, S.; Zafar, S.; Hussain, M. 27]. Their root systems facilitated the sorption of oil, and microbial activity in the rhizosphere contributed to the breakdown of contaminants. While phytoremediation is eco-friendly and sustainable, it is a slower process, and its effectiveness may be limited in areas with high contamination levels.

Hybrid Approaches: The hybrid approach, which combined microorganisms and plants, yielded the best results. The use of both microorganisms and plants increased the overall oil degradation efficiency to over 70%. The plants created a better environment for the microorganisms, enhancing their activity and accelerating the cleanup process. This approach is particularly useful for high-contamination areas where rapid cleanup is necessary.

Despite the promising potential of bioremediation, several challenges and limitations must be considered when applying these methods in Azerbaijan. One major issue is the high contamination levels present in certain oil-polluted sites. In such cases, bioremediation alone may not be sufficient, and supplementary chemical or mechanical cleanup techniques may be required to achieve effective remediation [Perelomov, L.V.; Gertsen, M.M.; Burachevskaya, M.; Hemalatha, S.; Vijayalakshmi, A.; Perelomova, I.; Atroshchenko, Y. 23-24]. Another limitation is the time factor: phytoremediation, in particular, is a long-term process and may not be suitable for large-scale or urgent cleanup efforts where rapid intervention is necessary. Additionally, microbial activity is highly temperature-dependent, which means that bioremediation may be less effective in colder climates or during winter months, potentially slowing the remediation process.

To address these challenges, several recommendations can be made. First, bioremediation programs should be expanded and widely implemented for cleaning oil-contaminated soils and water ecosystems across Azerbaijan. Second, further research should focus on identifying and developing local microorganisms that are especially effective in degrading oil contaminants under Azerbaijan's unique soil and climate conditions. Third, hybrid approaches that combine bioremediation with chemical or mechanical methods should be further developed, particularly for sites with severe contamination, to enhance cleanup efficiency. Finally, raising community awareness and providing education to local populations and experts about bioremediation methods is crucial, ensuring active participation and collaboration in the cleanup and environmental restoration process.

References:

1. Banat, I.M.; Makkar, R.S.; Cameotra, S.S. Potential commercial applications of microbial surfactants. Applied Microbiology and Biotechnology 2000, 53(5), 495-508.
2. Gertsen, M.M.; Arlyapov, V.A.; Perelomov, L.V.; Kharkova, A.S.; Golysheva, A.N.; Atroshchenko, Y.M.; Cardinale, A.M.; Reverberi, A.P. Environmental Implications of Energy Sources: A Review on Technologies for Cleaning Oil-Contaminated Ecosystems. Energies 2024, 17, 3561.
3. Kumar, A.; Kumar, A.; Singh, R.; Singh, R.; Pandey, S.; Rai, A.; Singh, V.K.; Rahul, B. Genetically Engineered Bacteria for the Degradation of Dye and Other Organic Compounds. In Abatement of Environmental Pollutants: Trends and Strategies; Pardeep Singh, P., Kumar, A., Borthakur, A., Eds.; Elsevier: Amsterdam, The Netherlands, 2020.
4. Perelomov, L.V.; Gertsen, M.M.; Burachevskaya, M.; Hemalatha, S.; Vijayalakshmi, A.; Perelomova, I.; Atroshchenko, Y. Organoclays Based on Bentonite and Various Types of Surfactants as Heavy Metal Remediants. Sustainability 2024, 16, 4804.
5. Rahman, K.S.; McClean, S.; Rhaman, K.; Banat, I.M. Microbial Degradation of Petroleum Hydrocarbons. In Applied Bioremediation: Overcoming the Challenges of Contaminated Environments; CRC Press: 2012.
6. Tariq, M.; Kausar, S.; Zafar, S.; Hussain, M. Phytoremediation of Oil Contaminated Soils: Current Status, Challenges, and Prospects. Environmental Science and Pollution Research 2020, 27(31), 38698-38711.

LOCAL ZEOLITES FOR WASTEWATER PURIFICATION

Shakhzod Toshev
Supervisor: R.F.Abbasova
Bukhara State Technological University, Bukhara, Uzbekistan
shakhzod.toshev@bhos.edu.az

Keywords: Natural zeolites Clinoptilolite Mordenite Iron-modified zeolite Heavy metal removal Electroplating wastewater

Under conditions of rapid industrialization, contamination of wastewater with heavy metals has become an increasingly serious environmental problem. One of the essential technologies used in many industrial sectors is electroplating. This technology is applied to protect various products from corrosion, enhance wear resistance, improve electrical conductivity, and provide an attractive surface finish. Electroplating production in Azerbaijan serves several industrial sectors, including the aluminum industry. Without proper treatment, wastewater from electroplating facilities poses a significant threat to the ecosystem of the Caspian Sea and to groundwater resources. In order to minimize environmental impact, local wastewater treatment systems are being implemented at industrial enterprises. Priority is given to environmentally friendly and cost-effective methods, particularly those utilizing local raw materials. Azerbaijan possesses significant deposits of natural zeolites, including clinoptilolite and mordenite. Zeolites are considered highly effective adsorbents and therefore attract considerable research interest. In this study, we investigated the adsorption properties of the following zeolites: natural clinoptilolite from the Aydag deposit (Tovuz region), mordenite from the Chanalab deposit (Nakhchivan), as well as iron-modified Nakhchivan mordenite. Clinoptilolite is characterized by high cation-exchange capacity, a well-developed channel system, and strong selectivity toward divalent metal ions. Mordenite, in contrast, has narrower channels and higher thermal stability but exhibits lower accessibility of exchange sites (Sebghatullah Mudaber, 20023) (Lofù A., 2023) (Velarde L., 2023).

The experiments were conducted using model solutions containing metals commonly found in electroplating wastewater: Zn^{2+}, Cu^{2+}, Cr^{6+}, Fe^{2+}, and Ni^{2+}.Sample preparation of natural zeolites was necessary to remove impurities and obtain reproducible sorption characteristics. The preparation process included crushing, washing with distilled water, and drying at 105–110 °C for 6–12 hours. To create additional mesoporosity through partial dissolution of the silica phase and to increase the accessibility of active sites, alkaline treatment with NaOH solutions (0.1–0.5 M) was performed. Since chromium in the model solution was present as Cr^{6+} in the form of dichromate, mordenite was modified with trivalent iron in order to alter the surface charge and introduce redox-active centers. Model solutions of Zn^{2+},

Cu^{2+}, Ni^{2+}, and Fe^{2+} were prepared from sulfate salts within a concentration range of 10–200 mg/L. The Cr^{6+} solution was prepared from $K_2Cr_2O_7$. The pH was adjusted using HCl or NaOH solutions. Infrared (IR) spectroscopy was used to analyze structural changes in the zeolites after alkaline treatment. Metal concentrations were determined photometrically. During the experiments, the adsorption capacity of the zeolites and the metal removal efficiency were calculated in order to construct adsorption isotherms and kinetic curves.

Our studies demonstrated that Fe-mordenite exhibits the highest sorption capacity for all metals, including hexavalent chromium, clinoptilolite also exhibits high cation-exchange capacity and better channel accessibility, resulting in more efficient sorption of divalent metals. Mordenite is characterized by narrower channels, which restrict ion diffusion; however, it shows greater resistance to high temperatures and aggressive environments. Most studies indicate that clinoptilolite is more effective than mordenite in removing Zn^{2+}, Cu^{2+}, and Ni^{2+}, whereas differences in Cr^{6+} sorption are minimized after iron modification. Thus, natural and modified zeolites from local deposits represent low-cost, effective, and environmentally friendly adsorbents for the post-treatment of wastewater containing heavy metals, particularly electroplating effluents.

References

1. Sebghatullah Mudaber, Jenaidullah Batur (2023) Zeolites as effective adsorbents for heavy metal removal in wastewater treatment of Kabul city-A review. IAR J Eng Tech; 4, 2, 20-31.
2. Lofù A., Mastrorilli P., Dell'Anna M. M., Mali M., Sisto R., Vignola R. (2016). Iron-modified zeolites for enhanced adsorption of hexavalent chromium from aqueous solutions. Archives of Environmental Protection. 42, 1, 35–40
3. Velarde L, Sadegh M., Escalera E., Antti M.-L., Akhtar F. (2023) Adsorption of heavy metals on natural zeolites: A review. Chemosphere 328, 1-16

MALEIN ANHIDRIDININ A-METILSTIROLLA OLIQOMERININ DIETILENTRIAMINLƏ TIKILI SOPOLIMERI SULU SISTEMLƏRDƏN URANIL IONLARININ SORBENTLƏRI KIMI

M.R.Bayramov, G.M.Mehdiyeva, M.A.Ağayeva, M.Ə.Cavadov, R.V.Rüstəmov
Bakı Dövlət Universiteti, Kimya Fakültəsi, Bakı, Azərbaycan
gunaymehdiyeva@bsu.edu.az

Xülasə - Təqdim olunan tezisdə sulu məhlullardan uranil ionlarını sorbsiya etmək məqsədilə tərəfimizdən sintetik sorbsiya materialının sintezi üzrə tədqiqatların nəticələri, yəni malein anhidridinin α-metilstirol ilə radikal blok polimerləşməsindən alınan məhsulun dietilentriaminlə tikilmə məhsulunun sorbsiya xassələrinin tədqiqinin nəticələri təqdim olunmuşdur.

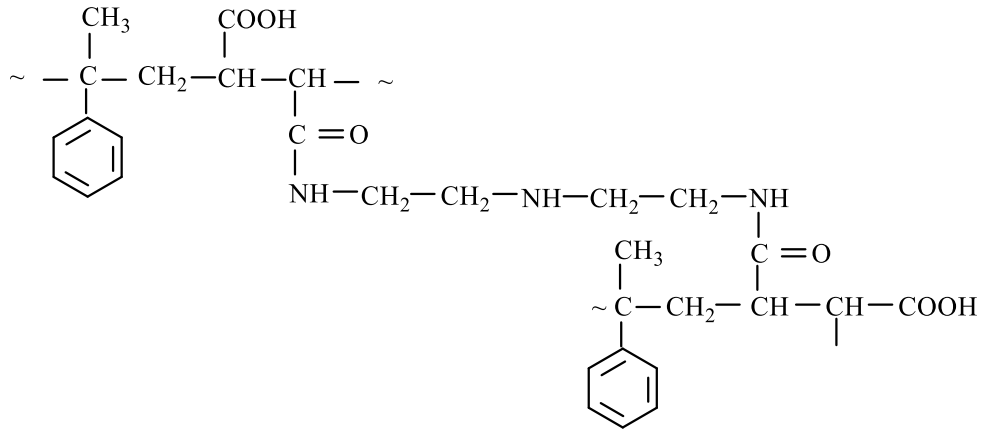
Açar sözlər: malein anhidridi, α-metilstirol, aminlər, tikili polimerlər, sorbentlər

Giriş:

Tərkibində funksional qruplar saxlayan, modifikasiya oluna bilən polimer materialların, sorbentlərin, yağ və yanacaq əlavələrinin, əczaçılıqda istifadə olunan məhsullarının, metalların korroziyasının qarşısını alan inhibitorlarının və s. istehsalı ilə bağlı müasir texnologiyalarda müxtəlif quruluşlu vinil monomerləri (stirol, akrilonitril, malein anhidridi, vinil asetat, vinil xlorid, divinil və s.) bu günə qədər ən çox tələb olunan sənaye məhsulları olaraq qalmaqdadır [Aliyev, 2014, 82-84; Mehdiyeva, 2024, 273-283]. Bu, əsasən onların yüksək reaksiya qabiliyyəti və onlardan əldə edilən məhsulların funksional xüsusiyyətlərinin müxtəlifliyi ilə əlaqədardır.

Təcrübi hissə:

Sulu məhlullardan uranil ionlarını sorsiyası məqsədilə istifadə olunan sorbsiya materialının sintezi məlum klassik üsulla - malein anhidridinin α-metilstirolla radikal blok sopolimerləşməsi aparılmışdır. Reaksiya ilkin monomerlərin 1:1 mol nisbətində, 130-140°C temperaturda, 2% di-tert-butil peroksid inisiatoru iştirakında, 10 saat müddətində aparılmışdır. Alınmış polimerin anhidrid hissəsi dietilentriaminlə 60-70°C temperaturda, 3 saat müddətində modifikasiya olunaraq aşağıda göstərilən quruluşa malik 97.5% çıxımla üçölçülü polimer materialı əldə edilmişdir:



Nəticələr və onların müzakirəsi:

Alınan tikili quruluşlu polimerin quruluşunda sorbsiya prosesləri üçün potensial olaraq zəruri olan funksional qrupların (-NH2, -COOH, C=O və s.) olması səbəbindən, o, yalnız radionuklidləri deyil, həm də ekoloji cəhətdən təhlükəli ağır metalları (civə, qalay, qurğuşun, xrom, mis və s.) tutmaq üçün tətbiq oluna bilən potensial sorbsiya materialı hesab edilə bilər. Bu cür sintetik materiallara (təbii materiallarla yanaşı) tələbat ildən-ilə artmaqdadır.

Müxtəlif qatılıqlı sulu uranil nitrat məhlullarından istifadə etməklə (müxtəlif pH-da, 25°C-də, 24 saat ərzində) model tədqiqatlar aparılmışdır. Müəyyən edilmişdir ki, tikili quruluşlu polimer uranil ionlarını pH 7-8-də effektiv şəkildə sorbsiya edir.

Təkliflər:

Aparılan tədqiqatlar nəticəsində müəyyən olunmuşdur ki, uranil ionlarının ilkin qatılığında, onların sorbent tərəfindən sorbsiya dərəcəsi 90%-dən çox olmuşdur. Qeyd etmək lazımdır ki, alınmış tikili quruluşlu sorbent hətta durulaşdırılmış məhlullarda da istifadə edilə bilər (nəzərə alsaq ki, qatılaşdırılmış məhlullarda bir sıra məlum sorbentlər durulaşdırılmış məhlullarda həmişə istifadə edilə bilməz).

Ədəbiyyat:

1. Aliyev, F.Y., Hasanova, A.M. Synthesis cooligomers – hexene with α-methylstyrene. JSPC European innovation, 2014, 17(9), 82-84
2. Mehdiyeva, G.M., Bayramov, M.R. Condensation products of 2-propenylphenol, formaldehyde, and methylamine and their property. Russian Journal of General Chemistry, 2024. 94(2), 273-283

YENI IZO-DESIL ƏVƏZLI 1,3-BENZOKSAZIN TÖRƏMƏLƏRININ SINTEZI VƏ ONLARIN SULFAT TURŞUSU MÜHITINDƏ KORROZIYA INHIBITORU XASSƏLƏRININ TƏDQIQI

M.R.Bayramov[1], G.M.Mehdiyeva[1], S.X.İsmayilova[2], L.Z.Əzimli[1], M.A.Ağayeva[1], M.Ə.Cavadov[1]
[1]Bakı Dövlət Universiteti, Kimya Fakültəsi, Bakı, Azərbaycan
[2]"Neftqazelmitədqiqatlayihə" İnstitutu, SOCAR, Bakı, Azərbaycan
*gunaymehdiyeva@bsu.edu.az

Xülasə - Təqdim olunan tezisdə yeni azot saxlayan üzvi birləşmələrin – izo-desil əvəzli 1,3-benzoksazin törəmələrinin - sintezi və onların 0,5 N H_2SO_4-də St.3 poladına qarşı inhibitor xassələrinin qravimetrik metodla tədqiqinin nəticələri təqdim olunmuşdur. Sintez olunmuş birləşmələrin quruluşu NMR və İQ spektroskopiyası vasitəsi ilə müəyyən edilmişdir. Onların korroziyaya qarşı xassələrinə temperaturun (25, 35°C) və qatılığın (50, 75, 100 mq/L) təsiri öyrənilmişdir.

Açar sözlər: decylphenol, 1,3-benzoksazinlər, aminlər, korroziya inhibitorları

Giriş:

Neftçıxarma sənayesinin aktual problemlərindən biri də istifadə olunan avadanlıqların aqressiv mühitlərdə korroziyadan qorunmasıdır [Ramaganthan, 2019, 32-54].

Dünya miqyasında neftin hasilatı proseslərini intensivləşdirmək üçün vaxtaşırı olaraq quyuların və boru kəmərlərinin daxili səthlərini çöküntülərdən, ağır neft qalıqlarından və digər arzu olunmaz maddələrdən təmizləmək üçün müxtəlif turşularla təmizlənməsi həyata keçirilir. Nəticədə metal avadanlıqlar korroziyaya uğrayır. Buna görə də, bu məqsədlərlə istifadə olunan mineral turşularının sulu məhlulların istifadəsində yüksək səthi aktivliyinə malik effektiv korroziya inhibitorları daxil edilir [Elhadi, 2016, 731-736; Mehdiyeva, 2023, 394-402].

Son illərdə tədqiqatlar aminlərə, fenollar və "yaşıl kimya" tələblərinə cavab verən, yüksək qoruyucu xüsusiyyətlərə malik olan və digər asanlıqla əldə edilə bilən birləşmələrə əsaslanan yeni, ekoloji cəhətdən təmiz korroziya inhibitorlarının hazırlanması istiqamətində xeyli işlər aparılmışdır [Chapagain, 2022, 211-224].

Bu məqsədlə tərəfimizdən yeni heteroatom saxlayan birləşmələr - izodesil əvəzli 1,3-benzoksazinlər - sintez edilmiş və sulfat turşusu iştirakında polad St.3-ün korroziyasına qarşı inhibitorlar kimi tədqiq edilmişdir. 1,3-benzoksazin, izodesil və digər fraqmentlərin olması bu birləşmələrə kifayət qədər yüksək inhibitor xassələri verməlidir. Aparılan korroziya tədqiqatlarının nəticələri bu məqalədə təqdim olunur.

Təcrübi hissə:

Sintez edilmiş birləşmələrin quruluşları NMR və İQ spektroskopiyası vasitəsi ilə təsdiq edilmişdir. Sintez edilmiş birləşmələrin ^{1}H və ^{13}C NMR spektrləri NMR spektrometrindən (AVANCE 300) (Bruker) istifadə edilərək qeydə alınmışdır. Həlledici kimi $CDCl_3$ (99.8%, kataloq № 151831) istifadə edilmişdir. Birləşmələrin İQ spektrləri Nikoled IS10 FTIR spektrofotometrində 4000-400 sm^{-1} diapazonunda qeydə alınmışdır.

Sintez olunmuş birləşmələrinin qravimetrik metodla korroziyaya qarşı inhibitor xassələri St.3 poladının lövhələri iştirakında 0,5 N sulu H_2SO_4 məhlulunda 3 saat müddətində birləşmələrin müxtəlif qatılıqlarında (50, 75 və 100 mq/l) və temperaturlarda (25 və 35°C) tədqiq edilmişdir.

Sintez edilmiş birləşmələrin iştirakında və onların iştirakı olmadan korroziya sürəti və poladın korroziyadan mühafizə dərəcəsi aşağıda göstərilən tənliklərə uyğun olaraq müəyyən edilmişdir:

$$K = \frac{m_1 - m_2}{S \cdot \tau}$$

Burada, m_1 və m_2 polad lövhələrin sınaqdan əvvəl və sonra olan kütləsidir, q

S polad lövhələrin səthinin sahəsi, m^2

τ - zaman, saat

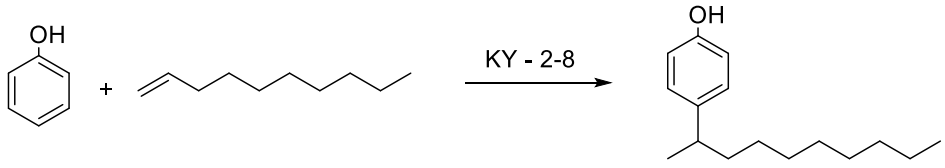
$$Z = \frac{k_1 - k_2}{k_1} \cdot 100\%$$

burada, k_1 – inhibitorsuz mühitdə korroziya sürəti, q/m^2 h

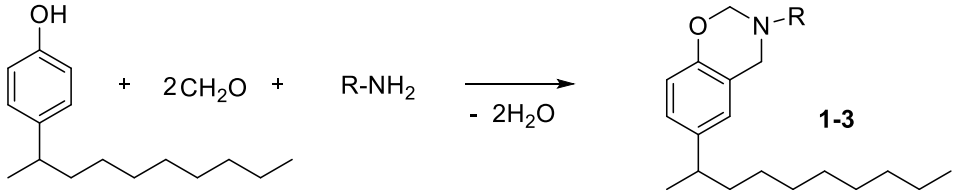
k_2 – inhibitor iştirakında korroziya sürəti, q/m^2 h.

Nəticələr və onların müzakirəsi:

Sintez olunmuş birləşmələrin sintezi üçün əvvəlcə 4-(dekan-2-il)fenol aşağıdakı reaksiya sxeminə uyğun olaraq fenolun desen-1-lə alkilləşdirilməsi aparılmışdır:



Sintez olunmuş birləşmələr aşağıda göstərilən sxem üzrə sintez olunmuşdur:



R = -CH_3 (**1**), - C_4H_9 (2), H_2C  (**3**)

1-3 birləşmələri yüksək çıxımlarla (uyğun olaraq 85, 83 və 80%) sintez edilmişdir.

Alınan nəticələrə əsasən, tədqiq olunan bütün birləşmələr 25 və 35°C temperaturda, 50, 75 və 100 mq/l qatılıqlarda 0,5 N sulfat turşusu mühitində korroziyaya qarşı inhibitor xassələrə malikdir.

Tədqiq olunan birləşmələrin 100 mq/l qatılığında maksimal inhibitor xassələri aşkar edilmişdir. Göstərilən qatılıqda (100 mq/l) poladın korroziyadan mühafizə dərəcələri 25°C-də müvafiq olaraq 90, 87 və 92,5%, 35°C-də isə 81,2, 85,2 və 90,2% təşkil edir. Birləşmələrin qatılıqları azaldıqca (50 və 75 mq/l) korroziyadan mühafizə dərəcələri azalır. Məsələn, birləşmələrin 75 mq/l qatılığında qorunma dərəcəsi 25°C-də 87,2, 84,2, 92,1%, 35°C-də isə müvafiq olaraq 80,2, 80,3, 87,1% təşkil edir.

Təkliflər:

İzo-desil fenolun formaldehid və birli aminlərlə (metilamin, n-butilamin, benzilamin) üçqat kondensləşməsi nəticəsində 80-85% çıxımlarla benzoksazinlər sintez edilmiş, onların 0,5 N sulfat turşusu mühitində 50, 75 və 100 mq/l qatılıqlarında korroziyaya qarşı xassələri aşkar olunmuşdur (3-cü birləşmə üçün maksimal qoruma dərəcəsi 100 mq/l qatılıqda 92,5% olmuşdur). Göstərilmişdir ki, nəticədə tədqiq olunan birləşmələr St.3 poladının turş mühitdə korroziyasına qarşı inhibitor kimi tövsiyə edilə bilər.

Ədəbiyyat:

1. Elhadi, S.M., Bilel, M., Abdelmalek, B. et al. Experimental evaluation of quinolinium and isoquinolinium derivatives as corrosion inhibitors of mild steel in 0.5 M H2SO4 solution. Prot Met Phys Chem Surf 52, 731–736 (2016). https://doi.org/10.1134/S2070205116040092
2. Mehdiyeva, G.M. 8-Allyl-1,3-benzoxazines as Hydrogen Sulfide Corrosion Inhibitors and Biocides in Crude Oil Extraction. *Pet. Chem.* **63**, 394–402 (2023). https://doi.org/10.1134/S0965544123030039
3. Chapagain, R. K., Gurung, S. K., Ranabhat, D., Adhikari, S., Gurung, P. Relationship between Training Effectiveness and Work Performance: Mediation of Workplace Environment. Quest Journal of Management and Social Sciences, 4(1), 58–70. (2022) https://doi.org/10.3126/qjmss.v4i1.45867

TULLANTILARIN BƏRPASI VƏ ƏTRAF MÜHİTİN REABİLİTASİYASINDA İNNOVATİV TEXNOLOGİYALAR

Dosent, Nəsirova Nəsibə Volodiya qızı[1]
Talıbzadə Zeynəb Şahin qızı[2]
Azərbaycan Texnologiya Universiteti
Gəncə, Azərbaycan
nasir.nasirova@rambler.ru, z.talibzade@atu.edu.az

Xülasə - İnnovativ texnologiyalar ətraf mühitin bərpasında və tullantıların dəyərli resurslara çevrilməsində mühüm rol oynayır. Müasir sənaye, kənd təsərrüfatı və şəhər fəaliyyətləri torpaq, su və hava keyfiyyətinə mənfi təsir göstərən böyük həcmdə tullantıların yaranmasına səbəb olur. Bu məqalədə tullantıların bərpası və ətraf mühitin reabilitasiyası üzrə yanaşmalar araşdırılır, üzvi tullantılardan bioqaz istehsalı, plastiklərin pirolizi, kompostlaşdırma, bio- və fitoremediasiya üsullarının tətbiqi kimi praktiki nümunələr təqdim olunur. Rəqəmsal monitorinq sistemlərinin və dövri iqtisadiyyat prinsiplərinin inteqrasiyası bu proseslərin səmərəliliyini artıraraq dayanıqlı resurs idarəetməsinə və ekosistemlərin bərpasına töhfə verir. Bu innovativ həllərin tətbiqi həm ekoloji mühafizəni, həm də iqtisadi faydaları təmin edərək uzunmüddətli ekoloji davamlılıq və dayanıqlılığın gücləndirilməsinə xidmət edir.

Açar sözlər: Tullantıların dəyərə çevrilməsi, ətraf mühitin bərpası, innovativ texnologiyalar, dövri iqtisadiyyat, dayanıqlı resurs idarəetməsi

Ətraf mühitin qorunması və dayanıqlı inkişaf qlobal ekoloji siyasətin prioritet istiqamətlərindən biridir. Sənayenin inkişafı, şəhərləşmə və intensiv kənd təsərrüfatı fəaliyyəti nəticəsində yaranan tullantılar ekosistemlərin funksional stabilliyini pozur, su, torpaq və hava keyfiyyətinə mənfi təsir göstərir. Eyni zamanda, tullantıların qeyri səmərəli idarə olunması insan sağlamlığını təhlükə altına alır və iqtisadi resurs itkisinə səbəb olur. Müasir innovativ texnologiyaların son illərdə geniş istifadəsi tullantıların bərpa olunmasınıda və ətraf aləmin reabilitasiyasında mühüm əhəmiyyət kəsb etməyə başlamışdır. Bu yanaşmalar yalnız ətraf mühitin qorunmasını təmin etmir, həm də iqtisadi cəhətdən resursların səmərəli dövriyyəsini təşviq edir.

Müasir innovativ texnologiyalar tullantıların dövri dəyərə çevrilməsini müxtəlif istiqamətlərdə reallaşdırır. Məsələn, bioloji tullantılar üzərində aparılan anaerob fermentasiya prosesi biogaz istehsalına imkan verir. Bu yanaşma həm enerji əldə edilməsinə, həm də üzvi tullantıların torpağa təhlükəsiz şəkildə qaytarılmasına şərait yaradır. Eyni zamanda, plastik və sənaye tullantılarının piroliz və termal qalıqlar vasitəsilə yanacaq və enerji resurslarına çevrilməsi artıq bir sıra ölkələrdə geniş tətbiq olunur. Bu texnologiyalar ətraf mühitin çirklənməsinin qarşısını alır və tullantıların iqtisadi dəyərini artırır. [Əliyev, R. M., Həsənov, F. Q.2020]

Tullantıların bərpasında innovativ yanaşmalardan biri də təkrar emal və up-sayklinqdir. Up-sayklinq- həm ekoloji, həm iqtisadi, həm də yaradıcı perspektivdən tullantıları dəyərli resurslara çevirmək deməkdir Məsələn, şəhər tullantılarından əldə olunan kağız, plastik və metal materiallar sənaye

və tikinti sektorunda xammal kimi istifadə edilə bilər. Bu proseslər həm təbii resursların qorunmasına, həm də tullantı həcminin azalmasına töhfə verir. Azərbaycanda şəhər tullantılarının təkrar emalı sahəsində pilot layihələr artıq həyata keçirilir ki, bu da tullantıların dəyərli resursa çevrilməsi potensialını nümayiş etdirir.

Ətraf mühitin reabilitasiyasında innovativ texnologiyalar yalnız tullantıların idarə olunması ilə məhdudlaşmır; onlar ekosistemlərin funksional stabilliyini bərpa etmək, biomüxtəlifliyi qorumaq və ekoloji xidmətləri bərpa etmək məqsədini daşıyır. Xüsusilə bioremidasiya və fitoremidasiya texnologiyaları çirklənmiş torpaqların bərpasında geniş tətbiq olunur. Bioremidasiya, mikroorqanizmlərin biokimyəvi fəaliyyəti vasitəsilə zərərli maddələri parçalamağa və toksik komponentləri neytrallaşdırmağa imkan verir. Fitoremidasiya isə bitkilərin torpaq və sudakı çirkləndiriciləri, ağır metalları və digər toksinləri udaraq və ya metabolizə edərək ətraf mühitin təmizlənməsinə xidmət edir.

Məsələn, neft çirklənməsi ilə zədələnmiş torpaqlarda hidrokarbonları parçalaya bilən bakteriya və göbələklərin tətbiqi, eləcə də müəyyən bitki növlərinin əkməsi torpağın bioloji balansını bərpa edir, toksik maddələrin səviyyəsini azaldır və torpağın mikrobioloji müxtəlifliyini artırır. Ağır metal çirklənməsi hallarında isə fitoremidasiya texnologiyaları metalların torpaqdan yığılmasına və daha sonra təhlükəsiz şəkildə çıxarılmasına imkan verir. Bu yanaşma ekosistem funksiyalarının bərpasını təmin edir, torpağın məhsuldarlığını artırır və landşaftın uzunmüddətli ekoloji dayanıqlığını gücləndirir.

Bundan əlavə, bioremidasiya və fitoremidasiya texnologiyaları yalnız ekoloji baxımdan deyil, həm də iqtisadi baxımdan effektivdir. Çirklənmiş torpaqların bərpası nəticəsində onlar təkrar kənd təsərrüfatı və ya sənaye fəaliyyətində istifadə oluna bilir, beləliklə əlavə torpaq resurslarının istismarı azalır və ətraf mühitə yük minimuma endirilir. Eyni zamanda, bərpa proseslərində istifadə olunan bitki və mikroorqanizm növləri regional şəraitə uyğun seçildikdə, yerli biomüxtəlifliyin qorunmasına da töhfə verir. [Hüseynov, F. H. 2017, 33-44]

Beləliklə, bioremidasiya və fitoremidasiya texnologiyaları innovativ və dayanıqlı yanaşmalar kimi ətraf mühitin reabilitasiyasında strateji əhəmiyyətə malikdir. Onlar yalnız çirklənməni aradan qaldırmaqla kifayətlənmir, həm də ekosistem xidmətlərinin bərpasını təmin edir, torpağın funksional sağlamlığını qoruyur və uzunmüddətli perspektivdə həm ekoloji, həm iqtisadi, həm də sosial fayda yaradır.

Aqrar sahədə tullantıların bərpası və torpağın reabilitasiyası innovativ texnologiyalarla birləşdirildikdə həm məhsuldarlıq artır, həm də ekosistem xidmətləri qorunur. Məsələn, üzvi tullantıların kompostlaşdırılması nəticəsində torpağın münbitliyi artır, su tutma qabiliyyəti yüksəlir və torpaq biotasının aktivliyi stimullaşır. Eyni zamanda, kompostlaşdırma nəticəsində

yaranan bioresurslar kənd təsərrüfatında gübrə kimi istifadə edilərək kimyəvi maddələrə olan tələbat azaldılır və ətraf mühitin kimyəvi yüklənməsi minimuma endirilir.[İbrahimov, A. İ. 2021, 55-67]

Tullantıların enerji resurslarına çevrilməsi sahəsində innovativ texnologiyalar həm ekoloji, həm də iqtisadi baxımdan mühüm əhəmiyyət kəsb edir. Biogaz və bioenerji sistemləri kənd yerlərində enerji təminatını artırmaqla yanaşı, üzvi tullantıların həcmini azaldır, bioloji tullantıların torpağa və suya zərərli təsirini minimuma endirir. Bu texnologiyalar anaerob fermentasiya, piroliz və biokimyəvi çevrilmə prinsiplərinə əsaslanır, beləliklə tullantılar yalnız atılmır, həm də enerji və resurs kimi istifadəyə verilir. Məsələn, kənd təsərrüfatı tullantılarından, mal-qaranın gübrəsindən və qida sənayesinin tullantılarından əldə olunan biogaz elektrik və istilik enerjisi istehsalında istifadə olunur. Bu, kənd yerlərində enerji müstəqilliyini gücləndirir və xarici enerji mənbələrinə asılılığı azaldır. [FAO. 2017.]

Eyni zamanda, bu yanaşmalar karbon emissiyalarını azaldır və iqlim dəyişikliyi ilə mübarizədə mühüm rol oynayır. Bioenerji sistemləri kömür və neft kimi fosil yanacaqlardan istifadəni əvəz edir, nəticədə istixana qazlarının atmosferə buraxılmasını azaldır. Bu, qlobal iqlim siyasətində Paris sazişi və digər ekoloji öhdəliklərlə uzlaşdırılan strateji bir həll olaraq dəyərləndirilir.

Bundan əlavə, innovativ bioenerji texnologiyaları iqtisadi baxımdan da üstünlüklər təqdim edir. Tullantıların enerji resurslarına çevrilməsi yeni iş yerlərinin yaradılmasına, yerli icmalar üçün əlavə gəlir mənbələrinin formalaşmasına və kənd təsərrüfatı tullantılarının iqtisadi dəyərinin artırılmasına imkan verir. Eyni zamanda, bioenerji istehsalından qalan qatı və maye qalıqlar torpağın münbitliyini artırmaq üçün üzvi gübrə kimi istifadə oluna bilər, beləliklə həm enerji, həm də kənd təsərrüfatı sahəsində sinerji yaradılır.

Beləliklə, tullantıların enerji resurslarına çevrilməsi yalnız qısa müddətli tullantı idarəçiliyi deyil, həm də davamlı enerji təminatı, karbon emissiyalarının azaldılması və ekoloji dayanıqlığın artırılması baxımından strateji əhəmiyyətə malikdir. Bu yanaşma qlobal iqlim dəyişikliyi ilə mübarizədə praktik və elmi əsaslı həll yollarını birləşdirir və davamlı inkişafın əhəmiyyətli komponenti kimi qiymətləndirilir.[Məmmədov, Q. Ş., İsmayılov, T. K. 2018, 47-57]

Bundan əlavə, rəqəmsal texnologiyalar tullantıların idarə olunmasında innovasiyaların sürətini artırır. IoT sensorları və məlumat analitikası vasitəsilə tullantıların miqdarı, tərkibi və daşınması real vaxt rejimində izlənilə bilir. Bu, tullantı axınlarını optimallaşdırmaq, bərpa proseslərini effektiv planlaşdırmaq və ətraf mühitin monitorinqini gücləndirmək üçün imkan yaradır.

Ümumilikdə, innovativ texnologiyaların tətbiqi tullantıların dövri dəyərə çevrilməsi və ətraf mühitin bərpası sahəsində həm ekoloji, həm də iqtisadi perspektivləri birləşdirir. Bu yanaşmalar yalnız qısamüddətli ətraf mühit problemlərini həll etməklə kifayətlənmir; onlar eyni zamanda tullantı

axınlarının effektiv idarə olunmasını təmin edir, resursların səmərəli dövriyyəsini təşviq edir və təbii sərvətlərin qorunmasına töhfə verir. Məsələn, bio-tullantıların kompostlaşdırılması torpağın münbitliyini artıraraq kənd təsərrüfatında kimyəvi gübrələrin istifadəsini azaldır və ekosistem xidmətlərinin dayanıqlığını təmin edir. Plastik və sənaye tullantılarının up-sayklinq və piroliz texnologiyaları vasitəsilə enerji və xammala çevrilməsi isə iqtisadi fayda gətirir və karbon emissiyalarının azaldılmasına xidmət edir.

Bundan əlavə, innovativ texnologiyalar sosial və institusional baxımdan da əhəmiyyətlidir. Onlar cəmiyyətin tullantıların idarə olunmasına münasibətini dəyişdirir, ekoloji şüurun formalaşmasına töhfə verir və iş yerlərinin yaradılması, yeni biznes imkanlarının təşviqi kimi iqtisadi faydalar yaradır. Eyni zamanda, rəqəmsal texnologiyalar və məlumat analitikası tullantı axınlarının optimallaşdırılmasına imkan verir, monitorinq və idarəetmə proseslərini daha şəffaf və effektiv edir.

İnnovativ texnologiyaların inteqrasiyası həm ekoloji dayanıqlığı, həm iqtisadi səmərəliliyi, həm də sosial faydanı birləşdirən strateji yanaşma kimi çıxış edir. Bu, yalnız lokal və qısamüddətli həlləri deyil, həm də uzunmüddətli resurs təhlükəsizliyi və davamlı inkişaf perspektivlərini təmin edən bir modeldir. Belə yanaşmalar qlobal ərzaq və enerji sistemlərinin optimallaşdırılmasında, ekosistem xidmətlərinin qorunmasında və tullantıların dəyərə çevrilməsi sahəsində strateji əhəmiyyət kəsb edir.

Nəticə olaraq, tullantıların bərpası və ətraf mühitin reabilitasiyasında innovativ texnologiyaların tətbiqi davamlı inkişafın ayrılmaz hissəsi hesab edilməlidir. Bio-remediya, fitoremediya, kompostlaşdırma, enerji istehsalı və rəqəmsal idarəetmə sistemləri ətraf mühitin qorunmasını və resursların səmərəli dövriyyəsini təmin edir. Gələcək tədqiqatlar bu texnologiyaların iqlim dəyişiklikləri, şəhər inkişafı və sənaye tullantılarının idarə olunması kontekstində optimallaşdırılmasına yönəlməlidir.

İstinadlar:

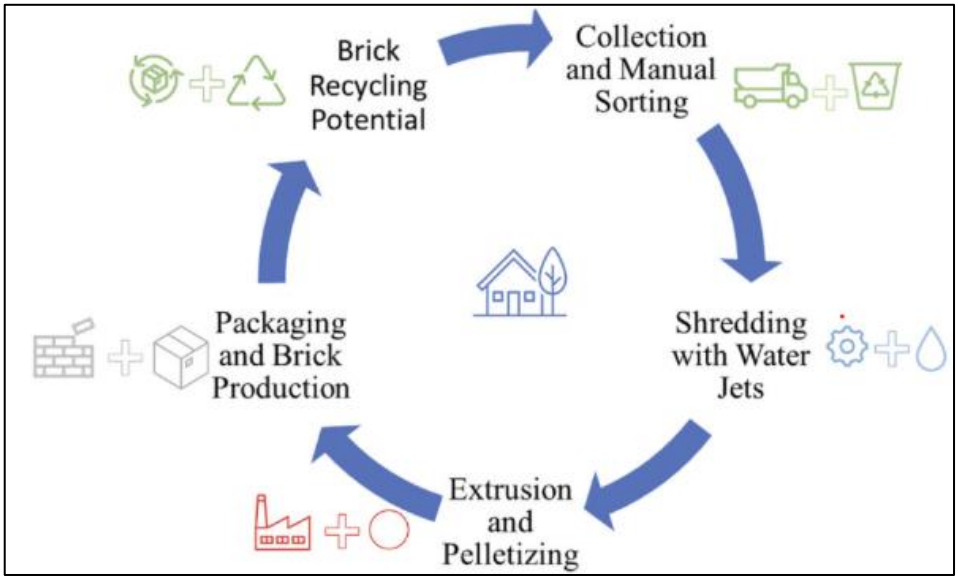
1. Əliyev, R. M., Həsənov, F. Q. Ətraf mühitin bərpasında innovativ texnologiyalar və bioremidasiya üsulları, Bakı: Elm Nəşriyyatı. 2020.
2. Məmmədov, Q. Ş., İsmayılov, T. K. 2018. Tullantıların dövri dəyərə çevrilməsi və bioenerji texnologiyaları. Azərbaycan Aqrar Elm Jurnalı, 12(3), 45–57.
3. Hüseynov, F. H. 2017. Ekosistem xidmətlərinin qorunmasında fitoremidasiya və bioremidasiya üsullarının rolu. Azərbaycan Biologiya Elmləri Jurnalı, 25(2), 33–44.
4. İbrahimov, A. İ. 2021. Davamlı tullantı idarəçiliyi və ətraf mühitin reabilitasiyasında innovativ texnologiyaların tətbiqi. AMEA-nın Xəbərləri (Ekologiya və Təbii Sərvətlər), 78(1), 55–67.
5. FAO. 2017. Circular Economy and Waste Valorization in Agriculture.

VALORISATION OF INDUSTRIAL WASTE INTO CARBON-MINERALIZED COMPOSITE MASONRY UNITS VIA COLD-CURE TECHNOLOGY: THE RENEWBLOCKS PROJECT

Ziyad Shiraliyev
Farid Valimammadov
Rima Guliyeva
Baku Higher Oil School (SOCAR)
Baku, Azerbaijan
ziyad.shiraliyev.std@bhos.edu.az
farid.valimammadov.std@bhos.edu.az
rima.guliyeva@bhos.edu.az

Summary - In Azerbaijan, the most relied source for structural blocks is natural saw stone “Kubik”. But these stone materials are too heavy that they create extra expense for steel foundations, and they are not thermally insulative. Also, local industries generate bug chunks of waste, such as limestone dust, silica fumes, and most importantly plastic waste. This proposal introduces “RenewBlocks” that can solve all these issues. We use a cold-cure carbonation process instead of melting plastic or using expensive chemical glues. The mixture is made out of Portland cement, limestone dust, shredded waste plastic, silica fume, and recycled other recycled materials. The silica fume densifies and suffocates the plastic parts to lock them in place. The use of CCUS allows blocks to cure on 1 day instead of 28, and saves storage costs. Although the composition of materials costs higher than natural stone, the cost of labour bridges the gaps and achieves 30% less cost. The product meets international and regional standards and uses recycled materials. Created blocks are salt-resistant, waterproof, self-healing for microcracks, and micro-flexible that ensures better resistance to earthquakes.

Keywords: Carbon Mineralization, Circular Economy, Composite Masonry, Waste Valorization



Introduction

Modern cities including Baku have a growth for high rise buildings. But for construction, still traditional methods are used. Natural limestone blocks are too heavy 2100kg/m³. In the areas with earthquake risks, such as Azerbaijan, the seismic force is tied to this weight. Because of the heaviness, buildings must be designed with steel and concrete foundations even for the internal walls. In addition, these blocks are prone to transferring heat easily, which drives the winter energy bills up.

Moreover, most of the industries are struggling with their waste disposal. Stonecutters generate limestone dust, metallurgical plants produce silica fume as a byproduct. Every sector throw awas a vast amount of plastic waste to the environment, making hazard and wasted potential of reuse.

The goal of this research is to introduce a product for non-load bearing walls that is almost completely made out of local waste. By using Carbon Capture, Utilization, and Storage (CCUS) technology, the product is enhanced for mechanical properties and becomes a collector of atmospheric waste -CO^2.

Experimental part

The production process maintained the use of maximum waste, while keeping the blocks mechanically strong. We avoided the use of synthetic chemical glues and relied on advanced particle packing to bind the materials.



The base binder is standard Portland Cement (CPC30), and the main filler is limestone dust from Garadagh quarries, which densifies the mixture, and provides a surface for carbon capture. The aggregate is shredded plastic waste (HDPE/LDPE). Friction shredding method is chosen for getting rough and jacked flakes of plastic that can physically grip the cement.

The plastic naturally repels water and Cement, not sticking to each other. The problem was solved via addition of silica fume, as the particles are microscopic they pack the tiny gaps between plastic and cement. Finally, waste cellulose was added for micro-reinforcement and internal water reservoir.

The manufacture process follows "Cold-Cure" sequence. Firstly, limestone dust, cement, and silica fume were mixed together. Then cellulose pulp and plastic shred are added, which are ensured to be fully covered with the mixture of dust. Amount of water is limited and carefully added for semi dry, zero slump consistency. After this step, the mixture is pressed onto the moulds using high frequency vibration to squeeze all the air out.

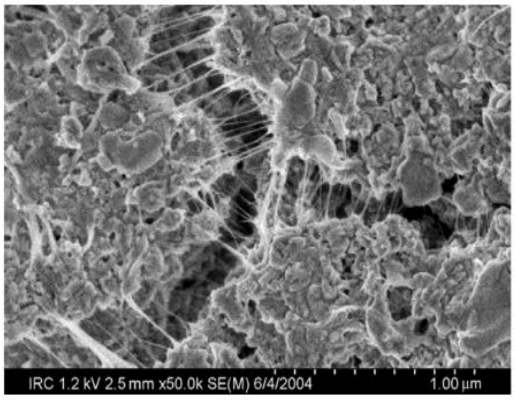
After demoulding, the stones sits on air for 3 hours to allow surface moisture to evaporate and open the tiny pathways inside the block. At the end, blocks are placed onto sealed industrial CO^2 chamber to cure for 24 hours before being tested.

Results and their discussion

The conducted tests proves that these blocks meet the strict requirements of partition walls and can show major advantages on other competitors.

For the test of first manually pressed prototype, the block fractured under hydraulic press at just 0.2 MPa. However, this pressure number is a failure, as the problem was in the testing method rather than the materials. The surface of the prototype was uneven and not properly capped. This roughness caused machine to apply all the force to single high point of the block, causing it to shatter instantly. Based on the research made of similar studies, under industrial conditions like proper pressing and standard flat capping the true compressive strength value is 5-6 MPa.

This much of strength is achieved through a method called "Pozzolanic Densification" by using silica fume. The avoidance of chemical glues allowed the block to rely entirely on the compounds of silica fume and hold together. The micro silica reacts with cement and forms a highly dense gel. This gel fills the microscopic gaps around plastic flakes, effectively suffocating and locking the plastic inside the rock.



Furthermore, the carbonation curing provides early strength to the blocks as injected CO_2 reacts with available Calcium ($Ca(OH)_2 + CO_2 \rightarrow CaCO_3 + H_2O$) and forms a hard calcite shell in just 24 hours. In the first

curing process, cellulose fibres prevents the blocks to cure rapidly and dry out to fast, ensuring that the stones are not going to crack in this process. When microcracks happen, the unreacted calcium inside the block activates and forms the calcite shell again, that gives the block self healing properties.

The aggregate as plastic material lowered the density of the material to 1150 kg/m³, achieving a product that is 2 times lighter than the natural limestone. This reduced dead load on building allows for much safer place during earthquakes. The plastic also interrupts the transfer of heat and gives the block a thermal conductivity of roughly 0.42 W/mK. This is a very strong parameter for a stone and reduces the heating/cooling costs for the residents.

In business case, the renewblocks are highly competitive. Thought the cost of one unit block is slightly higher than the cheapest option- natural stone, developers must care about the installation cost too. Because RenewBlocks are moulded and has flat surfaces, up to 70% less mortar is needed rather than raw limestones. In addition, as they are lighter, RenewBlocks are easier to lift and install, which decreases the building time twice for the walls. When these costs of labour, mortar, and logistics are considered, the final price of the wall is significantly cheaper than the stone wall.



At last, the stones meet all necessary construction standards. For a mechanical strength of 5-6 MPa, it exceeds the ASTM C129 standard (4.14 MPa minimum) for non load bearing concrete masonary units, as well as the regional Azerbaijan State Standard AZS 418-2010 (Grade M50) for partition walls. Regarding fire safety, the plastics inside the stone can melt under high temperature of fire. However, it's suffocated inside a mineral shell that holds the structure all together. When covered with architectural gypsum plaster, the wall system meets the EN 13501-1 safety rules for international partitions.

Offers

Based on this research, these recommendations can be proposed for the region:

1. Industrial Partnerships: the construction material factories should be built next to heavy industries that produce CO2. Thus, the gas can go straightly from the source for capturing for curation of bricks, lowering the carbon capture logistics costs to nearly zero.
2. Update Building Codes: City planners and policymakers can incentivize the use of lightweight materials for internal partition walls by updating building costs. This change would lower the used amount of steel, and overall carbon footprint.
3. Direct Waste Routing: Ministry of Ecology must create a circular system that diverts specific industrial waste to authorized construction manufacturers. The waste would be treated more as a commodity and bypass municipal landfills.

References

1. [Díaz, A. E., Di Lalla, N., & Hernández, A., 2025, 1-12] Analysis of a new brick design using plastic waste. *Cleaner Waste Systems*.
2. [Fu, T., Moon, R. J., Zavattieri, P., Youngblood, J., & Weiss, W. J., 2017, 456-479] Cellulose nanomaterials as additives for cementitious materials. *Cellulose-Reinforced Nanofibre Composites*.
3. [Kougnigan, A. M., Mwero, J., & Mutuku, R., 2023, 1-18] Modeling of Thermal Performance and Mechanical Properties of Concrete Blocks Incorporating Plastic Bottle Waste. *Cogent Engineering*.
4. [Tu, Z., Jian, Y., & Shao, Y., 2016, 420-427] Thermodynamics of reaction between carbon dioxide and calcium silicate hydrates. *Journal of CO2 Utilization*.
5. [Wang, R., Wang, P. M., & Li, X. G., 2005, 900-906] Physical and mechanical properties of styrene–butadiene rubber emulsion modified cement mortars. *Cement and Concrete Research*.
6. [Zhang, D., Ghouleh, Z., & Shao, Y., 2018, 1-11] Effect of Limestone Powder Content on the Early-Age Properties of CO2-Cured Concrete. *Journal of Materials in Civil Engineering*.

INVESTIGATION OF THE SORPTION OF CO^{2+} IONS FROM INDUSTRIAL WASTEWATER USING MODIFIED BENTONITE

Rzaeva A.A.[1], Imanova N.A.[2], Mammadova S.A. [2], Mahmudov F.T[2], Adigozalova M.N. [2], Asgarova T.N. [2]
[1]Baku Higher Oil School
Baku, Azerbaijan
[2]Institute of Chemistry of the Ministry of Science and Education of the Republic of Azerbaijan,
Baku, Azerbaijan
aysel.orujova@bhos.edu.az

Nowadays, the rapid development of industry is considered one of the major factors negatively affecting the environment, especially water resources. Wastewater generated in metallurgy, electrochemistry, chemical production, and mechanical engineering industries is often contaminated with heavy metal ions, posing a serious threat to ecosystems. In this regard, the effective removal of harmful components, particularly cobalt (Co^{2+}) ions, from industrial wastewater remains an important scientific and practical issue.

Cobalt ions are highly toxic and can accumulate in living organisms, causing various health problems. Their discharge into water bodies leads to reduced biodiversity and increased risks to human health. Therefore, the development of efficient and economically feasible technologies for removing these ions from wastewater is of great importance.

Various methods are used for the removal of heavy metal ions, including chemical precipitation, ion exchange, membrane technologies, and electrochemical methods. However, many of these techniques have disadvantages such as high cost, low selectivity, and the formation of secondary waste. In contrast, sorption methods attract attention due to their simplicity, high efficiency, economic viability, and environmental safety.

The sorption process enables the removal of heavy metal ions from aqueous solutions using natural or synthetic sorbents. This method is especially effective at low concentrations and has a wide range of applications. In recent years, nanomaterials and modified sorbents have become major subjects of research in this field.

The main aim of the present study was to investigate the removal of cobalt (Co^{2+}) ions from industrial wastewater using the sorption method, to evaluate the influence of key process parameters, and to determine the optimal conditions for adsorption. Different sorbent materials were tested, and the obtained results were analyzed in terms of their practical applicability.

Bentonite clays are natural minerals widely used in various technological fields, including the oil industry, agriculture, and chemical industry,

particularly for the purification of wastewater from heavy metal cations. Although numerous studies have investigated the removal of cobalt ions using bentonite, natural bentonite generally exhibits relatively low adsorption capacity. Therefore, studying cobalt ion removal using modified bentonite may provide valuable insight into improving adsorption efficiency.

For this purpose, bentonite obtained from the Ag-Dara deposit of Azerbaijan was modified into Na- and Ca-bentonite forms and used in this study. Na-bentonite can adsorb large amounts of water and form highly viscous thixotropic suspensions, whereas Ca-bentonite absorbs less water, swells less, and cannot remain suspended in water for long periods. Due to its lower water adsorption ability, the moisture content of Ca-bentonite is lower compared to Na-bentonite [1].

The purpose of the research was to investigate the adsorption potential of thermally treated nano-bentonite in Na- and Ca-bentonite forms for the removal of cobalt ions. The overall adsorption rate constants and thermodynamic parameters (ΔH, ΔS, and ΔG) were calculated. In addition, the equilibrium and kinetics of cobalt ion adsorption on modified nano-bentonite were studied.

The thermally treated Na- and Ca-bentonite samples were characterized using Scanning Electron Microscopy (SEM). Figure 1 presents the SEM images of Na- and Ca-bentonite. The images show that the nano-bentonite samples consist of particles with different phases and particle sizes below 200 nm.

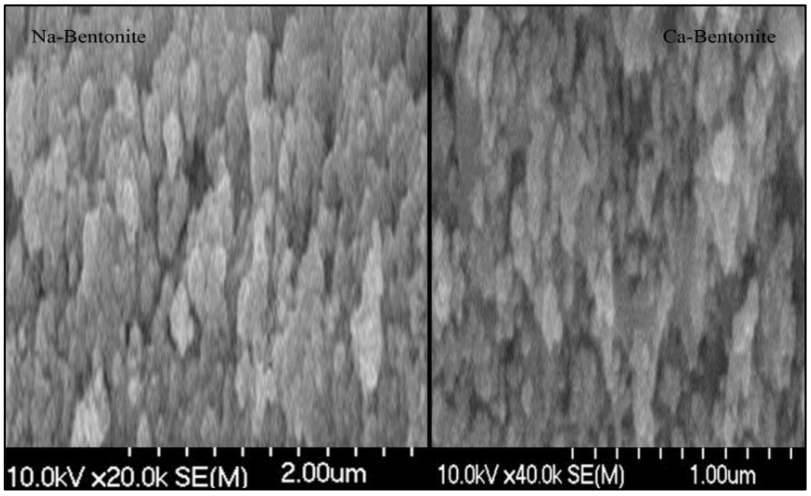


Figure 1. Scanning Electron Microscopy analysis of thermally treated Na- and Ca-bentonite.

The optimal pH value for cobalt ion adsorption on bentonite was found to be 8. Therefore, the kinetics and thermodynamics of cobalt ion adsorption

on thermally treated Na- and Ca-bentonite were investigated within the temperature range of 20–60°C and at cobalt ion concentrations of 2.58×10^{-5}–8.37×10^{-4} mol/L. Adsorption experiments were carried out at temperatures of 293.2, 303.1, 323.2, and 333.1 K, as well as at the standard temperature of 298.1 K under pH 7.80 ± 0.05 conditions. The initial and equilibrium concentrations of cobalt ions in solution were determined using UV spectrophotometry (SF-26) and atomic absorption spectroscopy on a Perkin-Elmer 180 instrument.

Table 1 presents the thermodynamic parameters of the adsorption process, including the entropy (ΔS^0), enthalpy (ΔH^0), and Gibbs free energy (ΔG^0) of activation. The positive ΔH^0 values confirm the endothermic nature of the adsorption process, while the ΔS^0 values reflect changes in the degree of disorder within the system during adsorption. The ΔG^0 values indicate the feasibility of the reaction at different temperatures.

Table 1. Entropy, enthalpy and free energy of activation of adsorption of cobalt ions

Sorbent	C_0, mol/l	ΔH^0, kJ/mol	ΔS^0,J/mol^{-1} grad^{-1}	ΔG^0, kJ/mol
Na-bentonite	$2.58\cdot10^{-5}$	23.72	147.69	−20.30
	$7.54\cdot10^{-5}$	23.29	143.37	−19.41
	$1.77\cdot10^{-4}$	25.03	144.70	−18.26
	$8.37\cdot10^{-4}$	25.67	104.20	−15.42
Ca-bentonite	$2.58\cdot10^{-5}$	39.31	197.41	−19.51
	$7.54\cdot10^{-5}$	39.43	193.89	−18.42
	$1.77\cdot10^{-4}$	31.57	166.01	−17.81
	$8.37\cdot10^{-4}$	21.86	125.72	−15.58

The calculated ΔG^o values show that the adsorption of cobalt ions onto Na- and Ca-bentonite is thermodynamically favorable. At the same time, the increase in ΔG^o at higher temperatures suggests that the adsorption process can still proceed effectively under elevated temperature conditions.

The positive ΔH^o values indicate the endothermic character of the adsorption reaction of Co^{2+} ions, demonstrating that a significant amount of thermal energy is required for the transfer of cobalt ions from the liquid phase to the solid phase.

The obtained results also show that heavy metal ions are adsorbed more effectively at higher temperatures. As temperature increases, the mobility of cations also increases, facilitating the removal of doubly charged ions from the liquid phase. This is supported by the positive ΔS^o values, which indicate an increase in system disorder during adsorption.

References

1. Ilyasova H.N., Yagubov A.I., Muradova N.M., Imanova N.A., Nuriyev A.N. *Sorption of Co^{2+} and Cd^{2+} ions from model solutions on modified bentonite and their colloid characteristics.* Azerbaijan Chemical Journal, 2017, No. 1, pp. 34–37.

MÜNDƏRİCAT / CONTENTS

MODERN APPROACHES TO IMPROVING THE EFFICIENCY OF GAS PURIFICATION FROM ACIDIC COMPONENTS
O.B. Akhmedova, M.Z. Nuriddinov, A.Sh. Qayumov, R.D.Asadova, N.Maxmudov.....2

C VİTAMİNİ (ASKORBİN TURŞUSU) ƏSASLI TƏBİİ ANTİOKSİDANT SİSTEMLƏRİN QİDA TEXNOLOGİYASINDA TƏTBİQİ VƏ ONLARIN KİMYƏVİ STABİLLİYİNİN ARAŞDIRILMASI
Əsgərli Rəvanə.....16

KARTOF NİŞASTA ƏSASLI BİOPOLİMER MATRİSİNƏ ANTOSİANLARIN İMMOBİLİZASİYASI: QİDA TƏHLÜKƏSİZLİYİ ÜÇÜN İNTELLEKTUAL İNDİKATOR PLYONKANIN NƏZƏRİ MODELİNİN QURULMASI
Əsgərli Rəvanə.....18

OBTAINING A BINARY SYSTEM BASED ON STYRENE–BUTADIENE–STYRENE POLYMER USING CARBON NANOTUBES AND DETERMINATION OF THE FLOW INDEX OF THE COMPOSITION MELT
Sharif Hajiyev Mahir, Aysun Rzazadə Mubariz.....20

PREPARATION AND STUDY OF A COMPOSITION BASED ON BUTADIENE-STYRENE POLYMER USING WOOD TAR
Maryam Huseyinova.....26

OBTAINING AND INVESTIGATION OF COMPOSITIONS WITH IMPROVED PERFORMANCE PROPERTIES BASED ON SKI-3 RUBBER
Rashad Alizade.....31

PREPARATION OF TETRACYCLIC HOMOPOLYMER AND A COPOLYMER WITH ACRYLIC FRAGMENTS
Kh. M. Mamedova, V. S. Kadyrly, E. G. Makhmudova, R. A. Rasulova, M. D. Ibragimova, I. R. Safarova, J. G. Ismailova.....36

PRODUCTION OF SYNTHETIC PETROLEUM ACIDS AND OXY-PETROLEUM ACIDS VIA LIQUID-PHASE OXIDATION OF NAPHTHENIC–PARAFFINIC HYDROCARBONS IN THE PRESENCE OF Mn, Cr, Co, Ni, AND Zn ACETYLACETONATES AS CATALYSTS
V.M. Abbasov, L.M. Afandiyeva, N.N. Babanli, N.N. Aliyeva, Sh.N. Ibrahimli.....38

STUDY OF THE INHIBITORY PROPERTIES OF AMINOESTERS OBTAINED BASED ON SYNTHETIC PETROLEUM ACIDS
V.M. Abbasov, L.M. Afandiyeva, G.Y. Rustamli, Ch.Z. Musaeva, S.A. Süleymanova.....41

OLEİN TURŞUSUNUN 2-AMİNOPİRİDİN KOMPLEKSİNİN CO_2 KORROZİYASINA QARŞI İNHİBİTOR KİMİ TƏDQİQİ
V.M .Abbasov, D.B. Ağamalıyeva, G.Ə.Abbasova, S.Z.Əhmədova, K.V.Əzizova....45

SYNTHESIS AND IR SPECTROSCOPIC STUDY OF A Cu(II) COMPLEX WITH A NITROGEN- AND SULFUR-DONOR HETEROCYCLIC LIGAND
Bayim Isakova, Afsun Sujayev, Nazar Nazarov, Mir Ali Isakov.....48

SYNTHESIS OF AN OPTICALLY TRANSPARENT COPOLYMER BASED ON N-VINYLCARBAZOLE AND METHYL METHACRYLATE
Seide Mamedli, Huseyn Nuriyev, Samira Mustafayeva, Gulshan Novruzova.....50

SYTHESIS AND CHARACTERIZATION OF BIODEGRADABLE GREASES DERIVED FROM SONFLOWER AND CORN OILS MODIFIED WITH CuO NANOPARTICLES
Sabina Garayeva, Aydan Baghirova.....53

СИНТЕЗ ОПТИЧЕСКИ ПРОЗРАЧНОГО СОПОЛИМЕРА НА ОСНОВЕ N-ВИНИЛКАРБАЗОЛА И БУТИЛМЕТАКРИЛАТА
Саида Мамедли, Рауф Джаббарбейли, Шабнам Гараева, Фарида Юсифли.....56

ARYLAMINE-SUBSTITUTED THIETANES AND FUNCTIONALLY SUBSTITUTED THIIRANES AS ANTIOXIDANTS FOR HYDROCARBON OXIDATION
Irada A. Rzayeva, Nazar M. Nazarov, Sabir S. Babayev, Ibadulla H. Mahmudov, Camila C.Ahmadova.....59

EKOLOJİ TƏMİZ DİZEL YANACAĞININ ALINMASINDA ULTRASƏSLİ KAVİTASİYASININ TƏSİRİ
Təranə Məmmədova, Zümrüd Köçərli.....61

СИНТЕЗ ФУРИЛЗАМЕЩЁННЫХ *α,β*-НЕНАСЫЩЕННЫХ КЕТОНОВ И ИХ АМИНПРОИЗВОДНЫХ
Т.Р. Сафарова, А.Р.Караева, М.И.Шатирова, Г.М.Мамедова.....63

НОВАЯ ТЕХНОЛОГИЯ ДЛЯ БОРЬБЫ С ОСЛОЖНЕНИЯМИ В ПРОЦЕССЕ ДОБЫЧИ НЕФТИ
Абдуллаев Вугар Джамил, Алсафарова Матанат Эльдар, Халилов Нурлан Назим, Алышова Джамала Гулу.....67

THE EFFECT OF AN ADDITIVE SYNTHESIZED FROM NATURAL PETROLEUM ACIDS ON THE PRODUCTION OF ROAD BITUMEN
Vagif Abbasov, Lala Afandiyeva, Yutta Cherepnova, Gunay Nasibova, Shafag Mammadova, Balacakhanim Babayeva, Nazile Afandiyeva 71

INVESTIGATION OF THE AEROBIC OXIDATION OF HYDROCARBONS IN THE PRESENCE OF METAL-CONTAINING HOMOGENEOUS CATALYTIC SYSTEMS
Vagif Abbasov, Lala Afandiyeva, Gunay Nasibova, Shafag Mammadova, Turan Mazamova, Fidan Hasanova.....74

OPTIMIZATION OF HYDRODENITROGENATION OF ALGAL CRUDE BIO-OIL USING NiCo/γAL$_2$O$_3$
Laman Talibova.....76

TEMPERATUR AMİLİNİN PARAFİNSİZLƏŞMƏ PROSESİNDƏ ROLU
Sevinc Hacıyeva, Nəzərova Müşkünaz.....78

MÜXTƏLİF METİLLƏŞDİRİCİ REAGENTLƏRİN NAFTOLLARLA REAKSİYASİNİN İLKİN TƏDQİQİ
Fərəcova Günay, Nəzərova Müşkünaz.....81

HoSbTe$_3$ VƏ HoBiTe$_3$ BİRLƏŞMƏLƏRİNİN ELEKTRİKKEÇİRİCİLİYİNİN VƏ TERMOELEKTRİK XASSƏSİNİN TEMPERATURDAN ASILILIĞI
Nərmin Məmmədova, Fuad Sadıqov, Teymur İlyaslı, Yasin Cəfərov, Ç.I.Abilov.....83

OBTAINING FOAM EXTINGUISHERS BASED ON PMS-10 AND ETHANOL AND STUDYING THEIR EFFECT ON FOAM STABILITY
Makhmudov Mukhtor Jamolovich, Nematov Khusan Ibodullayevich, Shoymardonov Olmasbek Bolta ogli.....86

ДИВЕРГЕНТНЫЙ СИНТЕЗ 6-АЛКИЛ-2-(4-ГИДРОКСИФЕНИЛ)-4-МЕТИЛ-1Н-ПИРРОЛО[3,4-С]ПИРИДИН-3(2Н)-ОНОВ И ИХ ПРОИЗВОДНЫХ
М.И.Шатирова, Ш.К.Шейдаева, А.Р.Караева, Г.М. Мамедова, С.Ш.Гулиева.....92

POLİSTİROL TƏRKİBLİ TULLANTILARIN DEPOLİMERLƏŞDİRİLMƏSİ PROSESİNİN TƏDQİQİ VƏ BƏRPA OLUNAN STİROL MONOMERİNİN XASSƏLƏRİNİN ANALİZİ
Babayeva Ülkər, Qarayeva İradə.....95

YÜKSƏK SIXLIQLI POLİETİLENİN (HDPE) İSTEHSAL PROSESİNDƏ HİDROGEN KONSENTRASİYASİNİN ƏRİMƏ İNDEKSİ VƏ STRUKTUR XASSƏLƏRİNƏ TƏSİRİNİN TƏDQİQİ
Manaflı Zaur, Qarayeva İradə 97

HEKSILAMMONIUM DODESIL SULFATIN SINTEZI VƏ ONUN SƏTHI AKTIV MADDƏ KIMI TƏTQIQI
İbrahimova Minavər, Xamiyeva Günay, Bağırova Şəfəq, Quliyeva Təranə, Əzizbəyli Emin 99

YENİ XALKON TÖRƏMƏLƏRİNİN SİNTEZİ VƏ QURULUŞUNUN TƏDQİQİ
A.R.Qarayeva, G.A.Məmmədli, M.İ Şatirova, G.M.Məmmədova, Ş.K.Şeydayeva . 102

SYNTHESIS AND THEORETICAL CALCULATIONS OF 2-(2,4-DICHLOROPHENYL)-4,5-DIPHENYL-1-(4-(PHENYLDIAZENYL)PHENYL)PHENYL)-1 H-IMIDAZOLE
Nargiz Orujova 105

ANALYSIS OF THE ISOMERIZATION PROCESS OF LOW-OCTANE GASOLINE
Turakulova Marjona, Seyedmeysam Kosari, Laziz Saidov 109

ENHANCED ALKYLATION OF PHENOL WITH ISOPRENE CYCLODIMERS USING ZEOLITE-CONTAINING KN-30 CATALYST
U.R. Gurbanova, Ch.K.Rasulov 113

MODERN ABSORPTION TECHNOLOGIES FOR ACID GAS REMOVAL FROM HYDROCARBON GASES: A GLOBAL ANALYSIS
Sh.U. Akhmedova, O.B. Akhmedova 116

DESIGN AND PERFORMANCE ANALYSIS OF SANDWICH-STRUCTURED WATER STORAGE TANKS
Aytaj Aliyeva, Zilan Mansurova, Aysel Mammadova 120

DECOMPOSITION OF HIGH-STABLE WATER-OIL EMULSIONS OF HEAVY OILS IN AN OIL PREPARATION DEVICE
Ochilov Abdurakhim Abdurasulovich, Uzakbaev Kamal Axmet uli 124

STUDY AND ANALYSIS OF THE STABILITY OF WATER-OIL EMULSIONS IN LOCAL OIL PREPARATION EQUIPMENT.
Ochilov Abdurakhim Abdurasulovich, Uzakbaev Kamal Axmet uli 133

SYNTHESIS OF MORPHOLINE-BASED AMINOMETHYLATED DERIVATIVES OF STERICALLY HINDERED CYCLOALKYLPHENOLS
Hajiyeva G.F., Naghiyeva M.V. 140

ALKİLFENOLLARIN AZTULLANTI ÜSULU İLƏ SİNTEZİ
Mahmudov Emin , Əliyeva Nailə 142

OPTIMIZATION OF CMC-PVA TERNARY BLEND FORMULATIONS FOR HIGH-EFFICIENCY SEED COATING: IMPACT ON GERMINATION RATE AND SEEDLING DEVELOPMENT
Asmar Eyvazli, Aysu Rzayeva, Garanfil Ahmadova 144

DEVELOPMENT OF ECO-FRIENDLY AND SELF-HEALING CHITOSAN-CITRATE BIOCOMPOSITE COATINGS FOR ADVANCED CORROSION PROTECTION OF METALLIC ASSETS
Leyla Muradova, Nazrin Ibadzade, Alishan Alishanov 149

COPPER-BASED ANODE DESIGN FOR METHANOL MICROFLUIDIC FUEL CELLS: MECHANISTIC INSIGHTS AND PERFORMANCE EVALUATION
Ilkana Mehdiyeva 154

CATALYTIC ALKYLATION OF P-CRESOL WITH ISOPRENE CYCLODIMERS USING A ZEOLITE-CONTAINING CATALYST
Naghiyev A.V., Aghamaliyev Z.Z. 158

PEPA-BASED OLEIC ACID DERIVATIVES AS EFFICIENT ANTISTATIC ADDITIVES FOR DIESEL FUEL
V.M. Abbasov, A.A. Kangarli, N.I. Mursalov, N.K. Dadashova, N.Sh. Rzayeva, F.J.Gurbanova *161*

OBTAINING STABLE SILVER NANOPARTICLES BASED ON SODIUM CITRATE
Lutpillayeva Masuda, Xoshimov Farxod *164*

ANİLİNİN SEOLİT KATALİZATORLARI İŞTİRAKINDA METANOLLA ALKİLLƏŞMƏ PROSESİNİN TƏDQİQİ
İsmayılov Səbuhi, Əliyeva Nailə *169*

ZN-CR LAYLI İKİLİ HİDROKSİDLƏRİ VƏ ONUN KARBON ƏSASLI NANOKOMPOZİTLƏRİNİN SİNTEZİ VƏ OPTİKİ XASSƏLƏRİNİN TƏDQİQİ
Hüsna Abuzərova, Ofeliya Balayeva,İradə Buniatzadə *171*

EP-300 QURĞUSUNDA YAN MƏHSUL KİMİ ALINAN TSİKLOPENTADİENİN AMİNLƏŞMƏSİ VƏ BƏZİ ÇEVRİLMƏLƏRNİN ÖYRƏNİLMƏSİ
Şahgəldiyev F.X., Babazadə Mənzər Zavur *174*

PİRROL TÖRƏMƏLƏRİNİN SİNTEZI REAKSİYASINDA YAŞIL KİMYANIN PRİNSİPLƏRİ VƏ PERSPEKTİVLƏRİ
Məmmədova A. A., Məmmədova Fidan Rafiq *180*

SYNERGISTIC $BASO_4$-BASED REFLECTIVE TOP COAT AND FORM-STABLE LAURIC-STEARIC ACID/FUMED SILICA PCM COMPOSITE FOR COMPLETE PASSIVE SOLAR ENERGY MANAGEMENT IN BUILDINGS
Fidan Sadigova, Nihat Guliyev, Elmar Esgerzade, Aliya Laylabashova *186*

RESEARCH OF CORROSION PROCESS AND DEVICES FOR ITS PREVENTION, THEIR TYPES AND SOLUTIONS
Khurbonova Firuza Solekhovna *190*

PROCESSING AND CHARACTERIZING ALTERNATIVE AND PARTNER MATERIAL FOR CUBIC SILICON
Murad Niftaliyev *193*

INVESTIGATION OF THE ANTIMICROBIAL ACTIVITY OF NITRO DERIVATIVES OF DICYCLOPENTADIENE AGAINST COLIFORM, ENTEROCOCCUS, AND *E. COLI* BACTERIA
Vagif Abbasov, Durna Aghamaliyeva, Chira Musaeva, Sabina Ahmadova, Könül Azizova, Nigar Aliyeva *195*

TOWARDS SUSTAINABLE HEATING SYSTEMS: ADVANCED MATERIALS AND OPTIMIZATION STRATEGIES FOR CO_2 MITIGATION
Aytaj Mammadli, Rabiyanur Mammadova *199*

ASFALTEN FRAKSİYALARINDA OKSİDLƏŞMƏ MEXANİZMLƏRİNİN RADİKAL TƏBİƏTİNİN TƏDQİQİ
Yolçuyeva Ü.C., Hacıyeva G.A., Nazli A. Mehdiyeva, Əzizbəyli E.İ., Murad Bayramov *203*

DEVELOPMENT AND CHARACTERIZATION OF STARCH-BASED pH-SENSITIVE FILMS INCORPORATED WITH RED CABBAGE ANTHOCYANIN FOR SMART FOOD PACKAGING APPLICATION
Nuybar Jafarli, Nargiz Atamova *205*

PREPARATION OF A SODIUM NAPHTHENATE–BASED FOAMING AGENT AND COMPARATIVE ANALYSIS OF ITS SURFACE-ACTIVE PROPERTIES
Vaqif Abbasov, Durna Ağamalıyeva, Lalə Əfəndiyeva, Rüfət Əzizov, Fariz Əmirli, Məhəbbət Rəcəbli *210*

DEVELOPMENT OF A CARBOXYMETHYL CELLULOSE – ALGINATE HYBRID SUPERABSORBENT HYDROGEL DESIGNED FOR WATER MANAGEMENT IN AGRICULTURE
Aynur Movsumova, Nigar Jafarli, Garanfil Ahmadova 213

pH SENSITIVE HYDROGELS IN DRUG DELIVERY
Aytaj Valiyeva, Aysel Mammadova 218

STUDY OF THE INORGANIC COMPLEX OF SYNTHETIC PETROLEUM ACIDS WITH TRIETHYLENETETRAMINE AND IMIDAZOLINE AS A SCALE INHIBITOR
Vaqif Abbasov, Durna Ağamalıyeva, Lalə Əfəndiyeva, Zaur Ağamalıyev, Sevda Rzayeva, Fəridə Qurbanova, Firəngiz Rəhimova Şükürova, Zəhra Qocayeva 226

EFFECT OF CARBON CHAIN LENGTH ON THE CORROSION INHIBITION EFFICIENCY OF SURFACTANTS
Nurana Ziyadzada, Murad Hasanov, Hajar Nabiyeva 230

ELECTROCHEMICAL INVESTIGATION OF BENZYLAMIDE OF NATURAL PETROLEUM ACIDS AS A CORROSION INHIBITOR FOR CARBON STEEL IN CO_2-SATURATED NaCl SOLUTION
N. K. Dadashova, V. M. Abbasov, D. B. Aghamaliyeva, N. I. Mursalov, F.J. Kurbanova 235

DESIGN AND BENCHTOP VALIDATION STRATEGY OF A FLEXIBLE ELECTROCHEMICAL IMPEDANCE SMART BANDAGE FOR SUSTAINABLE WOUND MONITORING
Shahriyar Eminzada 239

IMMOBILIZATION OF LACCASE IN CALCIUM ALGINATE BEADS FOR ENHANCED BIODEGRADATION OF AZO DYES IN AQUEOUS SYSTEMS
Shams Rzayeva, Nurana Askarova, Shafa Rahmanova, Aysel Mammadova 245

STUDY OF THE KINETICS OF CORROSION PROCESSES IN PRODUCED WATER CONTAINING CO_2 AND H_2S AND APPLICATION OF NEW INHIBITORS
Heydarova Almaz 249

BIOINSPIRED PLASMONIC AEROGEL FOR EFFICIENT AND SALT-RESISTANT SOLAR DESALINATION OF SALINE OR CONTAMINATED WATER
Laman Aliyeva, Mahira Ganbarova, Aliya Laylabashova 251

SUSTAINABLE NANO-BIOPOLYMER SPRAY FOR PREVENTING FUNGAL DISEASE OF PLANT-BASED FOODS
Revane Abdullayeva, Ayan Guliyeva, Rima Guliyeva 254

INVESTIGATION OF THE INFLUENCE OF ALKYLPHENOL-BASED ANTIOXIDANTS ON THE PROPERTIES OF SKN-26-BASED ELASTOMER COMPOSITIONS
Ayshe Gojazade 258

ПРОТОЧНЫЙ ЭЛЕКТРОЛИЗЕР « ГИПОНАТ » ДЛЯ ПОЛУЧЕНИЯ ГИПОХЛОРИТА НАТРИЯ
Гулиева Лейла Ильхам 260

SYNTHESIS STUDY OF BIOCHAR-CELLULOSE-BASED BIOCOMPOSITES FOR WASTEWATER TREATMENT FROM HEAVY METALS
Alishan Alishanov, Jala Nabiyeva, Madina Suleymanova 266

MECHANİSM OF THE ELECTROCHEMİCAL REDUCTİON PROCESS OF MO İONS
Ayan Alizada, Samira Jafarova 270

ORANGE PEEL REINFORCED POLY(LACTIC ACID) COMPOSITES: MECHANICAL PROPERTIES AND ACCELERATED BIODEGRADATION
Nihad Mirzazada, Ayla Abbasli 271

PREPARATION AND TESTING OF ENVIRONMENTALLY SAFE CORROSION INHIBITOR BASED ON REAGENTS OF NATURAL ORIGIN
Elnura Aliyeva, Durna Aghamaliyeva *275*

PRODUCTION OF SUSTAINABLE DIMETHYL ETHER THROUGH CARBON DIOXIDE HYDROGENATION
Ezozbek Turaev, Rima Guliyeva *279*

RADIATION PROTECTION POTENTIAL OF NBR-Bi_2O_3-$BaSO_4$ COMPOSITES
Fatima Azizli, Rana Khankishiyeva *283*

HIDROGEN ISTEHSALI ÜÇÜN ELEKTROKIMYƏVI SUYUN PARÇALANMASINDA Sb_2Se_3 ELEKTROKATALIZATORUN ROLU
Günel Xəlilova *288*

ETHYL 6-(ETHOXYMETHYL -4-(THIOPHEN-2)-2-THIOXO-1,2,3,4 TETRAHYDROPRIMIDINE-5-CARBOXILATE COMPLEXES WITH NICKEL
Ibadulla H. Mahmudov, Nazar M. Nazarov, Sabir S. Babayev, Camila C. Ahmadova, Irada A. Rzayeva *290*

THE ROLE OF Sb-Se-Te SYSTEMS IN SOLAR ENERGY CONVERSION: A HEORETICAL STUDY
Ilkane Mammadova Shakir, Pervin Guliyev Heydar *292*

INTERACTION BETWEEN CORROSION AND SALT DEPOSITION PROCESSES IN PRODUCED WATERS AND PREPARATION OF MULTIFUNCTIONAL INHIBITORS
Rasul Musayev *295*

SƏNAYE ÜSULU İLƏ ANİLİNİNİN N-ALKİLANİL TÖRƏMƏLƏRİNİN ALINMASININ TEXNOLOJİ PRİNSİPLƏRİ
Yusibov Kənan, Əliyeva Nailə *299*

AN INNOVATIVE ELECTROCHEMICAL APPROACH FOR FOOD SAFETY: FAST AND SENSITIVE DETECTION OF ACEPHATE IN VEGETABLE SAMPLES USING ZN-CU MOF (METALLIC ORGANIC FRAMEWORK) NANOCOMPOSITES
Elnur Mardiyev, Murad Imamverdizada *301*

SYNTHESIS OF 2-(4-AMINO-6-METHYL-5,6-DIHYDRO-1,3,5-TRIAZIN-2(1H)-YLIDENE)MALONONITRILE AND ITS PHARMACOLOGICAL AND BIOLOGICAL PROPERTIES
Mir Ali Isakov, Afsun Sujayev, Bayim Isakova, Lala Aliyeva *306*

SUSTAINABLE SYNTHESIS OF GRAPHENE-BASED SHEETS BY ELECTROCHEMICAL EXFOLIATION METHOD.
Murad Amirli, Arzu Abdullayeva, Rena Abbasova *309*

CHARACTERISTICS OF BIOCOMPOSITES BASED ON COMPATIBILIZED ETHYLENE HEXENE-1 COPOLYMER: THE INFLUENCE OF CORN HUSK MICRO-SIZED PARTICLES CONTENT ON THE MELT FLOW INDEX
Fatima Mustafayeva, Eltaj Mustafayev, Najaf Kakhramanov *314*

MÖHKƏMLİK GÖSTƏRİCİLƏRİ YAXŞILAŞDIRILMIŞ POLİMER MATERİALLAR
Vəlizadə N.Y., Qasımova G.Ş., Ağayeva F.A., Tağıyeva A.L. *316*

INVESTIGATION OF ELECTROCHEMICAL CORROSION BEHAVIOR OF CARBON STEEL IN FORMATION WATER USING EIS AND TAFEL METHODS
Sabina Rustamova *317*

STUDY OF THE ELECTROCHEMICAL REDUCTION PROCESS OF Bi IONS
Aisha Shikhaliyeva, Vusala Majidzade *321*

EVALUATION OF THE MELT FLOW INDEX OF COMPATIBILIZED POLYPROPYLENE RANDOM COPOLYMER - MICRO SIZED CORN HUSK BASED BIOCOMPOSITES
Fatima Mustafayeva, Farid Suleymanli, Ruhangiz Alasgarova *322*

2-ALLİLFENOLUN FORMALDEHİD VƏ BENZİLAMİNLƏ KONDENSLƏŞMƏ MƏHSULUNUN SİNTEZİ VƏ TƏDQİQİ
G.M.Mehdiyeva, F.O.İbadzadə, M.R.Bayramov, N.Y.Zeynalov *325*

2-ALLİLFENOL ƏSASINDA AZOT SAXLAYAN BİRLƏŞMƏLƏRİN SİNTEZİ VƏ TƏDQİQİ
G.M.Mehdiyeva, Ş.E. Səfərova, M.R.Bayramov, M.A.Ağayeva *326*

SYNTHESIS OF CYCLOPROPANE-CONTAINING DIESTER AND PREPARATION OF POLYESTER ON ITS BASIS
Leman Guliyeva, Khayyam Nazaraliyev, Rita Shahnazarli, Malahat Abdurahmanova *327*

CUOTEXTILE: A BIO-RESPONSIVE, NANOCLAY-ENCAPSULATED TEXTILE FOR HOSPITAL INFECTION CONTROL
Ziyad Shiraliyev, Rima Guliyeva *322*

AUTONOMOUS SOLID-STATE ELECTROCHROMIC GLAZING: INTEGRATING BIOMASS-DERIVED SOLAR CONCENTRATORS WITH ANTI-FREEZING ORGANOHYDROGELS
Ziyad Shiraliyev, Adil Ismayilzada, Rima Guliyeva *336*

BƏRPA OLUNAN XAMMALDAN TƏBİİ SEOLİT KATALİZATORLARI İLƏ BİOYANACAQ İSTEHSALI
Aişə Süleymanova, Gülbəniz Muxtarova *340*

GO/ZnAl-LDH NANOKOMPOZİTİ ƏSASINDA METİLEN GÖYÜNÜN FOTODEQRADASİYA VƏ ADSORBSİYASI QABİLİYYƏTİNİN ÖYRƏNİLMƏSİ.
Quluzadə Nuray, Balayeva Ofeliya *345*

EVALUATION OF THE CORROSION INHIBITION EFFICIENCY OF INHIBITOR SYSTEMS SYNTHESIZED FROM NATURAL PETROLEUM ACIDS
Ulviyya Abbasova, Sara Abbaszadeh, Rufana Alizadeh, Vugar Gasimov *348*

NANO-BIOREMEDIASIYA: EKOSISTEMLƏRIN BƏRPASINDA NANOHISSƏCIKLƏRIN VƏ MIKROORQANIZMLƏRIN SINERGETIK GÜCÜ
Aygün Almənmədova, İradə Eyvazova, Təranə İbrahimova, Könül Qəhrəmanova, Gülşən Qasımlı, Inarə Sədirzadə, Gülzar Məmmədova *352*

YAŞIL TRANSFORMASİYA DÖVRÜNDƏ DAYANIQLI İNKİŞAFIN YENI PARADİQMASI
Abbasova Günay Firdovsi qızı, Məstalıyev Seymur Ruslan oğlu *353*

SƏNAYE SULARININ TƏMİZLƏNMƏSİ PROSESLƏRİNDƏ TƏHLÜKƏSİZLİK RİSKLƏRİNİN AZALDILMASI
Vəfa Kərimli, Elnur Rüstəmzadə, Elton Qasımov *356*

DISCRETE ELEMENT SIMULATION OF PARTICLE SETTLING IN SHEARED SUSPENSIONS UNDER GRAVITY
Madina Ziyadkhanova *359*

KATALİTİK KREKİNQİN YÜNGÜL FLEQMASI ƏSASINDA NİTROTÖRƏMƏLƏRİN SİNTEZİ VƏ TƏDQİQİ
Dəmir Nağıyev, Sara Abbaszadə, Rufanə Əlizadə, Fəridə Tahirova, Məhsəti Qafarova *365*

YÜNGÜL FLEQMANIN NİTROLAŞMASI VƏ MAYE KAUÇUK ƏSASLI KOMPOZİSİYALARIN HAZIRLANMASI
Mehin Dadaşova, Sara Abbaszadə, Yeganə Ağazadə, Rufanə Əlizadə, Gülnar Vəliyeva, Tofiq Əliyev *369*

İSTİXANA VƏ BAĞ TULLANTILARINDAN KOMPOSTUN HAZIRLANMASI
Samirə Bağırova, Leyla Cavadova, Lalə Nəsirli, Arzu Axundova, Cəmalə Ağayeva, Mirhüseyin Səfərov, Lalə Cəlilova *373*

KOMPLEKS EMAL, ALTERNATİV VƏ BƏRPA OLUNAN ENERJİ MƏNBƏLƏRİ
İmran Qasım oğlu Qasımov, Günel Anar qızı Tomuyeva, Sədaqət Yaqub qızı Adıgözəlova, Şahnaz Qədir qızı Əliyeva, Zərifə Fuad qızı Yusubova 377

SYNTHESIS AND EVALUATION OF CATIONIC POLYASPARTAMIDES FOR THE REMOVAL OF AZO DYES FROM AQUEOUS SOLUTIONS.
Rizokulov Ramazon, Mehri Nizomova, Sunnatbek Teshayev, Aysel Mammadova. 382

TYPES OF COAGULANTS OBTAINED FROM ALUMINUM AND THEIR MAIN CHARACTERISTICS
Makhmudov Mukhtor Jamolovich, Sunatov Shokhrukh Shamsi ugli 385

PREDICTING THE KINETICS OF OIL BIODEGRADATION IN SEAWATER WHEN INOCULATED WITH ACTIVE HYDROCARBON-OXIDISING MICROORGANISMS
Konul Gahramanova, Parvin Mammadova, Gulshan Gasimli, Tarana İbragimova, İnara Sadirzade, Aygun Almammadova, Aytaj İsmayilli 391

SPECTROPHOTOMETRIC DETERMINATION OF Fe(III), Mo(VI), AND Cu(II) IONS IN NANOANALYTICAL SYSTEMS
Ayten Imamaliyeva, Famil Chyragov, Flora Hajiyeva 392

SYNTHESIS AND APPLICATION OF PET-DERIVED HYDROGEL ADSORBENTS FOR EFFICIENT TREATMENT OF DYE-CONTAMINATED WATER
Bafoev Asliddin, Ahmadova Garanfil..... 395

DESIGN AND EVALUATION OF BIODEGRADABLE POLYASPARTAMIDES FOR OIL/WATER SEPARATION
Bobajanov Sardor, Qandimov Sardor, Aysel Mamadova 400

OBTAINING PRODUCTION OF HIGH-QUALITY DIESEL FUEL BY COMBINING MILD HYDROTREATING AND EXTRACTION WITH IONIC LIQUIDS
Sabina Seidova, Minaver Ibrahimova, Sayara Aliyeva, Khadija Abdullayeva 403

PECTIN-BASED HYDROGEL DERIVED FROM CITRUS PEEL WASTE FOR REMOVAL OF HEAVY METALS AND DYES FROM AGRICULTURAL WASTEWATER
Sabina Gasimova, Lala Mahammadova, Garanfil Ahmadova..... 407

BİODİZELİN ALINMASINDA YENİ YAŞIL KATALİZATOR
Fərid Quliyev, Ofelya Cavadova, Azər Əmirov, İbrahim Məmmədov 412

MODERNIZATION OF OIL REFINING PROCESSES FOR PRODUCING HIGH-OCTANE GASOLINE
Turakulova Marjona, Panoev Erali..... 414

ECOLOGIK TRANSFORMATION OF THE OIL AND INDUSTRY IN THE CONTEXT OF THE GLOBAL CLIMATE AGENDA
Zoirova Aziza Irgashevna..... 419

DETERMINATION OF THE SORPTION CAPACITY OF SILICA GEL KSK AND ZEOLITE GRADE CaA FOR BENZENE AND n-HEXANE
Bekhruz Mansurov, Ruslan Khayitov 424

PROTECTION OF THE ATMOSPHERE FROM WASTE GASES OF OIL REFINERIES
Bozorov Gayrat..... 428

SOLVENT SELECTION IN ORGANIC CHEMISTRY: REPLACING TOXIC MEDIA WITH GREEN ALTERNATIVES
Sevgi Babayeva, Gulay Muradova, Nilufer Allahverdiyeva, Peri Huseynova 432

DEVELOPMENT OF EFFECTIVE TECHNOLOGY OF UTILIZATION OF SOUR GASES CONTAINING HYDROGEN SULFIDE
Turakulova Marjona, Panoev Erali, Jalilova Marjona 436

MATHEMATICAL MODELING OF SUSTAINABLE MATERIALS LIFECYCLE FOR ENVIRONMENTAL RESTORATION
Bakhronova Sayyora kizi, Qosimova Dilnura Uygunovna.....442

APPLICATION OF MATHEMATICAL MODELING AND FORECASTING METHODS TO IMPROVE THE EFFICIENCY OF WASTE RECYCLING SYSTEMS
Bakhronova Sayyora kizi, Amonova Gulbegim Alijon kizi.....445

VECTOR-BASED MODELING METHODS FOR ENVIRONMENTAL RESTORATION USING YEAR-ROUND REUSABLE WASTE
Botirova Jasmina Xurshidovna, Jo'rayev Shaxzod Shuhratjonvich.....448

SEPARATION AND PURIFICATION OF THE OLIVE BRINE USING TAILOR-MADE POLYMERS
Elchin Bilalov, Rolando C. S. Dias.....453

AQRO – SƏNAYE TULLANTILARINDAN BİOPLASTİK SİNTEZİ: NAR QABIĞININ (PUNICA GRANATUM) İNNOVATİV TƏTBİQİ VƏ ANALİZİ
Abbasova Ayla.....456

MULTI-STAGE VALORİZATİON OF SPENT GREEN AND BLACK TEA: FROM ETHANOL-BASED ANTIOXIDANT RECOVERY TO HIGH-EFFICIENCY BIODIESEL PRODUCTION
Aysun Pirkhiyeva, Laman Gahramanzada, Garanfil Ahmadova.....458

BİODİZELİN ALINMASINDA AKTİV BİOKARBON KATALİZATORUNUN TƏDQİQİ
Nəzrin Nəzirova, Ofelya Cavadova, Azər Əmirov, İbrahim Məmmədov.....461

INVESTIGATION OF ACETAL-EUCALYPTUS OIL MIXTURE AS ADDITIVE TO B10 FUEL BLEND
Mehin Bakhtiyarova, Nargiz Azimova, Yegana Mamedova, Ibrahim Mamedov.....463

İZOPRENİN TSİKLODİMERLƏRİ ƏSASINDA TSİKLOALKİLFENOLLARIN VƏ ONLARIN KARBONİL TÖRƏMƏLƏRİNİN ALINMASI
Heydərli G.Z., Bağırzadə R.Z., İsmayilova L.A., Məmmədli Ü.E., Atamov N.R., Əlili F.V. 465

HYBRID HYDROGEL SYNTHESIS
Ibroximova Mohinbonu, Xoshimov Farxod 466

WIDE-AREA DAMPING STRATEGIES FOR RENEWABLE-DOMINATED POWER SYSTEMS: STRUCTURE, LIMITATIONS AND FUTURE DIRECTIONS
Jalal Ibrahimov, Jamila Rzali.....470

CARBON FOOTPRINT ANALYSIS OF PRIMARY ALUMINUM PRODUCTION
Chingiz Hajiyev.....475

SCIENTIFIC AND TECHNOLOGICAL FOUNDATIONS FOR ENSURING ENVIRONMENTAL SUSTAINABILITY IN THE PROCESS OF BITUMEN MODIFICATION
Abdullaeva Shokhista Shukhratovna, Khujakulov Aziz Fayzullayevich 480

THERMAL DEGRADATION AND RECYCLING POTENTIAL OF FOOD PACKAGING POLYMERS: A REVIEW ON THE STRUCTURAL AND FUNCTIONAL CHANGES UNDER HEAT EXPOSURE
Aysu Jafarzade, Rasim Alosmanov.....485

GÜNƏBAXAN YAĞI TRİQLİSERİDLƏRİ VƏ N-(2-AMİNOETİL)-1,2-ETANDİAMİN ƏSASINDA ALINMIŞ SƏTHİ AKTİV MADDƏLƏRİN SİNTEZİ VƏ ONLARIN NEFT SƏNAYESİNDƏ TƏTBİQİ
Ilhama Agalar Zarbaliyeva, Sayat Knyaz Agasanova, Asgerzadeh Elmar Etibar, Amina Nadir Alimova, Hajar Tahir Nabiyeva.....490

INFLUENCE OF PROCESS PARAMETERS AND EXTRACTION STAGES ON THE EFFICIENCY OF AROMATIC HYDROCARBON SEPARATION
Gaybullaev Saidjon Abdusalimovich 494

OPTIMIZING THE AL/SI RATIO FOR DIRECT CO_2 HYDROGENATION
B.V. Guliyev, A. Zahidova, F.Ə. Nəsirov..... 500

MATHEMATICAL MODELING OF SUSTAINABLE WASTE VALORIZATION PROCESSES
Ramazonova Shohida Shomuhammadovna,
Rakhmatullayeva Ruxshona Bahromovna..... 502

ADSORPTION OF ANTIBIOTICS USING RICE HUSK HYDROCHARS PRODUCED VIA VARIOUS POST-TREATMENT METHODS
Ulduz Nazarli, Aysun Aghazada, Kifayat Gambarova,
Shalala Tanriverdiyeva, Rima Guliyeva..... 505

DEVELOPMENT OF A SUSTAINABLE YEAST-CHITOSAN BIO-COMPOSITE FILTRATION NET FOR HEAVY METAL REMOVAL AND WATER HARDNESS REDUCTION
Leyla Huseynova, Dilber Huseynova; Rima Guliyeva 509

KARBON VƏ DES ƏSASİNDA ALINMIŞ YENİ YAŞIL KATALİZATOR İŞTİRAKİNDA BİODİZEL SİNTEZİ
Gülbən Məmmədova, Yeganə Məmmədova, İbrahim Məmmədov 512

PREPARATION OF SURFACTANTS TO REMOVE OR COLLECT OIL SPILLS
Kanan Maharramli, Said Guliyev, Arzu Abdullayeva 514

DEVELOPMENT OF A MULTIFUNCTIONAL BIODEGRADABLE MULCHING FILM BASED ON PBSA INCORPORATING COFFEE SILVER SKIN AND COFFEE WASTE
Rana Rahimli, Elvira Sarsanova, Rima Guliyeva 519

ENHANCEMENT OF SULFURIC ACID PRODUCTION TECHNOLOGY BY PROCESSING SULFUR-CONTAINING WASTE GASES GENERATED DURING GAS PURIFICATION
Turakulova Marjona 524

PHYSICOCHEMICAL ANALYSIS OF FUEL DISTILLATES OBTAINED FROM WASTE TIRE
Ruxsora Khojiyeva, Ruslan Khayitov 531

AMINES USED IN THE ABSORPTION PURIFICATION OF GAS AND THE CAUSES OF FOAMING IN MDEA SOLUTION
E.R.Panoev, S.O'.Toshboev, Bozorov Gayrat, S.Yu.Begutjanova 536

THE CONCEPT OF OIL REFINING AND PETROCHEMICAL SYNTHESIS AND CLOSED-LOOP ECONOMICS FOR SOLVING ENVIRONMENTAL PROBLEMS IN OIL REFINING, PETROCHEMICAL SYNTHESIS, AND OIL AND GAS PRODUCTION
Ramin Musaev..... 541

METHANOL PRODUCTION FROM CO2 AND INDUSTRIAL OFF-GASES: ADVANCED CATALYTIC DESIGN AND HIERARCHICAL PROCESS INTEGRATION FOR A CIRCULAR ECONOMY
Suleymanova Dinara..... 546

ECO-FRIENDLY SYNTHESIS OF SOLID BASE CATALYSTS FROM LOCAL AGRICULTURAL, FOOD, AND MARINE WASTES FOR BIODIESEL PRODUCTION
Aliya Kurmayeva, Sara Malik-Aslanova..... 550

LAB-SCALE ZERO-WASTE VALORIZATION OF SPENT COFFEE GROUNDS AND SPENT DRILLING MUD
Teymur Ismayilov, Sabir Aliyev, Aliya Laylabashova..... 556

KAĞIZ TULLANTILARINDAN NEFTYIĞICI ADSORBENTİN ALINMASI
Nübar Rəhimova Rahim, Şahgəldiyev F.X. 559

PRODUCTION OF HIGH-PERFORMANCE BIO-BASED AEROGELS FROM SUGARCANE WASTE FOR CRUDE OIL REMEDIATION
Ayan Guliyeva, Revane Abdullayeva, Garanfil Ahmadova 563

IMPROVING THE ENVIRONMENTAL PERFORMANCE OF CATALYTIC CRACKING GASOLINE BY FRACTIONATION AND HYDROTREATING OF THE HEAVY FRACTION
Elvira Kazimova, Zaira Gasimova 567

STUDY OF MOLECULAR DYNAMICS SIMULATION OF SELECTIVE HEAVY METAL CAPTURE FROM HIGH-SALINITY PRODUCED WATER USING CHITOSAN OLIGOMERS
Mahabbat Aslanov 569

ENHANCING MACRONUTRIENT BIOAVAILABILITY IN SEWAGE SLUDGE-DERIVED BIOCHAR
Amil Ibadov 570

ENVİRONMENTAL ASPECT OF ELECTRİC VEHİCLES
Anar Aghayev, Azar Salimov 572

INVESTIGATION OF THE PRODUCTION OF ENVIRONMENTALLY BENIGN MIDDLE-DISTILLATE FRACTIONS VIA HYDROGENATION OF VARIOUS VEGETABLE OILS
Mammadova T., Karimli R., Aliyeva H., Mmikayilova A., Allahverdiyeva G. Z. 575

WASTE FROM AGRO-INDUSTRIAL ENTERPRISES AS PROMISING SORBENTS FOR OIL POLLUTION
Farkhod Azimov, R.F.Abbasova 578

SUSTAINABLE BIOCHEMICAL ENGINEERING FOR SPACE HABITATS: A MULTI-OMICS PLATFORM FOR FUNCTIONAL FOOD DESIGN AND CLOSED-LOOP NUTRITIONAL SYSTEMS
Fidan Guliyeva 580

STUDY OF THE EFFECT OF PRODUCED WATER COMPOSITION ON THE CORROSION PROCESS AND THE EFFECTIVENESS OF INHIBITORS
Gular Humbatzada, Agamaliyev Zaur 583

QIZIL ÇIXARMA MÜƏSİSSƏLƏRİNDƏ YARANAN SİANİD TƏRKİBLİ TULLANTI SULARININ FOTOKATALİTİK TƏMİZLƏNMƏ PROSESLƏRİ
Həsənova Seynurə Azər 585

MODIFIED NATURAL CLAY AS A POTENTIAL CD(II) ADSORBENT FROM WASTEWATER
Israfil Movsumzada, Tahir Javadzade 590

SCREENING OF IONIC LIQUIDS USING THE COSMO-RS METHOD FOR CO_2 CAPTURE
Hamida Azizbayli, Gulnar Atakishizada, Aydan Nadirova, Lala Huseynli, Fariz Amirli, Reyhan Aliyeva, Minaver Ibrahimova 592

SUSTAINABLE SOLUTIONS FOR OIL CONTAMINATION IN AZERBAIJAN: A COMPREHENSIVE STUDY ON BIOREMEDIATION AND HYBRID METHODS
Safura Ismayilova 596

LOCAL ZEOLITES FOR WASTEWATER PURIFICATION
Shakhzod Toshev, R.F.Abbasova 600

MALEIN ANHIDRIDININ A-METILSTIROLLA OLIQOMERININ DIETILENTRIAMINLƏ TIKILI SOPOLIMERI SULU SISTEMLƏRDƏN URANIL İONLARININ SORBENTLƏRİ KİMİ
M.R.Bayramov, G.M.Mehdiyeva, M.A.Ağayeva, M.Ə.Cavadov, R.V.Rüstəmov 601

YENI IZO-DESIL ƏVƏZLI 1,3-BENZOKSAZIN TÖRƏMƏLƏRININ SINTEZI VƏ ONLARIN SULFAT TURŞUSU MÜHITINDƏ KORROZIYA INHIBITORU XASSƏLƏRININ TƏDQIQI
M.R.Bayramov, G.M.Mehdiyeva, S.X.İsmayilova, L.Z.Əzimli, M.A.Ağayeva, M.Ə.Cavadov *603*

TULLANTILARIN BƏRPASI VƏ ƏTRAF MÜHİTİN REABİLİTASİYASINDA İNNOVATİV TEXNOLOGİYALAR
Nəsirova Nəsibə Volodiya qızı, Talıbzadə Zeynəb Şahin qızı *606*

VALORISATION OF INDUSTRIAL WASTE INTO CARBON-MINERALIZED COMPOSITE MASONRY UNITS VIA COLD-CURE TECHNOLOGY: THE RENEWBLOCKS PROJECT
Ziyad Shiraliyev, Farid Valimammadov, Rima Guliyeva *610*

INVESTIGATION OF THE SORPTION OF CO^{2+} IONS FROM INDUSTRIAL WASTEWATER USING MODIFIED BENTONITE
Rzaeva A.A., Imanova N.A., Mammadova S.A., Mahmudov F.T, Adigozalova M.N., Asgarova T.N. *615*

THANK YOU FOR YOUR SUPPORT AND CONTRIBUTION!

SOCAR POLYMER

SOCAR DOWNSTREAM

AzerGold
QAPALI SƏHMDAR CƏMİYYƏTİ

MAIRE



Bakı Ali Neft Məktəbinin Kampusu
Azərbaycan Respublikası, Bakı şəhəri,
Səbail rayonu, Yeni Salyan yolu 3-cü km. 25

Baku Higher Oil School Campus
25, the 3rd km., Yeni Salyan Highway,
Sabail district, Baku, Azerbaijan

Telefon / Phone: (+994 12) 521 31 11, 521 33 60;
Faks/Fax: (+994 12) 521 33 64;
info@bhos.edu.az

www.facebook.com/BakiAliNeftMektebi
www.bhos.edu.az

ISBN: 978-9952-8513-5-9